

N76-19643

Camera-ready copy of cover at NASA Hq., Code KSP

NASA SP-7601

THE ORBITING GEOPHYSICAL
 OBSERVATORIES
 OGO
 PROGRAM
 SUMMARY

Nov. 10, 1975

NATIONAL AERONAUTICS AND SPACE ADMINISTRATION



THE ORBITING GEOPHYSICAL
OBSERVATORIES
OGO
PROGRAM
SUMMARY

By

John E. Jackson and James I. Vette

Prepared by

National Space Science Data Center
NASA Goddard Space Flight Center



Scientific and Technical Information Office

1975
NATIONAL AERONAUTICS AND SPACE ADMINISTRATION
Washington, D.C.

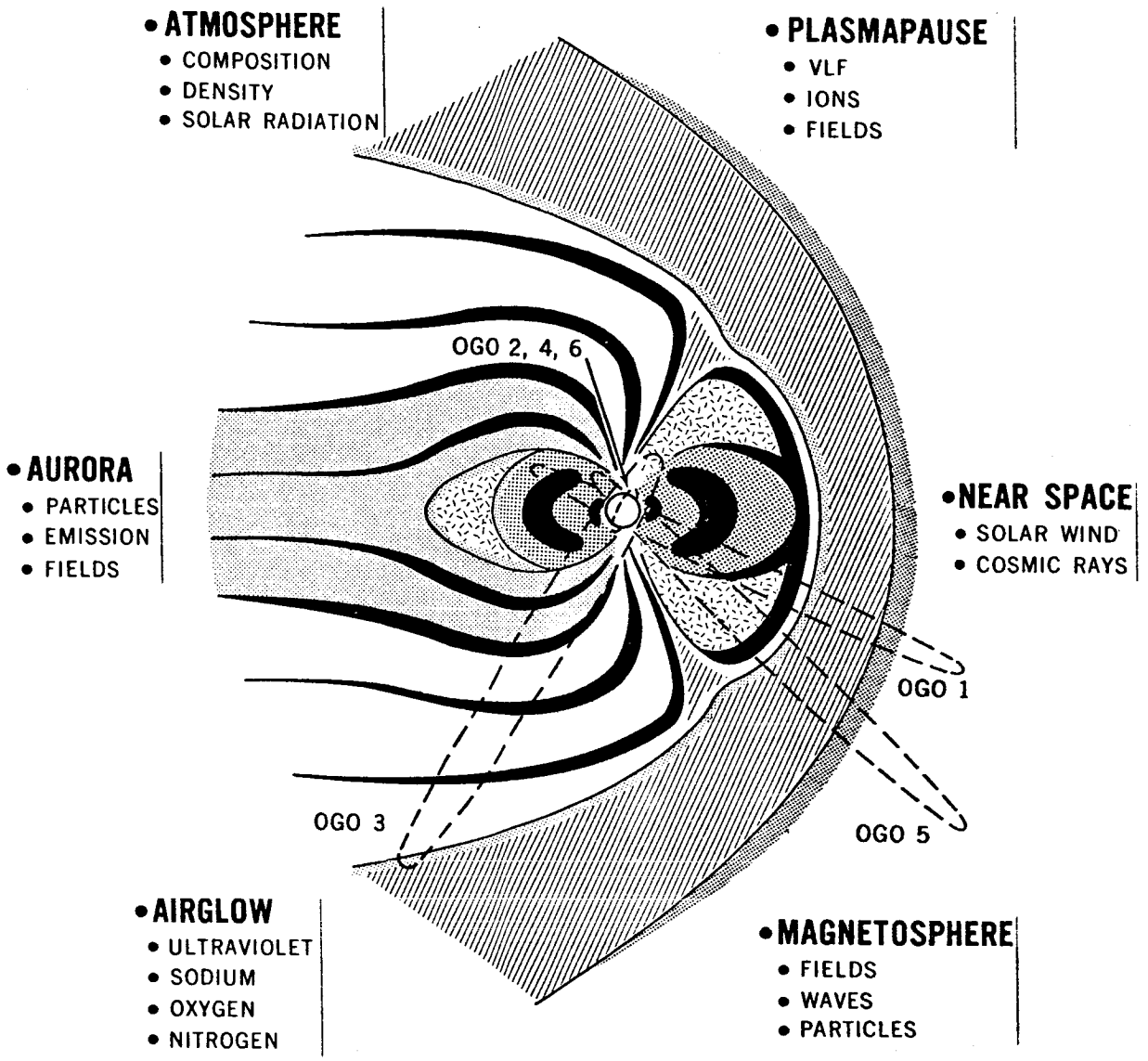
Nov. 10, 1975

Camera-ready copy of spine at NASA Hq., KSP

NASA
SP-7601

OGO PROGRAM SUMMARY

Jackson
and
Vette



December 10, 1975

**ORBITING GEOPHYSICAL OBSERVATORIES
1964-1971**

CONTENTS

	PAGE
I. FOREWORD	I-1
II. INTRODUCTION	II-1
III. OVERVIEW OF THE OGO PROGRAM	III-1
A. The OGO Program	III-1
1. Objectives and Background	III-1
2. Approach and Mission Profiles	III-1
3. Description of the OGO Spacecraft	III-2
3.1 Overall Configuration	III-2
3.2 Deployment Considerations	III-4
3.3 Major Subsystems	III-5
4. Technological Accomplishments	III-6
4.1 Operation Summary	III-6
4.2 Performance of Spacecraft Systems	III-7
4.3 Summary of Technological Accomplishments	III-7
B. Scientific Results	III-7
1. OGO 1 Results	III-7
2. OGO 2 Results	III-10
3. OGO 3 Results	III-12
4. OGO 4 Results	III-15
C. References	III-21
IV. SPACECRAFT AND EXPERIMENT CHARACTERISTICS WITH LITERATURE REFERENCES	IV-1
A. OGO 1	IV-1
B. OGO 2	IV-9
C. OGO 3	IV-16
D. OGO 4	IV-24
E. OGO 5	IV-32
F. OGO 6	IV-42
V. INDEXES TO EXPERIMENT CHARACTERISTICS	V-1
A. Index of Principal and Co-Investigators and Experiments	V-1
B. Index of Original Institutions of Principal Investigators and Experiments	V-13
C. Index of Spacecraft and Experiments	V-17
VI. LITERATURE CITATIONS AND ABSTRACTS	VI-1
A. Literature Cited in IAA	VI-1
B. Literature Cited in STAR	VI-82
C. Literature Cited in Other Series	VI-108
D. Literature Not Cited in the NASA System	VI-111
VII. INDEXES TO LITERATURE CITATIONS AND ABSTRACTS	VII-1
A. Subject Index	VII-1
B. Personal Author Index	VII-49
C. Corporate Source Index	VII-71
VIII. GLOSSARY OF ACRONYMS AND ABBREVIATIONS	VIII-1

II. INTRODUCTION

Data from OGO satellites have provided new knowledge concerning the solar wind, the near-interplanetary environment, the bow shock, the transition region, the magnetopause, the magnetotail, the radiation belts, the plasmasphere, the terrestrial magnetic fields, the auroral regions, and the upper atmosphere. The OGO data acquisition period, which extended from September 1964 to June 1971, encompassed a complete range of solar activity and a time interval when other satellites such as IMPs B-G, ATS 1 & 3, and INJUN 4 & 5 were measuring similar phenomena throughout the magnetosphere and interplanetary medium near the Earth. The extremely high data rate of OGO allowed measurement of various processes on a time scale previously unavailable for space experiments. All of these factors contributed to the extensive role which OGO data have played in our understanding of the near-Earth environment.

Although there continue to be articles appearing in the published literature concerning OGO, the majority of them have been written, particularly for OGOs 1-4, and one is now able to take a measure of the accomplishments of this program. Since the OGOs were in many ways the most complex scientific spacecraft ever attempted by NASA, it is not surprising that some of the scientific objectives were not achieved on the earlier missions. All OGOs, however, yielded useful results from at least one half of their experiments and at least 96 of the 132 OGO experiments can be considered successful. There has been an average of 3.3 papers per OGO experiment in refereed journals. Some additional interesting statistical data pertaining to the literature will be discussed later.

In the following section of this document an overview of the OGO program is presented which provides a discussion of the objectives, the relationships to other programs, spacecraft major characteristics, typical orbits and mission profiles, technological accomplishments, as well as the scientific results of OGOs 1-4. (Since many research papers based upon OGOs 5 and 6 continue to appear in the literature, the scientific results of OGOs 5 and 6 will be presented as a supplement to this Program Summary.) Brief descriptions of the six OGO spacecraft and of the experiments on each are given in Section IV which

includes statements concerning flight performance from which one can appraise the potential success of each spacecraft and experiment. This section is ordered by spacecraft and last name of the principal investigators of the experiments.

In order to provide some measure of final accomplishment and to provide the interested reader with more extensive details, a bibliography for each spacecraft and for each experiment is identified in that section. Because a large number of the cited documents are concerned with more than one OGO experiment or spacecraft, the actual citations and abstracts are provided in accession order in Section VI. The documents are identified by their A, N, or B accession numbers. These numbers are explained in the beginning of Section VI. Since the Spacecraft and Experiments Characteristics section provides identification and affiliation of project and experiment personnel as well as common names, other names and identification numbers of individual spacecraft and experiments, an index section directly follows the Characteristics section. The personnel affiliations given are those at the main phase of the program, not current affiliations. There are three experiment indexes: the first is ordered by spacecraft name and principal investigator last name, the second gives original institution of the principal investigator, and the last gives principal and co-investigator names.

NSSDC maintains a computerized file on all spacecraft and experiments known as its Automated Internal Management File. All of the information presented in Section IV, with the exception of the bibliographies, were extracted from this file. Many other characteristics of spacecraft, experiments, and data obtained by them exist in this file. Two major, periodic publications of NSSDC, *Report on Active and Planned Spacecraft and Experiments* and the *Data Catalog of Spacecraft Experiments* are produced directly from the AIM file. Any one interested in obtaining more information on these documents and other Data Center publications should request *NSSDC and WDC-A-R&S Document Availability and Distribution Services* (NSSDC 74-10) by writing to:

Code 601
Goddard Space Flight Center
Greenbelt, Maryland 20771

In Section III the experiments are identified by the project number. NSSDC uses an identification number that is based on the spacecraft international designation assigned on behalf of COSPAR by the IUWDS World Warning Agency for Satellites. To assist readers in translating between the project number, NSSDC-ID, and the principal investigator last name, Tables II-1 through II-4 are provided. Since the experiments on OGO 1 and OGO 3 were nearly

TABLE II-1

OGO 1 Experiments				OGO 3 Experiments	
Project No.	NSSDC ID	Principal Investigator	Institution	Project No.	NSSDC ID
A-01	64-054A-12	Anderson, K.A.	U of California, Berkeley	B-01	66-049A-01
A-02	64-054A-13	Wolfe, J. H.	ARC	B-02	66-049A-05
A-03	64-054A-14	Bridge, H. S.	MIT	B-03	66-049A-06
A-04	64-054A-15	Cline, T. L.	GSFC	B-04	66-049A-04
A-05	64-054A-16	Konradi, A.	GSFC	B-05	66-049A-10
A-06	64-054A-17	McDonald, F. B.	GSFC	B-06(P)	66-049A-02
		Evans, D.S.	GSFC	B-06(P)	66-049A-07
A-07	64-054A-18	Simpson, J. A.	U of Chicago	B-07	66-049A-03
A-08	64-054A-19	Van Allen, J. A.	SUI		
		Frank, L. A. (1)	SUI	B-08	66-049A-08
A-09(P)	64-054A-20	Winckler, J. R.	U of Minnesota	B-09(P)	66-049A-23
A-09(P)	64-054A-21	Winckler, J. R.	U of Minnesota	B-09(P)	66-049A-22
A-10	64-054A-01	Smith, E. J.	JPL	B-10	66-049A-12
A-11	64-054A-02	Heppner, J. P.	GSFC	B-11	66-049A-11
A-12	64-054A-03	Sagalyn, R. C.	AFCRL	B-12	66-049A-13
A-13	64-054A-04	Whipple, E. C.	ESSA-Boulder	B-13	66-049A-14
A-14	64-054A-05	Hargreaves, J. K.(2)	ESSA-Boulder		
		Fritz, R. B.(3)	ESSA-Boulder	B-14	66-049A-16
A-15	64-054A-06	Taylor, H. A., Jr.	GSFC	B-15	66-049A-15
A-16	64-054A-07	Bohn, J. L.(4)	Temple U	B-16	66-049A-21
A-17	64-054A-08	Helliwell, R. A.	Stanford U	B-17	66-049A-17
A-18	64-054A-09	Haddock, F. T.	U of Michigan	B-18	66-049A-18
A-19	64-054A-10	Mange, P. W.	NRL	B-19	66-049A-19
A-20	64-054A-11	Wolff, C. L.	GSFC	B-20	66-049A-20

- (1) J. A. Van Allen, Univ. of Iowa, was original PI
- (2) R. S. Lawrence, ESSA-Boulder, was original PI
- (3) J. K. Hargreaves, ESSA-Boulder, was original PI
- (4) W. M. Alexander, GSFC, was original PI
- (P) Part of

Nov. 10, 1975

TABLE II-2

OGO 2 Experiments				OGO 4 Experiments	
Project No.	NSSDC ID	Principal Investigator	Institution	Project No.	NSSDC ID
C-01(P)	65-081A-01	Haddock, F. T.	U of Michigan	D-01	67-073A-01
C-01(P)	65-081A-21	Haddock, F. T.	U of Michigan		
C-02	65-081A-02	Helliwell, R. A.	Stanford U	D-02	67-073A-02
C-03	65-081A-03	Morgan, M. G.	Dartmouth College	D-03	67-073A-03
C-05	65-081A-04	Smith, E. J.	JPL	D-05	67-073A-05
C-06	65-081A-05	Cain, J. C.	GSFC	D-06	67-073A-06
C-07	65-081A-06	Anderson, H. R.	Rice U	D-07	67-073A-07
C-08	65-081A-07	Simpson, J. A.	U of Chicago	D-08	67-073A-08
C-09	65-081A-08	Webber, W. R.	U of Minnesota	D-09	67-073A-09
C-10	65-081A-18	Van Allen, J. A.	SUI	D-10	67-073A-10
C-11	65-081A-09	Hoffman, R. A.	GSFC	D-11	67-073A-11
C-12	65-081A-10	Reed, E. I.	GSFC	D-12	67-073A-12
C-13	65-081A-11	Mange, P. W.	NRL	D-13	67-073A-13
C-14	65-081A-12	Barth, C. A.	U of Colorado	D-14	67-073A-14
C-15	65-081A-13	Jones, L. M.	U of Michigan	D-15	67-073A-15
C-16	65-081A-15	Taylor, H. A.	GSFC	D-16	67-073A-16
C-17	65-081A-20	Newton, G. P.	GSFC	D-17	67-073A-17
C-18	65-081A-14	Nilsson, C. S.	SAO	D-18	67-073A-18
C-19	65-081A-19	Donley, J. L.(1)	GSFC		
		Chandra, S.(2)	GSFC	D-19	67-073A-19
C-20	65-081A-17	Hinteregger, H. E.	AFCRL	D-20	67-073A-20
C-21	65-081A-16	Kreplin, R. W.	NRL	D-21	67-073A-21

(1) R. E. Bourdeau, GSFC, was original PI
 (2) J. L. Donley, GSFC, was original PI
 (P) Part of

TABLE II-3
OGO 5 Experiments

Project No.	NSSDC ID	Principal Investigator	Institution
E-01	68-014A-01	Boyd, R. L. F.	U College London
E-02	68-014A-02	Sagalyn, R. C.	AFCRL
E-03	68-014A-03	Serbu, G. P.	GSFC
E-04	68-014A-04	Anderson, K. A.	U of California, Berkeley
E-05	68-014A-05	Cline, T. L.	GSFC
E-06	68-014A-06	West, H. I., Jr.	LRL
E-07	68-014A-07	Frank, L. A.	SUI
E-08	68-014A-08	Hutchinson, G. W.	U of Southampton
E-09	68-014A-09	Meyer, P.	U of Chicago
E-10	68-014A-10	McDonald, F. B.	GSFC
E-11	68-014A-11	Ogilvie, K. W.	GSFC
E-12	68-014A-12	Van De Hulst, H. C.	Netherlands Inst
E-13	68-014A-13	Coleman, P. J., Jr.	UCLA
E-14	68-014A-14	Coleman, P. J., Jr.	UCLA
E-15	68-014A-15	Heppner, J. P.	GSFC
E-16	68-014A-16	Smith, E. J.	JPL
E-17	68-014A-17	Snyder, C. W.	JPL
E-18	68-014A-18	Sharp, G. W.	Lockheed
E-20	68-014A-20	Haddock, F. T.	U of Michigan
E-21	68-014A-21	Thomas, G. E.	U of Colorado
E-22	68-014A-22	Blamont, J. E.	CNES, France
E-23	68-014A-23	Kreplin, R. W.	NRL
E-24	68-014A-24	Crook, G. M.	TRW
E-26	68-014A-26	Aggson, T. L.	GSFC
E-27	68-014A-27	Simpson, J. A.	U of Chicago

Nov. 10, 1975

TABLE II-4
OGO 6 Experiments

pl

Project No.	NSSDC ID	Principal Investigator	Institution
F-01	69-051A-01	Sharp, G. W.	Lockheed
F-02	69-051A-02	Nagy, A. F.	U of Michigan
F-03	69-051A-03	Hanson, W. B.	University of Texas, Dallas
F-04	69-051A-04	Reber, C. A.	GSFC
F-05	69-051A-05	Taylor, H. A., Jr.(1)	GSFC
F-06	69-051A-06	Hanson, W. B.	University of Texas, Dallas
F-07	69-051A-07	McKeown, D.	GD, San Diego
F-08	69-051A-08	Kreplin, R. W.	NRL
F-09	69-051A-09	Bedo, D. E.	AFCLR
F-10	69-051A-10	Regener, V. H.	U of New Mexico
F-11	69-051A-11	Blamont, J. E.	CNES, France
F-12	69-051A-12	Clark, M. A.	Aerospace Corp.
F-13	69-051A-13	Barth, C. A.	U of Colorado
F-14	69-051A-14	Blamont, J. E.	CNES, France
F-15	69-051A-15	Evans, D. S.	GSFC
F-16	69-051A-16	Farley, T. A.	UCLA
F-17	69-051A-17	Williams, D. J.	GSFC
F-18	69-051A-18	Lockwood, J. A.	U of New Hampshire
F-19	69-051A-19	Masley, A. J.	MD
F-20	69-051A-20	Stone, E. C.	Cal Tech
F-21	69-051A-21	Cain, J. C.	GSFC
F-22	69-051A-22	Smith, E. J.	JPL
F-23	69-051A-23	Aggson, T. L.	GSFC
F-24	69-051A-24	Helliwell, R. A.	Stanford U
F-25	69-051A-25	Laaspere, T.	Dartmouth College
F-26	69-051A-26	Donahue, T. M.	U of Pittsburgh

(1) R. A. Pickett, GSFC, was original PI

December 17, 1975

TABLE II-4
OGO 6 Experiment S

Project No.	NSSDC ID	Principal Investigator	Institution
F-01	69-051A-01	Sharp, G. W.	Lockheed
F-02	69-051A-02	Nagy, A. F.	U of Michigan
F-03	69-051A-03	Hanson, W. B.	University of Texas, Dallas
F-04	69-051A-04	Reber, C. A.	GSFC
F-05	69-051A-05	Taylor, H. A., Jr.(1)	GSFC
F-06	69-051A-06	Hanson, W. B.	University of Texas, Dallas
F-07	69-051A-07	McKeown, D.	GD, San Diego
F-08	69-051A-08	Kreplin, R. W.	NRL
F-09	69-051A-09	Bedo, D. E.	AFCRL
F-10	69-051A-10	Regener, V. H.	U of New Mexico
F-11	69-051A-11	Blamont, J. E.	CNES, France
F-12	69-051A-12	Clark, M. A.	Aerospace Corp.
F-13	69-051A-13	Barth, C. A.	U of Colorado
F-14	69-051A-14	Blamont, J. E.	CNES, France
F-15	69-051A-15	Evans, D. S.	GSFC
F-16	69-051A-16	Farley, T. A.	UCLA
F-17	69-051A-17	Williams, D. J.	GSFC
F-18	69-051A-18	Lockwood, J. A.	U of New Hampshire
F-19	69-051A-19	Masley, A. J.	MD
F-20	69-051A-20	Stone, E. C.	Cal Tech
F-21	69-051A-21	Cain, J. C.	GSFC
F-22	69-051A-22	Smith, E. J.	JPL
F-23	69-051A-23	Aggson, T. L.	GSFC
F-24	69-051A-24	Helliwell, R. A.	Stanford U
F-25	69-051A-25	Laaspere, T.	Dartmouth College
F-26	69-051A-26	Donahue, T. M.	U of Pittsburgh

(1) R. A. Pickett, GSFC, was original PI

Nov. 10, 1975

INTRODUCTION

identical and similarly on OGO 2 and OGO 4, these pairs are shown together in Tables II-1 and II-2, respectively. It should be noted that a few experiments have been separated by NSSDC into two uniquely identified parts. This is done when the Data Center recognizes that the data will be provided independently for archival use and where many of the publications are related only to the separate parts of that experiment. In a few cases the original principal investigator selected by NASA Headquarters was replaced. The names shown in Tables II-1 through II-4 are the investigators who served as principals throughout the most important phases of each mission and the analysis of the data. For these cases, the originally selected PIs are given in footnotes.

As discussed in the Foreword, the Data Center maintains a computerized literature file which contains fields for the identification of experiments discussed in the document. This file is known as the Technical Reference File. Because the NASA Scientific and Technical Information Facility maintains abstracts, author affiliations, and contract or grant numbers, these items are not present in the TRF. There is an item or field in the TRF which classifies a document for each associated experiment as to whether it was written by: (a) people associated with the principal or other investigators directly connected with the experiment, (b) scientists not directly associated with the above group, or (c) personnel under contract to the principal investigator -- these contractors are usually involved with the construction and/or calibration of the instrument or with certain phases of the data analysis. In addition, this field also allows the classification of the content of the article as to whether it deals with the experiment or the data derived from the experiment in a major or secondary manner.

In most scientific papers, the introduction discusses previous work in the fields of interest and refers implicitly or explicitly to other spacecraft experiment results. Such references do not merit secondary recognition in the TRF classification scheme. Only if data from experiments are used or discussed in some explicit manner to support conclusions or to compare with the data of the main experiments presented in the paper are those experiments identified and classified as secondary. In a general review article where numerous experiments are mentioned, each such experiment is classified as secondary.

In the bibliography portion of Section IV, a two letter code is used to classify the article. A first letter P is used to denote the principal investigator group, including other investigators associated formally with the experiment although they may be in a different institution from that of the PI. A first letter O is used to denote all other authors except those under contract to the PI. This latter group is denoted by the two letter code PC, and it is a safe assumption

that such a paper will deal with the given experiment in a major way. The major or secondary content appears as the second letter M or S. Consequently, the five classifications for the experiment papers are: PM, PS, PC, OM, and OS. A similar classification of spacecraft papers into these five categories is also made. However, since the meaning is slightly different in this case, the explicit description of each appears with each spacecraft/mission bibliography.

The classification of author type is straightforward but the major or secondary classification is somewhat subjective. In order to provide some measure of consistency, only one person (JIV) has made this classification for all the articles which appear in this Summary. It is recognized that differences of opinion may exist as to the secondary classification. It has been our intent in so classifying the articles that the less experienced reader can be guided to those papers which clearly provide a major discussion of the given experiment and the data obtained from it. It has not been our intent to downgrade the implicit influence that another measurement may have had on the author in reaching his conclusions.

In order to obtain as complete a bibliography as possible for this OGO Summary, the following procedure was used. All articles in the TRF with identifiers for each of the six OGO spacecraft and its associated experiments were printed out with author, title, and citation. All articles in the three files *IAA*, *STAR*, and *OSTARE* (See Section VI) of the NASA system with keywords of the common name or alternate names of the OGO spacecraft listed in Section IV, as well as the keyword "Geophysical Observatories," were printed out. A comparison of these two printouts was made and missing articles were added appropriately to both the NASA files and the NSSDC TRF. The NASA accession numbers for each article were entered into the TRF. Similar comparisons were made at different times; the final such comparison was made with the printouts of July 1, 1974. In November 1974, a search on contract or grant number on the NASA files produced about 15 previously unidentified documents.

Because of certain problems with older documents for which NSSDC no longer possessed a hard copy version, it was not possible to enter these into the NASA system. In addition, in attempting to include OGO-related preprints which were acquired by NSSDC after July 1, 1974, and previously identified preprints which were published in journals or symposium proceedings after this date, it was necessary to identify these by the TRF accession number (B number) if time had not permitted the assignment of a NASA system number.

One other point should be clarified. A preprint which enters the NASA system will receive an N

INTRODUCTION

identical and similarly on OGO 2 and OGO 4, these pairs are shown together in Tables II-1 and II-2, respectively. It should be noted that a few experiments have been separated by NSSDC into two uniquely identified parts. This is done when the Data Center recognizes that the data will be provided independently for archival and where many of the publications are related only to the separate parts of that experiment. In a few cases the original principal investigator selected by NASA Headquarters was replaced. The names shown in Tables II-1 through II-4 are the investigators who served as principals throughout the most important phases of each mission and the analysis of the data. For these cases, the originally selected PIs are given in footnotes.

As discussed in the Foreword, the Data Center maintains a computerized literature file which contains fields for the identification of experiments discussed in the document. This file is known as the Technical Reference File. Because the NASA Scientific and Technical Information Facility maintains abstracts, author affiliations, and contract or grant numbers, these items are not present in the TRF. There is an item or field in the TRF which classifies a document for each associated experiment as to whether it was written by: (a) people associated with the principal or other investigators directly connected with the experiment; (b) scientists not directly associated with the above group; or (c) personnel under contract to the principal investigator. These contractors are usually involved with the construction and/or calibration of the instrument or with certain phases of the data analysis. In addition, this field also allows the classification of the content of the article as to whether it deals with the experiment or the data derived from the experiment in a major or secondary manner.

In most scientific papers, the introduction discusses previous work in the fields of interest and refers implicitly or explicitly to other spacecraft experiment results. Such references do not merit secondary recognition in the TRF classification scheme. Only if data from experiments are used or discussed in some explicit manner to support conclusions or to compare with the data of the main experiments presented in the paper are those experiments identified and classified as secondary. In a general review article where numerous experiments are mentioned, each such experiment is classified as secondary.

In the bibliography portion of Section IV, a two letter code is used to classify the article. A first letter P is used to denote the principal investigator group, including other investigators associated formally with the experiment although they may be in a different institution from that of the PI. A first letter O is used to denote all other authors except those under contract to the PI. This latter group is denoted by the two letter code PC, and it is a safe assumption

that such a paper will deal with the given experiment in a major way. The major or secondary content appears as the second letter M or S. Consequently, the five classifications for the experiment papers are: PM, PS, PC, OM, and OS. A similar classification of spacecraft papers into these five categories is also made. However, since the meaning is slightly different in this case, the explicit description of each appears with each spacecraft/mission bibliography.

The classification of author type is straightforward but the major or secondary classification is somewhat subjective. In order to provide some measure of consistency, only one person (JIV) has made this classification for all the articles which appear in this Summary. It is recognized that differences of opinion may exist as to the secondary classification. It has been our intent in so classifying the articles that the less experienced reader can be guided to those papers which clearly provide a major discussion of the given experiment and the data obtained from it. It has not been our intent to downgrade the implicit influence that another measurement may have had on the author in reaching his conclusions.

In order to obtain as complete a bibliography as possible for this OGO Summary, the following procedure was used. All articles in the TRF with identifiers for each of the six OGO spacecraft and its associated experiments were printed out with author, title, and citation. All articles in the three files IAA, STAR, and OSTARE (See Section VI) of the NASA system with keywords of the common name or alternate names of the OGO spacecraft listed in Section IV, as well as the keyword "Geophysical Observatories," were printed out. A comparison of these two printouts was made and missing articles were added appropriately to both the NASA files and the NSSDC TRF. The NASA accession numbers for each article were entered into the TRF. Similar comparisons were made at different times; the final such comparison was made with the printouts of July 1, 1974. In November 1974, a search on contract or grant number on the NASA files produced about 15 previously unidentified documents.

Because of certain problems with older documents for which NSSDC no longer possessed a hard copy version, it was not possible to enter these into the NASA system. In addition, in attempting to include OGO-related preprints which were acquired by NSSDC after July 1, 1974, and previously identified preprints which were published in journals or symposium proceedings after this date, it was necessary to identify these by the TRF accession number (B number) if time had not permitted the assignment of a NASA system number.

One other point should be clarified. A preprint which enters the NASA system will receive an N

INTRODUCTION

number. When that preprint or some slightly altered version including title (because of a referee's or editor's comments) appears in a published journal or book, it will receive, after some time delay, an A number. The A number has been used to identify the article in all such cases.

There are a large number of documents (either N or B numbered) which have not been included in the bibliography because they would add considerably to the bulk of this Summary without being very useful to most readers. The classes of these OGO documents are listed below and many are available, mainly in microfiche, from NSSDC.

1. Certain NASA News Releases
2. Flight Evaluation Reports
3. Operations Summary Reports
4. Brochures for Experiments
5. Specifications for Spacecraft
6. Specifications for Experiment Interfaces
7. Tracking and Data Acquisition Support Plans
8. Working Group Transactions
9. Experiment Test Gathering Minutes by the Project
10. Experiments Proposals
11. Telemetry Data Processing Plans
12. Operations Requirements Documents
13. Thermal Analysis Reports
14. Schematic Drawings
15. Experiment Bulletins
16. Program Bibliographies (superseded by this one)
17. Description of Tape Formats for Experiments (available in NSSDC Data Catalogs)
18. Orbital Operations Final Reports
19. Post Launch Reports
20. Data Index and Catalog for Telemetry Data
21. National and Organizational Annual Reports to COSPAR
22. Project Development Plan
23. Data User's Notes (written by NSSDC personnel)
24. System Engineering Documents

All the available experiment progress reports have been included because they contain some useful information and summaries of results. In addition, it was our desire to demonstrate that only a few of these reports reach NSSDC or the NASA Facility.

We conclude this section with some statistical information on the bibliography contained in Section VI. There are 774 documents included; 415 are articles in refereed scientific or technical journals; 150 are

articles in proceedings of symposia (we have lumped proceedings from all types of publications except refereed journals, including books, NASA special publications, university, industry, and the COSPAR publication, Space Research). The remaining reports are classified as: Book Articles (6), Government (68), University (101), and Industry (34). The journals in which most of the articles have been found and the number of articles are given in Table II-5.

TABLE II-5

Journals Where Most OGO Experiment Articles Appear

Journal Name	No. of Articles	
Annales de Géophysique	7	
Astrophysical Journals Pts. 1, 2, & 3	22	<i>Sci accents</i>
Journal of Geophysical Research - Space Science	243	<i>10TR</i>
IEEE Proceedings (all)	21	
Journal of Atmospheric & Terrestrial Physics	9	
Physical Review Letters	6	
Planetary and Space Science	19	
Radio Science	8	
Solar Physics	23	
Space Research (COSPAR)	31	
Space Science Reviews	9	
Other Journals	17	

It is clear by examining Table II-5 that the predominant journal for publication of OGO results was the Journal of Geophysical Research and, since that journal divided into 3 separate parts, the Space Science part. Included in the university reports are approximately 25 PhD theses.

Of the 736 documents which were related to experiments, as opposed to spacecraft, the distribution was PM = 588, OM = 17, PS = 59, OS = 63, and PC = 9. Since a given document could be related to more than one OGO experiment, a single code assignment was made on the basis of the hierarchy PM, OM, PS, OS, PC. As expected, the majority of documents cited were written by the PI group and discussed as a major topic of an OGO experiment.

In order to demonstrate the time period required to produce OGO scientific results in the archival literature, the graphs, Figures II-1 and II-2, are given. The abscissa is the time after launch, and the ordinate shows the cumulative number of experiment-related articles published in journals in 6-month intervals for each spacecraft. Any article associated with two or more spacecraft is included in the most recently launched spacecraft. Consequently, any paper associated with an OGO 1 experiment and some other OGO

Nov. 10, 1975

INTRODUCTION

experiment will not appear in the OGO 1 graph. The peak publication rate occurs for 2 to 3 years beginning some 2 1/2 to 3 years after launch. About 50% of the publications occur later than 3 to 3 1/2 years after launch, allowing an average time of 6 months for publication. From this it is clear that a large fraction of the important experimental results are produced well after prime data analysis funding has ended. These charts indicate that additional support after prime data analysis is essential if most of the scientific results are to be understood and made accessible to the scientific community in an acceptable manner.

The last data point for each of the OGO publications graphs in Figures II-1 and II-2 represents the total number of publications for the corresponding

OGO missions near the end of 1974. Figure II-1 indicates that the number of publications for OGO 1, OGO 2, and OGO 3 had increased very little during the previous 2 years. Figure II-2, however, shows that the total number of publications for OGO 4, OGO 5, and OGO 6 was still increasing at a high rate. The OGO 4 overview had to be revised several times because of the continued growth in publications during the preparation of this report. Numerous revisions were required in other sections of the report as well. It was therefore decided to publish the overview of OGO 5 and OGO 6, as a supplement to the present report. The supplement will include an updating of the publications by experiments, additions, and corrections to the bibliographic citations (and abstracts). Comments from OGO participants concerning any portion of this report will be most welcome.

JOURNAL ARTICLES PUBLISHED, CUMULATIVE

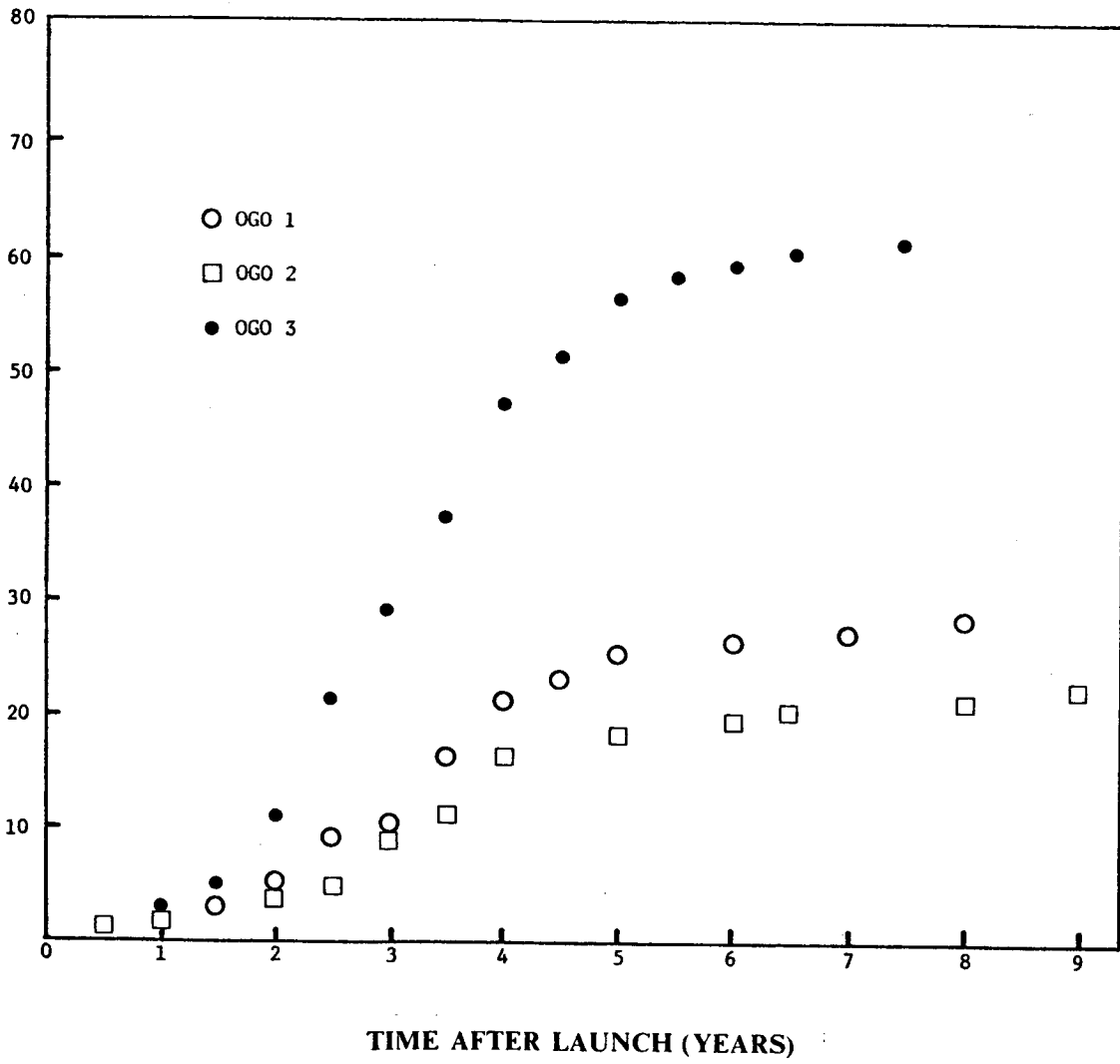


FIGURE II-1

JOURNAL ARTICLES PUBLISHED, CUMULATIVE

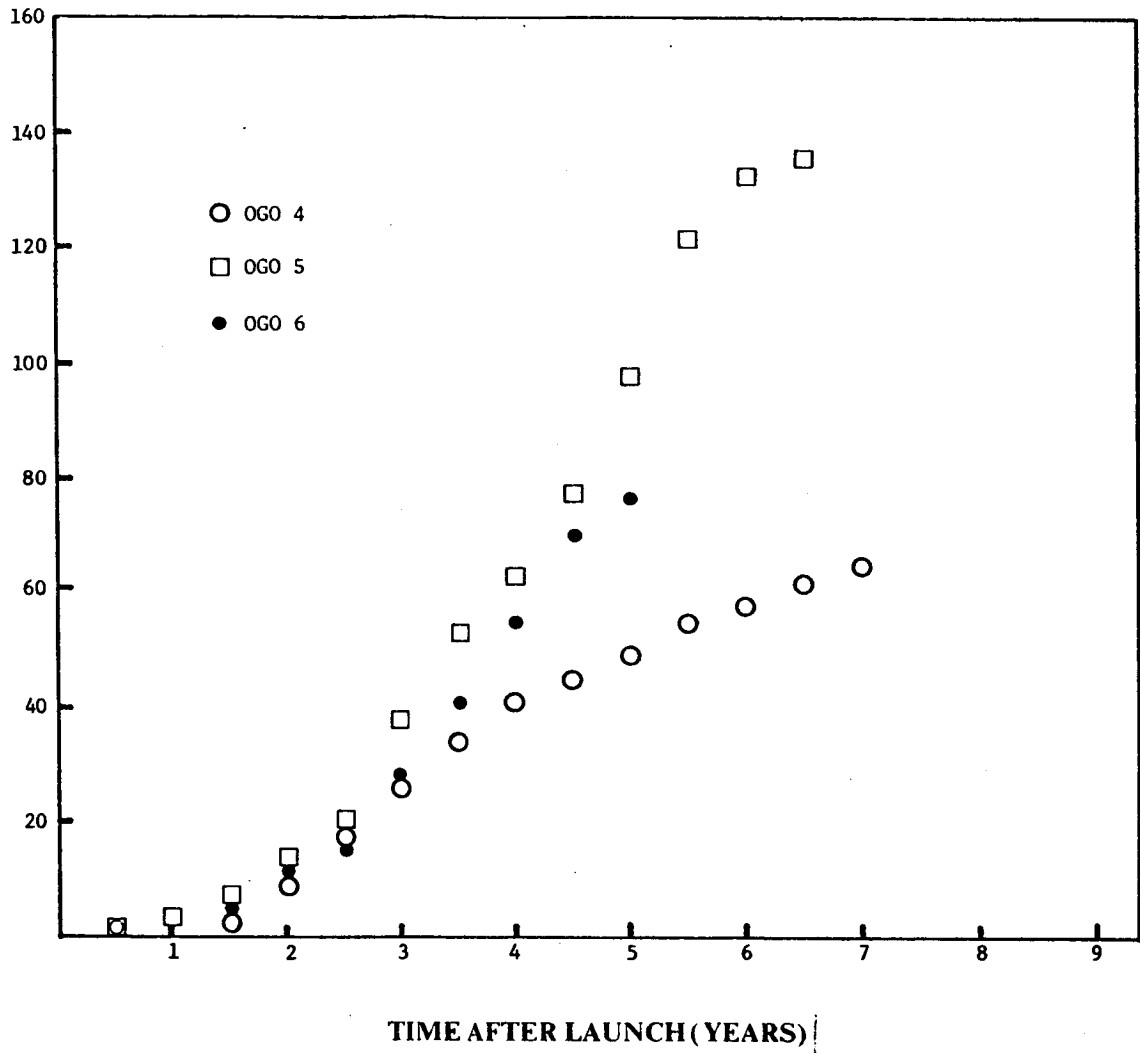


FIGURE II-2

A. The OGO Program

I. Objectives and Background

An overview of the OGO program might begin with some reflection upon the explosive growth of the Space Program in the United States during the late fifties and the early sixties and with the realization that the development of OGO as a 'third-generation' spacecraft was already well underway in 1960, three years after the launch of Sputnik I. Many of the great discoveries of our near-Earth environment, such as the radiation belts, the magnetosphere, and the solar wind, had already been made by the early exploratory satellites, such as Explorers I, III, IV, and XI, Vanguard I, and Pioneers III and IV. In the early sixties (1960-1963), these discoveries were investigated in greater detail by a dozen or so 'second-generation' spacecraft characterized by greater weight and experiment carrying capability. By 1960, however, it had become evident that the more definitive space investigations would require third-generation research tools, i.e. large spacecraft which would allow simultaneous observations by many different experiments and would provide a very-high bit rate telemetry. The third generation spacecraft were named observatories to emphasize the more comprehensive nature of the research program which would be conducted. The Orbiting Geophysical Observatory (OGO) is one of several types of observatories conceived and initiated circa 1960.

The concept of the OGO was developed by the Goddard Space Flight Center (GSFC) of the National Aeronautics and Space Administration (NASA). The prime contractor for the OGO spacecraft, the TRW Systems Group, Redondo Beach, California, was directed to proceed on the OGO effort through a Letter Contract, dated 6 January, 1961. The definitive NASA Contract was received by TRW on 3 August 1962 and by this date the NASA selection of experiments for OGO 1 had also been completed.

The scientific objective of the OGO program was to conduct a large number of diversified and interrelated physical experiments within the Earth's atmosphere and magnetosphere and in cis-lunar space in order to gain better understanding of Earth-Sun relationships and of the Earth itself, as a planet. The technological objective of the program—to enable achievement of the scientific objectives—was to develop and operate a three-axis stable 'standard observatory' which could be used repeatedly to carry large numbers of easily integrated scientific experiments into appropriate orbits.

As indicated earlier, the exploration of the near-Earth environment was well under way when the OGO program was initiated. The programs used for these preliminary explorations became, to some extent, parallel or even competing efforts after the launch of OGO 1. This was usually a very healthy situation for the OGO program, leading to extensive interchange of ideas and providing a strong incentive for the rapid dissemination of important results. The objectives of related programs such as the Energetic Particle Explorers, the Interplanetary Monitoring Platform (IMP) series, and the International Satellites for Ionospheric Studies (ISIS) were actually quite different from the OGO objectives, and the results related to OGO were, in most cases, complementary. For example, multi-satellite exploration of the magnetosphere and near-interplanetary space made possible the concurrent performance of related experiments studying energetic particles and their magnetic field at various positions in space. Correlation of the data from these experiments with data from the OGO experiments assisted in the separation of the spatial and temporal characteristics of cosmic rays, solar particles, geomagnetically trapped particles, and the galactic, interplanetary, and terrestrial magnetic fields.

In some cases, however, effort on the analysis of certain marginal OGO 1 and OGO 2 experiments was terminated and re-directed toward the analysis of more promising data from other programs.

2. Approach and Mission Profiles

The scientific goals of the OGO program were accomplished through a series of regularly scheduled launches in two basic orbits. An eccentric orbit (EGO) mission with apogee at about 150,000 km (95,000 mi) and initial perigee at about 300 km (190 mi) allowed the observatory to sweep through the natural radiation belts surrounding the Earth, providing a capability for a thorough mapping and study of phenomena associated with the magnetosphere and the near interplanetary space. The polar orbit (POGO) mission was conducted at lower altitudes with apogee and perigee typically at 1000 and 400 km (620 to 250 mi), respectively. This orbit, with inclination of 85 degrees or greater, provided thorough coverage of the Earth's atmosphere and lower ionosphere including the polar regions. The OGO spacecraft were launched one each year over a period of six years beginning in 1964, as shown in Table III-1, with the two subseries alternating in sequence.

TABLE III-1

Spacecraft	E/P	Launch date
OGO 1	E	5 September 1964
OGO 2	P	14 October 1965
OGO 3	E	7 June 1966
OGO 4	P	28 July 1967
OGO 5	E	4 March 1968
OGO 6	P	5 June 1969

The scientific program planned for the six OGO's is summarized in Figure III-1. Also shown in Figure III-1 is the alternating EGO/POGO launch sequence. The OGO 1 and 2 spacecraft were launched during a period of minimum solar activity. The OGO 1 and 2 experiments were essentially duplicated on OGO 3 and 4, respectively, because the original plan was that OGO 3 and 4 would continue the OGO 1 and 2 studies during the rising and maximum periods of the solar cycle. The OGO orbits are indicated in the frontispiece in relation to a somewhat stylized rendition of the magnetosphere in the noon-midnight meridian plane. Some of the scientific highlights are also indicated in the frontispiece, with the items listed on the right-hand side pertaining to EGO missions and the items on the left relating to POGO missions. The OGO 1 and OGO 3 orbits are also illustrated in Figure III-2 essentially as they would project on the plane of the ecliptic. The magnetosphere cross section outlined in Figure III-2 is essentially at right angle to the magnetosphere cross-section shown by the frontispiece. Both the frontispiece and Figure III-2 illustrate the thorough coverage of the magnetosphere, particularly of the magnetopause and bow shock, which was possible with the EGO missions.

Because of their long lifetimes, the EGO missions overlapped, making it possible to obtain data simultaneously from two (and even three) EGO missions. The magnetospheric regions which could be explored simultaneously by OGO 1 and OGO 3 are indicated in Figure III-2 for the period 1 September 1967 to 30 November 1967. It is seen that the local times for OGO 1 and OGO 3 apogees were actually seven hours apart. Thus, for example, OGO 1 could provide information for the magnetospheric tail region while OGO 3 was gathering data in the magnetosheath or at one of the magnetospheric boundaries. Figure III-2 also shows that the local time at apogee for OGO 1 and OGO 3 changed by about six hours in a three-month period, making it possible for either spacecraft to survey all local times in a one year period.

An essential feature of the technological approach was the standard-observatory concept: an orbiting 'experiment box.'

December 1, 1975

OVERVIEW

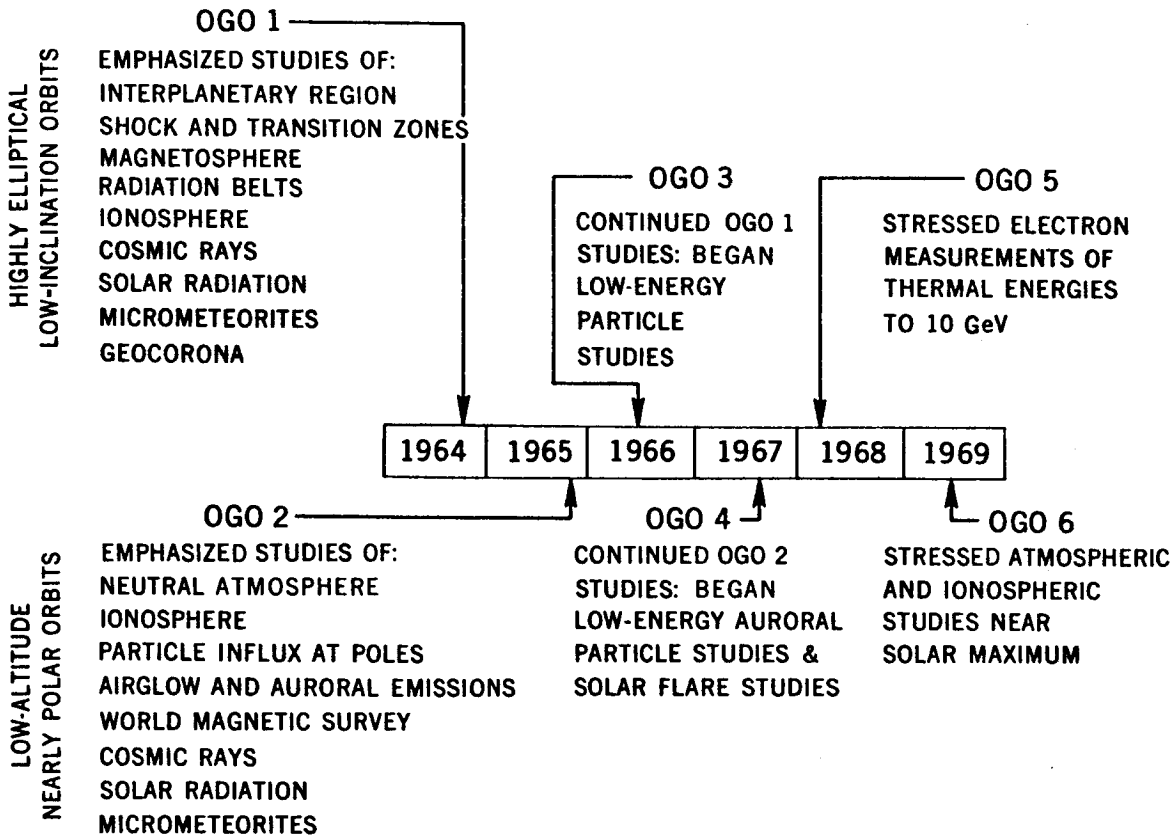
complete with solar power, attitude control, data storage, and telemetry, which would provide well-defined interfaces between the spacecraft subsystems and the experiments, thus allowing each experimenter to integrate his instruments with a minimum of effort. This concept (sometimes referred to as the 'street-car' principle), together with the relatively large payload capability, not only provided flexibility in selecting experiments, but also allowed incorporation of a limited number of high-risk experiments whose subsystem support requirements would have been prohibitive in smaller spacecraft where experiments and subsystems were highly intermingled. The same basic spacecraft (except for minor alterations) was used for the two types of orbit. The eccentric and polar orbits, however, required different launch vehicles (Atlas -

Agena and thrust-augmented Thor-Agena) and different launch sites (Eastern and Western Test Ranges), respectively. Total weight in orbit ranged from 479 to 635 kg (1050 to 1394 lb), of which 68.1 to 118.0 kg (150 to 260 lb) were assigned to experiment sensors and electronics.

3. Description of the OGO Spacecraft

3.1 Overall Configuration

A typical OGO deployed configuration is shown in Figure III-3. The main body was a 0.9 x 0.9 x 1.8 m (3 x 3 x 6 ft) rectangular prism, and its orientation (maintained by the spacecraft attitude



Orbiting Geophysical Observatories Program

FIGURE III-1.

OVERVIEW

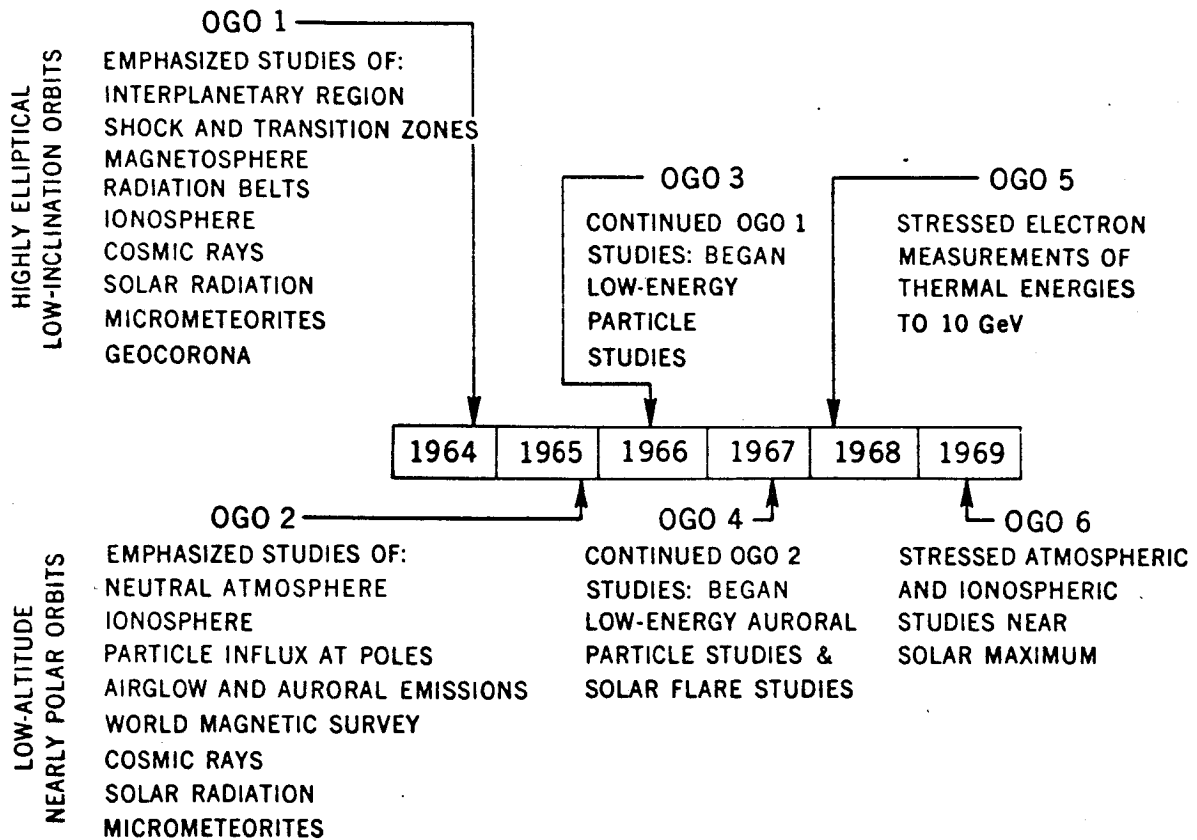
complete with solar power, attitude control, data storage, and telemetry, which would provide well-defined interfaces between the spacecraft subsystems and the experiments, thus allowing each experimenter to integrate his instruments with a minimum of effort. This concept (sometimes referred to as the 'street-car' principle), together with the relatively large payload capability, not only provided flexibility in selecting experiments, but also allowed incorporation of a limited number of high-risk experiments whose subsystem support requirements would have been prohibitive in smaller spacecraft where experiments and subsystems were highly intermingled. The same basic spacecraft (except for minor alterations) was used for the two types of orbit. The eccentric and polar orbits, however, required different launch vehicles (Atlas -

Agena and thrust-augmented Thor-Agena) and different launch sites (Eastern and Western Test Ranges), respectively. Total weight in orbit ranged from 479 to 635 kg (1050 to 1394 lb), of which 68.1 to 118.0 kg (150 to 260 lb) were assigned to experiment sensors and electronics.

3. Description of the OGO Spacecraft

3.1 Overall Configuration

A typical OGO deployed configuration is shown in Figure III-3. The main body was a 0.9 x 0.9 x 1.8 m (3 x 3 x 6 ft) rectangular prism, and its orientation (maintained by the spacecraft attitude



Orbiting Geophysical Observatories Program

Figure III-1 ← Set (10TRB)

Nov. 10, 1975

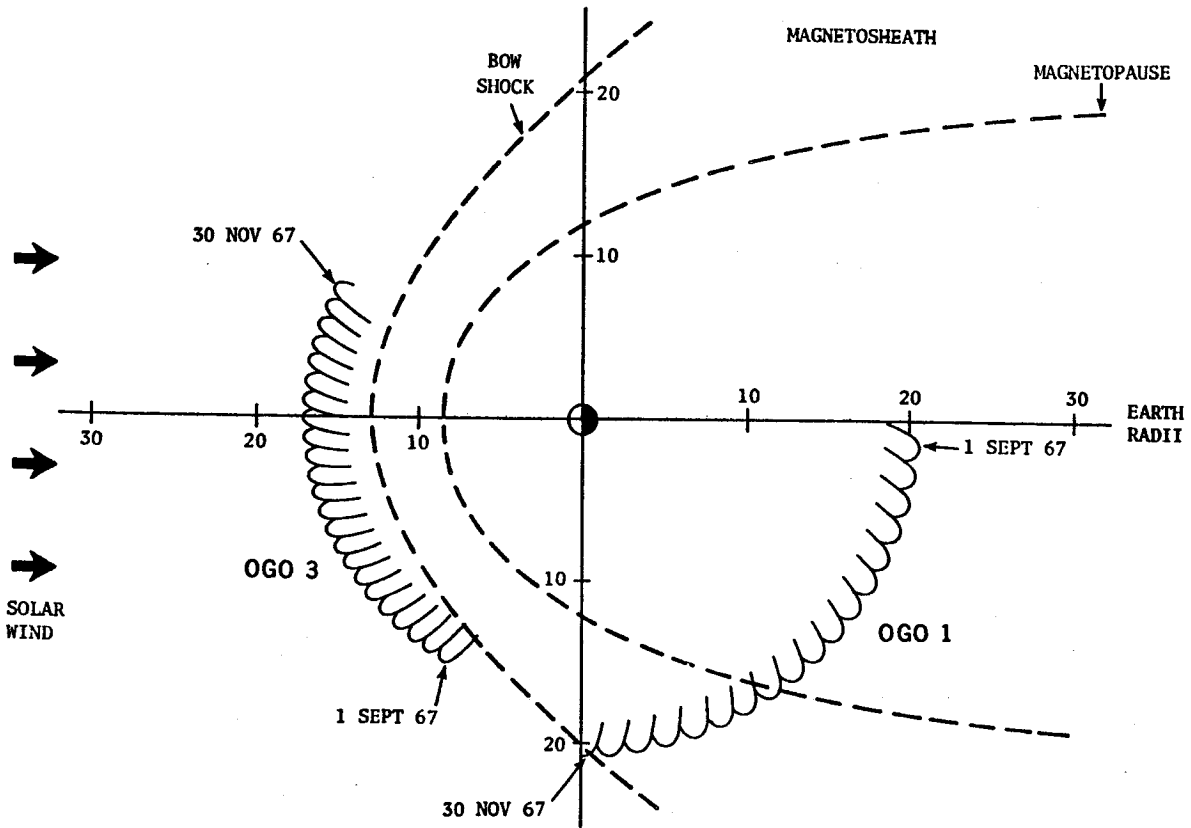
OVERVIEW

has been corrected

control system) was intended to be such that one 0.9 x 1.8 m (3 x 6 ft) face would be continuously pointed toward the Earth. This face and its opposite each had 0.6 sq m (6 sq ft) of area on which experiments could be mounted. The second purpose of the attitude control system was to maintain the solar arrays perpendicular to the rays of the sun. The cubical boxes near their extremities are the solar oriented experiment packages (SOEP's), each providing 0.1 sq m (1 sq ft) of experiment-mounting area on both the Sun-facing and anti-Sun-facing surfaces. At one end of the main body was a shaft mounted normal to the face which is pointed toward the Earth. Attached to this shaft were two orbit plane experiment

packages, OPEP-1 and OPEP-2. The third purpose of the attitude control system was to keep one face of each OPEP always faced forward along the velocity vector.

Two 6.7 m (22-ft) long booms (EP-5 and EP-6) and four 1.8 m (6-ft) long booms (EP-1 through EP-4) were provided to house experiment sensors whose sensitivity or viewing requirements made it necessary to remove them from the main body. Additional booms were provided for antennas; the most prominent in the figure is the turnstile Yagi directional antenna in the right foreground. Also shown in the figure are two antennas, typical of special experiment characteristics which can be accommodated. One was a long



Apogee distance, in Earth radii (R_E), and projection on the plane of the ecliptic of the Sun-Earth-probe (SEP) angle for OGO 1 and OGO 3. The inclination of the orbits is not illustrated.

FIGURE III-2

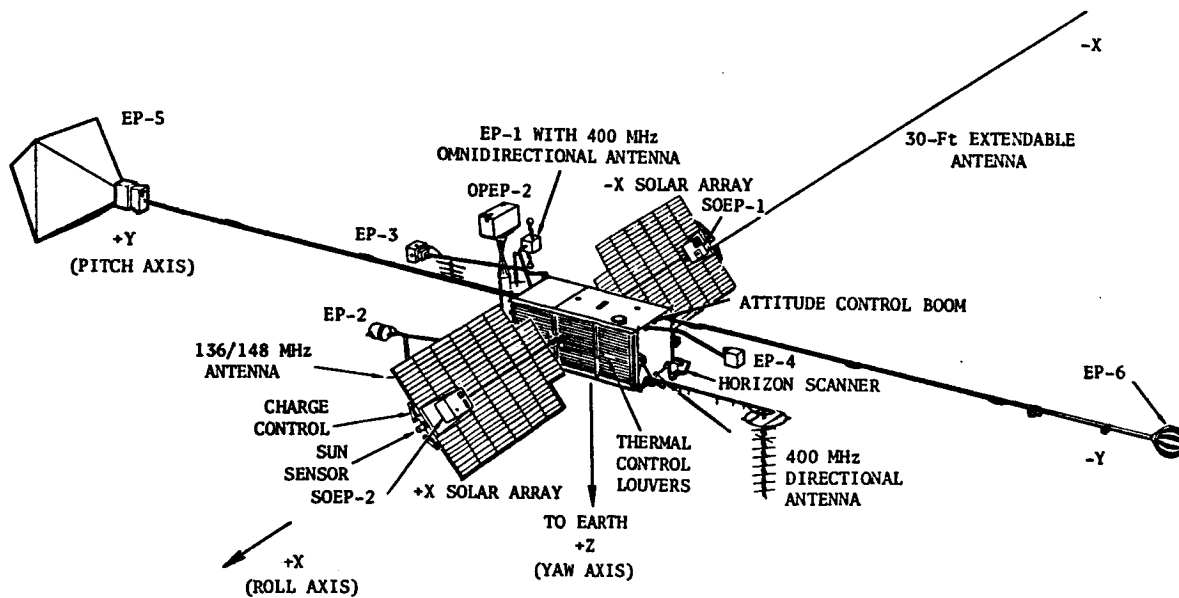
December 10, 1975

OVERVIEW

tubular spring bronze antenna, supplied by an experimenter, which could be extended from the end of the paddle after the spacecraft was in orbit, to a distance of 9.1 m (30 ft). The other was a rhomboid antenna made of metal tape and mounted to one of the long booms. This antenna was also deployed by radio command after the spacecraft had been stabilized in orbit. Several sensors for the same experiment could be installed in different appendages if data correlation or weight limitation reasons necessitated this. Interconnection was accomplished at the central junction box. This arrangement made it possible to accommodate installation of an experiment late in the prelaunch test cycle, should this have proved to be desirable.

3.2 Deployment Considerations

OGO had 13 major appendages which were deployed in orbit, subsequent to spacecraft separation, from a folded or stored configuration (Figure III-4) to the operational or deployed configuration (Figure III-3). The rather weird deployed configuration geometry (which resembled an oversized insect) was chosen to achieve the necessary mass properties control and experiment location with respect to the spacecraft and other experimental equipment, as well as support rigidity and minimum envelope in the folded configuration. The deployment operation was divided into two major sequences to avoid interference during appendage deployment.



Typical OGO Deployed Configuration

This figure actually shows OGO 5; other OGOS were very similar in appearance. The letters "X," "Y," and "Z" refer to the OGO coordinate system. The experiment package OPEP-1 (not shown) is directly below OPEP-2. The OGO dimensions are approximately 60 ft along the Y axis and 20 ft across the tips of the solar array.

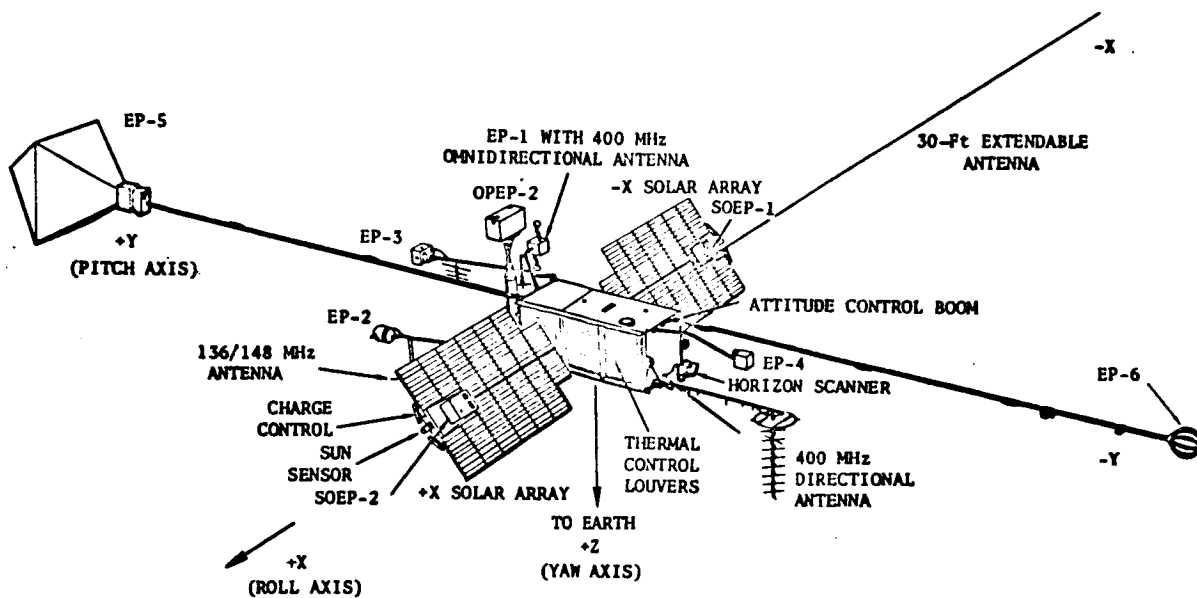
FIGURE III-3

OVERVIEW

...bular spring bronze antenna, supplied by an experimenter, which could be extended from the end of the paddle after the spacecraft was in orbit, to a distance of 9.1 m (30 ft). The other was a rhomboid antenna made of metal tape and mounted to one of the long booms. This antenna was also deployed by radio command after the spacecraft had been stabilized in orbit. Several sensors for the same experiment could be installed in different appendages if data correlation or weight limitation reasons necessitated this. Interconnection was accomplished at the central junction box. This arrangement made it possible to accommodate installation of an experiment late in the prelaunch test cycle, should this have proved to be desirable.

3.2 Deployment Considerations

OGO had 13 major appendages which were deployed in orbit, subsequent to spacecraft separation, from a folded or stored configuration (Figure III-4) to the operational or deployed configuration (Figure III-3). The rather weird deployed configuration geometry (which resembled an oversized insect) was chosen to achieve the necessary mass properties control and experiment location with respect to the spacecraft and other experimental equipment, as well as support rigidity and minimum envelope in the folded configuration. The deployment operation was divided into two major sequences to avoid interference during appendage deployment.



Typical OGO Deployed Configuration

This figure actually shows OGO 5; other OGOS were very similar in appearance. The letters "X," "Y," and "Z" refer to the OGO coordinate system. The experiment package OPEP-1 (not shown) is directly below OPEP-2. The OGO dimensions are approximately 60 ft along the Y axis and 20 ft across the tips of the solar array.

Figure III-3

The appendages deployed in the first sequence were EP-1 (400 MHz antenna included), EP-2 (136 MHz antenna included), EP-5, EP-6, and the +X and -X solar paddles. Total elapsed time from explosive valve actuation to hinge locking of EP-5 was to be less than 20 seconds. The appendages deployed in the second sequence were EP-3, EP-4, two attitude control nozzle support booms, OPEP-1, OPEP-2, and the high gain antenna, which was supported by and released simultaneously with OPEP-1. The total elapsed time from explosive valve actuation to hinge locking of EP-3 was less than 10 seconds.

3.3 Major Subsystems

The observatory concept led to the development of a standard spacecraft, incorporating a high degree of flexibility for accommodating many types of experiments. This was a marked departure from design practices used in earlier spacecraft, where weight limitations had led to a very tight integration of experiments and spacecraft systems. To achieve the desired flexibility, the OGO spacecraft included five separate and well-defined systems:* (1) the spacecraft main body and appendages where experiments could be mounted, (2) the attitude control system, (3) the thermal control system, (4) the power supply, and (5) the communication and data handling systems. This standardized arrangement made it possible to use the same basic spacecraft for the six OGO missions.

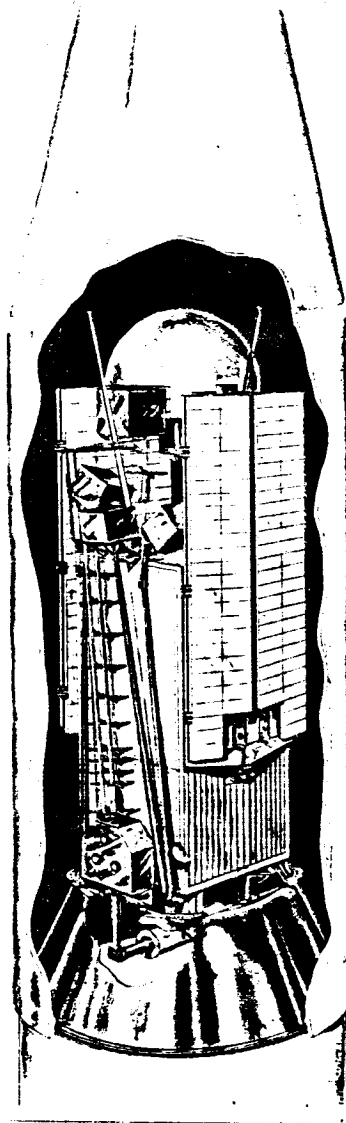
The overall configuration of the OGO spacecraft (described earlier) made it possible to accommodate simultaneously a large number of experiment requirements, such as Sun or anti-Sun orientation, Earth or anti-Earth viewing, specified attitude relative to the velocity vector, or a high degree of isolation when needed from the spacecraft and other experiments.

The attitude control system consisted of horizon scanners, servo-mechanisms, gas jets, electrically-driven flywheels and associated electronics. The system could stabilize the spacecraft in all three axes to within 2 deg of the local vertical, 5 deg of the Sun, and 5 deg of the velocity vector.

The thermal control system combined active and passive thermal-control techniques. Aluminized Mylar insulation was provided for the main body +Z, -Z, and -Y faces intermittently exposed to the Sun, and controllable radiating surface areas (louvers) were provided on the +X, -X, and +Y faces always exposed to outer space. Bimetallic actuators operating between 10 deg and 24 deg C moved the louvers from the fully closed to the fully opened position. Individual thermal control was provided as needed for externally mounted experiments.

Electrical power was supplied by two solar panel arrays providing about 550 w to two 28-volt nickel-cadmium storage batteries. The average power allotted for experiments was 50 w.

The Communication and Data Handling System included the following: (1) tracking equipment, consisting of two redundant 100-mw, 136 MHz Beacon transmitters and one 10-w, 136 MHz Beacon transmitter; (2) command equipment, consisting of two parallel 120 MHz command receivers, two redundant digital decoders (providing up to 254 relay commands), and one tone command decoder (providing up to 12 extra commands); and (3) telemetry equipment consisting of two redundant wide-band PCM Systems, each using a 400 MHz, 4-w transmitter, and a special purpose analog telemetry system, using a 400 MHz, 0.5-w transmitter. The real-time data



Typical OGO Folded Configuration

FIGURE III-4

* For a detailed description of the OGO spacecraft system, see 'The Orbiting Geophysical Observatories', by W.E. Scull and G.H. Ludwig, Proceedings of the IRE, 50, 2287-2296, Nov. 1962.

OVERVIEW

rates were 1, 4, 8, 16, and 64 kilobits per sec. A total data storage capacity of 86 million bits was provided by two recorders. The data could be stored at 1 or 4 kilobits per sec and played back at 64 or 128 kilobits per sec. Up to 32 alternate formats could be selected by ground command for experiment data sampling.

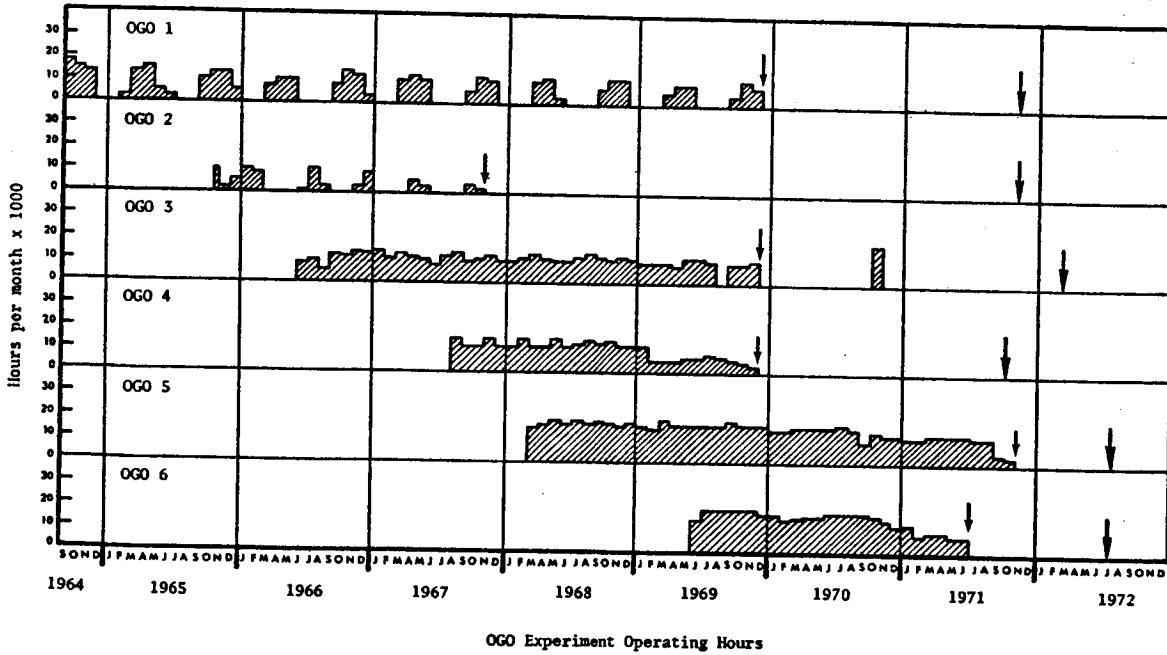
4. Technological Accomplishments

The technological accomplishments of the OGO programs can be divided into two major categories. The first includes the overall performance of the six OGO missions, i.e., basically the length of time for which each spacecraft provided useful data. The second includes the performance of specific subsystems, particularly those for which new and challenging technological problems had to be solved.

4.1 Operation Summary

A very good indication of the overall success of the OGO missions is the phenomenal volume of data (see Figure III-5)

which was acquired from the six OGO Spacecraft. During the period 1964 to 1971, over two million experiment hours of data were acquired, divided as follows: 364,000 from OGO 1; 72,000 from OGO 2; 440,000 from OGO 3; 260,000 from OGO 4; 636,000 from OGO 5 and 312,000 from OGO 6. This is comparable to the combined total of all other scientific satellites previously orbited by NASA. The longevity of the OGO spacecraft, as indicated by Figure III-5, was also quite spectacular. The duration of routine operations for the six spacecraft ranged from a minimum of 2 years (OGO 2) to a maximum of 5 1/2 years (OGO 1). The periods of routine operations were in all cases followed by a stand-by period (during which the spacecraft were still operable). The duration of these stand-by periods ranged from 1 to 4 years, the shorter stand-by periods being the result of a general termination of OGO spacecraft support during 1971 - 1972. All spacecraft, however, were still operable when operational support was terminated. Figure III-5 also illustrates the manner in which the OGO Missions overlapped, making it possible to obtain data simultaneously (but in different locations) from at least three OGO Spacecraft from 1966 to 1971.



OGO Experiment Operating Hours
 For each OGO there was a period of routine operations, which terminated at the date indicated by the first arrow. Afterwards, each OGO had standby status (with occasional special operations) until the date indicated by the second (heavier) arrow where all operational support was terminated.

FIGURE III-5

December 17, 1975

OVERVIEW

rates were 1, 4, 8, 16, and 64 kilobits per sec. A total data storage capacity of 86 million bits was provided by two recorders. The data could be stored at 1 or 4 kilobits per sec and played back at 64 or 128 kilobits per sec. Up to 32 alternate formats could be selected by ground command for experiment data sampling.

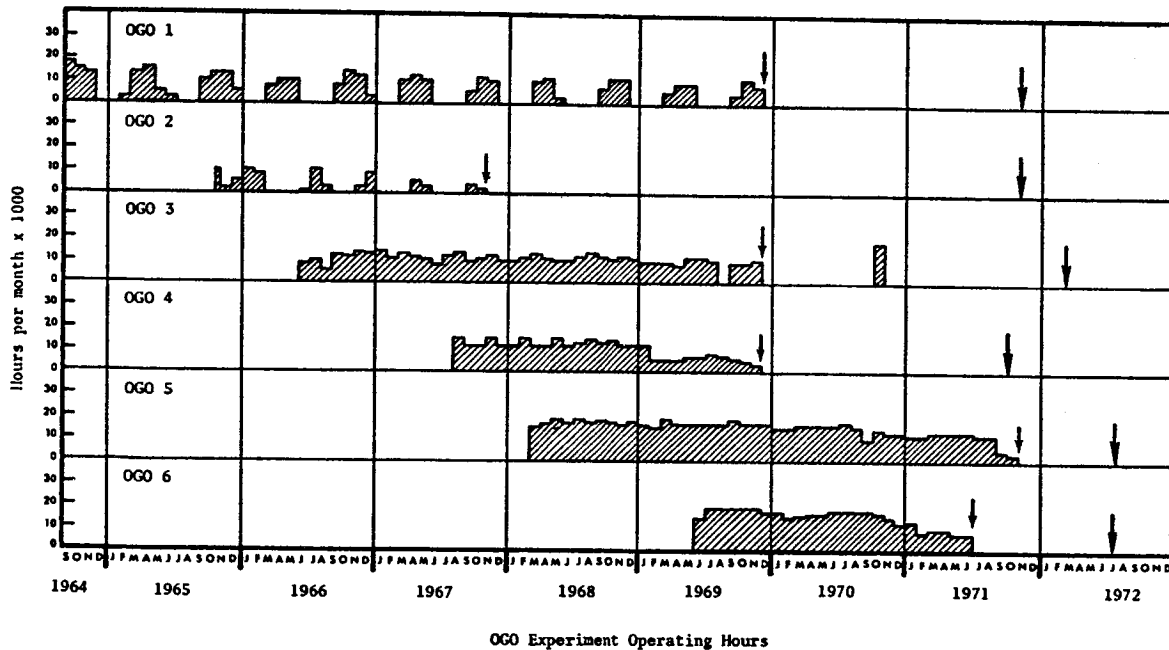
4. Technological Accomplishments

The technological accomplishments of the OGO programs can be divided into two major categories. The first includes the overall performance of the six OGO missions, i.e. basically the length of time for which each spacecraft provided useful data. The second includes the performance of specific subsystems, particularly those for which new and challenging technological problems had to be solved.

4.1 Operation Summary

A very good indication of the overall success of the OGO missions is the phenomenal volume of data (see Figure III-5)

which was acquired from the six OGO Spacecraft. During the period 1964 to 1971, over two million experiment hours of data were acquired, divided as follows: 364,000 from OGO 1; 72,000 from OGO 2; 440,000 from OGO 3; 260,000 from OGO 4; 636,000 from OGO 5 and 312,000 from OGO 6. This is comparable to the combined total of all other scientific satellites previously orbited by NASA. The longevity of the OGO spacecraft, as indicated by Figure III-5, was also quite spectacular. The duration of routine operations for the six spacecraft ranged from a minimum of 2 years (OGO 2) to a maximum of 5 1/2 years (OGO 1). The periods of routine operations were in all cases followed by a stand-by period (during which the spacecraft were still operable). The duration of these stand-by periods ranged from 1 to 4 years, the shorter stand-by periods being the result of a general termination of OGO spacecraft support during 1971 - 1972. All spacecraft, however, were still operable when operational support was terminated. Figure III-5 also illustrates the manner in which the OGO Missions overlapped, making it possible to obtain data simultaneously (but in different locations) from at least three OGO Spacecraft from 1966 to 1971.



For each OGO there was a period of routine operations, which terminated at the date indicated by the first arrow. Afterwards, each OGO had standby status (with occasional special operations) until the date indicated by the second (heavier) arrow where all operational support was terminated.

FIGURE III-5

OVERVIEW

ities were 1, 4, 8, 16, and 64 kilobits per sec. A total data storage capacity of 86 million bits was provided by two recorders. The data could be stored at 1 or 4 kilobits per sec and played back at 64 or 128 kilobits per sec. Up to 32 alternate formats could be selected by ground command for experiment data sampling.

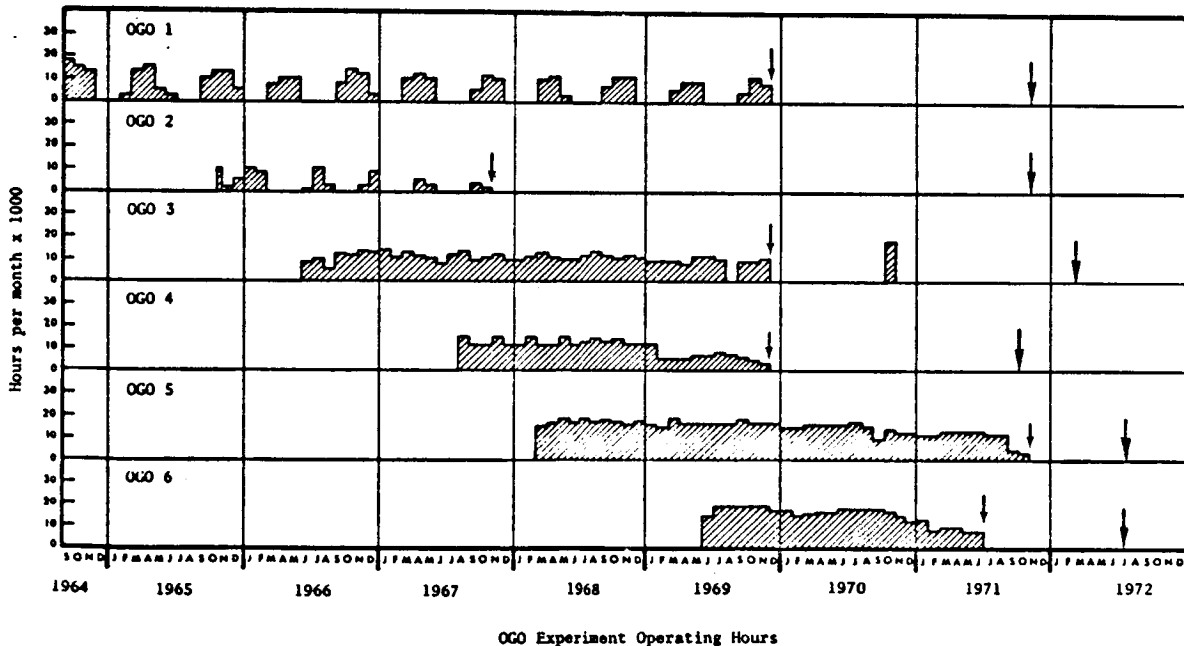
4. Technological Accomplishments

The technological accomplishments of the OGO programs can be divided into two major categories. The first includes the overall performance of the six OGO missions, i.e. basically the length of time for which each spacecraft provided useful data. The second includes the performance of specific subsystems, particularly those for which new and challenging technological problems had to be solved.

4.1 Operation Summary

A very good indication of the overall success of the OGO missions is the phenomenal volume of data (see Figure III-5)

which was acquired from the six OGO Spacecraft. During the period 1964 to 1971, over two million experiment hours of data were acquired, divided as follows: 364,000 from OGO 1; 72,000 from OGO 2; 440,000 from OGO 3; 260,000 from OGO 4; 636,000 from OGO 5 and 312,000 from OGO 6. This is comparable to the combined total of all other scientific satellites previously orbited by NASA. The longevity of the OGO spacecraft, as indicated by Figure III-5, was also quite spectacular. The duration of routine operations for the six spacecraft ranged from a minimum of 2 years (OGO 2) to a maximum of 5 1/2 years (OGO 1). The periods of routine operations were in all cases followed by a stand-by period (during which the spacecraft were still operable). The duration of these stand-by periods ranged from 1 to 4 years, the shorter stand-by periods being the result of a general termination of OGO spacecraft support during 1971 - 1972. All spacecraft, however, were still operable when operational support was terminated. Figure III-5 also illustrates the manner in which the OGO Missions overlapped, making it possible to obtain data simultaneously (but in different locations) from at least three OGO Spacecraft from 1966 to 1971.



OGO Experiment Operating Hours
For each OGO there was a period of routine operations, which terminated at the date indicated by the first arrow. Afterwards, each OGO had standby status (with occasional special operations) until the date indicated by the second (heavier) arrow where all operational support was terminated.

Figure III-5

NOV. 10, 1975

12/15/75

4.2 Performance of Spacecraft Systems

4.2.1 Overall Performance

The longevity and the data output of the various OGO missions (as summarized by Figure III-5) provide ample proof that the power, thermal, and data handling systems functioned extremely well. The basic spacecraft design for OGO 1 was sound, and it was used essentially unchanged (except for minor corrections and modifications) for the other five OGOs. The OGO spacecraft could also (and did) yield very useful data in the spin-stabilized back-up mode, whenever the attitude control system failed to maintain the desired three-axis stabilization.

4.2.2 The Attitude Control System

From the technological viewpoint, perhaps the major challenge offered by the OGO design was the stabilization and orientation requirements. Although--in principle--the pointing accuracies required of OGO, were not difficult to achieve (they varied from 2 to 5 deg), the three-axis stabilization was difficult to achieve with the complex configuration and deployment geometry of the OGO spacecraft.

The stabilization history of the six OGO spacecraft was as follows: OGO 1 failed to stabilize because of incomplete boom deployment; OGO 2 was stabilized for 10 days only, because of faulty horizon sensors causing premature control gas depletion; OGO 3 was stabilized for 46 days until a power converter failure occurred; OGO 4 was stabilized for 18 months; OGO 5 was stabilized for 41 months; and OGO 6 was stabilized for 24 months, i.e. until the end of its mission.

The failure to achieve or maintain stabilization on OGO 1, 2, and 3 was in general traceable to somewhat sophisticated aspects of design which were very difficult to anticipate and were not revealed by ground testing. The in-orbit problems were in general not due to quality control or test oversight; and because of their complexity, these problems revealed themselves gradually, i.e. following the successive design corrections. Thus the OGO 2 horizon sensor problems could not be detected, until the OGO 1 deployment problem was corrected. Similarly, the 10-day OGO 2 attitude-controlled operation did not last long enough to lead to the power converter failure eventually seen on OGO 3. Once corrected, however, a given problem never occurred again.

4.3. Summary of Technological Accomplishments

Compared to earlier space investigations, the orbiting geophysical observatories represent major advances in both precision and comprehensiveness. The technological accomplishments of the OGO program include:

- (1) near-perfect orbits for all six missions;
- (2) the successful deployment of a very complex spacecraft configuration in all cases except OGO 1, for which a partial deployment failure occurred;
- (3) three-axis stabilization accomplished for 10 days on the second OGO and maintained much longer on subsequent OGOs;
- (4) the successful simultaneous operation of a large number of experiments with very different requirements;
- (5) an extremely high information handling capacity;
- (6) a very high reliability of experiments and spacecraft systems, which, combined with the high data rate, resulted in a record breaking volume of scientific data;
- (7) the skillful use of backup modes of operation to overcome in-orbit problems and extend the usefulness of a mission.

B. SCIENTIFIC RESULTS

1. OGO 1 Results

Although all the OGO 1 experiments operated in orbit and acquired data, approximately half of these were severely degraded

because of the failure of the attitude control system and because two of the eleven appendages failed to deploy properly. The experiments which failed to yield significant results, and the major reasons for their degraded operations were as follows. Experiments A-19 (Geocoronal Lyman-Alpha) and A-20 (Gegenschein Photometry) were critically dependent upon anti-solar orientation. Experiment A-1 (Solar Cosmic Rays) required solar orientation to meet its objectives. Experiment A-18 (Radio Astronomy) could not operate properly because of incomplete antenna deployment. Spin modulation was very detrimental to experiments A-13 (Planar Ion and Electron Trap), A-16 (Interplanetary Dust Particles), and A-5 (Trapped Radiation and Scintillation Counter). Experiment A-8 (Trapped Radiation Omnidirectional Counter) also suffered from degraded OGO 1 operation, and although some measurements were made, the results were not considered of sufficient value for publication in the open literature. Insufficient protection against electrical interference led to a very high noise level in the data from experiment A-4 (Positron Search and Gamma-Ray Spectrum). Although experiment A-4 has not yet led to any publication, the data are currently (1975) being re-examined to see if they reveal any of the recently discovered gamma-ray bursts.

Very significant scientific results were nevertheless obtained with OGO 1 because:

- a) many of the experiments were not critically dependent upon specific spacecraft orientation;
- b) high-resolution measurements were made possible (for the first time) by the high data rate of the OGO telemetry system; and
- c) the OGO 1 orbit was very well suited for a detailed investigation of the magnetosphere, in particular the magnetopause, magnetosheath, and bow shock (see Figure III-2).

1.1 Magnetic Field Experiments

The extensive study of the outer magnetospheric regions by the two magnetic field experiments on OGO 1 was a major accomplishment, and the scientific results have been extensively quoted in review articles and in textbooks. Historically, magnetometers have provided the most comprehensive coverage of magnetospheric activities, and this was certainly true of the two magnetometer experiments on OGO 1, namely Smith's search coil magnetometer (Experiment A-10) and Heppner's fluxgate magnetometer (Experiment A-11).

1.1.1 Shock Structure (A-11)

From a study of numerous OGO 1 shock crossings observed with experiment A-11, Heppner et al (1967) derived a model of the average field profile for a typical shock crossing. The shock thickness was described in terms of three dimensions. As the shock is first encountered from the interplanetary space side, there is a narrow 'outer shell' less than 20 km (12 mi) thick where the interplanetary field becomes slightly disturbed. This is followed by a second region about 70 km (45 mi) thick where the field changes rapidly to a new level. In the third region the field settles gradually to its magnetosheath value over a distance of about 200 km (120 mi).

Two classes of field oscillations were frequently observed superimposed on this average shock structure: 1) coherent circularly polarized ULF waves with frequencies typically between 0.5 and 1.5 Hz, and 2) higher frequency (ELF) fluctuations.

The thin nature of the bow shock and the associated wave phenomena were important observations which henceforth had to be considered in theoretical models of the bow shock (Tidman 1967, Tidman and Northrop 1968).

1.1.2 Waves in the Magnetosheath (A-10)

Smith's search coil magnetometer experiment (A-10) was particularly well suited for the study of ELF magnetic fluctuations and it was shown by Smith et al (1967) that 3-300 Hz magnetic

4.2 Performance of Spacecraft Systems

4.2.1 Overall Performance

The longevity and the data output of the various OGO missions (as summarized by Figure III-5) provide ample proof that the power, thermal, and data handling systems functioned extremely well. The basic spacecraft design for OGO 1 was sound, and it was used essentially unchanged (except for minor corrections and modifications) for the other five OGOs. The OGO spacecraft could also (and did) yield very useful data in the spin-stabilized back-up mode, whenever the attitude control system failed to maintain the desired three-axis stabilization.

4.2.2 The Attitude Control System

From the technological viewpoint, perhaps the major challenge offered by the OGO design was the stabilization and orientation requirements. Although--in principle--the pointing accuracies required of OGO, were not difficult to achieve (they varied from 2 to 5 deg), the three-axis stabilization was difficult to achieve with the complex configuration and deployment geometry of the OGO spacecraft.

The stabilization history of the six OGO spacecraft was as follows: OGO 1 failed to stabilize because of incomplete boom deployment; OGO 2 was stabilized for 10 days only, because of faulty horizon sensors causing premature control gas depletion; OGO 3 was stabilized for 46 days until a power converter failure occurred; OGO 4 was stabilized for 18 months; OGO 5 was stabilized for 41 months; and OGO 6 was stabilized for 24 months, i.e. until the end of its mission.

The failure to achieve or maintain stabilization on OGO 1, 2, and 3 was in general traceable to somewhat sophisticated aspects of design which were very difficult to anticipate and were not revealed by ground testing. The in-orbit problems were in general not due to quality control or test oversight; and because of their complexity, these problems revealed themselves gradually, i.e. following the successive design corrections. Thus the OGO 2 horizon sensor problems could not be detected, until the OGO 1 deployment problem was corrected. Similarly, the 10-day OGO 2 attitude-controlled operation did not last long enough to lead to the power converter failure eventually seen on OGO 3. Once corrected, however, a given problem never occurred again.

4.3. Summary of Technological Accomplishments

Compared to earlier space investigations, the orbiting geophysical observatories represent major advances in both precision and comprehensiveness. The technological accomplishments of the OGO program include:

- (1) near-perfect orbits for all six missions;
- (2) the successful deployment of a very complex spacecraft configuration in all cases except OGO 1, for which a partial deployment failure occurred;
- (3) three-axis stabilization accomplished for 10 days on the second OGO and maintained much longer on subsequent OGOs;
- (4) the successful simultaneous operation of a large number of experiments with very different requirements;
- (5) an extremely high information handling capacity;
- (6) a very high reliability of experiments and spacecraft systems, which, combined with the high data rate, resulted in a record breaking volume of scientific data;
- (7) the skillful use of backup modes of operation to overcome in-orbit problems and extend the usefulness of a mission.

B. SCIENTIFIC RESULTS

1. OGO 1 Results

Although all the OGO 1 experiments operated in orbit and acquired data, approximately half of these were severely degraded

because of the failure of the attitude control system and because two of the eleven appendages failed to deploy properly. The experiments which failed to yield significant results, and the major reasons for their degraded operations were as follows. Experiments A-19 (Geocoronal Lyman-Alpha) and A-20 (Gegenschein Photometry) were critically dependent upon anti-solar orientation. Experiment A-1 (Solar Cosmic Rays) required solar orientation to meet its objectives. Experiment A-13 (Radio Astronomy) could not operate properly because of incomplete antenna deployment. Spin modulation was very detrimental to experiments A-13 (Planar Ion and Electron Trap), A-16 (Interplanetary Dust Particles), and A-5 (Trapped Radiation and Scintillation Counter). Experiment A-8 (Trapped Radiation Omnidirectional Counter) also suffered from degraded OGO 1 operation, and although some measurements were made, the results were not considered of sufficient value for publication in the open literature. Insufficient protection against electrical interference led to a very high noise level in the data from experiment A-4 (Positron Search and Gamma-Ray Spectrum). Although experiment A-4 has not yet led to any publication, the data are currently (1975) being re-examined to see if they reveal any of the recently discovered gamma-ray bursts.

Very significant scientific results were nevertheless obtained with OGO 1 because:

- a) many of the experiments were not critically dependent upon specific spacecraft orientation;
- b) high-resolution measurements were made possible (for the first time) by the high data rate of the OGO telemetry system; and
- c) the OGO 1 orbit was very well suited for a detailed investigation of the magnetosphere, in particular the magnetopause, magnetosheath, and bow shock (see Figure III-2).

1.1 Magnetic Field Experiments

The extensive study of the outer magnetospheric regions by the two magnetic field experiments on OGO 1 was a major accomplishment, and the scientific results have been extensively quoted in review articles and in textbooks. Historically, magnetometers have provided the most comprehensive coverage of magnetospheric activities, and this was certainly true of the two magnetometer experiments on OGO 1, namely Smith's search coil magnetometer (Experiment A-10) and Heppner's fluxgate magnetometer (Experiment A-11).

1.1.1 Shock Structure (A-11)

From a study of numerous OGO 1 shock crossings observed with experiment A-11, Heppner et al. (1967) derived a model of the average field profile for a typical shock crossing. The shock thickness was described in terms of three dimensions. As the shock is first encountered from the interplanetary space side, there is a narrow 'outer shell' less than 20 km (12 mi) thick where the interplanetary field becomes slightly disturbed. This is followed by a second region about 70 km (45 mi) thick where the field changes rapidly to a new level. In the third region the field settles gradually to its magnetosheath value over a distance of about 200 km (120 mi).

Two classes of field oscillations were frequently observed superimposed on this average shock structure: 1) coherent circularly polarized ULF waves with frequencies typically between 0.5 and 1.5 Hz, and 2) higher frequency (ELF) fluctuations.

The thin nature of the bow shock and the associated wave phenomena were important observations which henceforth had to be considered in theoretical models of the bow shock (Tidman 1967, Tidman and Northrop 1968).

1.1.2 Waves in the Magnetosheath (A-10)

Smith's search coil magnetometer experiment (A-10) was particularly well suited for the study of ELF magnetic fluctuations and it was shown by Smith et al (1967) that 3-300 Hz magnetic

4.2 Performance of Spacecraft Systems

4.2.1 Overall Performance

The longevity and the data output of the various OGO missions (as summarized by Figure III-5) provide ample proof that the power, thermal, and data handling systems functioned extremely well. The basic spacecraft design for OGO 1 was sound, and it was used essentially unchanged (except for minor corrections and modifications) for the other five OGOs. The OGO spacecraft could also (and did) yield very useful data in the spin-stabilized back-up mode, whenever the attitude control system failed to maintain the desired three-axis stabilization.

4.2.2 The Attitude Control System

From the technological viewpoint, perhaps the major challenge offered by the OGO design was the stabilization and orientation requirements. Although--in principle--the pointing accuracies required of OGO, were not difficult to achieve (they varied from 2 to 5 deg), the three-axis stabilization was difficult to achieve with the complex configuration and deployment geometry of the OGO spacecraft.

The stabilization history of the six OGO spacecraft was as follows: OGO 1 failed to stabilize because of incomplete boom deployment; OGO 2 was stabilized for 10 days only, because of faulty horizon sensors causing premature control gas depletion; OGO 3 was stabilized for 46 days until a power converter failure occurred; OGO 4 was stabilized for 18 months; OGO 5 was stabilized for 41 months; and OGO 6 was stabilized for 24 months, i.e. until the end of its mission.

The failure to achieve or maintain stabilization on OGO 1, 2, and 3 was in general traceable to somewhat sophisticated aspects of design which were very difficult to anticipate and were not revealed by ground testing. The in-orbit problems were in general not due to quality control or test oversight; and because of their complexity, these problems revealed themselves gradually, i.e. following the successive design corrections. Thus the OGO 2 horizon sensor problems could not be detected, until the OGO 1 deployment problem was corrected. Similarly, the 10-day OGO 2 attitude-controlled operation did not last long enough to lead to the power converter failure eventually seen on OGO 3. Once corrected, however, a given problem never occurred again.

4.3. Summary of Technological Accomplishments

Compared to earlier space investigations, the orbiting geophysical observatories represent major advances in both precision and comprehensiveness. The technological accomplishments of the OGO program include:

- (1) near-perfect orbits for all six missions;
- (2) the successful deployment of a very complex spacecraft configuration in all cases except OGO 1, for which a partial deployment failure occurred;
- (3) three-axis stabilization accomplished for 10 days on the second OGO and maintained much longer on subsequent OGOs;
- (4) the successful simultaneous operation of a large number of experiments with very different requirements;
- (5) an extremely high information handling capacity;
- (6) a very high reliability of experiments and spacecraft systems, which, combined with the high data rate, resulted in a record breaking volume of scientific data;
- (7) the skillful use of backup modes of operation to overcome in-orbit problems and extend the usefulness of a mission.

B. SCIENTIFIC RESULTS

1. OGO 1 Results

Although all the OGO 1 experiments operated in orbit and acquired data, approximately half of these were severely degraded

because of the failure of the attitude control system and because two of the eleven appendages failed to deploy properly. The experiments which failed to yield significant results, and the major reasons for their degraded operations were as follows. Experiments A-19 (Geocoronal Lyman-Alpha) and A-20 (Gegenschein Photometry) were critically dependent upon anti-solar orientation. Experiment A-1 (Solar Cosmic Rays) required solar orientation to meet its objectives. Experiment A-18 (Radio Astronomy) could not operate properly because of incomplete antenna deployment. Spin modulation was very detrimental to experiments A-13 (Planar Ion and Electron Trap), A-16 (Interplanetary Dust Particles), and A-5 (Trapped Radiation and Scintillation Counter). Experiment A-8 (Trapped Radiation Omnidirectional Counter) also suffered from degraded OGO 1 operation, and although some measurements were made, the results were not considered of sufficient value for publication in the open literature. Insufficient protection against electrical interference led to a very high noise level in the data from experiment A-4 (Positron Search and Gamma-Ray Spectrum). Although experiment A-4 has not yet led to any publication, the data are currently (1975) being re-examined to see if they reveal any of the recently discovered gamma-ray bursts.

Very significant scientific results were nevertheless obtained with OGO 1 because:

- a) many of the experiments were not critically dependent upon specific spacecraft orientation;
- b) high-resolution measurements were made possible (for the first time) by the high data rate of the OGO telemetry system; and
- c) the OGO 1 orbit was very well suited for a detailed investigation of the magnetosphere, in particular the magnetopause, magnetosheath, and bow shock (see Figure III-2).

1.1 Magnetic Field Experiments

The extensive study of the outer magnetospheric regions by the two magnetic field experiments on OGO 1 was a major accomplishment, and the scientific results have been extensively quoted in review articles and in textbooks. Historically, magnetometers have provided the most comprehensive coverage of magnetospheric activities, and this was certainly true of the two magnetometer experiments on OGO 1, namely Smith's search coil magnetometer (Experiment A-10) and Heppner's fluxgate magnetometer (Experiment A-11).

1.1.1 Shock Structure (A-11)

From a study of numerous OGO 1 shock crossings observed with experiment A-11, Heppner et al (1967) derived a model of the average field profile for a typical shock crossing. The shock thickness was described in terms of three dimensions. As the shock is first encountered from the interplanetary space side, there is a narrow 'outer shell' less than 20 km (12 mi) thick where the interplanetary field becomes slightly disturbed. This is followed by a second region about 70 km (45 mi) thick where the field changes rapidly to a new level. In the third region the field settles gradually to its magnetosheath value over a distance of about 200 km (120 mi).

Two classes of field oscillations were frequently observed superimposed on this average shock structure: 1) coherent circularly polarized ULF waves with frequencies typically between 0.5 and 1.5 Hz, and 2) higher frequency (ELF) fluctuations.

The thin nature of the bow shock and the associated wave phenomena were important observations which henceforth had to be considered in theoretical models of the bow shock (Tidman 1967, Tidman and Northrop 1968).

1.1.2 Waves in the Magnetosheath (A-10)

Smith's search coil magnetometer experiment (A-10) was particularly well suited for the study of ELF magnetic fluctuations and it was shown by Smith et al (1967) that 3-300 Hz magnetic

Nov. 10, 1975

etal

12/15/75

OVERVIEW

noise was present throughout the entire magnetosheath with higher amplitudes near the boundaries, especially near the shock. It was found that the power spectral density in the 3- to 300-Hz frequency range had an inverse cube dependence on frequency. The results of experiment A-10 extended upward the previous observations, which had been limited to the 10^3 to 10^1 Hz range, and suggested that a change in frequency dependence occurred somewhere between 0.1 and 1.0 Hz.

1.1.3 Shock and Magnetopause Motions (A-10, A-11, A-2, A-3)

Observations made prior to the OGO 1 launch had revealed that the shock and magnetopause were capable of considerable motion. The extent and persistence of this motion became fully appreciated with the OGO 1 observations which frequently revealed multiple shock and magnetopause crossings in a single orbit pass. As many as 15 identifiable magnetopause crossings were observed on a single OGO 1 pass. Multiple crossings were observed by experiments A-10 (Holzer et al, 1966) and A-11 (Heppner et al, 1967) discussed earlier and by experiment A-2 (Wolfe et al, 1966) to which we will return later. These multiple crossings suggested an oscillatory motion of the boundaries. The average amplitude, period, and mean velocity were estimated by Holzer et al, (1966) to be $1.5 R_E$, 60 min., and 10 km/sec (6.2 mi/sec), respectively for the shock front; and for the magnetopause $0.25 R_E$, 20 min., and 10 km/sec (6.2 mi/sec), respectively. Heppner et al, (1967) arrived at similar estimates for the motion of the bow shock, but concluded that the average velocity of the magnetopause motion had to be at most 2 km/sec (1.2 mi/sec). This minor disagreement was probably due to the great variability of the boundary motion and to the difficulty of defining average parameters, particularly with a single spacecraft. In any event, these results contributed new and significant information concerning typical boundary motions under quiet geomagnetic conditions.

Large-scale motions of the shock that occur during geomagnetic storms were investigated by Binsack and Vasyliunas (1968), using data from the OGO 1 Faraday cup experiment (A-3, Bridge) and simultaneous IMP 1 and IMP 2 observations. The conclusion was that the large-scale motion is associated with an overall compression of the entire magnetosphere-magnetosheath system in response to the enhanced solar wind dynamic pressure.

1.1.4 Mapping of the Dayside Magnetosheath (A-10, A-11)

The OGO 1 orbit (see Fig. 2) made it possible to conduct a detailed mapping of the dayside magnetosheath over a period of approximately 6 months. Another accomplishment of experiments A-10 (Holzer et al, 1966) and A-11 (Heppner et al, 1967) was to provide the first detailed dusk-to-dawn mapping of the magnetosheath. This study revealed the slight 3- to 6-deg misalignment between the axis of symmetry of the magnetosheath and the Earth-Sun line, which had been expected from the aberration effect caused by the orbital motion of the Earth around the Sun.

The magnetopause in the sunward hemisphere was most typically observed by experiment A-11 (Heppner et al, 1967) as a smooth transition over a distance of about 100 km (62 mi), i.e., comparable to the ion cyclotron radius.

1.1.5 Nightside Magnetosphere (A-10)

A number of important observations were made in the nightside magnetosphere by experiment A-10 (Heppner et al, 1967). For example, near the magnetopause in the dawn sector and within geomagnetic latitudes $+ or - 15$ deg, the field was found weaker than in the transition region, implying that the plasma pressure had to be greater than the magnetic pressure. In such a region the magnetopause boundary is poorly defined magnetically and difficult to identify from field data. Inferences concerning the magnetospheric plasma were also made, based upon middle latitude data obtained between 5 and $10 R_E$ near midnight, which showed that the magnetic field was greater than predicted. This was interpreted as being the result of plasma pressure near the equator at similar distances and times. To illustrate further the versatility of magnetometer experiments, one can mention the correlations which were made

between the nightside field observations and auroral activities which led to the conclusion that the onset of a negative bay had to originate within the closed magnetosphere.

1.2 Low-Energy Plasma Experiments

Some of the most important OGO 1 results were obtained from experiments designed to investigate low-energy plasmas in the magnetosphere with energies from thermal up to about 50 keV. These experiments have produced two notable 'firsts,' namely the first clear identification of the plasmasphere and the first radial mapping of the plasma sheet.

1.2.1 Mapping of the Plasmapause (A-15, A-12)

A clear concept of the plasmapause, the envelope or outer-boundary of the terrestrial ionosphere, did not exist before the OGO 1 launch. Prior in situ measurements were limited to those made during two crossings by Soviet lunar vehicles, which showed that the ionospheric electron density decreased rather abruptly at middle geomagnetic latitudes at a geocentric distance of about $4 R_E$. Strong but indirect evidence for the existence of a sharp decrease, or 'knee', in the equatorial electron density profile at about $4 R_E$ had been provided by ground-based whistler observations (Carpenter, 1963).

The in situ observations were considerably widened in scope and detail through the mass spectrometer measurements on OGO 1 (Experiment A-15, Taylor). Taylor et al, (1965) described the observations as revealing 'a belt of thermal ions that appears to expand and contract with changes in magnetic activity'. They referred to 'an outer boundary characterized by a reduction in both the H and He concentrations by a factor of 10 or more' and they also stated that there was a significant correlation between their findings and Carpenter's whistler knee.

Although Taylor et al exercised commendable caution and restraint in presenting their results, it was obvious that the existence of Carpenter's knee was now spectacularly confirmed, not only in the equatorial plane, but also at other latitudes. It was clearly a three-dimensional phenomenon, and its geomagnetic control had been clearly established. The next step was to find a more suitable name for this new geomagnetic boundary. Carpenter (1966), hastening the demise of the anthropomorphic Carpenter's knee designation, proposed the terms plasmapause for the boundary and plasmasphere for the region inside. Both terms have now gained wide acceptance.

Information concerning the plasmapause was also obtained with the spherical electrostatic analyzer (SEA) aboard OGO 1 (Experiment A-12, Sagalyn). The results presented by Ahmed and Sagalyn (1972) are consistent with those from the ion mass spectrometer (Taylor et al, 1965), although some differences exist. For example, the densities from the SEA experiment can be greater by a factor of two or more than the densities from the mass spectrometer. The SEA measurements showed more fine structure and greater variability in the sharpness of the plasmapause. The SEA results, unfortunately, lost much of their value because of their late publication date (1972). By 1972, a number of additional plasmapause studies conducted with OGO 3 and OGO 5 had already been published.

1.2.2 Mapping of the Plasma Sheet (A-3)

Bame et al (1967), using data from the Vela 2B satellite (launched 2 months ahead of OGO 1), showed that a plasma sheet of low-energy electrons stretched across the Earth's magnetotail from the dusk-to-dawn boundaries of the magnetosphere. The Vela data showed that these electrons had a quasi-thermal energy spectrum peaking anywhere between a few hundred eV and a few keV. Because of the circular Vela 2B orbit, the observations were limited to geocentric distances between 15.5 and $20.5 R_E$.

The radial extent of the plasma sheet was first revealed by the OGO 1 Faraday cup data (Experiment A-3, Bridge). These data were obtained in the evening sector of the magnetosphere, and they showed that the plasma sheet had an inner boundary, characterized by a rapid and substantial decrease in electron flux

OVERVIEW

noise was present throughout the entire magnetosheath with higher amplitudes near the boundaries, especially near the shock. It was found that the power spectral density in the 3- to 300-Hz frequency range had an inverse cube dependence on frequency. The results of experiment A-10 extended upward the previous observations, which had been limited to the 10^3 to 10^1 Hz range, and suggested that a change in frequency dependence occurred somewhere between 0.1 and 1.0 Hz.

1.1.3 Shock and Magnetopause Motions (A-10, A-11, A-2, A-3)

Observations made prior to the OGO 1 launch had revealed that the shock and magnetopause were capable of considerable motion. The extent and persistence of this motion became fully appreciated with the OGO 1 observations which frequently revealed multiple shock and magnetopause crossings in a single orbit pass. As many as 15 identifiable magnetopause crossings were observed on a single OGO 1 pass. Multiple crossings were observed by experiments A-10 (Holzer et al, 1966) and A-11 (Heppner et al, 1967) discussed earlier and by experiment A-2 (Wolfe et al, 1966) to which we will return later. These multiple crossings suggested an oscillatory motion of the boundaries. The average amplitude, period, and mean velocity were estimated by Holzer et al. (1966) to be $1.5 R_E$, 60 min., and 10 km/sec (6.2 mi/sec), respectively for the shock front; and for the magnetopause $0.25 R_E$, 20 min., and 10 km/sec (6.2 mi/sec), respectively. Heppner et al. (1967) arrived at similar estimates for the motion of the bow shock, but concluded that the average velocity of the magnetopause motion had to be at most 2 km/sec (1.2 mi/sec). This minor disagreement was probably due to the great variability of the boundary motion and to the difficulty of defining average parameters, particularly with a single spacecraft. In any event, these results contributed new and significant information concerning typical boundary motions under quiet geomagnetic conditions.

Large-scale motions of the shock that occur during geomagnetic storms were investigated by Binsack and Vasyliunas (1968), using data from the OGO 1 Faraday cup experiment (A-3, Bridge) and simultaneous IMP 1 and IMP 2 observations. The conclusion was that the large-scale motion is associated with an overall compression of the entire magnetosphere-magnetosheath system in response to the enhanced solar wind dynamic pressure.

1.1.4 Mapping of the Dayside Magnetosheath (A-10, A-11)

The OGO 1 orbit (see Fig. 2) made it possible to conduct a detailed mapping of the dayside magnetosheath over a period of approximately 6 months. Another accomplishment of experiments A-10 (Holzer et al, 1966) and A-11 (Heppner et al, 1967) was to provide the first detailed dusk-to-dawn mapping of the magnetosheath. This study revealed the slight 3- to 6-deg misalignment between the axis of symmetry of the magnetosheath and the Earth-Sun line, which had been expected from the aberration effect caused by the orbital motion of the Earth around the Sun.

The magnetopause in the sunward hemisphere was most typically observed by experiment A-11 (Heppner et al, 1967) as a smooth transition over a distance of about 100 km (62 mi), i.e. comparable to the ion cyclotron radius.

1.1.5 Nightside Magnetosphere (A-10)

A number of important observations were made in the nightside magnetosphere by experiment A-10 (Heppner et al, 1967). For example, near the magnetopause in the dawn sector and within geomagnetic latitudes \pm or $-$ 15 deg, the field was found weaker than in the transition region, implying that the plasma pressure had to be greater than the magnetic pressure. In such a region the magnetopause boundary is poorly defined magnetically and difficult to identify from field data. Inferences concerning the magnetospheric plasma were also made, based upon middle latitude data obtained between 5 and $10 R_E$ near midnight, which showed that the magnetic field was greater than predicted. This was interpreted as being the result of plasma pressure near the equator at similar distances and times. To illustrate further the versatility of magnetometer experiments, one can mention the correlations which were made

between the nightside field observations and auroral activities which led to the conclusion that the onset of a negative bay had to originate within the closed magnetosphere.

1.2 Low-Energy Plasma Experiments

Some of the most important OGO 1 results were obtained from experiments designed to investigate low-energy plasmas in the magnetosphere with energies from thermal up to about 50 keV. These experiments have produced two notable 'firsts,' namely the first clear identification of the plasmasphere and the first radial mapping of the plasma sheet.

1.2.1 Mapping of the Plasmapause (A-15, A-12)

A clear concept of the plasmapause, the envelope or outer-boundary of the terrestrial ionosphere, did not exist before the OGO 1 launch. Prior in situ measurements were limited to those made during two crossings by Soviet lunar vehicles, which showed that the ionospheric electron density decreased rather abruptly at middle geomagnetic latitudes at a geocentric distance of about $4 R_E$. Strong but indirect evidence for the existence of a sharp decrease, or 'knee', in the equatorial electron density profile at about $4 R_E$ had been provided by ground-based whistler observations (Carpenter, 1963).

The in situ observations were considerably widened in scope and detail through the mass spectrometer measurements on OGO 1 (Experiment A-15, Taylor). Taylor et al (1965) described the observations as revealing 'a belt of thermal ions that appears to expand and contract with changes in magnetic activity'. They referred to 'an outer boundary characterized by a reduction in both the H and He concentrations by a factor of 10 or more' and they also stated that there was a significant correlation between their findings and Carpenter's whistler knee.

Although Taylor et al exercised commendable caution and restraint in presenting their results, it was obvious that the existence of Carpenter's knee was now spectacularly confirmed, not only in the equatorial plane, but also at other latitudes. It was clearly a three-dimensional phenomenon, and its geomagnetic control had been clearly established. The next step was to find a more suitable name for this new geomagnetic boundary. Carpenter (1965), hastening the demise of the anthropomorphic Carpenter's knee designation, proposed the terms plasmapause for the boundary and plasmasphere for the region inside. Both terms have now gained wide acceptance.

Information concerning the plasmapause was also obtained with the spherical electrostatic analyzer (SEA) aboard OGO 1 (Experiment A-12, Sagalyn). The results presented by Ahmed and Sagalyn (1972) are consistent with those from the ion mass spectrometer (Taylor et al, 1965), although some differences exist. For example, the densities from the SEA experiment can be greater by a factor of two or more than the densities from the mass spectrometer. The SEA measurements showed more fine structure and greater variability in the sharpness of the plasmapause. The SEA results, unfortunately, lost much of their value because of their late publication date (1972). By 1972, a number of additional plasmapause studies conducted with OGO 3 and OGO 5 had already been published.

1.2.2 Mapping of the Plasma Sheet (A-3)

Bame et al (1967), using data from the Vela 2B satellite (launched 2 months ahead of OGO 1), showed that a plasma sheet of low-energy electrons stretched across the Earth's magnetotail from the dusk-to-dawn boundaries of the magnetosphere. The Vela data showed that these electrons had a quasi-thermal energy spectrum peaking anywhere between a few hundred eV and a few keV. Because of the circular Vela 2B orbit, the observations were limited to geocentric distances between 15.5 and $20.5 R_E$.

The radial extent of the plasma sheet was first revealed by the OGO 1 Faraday cup data (Experiment A-3, Bridge). These data were obtained in the evening sector of the magnetosphere, and they showed that the plasma sheet had an inner boundary, characterized by a rapid and substantial decrease in electron flux

12/15/75

etal, Nov. 10, 1975

and electron energy in the Earth's direction (Vasyliunas, 1968a). The inner boundary was typically found at $11 \pm 1 R_E$ under geomagnetically quiet conditions, and at $7 \pm 1 R_E$ under disturbed (storm) conditions. The existence of a sharp, well-defined inner boundary was a remarkable and unexpected feature; it showed conclusively that the plasma sheet and the radiation belt were distinct entities, each containing its own particle population.

1.2.3 Investigation of the Magnetosheath Plasma (A-2)

The general characteristics of the magnetosheath emerged very gradually during the 1959 to 1963 period from data obtained by many spacecraft (Luna 1, 2, and 3; Explorer 10, 12, and 14; IMP 1, etc.). By 1964, it was known that the magnetosheath plasma was significantly hotter than the solar wind and that its energy spectrum measured in the spacecraft coordinate system was much broader than the more nearly mono-energetic solar wind spectrum. Some disagreement existed, however, concerning the extent of plasma flow (if any) in the magnetosheath.

Results obtained with the Ames plasma probe on OGO 1 (Experiment A-2, Wolfe) provided qualitative information which helped clarify the earlier findings, due partly to improved resolution (100 to 19,000 eV in 30 steps) and partly to the opportunity of making simultaneous measurements from several spacecraft at widely separated locations. The plasma probe on OGO 1 (Wolfe et al, 1966) showed that the magnetosheath plasma was flowing around the magnetopause at a velocity at least one-half that of the solar wind. Comparisons between similar Ames probes on OGO 1 and IMP 2 (Wolfe et al, 1966) showed that the plasma temperature in the transition region was about an order of magnitude greater than the plasma temperature in nearby interplanetary space. Finally, by comparing observations made within a relatively short time interval inside the magnetosheath by the Ames plasma probes on OGO 1 and IMP 2 with observations made by the Los Alamos Scientific Laboratory on Vela 2B, it was shown (Wolfe et al, 1966) that plasma characteristics were remarkably uniform throughout the magnetosheath (for a given interplanetary solar wind condition).

Because of the clear and prompt presentation of the data by Wolfe et al (1966), the above observations have been quoted extensively in review articles. In many cases these reviews included also a reproduction of the energy spectra which Wolfe et al (1966) used to illustrate their findings.

1.3 Energetic Particle Measurements

Another group of experiments which contributed significantly to the success of the OGO 1 mission was concerned with the measurement of particles having energy typically in the range 0.1 to 100 MeV. These included experiments to investigate cosmic rays (galactic and solar) and the trapped radiation belts.

Some of the major scientific results of the OGO 1 mission were obtained with the electron spectrometer and ionization chamber experiments from the University of Minnesota (Experiment A-9, Winckler). In this case, however, it is often difficult to make a clear distinction between the OGO 1 results and the results from identical experiments on OGO 3, because Winckler and his colleagues treated the two sets of data as one continuous set of observations for the period September 1964 to July 1968. Since the OGO 1 data base was the most extensive (4 years of OGO 1 data compared to 2 years of OGO 3 data), it seems appropriate to include this topic under the OGO 1 results.

1.3.1 Radiation Belt Studies (A-9)

The magnetic deflection electron spectrometer on OGO 1 was the first instrument to measure the electron spectrum of the inner radiation zone without bremsstrahlung and proton contamination. The early OGO 1 observations revealed a pronounced slot in the energetic electron distribution near $L = 3$, presumably enhanced because of sunspot minimum, and most clearly seen because of improved directional and energy selection, (Pfitzer et al, 1966). The extended data coverage (provided by OGO 1 and OGO 3) made possible a definitive study of the long term variation of the

electron population in the inner radiation zone (Pfitzer and Winckler, 1968).

The natural injection of electrons into the inner zone was observed for the first time following the solar event of September 2, 1966 (Pfitzer and Winckler, 1968). It was shown that following large magnetic storms subsequent to solar flares, natural increases of one order of magnitude of the electron fluxes between 40 keV and 700 keV can appear far into the heart of the inner zone. Pfitzer (1972) also investigated the time history of the inner-zone flux intensity (following natural or artificial injections) and showed that the depletion could be explained quantitatively by the radial diffusion theory.

A unique study (Pfitzer, 1972) made possible by the varying orbit inclination of OGO 1 and OGO 3 was the study of the high-energy trapping boundary. The OGO 1 and OGO 3 satellites experienced a gradual increase in their orbit inclination from nearly equatorial at launch to nearly polar several years later. Thus, the complete high-energy trapping boundary could be sampled during the lifetime of the satellite, and a full three-dimensional survey of the radiation belt could be carried out. An interesting result was the observation that the trapping boundary was relatively insensitive to magnetic activity. The ionization chamber was used to map the trapping boundary because this instrument had a sensitivity threshold several orders of magnitude lower than that of the electron spectrometer.

Because of its high quality and extensive time (and space) coverage, the University of Minnesota data are the best source of information for the radiation zone particle population during the period September 1964 to July 1968. These data were made available to NSSDC, and they were used extensively for studies of the radiation belt. For example, the AE-5 model (Teague and Vette, 1972) is based largely upon the OGO 1 and OGO 3 electron spectrometer data provided to NSSDC by Professor Winckler.

1.3.2 Solar X-rays and Total Radiation in Space (A-9)

The University of Minnesota ionization chamber was a multi-purpose instrument which could be used to monitor a wide variety of radiation. A major study was made with this instrument of the solar X-ray and radio emission correlations (Arnoldy et al, 1968). Using OGO 1 and OGO 3 data approximately thirty X-ray events associated with solar flares were investigated between September 5, 1965 and June 20, 1966. This study made more certain than ever the close relationship between X-ray bursts and microwave (and a lack of correlation with metric bursts). A new result of this study was the finding of an approximate proportionality between the X-ray and radio emission over a limited range of radio frequencies and for a portion of the energetic X-ray spectrum.

The total radiation in space was monitored with the ionization chamber on OGO 1 and OGO 3 at distances varying from 15 to 25 earth radii. A most intriguing phenomenon observed was the solar cycle 'hysteresis' effect on galactic cosmic-ray modulation, characterized by the high-energy particles dropping first with the onset of new solar activity and the low energy particles afterward (Kane and Winckler, 1969).

1.3.3 Cosmic-ray Spectra and Fluxes (A-7, A-6)

The cosmic-ray experiment from the University of Chicago (Experiment A-7, Simpson) extended the knowledge of cosmic-ray spectra and fluxes to the previously unexplored energy region below 200 MeV per nucleon. This work led to the first precise determination of the low-energy fluxes of proton and alpha particles in the energy range of 2 to 20 MeV/nucleon under 'quiet' solar conditions (Fan et al, 1965). Of particular interest also was the investigation by the University of Chicago experimenters of the energetic proton streams which co-rotate with the Sun (Fan et al, 1965). This led to the discovery of a helium component, continuously associated with the protons, with an energy spectrum of E^{-2} MeV/nucleon in the energy range 2 to 20 MeV/nucleon. It was also found that the proton flux was not confined to the co-rotating regions, as previously believed, but was instead present at all times with lower intensity and different spectra.

Another significant first was the measurement of the relative abundances of the low-energy (30 to 300 MeV/nucleon) stripped

OVERVIEW

nuclei in the cosmic radiation (Comstock et al, 1966). These measurements of cosmic ray composition and fluxes at low energy have provided new and important constraints on hypotheses for the origin of galactic cosmic radiation.

Experiment A-6 (McDonald) on OGO 1 yielded cosmic-ray composition data (Balasubrahmanyam et al, 1966) in agreement with those of Comstock et al (1966). The data from experiment A-6 were of poorer quality, however, having suffered some degradation from the failure of boom EP-6 to deploy and clear the cosmic-ray telescope.

1.4 Radio Physics Experiments

The OGO 1 mission also led to some significant progress in Radio Physics, a discipline which includes a number of research activities based upon the propagation of radio waves in ionized media. The OGO 1 experiments belonging to this discipline were the VLF studies, the ionospheric profile measurements, and the radio astronomy investigations.

1.4.1. VLF Investigations (A-17)

The OGO 1 satellite was the first to provide VLF data (Experiment A-17, Helliwell) at altitudes of 6,000 - 12,000 km (3,700 to 7,400 mi) and at magnetic latitudes of 15 - 30 deg, a region previously unexplored by vehicles carrying VLF receivers. These data revealed a number of phenomena which could not or had not been observed at lower altitudes.

Two new types of non-ducted whistlers were discovered and interpreted, the MR and the Nu whistlers (Smith and Angerami, 1968). It was shown that the magnetospherically reflected (MR) whistler results from dispersive propagation of lightning energy in the magnetosphere. The MR whistlers usually exhibit multiple traces due to successive reflections in the magnetosphere. The Nu whistler, which derived the name from its resemblance to the Greek letter ν , is a modified MR whistler. The minimum 'cross-over' frequency of the Nu whistler was found to be related to the electron density near the satellite, a result which offered possibilities for studying the properties of the ambient medium.

The OGO 1 data have also provided the first in situ observations of whistler ducts. Near $L = 3$, the equatorial separation between ducts ranged from 50 to 500 km, (31 to 310 mi) and the equatorial thicknesses were about 400 km (250 mi) according to Smith and Angerami (1968).

Three distinct types of noise were discovered in the OGO 1 data and studied in detail: banded chorus, high-pass noise, and broadband noise. From their study of the banded chorus, Burtis and Helliwell (1969) concluded that these discrete emissions are generated inside the magnetosphere beyond the plasmapause and near the equatorial plane.

A survey of VLF noise observed by OGO 1 was carried out over the first hundred orbits. The region surveyed includes all local times and the range of dipole latitude from 0 to 50 degrees. It was found that high-pass and broadband noise occur primarily in the dark hemisphere (Dunckel et al, 1970), whereas whistler-mode (audio-frequency) noise occurs mainly near the noon meridian (Dunckel and Helliwell, 1969).

The upper frequency of the VLF receiver on OGO 1 (100 kHz) was too low to reach the peak of the high-pass noise. It has been shown more recently (Gurnett, 1974) that the high-pass noise discovered on OGO 1 extends up to 500 kHz with a peak near 200 kHz. Because of the intensity of this emission, the Earth is a significant planetary radio source.

1.4.2 Protonospheric Electron Density Profiles (A-14)

The OGO 1 propagation experiment (A-14 Hargreaves) was the first attempt to measure the electron concentrations in the protonosphere* by a combination of Faraday and differential Doppler measurements. In spite of experiment degradation caused by the failure to achieve three-axis stabilization, a few electron

* The upper region of the terrestrial ionosphere where H^+ is the predominant ionic constituent is sometimes called the protonosphere. At midlatitudes, this would correspond typically to altitudes greater than 2000 km.

density profiles were obtained by da Rosa and Garriott (1969) during the early months of the OGO 1 mission, at altitudes between 6,000 and 15,000 km (3,700 to 9,300 mi).

2. OGO 2 Results

The failure of the OGO 2 spacecraft attitude control, 10 days after launch, had a crippling effect on at least 12 of the 20 OGO 2 experiments. Proper orientation was an essential requirement for the two solar monitoring experiments (C-20 and C-21), for the radio astronomy experiment (C-01), for the three photometric experiments (C-12, C-13, and C-14), for three in-situ atmosphere/ionosphere experiments (C-15, C-16, and C-19), for two cosmic-ray experiments (C-08 and C-09), and for one directional trapped particle experiment (C-11). Experiment C-17, also critically dependent upon proper attitude, failed at launch and experiment C-18 yielded no useful data because its design was based upon incorrect dust particle information, causing the sensitivity threshold to be set much too high. The data from the magnetic field experiment C-05 were of very poor quality because of spacecraft spin.

Thus 10 days after launch, 15 of the OGO 2 experiments were either severely handicapped or completely useless. Much effort was spent trying to extract useful information from some of these experiments, but these attempts were eventually abandoned because of the difficulties involved* and because the experimenters could accomplish much more with their very successful (but otherwise identical) OGO 4 experiments. Thus in many cases the OGO 2 data analysis effort was transferred to OGO 4.

As a result of the OGO 2 attitude control failure, the OGO program failed to provide the planned measurements in the terrestrial atmosphere and lower ionosphere under conditions of minimum and rising solar activities. Although only 21 months separated the OGO 2 and OGO 4 launches, the solar activity rose during this period from its minimum value to 83 percent of its maximum value. The OGO 4, 5, and 6 missions were all conducted under conditions of sunspot maximum, and when the OGO program was terminated, the next solar minimum was still at least 3 years away. The current ISIS 2 and AE-C missions began in late 1974 to provide some of the 'near sunspot minimum' measurements which OGO 2 had failed to obtain in late 1965 and early 1966.

A number of important results were nevertheless obtained by some of the attitude sensitive OGO 2 experiments during the first 10 days of operation while three-axis stabilization was maintained, particularly in the case of experiments performed for the first time where even a few hours of good data could provide valuable new scientific information. In most cases the attitude sensitive experiments operated long enough with proper orientation to check their in-orbit performance and to discover design deficiencies, if any, which were subsequently corrected for the OGO 4 instrumentation. Thus the technological information obtained from the OGO 2 flight experience was an important factor in the overall success of the OGO 4 mission.

A considerable amount of scientific information was obtained, however, from a number of experiments for which attitude was not critical; namely the magnetic field measurements, the VLF studies, and the omnidirectional cosmic-ray investigations. The various scientific accomplishments of the OGO 2 mission will be summarized by disciplines using the same order as was used for OGO 1, and adding new disciplines afterwards, as required.

2.1 Magnetic Field Experiments

2.1.1 World Magnetic Survey (C-06)

One of the major goals of the IQSY cooperation was the measurement of the Earth's main magnetic field on a global basis. To carry out this World Magnetic Survey, the routine ground-based monitoring at fixed locations was supplemented by aircraft, surface ship, and satellite measurements. Magnetic surveys by satellites were given additional importance by being designated as one of the three areas of peaceful cooperation in outer space between the

* The lack of journal publications from the low energy particle experiment C-10 may also have been due to data processing difficulties.

OVERVIEW

nuclei in the cosmic radiation (Comstock et al, 1966). These measurements of cosmic ray composition and fluxes at low energy have provided new and important constraints on hypotheses for the origin of galactic cosmic radiation.

Experiment A-6 (McDonald) on OGO 1 yielded cosmic-ray composition data (Balasubrahmanyam et al, (1966) in agreement with those of Comstock et al (1966). The data from experiment A-6 were of poorer quality, however, having suffered some degradation from the failure of boom EP-6 to deploy and clear the cosmic-ray telescope.

1.4 Radio Physics Experiments

The OGO 1 mission also led to some significant progress in Radio Physics, a discipline which includes a number of research activities based upon the propagation of radio waves in ionized media. The OGO 1 experiments belonging to this discipline were the VLF studies, the ionospheric profile measurements, and the radio astronomy investigations.

1.4.1. VLF Investigations (A-17)

The OGO 1 satellite was the first to provide VLF data (Experiment A-17, Helliwell) at altitudes of 6,000 - 12,000 km (3,700 to 7,400 mi) and at magnetic latitudes of 15 - 30 deg, a region previously unexplored by vehicles carrying VLF receivers. These data revealed a number of phenomena which could not or had not been observed at lower altitudes.

Two new types of non-ducted whistlers were discovered and interpreted, the MR and the Nu whistlers (Smith and Angerami, 1968). It was shown that the magnetospherically reflected (MR) whistler results from dispersive propagation of lightning energy in the magnetosphere. The MR whistlers usually exhibit multiple traces due to successive reflections in the magnetosphere. The Nu whistler, which derived the name from its resemblance to the Greek letter ν , is a modified MR whistler. The minimum 'cross-over' frequency of the Nu whistler was found to be related to the electron density near the satellite, a result which offered possibilities for studying the properties of the ambient medium.

The OGO 1 data have also provided the first in situ observations of whistler ducts. Near $L = 3$, the equatorial separation between ducts ranged from 50 to 500 km, (31 to 310 mi) and the equatorial thicknesses were about 400 km (250 mi) according to Smith and Angerami (1968).

Three distinct types of noise were discovered in the OGO 1 data and studied in detail: banded chorus, high-pass noise, and broadband noise. From their study of the banded chorus, Burtis and Helliwell (1969) concluded that these discrete emissions are generated inside the magnetosphere beyond the plasmapause and near the equatorial plane.

A survey of VLF noise observed by OGO 1 was carried out over the first hundred orbits. The region surveyed includes all local times and the range of dipole latitude from 0 to 50 degrees. It was found that high-pass and broadband noise occur primarily in the dark hemisphere (Dunckel et al, 1970), whereas whistler-mode (audio-frequency) noise occurs mainly near the noon meridian (Dunckel and Helliwell, 1969).

The upper frequency of the VLF receiver on OGO 1 (100 kHz) was too low to reach the peak of the high-pass noise. It has been shown more recently (Gurnett, 1974) that the high-pass noise discovered on OGO 1 extends up to 500 kHz with a peak near 200 kHz. Because of the intensity of this emission, the Earth is a significant planetary radio source.

1.4.2 Protonospheric Electron Density Profiles (A-14)

The OGO 1 propagation experiment (A-14 Hargreaves) was the first attempt to measure the electron concentrations in the protonosphere* by a combination of Faraday and differential Doppler measurements. In spite of experiment degradation caused by the failure to achieve three-axis stabilization, a few electron

* The upper region of the terrestrial ionosphere where H+ is the predominant ionic constituent is sometimes called the protonosphere. At midlatitudes, this would correspond typically to altitudes greater than 2000 km.

density profiles were obtained by da Rosa and Garriott (1969) during the early months of the OGO 1 mission, at altitudes between 6,000 and 15,000 km (3,700 to 9,300 mi).

2. OGO 2 Results

The failure of the OGO 2 spacecraft attitude control, 10 days after launch, had a crippling effect on at least 12 of the 20 OGO 2 experiments. Proper orientation was an essential requirement for the two solar monitoring experiments (C-20 and C-21), for the radio astronomy experiment (C-01), for the three photometric experiments (C-12, C-13, and C-14), for three in-situ atmosphere/ionosphere experiments (C-15, C-16, and C-19), for two cosmic-ray experiments (C-08 and C-09), and for one directional trapped particle experiment (C-11). Experiment C-17, also critically dependent upon proper attitude, failed at launch and experiment C-18 yielded no useful data because its design was based upon incorrect dust particle information, causing the sensitivity threshold to be set much too high. The data from the magnetic field experiment C-05 were of very poor quality because of spacecraft spin.

Thus 10 days after launch, 15 of the OGO 2 experiments were either severely handicapped or completely useless. Much effort was spent trying to extract useful information from some of these experiments, but these attempts were eventually abandoned because of the difficulties involved* and because the experimenters could accomplish much more with their very successful (but otherwise identical) OGO 4 experiments. Thus in many cases the OGO 2 data analysis effort was transferred to OGO 4.

As a result of the OGO 2 attitude control failure, the OGO program failed to provide the planned measurements in the terrestrial atmosphere and lower ionosphere under conditions of minimum and rising solar activities. Although only 21 months separated the OGO 2 and OGO 4 launches, the solar activity rose during this period from its minimum value to 83 percent of its maximum value. The OGO 4, 5, and 6 missions were all conducted under conditions of sunspot maximum, and when the OGO program was terminated, the next solar minimum was still at least 3 years away. The current ISIS 2 and AE-C missions began in late 1974 to provide some of the 'near sunspot minimum' measurements which OGO 2 had failed to obtain in late 1965 and early 1966.

A number of important results were nevertheless obtained by some of the attitude sensitive OGO 2 experiments during the first 10 days of operation while three-axis stabilization was maintained, particularly in the case of experiments performed for the first time where even a few hours of good data could provide valuable new scientific information. In most cases the attitude sensitive experiments operated long enough with proper orientation to check their in-orbit performance and to discover design deficiencies, if any, which were subsequently corrected for the OGO 4 instrumentation. Thus the technological information obtained from the OGO 2 flight experience was an important factor in the overall success of the OGO 4 mission.

A considerable amount of scientific information was obtained, however, from a number of experiments for which attitude was not critical; namely the magnetic field measurements, the VLF studies, and the omnidirectional cosmic-ray investigations. The various scientific accomplishments of the OGO 2 mission will be summarized by disciplines using the same order as was used for OGO 1, and adding new disciplines afterwards, as required.

2.1 Magnetic Field Experiments

2.1.1 World Magnetic Survey (C-06)

One of the major goals of the IQSY cooperation was the measurement of the Earth's main magnetic field on a global basis. To carry out this World Magnetic Survey, the routine ground-based monitoring at fixed locations was supplemented by aircraft, surface ship, and satellite measurements. Magnetic surveys by satellites were given additional importance by being designated as one of the three areas of peaceful cooperation in outer space between the

* The lack of journal publications from the low energy particle experiment C-10 may also have been due to data processing difficulties.

OVERVIEW

nuclei in the cosmic radiation (Comstock et al, 1966). These measurements of cosmic ray composition and fluxes at low energy have provided new and important constraints on hypotheses for the origin of galactic cosmic radiation.

Experiment A-6 (McDonald) on OGO 1 yielded cosmic-ray composition data (Balasubrahmanyam et al (1966)) in agreement with those of Comstock et al. (1966). The data from experiment A-6 were of poorer quality, however, having suffered some degradation from the failure of boom EP-6 to deploy and clear the cosmic-ray telescope.

1.4 Radio Physics Experiments

The OGO 1 mission also led to some significant progress in Radio Physics, a discipline which includes a number of research activities based upon the propagation of radio waves in ionized media. The OGO 1 experiments belonging to this discipline were the VLF studies, the ionospheric profile measurements, and the radio astronomy investigations.

1.4.1. VLF Investigations (A-17)

The OGO 1 satellite was the first to provide VLF data (Experiment A-17, Helliwell) at altitudes of 6,000 - 12,000 km (3,700 to 7,400 mi) and at magnetic latitudes of 15 - 30 deg, a region previously unexplored by vehicles carrying VLF receivers. These data revealed a number of phenomena which could not or had not been observed at lower altitudes.

Two new types of non-ducted whistlers were discovered and interpreted, the MR and the Nu whistlers (Smith and Angerami, 1968). It was shown that the magnetospherically reflected (MR) whistler results from dispersive propagation of lightning energy in the magnetosphere. The MR whistlers usually exhibit multiple traces due to successive reflections in the magnetosphere. The Nu whistler, which derived the name from its resemblance to the Greek letter ν , is a modified MR whistler. The minimum 'cross-over' frequency of the Nu whistler was found to be related to the electron density near the satellite, a result which offered possibilities for studying the properties of the ambient medium.

The OGO 1 data have also provided the first in situ observations of whistler ducts. Near $L = 3$, the equatorial separation between ducts ranged from 50 to 500 km, (31 to 310 mi) and the equatorial thicknesses were about 400 km (250 mi) according to Smith and Angerami (1968).

Three distinct types of noise were discovered in the OGO 1 data and studied in detail: banded chorus, high-pass noise, and broadband noise. From their study of the banded chorus, Burtis and Helliwell (1969) concluded that these discrete emissions are generated inside the magnetosphere beyond the plasmopause and near the equatorial plane.

A survey of VLF noise observed by OGO 1 was carried out over the first hundred orbits. The region surveyed includes all local times and the range of dipole latitude from 0 to 50 degrees. It was found that high-pass and broadband noise occur primarily in the dark hemisphere (Dunckel et al, 1970), whereas whistler-mode (audio-frequency) noise occurs mainly near the noon meridian (Dunckel and Helliwell, 1969).

The upper frequency of the VLF receiver on OGO 1 (100 kHz) was too low to reach the peak of the high-pass noise. It has been shown more recently (Gurnett, 1974) that the high-pass noise discovered on OGO 1 extends up to 500 kHz with a peak near 200 kHz. Because of the intensity of this emission, the Earth is a significant planetary radio source.

1.4.2 Protonospheric Electron Density Profiles (A-14)

The OGO 1 propagation experiment (A-14 Hargreaves) was the first attempt to measure the electron concentrations in the protonosphere* by a combination of Faraday and differential Doppler measurements. In spite of experiment degradation caused by the failure to achieve three-axis stabilization, a few electron

* The upper region of the terrestrial ionosphere where H^+ is the predominant ionic constituent is sometimes called the protonosphere. At midlatitudes, this would correspond typically to altitudes greater than 2000 km.

density profiles were obtained by da Rosa and Garriott (1969) during the early months of the OGO 1 mission, at altitudes between 6,000 and 15,000 km (3,700 to 9,300 mi).

2. OGO 2 Results

The failure of the OGO 2 spacecraft attitude control, 10 days after launch, had a crippling effect on at least 12 of the 20 OGO 2 experiments. Proper orientation was an essential requirement for the radio astronomy experiment (C-01), for the three photometric experiments (C-12, C-13, and C-14), for three in-situ atmosphere/ionosphere experiments (C-15, C-16, and C-19), for two cosmic-ray experiments (C-08 and C-09), and for one directional trapped particle experiment (C-11). Experiment C-17, also critically dependent upon proper attitude, failed at launch and experiment C-18 yielded no useful data because its design was based upon incorrect dust particle information, causing the sensitivity threshold to be set much too high. The data from the magnetic field experiment C-05 were of very poor quality because of spacecraft spin.

Thus 10 days after launch, 15 of the OGO 2 experiments were either severely handicapped or completely useless. Much effort was spent trying to extract useful information from some of these experiments, but these attempts were eventually abandoned because of the difficulties involved* and because the experimenters could accomplish much more with their very successful (but otherwise identical) OGO 4 experiments. Thus in many cases the OGO 2 data analysis effort was transferred to OGO 4.

As a result of the OGO 2 attitude control failure, the OGO program failed to provide the planned measurements in the terrestrial atmosphere and lower ionosphere under conditions of minimum and rising solar activities. Although only 21 months separated the OGO 2 and OGO 4 launches, the solar activity rose during this period from its minimum value to 83 percent of its maximum value. The OGO 4, 5, and 6 missions were all conducted under conditions of sunspot maximum, and when the OGO program was terminated, the next solar minimum was still at least 3 years away. The current ISIS 2 and AE-C missions began in late 1974 to provide some of the 'near sunspot minimum' measurements which OGO 2 had failed to obtain in late 1965 and early 1966.

A number of important results were nevertheless obtained by some of the attitude sensitive OGO 2 experiments during the first 10 days of operation while three-axis stabilization was maintained, particularly in the case of experiments performed for the first time where even a few hours of good data could provide valuable new scientific information. In most cases the attitude sensitive experiments operated long enough with proper orientation to check their in-orbit performance and to discover design deficiencies, if any, which were subsequently corrected for the OGO 4 instrumentation. Thus the technological information obtained from the OGO 2 flight experience was an important factor in the overall success of the OGO 4 mission.

A considerable amount of scientific information was obtained, however, from a number of experiments for which attitude was not critical; namely the magnetic field measurements, the VLF studies, and the omnidirectional cosmic-ray investigations. The various scientific accomplishments of the OGO 2 mission will be summarized by disciplines using the same order as was used for OGO 1, and adding new disciplines afterwards, as required.

2.1 Magnetic Field Experiments

2.1.1 World Magnetic Survey (C-06)

One of the major goals of the IQSY cooperation was the measurement of the Earth's main magnetic field on a global basis. To carry out this World Magnetic Survey, the routine ground-based monitoring at fixed locations was supplemented by aircraft, surface ship, and satellite measurements. Magnetic surveys by satellites were given additional importance by being designated as one of the three areas of peaceful cooperation in outer space between the

* The lack of journal publications from the low energy particle experiment C-10 may also have been due to data processing difficulties.

U. S. and the U.S.S.R.* Experiment C-06 (Cain) was selected for OGO 2 as the U.S. space contribution to the IQSY World Magnetic Survey and to the cooperative venture between the U.S. and the U.S.S.R. It was therefore particularly gratifying that experiment C-06 turned out to be one of the few successful OGO 2 experiments. The objectives of experiment C-06 were fully met and the resulting data led to a description of the geomagnetic field improved by an order of magnitude over previous models (Cain et al, 1967). It was also shown that a globally accurate description of the main terrestrial field could be maintained using only satellite data. A comparison of OGO 2 and U.S.S.R. results in the region of the Brazilian anomaly showed excellent agreement (Cain et al, 1968).

2.1.2. Secular Field Variations (C-06)

OGO 2 data were also used in conjunction with older survey data to define the gross secular change of the main field during the first half of this century. It was shown by Cain and Hendricks (1969) that the main dipole was drifting westward at an increasing rate ($0.07^\circ/\text{year}$ in 1969) after a reversal of its eastward drift in about 1920. A slight slowing of the rate of decrease of the dipole moment was also observed.

2.1.3 Magnetic Storm Studies (C-06)

OGO 2 studies by Langel and Cain (1968) of the first major sequence of magnetic storms since the solar minimum in March 1966 resulted in information on the structure of polar ionospheric electrojets and the asymmetric ring current. The polar electrojets were seen to follow the classical 'two-cell' model and be definitely located at ionospheric altitudes. The source of the lower-latitude disturbance was seen to be extra-ionospheric both in its symmetric (Dst) and asymmetric (DS) components. The strong polar currents were seen to follow contours of L, to appear prior to the main phase of the magnetic storm, and almost to vanish at the beginning of the recovery phase when the ring current became symmetric. An extension of this study was published by Langel and Sweeney (1971).

2.2 Low-Energy Plasma Experiments

2.2.1 Global Sampling of Ion Composition (C-16)

Excellent data were acquired by experiment C-16 (Taylor) from October 14 to 24, 1965, while three-axis stabilization was maintained. These data yielded the first detailed description of the latitudinal variation of the ion composition, and it provided evidence of strong solar and geomagnetic control of the topside ionosphere and plasmasphere (Taylor et al, 1968b). These measurements made in a dawn-dusk orbit showed that in the altitude range of 415-1525 km (260-950 mi) the major ions were O^+ and H^+ , and the minor constituents were N^+ and He^+ . Solar control was revealed by the latitudinal asymmetry in the distribution of O^+ and N^+ , while the greater symmetry in the distribution of H^+ and He^+ was evidence of the strong solar-geomagnetic control of the light ions.

2.2.2. The High Latitude Plasmopause (C-16, C-02)

Experiment C-16 also revealed a pronounced light ion trough near 60 deg invariant latitude ($L = 4$) corresponding to the high latitude boundary of the plasmasphere. The light ion trough was found to correlate extremely well (Taylor et al, 1969) with similar rapid reductions in the propagation of both man-made and natural VLF signals received at the satellite by experiment C-02 (Helliwell).

2.3 Energetic Particle Measurements

The ionization chamber used for experiment C-07 (Anderson) had an isotropic response to incident radiation except for 2

percent of 4π steradians subtended by the OGO body and ion chamber neck. This omnidirectional characteristic made experiment C-07 insensitive to spacecraft orientation. During its 6 months of operation, experiment C-07 provided a complete sampling of local times.*

2.3.1 Radiation Belt Studies (C-07)

The high latitude boundary of 'trapped' radiation was found to occur at invariant latitude 67 - 70 deg, (Anderson et al, 1968). A few degrees lower, narrow spikes of intensity were observed on about 34 percent of all passes (McCoy, 1969). Their frequency of occurrence increased markedly with increased values of the magnetic disturbance index K_p , and they were seen at all local times. Spikes observed above the boundary appeared predominantly in the dawn hemisphere. The spikes above the boundary were attributed to quasi-trapped electrons, injected from the magnetospheric tail and drifting part way around the earth.

2.3.2 Solar Cosmic Rays over the Polar Caps (C-07)

Hudson and Anderson (1969) reported large fluctuations in the intensity of solar protons over the polar regions during two solar proton events on March 24, 1966, separated by 3.5 hours. Simultaneous observations made on OGO 1, 13 R_E sunward of the Earth by Kane and Winckler (Experiment A-9) showed no such fluctuations. These differences were interpreted as spatial effects due to the field structure over the poles.

2.3.3 Galactic Cosmic Radiation (C-07)

The cosmic ray knee (using balloon observation terminology) was investigated extensively with experiment C-07 (George, 1970a). The knee was interpreted as a position in the geomagnetic field where the cosmic-ray cutoff rigidity was about 1.2 Gv for the OGO 2 measurements. The invariant latitude of the knee was found to decrease with altitude at the rate of $(2.5 \pm 0.5) \times 10^3$ deg / km and to have a value of 59.1 deg at the Earth's surface in 1965-1966. Measurements of cosmic ray ionization over the polar regions with experiment C-07 (George, 1970b) yielded the following results. Extrapolating to the top of the atmosphere and to infinity, the ionization values were 550 ± 10 and 985 ± 6 ion pairs / (cm² sec atm), respectively, and splash albedo contributed 10.4 ± 2.3 percent of the total ionization at the top of the ionosphere. These results were for early November 1965.

2.4 Radio Physics Experiments

2.4.1 VLF Investigations (C-02, C-03)

A study with experiment C-02 (Heyborne et al 1969) of signals received from ground-based VLF transmitters revealed an abrupt signal cut-off (as severe as 40 db within a latitude change of 2 deg) occurring near 60 deg invariant latitude. The correlation of this cut-off with the plasmopause is discussed under section 2.2.2.

Propagation studies with experiment C-02 also led to the identification of a new type of non-ducted whistler: the walking-trace (WT) whistler, (Walter and Angerami, 1969). The WT whistlers are characterized by rising tones, occurrence localized within a few degrees of 51 deg invariant latitude, and rapid increases in travel times with latitude so that on frequency-time spectra a succession of WT whistlers appear to 'walk through' other whistlers with unchanged dispersion. The WT whistlers have been explained by magnetospheric equatorial ionization profiles incorporating small gradients across L shells.

A unique, stationary type of VLF auroral hiss was discovered with experiment C-02. This unusual type of hiss is limited to the

* Exchange of letters between President Kennedy and Chairman Krushchev in 1962.

* For the OGO 2 orbit the local time decreased by one hour in 12 days due to the combined effects of precession and of the Earth's motion around the Sun.

OVERVIEW

region of the auroral oval and it provides a tool for monitoring the auroral oval by means of satellite VLF observations (Jorgensen and Bell, 1968).

VLF observations made with experiment C-03 (Morgan), which used a 2.7 m (9 ft) electric dipole antenna, revealed phenomena somewhat different from those detected by the (magnetic) loop antenna on experiment C-02. The most significant result obtained with experiment C-03 was the frequent observation of lower-hybrid resonance (LHR) emissions. Since these LHR emissions were not seen by experiment C-02, it was definitely established that the LHR emission was an electric wave phenomenon (Laaspere et al, 1969).

2.4.2. Satellite Wake Study (C-01)

Although the Cosmic Radio Noise mapping planned with experiment C-01 (Haddock) was not possible due to the OGO 2 orientation problem, the observations made with experiment C-01 yielded useful information concerning the OGO 2 wake. (Yorks and Weil, 1970). The wake study was possible because experiment C-01 included an antenna impedance measuring capability at 2.5 MHz and because the impedance of a short dipole in the ionosphere is very sensitive to nearby electron concentrations (or electron depletions caused by a satellite wake).

2.5. Airglow and Auroral Measurements (C-12)

During the 10 days of stabilized operation, experiment C-12 (Blamont / Reed) obtained approximately 2 hours of airglow data while OGO 2 was in the Earth's shadow. These limited observations were of interest because they were the first of their kind. They confirmed the suspected extensive latitudinal extent of airglow and revealed very clearly the two airglow layers, (the lower one centered near 100 km (62 mi) and the upper one centered near 250 km (155 mi)) showing conclusively that vertical airglow profiles could indeed be derived from satellite measurements. A few auroras were also seen over the northern polar cap (Reed and Blamont, 1966).

An unexpected high background noise level present in the main body photometer showed the need for additional shielding. The observed background noise was due to energetic particles and it led to a useful mapping of energetic particle intensity (Reed et al, 1967). The OGO 4 main photometer was provided with the additional shielding and the background noise was reduced by two orders of magnitude.

3. OGO 3 Results

As originally planned, the OGO 3 mission was a continuation (during a period of rapidly increasing solar activity) of the OGO 1 mission (launched at sun spot minimum). The two spacecraft carried the same experiments (except for one very important new experiment on OGO 3, Frank's LEPEDEA experiment, B-8), and the observations from the two missions should have provided essentially a continuous data base. This was indeed the case for a number of experiments which were not critically dependent upon orientation and, as pointed out earlier, many of the findings described under the OGO 1 results were based upon both OGO 1 and OGO 3 data. A number of orientation-sensitive experiments were able to obtain for the first time a limited amount of high-quality data during the initial 46 days of OGO 3 stabilized operation. Also the proper boom deployment on OGO 3 led to improved performance of some experiments, particularly the fluxgate and rubidium magnetometers (Experiment B-11, Heppner).

The most important difference between OGO 1 and 3, however, was in the continuity of data coverage. As shown in Figure III-5, the OGO 1 operation was restricted to spring (March, April, and May) and fall (September, October, and November). This was due to the inertially fixed orientation of the OGO 1 spin axis, causing the solar aspect to be periodically unfavorable for the OGO 1 solar cells. Control of the spin axis orientation was maintained on OGO 3, resulting in continuous data coverage as shown in Figure III-5, and making possible a more complete study of the magnetosphere than could be done with the OGO 1 data.

Nineteen of the twenty-three experiments on OGO 3 yielded useful data, and each of these experiments led to at least one

major publication. The four unsuccessful OGO 3 experiments included B-02 (Wolfe), which could not operate properly due to spacecraft spin, experiment B-06a (McDonald), which failed 90 hours after initial turnon, experiment B-06b (Evans), which suffered from a very high background noise, and experiment B-14 (Fritz), which interfered with the command receiver. Before the interference problem from experiment B-14 could be overcome, the attitude system failed causing subsequent data from experiment B-14 to be useless.

3.1 Magnetic Field Experiments

On OGO 1 the 3-to-14,000 gamma rubidium vapor magnetometer (Experiment B-11, Heppner) was inoperative because the 6.9 m (22 ft) boom EP-6 (on which the experiment B-11 magnetometers were located) failed to deploy. The 0-to-500 gamma fluxgate magnetometer worked on OGO 1 in spite of the EP-6 failure but at a somewhat reduced accuracy. The proper operation of these magnetometers on OGO 3 (and the continuous OGO 3 operation) made it possible for the first time to acquire extensive and very accurate data throughout the inner magnetosphere (2 to 8 R_E). Measurements with improved accuracy also became possible at greater distances. An important aspect of the data analysis effort on experiment B-11 was therefore to conduct a comprehensive magnetic field survey of the inner magnetosphere.

3.1.1 Detailed Mapping of the Magnetic Field in the Magnetosphere (B-11, E-15)

Since fairly good models of the geomagnetic field B were already available when the study was undertaken, the new observed values $|B_{obs}|$ were compared (Sugiura et al, 1971) to the value predicted by the existing theoretical field model $|B_{theory}|$, and the new measurements were expressed in terms of the parameter ΔB ,

$$\text{where: } \Delta B = |B_{obs}| - |B_{theory}|$$

It was concluded from this study that the ΔB values could be viewed as perturbations (at magnetospheric heights) upon an otherwise essentially correct model of the geomagnetic field. It was found that a negative ΔB region existed near the dipole equator and that there was a positive ΔB region at middle to high latitudes in the nightside magnetosphere. The magnitude of the perturbation was found to increase with the value of the K_p index.

The very large volume of the magnetosphere, the gradual manner in which this volume is explored by an EGO satellite (see Figure III-2), the gradual increase in orbit inclination and in perigee altitude, and the effect of K_p upon the ΔB data made it difficult to obtain an adequate number of data points with one satellite. The ΔB study was initiated with the OGO 3 data, but the published results (Sugiura et al, 1971) included approximately an equal number of OGO 3 and OGO 5 observations.

3.1.2 The Equatorial Ring Current (B-11, E-15)

The interpretation of the equatorial ΔB region (discussed under 3.1.1) led to a new concept of the terrestrial ring current (Sugiura, 1972). The existence of an equatorial ring current at a distance of a few earth radii was originally postulated to explain ground-based observations of geomagnetic disturbances. A toroidal shape was the commonly accepted image of the ring current.

On the basis of the ΔB distribution, Sugiura (1972) showed that the ring current was a quasi-permanent feature of the magnetosphere and that this current was disk-like rather than toroidal, extending from a geocentric distance of about 2.5 R_E out to the neutral sheet in the magnetospheric tail. This conclusion led Sugiura and Poros (1973) to propose a revised model of the geomagnetic field which included the effect of this concentric disk-like ring current.

3.1.3 ELF Noise in the Magnetosphere (B-10)

The data from the OGO 3 triaxial search coil magnetometer (Experiment B-10, Smith) was used to describe the morphology of

OVERVIEW

region of the auroral oval and it provides a tool for monitoring the auroral oval by means of satellite VLF observations (Jorgensen and Bell, 1968).

VLF observations made with experiment C-03 (Morgan), which used a 2.7 m (9 ft) electric dipole antenna, revealed phenomena somewhat different from those detected by the (magnetic) loop antenna on experiment C-02. The most significant result obtained with experiment C-03 was the frequent observation of lower-hybrid resonance (LHR) emissions. Since these LHR emissions were not seen by experiment C-02, it was definitely established that the LHR emission was an electric wave phenomenon (Laaspere et al, 1969).

2.4.2. Satellite Wake Study (C-01)

Although the Cosmic Radio Noise mapping planned with experiment C-01 (Haddock) was not possible due to the OGO 2 orientation problem, the observations made with experiment C-01 yielded useful information concerning the OGO 2 wake. (Yorks and Weil, 1970). The wake study was possible because experiment C-01 included an antenna impedance measuring capability at 2.5 MHz and because the impedance of a short dipole in the ionosphere is very sensitive to nearby electron concentrations (or electron depletions caused by a satellite wake).

2.5. Airglow and Auroral Measurements (C-12)

During the 10 days of stabilized operation, experiment C-12 (Blamont / Reed) obtained approximately 2 hours of airglow data while OGO 2 was in the Earth's shadow. These limited observations were of interest because they were the first of their kind. They confirmed the suspected extensive latitudinal extent of airglow and revealed very clearly the two airglow layers, (the lower one centered near 100 km (62 mi) and the upper one centered near 250 km (155 mi)) showing conclusively that vertical airglow profiles could indeed be derived from satellite measurements. A few auroras were also seen over the northern polar cap (Reed and Blamont, 1966).

An unexpected high background noise level present in the main body photometer showed the need for additional shielding. The observed background noise was due to energetic particles and it led to a useful mapping of energetic particle intensity (Reed et al, 1967). The OGO 4 main photometer was provided with the additional shielding and the background noise was reduced by two orders of magnitude.

3. OGO 3 Results

As originally planned, the OGO 3 mission was a continuation (during a period of rapidly increasing solar activity) of the OGO 1 mission (launched at sun spot minimum). The two spacecraft carried the same experiments (except for one very important new experiment on OGO 3, Frank's LEPDEA experiment, B-8), and the observations from the two missions should have provided essentially a continuous data base. This was indeed the case for a number of experiments which were not critically dependent upon orientation and, as pointed out earlier, many of the findings described under the OGO 1 results were based upon both OGO 1 and OGO 3 data. A number of orientation-sensitive experiments were able to obtain for the first time a limited amount of high-quality data during the initial 46 days of OGO 3 stabilized operation. Also the proper boom deployment on OGO 3 led to improved performance of some experiments, particularly the fluxgate and rubidium magnetometers (Experiment B-11, Heppner).

The most important difference between OGO 1 and 3, however, was in the continuity of data coverage. As shown in Figure III-5, the OGO 1 operation was restricted to spring (March, April, and May) and fall (September, October, and November). This was due to the inertially fixed orientation of the OGO 1 spin axis, causing the solar aspect to be periodically unfavorable for the OGO 1 solar cells. Control of the spin axis orientation was maintained on OGO 3, resulting in continuous data coverage as shown in Figure III-5, and making possible a more complete study of the magnetosphere than could be done with the OGO 1 data.

Nineteen of the twenty-three experiments on OGO 3 yielded useful data, and each of these experiments led to at least one

major publication. The four unsuccessful OGO 3 experiments included B-02 (Wolfe), which could not operate properly due to spacecraft spin, experiment B-06a (McDonald), which failed 90 hours after initial turnon, experiment B-06b (Evans), which suffered from a very high background noise, and experiment B-14 (Fritz), which interfered with the command receiver. Before the interference problem from experiment B-14 could be overcome, the attitude system failed causing subsequent data from experiment B-14 to be useless.

3.1 Magnetic Field Experiments

On OGO 1 the 3-to-14,000 gamma rubidium vapor magnetometer (Experiment B-11, Heppner) was inoperative because the 6.9 m (22 ft) boom EP-6 (on which the experiment B-11 magnetometers were located) failed to deploy. The 0-to-500 gamma fluxgate magnetometer worked on OGO 1 in spite of the EP-6 failure but at a somewhat reduced accuracy. The proper operation of these magnetometers on OGO 3 (and the continuous OGO 3 operation) made it possible for the first time to acquire extensive and very accurate data throughout the inner magnetosphere (2 to 8 R_E). Measurements with improved accuracy also became possible at greater distances. An important aspect of the data analysis effort on experiment B-11 was therefore to conduct a comprehensive magnetic field survey of the inner magnetosphere.

3.1.1 Detailed Mapping of the Magnetic Field in the Magnetosphere (B-11)

Since fairly good models of the geomagnetic field B were already available when the study was undertaken, the new observed values $|B_{obs}|$ were compared (Sugiura et al, 1971) to the value predicted by the existing theoretical field model $|B_{theory}|$, and the new measurements were expressed in terms of the parameter ΔB ,

$$\text{where: } \Delta B = |B_{obs}| - |B_{theory}|$$

It was concluded from this study that the ΔB values could be viewed as perturbations (at magnetospheric heights) upon an otherwise essentially correct model of the geomagnetic field. It was found that a negative ΔB region existed near the dipole equator and that there was a positive ΔB region at middle to high latitudes in the nightside magnetosphere. The magnitude of the perturbation was found to increase with the value of the K_p index.

The very large volume of the magnetosphere, the gradual manner in which this volume is explored by an EGO satellite (see Figure III-2), the gradual increase in orbit inclination and in perigee altitude, and the effect of K_p upon the ΔB data made it difficult to obtain an adequate number of data points with one satellite. The ΔB study was initiated with the OGO 3 data, but the published results (Sugiura et al, 1971) included approximately an equal number of OGO 3 and OGO 5 observations.

3.1.2 The Equatorial Ring Current (B-11)

The interpretation of the equatorial ΔB region (discussed under 3.1.1) led to a new concept of the terrestrial ring current (Sugiura, 1972). The existence of an equatorial ring current at a distance of a few earth radii was originally postulated to explain ground-based observations of geomagnetic disturbances. A toroidal shape was the commonly accepted image of the ring current.

On the basis of the ΔB distribution, Sugiura (1972) showed that the ring current was a quasi-permanent feature of the magnetosphere and that this current was disk-like rather than toroidal, extending from a geocentric distance of about 2.5 R_E out to the neutral sheet in the magnetospheric tail. This conclusion led Sugiura and Poros (1973) to propose a revised model of the geomagnetic field which included the effect of this concentric disk-like ring current.

3.1.3 ELF Noise in the Magnetosphere (B-10)

The data from the OGO 3 triaxial search coil magnetometer (Experiment B-10, Smith) was used to describe the morphology of

ELF noise (0.1 to 1.0 kHz) in the magnetosphere. This study revealed two distinct populations of noise within the magnetosphere: steady noise (ELF hiss) occurring primarily in the plasmasphere and in the dayside outer magnetosphere at magnetic latitudes near 45 deg; and noise bursts (chorus and whistlers) at low latitude in the dayside outer magnetosphere (Russell et al, 1969, Russell and Holzer, 1970).

Although the ELF hiss band is variable, it extends typically from 500 to 700 hertz. An ELF emission having a frequency typically 1/10 that of the ELF hiss was discovered by Russell et al (1970) during their very comprehensive survey of ELF hiss. This lower frequency has been named the sub LHR hiss because its frequency spectrum is always below the Lower Hybrid Resonance frequency. The sub LHR hiss is extremely localized in space. It has been observed only within about 2 deg of the magnetic equator and only in the outer two earth radii of the plasmasphere. No explanation has yet been proposed for this emission.

3.1.4 Bow Shock Structure (B-10)

A very comprehensive study of the bow shock structure was conducted with the search coil magnetometer data (Experiment B-10, Smith) using OGO 3 data obtained during the first six months after launch. During this period OGO 3 crossed the Earth's bow shock over 500 times, and from these events a set of 494 crossings was selected for analysis (Olson and Holzer, 1974). Most of these data were obtained at the 1 kbs telemetry sampling rate, which placed an upper limit of 2.17 Hz for the frequency of the observed waveforms. This study showed that the dominant pattern, comprising about 85 percent of the shock crossings, consisted of waves having frequencies ranging from one to a few hertz upstream of the main shock compression and lower frequency waves, typically 0.3 Hz, downstream. The remaining 15 percent of the crossings exhibited a much more complex pattern, at times apparently chaotic.

On approximately thirty occasions the crossings were monitored at the high data rate (64 kbs). Of these, eleven crossings were suitable for analysis. This unique data set made it possible for the first time* to observe the high frequency structure of the magnetic fluctuations at the bow shock (Olson et al, 1969). Power spectra for frequencies between 1 and 140 Hz were obtained at successive positions near the shock, showing how the special characteristics of the quiet interplanetary medium is gradually modified, first upstream in the presence of the shock precursor, then at various positions within the shock, and finally in the magnetosheath downstream from the shock. The average energy density in the region $1 < f < 140$ Hz was found to be 4.9×10^{-11} , 4.3×10^{-11} , and 6.8×10^{-13} erg/cm³ for the quiet interplanetary medium, the maximum shock noise, and the magnetosheath, respectively.

3.2 Low-Energy Plasma Experiments

3.2.1. Mapping of the Plasmopause (B-15)

The mapping of the plasmopause, which was started with OGO 1 experiment A-15 (see section 1.2.1 of the Overview), was continued with the similar B-15 experiment on OGO 3. Using data obtained during stabilized operation, Taylor et al (1968a) investigated the position of the plasmopause as a function of the magnetic index K_p and found that the position of the plasmopause moved inward and outward from the earth in an inverse correlation with K_p , indicating significant expansion and contractions of the plasmopause. As the OGO 3 apogee moved gradually into the duskside and nightside magnetosphere during the initial stabilized period, a detailed in situ study of the duskside plasmopause was made possible for the first time (Taylor et al, 1970a). This study showed that the duskside bulge (Carpenter, 1966) was indeed a persistent feature of the plasmopause and that it was frequently characterized by sharply structured concentrations of hydrogen ions. This structured appearance lent further support to the plasma

* The high data rate could not be used on OGO 1 when the spacecraft was more than 10 RE away, because of the fast OGO 1 spin rate (5 rpm). The OGO 3 was not subject to this restriction because the spin rate was much slower (0.5 rpm).

convection models of Nishida (1966) and Brice (1967), which predicted a region of plasma turbulence in the afternoon sector. The turbulent region corresponded to the interface between the maximum opposing flow regimes of plasma, which either corotated with the Earth or flowed outside the plasmopause in a non-corotating manner. It was also found (Kikuchi and Taylor, 1972) that the irregular structure in the bulge region (and at other locations in the nighttime plasmopause) correlated quite well with ground-based Pc 1 observations.* This correlation suggested that Pc 1 events were associated primarily with the plasmopause.

3.2.2 Effects of Satellite Potential (B-13)

Whipple et al (1974) showed theoretically that typical satellite potentials could have large effects upon the ion currents measured by an experiment such as an ion-mass spectrometer or an ion trap. The above theoretical considerations yielded calculated current-voltage curves in excellent agreement with the ion current-voltage data obtained near the plasmopause with experiment B-13 (Planar Ion and Electron Trap, Whipple). The ion densities which Whipple et al (1974) inferred from their analysis were shown to be as much as one order of magnitude different from what would have been inferred from previous analyses.

3.2.3 Study of the 0 to 1000 eV Plasma (B-12)

The low-energy magnetospheric plasma was also investigated by Sagalyn and Smiddy (1967), using the data from two omnidirectional spherical plasma probes (Experiment B-12, Sagalyn). The flux, energy distribution and concentration of ions and electrons were measured in the energy range 0-1 keV over the altitude region 1.1 - 20 RE. One interesting result of this investigation was the very rapid variation in the ion-electron densities which was observed, at geocentric distances ranging from 2 to 4 RE, as the spacecraft went into and out of the shadow of the earth. The average energy of these low-energy particles was found to increase from about 0.2 eV at 1.1 RE to 6 ± 2 eV at 5 - 7 RE. The flux of particles in the 25 - 1000 eV range was measured in the outer magnetosphere and found to decrease by a factor of 4 following solar flares.

3.2.4 Study of the 40 to 2000 eV Plasma (B-3)

Experiment B-3 (Bridge) on OGO 3 provided the first detailed mapping of the low-energy (40- to 2000-eV) electron distribution in the dayside magnetosphere. This study was a continuation of the plasma sheet mapping initiated with the corresponding A-3 experiment on OGO 1 (see section 1.2.2). It was found (Vasyliunas, 1968b) that low energy electrons, in the 40 to 2000 eV range, were present throughout most of the dayside magnetosphere. In contrast to the distribution of more energetic electrons ($E > 40$ keV), which is roughly symmetrical with respect to the noon-midnight meridian, the low-energy electron flux was observed to be much more intense in the dawn sector than in the dusk sector.

3.2.5 Study of the 100 to 50,000 eV Plasma (B-8)

A remarkable wealth and diversity of information was obtained with experiment B-8 (Frank), the only OGO 3 experiment which had not been previously carried on OGO 1. Better known as the LEPEDEA experiment (Low-Energy Proton and Electron Differential Energy Analyzer), experiment B-8 was designed specifically for studying the magnetospheric plasma within the energy range 100 eV to 50,000 eV. The energy range was subdivided into 13 energy intervals, and the sensitivity was about 100 times greater than the sensitivity of instruments previously used for this purpose. Excellent data were acquired during the initial 46 days of attitude-controlled operation, and these were used to provide a comprehensive survey of the low-energy proton and electron intensities in the evening-to-midnight quadrant of the magnetosphere for L values ranging from 3 to 15.

The proton data (Frank and Owens, 1970) revealed the persistent presence of a partial ring current of protons, centered at

* Pc 1 events are geomagnetic micropulsations with periods ranging from 0.2 to 5 seconds.

ELF noise (0.1 to 1.0 kHz) in the magnetosphere. This study revealed two distinct populations of noise within the magnetosphere: steady noise (ELF hiss) occurring primarily in the plasmasphere and in the dayside outer magnetosphere at magnetic latitudes near 45 deg; and noise bursts (chorus and whistlers) at low latitude in the dayside outer magnetosphere (Russell et al, 1969, Russell and Holzer, 1970).

Although the ELF hiss band is variable, it extends typically from 500 to 700 hertz. An ELF emission having a frequency typically 1/10 that of the ELF hiss was discovered by Russell et al (1970) during their very comprehensive survey of ELF hiss. This lower frequency has been named the sub LHR hiss because its frequency spectrum is always below the Lower Hybrid Resonance frequency. The sub LHR hiss is extremely localized in space. It has been observed only within about 2 deg of the magnetic equator and only in the outer two earth radii of the plasmasphere. No explanation has yet been proposed for this emission.

3.1.4 Bow Shock Structure (B-10)

A very comprehensive study of the bow shock structure was conducted with the search coil magnetometer data (Experiment B-10, Smith) using OGO 3 data obtained during the first six months after launch. During this period OGO 3 crossed the Earth's bow shock over 500 times, and from these events a set of 494 crossings was selected for analysis (Olson and Holzer, 1974). Most of these data were obtained at the 1 kbs telemetry sampling rate, which placed an upper limit of 2.17 Hz for the frequency of the observed waveforms. This study showed that the dominant pattern, comprising about 85 percent of the shock crossings, consisted of waves having frequencies ranging from one to a few hertz upstream of the main shock compression and lower frequency waves, typically 0.3 Hz, downstream. The remaining 15 percent of the crossings exhibited a much more complex pattern, at times apparently chaotic.

On approximately thirty occasions the crossings were monitored at the high data rate (64 kbs). Of these, eleven crossings were suitable for analysis. This unique data set made it possible for the first time* to observe the high frequency structure of the magnetic fluctuations at the bow shock (Olson et al, 1969). Power spectra for frequencies between 1 and 140 Hz were obtained at successive positions near the shock, showing how the special characteristics of the quiet interplanetary medium is gradually modified, first upstream in the presence of the shock precursor, then at various positions within the shock, and finally in the magnetosheath downstream from the shock. The average energy density in the region $1 < f < 140$ Hz was found to be 4.9×10^{-14} , 4.3×10^{-11} , and 6.8×10^{-13} erg/cm³ for the quiet interplanetary medium, the maximum shock noise, and the magnetosheath, respectively.

3.2 Low-Energy Plasma Experiments

3.2.1. Mapping of the Plasmapause (B-15)

The mapping of the plasmapause, which was started with OGO 1 experiment A-15 (see section 1.2.1 of the Overview), was continued with the similar B-15 experiment on OGO 3. Using data obtained during stabilized operation, Taylor et al, (1968a) investigated the position of the plasmapause as a function of the magnetic index Kp and found that the position of the plasmapause moved inward and outward from the earth in an inverse correlation with Kp, indicating significant expansion and contractions of the plasmapause. As the OGO 3 apogee moved gradually into the duskside and nightside magnetosphere during the initial stabilized period, a detailed in situ study of the duskside plasmapause was made possible for the first time (Taylor et al, 1970a). This study showed that the duskside bulge (Carpenter, 1966) was indeed a persistent feature of the plasmapause and that it was frequently characterized by sharply structured concentrations of hydrogen ions. This structured appearance lent further support to the plasma

* The high data rate could not be used on OGO 1 when the spacecraft was more than 10 RE away, because of the fast OGO 1 spin rate (5 rpm). The OGO 3 was not subject to this restriction because the spin rate was much slower (0.5 rpm).

convection models of Nishida (1966) and Brice (1967), which predicted a region of plasma turbulence in the afternoon sector. The turbulent region corresponded to the interface between the maximum opposing flow regimes of plasma, which either corotated with the Earth or flowed outside the plasmapause in a non-corotating manner. It was also found (Kikutchi and Taylor, 1972) that the irregular structure in the bulge region (and at other locations in the nighttime plasmapause) correlated quite well with ground-based Pc 1 observations.* This correlation suggested that Pc 1 events were associated primarily with the plasmapause.

3.2.2 Effects of Satellite Potential (B-13)

Whipple et al, (1974) showed theoretically that typical satellite potentials could have large effects upon the ion currents measured by an experiment such as an ion-mass spectrometer or an ion trap. The above theoretical considerations yielded calculated current-voltage curves in excellent agreement with the ion current-voltage data obtained near the plasmapause with experiment B-13 (Planar Ion and Electron Trap, Whipple). The ion densities which Whipple et al, (1974) inferred from their analysis were shown to be as much as one order of magnitude different from what would have been inferred from previous analyses.

3.2.3 Study of the 0 to 1000 eV Plasma (B-12)

The low-energy magnetospheric plasma was also investigated by Sagalyn and Smiddy (1967), using the data from two omnidirectional spherical plasma probes (Experiment B-12, Sagalyn). The flux, energy distribution and concentration of ions and electrons were measured in the energy range 0-1 keV over the altitude region 1.1 - 20 RE. One interesting result of this investigation was the very rapid variation in the ion-electron densities which was observed, at geocentric distances ranging from 2 to 4 RE, as the spacecraft went into and out of the shadow of the earth. The average energy of these low-energy particles was found to increase from about 0.2 eV at 1.1 RE to 6 ± 2 eV at 5 - 7 RE. The flux of particles in the 25 - 1000 eV range was measured in the outer magnetosphere and found to decrease by a factor of 4 following solar flares.

3.2.4 Study of the 40 to 2000 eV Plasma (B-3)

Experiment B-3 (Bridge) on OGO 3 provided the first detailed mapping of the low-energy (40- to 2000-eV) electron distribution in the dayside magnetosphere. This study was a continuation of the plasma sheet mapping initiated with the corresponding A-3 experiment on OGO 1 (see section 1.2.2). It was found (Vasyliunas, 1968b) that low energy electrons, in the 40 to 2000 eV range, were present throughout most of the dayside magnetosphere. In contrast to the distribution of more energetic electrons ($E > 40$ keV), which is roughly symmetrical with respect to the noon-midnight meridian, the low-energy electron flux was observed to be much more intense in the dawn sector than in the dusk sector.

3.2.5 Study of the 100 to 50,000 eV Plasma (B-8)

A remarkable wealth and diversity of information was obtained with experiment B-8 (Frank), the only OGO 3 experiment which had not been previously carried on OGO 1. Better known as the LEPEDEA experiment (Low-Energy Proton and Electron Differential Energy Analyzer), experiment B-8 was designed specifically for studying the magnetospheric plasma within the energy range 100 eV to 50,000 eV. The energy range was subdivided into 13 energy intervals, and the sensitivity was about 100 times greater than the sensitivity of instruments previously used for this purpose. Excellent data were acquired during the initial 46 days of attitude-controlled operation, and these were used to provide a comprehensive survey of the low-energy proton and electron intensities in the evening-to-midnight quadrant of the magnetosphere for L values ranging from 3 to 15.

The proton data (Frank and Owens, 1970) revealed the persistent presence of a partial ring current of protons, centered at

* Pc 1 events are geomagnetic micropulsations with periods ranging from 0.2 to 5 seconds.

ELF noise (0.1 to 1.0 kHz) in the magnetosphere. This study revealed two distinct populations of noise within the magnetosphere: steady noise (ELF hiss) occurring primarily in the plasmasphere and in the dayside outer magnetosphere at magnetic latitudes near 45 deg; and noise bursts (chorus and whistlers) at low latitude in the dayside outer magnetosphere (Russell et al, 1969, Russell and Holzer, 1970).

Although the ELF hiss band is variable, it extends typically from 500 to 700 hertz. An ELF emission having a frequency typically 1/10 that of the ELF hiss was discovered by Russell et al (1970) during their very comprehensive survey of ELF hiss. This lower frequency has been named the sub LHR hiss because its frequency spectrum is always below the Lower Hybrid Resonance frequency. The sub LHR hiss is extremely localized in space. It has been observed only within about 2 deg of the magnetic equator and only in the outer two earth radii of the plasmasphere. No explanation has yet been proposed for this emission.

3.1.4 Bow Shock Structure (B-10)

A very comprehensive study of the bow shock structure was conducted with the search coil magnetometer data (Experiment B-10, Smith) using OGO 3 data obtained during the first six months after launch. During this period OGO 3 crossed the Earth's bow shock over 500 times, and from these events a set of 494 crossings was selected for analysis (Olson and Holzer, 1974). Most of these data were obtained at the 1 kbs telemetry sampling rate, which placed an upper limit of 2.17 Hz for the frequency of the observed waveforms. This study showed that the dominant pattern, comprising about 85 percent of the shock crossings, consisted of waves having frequencies ranging from one to a few hertz upstream of the main shock compression and lower frequency waves, typically 0.3 Hz, downstream. The remaining 15 percent of the crossings exhibited a much more complex pattern, at times apparently chaotic.

On approximately thirty occasions the crossings were monitored at the high data rate (64 kbs). Of these, eleven crossings were suitable for analysis. This unique data set made it possible for the first time* to observe the high frequency structure of the magnetic fluctuations at the bow shock (Olson et al, 1969). Power spectra for frequencies between 1 and 140 Hz were obtained at successive positions near the shock, showing how the special characteristics of the quiet interplanetary medium is gradually modified, first upstream in the presence of the shock precursor, then at various positions within the shock, and finally in the magnetosheath downstream from the shock. The average energy density in the region $1 < f < 140$ Hz was found to be 4.9×10^{-14} , 4.3×10^{-11} , and 6.8×10^{-13} erg/cm³ for the quiet interplanetary medium, the maximum shock noise, and the magnetosheath, respectively.

3.2 Low-Energy Plasma Experiments

3.2.1. Mapping of the Plasmopause (B-15)

The mapping of the plasmopause, which was started with OGO 1 experiment A-15 (see section 1.2.1 of the Overview), was continued with the similar B-15 experiment on OGO 3. Using data obtained during stabilized operation, Taylor et al, (1968a) investigated the position of the plasmopause as a function of the magnetic index Kp and found that the position of the plasmopause moved inward and outward from the earth in an inverse correlation with Kp, indicating significant expansion and contractions of the plasmopause. As the OGO 3 apogee moved gradually into the duskside and nightside magnetosphere during the initial stabilized period, a detailed in situ study of the duskside plasmopause was made possible for the first time (Taylor et al, 1970a). This study showed that the duskside bulge (Carpenter, 1966) was indeed a persistent feature of the plasmopause and that it was frequently characterized by sharply structured concentrations of hydrogen ions. This structured appearance lent further support to the plasma

* The high data rate could not be used on OGO 1 when the spacecraft was more than 10 RE away, because of the fast OGO 1 spin rate (5 rpm). The OGO 3 was not subject to this restriction because the spin rate was much slower (0.5 rpm).

convection models of Nishida (1966) and Brice (1967), which predicted a region of plasma turbulence in the afternoon sector. The turbulent region corresponded to the interface between the maximum opposing flow regimes of plasma, which either corotated with the Earth or flowed outside the plasmopause in a non-corotating manner. It was also found (Kikuchi and Taylor, 1972) that the irregular structure in the bulge region (and at other locations in the nighttime plasmopause) correlated quite well with ground-based Pc 1 observations.* This correlation suggested that Pc 1 events were associated primarily with the plasmopause.

3.2.2 Effects of Satellite Potential (B-13)

Whipple et al (1974) showed theoretically that typical satellite potentials could have large effects upon the ion currents measured by an experiment such as an ion-mass spectrometer or an ion trap. The above theoretical considerations yielded calculated current-voltage curves in excellent agreement with the ion current-voltage data obtained near the plasmopause with experiment B-13 (Planar Ion and Electron Trap, Whipple). The ion densities which Whipple et al (1974) inferred from their analysis were shown to be as much as one order of magnitude different from what would have been inferred from previous analyses.

3.2.3 Study of the 0 to 1000 eV Plasma (B-12)

The low-energy magnetospheric plasma was also investigated by Sagalyn and Smiddy (1967), using the data from two omnidirectional spherical plasma probes (Experiment B-12, Sagalyn). The flux, energy distribution and concentration of ions and electrons were measured in the energy range 0-1 keV over the altitude region 1.1 - 20 RE. One interesting result of this investigation was the very rapid variation in the ion-electron densities which was observed, at geocentric distances ranging from 2 to 4 RE, as the spacecraft went into and out of the shadow of the earth. The average energy of these low-energy particles was found to increase from about 0.2 eV at 1.1 RE to 6 ± 2 eV at 5 - 7 RE. The flux of particles in the 25 - 1000 eV range was measured in the outer magnetosphere and found to decrease by a factor of 4 following solar flares.

3.2.4 Study of the 40 to 2000 eV Plasma (B-3)

Experiment B-3 (Bridge) on OGO 3 provided the first detailed mapping of the low-energy (40- to 2000-eV) electron distribution in the dayside magnetosphere. This study was a continuation of the plasma sheet mapping initiated with the corresponding A-3 experiment on OGO 1 (see section 1.2.2). It was found (Vasyliunas, 1968b) that low energy electrons, in the 40 to 2000 eV range, were present throughout most of the dayside magnetosphere. In contrast to the distribution of more energetic electrons ($E > 40$ keV), which is roughly symmetrical with respect to the noon-midnight meridian, the low-energy electron flux was observed to be much more intense in the dawn sector than in the dusk sector.

3.2.5 Study of the 100 to 50,000 eV Plasma (B-8)

A remarkable wealth and diversity of information was obtained with experiment B-8 (Frank), the only OGO 3 experiment which had not been previously carried on OGO 1. Better known as the LEPDEA experiment (Low-Energy Proton and Electron Differential Energy Analyzer), experiment B-8 was designed specifically for studying the magnetospheric plasma within the energy range 100 eV to 50,000 eV. The energy range was subdivided into 13 energy intervals, and the sensitivity was about 100 times greater than the sensitivity of instruments previously used for this purpose. Excellent data were acquired during the initial 46 days of attitude-controlled operation, and these were used to provide a comprehensive survey of the low-energy proton and electron intensities in the evening-to-midnight quadrant of the magnetosphere for L values ranging from 3 to 15.

The proton data (Frank and Owens, 1970) revealed the persistent presence of a partial ring current of protons, centered at

* Pc 1 events are geomagnetic micropulsations with periods ranging from 0.2 to 5 seconds.

OVERVIEW

$L = 6.5$ during all magnetic conditions. Increased proton intensities and penetration to L values (of 3 or less) deep within the outer radiation zone were observed during geomagnetic storms. The above observations constituted the first in situ detection and survey of the extraterrestrial, 'storm-time,' ring current protons. Frank's conclusion that the elusive ring current had finally been detected was based upon: 1) excellent correlations between observed proton intensities and typical magnetic storm histories and 2) theoretical calculations showing that the total energy of the measured particles was adequate to account for the disturbance field (Frank 1967b).

The peak in the proton distribution at $L = 6.5$ under magnetic quiescence was identified as the 'quiet-time' ring current (Frank and Owens, 1970). It was subsequently shown by Sugiura (see section 3.1.2) that the 'quiet-time' ring current must extend over a range of geocentric distances greater than that indicated by Frank. Thus Frank's 'quiet-time' ring current must be only a part of the total equatorial current, responsible for 'quiet-time' geomagnetic perturbations at magnetospheric heights. It should be noted that Sugiura's refinement of the 'quiet-time' ring current concept has had no adverse impact upon Frank's 'storm-time' ring current concept. Frank's conclusions concerning the major 'storm-time' component continue to be widely accepted.

The electron data also displayed a rich and varied behavior (Frank, 1967a). These data were used to investigate the earthward edge of the plasma sheet and its relationship to the plasma pause (Shield and Frank, 1970). The importance of the proton and of the electron data was further enhanced by the fact that high-resolution spectra of low-energy protons and electrons had—for the first time—been obtained simultaneously. These simultaneous observations permitted detailed investigations of the relationship between the plasma sheet, the ring current, the trapping boundary, and the plasmopause (Frank 1971).

3.3 Energetic Particle Measurements

Some results from the OGO 3 energetic particle measurements have already been discussed in sections 1.3.1, 1.3.2, and 1.3.3. This was done whenever the OGO 3 experimenters had treated the data from their identical OGO 1 and OGO 3 experiments as one continuous data base. In such cases, the OGO 3 data were used mainly to extend the time or space coverage provided by OGO 1. Some of the results described under 3.3 are based upon joint OGO 1 and OGO 3 data, but in these cases a two satellite operation was an essential aspect of the experimental procedure.

3.3.1 Radiation Belts (B-9)

The major contribution of experiment B-9 to our knowledge of the radiation belts has already been discussed under sections 1.3.1 and 1.3.2. A result not previously mentioned was the insight into the nature of the outer zone variation which was gained by a close comparison of the electron fluxes measured with similar spectrometers on OGO 3 and ATS 1 (Pfitzer and Winckler, 1969). By comparing these two satellites at different places on a common drift shell, it was possible to measure the time delay of increases of electron flux, which could be identified as drifting eastward due to the gradient of the magnetospheric field and originating near local midnight during a magnetospheric substorm. The importance of the magnetospheric distortion which accelerated electrons as a source for the outer radiation belt was established.

3.3.2 Solar X Rays and Total Radiation in Space (B-4, B-9)

The knowledge of solar X rays was advanced significantly by experiment B-4 (Cline), which was the first to provide differential energy spectra in the range 80 keV to 1 MeV. (Experiment B-4 provided measurements at 16 energy levels equally spread between 80 keV and 1 MeV.) Investigations conducted with experiment B-4 during the solar flare of July 7, 1966, revealed a greater intensity in hard X rays than ever observed in a solar event previously, and indicated a non-thermal bremsstrahlung origin for the X rays (Cline et al, 1968). The investigation of solar X rays conducted with experiment B-9 (Winckler) was discussed under section 1.3.2.

A study, which required simultaneous observations by the identical OGO 1 and OGO 3 ionization chambers (experiments A-9 and B-9), was conducted to determine whether or not solar protons with energies greater than 12 MeV have free access to the outer magnetosphere. The 'screening' effect of the magnetosphere was determined by comparing simultaneous measurements of the particle intensity inside the magnetosphere and near the outer magnetospheric boundaries. (Kane et al, 1968). It was found that magnetospheric screening was indeed observable and could at times be complete for a duration of as much as 110 minutes in the tail of the magnetosphere.

3.3.3 Cosmic-Ray Spectra and Fluxes (B-7)

It is well known that the sun can produce large fluxes of cosmic-ray particles with energies less than 20 MeV per nucleon. These fluxes, which are easily observed during solar flares, are much more difficult to measure during 'quiet' periods. The study of 'quiet-time' protons and alpha particles, in the energy range 2 to 20 MeV/nucleon, was begun in 1964 at the University of Chicago using a cosmic-ray telescope on OGO 1 (see section 1.3.3). This study was continued during 1967 with an identical experiment (B-7) on OGO 3 (Fan et al, 1969). No significant changes were observed in spite of increased solar activity. These later results were not consistent with the assumed presence of a 'quiet-time' solar component, which would presumably be a function of the solar activity.

3.3.4 Solar Flare Protons (B-1 and B-5)

The proton event of July 7, 1966, was studied simultaneously by detectors on OGO 3 (Experiment B-1, Anderson), Imp 3, and Explorer 33. The measurements (Lin et al, 1968) revealed a narrow 'core,' about 3 degrees wide for electrons >40 keV, surrounded by a symmetric 'halo' of less intense >40 keV electrons and 0.5- to 20-MeV proton fluxes. The core was connected magnetically back to the flare region.

The same proton event was investigated by Konradi (1969) in the energy range 135 to 1650 keV using the data from experiment B-5. The results were similar to those of experiment B-1 (above), i.e. the observations in the lower energy range also revealed a halo, trapped on field lines which connected back to the flare region. Two additional features of the protons were observed in Konradi's study; namely, the isotropy of the incident flux in the magnetosheath and the tail, and a relative depression of proton intensity in the magnetosheath.

3.3.5 Search for Positrons (B-4)

Experiment B-4 (mentioned earlier under section 3.3.2) was used also to search for interplanetary positrons. The observed positron intensity in the range $E > 0.5$ MeV was 2 decades higher than the maximum value expected from cosmic ray meson production (Cline and Hones, 1970). This indicated either that the low-energy end of the galactic cosmic-ray spectrum was more intense than commonly believed, or that the positron origin was different than assumed.

3.4 Radio Physics Experiments

3.4.1 VLF Investigations (B-17)

Although the MR whistlers, the Nu whistlers, the banded chorus and the whistler ducts were first observed and clearly identified with the OGO 1 experiment A-17, the detailed investigations of these VLF phenomena by Helliwell and his associates were based upon both OGO 1 and OGO 3 data. Experiment B-17 (Helliwell) on OGO 3 was essentially the same as A-17 except for one important difference. The antenna on B-17 could be connected either as an electric sensor or as a magnetic sensor. The electric antenna was a new feature, which made it possible to observe on OGO 3 lower hybrid resonance noise bands. It was shown by Burtis (1973) that the LHR data could be used

to calculate electron densities near the plasmopause and that the calculated values agreed with the ion-mass spectrometer results (Experiment B-15) within a factor of 2.

As mentioned under Section 1.4.1, the first in situ evidence for the existence of VLF ducts was provided by the data from A-17 on OGO 1. The OGO 3 data have provided similar, but much more elaborate, examples of in situ observations, thus making possible the most complete study of duct properties conducted up to that time (Angerami, 1970). Some of the major conclusions reached from this study are as follows: it was confirmed that whistler ducts are enhancements of ionization, the relative enhancements ranging from 6 to 20 percent over the background; it was concluded that the duct thicknesses in L space were about $0.05 R_E$, and their width in longitude 4 to 8 times as much at the equator. The rising tones associated with these whistlers were interpreted as leakages from ducts that are beyond the satellite in L space.

Abrupt changes of whistler occurrence and noise characteristics were observed during plasmopause crossings on both OGO 1 and OGO 3. The plasmopause positions detected on one OGO 1 crossing and on one OGO 3 crossing were compared with the corresponding data from Taylor's ion mass spectrometers on OGO 1 and OGO 3, respectively; both comparisons yielded plasmopause positions which agreed within $0.1 R_E$ in L value (Carpenter et al, 1969).

3.4.2 Radio Astronomy (B-18)

The objective of experiment B-18 was to measure the dynamic radio spectrum of solar radio-noise bursts in the 2- to 4-MHz range. The planned observations included frequency drift rates, frequency bandwidth, and duration of bursts. The investigation program conducted with experiment B-18 followed very closely the stated objectives, and it led to the first large sample of high time-resolution information on low-frequency solar bursts (Haddock and Graedel, 1970). During the period June 7, 1966 to September 30, 1967, 218 type III* bursts were detected in the 2 to 4 MHz band. The type V continuum radiation following type III was seen in only 4 cases, and other types of bursts (I, II, and IV) were not seen at all. Approximately 70 percent of the observed type III solar bursts were found to be associated with flares (Graedel, 1970).

It is of interest to note that type III solar noise bursts were also observed below 100 kHz on OGO 3 (Dunckel et al, 1972). These bursts tend to follow type III bursts observed at 2-4 MHz by about 10 minutes. Observed drift rates and decay times correspond roughly to those extrapolated from higher frequency measurements.

3.5 Optical Experiments

3.5.1 Geocoronal Lyman Alpha (B-19)

Experiment B-19 (Mange) yielded the first profiles of the hydrogen Lyman-alpha intensity as a function of geocentric distance (Mange and Meier, 1970). The data were acquired during the first six weeks of OGO 3 operation, while attitude control was maintained. A total of eleven profiles was obtained for altitudes ranging from 5 to 19 earth radii. The variation of intensity with distance implied a hydrogen density at 50,000 km of about 20 atoms/cc for the summer 1966 epoch in the antisolar hemisphere. An extraterrestrial background of about 750 rayleighs was observed at apogee. The data suggested that regions near the galactic plane were brighter by about 150 rayleighs. The background intensity seemed to correlate with solar activity, suggesting that a portion of the background was solar-related.

* The classification of solar bursts is based upon their frequency-vs-time characteristics. The type III burst is characterized by a short duration (about 10 seconds) and by a rapid drift from high to low frequencies.

3.5.2 Sky Brightness at Visible Wavelengths (B-20)

Some useful data concerning the optical environment were obtained by the Gegenschein experiment (B-20, Wolff) during the initial stabilized OGO 3 operation (Wolff, 1967). An upper limit to the brightness of the daytime sky near a large unmanned satellite was obtained and found to be about 30 times less than the darkest daytime sky brightness previously reported by astronauts. The Gegenschein experiment, however, was unable to monitor the brightness of the antisolar region of the sky (its primary objective), because of light scattered by a very long radio antenna. The maximum value of the sky brightness was actually inferred from an investigation of this scattering effect, as the angle between the antenna and the optical axis varied during the OGO 3 orbit.

3.6 Interplanetary Dust Particles (B-16)

The data from experiment B-16 (Bohn) on OGO 3 represented the first measurements of dust particles in cislunar space since Pioneer 1 (1958). Data were obtained for 1505 hours and at altitudes primarily between 50,000 and 110,000 km. The flux derived from these observations was: $\Phi = 2 \times 10^{-3}$ events $m^{-2}s^{-1}(2\pi \text{ ster})^{-1}$ for particles greater than 2.0×10^{-13} gram (Alexander et al, 1973).

More recent measurements, however, have raised doubts concerning the validity of the data from experiment B-16. Berg and Grün (1973) have shown that microphone data (such as those of experiment B-16) can be severely contaminated by cosmic rays.

3.7 The Storm of January 13 - 14, 1967 (B-10)

Major distortions of the Earth's magnetosphere were observed during the geomagnetic storm of January 13-14, 1967. Although the OGO 3 study of this storm could have been discussed under section 3.1, various aspects of this study justify a departure from a strictly discipline-oriented presentation. The event was apparently the strongest storm ever encountered in space up to that time, and it led to the greatest compression of the magnetosphere ever recorded on the sunward side. The locations and instrumentation on five spacecraft (Imp-D, Vela 3A, Vela 3B, ATS 1, and OGO 3) during the storm permitted an unusually complete and large-scale measurement of this event.

The shock front from the sun was first detected (1150 UT January 13) by IMP-D at a range of $66 R_E$ and at an angle of 23 deg (forward) with the Sun-Earth line. The IMP-D observations yielded the average velocity of the shock front and its deceleration by the preceding slower moving solar plasma (Cummings and Coleman 1968). At 1204 UT the shock front encountered Vela 3A at $19 R_E$ and at 55 deg from the Sun-Earth line (Bame et al, 1968). Shortly afterwards the shock was seen at Vela 3B on the opposite side of the earth ($20 R_E$ and -54 deg). Twelve hours later, the ATS 1 satellite at $6.6 R_E$ had moved to the sunward side of the Earth, and it crossed the magnetopause at 0007 on January 14, showing that the magnetopause had penetrated substantially below $6.6 R_E$ (Opp, 1968 and references quoted therein).

At 0055 on January 14, OGO 3 encountered the bow shock abnormally close to the earth, which confirmed the ATS 1 observations. At 1900 January 14, OGO 3 crossed the bow shock at a point as far out as it had ever been measured, showing that the magnetosphere had reacted to the storm-induced compression by rebounding to abnormally large dimensions. (Russell et al, 1968). The post storm inflation was confirmed by VELA 3A and 3B, when they crossed the magnetopause on January 14 at 1100 UT and 1900 UT, respectively (Bame et al, 1968).

Other examples of space research based upon data from OGO 3 and from one or more additional spacecraft have been given earlier under the appropriate disciplines. The study of the January 13-14, 1967 storm has been singled out, however, as representing perhaps the best example of OGO 3 participation in a multi-satellite study requiring observations from many points in space and time.

4. OGO 4 Results

By maintaining 3-axis stabilization for nearly 18 months, the OGO 4 spacecraft far exceeded the performance of its

OVERVIEW

predecessors (the longest previous stabilized operation was 45 days with OGO 3), and many POGO experimenters were able for the first time to make measurements on an extended time scale. Except for an oscillation problem caused by the 18.3 m (60 ft) radio-astronomy antenna (Experiment D-01), which required extensive manual controls from the ground during the entire stabilized period, the OGO 4 spacecraft would have been the first "nearly perfect" spacecraft of the OGO program. The oscillation problem was solved on the next OGO simply by reducing the antenna length to 9.1 m (30 ft), and the completely normal spacecraft envisioned by the designers at the beginning of the program was finally achieved with OGO 5.

About 15 of the 20 OGO 4 experiments can be considered completely successful since each of these 15 experiments led to at least one major journal publication. For about half of the successful experiments the number of significant publications is five or greater. The five experiments which cannot be considered "completely successful" include: D-20 (Hinterreger) which failed two weeks after launch before it could yield any useful data; D-17 (Newton) which developed a large background ion current preventing the measurement of atmospheric densities at OGO altitudes; D-18 (Nilsson) which experienced a severe degradation due to a high level of noise in the data; D-01 (Haddock) which was also partially disabled by high noise levels in the data; and D-15 (Jones) which yielded data in a commutated format too complex for analysis. Most of the above unsuccessful experiments had not been previously performed in a satellite (except in the very unsatisfactory OGO 2 mission). These new and untried experiments were nevertheless included in OGO missions because a few "high risk" experiments could be included in the very large OGO payloads (see last paragraph of section 2 under III.A).

The OGO 4 results are presented by major scientific disciplines, following the order used previously for OGO 1, OGO 2, and OGO 3.

4.1 Magnetic Field Experiments

4.1.1 World Magnetic Survey (D-06)

One of the major objectives of the OGO 4 mission was to continue, extend, and refine the World Magnetic Survey which had been initiated with OGO 2. The magnetic field experiment D-06 (Cain) on OGO 4 obtained over 500 days of data, which were equivalent to about 50 pole-to-pole magnetic surveys. When the processing of the OGO 4 data for the period July 1967 to December 1967 was completed, the resulting measurements were combined with the OGO 2 data for the period October 1965 to September 1967 to produce the POGO (10/68)* geomagnetic field model (Cain and Langel, 1968). The same OGO 2 and OGO 4 data were used with data from other sources to derive the International Geomagnetic Reference Field (Cain and Cain, 1971). By adding the OGO 4 measurements for the period January 1968 to May 1968 to the POGO (10/68) data base, an improved POGO (8/69) model was derived (Cain and Sweeney, 1970). These measurements showed that accurate vector maps of the Earth's field could be derived using only total field data.** The POGO geomagnetic field models have been used extensively as supporting data for other satellite experiments.

4.1.2 Secular Field Variations (C-06)

Because of the extent and quality of the data, the magnetometer data analysis was extended well beyond the basic objectives of the World Magnetic Survey. Thus the data were used to study the secular changes in the geomagnetic field. It was found that the Earth's main dipole (as represented by the first

two spherical harmonic components of the field) continues to collapse although the total field (which includes the higher order harmonics) remains approximately constant (Cain, 1971 and Cain, 1968).

4.1.3 Crustal Anomalies (C-06, D-06, F-21)

Magnetic materials in the Earth's crust (i.e., down to a maximum depth of 20 km) produce magnetic anomalies, which can be quite strong near the Earth's surface. These effects, however, weaken rapidly with altitude, and at satellite altitudes of 250 to 500 km, the effects are comparable to the time variations of external sources. It had therefore been assumed that crustal anomalies would be undetectable from satellite altitudes. The data from Cosmos 49 (launched October 24, 1964 in a very low 250-400 km orbit) gave the first indications that these crustal anomalies might be detectable. A subsequent statistical analysis of the low-altitude, minimal-geomagnetic-activity data from OGO 2 (C-06), OGO 4 (D-06) and OGO 6 (F-21) showed conclusively that crustal anomalies could indeed be detected. (Regan et al, 1973)

4.1.4 Studies of the Equatorial Electrojet (D-06, F-21)

The term "equatorial electrojet" refers to an ionospheric current assumed responsible for the very large values of the solar quiet (Sq) daily magnetic variation (ΔF) observed near the magnetic dip equator. A very comprehensive investigation of this phenomenon was conducted using data from experiment D-06 on OGO 4 and from experiment F-21 on OGO 6, which jointly provided over 2000 mid-day traversals over the electrojet during the interval 1967 to 1970. The electrojet was typically characterized by a sharp negative V-Signature in the ΔF data, centered within 0.5 deg of the dip equator. Numerous departures from the basic V-pattern were also noted, particularly, but not always, during geomagnetic disturbances (Cain and Sweeney, 1972).

4.1.5 Detection of Field-Aligned Current (D-05, D-11)

One particularly interesting result obtained with the OGO 4 search coil magnetometer (Experiment D-05, Smith) was the detection at high latitudes of magnetic fluctuations which seemed to be produced by field-aligned currents. To test this interpretation the measured magnetic field disturbances were compared with simultaneous observations of low-energy precipitated electron fluxes measured with the OGO 4 auroral particles detector (Experiment D-11, Hoffman). Definite correlations were found by Berko et al (1975) during many nighttime satellite passes between the magnetic fluctuations and the electron fluxes (with energies greater than 1 keV) measured by experiment D-11. The absence of correlations for daytime observations suggested that the daytime magnetic fluctuations were due to current fluxes with energy less than 1 keV.

4.2 Low-Energy Plasma Experiments

4.2.1 Global Sampling of Ion Composition (D-16, F-05)

The data from experiment D-16 (Taylor) on OGO 4 and experiment F-05 (Taylor) on OGO 6 represent the most comprehensive set of ion composition data acquired prior to 1974 in the 400- to 1100-km altitude range. A statistical study of this extensive data base was undertaken to determine the average global characteristics of the principal ionic species (Taylor, 1973). The results of this continuing study will provide a major ion composition input to the current international effort for the development of an empirical ionospheric model between the altitudes of 100 and 1000 km.

4.2.2 The High-Latitude Light-Ion Trough (D-16, F-05)

It was discovered with OGO 2 (see section 2.2.2) that light ions such as H⁺ and He⁺ exhibit a sharp drop in density at 60 deg invariant latitude, i.e. at the high-latitude boundary of the plasmasphere. This drop or "trough" was much less pronounced

* The parenthetical notation (10/68) refers to the date when the model was completed.

** Typical accuracies at POGO altitudes for the X, Y and Z field components were 20, 40 and 50 gammas respectively.

OVERVIEW

predecessors (the longest previous stabilized operation was 45 days with OGO 3), and many POGO experimenters were able for the first time to make measurements on an extended time scale. Except for an oscillation problem caused by the 18.3 m (60 ft) radio-astronomy antenna (Experiment D-01), which required extensive manual controls from the ground during the entire stabilized period, the OGO 4 spacecraft would have been the first "nearly perfect" spacecraft of the OGO program. The oscillation problem was solved on the next OGO simply by reducing the antenna length to 9.1 m (30 ft), and the completely normal spacecraft envisioned by the designers at the beginning of the program was finally achieved with OGO 5.

About 15 of the 20 OGO 4 experiments can be considered completely successful since each of these 15 experiments led to at least one major journal publication. For about half of the successful experiments the number of significant publications is five or greater. The five experiments which cannot be considered "completely successful" include: D-20 (Hinterreger) which failed two weeks after launch before it could yield any useful data; D-17 (Newton) which developed a large background ion current preventing the measurement of atmospheric densities at OGO altitudes; D-18 (Nilsson) which experienced a severe degradation due to a high level of noise in the data; D-01 (Haddock) which was also partially disabled by high noise levels in the data; and D-15 (Jones) which yielded data in a commutated format too complex for analysis. Most of the above unsuccessful experiments had not been previously performed in a satellite (except in the very unsatisfactory OGO 2 mission). These new and untried experiments were nevertheless included in OGO missions because a few "high risk" experiments could be included in the very large OGO payloads (see last paragraph of section 2 under III.A).

The OGO 4 results are presented by major scientific disciplines, following the order used previously for OGO 1, OGO 2, and OGO 3.

4.1 Magnetic Field Experiments

4.1.1 World Magnetic Survey (D-06)

One of the major objectives of the OGO 4 mission was to continue, extend, and refine the World Magnetic Survey which had been initiated with OGO 2. The magnetic field experiment D-06 (Cain) on OGO 4 obtained over 500 days of data, which were equivalent to about 50 pole-to-pole magnetic surveys. When the processing of the OGO 4 data for the period July 1967 to December 1967 was completed, the resulting measurements were combined with the OGO 2 data for the period October 1965 to September 1967 to produce the POGO (10/68)* geomagnetic field model (Cain and Langel, 1968). The same OGO 2 and OGO 4 data were used with data from other sources to derive the International Geomagnetic Reference Field (Cain and Cain, 1971). By adding the OGO 4 measurements for the period January 1968 to May 1968 to the POGO (10/68) data base, an improved POGO (8/69) model was derived (Cain and Sweeney, 1970). These measurements showed that accurate vector maps of the Earth's field could be derived using only total field data.** The POGO geomagnetic field models have been used extensively as supporting data for other satellite experiments.

4.1.2 Secular Field Variations (C-06)

Because of the extent and quality of the data, the magnetometer data analysis was extended well beyond the basic objectives of the World Magnetic Survey. Thus the data were used to study the secular changes in the geomagnetic field. It was found that the Earth's main dipole (as represented by the first

two spherical harmonic components of the field) continues to collapse although the total field (which includes the higher order harmonics) remains approximately constant (Cain, 1971 and Cain, 1968).

4.1.3 Crustal Anomalies (C-06, D-06, F-21)

Magnetic materials in the Earth's crust (i.e., down to a maximum depth of 20 km) produce magnetic anomalies, which can be quite strong near the Earth's surface. These effects, however, weaken rapidly with altitude, and at satellite altitudes of 250 to 500 km, the effects are comparable to the time variations of external sources. It had therefore been assumed that crustal anomalies would be undetectable from satellite altitudes. The data from Cosmos 49 (launched October 24, 1964 in a very low 250-400 km orbit) gave the first indications that these crustal anomalies might be detectable. A subsequent statistical analysis of the low-altitude, minimal-geomagnetic-activity data from OGO 2 (C-06), OGO 4 (D-06) and OGO 6 (F-21) showed conclusively that crustal anomalies could indeed be detected. (Regan et al, 1973)

4.1.4 Studies of the Equatorial Electrojet (D-06, F-21)

The term "equatorial electrojet" refers to an ionospheric current assumed responsible for the very large values of the solar quiet (Sq) daily magnetic variation (ΔF) observed near the magnetic dip equator. A very comprehensive investigation of this phenomenon was conducted using data from experiment D-06 on OGO 4 and from experiment F-21 on OGO 6, which jointly provided over 2000 mid-day traversals over the electrojet during the interval 1967 to 1970. The electrojet was typically characterized by a sharp negative V-Signature in the ΔF data, centered within 0.5 deg of the dip equator. Numerous departures from the basic V-pattern were also noted, particularly, but not always, during geomagnetic disturbances (Cain and Sweeney, 1972).

4.1.5 Detection of Field-Aligned Current (D-05, D-11)

One particularly interesting result obtained with the OGO 4 search coil magnetometer (Experiment D-05, Smith) was the detection at high latitudes of magnetic fluctuations which seemed to be produced by field-aligned currents. To test this interpretation the measured magnetic field disturbances were compared with simultaneous observations of low-energy precipitated electron fluxes measured with the OGO 4 auroral particles detector (Experiment D-11, Hoffman). Definite correlations were found by Berko et al (1975) during many nighttime satellite passes between the magnetic fluctuations and the electron fluxes (with energies greater than 1 keV) measured by experiment D-11. The absence of correlations for daytime observations suggested that the daytime magnetic fluctuations were due to current fluxes with energy less than 1 keV.

4.2 Low-Energy Plasma Experiments

4.2.1 Global Sampling of Ion Composition (D-16, F-05)

The data from experiment D-16 (Taylor) on OGO 4 and experiment F-05 (Taylor) on OGO 6 represent the most comprehensive set of ion composition data acquired prior to 1974 in the 400- to 1100-km altitude range. A statistical study of this extensive data base was undertaken to determine the average global characteristics of the principal ionic species (Taylor, 1973). The results of this continuing study will provide a major ion composition input to the current international effort for the development of an empirical ionospheric model between the altitudes of 100 and 1000 km.

4.2.2 The High-Latitude Light-Ion Trough (D-16, F-05)

It was discovered with OGO 2 (see section 2.2.2) that light ions such as H⁺ and He⁺ exhibit a sharp drop in density at 60 deg invariant latitude, i.e., at the high-latitude boundary of the plasmasphere. This drop or "trough" was much less pronounced

* The parenthetical notation (10/68) refers to the date when the model was completed.

** Typical accuracies at POGO altitudes for the X, Y and Z field components were 20, 40 and 50 gammas respectively.

December 17, 1975

2
1
1.2.

for the heavy ions (O^+ , N^+). Although the OGO 2 discovery was based upon only 10 days of dawn-dusk observations, it was a first step in clearing a puzzling observation resulting from the Alouette 1 electron density data. The Alouette 1 data exhibited a well-defined trough in electron density at 60 deg invariant on the nightside of the earth, but this trough was not seen on the dayside (Muldrew, 1965).

A much more comprehensive study of high-latitude trough occurrence for light and heavy ions was conducted by Taylor and Walsh (1972) using data from OGO 4 (Experiment D-16) and from OGO 6 (Experiment F-05). It was found that the trough was present at all local times for light ions, but only at night for the heavy ions. Thus in the daytime when O^+ is typically the dominant ion, the total ion density (and hence the electron density) does not exhibit a trough. The OGO results therefore showed that the plasmapause is primarily a light-ion boundary.

4.2.3 Plasmapause Structure (D-16)

Under quiet magnetic conditions, the plasmapause is typically characterized by a sharp and smooth drop in proton density. Under disturbed conditions, the plasmapause is often poorly defined due to large and irregular variations in the proton density. These structured variations were investigated by Taylor et al. (1971) using OGO 4 data (Experiment D-16) obtained at high latitude during five consecutive satellite orbits following the peak of the magnetic storm on September 21, 1967. The observations were interpreted as evidence of a plasmatail (or elongation of the plasmasphere) which tends to corotate with the Earth. The general features of the plasmapause structure were found consistent with the dynamic plasmapause model developed theoretically by Grebowsky (1971).

4.2.4 The Equatorial Helium-Ion Trough (D-19, D-16)

The data from experiment D-19 (Chandra) and from experiment D-16 (Taylor) both revealed the presence of a pronounced nighttime depletion of helium ions at the equator in the altitude range of 700 to 900 km (Chandra et al, 1970; Taylor et al, 1970b). It was concluded very recently by Chandra (1975) that the nighttime He^+ trough at 700 - 900 km was produced by the same basic mechanism which produces the well-known *daytime* ionospheric equatorial anomaly* at lower altitudes.

4.2.5 Measurements of Ionospheric Temperatures (D-19)

Using data from experiment D-19, Chandra et al. (1970) investigated the latitudinal variation of electron temperature for both nighttime and daytime conditions, and the latitudinal variation of ion temperature for nighttime only.** The daytime electron

* The equatorial anomaly refers to the fact that a graph of noon values of electron density at fixed height versus latitude exhibits a trough centered at the magnetic dip equator with peaks 15 to 20 deg north and south. This behavior was considered anomalous when first discovered because simple theoretical considerations had predicted a single low-latitude peak at the subsolar point with densities decreasing monotonically north and south towards the poles.

** A highly negative (-2 to -7 volts) spacecraft potential in the daytime on OGO 4 interfered with the daytime ion temperature measurements. This negative potential also interfered with the daytime ion composition measurements of experiment D-16.

temperatures were typically 2000 deg K at the equator and 3000 deg K at high latitudes. The nighttime ion temperatures were found to be about 1500 deg K and relatively independent of latitude.

It should be mentioned at this point that some disagreements have existed in the past among the results obtained by the various plasma temperature measuring techniques (Benson, 1973). Many comparisons have been made to evaluate the true extent of the disagreements and hopefully to help resolve the differences. Such a comparison was made at night between the ion temperatures measured by experiment D-19 and the ion temperatures measured simultaneously by the Jicamarca Incoherent Scatter Radar. It was found by McClure and Troy (1971) that the OGO 4 measurements yielded values greater by a factor of 1.4. Recent investigations show that these discrepancies could be explained by a two-temperature plasma (Benson and Hoegy, 1973; Benson, 1973).

4.2.6 Ionospheric Phenomena Associated with Midlatitude Red Arcs (D-19)

Data from the OGO 4 retarding potential analyzer (experiment D-19) and from a similar experiment on Explorer 31, were used by Chandra et al (1971) to investigate the relative merits of three competing theories for the production of midlatitude (subauroral) red arcs. This investigation produced the first experimental evidence for accepting the thermal conduction mechanism proposed by Cole (1965) and for rejecting the dc electric field theory and the low-energy electron precipitating flux theory.

4.2.7 Field-Aligned 2.3 keV Electron Precipitation (D-11)

The OGO 4 Auroral Particle experiment (D-11, Hoffman) was the first experiment capable of measuring unambiguously the pitch angle distribution of electrons at a given energy level in the auroral regions.* This experiment provided a remarkable set of data which led to 13 publications in refereed journals. One of the major accomplishments was the discovery of field-aligned electrons (Hoffman and Evans, 1968), which led to the conclusion that the electron acceleration mechanism was due to electric fields parallel to the magnetic field.** A synoptic study of these field-aligned electrons was conducted by Berko (1973) to determine their spatial distributions and spectral characteristics, and by Berko and Hoffman (1974) to investigate their altitude and seasonal variations.

4.2.8 Identification of Particles Associated with Auroras (D-11)

Hoffman (1970) showed that the relatively steady, diffuse, subvisual aurora known as the mantle aurora was associated with electron fluxes having their peak energy at several keV. At slightly higher latitudes, within the auroral oval, Hoffman and Berko (1971) found that the dominant flux was at 0.7 keV which was the lowest energy level monitored by experiment D-11. They showed that these very low-energy fluxes were the cause of the high-altitude red auroral forms which define the auroral oval on the dayside. A more extensive investigation of electron fluxes measured by this experiment and of their relationship to the auroral oval was conducted by Gustafsson (1973).

* In the auroral zone the magnetic field is nearly vertical, i.e. aligned with the vertical Z axis of the stabilized spacecraft. The D-11 detectors therefore measured pitch angles which were essentially the same as their respective spacecraft angles.

** The existence of these electric fields was not consistent with the conductivity concepts of the early sixties. The electric fields, however, could be explained by the newly developed theories of anomalous plasma resistivity.

for the heavy ions (O^+ , N^+). Although the OGO 2 discovery was based upon only 10 days of dawn-dusk observations, it was a first step in clearing a puzzling observation resulting from the Alouette 1 electron density data. The Alouette 1 data exhibited a well-defined trough in electron density at 60 deg invariant on the nightside of the earth, but this trough was not seen on the dayside (Muldrew, 1965).

A much more comprehensive study of high-latitude trough occurrence for light and heavy ions was conducted by Taylor and Walsh (1972) using data from OGO 4 (Experiment D-16) and from OGO 6 (Experiment F-05). It was found that the trough was present at all local times for light ions, but only at night for the heavy ions. Thus in the daytime when O^+ is typically the dominant ion, the total ion density (and hence the electron density) does not exhibit a trough. The OGO results therefore showed that the plasmapause is primarily a light-ion boundary.

4.2.3 Plasmapause Structure (D-16)

Under quiet magnetic conditions, the plasmapause is typically characterized by a sharp and smooth drop in proton density. Under disturbed conditions, the plasmapause is often poorly defined due to large and irregular variations in the proton density. These structured variations were investigated by Taylor et al. (1971) using OGO 4 data (Experiment D-16) obtained at high latitude during five consecutive satellite orbits following the peak of the magnetic storm on September 21, 1967. The observations were interpreted as evidence of a plasmatail (or elongation of the plasmasphere) which tends to corotate with the Earth. The general features of the plasmapause structure were found consistent with the dynamic plasmapause model developed theoretically by Grebowsky (1971).

4.2.4 The Equatorial Helium-Ion Trough (D-19, D-16)

The data from experiment D-19 (Chandra) and from experiment D-16 (Taylor) both revealed the presence of a pronounced nighttime depletion of helium ions at the equator in the altitude range of 700 to 900 km (Chandra et al, 1970; Taylor et al, 1970b). It was concluded very recently by Chandra (1975) that the nighttime He^+ trough at 700 - 900 km was produced by the same basic mechanism which produces the well-known daytime ionospheric equatorial anomaly* at lower altitudes.

4.2.5 Measurements of Ionospheric Temperatures (D-19)

Using data from experiment D-19, Chandra et al., (1970) investigated the latitudinal variation of electron temperature for both nighttime and daytime conditions, and the latitudinal variation of ion temperature for nighttime only.** The daytime electron

* The equatorial anomaly refers to the fact that a graph of noon values of electron density at fixed height versus latitude exhibits a trough centered at the magnetic dip equator with peaks 15 to 20 deg north and south. This behavior was considered anomalous when first discovered because simple theoretical considerations had predicted a single low-latitude peak at the subsolar point with densities decreasing monotonically north and south towards the poles.

** A highly negative (-2 to -7 volts) spacecraft potential in the daytime on OGO 4 interfered with the daytime ion temperature measurements. This negative potential also interfered with the daytime ion composition measurements of experiment D-16.

temperatures were typically 2000 deg K at the equator and 3000 deg K at high latitudes. The nighttime ion temperatures were found to be about 1500 deg K and relatively independent of latitude.

It should be mentioned at this point that some disagreements have existed in the past among the results obtained by the various plasma temperature measuring techniques (Benson, 1973). Many comparisons have been made to evaluate the true extent of the disagreements and hopefully to help resolve the differences. Such a comparison was made at night between the ion temperatures measured by experiment D-19 and the ion temperatures measured simultaneously by the Jicamarca Incoherent Scatter Radar. It was found by McClure and Troy (1971) that the OGO 4 measurements yielded values greater by a factor of 1.4. Recent investigations show that these discrepancies could be explained by a two-temperature plasma (Benson and Hoegy, 1973; Benson, 1973)

4.2.6 Ionospheric Phenomena Associated with Midlatitude Red Arcs (D-19)

Data from the OGO 4 retarding potential analyzer (experiment D-19) and from a similar experiment on Explorer 31, were used by Chandra et al (1971) to investigate the relative merits of three competing theories for the production of midlatitude (subauroral) red arcs. This investigation produced the first experimental evidence for accepting the thermal conduction mechanism proposed by Cole (1965) and for rejecting the dc electric field theory and the low-energy electron precipitating flux theory.

4.2.7 Field-Aligned 2.3 keV Electron Precipitation (D-11)

The OGO 4 Auroral Particle experiment (D-11, Hoffman) was the first experiment capable of measuring unambiguously the pitch angle distribution of electrons at a given energy level in the auroral regions.* This experiment provided a remarkable set of data which led to 13 publications in refereed journals. One of the major accomplishments was the discovery of field-aligned electrons (Hoffman and Evans, 1968), which led to the conclusion that the electron acceleration mechanism was due to electric fields parallel to the magnetic field.** A synoptic study of these field-aligned electrons was conducted by Berko (1973) to determine their spatial distributions and spectral characteristics, and by Berko and Hoffman (1974) to investigate their altitude and seasonal variations.

4.2.8 Identification of Particles Associated with Auroras (D-11)

Hoffman (1970) showed that the relatively steady, diffuse, subvisual aurora known as the mantle aurora was associated with electron fluxes having their peak energy at several keV. At slightly higher latitudes, within the auroral oval, Hoffman and Berko (1971) found that the dominant flux was at 0.7 keV which was the lowest energy level monitored by experiment D-11. They showed that these very low-energy fluxes were the cause of the high-altitude red auroral forms which define the auroral oval on the dayside. A more extensive investigation of electron fluxes measured by this experiment and of their relationship to the auroral oval was conducted by Gustafsson (1973).

* In the auroral zone the magnetic field is nearly vertical, i.e. aligned with the vertical Z axis of the stabilized spacecraft. The D-11 detectors therefore measured pitch angles which were essentially the same as their respective spacecraft angles.

** The existence of these electric fields was not consistent with the conductivity concepts of the early sixties. The electric fields, however, could be explained by the newly developed theories of anomalous plasma resistivity.

for the heavy ions (O^+ , N^+). Although the OGO 2 discovery was based upon only 10 days of dawn-dusk observations, it was a first step in clearing a puzzling observation resulting from the Alouette 1 electron density data. The Alouette 1 data exhibited a well-defined trough in electron density at 60 deg invariant on the nightside of the earth, but this trough was not seen on the dayside (Muldrew, 1965).

A much more comprehensive study of high-latitude trough occurrence for light and heavy ions was conducted by Taylor and Walsh (1972) using data from OGO 4 (Experiment D-16) and from OGO 6 (Experiment F-05). It was found that the trough was present at all local times for light ions, but only at night for the heavy ions. Thus in the daytime when O^+ is typically the dominant ion, the total ion density (and hence the electron density) does not exhibit a trough. The OGO results therefore showed that the plasmapause is primarily a light-ion boundary.

4.2.3 Plasmapause Structure (D-16)

Under quiet magnetic conditions, the plasmapause is typically characterized by a sharp and smooth drop in proton density. Under disturbed conditions, the plasmapause is often poorly defined due to large and irregular variations in the proton density. These structured variations were investigated by Taylor et al. (1971) using OGO 4 data (Experiment D-16) obtained at high latitude during five consecutive satellite orbits following the peak of the magnetic storm on September 21, 1967. The observations were interpreted as evidence of a plasmatail (or elongation of the plasmasphere) which tends to corotate with the Earth. The general features of the plasmapause structure were found consistent with the dynamic plasmapause model developed theoretically by Grebowsky (1971).

4.2.4 The Equatorial Helium-Ion Trough (D-19, D-16)

The data from experiment D-19 (Chandra) and from experiment D-16 (Taylor) both revealed the presence of a pronounced nighttime depletion of helium ions at the equator in the altitude range of 700 to 900 km (Chandra et al, 1970; Taylor et al, 1970b). It was concluded very recently by Chandra (1975) that the nighttime He^+ trough at 700 - 900 km was produced by the same basic mechanism which produces the well-known *daytime* ionospheric equatorial anomaly* at lower altitudes.

4.2.5 Measurements of Ionospheric Temperatures (D-19)

Using data from experiment D-19, Chandra et al. (1970) investigated the latitudinal variation of electron temperature for both nighttime and daytime conditions, and the latitudinal variation of ion temperature for nighttime only.** The daytime electron

* The equatorial anomaly refers to the fact that a graph of noon values of electron density at fixed height versus latitude exhibits a trough centered at the magnetic dip equator with peaks 15 to 20 deg north and south. This behavior was considered anomalous when first discovered because simple theoretical considerations had predicted a single low-latitude peak at the subsolar point with densities decreasing monotonically north and south towards the poles.

** A highly negative (-2 to -7 volts) spacecraft potential in the daytime on OGO 4 interfered with the daytime ion temperature measurements. This negative potential also interfered with the daytime ion composition measurements of experiment D-16.

temperatures were typically 2000 deg K at the equator and 3000 deg K at high latitudes. The nighttime ion temperatures were found to be about 1500 deg K and relatively independent of latitude.

It should be mentioned at this point that some disagreements have existed in the past among the results obtained by the various plasma temperature measuring techniques (Benson, 1973). Many comparisons have been made to evaluate the true extent of the disagreements and hopefully to help resolve the differences. Such a comparison was made at night between the ion temperatures measured by experiment D-19 and the ion temperatures measured simultaneously by the Jicamarca Incoherent Scatter Radar. It was found by McClure and Troy (1971) that the OGO 4 measurements yielded values greater by a factor of 1.4. Recent investigations show that these discrepancies could be explained by a two-temperature plasma (Benson and Hoegy, 1973; Benson, 1973)

4.2.6 Ionospheric Phenomena Associated with Midlatitude Red Arcs (D-19)

Data from the OGO 4 retarding potential analyzer (experiment D-19) and from a similar experiment on Explorer 31, were used by Chandra et al (1971) to investigate the relative merits of three competing theories for the production of midlatitude (subauroral) red arcs. This investigation produced the first experimental evidence for accepting the thermal conduction mechanism proposed by Cole (1965) and for rejecting the dc electric field theory and the low-energy electron precipitating flux theory.

4.2.7 Field-Aligned 2.3 keV Electron Precipitation (D-11)

The OGO 4 Auroral Particle experiment (D-11, Hoffman) was the first experiment capable of measuring unambiguously the pitch angle distribution of electrons at a given energy level in the auroral regions.* This experiment provided a remarkable set of data which led to 13 publications in refereed journals. One of the major accomplishments was the discovery of field-aligned electrons (Hoffman and Evans, 1968), which led to the conclusion that the electron acceleration mechanism was due to electric fields parallel to the magnetic field.** A synoptic study of these field-aligned electrons was conducted by Berko (1973) to determine their spatial distributions and spectral characteristics, and by Berko and Hoffman (1974) to investigate their altitude and seasonal variations.

4.2.8 Identification of Particles Associated with Auroras (D-11)

Hoffman (1970) showed that the relatively steady, diffuse, subvisual aurora known as the mantle aurora was associated with electron fluxes having their peak energy at several keV. At slightly higher latitudes, within the auroral oval, Hoffman and Berko (1971) found that the dominant flux was at 0.7 keV which was the lowest energy level monitored by experiment D-11. They showed that these very low-energy fluxes were the cause of the high-altitude red auroral forms which define the auroral oval on the dayside. A more extensive investigation of electron fluxes measured by this experiment and of their relationship to the auroral oval was conducted by Gustafsson (1973).

* In the auroral zone the magnetic field is nearly vertical, i.e., aligned with the vertical Z axis of the stabilized spacecraft. The D-11 detectors therefore measured pitch angles which were essentially the same as their respective spacecraft angles.

** The existence of these electric fields was not consistent with the conductivity concepts of the early sixties. The electric fields, however, could be explained by the newly developed theories of anomalous plasma resistivity.

OVERVIEW

4.2.9 Erosion of the Dayside Magnetosphere (D-11)

The magnetopause has been observed to move inward following a reversal of the vertical component of the interplanetary field from northward to southward. This inward motion has been explained by an erosion mechanism whereby the outer, closed, dayside magnetic lines combine with the interplanetary field and become open tail lines. The transition region between open and closed field lines moves southward as a result of this field-line transfer. The transition region is of considerable interest since it appears to provide a funnel (polar cusp*) through which low-energy electrons can travel from the magnetosheath down to the lower atmosphere. The position of the transition region can therefore be determined from a mapping of the low-energy electron flux.

Burch (1972), using the low-energy electron-flux data from experiment D-11, found that the polar cusp moved southward at a rate of 0.1 degree per minute following an abrupt north-to-south reversal of the interplanetary field. This was the first time that such a measurement was made and it provided the first quantitative results concerning the erosion rate of the dayside magnetosphere. The initial study which applied to abrupt reversals of the interplanetary field was later extended to include gradual changes in the interplanetary field (Burch, 1973).

4.2.10 Electron Precipitation Patterns and Substorm Morphology (D-11)

Closely related to the topics discussed under 4.2.7, 4.2.8, and 4.2.9 is the subject of soft electron fluxes associated with the development and recovery of auroral substorms. A major study of this subject was conducted by Hoffman and Burch (1973) who identified five phases in typical substorms and the corresponding electron-flux patterns and auroral forms. This investigation also provided some evidence suggesting the existence of neutral lines in the magnetospheric tail.

4.3 Energetic Particle Measurements

4.3.1 Radiation Belt Studies (D-10)

Using the data from the trapped particle detectors in experiment D-10 (Van Allen, Fritz and Krimigis (1969) measured the ratio of trapped alpha particles to trapped protons, at energies lower than had previously been measured and within several energy intervals. The results indicated that solar wind protons and alpha particles of the same velocity were most probably thermalized upon entering the shock transition region.

4.3.2 Solar X-rays (D-21)

The Solar X-ray Emission experiment (D-21, Kreplin) provided solar X-ray fluxes in four bands, 0.5-3 A, 1-8 A, 8-16 A, and 44 to 60 A with much greater time resolution and dynamic range than had previously been available. The data from experiment D-21 made it possible to investigate for the first time the detailed history of X-ray emissions during solar X-ray flares in several wavelength bands (Kreplin et al., 1969). It was shown that the 1-8 A flux maximum occurred 1.5 min after the 0.5-3 A flux maximum, and that the 8-20 A flux reached its maximum 5 min later. The 0.5-3 A flux was observed to rise and fall more rapidly than the softer radiation.

The improved data obtained with experiment D-21 were also used as a data base for other studies. For example, it was first shown by Kreplin et al. (1970) that X-ray flares of photon energy greater than 20 keV (0.6 A) matched microwave bursts closely in initial time, total duration, and detailed structure. Matching

* Although not labelled, the polar cusps can be seen on the frontispiece; the magnetosheath flux leakage is indicated by the use of identical cross hatching in the magnetosheath and in the polar cusps.

structures were not evident, however, for the softer X-ray bursts (with energy less than 20 keV). Other examples of studies based upon the D-21 data include the first detailed correlation between enhanced solar X-ray flux and short wave fade-outs (Schwentek et al., 1971) and one of the first efforts to derive solar electron temperatures and emission measures* associated with solar flares (Horan, 1970).

4.3.3 Latitude Dependence of Cosmic-Ray Cut-off (D-08, D-09, D-07)

Using data from experiment D-08 (Low-Energy Proton and Alpha-Particle Measurements, Simpson) Fanselow and Stone (1972) investigated the vertical geomagnetic cut-off for cosmic-ray protons at seven energy intervals between 1.2 and 39 MeV. This study yielded nearly one order of magnitude more data during geomagnetically quiet times ($K_p < 1+$) than had previously been reported at even one of these energies. In addition, the energy resolution was significantly better than for previous instruments. The observations, which were organized as a function of magnetic equatorial time, showed that the cosmic-ray cut-off at midnight occurred essentially at the same invariant latitude (65 deg) for the seven energy intervals. The cut-off latitude at noon exhibited a much greater energy dependence (66 deg for 24.4 MeV protons and 72 deg for 1.3 MeV protons).

The Galactic and Solar Cosmic-Ray experiment (D-09, Webber) was basically capable of resolving both the energy (within the range 50 to 2000 MeV/nucleon) and the composition (up to $Z = 10$) of cosmic rays. Considerably improved data, however, became available from later spacecraft shortly after the OGO 4 data analysis had gotten under way, and the OGO 4 studies were limited to a few weeks' worth of proton and alpha-particle data. The OGO 4 effort (Sawyer, 1975) yielded proton cut-off rigidities in the Earth's magnetic field under both quiet and solar flare conditions. The results, which included much higher energies than previously measured, showed that the quiet time cut-offs were at lower latitudes than predicted from field models. From the latitude dependence of this cut-off, it was concluded that ring currents were the main cause of the cut-off depression.

The data from the Ionization Chamber (Experiment D-07, Anderson) was used to extend the study of the cosmic-ray knee initiated with the corresponding OGO 2 experiment (see section 2.3.3). The OGO 4 results showed that the knee latitude was 0.6 deg lower (closer to the equator) in August 1967 than measured by OGO 2 during the October 1965 to February 1966 period (George, 1970).

4.3.4 Electron Polar Cap (D-08)

Observations of energetic electron flux (with energy greater than a few hundred keV) reveal a nearly constant flux in the polar regions corresponding to the open geomagnetic field lines. This region, known as the electron polar cap, exhibits a sharp boundary at the latitude separating open and closed field lines. Using electron data ($E > 530$ keV) from experiment D-08, Evans and Stone (1972) conducted a mapping of the boundary between open and closed field lines (under geomagnetically quiet conditions) which was much more comprehensive than that previously available.

The electron flux near the edge of the polar cap frequently exhibits brief and rapid increases, by typically one order of magnitude. These increases, known as electron spikes, have been investigated extensively by Brown and Stone (1972). This study which included over 750 spike observations, showed that the

* The emission measure which is defined as $\int N_e^2 dV$ provides some indication of the size and density of the emission region. The only previous attempt to measure electron temperature and emission measure during an X-ray flare was by Hudson et al. (1969).

OVERVIEW

4.2.9 Erosion of the Dayside Magnetosphere (D-11)

The magnetopause has been observed to move inward following a reversal of the vertical component of the interplanetary field from northward to southward. This inward motion has been explained by an erosion mechanism whereby the outer, closed, dayside magnetic lines combine with the interplanetary field and become open tail lines. The transition region between open and closed field lines moves southward as a result of this field-line transfer. The transition region is of considerable interest since it appears to provide a funnel (polar cusp*) through which low-energy electrons can travel from the magnetosheath down to the lower atmosphere. The position of the transition region can therefore be determined from a mapping of the low-energy electron flux.

Burch (1972), using the low-energy electron-flux data from experiment D-11, found that the polar cusp moved southward at a rate of 0.1 degree per minute following an abrupt north-to-south reversal of the interplanetary field. This was the first time that such a measurement was made and it provided the first quantitative results concerning the erosion rate of the dayside magnetosphere. The initial study which applied to abrupt reversals of the interplanetary field was later extended to include gradual changes in the interplanetary field (Burch, 1973).

4.2.10 Electron Precipitation Patterns and Substorm Morphology (D-11)

Closely related to the topics discussed under 4.2.7, 4.2.8, and 4.2.9 is the subject of soft electron fluxes associated with the development and recovery of auroral substorms. A major study of this subject was conducted by Hoffman and Burch (1973) who identified five phases in typical substorms and the corresponding electron-flux patterns and auroral forms. This investigation also provided some evidence suggesting the existence of neutral lines in the magnetospheric tail.

4.3 Energetic Particle Measurements

4.3.1 Radiation Belt Studies (D-10)

Using the data from the trapped particle detectors in experiment D-10 (Van Allen), Fritz and Krimigis (1969) measured the ratio of trapped alpha particles to trapped protons, at energies lower than had previously been measured and within several energy intervals. The results indicated that solar wind protons and alpha particles of the same velocity were most probably thermalized upon entering the shock transition region.

4.3.2 Solar X-rays (D-21)

The Solar X-ray Emission experiment (D-21, Kreplin) provided solar X-ray fluxes in four bands, 0.5-3 A, 1-8 A, 8-16 A, and 44 to 60 A with much greater time resolution and dynamic range than had previously been available. The data from experiment D-21 made it possible to investigate for the first time the detailed history of X-ray emissions during solar X-ray flares in several wavelength bands (Kreplin et al., 1969). It was shown that the 1-8 A flux maximum occurred 1.5 min after the 0.5-3 A flux maximum, and that the 8-20 A flux reached its maximum 5 min later. The 0.5-3 A flux was observed to rise and fall more rapidly than the softer radiation.

The improved data obtained with experiment D-21 were also used as a data base for other studies. For example, it was first shown by Kreplin et al. (1970) that X-ray flares of photon energy greater than 20 keV (0.6 A) matched microwave bursts closely in initial time, total duration, and detailed structure. Matching

* Although not labelled, the polar cusps can be seen on the frontispiece; the magnetosheath flux leakage is indicated by the use of identical cross hatching in the magnetosheath and in the polar cusps.

structures were not evident, however, for the softer X-ray bursts (with energy less than 20 keV). Other examples of studies based upon the D-21 data include the first detailed correlation between enhanced solar X-ray flux and short wave fade-outs (Schwentek et al, 1971) and one of the first efforts to derive solar electron temperatures and emission measures* associated with solar flares (Horan, 1970).

4.3.3 Latitude Dependence of Cosmic-Ray Cut-off (D-08, D-09, D-07)

Using data from experiment D-08 (Low-Energy Proton and Alpha-Particle Measurements, Simpson) Faselow and Stone (1972) investigated the vertical geomagnetic cut-off for cosmic-ray protons at seven energy intervals between 1.2 and 39 MeV. This study yielded nearly one order of magnitude more data during geomagnetically quiet times ($K_p < 1+$) than had previously been reported at even one of these energies. In addition, the energy resolution was significantly better than for previous instruments. The observations, which were organized as a function of magnetic equatorial time, showed that the cosmic-ray cut-off at midnight occurred essentially at the same invariant latitude (65 deg) for the seven energy intervals. The cut-off latitude at noon exhibited a much greater energy dependence (66 deg for 24.4 MeV protons and 72 deg for 1.3 MeV protons).

The Galactic and Solar Cosmic-Ray experiment (D-09, Webber) was basically capable of resolving both the energy (within the range 50 to 2000 MeV/nucleon) and the composition (up to $Z = 10$) of cosmic rays. Considerably improved data, however, became available from later spacecraft shortly after the OGO 4 data analysis had gotten under way, and the OGO 4 studies were limited to a few weeks' worth of proton and alpha-particle data. The OGO 4 effort (Sawyer, 1975) yielded proton cut-off rigidities in the Earth's magnetic field under both quiet and solar flare conditions. The results, which included much higher energies than previously measured, showed that the quiet time cut-offs were at lower latitudes than predicted from field models. From the latitude dependence of this cut-off, it was concluded that ring currents were the main cause of the cut-off depression.

The data from the Ionization Chamber (Experiment D-07, Anderson) was used to extend the study of the cosmic-ray knee initiated with the corresponding OGO 2 experiment (see section 2.3.3). The OGO 4 results showed that the knee latitude was 0.6 deg. lower (closer to the equator) in August 1967 than measured by OGO 2 during the October 1965 to February 1966 period (George, 1970).

4.3.4 Electron Polar Cap (D-08)

Observations of energetic electron flux (with energy greater than a few hundred keV) reveal a nearly constant flux in the polar regions corresponding to the open geomagnetic field lines. This region, known as the electron polar cap, exhibits a sharp boundary at the latitude separating open and closed field lines. Using electron data ($E > 530$ keV) from experiment D-08, Evans and Stone (1972) conducted a mapping of the boundary between open and closed field lines (under geomagnetically quiet conditions) which was much more comprehensive than that previously available.

The electron flux near the edge of the polar cap frequently exhibits brief and rapid increases, by typically one order of magnitude. These increases, known as electron spikes, have been investigated extensively by Brown and Stone (1972). This study which included over 750 spike observations, showed that the

* The emission measure which is defined as $\int N_p^2 dV$ provides some indication of the size and density of the emission region. The only previous attempt to measure electron temperature and emission measure during an X-ray flare was by Hudson et al (1969).

OVERVIEW

4.2.9 Erosion of the Dayside Magnetosphere (D-11)

The magnetopause has been observed to move inward following a reversal of the vertical component of the interplanetary field from northward to southward. This inward motion has been explained by an erosion mechanism whereby the outer, closed, dayside magnetic lines combine with the interplanetary field and become open tail lines. The transition region between open and closed field lines moves southward as a result of this field-line transfer. The transition region is of considerable interest since it appears to provide a funnel (polar cusp*) through which low-energy electrons can travel from the magnetosheath down to the lower atmosphere. The position of the transition region can therefore be determined from a mapping of the low-energy electron flux.

Burch (1972), using the low-energy electron-flux data from experiment D-11, found that the polar cusp moved southward at a rate of 0.1 degree per minute following an abrupt north-to-south reversal of the interplanetary field. This was the first time that such a measurement was made and it provided the first quantitative results concerning the erosion rate of the dayside magnetosphere. The initial study which applied to abrupt reversals of the interplanetary field was later extended to include gradual changes in the interplanetary field (Burch, 1973).

4.2.10 Electron Precipitation Patterns and Substorm Morphology (D-11)

Closely related to the topics discussed under 4.2.7, 4.2.8, and 4.2.9 is the subject of soft electron fluxes associated with the development and recovery of auroral substorms. A major study of this subject was conducted by Hoffman and Burch (1973) who identified five phases in typical substorms and the corresponding electron-flux patterns and auroral forms. This investigation also provided some evidence suggesting the existence of neutral lines in the magnetospheric tail.

4.3 Energetic Particle Measurements

4.3.1 Radiation Belt Studies (D-10)

Using the data from the trapped particle detectors in experiment D-10 (Van Allen), Fritz and Krimigis (1969) measured the ratio of trapped alpha particles to trapped protons, at energies lower than had previously been measured and within several energy intervals. The results indicated that solar wind protons and alpha particles of the same velocity were most probably thermalized upon entering the shock transition region.

4.3.2 Solar X-rays (D-21)

The Solar X-ray Emission experiment (D-21, Kreplin) provided solar X-ray fluxes in four bands, 0.5-3 A, 1-8 A, 8-16 A, and 44 to 60 A with much greater time resolution and dynamic range than had previously been available. The data from experiment D-21 made it possible to investigate for the first time the detailed history of X-ray emissions during solar X-ray flares in several wavelength bands (Kreplin et al, 1969). It was shown that the 1-8 A flux maximum occurred 1.5 min after the 0.5-3 A flux maximum, and that the 8-20 A flux reached its maximum 5 min later. The 0.5-3 A flux was observed to rise and fall more rapidly than the softer radiation.

The improved data obtained with experiment D-21 were also used as a data base for other studies. For example, it was first shown by Kreplin et al (1970) that X-ray flares of photon energy greater than 20 keV (0.6 A) matched microwave bursts closely in initial time, total duration, and detailed structure. Matching

* Although not labelled, the polar cusps can be seen on the frontispiece; the magnetosheath flux leakage is indicated by the use of identical cross hatching in the magnetosheath and in the polar cusps.

structures were not evident, however, for the softer X-ray bursts (with energy less than 20 keV). Other examples of studies based upon the D-21 data include the first detailed correlation between enhanced solar X-ray flux and short wave fade-outs (Schwentek et al, 1971) and one of the first efforts to derive solar electron temperatures and emission measures* associated with solar flares (Horan, 1970).

4.3.3 Latitude Dependence of Cosmic-Ray Cut-off (D-08, D-09, D-07)

Using data from experiment D-08 (Low-Energy Proton and Alpha-Particle Measurements, Simpson) Fanelow and Stone (1972) investigated the vertical geomagnetic cut-off for cosmic-ray protons at seven energy intervals between 1.2 and 39 MeV. This study yielded nearly one order of magnitude more data during geomagnetically quiet times ($K_p < 1+$) than had previously been reported at even one of these energies. In addition, the energy resolution was significantly better than for previous instruments. The observations, which were organized as a function of magnetic equatorial time, showed that the cosmic-ray cut-off at midnight occurred essentially at the same invariant latitude (65 deg) for the seven energy intervals. The cut-off latitude at noon exhibited a much greater energy dependence (66 deg for 24.4 MeV protons and 72 deg for 1.3 MeV protons).

The Galactic and Solar Cosmic-Ray experiment (D-09, Webber) was basically capable of resolving both the energy (within the range 50 to 2000 MeV/nucleon) and the composition (up to $Z = 10$) of cosmic rays. Considerably improved data, however, became available from later spacecraft shortly after the OGO 4 data analysis had gotten under way, and the OGO 4 studies were limited to a few weeks' worth of proton and alpha-particle data. The OGO 4 effort (Sawyer, 1975) yielded proton cut-off rigidities in the Earth's magnetic field under both quiet and solar flare conditions. The results, which included much higher energies than previously measured, showed that the quiet time cut-offs were at lower latitudes than predicted from field models. From the latitude dependence of this cut-off, it was concluded that ring currents were the main cause of the cut-off depression.

The data from the Ionization Chamber (Experiment D-07, Anderson) was used to extend the study of the cosmic-ray knee initiated with the corresponding OGO 2 experiment (see section 2.3.3). The OGO 4 results showed that the knee latitude was 0.6 deg lower (closer to the equator) in August 1967 than measured by OGO 2 during the October 1965 to February 1966 period (George, 1970).

4.3.4 Electron Polar Cap (D-08)

Observations of energetic electron flux (with energy greater than a few hundred keV) reveal a nearly constant flux in the polar regions corresponding to the open geomagnetic field lines. This region, known as the electron polar cap, exhibits a sharp boundary at the latitude separating open and closed field lines. Using electron data ($E > 530$ keV) from experiment D-08, Evans and Stone (1972) conducted a mapping of the boundary between open and closed field lines (under geomagnetically quiet conditions) which was much more comprehensive than that previously available.

The electron flux near the edge of the polar cap frequently exhibits brief and rapid increases, by typically one order of magnitude. These increases, known as electron spikes, have been investigated extensively by Brown and Stone (1972). This study which included over 750 spike observations, showed that the

* The emission measure which is defined as $\int N_e^2 dV$ provides some indication of the size and density of the emission region. The only previous attempt to measure electron temperature and emission measure during an X-ray flare was by Hudson et al (1969).

spikes could be divided into three distinct populations depending on whether they occur at latitudes below, at, or above the local limit of trapping.

4.4 Radio Physics Experiments

4.4.1 VLF Investigations (D-02, D-03)

A remarkable variety of VLF phenomena, first identified with OGO experiments, has been described in sections 1.4.1 (OGO 1), 2.4.1 (OGO 2), and 3.4.1 (OGO 3). With the OGO 4 experiments the long list of accomplishments in the VLF discipline continued to grow very significantly.

The following phenomena were first identified with the data from experiment D-02 (Helliwell): equatorial erosion, which is a steady decrease in the high-frequency cut-off of whistlers as the satellite approaches the magnetic equator (Scarabucci, 1970); banded whistlers, which are broadly dispersed whistlers discontinuous at one or more frequencies (Paymar, 1972); whistler striations, which are amplitude enhancements in bands of frequencies exhibiting either a steady increase or decrease (in frequency) over extended periods of time, and giving rise to a striated appearance on compressed frequency-vs-time records (Kimura, 1971; Dantas, 1972); and band-limited ELF hiss (BLH), a continuous noise band observed from 10- to 55-deg dipole latitude and exhibiting an upper cut-off in the vicinity of 600 Hz, which is nearly independent of satellite altitude and latitude (Muzzio and Angerami, 1972).

Propagation studies conducted with experiment D-02 led to the identification of the pro-longitudinal (PL) mode, a new type of non-ducted whistler propagation in the magnetosphere. The original identification of the PL mode was greatly aided by measuring on OGO 4 the same signal with two receivers having very different bandwidths. This made it possible to estimate the Doppler shift, an essential parameter for the interpretation of these observations (Scarabucci, 1969).

The information obtained with experiment D-02 was also used as a data base for other studies, such as the investigation of magnetospheric substorms by Carpenter and Chappell (1973). In this particular case, the VLF data were used to monitor the gradual erosion of the plasmapause during a weak magnetic storm.

Some of the VLF data observed on OGO 2 with experiment C-03 were interpreted as LHR emissions (see section 2.4.1), an emission which depends upon the electron concentration, the ion composition, and the intensity of the Earth's magnetic field. The LHR interpretation was confirmed by comparing similar VLF observations from experiment D-03 (Morgan) on OGO 4 with simultaneous ion composition and density data from experiment D-16 (Laaspere and Taylor, 1970).

Auroral hiss data from experiment D-03 were compared with simultaneous low-energy electron precipitation measured by experiment D-11 because earlier work by Gurnett (1966) and Hartz (1970) had indicated that a direct relationship existed between hiss and precipitation. It was found that VLF hiss correlated well with precipitation events at 0.7 keV, but poorly with activity at 2.3 and 7.3 keV (Hoffman and Laaspere, 1972).

The VLF data from experiment D-03 also led to the first observations of harmonic ion cyclotron resonances (Kikuchi, 1970). Since only a few examples of these (still unexplained) resonances could be found, Kikuchi (1970) concluded that the excitation mechanism had to involve excitation conditions that can be satisfied only under very special circumstances.

4.4.2 Antenna Impedance Measurements (D-01)

Experiment D-01 (Haddock) was partially disabled by a high noise level in the radiometer data caused by radio-frequency interference generated within the spacecraft. The noise level made it impractical to conduct the planned radio astronomy experiment (mapping the brightness temperature of the sky at 2.5 MHz). The planned antenna impedance measurements, however, were not affected by the interference and they represent a useful body of data for the study of the behavior of antennas in the ionospheric plasma (Potter, 1970).

4.5 Optical Experiments

4.5.1 Visible and Near UV Airglow (D-12)

Experiment D-12 (Airglow and Auroral Study, Reed) provided the first global mapping of airglow in the visible and near-ultra-violet wavelengths (Reed et al, 1973). One of the most surprising results was the pronounced asymmetry in intensities observed between the southern and northern hemispheres (Chandra et al, 1973). Also unexpected were the large differences between the equinox and winter solstice data, particularly at 2630 Å and 5577 Å, giving support to the idea that there are large variations in the density of the neutral atmosphere at 100 km (62 mi) (Reed and Chandra, 1975).

This global mapping of airglow is a unique and valuable source of information. Although the primary data reduction is essentially completed, only a relatively small portion has been thoroughly analyzed and published. The correlations between electron temperatures and SAR arcs were discussed under section 4.2.6. New information continues to be derived from the data from experiment D-12 such as the correlations between red arcs in the northern and southern hemispheres (Reed and Blamont, 1974) and the possibility of using airglow data as an indicator of the altitude and density of the F-region maximum (Chandra et al, 1975).

4.5.2 Lyman-Alpha and UV Airglow (D-13, D-14)

Airglow measurements in the far ultraviolet by experiment D-13 (Lyman-Alpha and UV Airglow Study, Mange) have led to the discovery of far ultraviolet airglow in the equatorial zone (Hicks and Chubb, 1970). The detectors from experiment D-13 showed that these emissions occurred in the 1230- to 1350-Å band and in the 1350- to 1550-Å band. A more precise identification by the UV Spectrometer of experiment D-14 (Barth) showed that the equatorial UV airglow was caused by oxygen lines at 1304 and 1356 Å (Barth and Shaffner, 1970). The observations reported by Hicks and Chubb (1970) indicated a strong seasonal and local time dependence but more importantly a high degree of symmetry with respect to the magnetic dip equator. The symmetrical 1356-Å emission data (which depend primarily upon Nm, the maximum electron density at the F-2 peak) were combined with the asymmetrical 6300-Å data from experiment D-12 (which depend upon both Nm and hm, the height corresponding to Nm) to conduct the study mentioned at the end of section 4.5.1. This study showed that airglow data offer the possibility of mapping the height and density of the F-2 peak over extended areas, a measurement which has not yet been achieved by other techniques.

Other discoveries made with the data from experiment D-13 include the depressions in the Lyman-alpha and 1304-Å emissions over the poles (Meier, 1970), the 1304-Å conjugate enhancements (Meier, 1971), and the observations of Lyman-Birge-Hopfield emission in the daytime airglow (Prinz and Meier, 1971).

An entirely new look at the morphology of auroras has been obtained with the far ultraviolet data from experiment D-13. The results presented by Chubb and Hicks (1970) showed that auroral arcs were easily detectable even in full sunlight, and that the aurora was continuously present with little difference between southern and northern hemispheres. The morphology of the far ultraviolet aurora was found to be quite similar to that of the visible aurora.

The many results from experiment D-13 also include long term studies on the geocoronal Lyman-alpha emission (Meier and Mange, 1970) and on the temporal variation in the solar Lyman-alpha flux (Meier, 1969).

The first global measurements of nitric oxide from a satellite were made with the OGO 4 ultraviolet scanning spectrometer (Experiment D-14, Barth). The measurements, which are based upon observations of nitric oxide fluorescence at 2150 Å, showed that the nitric oxide content of the atmosphere is relatively stable between 40°N and 40°S above about 70 km (Rusch, 1973). Although similar measurements have been planned for the AE-C mission (launched Dec. 16, 1973), the AE-C results have not yet been published. Thus, at the present time (Spring, 1975), the OGO 4 measurements of nitric oxide are the only ones of this type.

OVERVIEW

4.6 Interplanetary Dust Particles (D-18)

The usefulness of experiment D-18 (Interplanetary Dust Particles, Nilsson) was very limited because of high noise levels in the rear sensor. Many of the observed microphone events were clearly triggered by noise. An upper limit to the flux of particles greater than 10^{-12} grams was calculated based upon 49 events which could have been real micrometeoroid impacts. The resulting flux value was: $\Phi = 7 \times 10^3$ particles/m² sec 2 π ster (Nilsson et al, 1969). The comment made under section 3.6 concerning the validity of microphone data is also applicable to experiment D-18.

December 1, 1975

REFERENCES

- Ahmed, M., and R. C. Sagalyn, "Thermal Positive Ions in the Outer Ionosphere and Magnetosphere from OGO 1," *J. Geophys. Res.*, **77**, 7, 1205-1220, Mar. 1972.
- Alexander, W. M., J. C. Smith, C. W. Arthur, and J. L. Bohn, "Four Years of Dust Particle Measurements in Cislunar and Selenocentric Space from Lunar Explorer and OGO 3," *Space Res.*, **13**, v-2, 1037-1046, 1973.
- Anderson, H. R., P. D. Hudson, and J. E. McCoy, "Observations of POGO Ion Chamber Experiment in the Outer Radiation Zone," *J. Geophys. Res.*, **73**, 19, 6285-6297, Oct. 1968.
- Angerami, J. J., "Whistler Duct Properties Deduced from VLF Observations Made with the OGO 3 Satellite near the Magnetic Equator," *J. Geophys. Res.*, **75**, 31, 6115-6135, Nov. 1970.
- Arnoldy, R. L., S. R. Kane, and J. R. Winckler, "Energetic Solar Flare X-rays Observed by Satellite and their Correlation with Solar Radio and Energetic Particle Emission," *Astrophys. J.*, Vol 151, 711-736, Feb. 1968.
- Balasubrahmanyam, V. K., D. E. Hagge, G. H. Ludwig, and F. B. McDonald, "The Multiply Charged Primary Cosmic Radiation at Solar Minimum, 1965," *J. Geophys. Res.*, **71**, 7, 1771-1779, Apr. 1966.
- Bame, S. J., J. R. Asbridge, H. E. Felthouser, F. W. Hones, and I. B. Strong, "Characteristics of the Plasma Sheet in the Earth's Magnetotail," *J. Geophys. Res.*, **72**, 1, 113-129, Jan. 1967.
- Bame, S. J., J. R. Asbridge, A. J. Hundhausen, and I. B. Strong, "Solar Wind and Magnetosheath Observations during the January 13-14, 1967, Geomagnetic Storm," *J. Geophys. Res.*, **73**, 17, 5761-5767, Sept. 1968.
- Barth, C. A. and S. Schaffner, "OGO 4 Spectrometer Measurements of the Tropical Ultraviolet Airglow," *J. Geophys. Res.*, **75**, 22, 4299-4306, Aug. 1970.
- Benson, R. F., "Simultaneous In Situ Electron Temperature Comparison of Alouette 2 Probe and Plasma Resonance Data," *J. Geophys. Res.*, **78**, 28, 6755-6759, Oct. 1973.
- Benson, R. F. and W. R. Hoegy, "Effect of an Isotropic Nonequilibrium Plasma on Electron Temperature Measurements," *J. Geophys. Res.*, **78**, 22, 4702-4706, Aug. 1973.
- Berg, O. E., and E. Grün, "Evidence of Hyperbolic Cosmic Dust Particles," *Space Res.*, **13**, v-2, 1047-1055, 1973.
- Berko, F. W., "Distributions and Characteristics of High-Latitude Field-Aligned Electron Precipitation," *J. Geophys. Res.*, **78**, 10, 1615-1626, Apr. 1973.
- Berko, F. W., and R. A. Hoffman, "Dependence of Field-Aligned Electron Precipitation Occurrence on Season and Altitude," *J. Geophys. Res.*, **79**, 25, 3749-3754, Sept. 1974.
- Berko, F. W., R. A. Hoffman, R. K. Burton, and R. E. Holzer, "Simultaneous Particle and Field Observations of Field-Aligned Currents," *J. Geophys. Res.*, **80**, 1, 37-46, Jan. 1975.
- Binsack, J. H., and V. M. Vasylunas, "Simultaneous IMP 2 and OGO 1 Observations of Bow Shock Compression," *J. Geophys. Res.*, **73**, 1, 429-433, Jan. 1968.
- Brice, N. M., "Bulk Motion of the Magnetosphere," *J. Geophys. Res.*, **72**, 21, 5193-5211, Nov. 1967.
- Brown, J. W., and E. C. Stone, "High-Energy Electron Spikes at High Latitudes," *J. Geophys. Res.*, **77**, 19, 3384-3396, July 1972.
- Burch, J. L., "Precipitation of Low-Energy Electrons at High Latitudes: Effects of Interplanetary Magnetic Field and Dipole Tilt Angle," *J. Geophys. Res.*, **77**, 34, 6696-6707, Dec. 1972.
- Burch, J. L., "Rate of Erosion of Dayside Magnetic Flux Based on a Quantitative Study of the Dependence of Polar Cusp Latitude on the Interplanetary Magnetic Field," *Radio Science*, 955-961, Nov. 1973.
- Burtis, W. J., "Electron Concentrations Calculated from the Lower Hybrid Resonance Noise Band Observed by OGO 3," *J. Geophys. Res.*, **78**, 25, 5515-5523, Sept. 1973.
- Burtis, W. J., and R. A. Helliwell, "Banded Chorus - A New Type of VLF Radiation Observed in the Magnetosphere by OGO 1 and OGO 3," *J. Geophys. Res.*, **74**, 11, 3002-3010, June 1969.
- Cain, J. C., "Accomplishments of the World Magnetic Survey by POGO Satellites," NASA SP-195, *Significant Accomplishments in Science*, GSFC, 46-49, 1968.
- Cain, J. C., "Geomagnetic Models from Satellite Surveys," *Review of Geophys. and Space Phys.*, **9**, No. 2, 259-273, May 1971.
- Cain, J. C., and S. J. Cain, "Derivation of the International Geomagnetic Reference Field (IGRF 10/68)" NASA, TN D-6237, Aug. 1971.

- Cain, J. C., and S. J. Hendricks. "Geomagnetic Secular Variation 1900-1965." NASA/GSFC X-612-67-479, Greenbelt, Md., Sept. 1967.
- Cain, J. C., and R. E. Sweeney. "Magnetic Field Mapping of the Inner Magnetosphere," *J. Geophys. Res.*, 75, 22, 4360-4362, Aug. 1970.
- Cain, J. C., and R. A. Langel, "The Geomagnetic Survey by the Polar Orbiting Geophysical Observatories OGO 2 and OGO 4 1965-1967," GSFC Report X-612-68-502, Greenbelt, Md., 1968.
- Cain, J. C., and R. E. Sweeney, "POGO Observations of the Equatorial Electrojet," NASA/GSFC, TMX-65995, Greenbelt, Md. Aug. 1972.
- Cain, J. C., S. J. Hendricks, R. A. Langel, and W. V. Hudson, "Proposed Model for the International Geomagnetic Reference Field--1965," *J. Geomagnetism and Geoelect.*, 19, 335-355, 1967.
- Cain, J. C., R. A. Langel, and S. J. Hendricks, "Magnetic Chart of the Brazilian Anomaly--A Verification" *Geomagnetism and Aeronomy.* 8, 84-87, 1968.
- Carpenter, D. L., "Whistler Evidence of a 'Knee' in the Magnetospheric Ionization Density Profile," *J. Geophys. Res.*, 68, 1675-1682, Mar. 15, 1963.
- Carpenter, D. L., "Whistler Studies of the Plasmopause in the Magnetosphere," *J. Geophys. Res.*, 71, 3, 693-725, Feb. 1966.
- Carpenter, D. L., and C. R. Chappell, "Satellite Studies of Magnetospheric Substorms on August 15, 1968 3. Some Features of Magnetospheric Convection," *J. Geophys. Res.*, 78, 16, 3062-3067, June 1973.
- Carpenter, D. L., C. G. Park, H. A. Taylor, Jr., and H. C. Brinton, "Multi-Experiment Detection of the Plasmopause from EOGO Satellites and Antarctic Ground Stations," *J. Geophys. Res.*, 74, 7, 1837-1847, Apr. 1969.
- Chandra, S., "The Equatorial Helium Ion Trough and the Geomagnetic Anomaly," *J. Atmos. Terr. Phys.*, 359-367, Feb. 1975.
- Chandra, S., B. E. Troy, Jr., J. L. Donley, and R. E. Bourdeau, "OGO 4 Observations of Ion Composition and Temperatures in the Topside Ionosphere," *J. Geophys. Res.*, 75, 19, 3867-3878, July 1970.
- Chandra, S., E. J. Maier, B. E. Troy, Jr., and B. C. Narasingo Rao, "Subauroral Red Arcs and Associated Ionospheric Phenomena," *J. Geophys. Res.*, 76, 4, 920-925, Feb. 1971.
- Chandra, S., E. I. Reed, B. E. Troy, Jr., and J. E. Blamont, "Equatorial Airglow and the Ionospheric Geomagnetic Anomaly," *J. Geophys. Res.*, 78, 22, 4630-4640, Aug. 1973.
- Chandra, S., E. I. Reed, R. R. Meier, C. B. Opal, and G. T. Hicks, "Remote Sensing of the Ionospheric F-layer by Use of OI-6300 A and OI-1356 A Observations," *J. Geophys. Res.*, 80, 16, 2327-2332, June 1975.
- Chubb, T. A., and G. T. Hicks, "Observations of the Aurora in the Far Ultraviolet from OGO 4," *J. Geophys. Res.*, 75, 7, 1290-1311, Mar. 1970.
- Cline, T. L., and E. W. Hones, Jr., "Interplanetary Positrons Near 1 MeV from Other than the Pion Yields Muon Yields Electron Process," *Acta Physica.* 29, Suppl. 1, 159-164, 1970 (Proc. of 11th International Conference on Cosmic Rays, Budapest, Hungary, Aug. 25 - Sept. 4, 1969).
- Cline, T. L., S. S. Holt, and E. W. Hones, Jr., "High-Energy X-rays from the Solar Flare of July 7, 1966," *J. Geophys. Res.*, 73, 1, 434-437, Jan. 1968.
- Cole, K. D., "Stable Auroral Red Arcs, Sinks for Energy of Dst Main Phase," *J. Geophys. Res.*, 70, 7, 1689-1706, Apr. 1965.
- Comstock, G. M., C. Y. Fan, and J. A. Simpson, "Abundances and Energy Spectra of Galactic Cosmic-Ray Nuclei Above 20 MeV per Nucleon in the Nuclear Charge Range $2 < Z < 26$," *Astrophys. J.*, 146, 51-77, Oct. 1966.
- Cummings, W. D., and P. J. Coleman, Jr., "Magnetic Fields in the Magnetopause and Vicinity at Synchronous Altitude," *J. Geophys. Res.*, 73, 17, 5699-5718, Sept. 1968.
- Dantas, H. H., "OGO 4 Satellite Observations of Whistler-Mode Propagation Effects Associated with Caustics in the Magnetosphere," Stanford Univ., Ph.D. Thesis, Stanford, California, Oct. 1972.
- da Rosa, A. V., and O. K. Garriott, "Protonospheric Electron Concentration Profiles," *J. Geophys. Res.*, 74, 26, 6386-6402, Dec. 1969.
- Dunckel, N., and R. A. Helliwell, "Whistler-Mode Emissions on the OGO 1 Satellite," *J. Geophys. Res.*, 74, 26, 6371-6385, Dec. 1969.

- Dunckel, N., B. Ficklin, L. Rorden, and R. A. Helliwell, "Low-Frequency Noise Observed in the Distant Magnetosphere with OGO 1," *J. Geophys. Res.*, 75, 10, 1854-1862, Apr. 1970.
- Dunckel, N., R. A. Helliwell, and J. Vesecky, "Type III Solar Noise Observed Below 100 kHz on OGO 3," *Solar Physics*, 25, 197-209, 1972.
- Evans, L. C., and E. C. Stone, "Electron Polar Cap and the Boundary of Open Geomagnetic Field Lines," *J. Geophys. Res.*, 77, 28, 5580-5584, Oct. 1972.
- Fan, C. Y., G. Gloeckler, and J. A. Simpson, "Protons and Helium Nuclei Within Interplanetary Regions Which Co-rotate with the Sun" Proc. 9th Int. Conf. Cosmic Rays, 109-111, London, 1965.
- Fan, C. Y., G. Gloeckler, and R. B. McKibben, "Quiet Time Fluxes of Protons and Alpha Particles in the Energy Range 2-20 MeV/Nucleon in 1967" *Acta Phys. Acad. Sci. Hungary*, 29, Suppl. 2, 261-267, 1970, (Proc. 11th Conf. on Cosmic Rays, Budapest, Hungary, Aug. 25-Sept. 4, 1969).
- Fanselow, J. L., and E. C. Stone, "Geomagnetic Cutoffs for Cosmic-Ray Protons for Seven Energy Intervals Between 1.2 and 39 MeV," *J. Geophys. Res.*, 77, 22, 3999-4009, Aug. 1972.
- Frank, L. A., "Initial Observations of Low-Energy Electrons in the Earth's Magnetosphere with OGO 3," *J. Geophys. Res.*, 72, 1, 185-195, Jan. 1967a.
- Frank, L. A., "On the Extraterrestrial Ring Current During Geomagnetic Storms," *J. Geophys. Res.*, 72, 15, 3753-3767, Aug. 1967b.
- Frank, L. A., "Relationship of the Plasma Sheet, Ring Current, Trapping Boundary, And Plasmapause Near the Magnetic Equator and Local Midnight," *J. Geophys. Res.*, 76, 10, 2265-2275, Apr. 1971.
- Frank, L. A., and H. D. Owens, "Omnidirectional Intensity Contours of Low-Energy Protons ($0.5 \leq E \leq 50$ keV) in the Earth's Outer Radiation Zone at the Magnetic Equator," *J. Geophys. Res.*, 75, 7, 1269-1278, Mar. 1970.
- Fritz, T. A., and S. M. Krimigis, "Initial Observations of Geomagnetically Trapped Protons and Alpha Particles with OGO 4," *J. Geophys. Res.*, 74, 21, 5132-5138, Oct. 1969.
- George, M. J., "Observations of the Cosmic Ray Knee with a Polar Orbiting Ionization Chamber," *J. Geophys. Res.*, 75, 16, 3159-3166, June 1970a.
- George, M. J., "The Altitude Dependence of the Quiet Time Cosmic Ray Ionization Over the Polar Regions at Solar Minimum," *J. Geophys. Res.*, 75, 16, 3154-3158, June 1970b.
- Graedel, T. E., "The Association of Solar Optical Flares with Type III Solar Bursts from 4 to 2 MHz Observed by OGO III," *The Astrophysical Journal*, Vol. 160, 301-307, Apr. 1970.
- Grebowsky, J. M., "Time-Dependent Plasmapause Motion," *J. Geophys. Res.*, 76, 25, 6193-6197, Sept. 1971.
- Gurnett, D. A., "A Satellite Study of VLF Hiss," *J. Geophys. Res.*, 71, 23, 5599-5615, Dec. 1966.
- Gurnett, D. A., "The Earth as a Radio Source: Terrestrial Kilometric Radiation," *J. Geophys. Res.*, 79, 28, 4227-4238, Oct. 1974.
- Gustafsson, G., "Latitude and Local Time Dependence of Precipitated Low-Energy Electrons at High Latitudes," *J. Geophys. Res.*, 78, 25, 5537-5552, Sept. 1973.
- Haddock, F. T., and T. E. Graedel, "Dynamic Spectra of Type III Solar Bursts from 4 to 2 MHz Observed by OGO III," *The Astrophysical Journal*, Vol. 160, 293-300, Apr. 1970.
- Hartz, T. R., "Low Frequency Noise Emissions and Their Significance for Energetic Particle Processes in the Polar Ionosphere," *The Polar Ionosphere and Magnetospheric Processes*, edited by G. Skouli, Gordon and Breach, New York, 1970.
- Heppner, J. P., M. Sugiura, T. L. Skillman, B. G. Ledley, and M. Campbell, "OGO-A Magnetic Field Observations," *J. Geophys. Res.*, 72, 21, 5417-5471, Nov. 1967.
- Heyborne, R. L., R. L. Smith, and R. A. Helliwell, "Latitudinal Cutoff of VLF Signals in the Ionosphere," *J. Geophys. Res.*, 74, 9, 2393-2397, May 1969.
- Hicks, G. T., and T. A. Chubb, "Equatorial Aurora/Airglow in the Far Ultraviolet," *J. Geophys. Res.*, 75, 31, 6233-6248, Nov. 1970.
- Hoffman, R. A., "Auroral Electron Drift and Precipitation: Cause of the Mantle Aurora," GSFC document X-646-70-205, June 1970.

- Hoffman, R. A., and F. W. Berko, "Primary Electron Influx to Dayside Auroral Oval," *J. Geophys. Res.*, **76**, 13, 2967-2976, May 1971.
- Hoffman, R. A., and J. L. Burch, "Electron Precipitation Patterns and Substorm Morphology," *J. Geophys. Res.*, **78**, 16, 2867-2884, June 1973.
- Hoffman, R. A., and D. S. Evans, "Field-Aligned Electron Bursts at High Latitudes Observed by OGO 4," *J. Geophys. Res.*, **73**, 19, 6201-6214, Oct. 1968.
- Hoffman, R. A., and T. Laaspere, "Comparison of Very-Low-Frequency Auroral Hiss With Precipitating Low-Energy Electrons by the Use of Simultaneous Data From Two OGO 4 Experiments," *J. Geophys. Res.*, **77**, 640-650, Feb. 1972.
- Holzer, R. E., M. G. McLeod, and E. J. Smith, "Preliminary Results from the OGO 1 Search Coil Magnetometer: Boundary Positions and Magnetic Noise Spectra," *J. Geophys. Res.*, **71**, 5, 1481-1486, Mar. 1966.
- Horan, D. M., "Coronal Electron Temperatures Associated with Solar Flares," Ph.D. Thesis, Catholic University of America, Washington, D.C., 1970.
- Hudson, P. D., and H. R. Anderson, "Nonuniformity of Solar Protons Over the Polar Caps on March 24, 1966," *J. Geophys. Res.*, **74**, 11, 2881-2890, June 1969.
- Hudson, H. S., L. E. Peterson, and D. A. Schwartz, "Hard Solar X-ray Spectrum Observed from the Third Orbiting Solar Observatory," *Astrophys. J.* **157**, 389-415, July 1969.
- Jorgensen, T. S., and F. T. Bell, "Observations of Naturally Occurring VLF and Man-made HF Plasma Waves in Auroral Regions of the Ionosphere," Proc. of the NATO Advan. Study Inst., Roros, Norway, Apr. 17-26, 1968 in *Plasma Waves in Space and in the Laboratory*, **2**, 377-387, ed. J. O. Thomas and B. J. Landmark, Am. Elsevier Pub. Co., New York, N. Y., 1970.
- Kane, S. R., and J. R. Winckler, "'Hysteresis' Effect in Cosmic Ray Modulation and the Cosmic Ray Gradient Near Solar Minimum," *J. Geophys. Res.*, **74**, 26, 6247-6255, Dec. 1969.
- Kane, S. R., J. R. Winckler, and D. J. Hoffman, "Observations of the Screening of Solar Cosmic Rays by the Outer Magnetosphere," *Planetary Space Science*, **16**, 1381-1404, 1968.
- Kikuchi, H., "Harmonic Ion Cyclotron Resonances Observed by the OGO 4 Satellite," *Nature*, Vol. 225, 257-258, Jan. 17, 1970.
- Kikuchi, H., and H. A. Taylor, Jr., "Irregular Structure of Thermal Ion Plasma Near the Plasmapause Observed from OGO 3 and PC 1 Measurements," *J. Geophys. Res.*, **77**, 131-142, Jan. 1972.
- Kimura, I., "Drifting Whistler Cut-off Phenomena-Striations-Observed by POGO Satellites," *Space Research 11*, No. 2, 1331-1336, 1971 (Proc. 13th COSPAR Meeting, Leningrad USSR, May 20-29, 1970).
- Konradi, A., "135-1650 keV Solar Protons After the Flare of July 7, 1966, Observed in the Magnetotail and Magnetosheath," *J. Geophys. Res.*, **74**, 5, 1158-1163, March 1969.
- Kreplin, R. W., D. M. Horan, T. A. Chubb, and H. F. Friedman, "Measurements of Solar X-ray Emission from the OGO-IV Spacecraft," *Solar Flares and Space Research* (Z. Svestka and C. de Jager, ed.) North-Holland, Amsterdam, 121-130, 1969.
- Kreplin, R. W., P. J. Moser, and J. P. Castelli, "Flare X-ray and Radio Wave Emission," *Space Research X, North-Holland Publishing Company, Amsterdam*, 920-927, 1970.
- Laaspere, T., and H. A. Taylor, Jr., "Comparison of Certain VLF Noise Phenomena With the Lower Hybrid Resonance Frequency Calculated from Simultaneous Ion Composition Measurements," *J. Geophys. Res.*, **75**, 1, 97-106, Jan. 1970.
- Laaspere, T., M. G. Morgan, and W. C. Johnson, "Observations of Lower Hybrid Resonance Phenomena on the OGO 2 Spacecraft," *J. Geophys. Res.*, **74**, 1, 141-152, Jan. 1969.
- Langel, R. A., and J. C. Cain, "OGO 2 Magnetic Field Observations During the Magnetic Storm of March 13-15, 1966," *Ann. Geophys.*, **24**, No. 3, 857-869, 1968.
- Langel, R. A., and R. E. Sweeney, "Asymmetric Ring Current at Twilight Local Time," *J. Geophys. Res.*, **76**, 19, 4420-4427, July 1971.
- Lin, R. P., S. W. Kahler, and E. C. Roelof, "Solar Flare Injection and Propagation of Low-Energy Protons and Electrons in the Event of July 7-9, 1966," *Solar Phys.*, Vol. 4, 338-360, 1968.
- McClure, J. P., and B. E. Troy, Jr., "Equatorial Ion Temperature: A Comparison of Conflicting Incoherent Scatter and OGO 4 Retarding Potential Analyzer Values," *J. Geophys. Res.*, **76**, 19, 4534-4540, July 1971.
- McCoy, J. E., "High-Latitude Ionization Spikes Observed by the POGO Ion Chamber Experiment," *J. Geophys. Res.*, **74**, 9, 2309-2318, May 1969.

- Mange, P., and R. R. Meier, "OGO 3 Observations of the Lyman Alpha Intensity and the Hydrogen Concentration Beyond 5 R_E ," *J. Geophys. Res.*, 75, 10, 1837-1847, Apr. 1970.
- Meier, R. R., "Temporal Variations of Solar Lyman Alpha," *J. Geophys. Res.*, 74, 26, 6487-6490, Dec. 1969.
- Meier, R. R., "Depressions in the Far-Ultraviolet Airglow Over the Poles," *J. Geophys. Res.*, 75, 31, 6218-6232, Nov. 1970.
- Meier, R. R., "Observations of Conjugate Excitation of the OI1304-A Airglow," *J. Geophys. Res.*, 76, 1, 242-247, Jan. 1971.
- Meier, R. R., and P. Mange, "Geocoronal Hydrogen: An Analysis of the Lyman-Alpha Airglow Observed from OGO 4," *Planet. Space Sci.*, 18, 803, 1970.
- Muldrew, D. B., "F-Layer Ionization Troughs Deduced from Alouette Data," *J. Geophys. Res.*, 70, 11, 2635-2650, June 1965.
- Muzzio, J. L. R., and J. J. Angerami, "OGO 4 Observations of Extremely Low Frequency Hiss," *J. Geophys. Res.*, 77, 7, 1157-1173, Mar. 1972.
- Nilsson, C. S., F. W. Wright, and D. Wilson, "Attempts to Measure Micrometeoroid Flux on the OGO 2 and 4 Satellites," *J. Geophys. Res.*, 74, 5268-5276, Oct. 15, 1969.
- Nishida, A., "Formation of Plasmapause, or Magnetospheric Plasma Knee, by the Combined Action of Magnetospheric Convection and Plasma Escape from the Tail," *J. Geophys. Res.*, 71, 23, 5669-5679, Dec. 1966.
- Olson, J. V., and R. E. Holzer, "On the Local Time Dependence of the Bow Shock Wave Structure," *J. Geophys. Res.*, 79, 7, 939-947, Mar. 1974.
- Olson, J. V., R. E. Holzer, and E. J. Smith, "High-Frequency Magnetic Fluctuations Associated with the Earth's Bow Shock," *J. Geophys. Res.*, 74, 19, 4601-4617, Sept. 1969.
- Opp, A. G., "Penetration of the Magnetopause Beyond 6.6 R_E During the Magnetic Storm of January 13-14, 1967: Introduction," *J. Geophys. Res.*, 73, 17, 5697-5698, Sept. 1968.
- Paymar, E. M., "Banded Whistlers Observed on OGO 4," Stanford University Report SU-SEL-71-054, Jan. 1972.
- Pfizer, K. A., "OGO 1 and OGO 3 Electron Spectrometer and Ion Chamber Data," Final Report, McDonnell Douglas Astronautics Co., May 1972.
- Pfizer, K. A., and J. R. Winckler, "Experimental Observation of a Large Addition to the Electron Inner Radiation Belt After a Solar Flare Event," *J. Geophys. Res.*, 73, 17, 5792-5797, Sept. 1968.
- Pfizer, K. A., and J. R. Winckler, "Intensity Correlations and Substorm Electron Drift Effects in the Outer Radiation Belt Measured with the OGO 3 and ATS 1 Satellites," *J. Geophys. Res.*, 74, 21, 5005-5018, Oct. 1969.
- Pfizer, K. A., S. R. Kane, and J. R. Winckler, "Spectra and Intensity of Electrons in the Radiation Belts," *Space Res.*, 6, 702-713, 1966.
- Potter, W. H., "The Reduction and Analysis of Data From the Low-Frequency Radio Astronomy Experiment Aboard the OGO-IV Spacecraft," University of Michigan/Radio Astronomy Observatory, Report 70-5, July 1970.
- Prinz, D. K., and R. R. Meier, "OGO 4 Observations of the Lyman-Birge-Hopfield Emissions in the Day Airglow," *J. Geophys. Res.*, 76, 25, 6146-6158, Sept. 1971.
- Reed, E. I., and J. E. Blamont, "Some Results Concerning the Principal Airglow Lines as Measured From the OGO-II Satellite," *Proc. of the 7th Int. Space-Science Symposium, Vienna, 10-18 May 1966. Space Res.*, 7, 337-352, 1967.
- Reed, E. I., and J. E. Blamont, "Observations of the Conjugate SAR Arcs of September 28-30, 1967," *J. Geophys. Res.*, 79, 16, 2524-2525, June 1974.
- Reed, E. I., and S. Chandra, "The Global Characteristics of Atmospheric Emission in the Lower Thermosphere and Their Aeronomic Implications," to be published in *J. Geophys. Res.*, 1975.
- Reed, E. I., W. B. Fowler, C. W. Aitken, and J. F. Brun, "Some Effects of MeV Electrons on the OGO II (POGO) Airglow Photometers," NASA/GSFC Document X-613-67-132, Mar. 1967.
- Reed, E. I., W. B. Fowler, and J. E. Blamont, "An Atlas of Low-Latitude 6300-A (OI) Night Airglow from OGO 4 Observations," *J. Geophys. Res.*, 78, 25, 5658-5675, Sept. 1973.

- Regan, R. D., W. M. Davis, and J. C. Cain, "Detection of 'Intermediate Size' Magnetic Anomalies in Cosmos 49 and OGO 2, 4, and 6 Data", *Space Res.* 13, 2, 613-623, 1973.
- Rusch, D. W., "Satellite Ultraviolet Measurements of Nitric Oxide Fluorescence With a Diffusive Transport Model," *J. Geophys. Res.*, 78, 25, 5676-5686, Sept. 1973.
- Russell, C. T. and R. E. Holzer, "AC Magnetic Fields" in B. M. McCormac (ed.), *Particles and Fields in the Magnetosphere*, 1970, pp. 195-212, D. Reidel Publishing Co., Dordrecht, Holland.
- Russell, C. T., J. V. Olson, R. E. Holzer, and E. J. Smith, "OGO 3 Search Coil Magnetometer Data Correlated With the Reported Crossing of the Magnetopause at $6.6 R_E$ by ATS 1," *J. Geophys. Res.*, 73, 17, 5769-5775, Sept. 1968.
- Russell, C. T., R. E. Holzer, and E. J. Smith, "OGO 3 Observations of ELF Noise in the Magnetosphere, 1, Spatial Extent and Frequency of Occurrence," *J. Geophys. Res.*, 74, 3, 755-777, Feb. 1969.
- Russell, C. T., R. E. Holzer, and E. J. Smith, "OGO 3 Observations of ELF Noise in the Magnetosphere, 2, The Nature of the Equatorial Noise," *J. Geophys. Res.*, 75, 4, 755-768, Feb. 1970.
- Sagalyn, R. C., and M. Smiddy, "Magnetosphere Plasma Properties During a Period of Rising Solar Activity-OGO-III," *Space Res.* 8, 139-149, Proceedings of London Meeting, July 25-28, 1967.
- Sawyer, D., NSSDC, NASA/GSFC, to be published (private communication 1975).
- Scarabucci, R. R., "Analytical and Numerical Treatment of Wave Propagation in the Lower Ionosphere," Ph.D. Dissertation, Radioscience Lab., Stanford Electronics Labs., Stanford University, Stanford, Calif., Oct. 1969.
- Scarabucci, R. R., "Satellite Observations of Equatorial Phenomena and Defocusing of VLF Electromagnetic Waves," *J. Geophys. Res.*, 75, 1, 69-84, Jan. 1970.
- Schild, M. A., and L. A. Frank, "Electron Observations Between the Inner Edge of the Plasma Sheet and the Plasmasphere," *J. Geophys. Res.*, 75, 28, 5401-5414, Oct. 1970.
- Schwentek, H., G. Hartman, and R. W. Kreplin, "The Trend of Ionospheric Absorption During Shortwave Fade-Outs Related to the Trend of Enhancement of Solar X-ray Flux," *Radio Science*, 35-40, Jan. 1971.
- Scull, W. E., and G. H. Ludwig, "The Orbiting Geophysical Observatories," *Proceedings of the IRE*, 50, 2287-2296, Nov. 1962.
- Smith, R. L., and J. J. Angerami, "Magnetospheric Properties Deduced from OGO 1 Observations of Ducted and Nonducted Whistlers," *J. Geophys. Res.*, 73, 1, 1-20, Jan. 1968.
- Smith, E. J., R. E. Holzer, M. B. McLeod, and C. T. Russell, "Magnetic Noise in the Magnetosheath in the Frequency Range 3-300 Hz," *J. Geophys. Res.*, 72, 19, 4803-4813, Oct. 1967.
- Sugiura, M., "Equatorial Current Sheet in the Magnetosphere," *J. Geophys. Res.*, 77, 31, 6093-6103, Nov. 1972.
- Sugiura, M., and D. J. Poros, "A Magnetospheric Field Model Incorporating the OGO 3 and 5 Magnetic Field Observations," *Planet. Space Sci.*, 21, 1763-1773, Oct. 1973.
- Sugiura, M., B. G. Ledley, T. L. Skillman, and J. P. Heppner, "Magnetospheric-Field Distortions Observed by OGO 3 and 5," *J. Geophys. Res.*, 76, 31, 7552-7565, Nov. 1971.
- Taylor, Jr., H. A., "Parametric Description of Thermospheric Ion Composition Results," *J. Geophys. Res.*, 78, 1, 315-319, Jan. 1973.
- Taylor, Jr., H. A., and W. J. Walsh, "The Light-Ion Trough, the Main Trough and the Plasmapause," *J. Geophys. Res.*, 77, 34, 6716-6723, Dec. 1972.
- Taylor, Jr., H. A., H. C. Brinton, and M. W. Pharo, III, "Contraction of the Plasmasphere During Geomagnetically Disturbed Periods," *J. Geophys. Res.*, 73, 3, 961-968, Feb. 1968a.
- Taylor, Jr., H. A., H. C. Brinton, M. W. Pharo, III, and N. K. Rahman, "Thermal Ions in the Exosphere: Evidence of Solar and Geomagnetic Control," *J. Geophys. Res.*, 73, 17, 5521-5533, Sept. 1968b.
- Taylor, Jr., H. A., H. C. Brinton, D. L. Carpenter, F. M. Bonner, and R. L. Heyborne, "Ion Depletion in the High-Latitude Exosphere: Simultaneous OGO 2 Observations of the Light Ion Trough and the VLF Cutoff," *J. Geophys. Res.*, 74, 14, 3517-3528, July 1969.
- Taylor, Jr., H. A., H. C. Brinton, and A. C. Deshmukh, "Observations of Irregular Structure in Thermal Ion Distributions in the Duskside Magnetosphere," *J. Geophys. Res.*, 75, 13, 2481-2489, May 1970a.

Taylor, Jr., H. A., H. G. Mayr, and H. C. Brinton, "Observations of Hydrogen and Helium Ions During a Period of Rising Solar Activity," *Space Research* 10, 663-678, 1970b.

Taylor, Jr., H. A., J. M. Grebowsky, and W. J. Walsh, "Structured Variations of the Plasmapause: Evidence of a Corotating Plasma Tail," *J. Geophys. Res.*, 76, 28, 6806-6814, Oct. 1971.

Taylor, Jr., H. A., H. C. Brinton, and C. R. Smith, "Positive Ion Composition in the Magnetoionosphere Obtained from the OGO-A Satellite," *J. Geophys. Res.*, 70, 23, 5769-5781, Dec. 1975.

Teague, M. J., and J. I. Vette, "The Inner Zone Electron Model AE-5," NSSDC 72-10, Nov. 1972.

Tidman, D. A., "The Earth's Bow Shock Wave," *J. Geophys. Res.*, 72, 7, 1799-1808, Apr. 1967.

Tidman, D. A., and T. G. Northrop, "Emission of Plasma Waves by the Earth's Bow Shock," *J. Geophys. Res.*, 73, 5, 1543-1553, Mar. 1968.

Vasyliunas, V. M., "A Survey of Low-Energy Electrons in the Evening Sector of the Magnetosphere with OGO 1 and OGO 3," *J. Geophys. Res.*, 73, 9, 2839-2884, May 1968a.

Vasyliunas, V. M., "Low-Energy Electrons on the Day Side of the Magnetosphere," *J. Geophys. Res.*, 73, 23, 7519-7523, Dec. 1968b.

Walter, F., and J. J. Angerami, "Nonducted Mode of VLF Propagation Between Conjugate Hemispheres: Observations on OGO's 2 and 4 of the 'Walking-Trace' Whistler and of Doppler Shifts in Fixed Frequency Transmissions," *J. Geophys. Res.*, 74, 26, 6352-6370, Dec. 1969.

Whipple, E. C., J. M. Warnock, and R. H. Winkler, "Effect of Satellite Potential on Direct Ion Density Measurements Through the Plasmapause," *J. Geophys. Res.*, 79, 1, 179-185, Jan. 1974.

Wolfe, J. H., R. W. Silva, and M. A. Myers, "Preliminary Results from the Ames Research Center Plasma Probe Observations of the Solar Wind-Geomagnetic Field Interaction Region on IMP 2 and OGO 1," *Space Res.* 6, 680-700, 1966.

Wolff, C. L., "Optical Environment About the OGO 3 Satellite," *Science*, Vol. 158, 1045-1046, Nov. 24, 1967.

Yorks, R. G., and H. Weil, "OGO 2 Data Analysis Satellite Plasma Wake Study," U. of Michigan, Radio Astronomy Observatory, Report No. 70-1, Feb. 1970.

IV. SPACECRAFT AND EXPERIMENT CHARACTERISTICS WITH LITERATURE REFERENCES

OGO 1

SPACECRAFT CHARACTERISTICS

COMMON NAME OGO 1
 ALTERNATE NAMES EOGO 1, EGO-1,
 EGO-A, OGO-A, 00879,
 S49
 NSSDC ID 64-054A
 LAUNCH DATE 09/05/64
 WEIGHT IN ORBIT 487 kg
 LAUNCH SITE Cape Canaveral, United
 States
 LAUNCH VEHICLE Atlas-Agena B
 SPONSORING COUNTRY United States
 SPONSORING AGENCY NASA-OSSA

ORBIT PARAMETERS	INITIAL	LATER
Epoch Date	09/07/64	03/03/69
Apogee (km alt)	149,385	111,135
Perigee (km alt)	281	38,581
Period (min)	3839	3839
Inclination (deg)	31.2	58.1

PERSONNEL

Project Manager -
 W. E. Scull - NASA-GSFC - Greenbelt, Maryland
 Project Scientist -
 G. H. Ludwig - NASA-GSFC - Greenbelt, Maryland
 Program Manager -
 C. D. Ashworth - NASA Hq - Washington, DC
 Program Scientist -
 A. W. Schardt - NASA Hq - Washington, DC

BRIEF DESCRIPTION

The purpose of the OGO 1 spacecraft, the first of a series of six orbiting geophysical observatories, was to conduct many diversified geophysical experiments to obtain a better understanding of the Earth as a planet and to develop and operate a standardized observatory-type satellite. OGO 1 consisted of a main body that was parallelepiped in form, two solar panels, each with a solar-oriented experiment package (SOEP), two orbital plane experiment packages (OPEP), and six appendages EP-1 through EP-6 supporting the boom experiments. One face of the main body was designed to point toward the Earth (+z axis), and the line connecting the two solar panels (x axis) was intended to be perpendicular to the Earth-Sun-Spacecraft plane. The solar panels were able to rotate about the x axis. The OPEPs were mounted on and could rotate about an axis that was parallel to the z axis and attached to the main body. Due to a boom deployment failure shortly after orbital injection, the spacecraft was put into a permanent spin mode of 5 rpm about the z axis. This spin axis remained fixed with a declination of about -10 deg and right ascension of about 40 deg at launch. The local time of apogee was 2100 hr. OGO 1 carried 20 experiments. Twelve of these were particle studies and two were magnetic field studies. In addition, there was one experiment for each of the following types of studies -- Interplanetary Dust, VLF, Lyman-Alpha, Gegenschein, Atmospheric Mass, and Radio Astronomy. Real-time data were transmitted at 1, 8, or 64 kbs depending on the distance of the spacecraft from the Earth. Playback data were tape recorded at 1

kbs and transmitted at 64 kbs. Two wideband transmitters, one feeding into an omnidirectional antenna and the other feeding into a directional antenna, were used to transmit data. A special-purpose telemetry system, feeding into either antenna, was also used to transmit wideband data in real time only. Tracking was accomplished by using radio beacons and a range and range-rate S-band transponder. Because of the boom deployment failure, the best operating mode for the data handling system was the use of one of the wideband transmitters and the directional antenna. All data received from the omnidirectional antenna were noisy. During September 1964, acceptable data were received over 70 percent of the orbital path. Spacecraft operation was restricted to spring (approximately March, April, and May) and fall (approximately September, October, and November) due to spacecraft power supply limitations. There were 11 of these 3-month periods prior to spacecraft turnoff on November 25, 1969, after 22,631 hr of experiment operation. The spacecraft was then placed in a stand-by status until November 1, 1971, at which time all OGO 1 support was terminated.

SPACECRAFT/MISSION BIBLIOGRAPHY

Papers with major discussion of spacecraft, mission, testing, subsystems, or ground systems prepared by NASA project or project support personnel.
 A63-10333, A63-21527, A65-14349, A65-19503,
 A65-22431, A69-36674, A70-35303,
 N62-15053, N64-27251, N65-21656, N65-29296,
 N66-21006, N74-76913, N74-76932,
 B04384-000, B08396-000.

Papers with minor discussion of spacecraft, mission, testing, subsystems, or ground systems prepared by NASA project or project support personnel.
 N65-29783, N74-76912

Papers about spacecraft, mission, testing, subsystems, or ground systems prepared by NASA contractor personnel.
 A63-13537, A63-13629, A63-21528, A63-23249,
 A64-10864, A64-11240, A64-24447, A64-27303,
 A65-19528, A66-15919,
 N67-22257, N69-33977, N74-74623.

EXPERIMENTS

OGO 1, Anderson

EXPERIMENT NAME Solar Cosmic Rays
 NSSDC ID 64-054A-12
 PROJECT DESIGNATION 4901, A-01
 PERSONNEL
 PI - K.A. Anderson
 University of California - Berkeley, California
 OI - G.H. Pitt
 University of California - Berkeley, California

SPACECRAFT AND EXPERIMENT CHARACTERISTICS

BRIEF DESCRIPTION

This instrumentation consisted of a CsI crystal surrounded by a plastic anticoincidence shield and optically coupled to a photomultiplier tube. The system also contained a 32-channel pulse height analyzer. Although the principal objective of this experiment was to measure 3- to 90-MeV solar protons, the detector had no ability to discriminate between different kinds of particles. The system was mounted in SOEP-1 and had a 38-deg acceptance cone angle. Inflight calibration was provided. Counts in groups of four channels, accumulated over 31/32 of the telemetry frame time (1.152, 0.144, or 0.018 sec), were read out during successive telemetry frames. Some time before the experiment was turned on, the anticoincidence system failed. This resulted in high background rates due to galactic cosmic rays. Thus, the data were useful for studies of event morphology but not for determination of absolute fluxes. Although the detector axis was intended to point toward the Sun, a malfunction in the OGO 1 attitude control system prevented this. Otherwise, the experiment performed well from launch through November 25, 1969, when all experiments aboard OGO 1 were turned off.

BIBLIOGRAPHY

- PM: A67-41233, A69-31967, A71-19825,
B03937-000, B03944-000.
- OS: N69-34536.

OGO 1, Bohn

EXPERIMENT NAME Interplanetary Dust Particles

NSSDC ID 64-054A-07

PROJECT DESIGNATION 4916, A-16

PERSONNEL

PI - J.L. Bohn
Temple University - Philadelphia, Pennsylvania

OI - W.M. Alexander
Baylor University - Waco, Texas

BRIEF DESCRIPTION

This experiment was designed to measure the velocity and mass distributions of interplanetary dust particles with diameters of the order of 1 micron. The instrumentation consisted of four nearly identical meteoroid sensors located in a container mounted on the end of the 1.8-m EP-3 boom. Each sensor tube consisted of two thin films (1000-A thick aluminum and aluminum oxide), a grid, and a microphone. The sensors had openings in the plus or minus x, + y, and - z directions. Penetration of the aluminum film by a micrometeoroid produced a plasma cloud that was collected by the aluminum oxide film and started a 2-MHz clock. A plasma cloud was also produced when the micrometeoroid struck the microphone plate. The plasma cloud was collected by the grid, which stopped the clock and provided a measurement of the velocity of the particle. The resulting pulse height signal from the grid provided information on the kinetic energy and/or momentum of the particle. The + y sensor had an apparent failure. Moreover, the directionality of the particles could not be determined owing to the spin of OGO 1 and the low data sampling rate. The actual flux was so much lower than expected that only a few micrometeoroid events were observed.

BIBLIOGRAPHY

- PM: A66-15266,
N67-32070.
- PS: A68-29467.

OGO 1, Bridge

EXPERIMENT NAME Plasma Probe, Faraday Cup

NSSDC ID 64-054A-14

PROJECT DESIGNATION 4903, A-03

PERSONNEL

PI - H.S. Bridge
MIT - Cambridge, Massachusetts

OI - A.M. Bonetti
University of Florence - Florence, Italy

OI - B. Rossi
MIT - Cambridge, Massachusetts

OI - A.J. Lazarus
MIT - Cambridge, Massachusetts

OI - F. Scherb
MIT - Cambridge, Massachusetts

OI - V. Vasyliunas
MIT - Cambridge, Massachusetts

BRIEF DESCRIPTION

Two multigrad Faraday cups were used to study the directional intensity of protons and electrons of the solar wind, magnetosheath, and magnetotail. One single collector Faraday cup, located in SOEP-2, was used to study electrons in four energy windows between 125 eV and 2 keV. Currents in all four energy windows were measured every 9.2 seconds. The detector worked well from launch until November 25, 1969, when the spacecraft was turned off. Useful data were obtained, although observatory spin complicated data reduction. One split-collector Faraday cup was to be used to study protons but due to the unexpected spinup of the spacecraft, the data collected were useless.

BIBLIOGRAPHY

- PM: A68-17768, A68-28348, A69-19373, A71-30029,
N72-18715.
- PS: A73-33436.
- OS: N70-27302.

OGO 1, Cline

EXPERIMENT NAME Positron Search and Gamma Ray Spectrum

NSSDC ID 64-054A-15

PROJECT DESIGNATION 4904, A-04

PERSONNEL

PI - T.L. Cline
NASA-GSFC - Greenbelt, Maryland

OI - E.W. Hones, Jr.
IDA - Washington, DC

SPACECRAFT AND EXPERIMENT CHARACTERISTICS

BRIEF DESCRIPTION

This experiment was designed to determine whether low-energy (0 to 3 MeV) positrons are trapped temporarily or permanently in the Van Allen radiation region and whether low-energy solar and interplanetary positrons exist at the edge of the magnetic field of the Earth. It was also designed to detect gamma-ray bursts from the Sun in the energy interval from 80 keV to 1 MeV. The experimental apparatus, located in SOEP-1, consisted of three CsI crystals surrounded by a plastic anticoincidence shield, with the output of the whole unit being monitored by three PMs. It was primarily designed to search for interplanetary positrons by measuring the spectra of single or paired X-rays produced by the stopping of a positron. In another possible mode of data acquisition, single X-rays were monitored in one of the CsI spectrometers with 4π particle anticoincidence, which was virtually X-ray transparent above 80 keV. Once every 18.5 seconds, integral intensity measurements were made in each of the 16 energy levels equally spaced between 80 keV and 1 MeV, allowing for both temporal and spectral analysis of the data. Inflight calibration of the spectrometer was accomplished by monitoring the 511-keV annihilation line. The experiment did not achieve the desired objectives, but did obtain useful data. The basic difficulties were electrical interference and secular degradation of the response of the PMs. No important papers were produced using the data. The data, however, are currently (1975) being reexamined to see if they contain any information on gamma-ray bursts that have recently been noted in data from the Vela spacecraft.

BIBLIOGRAPHY

PM: A68-41427.
N74-77446.

PS: A74-30149.

OGO 1, Haddock

EXPERIMENT NAME Radio Astronomy
NSSDC ID 64-054A-09
PROJECT DESIGNATION 4918, A-18
PERSONNEL
PI - F.T. Haddock
University of Michigan - Ann Arbor, Michigan

BRIEF DESCRIPTION

This experiment was designed to measure the dynamic radio spectrum of solar radio noise bursts by observing frequency drift rate, frequency bandwidth, duration of fast-drift solar bursts, cosmic noise intensity, ionospheric electron densities (50 to 500 electrons/cc), atmospheric, auroral noise from the Earth to spacecraft, and radio noise generated in the terrestrial ionosphere and in interplanetary plasmas. The experiment was also capable of observing radio bursts from the planet Jupiter. The instrumentation, located in SOEP-1, consisted of a 9-m monopole antenna and a sweep frequency superheterodyne receiver. The receiver had automatic repetitive tuning from 2 to 4 MHz with a 2-sec sweep period. Automatic amplitude and frequency calibration was provided by a crystal calibrator that provided controlled amplitude pulses at 500-kHz intervals across the 2- to 4-MHz band. The antenna was a rolled beryllium copper strip that extended to about 9 m in a 1.27-cm tubular configuration. It was stored in a flat shape on a drum prior to the flight and was supposed to be deployed by a shunt-wound motor upon ground command after launch. However, problems were experienced with the deployment of the antenna, and, although a number of attempts were made, no indications of full deployment were ever received. Even though the antenna did not fully deploy, data were obtained because the experiment was not affected by the spin of OGO 1. The data, however, were of

little value because of the antenna problem and the high-noise environment. The experiment has been inoperable since November 1969.

BIBLIOGRAPHY

PM: N69-31345, N74-74631.

PS: N69-25437.

OGO 1, Hargreaves

EXPERIMENT NAME Radio Propagation
NSSDC ID 64-054A-05
PROJECT DESIGNATION 4914, A-14
PERSONNEL
PI - J.K. Hargreaves
ESSA - Boulder, Colorado
OI - R.S. Lawrence
ESSA - Boulder, Colorado
OI - R.B. Fritz
ESSA - Boulder, Colorado
OI - O.K. Garriott
Stanford University - Stanford, California

BRIEF DESCRIPTION

This experiment was used to explore the exosphere by studying the behavior of the columnar electron content between ground and spacecraft as the spacecraft rose from perigee in its very eccentric orbit. Simultaneous measurements were made of the differential doppler frequency and the Faraday rotation angle. The instrumentation consisted of a pair of radio beacons operating at harmonically related frequencies (40.01 and 360.09 MHz), which were modulated by 20- and 200-kHz signals. The 40-MHz transmitting antenna, located on EP-2, was a simple dipole with a gain of 2 db, while the 360-MHz antenna, located on EP-3, was a yagi with a gain of 8 db. Signals were received at a tracking antenna at Boulder from a maximum distance of 60,000 km. OGO 1 was planned as an Earth-stabilized spacecraft, but difficulties that appeared immediately after launch caused the spacecraft to spin at a rate of about 5 rpm. This introduced a number of unexpected complications in the interpretation and analysis of the data. The spin-axis orientation was not precisely known. Values of 42.5 deg in right ascension and -9 deg in inclination, suggested by independent experiments, were used in interpreting the beacon data, although the results did not require an accurate knowledge of this orientation.

BIBLIOGRAPHY

PM: A68-38439.
N66-12993, N69-24521.
B18548-000.

OM: A66-10892.

OGO 1, Helliwell

EXPERIMENT NAME VLF Noise and
Propagation
NSSDC ID 64-054A-08
PROJECT DESIGNATION 4917, A-17

SPACECRAFT AND EXPERIMENT CHARACTERISTICS

PERSONNEL

- PI - R.A. Helliwell
Stanford University - Stanford, California
- OI - J.J. Angerami
Stanford University - Stanford, California
- OI - L.H. Rorden
Stanford University - Stanford, California

BRIEF DESCRIPTION

This experiment consisted of four VLF radio receivers to be used for study of natural VLF noise occurrences at orbital altitudes. The receiver systems consisted of an inflatable 2.9-m loop antenna, a preamplifier stage at the end of a long boom (EP-5), and the receiver electronics packages in the main body of the spacecraft. Three step-frequency receivers, covering frequency ranges of 0.2 to 1.6 kHz, 1.6 to 12.5 kHz, and 12.5 to 100 kHz, each observed a complete spectrum of 256 signal strength values once every 2.3, 18.4, or 147.2 sec depending upon the selected mode of operation. Observations from these three receivers were tape recorded at 1 kbs or observed in real time at 1, 8, or 64 kbs. The tape is read out upon command at the 64-kbs rate. The other receiver is a broadband receiver observing signals from 0.3 to 12.5 kHz. These data were not tape recorded, but observed only in real time on the special purpose telemetry channel. Data from the three receivers (PCM data) were recorded for over half the time in orbit with high bit rate usually when the spacecraft was near perigee, and low bit rate near apogee. Broadband resolution depended upon the rayspan spectrum analyzer used to process the tape. This equipment can provide up to 10-msec time resolution and up to 30-Hz frequency resolution. The broadband data are available only for relatively short portions of the spacecraft operating lifetime since they were received only when the spacecraft was scheduled to transmit in range of a telemetry station. This experiment operated nominally during the active spacecraft lifetime.

BIBLIOGRAPHY

- PM: A68-17728, A69-25153, A69-31981, A70-15117, A70-27183, N67-30831, N67-37021, N70-15678, N70-33156, N73-16344.
- PS: A68-38428.
- PC: N74-74765.
- OS: A68-14098, A70-30078, A70-40479, A72-21189, B00969-000.

OGO 1, Heppner

EXPERIMENT NAME Magnetic Survey Using Two Magnetometers
NSSDC ID 64-054A-02
PROJECT DESIGNATION 4911, A-11
PERSONNEL
PI - J.P. Heppner
NASA-GSFC - Greenbelt, Maryland
OI - B.G. Ledley
NASA-GSFC - Greenbelt, Maryland
OI - M. Sugiura
NASA-GSFC - Greenbelt, Maryland
OI - R.M. Campbell
NASA-GSFC - Greenbelt, Maryland
OI - T.L. Skillman
NASA-GSFC - Greenbelt, Maryland

BRIEF DESCRIPTION

OGO 1 was equipped with a three-axis, dual range, fluxgate magnetometer for measuring vector fields up to 30 and 500 gammas full-scale, and a four-cell rubidium vapor magnetometer for measuring scalar fields of 3 to 14,000 gammas, with programmed bias fields incorporated for vector measurements in weak fields. The instrument was intended to measure magnetospheric, transition region, and interplanetary magnetic fields. The sensors were located on the EP-6 boom. At launch, boom EP-6 apparently failed to deploy, causing the rubidium vapor magnetometer to be left in a high-gradient field where it could not operate, and the fluxgate to be left in a position where spacecraft fields limited its accuracy to about three gammas. In the 1-kb mode, each fluxgate was sampled 1.7 times per sec and 8 and 64 times faster in the other modes.

BIBLIOGRAPHY

- PM: A68-11011, A68-12172, A72-12084.
- PS: N70-19313.
- OS: A71-30028.

OGO 1, Konradi

EXPERIMENT NAME Trapped Radiation Scintillation Counter
NSSDC ID 64-054A-16
PROJECT NAME 4905, A-05
PERSONNEL
PI - A. Konradi
NASA-GSFC - Greenbelt, Maryland
OI - L.R. Davis
NASA-GSFC - Greenbelt, Maryland
OI - R.A. Hoffman
NASA-GSFC - Greenbelt, Maryland
OI - J.M. Williamson
NASA-GSFC - Greenbelt, Maryland

BRIEF DESCRIPTION

The objectives of this experiment were (1) to study the temporal and spatial variations of the trapped particle intensities, pitch angle distributions, and energy spectra of electrons (10 to 100 keV) and protons (120 to 4500 keV), and (2) to determine particle lifetimes, isolate processes by which trapped particles are lost, and define the sources and accelerating mechanisms of trapped particles. The experiment, located in OPEP-2, consisted of a filter wheel, wheel stepping motor, phosphor scintillator, PM, electrometer, and count rate meter. The detector had two entrance apertures for particles, one aligned with the phototube axis and one at 90 deg to this axis. Both protons and electrons could enter the aligned opening and reach the phosphor. Only electrons could enter the 90-deg opening, scatter off a gold disc, and reach the phosphor. The counting rate in the aligned opening measured proton flux, and the current therein measured the total energy flux of electrons, protons, etc. The current in the 90-deg opening measured the electron energy flux. Different thickness absorbers on the wheel provided spectral information. The experiment worked until the absorber wheel stopped on December 2, 1964. Data recorded after this date are unusable.

BIBLIOGRAPHY - None found

SPACECRAFT AND EXPERIMENT CHARACTERISTICS

OGO 1, Mange

EXPERIMENT NAME Geocoronal
Lyman-Alpha Scattering

NSSDC ID 64-054A-10

PROJECT DESIGNATION 4919, A-19

PERSONNEL

PI - P.W. Mange
Naval Research Laboratory - Washington, D.C.

BRIEF DESCRIPTION

The objective of this experiment was to measure the intensity of hydrogen Lyman-Alpha radiation (1216 Å) scattered by neutral hydrogen at 5 to 20 R_E . This wavelength is the fundamental resonance line of neutral atomic hydrogen, and these intensity measurements, therefore, provide a measure of the density of neutral hydrogen in the hydrogen geocorona. The instrumentation consisted of four ion chambers mounted on the anti-Earth door of OGO 1. Each ion chamber was filled with nitric oxide gas and had lithium fluoride windows. The ion chambers were sensitive in the 1050- to 1350-Å band. The instrumentation faced the Sun steadily for more than 4 months before viewing the Sun-free sky, causing detector degradation. The maximum intensities observed were lower than those measured by the OGO 3 ion chambers by a factor of more than 30. This difference has been attributed primarily to the spurious response of the damaged detectors to radiation belt particles. The data obtained from the experiment were not a measure of the Lyman-Alpha intensity because of the detector degradation.

BIBLIOGRAPHY -- None found

OGO 1, McDonald

EXPERIMENT NAME Cosmic-Ray Isotopic
Abundance

NSSDC ID 64-054A-17

PROJECT DESIGNATION 4906, A-06

PERSONNEL

PI - F.B. McDonald
NASA-GSFC - Greenbelt, Maryland

OI - G.H. Ludwig
NASA-GSFC - Greenbelt, Maryland

BRIEF DESCRIPTION

To analyze the charge and energy spectra of the primary cosmic radiation, a dE/dx vs E plastic scintillator telescope measured ions with Z values between 1 and 8 and with energies in a Z -dependent range (for example, for $Z=1$ or 2, the range was 15 to 80 MeV/nucleon, for $Z=6$, the range was 25 to 145 MeV/nucleon). Pulse height analysis is performed on 1, 8, or 64 events per sec. Count rates in various telescope modes are also obtained. Three orthogonal GM telescopes were also used to monitor protons above 28 MeV and 70 MeV. The detectors, located in the main body, functioned normally while the spacecraft was tracked. The boom which was folded across this experiment failed to deploy, and this resulted in significant degradation of the experimental data. Data were obtained from launch until November 1969. Coverage was high during fall and spring of each year, and low during winter and summer.

BIBLIOGRAPHY

PM: A63-20022, A66-26348, A66-34847, A67-19913,
A68-41421, A68-41431, A71-18137,
B01634-000.

OGO 1, Sagalyn

EXPERIMENT NAME Spherical Ion and
Electron Trap

NSSDC ID 64-054A-03

PROJECT DESIGNATION 4912, A-12

PERSONNEL

PI - R.C. Sagalyn
AFCRL - Bedford, Massachusetts

OI - M. Smiddy
AFCRL - Bedford, Massachusetts

BRIEF DESCRIPTION

The objective of this experiment was to measure the flux, temperature, and energy distribution of electrons and positive ions having energies ranging from thermal up to 1000 eV, as a function of position (altitude, L-shell, etc.) and of time (solar and magnetic activity). Two spherical electrostatic sensors, used as omnidirectional plasma probes, were mounted on a short boom (EP-1). One detector was designed for electron measurements and consisted of two concentric spheres. The outer sphere was a grid that allowed the ambient electrons to pass through and be collected by the inner sphere. The second sensor, which was designed to measure positive ions, consisted of three concentric spheres, an outer aperture grid, an inner collecting sphere, and a suppressor grid between them. Collector currents were measured with electrometers. Logic circuits controlled the sequence of the measurement operations, so that different potentials were applied between the spheres in prescribed patterns. A complete measurement cycle took 25.6 min. Essentially, the experiment was designed to cycle in three major modes of operation to provide data on the flux of charged particles, the mean particle temperatures, and the energy distributions of the plasma particles, respectively. The output currents from each sensor were calibrated once per experiment cycle. The instrument operated 7251 hr and failed in September 1966.

BIBLIOGRAPHY

PM: A72-23011.

PC: N70-28003.

OGO 1, Simpson

EXPERIMENT NAME Cosmic-Ray Spectra and
Fluxes

NSSDC ID 64-054A-18

PROJECT DESIGNATION 4907, A-07

PERSONNEL

PI - J.A. Simpson
University of Chicago - Chicago, Illinois

OI - C.Y. Fan
University of Chicago - Chicago, Illinois

Nov. 10, 1975

SPACECRAFT AND EXPERIMENT CHARACTERISTICS

BRIEF DESCRIPTION

Three solid-state particle telescopes were used to measure the intensity and energy distribution of cosmic rays. A dE/dx vs E telescope resolved the nuclear composition of cosmic rays in the energy range from 22 to 103 MeV/nucleon (charge resolution ranged through $Z = 26$, energy per nucleon intervals approximately proportional to Z^2/A). A dE/dx vs range telescope (proton-alpha telescope) detected protons and alpha particles in the energy range from 1.4 to 33 MeV/nucleon, and a single-element low-energy proton telescope (OPEP telescope) was primarily sensitive to protons in the energy range from 1.4 to 3.7 MeV. The composition and proton-alpha telescopes were located in the main body and oriented parallel to the spacecraft z axis. Pulse height information was obtained from the composition telescope using one 256-channel and two 512-channel pulse height analyzers. This allowed pulse height analysis of particles in four energy intervals -- for protons 5 to 11 MeV, 11 to 22 MeV, 22 to 103 MeV, and greater than 103 MeV. Pulse height information sent back from the proton-alpha telescope allowed pulse height analysis of particles in two energy ranges, protons 1.4 to 8.6 MeV and 8.6 to 33 MeV. This transmission used one 256-channel pulse height analyzer, while count rate information was sent back from all three telescopes. The time resolution ranged from about one measurement per 0.02 sec to about one measurement per 147 sec, depending on the counting mode and the telemetry bit rate. The experiment was not affected by the observatory spin, and useful data were obtained.

BIBLIOGRAPHY

PM: A66-34754, A66-34833, A67-11687, A67-27249, A67-37412, A68-41420, A68-41434, A69-20067, A69-20068, B03716-000.

OGO 1, Smith

EXPERIMENT NAME Triaxial Search Coil Magnetometer
NSSDC ID 64-054A-01
PROJECT DESIGNATION 4910, A-10
PERSONNEL
PI - E.J. Smith
NASA-JPL - Pasadena, California
OI - R.E. Holzer
University of California - Los Angeles, California

BRIEF DESCRIPTION

The OGO 1 triaxial search coil magnetometer was designed to measure the magnetic field fluctuations from 0.01 to 1 kHz. Due to a spacecraft malfunction, the OGO spacecraft assumed a spin-stabilized mode with a 12-sec period. This meant the magnetometer output was modulated with an approximately sinusoidal signal, providing a measure of the direct current (dc) component of the magnetic field perpendicular to the spin axis as well as the alternating current (ac) data. The magnetometer assembly was on EP-5, a 6.1-m boom, and the electronics system was in the body of the spacecraft. The sensitivity was 10 microvolts per gamma-sec. The low-frequency channel was sampled five times every 1.152 sec by the telemetry system when the data rate was 1 kbs, and proportionally faster for the higher telemetry rates of 8 and 64 kbs. However, due to the spacecraft spin, the highest bit rate could not be used when the spacecraft was more than 10 R_E away. The upper frequency cutoff (to avoid aliasing in the data) was 2 Hz for the 1- and 8-kbs telemetry rates, and 130 Hz for the 64-kbs rate. The high-frequency channel provided spectral analysis information for frequencies from 1 to 10 kHz in five steps. The experiment operated satisfactorily, averaging about 4000 hr of data per year.

IV-6

BIBLIOGRAPHY

PM: A66-23148, A67-40804, A69-36675, A70-15127, A72-44857.
PS: A68-13469, N73-10791.
PC: N69-72494.
OS: A70-27594, A72-21189.

OGO 1, Taylor

EXPERIMENT NAME Positive Ion Composition
NSSDC ID 64-054A-06
PROJECT DESIGNATION 4915, A-15
PERSONNEL
PI - H.A. Taylor, Jr.
NASA-GSFC - Greenbelt, Maryland
OI - N.W. Spencer
NASA-GSFC - Greenbelt, Maryland

BRIEF DESCRIPTION

The instrumentation for this OPEP-1 experiment consisted of two ceramic Bennett radio-frequency mass spectrometers to measure thermal atmospheric positive ions in the range 1 to 45 amu. The low-range mass spectrometer measured ions with mass-to-charge ratios from 1 to 6 amu, with a resolution of 0.5 amu. The high-range mass spectrometer measured ions with mass/energy values from 7 to 45 amu, with a resolution of 1 in 20 amu. Ion concentrations from 5 ions to 10^6 ions per cc could be measured. The time required for a complete scan of the mass range was 64 sec, which corresponded to a spatial resolution of about 300 km. The successful operation of the experiment provided the first high-resolution in situ direct measurements of the positive ion composition, from an altitude of less than 1000 km to interplanetary space and beyond the boundary of the magnetosphere.

BIBLIOGRAPHY

PM: A63-12209, A66-14781, A68-19744, A68-37114, A69-23777, A70-26568.
PS: A68-41673.
OM: A69-25153, A69-25157.
OS: A68-37940, A70-41087, A71-30951, N74-74635.

OGO 1, Van Allen

EXPERIMENT NAME Trapped Radiation and High-Energy Protons
NSSDC ID 64-054A-19
PROJECT DESIGNATION 4908, A-08

SPACECRAFT AND EXPERIMENT CHARACTERISTICS

PERSONNEL

PI - J.A. Van Allen
University of Iowa - Iowa City, Iowa
OI - L.A. Frank
University of Iowa - Iowa City, Iowa

BRIEF DESCRIPTION

This experiment was designed to detect charged particles and measure omnidirectional intensities of outer belt electrons to understand the origin of the belts and the fluctuations in the belts. The detector composed of GM tubes and solid-state junction devices was capable of measuring electrons of energies greater than 40, 150, and 1600 keV and protons of energies greater than 0.5, 3.5, and 16 MeV. The instrumentation was located on the EP-2 boom. The experiment was not seriously affected by observatory spin, and useful data were obtained.

BIBLIOGRAPHY

PM: N67-31362, N67-40126, N69-12899, N74-76911.

OGO 1, Whipple

EXPERIMENT NAME Planar Ion and Electron Trap
NSSDC ID 64-054A-04
PROJECT DESIGNATION 4913, A-13

PERSONNEL

PI - E.C. Whipple
ESSA - Boulder, Colorado
OI - B.E. Troy, Jr.
NASA-GSFC - Greenbelt, Maryland

BRIEF DESCRIPTION

This experiment was flown to measure densities and energy distributions of thermal ions and electrons over the altitude range from below the F-maximum region of the ionosphere to several R_E . In addition the experiment was capable of yielding some data concerning ion masses, fluxes and directions of quasi-energetic particles, and the polarity and magnitude of the vehicle potential. The sensor, located in OPEP-1, was an electron and ion trap that consisted of four parallel circular plane grids in front of a collecting plate. The current to the collector was measured by a vibrating reed electrometer with an automatic range change for each decade of current from 10^{-1} to 10^{-6} amp. Four modes of experiment operation were used, namely a low-resolution and a high-resolution mode for both ions and electrons. In each mode, a variable potential was applied to one grid in the trap, while the potentials on each of the other grids and the collector were held constant. The average time to complete a mode was between 12 and 15 sec, and the complete cycle of four modes averaged less than 1 min. The measured current and applied varied voltages were digitized and stored in the experiment shift register until read out to the spacecraft telemetry system. The sensors worked, but, because of observatory spin, the data were of very little value. The experiment failed in December 1967.

BIBLIOGRAPHY

PM: N74-74638.
PS: A69-31976, A70-13994, A73-33436.

OGO 1, Winckler

EXPERIMENT NAME Ionization Chamber
NSSDC ID 64-054A-20
PROJECT DESIGNATION 4909, A-09

PERSONNEL

PI - J.R. Winckler
University of Minnesota - Minneapolis, Minnesota
OI - S.R. Kane
University of Minnesota - Minneapolis, Minnesota
OI - R.L. Arnoldy
University of Minnesota - Minneapolis, Minnesota

BRIEF DESCRIPTION

This experiment, designed to measure the ionization due to primary cosmic rays, consisted of a 17.8-cm integrating ionization chamber with a resetting drift-type electrometer. The system was mounted on a 1.2-m boom (EP-4) extending from the main body of the spacecraft along the y axis. The chamber responded to electrons and protons with energies greater than 0.6 and 12 MeV, respectively, and to X-rays from 10 to 50 keV. The ionization current was measured by a vacuum tube electrometer the output of which, as a function of time, was an automatically resetting sawtooth ramp voltage between 0 and 5 volts. Data were telemetered in three independent forms through three digital words and one analog word, each of which was telemetered once every 1.152 sec when the OGO system was operating at 1 kbs. The sampling rate linearly increased with the telemetry rate. This experiment performed well from launch through November 25, 1969, when all experiments aboard OGO 1 were turned off.

BIBLIOGRAPHY

PM: A65-33664, A67-25807, A67-41232, A68-22450, A68-35480, A69-12740, A69-22182, A70-15106, A71-18128, N67-13710, N68-10422, N68-23026, N70-17448, N70-17624, N72-28802, N74-18420, N74-21445, N74-74639.

PS: A66-34768.

OS: A69-33055, A69-34227, A70-30059, A71-27654, A73-14962.

OGO 1, Winckler

EXPERIMENT NAME Electron Spectrometer
NSSDC ID 64-054A-21
PROJECT DESIGNATION 4909, A-09

PERSONNEL

PI - J.R. Winckler
University of Minnesota - Minneapolis, Minnesota
OI - K.A. Pfitzer
University of Minnesota - Minneapolis, Minnesota
OI - R.L. Arnoldy
University of Minnesota - Minneapolis, Minnesota

BRIEF DESCRIPTION

The objective of this experiment was to measure the electron energy spectrum in the radiation belts for the energy range from 50 keV to 4 MeV. The experiment consisted of a five-channel electron spectrometer containing an analyzing electromagnet, a plastic scintillator crystal, a PM, and a pulse height analyzer. The

SPACECRAFT AND EXPERIMENT CHARACTERISTICS

analyzing electromagnet was used to define the five energy channels. The pulse height analyzer accepted only pulses corresponding to the particular energy channel being sampled. In this way, the background due to Bremsstrahlung and penetrating particles was reduced because only those background pulses in the narrow energy band being analyzed were counted. This system was mounted in the main body of the spacecraft and looked out in a direction 10 deg off the spacecraft z axis, with a 15-deg acceptance cone. Since OGO 1 was spin stabilized (about its z axis) shortly after launch, the acceptance cone was effectively increased to 35 deg. Directional measurements of electrons were made in five contiguous, logarithmically equispaced energy channels between 50 and 4000 keV. Background particles were counted by operating the spectrometer without the electromagnet. The system sampled the five spectral intervals and five background intervals every 2.304 sec when the OGO 1 system was operating at 1 kbs. The sampling rate increased linearly with the telemetry bit rate. Data from each of the five channels were telemetered as one digital word. This experiment performed well from launch through November 25, 1969, when all experiments aboard OGO 1 were turned off.

BIBLIOGRAPHY

- PM: A67-25807, A68-41697, A70-30090,
N67-13710, N69-19899, N70-17448, N70-17624,
N72-28802, N74-74639.
- OM: N73-20842, N74-20502, N74-20503.
- OS: A70-30358, A71-33948,
N66-35685, N67-19899, N74-74636.

OGO 1, Wolfe

EXPERIMENT NAME Electrostatic Plasma
Analysis (Protons
0.1-18keV)

NSSDC ID 64-054A-13

PROJECT DESIGNATION 4902, A-02

PERSONNEL

PI - J.H. Wolfe
NASA-ARC - Moffett Field, California

BRIEF DESCRIPTION

This experiment was designed to study the positive ion component of the solar wind plasma. Three quadrispherical electrostatic analyzers, two looking into the orbital plane OPEP-2 and one solar oriented SOEP-2, were to be used to detect protons in 30 steps in the range 100 to 18,000 eV. The unintended spacecraft spin made the data analysis very complicated. The sensors could serve as a detector for the magnetopause and bow shock, however.

BIBLIOGRAPHY

- PM: A65-25921, A65-29239.

OGO 1, Wolff

EXPERIMENT NAME Gegenschein
Photometry

NSSDC ID 64-054A-11

IV-8

PROJECT DESIGNATION 4920, A20

PERSONNEL

- PI - C.L. Wolff
NASA-GSFC - Greenbelt, Maryland
- OI - K.L. Hallam
NASA-GSFC - Greenbelt, Maryland
- OI - S.P. Wyatt
University of Illinois - Urbana, Illinois

BRIEF DESCRIPTION

This experiment was designed to measure the amount of solar light that is scattered by particles in space (dust, etc.) in the neighborhood of the anti-solar point. This light contribution to the night sky is called the gegenschein. The basic data from this experiment were to be pictures of the sky at the antisolar point taken by a television (TV) camera and telemetered to Earth as a 22 x 32 matrix. The experimental package, located in SOEP-2, was a photoelectric camera that formed images of the sky in the visible and near-visible light. The data from this assembly were transmitted back to Earth where they were reconstructed into pictures. Each of these pictures covered about 100 square degrees of sky with a resolution of 0.5 deg. The package consisted of -- (1) a four element f/1.5 objective lens, (2) a filter wheel containing five filters that covered the range from 3000 to 7000 A, (3) an S-20 cathode deposited on a thin, curved window of Corning 9741 ultraviolet transmitting glass, (4) an image dissector tube named the Star Tracker FW 143B made by the IIT Corporation, and (5) an electronic unit that amplified and counted the current pulses coming from the tube due to the individual photons arriving at the photocathode. The system was designed to operate at low light levels. Its overall quantum efficiency was of the order of 5 percent. Unfortunately, upon attaining orbit, OGO 1 went into an uncontrolled spin, and the experiment failed to achieve its experimental objective. In addition, after three months in orbit, the filter wheel refused to rotate due to an electrical failure in the wheel drive circuit. Despite the failure to achieve the initial goals of the experiment, an interesting study was made determining the effects of the Van Allen belt particle fluxes on the scientific package.

BIBLIOGRAPHY

- PM: A67-12055.
- PS: N64-27813.

OGO 2

SPACECRAFT CHARACTERISTICS

COMMON NAME OGO 2
 ALTERNATE NAMES OGO-C, POGO 1, S 50,
 01620
 NSSDC ID 65-081A
 LAUNCH DATE 10/14/65
 WEIGHT IN ORBIT 520 kg
 LAUNCH SITE Vandenberg AFB,
 United States
 LAUNCH VEHICLE Thrust-Augmented
 Thor-Agena D
 SPONSORING COUNTRY United States
 SPONSORING AGENCY NASA-OSSA

ORBIT PARAMETERS INITIAL LATER

Epoch Date	10/15/65	01/27/72
Apogee (km alt)	1510	1272
Perigee (km alt)	414	415
Period (min)	104	101.7
Inclination (deg)	87.4	87.4

PERSONNEL

Project Manager -
 W. E. Scull - NASA-GSFC - Greenbelt, Maryland

Project Scientist -
 N. W. Spencer - NASA-GSFC - Greenbelt, Maryland

Program Manager
 C. D. Ashworth - NASA Hq - Washington, D.C.

Program Scientist
 R. F. Fellows - NASA Hq - Washington, D.C.

BRIEF DESCRIPTION

OGO 2 was a large observatory instrumented with 20 experiments designed to make simultaneous correlative observations of aurora and airglow emissions, energetic particles, magnetic field variations, ionospheric properties, etc., especially over the polar areas. OGO 2 consisted of a main body, generally parallelepiped in form, two rectangular solar panels, each with a solar-oriented experiment package (SOEP), and two orbital-plane experiment packages (OPEP). It also included six experiment packages (EP-1, -2, -3, -4, -5 and -6) mounted on booms extending generally fore and aft of the spacecraft along the y axis. Antenna and attitude control fixtures also extended from separate and/or EP booms. The main body was attitude-controlled by use of horizon scanners and gas jets and was designed to point toward the Earth (z axis). The axis connecting the two solar panels (x axis) was designed to oscillate to remain perpendicular to the Earth-Sun-spacecraft plane. The solar panels activated by sun sensors could rotate about this x axis to obtain maximum radiation for the solar cells and concurrently orient the SOEP properly. The OPEPs were reoriented on either end of an axis that was parallel to the z axis and attached to the forward end of the main body. These OPEP sensors normally were maintained looking forward in the orbital plane of the satellite. To maintain this orientation, the OPEP axis could rotate over a 90-deg region. In addition, an angular difference of over 90 deg was possible between the orientation of the upper and lower OPEP packages. The SOEP contained four experiments, and the OPEP contained five experiments. Newton's particle experiment failed on launch, and Kreplin's solar X-ray experiment failed shortly thereafter. Soon after achieving orbit, difficulties in maintaining earth lock with horizon scanners caused exhaustion of attitude control gas by October 23, 1965, 10 days after launch. At this time, the spacecraft entered a spin mode (about 0.11 rpm) with a large coning angle about the previously vertical axis. Five experiments became useless when the satellite went into this spin

mode. Six additional experiments were degraded by this loss of attitude control. By April 1966, both batteries had failed, so subsequent observations were limited to sunlit portions of the orbit. By December 1966, only eight experiments were operational, five of which were not degraded by the spin mode operation. By April 1967, the tape recorders had malfunctioned and only one third of the recorded data could be processed. Spacecraft power and periods of operational scheduling conflicts created six large data gaps, so that data were observed on a total of about 306 days of the two-year 18-day total span of observed satellite data to November 1, 1967. The data gaps were -- (a) October 24, 1965, to November 5, 1965, (b) December 6, 1965, to January 7, 1966, (c) April 9, 1966, to June 21, 1966, (d) September 2, 1966, to November 18, 1966, (e) December 27, 1966, to April 11, 1967, and (f) May 9, 1967 to September 19, 1967. The spacecraft was shut down on November 1, 1967, with eight experiments still operational. It was reactivated for two weeks in February 1968 to operate Experiment C-O6 (J. Cain). The spacecraft was kept in a stand-by status until November 1, 1971, at which time OGO 2 operations were completely terminated.

SPACECRAFT/MISSION BIBLIOGRAPHY

Papers with major discussion of spacecraft, mission, testing, subsystems, or ground systems prepared by NASA project or project support personnel.

A63-10333, A63-21527, A65-14349, A69-36674,
 A70-35303.
 N64-23517, N65-18269, N74-76913, N74-76932.

Papers with minor discussion of spacecraft, mission, testing, subsystems, or ground systems prepared by NASA project or project support personnel.

N67-18763.

Papers about spacecraft, mission, testing, subsystems, or ground systems prepared by NASA contractor personnel.

A63-13537, A63-13629, A63-21528, A64-10864,
 A65-19528.
 N64-13388, N74-74623, N74-74661.
 B00570-000.

EXPERIMENTS

OGO 2, Anderson

EXPERIMENT NAME Cosmic-Ray Ionization
 NSSDC ID 65-081A-06
 PROJECT DESIGNATION 5007, C-07

PERSONNEL

PI - H.R. Anderson
 Rice University - Houston, Texas

OI - V.H. Neher
 Cal Tech - Pasadena, California

BRIEF DESCRIPTION

This experiment was designed to measure cosmic-ray and solar flare particle intensities (protons above 10 MeV, electrons above 0.5 MeV) using an ion chamber. The ion chamber was mounted at the end of spacecraft boom EP-1, about 2.5 m from the main body of the spacecraft. Because the ion chamber had omnidirec-

SPACECRAFT AND EXPERIMENT CHARACTERISTICS

tional sensitivity, except for negligible shadowing by the spacecraft, the slow rolling of the spacecraft did not adversely affect the instrument. The experiment operated normally from October 14, 1965, to April 2, 1966.

BIBLIOGRAPHY

PM: A68-43450, A69-28950, A69-31967, A70-31902,
A70-31903,
N74-74624, N74-76923.
PS: N69-34536.

OGO 2, Barth

EXPERIMENT NAME UV Spectrometer,
1100-3400A
NSSDC ID 65-081A-12
PROJECT DESIGNATION 5014, C-14
PERSONNEL
PI - C.A. Barth
University of Colorado - Boulder, Colorado
OI - L.J. Wallace
Kitt Peak National Observatory - Tucson, Arizona
OI - E.F. Mackey
Packard-Bell - Newbury Park, California

BRIEF DESCRIPTION

The purpose of this experiment was to measure the Earth's ultraviolet spectra caused by the aurora, dayglow, twilight glow, and nightglow. The experiment objectives included measurements of the atomic hydrogen Lyman-Alpha 1216-A airglow on both the day and night sides of the Earth, the atomic oxygen 1304-A dayglow and twilight glow, and the emission features of the ultraviolet aurora. These measurements, obtained as a function of location and time, were to be correlated with other appropriate data. The instrumentation consisted of an Ebert-Fastie scanning spectrometer and an electronic subsystem located in the main body. The spectral region of measurement, from 1100 to 3400 A, was scanned with a resolution of 20 A. This experiment did not achieve the desired objectives, as the satellite was not properly stabilized. Little good data were received, and the experiment operated only 499 hrs.

BIBLIOGRAPHY

OS: N69-18074.

OGO 2, Cain

EXPERIMENT NAME Magnetic Survey,
Rubidium Vapor
Magnetometer
NSSDC ID 65-081A-05
PROJECT DESIGNATION 5006, C-06
PERSONNEL
PI - J.C. Cain
NASA-GSFC - Greenbelt, Maryland
OI - R.A. Langel
NASA GSFC - Greenbelt, Maryland

BRIEF DESCRIPTION

The primary objectives of this experiment were to refine the then available analytical description of the main geomagnetic field (as part of the U.S. contribution to the World Magnetic Survey) and to measure the secular change in the main field. The detector system, located in EP-6, consisted of two dual-cell, optically pumped, self-oscillating, rubidium-85 vapor magnetometers. The oscillation frequency of the system was directly proportional to the magnitude of the ambient magnetic field. This frequency was counted by two electronic scalars for alternate half-seconds. The oscillation frequency of the magnetometer was also transmitted in real time on one channel of the spacecraft's special-purpose telemeter to provide information on field fluctuations. This magnetometer system made scalar measurements over a range from 15,000 to 64,000 gammas, and had an accuracy of 0.5 to 1.5 gammas over this range. In spite of the spacecraft attitude control system problems, the magnetometer functioned well. The instrument operation was nominal for the first six months of the satellite lifetime, after which a failure of one scalar power supply caused the loss of the special purpose telemetry signal and half of the digital data. The reduction in the scientific usefulness of the data received from the remaining scalar was minor, however, because of the redundancies built into the system. The rest of the data from the magnetometer were obtained with the remaining scalar until May 1967, and then in the interval from September 19 to October 2, 1967, during which time data collection was very intermittent.

BIBLIOGRAPHY

PM: A67-23244, A67-36513, A67-36901, A68-26625,
A68-42083, A69-11125, A69-37490, A69-42428,
A70-39349, A71-29903, A71-33946, A72-12081,
A74-34019,
N67-30147, N67-37398, N71-32190, N74-13566,
N74-17058.
PS: A73-41374.
N64-27355, N72-23341, N74-20982.

OGO 2, Donley

EXPERIMENT NAME Positive Ion Study
NSSDC ID 65-081A-19
PROJECT DESIGNATION 5019, C-19
PERSONNEL
PI - J.L. Donley
NASA-GSFC - Greenbelt, Maryland
OI - R.E. Bourdeau
NASA-GSFC - Greenbelt, Maryland

BRIEF DESCRIPTION

This instrument was a planar retarding potential analyzer designed to measure ion composition and density and temperature of electrons and ions. The sensor, located in OPEP-1, consisted of three grids and a collector. Voltage-versus-current profiles could be obtained by means of controlled voltages and voltage sweeps on the grids. From these profiles, density, temperature, and composition data could be calculated. The instrument was designed so that the aperture grid faced in the direction of spacecraft motion. Due to the failure of the three-axis stabilization system ten days after launch, the instrument could not be oriented properly. The subsequent data obtained were not scientifically useful.

BIBLIOGRAPHY - None found

SPACECRAFT AND EXPERIMENT CHARACTERISTICS

OGO 2, Haddock

EXPERIMENT NAME Radio Astronomy
 NSSDC ID 65-081A-01
 PROJECT DESIGNATION 5001, C-01
 PERSONNEL
 PI - F.T. Haddock
 University of Michigan - Ann Arbor, Michigan

BRIEF DESCRIPTION

The purpose of this experiment was to map the brightness temperature of the sky at a frequency of 2.5 MHz, using an 18-m monopole antenna and depending upon ionospheric focusing to achieve angular resolution. The experiment, located in SOEP-1, included a two-channel radiometer (2.0 and 2.5 MHz) and an impedance probe operating at 2.5 MHz. No mapping information could be obtained from this experiment due to the high noise level, the failure of the spacecraft to stabilize, and the high orbit of the satellite. It was possible to utilize the resulting data for a study of the wake produced by the spacecraft as it moved through the ionosphere (see experiment 65-081A-21).

BIBLIOGRAPHY

PM: A71-26144.
 N69-14393, N70-23999.
 PS: N69-25437.

OGO 2, Haddock

EXPERIMENT NAME Electron Density
 Measurements
 NSSDC ID 65-081A-21
 PROJECT DESIGNATION 5001, C-01
 PERSONNEL
 PI - F.T. Haddock
 University of Michigan - Ann Arbor, Michigan
 OI - H. Weil
 Naval Research Laboratory - Washington, D.C.
 OI - R.G. York
 Naval Research Laboratory - Washington, D.C.

BRIEF DESCRIPTION

The purpose of this experiment was to obtain a model of the variations of electron density distribution around a satellite as it travelled through the ionosphere. The reliable identification of a wake could be used for attitude determination of the satellite. This experiment was a by-product of a radio astronomy experiment (65-081A-01). This wake-probing aspect of the experiment was not planned. In fact, it was made possible only by a failure of the spacecraft stabilization system to maintain the planned three-axis stabilization. The ionospheric probe was an 18-m monopole antenna, located on SOEP-1. A 2.5-MHz impedance bridge measured the antenna impedance on a time-sharing basis, taking samples every 0.288 sec at the slowest data rate. Since the spacecraft spin axis was roughly perpendicular to the satellite orbit plane, an electron density minimum could be determined once each spin cycle (approximately four min). The measurement of the antenna impedance therefore indicated the ambient electron density of the wake to be less than that of a relatively unperturbed ionosphere. The data yielded by this experiment were excellent.

BIBLIOGRAPHY

PM: A70-35771, A73-34783.
 N70-23999.

OGO 2, Helliwell

EXPERIMENT NAME VLF Noise and
 Propagation
 NSSDC ID 65-081A-02
 PROJECT DESIGNATION 5002, C-02
 PERSONNEL
 PI - R.A. Helliwell
 Stanford University - Stanford, California
 OI - L.H. Rorden
 Stanford University - Stanford, California
 OI - J.J. Angerami
 Stanford University - Stanford, California

BRIEF DESCRIPTION

This experiment consisted of five VLF radio receivers that studied natural and man-made VLF noise occurrences at orbital altitudes. The receiver systems consisted of an inflatable 2.9-m loop antenna, a preamplifier stage at the end of a long boom (EP-5), and a receiver electronics package in the main body of the satellite. Three step-frequency receivers covered frequency ranges from 0.2 to 1.6, 1.6 to 12.5, and 12.5 to 100 kHz. Observations from these three receivers were tape recorded, and the tape was read out upon command. The fourth receiver was tunable between 14.4 and 26.3 kHz, and the data were recorded and transmitted in the same way as the data from the three step-frequency receivers. The fifth receiver was a broadband receiver operating between 0.3 and 12.5 kHz. These data were not tape recorded, but were observed only in real time on the special-purpose telemetry channel. Data from the narrowband receivers were obtained intermittently for about one-third of the approximately 2 years of spacecraft operation. The wideband data observations covered only a very small portion of the satellite lifetime, due to the limitation of real time operation only and difficulties experienced with spacecraft power. This experiment operated for seven 1-to-2 month periods, beginning respectively on October 17, 1965, January 17, 1966, March 15, 1966, June 21, 1966, November 18, 1966, April 11, 1967, and September 2, 1967. This experiment operated for a total of 6,748 hours.

BIBLIOGRAPHY

PM: A68-19752, A68-31481, A69-14029, A69-28958,
 A69-34939, A70-15116, A70-29924, A71-31757.
 N67-30831, N70-15525, N70-32928.
 B01263-000.
 PS: A68-37940.
 PC: N74-74765.
 OS: A69-11125, A69-38495, A70-30078, A72-21189.
 B00969-000.

Nov. 10, 1975

SPACECRAFT AND EXPERIMENT CHARACTERISTICS

OGO 2, Hinteregger

EXPERIMENT NAME Solar UV Emissions
NSSDC ID 65-081A-17
PROJECT DESIGNATION 5020, C-20
PERSONNEL
PI - H.E. Hinteregger
AFCRL - Bedford, Massachusetts
OI - D.E. Bedo
AFCRL - Bedford, Massachusetts

BRIEF DESCRIPTION

This experiment was designed to measure solar photon flux as a function of wavelength between 170 and 1700 Å. The experiment was located on SOEP-2, a solar-oriented panel on the spacecraft. Solar radiation entered the experiment package through an aperture equipped with a set of electrically charged grids to reject charged particles. Then the radiation illuminated a stack of six small gratings and was diffracted onto six photocathodes. These photocathodes were located in two PMs (two per PM). By electronic discrimination, only one photocathode was used at any given time in each PM. The gratings were all illuminated at the same angle of incidence, and were stepped through the spectral range in 512 intervals every seven minutes during normal operation. An alternative mode provided for a short scan of 32 steps, beginning at any of 16 different points in the 512-step scan. This experiment failed to yield any useful scientific data due to the failure of the spacecraft to orient properly. It provided useful engineering data and was operational for over two years in space.

BIBLIOGRAPHY

PM: A66-27326.
N65-29678.
PC: N65-14504.

OGO 2, Hoffman

EXPERIMENT NAME Scintillation Detector
NSSDC ID 65-081A-09
PROJECT DESIGNATION 5011, C-11
PERSONNEL
PI - R.A. Hoffman
NASA-GSFC - Greenbelt, Maryland

BRIEF DESCRIPTION

This experiment was designed to study fluctuations in the trapped radiation by measuring low-energy trapped radiation and auroral particles. Two scintillator/PMs located on EP-2 were designed to observe electrons between 10 and 100 keV and protons between 100 keV and 4.5 MeV. One scintillator was intended to point radially away from the Earth. The other scintillator was to have looked at 90 deg to this. One of the two photomultiplier tubes lost three orders of magnitude gain when turned on after launch. This, coupled with the failure of the attitude control system, made the data from the remaining detector worthless. The detector failed on October 14, 1965. No useful data were obtained from this experiment.

BIBLIOGRAPHY - None found

IV-12

OGO 2, Jones

EXPERIMENT NAME Neutral Particle and Ion
Composition
NSSDC ID 65-081A-13
PROJECT DESIGNATION 5015, C-15
PERSONNEL
PI - L.M. Jones
University of Michigan - Ann Arbor, Michigan
OI - R.J. Leite
University of Michigan - Ann Arbor, Michigan

BRIEF DESCRIPTION

A quadrupole mass spectrometer, located in OPEP-2, was used to measure neutral particle and positive ion composition in the mass range from 1 to 44 amu, between 300 and 900 km. The mass range was swept six times at six different sensitivity levels, with a seventh sweep devoted to calibration, for both the ion and neutral samples. Each sweep had a 6-sec duration, and in this time the mass scale was swept from approximately 50 to 0 amu in a spectral mode and approximately 40 to 0 amu in an integral mode. Therefore, a full cycle of operation required 14 sweeps and 84 sec. The experiment failed to achieve the desired objective due to spacecraft problems, mainly loss of attitude control. The data obtained were of little value, but they did indicate that the spacecraft expelled large amounts of water vapor over an extended period of time. A failure in the command distribution unit of the spacecraft, which supplied electrical power to the spectrometer, prevented activation of the experiment after April 11, 1966.

BIBLIOGRAPHY

PM: N70-14425, N74-77537.

OGO 2, Kreplin

EXPERIMENT NAME Solar X-ray Emissions
NSSDC ID 65-081A-16
PROJECT DESIGNATION 5021, C-21
PERSONNEL
PI - R.W. Kreplin
Naval Research Laboratory - Washington, D.C.
OI - T.A. Chubb
Naval Research Laboratory - Washington, D.C.
OI - H.D. Friedman
Naval Research Laboratory - Washington, D.C.

BRIEF DESCRIPTION

This experiment utilized four ion chambers to observe broadband solar emissions in the wavelength ranges of 0.5 to 3 Å, 2 to 8 Å, 8 to 16 Å, and 44 to 60 Å, which play an important role in the formation of the D- and E regions of the ionosphere. To minimize contamination from charged particles, the field of view of each ion chamber was limited to 0.1 steradian, and the experiment package was located on SOEP-2. The instrument cycled each detector through a zero-current calibration check once each 640 sec. Each detector except the 44 to 60 Å one incorporated automatic range changing to avoid saturation. However, this feature could be overridden by a command from the ground. The experiment failed in November 1965, a month after launch.

BIBLIOGRAPHY - None found

SPACECRAFT AND EXPERIMENT CHARACTERISTICS

OGO 2, Mange

EXPERIMENT NAME Lyman-Alpha and UV
Airglow Study
NSSDC ID 65-081A-11
PROJECT DESIGNATION 5013, C-13
PERSONNEL
PI - P.W. Mange
Naval Research Laboratory - Washington, DC

BRIEF DESCRIPTION

There were two parts to this experiment -- A Far-UV Experiment (1230-1350 A) and a Lyman-Alpha Experiment (1050-1350 A). The sensors, located on the main body, were UV ion chambers. The Far-UV Experiment yielded information about the rate at which energy is absorbed. The Lyman-Alpha Glow Experiment measured Lyman-Alpha radiation from the direction of the Earth and from space. The sensors functioned properly, but the spacecraft spin made the data useless.

BIBLIOGRAPHY - None found

OGO 2, Morgan

EXPERIMENT NAME Whistler and
Audio-Frequency
Electromagnetic Waves
NSSDC ID 65-081A-03
PROJECT DESIGNATION 5003, C-03
PERSONNEL
PI - M.G. Morgan
Dartmouth College - Hanover, New Hampshire

BRIEF DESCRIPTION

This experiment was designed to study ionospheric effects on whistler-mode waves and on propagation of whistlers in the 0.5- to 18-kHz band. It consisted of a dipole electric carpenter-tape antenna, located on EP-1, which was extendable to 3 m. This antenna fed a wideband receiver with a 60-db dynamic range. Receiver gain was controlled from the ground and operated in four ranges. Receiver gain stepped down 15 db in each sequence step. The resulting data were records of noise frequency versus time, which could be played for aural review or processed into sonograms for visual study. It is doubtful that the antenna was completely extended. Probable extension was only 2.5 m. Adjustments required as a result of prelaunch spacecraft testing resulted in the antenna extending closer to the SOEP than desirable. Interference difficulties were also encountered from the 400-Hz power supply used in the attitude control system. Unknown and variable amounts of signal loss occurred due to the spacecraft plasma sheath and prevented reliable measurement of signal intensity. This experiment operated for nearly 5624 hr before the spacecraft operation was terminated.

BIBLIOGRAPHY

PM: A69-16257.
N69-17928.
OM: N67-30831.
OS: A72-21189.
B00969-000.

OGO 2, Newton

EXPERIMENT NAME Neutral Particle Study
NSSDC ID 65-081A-20
PROJECT DESIGNATION 5017, C-17
PERSONNEL
PI - G.P. Newton
NASA-GSFC - Greenbelt, Maryland

BRIEF DESCRIPTION

The purpose of this experiment was to measure the neutral particle density and temperature along the OGO 2 orbit. The instrumentation, located in OPEP-2, contained a Bayard-Alpert ionization gauge, which consisted of a gridded tube open to the neutral atmosphere. The experiment failed immediately after launch, when the breakaway device, which should have opened the sensor to the space environment, could not be deployed. The reason for failure could not be uniquely established. It was believed to be a deficiency in the spacecraft/experiment wiring.

BIBLIOGRAPHY - None found

OGO 2, Nilsson

EXPERIMENT NAME Interplanetary Dust
Particles
NSSDC ID 65-081A-14
PROJECT DESIGNATION 5018, C-18
PERSONNEL
PI - C.S. Nilsson
SAO - Cambridge, Massachusetts
OI - D. Wilson
SAO - Cambridge, Massachusetts

BRIEF DESCRIPTION

Four thin-film capacitor micrometeorite detectors were carried aboard OGO 2 to obtain measurements of the velocities, masses, and orbits of dust particles in the Earth's dust cloud. The detectors, located on EP-3, were circular tubes, 2.5 cm in diameter and 10 cm long, each containing three sensors -- two thin-film capacitors and a microphone crystal. The front sensor consisted of two 500-A layers of aluminum oxide, each coated front and back with 500 A of aluminum. The rear sensor was a 1-micron silicon oxide layer, coated front and back with 1000 A of aluminum and deposited on a glass disk. The third sensor was a lead zirconate crystal transducer that was bonded to the rear of each glass disk. A particle that passed through the front sensor would give rise to a small plasma pulse, which was detected and used to start an oscillator that measured the time of flight down the tube. After traversing the length of the tube, the particle would impact destructively on the rear capacitor sensor, producing another plasma pulse which was used to stop the time-of-flight oscillator and provide the particle's velocity. The impulse imparted to the glass disk by the particle impact provided information on the momentum of the particle. A reasonable mass threshold for both thin-film capacitor sensors was estimated to be 10^{-12} grams. Three of the four tubes were pointed in mutually orthogonal directions. One of the detectors was shielded from particle impacts to serve as a control against electrical interference. The only sensor to fail was the rear capacitor on the shielded detector. The experiment heater failed after 1 week of operation, introducing numerous false counts into the transducer data output due to the transducer-noise temperature dependence. Electrical interference arising from commands sent to the spacecraft caused the rear capacitor sensor

SPACECRAFT AND EXPERIMENT CHARACTERISTICS

data to contain many false counts. In 1370 hr of data, only two possible micrometeoroid impacts were found. However, the flux rate determined from these data compared favorably with flux rates obtained from experiments on earlier spacecraft.

BIBLIOGRAPHY

PM: A66-41213, A68-35397, A70-10444,
N69-23367.

PS: A68-29467.

OGO 2, Reed

EXPERIMENT NAME Airglow and Auroral
Study

NSSDC ID 65-081A-10
PROJECT DESIGNATION 5012, C-12

PERSONNEL

PI - E.I. Reed
NASA-GSFC - Greenbelt, Maryland
OI - J.E. Blamont
CNES - Bretigny, France

BRIEF DESCRIPTION

The objective of this experiment was to study airglow and auroral activity by obtaining photometric measurements at the following wavelengths (Angstroms): 2630 (E-region airglow -- Herzberg molecular oxygen emission, and aurora -- Vegard-Kaplan molecular nitrogen emission); 3914 (visible aurora -- molecular nitrogen ion emission); 5577 (airglow and aurora -- green atomic oxygen emission); 5890 (E-region airglow -- yellow sodium emission); 6225 (E-region airglow -- red hydroxyl emission); and 6300 (F-region airglow -- red atomic oxygen emission). The photometers were mounted in the main body and in OPEP-1. All of the above spectral lines were sensed by the main-body photometer oriented in the Earth's direction. The 6300-A line was also observed in the anti-Earth direction and by the OPEP photometer. In the main-body photometer, the incident light was alternately directed through six filters corresponding to the six wavelengths by an automatic stepping mirror system. The mirrors could be commanded to remain in any of the spectral positions for a more comprehensive study of the distribution of a particular line. The field of view of the main body spectrometer had a half-angle of slightly less than 5 deg. The field of view of the OPEP spectrometer was 1/2 deg in height and 6 deg in width. A mirror scan system moved the center of the OPEP field of view from horizontal to 30 deg below horizontal in 1/2-deg steps. The time required to scan across these 30 deg was 34.7 sec, a time interval in which the spacecraft moved approximately 250 km. When one scan was completed, the motion reversed direction and a new scan started at the same rate. Every 200 sec, there was an 8-sec calibration cycle. The instruments performed satisfactorily, but the scientific objectives could not be achieved due to the failure of the spacecraft attitude system.

BIBLIOGRAPHY

PM: A67-23278,
N67-27576, N67-27578, N72-27423.

PS: N69-18074.

IV-14

OGO 2, Simpson

EXPERIMENT NAME Low-Energy Proton,
Alpha Particle
Measurement

NSSDC ID 65-081A-07
PROJECT DESIGNATION 5008, C-08

PERSONNEL

PI - J.A. Simpson
University of Chicago - Chicago, Illinois
OI - E.C. Stone
University of Chicago - Chicago, Illinois
OI - C.Y. Fan
University of Chicago - Chicago, Illinois

BRIEF DESCRIPTION

Two solid-state particle telescopes, located in the main body, were used to study low-energy cosmic-ray protons and alpha particles. One of these detectors was a three-element range telescope ('vertical') that was capable of identifying two energy ranges of protons and alpha particles (1.22 to 39.2 and 9.32 to 39.2 MeV/nucleon) and electrons (energy greater than 400 keV and 700 keV). The other detector was a one-element telescope ('horizontal') sensitive to protons and alpha particles in the energy range from 0.72 to about 11 MeV/nucleon. The vertical telescope axis of symmetry was parallel to the spacecraft z axis, which later unintentionally became the spin axis. The horizontal telescope symmetry axis was nearly parallel to the spacecraft y axis (perpendicular to the z axis). Pulse height information was sent back from the vertical telescope, allowing pulse height analyses of protons (energies from 1.22 to 39.2 MeV), alpha particles (energies from 4.88 to 156.8 MeV), and electrons (energy greater than 400 keV) using a 256-channel pulse height analyzer. Count rate information was sent back from both telescopes. The experiment was performing normally at the time the spacecraft systems were deactivated (November 1, 1967). However, the spinning of the spacecraft caused difficulty in interpreting the data after October 23, 1965.

BIBLIOGRAPHY

OS: N69-34536.

OGO 2, Smith

EXPERIMENT NAME Triaxial Search-Coil
Magnetometer

NSSDC ID 65-081A-04
PROJECT DESIGNATION 5005, C-05

PERSONNEL

PI - E.J. Smith
NASA-JPL - Pasadena, California
OI - R.E. Holzer
University of California - Los Angeles, California

BRIEF DESCRIPTION

This experiment was used to study the ELF range of magnetic fluctuations of the Earth's magnetic field. The search coil sensor consisted of a coil of 100,000 turns of wire, wound around a nickel-steel-laminated core. The coil sensitivity was approximately 10 microvolt-sec per gamma. A low-noise preamplifier with a gain of 100 was mounted on an auxiliary housing near the search coil. The three orthogonal sensors and their associated preamplifiers were mounted at the end of the EP-5 six-m boom to reduce

SPACECRAFT AND EXPERIMENT CHARACTERISTICS

interference from spacecraft-generated fields. Magnetic-field fluctuation measurements were made in the frequency range from below 0.01 Hz to above 1000 Hz. The signals were divided into a high-frequency and a low-frequency channel, which overlapped near the center of the five-decade frequency band. The low-frequency wave forms were digitized and telemetered. The high-frequency information was obtained continuously by using an on-board low-resolution spectrum analyzer consisting of five comb filters centered at 10, 32, 100, 320 and 800 Hz. The high-frequency wave forms were also telemetered (on a part-time basis) in analog form for subsequent high-resolution, ground-based processing. Spacecraft spin made the data obtained very poor in quality. The experiment was turned off after operating for 5518 hr.

BIBLIOGRAPHY

PM: A69-36675.
 PC: B21207-000.
 OS: A72-21189.

OGO 2, Taylor

EXPERIMENT NAME	Positive Ion Composition
NSSDC ID	65-081A-15
PROJECT DESIGNATION	5016, C-16
PERSONNEL	
PI - H.A. Taylor, Jr.	
	NASA-GSFC - Greenbelt, Maryland
OI - N.W. Spencer	
	NASA-GSFC - Greenbelt, Maryland

BRIEF DESCRIPTION

A ceramic Bennett radio-frequency ion mass spectrometer tube, located in OPEP-1, was used to measure thermal atmospheric ions having mass-to-charge values from 1 to 45 amu, with a mass resolution of approximately 1 in 20 amu. Concentrations from 1.0 to 10^6 ions per cc were measured. The time between consecutive samples of each ion detected, i.e., the spectral sweep rate, was 25.6 sec. This time interval corresponded to a spatial resolution of from 175 to 200 km along the orbit path, or to 1.5 deg in latitude. Mean ion mass and total ion concentration were also calculated. The experiment provided useful data for about one year. It failed on October 18, 1967.

BIBLIOGRAPHY

PM: A68-37114, A68-41673, A69-31326, A69-34939,
 A71-33762, A73-11904, A73-15533.
 PS: A68-38423, A71-30037.
 OS: A72-10361.

OGO 2, Van Allen

EXPERIMENT NAME	Corpuscular Radiation Experiment
NSSDC ID	65-081A-18
PROJECT DESIGNATION	5010, C-10

PERSONNEL

PI - J.A. Van Allen
 University of Iowa - Iowa City, Iowa
 OI - L.A. Frank
 University of Iowa - Iowa City, Iowa
 OI - S.M. Krimigis
 University of Iowa - Iowa City, Iowa
 OI - T.P. Armstrong
 University of Iowa - Iowa City, Iowa

BRIEF DESCRIPTION

This experiment was to study the precipitation of low-energy particles (75 to 75,000 eV) at high latitudes, including solar cosmic rays and geomagnetically trapped particles. The experiment used a cylindrical electrostatic analyzer and surface barrier silicon detectors located in EP-4. The experiment was operating normally when the spacecraft was shut down on November 1, 1967.

BIBLIOGRAPHY

PM: N69-20849, N74-76909.

OGO 2, Webber

EXPERIMENT NAME	Galactic and Solar Cosmic Ray
NSSDC ID	65-081A-08
PROJECT DESIGNATION	5009, C-09
PERSONNEL	
PI - W.R. Webber	
	University of Minnesota - Minneapolis, Minnesota

BRIEF DESCRIPTION

The Cosmic-Ray Telescope Experiment was designed to measure the differential energy spectra of protons, helium nuclei, and heavier nuclei up to $Z = 10$, within the energy range from 50 to 2000 MeV/nucleon. The telescope had a maximum sampling rate of one count per 288 msec. The telescope, located in the main body, consisted of two detectors, a scintillator with its associated PM, and a scintillator and a Cerenkov element sandwich with both elements optically coupled to the same PM. A 70-nsec coincidence circuit coupled the two detectors to form the telescope. Pulses from each detector were pulse height analyzed. Sample pulse heights, the coincidence count rate, and the count rate of the first detector were telemetered. The noise levels of the spacecraft increased to sufficient amplitude to render the first detector count rate data unusable except during eclipse periods. All the useful data from this experiment were obtained between October 15 and October 24, 1965, and about 17 percent of the data obtained during this period contain useful information.

BIBLIOGRAPHY

PM: A66-23684, A68-41562.
 PS: N74-19088.

SPACECRAFT AND EXPERIMENT CHARACTERISTICS

OGO 3, Bohn

EXPERIMENT NAME Interplanetary Dust Particles
 NSSDC ID 66-049A-21
 PROJECT DESIGNATION 4916, B-16
 PERSONNEL
 PI - J.L. Bohn
 Temple University - Philadelphia, Pennsylvania
 OI - W.M. Alexander
 Baylor University - Waco, Texas

BRIEF DESCRIPTION

The objective of this experiment was to measure over a long period of time the velocity and mass distributions of interplanetary dust particles with diameters on the order of 1 micron. The instrumentation was very similar to that of the dust particle experiment flown on OGO 1 and consisted of a combination of acoustical and ionization sensors located on EP-3. The basic detector was a 2.54-cm tube containing three sensor elements. The first element was a thin film (1500 Å), the second was a metallic disc to which a piezoelectric ceramic transducer was bonded, and the third was a metallic grid in front of the disc. Penetration of the front film by a micrometeoroid produced a plasma cloud that was detected and activated a 2-MHz clock. If the particle then impacted on the metallic disc, the impulse was sensed by the ceramic transducer. The ionization produced by this collision was detected by the grid, which in turn stopped the clock, providing measurement of the particle velocity. The pulse height signal produced by the grid provided information on the kinetic energy and/or momentum of the particle. The total exposed area was 15 cm². The experiment incorporated automatic inflight continuous calibration that enabled a distinction to be made between events, noise, and normal signals. All events occurred at an altitude between 50,000 and 110,000 km. The data were obtained from both real-time and tape storage/playback modes. Only the real-time data, however, were considered reliable. Although the determination of the micrometeoroid directionality was difficult to determine, owing to the spin of OGO 3 and the low data sampling rate, good data were obtained from the front film counters and the grid over an extended period of time.

BIBLIOGRAPHY

PM: A68-29457, A68-29468, A71-14014, A71-33741,
 N71-33768,
 B15918-000.
 PS: A68-29467.

OGO 3, Bridge

EXPERIMENT NAME Plasma Probe, Faraday Cup
 NSSDC ID 66-049A-06
 PROJECT DESIGNATION 4903, B-03

PERSONNEL

PI - H.S. Bridge
 MIT - Cambridge, Massachusetts
 OI - A.M. Bonetti
 University of Florence - Florence, Italy
 OI - B. Rossi
 MIT - Cambridge, Massachusetts
 OI - A.J. Lazarus
 MIT - Cambridge, Massachusetts
 OI - F. Scherb
 MIT - Cambridge, Massachusetts
 OI - V.M. Vasylunas
 MIT - Cambridge, Massachusetts

BRIEF DESCRIPTION

Two multi-grid Faraday cups were used to study the directional intensity of protons and electrons of the solar wind, magnetosheath, and magnetotail. One single collector Faraday cup, located in SOEP-2, was used to study electrons in four energy windows between 40 eV and 2 keV. Currents in all four energy windows were measured every 4.6 sec. The detector worked well from launch until December 1, 1969, when the experiment was turned off. One split-collector Faraday cup was to be used to study protons, but due to the unexpected spinup of the spacecraft, the data are useless.

BIBLIOGRAPHY

PM: A68-28348, A69-14027, A69-19373, A71-30029,
 N72-18715.
 OS: A73-33436.

OGO 3, Cline

EXPERIMENT NAME Positron Search and Gamma-Ray Spectrum
 NSSDC ID 66-049A-04
 PROJECT DESIGNATION 4904, B-04
 PERSONNEL
 PI - T.L. Cline
 NASA-GSFC - Greenbelt, Maryland
 OI - E.W. Hones, Jr.
 LASL - Los Alamos, New Mexico

BRIEF DESCRIPTION

This experiment was designed to determine whether low-energy (0 to 3 MeV) positrons are trapped temporarily or permanently in the Van Allen radiation region, and whether low-energy solar and interplanetary positrons exist at the edge of the magnetic field of the Earth. It was also designed to detect gamma-ray bursts from the Sun, for gamma rays in the energy interval from 80 keV to 1 MeV. The arrangement was virtually identical to that flown on OGO 1, except that the PMs used were of an improved variety. The experimental apparatus, located in SOEP-1, consisted of three CsI crystals surrounded by a plastic anticoincidence shield, with the output of the whole unit being monitored by three photomultipliers. It was primarily designed to search for interplanetary positrons by measuring the spectra of single or paired X-rays produced by the stopping of a positron. In another possible mode of data acquisition, single gamma rays were monitored in one of the CsI spectrometers with a 4 π particle anticoincidence, which is virtually gamma-ray transparent above 80 keV. Once each 18.5 sec, integral intensity measurements were made in each of the 16 energy levels equally spaced between 80 keV and 1 MeV, allowing for both temporal and spectral analysis.

SPACECRAFT AND EXPERIMENT CHARACTERISTICS

of the data. Inflight calibration of the spectrometer was accomplished by monitoring the 511-keV annihilation line. The experiment was successful.

BIBLIOGRAPHY

PM: A68-17769, A68-41427, A69-23753, A70-38098.

PS: A74-30149.

OGO 3, Evans

EXPERIMENT NAME Low-Energy Proton
Experiment
NSSDC ID 66-049A-07
PROJECT DESIGNATION 4906, B-06b
PERSONNEL
PI - D.C. Evans
NASA-GSFC - Greenbelt, Maryland
OI - L.R. Davis
NASA-GSFC - Greenbelt, Maryland

BRIEF DESCRIPTION

This experiment was designed to measure the intensity and energy spectrum of 5- to 100-keV protons. It was located in the main body, and it employed channeltron detectors, cylindrical electrostatic analyzers, and a broom magnetic analyzer to reject electrons. It was designed to replace the GM portion of the cosmic-ray isotopic abundance experiment (66-049A-02) and utilized a power supply and data accumulators from experiment -02. An unexpected and unexplained high background counting rate prevented the acquisition of useful data.

BIBLIOGRAPHY - None found

OGO 3, Frank

EXPERIMENT NAME Low-Energy Electrons
and Protons
NSSDC ID 66-049A-08
PROJECT DESIGNATION 4908, B-08
PERSONNEL
PI - L.A. Frank
University of Iowa - Iowa City, Iowa
OI - J.A. Van Allen
University of Iowa - Iowa City, Iowa

BRIEF DESCRIPTION

This experiment measured the differential energy spectra of protons and electrons over the energy range 100 eV to 50 keV (subdivided into 13 energy intervals) within and in the vicinity of the magnetosphere of the Earth. The instrumentation, located on EP-2, consisted of two curved-plate, cylindrical, electrostatic analyzers, used as a low-energy proton and electron differential energy analyzer (LEPEDEA), and two Bendix continuous channel multipliers. The accumulation time per channel was about 1 sec. Approximately 5 min were required to complete a scan of the entire energy range. After the spacecraft attitude control system failed on July 23, 1966, one of the LEPEDEAs was oriented parallel to the spacecraft spin axis, and the other was oriented perpendicular

IV-18

to the spin axis. (The spin period varied from about 91 to 122 sec.) The experiment performed normally until it failed on May 23, 1967.

BIBLIOGRAPHY

PM: A67-19926, A67-26312, A67-37401, A68-17771,
A68-34245, A68-41684, A69-19358, A70-23490,
A70-23491, A70-30089, A70-43834, A71-17261,
A71-24781.
N66-13640, N68-15232.

PS: A69-29565.

OS: A69-37967, A70-30358, A70-31905, A70-37487,
A71-17263.
B18378-000.

OGO 3, Fritz

EXPERIMENT NAME Radio Propagation
NSSDC ID 66-049A-16
PROJECT DESIGNATION 4914, B-14
PERSONNEL
PI - R.B. Fritz
ESSA - Boulder, Colorado
OI - J.K. Hargreaves
ESSA - Boulder, Colorado
OI - R.S. Lawrence
ESSA - Boulder, Colorado
OI - O.K. Garriott
Stanford University - Stanford, California

BRIEF DESCRIPTION

In this experiment a radio beacon transmitted at two coherent frequencies, 40.01 and 360.09 MHz, using antennas located on EP-2 and EP-3, respectively. Both frequencies were modulated by 20-kHz and 200-kHz sine waves. The signals were received by two sets of tracking antennas near Boulder, Colorado. Each antenna system consisted of a 28-ft paraboloid to receive the 360-MHz signal, and a 6-element yagi for the 40-MHz signal. In using Faraday rotation techniques on the 40-MHz signal, the computed total electron content depends on the distribution of electron density; i.e., the total number of electrons affecting the signal were assumed to occur near the electron density maximum. In the modulation-phase or 'group-delay' technique, the determination of t_{ec} is independent of the electron density distribution. The two measurements then should be comparable at lower spacecraft altitudes, but at high altitudes the two measurements should differ due to electrons well removed from the ionospheric maximum. This experiment caused severe interference with the command receiver. Before a means of successful operation could be devised to counteract the interference effect, the spacecraft attitude system failed. The subsequent spin-stabilized mode was not suitable for experiment operation, so no useful data were obtained.

BIBLIOGRAPHY

PM: B18548-000.

SPACECRAFT AND EXPERIMENT CHARACTERISTICS

OGO 3, Haddock

EXPERIMENT NAME Radio Astronomy
 NSSDC ID 66-049A-18
 PROJECT DESIGNATION 4918, B-18
 PERSONNEL
 PI - F.T. Haddock
 University of Michigan - Ann Arbor, Michigan

BRIEF DESCRIPTION

The objective of this experiment was to measure the spectrum of solar radio noise bursts in the 2- to 4-MHz band. The instrumentation included a 9-m antenna in SOEP-1 and a swept-frequency receiver in the main body. Forty-five days after launch, a malfunction occurred in the sweeping trigger pulse, intermittently causing the sweep to change from a 4- to 2-MHz sweep once every 2 sec to a 4- to 3-MHz sweep every second. By October 10, 1966, the experiment operated in the 1-sec sweep mode (4 to 3 MHz) only. A large quantity of useful data was obtained from this experiment.

BIBLIOGRAPHY

PM: A70-34835, A71-19724, A71-43176,
 N70-11147, N70-12221, N74-74631, N74-74660,
 N74-76907.
 PS: N69-25437.
 OS: N70-33175.

OGO 3, Helliwell

EXPERIMENT NAME VLF Noise and
 Propagation
 NSSDC ID 66-049A-17
 PROJECT DESIGNATION 4917, B-17
 PERSONNEL
 PI - R.A. Helliwell
 Stanford University - Stanford, California
 OI - L.H. Rorden
 Stanford University - Stanford, California

BRIEF DESCRIPTION

This experiment measured naturally occurring VLF noise phenomena within the spacecraft orbit region, such as terrestrial noise produced below 70 km, emissions from charged particles trapped in the magnetic field of the Earth, cosmic noise, and proton and helium whistlers. The instrumentation consisted of a loop antenna and preamplifier at the end of a long boom (EP-5) and the receiver electronics package in the spacecraft main body. The receiver system provided a wide frequency coverage, from 0.2 to 100.0 kHz contiguous narrowband measurements and from 0.015 to 12.5 kHz broadband measurements. It had a dynamic range of about 80 db. The antenna bias capability was lost in July 1968, and for one month (August 1969) the spacecraft was shut down due to a power loss. Observations were made for a total of 27,810 hours during the active spacecraft lifetime.

BIBLIOGRAPHY

PM: A69-25153, A69-31981, A70-27183, A71-11499,
 A72-42043, A73-41912,
 N67-30831, N68-14025, N70-15678, N70-33156,
 N73-16344,
 B01263-000, B01265-000.
 PS: A68-37940,
 N68-17981.
 OS: A70-30078, A70-40479, A71-30952, A72-21189,
 B00969-000.

OGO 3, Heppner

EXPERIMENT NAME Magnetic Survey Using
 Two Magnetometers
 NSSDC ID 66-049A-11
 PROJECT DESIGNATION 4911, B-11
 PERSONNEL
 PI - J.P. Heppner
 NASA-GSFC - Greenbelt, Maryland
 OI - B.G. Ledley
 NASA-GSFC - Greenbelt, Maryland
 OI - R.M. Campbell
 NASA-GSFC - Greenbelt, Maryland
 OI - T.L. Skillman
 NASA-GSFC - Greenbelt, Maryland
 OI - M. Sugiura
 NASA-GSFC - Greenbelt, Maryland

BRIEF DESCRIPTION

The primary objective of this experiment was to study the geomagnetic field and its interactions with the environment. The detector system, located in EP-6, consisted of a boom-mounted, triaxial, dual range, fluxgate magnetometer and two boom-mounted, dual-cell, optically pumped, self-oscillating rubidium vapor magnetometers. The triaxial fluxgate magnetometer provided simultaneous measurements of the three magnetic-field vector components in two different ranges, plus or minus 30 gammas and plus or minus 300 gammas. The accuracy for the fluxgate was plus or minus 2 gammas in field intensities up to 30 gammas and reached a maximum of 10 gammas in field intensities of 300 gammas (checked by means of inflight comparison with the rubidium magnetometer). The accuracy of the rubidium vapor magnetometer is about 2 gammas for large field values. The instrument is not reliable for fields less than 10 gammas. The fluxgate and rubidium sensors returned nominal data until about July 23, 1966, when the spacecraft attitude control system failed. Fluxgate data taken after this date are of poor-to-useless quality due to the difficulty of correcting these data for spacecraft spin. The vector data from the rubidium instrument suffer from this same problem. However, the field magnitudes obtained by the rubidium magnetometers remain useful, with about 50 percent data coverage from July 1966 to August 1968.

BIBLIOGRAPHY

PM: A69-11226, A70-30076, A71-23635, A72-10886,
 A72-12084, A73-11732, A73-43693,
 N71-25271, N71-32436,
 B19906-000.
 PS: A71-17258,
 N70-19313.

SPACECRAFT AND EXPERIMENT CHARACTERISTICS

OM: A73-13871.

OS: A71-17686, A71-34777, A72-42902.

OGO 3, Konradi

EXPERIMENT NAME Trapped Radiation
Scintillation Counter
NSSDC ID 66-049A-10
PROJECT NAME 4905, B-05
PERSONNEL

- PI - A. Konradi
NASA-GSFC - Greenbelt, Maryland
- OI - L.R. Davis
NASA-GSFC - Greenbelt, Maryland
- OI - R.A. Hoffman
NASA-GSFC - Greenbelt, Maryland
- OI - J.M. Williamson
NASA-GSFC - Greenbelt, Maryland

BRIEF DESCRIPTION

The objectives of this experiment were (1) to study the temporal and spatial variations of the trapped particle intensities, pitch angle distributions, and energy spectra of electrons (10 to 100 keV) and protons (100 to 1000 keV) and (2) to determine particle lifetimes, processes by which trapped particles are lost, and the sources and accelerating mechanisms of trapped particles. The experiment, located in OPEP-2, consisted of a filter wheel, wheel stepping motor, phosphor scintillator, PM, electrometer, and count-rate meter. The detector had two entrance apertures for particles, one aligned with the phototube axis and one at 90 deg to this axis. Both protons and electrons could enter the aligned opening and reach the phosphor. Only electrons could enter the 90-deg opening, scatter off a gold disc, and reach the phosphor. The counting rate with the aligned opening measured proton flux, and the current measured the total energy flux of electrons, protons, etc. The current with the 90-deg opening measured the electron energy flux. Different thickness absorbers on the wheel provided spectral information. The experiment worked well until the absorber wheel stopped in January 1967.

BIBLIOGRAPHY

PM: A69-21699.

OGO 3, Mange

EXPERIMENT NAME Geocoronal
Lyman-Alpha Scattering
NSSDC ID 66-049A-19
PROJECT DESIGNATION 4919, B-19
PERSONNEL

- PI - P.W. Mange
Naval Research Laboratory - Washington, D.C.

BRIEF DESCRIPTION

This experiment was designed to measure the intensity of hydrogen Lyman-Alpha radiation (1216 Å) scattered by neutral hydrogen at 5 to 19 R_E. This wavelength is the fundamental resonance line of neutral atomic hydrogen, and these intensity measurements, therefore, provide a measure of the density of neutral

hydrogen in the hydrogen geocorona. The instrumentation consisted of four ion chambers mounted on the anti-Earth door of the main body. Each ion chamber was filled with nitric oxide gas and had lithium fluoride windows. The ion chambers were sensitive in the 1050- to 1350-Å band. The experiment functioned well from launch until July 23, 1966. On this date, OGO 3 was commanded to the spin mode, and the experiment faced the Sun, causing detector degradation. The experiment has been inoperable since.

BIBLIOGRAPHY

PM: A70-27181, A71-14028.
PS: A69-30191.
OS: A71-24439.

OGO 3, McDonald

EXPERIMENT NAME Cosmic-Ray Isotopic
Abundance
NSSDC ID 66-049A-02
PROJECT DESIGNATION 4906, B-06a
PERSONNEL

- PI - F.B. McDonald
NASA-GSFC - Greenbelt, Maryland
- OI - G.H. Ludwig
NASA-GSFC - Greenbelt, Maryland

BRIEF DESCRIPTION

To analyze the charge and energy spectra of the primary cosmic radiation, a dE/dx vs E plastic scintillator telescope measured ions with Z values between 1 and 8 and with energies in a Z-dependent range (for example, for Z=1 or 2, the range was 15 to 80 MeV/nucleon; for Z=6, the range was 25 to 145 MeV/nucleon). Pulse height analysis was performed on 1, 8, or 64 events per sec. Count rates in various telescope modes were also obtained. The instrumentation was located on the anti-Earth panel of the main body. The channel-multiplier portion of the experiment failed 90 hours after initial turn-on, resulting in a serious degradation of the experiment.

BIBLIOGRAPHY - None found

OGO 3, Sagalyn

EXPERIMENT NAME Spherical Ion and
Electron Trap
NSSDC ID 66-049A-13
PROJECT DESIGNATION 4912, B-12
PERSONNEL

- PI - R.C. Sagalyn
AFCL - Bedford, Massachusetts
- OI - M. Smiddy
AFCL - Bedford, Massachusetts

BRIEF DESCRIPTION

Two independent spherical electrostatic analyzers were used to measure the flux, energy distribution, temperature, and density of ions and electrons from perigee up to spacecraft apogee. Electron and ion densities were measured in the range 1 to 10⁸ particles/cubic centimeter. The range of measurements of thermal ion and electron temperatures was from 700 to approximately 100,000 deg K. The

SPACECRAFT AND EXPERIMENT CHARACTERISTICS

data obtained were used to study the low-energy plasma properties of the magnetosphere during quiet and disturbed solar periods. Each analyzer, composed of a mesh ball surrounding a collector, was mounted on boom EP-1 that extended 2.4 m from the vehicle surface. The experiment had a basic cycle time of 25.6 min. Density, spacecraft potential, and differential energy distribution were measured repeatedly for approximately 13 min during a cycle. High-energy flux and energy distribution were measured during the remaining 13 min. Inflight calibrations were applied to the electrometers of both sensors once per cycle. The measurements were judged to be accurate to approximately 30 percent. The experiment provided good data during the first 3 months of operation in spite of some degradation due to observatory spin. The failure of the mode commutator in October 1966 caused further degradation of the experiment.

BIBLIOGRAPHY

PM: A68-29421.

OGO 3, Simpson

EXPERIMENT NAME Cosmic-Ray Spectra and Fluxes
 NSSDC ID 66-049A-03
 PROJECT DESIGNATION 4907, B-07
 PERSONNEL
 PI - J.A. Simpson
 University of Chicago - Chicago, Illinois
 OI - C.Y. Fan
 University of Chicago - Chicago, Illinois
 OI - P. Meyer
 University of Chicago - Chicago, Illinois

BRIEF DESCRIPTION

Three solid-state particle telescopes were used to measure the intensity and energy distribution of cosmic rays. A dE/dx vs E telescope (composition telescope) resolved the nuclear composition of cosmic rays in the energy range from 30 to 100 MeV/nucleon (charge resolution range through $Z=26$, energy per nucleon intervals approximately proportional to Z^2/A). A dE/dx vs range telescope (proton-alpha telescope) detected protons and alpha particles in the energy range from 1.6 to 33 MeV/nucleon, and a single-element low-energy proton telescope (OPEP telescope) was primarily sensitive to protons in the energy range from 1.4 to 3.7 MeV. The composition and proton-alpha telescopes were located in the main body and oriented parallel to the spacecraft z axis, whereas the OPEP telescope was oriented perpendicular to the z axis. Pulse height information was obtained from the composition telescope using one 256-channel and two 512-channel pulse height analyzers. This allowed pulse height analysis of particles in four energy intervals -- for protons 5 to 11 MeV, 11 to 22 MeV, 22 to 103 MeV, and greater than 103 MeV. Pulse height information was sent back from the proton-alpha telescope using one 256-channel pulse height analyzer. This allowed pulse height analysis of particles in two energy ranges -- for protons 1.6 to 8.6 MeV and 8.6 to 33 MeV. Count rate information was obtained from all three telescopes. The time resolution ranged from about one measurement per 0.02 sec to about one measurement per 147 sec, depending on the counting mode and the telemetry bit rate. The experiment was not affected by observatory spin, and useful data were obtained.

BIBLIOGRAPHY

PM: A68-41420, A71-18127.
 B03716-000.

OGO 3, Smith

EXPERIMENT NAME Triaxial Search-Coil Magnetometer
 NSSDC ID 66-049A-12
 PROJECT DESIGNATION 4910, B-10
 PERSONNEL
 PI - E.J. Smith
 NASA-JPL - Pasadena, California
 OI - R.E. Holzer
 University of California - Los Angeles, California

BRIEF DESCRIPTION

In this experiment magnetic field variations were measured triaxially from 0.01 to 800 Hz by a search-coil magnetometer with high-permeability core mounted on boom EP-5. The signals were divided into a high-frequency and a low-frequency channel which overlapped near the center of the five-decade frequency band. The low-frequency wave forms were digitized and telemetered. The high-frequency information was obtained continuously by using an on-board low-resolution spectrum analyzer consisting of five comb filters centered at 10, 32, 100, 320 and 800 Hz. The high-frequency wave forms were also telemetered (on a part-time basis) in analog form for subsequent high-resolution, ground-based processing. The instrument performed throughout the operational life of the spacecraft, but the usefulness of the three broadband channels was reduced by spacecraft interference.

BIBLIOGRAPHY

PM: A68-41693, A69-18834, A69-36675, A69-40501,
 A70-21380.
 PS: A70-30078,
 N73-10791.
 PC: N69-72494.
 OS: A72-21189.

OGO 3, Taylor

EXPERIMENT NAME Positive Ion Composition
 NSSDC ID 66-049A-15
 PROJECT DESIGNATION 4915, B-15
 PERSONNEL
 PI - H.A. Taylor, Jr.
 NASA-GSFC - Greenbelt, Maryland
 OI - N.W. Spencer
 NASA-GSFC - Greenbelt, Maryland

BRIEF DESCRIPTION

This experiment was designed to study the global nature of the thermal ions surrounding the Earth. The experiment contained two ceramic Bennett RF mass spectrometers mounted in OPEP-1. Each tube contained 17 grids, a collector, and an external guard ring. Voltages on the guard ring and on some of the grids were set at fixed or controlled negative dc voltage levels. When a positive ion of proper mass and velocity was resonant with the RF voltage, it passed the final positive grid and struck the collector. These impinging positive ions caused a current flow that was converted by an electrometer to a voltage directly proportional to the current. The resultant voltage was processed by the decade amplifier into

SPACECRAFT AND EXPERIMENT CHARACTERISTICS

analog data outputs for each tube, one output for each decade of collector current between 10^{-14} and 10^{-8} amp. The low mass spectrometer measured ions with mass-to-charge ratios from 1 to 6 amu, with a resolution of 0.5 amu. The high-mass spectrometer measured m/e values from 7 to 45 amu, with a resolution of 1 in 20. A complete mass scan took 64 sec. The instruments had a dynamic range from 5 ions/cc to 10^6 ions/cc. Excellent data were obtained during the first 40 days of attitude-controlled operation. Useful data were also obtained during the subsequent spin mode operation but with complications due to attitude effects. The gradual increase in perigee height also placed some limitations on the usefulness of this experiment.

BIBLIOGRAPHY

PM: A68-19744, A68-37114, A69-23777, A70-26568,
A70-29185, A70-38377, A72-17453.

PS: A68-41673.

OM: A69-25153, A69-25157.

OS: A70-30358.

OGO 3, Whipple

EXPERIMENT NAME Planar Ion and Electron
Trap
NSSDC ID 66-049A-14
PROJECT DESIGNATION 4913, B-13
PERSONNEL
PI - E.C. Whipple
ESSA - Boulder, Colorado
OI - B.E. Troy, Jr.
NASA-GSFC - Greenbelt, Maryland

BRIEF DESCRIPTION

This experiment was designed to measure the distributions of ions and electrons near thermal energy from perigee to apogee. The data also specified the magnitude and polarity of the spacecraft charge. The instrumentation consisted of a plasma detector and an electrometer, mounted together on the OPEP-1, and ancillary electronics that included logic and detection circuits. The plasma sensor contained three parallel circular grids and a collector. The aperture grid was 3.3 cm in diameter, and the two interior grids were 7.3 cm in diameter. A gold-plated magnesium collector was mounted behind the grids. The detector shell provided a ground plane flush with the spacecraft skin. The experiment was operated in both low-resolution and high-resolution modes for electrons and ions. The average time to complete an observation in any one mode was 15 sec. The collector current was measured with a vibrating reed electrometer in the range from 10^{-13} to 10^{-6} amp. This experiment operated on a reduced schedule to minimize interference with the triaxial search coil magnetometer experiment. The data were also seriously degraded by observatory spin.

BIBLIOGRAPHY

PM: A74-18372,
N74-74638.

PS: A69-31976, A70-13994, A73-33436.

IV-22

OGO 3, Winckler

EXPERIMENT NAME Electron Spectrometer
NSSDC ID 66-049A-22
PROJECT DESIGNATION 4909, B-09
PERSONNEL
PI - J.R. Winckler
University of Minnesota - Minneapolis, Minnesota
OI - R.L. Arnoldy
University of Minnesota - Minneapolis, Minnesota
OI - K.A. Pfitzer
University of Minnesota - Minneapolis, Minnesota

BRIEF DESCRIPTION

The objective of this experiment was to measure the electron energy spectrum in the radiation belts for the range from 50 keV to 4 MeV. The experiment consisted of a five-channel electron spectrometer containing an analyzing electromagnet, a plastic scintillator crystal, a PM, and a pulse height analyzer. The analyzing electromagnet was used to define the five energy channels. The pulse height analyzer accepted only the pulses corresponding to the particular energy channel being sampled. In this way the background due to bremsstrahlung and penetrating particles was reduced because only those background pulses in the narrow energy band being analyzed were counted. This system was mounted in the main body in a direction 10 deg off the spacecraft z-axis with a 15-deg acceptance cone. Since OGO 3 was spin stabilized about its z-axis shortly after launch, the acceptance cone was effectively increased to 35 deg. Directional measurements of electrons were made in five contiguous, logarithmically equispaced energy channels between 50 and 4000 keV. Background particles were counted by operating the spectrometer without the electromagnet. The system sampled the five spectral intervals and five background intervals every 2.3 sec when the OGO 3 system was operating at 1 kbs. The sampling rate increased linearly with the telemetry bit rate. Data from each of the five channels were telemetered as one digital word. This experiment performed well from launch to December 1, 1969, when all experiments aboard OGO 3 were turned off.

BIBLIOGRAPHY

PM: A68-41697, A69-40508, A69-43172, A70-30090,
N67-13710, N69-19899, N70-17448, N70-17624,
N72-28802, N74-74639.

OM: N73-20842, N74-20502, N74-20503.

OS: N74-74636.

OGO 3, Winckler

EXPERIMENT NAME Ionization Chamber
NSSDC ID 66-049A-23
PROJECT DESIGNATION 4909, B-09
PERSONNEL
PI - J.R. Winckler
University of Minnesota - Minneapolis, Minnesota
OI - R.L. Arnoldy
University of Minnesota - Minneapolis, Minnesota
OI - S.R. Kane
University of Minnesota - Minneapolis, Minnesota

Nov. 10, 1975

SPACECRAFT AND EXPERIMENT CHARACTERISTICS

BRIEF DESCRIPTION

This experiment was designed to measure the ionization due to primary cosmic rays. The instrumentation consisted of a 17.8-cm diameter integrating ionization chamber with a resetting drift-type electrometer. The system was mounted on the 1.2-m EP-4 boom extending from the main body of the spacecraft along the y axis. The chamber responded to electrons and protons with energies greater than 0.6 and 12 MeV, respectively, and to X-rays in the range 10 to 50 keV. The ionization current was measured by a vacuum tube electrometer the output of which, as a function of time, was an automatically resetting sawtooth ramp voltage between 0 and 5 V. Data were telemetered in three independent forms through three digital words and one analog word, each of which was telemetered once every 1.152 sec when the OGO 3 system was operating at 1 kbs. The sampling rate linearly increased with the telemetry rate. This experiment performed well from launch to December 1969 when all experiments aboard OGO 3 were turned off.

BIBLIOGRAPHY

- PM: A67-41232, A68-22450, A68-35480, A69-12740, A69-22182, A69-40508, A69-43172, A70-15106, A71-18128, N67-13710, N68-10422, N68-23026, N70-17448, N70-17624, N72-28802, N74-18420, N74-21445, N74-74639.
- OS: A69-33055, A69-34227, A70-30059, A71-17918, A71-27654, A73-14962.

OGO 3, Wolfe

EXPERIMENT NAME Electrostatic Plasma Analysis (Protons 0.1-18 keV)
 NSSDC ID 66-049A-05
 PROJECT DESIGNATION 4902, B-02
 PERSONNEL
 PI - J.H. Wolfe
 NASA-ARC - Moffett Field, California

BRIEF DESCRIPTION

This experiment was designed to study the positive ion component of the solar wind plasma. Three quadrispherical electrostatic analyzers, two looking into the orbital plane (OPEP-2) and one solar-oriented (SOEP-2), were to be used to detect protons in 30 steps in the range 100 to 18,000 eV. Owing to the unintended spacecraft spin, little useful data were obtained. The data may be used to indicate the location of the magnetopause and bow shock.

BIBLIOGRAPHY

- PM: A65-29239.

OGO 3, Wolff

EXPERIMENT NAME Gegenschein Photometry
 NSSDC ID 66-049A-20
 PROJECT DESIGNATION 4920, B-20

PERSONNEL

- PI - C.L. Wolff
 NASA-GSFC - Greenbelt, Maryland
 OI - K.L. Hallam
 NASA-GSFC - Greenbelt, Maryland
 OI - S.P. Wyatt
 University of Illinois - Urbana, Illinois

BRIEF DESCRIPTION

This experiment was designed to measure the amount of solar light that is scattered by particles in space (dust, etc.) in the neighborhood of the antisolar point. This light contribution to the night sky is called the Gegenschein. The data from the experiment were to be pictures of the sky at the antisolar point taken by a TV camera and telemetered to Earth in the form of a matrix of pulse counts. The apparatus was similar, except in minor details, to that flown on OGO 1 (64-054A-11). The experimental package, located in SOEP-2, was a photoelectric camera that formed images of the sky in the visible and near-infrared regions of the spectrum. The data from this assembly were transmitted back to Earth where they were reconstructed into pictures. Each of these pictures covered less than 100 square degrees of the sky, with a resolution on the order of 0.25 deg. The package consisted of -- (1) an f/1.5 objective lens, (2) a filter wheel containing three filters centered at 3000, 5000, and 7000 A, with passbands of 500 A, (3) an S-20 cathode deposited on a thin, curved ultraviolet transmitting glass, (4) an image dissector named the Star Tracker FW 143B made by the ITT Corporation, and (5) an electronic unit that amplified and counted the current pulses coming from the tube due to the individual photons arriving at the photocathode. The experiment failed to achieve its initial objective for the following reasons--(1) during the first six weeks of orbit the antisolar point was within the Milky Way and could not be detected, (2) after the first six weeks of orbit the spacecraft was spun up, making it impossible to take pictures, and (3) the signal-to-noise ratio was not as large as expected due to scattered sunlight from other parts of the spacecraft. Despite the failure to achieve the original goals, an interesting study on the optical environment about the spacecraft was made.

BIBLIOGRAPHY

- PM: A68-12548.
 N67-35595.

Nov. 10, 1975

SPACECRAFT AND EXPERIMENT CHARACTERISTICS

OGO 4

SPACECRAFT CHARACTERISTICS

COMMON NAME OGO 4
 ALTERNATE NAMES OGO-D, POGO 2,
 02895, S 50A
 NSSDC ID 67-073A
 LAUNCH DATE 07/28/67
 WEIGHT IN ORBIT 562 kg
 LAUNCH SITE Vandenberg Air Force
 Base, United States
 LAUNCH VEHICLE Thrust-Augmented
 Thor-Agena D
 SPONSORING COUNTRY United States
 SPONSORING AGENCY NASA-OSSA

ORBIT PARAMETERS

	INITIAL	LATER
Epoch Date	07/27/67	01/28/72
Apogee (km alt)	900	505
Perigee (km alt)	416	364
Period (min)	98	93
Inclination (deg)	86.0	86.0

PERSONNEL

Project Manager -
 W. E. Scull - NASA-GSFC - Greenbelt, Maryland
 Project Scientist -
 N. W. Spencer - NASA-GSFC - Greenbelt, Maryland
 Program Manager -
 C. D. Ashworth - NASA Hq. - Washington, D.C.
 Program Scientist -
 R. F. Fellows - NASA Hq. - Washington, D.C.

BRIEF DESCRIPTION

OGO 4 was a large observatory instrumented with experiments designed to study the interrelationships between the aurora and airglow emissions, energetic particle activity, geomagnetic field variation, ionospheric ionization and recombination, and atmospheric heating which take place during a period of increased solar activity. OGO 4 consisted of a main body, generally parallelepiped in form, two rectangular solar panels each including a solar-oriented experiment package (SOEP), two Orbital-Plane experiment packages (OPEP), and six appendages EP-1 through EP-6, supporting the boom experiment packages. The main body was attitude controlled by horizon scanners and gas jets and was designed to be pointed toward the Earth (z axis). The axis connecting the two solar panels (x axis) was designed to oscillate and remain perpendicular to the Earth-Sun-spacecraft plane. The solar panels, activated by Sun sensors, could rotate about this axis to obtain maximum radiation for the solar cells and, concurrently, orient the SOEP properly. The OPEPs were mounted on either end of an axis which was parallel to the z axis and attached to the forward end of the main body. The OPEP sensors normally were maintained looking forward in the orbital plane of the satellite. To maintain this orientation, the OPEP axis could rotate over 90 deg, and, in addition, an angular difference of over 90 deg was possible between the orientation of the upper and lower OPEP packages. The SOEP contained four experiments, and the OPEP contained five experiments. After the spacecraft achieved orbit and the experiments were deployed into an operating mode, an attitude-control problem occurred. This condition was corrected by ground-control procedures, and three-axis stabilization was maintained for 18 months until complete failure of the tape recording systems in mid-January 1969. At that time, due to the difficulty of maintaining attitude control without the tape recorders, the attitude control system was commanded off, and the spacecraft was placed into a spin-stabilized mode about the axis which was previously maintained

IV-24

vertically. Initial spin period was 202 sec with the mean spin axis approximately perpendicular to the orbit plane (spin period as of March 12, 1969, was 217 sec). The precession period of the mean spin axis was about 5 days. In this mode, seven of the remaining experiments were turned off since no meaningful data could be observed by them. On October 23, 1969, the satellite was placed in a stand-by status. It was reactivated to obtain VLF observations from February 1, 1970, to March 9, 1970; from January 27, 1971, to February 2, 1971; and from August 17, 1971, to September 27, 1971. Operational support of OGO 4 was terminated on September 27, 1971.

SPACECRAFT/MISSION BIBLIOGRAPHY

Papers with major discussion of spacecraft, mission, testing, subsystems, or ground systems prepared by NASA project or project support personnel.
 A63-10333, A69-36674, A70-35303,
 N74-76932.

Papers about spacecraft, mission, testing, subsystems, or ground systems prepared by NASA contractor personnel.
 A64-10864.
 N69-33977.

EXPERIMENTS

OGO 4, Anderson

EXPERIMENT NAME Cosmic-Ray Ionization
 NSSDC ID 67-073A-07
 PROJECT DESIGNATION 5007, D-07
 PERSONNEL
 PI - H.R. Anderson
 Rice University - Houston, Texas
 OI - V.H. Neher
 Cal Tech - Pasadena, California

BRIEF DESCRIPTION

This experiment was designed to measure cosmic-ray and solar flare particle intensities (protons above 10 MeV, electrons above 0.5 MeV) using an ion chamber. The ion chamber was mounted at the end of spacecraft boom EP-1 about 2.5 m from the main body of the spacecraft. The ion chamber operated successfully for only the first 160 orbits of the satellite. The reason for the failure is not known.

BIBLIOGRAPHY

PM: A70-31903.
 N74-74624, N74-76923.
 PS: N69-34536.

SPACECRAFT AND EXPERIMENT CHARACTERISTICS

OGO 4, Barth

EXPERIMENT NAME UV Spectrometer,
1100-3400 A
 NSSDC ID 67-073A-14
 PROJECT DESIGNATION 5014, D-14
 PERSONNEL
 PI - C.A. Barth
 University of Colorado - Boulder, Colorado
 OI - L.J. Wallace
 Kitt Peak National Observatory - Tucson, Arizona
 OI - E.F. Mackey
 Packard-Bell - Newbury Park, California

BRIEF DESCRIPTION

An Ebert-Fastie scanning spectrometer was used to measure the ultraviolet (UV) spectrum of the Earth in the wavelength range from 1100 to 3400 A, with a 20-A resolution. The objectives of this experiment included the measurement of the intensity of the following emissions -- (a) the hydrogen Lyman-Alpha on both the day and night sides, (b) the atomic oxygen 1304-A day and twilight glow, and (c) the atomic oxygen 1356-A line, the atomic nitrogen 1493-A line, and the molecular nitrogen Lyman-Birge-Hopfield bands of the photoelectron-excited dayglow. Another objective was the determination of the vertical distribution of ozone from the measurement of the back-scattered UV daylight in the 2000- to 3400-A range. The focal length of the Ebert mirror was 250 mm, and the grating used had 2160 lines per millimeter. The spectral scan period was 74.5 sec. However, during about 7 percent of the time, this scan period was reduced to 18.6 sec. The instrument was mounted on the main body looking to nadir. The F channel was the output of a PM with a sapphire window and a cesium telluride cathode. The wavelength interval measured here extended from 1750 to 3400 A, with a dynamic range of 10⁸. The G-data channel was the output of a PM with a lithium fluoride window and a cesium iodide cathode. On this channel the wavelength ranges scanned extended from 1100 to 1750 A, and the measured intensity could vary over a range from 1 to 1000. Prefocused light sources, some operated by command, provided in-orbit calibrations. This experiment remained operational until the support of OGO 4 was ended in September 1971.

BIBLIOGRAPHY

PM: A69-31400, A69-32645, A69-36682, A70-39338,
A73-10878, A73-41925,
N69-26549.
 OM: A72-26402.
 OS: A69-34957, A70-39344, A72-42418.

OGO 4, Cain

EXPERIMENT NAME Magnetic Survey,
Rubidium Vapor
Magnetometer
 NSSDC ID 67-073A-06
 PROJECT DESIGNATION 5006, D-06
 PERSONNEL
 PI - J.C. Cain
 NASA-GSFC - Greenbelt, Maryland
 OI - R.A. Langel
 NASA-GSFC - Greenbelt, Maryland

BRIEF DESCRIPTION

The OGO 4 rubidium vapor magnetometer, located in EP-6, was an optically pumped, self-oscillating dual cell instrument used to measure the scalar field from polar orbit. The instrument was sampled every 0.5 sec, and operated almost continuously from launch until January 19, 1969. The measurements were accurate to within 0.4 gamma, with an absolute accuracy expected to be about 2 gammas. The accuracy of the measurements was limited by spacecraft fields.

BIBLIOGRAPHY

PM: A69-37490, A69-42428, A70-39349, A71-29903,
A72-12081, A73-31768, A73-31773, A74-34019,
N71-32190, N72-30823, N73-20866, N74-13566,
N74-17058.
B15846-000, B15849-000.

PS: A73-31772, A73-41374,
N72-23341, N74-20982.

OGO 4, Chandra

EXPERIMENT NAME Positive Ion Study
 NSSDC ID 67-073A-19
 PROJECT DESIGNATION 5019, D-19
 PERSONNEL
 PI - S.S. Chandra
 NASA-GSFC - Greenbelt, Maryland
 OI - J.L. Donley
 NASA-GSFC - Greenbelt, Maryland
 OI - R.E. Bourdeau
 NASA-GSFC - Greenbelt, Maryland

BRIEF DESCRIPTION

This instrument was a planar retarding potential analyzer (RPA) which was designed to measure ion composition and density, and the temperature of ions and electrons. The sensor unit in OPEP-1 was oriented to face the spacecraft velocity vector. It consisted of three circular gold-plated wire-mesh grids mounted in front of a circular gold-plated collector. All elements were separated by 0.4 cm. The outer grid was 2.5 cm in diameter, and the remaining elements were 6.4 cm in diameter. This outer grid was mounted on a 7-cm guard ring, flush with, but electrically isolated from, the OPEP. A sweep of stepping voltages (128 steps) was applied in alternating ion (middle grid swept from 12.6 to -0.1 v) and electron (outer two grids swept from -3.2 to 7.0 v) modes. Raw data consisted of plots of retarding potential values versus current flowing to the collector. These were analyzed to obtain temperature, density, and composition data. The 128 voltage steps required for each curve took 36.6 seconds to sweep, during which time the spacecraft moved a distance of 1.5 to 2.5 deg latitude. The densities observable ranged from about 100 to 100,000 particles/cc. The composition determinations could not satisfactorily distinguish N+ from O+, but HE+ and H+ were consistently identifiable. This experiment operated satisfactorily for 13,563 hr over a period of about 18 months. Data collected after the spacecraft stabilization was lost were not usable.

SPACECRAFT AND EXPERIMENT CHARACTERISTICS

BIBLIOGRAPHY

PM: A70-36016, A71-19663, A71-33956, A73-38939,
N68-35999,
B22334-000.

PS: A71-30037, A71-30951.

PC: N74-76910.

OS: A72-26411, A73-33436.

OGO 4, Haddock

EXPERIMENT NAME Radio Astronomy
NSSDC ID 67-073A-01
PROJECT DESIGNATION 5001, D-01
PERSONNEL
PI - F.T. Haddock
University of Michigan - Ann Arbor, Michigan
OI - W. Potter
University of Michigan - Ann Arbor Michigan

BRIEF DESCRIPTION

The purpose of this experiment was to map the brightness temperature of the sky at a frequency of 2.5 MHz, using an 18-m monopole antenna on the spacecraft and depending upon ionospheric focusing to achieve angular resolution. The experiment, located in SOEP-1, operated for the life of the spacecraft, returning data from radiometers operating at 2.0 and 2.5 MHz and measurements of the complex impedance of the antenna at 2.5 MHz. Radio-frequency interference generated within the spacecraft made interpretation of the radiometer data very difficult, and it appears to be impractical to extract mapping information. The antenna impedance measurements were unaffected and represent a body of data useful for the study of the properties of the ionosphere and the behavior of antennas in plasma.

BIBLIOGRAPHY

PM: A71-26144,
N70-42352.

PS: N69-25437.

OGO 4, Helliwell

EXPERIMENT NAME VLF Noise and
Propagation
NSSDC ID 67-073A-02
PROJECT DESIGNATION 5002, D-02
PERSONNEL
PI - R.A. Helliwell
Stanford University - Stanford, California
OI - L.H. Rorden
Stanford University - Stanford, California

BRIEF DESCRIPTION

This experiment consisted of six VLF radio receivers that studied natural and man-made VLF noise occurrences at orbital altitudes. The receiver systems consisted of an inflatable 2.9-m loop antenna,

a preamplifier stage at the end of the EP-5 boom, and a receiver electronics package in the main body of the satellite. Three step-frequency receivers covered the frequency ranges from 0.2 to 1.6, 1.6 to 12.5, and 12.5 to 100 kHz. Observations from these receivers were tape recorded and read out upon command. These three step-frequency receivers could be tuned, on command, to any fixed frequency in their range. The fourth (phase-tracking) receiver operated between 14.4 and 26.3 kHz and was tuned on command to receive signals from any VLF station transmitting in this range. These data were recorded and transmitted in the same way as the step-frequency receiver data. The fifth and sixth receivers were broadband, operating from 0.015 to 0.30 kHz (ELF) and from 0.30 to 12.5 kHz (VLF). These data were not tape recorded, but were observed only in real time on the special purpose telemetry channel. A matching transformer connected on command to the antenna allowed either electric field or magnetic field observations. This experiment was the same as that for OGO 2, except for the addition of the ELF receiver and the ability to make electric-field observations. The experiment operated nominally through February 1968, when the electric field observing mode failed. Subsequent operation continued until spacecraft shut-down in November 1969. The experiment was reactivated in 1970 (1 February - 9 March), and twice in 1971 (27 January - 2 February, and 17 August - 27 September). It was turned on once in 1971 for Apollo support, and once to obtain correlative data for USAF Cannonball (71-067C) observations.

BIBLIOGRAPHY

PM: A69-14029, A70-15116, A70-18532, A71-31757,
A71-39746, A72-23008, A73-33451, A73-33876,
N68-14025, N70-15525, N70-15768, N70-32928,
N73-16126, N73-22079, N74-12109.

PS: N74-15857.

OM: A70-18534.

OS: A70-30078, A72-19149, A72-21189.

OGO 4, Hinteregger

EXPERIMENT NAME Solar UV Emissions
NSSDC ID 67-073A-20
PROJECT DESIGNATION 5020, D-20
PERSONNEL
PI - H.E. Hinteregger
AFCRL - Bedford, Massachusetts
OI - D.E. Bedo
AFCRL - Bedford, Massachusetts

BRIEF DESCRIPTION

This experiment was designed to measure solar photon flux as a function of wavelength between 170 and 1700 Å. The experiment was located on SOEP-2, a solar-oriented panel on the spacecraft. Solar radiation entered the experiment package through an aperture equipped with a set of electrically charged grids to reject charged particles. Then the radiation illuminated a stack of six small gratings and was diffracted onto six photocathodes. These photocathodes were located in two PMs (two per PM). By electronic discrimination, only one photocathode was used at any given time in each photomultiplier. The gratings were all illuminated at the same angle of incidence, and were stepped through the spectral range in 512 intervals every seven minutes during normal operation. An alternative mode provided for a short scan of 32 steps, beginning at any of 16 different points in the 512-step scan. The experiment failed after two weeks in orbit (August 12, 1967). The two-week period was used to check out the instrument rather than to collect data, so no data resulted.

SPACECRAFT AND EXPERIMENT CHARACTERISTICS

BIBLIOGRAPHY

PM: N65-29678.

PC: N65-14504.

OGO 4, Jones

EXPERIMENT NAME Neutral Particle and Ion
Composition
NSSDC ID 67-073A-15
PROJECT DESIGNATION 5015, D-15
PERSONNEL
PI - L.M. Jones
University of Michigan - Ann Arbor, Michigan
OI - R.J. Leite
University of Michigan - Ann Arbor, Michigan

OGO 4, Hoffman

EXPERIMENT NAME Low-Energy Auroral
Particle Detector
NSSDC ID 67-073A-11
PROJECT DESIGNATION 5011, D-11
PERSONNEL
PI - R.A. Hoffman
NASA-GSFC - Greenbelt, Maryland
OI - D.S. Evans
NASA-GSFC - Greenbelt, Maryland

BRIEF DESCRIPTION

The auroral particles experiment, located in EP-2, contained eight detectors, each comprised of a cylindrical electrostatic analyzer with a channel electron multiplier. Seven of these detectors were capable of measuring protons or electrons as selected by ground command, and the eighth detector measured background. Five of the detectors looked along a vector pointing radially away from the Earth, while three others looked out at 30 deg, 60 deg, and 90 deg to the radius vector pointing away from the Earth. The look directions of all the detectors lay in a single plane. Four of the detectors that looked directly away from the Earth measured electrons or protons at either 0.7, 2.3, 7.4, or 23.8 keV, and the fifth measured the background. Those detectors at other angles measured electrons or protons at 2.3 keV. Most of the data were taken over the north and south auroral zones and polar caps, but a small amount of lower latitude data were taken. The data taken over the south auroral zone amounted to less than 5 percent of the data. Since the magnetic field of the Earth is nearly vertical in the auroral zone, the detectors that pointed away from the Earth measured precipitating particles, and the angled detectors measured particles having pitch angles nearly comparable to their respective spacecraft angles. All detectors, except for the 6 keV and the 90 deg 2 keV, developed some noise problems preventing the measurement of small fluxes. Otherwise the detectors functioned normally from initial turn-on (July 30, 1967) until January 25, 1969, when the experiment was turned off. The experiment was operated in the electron mode continuously for about six days out of every seven.

BIBLIOGRAPHY

PM: A68-43443, A69-28964, A71-27911, A71-30032,
A72-19149, A72-39541, A73-15531, A73-26988,
A73-41914, A74-14274,
N70-29987, N71-25272, N73-10392, N73-11345,
N73-21367, N73-25868, N74-74628.
B16576-000, B22333-000.

BRIEF DESCRIPTION

The objective of this experiment was to obtain ambient composition data, for both neutral and ionized species, that would contribute to an understanding of several atmospheric processes and phenomena such as diffusive separation, photochemical production, and photoionization. The OGO 4 electron-impact, open-ion-source quadrupole mass spectrometer was programmed to measure the concentration of both neutral and charged particles over the mass-to-charge ratio range from 50 to 0. The resolution was such that mass-to-charge ratio (m divided by e) values 19, 20, and 21 could easily be distinguished. The maximum sensitivity for positive ions was 10 ions/cc/V output and for neutral species 100,000 neutral particles/cc/V output. The lower sensitivity for neutrals resulted from low-ionization efficiency of the ion source. There were six linear decade output ranges. To avoid sequential switching of all six decades, two amplifiers were provided at the electrometer output, one with unity gain and the other with a gain of 10. Each amplifier was connected to a separate analog data channel with this arrangement. The six-decade output range was achieved with only three range-switching operations. The remaining analog data channel assigned to this experiment was devoted to spectrometer housekeeping data. Each sweep cycle, i.e., scan of m/e values from 50 to 1, took 6 sec and resulted in a spatial resolution of 0.8 km per mass unit of sweep. A complete measurement consisted of 14 mass sweeps, which were divided equally between the collection of charged and neutral particles, with two sweeps devoted to instrument calibration. The spectrometer was operated in two modes - a normal or spectral mode and a zero resolution or 'staircase' mode where the output corresponded approximately to an integral spectrum. The experiment, which weighed 3.8 kg, was mounted in OPEP-2, an orbital plane experiment package. This experiment remained operational until the OGO 4 support was ended in September 1971.

BIBLIOGRAPHY

PM: A69-36681,
N71-21544, N71-23238.
B05000-000.

OGO 4, Kreplin

EXPERIMENT NAME Solar X-ray Emissions
NSSDC ID 67-073A-21
PROJECT DESIGNATION 5021, D-21
PERSONNEL
PI - R.W. Kreplin
Naval Research Laboratory - Washington, D.C.
OI - T.A. Chubb
Naval Research Laboratory - Washington, D.C.
OI - H.D. Friedman
Naval Research Laboratory - Washington, D.C.

SPACECRAFT AND EXPERIMENT CHARACTERISTICS

BRIEF DESCRIPTION

The objective of this experiment was to measure the solar X-ray emission flux for correlations with phenomena in the D and E regions of the Earth's ionosphere. The experiment was composed of four ionization chambers that were sensitive in nominal 0.5- to 3.0-A, 1- to 8-A, 8- to 16-A (or 8- to 20-A), and 44- to 60-A passbands. The detectors were mounted in SOEP-2, a solar-oriented experiment package of the spacecraft, and were pointed continuously at the Sun. The currents generated in the ionization chambers were amplified by linear electrometers, three of which changed ranges automatically to provide the appropriate sensitivity for observations during both intense solar flares and solar quiet periods. The outputs from the electrometers were digitized and either transmitted directly to the ground or stored in the spacecraft tape recorders for later transmission. The worst-time resolution, obtained with the spacecraft multiplexer operating at 4 kbs, was 4.6 sec for the 8- to 16-A and 44- to 60-A detectors. The time resolution was considerably better for the 0.5- to 8-A detectors. The 44- to 60-A detector failed in November 1967, but the other three detectors produced useful data until the spacecraft tape recorder was disabled in January 1969.

BIBLIOGRAPHY

- PM: A69-43611, A71-14046, A71-14212, A71-20318,
N74-74629.
- PS: A70-43301,
N69-32730.
- OS: A72-35089,
N69-17412, N71-36131.

OGO 4, Mange

EXPERIMENT NAME Lyman-Alpha and UV
Airglow Study

NSSDC ID 67-073A-13

PROJECT DESIGNATION 5013, D-13

PERSONNEL

PI - P.W. Mange
Naval Research Laboratory - Washington, D.C.

OI - R.R. Meier
Naval Research Laboratory - Washington, D.C.

BRIEF DESCRIPTION

This experiment was designed to measure the Lyman-Alpha night skyglow radiation from Earth (1050 to 1350 A), the Lyman-Alpha background radiation from space (1050 to 1350 A), and the Far-UV airglow radiation from Earth (1230 to 1350 A and 1350 to 1550 A) using eight detectors located on the main body. Seven of the detectors were pointed toward the Earth to measure the Far-UV airglow and Lyman-Alpha night skyglow, and one was directed toward space to measure the Lyman-Alpha background radiation. The 1050- to 1350-A detectors had lithium fluoride windows and nitric-oxide gas filler, the 1230- to 1350-A detectors had calcium fluoride windows and nitric-oxide gas filler, and the 1350- to 1550-A detectors had barium fluoride windows and a symmetrical dimethyl-hydrazine gas filler. These detectors observed zenith and nadir intensities in the night sky at altitudes of 400 to 900 km. The output consisted of intensities taken at 2-min intervals covering the period from July 29, 1967, to January 20, 1969. The satellite tape recorder failed on January 20, 1969, limiting the data to real time only. Prior to this equipment failure, the radiation detectors operated with negligible loss of sensitivity with the exception of the 1230- to 1350-A detectors which, for no known reason, steadily decreased in sensitivity and became useless after 6 weeks of operation. In general, the operation of the instrumentation was nominal.

IV-28

BIBLIOGRAPHY

- PM: A70-15128, A70-23493, A70-35764, A71-11503,
A71-11504, A71-14028, A71-17279.
- PS: A69-30191.
- OM: A73-38939.
- OS: A69-34957, A72-42418,
N71-34333.

OGO 4, Morgan

EXPERIMENT NAME Whistler and
Audio-Frequency
Electromagnetic Waves

NSSDC ID 67-073A-03

PROJECT DESIGNATION 5003, D-03

PERSONNEL

PI - M.G. Morgan
Dartmouth College - Hanover, New Hampshire

BRIEF DESCRIPTION

This experiment was designed to study ionospheric effects on whistler-mode waves and on propagation of whistlers in the 0.3- to 18-kHz band. It consisted of a dipole electric field carpenter tape antenna, located on EP-1, which was extended to 3 m. This antenna fed a wideband receiver with a 60-db dynamic range. The receiver gain, controlled by ground command, operated in four ranges, stepping down 15 db in each sequential step. An 8-kHz continuous calibration signal of known intensity was fed to the receiver. The resulting data were records of noise frequency versus time. These could be reviewed aurally, or be processed into sonograms for visual study. This experiment worked satisfactorily and was operated over a period of 27 months until spacecraft operation was discontinued.

BIBLIOGRAPHY

- PM: A70-18534, A72-19149.
- OM: A70-19630.
- OS: A72-21189, A72-39541

OGO 4, Newton

EXPERIMENT NAME Neutral Particle Study

NSSDC ID 67-073A-17

PROJECT DESIGNATION 5017, D-17

PERSONNEL

PI - G.P. Newton
NASA-GSFC - Greenbelt, Maryland

BRIEF DESCRIPTION

This experiment was designed to measure neutral atmospheric density and temperature in the upper thermosphere and exosphere

OGO 4, Reed

as a function of spatial and temporal changes. In addition, correlations between changes in the atmospheric parameters and variations of solar and magnetic activity were to be studied. A Bayard-Alpert pressure gauge was used as the sensor. This hot-filament detector had a helical grid around an axial cylindrical collector. Electrons emitted from one of the three redundant filaments, mounted outside the grid, ionized the neutral particles by collision. The positively charged grid not only accelerated the electrons, but it also repelled the positive ions toward the collector and produced a measurable collector current, which was proportional to the number density of particles inside the gauge. Located in OPEP-2, the sensor was scanned about the velocity vector to determine the neutral-particle velocity distribution from which atmospheric temperature can be deduced. The instrument yielded data during the 18 months of attitude controlled OGO 4 operation. It was discovered, however, that the sensor develops a large background ion current which limits its ability to make atmospheric density measurements to relatively low altitudes. The perigee altitude of OGO 4 appear to be too high to allow highly useful atmospheric density data to be obtained.

EXPERIMENT NAME Airglow and Auroral Study
 NSSDC ID 67-073A-12
 PROJECT DESIGNATION 5012, D-12
 PERSONNEL
 PI - E.I. Reed
 NASA-GSFC - Greenbelt, Maryland
 OI - J.E. Blamont
 CNES - Bretigny, France

BIBLIOGRAPHY - None found

BRIEF DESCRIPTION

The objective of this experiment was to study airglow and auroral activity by obtaining photometric measurements at the following wavelengths (Angstroms): 2630 (E-region airglow -- Herzberg molecular oxygen emission, and aurora -- Vegard-Kaplan molecular nitrogen emission); 3914 (visible aurora -- molecular nitrogen ion emission); 5577 (airglow and aurora -- green atomic oxygen emission); 5890 (E-region airglow -- yellow sodium emission); 6225 (E-region airglow--red hydroxyl emission); and 6300 (F-region airglow -- red atomic oxygen emission). The photometers were mounted in the main body and in OPEP-1, an orbital-plane experiment package. All of the above spectral lines were sensed by the main body photometer oriented in the Earth direction. The 6300-A line was also observed in the anti-Earth direction and by the OPEP photometer. In the main body photometer, the incident light was alternately directed through six filters corresponding to the six wavelengths by an automatic stepping-mirror system. The mirrors could be commanded to remain in any of the spectral positions for a more comprehensive study of the distribution of a particular line. The field of view of the main body spectrometer had a half-angle of slightly less than 5 degrees. The field of view of the OPEP spectrometer was 1/2 degree in height and 6 degrees in width. A mirror scan system moved the center of the OPEP field of view from horizontal to 30 degrees below horizontal in 1/2-degree steps. The main body photometer provided data for six months in the Earth direction. The zenith and OPEP photometers worked for the duration of the OGO 4 operations.

OGO 4, Nilsson

EXPERIMENT NAME Interplanetary Dust Particles
 NSSDC ID 67-073A-18
 PROJECT DESIGNATION 5018, D-18
 PERSONNEL
 PI - C.S. Nilsson
 SAO - Cambridge, Massachusetts

BRIEF DESCRIPTION

The objective of this experiment was to measure over a long period of time the velocity and mass distribution of interplanetary dust particles in the mass range from one nanogram to less than one picogram (10^{-9} to 10^{-12} gram). The experiment also attempted to determine the importance of geomagnetic control on the dynamics of dust particles by correlating the various measurements with geophysical, geomagnetic, and solar phenomena. The instrumentation was very similar to that used for micrometeoroid experiments flown on previous OGO flights. The dust particles were detected by four tubular detectors mounted on EP-3 and aligned along the body axes of OGO 4. The tubular detectors were a combination of acoustical and ionization sensors. An incoming dust particle first penetrated a thin film sensor. The ionization caused by this collision formed a plasma cloud which, in turn, triggered a 4-MHz clock. If the particle had sufficient energy, it impacted on the second sensor, a metallic disc with a transducer bonded to it. The signal from the transducer gave a measure of the momentum of the particle. The ionization caused by this second collision produced a plasma cloud, which was detected by a metallic grid and stopped the clock. This allowed the velocity of the particle to be determined. The micrometeoroid detectors were oriented correctly for a good deal of the experiment life. However, some unknown noise in the rear-sensor system limited the amount of useful data concerning rear-sensor events. The microphone system emitted noise in a manner similar to that on OGO 2, and microphone-only events were deleted from the data analysis.

BIBLIOGRAPHY

PM: A70-15522, A70-15645, A72-13428, A73-38939, A74-34042, N71-25268, N72-26309, N72-27423, N72-28353.
 PS: A71-19663, N69-18074.
 PC: N74-74637.

OGO 4, Simpson

EXPERIMENT NAME Low-Energy Proton, Alpha Particle Measurement
 NSSDC ID 67-073A-08
 PROJECT DESIGNATION 5008, D-08
 PERSONNEL
 PI - J.A. Simpson
 University of Chicago - Chicago, Illinois
 OI - C.Y. Fan
 University of Arizona - Tucson, Arizona
 OI - E.C. Stone
 University of Chicago - Chicago, Illinois

BIBLIOGRAPHY

PM: A70-10444, A71-28700, B04201-000.

Nov. 10, 1975

SPACECRAFT AND EXPERIMENT CHARACTERISTICS

BRIEF DESCRIPTION

Two solid-state particle telescopes, located in the main body, were used to study low-energy cosmic-ray protons and alpha particles. One of these was a three-element range telescope ('vertical' telescope) that was capable of identifying two energy ranges of protons and alpha particles (from 1.22 to 39.2 and 9.32 to 39.2 MeV/nucleon) and electrons (energy greater than 400 keV and energy greater than 620 keV). The other detector was a one-element telescope ('horizontal' telescope) sensitive to protons and alpha particles having energy greater than 720 keV/nucleon. The vertical telescope axis of symmetry was parallel to the spacecraft z axis which became the spin axis after January 1969. The horizontal telescope symmetry axis was nearly parallel to the spacecraft y axis (perpendicular to the z axis). Pulse height information was sent back from the vertical telescope allowing pulse height analyses of protons (energies from 1.22 to 39.2 MeV), alpha particles (energies from 4.88 to 156.8 MeV), and electrons (energy greater than 400 keV) using a 256-channel pulse height analyzer. Count rate information was sent back from both telescopes. The experiment performed normally from launch until the spacecraft was placed in a stand-by status on October 23, 1969. However, the spinning of the spacecraft made it difficult to interpret data after mid-January 1969.

BIBLIOGRAPHY

PM: A69-43183, A72-35591, A72-38728, A72-44522,
N72-25727.

PS: A72-21510.

OS: A71-11494, A73-14962,
N69-34536.

OGO 4, Smith

EXPERIMENT NAME Triaxial Search-Coil
Magnetometer

NSSDC ID 67-073A-05

PROJECT DESIGNATION 5005, D-05

PERSONNEL

PI - E.J. Smith
NASA-JPL - Pasadena, California

OI - R.E. Holzer
University of California - Los Angeles, California

BRIEF DESCRIPTION

The OGO 4 triaxial search-coil magnetometer, located on the EP-5 boom, was designed to measure the alternating component of the magnetic field from a low-altitude polar orbit. Measurements were made in the frequency range from 0.01 Hz to 1000 Hz. The signals were divided into a high-frequency and a low-frequency channel which overlapped near the center of the five-decade frequency band. The low-frequency wave forms were digitized and telemetered. The high-frequency information was obtained continuously by using an on-board low-resolution spectrum analyzer consisting of five comb filters centered at 10, 32, 100, 320, and 800 Hz. The high-frequency wave forms were also telemetered (on a part-time basis) in analog form for subsequent high-resolution, ground-based processing. Data were of good quality for the operational life of the spacecraft, including the two months of special operation from January to March of 1970.

IV-30

BIBLIOGRAPHY

PM: A69-18834, A69-36675,
N73-21367.

PS: A70-30078.

PC: B21207-000.

OS: A72-21189.

OGO 4, Taylor

EXPERIMENT NAME Positive Ion
Composition

NSSDC ID 67-073A-16

PROJECT DESIGNATION 5016, D-16

PERSONNEL

PI - H.A. Taylor, Jr.
NASA-GSFC - Greenbelt, Maryland

OI - N.W. Spencer
NASA-GSFC - Greenbelt, Maryland

BRIEF DESCRIPTION

The specific objectives of this experiment included (1) a study of the ion composition as a function of magnetic coordinates (latitude, longitude, time, and McIlwain's L-parameter) to investigate the means and degree of magnetic control of the ion distribution, (2) a comparison of measurements obtained from the same experiment on both the POGO and EOGO spacecraft, with special attention given to ionic diffusion along L-shells, and (3) a study of the temporal, solar, and geomagnetic effects on the ion distribution and transition levels. A ceramic Bennett radio-frequency ion mass spectrometer tube, located in OPEP-1, was used to measure thermal atmospheric ions having mass-to-charge ratio values from 1 to 45, with a mass resolution of about 1 in 20 amu. Concentrations from 10 to 10⁶ ions/cc could be measured. The time between consecutive samples of each ion detected, i.e., the spectral sweep rate, was 25.6 sec, a time interval corresponding to a spatial resolution from 175 to 200 km along orbit path, or to 1.5 deg in latitude. The instrument provided good data for the operational life of the spacecraft.

BIBLIOGRAPHY

PM: A69-31326, A70-18534, A70-38377, A70-41057,
A71-24555, A71-33762, A71-43166, A73-15533,
A73-19255,
N71-25270, N72-23334, N73-17948, N74-10366.

OS: B22333-000.

OGO 4, Van Allen

EXPERIMENT NAME Low-Energy Proton and
Electron Differential
Energy Analyzer
(LEPEDEA)

NSSDC ID 67-073A-10

PROJECT DESIGNATION 5010, D-10

Nov. 10, 1975

SPACECRAFT AND EXPERIMENT CHARACTERISTICS

PERSONNEL

PI - J.A. Van Allen
University of Iowa - Iowa City, Iowa
OI - L.A. Frank
University of Iowa - Iowa City, Iowa

BIBLIOGRAPHY

PM: A66-23684.
N74-19088.

BRIEF DESCRIPTION

The objectives of this experiment were: 1) to conduct a comprehensive latitude and temporal study of the intensities and energy spectra of electrons and protons precipitating into the Earth's upper atmosphere and 2) to provide information on the spatial, angular, and temporal distribution of geomagnetically trapped proton and alpha particles. The instrumentation used for the study of precipitating particles was a Low-Energy Proton and Electron Differential Energy Analyzer (LEPEDEA) with 16 energy bands in the range 5 to 50,000 eV. A single thin-window GM was provided for an integral measurement of electron flux above 40 keV and of proton flux above 500 eV. Two solid-state detectors were used for the trapped-particles study. One was an alpha-particle experiment with four energy bands in the range 1.05 MeV to 7.8 MeV. The other was a proton experiment with four energy bands in the range 0.37 MeV to 9.9 MeV. The experiment package was mounted on the short boom EP-4, and it yielded data from launch until October 1969, at which time the spacecraft was placed in a stand-by status. The data, however, were of very limited value because of a severe temperature problem in the instrument package.

BIBLIOGRAPHY

PM: A69-43184.
N74-76909.

PS: A69-29565.

OGO 4, Webber

EXPERIMENT NAME Galactic and Solar
Cosmic Ray
NSSDC ID 67-073A-09
PROJECT DESIGNATION 5009, D-09
PERSONNEL
PI - W.R. Webber
University of Minnesota - Minneapolis, Minnesota

BRIEF DESCRIPTION

This cosmic-ray telescope experiment was designed to measure the differential energy spectra of protons, helium nuclei, and heavier nuclei up to $Z = 10$ within the energy range from 50 to 2000 MeV/nucleon and at a maximum sampling rate of one per 288 msec. The telescope, located in the main body, consisted of two detectors, a scintillator with its associated PM and a scintillator and a Cerenkov element sandwich, with both elements optically coupled to the same PM tube. A 70-nanosec coincidence circuit coupled the two detectors to form the telescope. Pulses from each PM were pulse-height analyzed. Sampled pulse heights, the coincidence count rate, and the count rate of the first detector were telemetered. The resolution of the OGO 4 detector deteriorated at launch, probably due to partial separation of an optical interface in one element of the telescope. This resulted in a reduced efficiency for detecting protons greater than about 200 MeV, with the worst resolution near the Cerenkov threshold of 320 MeV. Otherwise, the experiment functioned as planned until October 23, 1969.

Nov. 10, 1975

SPACECRAFT AND EXPERIMENT CHARACTERISTICS

OGO 5

Operational support of OGO 5 was terminated on July 14, 1972.

SPACECRAFT CHARACTERISTICS

COMMON NAME OGO 5
 ALTERNATE NAMES OGO-E, EGO-3,
 EGO-3, 03138, S 59
 NSSDC ID 68-014A
 LAUNCH DATE 03/04/68
 WEIGHT IN ORBIT 611 kg
 LAUNCH SITE Cape Canaveral, United
 States
 LAUNCH VEHICLE Atlas-Agena D
 SPONSORING COUNTRY United States
 SPONSORING AGENCY NASA-OSSA

ORBIT PARAMETERS	INITIAL	LATER
Epoch Date	03/04/68	04/04/71
Apogee (km alt)	148,228	120,666
Perigee (km alt)	272	26,405
Period (min)	3796	3796
Inclination (deg)	31.1	54.0

PERSONNEL

Project Manager -
 W. E. Scull - NASA-GSFC - Greenbelt, Maryland
 Project Scientist -
 J. P. Heppner - NASA-GSFC - Greenbelt, Maryland
 Program Manager -
 T. L. Fischetti - NASA Hq. - Washington, D.C.
 Program Scientist -
 A. W. Schardt - NASA Hq. - Washington, D.C.

BRIEF DESCRIPTION

The purpose of the OGO 5 spacecraft, the fifth of a series of six orbiting geophysical observatories, was to conduct many diversified geophysical experiments to obtain a better understanding of the Earth as a planet and to develop and operate a standardized observatory-type spacecraft. OGO 5 consisted of a main body that was parallelepiped in form, two solar panels, each with a solar-oriented experiment package (SOEP), two orbital-plane experiment packages (OPEP), and six appendages EP-1 through EP-6 supporting the boom experiment packages. One face of the main body was Earth-pointing (z axis), and the line connecting the two solar panels (x axis) was perpendicular to the Earth-Sun-spacecraft plane. The solar panels were able to rotate about the x axis. The OPEPs were mounted on and could rotate about an axis that was parallel to the z axis and that was attached to the main body. At launch, the initial local time of apogee was 0944 hr. OGO 5 carried 25 experiments. Seventeen of these were particle studies, and two were magnetic field studies. In addition, there was one each of the following types of experiments -- radio astronomy, UV spectrum, Lyman-Alpha, solar X-ray, plasma waves, and electric field. Real-time data were transmitted at 1, 8, and 64 kbs, depending on the distance from the spacecraft to the Earth. Playback data were tape recorded at 1 kbs and transmitted at 64 kbs. Two wide-band transmitters, one feeding into an omnidirectional antenna and the other feeding into a directional antenna, were used to transmit data. A special purpose telemetry system, feeding into either antenna, was also used to transmit wideband data in real time only. Tracking was accomplished by using radio beacons and a range and range-rate S-band transponder. One wideband telemetry transmitter had a partial failure 30 days after launch, resulting in a 10 to 1 power output reduction. The spacecraft attitude control failed on August 6, 1971, after 41 months of normal operation. The spacecraft was placed in a stand-by status on October 8, 1971. Three experiments were reactivated for the period from June 1 to July 13, 1972 (68-014A-09, 68-014A-22, and 68-014A-27).

IV-32

SPACECRAFT/MISSION BIBLIOGRAPHY

Papers with major discussion of spacecraft, mission, testing, subsystems, or ground systems prepared by NASA project or project support personnel.
 A63-10333, A69-36674, A70-35303,
 N74-76932.

Papers with minor discussion of spacecraft, mission, testing, subsystems, or ground systems prepared by NASA project or project support personnel.
 N74-76912.

Papers about spacecraft, mission, testing, subsystems, or ground systems prepared by NASA contractor personnel.
 A64-10864,
 N69-33977.

EXPERIMENTS

OGO 5, Aggson

EXPERIMENT NAME Electric Field
 Measurement
 NSSDC ID 68-014A-26
 PROJECT DESIGNATION E-26
 PERSONNEL
 PI - T.L. Aggson
 NASA-GSFC - Greenbelt, Maryland
 OI - N.C. Maynard
 NASA-GSFC - Greenbelt, Maryland
 OI - J.P. Heppner
 NASA-GSFC - Greenbelt, Maryland

BRIEF DESCRIPTION

This experiment was designed to observe electric fields in the outer regions of the magnetosphere, in the transition region, and in the solar wind. The experiment technique used was that of double floating probes, the probes being the plus and minus x-axis antennas. Electric field measurements were normal from launch until June 1968, when a preamplifier failed. From that time until December 1968 some useful ac field data were obtained. No data were obtained after December 1968.

BIBLIOGRAPHY--None found

OGO 5, Anderson

EXPERIMENT NAME Energetic Radiations
 from Solar Flares
 NSSDC ID 68-014A-04
 PROJECT DESIGNATION E-04

December 10, 1975

SPACECRAFT AND EXPERIMENT CHARACTERISTICS

PERSONNEL

PI - K.A. Anderson
 University of California - Berkeley, California
 OI - S.R. Kane
 University of California - Berkeley, California
 OI - H. Mark
 University of California - Berkeley, California

BRIEF DESCRIPTION

This experiment was designed to study the spectrum of energetic X-rays, protons, alpha particles, and electrons emitted by the Sun in association with solar flares. The experiment, located in SOEP-1, used three separate detecting systems. First, an omnidirectional NaI (thallium) scintillation counter measured solar X-rays in eight energy channels from 9.6 to 19.2, 19.2 to 32, 32 to 48, 48 to 64, 64 to 80, 80 to 104, 104 to 128, and greater than 128 keV. The data were sampled for 1.15 sec once every 2.3 sec. Second, a particle telescope composed of seven solid-state detectors -- D1, D2, D3, D4, D5, D6, D7, and an anticoincidence shield -- measured protons in the six energy channels from 7 to 20, 20 to 45, 45 to 80, 80 to 130, 130 to 200, and greater than 200 MeV. These channels had a nonseparable alpha particle component. The lowest energy channel was sampled once every 147 sec, while all other channels were sampled once every 9.2 sec. The third system consisted of a directional GM magnetic spectrometer that measured electrons in two channels, from 22 to 27 and 50 to 90 keV. These data were sampled once every 147 sec. To reduce the possible contribution of magnetospheric radiation to the background counting rates of the detectors, the experiment only operated at satellite altitudes above 80,000 km, i.e., about 48 hr or 67 percent of each orbit. The X-ray detector operated satisfactorily throughout the mission. The D7 detector element in the proton-alpha telescope was found to be very noisy just prior to launch. It was therefore disabled electronically, and no data were available for protons or alpha particles above 200 MeV/nucleon. The rest of this telescope performed normally throughout the mission. The electron spectrometer performed normally from launch until September 23, 1969, when the 22- to 27-keV channel became erratic and later stopped counting completely. The other electron channel performed normally throughout the mission.

BIBLIOGRAPHY

PM: A69-40775, A71-15937, A71-19825, A72-14561,
 A73-11389, A73-20766, A74-30287, A74-38468,
 N72-28812, N74-21445, N74-21458,
 B03940-000.
 PS: A70-25746, A73-17041, A74-30908,
 B22607-000.
 OS: A71-20945, A72-13507,
 B22602-000.

OGO 5, Blamont

EXPERIMENT NAME Geocoronal
 Lyman-Alpha
 Measurements
 NSSDC ID 68-014A-22
 PROJECT DESIGNATION E-22
 PERSONNEL
 PI - J.E. Blamont
 CNES - Paris, France

BRIEF DESCRIPTION

The objective of this experiment was to determine the hydrogen distribution in the geocorona and the geocorona's temperature from the measurements of the intensity and line width of the emerging Lyman-Alpha radiation. In addition, the experiment provided data on extraterrestrial sources of Lyman-Alpha, such as interstellar wind, comets, planets, and numerous stars. The sensor was a photometer with a field of view of 40 min of arc and a bandwidth of 80 Å centered at Lyman-Alpha wavelength (1216 Å). Specifically, a plane mirror which could rotate about a horizontal axis was used to move the field of view in 1/2 deg steps. Leaving this mirror, the radiation struck a spherical mirror that focused it onto a diaphragm. Subsequently the image of the diaphragm was focused on the entrance window of a photomultiplier via a system consisting of an aspherical mirror and a plane grating. A hydrogen cell, filled with hydrogen gas at a pressure of 0.5 mm of mercury and containing two magnesium fluoride windows, was placed in front of the photomultiplier and provided the measurement of line width. Pulses produced by the PM were counted for 0.432 sec, a time span during which the plane mirror position did not change. The number of pulses in this time interval was a measurement of intensity. A shutter was closed every third minute to measure the dark current level of the photometer. The experiment was mounted in OPEP-1. Instrument scanning caused the field-of-view axis to move inside a cone of 16 deg half-angle, with the local vertical as axis. Two modes of operation were possible and the choice was made by ground command. In the scanning mode the plane mirror would scan continuously. In the stepping mode this mirror would be placed in a specified position. The experiment was turned off when the spacecraft was deactivated on October 8, 1971, after operating for 23,170 hr.

BIBLIOGRAPHY

PM: A69-31412, A70-42468, A71-24438, A71-33834,
 A73-19233,
 N73-10812,
 B22614-000.
 PS: N65-30651.
 OS: A73-12323, A73-39074,
 N73-10813.

OGO 5, Boyd

EXPERIMENT NAME Electron Temperature
 and Density
 NSSDC ID 68-014A-01
 PROJECT DESIGNATION E-01
 PERSONNEL
 PI - R.L.F. Boyd
 University College - London, England
 OI - P.A. Willmore
 University College - London, England
 OI - K. Norman
 University College - London, England

BRIEF DESCRIPTION

The purpose of this experiment, located on EP-1, was to study the electron temperature and density in the magnetosphere to understand the effects of the solar wind on the geomagnetic field. The current-voltage characteristics for a Langmuir probe immersed in the ionospheric plasma were analyzed, and from this information the local electron temperature and concentration could be deduced. The instrument was capable of measuring electron temperatures over the range from 700 to 25,000 deg K and concentrations over the range from 1 to 10⁵ electrons/cc. The experiment operated normally for 30.465 hr (until spacecraft shutdown).

SPACECRAFT AND EXPERIMENT CHARACTERISTICS

BIBLIOGRAPHY

PM: A70-37513, A74-17648.
 OS: A73-33456.
 B22612-000.

OGO 5, Cline

EXPERIMENT NAME Interplanetary,
 Electrons, Positrons, and
 Protons
 NSSDC ID 68-014A-05
 PROJECT DESIGNATION E-05
 PERSONNEL
 PI - T.L. Cline
 NASA-GSFC - Greenbelt, Maryland

BRIEF DESCRIPTION

This experiment was intended primarily to study solar and galactic electrons and positrons in the energy range from 2 to 9.5 MeV. It also measured solar electrons above several hundred keV, solar X-rays above 80 keV, and medium-energy galactic and solar protons and alpha particles. The instrument, mounted on EP-3, was a dE/dx vs E plastic scintillator telescope surrounded by an anticoincidence plastic scintillator. Between the residual-E sensor and the anticoincidence sensor was a CsI scintillator that observed gamma rays associated with electrons and positrons stopping in the residual-E sensor. Analysis of the CsI scintillator output permitted differentiation between electrons and positrons. Pulse height analysis of the dE/dx and residual-E sensor outputs was performed, as was inflight calibration. The experiment functioned normally from launch to September 14, 1969, after which no further useful data were obtained.

BIBLIOGRAPHY

PM: A70-38096.
 N69-38983.
 PS: A74-30149.

OGO 5, Coleman

EXPERIMENT NAME Hydromagnetic Waves
 and Trapped Particles
 NSSDC ID 68-014A-13
 PROJECT DESIGNATION E-13
 PERSONNEL
 PI - P.J. Coleman, Jr.
 University of California - Los Angeles, California
 OI - T.A. Farley
 University of California - Los Angeles, California
 OI - D.L. Judge
 University of Southern California - Los Angeles,
 California

BRIEF DESCRIPTION

This experiment, located in EP-1, consisted of six plastic scintillator detectors to measure the unidirectional flux of electrons in eight energy intervals between 50 keV and 1.2 MeV. Two of

the detectors pointed in opposite directions while the remainder pointed in various other directions. The experiment was designed to determine the magnetohydrodynamic properties of disturbances in the magnetosphere and beyond. It was conducted in conjunction with the UCLA fluxgate magnetometer experiment (68-014A-14). A thermal problem adversely affected the data quality for the second half of 1969. However, prior to that time and until October 8, 1971, when it was turned operationally off, the experiment was performing normally.

BIBLIOGRAPHY

PM: A71-43162, A72-42406, A72-44513, A73-29964,
 A73-33437, A73-33453, A73-33457, A73-36273,
 A74-24766.
 PS: A74-14283, A74-17742.
 B22611-000.
 OM: A73-33449.
 OS: A72-44850, A73-13883, A73-33454, A73-33456.
 N74-17126.

OGO 5, Coleman

EXPERIMENT NAME Triaxial Fluxgate
 Magnetometer
 NSSDC ID 68-014A-14
 PROJECT DESIGNATION E-14
 PERSONNEL
 PI - P.J. Coleman, Jr.
 University of California - Los Angeles, California
 OI - T.A. Farley
 University of California - Los Angeles, California
 OI - D.L. Judge
 University of Southern California - Los Angeles,
 California
 OI - C.T. Russell
 University of California - Los Angeles, California

BRIEF DESCRIPTION

This experiment consisted of a triaxial fluxgate magnetometer mounted on the EP-5, 6.1-m boom. The range of each sensor was 16 gammas, with 0.125-gamma digitization windows. For a given ambient field, a known offset field could be applied to the sensor by a surrounding current-carrying coil. In this way, ambient fields of $\pm 64,000$ gammas per axis were measurable with 0.125-gamma digitization accuracy. The sensor output signals were passed through a filter that removed frequency components higher than the sampling frequency. The filtered signals were then sampled in real time at 0.87, 6.96, or 55.5 vector measurements per second, depending on the satellite bit rate, and at 0.87 vector measurement per second in the tape-recorded channel. As the instrument shifted offset field ranges, the first six data points taken after the shift were affected in an understood, and therefore correctable, way. Also, the instrument housing was equipped with an electric heater that introduced a correctable offset field when it came on. Further, the zero offset on each sensor drifted slowly as a function of sensor electronic temperature. By using simultaneous fluxgate and rubidium magnetometer data from the GSFC experiment, this offset correction could be determined within ± 3 gammas over most of the satellite orbit. Data were received until September 20, 1971, when the experiment was turned off. Temperature plots are available from NSSDC for orbits 38 and thereafter. During low-temperature times, offsets could be as much as 10 gammas.

SPACECRAFT AND EXPERIMENT CHARACTERISTICS

BIBLIOGRAPHY

- PM:** A67-15724, A69-42693, A70-13980, A70-36006, A70-43851, A71-14515, A71-14550, A71-19656, A71-21631, A71-21643, A71-27913, A71-33943, A71-43162, A72-23004, A72-29379, A72-35599, A72-35610, A72-44513, A72-44856, A72-44857, A73-29964, A73-29966, A73-33437, A73-33449, A73-33450, A73-33452, A73-33457, A73-36273, A74-21679, A74-21680, N73-10792, N73-20498, N74-74633, B12880-000, B18269-000, B22611-000, B22612-000.
- PS:** A70-30078, A71-23711, A71-33944, A72-19145, A72-42406, A72-42902, A73-33453, A74-14283, A74-17742, N69-33963, N73-10791.
- OM:** A70-30069, A72-21223, A72-29378, A73-33456, A74-12627, N72-11325.
- OS:** A69-33452, A70-36005, A71-11491, A71-17263, A71-30952, A71-37353, A72-26399, A72-44850, A73-13883, A73-24744, A73-33454, A73-33455, A73-36275, A74-18364, A74-43688, N73-10795, N74-17126, B14580-000.

OGO 5, Crook

EXPERIMENT NAME Plasma Wave Detector
 NSSDC ID 68-014A-24
 PROJECT DESIGNATION E-24
 PERSONNEL
 PI - G.M. Crook
 TRW Systems Group - Redondo Beach, California
 OI - F.L. Scarf
 TRW Systems Group - Redondo Beach, California
 OI - R.W. Fredricks
 TRW Systems Group - Redondo Beach, California
 OI - I.M. Green
 TRW Systems Group - Redondo Beach, California

BRIEF DESCRIPTION

The plasma wave detector included five electric dipoles and three orthogonal search-coil magnetometers mounted on the EP-5 6.7-m boom. The three 0.5-m orthogonal electric dipoles were normal to the planes of the magnetometers. Each of the orthogonal components of the dipole and magnetometer was sampled simultaneously for 9.2 sec through 15-percent bandpass filters in the following sequence -- 0.56, 1.3, 3.0, 7.35, 14.5, 30.0, and 70.0 kHz for each dipole concurrent with 0.56, 0.56, 0.56, 0.56, 70.0, 70.0, and 70.0 kHz for each magnetometer. Repeat time for this sequence was 3.26 min. Onboard autocorrelation was performed between each electric field and magnetic field measurement. The remaining two boom-mounted dipoles were colinear, differing only in length. Each dipole was monitored through a 200-Hz 10-percent filter for 2 sec once every 9.2 sec. In addition to the digital data, 1- to 22-Khz electric-field data taken from one main dipole and yielding power spectrum information for that axis were continuously monitored by a special purpose analog telemetry system. Threshold sensitivity of these measurements was telemetered with the digital data. Intense emissions below 1 kHz and above 22 kHz may still be detectable. The experiment operated normally, but much of the data returned after April 1968 were of poor quality due to a telemetry transmitter failure.

BIBLIOGRAPHY

- PM:** A69-14681, A69-36683, A69-42693, A70-17376, A70-29111, A70-30069, A70-30085, A70-36005, A70-36006, A70-37483, A71-11500, A71-14550, A71-23711, A71-24788, A71-30956, A71-37353, A71-43158, A71-43162, A72-23019, A72-26399, A72-29380, A72-35610, A72-44523, A73-13883, A73-19254, A73-26985, A73-29964, A73-29966, A73-33437, A73-33456, A73-36273, A74-21680, N72-22383, N73-10789, N73-10795, N74-77109, B18269-000, B22612-000.
- PS:** A69-33452, A70-17376, A70-30083, A71-14068, A71-37368, A74-43688.
- OM:** A73-33457, B14583-000.
- OS:** A71-11491, A71-30952, A71-31774, A72-21189, A72-44850, A73-22069, A74-14283.

OGO 5, Frank

EXPERIMENT NAME Low-Energy Proton and
 Electron Differential
 Energy Analyzer
 (LEPEDEA)
 NSSDC ID 68-014A-07
 PROJECT DESIGNATION E-07
 PERSONNEL
 PI - L.A. Frank
 University of Iowa - Iowa City, Iowa
 OI - J.A. Van Allen
 University of Iowa - Iowa City, Iowa
 OI - T.A. Fritz
 University of Iowa - Iowa City, Iowa
 OI - T.P. Armstrong
 University of Iowa - Iowa City, Iowa
 OI - S.M. Krimigis
 University of Iowa - Iowa City, Iowa

BRIEF DESCRIPTION

This experiment was designed to measure the differential energy spectrum of protons and electrons over the range from 5 eV to 100 keV in the Earth's magnetosphere and its environment. The experiment was also to measure trapped alpha particles over the range from 0.4 to 200 MeV. The detector, located in EP-2, was an electrostatic analyzer using Bendix channeltron electron multipliers. The experiment failed March 12, 1968, nine days after launch.

BIBLIOGRAPHY

- PM:** A71-14550, A71-37353, A71-43158, N66-13640.
- PS:** A69-29565.

NOV. 10, 1975

SPACECRAFT AND EXPERIMENT CHARACTERISTICS

OGO 5, Haddock

EXPERIMENT NAME Radio Astronomy
 NSSDC ID 68-014A-20
 PROJECT DESIGNATION E-20
 PERSONNEL
 PI - F.T. Haddock
 University of Michigan - Ann Arbor, Michigan

PERSONNEL
 PI - J.P. Heppner
 NASA-GSFC - Greenbelt, Maryland
 OI - B.G. Ledley
 NASA-GSFC - Greenbelt, Maryland
 OI - M. Sugiura
 NASA-GSFC - Greenbelt, Maryland
 OI - T.L. Skillman
 NASA-GSFC - Greenbelt, Maryland
 OI - R.M. Campbell
 NASA-GSFC - Greenbelt, Maryland

BRIEF DESCRIPTION

This experiment, used primarily to observe Type-3 solar radio bursts, consisted of a 9.12-m monopole antenna and a step-frequency superheterodyne receiver tunable through the eight frequencies of 0.05, 0.10, 0.20, 0.35, 0.60, 0.90, 1.80, and 3.50 MHz in 9.2 sec (1.152 sec at each frequency, regardless of spacecraft telemetry rate). This experiment operated both during real-time coverage and during tape-recorded coverage. The experiment package was located in SOEP-1, with the monopole antenna oriented perpendicular to the Earth-Sun-spacecraft plane (-x direction). The receiver bandwidth was 10 kHz (6 db points), and the intermediate frequency stage had an automatic gain control yielding a dynamic range of 44 db. A solid-state, four-level noise generator was connected in place of the antenna for inflight calibration every 9.85 min (36.9 sec were required for calibration). The receiver operated in either of two modes. During normal operation, the receiver was stepped through the eight frequencies. In a nonstepping mode, the receiver was locked on only one of the available frequency channels. The radiometer operated in the stepping mode except for the periods from April 25 to June 18, 1968 (3.5 MHz), September 12 to 14, 1968 (0.6 MHz), and December 15 to 17, 1969 (0.6 MHz). Both impulsive and nonimpulsive interference occurred, with the four lower frequency channels usually being affected by some impulsive interference assumed due to other experiments on board the spacecraft. Nonimpulsive interference, manifested as permanent noise levels higher than preflight receiver noise, occurred in the case of the 1.80- and 0.35-MHz channels. The system stability was checked approximately every 2 months from March 1968 through December 1969, and the output levels were found to be constant to within a few percent. This experiment remained fully operational until the OGO 5 support was terminated on July 14, 1972.

BIBLIOGRAPHY

PM: A73-17047, A73-32964, A73-32965, A73-41497,
 A74-14811,
 N69-14392, N72-23118,
 B14718-000.
 PS: N69-25437.

OGO 5, Heppner

EXPERIMENT NAME Magnetic Survey Using
 Two Magnetometers
 NSSDC ID 68-014A-15
 PROJECT DESIGNATION E-15

BRIEF DESCRIPTION

The primary objective of this experiment was to study the geomagnetic field and its interactions with the environment. The detector system consisted of a triaxial fluxgate magnetometer and two dual-cell, optically pumped, self-oscillating, rubidium-87 vapor magnetometers. Both magnetometers were mounted on boom EP-6 to minimize effects of spacecraft fields. The triaxial fluxgate magnetometer provided simultaneous measurements of the three magnetic-field vector components in the range ± 4000 gammas (over a frequency range from 0 to 120 Hz). A 10-gamma inflight calibration was applied on command as a check on sensitivity changes. The accuracy was ± 1 gamma (checked by means of inflight comparison with the rubidium magnetometers). The rubidium vapor magnetometers provided scalar measurements of the magnetic field magnitude. However, a triaxial coil system was built into the sphere surrounding the rubidium magnetometers to allow vector measurements to be made. This was used to monitor the output of the fluxgate magnetometer as a check on zero drifts. The rubidium vapor magnetometers had an absolute accuracy of ± 0.5 gamma. Six weeks after launch, the frequency counter failed, causing the loss of the rubidium magnetometer data for fields greater than 14,000 gammas. A problem that developed with time and had an effect on the quality of the rubidium data was a lamp oscillation of one of the two rubidium magnetometers. This led to turning off the malfunctioning rubidium magnetometer in April 1968. With this magnetometer off, the operation was normal but caused the rubidium system to have larger null zones. As a result, some of the data are either of lower quality or absent. In December 1970, owing to further problems with the lamp oscillations, it was decided to turn on the rubidium magnetometers only briefly at selected time intervals in order to check the operations of the fluxgate magnetometer. The accuracy of the fluxgate data after correction was from 1.5 to 3 gammas. The fluxgate magnetometer remained fully operational until the OGO 5 support was terminated on July 14, 1972.

BIBLIOGRAPHY

PM: A70-30045, A70-30076, A71-23635, A71-31754,
 A71-43161, A72-10886, A73-11732, A73-33464,
 A73-43693,
 N71-25271, N71-32519,
 B19906-000, B22604-000.
 PS: A72-13507.
 OM: A73-13871.
 OS: A71-17686, A71-34777, A72-42902, A73-45112.

OGO 5, Hutchinson

EXPERIMENT NAME Energetic Photons in
 Primary Cosmic Rays
 NSSDC ID 68-014A-08

SPACECRAFT AND EXPERIMENT CHARACTERISTICS

PROJECT DESIGNATION E-08
PERSONNEL

- PI - G.W. Hutchinson
Southampton University - Southampton, England
- OI - D. Ramsden
Southampton University - Southampton, England
- OI - R.D. Wills
Southampton University - Southampton, England

BRIEF DESCRIPTION

This experiment was used to study galactic gamma radiation. The instrumentation included a six-gap acoustic spark chamber with a sensitive area of 102 sq cm, surrounded by a scintillation plastic anticoincidence counter. The chamber was triggered by a counter telescope with an acceptance solid angle of 0.2 steradian, consisting of a directional Cerenkov counter and a plastic scintillator. The experiment was mounted in the main body of the spacecraft, so that the center of its acceptance solid angle was directed away from the Earth. The experiment operation was limited to the period when the spacecraft was outside the radiation belts, because the high flux of charged particles would have rendered the anticoincidence counter inoperative and could permanently have changed the characteristics of the PMs. Photons of energy 25 to 100 MeV were measured in determining whether the gamma-ray component of primary cosmic rays has preferred directions. In orbit it was found that the triggering rate of the experiment was much higher than expected, presumably due to improper instrument performance. This improper operation reduced the useful life of the spark chamber to about five months. After November 6, 1968, the experiment operated only on request of the experimenter. The total operating time of the experiment was 2836 hrs.

BIBLIOGRAPHY

PM: A70-40691.
B18277-000.

OGO 5, Kreplin

EXPERIMENT NAME Solar X-ray Emissions
NSSDC ID 68-014A-23
PROJECT DESIGNATION E-23
PERSONNEL

- PI - R.W. Kreplin
Naval Research Laboratory - Washington, D.C.
- OI - T.A. Chubb
Naval Research Laboratory - Washington, D.C.
- OI - H.D. Friedman
Naval Research Laboratory - Washington, D.C.
- OI - S. Bowyer
University of California - Berkeley, California

BRIEF DESCRIPTION

The objective of this experiment was to measure solar X-ray emissions in the 0.6-A to 6.0-A region. The instrumentation consisted of a proportional counter connected to an eight-channel pulse height analyzer. The detector operated only at altitudes greater than 60,000 km within the highly eccentric orbit of the satellite. The resulting data cover about three-quarters of each 2.6-day orbit. The detector package, located in SOEP-1, was continuously oriented toward the sun. The proportional counter was filled with a mixture of xenon (97 percent) and carbon dioxide (3 percent) at a pressure of 204 cm Hg. The window, with a diameter of 0.250 in., consisted of 10 mil of beryllium overlaid with one mil of aluminum. The pulse height analyzer separated pulses from the proportional counter into eight energy channels, ranging initially

from 2 to 20 keV. The energy levels of the eight channels changed continuously after launch, stabilizing at a range approximately 4 to 40 keV by July 1968. In-flight calibration was carried out twice during each orbit, using an iron-55 source mounted on a movable arm. The detector was not designed to reject particle counts. The beryllium-window particle thresholds were 170 keV for electrons and 5.5 MeV for protons. Nominal quiet-time background count rates were about one count/sec due to penetrating cosmic rays. Occasional particle interference due to the Outer Van Allen Belt was observed, and the data are not usable during energetic solar proton events. This experiment was turned off April 24, 1970, due to a loss in proportional counter resolution.

BIBLIOGRAPHY

PM: A70-45768, A73-11391.
N74-21450.

OGO 5, McDonald

EXPERIMENT NAME Galactic and Solar
Cosmic-Ray Studies
NSSDC ID 68-014A-10
PROJECT DESIGNATION E-10
PERSONNEL

- PI - F.B. McDonald
NASA-GSFC - Greenbelt, Maryland
- OI - G.H. Ludwig
NASA-GSFC - Greenbelt, Maryland
- OI - V.K. Balasubrahmanyam
NASA-GSFC - Greenbelt, Maryland
- OI - D.E. Hagge
NASA-GSFC - Greenbelt, Maryland

BRIEF DESCRIPTION

This experiment was designed to measure the chemical composition (Z from 1 to 14) and energy spectrum (Energy/nucleon from 4 to 800 MeV) of the cosmic radiation. The instrumentation, located in the main body, consisted of three telescopes -- the low-, medium-, and high-energy detectors (LED, MED, HED, respectively). The LED was a solid-state telescope which covered the energy range from 4 to 20 MeV for protons through the range from 8 to 40 MeV/nucleon for carbon and oxygen. The MED was a scintillator telescope. It operated in a dE/dx vs E mode for 20- to 80-MeV/nucleon stopping particles and in a triple dE/dx mode for 80- to 200-MeV/nucleon penetrating particles. The HED was a double dE/dx and Cerenkov telescope covering the energy range from 200 to 800 MeV/nucleon. The instruments provided nearly 100 percent coverage during each April-November interval and, due to thermal problems, only about 30 percent coverage during each December-March interval. Otherwise the instruments functioned well until spacecraft turnoff.

BIBLIOGRAPHY

PM: A67-25852, A70-38127.
N69-38984.

OGO 5, Meyer

EXPERIMENT NAME Cosmic-Ray Electrons
NSSDC ID 68-014A-09

SPACECRAFT AND EXPERIMENT CHARACTERISTICS

PROJECT DESIGNATION E-09

PERSONNEL

- PI - P. Meyer
University of Chicago - Chicago, Illinois
- OI - C.Y. Fan
University of Arizona - Tucson, Arizona
- OI - J.J. L'Heureux
University of Arizona - Tucson, Arizona

BRIEF DESCRIPTION

This experiment measured the flux and energy spectrum of primary cosmic-ray electrons with energies between 15 and 45 MeV, and flux and energy spectrum of protons with energies between 143 and 169 MeV, and below 16 GeV. The detector used was a particle telescope composed of a scintillation counter, a gas Cerenkov counter, a solid-state detector, and a CsI scintillation counter surrounded by two plastic scintillators. The experiment was located in the main body and it was turned on only when the satellite's McIlwain parameter, L , was greater than $12 R_E$. The experiment was fully operational when the spacecraft was put in a stand-by status on October 8, 1971. The experiment was reactivated from June 1 to July 13, 1972.

BIBLIOGRAPHY

PM: A70-12902, A71-18170, A71-29057, A72-16719,
A73-33293, A74-30204, A74-31942
B08373-000.

OM: B13262-000.

OGO 5, Ogilvie

EXPERIMENT NAME Triaxial Electron Analyzer

NSSDC ID 68-014A-11

PROJECT DESIGNATION E-11

PERSONNEL

- PI - K.W. Ogilvie
NASA-GSFC - Greenbelt, Maryland
- OI - T.D. Wilkerson
University of Maryland - College Park, Maryland

BRIEF DESCRIPTION

The objective of this experiment was to determine the energy spectra of electrons arriving at the spacecraft from three mutually orthogonal directions. Electrons were analyzed by three 127-deg electrostatic analyzers with channeltron detectors. They were mounted in the spacecraft main body. Look-directions of the mutually orthogonal detectors formed equal angles to the Earth-satellite line, and always pointed away from the Earth. Each analyzer was stepped simultaneously through 14 energy windows with center energies of 10, 25, 45, 80, 130, 210, 340, 550, 890, 1400, 2300, 3800, and 9900 eV. Each window was sampled for 1.15 sec. Each detector had a 10-deg acceptance cone. A radioactive source was used to calibrate each instrument in flight. The instrument was operated only on the outward-bound portion of each orbit because of a spacecraft heat problem. Degradation of the channeltrons limited useful operation to only about 30 days, with increasingly poor data quality received toward the end of the operating period.

IV-38

BIBLIOGRAPHY

PM: A66-23689, A67-33595, A68-25969, A71-31754,
A72-13507, A73-45112.
N71-25273

OGO 5, Sagalyn

EXPERIMENT NAME Thermal and Epithermal Plasma

NSSDC ID 68-014A-02

PROJECT DESIGNATION E-02

PERSONNEL

- PI - R.C. Sagalyn
AFCRL - Bedford, Massachusetts
- OI - M. Smiddy
AFCRL - Bedford, Massachusetts

BRIEF DESCRIPTION

This experiment consisted of two spherical retarding potential probes, one each for electron and ion observations. They were mounted on the EP-4 boom extending along the y-axis of the spacecraft, generally opposite the velocity vector. There were 7.5-cm spherical mesh grids for both sensors, a second internal grid for one of the sensors, and a spherical collector about 3 cm in diameter. Five modes of operation provided current and voltage curves for each sensor. From these curves one could calculate density (from 1 to 10^6 particles per cubic centimeter), temperature (700 to 100,000 deg K), and energy (25 to 2,000 eV) for both ions and electrons. Spacecraft potential, electron flux (from 3×10^5 to 5×10^{11} electrons/cm²-sec), and proton flux (from 10^5 to 10^{11} protons/cm²-sec) could also be measured. A failure in the experiment power supply two weeks after launch caused severe degradation and prevented the acquisition of useful data.

BIBLIOGRAPHY - None found

OGO 5, Serbu

EXPERIMENT NAME Thermal Ions and Electrons

NSSDC ID 68-014A-03

PROJECT DESIGNATION E-03

PERSONNEL

- PI - G.P. Serbu
NASA-GSFC - Greenbelt, Maryland
- OI - E.J. Maier
NASA-GSFC - Greenbelt, Maryland

BRIEF DESCRIPTION

A planar multi-grid sensor, located in OPEP-2 and programmed as a retarding potential analyzer, was used to observe the directional intensity of the electron and ion components of the low-energy plasma in interplanetary space and near-Earth. Spectra were obtained for both ions and electrons in the energy range from 0 to 500 eV. A complete spectrum was obtained every 16 or 128 sec. The experiment worked continuously from launch until the spacecraft was turned off. However, much of the data was difficult to analyze because of the velocity vector scanning done by OPEP-2 to meet the requirements of experiment 68-014A-06.

SPACECRAFT AND EXPERIMENT CHARACTERISTICS

BIBLIOGRAPHY

PM: A71-11498, A72-26399.

OGO 5, Sharp

EXPERIMENT NAME Light-Ion Magnetic
Mass Spectrometer

NSSDC ID 68-014A-18

PROJECT DESIGNATION E-18

PERSONNEL

PI - G.W. Sharp
Lockheed - Palo Alto, California
OI - T.J. Crowther
Lockheed - Palo Alto, California
OI - K.K. Harris
Lockheed - Palo Alto, California

BRIEF DESCRIPTION

This experiment was designed to determine the concentration of light ion species in the topside ionosphere and exosphere and to measure these concentrations throughout the plasmasphere. The experiment was also designed to monitor the locations of the plasmopause, magnetopause and bow shock. The instrument consisted of an automatic, multiranged, magnetic-focus ion mass spectrometer. The instrument was capable of measuring singly ionized atomic oxygen, hydrogen, and helium concentrations. A complete measurement of these concentrations plus a calibration was completed in 4.6 sec. The accuracy of the measured data was estimated to be 10 percent. The instrument was located on OPEP-1 so that the velocity vector was essentially normal to the instrument aperture. The instrument acquired useful data from launch until May 31, 1969. In early July 1969 the instrument was turned off due to degradation of the experiment sensing element. At that time the experiment had operated for more than 14,000 hr.

BIBLIOGRAPHY

PM: A69-36679, A70-18530, A70-18546, A70-30074,
A70-36014, A70-43851, A71-11491, A71-24787,
A71-39833, A71-43162, A72-10892, A72-39544,
A73-12320, A73-22054, A73-26985, A73-29966,
A73-33451, A73-33876,
N73-16432, N74-76914,
B22600-000, B22610-000.

PS: N74-17126.

OM: A70-36006, A73-20652, A73-33457,
B20951-000.

OS: A69-33452, A70-30069, A70-36005, A70-37483,
A71-14515, A71-23711, A73-33456, A74-14283,
A74-18364,
N70-27302,
B22612-000.

OGO 5, Simpson

EXPERIMENT NAME Low-Energy Heavy
Cosmic-Ray Particles
(High-Z Low-E)

NSSDC ID 68-014A-27

PROJECT DESIGNATION E-27

PERSONNEL

PI - J.A. Simpson
University of Chicago - Chicago, Illinois

BRIEF DESCRIPTION

This experiment was designed to detect particles in the energy range from 2 to 50 MeV/nucleon, and to accomplish the following -- (1) examine the shape of the differential energy spectrum, (2) extend the measurement of relative abundance of the elements up through iron, (3) search for nuclei of very high charge (Z from 5 to 50), and (4) extend observations of very heavy nuclei from solar flares to 2 MeV/nucleon. The detector (a solid-state, windowless, lithium-drifted device surrounded by an anticoincidence cup) was located on the main body panel facing away from the Earth. It was used in conjunction with a 500-channel and a 1000-channel analyzer. The experiment was considered operational and was transmitting data when the spacecraft was turned off in October 1971. The experiment was reactivated between June 1 and July 13, 1972.

BIBLIOGRAPHY

PM: A71-13475, A72-15366, A72-32959, A73-13719,
A74-30156,
N73-25870.

OS: A73-23538,
B17665-000.

OGO 5, Smith

EXPERIMENT NAME Triaxial Search-Coil
Magnetometer

NSSDC ID 68-014A-16

PROJECT DESIGNATION E-16

PERSONNEL

PI - E.J. Smith
NASA-JPL - Pasadena, California
OI - R.E. Holzer
University of California - Los Angeles, California

BRIEF DESCRIPTION

The OGO 5 triaxial search coil magnetometer, located on the EP-5 boom, was designed to measure magnetic field fluctuations in and beyond the magnetosphere. Measurements were made in the frequency range from 0.01 Hz to 1000 Hz. The signals were divided into high-frequency and low-frequency channels, which overlapped near the center of the five-decade frequency band. The low-frequency wave forms were digitized and telemetered. The high-frequency information was obtained continuously by using an on-board low-resolution spectrum analyzer consisting of seven comb filters centered at 10, 22, 47, 100, 216, 467, and 1000 Hz. The high-frequency wave forms were also telemetered (on a part-time basis) in analog form for subsequent high-resolution, ground-based processing. Interference occurred between the seven-channel spectrum analyzer and the high-frequency analog channels, seriously degrading the high-frequency analog data throughout the

SPACECRAFT AND EXPERIMENT CHARACTERISTICS

operational life of the experiment. The experiment operated adequately throughout the mission.

BIBLIOGRAPHY

- PM: A69-36675, A70-37483, A71-33943, A72-26399, A72-29378, A74-18364, A74-21679, A74-24767.
- PS: A70-30078, A74-14283, N73-10791.
- PC: N69-72494.
- OM: A70-43851, A73-33457, A74-12627.
- OS: A69-33452, A70-36005, A71-11491, A71-23711, A72-21189, A73-13855, A73-13883, A73-33453, A73-33456, N74-17126, B22612-000.

OGO 5, Snyder

EXPERIMENT NAME Plasma Spectrometer
NSSDC ID 68-014A-17
PROJECT DESIGNATION E-17
PERSONNEL
PI - C.W. Snyder
NASA-JPL - Pasadena, California
OI - M.M. Neugebauer
NASA-JPL - Pasadena, California
OI - J.L. Lawrence, Jr.
NASA-JPL - Pasadena, California

BRIEF DESCRIPTION

Two pairs of detectors, one mounted on a solar panel always facing the Sun and one mounted on the spacecraft body always facing radially away from the Earth, were used to measure the flux of solar plasma in the vicinity of the spacecraft. Energy spectra of positive ions and electrons could be measured by the 120-deg curved plate analyzers, with a 5-deg conic field of view in 128 logarithmically equispaced E/Q channels from 2.54 v to 16,900 v. Total flux and angular distribution of positive ions were measured by Faraday cups with a 20-deg field of view in one E/Q range from 100 to 11,000 v. Each pair of Faraday cup/electrostatic analyzer combinations was capable of making two plasma flux and angle of flow measurements, and one proton density, alpha particle density, bulk speed, and temperature measurement about every 10 sec at 8 bps. During almost all the time the spacecraft was in the solar wind, only the solar-panel-mounted sensor pair was able to make the usual solar wind plasma parameter measurements. The electrostatic analyzers suffered data degradation from sensitivity scale switching and contamination of the positive ion spectra by photoelectrons leaking into the detector. Scale-switching transients affected mainly the alpha data, while photoelectron contamination affected mainly the location of the proton peak flux. Due to these effects, errors appeared in the measured parameters of temperature, bulk speed, and density, but not angle flow and plasma flux. Plasma parameters were calculated by an iterative calculation involving correction of the Faraday cup density and angle by the proton bulk speed, and correction of the curved-plate-determined bulk speed by the Faraday-cup-determined angle of flow. The instrumentation operated satisfactorily for the duration of the OGO 5 mission.

BIBLIOGRAPHY

- PM: A68-42739, A70-21377, A70-36005, A71-14550, A71-33943, A71-37353, A71-43162, A72-29378, A72-35610, A73-23539, A73-29966, A73-36273, A74-12627, A74-21679, A74-21680, N72-14808, B22612-000.
- OM: A70-29111, A70-36006, A73-29964, A73-33437.
- OS: A70-37483, A71-14515, A71-19656, A71-23711, A71-33944, A72-26399, A73-13883, B22609-000.

OGO 5, Thomas

EXPERIMENT NAME UV Photometer
NSSDC ID 68-014A-21
PROJECT DESIGNATION E-21
PERSONNEL
PI - G.E. Thomas
University of Colorado - Boulder, Colorado
OI - C.A. Barth
University of Colorado - Boulder, Colorado
OI - J.B. Pearce
University of Colorado - Boulder, Colorado
OI - E.F. Mackey
Packard-Bell - Newbury Park, California

BRIEF DESCRIPTION

The UV Photometer Experiment on OGO 5 was flown to measure the distribution of terrestrial airglow in the hydrogen Lyman-Alpha emission at 1216 A and the atomic oxygen emission at 1304 A. The photometer was mounted on the side of the main body facing away from the Earth to view the airglow in the local zenith. The field of view was 3 deg at half maximum. Radiation measurements between 1050 and 1800 A were obtained with this two-channel photometer experiment. The B-channel data (from 1250 to 1800 A) were used to remove the contribution of non-Lyman-Alpha radiation from the A-channel (1050 to 1800 A) data. Each photometer had its own amplifier and high-voltage servo-control system. The telemetered data were approximately proportional to the logarithm of the UV source intensity. Inflight calibration checks and automatic drift corrections were incorporated in the flight experiment. A lens cover, mounted at the edge of the photometer aperture and operated on ground command, not only provided increased protection from incident sunlight, but on several occasions enabled the experimenter to identify spurious signals. Both channels had a nominal sensitivity of 10 Rayleighs. Several measurements of the 1216-A extraterrestrial background radiation were made by placing the OGO 5 spacecraft into a spinning mode. This was done while OGO 5 was at altitudes greater than 80,000 km, i.e. when it was beyond the geocoronal scattering region. Background measurements were made during the periods September 12 to 14 and December 15 to 17, 1969, April 1 to 3 and September 1 to 6, 1970, and March 18 to 22, 1971. The experiment functioned normally throughout the OGO 5 mission.

BIBLIOGRAPHY

- PM: A69-31400, A71-24439, A72-32955, A74-15496, A74-22345.
- PS: N73-10813.

SPACECRAFT AND EXPERIMENT CHARACTERISTICS

OM: A71-33834.

OS: A71-35409, A73-12323, A73-39074.

OGO 5, Van De Hulst

EXPERIMENT NAME Measurement of the
Absolute Flux and
Energy Spectra of
Electrons
NSSDC ID 68-014A-12
PROJECT DESIGNATION E-12
PERSONNEL
PI - H.C. Van De Hulst
Netherlands Institute - Leiden, The Netherlands
OI - D. Tanka
Netherlands Institute - Leiden, The Netherlands
OI - M.N. Lind
Netherlands Institute - Leiden, The Netherlands

BRIEF DESCRIPTION

This experiment measured the absolute flux and energy spectrum of energetic galactic cosmic ray electrons (from 0.5 to 10 GeV) that are believed to be the source of synchrotron radiation which causes the nonthermal galactic radio noise. Protons (from 20 to 100 GeV) and gamma rays above 500 MeV were also measured. The instrumentation, a detector with six counters, was located on the side of the main body facing away from the Earth. The experiment functioned normally throughout the mission.

BIBLIOGRAPHY

PM: A69-19198, A70-37522, A70-38105, A70-38106,
A70-40690, A70-45769, A72-33869, A73-19252,
A74-27700, A74-31903.
B14744-000, B14745-000.

OGO 5, West

EXPERIMENT NAME Electron and Proton
Spectrometer
NSSDC ID 68-014A-06
PROJECT DESIGNATION E-06
PERSONNEL
PI - H.I. West, Jr.
Lawrence Radiation Laboratory - Livermore, California
OI - R.G. D'Arcy, Jr.
Lawrence Radiation Laboratory - Livermore, California
OI - L. Mann
Lawrence Radiation Laboratory - Livermore, California

BRIEF DESCRIPTION

This experiment was designed to measure the spectra, fluxes, and directional properties of electrons, protons, and alpha particles. Electrons were sensed by solid-state detectors found within each of two permanent magnet spectrometers. These spectrometers measured electrons in narrow energy windows centered at 79, 158, 266, 479, 822, 1530, and 2820 keV. Protons in six contiguous energy intervals (at 0.23, 0.57, 1.35, 5.60, 14.0, and 43 MeV), alpha particles in three contiguous intervals (at 5.9, 22.7, and 56.4 MeV), and electrons above 4 MeV were separately measured by a

four-sensor solid-state telescope. This telescope was physically located inside the larger of the two electron spectrometer magnets and in line with the spectrometer entrance aperture. Protons between 100 and 150 keV were also measured by a single solid-state detector adjacent to the telescope. The instruments were mounted on OPEP-2 and had their apertures looking perpendicular to the radius vector from the Earth. OPEP-2 was rotated back and forth about this radius vector through 230 deg at 3 deg/sec, permitting the determination of particle directional distributions. The experiment worked normally as long as data were telemetered from OGO 5. Thus, nearly 100 percent coverage was obtained between March 1968 and August 1971.

BIBLIOGRAPHY

PM: A66-23690, A71-21037, A73-12442, A73-24732,
A73-33454, A73-33455.
N70-28103, N73-31150, N74-13165.
B07587-000, B15152-000.
PS: N67-30930.
OM: A73-33449, A73-33457.
N73-20842.
OS: A72-35597, A73-33453, A73-33456, A74-11742.
N71-25273.

SPACECRAFT AND EXPERIMENT CHARACTERISTICS

OGO 6

SPACECRAFT CHARACTERISTICS

COMMON NAME OGO 6
 ALTERNATE NAMES PL-691D, OGO-F, S 60,
 POGO 3, 03986
 NSSDC ID 69-051A
 LAUNCH DATE 06/05/69
 WEIGHT IN ORBIT 632 kg
 LAUNCH SITE Vandenberg AFB,
 United States
 LAUNCH VEHICLE Thrust-Augmented
 Thor-Agena D
 SPONSORING COUNTRY United States
 SPONSORING AGENCY NASA-OSSA

ORBIT PARAMETERS INITIAL LATER

Epoch Date 06/04/69 01/28/72
 Apogee (km alt) 1077 967
 Perigee (km alt) 413 392
 Period (min) 99.7 98.3
 Inclination (deg) 82.0 82.0

PERSONNEL

- Project Manager -
 W. E. Scull - NASA-GSFC - Greenbelt, Maryland
- Project Scientist -
 N. W. Spencer - NASA-GSFC - Greenbelt, Maryland
- Program Manager -
 T. L. Fischetti - NASA Hq - Washington, D.C.
- Program Scientist -
 R. F. Fellows - NASA Hq - Washington, D.C.

BRIEF DESCRIPTION

OGO 6 was a large observatory instrumented with 26 experiments designed to study the various interrelationships between, and latitudinal distributions of, high-altitude atmospheric parameters during a period of increased solar activity. The main body of the spacecraft was attitude controlled by means of horizon scanners and gas jets so that its orientation was maintained constant with respect to the Earth and the Sun. The solar panels rotated on a horizontal axis extending transversely through the main body of the spacecraft. The rotation of the panels was activated by sun-sensors so that the panels received maximum sunlight. Seven experiments were mounted on the solar panels (the SOEP package). An additional axis, oriented vertically across the front of the main body, carried seven experiments (the OPEP package). Nominally, these sensors observed in a forward direction in the orbital plane of the satellite. The sensors could be rotated more than 90 deg relative to the nominal observing position and more than 90 deg between the upper and lower OPEP groups mounted on either end of this axis. On June 22, 1969, a failure occurred in the solar paddle array. This gave the vehicle a negative potential of more than 20 volts when the paddles were exposed to sunlight. This potential shift affected seven experiments which made measurements dependent upon knowledge of the spacecraft plasma sheath. During October 1969, a string of solar cells failed, but the only effect of the decreased power was to cause two experiments to change their mode of operation. Also during October 1969, a combination of manual and automatic attitude control was initiated, which extended the control gas lifetime of the attitude control system. In August 1970, tape recorder 1 operation degraded so that all recorded data were subsequently taken with tape recorder 2. By September 1970, power and equipment degradation left 14 experiments operating normally, three partially, and nine off. From October 14, 1970, tape recorder 2 was used only on Wednesdays (World Days) to conserve power and extend tape recorder operation.

In June 1971, the number of 'on' experiments decreased from 13 to 7, and on June 28, 1971, the spacecraft was placed in a spin-stabilized mode about the yaw (z) axis and turned off due to difficulties with spacecraft power. The attitude control system had operated properly until that time, and enough control gas remained for an additional 6 months of 3-axis stabilization. OGO 6 was turned on again from October 10, 1971, through March 1972, for operation of experiment 25 by Radio Research Laboratory, Japan. OGO 6 was kept in a stand-by status until July 14, 1972, at which time all operational support of OGO 6 was terminated.

SPACECRAFT/MISSION BIBLIOGRAPHY

Papers with major discussion of spacecraft, mission, testing, subsystems, or ground systems prepared by NASA project or project support personnel.
 A69-36674, A69-43132, A70-35303,
 N74-76932.

Papers about spacecraft, mission, testing, subsystems, or ground systems prepared by NASA contractor personnel.
 A64-10864.

EXPERIMENTS

OGO 6, Aggson

EXPERIMENT NAME DC Electric Field
 Measurements
 NSSDC ID 69-051A-23
 PROJECT DESIGNATION F-23

PERSONNEL

- PI - T.L. Aggson
 NASA-GSFC - Greenbelt, Maryland
- OI - N.C. Maynard
 NASA-GSFC - Greenbelt, Maryland
- OI - J.P. Heppner
 NASA-GSFC - Greenbelt, Maryland

BRIEF DESCRIPTION

Ambient dc electric fields were to be measured by determining the potential difference between two oppositely directed, 30-ft antennas with a high-input impedance voltmeter. The antennas, located on SOEP-1 and SOEP-2 (and shared with Experiment 25), were always parallel to the Earth's surface, being north-south in the dawn-dusk plane and east-west in the midnight plane. Direct-current electric fields and 4-Hz to 4-kHz ac fields were measured. On June 22, 1969 (12 days after launch), the floating potential required by this experiment was lost due to a spacecraft electrical failure. After this time, the only good electric field data obtained during the spacecraft's operational life were taken during eclipse time, which was estimated to be 10 percent of the total time.

BIBLIOGRAPHY

PM: A70-30082, A72-35989, A72-39980, A72-42432,
 A72-44854,
 N74-19023, N74-74627,
 B22605-000.

SPACECRAFT AND EXPERIMENT CHARACTERISTICS

OM: A72-42901.

OS: N74-74632.

OGO 6, Barth

EXPERIMENT NAME UV Photometer
 NSSDC ID 69-051A-13
 PROJECT DESIGNATION F-13
 PERSONNEL

- PI - C.A. Barth
University of Colorado - Boulder, Colorado
- OI - J.B. Pearce
University of Colorado - Boulder, Colorado
- OI - E.F. Mackey
Packard-Bell - Newbury Park, California

BRIEF DESCRIPTION

The scientific objectives of this experiment were: (1) to measure the intensity of the hydrogen Lyman-Alpha emission at 1216 A and of the atomic oxygen emission at 1304 A in the airglow, (2) to measure the columnar densities of the neutral atomic hydrogen and oxygen species above the orbit, and (3) to measure the spatial distribution (in local time and latitude) and the temporal changes (with solar and geophysical activity) of the above mentioned densities and emission intensities. The photometer was located on the main body, facing away from the earth. The field of view was 3 deg FWHM. Radiation measurements were made with a two-channel photometer. Channel B data, in the wavelength interval from 1250 to 1800 A, were used to remove the contribution of the non-Lyman-Alpha radiation from the Channel A data, which ranged from 1050 A to 1800 A. Thus, the intensity of the airglow emissions at 1216 and 1304 A could be inferred directly from the quantities Channel-A-Output-Minus-Channel-B, and Channel-B-Output. Both channels had a dynamic range from 10 Rayleighs to 100 kiloRayleighs. A commandable shutter was included to allow measurements of background and spurious signals. Since scattered sunlight affected the measurements when the sun was within 34 deg of the -z axis, suitable shielding was provided. The telemetered data were approximately proportional to the logarithm of the ultraviolet source intensity. Inflight calibration checks and automatic drift corrections were incorporated in the experiment. Spacecraft operations were terminated on June 28, 1971. At that time, this experiment was still operational, having functioned for more than 14,000 hr.

BIBLIOGRAPHY - None found

OGO 6, Bedo

EXPERIMENT NAME Solar UV Emissions,
160-1600 A
 NSSDC ID 69-051A-09
 PROJECT DESIGNATION F-09
 PERSONNEL

- PI - D.E. Bedo
AFRL - Bedford, Massachusetts
- OI - H.E. Hinteregger
AFRL - Bedford, Massachusetts

BRIEF DESCRIPTION

The purpose of this experiment was to measure solar radiation intensity in the wavelength range from 160 to 1600 A, with a total passband from 7 to 20 A in width. Solar radiation entered the instrument, located in SOEP-2, through polarized apertures which served to minimize the background signal noise due to charged particles and secondary electron emissions. This radiation struck a vertical stack of six gratings at an angle of 86 deg from the grating normal. The six gratings had different grating constants. The diffracted radiation was observed with a photomultiplier detector. Normal operation consisted of scanning the entire spectrum in 512 steps. In another mode, fifteen overlapping short scans of about 65 steps each were available for more continuous coverage of a shorter spectral range. The experiment worked well, but data were not taken after about March 1, 1970, due to degradation of the channel electron multipliers.

BIBLIOGRAPHY

PM: N71-10358.

PC: N74-16940.

OGO 6, Blamont

EXPERIMENT NAME Airglow and Auroral
Emissions
 NSSDC ID 69-051A-11
 PROJECT DESIGNATION F-11
 PERSONNEL

- PI - J.E. Blamont
CNES - Bretigny, France

BRIEF DESCRIPTION

This experiment had as its broad objective the study of airglow and auroral emissions at two wavelengths -- (1) the 6300-A red line of atomic oxygen, and (2) the 3914-A radiation from the molecular nitrogen ion. In addition, correlative investigations were planned. A photometer mounted on the EP-3 boom was used to measure the altitude distribution of the intensities of these emissions. The instrument could scan above or below the horizontal (x-y) plane in sixty 0.5-deg steps. The viewing angle was 6 deg parallel to the x-y plane and 0.5 deg perpendicular to the plane. A scan cycle from the x-y plane and back was completed using the 6300-A filter. Another cycle was then completed with the 3914-A filter in place. A complete cycle period lasted approximately 34 sec for each interference filter. All scheduled spacecraft operations were terminated in May 1971.

BIBLIOGRAPHY

OS: B19920-000.

OGO 6, Blamont

EXPERIMENT NAME Line Shape of the
6300-A Airglow
Emission
 NSSDC ID 69-051A-14
 PROJECT DESIGNATION F-14
 PERSONNEL

- PI - J.E. Blamont
CNES - Bretigny, France

SPACECRAFT AND EXPERIMENT CHARACTERISTICS

BRIEF DESCRIPTION

The objectives of this experiment were to measure the shape and width of the atomic oxygen red line at 6300 A emitted in the airglow and to study neutral atmospheric temperatures deduced from these measurements. The sensing optical system was mounted on the earthside of the main body and consisted of an interference filter at 6300 A, a spherical Fabry-Perot interferometer, and a PM. The emission layer, which is centered at about 250 km, was viewed tangentially by the optical system. Since the spacecraft altitude varied between 400 and 1000 km, a moving flat mirror was placed in front of the equipment to keep the sensor optical axis in the direction of the emission layer. The experiment had a circular field of view of 1 deg. Measurements were made at four heights, corresponding to four mirror positions. One mirror position provided tangential viewing at about 250 km. The other mirror positions changed the optical axis by +2, +4 and -2 degrees. At perigee, the four observed altitudes were at 240, 280, 320, and 360 km. At apogee, these altitudes were 100, 200, 300, and 400 km. After being reflected by the mirror, the beam passed through an interference filter centered at 6300 A. Every 11 sec, a second filter centered at 6200 A was switched in place of the original filter for 2 sec to determine that portion of the input due to background stray light. The interferometer consisted essentially of two quartz plano-concave lenses 13.2 mm apart. The two spherical surfaces were coated with multilayer dielectric reflecting films. Scanning of the interferometer was achieved by varying the distance between the two lenses using the piezoelectric effect. Once every 2 days the calibration of the interferometer was adjusted in orbit by operating a cadmium discharge source on ground command. The sensitivity of the photomultiplier and the transmission of the interference filters were monitored from the response of the equipment to light emitted by two tungsten lamps. The experiment became inoperable in September 1970.

BIBLIOGRAPHY

PM: A72-35603, A74-23679.

OGO 6, Cain

EXPERIMENT NAME Magnetic Survey,
Rubidium Vapor
Magnetometer
NSSDC ID 69-051A-21
PROJECT DESIGNATION F-21
PERSONNEL
PI - J.C. Cain
NASA-GSFC - Greenbelt, Maryland
OI - R.A. Langel
NASA-GSFC - Greenbelt, Maryland

BRIEF DESCRIPTION

The OGO 6 rubidium vapor magnetometer was an optically pumped, self-oscillating, dual-cell instrument used to measure the scalar magnetic field in polar orbit. The instrument, located on boom EP-6, was sampled every 0.288 sec, and operated almost continuously from launch until June 28, 1971. The precision of the measurements was plus or minus 0.6 gamma with an absolute accuracy of approximately 2 gammas. The accuracy of the measurements was limited by spacecraft fields.

BIBLIOGRAPHY

PM: A70-39349, A71-29903, A73-31768, A74-34019,
N72-30823, N73-20866, N74-13566, N74-17058,
B15846-000, B15849-000.

PS: A73-31772, A73-41374,
N72-23341, N74-20982.

OS: A73-31769.

OGO 6, Clark

EXPERIMENT NAME Celestial Lyman-Alpha
Measurement
NSSDC ID 69-051A-12
PROJECT DESIGNATION F-12
PERSONNEL
PI - M.A. Clark
Aerospace Corporation - El Segundo, California
OI - D.D. Elliott
Aerospace Corporation - El Segundo, California
OI - P.H. Metzger
Aerospace Corporation - El Segundo, California

BRIEF DESCRIPTION

This experiment was designed to measure the zenith angle distribution of Lyman-Alpha radiation on a global basis. The experiment consisted of a photometer centered at 1216 A, with a 3-A bandwidth and a 6-deg field of view. It used a rotation mirror to make a circular scan of the sky once each 40 sec. The photometer was mounted outside the main body facing away from the earth, allowing a clear view of both horizons. The scanner plane was canted 20 deg from the spacecraft axis to avoid direct observation of the sun, and therefore the instrument scanned most of the celestial sphere exclusive of a cone of 20 deg half-angle around the solar and antisolar points. The photometer sensitivity was about 1 Rayleigh during early operations but decayed to approximately 10 Rayleighs after a few days. Count-rate data were obtained during the period from June 6 to 18, 1969, and were of excellent quality. The scanner failed on June 23, 1969.

BIBLIOGRAPHY

PM: A70-43852, A71-17975,
N71-36136, N72-23429, N74-74625.
OS: A71-24439.

OGO 6, Donahue

EXPERIMENT NAME Sodium Airglow
Photometer
NSSDC ID 69-051A-26
PROJECT DESIGNATION F-26
PERSONNEL
PI - T.M. Donahue
University of Pittsburgh - Pittsburgh, Pennsylvania
OI - J.E. Blamont
CNES - Bretigny, France

BRIEF DESCRIPTION

The primary objective of this experiment was to provide measurements of the yellow airglow of sodium at 5890 A and 5896 A and of the green airglow of atomic oxygen at 5577 A. The airglow was viewed slantwise with a horizon-scanning photometer. The resulting large optical path produced amplifications

SPACECRAFT AND EXPERIMENT CHARACTERISTICS

in surface brightness of a factor of 10 to 20. The sensor, which was mounted on the Earth-facing side of the main body, consisted of an optical system, interference filters, and a photomultiplier. The photometer was equipped with a mirror that was pivoted to scan the sky near the horizon. This mirror scan required 18.4 sec, extended from 10 deg below the horizon to about 25 deg below the horizon, and was divided into 127 positions, each separated by 7.5 min of arc. For a complete cycle, the photometer scanned up and down with the green filter (5577 Å) and then repeated the motion with the yellow filter (5890 Å). The vertical field of view was 7.5 min of arc, and the horizontal field of view was 4.2 deg. When the satellite was at an altitude of 500 km, the sampled emission feature at 250 km was less than 4 km high for a single mirror position. The experiment remained operational throughout the useful life of OGO 6 and yielded 8251 hours of data. After October 1970, however, the experiment was operated only one day per week to minimize PM fatigue.

BIBLIOGRAPHY

PM: A72-35604, A73-45121, A74-30670.
N73-16436.
B22606-000.

OGO 6, Evans

EXPERIMENT NAME Auroral Particle
Measurement
NSSDC ID 69-051A-15
PROJECT DESIGNATION F-15
PERSONNEL
PI - D.S. Evans
NASA-GSFC - Greenbelt, Maryland
OI - D.E. Stilwell
NASA-GSFC - Greenbelt, Maryland

BRIEF DESCRIPTION

The purpose of this experiment was to measure the directional intensity and energy spectrum of auroral electrons and protons in the range from 1 to 20 keV. The instrumentation, located at the end of the EP-4 boom, consisted of a curved plate electrostatic analyzer with an open-window electron multiplier. The overall performance of the experiment was good. However, the experiment tape recorder output modulation became erratic about August 15, 1969. Therefore, a real-time special purpose system had to be used. This limited the operation of the experiment to three days of the special purpose six-day cycle of operation. In June 1972, after 16,893 hr of operation, the instrument was turned off together with the spacecraft.

BIBLIOGRAPHY - None found

OGO 6, Farley

EXPERIMENT NAME Trapped and
Precipitating Electrons
UCLA
NSSDC ID 69-051A-16
PROJECT DESIGNATION F-16

PERSONNEL

PI - T.A. Farley
University of California - Los Angeles, California
OI - M.C. Chapman
TRW Systems Group - Redondo Beach, California

BRIEF DESCRIPTION

The objectives of this experiment were to study the precipitation of electrons into the atmosphere, to relate particle precipitation and particle trapping, and to determine the effects of these phenomena upon magnetospheric structure. Six plastic scintillator detectors located at the end of the EP-1 boom measured the unidirectional electron fluxes in eight energy intervals between 50 keV and 1.2 MeV. A seventh plastic scintillator measured omnidirectional electron fluxes in the same energy intervals. One unidirectional detector experienced a large reduction in efficiency shortly after launch. Other detectors functioned normally from launch until June 28, 1971, when the experiment was turned off. Unfortunately, these data are contaminated by protons whenever they are present.

BIBLIOGRAPHY

PM: N73-15863.

OGO 6, Hanson

EXPERIMENT NAME Planar Ion and Electron
Trap
NSSDC ID 69-051A-03
PROJECT DESIGNATION F-03
PERSONNEL
PI - W.B. Hanson
University of Texas - Dallas, Texas
OI - T.W. Flowerday
University of Texas - Dallas, Texas

BRIEF DESCRIPTION

This experiment was used to determine the following characteristics of the ionosphere -- the ion concentration, the ion composition, the ion temperature, the fast electron flux with a normal energy component greater than 9.1 eV, and the horizontal irregularities in the ion concentration. The retarding potential analyzer consisted of a sensor head and an electronics box. The sensor head contained an 8-cm cylinder with a concentric 2-cm aperture. Charged particles passed through this aperture before striking a solid collector. The path between the aperture and collector was segmented by four grids, whose potentials were controlled by the electronics box. The sensor head was flush-mounted with the front face of the OPEP-2. During normal operation, the sensor face was perpendicular to the vehicle velocity vector. There were two basic modes of operation -- an ion-analysis mode and a duct mode. These modes were alternately employed. A complete cycle time of either 40 or 10 sec could be selected for both modes by ground command. The spatial resolution was from 40 to 160 m, depending on the cycle time selected. The experiment was first turned on during orbit 20. Because of the 20-v negative vehicle potential, which developed 17 days after launch, reliable ion temperature, ion composition, and photoelectron flux data could not be obtained except upon spacecraft entry into eclipse, when the vehicle potential recovered quite rapidly. However, ion-concentration and duct-mode data were still valid during sunlight. In October 1969, the vehicle potential diminished to the extent that ion temperature and dominant component ions could be determined even in sunlight. During each eclipse, the vehicle potential returned to normal, and complete data were obtained

SPACECRAFT AND EXPERIMENT CHARACTERISTICS

during approximately 30 percent of each orbit. The performance of the instrument was excellent from turn-on, and the experiment yielded excellent data. It was normally operated 100 percent of the time. After operating for 17,180 hr, the experiment was turned off during June 1971.

BIBLIOGRAPHY

PM: A70-43840, A70-43841, A72-44516, A73-19241,
A73-22066, A73-24738, A73-41919, A74-12640,
A74-18754, A74-27695.
N73-32286, N74-20542.
B20340-000, B22605-000.

PS: A72-26411.

OS: A72-42416.
N71-35437.

OGO 6, Hanson

EXPERIMENT NAME Ion Mass Spectrometer,
UTD
NSSDC ID 69-051A-06
PROJECT DESIGNATION F-06
PERSONNEL
PI - W.B. Hanson
University of Texas - Dallas, Texas
OI - T.W. Flowerday
University of Texas - Dallas, Texas

BRIEF DESCRIPTION

An ion mass spectrometer was employed to measure the composition of positive ions in the mass range from 1 to 34 amu. The instrumentation, located in OPEP-1, consisted of a 90-deg-sector magnetic analyzer, an electron multiplier detector, and a linear automatic-ranging electrometer. The different ion species were sampled by applying a varying voltage to the analyzer. The spectrometer could operate in a sweep mode and a step mode. In the sweep mode the voltage was swept exponentially from -4000 V to -94 V. In the step mode the voltage could be stepped through a sequence of 11 values (corresponding to mass peaks at 1, 2, 4, 7, 8, 14, 16, 18, 28, 30, and 32 amu) or four values (corresponding to mass peaks at 1, 4, 14, and 16 amu). There were no scientific results from this experiment because the instrument was irreparably damaged at turn-on by high-voltage arcing. Data were collected for a 57-hr period but were subsequently proven to be invalid.

BIBLIOGRAPHY

PM: A72-10902, A72-35989, A72-42016.
N71-10588.

PS: A73-29988.

OGO 6, Helliwell

EXPERIMENT NAME VLF Noise and
Propagation
NSSDC ID 69-051A-24
PROJECT DESIGNATION F-24

IV-46

PERSONNEL

PI - R.A. Helliwell
Stanford University - Stanford, California
OI - L.H. Rorden
Stanford University - Stanford, California

BRIEF DESCRIPTION

Three magnetic antennas and one electric antenna located at the end of the EP-5 boom were used to study the properties of waves in the ionosphere over the frequency range from 20 Hz to 30 kHz. The experiment provided information such as the polarization, wave-normal direction, and E/H ratio of signals in the frequency range of interest. Also, it measured the antenna impedance and current both with and without bias and the phase and amplitude of VLF transmitter signals. On July 25, 1969, the antenna extension was completed. On August 22, 1969, failure of a mode logic component limited observations to only the electric field spectrum. Subsequently, the special purpose data was limited to the narrow-band mode (0 to 30 kHz) and the spectrum mode (30 to 100 kHz). The experiment was turned off on June 28, 1971, when the spacecraft was turned off.

BIBLIOGRAPHY

PM: A71-14538.
N74-12842.

OS: A72-21189.

OGO 6, Kreplin

EXPERIMENT NAME Solar X-ray Emissions

NSSDC ID 69-051A-08
PROJECT DESIGNATION F-08
PERSONNEL

PI - R.W. Kreplin
Naval Research Laboratory - Washington, D.C.
OI - T.A. Chubb
Naval Research Laboratory - Washington, D.C.
OI - H.D. Friedman
Naval Research Laboratory - Washington, D.C.
OI - S. Bowyer
University of California - Berkeley, California

BRIEF DESCRIPTION

This experiment used a scintillating crystal/PM detector and a proportional counter to observe solar X-rays between 0.15 and 6.2 A. Each detector was coupled to an eight-channel pulse height analyzer. The detectors were located in SOEP-1. Although the detectors worked well, the data were virtually useless due to contamination from trapped particles. The experiment was turned off in September 1970.

BIBLIOGRAPHY - None found

SPACECRAFT AND EXPERIMENT CHARACTERISTICS

OGO 6, Laaspere

EXPERIMENT NAME Whistler and
 Audio-Frequency
 Electromagnetic Waves
 NSSDC ID 69-051A-25
 PROJECT DESIGNATION F-25
 PERSONNEL
 PI - T. Laaspere
 Dartmouth College - Hanover, New Hampshire
 OI - M.G. Morgan
 Dartmouth College - Hanover, New Hampshire

BRIEF DESCRIPTION

Two 30-ft electric dipole antennas (attached to SOEP-1 and SOEP-2 and shared with Experiment 23) were used to study the propagation and characteristics of whistler-mode waves in the ionosphere over an extended range of frequencies. Four 15-kHz bands (0.02 to 15 kHz, 15 to 30 kHz, 92.5 to 107.5 kHz, and 280 to 295 kHz) could be received in real time. Two 0.2-kHz bands (centered at 200 and 540 kHz) and a 0.02- to 1000-kHz broadband signal could be tape recorded. The tape-recorded data, consisting of digital values of signal intensities, were observed almost continuously from launch until spacecraft turnoff June 28, 1971. Real-time data were obtained from telemetry stations on all scheduled days (2 days out of 6, since this was one of three different experiments sharing the same special purpose telemetry system) over the same time period. The narrow-band receivers recorded signal intensities at 200 kHz from BBC, England, and at 540 kHz from New Mexico, or from other emitters at those frequencies. A special operation of the real-time broadband receivers was made by Radio Research Laboratories, Japan, with observations near Siple Station, Antarctica, and Kashima, Japan, from October 1, 1971, to March 1972.

BIBLIOGRAPHY

PM: A69-36677, A71-33951, A72-29384, A73-33438,
 A74-34020,
 B17973-000.
 PS: A72-23420.
 OS: A72-21189.

OGO 6, Lockwood

EXPERIMENT NAME Neutron Monitor
 NSSDC ID 69-051A-18
 PROJECT DESIGNATION F-18
 PERSONNEL
 PI - J.A. Lockwood
 University of New Hampshire - Durham, New
 Hampshire
 OI - E.L. Chupp
 University of New Hampshire - Durham, New
 Hampshire

BRIEF DESCRIPTION

A moderated helium-3 proportional counter, mounted on the EP-5 boom, was used to measure the total neutron flux in the energy interval from 1 keV to 10 MeV. Four sets of charged particle counters, placed on two pairs of opposing sides of the proportional counter, served as a charged particle rejection system

for the neutron measurements. These detectors also provided omnidirectional charged particle count rates (protons above 13 MeV and electrons above 1.5 MeV) and count rates for particles that gave coincident counts in detectors on opposing sides of the proportional counter (protons above 50 MeV and electrons above 13 MeV). A plastic scintillator was operated in coincidence with the proportional counter to measure 1- to 10-MeV neutrons in four energy intervals. The detector system performed normally until December 24, 1969, when the power supply failed. No useful data were obtained after that date.

BIBLIOGRAPHY

PM: A69-36678, A70-39326, A72-10877, A73-41498,
 A74-15356,
 N73-19841, N73-32639,
 B22608-000.
 PS: A73-36645.

OGO 6, Masley

EXPERIMENT NAME Low-Energy Solar
 Cosmic-Ray
 Measurement
 NSSDC ID 69-051A-19
 PROJECT DESIGNATION F-19
 PERSONNEL
 PI - A.J. Masley
 McDonnell-Douglas - Huntington Beach, California
 OI - P.R. Satterblom
 McDonnell-Douglas - Huntington Beach, California

BRIEF DESCRIPTION

This experiment was designed to study solar cosmic radiation and geomagnetically trapped and precipitating radiation. The instrumentation, located on the main body, consisted of two solid-state detector discs mounted coaxially to form a telescope that looked away from the Earth with a 28-deg conical half-angle. Protons in 14 contiguous energy intervals between 5 and 78 MeV and alpha particles in 12 intervals between 17 and 125 MeV were counted. The sum of counts of protons above 78 MeV and electrons above 250 keV was also obtained. This experiment functioned normally from launch until August 29, 1970, at which time a spacecraft failure prevented the transmission of any further experiment data.

BIBLIOGRAPHY

PM: A68-27616, A71-18158, A72-31965, A74-30263,
 N73-16795,
 B11181-000

OGO 6, McKeown

EXPERIMENT NAME Energy Transfer Probe
 for Atmospheric Density
 NSSDC ID 69-051A-07
 PROJECT DESIGNATION F-07

NOV. 10, 1975

SPACECRAFT AND EXPERIMENT CHARACTERISTICS

PERSONNEL

- PI - D. McKeown
General Dynamics - San Diego, California
- OI - H.R. Poppa
General Dynamics - San Diego, California

BRIEF DESCRIPTION

The primary objective of this experiment was to measure the kinetic energy imparted by the atmosphere to the surface of an orbiting satellite. A secondary purpose was to determine variations in atmospheric density as a function of time, latitude, and solar activity. Four dual-energy transfer probes were mounted on OPEP-1, normal to the velocity vector of the spacecraft. Each probe utilized a 1.27-cm, 15-MHz, temperature-sensitive quartz crystal detector for measuring the gas-to-surface energy transfer. Two of the crystal energy transfer surfaces were plated with aluminum, and the other two were plated with gold. The instrument was capable of detecting a kinetic energy transfer from 10^{-6} to 10^{-1} w/sq cm. Each probe was equipped with a shutter that periodically (every 111 sec) cut off the air flow to the instrument to allow for calibration. The change in probe surface mass due to contamination, impact, cleaning, etc., was continuously monitored by a quartz crystal microbalance. The experiment was a success, and good data were obtained from launch until August 29, 1970, when a failure in the spacecraft telemetry subsystem prevented the transmission of further experimental data. The instrumentation was used subsequently to monitor the status of this subsystem failure.

BIBLIOGRAPHY

- PM: A66-15922, A69-36680,
N71-20207, N74-74659,
B20296-000, B20953-000, B20954-000.
- PS: N74-10255,
B20297-000.

OGO 6, Nagy

- EXPERIMENT NAME Electron Temperature
and Density
- NSSDC ID 69-051A-02
- PROJECT DESIGNATION F-02
- PERSONNEL
- PI - A.F. Nagy
University of Michigan - Ann Arbor, Michigan
- OI - L.H. Brace
NASA-GSFC - Greenbelt, Maryland

BRIEF DESCRIPTION

The purpose of this experiment was to observe the worldwide distribution of electron densities and temperatures. It consisted of two cylindrical Langmuir probes, mounted on OPEP-2, at right angles to each other, with one probe aligned in the direction of the spacecraft velocity vector and the other parallel to the OPEP rotational axis. Each probe consisted of a collector 22.9 cm long and 5.6 mm in diameter, extending outward from a concentric guard 22.9 cm long and 16.5 mm in diameter. Both components were stainless steel and were insulated from each other with Teflon. The electronics package in the main spacecraft body provided sawtooth voltage sweeps to the probe, detected the ensuing current flow between ground and collector, provided a calibration sequence every 10 min, and provided control system circuitry necessary for varying the mode of operation and for processing the experiment-generated information for telemetry. Data resolution was no better than one observation per 80 km in the normal mode,

20 km in the fast mode. This experiment operated nominally until the daytime spacecraft potential shift occurred on June 22, 1969. After this time, daylight data were not useful. After September 1969, an attempt was made to make some of the daytime observations usable. Within these limitations, the experiment remained operational until the spacecraft was turned off on June 28, 1971.

BIBLIOGRAPHY

- PM: A72-35989, A73-19241,
N73-13376,
B22605-000.
- OS: A73-41919.

OGO 6, Reber

- EXPERIMENT NAME Neutral Atmospheric
Composition
- NSSDC ID 69-051A-04
- PROJECT DESIGNATION F-04
- PERSONNEL
- PI - C.A. Reber
NASA-GSFC - Greenbelt, Maryland
- OI - D.N. Harpold
NASA-GSFC - Greenbelt, Maryland
- OI - G.R. Carignan
University of Michigan - Ann Arbor, Michigan
- OI - D.R. Tausch
University of Michigan - Ann Arbor, Michigan

BRIEF DESCRIPTION

The primary objective of this experiment was to study the concentration of the major constituents (nitrogen, oxygen, helium, and hydrogen) of the Earth's neutral upper atmosphere during changing solar and magnetic activity as a function of time and location. The spectrometer system consisted of a quadrupole analyzer (in which mass separation occurred within a direct-current and a radio-frequency electric field), an enclosed dual-filament electron bombardment ion source, an electron multiplier, supporting electronics for operating the analyzer and source, and a break-off device for exposing the evacuated mass spectrometer to the atmosphere after the spacecraft achieved orbit. Located on OPEP-2 the spectrometer's entrance aperture normally faced into the direction of motion. This experiment was designed to operate in any one of three modes, depending on the command given. In Mode C the spectrometer was tuned to a particular neutral species mass and measured its concentration only. In the other two modes of operation, both pretuned stepping and mass sweeping approaches were used. A complete measurement in Mode A lasted 368 seconds and consisted of 28 stepping sequences and two sweeping sequences. A complete measurement cycle in Mode B also took 368 sec and consisted of six sweeping sequences and four stepping sequences. The experiment remained fully operational until the spacecraft was turned off June 28, 1971.

BIBLIOGRAPHY

- PM: A71-21647, A71-39711, A72-13518, A72-32964,
A72-42431, A73-26997, A73-27602, A73-31767,
A73-33441, A73-38941, A74-18376, A74-21693,
A74-27713, A74-34027,
N71-20638, N71-25267, N73-17946, N73-33320,
B16248-000.
- PS: A72-24957, A73-15538, A73-29975.

SPACECRAFT AND EXPERIMENT CHARACTERISTICS

OGO 6, Stone

EXPERIMENT NAME Cosmic-Ray Experiment
NSSDC ID 69-051A-20
PROJECT DESIGNATION F-20
PERSONNEL
PI - E.C. Stone
California Technology - Pasadena, California
OI - R.E. Vogt
California Technology - Pasadena, California

BRIEF DESCRIPTION

This experiment was designed to measure the energy spectra and chemical composition of cosmic-ray particles of both solar and galactic origin over selected energy intervals, using three charged-particle telescopes located on the main body and facing away from the Earth. The first was an energy-loss range telescope consisting of seven solid-state detectors separated by various absorbers, arranged in a single stack, and surrounded on the side by a plastic scintillator anticoincidence counter. Particles arriving within a cone of 30-deg half-angle with respect to the vertical were analyzed for energy loss in the first detectors and for range in the subsequent detectors and absorbers. The threshold energies were from 1.0 to 315 MeV/nucleon. The second telescope was an energy-loss Cerenkov type, which detected particles with energy greater than 400 MeV/nucleon arriving within a cone of 35 deg half-angle with respect to the vertical. These particles were analyzed for energy loss in a solid-state detector and for velocity in a quartz Cerenkov radiator. The third telescope was an energy-loss telescope that detected particles arriving within a cone of 4.5 deg half-angle with respect to the vertical, and also analyzed them for energy loss in a solid-state detector. The threshold energies for protons and alpha particles were 3.3 and 8.5 MeV/nucleon. The experiment performed normally throughout the mission. The time coverage was near 100 percent until August 1970, after which the coverage dropped due to the malfunction of the spacecraft tape recorder.

BIBLIOGRAPHY

PM: A68-27615, A71-22801, A73-15526, A73-24727,
A74-30190,
N72-27829, N72-29818, N73-15837, N73-33777,
N74-21466,
B10763-000.
PS: A72-21510, A72-39401.

OGO 6, Taylor

EXPERIMENT NAME Ion Mass Spectrometer,
GSFC
NSSDC ID 69-051A-05
PROJECT DESIGNATION F-05
PERSONNEL
PI - H.A. Taylor, Jr.
NASA-GSFC - Greenbelt, Maryland
OI - R.A. Pickett
NASA-GSFC - Greenbelt, Maryland
OI - F.R. Allum
University of Texas - Dallas, Texas

BRIEF DESCRIPTION

This experiment was designed to obtain data that would describe the global distribution of the ion composition of the upper ionosphere, with emphasis on temporal and spatial variations. The

objectives included the investigation of magnetic and solar control, and the study of polar-region phenomena. The detector, a Bennett radio-frequency ion mass spectrometer, consisted of a tube with a series of plane-parallel knitted grids mounted normal to the tube axis. Both ac and dc fields accelerated the ions down the length of the tube toward a collector. Only those ions satisfying the velocity and phase conditions established by the fields received sufficient energy from the fields to pass a retarding potential grid and impinge on the collector. Ambient thermal positive ions in the mass range from 1 to 45 amu were measured with a resolution of approximately 1 in 20 amu. The instrument's sensitivity ranged from approximately 10^6 ions/cc to approximately 10 ions/cc. Measurements of a given ion were repeated once every 36.8 sec, for an average spatial resolution of about 2 deg in latitude. The sensor was mounted on the OPEP-2 and was positioned to point into the direction of motion whenever possible. Periodic calibrations were performed. The experiment operated essentially continuously from launch until September 1, 1970, when the spacecraft's operation became intermittent as a result of spacecraft malfunction. All spacecraft operations were terminated on June 28, 1971. At that time the experiment was still operational after functioning for more than 14,000 hours.

BIBLIOGRAPHY

PM: A71-33762, A73-11904, A73-15533, A73-19255,
A74-18376,
N71-25265, N74-16064.
PS: A71-43166.
OS: B22334-000.

OGO 6, Williams

EXPERIMENT NAME Trapped and
Precipitating Electrons,
GSFC
NSSDC ID 69-051A-17
PROJECT DESIGNATION F-17
PERSONNEL
PI - D.J. Williams
NASA-GSFC - Greenbelt, Maryland
OI - J.H. Trainor
NASA-GSFC - Greenbelt, Maryland

BRIEF DESCRIPTION

The primary objective of this experiment was to study the temporal and spatial behavior of medium- to high-energy electrons at low altitudes in the outer zone. The experiment utilized the near-polar low-altitude orbit of OGO 6 to achieve (at high latitudes) a high sampling density of the outer zone field lines under relatively stable and well-known field configuration. The three-axis stabilization made it possible to orient detectors essentially parallel or perpendicular to the field lines in the high-latitude region of interest. A total of seven detectors were used at the end of the EP-2 boom. Four detectors oriented horizontally measured the intensities of trapped and precipitating electrons in the integral energy ranges E greater than 40 keV, 100 keV, 300 keV, and 1 MeV, respectively. Two detectors looking away from the Earth measured precipitating electrons in two ranges, E greater than 30 keV and 300 keV, respectively. One detector facing the Earth measured backscatter electrons in the range E greater than 30 keV. The detectors functioned normally until a spacecraft malfunction on August 29, 1970, prevented the telemetering of any further data.

BIBLIOGRAPHY

PM: A68-34540, A69-36676.
OS: N74-16072.

V. INDEXES TO EXPERIMENT CHARACTERISTICS

A. INDEX OF PRINCIPAL AND CO-INVESTIGATORS AND EXPERIMENTS

NAME, EXPERIMENT NAME	NSSDC ID	PI'S LAST NAME	PAGE
Aggson, T.L. - NASA-GSFC			
OGO 5, Electric Field Measurement	(68-014A-26)	Aggson	32
OGO 6, DC Electric Field Measurements	(69-051A-23)	Aggson	42
Alexander, W.M. - Baylor U			
OGO 1, Interplanetary Dust Particles	(64-054A-07)	Bohn	2
OGO 3, Interplanetary Dust Particles	(66-049A-21)	Bohn	17
Allum, F.R. - U of Texas, Dallas			
OGO 6, Ion Mass Spectrometer, GSFC	(69-051A-05)	Taylor	50
Anderson, H.R. - Rice U			
OGO 2, Cosmic-Ray Ionization	(65-081A-06)	Anderson	9
OGO 4, Cosmic-Ray Ionization	(67-073A-07)	Anderson	24
Anderson, K.A. - U of California, Berkeley			
OGO 1, Solar Cosmic Rays	(64-054A-12)	Anderson	1
OGO 3, Solar Cosmic Rays	(66-049A-01)	Anderson	16
OGO 5, Energetic Radiations From Solar Flares	(68-014A-04)	Anderson	32
Angerami, J.J. - Stanford U			
OGO 1, VLF Noise and Propagation	(64-054A-08)	Helliwell	3
OGO 2, VLF Noise and Propagation	(65-081A-02)	Helliwell	11
Armstrong, T.P. - U of Iowa			
OGO 2, Corpuscular Radiation Experiment	(65-081A-18)	Van Allen	15
OGO 5, Low-Energy Proton and Electron Differential Energy Analyzer (LEPEDEA)	(68-014A-07)	Frank	35
Arnoldy, R.L. - U of Minnesota			
OGO 1, Ionization Chamber	(64-054A-20)	Winckler	7
OGO 1, Electron Spectrometer	(64-054A-21)	Winckler	7
OGO 3, Electron Spectrometer	(66-049A-22)	Winckler	22
OGO 3, Ionization Chamber	(66-049A-23)	Winckler	22
Balasubrahmanyam, V.K. - NASA-GSFC			
OGO 5, Galactic and Solar Cosmic-Ray Studies	(68-014A-10)	McDonald	37
Barth, C.A. - U of Colorado			
OGO 2, UV Spectrometer, 1100 - 3400 A	(65-081A-12)	Barth	10
OGO 4, UV Spectrometer, 1100 - 3400 A	(67-073A-14)	Barth	25
OGO 5, UV Photometer	(68-014A-21)	Thomas	40
OGO 6, UV Photometer	(69-051A-13)	Barth	43
Bedo, D.E. - AFCRL			
OGO 2, Solar UV Emissions	(65-081A-17)	Hinterregger	12
OGO 4, Solar UV Emissions	(67-073A-20)	Hinterregger	26
OGO 6, Solar UV Emissions, 160 - 1600 A	(69-051A-09)	Bedo	43
Blamont, J.E. - CNES			
OGO 2, Airglow and Auroral Study	(65-081A-10)	Reed	14
OGO 4, Airglow and Auroral Study	(67-073A-12)	Reed	29

INDEX OF PRINCIPAL AND CO-INVESTIGATORS AND EXPERIMENTS

NAME, EXPERIMENT NAME	NSSDC ID	PI'S LAST NAME	PAGE
Blamont, J.E.-(CON'T)			
OGO 5, Geocoronal Lyman-Alpha Measurements	(68-014A-22)	Blamont	33
OGO 6, Airglow and Auroral Emissions	(69-051A-11)	Blamont	43
OGO 6, Line Shape of the 6300-A Airglow Emission	(69-051A-14)	Blamont	43
OGO 6, Sodium Airglow Photometer	(69-051A-26)	Donahue	44
Bohn, J.L. - Temple U			
OGO 1, Interplanetary Dust Particles	(64-054A-07)	Bohn	2
OGO 3, Interplanetary Dust Particles	(66-049A-21)	Bohn	17
Bonetti, A.M. - U of Florence			
OGO 1, Plasma Probe, Faraday Cup	(64-054A-14)	Bridge	2
OGO 3, Plasma Probe, Faraday Cup	(66-049A-06)	Bridge	17
Bourdeau, R.E. - NASA-GSFC			
OGO 2, Positive Ion Study	(65-081A-19)	Donley	10
OGO 4, Positive Ion Study	(67-073A-19)	Chandra	25
Bowyer, S. - U of California, Berkeley			
OGO 5, Solar X-ray Emissions	(68-014A-23)	Kreplin	37
OGO 6, Solar X-ray Emissions	(69-051A-08)	Kreplin	46
Boyd, R.L.F. - U College, London			
OGO 5, Electron Temperature and Density	(68-014A-01)	Boyd	33
Brace, L.H. - NASA-GSFC			
OGO 6, Electron Temperature and Density	(69-051A-02)	Nagy	48
Bridge, H.S. - MIT			
OGO 1, Plasma Probe, Faraday Cup	(64-054A-14)	Bridge	2
OGO 3, Plasma Probe, Faraday Cup	(66-049A-06)	Bridge	17
Cain, J.C. - NASA-GSFC			
OGO 2, Magnetic Survey, Rubidium Vapor Magnetometer	(65-081A-05)	Cain	10
OGO 4, Magnetic Survey, Rubidium Vapor Magnetometer	(67-073A-06)	Cain	25
OGO 6, Magnetic Survey, Rubidium Vapor Magnetometer	(69-051A-21)	Cain	44
Campbell, R.M. - NASA-GSFC			
OGO 1, Magnetic Survey Using Two Magnetometers	(64-054A-02)	Hepppner	4
OGO 3, Magnetic Survey Using Two Magnetometers	(66-049A-11)	Hepppner	19
OGO 5, Magnetic Survey Using Two Magnetometers	(68-014A-15)	Hepppner	36
Carignan, G.R. - U of Michigan			
OGO 6, Neutral Atmospheric Composition	(69-051A-04)	Reber	48
Chandra, S.S. - NASA-GSFC			
OGO 4, Positive Ion Study	(67-073A-19)	Chandra	25
Chapman, M.C. - TRW Systems Group			
OGO 6, Trapped and Precipitating Electrons, UCLA	(69-051A-16)	Farley	45
Chubb, T.A. - Naval Research Lab			
OGO 2, Solar X-ray Emissions	(65-081A-16)	Kreplin	12
OGO 4, Solar X-ray Emissions	(67-073A-21)	Kreplin	27
OGO 5, Solar X-ray Emissions	(68-014A-23)	Kreplin	37
OGO 6, Solar X-ray Emissions	(69-051A-08)	Kreplin	46
Chupp, E.L. - U of New Hampshire			
OGO 6, Neutron Monitor	(69-051A-18)	Lockwood	47

INDEX OF PRINCIPAL AND CO-INVESTIGATORS AND EXPERIMENTS

NAME, EXPERIMENT NAME	NSSDC ID	PI'S LAST NAME	PAGE
Clark, M.A. - Aerospace Corp OGO 6, Celestial Lyman-Alpha Measurement	(69-051A-12)	Clark	44
Cline, T.L. - NASA-GSFC OGO 1, Positron Search and Gamma Ray Spectrum	(64-054A-15)	Cline	2
OGO 3, Positron Search and Gamma-Ray Spectrum	(66-049A-04)	Cline	17
OGO 5, Interplanetary Electrons, Positrons, and Protons	(68-014A-05)	Cline	34
Coleman, Jr., P.J. - U of California OGO 5, Hydromagnetic Waves and Trapped Particles	(68-014A-13)	Coleman	34
OGO 5, Triaxial Fluxgate Magnetometer	(68-014A-14)	Coleman	34
Crook, G.M. - TRW Systems Group OGO 5, Plasma Wave Detector	(68-014A-24)	Crook	35
Crowther, T.J. - Lockheed OGO 5, Light-Ion Magnetic Mass Spectrometer	(68-014A-18)	Sharp	39
OGO 6, Microphone Atmospheric Density Gauge	(69-051A-01)	Sharp	49
D'Arcy, Jr., R.G. - Lawrence Livermore Lab OGO 5, Electron and Proton Spectrometer	(68-014A-06)	West	41
Davis, L.R. - NASA-GSFC OGO 1, Trapped Radiation Scintillation Counter	(64-054A-16)	Konradi	4
OGO 3, Low-Energy Proton Experiment	(66-049A-07)	Evans	18
OGO 3, Trapped Radiation Scintillation Counter	(66-049A-10)	Konradi	20
Donahue, T.M. - U of Pittsburgh OGO 6, Sodium Airglow Photometer	(69-051A-26)	Donahue	44
Donley, J.L. - NASA-GSFC OGO 2, Positive Ion Study	(65-081A-19)	Donley	10
OGO 4, Positive Ion Study	(67-073A-19)	Chandra	25
Elliott, D.D. - Aerospace Corp OGO 6, Celestial Lyman-Alpha Measurement	(69-051A-12)	Clark	44
Evans, D.S. - NASA-GSFC OGO 3, Low-Energy Proton Experiment	(66-049A-07)	Evans	18
OGO 4, Low-Energy Auroral Particle Detector	(67-073A-11)	Hoffman	27
OGO 6, Auroral Particle Measurement	(69-051A-15)	Evans	45
Fan, C.Y. - U of Chicago OGO 1, Cosmic-Ray Spectra and Fluxes	(64-054A-18)	Simpson	5
OGO 2, Low-Energy Proton, Alpha Particle Measurement	(65-081A-07)	Simpson	14
OGO 3, Cosmic-Ray Spectra and Fluxes	(66-049A-03)	Simpson	21
Fan, C.Y. - U of Arizona OGO 4, Low-Energy Proton, Alpha Particle Measurement	(67-073A-08)	Simpson	29
OGO 5, Cosmic-Ray Electrons	(68-014A-09)	Meyer	37
Farley, T.A. - U of California, LA OGO 5, Hydromagnetic Waves and Trapped Particles	(68-014A-13)	Coleman	34
OGO 5, Triaxial Fluxgate Magnetometer	(68-014A-14)	Coleman	34
OGO 6, Trapped and Precipitating Electrons UCLA	(69-051A-16)	Farley	45
Flowerday, T.W. - U of Texas, Dallas OGO 6, Planar Ion and Electron Trap	(69-051A-03)	Hanson	45
OGO 6, Ion Mass Spectrometer, UTD	(69-051A-06)	Hanson	46

NOV. 10, 1975

INDEX OF PRINCIPAL AND CO-INVESTIGATORS AND EXPERIMENTS

NAME, EXPERIMENT NAME	NSSDC ID	PI'S LAST NAME	PAGE
Frank, L.A. - U of Iowa			
OGO 1, Trapped Radiation and High-Energy Protons	(64-054A-19)	Van Allen	6
OGO 2, Corpuscular Radiation Experiment	(65-081A-18)	Van Allen	15
OGO 3, Low-Energy Electrons and Protons	(66-049A-08)	Frank	18
OGO 4, Low-Energy Proton and Electron Differential Energy Analyzer (LEPEDEA)	(67-073A-10)	Van Allen	30
OGO 5, Low-Energy Proton and Electron Differential Energy Analyzer (LEPEDEA)	(68-014A-07)	Frank	35
Fredericks, R.W. - TRW Systems Group			
OGO 5, Plasma Wave Detector	(68-014A-24)	Crook	35
Friedman, H.D. - Naval Research Lab			
OGO 2, Solar X-Ray Emissions	(65-081A-16)	Kreplin	12
OGO 4, Solar X-Ray Emissions	(67-073A-21)	Kreplin	27
OGO 5, Solar X-Ray Emissions	(68-014A-23)	Kreplin	37
OGO 6, Solar X-Ray Emissions	(69-051A-08)	Kreplin	46
Fritz, R.B. - ESSA-Boulder			
OGO 1, Radio Propagation	(64-054A-05)	Hargreaves	3
OGO 3, Radio Propagation	(66-049A-16)	Fritz	18
Fritz, T.A. - U of Iowa			
OGO 5, Low-Energy Proton and Electron Differential Energy Analyzer (LEPEDEA)	(68-014A-07)	Frank	35
Garriott, O.K. - Stanford U			
OGO 1, Radio Propagation	(64-054A-05)	Hargreaves	3
OGO 3, Radio Propagation	(66-049A-16)	Fritz	18
Green, I.M. - TRW Systems Group			
OGO 5, Plasma Wave Detector	(68-014A-24)	Crook	35
Haddock, F.T. - U of Michigan			
OGO 1, Radio Astronomy	(64-054A-09)	Haddock	3
OGO 2, Radio Astronomy	(65-081A-01)	Haddock	11
OGO 2, Electron Density Measurements	(65-081A-21)	Haddock	11
OGO 3, Radio Astronomy	(66-049A-18)	Haddock	19
OGO 4, Radio Astronomy	(67-073A-01)	Haddock	26
OGO 5, Radio Astronomy	(68-014A-20)	Haddock	36
Hagge, D.E. - NASA-GSFC			
OGO 5, Galactic and Solar Cosmic-Ray Studies	(68-014A-10)	McDonald	37
Hallam, K.L. - NASA-GSFC			
OGO 1, Gegenschein Photometry	(64-054A-11)	Wolff	8
OGO 3, Gegenschein Photometry	(66-049A-20)	Wolff	23
Hanson, W.B. - U of Texas, Dallas			
OGO 6, Planar Ion and Electron Trap	(69-051A-03)	Hanson	45
OGO 6, Ion Mass Spectrometer, UTD	(69-051A-06)	Hanson	46
Hargreaves, J.K. - ESSA-Boulder			
OGO 1, Radio Propagation	(64-054A-05)	Hargreaves	3
Hargreaves, J.K. - U of Lancaster			
OGO 3, Radio Propagation	(66-049A-16)	Fritz	18
Harpold, D.N. - NASA-GSFC			
OGO 6, Neutral Atmospheric Composition	(69-051A-04)	Reber	48

INDEX OF PRINCIPAL AND CO-INVESTIGATORS AND EXPERIMENTS

NAME, EXPERIMENT NAME	NSSDC ID	PI'S LAST NAME	PAGE
Harris, K.K. - Lockheed OGO 5, Light-Ion Magnetic Mass Spectrometer	(68-014A-18)	Sharp	39
Helliwell, R.A. - Stanford U			
OGO 1, VLF Noise and Propagation	(64-054A-08)	Helliwell	3
OGO 2, VLF Noise and Propagation	(65-081A-02)	Helliwell	11
OGO 3, VLF Noise and Propagation	(66-049A-17)	Helliwell	19
OGO 4, VLF Noise and Propagation	(67-073A-02)	Helliwell	26
OGO 6, VLF Noise and Propagation	(69-051A-24)	Helliwell	46
Heppner, J.P. - NASA-GSFC			
OGO 1, Magnetic Survey Using Two Magnetometers	(64-054A-02)	Heppner	4
OGO 3, Magnetic Survey Using Two Magnetometers	(66-049A-11)	Heppner	19
OGO 5, Magnetic Survey Using Two Magnetometers	(68-014A-15)	Heppner	36
OGO 5, Electric Field Measurement	(68-014A-26)	Aggson	32
OGO 6, DC Electric Field Measurements	(69-051A-23)	Aggson	42
Hinteregger, H.E. - AFRL			
OGO 2, Solar UV Emissions	(65-081A-17)	Hinteregger	12
OGO 4, Solar UV Emissions	(67-073A-20)	Hinteregger	26
OGO 6, Solar UV Emissions	(69-051A-09)	Bedo	42
Hoffman, R.A. - NASA-GSFC			
OGO 1, Trapped Radiation Scintillation Counter	(64-054A-16)	Konradi	4
OGO 2, Scintillation Detector	(65-081A-09)	Hoffman	12
OGO 3, Trapped Radiation Scintillation Counter	(66-049A-10)	Konradi	20
OGO 4, Low-Energy Auroral Particle Detector	(67-073A-11)	Hoffman	27
Holzer, R.E. - U of California, LA			
OGO 1, Triaxial Search-Coil Magnetometer	(64-054A-01)	Smith	6
OGO 2, Triaxial Search-Coil Magnetometer	(65-081A-04)	Smith	14
OGO 3, Triaxial Search-Coil Magnetometer	(66-049A-12)	Smith	21
OGO 4, Triaxial Search-Coil Magnetometer	(67-073A-05)	Smith	30
OGO 5, Triaxial Search-Coil Magnetometer	(68-014A-16)	Smith	39
OGO 6, Triaxial Search-Coil Magnetometer	(69-051A-22)	Smith	49
Hones, E.W. - IDA			
OGO 1, Positron Search and Gamma-Ray Spectrum	(64-054A-15)	Cline	2
Hones, E.W. - LASL			
OGO 3, Positron Search and Gamma-Ray Spectrum	(66-049A-04)	Cline	17
Hutchinson, G.W. - Southampton U			
OGO 5, Energetic Photons in Primary Cosmic Rays	(68-014A-08)	Hutchinson	36
Jones, L.M. - U of Michigan			
OGO 2, Neutral Particle and Ion Composition	(65-081A-13)	Jones	12
OGO 4, Neutral Particle and Ion Composition	(67-073A-15)	Jones	27
Judge, D.L. - USC			
OGO 5, Hydromagnetic Waves and Trapped Particles	(68-014A-13)	Coleman	34
OGO 5, Triaxial Fluxgate Magnetometer	(68-014A-14)	Coleman	34
Kane, S.R. - U of Minnesota			
OGO 1, Ionization Chamber	(64-054A-20)	Winckler	7
OGO 3, Ionization Chamber	(66-049A-23)	Winckler	22
Kane, S.R. - U of California, Berkeley			
OGO 5, Energetic Radiations from Solar Flares	(68-014A-04)	Anderson	32
Konradi, A. - NASA-GSFC			
OGO 1, Trapped Radiation Scintillation Counter	(64-054A-16)	Konradi	4
OGO 3, Trapped Radiation Scintillation Counter	(66-049A-10)	Konradi	20

INDEX OF PRINCIPAL AND CO-INVESTIGATORS AND EXPERIMENTS

NAME, EXPERIMENT NAME	NSSDC ID	PI'S LAST NAME	PAGE
Kreplin, R.W. - Naval Research Lab			
OGO 2, Solar X-Ray Emissions	(65-081A-16)	Kreplin	12
OGO 4, Solar X-Ray Emissions	(67-073A-21)	Kreplin	27
OGO 5, Solar X-Ray Emissions	(68-014A-23)	Kreplin	37
OGO 6, Solar X-Ray Emissions	(69-051A-08)	Kreplin	46
Krimigis, S.M. - U of Iowa			
OGO 2, Corpuscular Radiation Experiment	(65-081A-18)	Van Allen	15
OGO 5, Low-Energy Proton and Electron Differential Energy Analyzer (LEPEDEA)	(68-014A-07)	Frank	35
L'Heureux, J.J. - U of Arizona			
OGO 5, Cosmic-Ray Electrons	(68-014A-09)	Meyer	37
Laaspere, T. - Dartmouth College			
OGO 6, Whistler and Audio-Frequency Electromagnetic Waves	(69-051A-25)	Laaspere	47
Langel, R.A. - NASA-GSFC			
OGO 2, Magnetic Survey, Rubidium Vapor Magnetometer	(65-081A-05)	Cain	10
OGO 4, Magnetic Survey, Rubidium Vapor Magnetometer	(67-073A-06)	Cain	25
OGO 6, Magnetic Survey, Rubidium Vapor Magnetometer	(69-051A-21)	Cain	44
Lawrence, R.S. - ESSA-Boulder			
OGO 1, Radio Propagation	(64-054A-05)	Hargreaves	3
OGO 3, Radio Propagation	(66-049A-16)	Fritz	18
Lawrence, Jr., J.L. - NASA-JPL			
OGO 5, Plasma Spectrometer	(68-014A-17)	Snyder	40
Lazarus, A.J. - MIT			
OGO 1, Plasma Probe, Faraday Cup	(64-054A-14)	Bridge	2
OGO 3, Plasma Probe, Faraday Cup	(66-049A-06)	Bridge	17
Ledley, B.G. - NASA-GSFC			
OGO 1, Magnetic Survey Using Two Magnetometers	(64-054A-02)	Heppler	4
OGO 3, Magnetic Survey Using Two Magnetometers	(66-049A-11)	Heppler	19
OGO 5, Magnetic Survey Using Two Magnetometers	(68-014A-15)	Heppler	36
Leite, R.J. - U of Michigan			
OGO 2, Neutral Particle and Ion Composition	(65-081A-13)	Jones	12
OGO 4, Neutral Particle and Ion Composition	(67-073A-15)	Jones	27
Lind, M.N. - Netherlands Institute			
OGO 5, Measurement of the Absolute Flux and Energy Spectrum of Electrons	(68-014A-12)	Van De Hulst	41
Lockwood, J.A. - U of New Hampshire			
OGO 6, Neutron Monitor	(69-051A-18)	Lockwood	47
Ludwig, G.H. - NASA-GSFC			
OGO 1, Cosmic-Ray Isotopic Abundance	(64-054A-17)	McDonald	5
OGO 3, Cosmic-Ray Isotopic Abundance	(66-049A-02)	McDonald	20
OGO 5, Galactic and Solar Cosmic-Ray Studies	(68-014A-10)	McDonald	37
Mackey, E.F. - Packard-Bell			
OGO 2, UV Spectrometer, 1100-3400 A	(65-081A-12)	Barth	10
OGO 4, UV Spectrometer, 1100-3400 A	(67-073A-14)	Barth	25
OGO 5, UV Photometer	(68-014A-21)	Thomas	40
OGO 6, UV Photometer	(69-051A-13)	Barth	43

INDEX OF PRINCIPAL AND CO-INVESTIGATORS AND EXPERIMENTS

NAME, EXPERIMENT NAME	NSSDC ID	PI'S LAST NAME	PAGE
Maier, E.J. - NASA-GSFC OGO 5, Thermal Ions and Electrons	(68-014A-03)	Serbu	38
Mange, P.W. - Naval Research Lab OGO 1, Geocoronal Lyman-Alpha Scattering	(64-054A-10)	Mange	5
OGO 2, Lyman-Alpha and UV Airglow Study	(65-081A-11)	Mange	13
OGO 3, Geocoronal Lyman-Alpha Scattering	(66-049A-19)	Mange	20
OGO 4, Lyman-Alpha and UV Airglow Study	(67-073A-13)	Mange	28
Mann, L. - Lawrence Livermore Lab OGO 5, Electron and Proton Spectrometer	(68-014A-06)	West	41
Mark, H. - U of California OGO 5, Energetic Radiations from Solar Flares	(68-014A-04)	Anderson	32
Masley, A.J. - McDonnell-Douglas OGO 6, Low-Energy Solar Cosmic-Ray Measurement	(69-051A-19)	Masley	47
Maynard, N.C. - NASA-GSFC OGO 5, Electric Field Measurement	(68-014A-26)	Aggson	32
OGO 6, DC Electric Field Measurement	(69-051A-23)	Aggson	42
McDonald, F.B. - NASA-GSFC OGO 1, Cosmic-Ray Isotopic Abundance	(64-054A-17)	McDonald	5
OGO 3, Cosmic-Ray Isotopic Abundance	(66-049A-02)	McDonald	20
OGO 5, Galactic and Solar Cosmic-Ray Studies	(68-014A-10)	McDonald	37
McKeown, D. - General Dynamics OGO 6, Energy Transfer Probe for Atmospheric Density	(69-051A-07)	McKeown	47
Meier, R.R. - Naval Research Lab OGO 4, Lyman-Alpha and UV Airglow Study	(67-073A-13)	Mange	28
Metzger, P.H. - Aerospace Corp OGO 6, Celestial Lyman-Alpha Measurement	(69-051A-12)	Clark	44
Meyer, P. - U of Chicago OGO 3, Cosmic-Ray Spectra and Fluxes	(66-049A-03)	Simpson	21
OGO 5, Cosmic-Ray Electrons	(68-014A-09)	Meyer	37
Morgan, M.G. - Dartmouth College OGO 2, Whistler and Audio-Frequency Electromagnetic Waves	(65-081A-03)	Morgan	13
OGO 4, Whistler and Audio-Frequency Electromagnetic Waves	(67-073A-03)	Morgan	28
OGO 6, Whistler and Audio-Frequency Electromagnetic Waves	(69-051A-25)	Laaspere	47
Nagy, A.F. - U of Michigan OGO 6, Electron Temperature and Density	(69-051A-02)	Nagy	48
Neher, V.H. - Cal Tech OGO 2, Cosmic-Ray Ionization	(65-081A-06)	Anderson	9
OGO 4, Cosmic-Ray Ionization	(67-073A-07)	Anderson	24
Neugebauer, M.M. - NASA-JPL OGO 5, Plasma Spectrometer	(68-014A-17)	Snyder	40
Newton, G.P. - NASA-GSFC OGO 2, Neutral Particle Study	(65-081A-20)	Newton	13
OGO 4, Neutral Particle Study	(67-073A-17)	Newton	28

INDEX OF PRINCIPAL AND CO-INVESTIGATORS AND EXPERIMENTS

NAME. EXPERIMENT NAME	NSSDC ID	PI'S LAST NAME	PAGE
Nilsson, C.S. - SAO			
OGO 2, Interplanetary Dust Particles	(65-081A-14)	Nilsson	13
OGO 4, Interplanetary Dust Particles	(67-073A-18)	Nilsson	29
Norman, K. - U College, London			
OGO 5, Electron Temperature and Density	(68-014A-01)	Boyd	33
Ogilvie, K.W. - NASA-GSFC			
OGO 5, Triaxial Electron Analyzer	(68-014A-11)	Ogilvie	38
Pearce, J.B. - U of Colorado			
OGO 5, UV Photometer	(68-014A-21)	Thomas	40
OGO 6, UV Photometer	(69-051A-13)	Barth	43
Pfitzer, K.A. - U of Minnesota			
OGO 1, Electron Spectrometer	(64-054A-21)	Winckler	7
OGO 3, Electron Spectrometer	(66-049A-22)	Winckler	22
Pickett, R.A. - NASA-GSFC			
OGO 6, Ion Mass Spectrometer GSFC	(69-051A-05)	Taylor	50
Pitt, G.H. - U of California, Berkeley			
OGO 1, Solar Cosmic Rays	(64-054A-12)	Anderson	1
OGO 3, Solar Cosmic Rays	(66-049A-01)	Anderson	16
Poppa, H.R. - Gen Dynamics			
OGO 6, Energy Transfer Probe for Atmospheric Density	(69-051A-07)	McKeown	47
Potter, W. - U of Michigan			
OGO 4, Radio Astronomy	(67-073A-01)	Haddock	26
Ramsden, D. - Southampton U			
OGO 5, Energetic Photons in Primary Cosmic Rays	(68-014A-08)	Hutchinson	36
Reber, C.A. - NASA-GSFC			
OGO 6, Neutral Atmospheric Composition	(69-051A-04)	Reber	48
Reed, E.I. - NASA-GSFC			
OGO 2, Airglow and Auroral Study	(65-081A-10)	Reed	14
OGO 4, Airglow and Auroral Study	(67-073A-12)	Reed	29
Regener, V.H. - U of New Mexico			
OGO 6, Solar UV Survey, 1850 - 3500 A	(69-051A-10)	Regener	49
Rorden, L.H. - Stanford U			
OGO 1, VLF Noise and Propagation	(64-054A-08)	Helliwell	3
OGO 2, VLF Noise and Propagation	(65-081A-02)	Helliwell	11
OGO 3, VLF Noise and Propagation	(66-049A-17)	Helliwell	19
OGO 4, VLF Noise and Propagation	(67-073A-02)	Helliwell	26
OGO 6, VLF Noise and Propagation	(69-051A-24)	Helliwell	46
Rossi, B. - MIT			
OGO 1, Plasma Probe, Faraday Cup	(64-054A-14)	Bridge	2
OGO 3, Plasma Probe, Faraday Cup	(66-049A-06)	Bridge	17
Russell, C.T. - U of California, LA			
OGO 5, Triaxial Fluxgate Magnetometer	(68-014A-14)	Coleman	34

INDEX OF PRINCIPAL AND CO-INVESTIGATORS AND EXPERIMENTS

NAME, EXPERIMENT NAME	NSSDC ID	PI'S LAST NAME	PAGE
Sagalyn, R.C. - AFCRL			
OGO 1, Spherical Ion and Electron Trap	(64-054A-03)	Sagalyn	5
OGO 3, Spherical Ion and Electron Trap	(66-049A-13)	Sagalyn	20
OGO 5, Thermal and Epithermal Plasma	(68-014A-02)	Sagalyn	38
Satterblom, P.R. - McDonnell-Douglas			
OGO 6, Low-Energy Solar Cosmic-Ray Measurement	(69-051A-19)	Masley	47
Scarf, F.L. - TRW Systems Group			
OGO 5, Plasma Wave Detector	(68-014A-24)	Crook	35
Scherb, F. - MIT			
OGO 1, Plasma Probe, Faraday Cup	(64-054A-14)	Bridge	2
OGO 3, Plasma Probe, Faraday Cup	(66-049A-06)	Bridge	17
Serbu, G.P. - NASA-GSFC			
OGO 5, Thermal Ions and Electrons	(68-014A-03)	Serbu	38
Sharp, G.W. -- Lockheed			
OGO 5, Light-Ion Magnetic Mass Spectrometer	(68-014A-18)	Sharp	39
OGO 6, Microphone Atmospheric Density Gauge	(69-051A-01)	Sharp	49
Simpson, J.A. - U of Chicago			
OGO 1, Cosmic-Ray Spectra and Fluxes	(64-054A-18)	Simpson	5
OGO 2, Low-Energy Proton, Alpha Particle Measurement	(65-081A-07)	Simpson	14
OGO 3, Cosmic-Ray Spectra and Fluxes	(66-049A-03)	Simpson	21
OGO 4, Low-Energy Proton, Alpha Particle Measurement	(67-073A-08)	Simpson	29
OGO 5, Low-Energy Heavy Cosmic-Ray Particles (High-Z, Low-E)	(68-014A-27)	Simpson	39
Skillman, T.L. - NASA-GSFC			
OGO 1, Magnetic Survey Using Two Magnetometers	(64-054A-02)	Heppner	4
OGO 3, Magnetic Survey Using Two Magnetometers	(66-049A-11)	Heppner	19
OGO 5, Magnetic Survey Using Two Magnetometers	(68-014A-15)	Heppner	36
Smiddy, M. - AFCRL			
OGO 1, Spherical Ion and Electron Trap	(64-054A-03)	Sagalyn	5
OGO 3, Spherical Ion and Electron Trap	(66-049A-13)	Sagalyn	20
OGO 5, Thermal and Epithermal Plasma	(68-014A-02)	Sagalyn	38
Smith, E.J. - NASA-JPL			
OGO 1, Triaxial Search-Coil Magnetometer	(64-054A-01)	Smith	6
OGO 2, Triaxial Search-Coil Magnetometer	(65-081A-04)	Smith	14
OGO 3, Triaxial Search-Coil Magnetometer	(66-049A-12)	Smith	21
OGO 4, Triaxial Search-Coil Magnetometer	(67-073A-05)	Smith	30
OGO 5, Triaxial Search-Coil Magnetometer	(68-014A-16)	Smith	39
OGO 6, Triaxial Search-Coil Magnetometer	(69-051A-22)	Smith	49
Snyder, C.W. - NASA-JPL			
OGO 5, Plasma Spectrometer	(68-014A-17)	Snyder	40
Spencer, N.W. - NASA-GSFC			
OGO 1, Positive Ion Composition	(64-054A-06)	Taylor	6
OGO 2, Positive Ion Composition	(65-081A-15)	Taylor	15
OGO 3, Positive Ion Composition	(66-049A-15)	Taylor	21
OGO 4, Positive Ion Composition	(67-073A-16)	Taylor	30
Stillwell, D.E. - NASA-GSFC			
OGO 6, Auroral Particle Measurement	(69-051A-15)	Evans	45

INDEX OF PRINCIPAL AND CO-INVESTIGATORS AND EXPERIMENTS

NAME, EXPERIMENT NAME	NSSDC ID	PI'S LAST NAME	PAGE
Stone, E.C. - U of Chicago			
OGO 2, Low-Energy Proton, Alpha Particle Measurement	(65-081A-07)	Simpson	14
OGO 4, Low-Energy Proton, Alpha Particle Measurement	(67-073A-08)	Simpson	29
Stone, E.C. - Cal Tech			
OGO 6, Cosmic-Ray Experiment	(69-051A-20)	Stone	50
Sugiura, M. - NASA-GSFC			
OGO 1, Magnetic Survey Using Two Magnetometers	(64-054A-02)	Heppner	4
OGO 3, Magnetic Survey Using Two Magnetometers	(66-049A-11)	Heppner	19
OGO 5, Magnetic Survey Using Two Magnetometers	(68-014A-15)	Heppner	36
Tausch, D.R. - U of Michigan			
OGO 6, Neutral Atmospheric Composition	(69-051A-04)	Reber	48
Tanka, D. - Netherlands Institute			
OGO 5, Measurement of the Absolute Flux and Energy Spectra of Electrons	(68-014A-12)	Van De Hulst	41
Taylor, Jr., H.A. - NASA-GSFC			
OGO 1, Positive Ion Composition	(64-054A-06)	Taylor	6
OGO 2, Positive Ion Composition	(65-081A-15)	Taylor	15
OGO 3, Positive Ion Composition	(66-049A-15)	Taylor	21
OGO 4, Positive Ion Composition	(67-073A-16)	Taylor	30
OGO 6, Ion Mass Spectrometer, GSFC	(69-051A-05)	Taylor	50
Thomas, G.E. - U of Colorado			
OGO 5, UV Photometer	(68-014A-21)	Thomas	40
Trainer, J.H. - NASA-GSFC			
OGO 6, Trapped and Precipitating Electrons, GSFC	(69-051A-17)	Williams	50
Troy, Jr., B.E. - NASA-GSFC			
OGO 1, Planar Ion and Electron Trap	(64-054A-04)	Whipple	7
OGO 3, Planar Ion and Electron Trap	(66-049A-14)	Whipple	22
Van Allen, J.A. - U of Iowa			
OGO 1, Trapped Radiation and High-Energy Protons	(64-054A-19)	Van Allen	6
OGO 2, Corpuscular Radiation Experiment	(65-081A-18)	Van Allen	15
OGO 3, Low-Energy Electrons and Protons	(66-049A-08)	Frank	18
OGO 4, Low-Energy Proton and Electron Differential Energy Analyzer (LEPEDEA)	(67-073A-10)	Van Allen	30
OGO 5, Low-Energy Proton and Electron Differential Energy Analyzer (LEPEDEA)	(68-014A-07)	Frank	35
Van De Hulst, H.C. - Netherlands Institute			
OGO 5, Measurement of the Absolute Flux and Energy Spectra of Electrons	(68-014A-12)	Van De Hulst	41
Vasyliunas, V.M. - MIT			
OGO 1, Plasma Probe, Faraday Cup	(64-054A-14)	Bridge	2
OGO 3, Plasma Probe, Faraday Cup	(66-049A-06)	Bridge	17
Vogt, R.E. - Cal Tech			
OGO 6, Cosmic-Ray Experiment	(69-051A-20)	Stone	50
Wallace, L.J. - Kitt Peak Natl Obs			
OGO 2, UV Spectrometer, 1100 - 3400 A	(65-081A-12)	Barth	10
OGO 4, UV Spectrometer, 1100 - 3400 A	(67-073A-14)	Barth	25

NOV. 10, 1975

INDEX OF PRINCIPAL AND CO-INVESTIGATORS AND EXPERIMENTS

NAME, EXPERIMENT NAME	NSSDC ID	PI'S LAST NAME	PAGE
Webber, W.R. - U of Minnesota			
OGO 2, Galactic and Solar Cosmic Ray	(65-081A-08)	Webber	15
OGO 4, Galactic and Solar Cosmic Ray	(67-073A-09)	Webber	31
Weil, H. - Naval Research Lab			
OGO 2, Electron Density Measurements	(65-081A-21)	Haddock	11
West, Jr., H.I. - Lawrence Livermore Lab			
OGO 5, Electron and Proton Spectrometer	(68-014A-06)	West	41
Whipple, E.C. - ESSA-Boulder			
OGO 1, Planar Ion and Electron Trap	(64-054A-04)	Whipple	7
OGO 3, Planar Ion and Electron Trap	(66-049A-14)	Whipple	22
Wilkerson, T.D. - U of Maryland			
OGO 5, Triaxial Electron Analyzer	(68-014A-11)	Ogilvie	38
Williams, D.J. - NASA-GSFC			
OGO 6, Trapped and Precipitating Electrons, GSFC	(69-051A-17)	Williams	50
Williamson, J.M. - NASA-GSFC			
OGO 1, Trapped Radiation Scintillation Counter	(64-054A-16)	Konradi	4
OGO 3, Trapped Radiation Scintillation Counter	(66-049A-10)	Konradi	20
Willmore, P.A. - U College, London			
OGO 5, Electron Temperature and Density	(68-014A-01)	Boyd	33
Wills, R.D. - Southampton U			
OGO 5, Energetic Photons in Primary Cosmic Rays	(68-014A-08)	Hutchinson	36
Wilson, D. - SAO			
OGO 2, Interplanetary Dust Particles	(65-081A-14)	Nilsson	13
Winckler, J.R. - U of Minnesota			
OGO 1, Ionization Chamber	(64-054A-20)	Winckler	7
OGO 1, Electron Spectrometer	(64-054A-21)	Winckler	7
OGO 3, Electron Spectrometer	(66-049A-22)	Winckler	22
OGO 3, Ionization Chamber	(66-049A-23)	Winckler	22
Wolfe, J.H. - NASA-ARC			
OGO 1, Electrostatic Plasma Analysis (Protons 0.1 - 18 keV)	(64-054A-13)	Wolfe	8
OGO 3, Electrostatic Plasma Analysis (Protons 0.1 - 18 keV)	(66-049A-05)	Wolfe	23
Wolff, C.L. - NASA-GSFC			
OGO 1, Gegenschein Photometry	(64-054A-11)	Wolff	8
OGO 3, Gegenschein Photometry	(66-049A-20)	Wolff	23
Wyatt, S.P. - U of Illinois			
OGO 1, Gegenschein Photometry	(64-054A-11)	Wolff	8
OGO 3, Gegenschein Photometry	(66-049A-20)	Wolff	23
York, R.G. - Naval Research Lab			
OGO 2, Electron Density Measurements	(65-081A-21)	Haddock	11

B. INDEX OF ORIGINAL INSTITUTIONS OF PRINCIPAL INVESTIGATORS AND EXPERIMENTS

NAME, EXPERIMENT NAME	NSSDC ID	PI'S LAST NAME	PAGE
Aerospace Corp			
OGO 6, Celestial Lyman-Alpha Measurement	(69-051A-12)	Clark	44
AFCRL			
OGO 1, Spherical Ion and Electron Trap	(64-054A-03)	Sagalyn	5
OGO 2, Solar UV Emissions	(65-081A-17)	Hinteregger	12
OGO 3, Spherical Ion and Electron Trap	(66-049A-13)	Sagalyn	20
OGO 4, Solar UV Emissions	(67-073A-20)	Hinteregger	26
OGO 5, Thermal and Epithermal Plasma	(68-014A-02)	Sagalyn	38
OGO 6, Solar UV Emissions, 160 - 1600 A	(69-051A-09)	Bedo	43
Cal Tech			
OGO 6, Cosmic-Ray Experiment	(69-051A-20)	Stone	50
CNES			
OGO 5, Geocoronal Lyman-Alpha Measurements	(68-014A-22)	Blamont	33
OGO 6, Airglow and Auroral Emissions	(69-051A-11)	Blamont	43
OGO 6, Line Shape of the 6300-A Airglow Emission	(69-051A-14)	Blamont	43
Dartmouth College			
OGO 2, Whistler and Audio-Frequency Electromagnetic Waves	(65-081A-03)	Morgan	13
OGO 4, Whistler and Audio-Frequency Electromagnetic Waves	(67-073A-03)	Morgan	28
OGO 6, Whistler and Audio-Frequency Electromagnetic Waves	(69-051A-25)	Laaspere	47
ESSA			
OGO 1, Radio Propagation	(64-054A-05)	Hargreaves	3
OGO 3, Radio Propagation	(66-049A-16)	Fritz	18
Gen Dynamics			
OGO 6, Energy Transfer Probe for Atmospheric Density	(69-051A-07)	McKeown	47
Lawrence Livermore Lab			
OGO 5, Electron and Proton Spectrometer	(68-014A-06)	West	41
Lockheed			
OGO 5, Light-Ion Magnetic Mass Spectrometer	(68-014A-18)	Sharp	39
OGO 6, Microphone Atmospheric Density Gauge	(69-051A-01)	Sharp	49
McDonnell-Douglas			
OGO 6, Low-Energy Solar Cosmic-Ray Measurement	(69-051A-19)	Masley	47
MIT			
OGO 1, Plasma Probe, Faraday Cup	(64-054A-14)	Bridge	2
OGO 3, Plasma Probe, Faraday Cup	(66-049A-06)	Bridge	17
NASA-ARC			
OGO 1, Electrostatic Plasma Analysis (Protons 0.1 - 18 keV)	(64-054A-13)	Wolfe	8

NOV. 10, 1975

INDEX OF ORIGINAL INSTITUTIONS OF PRINCIPAL INVESTIGATORS AND EXPERIMENTS

INSTITUTIONS, EXPERIMENT NAME	NSSDC ID	PI'S LAST NAME	PAGE
NASA-ARC (CONT)			
OGO 3, Electrostatic Plasma Analysis (Protons 0.1 - 18 keV)	(66-049A-05)	Wolfe	22
NASA-GSFC			
OGO 1, Magnetic Survey Using Two Magnetometers	(64-054A-02)	Heppner	4
OGO 1, Planar Ion and Electron Trap	(64-054A-04)	Whipple	7
OGO 1, Positive Ion Composition	(64-054A-06)	Taylor	6
OGO 1, Gegenschein Photometry	(64-054A-11)	Wolff	8
OGO 1, Positron Search and Gamma-Ray spectrum	(64-054A-15)	Cline	2
OGO 1, Trapped Radiation Scintillation Counter	(64-054A-16)	Konradi	4
OGO 1, Cosmic-Ray Isotopic Abundance	(64-054A-17)	McDonald	5
OGO 2, Magnetic Survey, Rubidium Vapor Magnetometer	(65-081A-05)	Cain	10
OGO 2, Scintillation Detector	(65-081A-09)	Hoffman	12
OGO 2, Airglow and Auroral Study	(65-081A-10)	Reed	14
OGO 2, Positive Ion Composition	(65-081A-15)	Taylor	15
OGO 2, Positive Ion Study	(65-081A-19)	Donley	10
OGO 2, Neutral Particle Study	(65-081A-20)	Newton	13
OGO 3, Cosmic-Ray Isotopic Abundance	(66-049A-02)	McDonald	20
OGO 3, Positron Search and Gamma-Ray Spectrum	(66-049A-04)	Cline	17
OGO 3, Low-Energy Proton Experiment	(66-049A-07)	Evans	18
OGO 3, Trapped Radiation Scintillation Counter	(66-049A-10)	Konradi	20
OGO 3, Magnetic Survey Using Two Magnetometers	(66-049A-11)	Heppner	19
OGO 3, Planar Ion and Electron Trap	(66-049A-14)	Whipple	22
OGO 3, Positive Ion Composition	(66-049A-15)	Taylor	21
OGO 3, Gegenschein Photometry	(66-049A-20)	Wolff	23
OGO 4, Magnetic Survey, Rubidium Vapor Magnetometer	(67-073A-06)	Cain	25
OGO 4, Low-Energy Auroral Particle Detector	(67-073A-11)	Hoffman	27
OGO 4, Airglow and Auroral Study	(67-073A-12)	Reed	29
OGO 4, Positive Ion Composition	(67-073A-16)	Taylor	30
OGO 4, Neutral Particle Study	(67-073A-17)	Newton	28
OGO 4, Positive Ion Study	(67-073A-19)	Chandra	25
OGO 5, Thermal Ions and Electrons	(68-014A-03)	Serbu	38
OGO 5, Interplanetary Electrons, Positrons, and Protons	(68-014A-05)	Cline	34
OGO 5, Galactic and Solar Cosmic-Ray Studies	(68-014A-10)	McDonald	37
OGO 5, Triaxial Electron Analyzer	(68-014A-11)	Ogilvie	38
OGO 5, Magnetic Survey Using Two Magnetometers	(68-014A-15)	Heppner	36
OGO 5, Electric Field Measurement	(68-014A-26)	Aggson	32
OGO 6, Neutral Atmospheric Composition	(69-051A-04)	Reber	48
OGO 6, Ion Mass Spectrometer, GSFC	(69-051A-05)	Taylor	50
OGO 6, Auroral Particle Measurement	(69-051A-15)	Evans	45
OGO 6, Trapped and Precipitating Electrons, GSFC	(69-051A-17)	Williams	50
OGO 6, Magnetic Survey, Rubidium Vapor Magnetometer	(69-051A-21)	Cain	44
OGO 6, DC Electric Field Measurements	(69-051A-23)	Aggson	42
NASA-JPL			
OGO 1, Triaxial Search-Coil Magnetometer	(64-054A-01)	Smith	6
OGO 2, Triaxial Search-Coil Magnetometer	(65-081A-04)	Smith	14
OGO 3, Triaxial Search-Coil Magnetometer	(66-049A-12)	Smith	21
OGO 4, Triaxial Search-Coil Magnetometer	(67-073A-05)	Smith	30
OGO 5, Triaxial Search-Coil Magnetometer	(68-014A-16)	Smith	39
OGO 5, Plasma Spectrometer	(68-014A-17)	Snyder	40
OGO 6, Triaxial Search-Coil Magnetometer	(69-051A-22)	Smith	49
Naval Research Lab			
OGO 1, Geocoronal Lyman-Alpha Scattering	(64-054A-10)	Mange	5
OGO 2, Lyman-Alpha and UV Airglow Study	(65-081A-11)	Mange	13
OGO 2, Solar X-Ray Emissions	(65-081A-16)	Kreplin	12
OGO 3, Geocoronal Lyman-Alpha Scattering	(66-049A-19)	Mange	20
OGO 4, Lyman-Alpha and UV Airglow Study	(67-073A-13)	Mange	28
OGO 4, Solar X-Ray Emissions	(67-073A-21)	Kreplin	27
OGO 5, Solar X-Ray Emissions	(68-014A-23)	Kreplin	37
OGO 6, Solar X-Ray Emissions	(69-051A-08)	Kreplin	46
Netherlands Institute			
OGO 5, Measurement of the Absolute Flux and Energy Spectra of Electrons	(68-014A-12)	Van De Hulst	41

INDEX OF ORIGINAL INSTITUTIONS OF PRINCIPAL INVESTIGATORS AND EXPERIMENTS

INSTITUTIONS, EXPERIMENT NAME	NSSDC ID	PI'S LAST NAME	PAGE
Rice U			
OGO 2, Cosmic-Ray Ionization	(65-081A-06)	Anderson	9
OGO 4, Cosmic-Ray Ionization	(67-073A-07)	Anderson	24
SAO			
OGO 2, Interplanetary Dust Particles	(65-081A-14)	Nilsson	13
OGO 4, Interplanetary Dust Particles	(67-073A-18)	Nilsson	29
Stanford U			
OGO 1, VLF Noise and Propagation	(64-054A-08)	Helliwell	3
OGO 2, VLF Noise and Propagation	(65-081A-02)	Helliwell	11
OGO 3, VLF Noise and Propagation	(66-049A-17)	Helliwell	19
OGO 4, VLF Noise and Propagation	(67-073A-02)	Helliwell	26
OGO 6, VLF Noise and Propagation	(69-051A-24)	Helliwell	46
Temple U			
OGO 1, Interplanetary Dust Particles	(64-054A-07)	Bohn	2
OGO 3, Interplanetary Dust Particles	(66-049A-21)	Bohn	17
TRW Systems Group			
OGO 5, Plasma Wave Detector	(68-014A-24)	Crook	35
U College, London			
OGO 5, Electron Temperature and Density	(68-014A-01)	Boyd	33
U of California, Berkeley			
OGO 1, Solar Cosmic Rays	(64-054A-12)	Anderson	1
OGO 3, Solar Cosmic Rays	(66-049A-01)	Anderson	16
OGO 5, Energetic Radiations from Solar Flares	(68-014A-04)	Anderson	32
U of California, LA			
OGO 5, Hydromagnetic Waves and Trapped Particles	(68-014A-13)	Coleman	34
OGO 5, Triaxial Fluxgate Magnetometer	(68-014A-14)	Coleman	34
OGO 6, Trapped and Precipitating Electrons UCLA	(69-051A-16)	Farley	45
U of Chicago			
OGO 1, Cosmic-Ray Spectra and Fluxes	(64-054A-18)	Simpson	5
OGO 2, Low-Energy Proton, Alpha Particle Measurement	(65-081A-07)	Simpson	14
OGO 3, Cosmic-Ray Spectra and Fluxes	(66-049A-03)	Simpson	21
OGO 4, Low-Energy Proton, Alpha Particle Measurement	(67-073A-08)	Simpson	29
OGO 5, Cosmic-Ray Electrons	(68-014A-09)	Meyer	37
OGO 5, Low-Energy Heavy Cosmic-Ray Particles(High-Z, Low-E)	(68-014A-27)	Simpson	39
U of Colorado			
OGO 2, UV Spectrometer, 1100 - 3400 A	(65-081A-12)	Barth	10
OGO 4, UV Spectrometer, 1100 - 3400 A	(67-073A-14)	Barth	25
OGO 5, UV Photometer	(68-014A-21)	Thomas	40
OGO 6, UV Photometer	(69-051A-13)	Barth	43
U of Iowa			
OGO 1, Trapped Radiation and High-Energy Protons	(64-054A-19)	Van Allen	6
OGO 2, Corpuscular Radiation Experiment	(65-081A-18)	Van Allen	15
OGO 3, Low-Energy Electrons and Protons	(66-049A-08)	Frank	18
OGO 4, Low-Energy Proton and Electron Differential Energy Analyzer (LEPEDEA)	(67-073A-10)	Van Allen	30
OGO 5, Low-Energy Proton and Electron Differential Energy Analyzer (LEPEDEA)	(68-014A-07)	Frank	35
U of Michigan			
OGO 1, Radio Astronomy	(64-054A-09)	Haddock	3
OGO 2, Radio Astronomy	(65-081A-01)	Haddock	11
OGO 2, Neutral Particle and Ion Composition	(65-081A-13)	Jones	12

INDEX OF ORIGINAL INSTITUTIONS OF PRINCIPAL INVESTIGATORS AND EXPERIMENTS

INSTITUTIONS, EXPERIMENT NAME	NSSDC ID	PI'S LAST NAME	PAGE
U of Michigan-<i>CONV</i>			
OGO 2, Electron Density Measurements	(65-081A-21)	Haddock	11
OGO 3, Radio Astronomy	(66-049A-18)	Haddock	19
OGO 4, Radio Astronomy	(67-073A-01)	Haddock	26
OGO 4, Neutral Particle and Ion Composition	(67-073A-15)	Jones	27
OGO 5, Radio Astronomy	(68-014A-20)	Haddock	36
OGO 6, Electron Temperature and Density	(69-051A-02)	Nagy	48
U of Minnesota			
OGO 1, Ionization Chamber	(64-054A-20)	Winckler	7
OGO 1, Electron Spectrometer	(64-054A-21)	Winckler	7
OGO 2, Galactic and Solar Cosmic Ray	(65-081A-08)	Webber	15
OGO 3, Electron Spectrometer	(66-049A-22)	Winckler	22
OGO 3, Ionization Chamber	(66-049A-23)	Winckler	22
OGO 4, Galactic and Solar Cosmic Ray	(67-073A-09)	Webber	31
U of New Hampshire			
OGO 6, Neutron Monitor	(69-051A-18)	Lockwood	47
U of New Mexico			
OGO 6, Solar UV Survey, 1850 - 3500 A	(69-051A-10)	Regener	49
U of Pittsburgh			
OGO 6, Sodium Airglow Photometer	(69-051A-26)	Donahue	44
U of Southampton			
OGO 5, Energetic Photons in Primary Cosmic Rays	(68-014A-08)	Hutchinson	36
U of Texas, Dallas			
OGO 6, Planar Ion and Electron Trap	(69-051A-03)	Hanson	45
OGO 6, Ion Mass Spectrometer, UTD	(69-051A-06)	Hanson	46

Nov. 10, 1975

C. INDEX OF SPACECRAFT AND EXPERIMENTS

OGO 1			
Solar Cosmic Rays	(64-054A)		
Interplanetary Dust Particles	(64-054A-12)	Anderson	1
Plasma Probe, Faraday Cup	(64-054A-07)	Bohn	2
Positron Search and Gamma-Ray Spectrum	(64-054A-14)	Bridge	2
Radio Astronomy	(64-054A-15)	Cline	2
Radio Propagation	(64-054A-09)	Haddock	3
VLF Noise and Propagation	(64-054A-05)	Hargreaves	3
Magnetic Survey Using Two Magnetometers	(64-054A-08)	Helliwell	3
Trapped Radiation Scintillation Counter	(64-054A-02)	Heppner	4
Geocoronal Lyman-Alpha Scattering	(64-054A-16)	Konradi	4
Cosmic-Ray Isotopic Abundance	(64-054A-10)	Mange	5
Spherical Ion and Electron Trap	(64-054A-17)	McDonald	5
Cosmic-Ray Spectra and Fluxes	(64-054A-03)	Sagalyn	5
Triaxial Search-Coil Magnetometer	(64-054A-18)	Simpson	5
Positive Ion Composition	(64-054A-01)	Smith	6
Trapped Radiation and High-Energy Protons	(64-054A-06)	Taylor	6
Planar Ion and Electron Trap	(64-054A-19)	Van Allen	6
Ionization Chamber	(64-054A-04)	Whipple	7
Electron Spectrometer	(64-054A-20)	Winckler	7
Electrostatic Plasma Analysis (Protons 0.1-18 keV)	(64-054A-21)	Winckler	7
Gegenschein Photometry	(64-054A-13)	Wolfe	8
	(64-054A-11)	Wolff	8
OGO 2			
Cosmic-Ray Ionization	(65-081A)		
UV Spectrometer, 1100 - 3400 A	(65-081A-06)	Anderson	9
Magnetic Survey, Rubidium Vapor Magnetometer	(65-081A-12)	Barth	10
Positive Ion Study	(65-081A-05)	Cain	10
Radio Astronomy	(65-081A-19)	Donley	10
Electron Density Measurements	(65-081A-01)	Haddock	11
VLF Noise and Propagation	(65-081A-21)	Haddock	11
Solar UV Emissions	(65-081A-02)	Helliwell	11
Scintillation Detector	(65-081A-17)	Hinteregger	12
Neutral Particle and Ion Composition	(65-081A-09)	Hoffman	12
Solar X-Ray Emissions	(65-081A-13)	Jones	12
Lyman-Alpha and UV Airglow Study	(65-081A-16)	Kreplin	12
Whistler and Audio-Frequency Electromagnetic Waves	(65-081A-11)	Mange	13
	(65-081A-03)	Morgan	13
Neutral Particle Study	(65-081A-20)	Newton	13
Interplanetary Dust Particles	(65-081A-14)	Nilsson	13
Airglow and Auroral Study	(65-081A-10)	Reed	14
Low-Energy Proton, Alpha Particle Measurement	(65-081A-07)	Simpson	14
Triaxial Search-Coil Magnetometer	(65-081A-04)	Smith	14
Positive Ion Composition	(65-081A-15)	Taylor	15
Corpuscular Radiation Experiment	(65-081A-18)	Van Allen	15
Galactic and Solar Cosmic Ray	(65-081A-08)	Webber	15
OGO 3			
Solar Cosmic Rays	(66-049A)		
Interplanetary Dust Particles	(66-049A-01)	Anderson	16
Plasma Probe, Faraday Cup	(66-049A-21)	Bohn	17
Positron Search and Gamma-Ray Spectrum	(66-049A-06)	Bridge	17
Low-Energy Proton Experiment	(66-049A-04)	Cline	17
Low-Energy Electrons and Protons	(66-049A-07)	Evans	18
Radio Propagation	(66-049A-08)	Frank	18
Radio Astronomy	(66-049A-16)	Fritz	18
VLF Noise and Propagation	(66-049A-18)	Haddock	19
Magnetic Survey Using Two Magnetometers	(66-049A-17)	Helliwell	19
Trapped Radiation Scintillation Counter	(66-049A-11)	Heppner	19
Geocoronal Lyman-Alpha Scattering	(66-049A-10)	Konradi	20
Cosmic-Ray Isotopic Abundance	(66-049A-19)	Mange	20
Spherical Ion and Electron Trap	(66-049A-02)	McDonald	20
Cosmic-Ray Spectra and Fluxes	(66-049A-13)	Sagalyn	20
Triaxial Search-Coil Magnetometer	(66-049A-03)	Simpson	21
	(66-049A-12)	Smith	21

INDEX OF SPACECRAFT AND EXPERIMENTS

NAME	NSSDC ID	PI'S LAST NAME	PAGE
OGO 3-(CONT)			
Positive Ion Composition	(66-049A-15)	Taylor	21
Planar Ion and Electron Trap	(66-049A-14)	Whipple	22
Electron Spectrometer	(66-049A-22)	Winckler	22
Ionization Chamber	(66-049A-23)	Winckler	22
Electrostatic Plasma Analysis (Protons 0.1-18 keV)	(66-049A-05)	Wolfe	23
Gegenschein Photometry	(66-049A-20)	Wolff	23
OGO 4			
Cosmic-Ray Ionization	(67-073A)		
UV Spectrometer, 1100 - 3400 A	(67-073A-07)	Anderson	24
Magnetic Survey, Rubidium Vapor Magnetometer	(67-073A-14)	Barth	25
Positive Ion Study	(67-073A-06)	Cain	25
Radio Astronomy	(67-073A-19)	Chandra	25
VLF Noise and Propagation	(67-073A-01)	Haddock	26
Solar UV Emissions	(67-073A-02)	Helliwell	26
Low-Energy Auroral Particle Detector	(67-073A-20)	Hinteregger	26
Neutral Particle and Ion Composition	(67-073A-11)	Hoffman	27
Solar X-Ray Emissions	(67-073A-15)	Jones	27
Lyman-Alpha and UV Airglow Study	(67-073A-21)	Kreplin	27
Whistler and Audio-Frequency Electromagnetic Waves	(67-073A-13)	Mange	28
Neutral Particle Study	(67-073A-03)	Morgan	28
Interplanetary Dust Particles	(67-073A-17)	Newton	28
Airglow and Auroral Study	(67-073A-18)	Nilsson	29
Low-Energy Proton, Alpha Particle Measurement	(67-073A-12)	Reed	29
Triaxial Search-Coil Magnetometer	(67-073A-08)	Simpson	29
Positive Ion Composition	(67-073A-05)	Smith	30
Low-Energy Proton and Electron Differential Energy Analyzer (LEPEDEA)	(67-073A-16)	Taylor	30
Galactic and Solar Cosmic Ray	(67-073A-10)	Van Allen	30
	(67-073A-09)	Webber	31
OGO 5			
Electric Field Measurement	(68-014A)		
Energetic Radiations from Solar Flares	(68-014A-26)	Aggson	32
Geocoronal Lyman-Alpha Measurements	(68-014A-04)	Anderson	32
Electron Temperature and Density	(68-014A-22)	Blamont	33
Interplanetary Electrons, Positrons, and Protons	(68-014A-01)	Boyd	33
Hydromagnetic Waves and Trapped Particles	(68-014A-05)	Cline	34
Triaxial Fluxgate Magnetometer	(68-014A-13)	Coleman	34
Plasma Wave Detector	(68-014A-14)	Coleman	34
Low-Energy Proton and Electron Differential Energy Analyzer (LEPEDEA)	(68-014A-24)	Crook	35
Radio Astronomy	(68-014A-07)	Frank	35
Magnetic Survey Using Two Magnetometers	(68-014A-20)	Haddock	36
Energetic Photons in Primary Cosmic Rays	(68-014A-15)	Heppner	36
Solar X-Ray Emissions	(68-014A-08)	Hutchinson	36
Galactic and Solar Cosmic-Ray Studies	(68-014A-23)	Kreplin	37
Cosmic-Ray Electrons	(68-014A-10)	McDonald	37
Triaxial Electron Analyzer	(68-014A-09)	Meyer	37
Thermal and Epithermal Plasma	(68-014A-11)	Ogilvie	38
Thermal Ions and Electrons	(68-014A-02)	Sagalyn	38
Light-Ion Magnetic Mass Spectrometer	(68-014A-03)	Serbu	38
Low-Energy Heavy Cosmic-Ray Particles (High-Z, Low-E)	(68-014A-18)	Sharp	39
Triaxial Search-Coil Magnetometer	(68-014A-27)	Simpson	39
Plasma Spectrometer	(68-014A-16)	Smith	39
UV Photometer	(68-014A-17)	Snyder	40
Measurement of the Absolute Flux and Energy Spectra of Electrons	(68-014A-21)	Thomas	40
Electron and Proton Spectrometer	(68-014A-12)	Van De Hulst	41
	(68-014A-06)	West	41
OGO 6			
DC Electric Field Measurements	(69-051A)		
UV Photometer	(69-051A-23)	Aggson	42
Solar UV Emissions, 160 - 1600 A	(69-051A-13)	Barth	43
Airglow and Auroral Emissions	(69-051A-09)	Bedo	43
Line Shape of the 6300-A Airglow Emission	(69-051A-11)	Blamont	43
Magnetic Survey, Rubidium Vapor Magnetometer	(69-051A-14)	Blamont	43
Celestial Lyman-Alpha Measurement	(69-051A-21)	Cain	44
Sodium Airglow Photometer	(69-051A-12)	Clark	44
Auroral Particle Measurement	(69-051A-26)	Donahue	44
Trapped and Precipitating Electrons, UCLA	(69-051A-15)	Evans	45
Planar Ion and Electron Trap	(69-051A-16)	Farley	45
	(69-051A-03)	Hanson	45

INDEX OF SPACECRAFT AND EXPERIMENTS

NAME	NSSDC ID	PI'S LAST NAME	PAGE
OGO 6-(CONT)			
Ion Mass Spectrometer, UTD	(69-051A-06)	Hanson	46
VLF Noise and Propagation	(69-051A-24)	Helliwell	46
Solar X-Ray Emissions	(69-051A-08)	Kreplin	46
Whistler and Audio-Frequency Electromagnetic Waves	(69-051A-25)	Laaspere	47
Neutron Monitor	(69-051A-18)	Lockwood	47
Low-Energy Solar Cosmic-Ray Measurement	(69-051A-19)	Masley	47
Energy Transfer Probe for Atmospheric Density	(69-051A-07)	McKeown	47
Electron Temperature and Density	(69-051A-02)	Nagy	48
Neutral Atmospheric Composition	(69-051A-04)	Reber	48
Solar UV Survey, 1850 - 3500 A	(69-051A-10)	Regener	49
Microphone Atmospheric Density Gauge	(69-051A-01)	Sharp	49
Triaxial Search-Coil Magnetometer	(69-051A-22)	Smith	49
Cosmic-Ray Experiment	(69-051A-20)	Stone	50
Ion Mass Spectrometer, GSFC	(69-051A-05)	Taylor	50
Trapped and Precipitating Electrons, GSFC	(69-051A-17)	Williams	50

VI. Literature Citations and Abstracts

The literature that forms the bibliography for this OGO Program Summary has been given in Section IV in terms of the accession numbers of the NASA system. There are a small number of articles which were not in the NASA system when this summary was written that are given in terms of the NSSDC accession number. In this section the complete citation and abstract for each OGO selected article in the NASA system is presented. These are ordered by the accession numbers. Since abstracts are not included in the NSSDC TRF, only citations are given for the "B" number articles.

The accession number at the beginning of a citation is a unique number assigned for identification to each document processed into the NASA system. The letter starting an accession number indicates the series to which it belongs, and the two-digit number immediately following the letter consists of the last two digits of the year in which the document was processed.

A. Literature Cited in IAA

The "A" at the beginning of these accession numbers represents a series announced in *International Aerospace Abstracts (IAA)*. This series contains journal articles and books, meeting papers and conference proceedings issued by professional societies and academic organizations, and translations of journals. No meeting papers are used in the OGO Bibliography unless the actual written paper is available through the professional society or a document distribution center.

A63-10333*

THE ORBITING GEOPHYSICAL OBSERVATORIES.

G. H. Ludwig and W. E. Scull (NASA, Goddard Space Flight Center, Greenbelt, Md.) Nov. 1962 10 p IRE, Proceedings, vol. 50, Nov. 1962, p. 2287-2296.

Description of the Orbiting Geophysical Observatories which are systems designed to fulfill a primary objective of conducting large numbers of significant, diversified experiments for making scientific and technological measurements within the earth's atmosphere, the magnetosphere, and cislunar space, to obtain a better understanding of earth-Sun relationships and the earth as a planet. Configured to meet scientific requirements, the observatories include six booms of different lengths for experiments requiring locations at a distance from the main body. Five degrees of freedom allow the capability of continuously orienting solar and antisolar, geocentric and antigeocentric, and orbital experiments within relatively close limits. Weighing 1,000 lb, of which 150 lb are exclusively experiments, the observatories have potential of growth to 1,500 lb and carrying more experiments. Designed to include five basic subsystems of structure, stabilization and control, power supply, communications and data handling, and thermal control, the observatories have well-defined interfaces for experiments. This basic design fulfills a secondary objective of having available for launching at regular intervals, a standard-type spacecraft consisting of a basic design that can be used repeatedly to carry large numbers of easily integrated experiments in a wide variety of orbits.

A63-12209*

INSTRUMENTATION FOR ATMOSPHERIC COMPOSITION MEASUREMENTS.

H. C. Brinton, C. R. Smith, and H. A. Taylor, Jr. (NASA, Goddard Space Flight Center, Aeronomy and Meteorology, Div., Greenbelt, Md.) 1962 14 p Instrument Society of America, 1962 National Aero-Space Instrumentation Symposium, 8th, Washington, D.C., May 21-23, 1962. ISA Proceedings, vol. 8, 1962, p. 1-14.

Discussion of the research program on the pressure, density, temperature, composition, and ionization of the atmosphere, with emphasis on the indirect and direct methods of data gathering and the particular instruments utilized, such as spectrometers, pressure gages, and electrostatic probes. The objectives and the general scope of some of the aeronomy projects are briefly outlined. The Bennett RF mass spectrometer is described. The experimental packages carried by several satellites and sounding rockets are illustrated.

A63-13537

IMPLEMENTATION OF A DESIGN REVIEW.

A. S. Winthrop (Space Technology Laboratories, Inc., Redondo Beach, Calif.) 1962 16 p Institute of Radio

Engineers, Annual Seminar, 3rd, Reliability of Space Vehicles, Los Angeles, Calif., Oct. 26, 1962. In: Third Annual Seminar on Reliability of Space Vehicles. North Hollywood, Calif., Western Periodicals Co., 1962

Description of the theoretical development and actual implementation within a divisional organization of a comprehensive design review program. Successful application to the Orbiting Geophysical Observatory program is reported. The initial success of the pilot operation suggests a company-wide application.

A63-13629

INSIDE THE ORBITING GEOPHYSICAL OBSERVATORY.

P. F. Glaser and E. R. Spangler (Space Technology Laboratories, Inc., Redondo Beach, Calif.) 15 Feb. 1963 5 p Electronics, vol. 36, Feb. 15, 1963, p. 61-65.

Description of some of the equipment to be carried on board the Orbiting Geophysical Observatory (OGO). Detailed treatment is given to the battery charging system; the communications system, which will use three tracking transmitters and three wide-band transmitters for telemetry; and the digital and the analog data-handling assemblies.

A63-20022*

COSMIC RAY EXPERIMENTS FOR EXPLORER 12 AND THE ORBITING GEOPHYSICAL OBSERVATORY.

G. H. Ludwig and F. B. McDonald (NASA, Goddard Space Flight Center, Greenbelt, Md.) Edited by Wolfgang Priester. Amsterdam, North-Holland Publishing Co., New York, Interscience Publishers Division, John Wiley and Sons, Inc., 1963, p. 1129-1143. 1963 15 p In: Space Research 3 Proceedings of the Third International Space Science Symposium, Washington, D.C., May 2-8, 1962. Committee on Space Research - COSPAR and the U.S. National Academy of Sciences.

Description of the three detector arrays on the Explorer 12 (1961 Upsilon), and of the new instruments developed for the OGO. The cosmic-ray experiment on Explorer 12 consisted of a Geiger counter telescope, a thin CsI scintillation counter and a large area scintillation counter telescope. The thin scintillation counter was connected to an 8 level integral analyzer. The large area scintillation counter telescope, which measured the energy loss of the detected particles, was fed to a 32 channel differential pulse height analyzer with a storage capacity of 65,535 counts per channel. Both the Geiger counter telescope and single counter rates were telemetered. All information was multiplexed onto a single channel. Details of the instrumentation and the methods of encoding are discussed.

A63-21527*

THE MISSION OF THE ORBITING GEOPHYSICAL OBSERVATORIES.

W. E. Scull (NASA, Goddard Space Flight Center,

Orbiting Geophysical Observatories, Greenbelt, Md.) Edited by Irving E. Jeter. North Hollywood, Calif., Western Periodicals Co., 1963, p. 127-148. 1963 22 p In: Scientific Satellites. Advances in the Astronautical Sciences, vol. 12. NASA, American Association for the Advancement of Science, and American Astronautical Society, Symposium on Scientific Satellites-Mission and Design, Philadelphia, Pa., Dec. 27, 1962.

Review of the design and objectives of the OGO program. The primary objective is to conduct large numbers of experiments concerning the atmosphere of the Earth, the magnetosphere, and cislunar space, in order to obtain information of the Earth-sun relationship. A secondary objective is to design, develop, and make available for launching at relative intervals a standard observatory-type oriented spacecraft consisting of a basic system design that can be used repeatedly to carry large numbers of easily integrated experiments in a wide variety of orbits. The current program consists of two missions: the Eccentric Orbiting Geophysical Observatory, and the Polar Orbiting Geophysical Observatory.

A63-23249

THE ORBITING GEOPHYSICAL OBSERVATORY TEST PROGRAM.

M. C. Peterson (Space Technology Laboratories, Inc., Redondo Beach, Calif.) Aug. 1963 12 p Institute of Electric and Electronics Engineers, International Conference and Exhibit on Aerospace Support, Washington, D.C., Aug. 4-9, 1963. IEEE Transactions on Aerospace, vol. AS-1, Aug. 1963, p. 362-373.

Description of the Orbiting Geophysical Observatory Spacecraft and the electrical and mechanical checkout procedures and equipment used in its qualification and acceptance testing. The Integrated Systems Test approach incorporating semi-automatic test programming and spacecraft evaluation is described, after disclosure of previous test cycles and the test program objectives. Specific tests on the attitude control, power, and communications and data handling spacecraft subsystem are discussed, with consideration given to mechanical handling and test fixtures.

A64-10864

ATTITUDE CONTROL FOR AN ORBITING OBSERVATORY: OGO.

D. D. Otten (Space Technology Labs., Inc., Redondo Beach, Calif.) Dec. 1963 5 p Control Engineering, Vol. 10, Dec. 1963, p. 81-85.

Discussion of the challenging task of designing a seemingly simple attitude-positioning control system for a scientific satellite, from hard, irreducible specifications. In the orbiting geophysical observatory satellites, positioning must be accurate and nearly continuous for a design life of one year. High accuracy in continuous positioning is not consistent with the total energy that can be carried as compressed gas. The solution for OGO is a classic example of the control engineer's mating of electronics, optics, electromechanics, and pneumatics in a reliable system.

A64-11240

POWER SOURCES.

A. Krausz (Space Technology Labs., Redondo Beach, Calif.) Edited by A. V. Balakrishnan. New York, McGraw-Hill Book Co., Inc., 1963, p. 213-250. 1963 38 p refs In: Space Communications.

General considerations regarding power requirements for satellites or spacecraft carrying communications or data-processing equipment. The primary energy sources available are described, and methods of converting primary energy to usable electrical energy are discussed in some detail, including photovoltaic energy conversion, thermionic conversion, and batteries and fuel cells. Briefly described is the electric-power-supply subsystem for the orbiting geophysical observatory (OGO).

A64-24447

REAL TIME QUICK-LOOK ANALYSIS FOR THE OGO SATELLITES.

R. J. Coyle and J. K. Stewart (Datatrol Corp., Silver Spring, Md.) Baltimore, Spartan Books, Inc., London, Cleaver-Hume Press, 1964, p. 125-138. 1964 14 p In: American Federation of Information Processing Societies, Spring Joint Computer Conference, Washington, D.C., Apr. 1964, Proceedings. Volume 25. (AIAA Paper 64-218)

Description of the programming system (exclusive of the tracking and orbit determination) for Orbiting Geophysical Observatory (OGO) satellites. The system is divided into two distinct parts: the real time monitor control, and experiment processors. The monitor control is further divided into three sections: the schedule program, monitor processors, and interrupt processors. Definitions are given of the functions and characteristics of these various sections. It is felt that the presented techniques to minimize the execution time of a powerful real-time monitor and to allocate reusable storage in a flexible manner indicate the inherent efficiency of a real-time approach.

A64-27303

TESTING OGO's ATTITUDE CONTROLS.

N. H. Beachley, L. B. Martin, and D. D. Otten (Space Technology Labs., Inc., Redondo Beach, Calif.) Oct. 1964 6 p Control Engineering, vol. 11, Oct. 1964, p. 93-97.

Description of the attitude-control system for the Orbiting Geophysical Observatory (OGO) satellite and the facilities and procedures used in performing prelaunch operational checks. When individual attitude-control axes are decoupled sufficiently to permit testing the control systems one at a time, the single-axis simulator technique used on OGO is said to offer an excellent simulation of the low-torque environment of space, at low cost compared to other approaches. A suspended table (on a long, low-torsion wire served at the top to reduce torsion to the vanishing point) reportedly requires 170 hr to accumulate a position error of 1 millirad.

D.H.

A65-14349*

THE ORBITING GEOPHYSICAL OBSERVATORIES.

W. E. Scull (NASA, Goddard Space Flight Center, Greenbelt, Md.) Edited by Tsuyoshi Hayashi. Tokyo, Agne Corp., 1964, p. 771-784. 1964 14 p In: International Symposium on Space Technology and Science, 5th, Tokyo, Japan, Sep. 2-7, 1963, Proceedings.

Brief review of the development and objectives of the orbiting geophysical observatories. The following subjects are treated: (1) program objectives, (2) spacecraft, (3) structure, (4) thermal control, (5) power supply, (6) attitude control, (7) communications and data handling, (8) tracking and command, (9) data acquisition and control, (10) data processing, and (11) experiments. The experiments to be carried on EGO and POGO are listed in tables. M.M.

A65-19503*#

A SIMULATION OF THE RESPONSE OF THE OGO SPACECRAFT STRUCTURE TO THE LAUNCH ACOUSTIC ENVIRONMENT.

P. J. Alfonsi (NASA, Goddard Space Flight Center, Test and Evaluation Div., Greenbelt, Md.) 1965 8 p In: AIAA Unmanned Spacecraft Meeting, Los Angeles, Calif., Mar. 1-4, 1965 (AIAA Publication CP-12). New York, American Inst. of Aeronautics and Astronautics, 1965, p. 60-67.

Discussion of the acoustic test program of the Orbiting Geophysical Observatory (OGO) conducted at Langley Research Center in the sound field generated by the 9 ft by 6 ft thermal structures wind tunnel. The specific purpose of the program was to experimentally determine the magnitude and spectra of the vibration response of the OGO spacecraft structure due to the associated acoustic environment. The description includes the test facility, the test specimen, instrumentation, test requirements, and test procedure. The maximum and minimum octave band levels in the sound

field generated by the thermal structures wind tunnel and recorded at the reference location during the six low level runs are presented. It is shown that the repeatability of the sound field is excellent with no more than 1-db variation in the data from these runs. It is also shown that the overall runs vibration levels at the base of the interstage fitting on the Agena ring were virtually the same for each low level run. Plots of acceleration spectral density, including overall levels, are also presented.

M.L.

A65-19528#

THE ELECTRIC POWER SUPPLY OF THE ORBITING GEOPHYSICAL OBSERVATORY

A. Krausz and R. L. Robinson (Space Technology Labs., Inc., Redondo Beach, Calif.) 1965 9 p refs In: AIAA Unmanned Spacecraft Meetings, Los Angeles, Calif., Mar. 1-4, 1965 (AIAA Publication CP-12). New York, Amerikan Inst. of Aeronautics and Astronautics, 1965, p. 314-322.

Review of the design requirements of the Orbiting Geophysical Observatory (OGO) spacecraft electrical power subsystem. The major problems of the design requirements are identified. The batteries, solar array, power supply controls, and performance in space are considered. It is shown that a number of innovations were incorporated into the OGO power supply in order to meet the wide range of design constraints. The following are concluded to be the innovations: the capability for the use of ground commands to control operation of the power supply and to modify operating conditions to meet varying orbital conditions; the use of a partial shunt regulator for controlling solar array output; a battery charge control method which is simple to mechanize yet assures complete recharge under varying conditions and prevents operation which would cause battery degradation; development of a lightweight solar array, utilizing beryllium, which can withstand a 2-hr eclipse and cycle temperatures from 80 deg to -160 deg C; and development of a lithium-filled heat sink for power transistors which is thermally independent of the spacecraft and which limits transistor temperatures to the same values. It is hoped that the described solutions will be useful in improving the design of power supplies for future spacecraft.

(Author) M.L.

A65-22431#

OGO-I, FIRST US ORBITING GEOPHYSICAL OBSERVATORY - IGSY: RELATED INVESTIGATIONS IN SPACE.

Mar. 1965 7 p (IG Bulletin, no. 92, Feb. 1965) American Geophysical Union, Transactions, vol. 46, Mar. 1965, p. 326-332.

Description of the OGO-I, the first in a US series of large geophysical observatory satellites, launched into a highly elongated Earth orbit on Sept. 4, 1964. The OGO-I carries 20 experiments contributed by scientists from seven government laboratories and nine universities. The satellite's power supply, attitude- and thermal-control systems, and procedures for communications, and data handling and processing, are briefly discussed. OGO-I carries instrumentation for scientific investigations in the galactic, interplanetary, and planetary regions of space. In galactic space, the satellite is conducting experiments in cosmic rays, radio astronomy, and gegenschein. Interplanetary space experiments include energetic solar protons, solar wind, magnetic fields, solar X rays, ultraviolet radiation, and micrometeorites. Experiments in planetary space are concerned with composition of the neutral atmosphere, density and temperature of the ionosphere, micrometeorites, magnetic fields, geomagnetically trapped radiation, and vlf emissions. A table gives names of experimenters and their affiliation, together with titles of the experiments, brief descriptions of them, and their current status.

F.R.L.

A65-25921*#

PRELIMINARY RESULTS FROM THE AMES RESEARCH CENTER PLASMA PROBE

OBSERVATIONS OF THE SOLAR-WIND-GEOMAGNETIC FIELD INTERACTION REGION ON IMP-2 AND OGO-1.

M. A. Myers (NASA, Ames Research Center, Space Sciences Div., Moffett Field, Calif.), R. W. Silva, and J. H. Wolfe May 1965 38 p COSPAR, International Space Science Symposium, 6th, Buenos Aires, Argentina, May 13-19, 1965, Paper.

Review of satellite measurements on the characteristics of the plasma in the region of transition between the solar wind and the geomagnetic field. Data obtained with the Interplanetary Monitoring Platform, IMP 2, and with the Orbiting Geophysical Observatory, OGO 1, are discussed. The data indicate that there is, in general, a decrease of less than a factor of two in the convective velocity of the plasma as it passes from interplanetary space into the transition region. This is accompanied by a temperature increase of almost an order of magnitude. Evidence is presented for significant plasma acceleration in the transition region. Other features are discussed which apparently question the validity of interpreting the interaction of solar plasma with the geomagnetic field in terms of an aerodynamic analogy. A possible mechanism for the injection of high-energy particles into the magnetosphere is also presented.

P.K.

A65-29239*#

SOLAR WIND MEASUREMENT TECHNIQUES. 2: SOLAR PLASMA ENERGY SPECTROMETERS.

C. W. Beck, II, C. N. Burrous, T. B. Fryer, and R. C. Hedlund (NASA, Ames Research Center, Moffett Field, Calif.) 1965 13 p In: National Aerospace Electronics Conference, 17th, Dayton, Ohio, May 10-12, 1965, Proceedings. Conference sponsored by the Professional Group on Aerospace and Navigational Electronics, Dayton Section of the Inst. of Electrical and Electronics Engineers, and American Inst. of Aeronautics and Astronautics, Dayton, Inst. of Electrical and Electronics Engineers, Dayton Section, 1965, p. 82-94.

Description of the curved-plate electrostatic solar-plasma instruments designed by NASA for the Orbiting Geophysical Observatory and the Interplanetary Monitoring Platform. These instruments measure the flux, angle of incidence, and energy spectrum of the positive ions within the solar plasma. They are capable of detecting a flux of 100,000 protons/sq cm-sec (10 to the -14th power amperes with a capture area of 0.5 sq cm) over an energy range from 450 eV to 18 keV with an angular resolution of better than + or - 4 deg.

(Author) A.B.K.

A65-33664*#

RESPONSE OF ION CHAMBERS IN FREE SPACE TO THE LONG-TERM COSMIC-RAY VARIATION FROM 1960 TO 1965.

R. L. Arnoldy (Minnesota, U., School of Physics and Astronomy, Minneapolis, Honeywell, Inc., Research Center, Hopkins, Minn.), S. R. Kane, and J. R. Winckler (Minnesota, U., School of Physics and Astronomy, Minneapolis, Minn.) 1 Sep. 1965 9 p refs Journal of Geophysical Research, vol. 70, Sep. 1, 1965, p. 4107-4115. NSF/NASA supported research.

Computation of differential response curves and mean rigidity of response for an ion chamber in free space using the cosmic-ray spectrum at solar minimum and maximum observed by independent cosmic-ray measurements. The response is found to be confined predominantly to the rigidity interval 1.5 to 2.5 Bv during the entire solar cycle and is consistent with the observed modulation of He nuclei at these rigidities. The corresponding rigidity intervals for ion chambers flown on balloons at high latitudes and at Minneapolis are 2.5 to 3.5 Bv and 3.0 to 4.0 respectively. Using these results and the measurements made with ion chambers aboard the Pioneer 5 (1960) Mariner 2 (1962) and OGO A (1964) to (1965) spacecraft ion chambers flown on balloons at high latitudes and at Minneapolis and the He nuclei detectors the rigidity dependence of the long-term

variation during 1960 to 1965 is found to be consistent with the form p -beta where beta equals approximately 0.8. For the subperiods 1960 to 1962 and 1962 to 1964 beta is about 0.8 and 1.4 respectively. (Author) M.F.

A66-10892#

IONOSPHERIC EXPERIMENT USING THE ORBITING GEOPHYSICAL OBSERVATORY (OGO-A) AT THE IONOSPHERE RESEARCH LABORATORY, KYOTO UNIVERSITY.

T. Obayashi (Kyoto U., Ionosphere Research Lab., Kyoto, Japan.) 1965 11 p Report of Ionosphere and Space Research in Japan, vol. 19, no. 2, 1965, p. 214-224.

Description of radio propagation experiments using the transmitted VHF waves from the Orbiting Geophysical Observatory (OGO-A) made during the period from September to December 1964. Ingenious methods have been developed to deduce the electron density in the ionosphere and the magnetosphere from the observed Faraday fading and differential Doppler shifts. Some provisional results of the analysis are described briefly. (Author)

A66-14781*#

POSITIVE ION COMPOSITION IN THE MAGNETOSPHERE OBTAINED FROM THE OGO-A SATELLITE.

H. C. Brinton, C. R. Smith (NASA, Goddard Space Flight Center, Lab. for Atmospheric and Biological Science, Greenbelt, Md.), and H. A. Taylor, Jr. 1 Dec. 1965 13 p refs Journal of Geophysical Research, vol. 70, Dec. 1, 1965, p. 5769-5781.

First results from the OGO 1 positive ion spectrometer experiment are presented for the period Sept. 23 through Dec. 10, 1964. Thermal hydrogen and helium ion distributions extend from the lowest observations at 1500 km to an altitude of 30,000 km. The density obtained for $H(+)$ at 2000 km is of the order of 1000 ions/cu cm, and the $H(+)$ concentration is 1% of $H(+)$ over most of the altitude range. Whereas the concentration and distribution of $H(+)$ observed at the lower altitudes is in general agreement with theoretical models, the upper altitude profiles show significant departure from predictions based on diffusive equilibrium theory. Evidence is presented indicating that diffusion of ions is controlled by the geomagnetic field and that the ions are distributed in a beltlike region which exhibits a sharp gradient resulting in a plateau at its outer boundary, which is characterized by a reduction in both the $H(+)$ and $He(+)$ concentrations by a factor of 10 or more. The ion belt is observed to expand and contract over an altitude range of 8000 to 30,000 km in an inverse relationship with the magnetic activity index A_p . There is significant correlation between these results and the knee whistler observations as well as with high-altitude ionization gradients observed from other satellites. Although the data provide some indication of a direct coupling between the lower and upper ionosphere, more data will be required to describe this relationship adequately. (Author)

A66-15266*

MEASURED VELOCITIES OF INTERPLANETARY DUST PARTICLES.

W. M. Alexander, O. E. Berg, C. W. McCracken, C. S. Nilsson, and L. Secretan (NASA, Goddard Space Flight Center, Greenbelt, Md.) 13 Nov. 1965 2 p Nature, vol. 208, Nov. 13, 1965, p. 673, 674.

Review of measurements by OGO 1 (1964 54A) of the velocities of dust particles in cislunar space. The particle detector array is described. Due to difficulties with both the spacecraft and the experiment, only three probable dust particle impacts were recorded. The details of these impacts are discussed. None of the three particles were in closed earth orbit. P.K.

A66-15919#

MAGNETIC CONSIDERATIONS IN THE DESIGN AND TESTING OF THE OGO AND PIONEER SPACECRAFT.

G. J. Gleghorn and J. W. Lindner (Space Technology Labs., Inc., Spacecraft Systems Program Management Div., Redondo Beach, Calif.) Sep. 1965 35 p International Astronautical Federation, International Astronautical Congress, 16th, Athens, Greece, Sep. 13-18, 1965, Paper.

Discussion of some aspects of the magnetic design of the Orbiting Geophysical Observatory (OGO) and the Pioneer solar probe spacecraft as typical examples of problems in satellite design. The characteristics of some commonly used detectors are discussed, and representative data from satellite and space probe measurements are presented. These are shown to establish the basis for magnetic design and test requirements for the OGO and Pioneer programs. Topics discussed include instrumentation, magnetic environment of OGO and Pioneer, criteria for magnetic properties of spacecraft, mechanical equipment, electronic components, permanent magnets, electric currents, test methods, assembly magnetic tests, and observatory tests. Test data from OGO and Pioneer spacecraft have demonstrated that it is possible to design and build complex spacecraft which satisfy stringent magnetic requirements consistent with the measurement of magnetic fields in space. M.F.

A66-15922#

PROBE FOR MEASURING ENERGY TRANSFER BETWEEN A SATELLITE AND THE UPPER ATMOSPHERE.

M. G. Fox and D. McKeown (General Dynamics Corp., General Dynamics/Convair, Space Science Lab., San Diego, Calif.) Sep. 1965 18 p refs International Astronautical Federation, International Astronautical Congress, 16th, Athens, Greece, Sep. 13-18, 1965, Paper. (Nonr-3175(00))

A probe has been developed to measure energy transfer between a satellite surface and the upper atmosphere. It is cylindrical in shape, 3 cm in diameter, and 9 cm long. Energy transfer is detected by the frequency change of a temperature-sensitive quartz crystal located in the nose of the probe. Transfer rates down to 15 microwatt/sq cm can be measured. Data provided by the probe can be used to determine the accommodation coefficients of surfaces, and periodic variations in the atmospheric density. Laboratory results show that the probe will operate at altitudes up to 600 km where the atmospheric density is still great enough to produce measurable heating. (Author)

A66-23148*#

PRELIMINARY RESULTS FROM THE OGO-1 SEARCH COIL MAGNETOMETER: BOUNDARY POSITIONS AND MAGNETIC NOISE SPECTRA.

R. E. Holzer, M. G. McLeod (California, U., Inst. of Geophysics and Planetary Physics, Los Angeles, Calif.), and E. J. Smith (California Inst. of Tech., Jet Propulsion Lab., Pasadena, Calif.) 1 Mar. 1966 6 p refs Journal of Geophysical Research, vol. 71, Mar. 1, 1966, p. 1481-1486. (Contract JPL-950403)

Preliminary analysis of data on the character and location of the magnetopause and the characteristics of broad-band magnetic noise obtained with triaxial search coil magnetometer aboard the OGO 1 satellite. The magnetometer consists of three mutually perpendicular sensors each of which is a coil with a highly permeable magnetic core. The sensors and preamplifier are located in a package at the end of a 20-ft boom to minimize spacecraft interference. The results discussed were derived from observations made while apogee was above the sunlit hemisphere and the spacecraft was able to penetrate into the interplanetary medium in the outer part of its orbit. An attempt was made to locate the mean positions for both the magnetopause and the shockfront. The evidence obtained indicates that both the magnetopause and the shockfront are frequently in motion. D.P.F.

A66-23684*

TWO SATELLITE-BORNE COSMIC RADIATION DETECTORS.

R. G. Bingham, W. C. Erickson, R. L. Howard, J. Lezniak, D. Sawyer, and W. R. Webber (Minnesota, U., School of Physics and Astronomy, Minneapolis, Minn.) Feb. 1966 8 p Annual Nuclear Science Symposium, 12th, San Francisco, Calif., Oct. 18-20, 1965, Paper. IEEE Transactions on Nuclear Science, vol. NS-13, Feb. 1966, p. 478-485. (Contract NAS5-3096)

Description of experiments designed to measure the differential energy spectra of protons, helium nuclei and heavy nuclei up to a charge $Z = 14$ in the range 1.0 to 1200 Mev per nucleon. To carry out these experiments, cosmic radiation telescopes constructed at the University of Minnesota will be flown on the Polar Orbiting Geophysical Observatories, POGO C and D, and on the Pioneer Deep Space Probes C and D. The POGO telescope utilizes a combination of scintillation and Cerenkov counters together with a semiconductor detector. Use of the thresholds in the geomagnetic field extends the energy range for protons to 30 Bev. A Geiger tube, four lithium-drifted silicon detectors, and a Cerenkov counter comprise the Pioneer telescope.

M.F.

A66-23689*

PLASMA ELECTRON DETECTOR USING AN OPEN ELECTRON MULTIPLIER.

D. L. Lind and N. McIlwraith (NASA, Goddard Space Flight Center, Greenbelt, Md.) Feb. 1966 4 p Annual Nuclear Science Symposium, 12th, San Francisco, Calif., Oct. 18-20, 1965, Paper. IEEE Transactions on Nuclear Science, vol. NS-13, Feb. 1966, p. 511-514.

The triaxial electron spectrometer, scheduled for flight on the OGO 5 spacecraft, measures flux and energy distributions of electrons reaching the detector with from zero to 10 kv energy. Electrons are analyzed in a curved-plate, electrostatic analyzer, and detected with a windowless continuous-dynode electron multiplier. The multiplier is operated in a constant-output, variable-gain, current mode as the null detector in a feedback circuit. Five decades of dynamic range for flux measurements are obtained with a logarithmically compressed analog telemetry signal. Tests of the gain stability of two different channel multipliers have been made for periods of up to 850 hr. These tests indicate that the gain loss can be limited to a factor of two or three during the 1-yr lifetime of the spacecraft. (Author)

A66-23690

AN ELECTRON AND PROTON SPECTROMETER DETECTOR SYSTEM FOR AN OGO-E SATELLITE EXPERIMENT.

J. H. McQuaid (California, U., Lawrence Radiation Lab., Electronics Engineering Dept., Livermore, Calif.) Feb. 1966 8 p Annual Nuclear Science Symposium, 12th, San Francisco, Calif., Oct. 18-20, 1965, Paper. IEEE Transactions on Nuclear Science, vol. NS-13, Feb. 1966, p. 515-522. AEC sponsored research.

A detector system for use with a magnetic electron spectrometer and a proton telescope is described. The experiment will be included on the Orbiting Geophysical Observatory 5 (OGO 5) satellite. Electron measurements cover the range from 60 kev to 2.7 Mev in seven differential energy channels. Each channel consists of an electron-plus-background detector and a background detector. A method of handling information from both detectors with the same amplifier system is discussed. This scheme is used to ensure that the proper background subtraction is made in spite of electronic drifts. Coincidence and anticoincidence logic is used for routing the electron-plus-background and background signals to their respective scalars. The four-element proton telescope uses solid state detectors directly in line with the collimator. The telescope lies within the pole pieces of the electron spectrometer magnet. Seven proton channels are provided covering the range from 200 kev to 50 Mev. In addition, three alpha channels from 6 Mev to 130 Mev are obtained. Pulse height selection of the pulses from each detector plus coincidence and anticoincidence between these pulses will resolve the double

valued energy loss in the detectors and determine the energy channels. The alpha particles are differentiated from protons only through their greater dE/dx . A tunnel diode differential discriminator is discussed. This discriminator makes its logical decisions at the trailing edge of the input pulse. In this way pulses of varying widths cannot cause false decisions. Two charge-sensitive preamplifiers have been developed for this work. Optimum noise characteristics are obtained with RC differentiating and integrating time constants of approximately 1/3 microsec. The total standby power is less than 0.5 watt. This includes 14 preamplifiers and 26 amplifiers. All logic, including tunnel diode differential discriminators, operate on zero standby power. (Author)

A66-26348*#

THE MULTIPLY CHARGED PRIMARY COSMIC RADIATION AT SOLAR MINIMUM, 1965.

V. K. Balasubrahmanyam, D. E. Hage, G. H. Ludwig, and F. B. McDonald (NASA, Goddard Space Flight Center, Greenbelt, Md.) 1 Apr. 1966 10 p refs Journal of Geophysical Research, vol. 71, Apr. 1, 1966, p. 1771-1780.

The primary cosmic-ray charge and energy spectra have been obtained for helium through oxygen during the recent period when solar modulation effects were at a minimum. These spectra represent a synthesis of preliminary experimental results from cosmic-ray experiments flown on OGO 1, IMP 3, and high-altitude Skyhook balloon flights. The He energy spectrum is given from 35 to 750 Mev/nucleon. The energy spectra for lithium-oxygen covers the interval approximately 40-1200 Mev/nucleon. Integral flux values > 1200 Mev are obtained for He through Ne. L/M ratios of 0.29 plus or minus .07 at 100 Mev/nucleon and 0.30 plus or minus .03 above 600 Mev/nucleon are found. The C/He ratio of 0.023 plus or minus .005 at 100 Mev/nucleon is significantly less than the same integral ratio of 0.036 plus or minus .004 above 600 Mev/nucleon, indicating the effects of ionization losses during propagation through the interstellar gas under the assumption of similar source spectra.

(Author)

A66-27326*#

COLLIMATING GRATING MONOCHROMATORS FOR THE VACUUM ULTRAVIOLET.

D. E. Bedo and H. E. Hinteregger (USAF, Office of Aerospace Research, Cambridge Research Labs., Bedford, Mass.) 1965 5 p refs In: Conference on Photographic and Spectroscopic Optics, Tokyo, Japan, Sep. 1-5, 1964, and Kyoto, Japan, Sep. 7, 8, 1964, Proceedings (Japanese Journal of Applied Physics, Supplement 1, vol. 4, 1965). Conference sponsored by the International Commission for Optics, the Science Council of Japan, and the Japan Society of Applied Physics. Tokyo, Japanese Journal of Applied Physics, 1965, p. 473-477. NASA supported research.

A nonfocusing, grazing incidence monochromator which utilizes planar gratings and collimating slit systems is described. Such an instrument is capable of moderate spectral resolution in the vacuum ultraviolet and allows for relatively simple scanning mechanisms. Monochromators of this type have been built for laboratory studies and for incorporation in a satellite-borne experiment for monitoring solar intensities in the extreme ultraviolet. Measurements made on rare gas spectra indicate approximate agreement between computed and observed instrumental line widths. (Author)

A66-34754*#

PROTONS AND HELIUM NUCLEI WITHIN INTERPLANETARY MAGNETIC REGIONS WHICH CO-ROTATE WITH THE SUN.

C. Y. Fan, G. Gloeckler, and J. A. Simpson (Chicago, U., Enrico Fermi Inst. for Nuclear Studies, Chicago, Ill.) 1966 3 p refs In: International Conference on Cosmic Rays, 9th, Imperial Coll. of Science and Technology, London, English, Sep. 6-17, 1965, Proceedings Volume 1. Conference sponsored by the International Union of Pure and Applied Physics, the Inst. of Physics, and the Physical Society, London, Inst. of Physics and Physical Society, 1966, p. 109-111.

(Contracts NASS-2990; NASS-2133; AF 19(628)-2473)

From IMP-1 measurements we showed in 1964 that fluxes of protons of greater than 1-Mev energy appeared for several days in a sequence of six consecutive 27-day intervals. We concluded that these protons were confined within a region corotating with the sun which modulates the galactic cosmic radiation at the orbit of earth with same 27-day recurrence period. This region has persisted for more than 20 solar rotations and was observed with the IMP-1 magnetometer by Ness and Wilcox to possess special characteristics. The energy spectrum of the protons in the leading and trailing sides of the corotating region was measured. A helium component continuously associated with the protons has been found with an energy spectrum of the form proportional to E to the -2 power Mev/nucleon in the energy range 2 to 30 Mev/nucleon. Evidence from the OGO-1 satellite indicates that the proton and helium fluxes are not only present within corotating regions, but are also present at lower intensity and with different spectra at all times throughout a 2-1/2 month period. The source for continual acceleration of these protons and helium nuclei is discussed. (Author)

A66-34768#

STUDIES OF PRIMARY COSMIC RAYS WITH IONIZATION CHAMBERS.

R. L. Arnoldy (Honeywell Inc., Res. Center, Hopkins, Minn.), S. R. Kane, and J. R. Winckler (Minnesota Univ., School of Physics and Astronomy, Minneapolis, Minn.) 1966 4 p refs. Inst. of Physics and Physical Society (London), 1966 p 157-160. Proceedings of the Intern. Conf. on Cosmic Rays, 9th, Imperial Coll. of Sci. and Tech., London, 6-17 Sep. 1965 sponsored by Intern. Union of Pure and Applied Physics, the Inst. of Physics and the Physical Society. Avail: NTIS

A66-34833*#

ABUNDANCES AND ENERGY SPECTRA FOR NUCLEI OF GALACTIC ORIGIN ABOVE 20 MEV PER NUCLEON.

G. M. Comstock, C. Y. Fan, and J. A. Simpson (Chicago, U., Enrico Fermi Inst. for Nuclear Studies, Chicago, Ill.) 1966 4 p refs. In: International Conference on Cosmic Rays, 9th, Imperial Coll. of Science and Technology, London, England, Sep. 6-17, 1965. Proceedings, Volume 1. Conference sponsored by the International Union of Pure and Applied Physics, the Inst. of Physics, and the Physical Society, London, Inst. of Physics and Physical Society, 1966, p. 383-386. Discussion, P. H. Fowler (Bristol, U., H. H. Wills Physics Lab., Bristol, England), W. R. Webber (Minnesota, U., School of Physics and Astronomy, Minneapolis, Minn.), and B. R. Daniel (Tata Inst. of Fundamental Research, Bombay, India), p. 386. (Contract NASS-2133; Grants AF-AFOSR-521-65; NsG A.)

The individual chemical abundances of nuclei with charge Z extending from $Z = 2$ to $Z = 14$ in the energy range 20 to 300 Mev/nucleon have been measured in interplanetary space in the OGO-1 satellite for approximately 150 hr in Oct. and Nov. 1964. At higher Z , two charge groups were measured including the Fe group. The energy spectra for C, O and Ne are shown to be remarkably flat and different from the helium spectrum measured simultaneously over the same energy/nucleon range. It is concluded that these spectral differences exist in the cosmic radiation outside the solar system. The relative abundances for $6 < Z < 14$ or equal to 14 display an even-odd Z ratio of approximately 8:1. Li, Be and B, and the Fe group are present with about the same relative abundances as observed at higher energies. It is suggested that the rate of particle acceleration for a wide range of Z competes effectively with the rate of ionization loss at these low energies. The measurements were made with solid state silicon detectors and anticoincidence scintillators arranged to measure energy loss and total energy. (Author)

A66-34847*#

GALACTIC COSMIC RAYS AT SOLAR MINIMUM, 1965.

V. K. Balasubrahmanyam, D. E. Hagge, G. H. Ludwig, and F. B. McDonald (NASA, Goddard Space Flight Center, Greenbelt, Md.) 1966 10 p refs. In: International Conference on Cosmic Rays, 9th, Imperial Coll. of Science and Technology, London, England, Sep. 6-17, 1965. Proceedings, Volume 1. Conference sponsored by the International Union of Pure and Applied Physics, the Inst. of Physics, and the Physical Society, London, Inst. of Physics and Physical Society, 1966, p. 427-436.

A synthesis of preliminary experimental results from cosmic ray experiments flown on OGO 1, IMP 1, 2, and 3, and high-latitude Skyhook balloon flights provides charge and energy spectra extending from about 20 Mev per nucleon to 1 Gev/nucleon for hydrogen to neon. A multiple Geiger counter cosmic ray monitor flown on these four satellites provided information on the total flux greater than 50 Mev/nucleon. The period from Mar. to June 1965 appears to have minimum solar modulation effects and is operationally defined to be the solar cosmic ray minimum. Energy spectra for particles from H to Ne from 25 Mev/nucleon to 1 Gev/nucleon are presented. Results on the long-term temporal variation of He nuclei and protons are discussed. The L/M ratio at 100 Mev/nucleon and above 600 Mev/nucleon are found to be 0.29 ± 0.05 and 0.30 ± 0.03 . The C/He ratio at 100 Mev/nucleon is found to be 0.021 ± 0.005 whereas above 600 Mev/nucleon the same ratio is found to be 0.36 ± 0.004 . The change in this ratio appears to suggest the deceleration of the nuclei of higher Z in the interstellar gas due to ionization. (Author)

A66-41213*

SOME DOUBTS ABOUT THE EARTH'S DUST CLOUD.

C. Nilsson (NASA, Goddard Space Flight Center, Lab. for Space Sciences, Greenbelt, Md.) 9 Sep. 1966 5 p refs. Science, vol. 153, Sep. 9, 1966, p. 1242-1246.

Discussion of the dubious validity of past satellite measurements of micrometeoroid fluxes in which piezoelectric microphones were used as detectors. Data have been obtained from satellite and laboratory experiments which show that microphone crystals emit noise when subjected to slowly varying temperatures. The rate of noise is consistent with past flight data which were previously interpreted on the basis of micrometeoroid impacts. These measurements have given rise to the theory that the earth is surrounded by a cloud of dust, although no satisfactory mechanism has yet been found to explain this apparent phenomenon. Results are reported from which it appears that whether or not a concentration of dust exists in the vicinity of the earth, the data from satellite microphone measurements should not be used to support such a hypothesis. M.M.

A67-11687*

ABUNDANCES AND ENERGY SPECTRA OF GALACTIC COSMIC-RAY NUCLEI ABOVE 20 MEV PER NUCLEON IN THE NUCLEAR CHARGE RANGE 2 LESS THAN OR EQUAL TO Z LESS THAN OR EQUAL TO 26.

G. M. Comstock, C. Y. Fan (Chicago, U., Enrico Fermi Inst. for Nuclear Studies and Dept. of Physics, Chicago, Ill.), and J. A. Simpson (Chicago, U., Enrico Fermi Inst. for Nuclear Studies, Chicago, Ill.) Oct. 1966 28 p refs. Astrophysical Journal, vol. 146, Oct. 1966, p. 51-77. (Contracts NASS-2133; AF 49(638)-1642; Grant NsG 179-61)

Study of the abundances of the elements helium through silicon, in addition to the nuclear-charge group $15 < Z < 25$ and group, and measurement of the differential energy spectra of the elements, using a telescope composed of solid-state detectors on the OGO 1 satellite. The bearing of the experimental results on the origin and propagation of cosmic-ray nuclei is discussed. Energy degradation by ionization loss alone may not account for the results. The rate of particle acceleration for a wide range of the change number Z may compete effectively with the

rate of ionization loss at these low energies. Alternatively, a discrete and possibly nearby source in the Galaxy may account for the measurements. Since the technique of using solid-state devices for measuring multiply charged nuclei is novel, a description of the instrument and methods of analyzing the data is included. W.A.E.

A67-12055*

THE EFFECT OF THE EARTH'S RADIATION BELTS ON AN OPTICAL SYSTEM.

C. Wolff (NASA, Goddard Space Flight Center, Greenbelt, Md.) Nov. 1966 5 p refs Applied Optics, vol. 5, Nov. 1966, p. 1838-1842.

A photoelectric optical imaging system has survived one year in the earth's radiation belts with no measurable (< 20%) change in sensitivity. The system passes through all of the radiation belts twice every 64 hr, and experiences a noise level equivalent to 400 photons/sec when in their most intense regions. While this noise is far less than that of other photoelectric systems operating in the belts because of the small effective area of the photocathode, the noise per unit cathode area is $1.3 \times 100,000$ photons/sec-sq cm, and is similar to the best of the other systems. The number and energy distribution of incident particles is calculated and then combined with shielding estimates to give the total energy absorbed in the optical elements. Radiation damage reports in the literature are shown to be consistent with the lack of a sensitivity change in this orbiting optical system. The effects of particle radiation on optical systems in general is briefly summarized, with emphasis with emphasis on recent work of others. (Author)

A67-15724*

A MAGNETIC FIELD INSTRUMENT FOR THE OGO-E SPACECRAFT.

C. R. Benjamin (Marshall Labs., Torrance, Calif.) and R. C. Snare (California, U. Los Angeles, Calif.) Dec. 1966 8 p Inst. of Electrical and Electronics Engineers, Annual Conference on Nuclear and Space Radiation Effects, Stanford U., Palo Alto, Calif., Jul. 18-21, 1966, Paper. IEEE Transactions on Nuclear Science, vol. NS-13, Dec. 1966, p. 333-340. Research supported by the U. of California.

Description of a three-axis, fluxgate magnetometer which will provide data for the study of MHD waves and other magnetic field structures in space. The magnetometer has sufficient dynamic range to measure magnetic field values from the surface of the earth to apogee. In addition to this wide dynamic range, the instrument provides for a resolution at all field values of 1/16 gamma. This resolution and dynamic range are accomplished by employing a tightly fed-back, closed-loop magnetometer, and a digital offset field generator in each of the three mutually perpendicular axes. Packaging and construction techniques used in the instrument are discussed. M.F.

A67-19913*#

SOLAR MODULATION OF GALACTIC COSMIC RAYS.

V. K. Balasubrahmanyam, E. Boldt, and R. A. R. Palmeira (NASA, Goddard Space Flight Center, Greenbelt, Md.) 1 Jan. 1967 10 p refs Journal of Geophysical Research, vol. 72, Jan. 1, 1967, p 27-36.

The modulation of galactic protons and He nuclei during the last solar cycle is analyzed according to Parker's theory. The mechanism of modulation remains essentially the same during several years of low solar activity (1961-1965). The modulation near solar maximum (1959) implies that the scale sizes of the magnetic inhomogeneities in the solar wind are reduced below the values at solar minimum. An adequate description at solar maximum would require further refinements of the theory. The proton-to-He-nucleus ratio outside the solar system is shown to be consistent with the value approximately 6, in a kinetic-energy/nucleon representation, for the interval 100-1000 Mev/nucleon. (Author)

A67-19926*#

INITIAL OBSERVATIONS OF LOW-ENERGY ELECTRONS IN THE EARTH'S MAGNETOSPHERE WITH OGO-3.

L. A. Frank (Iowa, State U., Dept. of Physics and Astronomy, Iowa City, Iowa) 1 Jan. 1967 11 p Journal of Geophysical Research, vol. 72, Jan. 1, 1967, p. 185-195.

(Contract NASS-2054; Nonr-1509(06); Grant NsG-233-62)

Description of initial observations of electrons over the energy range extending from approximately 100 ev to 50 kev at geocentric radial distances 8-20RE in the dark hemisphere of the earth's magnetosphere with electrostatic analyzers borne on OGO 3, for June 12-13 1966. The electron-differential-energy spectra typically are characterized by a single peak in intensities occurring in the energy range approximately 0.8-10 kev and at lower energies with increasing geocentric radial distance, by broader widths with decreasing radial distance, and by greater slopes for electron energies $E >$ or equal kev with increasing radial distance. M.M.

A67-23244*

FIRST MAGNETIC FIELD RESULTS FROM THE OGO-2 SATELLITE.

J. C. Cain, S. J. Hendricks (NASA, Goddard Space Flight Center, Greenbelt, Md.), and R. A. Langel Edited by R. L. Smith-Rose. Amsterdam, North-Holland Publishing Co., 1967, p. 1466-1476. 1967 11 p refs In: Space Research 7, Proceedings of the Seventh International Space Science Symposium, Vienna, Austria, May 10-18, 1966. Volume 2. Symposium sponsored by the Committee on Space Research, the International Union of Geodesy and Geophysics, and the International Scientific Radio Union.

The OGO 2 (1965-81A) satellite was launched Oct. 14, 1965 into an orbit with an inclination of 87.4 deg, perigee of 414 km and apogee of 1510 km. Digital samples of the total magnetic field F were obtained with a rubidium vapor magnetometer at 0.5-sec intervals (accuracy + or - = 2 gamma). Root-mean-square differences between the measured field values and those computed from previously derived spherical harmonic expansions were computed. The best comparison of the data is with the GSFC September 1965 field which showed rms residuals of 47 gamma. Computation of fields fit to the limited data sample show rms deviations of 4.1 gamma using 143 internal spherical harmonics. The residuals from this field show oscillations near the north pole of a few tens of gammas amplitude and irregular structure elsewhere of the order of a few gammas. (Author)

A67-23278*

SOME RESULTS CONCERNING THE PRINCIPAL AIRGLOW LINES AS MEASURED FROM THE OGO-2 SATELLITE.

J. E. Blamont (Centre National de la Recherche Scientifique, Paris, France) and E. L. Reed (NASA, Goddard Space Flight Center, Greenbelt, Md.) 1967 16 p refs COSPAR, International Space Science Symposium, 7th, Vienna, Austria, May 10-18, 1966, Paper. In: Space Research 7, Proceedings of the Seventh International Space Science Symposium, Vienna, Austria, May 10-18, 1966. Volume 1. NASA sponsored research. Symposium sponsored by the Committee on Space Research, the International Union of Geodesy and Geophysics, and the International Scientific Radio Union. Edited by R. L. Smith-Rose. Amsterdam, North-Holland Publishing Co., 1967, p. 337-352.

Two photometers on the OGO 2 spacecraft (launched Oct. 14, 1965, 420 km perigee, 1520 km apogee, 87.4 deg inclination) scanned the airglow horizon through a filter centered at 6300 A, the nadir airglow at 6300, 6225, 5890, 5577, 3914, and 2630 A, and the zenith airglow at 6300 A. During its less than 10 days of stabilized operation approximately an hour of data were obtained while in the earth's shadow. The nadir measurements observed the blue enhancement at twilight, several aurorae, and typical nighttime airglow. The horizon scanning photometer observed the two airglow layers, a thick one generally above 200 km

A67-25807

attributed to the 6300 A line of atomic oxygen and a thin layer centered between 65 and 95 km attributed to the OH emissions which fall within the 40 A-wide passband of the interference filter. The maximum emission of the 6300-A line occurred generally between 200 and 300 km altitude with values of 1 to 25 photons $\text{cm}^2/\text{cm}^2/\text{sec}$ at night and about a factor of 10 greater in the twilight. (Author)

A67-25807*

THE SPECTRA AND INTENSITY OF ELECTRONS IN THE RADIATION BELTS.

S. R. Kane, K. Pfizter, and J. R. Winckler (Minnesota, U., School of Physics and Astronomy, Minneapolis, Minn.) Edited by R. L. Smith-Rose. Washington, D.C., Spartan Books, 1966, p. 702-713. 1966 12 p COSPAR, International Space Science Symposium, 6th, Buenos Aires, Argentina, May 13-19, 1965, Paper. In: Space Research 6, Proceedings of the Sixth International Space Science Symposium, Mar del Plata, Argentina, May 11-19, 1965. Symposium sponsored by the Committee on Space Research, the International Astronomical Union, the International Union of Geodesy and Geophysics, the International Union of Pure and Applied Chemistry, the International Union of Pure and Applied Physics, and the International Scientific Radio Union. NASA supported research.

A magnetic spectrometer measuring electrons in 5 channels and between 50-4000 keV and an integrating ionization chamber were launched into an eccentric orbit on Sept. 4, 1964 on the OGO 1 satellite. Electron spectra, pitch angle distributions, and total ionization are measured throughout the inner and outer belts. These measurements show the radiation region to be separated into two belts by a very pronounced slot near $L = 3$. The slot is always deep for electrons above 290 keV, but during times of magnetic disturbances may not be a clear feature for 50-120 keV electrons. The slot extends throughout all electron pitch angles and appears especially pronounced now during solar minimum. Typical fluxes observed by these detectors are tabulated. In the inner zone these fluxes are observed to be quite stable, and the spectrum steepens as L increases from 1.3 to 3.0. In the outer zone the fluxes and spectra are very dependent on magnetic activity. (Author)

A67-25852*

OGO-E COSMIC RADIATION: NUCLEAR ABUNDANCE EXPERIMENT.

S. L. Jones, G. H. Ludwig, D. E. Stilwell, J. H. Trainor, and S. H. Way (NASA, Goddard Space Flight Center, Greenbelt, Md.) Feb. 1967 8 p Nuclear Science Symposium on Instrumentation in Space and Lab., 13th, Boston, Mass., Oct. 19-21, 1966, Paper. IEEE Transactions on Nuclear Science, vol. NS-14, Feb. 1967, p. 56-63.

Description of equipment used to measure nuclear abundances of galactic and solar cosmic rays. Three detector assemblies used to measure the differential energy spectra of protons and heavier nuclei through calcium in the range from 400 keV to 1 BeV/nucleon are described, as well as an extensive electronics system used to implement the logic, perform pulse-height analysis, measure particle fluxes, monitor experiment performance, and interface with the OGO data system. A.B.K.

A67-26312*#

SEVERAL OBSERVATIONS OF LOW-ENERGY PROTONS AND ELECTRONS IN THE EARTH'S MAGNETOSPHERE WITH OGO-3.

L. A. Frank (Iowa, State U., Dept. of Physics and Astronomy, Iowa City, Iowa.) 1 Apr. 1967 12 p refs Journal of Geophysical Research, vol. 72, Apr. 1, 1967, p. 1905-1916. (Contracts NAS5-2054; Nonr-1509(06); Grant NSG 233-62)

Description of simultaneous observations of proton and electron differential energy spectra during segments of three outbound traversals of OGO 3 through the magnetosphere for the period from June 11 to 15, 1966, on L shells 3.3 to 16. A preliminary order-of-magnitude estimate of the total energy of trapped protons within the earth's atmosphere is

5×10 to the 21st power ergs, and the estimated contribution from this low-energy proton distribution to the quiettime terrestrial ring current field at the earth's surface is approximately -10 gamma. A transient, narrow peak of relatively high low-energy proton and electron intensities within the energy range from approximately 300 eV to 2 keV at L is approximately equal to 4 with width ΔL is approximately equal to 1 was also observed. M.M.

A67-27249*

COMPOSITION AND SPECTRA OF CHARGED PARTICLES OF SOLAR AND COSMIC ORIGIN MEASURED ON SATELLITES.

G. Comstock, C. Y. Fan, G. Gloeckler, and J. A. Simpson (Chicago, U., Enrico Fermi Inst. for Nuclear Studies, Chicago, Ill.) Edited by J. Gauger and A. J. Masley. North Hollywood, Calif., Western Periodicals Co. 1966, p. 129-145. 1966 17 p refs In: Recent Advances in Cosmic Ray Research, Proceedings of a Symposium, Huntington Beach, Calif., Apr. 4-6, 1966. Symposium sponsored by the Douglas Aircraft Co.

(Contracts NAS5-2990; NAS5-2133; AF 19(628)-2473; Grants NSG 179-61; AF-AFOSR-521-65)

Analysis of measurements performed by satellites OGO 1 and IMP 1 of the composition and spectra of particles of galactic and solar origin. The measurements of the chemical abundances of nuclei with charge Z extending from $Z = 2$ to $Z = 26$ in the energy range 30 to 300 MeV/nucleon were done with a cosmic ray telescope on board OGO 1 during the period of solar minimum. Results presented on abundances and energy spectra for nuclei suggest that the rate of particle acceleration for a wide range of Z compete effectively with the rate of ionization loss at low energies. Measurements of intensity variations of protons and helium nuclei within interplanetary magnetic regions which corotate with the sun are described. The presence of a helium component which correlates in time with the changes in energy spectrum and flux levels of the proton component is convincing evidence that both have the same origin. The nature of this origin is discussed as either solar or galactic. T.M.

A67-33595*

ELECTRON MEASUREMENTS NEAR A WEAK AURORA.

D. L. Lind, N. McIlwraith, and K. W. Ogilvie (NASA, Goddard Space Flight Center, Greenbelt, Md.) Edited by B. M. McCormac. New York, Reinhold Publishing Corp., 1967, p. 243-248. 1967 6 p In: Aurora and Airglow, NATO Advanced Study Inst., U. of Keele, Keele, Staffs., England, Aug. 15-26, 1966, Proceedings. Inst. supported by the North Atlantic Treaty Organization, the Cambridge Research Labs. of the U.S. Air Force, the Research Office of the U.S. Army, the Defense Atomic Support Agency, the Office of Naval Research of the U.S. Navy, and the Inst. for Telecommunication Sciences and Aeronomy of the Environmental Science Services Administration.

Description of electron measurements near a weak aurora during the flight of a Nike-Tomahawk rocket. The total energy obtained by integrating the observed electron intensities was compared with the readings of the 5577 and 3914 A photometers. The result showed reasonably good correlation between the two peaks at 165 sec. If isotropy is assumed in the upper atmosphere and the average of the two peak readings of electron energy is used, a figure of 11.0 ergs for approximately 970 R of λ 5577 is arrived at. The λ 3914 intensity measured at the time was 380 R. The commonly accepted figure would be about 2.0 ergs for 400 R of λ 3914, but the difference can be readily accounted for by calibration and geometrical ambiguities in the photometric data. No inconsistency seems to be indicated. M.M.

A67-36513*

RUBIDIUM VAPOR MAGNETOMETER FOR NEAR EARTH ORBITING SPACECRAFT.

W. H. Farthing and W. C. Folz (NASA, Goddard Space

Flight Center, Greenbelt, Md.) Aug. 1967 8 p refs Review of Scientific Instruments, vol. 38, Aug. 1967, p. 1023-1030.

The paper describes the instrumentation and in-flight performance of the rubidium vapor magnetometers being flown by NASA on the POGO satellites. An optically pumped, self-oscillating rubidium magnetometer was selected as being most compatible with the objectives of the study and with the spacecraft capabilities. A four absorption cell configuration is used to reduce the effect of the null zones inherent in these instruments and to obtain accuracies compatible with the scientific objectives of the program. Scalar magnetic field data are obtained in both digital (PCM) and analog (frequency multiplex) form. Instrument performance parameters are monitored through both main frame and subcommutated PCM data. The first instrument orbited was aboard OGO 2 which was launched on Oct. 14, 1965. This instrument has returned a large quantity of data, and is still operating when sufficient spacecraft power is available. The accuracy of the data is determined, apart from orbit accuracy, by spurious phase shifts within the instrument. These arise from such sources as optical axis misalignment, electronic nonlinearities and frequency dependence, and propagation delay over the long cables connecting sensor and electronics. The magnitude of the resulting error is inversely proportional to the phase slope of the dual cell absorption line. The total effect in the POGO instrument of these sources of error is an accuracy of better than 1.5 gamma over the entire instrument range of 15,000 to 64,000 gamma.

(Author)

A67-36901*

THE MAIN GEOMAGNETIC FIELD.

J. C. Cain (NASA, Goddard Space Flight Center, Greenbelt, Md.) Jun. 1967 5 p refs American Geophysical Union Transactions, vol. 48, Jun. 1967, p. 511-515.

Survey of data recently acquired for the study of the main geomagnetic field. The data contributed by the low polar satellite OGO 2 and by the U.S. Naval Oceanographic Office are discussed. It is pointed out that one of the most pressing needs in geomagnetism is the conversion of the available magnetic survey data to computer-readable form. Attempts to define accurately the main geomagnetic field by numerical functions are examined, and the secular change and source of the main field are studied. M.F.

A67-37401*#

ON THE EXTRATERRESTRIAL RING CURRENT DURING GEOMAGNETIC STORMS.

L. A. Frank (Iowa, State U., Dept. of Physics and Astronomy, Iowa City, Iowa) 1 Aug. 1967 15 p refs Journal of Geophysical Research, vol. 72, Aug. 1, 1967, p. 3753-3767. (Contracts NAS5-2054; Nonr-1509(06); Grant NsG 233-62)

Summary of first observations of the charged particles of the extraterrestrial ring current during two moderate geomagnetic storms. Measurements of the differential energy spectrums of protons and electrons, separately, over the energy range extending from approximately 200 ev to 50 kev with a sensitive array of electrostatic analyzers on board OGO 3 reveal large temporal variations in intensities of these low-energy charged particles at low and moderate latitudes in the outer radiation zone during two moderate geomagnetic storms in late June and early July 1966. The total energy of these low-energy protons and electrons within the earth's magnetosphere is sufficient to account for the depression of the geomagnetic field observed at the earth's surface over low and moderate latitudes; hence these charged particles may be identified as the major contributors to the storm-time extraterrestrial ring current. M.F.

A67-37412*#

A SEARCH FOR ALPHA PARTICLES TRAPPED IN THE GEOMAGNETIC FIELD.

K. B. Fenton (Chicago, U., Enrico Fermi Inst. for Nuclear Studies, Chicago, Ill.) 1 Aug. 1967 6 p refs Journal of Geophysical Research, vol. 72, Aug. 1, 1967, p. 3889-3894. (Contracts NAS5-2133; AF 49(638)-1642; Grant NsG

179-61)

Data from the charged-particle telescope on the satellite OGO 1 for the regions of the geomagnetic field in which protons of energy 26-85 Mev are trapped have been analyzed for the presence of alpha particles during a period near the minimum of solar activity (1964). The region of (B, L) space sampled is that for which $1.6 < \text{or} = \text{to } L < \text{or} = 3.3$ and $0.01 < \text{or} = \text{to } B < \text{or} = 0.25$. From an examination of samples of data in which a total of 15,000 trapped protons was observed, it is concluded that the upper limits for the alpha-particle proton ratio are 1 in 1500 for the energy range 26-85 Mev nucleon and less than 1 in 50 for the rigidity range 0.33-0.39 BV. It is inferred from the fact that the results indicate an almost pure proton source that the decay of energetic albedo neutrons must be the principal source of trapped protons at energies above 26 Mev. (Author)

A67-40804*#

MAGNETIC NOISE IN THE MAGNETOSHEATH IN THE FREQUENCY RANGE 3-300 HZ.

R. E. Holzer, M. G. McLeod, C. T. Russell (California, U., Inst. of Geophysics and Planetary Physics, Los Angeles, Calif.), and E. J. Smith (California Inst. of Tech., Jet Propulsion Lab., Space Sciences Div., Pasadena, Calif.) 1 Oct. 1967 11 p refs Journal of Geophysical Research, vol. 72, Oct. 1, 1967, p. 4803-4813.

(Contracts NAS7-100; JPL-950403)

(JPL-TR-32-1199)

Evaluation of preliminary results concerning rapid magnetic-field variations (3 to 300 Hz) observed in the magnetosheath by the OGO 1 search-coil-magnetometer spectrum analyzer. Broad-band signals are continuously present in the magnetosheath at these frequencies and are relatively intense and high available on time scale of tens of seconds. Power-spectral-density estimates for several representative intervals lead to a formula which extends previous estimates for the fluctuating magnetic fields in the magnetosheath up to 300 Hz, and reveals an apparent change in the frequency dependence of the spectrum somewhere between 0.1 and 1 Hz. The observations are discussed in terms of the two transverse modes of plasma wave propagation that exist at frequencies below the electron gyrofrequency. Arguments are presented suggesting that some high frequency bursts seen in interplanetary space just outside the bow shock are actually precursor waves propagating upstream against the solar wind. F.R.I.

A67-41232

A STUDY OF ENERGETIC SOLAR FLARE X-RAYS.

R. L. Arnoldy, S. R. Kane, and J. R. Winckler (Minnesota, U., School of Physics and Astronomy, Minneapolis, Minn.) Sep. 1967 8 p refs Solar Physics, vol. 2, Sep. 1967, p. 171-178.

A new series of solar flare energetic X-ray events has been detected by an ionization chamber on the OGO 1 and OGO 3 satellites in free space. These X-rays lie in the range 10-50 kev, and a study has been made of their relationship to 3- and 10-cm radio bursts and with the emission of electrons and protons observed in space. The onset times, times of maximum intensity and total duration are very similar for the radio and X-ray emission. Also, the average decay is similar and usually follows an exponential type behavior. However, this good correlation applies most often to the flash phase of flares, whereas subsequent surges of activity from the same eruption may produce microwave emission or further X-ray bursts not closely correlated. An approximate proportionality is found between the total energy content of the X-rays and of the 3- and 10-cm integrated radio fluxes. These measurements suggest that the X-ray and microwave emission have a common energizing process which determines the time profile of both. The recording of electrons greater than 40 kev by the IMP satellite has been found to correlate very well with flares producing X-ray and microwave emission provided the propagation path to the sun is favorable. There is evidence that the acceleration of solar protons may not

be closely associated with the processes responsible for the production of microwaves, X-rays, and interplanetary electrons. The OGO ionization chamber responds to energies (10-50 kev) intermediate between the soft X-rays giving SID disturbances (1-10 kev) and energetic quanta previously measured with balloons (50-500 kev). Proposed source mechanisms should be capable of covering this range of energies including the most energetic quanta occasionally observed. (Author)

A67-41233*

ENERGETIC PROTONS FROM THE SOLAR FLARE OF MARCH 24, 1966.

K. A. Anderson (California, U., Dept. of Physics and Space Sciences Lab., Berkeley, Calif.), S. W. Kahler, and J. H. Primbsch Sep. 1967 13 p refs Solar Physics, vol. 2, Sep. 1967, p. 179-191.

(Contract NAS5-2222)

Observation of ten to 100-mev protons from the solar flare of March 24, 1966, on the University of California scintillation counter on OGO 1. The short rise and decay times observed in the count rates of the 32 channels of pulse-height analysis show that scattering of the protons by the interplanetary field was much less important in this event than in previously observed proton flares. Small fluctuations of the otherwise smooth decay phase may be due to flare protons reflected from the back of a shock front which passed the earth on March 23. M.M.

A68-11011*#

OGO-A MAGNETIC FIELD OBSERVATIONS.

M. Campbell (NASA, Goddard Space Flight Center, Greenbelt, Md.), J. P. Heppner, B. G. Ledley, T. L. Skillman, and M. Sugiura 1 Nov. 1967 55 p refs Journal of Geophysical Research, vol. 72, p. 5417-5471.

Summary of new findings obtained from the initial study of the OGO-1 fluxgate-magnetometer measurements between 4 and 24.5 R sub E. A model magnetic field profile of the cross-sectional structure of the bow shock is derived in terms of the sharpness of the interface, the rise time, and the total time interval occupied by a field pileup at the shock. Superimposed on the average shock structure, two classes of field oscillations are frequently observed. A series of bow shock crossings during the main phase of the Apr. 18, 1965 magnetic storm are found to occur at an abnormally large distance from the earth, principally as a consequence of the strong (20 to 27 gamma) interplanetary field that lowers the Alfvén Mach number to 1.5. The magnetopause in the sunward hemisphere is most typically observed as a smooth transition over a dimension comparable to the ion cyclotron radius. The correlation of negative-bay onsets in the auroral belt with OGO-1 observations on the night side of the earth supports more general morphological arguments that the onset originates within the closed magnetosphere or auroral ionosphere and is not dependent on being triggered by a sudden change in the solar wind plasma or field. At middle latitudes between 5 and 10 R sub E near the midnight time sector, the total field intensity is found to be considerably stronger than predicted by existing field models. M.M.

A68-12172*#

RECENT MEASUREMENTS OF THE MAGNETIC FIELD IN THE OUTER MAGNETOSPHERE AND BOUNDARY REGIONS.

J. P. Heppner (NASA, Goddard Space Flight Center, Greenbelt, Md.) Space Science Reviews, vol. 7, p. 166-190. 16 Oct. 1967 25 p refs (European Space Research Organization, International Colloquium on Auroral and Associated Magnetospheric Phenomena at Very High Latitudes, Stockholm, Sweden, Nov. 16-18, 1965, Paper.

Interpretation of recent (EGO-A) magnetic-field measurements in an early stage of investigation. Initial findings, rather than final results, are given. This information is presented relative to the framework of earlier experiments, thus providing the review aspect of this presentation. Special

attention is given to the boundary regions of the magnetosphere and to the shock-front characteristics. P.V.T.

A68-12548*

OPTICAL ENVIRONMENT ABOUT THE OGO-3 SATELLITE.

C. Wolff (NASA, Goddard Space Flight Center, Greenbelt, Md.) Science, vol. 158, p. 1045, 1046. 24 Nov. 1967 2 p refs

Evaluation of photometric measurements made on the Orbiting Geophysical Observatory (OGO 3), establishing an upper limit to the brightness of the daytime sky. The work is related to attempts to determine why astronauts have such difficulty in viewing stars when the sun is above the horizon (or above the earth's limb). According to these measurements, this brightness is 30 times less than the darkest daytime reported from visual observations taken on Gemini. However, there still remains the danger that this background light (less than 5×10^{-10} to the minus 12th power as bright as the sun) will interfere with observations of the solar corona and zodiacal light. P.V.T.

A68-13469*#

SOME REMARKS ON THE POSITION AND SHAPE OF THE NEUTRAL SHEET.

K. I. Brody (California, U., Inst. of Geophysics and Planetary Physics, Los Angeles, Calif.) and C. T. Russell Journal of Geophysical Research, vol. 72, p. 6104-6106. 1 Dec. 1967 3 p refs NASA supported Research.

Discussion of a relatively simple empirical formula for the location of the neutral sheet in the geocentric solar magnetospheric coordinate system. It is concluded that for properly ordering data taken in the earth's geomagnetic tail, it is necessary to know the direction and velocity of the solar wind outside the tail at the same time as the observations within the tail are being made. Even if the coordinate system used to order the data were rotated with the X axis of the coordinate system pointing in a direction corrected for the nonradial solar wind flow and the associated aberration angle, the neutral sheet does not coincide with the X-Y plane, but rather is a curved surface touching the X-Y plane at the edges of the tail and furthest from the X-Y plane in the center of the tail. An expression is given which should prove useful in studying phenomena in the magnetotail whenever a knowledge of the distance from the neutral sheet is an important parameter. R.B.S.

A68-14098

A REVIEW OF SATELLITE OBSERVATIONS OF V.L.F. PHENOMENA IN THE MAGNETOSPHERE.

M. J. Rycroft (Southampton, U., Dept. of Geophysics, Southampton, England) London, Institution of Electrical Engineers /IEE Conference Publication no. 36/, p. 267-294. 1967 28 p refs In: Conference on M.F., L.F., and V.L.F. Radio Propagation, London, England, Nov. 8-10, 1967, Papers. Conference sponsored by the Electronics Div. of the Institution of Electrical Engineers and the Aerospace, Maritime and Military Systems Group of the Institution of Electronic and Radio Engineers.

Review of natural vlf phenomena observed aboard the Alouette, Injun 3, and OGO satellites in the earth's ionosphere and magnetosphere with emphasis on the frequency-time characteristics of whistlers, discrete emissions, and hiss. Other geophysical occurrences with which these phenomena are associated are discussed, and differences between electric- and magnetic-field measurements of ion-cyclotron whistlers are considered, as are those of noise bands having a lower frequency cutoff at the lower hybrid resonance frequency. Inferences are made concerning the ionic composition and temperature, and their spatial variations. B.B.

A68-17728*#

MAGNETOSPHERIC PROPERTIES DEDUCED FROM OGO-1 OBSERVATIONS OF DUCTED AND NON-DUCTED WHISTLERS.

J. J. Angerami (Stanford U., Stanford Radioscience Lab.,

Stanford, Calif.) and R. L. Smith *Journal of Geophysical Research*, vol. 73, p. 1-20. 1 Jan. 1968 20 p refs
(Contract NASS-2131; Grant NSF GA-775)

The OGO 1 satellite has yielded evidence for both ducted and nonducted modes of whistler propagation in the magnetosphere. Two new types of nonducted whistlers have been identified: the magnetospherically reflected whistler and the Nu whistler. These whistlers have never been observed on the ground. Their unique properties result in part from the presence of ions that permit reflection of whistler-mode energy in the magnetosphere. These phenomena provide a new tool for study of the distribution of ionization in the magnetosphere. Ducted whistlers from OGO 1 have provided the first in situ observations of whistler ducts. Near $L = 3$, the equatorial separations between ducts ranged from 50 to 500 km, and the equatorial thicknesses were about 400 km. The analysis yielded independent experimental support for the diffusive equilibrium model of distribution of ionization along the field lines in the plasmasphere. Some evidence was found of distortion of the magnetic field on the nightside at L is approximately 3, possibly due to oblique incidence of the solar wind on the earth's field. (Author)

A68-17768*#
SIMULTANEOUS IMP 2 AND OGO 1 OBSERVATIONS OF BOW SHOCK COMPRESSION.

J. H. Binsack (Massachusetts Inst. of Tech., Lab. for Nuclear Science and Center for Space Research, Cambridge, Mass.) and V. M. Vasyliunas (Massachusetts Inst. of Tech., Lab. for Nuclear Science and Dept. of Physics, Cambridge, Mass.) *Journal of Geophysical Research*, vol. 73, p. 429-433. 1 Jan. 1968 5 p refs
(Contracts NASS-2053; AT (30-1)2098; Grant NsG-386)

Quantitative investigation of the question of whether large-scale motions of the bow shock that occur during magnetic storms result primarily from the overall compression of the entire magnetosphere magnetosheath system by the enhanced solar-wind dynamic pressure. The investigation was made, using simultaneous observations from the MIT plasma probes on IMP 2 and OGO 1. It was verified that this shock motion occurs nearly simultaneously on the dawn and dusk sides of the magnetosheath. It was possible to use one satellite to monitor the solar-wind pressure, while the other was observing the shock. M.M.

A68-17769*#
HIGH-ENERGY X-RAYS FROM THE SOLAR FLARE OF JULY 7, 1966.

T. L. Cline, S. S. Holt (NASA, Goddard Space Flight Center, Greenbelt, Md.), and E. W. Hones, Jr. (California, U., Los Alamos Scientific Lab., Los Alamos, N. Mex.) *Journal of Geophysical Research*, vol. 73, p. 434-437. 1 Jan. 1968 4 p refs

Measurements of the highest differential energy range of X rays, from 80 Kev to 1 Mev, during the solar flare by July 7, 1966. The spectral shape, time characteristics, and radio correlation for this flare strongly suggest a nonthermal bremsstrahlung origin for the hard X rays. It is noted, however, that the NRL (Naval Research Laboratory) data for the 1959 events have very different spectral and temporal characteristics. It is entirely conceivable that the X-ray production in different flares may be governed by different mechanisms. It is pointed out that the attribution of hard-flare X rays to a thermal model in general would not be justified. M.M.

A68-17771*#
ENERGY FLUXES OF LOW-ENERGY PROTONS AND POSITIVE IONS IN THE EARTH'S INNER RADIATION ZONE.

L. A. Frank and R. L. Swisher (Iowa, U., Dept. of Physics and Astronomy, Iowa City, Iowa) *Journal of Geophysical Research*, vol. 73, p. 442-444. 1 Jan. 1968 3 p refs
(Contracts NASS-2054; Nonr-1509(06); Grant NsG 233-62)

Initial survey of measurements of the differential energy spectra of positive ions in the earth's inner radiation zone

with an array of sensitive electrostatic analyzer borne on the earth satellite OGO 3. On the basis of the present findings of upper limits for these energy fluxes over a large region of the inner zone that are less by factors of 10 to 100 in comparison with the energy fluxes reported by Freeman, it is considered likely that energy fluxes of 500-ev to 1-Mev positive ions of about 50 ergs/sq cm-sec-ster are not a feature of the inner radiation zone. M.M.

A68-19744*
CONTRACTION OF THE PLASMASPHERE DURING GEOMAGNETICALLY DISTURBED PERIODS.

H. C. Brinton, M. W. Pharo, III, and H. A. Taylor, Jr. (NASA, Goddard Space Flight Center, Lab. for Atmospheric and Biological Sciences, Greenbelt, Md.) *Journal of Geophysical Research*, vol. 73, p. 961-968. 1 Feb. 1968 8 p refs

Direct measurements of the thermal positive ions of hydrogen and helium have been obtained from positive ion mass spectrometers aboard OGOs 1 and 3. Observations made during 1965 and 1966 show distributions of H and He extending to altitudes as great as 40,000 km, corresponding to a magnetospheric coordinate of $L = 8$. The outer boundary of the plasmasphere is characterized by an abrupt decrease in the ion concentration. This boundary or plasmopause, defined by the reduction of H concentration to 5×10 ions/cu cm or less, is often quite sharp, with decreases in ion concentration of as much as an order of magnitude occurring within 250 km. The position of the plasmopause is observed to move inward and outward from the earth in an inverse correlation with the planetary magnetic activity index K_p , indicating significant large-scale expansion and contraction of the plasmasphere during periods of agitated magnetospheric conditions. The apparent correlation between measurements of the hydrogen ion boundary and the knee whistler evidence of the plasmopause suggests that the mechanism responsible for the depletion of the ionization is effective along the lines of the magnetic field, extending well into the earth's inner atmosphere, to 1000 km and below. (Author)

A68-19752*
INTERPRETATION OF AURORAL HISS MEASURED ON OGO 2 AND AT BYRD STATION IN TERMS OF INCOHERENT CERENKOV RADIATION.

T. S. Jorgensen (Stanford U., Stanford Radioscience Lab., Stanford, Calif.) *Journal of Geophysical Research*, vol. 73, p. 1055-1069. 1 Feb. 1968 15 p refs
(Contract NASS-3093; Grant NSF GA-214)

Observation of a wideband noise (termed auroral hiss) at low and very low frequencies at ground-based stations and on satellites at high magnetic latitudes. A model for a region in space in which the auroral hiss is believed to be generated is investigated, and it is indicated that the amount of power generated in this region is comparable to the observed power. It is concluded that the auroral hiss can be generated by incoherent Cerenkov radiation from electrons having energies of about 1 kev. B.B.

A68-22450*
ENERGETIC SOLAR FLARE X-RAYS OBSERVED BY SATELLITE AND THEIR CORRELATION WITH SOLAR RADIO AND ENERGETIC PARTICLE EMISSION.

R. L. Arnoldy, S. R. Kane, and J. R. Winckler (Minnesota, U., School of Physics and Astronomy, Minneapolis, Minn.) *Astrophysical Journal*, vol. 151, Pt-1, p. 711-736. Feb. 1968 26 p refs
(Contract NASS-2071)

Detection of about 30 solar-flare X-ray bursts by the OGO-1 and OGO-3 spacecraft between Sept. 5, 1964, and June 20, 1966. These energetic X-ray bursts have been correlated with 3- and 10-cm radio-emission and solar-flare electron and proton events measured in space. A proportionality is observed between the time-integrated X-ray and radio fluxes, and for a given flare the rise time, decay time, and total duration of the radio and X-ray bursts are similar. It

is shown that the results are consistent with a source in the flare region consisting of an active volume in a magnetic field containing hot or energetic electrons which lose energy predominantly by collision with a much cooler gas and produce X-rays by bremsstrahlung. The similarity of decay and proportionality between the X-rays and microwaves suggests that the same electrons might produce both emissions.
P.V.T.

A68-25969*#

AURORAL ELECTRON ENERGY SPECTRA.

K. W. Ogilvie (NASA, Goddard Space Flight Center, Greenbelt, Md.) *Journal of Geophysical Research*, vol. 73, p. 2325-2332. 1 Apr. 1968 8 p refs

Presentation of observations of differential energy spectra of electrons above a weak aurora at Fort Churchill, Canada. Measurements were made at altitudes between 180 and 250 km using an electrostatic analyzer and channeltron detector over the energy range 10 eV to 10 keV. Below about 100 eV scattering from the rocket was pronounced. Although between 1 and 10 keV the spectra can be well represented by power-exponential functions with maxima in the region 1 to 4 keV, between 1 keV and 100 eV the flux rises toward lower energies. An estimate of the number of secondaries in the energy region 100 eV to 1 keV generated by the higher energy primaries is made, and it proves to be too small to explain the observed electron flux at low energies. This flux is shown to vary so little with altitude that it is likely to be due to ambient electrons accelerated by electric fields.
Author

A68-26625#

A PROPOSED MODEL FOR THE INTERNATIONAL GEOMAGNETIC REFERENCE FIELD, 1965.

J. C. Cain, S. J. Hendricks, W. V. Hudson, and R. A. Langel *Journal of Geomagnetism and Geoelectricity*, vol. 19, no. 4, p. 335-355. 1967 21 p refs

Description of a current model of the main geomagnetic field by a series of 120 spherical harmonic coefficients and their first and second time derivatives from epoch 1960. This model was derived from a sample of all magnetic-survey data available for the interval from 1900 to 1964, plus a recent global distribution of preliminary total-field observations from the OGO 2 (1965-81A) spacecraft for epoch 1965.8. A duplicate data selection was made, and the resulting field model was compared with the original one to help evaluate the minimum error. It was noted that the rms difference between the two models was about 30 gamma in the force components, 0.04 deg in dip, and 0.3 deg in declination at the earth's surface for 1965.0.
M.F.

A68-27615*

A SOLAR AND GALACTIC COSMIC RAY SATELLITE EXPERIMENT.

W. E. Althouse, T. H. Harrington (Analog Technology Corp., Pasadena, Calif.), E. C. Stone, and R. E. Vogt (California Inst. of Tech., Pasadena, Calif.) Feb. 1968 9 p *Inst. of Electrical and Electronics Engineers, Nuclear Science Symposium, 14th, Los Angeles, Calif., Oct. 31-Nov. 2, 1967. IEEE Transactions on Nuclear Science*, vol. NS-15, p. 229-237.
(Contract NAS5-9312; Grant NsG-426)

Description of the cosmic-ray measuring device for the OGO-F spacecraft. An experiment is discussed which involves three charged-particle detector systems which measure the spectra and chemical composition of galactic and solar cosmic rays over selected energy intervals. Two of the detector systems, the Delta E-Range and Delta E-Cerenkov telescopes, will measure the galactic flux and smaller solar-flare fluxes, while a third detector system, the Flare telescope, will measure larger fluxes.
B.B.

A68-27616*

A LOW ENERGY SOLAR COSMIC RAY EXPERIMENT FOR OGO-F.

D. W. Burtis, A. J. Masley, P. R. Satterblom, and M. H.

Wolpert (McDonnell Douglas Corp., Douglas Aircraft Co., Missile and Space Systems Div., Space Science Dept., Santa Monica, Calif.) Feb. 1968 4 p *Inst. of Electrical and Electronics Engineers, Nuclear Science Symposium, 14th, Los Angeles, Calif., Oct. 31-Nov. 2, 1967. IEEE Transactions on Nuclear Science*, vol. NS-15, p. 238241.
(Contract NAS5-9324)

Discussion of the Douglas OGO-F low-energy solar cosmic ray experiment which measures the differential energy spectrum of 5 to 80-Mev protons and 18 to 160 Mev alphas, using two double-diffused, totally depleted silicon diodes. The pulse-amplitude discrimination system, the data multiplexing scheme, and the in-flight calibrator are considered.
B.B.

A68-28348*#

A SURVEY OF LOW-ENERGY ELECTRONS IN THE EVENING SECTOR OF THE MAGNETOSPHERE WITH OGO-1 AND OGO-3.

V. M. Vasyliunas (Massachusetts Inst. of Tech., Lab. for Nuclear Science and Dept. of Physics, Cambridge, Mass.) 1 May 1968 46 p refs *Journal of Geophysical Research*, vol. 73, p. 2839-2884.
(Contracts NAS5-2053; AT(30-1)-2098; Grant NsG-386)

Investigation of the low-energy electron population in the magnetosphere within the local-time range from approximately 17 to approximately 22 hours, using observations of electrons with energies from 125 eV to approximately 2 keV, obtained with the OGO 1 satellite, and of electrons with energies from 40 eV to approximately 2 keV, obtained with the OGO 3 satellite. Intense fluxes of these electrons are confined to a spatial region known as the plasma sheet, which is an extension of the magnetotail plasma sheet discovered by Vela satellites and is identified with the soft-electron band first detected by Gringauz. Weak or no electron fluxes are found between the inner boundary of the plasma sheet and the outer boundary of the plasmasphere. Detection of the very high ion densities within the plasmasphere gives positions for its boundary in good agreement with other determinations. During periods of magnetic-bay activity, the plasma sheet extends closer to the earth; the inner boundary of the plasma sheet is then found at equatorial distances of six to eight earth radii. Within the plasma sheet, the electron population is characterized by number densities from 0.3 to 30 cm⁻³ to the -3rd power and mean energies from 50 to 1600 eV and higher, with a strong anticorrelation between density and mean energy. It is pointed out that the lower energies and higher densities tend to occur during periods of geomagnetic disturbance.
R.B.S.

A68-29421*

MAGNETOSPHERE PLASMA PROPERTIES DURING A PERIOD OF RISING SOLAR ACTIVITY, OGO-3.

R. C. Sagalyn and M. Smiddy (USAF, Office of Aerospace Research, Cambridge Research Labs., Bedford, Mass.) Amsterdam, North-Holland Publishing Co., 1968 11 p refs In: *Space Research 8, Proceedings of the tenth COSPAR Plenary Meeting, Imperial Coll. of Science and Technology, London, England, Jul. 24-29, 1967, p. 139-149. NASA supported research.*

The flux, energy distribution, and concentration of ions and electrons were investigated by means of two omnidirectional plasma probes flown on the OGO 3 satellite launched June 7, 1966. The measurements cover the energy range 0 to 1 keV over the altitude region 1.1 to 20 earth radii. In the analysis, emphasis is placed on results obtained in the transition region, altitudes where whistler propagation may be significant, and during periods of high solar activity. The concentration of thermal charged particles decreases with height from 80,000 cm⁻³ to the -3rd power at perigee to a minimum of 5 cm⁻³ to the -3rd power at apogee. The most rapid changes in density with altitude occur between perigee 7 earth radii. The altitude of maximum density change with height is dependent both on magnetic latitude and position of the satellite with respect to the earth-sun line. The flux of nonthermal charged particles varying between 1

million and 3×10 to the 9th power cm to -2nd power/sec are correlated with the magnetic B and L parameters. Following the solar and magnetic storm which commenced Sept. 2, 1966, the particle flux in the energy range 25 ev to 1 kev decreased by a factor of four in the transition region accompanied by an increase in mean particle energy.

(Author)

A68-29457*

ZODIACAL DUST MEASUREMENTS IN CIS-LUNAR AND INTERPLANETARY SPACE FROM OGO-3 AND MARINER 4 EXPERIMENTS BETWEEN JUNE AND DECEMBER 1966.

W. M. Alexander and J. L. Bohn (Temple U., Philadelphia, Pa.) Amsterdam, North-Holland Publishing Co., 1968 7 p refs In: Space Research 8, Proceedings of the tenth COSPAR Plenary Meeting, Imperial Coll. of Science and Technology, London, England, Jul. 24-29, 1967, p. 489-495.

New measurements of the flux of interplanetary dust particles in cislunar and interplanetary space have been obtained from experiments on the OGO 3 and Mariner 4 spacecraft. The major portion of the OGO 3 measurement was made between 50,000 and 110,000 km from the surface of the earth. The 1966 Mariner 4 measurement was made over a heliocentric distance of 1.1 to 1.25 AU. The OGO 3 measurement represents the first measurement in cislunar space since Pioneer 1 and the only measurement which repeatedly sampled the cislunar dust particle flux over a considerable period of time. For the first time, the Mariner 4 measurement provides a second data sample over the same heliocentric distance in the zodiacal dust cloud by the same instrumentation. The results of these measurements are interpreted in terms of the recent hypervelocity calibration data and thermal effect studies and then compared to the previous satellite and space probe measurements. (Author)

A68-29467*

RESULTS OF STUDIES OF THERMAL GRADIENT EFFECTS ON CERAMIC TRANSDUCER SENSORS USED IN COSMIC DUST EXPERIMENTS.

W. M. Alexander, J. L. Bohn, and W. F. Simmons (Temple U., Philadelphia, Pa.) Amsterdam, North-Holland Publishing Co., 1968 8 p refs In: Space Research 8, Proceedings of the tenth COSPAR Plenary Meeting, Imperial Coll. of Science and Technology, London, England, Jul. 24-29, 1967, p. 588-595.

An extensive study of thermal gradient and temperature effects on ceramic transducer sensors used in cosmic dust experiments on rockets, satellites, and deep space probes has been conducted. The transducers used on the tests were sensors from experiments on Explorer 1, Pioneer 1, Vanguard 3, Explorer 8, Mariner 2, Mariner 4, OGOs 1, 2, and 3, Surveyor Lander and AIMP-E spacecraft. The sensors were subjected to temperatures over a range of $-20 \text{ C} < \text{or} = \text{to} t < \text{or} = \text{to} +46 \text{ C}$, and both positive and negative thermal gradients ($t \text{ sub } \text{gd}$) over a range of $0.01 \text{ C/min} < \text{or} = \text{to} t \text{ sub } \text{gd} < \text{or} = \text{to} 2.2 \text{ C/min}$. More than 350 transducer thermal cycles were conducted using the various transducer types of the above space experiments and simulating the different thermal conditions experienced by the sensors. The data from these tests show that thermal noise from the transducers has not been a major source of false data from the above experiments. The results of these new studies are discussed and interpreted with respect to the data from all previous dust particle experiments and other thermal studies. (Author)

A68-29468*

RESULTS OF RECENT MICROPARTICLE HYPERVELOCITY IMPACT STUDIES RELATED TO SENSORS OF COSMIC DUST EXPERIMENTS.

W. M. Alexander, J. L. Bohn, and A. Wever (Temple U., Philadelphia, Pa.) Amsterdam, North-Holland Publishing Co., 1968 10 p refs In: Space Research 8, Proceedings of the tenth COSPAR Plenary Meeting, Imperial Coll. of Science and Technology, London, England, Jul. 24-29, 1967, p. 596-605.

Study of the response of sensors used in cosmic-dust experiments to hypervelocity impacts of microparticles. Hypervelocity experiments show that the sensor response is related in a nonlinear fashion to the velocity of the impacting microparticles. The results of these experiments are used to present a new interpretation of the data from previous satellite experiments, in particular, those on Explorer 1, Explorer 8, and Vanguard 3, which have provided more than 90% of the data from experiments using microphone sensors.

F.R.L.

A68-31481*#

PROTON GYROFREQUENCY BAND EMISSIONS OBSERVED ABOARD OGO 2.

W. E. Blair, T. L. Crystal, B. P. Ficklin, H. Guthart, and T. J. Yung (Stanford Research Inst., Menlo Park, Calif.) 1 Jun. 1968 5 p refs Journal of Geophysical Research, vol. 73, p. 3592-3596.

(Contract NAS5-3093)

Discussion of preliminary results of OGO 2 satellite measurements of electromagnetic emissions in the vicinity of the proton gyrofrequency. The emissions were analyzed from two sources of data: the sweep-frequency receiver PCM data, showing the noise amplitude-frequency spectrum, and the Rayspan special-purpose data, showing the frequency-time spectrum. The emissions are characterized by a noise band whose sharp lower cutoff frequency is within 10% of the local proton gyrofrequency and whose upper cutoff frequency varies with magnetic latitude and can be as high as an order of magnitude above the proton gyrofrequency. M.F.J.

A68-31924#

THE 23 AND 28 MAY 1967 SOLAR COSMIC RAY EVENTS.

A. D. Goedeke and A. J. Masley (McDonnell Douglas Corp., Douglas Aircraft Co., Missile and Space Systems Div., Space Science Dept., Santa Monica, Calif.) May 1968 21 p COSPAR, Plenary Meeting, 11th, Tokyo, Japan, May 9-21, 1968. Paper.

(Contract NSF C-393)

Description of ground-based riometer data on the May 23 and 28, 1967, solar cosmic-ray events which were also observed in space by particle detectors on the IMP-F, OGO-III, and 1963-38C satellites. The May 23 event is the first large event since 1962 originating in a flare considerably east of the central meridian. This solar cosmic-ray event may be associated with several northeast flares in the McMath Plage Region 8818, including one of importance 3B at N27 E25, beginning at 1836 UT on May 23. An event on May 28 followed, beginning at 0630 UT and reaching over 3 db. This event was associated with a 3B flare at N28 W33 beginning at 0527 UT on May 28. The rapid rise to maximum absorption and exponential decay is typical of events originating in flares west of the central meridian.

M.M.

A68-34245*

ON THE DISTRIBUTIONS OF LOW-ENERGY PROTONS AND ELECTRONS IN THE EARTH'S MAGNETOSPHERE.

L. A. Frank (Iowa, U., Dept. of Physics and Astronomy, Iowa City, Iowa) New York, Reinhold Book Corp., 1968 21 p refs In: Earth's Particles and Fields, Proceedings of the NATO Advanced Study Inst., Freising, West Germany, Jul. 31-Aug. 11, 1967. Inst. supported by the North Atlantic Treaty Organization, the Advanced Research Projects Agency, the Office of Aerospace Research of the U.S. Air Force, the Research Office of the U.S. Army, the Defense Atomic Support Agency, and the Office of Naval Research of the U.S. Navy.

(Grant NGL-16-001-002)

Summary of the status of low-energy charged-particle observations within the earth's magnetosphere during 1965. The results provide a framework for discussions of the complex spatial distributions and temporal variations of

low-energy proton and electron intensities which have been detected and surveyed within the earth's radiation zones and their environs. B.B.

A68-34540*

A SOLID STATE DETECTOR EXPERIMENT FOR ELECTRON MEASUREMENTS ON OGO-F.

J. H. Trainor and D. J. Williams (NASA, Goddard Space Flight Center, Greenbelt, Md.) Jun. 1968 4 p refs IEEE Transactions on Nuclear Science, vol. NS-15, p. 562-565. (Scintillation and Semiconductor Counter Symposium, 11th, Washington, D.C., Feb. 28-Mar. 1, 1968.

Description of a solid-state detector system developed for a polar orbital flight on an Orbiting Geophysical Observatory to perform measurements of the electron flux and spectra above 35 KeV, for both precipitating and locally mirroring electrons, and also atmospheric backscatter. The physical need and the design requirements of such an experiment and its electronic realization, including the methods of monitoring detector and electronic performance in flight, are discussed. V.Z.

A68-35397*

THE FLUX OF METEORS AND MICROMETEORIODS IN THE NEIGHBORHOOD OF THE EARTH.

C. S. Nilsson and R. B. Southworth (Smithsonian Institution, Smithsonian Astrophysical Observatory, Cambridge, Mass.) Dordrecht, D. Reidel Publishing Co. 1968 8 p In: Physics and Dynamics of Meteors, International Astronomical Union, Symposium, Tatranska Lomnica, Czechoslovakia, Sep. 4-9, 1967, Proceedings. p. 280-287. International Astronomical Union Symposium no. 33, (Contract NAS5-11007; Grant NSR-09-015-033)

Results of some measurements of the cumulative influx of meteors and micrometeoroids during the period from 1965 to 1967. Analysis of measurements of radio-meteor rates made at Havana, Ill., indicate that the mean cumulative influx I of meteors/sqm/sec/2 pi ster from September 1965 to December 1966 is best described by the equation $\log I = -14.1 - 1.05 \log m$, where m is the lower mass limit in grams. Analysis of 700 hr of data from a micrometeoroid detection system on the OGO 2 satellite reveals no micrometeoroid events. Thus, to a probability of 0.86, the average flux of particles of mass greater than 10 to the minus 12th power g is calculated to be less than 6×0.001 particles/sqm/sec/2 pi ster. R.A.F.

A68-35480*

THE OBSERVATION OF 10-50 KEV SOLAR FLARE X-RAYS BY THE OGO SATELLITES AND THEIR CORRELATION WITH SOLAR RADIO AND ENERGETIC PARTICLE EMISSION.

R. L. Arnoldy, S. R. Kane, and J. R. Winckler (Minnesota, U., School of Physics and Astronomy, Minneapolis, Minn.) Dordrecht, D. Reidel Publishing Co. 1968 20 p refs In: Structure and Development of Solar Active Regions, International Astronomical Union, Symposium, Budapest, Hungary, Sep. 4-8, 1967, Proceedings. p. 490-509. International Astronomical Union Symposium no. 35, (Contract NAS5-2071)

Summary of the results of 70 observations of energetic solar-flare X-ray bursts by large ionization chambers on the OGO satellites in space, together with a discussion of the relationship of these events to microwave solar radio bursts and to observations of energetic electrons and protons ejected into space by the same flares. A strong correlation is shown to exist between X-ray bursts and interplanetary solar-flare electrons observed by satellites. This correlation is weak, however, for solar protons. A strong propagation asymmetry is inferred for solar-flare electrons along the spiral interplanetary magnetic field. R.A.F.

A68-37114*

THERMAL ION STRUCTURE OF THE PLASMAPAUSE.

H. C. Brinton, R. A. Pickett, and H. A. Taylor, Jr. (NASA,

Goddard Space Flight Center, Lab. for Atmospheric and Biological Sciences, Greenbelt, Md.) Jul. 1968 11 p refs Planetary and Space Science, vol. 16, p. 89-909.

Determination of the distribution of thermal positive ions of hydrogen and helium in the magnetosphere from the first Orbiting Geophysical Observatory (OGO 1) ion mass spectrometer measurements. The distribution is strongly controlled by the geomagnetic field, its chief feature being a region of toroidal form, the plasmasphere, bounded approximately by the $L = 4.5$ shell within which the ion concentration decreases slowly with increasing altitude from an initial value of 3000 ions/cu cm at 2000 km. At the boundary of this region, which is compressed during periods of high magnetic activity, a sharp decrease in the ion concentration by a factor of ten or more for an altitude increase of less than one earth radius is observed, leading to a concentration beyond the boundary of less than 100 ions/cu cm. An apparent diurnal expansion in the plasma distribution is centered at 2000 hr. Over most of the altitude range within the plasmasphere the concentrations of $H(+)$ and $He(+)$ are observed in a constant ratio of 300:1, indicating departure from simple diffusive equilibrium. M.G.

A68-37148*

SOLAR FLARE INJECTION AND PROPAGATION OF LOW ENERGY PROTONS AND ELECTRONS IN THE EVENT OF 7-9 JULY, 1966.

S. W. Kahler (California, U., Dept. of Physics and Space Sciences Lab., Berkeley, Calif.), R. P. Lin, and E. C. Roelof (Boeing Co., Boeing Scientific Research Labs., Seattle, Wash.; NASA, Goddard Space Flight Center, Greenbelt, Md.) Jul. 1968 23 p refs Solar Physics, vol. 4, p. 338-360. (Contracts NAS5-2989; NAS5-2222; NAS5-9077)

Simultaneous satellite observations of the solar particle event on July 7 to 9, 1966 are utilized to show that large spatial gradients are present in the fluxes of 0.5 to 20 MeV protons and > 45 keV electrons. The event is divided into three parts: the ordinary diffusive component, the halo, and the core. The core corotates with the interplanetary field, and therefore it and the surrounding halo are interpreted as spatial features which are connected by the interplanetary magnetic field lines to the vicinity of the flare region. Upper limits to the interplanetary transverse diffusion coefficient for 4 to 20 MeV protons at 1 AU are derived from the width of the halo. These are at least two orders of magnitude less than the parallel diffusion coefficient for the same energy particles. It is argued that the observed flux variations cannot be explained by an impulsive point source injection for any physically reasonable diffusion model. The geometry of the injection mechanism is discussed and it is suggested that some temporary storage of the flare particles occurs near the sun. (Author)

A68-37940#

RECENT RESEARCH ON THE MAGNETOSPHERIC PLASMAPAUSE.

D. L. Carpenter (Stanford U., Stanford Radioscience Lab., Stanford, Calif.) Jul. 1968 7 p refs Conjugate Point Symposium, Boulder, Colo., Jun. 13-16, 1967. Radio Science, vol. 3, p. 719-725. (Grants NSF GA-775; NSF GA-214; AF-AFOSR-783-67)

An investigation is made into the nature of the plasmapause - a three-dimensional field aligned boundary that divides the closed field-line portion of the earth's magnetosphere into two physically distinct regions. The boundary is asymmetric, usually exhibiting a minimum geocentric range near dawn and a maximum near dusk under conditions of moderate but steady geomagnetic agitation ($k_{sub} p = 2$ to 4). The mean equatorial radius of the plasmapause is typically about 4 $R_{sub} E$, but it may vary from about 5.5 $R_{sub} E$ during periods of extreme quiet to the range 2 to 3 $R_{sub} E$ during great storms. The approximately corotating thermal plasma within the boundary exhibits two types of radial drift motions. These may be visualized as: (1) slow breathing motions that follow the radial variations in a fixed, asymmetric boundary, (2) more rapid, transient (1 to 2 hr) motions that

occur when the boundary position varies, as is the case during a polar substorm. The plasmopause involves an abrupt (possibly on a scale of a few kilometers) change in electron density, in tube electron content above 1000 km, and possibly in plasma bulk velocity and mean thermal energy. Many wave propagation phenomena of conjugate interest are strongly affected by the presence of the plasmopause. For example, satellites moving poleward through the boundary observe a cutoff in whistlers propagating from the conjugate hemisphere; a decrease in the intensity of fixed-frequency VLF signals propagating upward, and dramatic changes in VLF noise such as the lower hybrid resonance (LHR) noise. In ground recordings made at Eights (L approximately 4) and Byrd (L approximately 7) in the austral winter, four distinct magnetospheric regions of propagation are identified. (Author)

A68-38423*
MODEL OF MAGNETOSPHERIC TEMPERATURE DISTRIBUTION.

H. G. Mayr and H. Volland (NASA, Goddard Space Flight Center, Aeronomy Branch, Greenbelt, Md.) 1 Aug. 1968 8 p refs Journal of Geophysical Research, vol. 73, p. 4851-4858.

In the magnetosphere, the equation of heat flux parallel to the magnetic field must be modified because of the low electron concentration and large mean free path. This leads to a density-dependent heat conductivity that is decreased such that the high temperatures in the magnetosphere observed by Serbu and Maier (1966) can be explained. In the upper magnetosphere, turbulent heat transfer in accordance with Bohm's diffusion coefficient can account for heat fluxes on the order of 10 to the -10th power erg/sq cm-sec (6.1×10 eV/sq cm-sec) across the magnetic field. Such heat fluxes are consistent with ion-electron temperature differences of $T_{\text{sub } i} - T_{\text{sub } e} = 10,000$ K also discovered by Serbu and Maier. This direct thermal energy input is negligible for the energy balance of the magnetosphere when compared with the heat fluxes .001 to .01 erg/sq cm-sec generated through nonlocal heating by fast ionospheric electrons. (Author)

A68-38428*
UNDUCTED WHISTLER EVIDENCE FOR A SECONDARY PEAK IN THE ELECTRON ENERGY SPECTRUM NEAR 10 keV.

R. M. Thorne (Stanford U., Stanford Radioscience Lab., Stanford, Calif.) 1 Aug. 1968 10 p refs Journal of Geophysical Research, vol. 73, p. 4895-4904. (Grants AF-AFOSR-783-67; NsG-174; NsG-05-020-088)

Resonant particle interactions between unducted, magneto spherically reflected (MR) whistler-mode radiation and the ambient plasma have been investigated. Because the frequencies of such waves are small compared to the local electron gyrofrequency and the wave normals practically perpendicular to the magnetic field, Landau electron interactions dominate. Resonant ion energies are well above 1 MeV and can consequently be ignored. The upper and lower frequency cutoffs, as well as the high-frequency region of growth of the multiple bounce MR traces observed near $L = 2.5$, can be accounted for by an ambient electron distribution that has a secondary peak in the vicinity of 10 keV. (Author)

A68-38439*
RESPONSE OF IONOSPHERIC AND EXOSPHERIC ELECTRON CONTENTS TO A PARTIAL SOLAR ECLIPSE.

R. B. Fritz, J. K. Hargreaves (ESSA, Research Labs., Boulder, Colo.), and E. R. Schiffmacher 1 Aug. 1968 5 p refs Journal of Geophysical Research, vol. 73, p. 4994-4998. (NASA Order S-20614-G; NASA Order R-101)

Discussion of observations made using radio beacon transmitters aboard the OGO 1 satellite at the time of the partial solar eclipse of May 9, 1967, for which the maximum obscuration near the peak of the ionospheric F2 region was

41%. Results obtained indicate a relative movement of ionization from topside to bottomside during the eclipse, which is consistent with scatter-radar data of Evans (1965) and the topside-sounder results of King et al (1967). The noted change of exospheric content during and shortly after the eclipse is also discussed. R.B.S.

A68-41420*
DIFFERENTIAL ENERGY SPECTRA AND INTENSITY VARIATION OF 1-20 MEV/NUCLEON PROTONS AND HELIUM NUCLEI IN INTERPLANETARY SPACE (1964-66).

C. Y. Fan, G. Gloeckler (Maryland, U., Dept. of Physics, College Park, Md.), B. McKibben, K. R. Pyle, and J. A. Simpson (Chicago, U., Enrico Fermi Inst. for Nuclear Studies and Dept. of Physics, Chicago Ill.) 15 May 1968 5 p refs /International Union of Pure and Applied Physics, International Conference on Cosmic Rays, 10th, Calgary, Canada, Jun. 19-30, 1967. Canadian Journal of Physics, vol. 46, Pt-3, p. S498-S502.

(Contracts NAS2-1758; AF 49(638)-1642; Grants NGL-14-001-006; NsG-179-61)

Measurements made in interplanetary space with a Delta E range telescope on the OGO 1 and OGO 3 satellites and on the Pioneer 7 space probe showed that protons and helium nuclei in the energy range 1 to 20 MeV/nucleon are present during quiet times in late 1964; in May, October and November 1965; and in August 1966. The intensities for both proton and helium nuclei are found to decrease with increasing energies. The spectra join those of the particles above 20 MeV/nucleon, which are known to be of galactic origin. For both protons and helium nuclei, the fluxes were higher in the period of minimum solar modulation in 1965 than in 1964. While in 1966 the helium flux decreased to its 1964 level, the proton flux showed a further increase over this period. It is believed that most of the particles observed during the period of minimum solar modulation were of galactic origin. As solar activity increases again, it seems that to the galactic low-energy fluxes, particularly for protons, there is added a steady contribution of solar origin. (Author)

A68-41421*
MEASUREMENT AND INTERPRETATION OF THE ISOTOPIC COMPOSITION OF HYDROGEN AND HELIUM COSMIC-RAY NUCLEI BELOW 75 MeV/NUCLEON.

D. E. Hagge (NASA, Manned Spacecraft Center, Houston, Tex.), F. B. McDonald (NASA, Goddard Space Flight Center, Greenbelt, Md.), and J. P. Meyer 15 May 1968 6 p refs /International Union of Pure and Applied Physics, International Conference on Cosmic Rays, 10th, Calgary, Canada, Jun. 19-30, 1967. Canadian Journal of Physics, vol. 46, Pt-3, p. S503-S508.

Measurement of hydrogen and helium isotopic abundance ratios and examination of the results of a propagation calculation studying the bearing of different source and propagation models on the two ratios. The creation of deuterons and He-3 through fragmentation of cosmic-ray and interstellar He-4 nuclei, and proton-proton reactions are investigated in order to understand the energy dependence of the hydrogen and helium ratios. A Monte Carlo technique is used to propagate the cosmic-ray protons and He-4 nuclei from the source to earth. Ionization loss, energy dependence of the cross sections, and reaction kinematics are taken into account, but elastic scattering, acceleration in space, and solar modulation are not. It is concluded that the present results completely rule out a total-energy, and favor a kinetic-energy source power spectrum. R.E.L.

A68-41427*
SEARCH FOR LOW-ENERGY INTERPLANETARY POSITRONS.

T. L. Cline (NASA, Goddard Space Flight Center, Greenbelt, Md.) and E. W. Hones, Jr. (California, U., Los Alamos Scientific Lab., Los Alamos, N. Mex.) 15 May 1968 3 p

refs /International Union of Pure and Applied Physics, International Conference on Cosmic Rays, 10th, Calgary, Canada, Jun. 19-30, 1967./ Canadian Journal of Physics, vol. 46, Pt-3, p. S527-S529.

Preliminary results of an experiment designed to detect and measure the intensity of interplanetary positrons of energy 0 to 3 MeV with the satellites OGO 1 and OGO 3 are outlined. Evidence for a statistically significant counting rate of detected positrons is presented, and the possibility that these particles represent a true primary component rather than a background effect, such as cosmic-ray induced secondaries in the detector, is considered. It is shown that the apparent intensity of low-energy positrons, assuming that value derived from their counting rate, would be consistent with an equilibrium charge ratio. This result would not be predicted with mechanisms involving the ionization of matter or the acceleration of electrons, but would be consistent with a strongly energy-dependent galactic trapping parameter allowing meson-decay electrons to slow down in great abundance or with the existence of an independent source. (Author)

A68-41431*

THE COMPOSITION OF LOW-ENERGY COSMIC RAYS IN 1965.

V. K. Balasubrahmanyam, D. E. Hagge (NASA, Manned Spacecraft Center, Houston, Tex.), and F. B. McDonald (NASA, Goddard Space Flight Center, Greenbelt, Md.) 15 May 1968 5 p /International Union of Pure and Applied Physics, International Conference on Cosmic Rays, 10th, Calgary, Canada, Jun. 19-30, 1967./ Canadian Journal of Physics, vol. 46, Pt-3, p. S539-S543.

Primary cosmic-ray energy spectra and charge composition were measured during the 1965 period of solar modulation minimum. A dE/dx vs E type of scintillator-photomultiplier detector on board the eccentric-orbiting NASA spacecraft OGO 1 was used. The charge composition was measured through neon over an energy range of 25 to 200 MeV/nucleon, depending upon the specific component. The spectra for all groups are nearly flat during this time, with the oxygen flux at about 0.005 nucleus/(sq m-ster-sec-MeV/nucleon). The relative abundances found are Li, 0.27; Be, 0.11; B, 0.37; C, 1.20; N, 0.30; O, 1.00; F, < 0.01; and Ne, 0.12. An L/M ratio of 0.30 + or - 0.06 is found. (Author)

A68-41434*

THE LOW-ENERGY COSMIC-RAY NUCLEI AND THEIR PROPAGATION IN INTERSTELLAR SPACE.

G. M. Comstock (Chicago, U., Enrico Fermi Inst. for Nuclear Physics and Dept. of Physics, Chicago, Ill.) 15 May 1968 4 p refs /International Union of Pure and Applied Physics, International Conference on Cosmic Rays, 10th, Calgary, Canada, Jun. 19-30, 1967./ Canadian Journal of Physics, vol. 46, Pt-3, p. S553-S556.

(Contract AF 49(638)-1642; Grants ; NGL-14-001-006; NsG-179-61)

The differential energy spectra of the cosmic-ray nuclei helium, carbon, nitrogen, and oxygen above 30 MeV/nucleon, boron, neon, magnesium, and silicon above 50 MeV/nucleon, and the iron group above 100 MeV/nucleon, measured in October to December 1964 and May to June 1965 by the University of Chicago charged-particle telescope on board the OGO 1 satellite (Comstock et al., 1966), have been corrected to take account of the effective depletion depth of the gold-silicon solid-state detectors used for rate-of-energy-loss measurement. Additional data from October to December 1965 are included. The magnitudes and relative shapes of the spectra deduced by extrapolation to nearly interstellar space place important constraints on the allowed modes of interstellar propagation for these nuclei. Two-component models are shown to account for most of the observed properties of the interstellar cosmic-ray nuclei. (Author)

A68-41562*

DIRECT MEASUREMENTS OF GEOMAGNETIC

CUTOFFS FOR COSMIC-RAY PARTICLES IN THE LATITUDE RANGE 45 DEG TO 70 DEG USING BALLOONS AND SATELLITES.

R. G. Bingham (Boeing Co., Seattle, Wash.), J. F. Ormes, D. M. Sawyer, and W. R. Webber (Minnesota, U., School of Physics and Astronomy, Minneapolis, Minn.) 15 May 1968 4 p refs /International Union of Pure and Applied Physics, International Conference on Cosmic Rays, 10th, Calgary, Canada, Jun. 19-30, 1967./ Canadian Journal of Physics, vol. 46, Pt-4, p. S1078-S1081.

Analysis of the results of direct measurement by balloon (Weber and Ormes, 1965) and satellite (Bingham et al., 1966) of the quiet-time cutoff rigidities for cosmic-ray particles. The measured cutoffs are seen to be consistently below those expected on the basis of detailed orbit calculations based on the surface field of the earth (Shea and Smart, 1967). These differences amount to an approximate 7% reduction at a geomagnetic latitude of 45 deg, increasing to about 25% at 60 deg. At 70 deg, the cutoff is apparently less than 12% of the expected internal field value at 190 MV at 2100 hours local time. It is concluded from the data that, at latitudes less than 60 deg, a limit can be set to the amount of reduction produced by a ring current within the magnetosphere. The most reasonable value for the magnetic moment of this ring current is 0.08 M sub e. Large diurnal changes in the cutoffs characterize the situation at latitudes greater than 60 deg. P.G.M.

A68-41673*

THERMAL IONS IN THE EXOSPHERE: EVIDENCE OF SOLAR AND GEOMAGNETIC CONTROL.

H. C. Brinton, M. W. Pharo, III, N. K. Rahman (NASA, Goddard Space Flight Center, Lab. for Atmospheric and Biological Sciences, Greenbelt, Md.), and H. A. Taylor 1 Sep. 1968 13 p refs Journal of Geophysical Research, vol. 73, p. 5521-5533.

Results of measurements of the latitudinal variation in the exosphere ion composition. Direct measurements of a pronounced latitudinal variation in the exospheric ion composition were obtained from the RF ion spectrometer experiment on OGO 2. Measurements of thermal positive ions obtained in a nearly polar dawn-dusk orbit during mid-October 1965 show that in the altitude range from 415 to 1525 km the major ions are O(+) and H(+) and the minor constituents are N(+) and He(+). Evidence of pronounced solar and geomagnetic control of the ion distributions is further examined by translating the data along magnetic field lines to both (1) a constant 100-km reference level and (2) the dipole equator, applying chemical and diffusive equilibrium theory. At 100 O(+) dominates in both the northern and southern polar ionospheres, yielding at lower latitudes where H(+) dominates. The resultant mean ion mass distribution, about 14 to 16 amu at the poles, and about 4 amu at the equator, is consistent with theory and other measurements. The high-latitude ionosphere is marked by two dominant features: (1) a persistent major trough in n(H(+)) and n(He(+)) where n(H(+)) drops to about 100 ions/cu cm near 60 deg dipole and (2) a variable poleward peak in which the total ion concentration approaches 10,000 ions/cu cm near 80 deg dipole. Z.W.

A68-41684*

LIFETIMES FOR LOW-ENERGY PROTONS IN THE OUTER RADIATION ZONE.

L. A. Frank (Iowa, U., Dept. of Physics and Astronomy, Iowa City, Iowa) and R. L. Swisher 1 Sep. 1968 8 p refs Journal of Geophysical Research, vol. 73, p. 5665-5672. (Contracts NASS-2054; Nonr-1509(06); Grants NGL-16-001-002; NsG-233-62)

The directional, differential intensities of protons over the energy range approximately 200 eV to 50 keV injected into the outer radiation zone - i.e., the extraterrestrial ring current - coincident with the initial phase of the geomagnetic storm during early July 1966 were monitored with a sensitive array of electrostatic analyzers borne on the earth satellite OGO 3. Proton intensities are greatly enhanced throughout

the outer radiation zone for L values \geq or \approx to 3 during the main phase of this moderate magnetic storm, and the injection mechanism ceases to be effective after the storm main phase for L values \leq or \approx to 5.5. Proton ($30 <$ or $=$ to $E <$ or $=$ to 50 keV) intensities are shown to exponentially decay with lifetimes ranging from 15 to 105 hr in substantial agreement with calculated lifetimes invoking measured charge-exchange cross sections for protons incident upon atomic hydrogen and a model of the atomic hydrogen concentration in the earth's exosphere. The atomic hydrogen concentration model for the terrestrial exosphere providing the best fit to the observed proton lifetimes over geocentric radial distances 2.5 to 4.8 R sub E (corresponding to observed concentrations approximately 200 to 30 hydrogen atoms/cm allows only atoms in ballistic orbits in the exosphere as opposed to a model geocorona that includes an additional atomic hydrogen population in captive elliptical orbits.

(Author)

A68-41693*

OGO-3 SEARCH COIL MAGNETOMETER DATA CORRELATED WITH THE REPORTED CROSSING OF THE MAGNETOPAUSE AT 6.6 R SUB E BY ATS 1.

R. E. Holzer (California, U., Inst. of Geophysics and Planetary Physics, Los Angeles, Calif.), J. V. Olson, C. T. Russell, and E. J. Smith (California Inst. of Tech., Jet Propulsion Lab., Pasadena, Calif.) 1 Sep. 1968 7 p refs Journal of Geophysical Research, vol. 73, p. 5769-5775.

OGO 3 passed from the outer magnetosphere through the magnetosheath and into the interplanetary medium between 2200 UT, Jan. 13, and 0300 UT, Jan. 14, 1967. This interval includes the time during which the ATS 1 satellite reportedly encountered the magnetopause and magnetosheath at 6.6 R sub E. Nearly two hours before the ATS 1 event, the OGO 3 search coil magnetometer recorded a normal magnetopause crossing. About half an hour later a sudden increase in the steady magnetic field to an unusually large amplitude for a magnetosheath field was observed. Then, within a minute of the first reported ATS 1 magnetopause crossing, an increase in the amplitude of the magnetic noise was noted. Finally about 45 min after the first ATS 1 crossing, the bow shock was crossed at a position extremely close to the earth. An analysis of the OGO 3 search coil data fully supports the interpretation of the unusual ATS 1 records as displacements of the magnetopause inside of the ATS 1 orbit.

(Author)

A68-41697*

EXPERIMENTAL OBSERVATION OF A LARGE ADDITION TO THE ELECTRON INNER RADIATION BELT AFTER A SOLAR FLARE EVENT.

K. A. Pfitzer and J. R. Winckler (Minnesota, U., School of Physics and Astronomy, Minneapolis, Minn.) 1 Sep. 1968 6 p refs Journal of Geophysical Research, vol. 73, p. 5792-5797.

(Contract NAS5-2071)

Detailed review of data obtained from the simultaneous detection of solar and galactic cosmic-ray fluxes by satellites in various regions of interplanetary space. These satellites include Venus 2 and 3, Pioneer 6, IMP 3, OGO 1, inside the earth's orbit, and Mariner 4 and Zond 3, beyond the earth's orbit. The projections of the trajectories of the satellites are illustrated. Data on the approximately $>$ 1-MeV proton detection obtained during the flights of these objects are illustrated, including data from the flares of July 29 and Aug. 17, 1965. It is seen that when the distance between space objects is short (not more than 10 to 20 million km), the proton flares were detected on various objects almost simultaneously. Data on the variations in protons of various energies obtained during the Zond 3 and Venus 2 flights are illustrated and compared. The detection of galactic cosmic particles by Zond 3, Venus 2 and 3, and Pioneer 6 is discussed.

R.E.L.

A68-42083*#

MAGNETIC CHART OF THE BRAZILIAN ANOMALY:

A VERIFICATION.

J. C. Cain, S. J. Hendricks (NASA, Goddard Space Flight Center, Greenbelt, Md.), and R. A. Langel 1968 4 p refs /Geomagnetism i Aeronomiia, vol. 8, no. 1, 1968, p. 107-111./ Geomagnetism and Aeronomy, vol. 8, no. 1, p. 84-87. Translation.

Comparison between the minimum geomagnetic field in southern Brazil, as mapped by Konovalov and Nalivaiko (1967) from Cosmos 26 and Cosmos 49 data, and a field model calculated by Frutkin (1965) on the basis of data obtained by OGO 2. The results prove that the Brazilian minimum is uniform without any noticeable internal structure.

V.P.

A68-42739***OGO-E PLASMA SPECTROMETER.**

R. A. Graham and F. E. Vesceles (California Inst. of Tech., Jet Propulsion Lab., Pasadena, Calif.) Pittsburgh, Pa., Instrument Society of America, 1967 43 p In: Instrument Society of America, National Aerospace Instrumentation Symposium, 13th, San Diego, Calif., Jun. 13-16, 1967, Proceedings, p. 111-153.

Description of the design, development, and implementation of the OGO 5 plasma spectrometers E-17-1 and E-17-2. The instruments are designed to measure both the total quantity of flux below 12,000 V in energy and to indicate, in a short span of time, the energy (spectral density) of this plasma. These units are to be flight instruments on the Orbiting Geophysical Observatory, model 5.

R.M.

A68-43443*

FIELD-ALIGNED ELECTRON BURSTS AT HIGH LATITUDES OBSERVED BY OGO-4.

D. S. Evans (NASA, Goddard Space Flight Center, Greenbelt, Md.) and R. A. Hoffman 1 Oct. 1968 14 p refs Journal of Geophysical Research, vol. 73, p. 6201-6214.

In a series of passes in the northern high-latitude region, short bursts of radiation were observed in the energy range from 0.7 to 24 keV by detectors aboard the polar orbiting satellite OGO 4. Among these bursts were a number in which the pitch-angle distributions at 2.3 keV displayed a maximum at small angles to the magnetic field lines. From the distributions and energy spectra, it is argued that a possible source mechanism for these particles is electric fields parallel to the magnetic field lines at distances of several earth radii. The source particles would then be the ambient thermal plasma, with two markedly different temperature components, one at a few electron volts, from which the field-aligned radiation originates, and the other greater than an order of magnitude hotter, which produces the isotropic portion of the pitch-angle distribution.

(Author)

A68-43450*

OBSERVATIONS OF POGO ION CHAMBER EXPERIMENT IN THE OUTER RADIATION ZONE.

H. R. Anderson, P. D. Hudson (William Marsh Rice U., Dept. of Space Sciences, Houston, Tex.), and J. E. McCoy (William Marsh Rice U., Dept. of Space Sciences., NASA, Manned Spacecraft Center, Houston, Tex.) 1 Oct. 1968 13 p refs Journal of Geophysical Research, vol. 73, p. 6285-6297.

(Contracts NAS7-100; NAS5-9317)

The ion chamber on OGO 2.4, (POGO) measures the total ionization produced by radiation able to penetrate 0.2 g/sq cm of iron ($E_p E_{sub p} > 10$ MeV, $E_{sub e} > 1$ MeV). The boundary of the outer radiation zone is observed at invariant latitude of 67 deg - 70 deg at 423 to 1525 km altitude, and on at least 34% of passes a narrow spike of intensity is observed a few degrees below the boundary. The spikes are distributed uniformly in local time, but correlate strongly with Kp. Spikes above the boundary occur preferentially on the dawn side. When perigee fell in the outer zone, the point conjugate to the observation point was below 100-km altitude at longitudes 300 deg - 50 deg E. During the period of Mar. 22 through Apr. 1, 1966, the ionization was very high at such points. We interpret this as being

due to intense injection of 1-10 MeV electrons at Lambda A = 57 deg - 62 deg, and we deduce that this is different from the lower injection that repopulates the outer zone in about half a longitudinal drift period. (Author)

A69-11125*

OGO-2 MAGNETIC FIELD OBSERVATIONS DURING THE MAGNETIC STORM OF MARCH 13-15, 1966.

J. C. Cain (NASA, Goddard Space Flight Center, Greenbelt, Md.) and R. A. Langel 1968 13 p refs (International Assn. of Geomagnetism and Aeronomy, Symposium on Special Events, Saint-Gall, Switzerland, Oct. 2, 1967./ Annales de Geophysique, vol. 24, p. 857-869.

Analysis of magnetic field data from the OGO 2 spacecraft and from surface magnetic observatories for the period from Mar. 13 to 15, 1966. During this interval there occurred a magnetic storm with a Dst decrease of 122 gamma. The results indicate a nonsymmetric inflation of the magnetosphere, with the field decrease in the dusk sector being a factor of about three more than that in the dawn sector. The evidence indicates that the sources of both Dst and Ds in low latitudes are external to the satellite altitudes (410 to 1510 km). Polar ionospheric currents were detected more than 1.5 hr before the main phase of the storm. These currents conform to the classical 2-celled model, which includes a concentrated eastward current in the evening local time sector, and a concentrated westward current in the morning local time sector. F.R.L.

A69-11226*

PROPAGATION OF THE SUDDEN COMMENCEMENT OF JULY 8, 1966, TO THE MAGNETOTAIL.

J. P. Heppner (NASA, Goddard Space Flight Center, Greenbelt Md.), B. G. Ledley, T. L. Skillman, and M. Sugiura 1 Nov. 1968 11 p refs Journal of Geophysical Research, vol. 73, p. 6699-6709.

A sudden magnetic field increase associated with the July 8, 1966, sudden commencement (SC) was observed by the OGO 3 satellite in the magnetotail. By use of the IMP 3 and Explorer 33 observations made by Ness and Taylor (1968) of the interplanetary shock that caused the SC, it is shown that the magnetospheric propagation of the field increase toward the tail is faster than the propagation of the interplanetary shock just outside the bow shock. Conclusions drawn include (1) that the observed magnetic field increase in the tail is unlikely to be due to an increased lateral pressure of the postshock solar wind gas from the side of the tail, and (2) that the transfer of additional polar magnetic flux to the tail due to the increase in the solar wind pressure on the front side of the magnetosphere can account for the observed tail field increase. (Author)

A69-12740*

OBSERVATIONS OF THE SCREENING OF SOLAR COSMIC RAYS BY THE OUTER MAGNETOSPHERE.

D. J. Hofmann (Wyoming, U., Dept. of Physics, Laramie, Wyo.), S. R. Kane, and J. R. Winckler (Minnesota, U., School of Physics and Astronomy, Minneapolis, Minn.) Nov. 1968 24 p refs Planetary and Space Science, vol. 16, p. 1381-1404. (Contract NAS5-2071)

Investigation of spatial variations in particle intensity near and inside the magnetosphere during the solar cosmic-ray events of September 1966, using simultaneous observations by identical ionization chambers aboard the satellites OGO 1 and OGO 3. Cross-correlation of the absolute proton flux computed from the chamber rate during three solar-particle events shows good agreement with the measurements by the IMP-6 Solar Proton Monitor during the same events. The peak dosage measured during the September 1966 solar cosmic-ray events varied from 4×0.0001 r/hr to 60 r/hr. The high sensitivity and absolute intercomparability of the instruments allow small intensity differences to be detected, and it is established that the observed differences can be explained by a magnetospheric screening effect when an anisotropic beam of particles is present in

space. Evidence shows that the screening is at times complete for a duration of as much as 110 min in the tail of the magnetosphere so that, during this period, the solar cosmic rays have virtually no access to that region of the magnetosphere. M.M.

A69-14027*

LOW-ENERGY ELECTRONS ON THE DAY SIDE OF THE MAGNETOSPHERE.

V. M. Vasyliunas (Massachusetts Inst. of Tech., Dept. of Physics and Center for Space Research, Cambridge, Mass.) 1 Dec. 1968 5 p refs Journal of Geophysical Research, vol. 73, p. 7519-7523. (Contract NAS5-2053; Grants NGR-22-009-015; NsG-386;)

Preliminary report on the observations made with the MIT electron detector on the OGO 3 satellite within the magnetosphere from August 1966 to February 1967. The observations apply to the satellite surveyed local times from approximately 18 hr through noon to approximately 4 hr. The results confirm a previous suggestion that a region of low-energy electrons completely envelops the Van Allen belt. M.G.

A69-14029*

ION CUTOFF WHISTLERS.

J. L. R. Muzzio (Stanford U., Radioscience Lab., Stanford, Calif.) 1 Dec. 1968 4 p refs Journal of Geophysical Research, vol. 73, p. 7526-7529. (Contract NAS5-3093; NASA Order SC-05-020-008; Grant NsG-174)

Discussion of a new phenomenon (ion cutoff whistlers) observed during a VLF experiment aboard the satellites OGO 2 and OGO 4. This phenomenon manifests itself by the turning up of a whistler trace at a frequency below 1 kHz. A possible application of ion cutoff whistlers to the determination of the relative proton concentration in the ionosphere is discussed. M.G.

A69-14681*

DETECTION OF ELECTRIC-FIELD TURBULENCE IN THE EARTH'S BOW SHOCK.

G. M. Crook, R. W. Fredricks, I. M. Green (TRW Systems Group, Space Sciences Lab., Redondo Beach, Calif.), C. F. Kennel (TRW Systems Group, Space Sciences Lab., Redondo Beach, Calif., California, U., Dept. of Physics, Los Angeles, Calif.), and F. L. Scard 23 Dec. 1968 4 p refs Physical Review Letters, vol. 21, p. 1761-1764. (Contract NAS5-9278)

Account of the observation of low-frequency fluctuating electric fields generated in the earth's bow shock. It is found that the wave amplitude is not a smooth function of space through the shock, but rather that it is strongly correlated with magnetic-field structures within the shock. (Author)

A69-16257*

OBSERVATIONS OF LOWER HYBRID RESONANCE PHENOMENA ON THE OGO 2 SPACECRAFT.

W. C. Johnson (Dartmouth Coll., Thayer School of Engineering, Radiophysics Lab., Hanover, N. H.), T. Laaspere, and M. G. Morgan 1 Jan. 1969 12 p refs Journal of Geophysical Research, vol. 74, p. 141-152. (Contract NAS5-3092)

Observation of audio frequency noise bands of continuous and triggered type that are evidently associated with the lower hybrid resonance frequency of the ionospheric medium, with Dartmouth's whistler receiver using a 9-ft electric dipole antenna on the OGO 2 spacecraft at heights up to 1500 km. Although the electric dipole on OGO 2 is much shorter than the antennas of Alouette, the results are similar to the Alouette observations. A new observation made is that the upper cutoff frequency of the lower hybrid resonance noise bands triggered by fractional-hop whistlers occasionally displays an envelope that has the shape of an Eckersley whistler. Whereas the results of the experiment are consistent with the interpretation that the lower cutoff frequency of noise bands triggered by whistlers is the lower hybrid

resonance frequency of the ionosphere in the vicinity of the satellite, there is at present no satisfactory explanation of the upper cutoff. P.v.T.

A69-18834*
OGO 3 OBSERVATIONS OF ELF NOISE IN THE MAGNETOSPHERE. I.

R. E. Holzer (California, U., Inst. of Geophysics and Planetary Physics, Los Angeles, Calif.), C. T. Russell, and E. J. Smith (California Inst. of Tech., Jet Propulsion Lab., Pasadena, Calif.) 1 Feb. 1969 23 p refs Journal of Geophysical Research, vol. 74, p. 755-777. (Contract JPL-950403)

The magnetic noise in the magnetosphere in the frequency range from 10 to 800 Hz has been extensively measured by the spectrum analyzers of the search coil magnetometer on OGO 3. The paper is a statistical study of the spatial extent and frequency of occurrence of noise at the higher end of this passband; at these frequencies noise above the detector thresholds is most common within the magnetosphere. Steady noise and noise bursts are found to constitute two distinct populations. Both the local-time and magnetic latitude distribution of both classes of signals are investigated. When the magnetic latitude distributions are extrapolated downward to 1000-km altitudes, the results are consistent with previous satellite observations at these low altitudes. However, the equatorial distributions cannot be inferred by simply projecting the magnetic noise measured at low altitudes on to the equator along flux tubes. The in situ measurements cannot determine the exact location of the source of all the noise observed. However, it is found that steady noise is definitely generated near 45 deg magnetic latitude on the dayside of the magnetosphere for L values from 6 to 10, and that bursts are generated near the equator above L = 6 from 0400 to 1800 local time. (Author)

A69-19198
PRIMARY ELECTRON DETECTOR EXPERIMENT FOR OGO-E.

J. R. Gilland (Ball Brothers Research Corp., Boulder, Colo., 04(Leiden, State U., Leiden, Netherlands), D. B. Hicks, L. K. Rogowski, and B. N. Swanenburg New York, Feb. 1969 7 p (Inst. of Electrical and Electronics Engineers, Nuclear Science Symposium, 15th, Montreal, Canada, Oct. 23-25, 1968.) IEEE Transactions on Nuclear Science, vol. NS-16, p. 352-358. Research supported by the Netherlands State U. (IEEE Paper 3C-4)

Description of a primary electron detector to measure the electron component in the primary cosmic radiation. The measurements are intended to reveal the absolute flux and energy spectrum of electrons in the energy range from 0.5 to 10 GeV. The experiment will also measure gamma rays above 500 MeV and protons between 20 and 100 GeV. The components of the detector system include five individual radiation counters grouped into subsystems comprising a lead/glass total-absorption spectrometer crystal, a cesium iodide/glass scintillator phoswich, and a cesium iodide/plastic phoswich. The experiment was launched on an Orbiting Geophysical Observatory (OGO 5) in early 1969. The final configuration has an envelope volume of about 950 cu in, weighs 16 lb. and operates on 1.1 W of power. B.H.

A69-19358*
RECENT OBSERVATIONS OF LOW-ENERGY CHARGED PARTICLES IN THE EARTH'S MAGNETOSPHERE.

L. A. Frank (Iowa, U., Dept. of Physics and Astronomy, Iowa City, Iowa) Dordrecht, D. Reidel Publishing Co. 1968 19 p refs In: Physics of the Magnetosphere, Proceedings of the Conference, Boston Coll., Chestnut Hill, Mass., Jun. 19-28, 1967, p. 271-289. Conference sponsored by the U.S. Air Force and Boston Coll. (Astrophysics and Space Science Library, volume 10), 1968. (Contracts NAS5-2054; Nonr-1509/06/; Grants NGL-16-001-002; NSG-233-62)

Summary of several recent observations of low-energy proton and electron intensities within the energy range of 100 eV to 50 keV in the earth's radiation zones with a sensitive array of electrostatic analyzers on the earth-satellite OGO 3 during 1966. Measurements of charged particles of the extraterrestrial ring current during a moderate geomagnetic storm, of the low-energy proton and electron distribution in the vicinity of the midnight trapping boundary near the magnetic equatorial plane, and of upper limits for proton and ion energy fluxes deep within the inner radiation zone are presented together with several introductory comments concerning the morphology of the omnidirectional intensities of energetic electrons at the magnetic equator in the outer radiation zone. (Author)

A69-19373*
LOW ENERGY ELECTRONS IN THE MAGNETOSPHERE AS OBSERVED BY OGO-1 AND OGO-3.

V. M. Vasyliunas (Massachusetts Inst. of Tech., Physics Dept. and Lab. for Nuclear Science, Cambridge, Mass.) Dordrecht, D. Reidel Publishing Co. 1968 19 p refs In: Physics of the Magnetosphere, Proceedings of the Conference, Boston Coll., Chestnut Hill, Mass., Jun. 19-28, 1967, p. 622. Conference sponsored by the U.S. Air Force and Boston Coll. (Astrophysics and Space Science Library, volume 10), 1968. (Contracts NAS5-2053; AT (30-1)-2098; Grant NSG-386)

Discussion of the general configuration of the plasma sheet, its termination on the earthward side, and its relation to magnetic-bay activity. During quiet times the inner boundary of the plasma sheet, located at an equatorial distance of approximately 11 R sub E, is characterized by a steep electron pressure gradient, with a length scale of approximately 0.4 R sub E, as well as by a steep temperature gradient, but has only a weak density gradient. During bay activity, the boundary now located at approximately 6 R sub E is still characterized by the same electron pressure gradient, with only a slightly longer length scale of approximately 0.6 R sub E. G.R.

A69-20067*
ENERGY SPECTRA AND ABUNDANCES OF THE COSMIC-RAY NUCLEI HELIUM TO IRON FROM THE OGO-1 SATELLITE EXPERIMENT.

G. M. Comstock, C. Y. Fan, and J. A. Simpson (Chicago, U., Enrico Fermi Inst. for Nuclear Studies, Chicago, Ill.) Feb. 1969 9 p refs Astrophysical Journal, vol. 155, Pt-1, p. 609-617. (Contracts NAS5-2133; AF 49(638)-1642; Grant NSG-179-61)

The differential energy spectra of He, B, C, N, Ne, Mg, Si, and the Fe group obtained above 20 MeV nucleon⁻¹ from an experiment on the OGO 1 satellite have been reevaluated by using new detector calibrations and an additional block of data. The results reported now cover the time interval from October 1964 to November 1965, which spans the period of minimum solar modulation in the 11-year solar-activity cycle. The shapes of the energy spectra are modified at low energy as a result of the new analysis. However, since the shapes of the spectra relative to one another remain essentially the same, the conclusions reached earlier remain unchanged. The relative abundances of the nuclei were reevaluated. The abundances for several nuclei have now been determined for the two energy intervals 50-100 and 100-200 MeV/nucleon. In addition to the abundances previously reported for He to Fe, the abundances for Na, Al, and the nuclear-charge groups (P-K) and (Ca-Cr) have been obtained at low energy for the first time. The implications of these abundances for the origin of the low-energy radiation are discussed briefly. The new methods for analysis are described, and the linearity of solid-state-detector response over the nuclear-charge range Z = 1 to Z = 26 is established. (Author)

A69-20068*
PROPAGATION AND SOURCE CHARACTERISTICS DERIVED FROM THE LOW-ENERGY, MULTIPLY CHARGED, COSMIC-RAY NUCLEI.

G. M. Comstock (Chicago, U., Enrico Fermi Inst. for Nuclear Studies and Dept. of Physics, Chicago, Ill.) Feb. 1969 25 p refs Astrophysical Journal, vol. 155, Pt- 1, p. 619-643. (Contracts NAS5-2133; AF 49(638)-1642; Grant NSG-179-61)

Models for the origin and propagation of the cosmic-ray nuclei which assume a uniform particle population defined by a single set of propagation and source characteristics (including recently proposed steady-state models with a broad path-length distribution function) do not look attractive in terms of the nearby interstellar energy spectra derived from recent low-energy measurements made on the OGO 1 satellite. Instead, the properties of these interstellar energy spectra strongly suggest the existence of two distinct particle populations or components. These two components would result from different types of sources or modes of propagation. It is shown quantitatively that such two-component models satisfy the present experimental results down to the lowest observed energies over the wide nuclear charge range of helium to iron. The constraints placed by the data on two-component models are discussed with the aid of calculated interstellar energy spectra of the nuclear charge groups He, B, CNO (6 or = to Z < or = to 8), LH (10 < or = to 15) and the Fe group (25 < or = to Z < or = to 28) derived for several different sets of source and propagation parameters. These calculated spectra are compared with the observed energy spectra of these charge groups corrected for solar modulation. Physical conditions which may give rise to two distinct particle populations are discussed briefly. (Author)

A69-21699*

THE 135-1650 KEV SOLAR PROTONS AFTER THE FLARE OF JULY 7, 1966, OBSERVED IN THE MAGNETOTAIL AND MAGNETOSHEATH.

A. Konradi (NASA, Goddard Space Flight Center, Greenbelt, Md.) 1 Mar. 1969 6 p refs Journal of Geophysical Research, vol. 74, p. 1158-1163.

Protons with energies $E > 135$ keV were observed in the tail of the magnetosphere after the flare of July 7, 1966. These protons have an isotropic pitch-angle distribution. The maximum intensity of the protons reached approximately $1.2 \times 10,000/(\text{sq cm sec ster})$ for particles with $E > 120$ keV between 1000 and 1100 UT and 1400 and 1500 UT July 8, 1966. The energy spectrum of the protons expressed as an exponential in rigidity indicates a monotonic softening; the characteristic rigidity, P_0 changing from about 50 to 10 MV. An hour-long excursion of the satellite into the magnetosheath during the peak of the proton flux showed that the proton intensity is lower in the magnetosheath than in the magnetosphere by a factor of 2. The observed pitch-angle distribution is flat in both regions. (Author)

A69-22181*

THE SOLAR PARTICLE EVENT OF JULY 16-19, 1966 AND ITS POSSIBLE ASSOCIATION WITH A FLARE ON THE INVISIBLE SOLAR HEMISPHERE.

H. W. Dodson, E. R. Hedeman (Michigan, U., McMath-Hulbert Observatory, Lake Angelus, Mich.), 04(California, U., Space Sciences Lab., Berkeley, Calif.), S. W. Kahler, and R. P. Lin Feb. 1969 10 p refs Solar Physics, vol. 6, p. 294-303. (Contracts NAS5-9077; NAS5-2222; Grant NGR-23-005-275)

An energetic solar proton and electron event was observed by particle detectors aboard Explorer 33 and OGO 3 during the period July 16-19, 1966. Optical and radio observations of the sun suggest that these particles were produced by a flare which may have occurred on July 16 near the central meridian of the invisible hemisphere. The active region to which the flare is assigned is known to have produced the energetic particle events of July 7 and 28, 1966. The propagation of the particles in the July 16-19 event over

the approximately 180 deg. extent of solar longitude from the flare to the earth is discussed, and it is concluded that there must exist a means of rapidly distributing energetic particles over a large area of the sun. Several possible mechanisms are suggested. (Author)

A69-22182*

OBSERVATIONS OF ENERGETIC X-RAYS AND SOLAR COSMIC RAYS ASSOCIATED WITH THE 23 MAY 1967 SOLAR FLARE EVENT.

S. R. Kane and J. R. Winckler (Minnesota, U., School of Physics and Astronomy, Minneapolis, Minn.) Feb. 1969 16 p refs Solar Physics, vol. 6, p. 304-319. (Contract NAS5-2071)

Description of observations of energetic solar flare X-rays by the OGO 3 ion chamber of May 21, 1967. The time-intensity profile for the X-ray event showed three distinct peaks at approximately 1810, 1841, and 1942 UT. The second peak is the largest X-ray burst observed so far by the OGO 1 and OGO 3 ion chambers. The soft X-ray observations reported by Van Allen (1968) also show similar peaks, roughly proportional in magnitude to the energetic X-ray peaks. However, the intensity of energetic X-rays peaked in each case from 5 to 10 min earlier than the soft X-ray intensity, indicating a relatively hard photon energy spectrum near the peak of the energetic X-ray emission. The corresponding time-intensity profile for the solar radio emission also showed three peaks in the microwave region nearly coincident with the energetic X-ray peaks. The third radio peak was relatively rich in the metric emission. Beyond this peak, both the energetic X-rays and the microwave emission decayed with a time constant of approximately 8 min, while the corresponding time constant for the soft X-rays was approximately 43 min. In view of the earlier findings about the energetic X-rays, it is indicated that the May 23 solar X-ray event was similar to those observed earlier.

M.M.

A69-23753*

VERY HIGH ENERGY SOLAR X-RAYS OBSERVED DURING THE PROTON EVENT OF 7 JULY 1966.

T. L. Cline, S. S. Holt (NASA, Goddard Space Flight Center, Greenbelt, Md.), and E. W. Hones, Jr. (California, U., Los Alamos Scientific Lab., Los Alamos, N. Mex.) Cambridge, Mass., MIT Press, 1969 5 p In: The Proton Flare Project (The Jul. 1966 event). Edited by A. C. Stickland. (Annals of the IQSY. Volume 3), p. 193-197.

The time history and spectral intensity of solar X-rays of energies from 80 keV to more than 500 keV were observed during the flare event of July 7, 1966. These measurements, made with the satellite OGO 3, cover the highest energy range available thus far and show this event to have the greatest measured hard X-ray intensity of any solar event studied in detail to date. Three intensity peaks at about 0027, 0029, and 0037 UT coincide with the times of microwave intensity maxima. A study of the spectral and temporal features of the X-ray emission, and comparison with the radio data, indicate a nonthermal bremsstrahlung origin for the X-rays. (Author)

A69-23777*

EVIDENCE OF CONTRACTION OF THE EARTH'S THERMAL PLASMASPHERE SUBSEQUENT TO THE SOLAR FLARE EVENTS OF 7 AND 9 JULY 1966.

H. C. Brinton, M. W. Pharo, III, and H. A. Taylor, Jr. (NASA, Goddard Space Flight Center, Aeronomy Branch, Greenbelt, Md.) Cambridge, Mass., MIT Press, 1969 6 p refs In: The Proton Flare Project (The Jul. 1966 Event). Edited by A. C. Stickland. (Annals of the IQSY. Volume 3), p.389-394.

Direct measurements of thermal H(+) and He(+) in the magnetosphere have been obtained from ion mass spectrometers on OGO 1 and 3 satellites. Typical H(+) profiles exhibit a gradual decrease in concentration with altitude within the plasmasphere, while the outer boundary of the plasmasphere is characterized by an abrupt decrease

in concentration to 5 ions/cu cm or less. This boundary, the plasmapause, is observed to move inward and outward in an inverse correlation with the magnetic activity index Kp. The magnetosphere was disturbed during the solar flare period July 7-9, 1966, and on July 9, the plasmapause was observed to be unusually low, at L = 3.3. This observation contrasted with measurements of the plasmapause on both preceding and succeeding orbits, when in the absence of flares and magnetic disturbance the H(-) boundary was observed to expand to L values as high as 6. These measurements correlate well with knee whistler observations of the plasmapause. (Author)

A69-25153*
MULTI-EXPERIMENT DETECTION OF THE PLASMAPAUSE FROM EOGO SATELLITES AND ANTARCTIC GROUND STATIONS.

H. C. Brinton (NASA, Goddard Space Flight Center, Lab. for Atmospheric and Biological Sciences, Greenbelt, Md.), D. L. Carpenter, C. G. Park (Stanford U., Stanford Radioscience Lab., Stanford, Calif.), and H. A. Taylor, Jr. 1 Apr. 1969 11 p refs Journal of Geophysical Research, vol. 74, p. 1837-1847. NSF supported research. (Contract NAS5-2131)

Correlation study of plasmapause position measured by three independent experiments involving: (1) ion mass spectrometers on OGO 1 and OGO 3 (2) broadband VLF receivers (0.3-12.5 kHz) on OGO 1 and OGO 3; and (3) broadband VLF recordings at Antarctica, near the 90 meridian. In the satellite VLF data, the plasmapause crossings are identified by abrupt changes in observed whistler and VLF noise activity, and by noise bands of limited duration. In two cases of simultaneous VLF and ion data from the same satellite, plasmapause crossings were detected by both experiments within less than 0.1 RE in L value. In eight cases of OGO 1 ion data and simultaneous ground whistler data spaced from 1 to 12 hours from OGO in local time, good agreement was found between the measured plasmapause positions. The comparisons provide new verification of the worldwide extent of the plasmapause. Previous indications that the radius of the plasmapause is frequently about constant, over large local-time sectors in the range 0-18 LT, are also verified. B.H.

A69-25157*
AN INTERPRETATION OF OGO LIGHT ION ABUNDANCE MEASUREMENTS.

L. Colin, S. W. Dufour, and D. S. Willoughby (NASA, Ames Research Center, Space Sciences Div., Moffett Field, Calif.) 1 Apr. 1969 4 p refs Journal of Geophysical Research, vol. 74, p. 1863-1866.

Investigation of a diffusive equilibrium theory to account for the light-ion abundance measurements of the OGO satellites. It is shown that reasonable latitudinal distributions of temperature, temperature gradient, and composition can be found that are compatible (using field-aligned diffusive equilibrium with positive temperature gradients) with published OGO data. G.R.

A69-28950*
HIGH-LATITUDE IONIZATION SPIKES OBSERVED BY THE POGO ION CHAMBER EXPERIMENT.

J. E. McCoy (William Marsh Rice U., Dept. of Space Science, NASA, Manned Spacecraft Center, Houston, Tex.) 1 May 1969 10 p refs Journal of Geophysical Research, vol. 74, p. 2309-2318. (Contract NAS5-9317)

Study of ionization spikes observed by the POGO spacecraft which was launched into a low polar orbit on Oct. 14, 1965, and carried an ion chamber experiment sensitive to electrons with energies greater than 1 MeV and protons greater than 10 MeV. These spikes were found to be present near the high-latitude boundary of stably trapped radiation on at least 30% of the satellite passes through this region. Their frequency of occurrence increases markedly with increased magnetic disturbance. Occurrence of those

spikes lying just inside the observed boundary of trapping appears to be evenly distributed with respect to local time, but the occurrence of spikes at latitudes outside the region of stable trapping is predominantly in the dawn hemisphere. It is argued that these spikes are the result of injection of high-energy electrons (E is approximately 1 MeV) onto field lines near the boundary of trapping and are associated with the electron islands reported in the magnetospheric tail by Anderson et al. (1965, 1967, 1968). It is shown that the spatial distribution of spikes as observed by POGO should be expected as a consequence of electron drift, in the postmidnight quadrant, into a region of pseudotrapping.

P.V.T.

A69-28958*
LATITUDINAL CUTOFF OF VLF SIGNALS IN THE IONOSPHERE.

R. A. Helliwell (Stanford U., Stanford Radioscience Lab., Stanford, Calif.), R. L. Heyborne (Utah State U. of Agriculture and Applied Science, Dept. of Electrical Engineering, Logan, Utah), and R. L. Smith 1 May 1969 5 p refs Journal of Geophysical Research, vol. 74, p. 2393-2397. (Grants NsG-05-020-008; NGR-05-020-288; NSF GK-1597; NsG-174)

Discussion of some preliminary results of a study of the latitudinal cutoff of manmade VLF (18 kHz) signals traveling over the short path to the OGO 2 satellite. The polar-orbiting OGO 2 satellite recorded a latitudinal cutoff of these signals between roughly 50 deg and 70 deg invariant latitude. The signal cutoff (which ranged from 10 to 40 dB magnetic field attenuation) was frequently followed by strong noise believed to be auroral hiss. G.R.

A69-28964*
LOW-ENERGY ELECTRON PRECIPITATION AT HIGH LATITUDES.

R. A. Hoffman (NASA, Goddard Space Flight Center, Greenbelt, Md.) 1 May 1969 8 p refs Journal of Geophysical Research, vol. 74, p. 2425-2432.

Discussion of data for low-energy electron fluxes at high latitudes, obtained from two detectors in a satellite launched on July 28, 1967, into a low-altitude polar orbit. The responses of the 0.7-keV and 7.3 keV detectors to precipitating electrons in the Northern Hemisphere during a number of orbits are discussed. G.R.

A69-29565*#
DEGRADATION OF CONTINUOUS-CHANNEL ELECTRON MULTIPLIERS IN A LABORATORY OPERATING ENVIRONMENT.

L. A. Frank, N. K. Henderson, and R. L. Swisher (Iowa, U., Dept. of Physics and Astronomy, Iowa City, Iowa) May 1969 5 p refs Review of Scientific Instruments, vol. 40, p. 685-689. (Contracts NAS5-9074; NAS5-9156)

Measurements of the counting rates (approximately 1,000 to 10,000 counts per second) of continuous-channel electron multipliers mounted in an electrostatic analyzer responding to a monoenergetic beam of electrons, while operating in a vacuum chamber at a pressure approximately 3×0.00001 torr attained with an oil diffusion pump, display a degradation of their gain (fatigue) proportional to the accumulated counts. The useful lifetime of these devices when employed with fixed-threshold pulse amplifiers is defined as the accumulated counts until gain degradation has produced a reduction of the counting rates to 15% of the initial responses at an operating bias voltage of 4000 V and constant stimuli. The lifetimes of these particle detectors in this laboratory environment are approximately 10 to the 10th power counts or, for example, an average counting rate of 300 counts per second for one year. Comparison of this laboratory lifetime with the responses of similar instrumentation which has been flown on OGO 3, 4, and 5 and IMP 4 demonstrates that the expected lifetimes for these electron multipliers in a spaceflight environment are several

years. Efficiencies of an electron multiplier for counting monoenergetic electrons over an energy range approximately 60 to 50,000 eV are also presented. (Author)

A69-30191#

THE HYDROGEN LYMAN-ALPHA AIRGLOW.

R. R. Meier (U.S. Navy, Naval Research Lab., E. O. Hulburt Center for Space Research, Washington, D.C.) May 1969 8 p refs Astronautics and Aeronautics, vol. 7, p. 68-75.

Investigation of the origin of the hydrogen Lyman-alpha airglow. Available experimental data from rocket and satellite measurements are examined with regard to the three principal models which have been proposed for the production of the Lyman-alpha nightglow. It is concluded that the Lyman-alpha radiation around earth comes principally from multiple scattering of solar photons within a hydrogen geocorona contained within some 3 earth radii. With the availability of complete satellite mappings of Lyman-alpha it should be possible to decide to what extent the theoretical models describe the hydrogen distribution. G.R.

A69-31326*#

OBSERVATIONS OF HYDROGEN AND HELIUM IONS DURING A PERIOD OF RISING SOLAR ACTIVITY.

H. C. Brinton (NASA, Goddard Space Flight Center, Lab. for Atmospheric and Biological Sciences, Greenbelt, Md.), H. G. Mayr, and H. A. Taylor, Jr. May 1969 38 p refs COSPAR, Plenary Meeting, 12th, Prague, Czechoslovakia, May 11-24, 1969. Paper.

Results of direct measurements of hydrogen and helium ion distributions during the period from 1967 to 1968 (a period approaching the maximum of solar cycle 20). The results indicate that no significant He(+) belt has formed near 1000 km. Variability with respect to season and local magnetic time, which is observed throughout the ion composition, is particularly pronounced in n(He(+)) and n(H(+)), and is presented in detail. Some implications of this variability for the investigation of ionospheric response to solar changes, and for the development of new ionospheric models, are discussed briefly. Comments are offered on the possible mechanisms which could be responsible for the observed anomalies. M.G.

A69-31400#

ULTRAVIOLET OBSERVATIONS OF ATOMIC HYDROGEN AND OXYGEN FROM THE OGO SATELLITES.

G. E. Thomas (Colorado, U., Dept. of AstroGeophysics and Lab. for Atmospheric and Space Physics, Boulder, Colo.) May 1969 5 p ref COSPAR, Plenary Meeting, 12th, Prague, Czechoslovakia, May 11-24, 1969. Paper.

Evaluation of two complementary satellite UV experiments conducted by the University of Colorado on the Orbiting Geophysical Observatories (OGO). A scanning UV spectrometer on OGO 4 measures the UV spectrum of the earth's airglow between 1100 and 3300 Å. Because of its polar orbit, OGO 4 has provided extensive coverage from July 1967 to the present of the emergent UV radiation over practically the entire globe. A dual-channel filter photometer, sensitive to the 1216 and 1304-Å resonance lines of atomic hydrogen (H) and oxygen (O), was carried in the OGO 5 satellite, launched in March 1968. The orbit of OGO 5 penetrates the entire radial extent of the hydrogen geocorona (about 15 earth radii) out to about 24 earth radii. Data from the radially-outlooking photometer yield vertical profiles of O and H up to 1000 km and 10 earth radii, respectively, in regions where the radiation-belt interference is not important. Some observations of these two resonance lines are presented, as well as the information they provide concerning the densities of H and O, and the modes of excitation of these lines. The OGO 5 results are compared with exospheric models of the hydrogen geocorona. P.v.T.

A69-31412#

OGO-5 MEASUREMENTS OF LYMAN-ALPHA INTENSITY DISTRIBUTION AND LINEWIDTH UP TO**6 EARTH RADII.**

J. L. Bertaux and J. E. Blamont (Centre National de la Recherche Scientifique, Service d'Aeronomie, Verrieres-le-Buisson, Essonne, France) May 1969 27 p refs COSPAR, Plenary Meeting, 12th, Prague, Czechoslovakia, May 11-24, 1969. Paper.

Discussion of OGO 5 satellite measurements of the intensity and width of the Lyman alpha line scattered by the hydrogen geocorona. The intensity profiles obtained present a maximum around 1.0 earth radii. Profiles of the reduction factor are computed from intensity profiles. A geocoronal temperature evaluation is conducted, and values of the equivalent Doppler temperature, deduced from the values of the reduction factors computed for different hypotheses, are presented. G.R.

A69-31967*

NONUNIFORMITY OF SOLAR PROTONS OVER THE POLAR CAPS ON MARCH 24, 1966.

H. R. Anderson (William Marsh Rice U., Dept. of Space Science, Houston, Tex.) and P. D. Hudson 1 Jun. 1969 10 p refs Journal of Geophysical Research, vol. 74, p. 2881-2890.

(Contract NAS5-9317)

Observations of approximately 10-MeV protons were made over the polar regions by an ionization chamber during two solar proton events on March 24, 1966, separated by approximately 3.5 hr. Short-term fluctuations in the ionization were observed with factor of two changes occurring in approximately 30 sec or approximately 220 km. A nearly identical ionization chamber at 10-16 RE sunward observed no short-term fluctuations, and these differences are interpreted as spatial effects due to the field structure over the poles. The fluctuations occur mainly when the proton density outside the magnetosphere is increasing rapidly and when the flux is highly anisotropic. Most of the fluctuations disappear in approximately 2 hr, but similarities between the fluctuations observed during the two solar proton events suggest that the modulation is not interplanetary in origin, and that the magnetospheric field structure causing the modulation retains the same pattern for a period of 3.5 hr. The fluctuations may be due to particles following different paths through the magnetosphere and connecting to different parts of the anisotropic flux behind the bow shock.

(Author)

A69-31976*

THEORY OF AN ELECTRON TRAP ON A CHARGED SPACECRAFT.

L. W. Parker (Mt. Auburn Research Associates, Inc., Cambridge, Mass.) and E. C. Whipple, Jr. (ESSA, Boulder, Colo.) 1 Jun. 1969 10 p refs Journal of Geophysical Research, vol. 74, p. 2962-2971. NASA supported research.

(Contract ESSA-F22-8-69N)

Description of a theory for the behavior of an electron trap on a slowly moving charged spacecraft in the limit of large Debye length and no magnetic field. Analytic expressions are obtained for the current to an aperture electrode and to an internal retarding electrode for all values of aperture and spacecraft potentials. When the spacecraft is repulsive and the aperture grid is less repulsive (or even attractive), a potential barrier exists that reduces the current. The extent of the reduction can be orders of magnitude. As a consequence, the knee in the current-voltage curve can yield incorrect values for the electron concentration and spacecraft potential if conventional Langmuir probe theory is used. When the spacecraft is more attractive than the aperture grid, the current is unaffected by the spacecraft potential. It is shown that in the so-called exponential regime of the retarded current, it is impossible for secondary electrons to reach the collector from the adjacent external surfaces of the spacecraft. In the attractive regime, the current characteristic is linear for large aperture potentials.

(Author)

A69-31981*

BANDED CHORUS: A NEW TYPE OF VLF RADIATION OBSERVED IN THE MAGNETOSPHERE BY OGO-1 AND OGO-3.

W. J. Burtis (Stanford U., Radioscience Lab., Stanford, NASA, Ames Research Center, Moffett Field, Calif.) and R. A. Helliwell (Stanford, U., Radioscience Lab., Stanford, Calif.) 1 Jun. 1969 9 p refs Journal of Geophysical Research, vol. 74, p. 3002-3010. (Contract NAS5-2131; Grants NsG-174-05-020-008; NGR-05-020-288)

Satellites OGO 1 and OGO 3 observe VLF discrete emissions in the magnetosphere primarily in a single, variable frequency band. The frequency, f , of this banded chorus depends on the equatorial electron gyrofrequency, f sub HO for the field line passing through the satellite, typical ratios of f/f sub HO being 0.2-0.5. Evidently the emissions are produced near the equator at a fraction of the electron gyrofrequency, as predicted by electron cyclotron resonance generation mechanisms. A secondary dependence of the banded chorus frequency on dipole latitude, such that the lower ratios of f/f sub HO are found at higher latitudes, is interpreted to mean that the emissions are generated at about half the electron gyrofrequency, but deviate inward from the field line to lower L values as they propagate earthward. Theoretical support is given by ray tracings showing the inward deviation of nonducted whistler-mode radiation due to the curvature of the magnetic field. Banded chorus has been observed at all local times, but is most common in the morning magnetosphere, outside the plasmapause.

(Author)

A69-32645*

SATELLITE OBSERVATIONS OF THE VERTICAL OZONE DISTRIBUTION IN THE UPPER STRATOSPHERE.

G. P. Anderson, C. A. Barth, F. Cayla, and J. London (Colorado, U., Dept. of Astro-Geophysics and Lab. For Atmospheric and Space Physics, Boulder, Colo.) Mar. 1969 5 p refs (Symposium International de l'Ozone, 10th, Monaco, Sep. 2-7, 1968.) Annales de Geophysique, vol. 25, p. 341-345. (Contract NAS5-9315; Grants NGL-06-003-052; NSF GP-3196)

An Ebert-Fastie UV spectrometer mounted on a polar-orbiting satellite was used to observe backscattered radiation in the spectral region 2500 to 3100 Å. A simultaneous set of ozone balloon and rocket observations (Krueger, 1968) was used as a calibration for the satellite data. A modified Phillips-Twomey inversion technique was applied to the data, resulting in a reasonable vertical ozone distribution in the region 35 to 55 km. Computations on independent data verified the dependability of the method.

(Author)

A69-33055

DIRECTIVITY OF SOLAR HARD X-RAY BURSTS.

K.-I. Ohki (Tokyo, U., Dept. of Astronomy, Tokyo, Japan) May 1969 8 p refs Solar Physics, vol. 7, p. 260-267.

Solar hard X-ray bursts (>0 keV) seem to show a center-to-limb variation, while softer X-ray bursts show no directivity. This effect of hard X-ray bursts may be due to the directivity of the emission itself. As the cause of the directivity, two possibilities are suggested. One is the inverse Compton effect, and the other is the bremsstrahlung from anisotropic electrons.

(Author)

A69-33452*#

THE FINE STRUCTURE OF THE EARTH'S COLLISION-LESS SHOCK WAVE.

R. W. Fredricks and F. L. Scarf (TRW Systems Group, Space Sciences Lab., Redondo Beach, Calif.) New York, American Inst. of Aeronautics and Astronautics, Jun. 1969 6 p refs American Inst. of Aeronautics and Astronautics, Fluid and Plasma Dynamics Conference, San Francisco, Calif., Jun. 16-18, 1969. (Contract NAS5-9278)

(AIAA Paper 69-676)

Instruments aboard the eccentric earth-orbiter OGO 5 have provided high time resolution plasma diagnostics from which the gross and fine structure of collision-free shocks can be deduced. Several types of shock structures were found in the high-beta, high Mach number flows of solar wind plasma impinging upon the magnetospheric obstacle. By far the most common structure is a large-amplitude MHD pulse structure having a characteristic length of the initial gradient and trailing wave train corresponding to a few times the electron inertial length. The dissipation mechanism in such shock structures is provided by electrostatic wave turbulence arising from current-driven electron-proton or proton-proton two-stream instabilities which saturate nonlinearly. Nonlinear whistler mode waves also occur in some shock structures, but provide much less efficient dissipation or proton thermalization compared with that due to the electrostatic turbulence.

(Author)

A69-34227#

SOME RELATIONS BETWEEN 3 CM SOLAR RADIO BURSTS, FLARES, X-RAYS AND GEOMAGNETIC CROCHETS.

S. Pinter (Slovenska Akademia Vied, Geofyzikalni Ustav, Hurbanovo, Czechoslovakia) 1969 6 p refs Astronomical Institutes of Czechoslovakia, Bulletin, vol. 20, no. 3, p. 151-156.

Examination of the geoactivity of solar flares and of the relations between geomagnetic crochets and X-rays, solar radio bursts, and flares. Time relations of soft and hard X-ray emission, centimeter radio bursts, and expansive and Y phases of flares with geomagnetic crochets are investigated. It is shown that not all flares are equally geoactive and that their wave geoactivity depends on the height at which they begin to expand in the solar atmosphere.

G.R.

A69-34939*

ION DEPLETION IN THE HIGH-LATITUDE EXOSPHERE: SIMULTANEOUS OGO-2 OBSERVATIONS OF THE LIGHT ION TROUGH AND THE VLF CUTOFF.

F. M. Bonner (Aero Geo Astro Co., College Park, Md.), H. C. Brinton (NASA, Goddard Space Flight Center, Greenbelt, Md.), D. L. Carpenter (Stanford U., Calif.), R.L. Heyborne (Utah State U., Logan, Utah), and H. A. Taylor, Jr. 1 Jul. 1969 12 p refs Journal of Geophysical Research, vol. 74, p. 3517-3528. NSF supported research. (Contract NAS5-3093; Grant NGR-05-020-288)

Description of the simultaneous observations of positive-ion composition, VLF earth-to-satellite transmission, and whistlers obtained from the OGO 2 satellite during October 1965 in a polar, dawn-dusk orbit. It is found that as the satellite moves poleward above about 55 deg invariant latitude, sudden depletions of the light ion components of the topside ionosphere are observed, wherein the concentrations of H(+) and He(+) decrease by as much as an order of magnitude within 3 Å. The possible mechanisms for this depletion are discussed.

Z.W.

A69-34957*

RADIATIVE RECOMBINATION OF ATOMIC OXYGEN IONS IN THE NIGHTTIME F REGION.

W. B. Hanson (Southwest Center for Advanced Studies, Dallas, Tex.) 1 Jul. 1969 3 p refs Journal of Geophysical Research, vol. 74, p. 3720-3722. (Grant NGL-44-004-001)

Discussion of nighttime observation of two longitudinal arcs of weak ultraviolet radiation located rather symmetrically about the magnetic dip equator. The radiation was detected by the polar-orbiting OGO 4 satellite and was identified as the 1304 and 1356-Å lines of atomic oxygen. Various possible explanations of the source of the observed radiation are discussed. It is concluded that correlation of the UV measurements with the direct plasma probes on OGO 4 will provide very strong evidence as to whether or not the detected emissions are in fact associated with enhanced plasma

concentrations, provided that the probes are at low enough altitudes to have access to the magnetic field lines passing through the anomaly regions. P.G.

A69-36674*

THE ORBITING GEOPHYSICAL OBSERVATORIES.

W. E. Scull (NASA, Goddard Space Flight Center, Greenbelt, Md.) Apr. 1969 6 p IEEE Transactions on Geoscience Electronics, vol. GE-7, p. 55-60.

The OGO systems are designed to fulfill a primary objective of conducting large numbers of significant, diversified experiments for making scientific and technological measurements within the earth's atmosphere, the magnetosphere, and cislunar space to obtain a better understanding of earth-sun relationships and the earth as a planet. The observatories include six appendages of different lengths for experiments requiring locations at a distance from the main body. Five degrees of freedom allow the capability of continuously orienting solar and antisolar, geocentric and antigeocentric, and orbital experiments within relatively close limits. Designed to include five basic subsystems of structure, stabilization and control, power, communications and data handling, and thermal control, the observatories have well defined interfaces for experiments. Five of the six observatories in the program have already been launched and have returned significant scientific information. Weights of the observatories range from 1073 to 1400 lb, including as many as 390 lb of experiments. One hundred six experiments have already been orbited on the five spacecraft, with 26 experiments scheduled for the last mission. Orbits have included three highly eccentric orbits inclined initially approximately 31 deg, and two low altitude nearly circular polar orbits. The orbit for the last mission, OGO 6, is of the latter type. (Author)

A69-36675*

OGO SEARCH COIL MAGNETOMETER EXPERIMENTS.

A. M. A. Frandsen, R. E. Holzer (California, U., Inst. of Geophysical and Planetary Physics, Los Angeles, Calif.), and E. J. Smith (California Inst. of Tech., Jet Propulsion Lab., Pasadena, Calif.) Apr. 1969 14 p refs IEEE Transactions on Geoscience Electronics, vol. GE-7, p. 61-74. (Contract JPL-950403)

The OGO triaxial search coil magnetometer measures naturally occurring magnetic fluctuations between 0.01 and 1000 Hz in the space around the earth. The instrument design is described and the design rationale is discussed. The results of the observations on the first five OGO spacecraft in the magnetosphere, magnetotail, magnetosheath, interplanetary medium, and hydromagnetic bow shock are summarized and discussed. (Author)

A69-36676*

DESIGN OF A LONG-LIFE RELIABLE NUCLEAR EXPERIMENT FOR SPACE FLIGHT.

J. H. Trainor and D. J. Williams (NASA, Goddard Space Flight Center, Greenbelt, Md.) Apr. 1969 4 p refs IEEE Transactions on Geoscience Electronics, vol. GE-7, p. 74-77.

Description of an experiment which has been developed for flight on OGO 6 in polar orbit. Measurements will be made of the electron flux and spectra above 30 keV, both for precipitating and locally mirroring electrons as well as atmospheric backscatter. The scientific purposes, detector and electronic systems, packaging, thermal design, internal calibration, and test philosophy are discussed. This work emphasizes the design features and philosophy used in the development, fabrication, and testing of the experiment in order to ensure a long, useful lifetime in space. (Author)

A69-36677

AN EXPERIMENT TO STUDY ELECTRIC AND ELECTROMAGNETIC FIELDS IN THE FREQUENCY RANGE 10 HZ TO 540 KHZ ON OGO-F.

R. C. Carden (Time-Zero Corp., Torrance, Calif.), T.

Laaspere, and B. Pratt (Dartmouth Coll., Thayer School of Engineering, Radiophysics Lab., Hanover, N.H.) Apr. 1969 11 p refs IEEE Transactions on Geoscience Electronics, vol. GE-7, p. 78-88.

Description of an experiment which will extend the frequency range over which whistler-mode waves can be observed in the ionosphere. The experiment uses an electric dipole antenna and will therefore also detect the essentially purely electric waves associated with the lower hybrid resonance noise bands. Emphasis is on broadband observations in the bands 0.01-15, 15-30, 92.5-107.5, and 280-295 kHz. The experiment also includes two narrow-band receivers (at 200 and 540 kHz) and a subsystem to measure the antenna impedance at four frequencies (8, 24, 104.5, and 285 kHz). (Author)

A69-36678*

COSMIC RAY NEUTRON MONITOR FOR OGO-F.

E. L. Chupp, R. W. Jenkins (New Hampshire, U., Dept. of Physics, Durham, N.H.), and J. A. Lockwood Apr. 1969 6 p refs IEEE Transactions on Geoscience Electronics, vol. GE-7, p. 88-93. (Contract NAS5-9313)

The objective of this experiment is to monitor the cosmic-ray neutron flux over a large region of space near the earth for an extended time with a simple neutron monitor. The basic detecting system to measure the integrated neutron flux from .01 eV to 15 MeV consists of a moderated He-3 proportional counter surrounded by a charged-particle rejection system. A plastic scintillator viewed by a photomultiplier is operated in coincidence with the neutron counter to determine the energy spectrum and flux in the 1-10 MeV range. In order to minimize contributions from neutrons produced within the OGO spacecraft, the sensor is located about 4.5 m out on the EP-5 boom. The experiment includes an in-flight calibrator to check pulse discriminator levels on neutron and charged-particle channels and a calibration-loop system to compensate for changes in the photomultiplier gain. The weight of the neutron sensor is 2.58 kg, with a length of 0.314 m and a diameter of 0.111 m. The total power requirements are 4.5 W. (Author)

A69-36679

OGO-5 ION SPECTROMETER.

K. K. Harris and G. W. Sharp (Lockheed Aircraft Corp., Research Labs., Palo Alto, Calif.) Apr. 1969 6 p IEEE Transactions on Geoscience Electronics, vol. GE-7, p. 93-98.

The ion spectrometer aboard OGO 5 is a most versatile instrument for topside ionospheric and magnetospheric investigations. The concentration profiles of positive O, He, and H ions are obtained in the topside ionosphere with excellent spatial resolution and with a sensitivity sufficient to measure less than 1 ion per cu cm. The dynamic range of the instrument is better than 8 orders of magnitude. These functions are accomplished with an absolute minimum of telemetry bandwidth. The instrument also functions as an energetic particle analyzer and is capable of measuring energy distributions of protons from 0 to 600 eV. The bow shock crossings of the vehicle are easily detected with the ion spectrometer, and temperature measurements within the magnetosheath are obtained. (Author)

A69-36680*

GAS-SURFACE ENERGY TRANSFER EXPERIMENT FOR OGO-F.

R. S. Dummer (Faraday Labs., La Jolla, Calif.) and D. McKeown Apr. 1969 9 p refs IEEE Transactions on Geoscience Electronics, vol. GE-7, p. 98-106. (Contracts NAS5-11163; N00014-68-C-0373)

Description of a gas-surface energy transfer experiment for the OGO 6 satellite. The experiment is to measure the kinetic energy flux of the upper atmosphere relative to the orbiting satellite, and what fraction of this energy is transferred at normal incidence to surfaces. Four probes that can detect energy transfer between 10 microwatts per sq cm

and .01 W per sq cm by the frequency change of temperature-sensitive oscillating quartz crystals are used to make the measurements. Probe accuracies of 3 per cent and precision of measurements of better than 1 per cent are maintained by periodic in-flight calibration of the crystal sensors. Data from the experiment will be used to determine the energy accommodation and drag coefficients of Al and Au, in O and diatomic nitrogen, the main components of the upper atmosphere between 400 and 1100 km. The kinetic energy flux measurement, being used in the determination of accommodation and drag coefficients, offers a novel method for determination of the upper atmospheric density and its scale height by relating measurements of the energy flux to the satellite ephemeris. (Author)

A69-36681*

A SWEEPING NEUTRAL AND POSITIVE ION MASS SPECTROMETER FOR ATMOSPHERIC COMPOSITION AT SATELLITE ALTITUDES.

B. B. Hinton, R. D. Kistler, R. J. Leite, and C. J. Mason (Michigan, U., Dept. of Aerospace Engineering, Ann Arbor, Mich.) Apr. 1969 8 p IEEE Transactions on Geoscience Electronics, vol. GE-7, p. 107-114. (Contract NAS5-3098)

Description of a sweeping mass spectrometer which performs both neutral particle and positive ion concentration measurements aboard an earth satellite. An open ion source design is utilized to adapt, with minimum degradation, both kinds of particles for the filtering action of the quadrupole field. Six linear ranges of sensitivity are provided to permit complete compositional analysis between altitudes of 300 and 1000 km. The mass range is 0-50 microns, and maximum sensitivities are 100,000 neutral particles per cu cm per volt output and 10 positive ions per cu cm per volt output. Neutral particle and positive ion measurements are made sequentially each requiring approximately 36 sec to complete using a sweep duration of approximately 6 sec. On OGO 4 this sweep duration provided a spatial resolution of 0.8 km per mass unit of sweep. Preliminary results show that the spectrometer is operating within design specifications and the SNR is excellent. Geophysical interpretations of these data should aid in the formation of more definitive model atmospheres which are important in such diverse fields as weather prediction, manned space flights, and radio propagation. (Author)

A69-36682

OGO-4 ULTRAVIOLET AIRGLOW SPECTROMETER.

C. A. Barth (Colorado, U., Dept. of Astrogeophysics, Boulder, Colo.) and E. F. Mackey (Packard Bell Electronics Corp., Space and Systems Div., Newbury Park, Calif.) Apr. 1969 6 p IEEE Transactions on Geoscience Electronics, vol. GE-7, p. 114-119. (Grant NGL-06-003-052)

The OGO 4 UV airglow spectrometer, which measures the earth's spectrum between 1100 and 3400 Å, consists of an Ebert-Fastie monochromator and two photomultipliers with wide-dynamic range electronics. The cesium telluride photomultiplier channel measures the backscattered UV daylight between 1750 and 3400 Å over a dynamic range of 10,000 with a spectral resolution of 20 Å. The cesium iodide photomultiplier channel measures airglow emission lines between 1100 and 1750 Å, even with the fully illuminated earth for a background. (Author)

A69-36683*

THE OGO-5 PLASMA WAVE DETECTOR-INSTRUMENTATION AND IN-FLIGHT OPERATION

G. M. Crook, R. W. Fredricks, I. M. Green, P. Lukas (TRW Systems Group, Space Science Lab., Redondo Beach, Calif.), and F. L. Scarf Apr. 1969 16 p refs IEEE Transactions on Geoscience Electronics, vol. GE-7, p. 120-135.

(Contract NAS5-9278)

The OGO 5 spacecraft includes in its payload an

experiment designed to measure electric field components of electrostatic and electromagnetic waves in the frequency range of 200 Hz to 70 kHz, using a variety of short, capacitively coupled antennas. In addition, the experiment has triaxial search coils, and onboard E-B correlations are performed to aid in distinguishing between the two types of waves. The design goals and instrumentation are described, and a brief account of the in-flight operation is presented.

(Author)

A69-37490*

PREDICTION OF GEOMAGNETIC SECULAR CHANGE CONFIRMED.

R. H. Ball (Rand Corp., Santa Monica, Calif.), J. C. Cain (NASA, Goddard Space Flight Center, Greenbelt, Md.), and A. B. Kahle 12 Jul. 1969 1 p refs Nature, vol. 223, p. 165.

Study of the correlation between the eccentric dipole motion and the change in length of day. A new model of the geomagnetic field was recently derived from data recorded by the OGO 2 and OGO 4 spacecraft. Using this model the eccentric dipole motion is westward at 0.114 deg/year. This new value confirms the predicted decrease some time during this period to a level about equivalent to that forty years earlier. G.R.

A69-37555*

A COMPARISON OF ENERGETIC STORM PROTONS TO HALO PROTONS.

S. W. Kahler (California, U., Space Sciences Lab., Berkeley, Calif.) Jul. 1969 20 p refs Solar Physics, vol. 8, p. 166-185. (Contract NAS5-2222)

Analysis of satellite observations of solar proton events with a halo structure or an energetic storm proton event and an SSC. It is pointed out that some SSC events are associated with a decrease in the few megaelectron volt cosmic ray fluxes while most are associated with a flux increase. The properties of halo protons and energetic storm protons are compared. It is hypothesized that the two events are similar in origin. The propagation mode of storm particles is discussed. Evidence is presented for a solar, rather than interplanetary origin of storm protons. (Author)

A69-37967

POSSIBLE INJECTION OF CHARGED PARTICLES INTO A RADIATION ZONE DURING THE MAIN PHASE OF A MAGNETIC STORM.

V. P. Shalimov Dec. 1968 3 p refs Cosmic Research, vol. 6, p. 785-787. Translated from Kosmicheskie Issledovaniia, vol. 6, Nov.-Dec. 1968, p. 941-943.

Analysis of data concerning protons with energies between 200 eV and 50 keV, found in the captured-radiation zone of the Van Allen belts. According to Frank (1967), these protons were injected into this zone from the equatorial zone during the initial stage of a magnetic storm. It is indicated that the injection of these protons might also have occurred during the main phase of the magnetic storm. V.Z.

A69-38495

VLF AND LF EMISSIONS IN AURORAL REGIONS OF THE IONOSPHERE.

T. S. Jorgensen (Dansk Meteorologisk Institut, Copenhagen, Denmark) New York, Van Nostrand Reinhold Co., 1969 10 p refs In: Atmospheric Emissions, Proceedings of the NATO Advanced Study Inst., Agricultural Coll. of Norway, As, Norway, Jul. 29-Aug. 9, 1968, p. 165-174. Inst. supported by NATO, the U.S. Air Force, and the U.S. Navy.

Discussion of the characteristic features and the mechanism of origin of VLF and LF emissions in auroral regions of the ionosphere. Observations of auroral hiss at various latitudes are reviewed. The information concerning the noise spectrum in space as observed by a satellite is considered. Studies are reported regarding the general shape and location of the hiss zones. Mechanisms of the generation of auroral hiss are discussed and reasons are cited

for the discrepancies between the theory and observations in earlier attempts to explain emissions by Cerenkov radiation. G.R.

A69-40501*

HIGH-FREQUENCY MAGNETIC FLUCTUATIONS ASSOCIATED WITH THE EARTH'S BOW SHOCK.

R. E. Holzer (California, U., Inst. of Geophysics and Planetary Physics, Los Angeles, Calif.), J. V. Olson, and E. J. Smith (California Inst. of Tech., Jet Propulsion Lab., Pasadena, Calif.) 1 Sep. 1969 17 p ref Journal of Geophysical Research, vol. 74, p. 4601-4617. NASA supported research. (Contract JPL-950403)

Investigation of magnetic fluctuations associated with the earth's bow shock in the frequency range from 0.5 to 500 Hz. These fluctuations have been detected with the search coil magnetometer on OGO 3. The analyzed shock crossings represent data taken at the 64,000 bit/sec data rate, where the instrumental Nyquist frequency is approximately 140 Hz. Power spectra have been computed for various intervals in the shock and show a broad band of noise to be present, which is of two basic types. First, there is a random background of frequencies that covers a range from below one to many hundreds of hertz. Superimposed upon this background are short-lived packets of coherent elliptically polarized radiation that occur randomly at frequencies from 10 to 500 Hz and range in amplitude from 0.01 to 0.1 gamma. Each packet is nearly monochromatic. The spectra computed from these data vary with position in the shock and are more than two orders of magnitude above interplanetary medium spectra and generally more than one order of magnitude above the magnetosheath spectra. P.G.

A69-40508*

EXPERIMENTAL VERIFICATION OF DRIFT-SHELL SPLITTING IN THE DISTORTED MAGNETOSPHERE.

T. W. Lezniak, K. A. Pfitzer, and J. R. Winckler (Minnesota, U., School of Physics and Astronomy, Minneapolis, Minn.) 1 Sep. 1969 7 p refs Journal of Geophysical Research, vol. 74, p. 4687-4693. (Grant NGL-24-005-008)

Investigation of drift-shell splitting in the nondipolar distorted magnetosphere as proposed by Roederer (1967). The theory is tested experimentally by using data from an electron spectrometer on the synchronous-orbit satellite ATS 1 and data from an electron spectrometer and ion chamber on the elliptical orbit satellite OGO 3. The agreement between calculated and measured fluxes is satisfactory not only in predicting the proper noon-to-midnight asymmetry but also in correctly predicting the pitch-angle distribution as a function of local time. P.G.

A69-40775*

OBSERVATIONS OF TWO COMPONENTS IN ENERGETIC SOLAR X-RAY BURSTS.

S. R. Kane (California, U., Space Sciences Lab., Berkeley, Calif.) Aug. 1969 4 p refs Astrophysical Journal, vol. 157, Pt-2, p. L139-L142. (Contract NAS5-9094)

Measurements made with the solar X-ray detector aboard the OGO 5 satellite show that some energetic (more than 9.6 keV) solar X-ray bursts consist of two components. An impulsive component reaches its peak early in the event, approximately in coincidence with the peak in the microwave burst, and has a photon spectrum consistent with a power law in energy. A slower component attains its maximum later in the event and has a photon spectrum steeper than that for the impulsive component. The measurements also show that in some X-ray bursts only the slower component is observable. The impulsive component is attributed to the bremsstrahlung emission from electrons with a nonthermal energy distribution. (Author)

A69-42428*

THE LOCATION OF THE DIP EQUATOR AT E-LAYER

ALTITUDE.

J. C. Cain (NASA, Goddard Space Flight Center, Greenbelt, Md.) Sep. 1969 4 p refs Radio Science, vol. 4, p. 781-784. (International Symposium on Equatorial Aeronomy, 3rd, Ahmedabad, India, Feb. 3-10, 1969.)

Tabulation of the position of the magnetic dip equator at 100 km, and of the gradient of position with time and altitude, using the POGO (19/68), GSFC (12/66), and IGRF (10/68) geomagnetic field models. The positions agree within a few tenths of a degree with each other but differ up to 2 deg from older models and charts. The maximum gradients with time (0.2 deg/yr) and altitude (minus 0.3 deg/100 km) occur to the west of Africa. (Author)

A69-42693**

OBSERVATIONS OF THE MICROSTRUCTURE OF THE EARTH'S BOW SHOCK.

P. J. Coleman, Jr. (California, U., Inst. of Geophysics and Planetary Physics, Los Angeles, Calif.) and R. W. Fredricks (TRW Systems Group, Space Sciences Lab., Redondo Beach, Calif.) New York, Gordon and Breach, Science Publishers, Inc., 1969 30 p refs In: Plasma Instabilities in Astrophysics, Proceedings of the Conference, Monterey, Calif., Oct. 14-17, 1968. p. 199-228. Conference Sponsored by the American Astronomical Society, the American Physical Society, Stanford U., and the U.S. Atomic Energy Commission. (Contracts NAS5-9278; NAS5-9098)

Discussion of some very recent observations of fluctuating electric fields and their apparent relationship to the MHD bow shock structure as defined by a low frequency fluxgate magnetometer. The observations were made by instruments aboard OGO 5 launched on March 4, 1968 into a highly elliptical earth orbit. Detailed magnetometer and ac electric field data for two bow shock traversals have been correlated. The raw data from some 58 other shock traversals are examined. A description is given of the electric field (or plasma wave) detector flown on OGO 5. G.R.

A69-43132#

LAST OF THE OGO'S.

P. J. Parker Oct. 1969 3 p Spaceflight, vol. 11, p. 363-365.

General description of the design and research program of the OGO 6 which is last of the OGO series and was launched on June 5, 1969. The initial orbit, inclined at 82 deg to the equator, ranged between 245 and 680 miles and had a period of about 100 min. The 1393-lb spacecraft carries 25 experiments for obtaining data over a complete range of latitudes, extending from the equator to the poles. These experiments relate to the earth's upper atmosphere and ionosphere, the auroral regions surrounding the poles, and the edges of the regions of trapped radiation. Particular emphasis is placed on the interrelationships between particle activity, aurora and airglow, the geomagnetic field, the neutral and ionized composition, wave propagation and noise, and the input solar energy contributing to ionization and heating. Z.W.

A69-43172*

INTENSITY CORRELATIONS AND SUBSTORM ELECTRON DRIFT EFFECTS IN THE OUTER RADIATION BELT MEASURED WITH THE OGO 3 AND ATS 1 SATELLITES.

K. A. Pfitzer and J. R. Winckler (Minnesota, U., School of Physics and Astronomy, Minneapolis, Minn.) 1 Oct. 1969 14 p refs Journal of Geophysical Research, vol. 74, p. 5005-5018. (Grant NGL-24-005-008)

Study of the space-time distribution of the radiation in the outer radiation belt using the correlated data of two satellites, ATS 1 and OGO 3. The applicability of known models of the distorted magnetosphere during quiet conditions is tested in order to verify that under these known conditions the spectrometers could be brought into simultaneous agreement at various points on common drift shells in the very slowly changing outer zone. This comparison is extended

to cases of large electron flux increases during magnetospheric substorms typified by auroral-zone bay events. Z.W.

A69-43183*

ACCESS OF SOLAR PROTONS INTO THE POLAR CAP: A PERSISTENT NORTH-SOUTH ASYMMETRY.

L. C. Evans and E. C. Stone (California Inst. of Tech., Pasadena, Calif.) 1 Oct. 1969 5 p refs Journal of Geophysical Research, vol. 74, p. 5127-5131. (Contract NAS5-3095; Grant NGL-05-002-007)

Before the magnetic storm sudden commencement during the Nov. 2, 1967, solar particle event, the access of 1.2 to 40 MeV protons into the high latitude portion of the northern polar region was delayed by about 20 hours. At the same time, the access delay for 10 to 40 MeV protons was less than one hour in the southern polar region and at middle northern latitudes. The implications of the north-south asymmetry are discussed. (Author)

A69-43184*

INITIAL OBSERVATIONS OF GEOMAGNETICALLY TRAPPED PROTONS AND ALPHA PARTICLES WITH OGO 4.

T. A. Fritz and S. M. Krimigis (Iowa, U., Dept. of Physics and Astronomy, Iowa City, Iowa) 1 Oct. 1969 7 p refs Journal of Geophysical Research, vol. 74, p. 5132-5138. Research supported by the National Research Council of Canada.

(Contract NAS5-3097; NASA Order R-21-009-004(13); Contracts Nonr-1509(06); Now-62-0604-C)

Discussion of observations obtained with two totally depleted solid-state detectors with thicknesses of 34 and 7.2 microns designed to measure protons and alpha particles, respectively, on the OGO 4 spacecraft. Both detectors have four electronically determined energy channels. Comparison of the data with various predictions of models that consider the solar wind as a source of trapped particles shows serious discrepancies between theory and observations. G.R.

A69-43611

MEASUREMENTS OF SOLAR X-RAY EMISSION FROM THE OGO-4 SPACECRAFT.

T. A. Chubb, H. Friedman (U.S. Navy, Naval Research Lab., E. O. Hulbert Center for Space Research, Washington, D.C.), D. M. Horan, and R. W. Kreplin (Amsterdam, North-Holland Publishing Co., 1969 10 p refs In: Solar flares and space research, COSPAR, Plenary Meeting, 11th, Symposium, Tokyo, Japan, May 9-11, 1968, Proceedings, p. 121-130. Symposium co-sponsored by the International Astronomical Union, the International Union of Geodesy and Geophysics, and the International Scientific Radio Union.

Instrumentation aboard OGO 4 monitors solar X-ray fluxes in four bands (0.5-3A, 1-8A, 8-16A, and 44-50A) with high time resolution and sufficient dynamic range to compare peak fluxes during flares with preflare and postflare conditions. Comparisons with SOLRAD X-ray data obtained with similar detectors during the IQSY show that the quiet sun base level in the 8-20 A band had risen in 1967 by a factor of about 30, while in the 1-8 A band the increase has been greater than a factor of 100. The 44-60 A flux has shown an increase of a factor of 10. From a number of large flares recorded by OGO 4 in July and August 1967, it is observed that the flare X-ray emission starts earliest in the shortest wavelengths; the 0.5-3 A band leads the 1-8 A and 8-16 A bands by about one minute. Peak fluxes are also reached earliest at the shortest wavelengths. (Author)

A70-10444*

ATTEMPTS TO MEASURE MICROMETEOROID FLUX ON THE OGO 2 AND OGO 4 SATELLITES.

C. S. Nilsson, D. Wilson (Smithsonian Institution, Smithsonian Astrophysical Observatory, Cambridge, Mass.), and F. W. Wright 15 Oct. 1969 9 p refs Journal of Geophysical Research, vol. 74, p. 5268-5276. (Contract NAS5-11007)

Description of the micrometeoroid experiments on the OGO 2 and OGO 4 satellites. The aim of the OGO 2 experiment was to measure the velocities, masses, and orbits of dust particles in the earth's dust cloud. No orbits were determined, and it is questionable whether any micrometeoroids of mass greater than 1 picogram impacted on the sensors during the 1300 hr in which good data were obtained. The OGO 4 experiment was modified in an attempt to measure a flux obviously much smaller than previously anticipated. No micrometeoroids capable of penetrating 4000 A of Al have impacted on ionization sensors with a total effective area of 5 sq cm ster during a 3000-hr exposure. The flux of micrometeoroids greater than 1 picogram in the neighborhood of the earth is less than .002 particles/sq m sec 2 pi ster. (Author)

A70-12902*

PRIMARY COSMIC-RAY ELECTRON ENERGY SPECTRUM FROM 10 TO 200 MEV OBSERVED IN INTERPLANETARY SPACE.

C. Y. Fan, J. L'Heureux, and P. Meyer (Chicago, U., Enrico Fermi Inst. for Nuclear Studies, Chicago, Ill.) 13 Oct. 1969 4 p refs Physical Review Letters, vol. 23, p. 877-880. (Contract NAS5-9096; Grant NGR-14-001-005)

Measurement of the quiet-time flux and energy spectrum of primary cosmic-ray electrons in the energy range from 10 to 200 MeV in interplanetary space. The investigation was carried out with an instrument on board the OGO 5 satellite and covers the period from Mar. 15 to Apr. 25, 1968. When these 1968 results are compared with the 1966 results of L'Heureux and Meyer (1968) and of Webber (1968), a difference of almost an order of magnitude exists which is probably due to an enhanced modulation at the time of the measurement. M.M.

A70-13980*

HELIOGRAPHIC LATITUDE DEPENDENCE OF THE DOMINANT POLARITY OF THE INTERPLANETARY MAGNETIC FIELD.

P. J. Coleman, Jr. (California, U., Inst. of Geophysics and Planetary Physics, Los Angeles, Calif.) and R. L. Rosenberg 1 Nov. 1969 12 p refs Journal of Geophysical Research, vol. 74, p. 5611-5622.

The measurements of the interplanetary magnetic field taken with the Mariners 2, 4, and 5, and the OGO 5 cover several parts of the interval from September 1962 to the present and several paths through the region between 0.7 and 1.5 AU and between plus and minus 7.3 deg in solar equatorial latitude. Evidence is found for a distinct dominant polarity effect in the magnetic field. Specifically, the dominant polarity of the field was inward (toward the sun) at heliographic latitudes above the solar equatorial plane and outward (away from the sun) at latitudes below this plane. Magnetographs of the polar regions of the sun indicate that the dipolar component of the sun's field has been inward over the northern hemisphere and outward over the southern hemisphere since the last maximum in solar activity, which occurred in 1958. The results suggest that over most of a solar cycle, the dominant polarity of the interplanetary field in either the northern or southern hemisphere of interplanetary space is just that of the dipolar component of the sun's field in the same hemisphere. (Author)

A70-13994*

EFFECTS OF SECONDARY ELECTRON EMISSION ON ELECTRON TRAP MEASUREMENTS IN THE MAGNETOSPHERE AND SOLAR WIND.

L. W. Parker (Mount Auburn Research Associates, Inc., Cambridge, Mass.) and E. C. Whipple, Jr. (ESSA, Research Labs., Aeronomy Lab., Boulder, Colo.) 1 Nov. 1969 12 p refs Journal of Geophysical Research, vol. 74, p. 5763-5774. NASA supported research. (Contract E-22-8-69(N))

Extension of a previously developed theory for the behavior of an electron trap mounted on a charged spacecraft to include the contributions of secondary electrons emitted

from the spacecraft surfaces. Analytic formulas are derived that reproduce the results of particle trajectory calculations for all probe and satellite potentials, in the limit of large Debye length and no magnetic field. The analysis is complicated by the possible presence of a potential barrier for a repulsive satellite, and also by the presence of more than one emitting surface. It is shown, in solar wind measurements where both hot and cold electron components are sometimes inferred, that while the hot component may be correctly attributed to the plasma, the cold component can at times be attributed to secondaries from the spacecraft surfaces. Incorrect interpretation of the observed currents has led in the past to overestimates of the electron concentration. A correct interpretation leads to electron concentrations in good agreement with positive ion densities measured by other techniques in the solar wind. (Author)

A70-15106*

"HYSTERESIS" EFFECTS IN COSMIC RAY MODULATION AND THE COSMIC RAY GRADIENT NEAR SOLAR MINIMUM.

S. R. Kane and J. R. Winckler (Minnesota, U., School of Physics and Astronomy, Minneapolis, Minn.) 1 Dec. 1969 9 p refs Journal of Geophysical Research, vol. 74, p. 6247-6255.

(Contract NAS5-2071)

Cosmic-ray total ionization measurements made in space near the earth with the OGO 1 and OGO 3 ion chambers during the period from September 1964 to December 1967 are compared with other cosmic-ray measurements in space and on the ground. As compared to the recovery phase (before May 1965), the apparent long-term modulation of the low-energy particles was relatively less during the early decreasing phase (June 1965 to December 1966) giving rise to the hysteresis effect. The observed effect disappeared completely by Apr. 22-28, 1967. The hysteresis effect is probably a characteristic of the modulation mechanism. It is not likely to be due to the time variation of a quiescent flux of energetic solar particles. (Author)

A70-15116*

NONDUCTED MODE OF VLF PROPAGATION BETWEEN CONJUGATE HEMISPHERES: OBSERVATIONS ON OGO'S 2 AND 4 OF THE "WALKING-TRACE" WHISTLER AND OF DOPPLER SHIFTS IN FIXED FREQUENCY TRANSMISSIONS.

J. J. Angerami (Stanford U., Stanford Radioscience Lab., Stanford, Calif.) and F. Walter 1 Dec. 1969 19 p refs Journal of Geophysical Research, vol. 74, p. 6352-6370. (Contracts NAS5-3093; N00014-67-A-0112-0012; Grants NGR-05-020-008; NSF GA-1151; NSF GA-1485; NSF GP-948; NsG-174)

Description of a new whistler phenomenon identified in mid-latitude (about 50 deg) spectrographic records from the VLF experiment aboard the low altitude polar satellites OGO 2 and OGO 4. Evidence for nonducted whistler-mode propagation from one hemisphere to the conjugate ionosphere has been found. The nonducted propagation manifests itself both in naturally occurring whistlers and in man-made signals. G.R.

A70-15117*

WHISTLER-MODE EMISSIONS ON THE OGO-1 SATELLITE.

N. Dunckel and R. A. Helliwell (Stanford U., Stanford Radioscience Lab., Stanford, Calif.) 1 Dec. 1969 15 p refs Journal of Geophysical Research, vol. 74, p. 6371-6385. (Contract NAS5-2131; Grants NsG-174; NGR-05-020-288; NGR-05-020-008; NSF GP-948)

Results of magnetospheric observations of whistler-mode emissions made by the OGO-1 satellite over the frequency range of 0.3 to 100 kHz. Taken during the geomagnetically quiet period from September 1964 through May 1965, the data cover geocentric distances from 2 to 24 earth radii and geomagnetic latitudes in the range of plus or minus 50 deg. The spectra of emissions resemble those of chorus and

midlatitude hiss observed on the ground. An important new result is the observation that the upper-frequency limit of most of these emissions is proportional to the minimum electron gyrofrequency along the magnetic field line passing through the satellite. This is interpreted to mean that the source of these emissions lies close to the equatorial plane. Estimates of the average intensity of these emissions agree with the intensity required to explain the precipitation of electrons through pitch-angle scattering by whistler-mode waves. (Author)

A70-15127

RESONANT COMPRESSIONAL WAVES IN THE GEOMAGNETIC TAIL.

G. L. Siscoe (McDonnell Douglas Corp., McDonnell Douglas Astronautics Co., Western Div., Santa Monica, California, U., Dept. of Meteorology, Los Angeles, Calif.) 1 Dec. 1969 5 p refs Journal of Geophysical Research, vol. 74, p. 6482-6486. Research supported by the McDonnell Douglas Independent Research and Development Program.

Irregularities in the solar wind can excite compression waves in the geomagnetic tail that have their maximum amplitude in the plasma sheet. Details such as the exact frequency and spatial distribution of the waves depend on the overall geometry of the tail. Estimates of these properties are obtained by use of a single-layered, two dimensional model. Symmetric and antisymmetric modes are studied. For the physical parameters chosen to represent the typical tail, the fundamental period of the antisymmetric mode is approximately 11 min and that of the symmetric mode is approximately 2 min. (Author)

A70-15128*

TEMPORAL VARIATIONS OF SOLAR LYMAN ALPHA

R. R. Meier (U.S. Navy, Naval Research Lab., E. O. Hulburt Center for Space Research, Washington, D. C.) 1 Dec. 1969 4 p refs Journal of Geophysical Research, vol. 74, p. 6487-6490. NASA supported research.

Geocoronal Lyman-alpha was observed by the OGO 4 spacecraft from August through December 1967. The emission rate at a fixed orientation with respect to the sun was found to have short-term fluctuations of less than plus or minus 5 per cent superimposed on a monthly (or 27-day) variation of as much as plus or minus 15 per cent. These phenomena are attributed to variability of the Lyman-alpha flux at the center of the solar emission line. (Author)

A70-15522*#

METEOROLOGICAL RESULTS FROM MULTI-SPECTRAL PHOTOMETRY IN AIRGLOW BANDS BY THE OGO-4 SATELLITE.

L. J. Allison (NASA, Goddard Space Flight Center, Greenbelt, Md.), J. E. Blamont (Centre National de la Recherche Scientifique, Paris, France), W. B. Fowler, E. R. Kreins (Applications Center, Washington, D.C.), E. I. Reed, and G. Warnecke Nov. 1969 11 p refs Journal of the Atmospheric Sciences, vol. 26, p. 1329-1339.

The presence or absence of clouds, their characteristics, and variations of surface albedo have been correlated with observations made at several different wavelengths in the visible spectrum. These were made at high and low nighttime light levels by an airglow photometer aboard the OGO 4 satellite during August 1967 through January 1968. The wavelength regions studied were approximately 50 Å bands centered at 3914, 5577, 5893, 6225, and 6300 Å, in the energy range of 10 to the minus 7th power to 10 to the minus 3rd power erg/sq cm-sec-Å ster with a field of view of approximately 10 deg. It was found that at the longer wavelengths (1225 and 6300 Å) the observations were strongly influenced by the variations of surface albedo. At the shorter wavelengths, the surface albedo variations were partly masked by the light returned through Rayleigh and Mie scattering. Preliminary analysis is made of surface and clouds by study of reflective radiance under moonlight and other nocturnal illuminations. Possibilities of further analysis are

examined, including methods of deducing cloud height information. (Author)

A70-15645*#

INFLIGHT RADIOMETRIC CALIBRATION OF OGO-IV AIRGLOW PHOTOMETER.

J. E. Blamont, W. B. Fowler (Centre National de la Recherche Scientifique, Paris, France), and E. I. Reed (NASA, Goddard Space Flight Center, Greenbelt, Md.) Oct. 1969 12 p Optical Society of America, Annual Meeting, Chicago, Ill., Oct. 21-24, 1969, Paper.

Description of the in-flight calibration of a low-brightness photometer which viewed the airglow in the visual and UV wavelengths directly below the spacecraft and at 6300 Å above the satellite. The stability of responsivity in orbit is checked by comparing moonlit earth radiance over the oceans on repeated orbits under varying cloud conditions. Studies of a number of orbits show the ratios of moonlit radiances at 3914 Å and 6225 Å follow closely the values predicted from calculations of reflected radiance of the earth's atmosphere. Absolute responsivity determined from the overhead transit of Saturn in October and Jupiter in December indicates a 33 per cent drop in responsivity from the laboratory calibration in March 1966. This decrease, applied to all filtered channels, gives radiance values in near agreement with ground-based airglow measurements at 6300 Å.

(Author)

A70-17376*

OBSERVATIONS OF PLASMA WAVES IN SPACE.

G. M. Crook, R. W. Fredricks, I. M. Green (TRW Systems Group, Redondo Beach, Calif.), C. F. Kennel (California, U., Berkeley, Calif.), and F. L. Scarf (New York American Elsevier Publishing Co., Inc., 1969 26 p refs In: Plasma Waves in Space and in the Lab., NATO, Advanced Study Inst., Roros, Norway, Apr. 17-26, 1968, Proceedings, Volume 1, p. 379-404. Research supported by the TRW Systems Group Independent Research Program.

(Contracts NAS2-3410; NAS2-4673; NAS5-9278; Grant NASw-1598)

Brief discussion of techniques used to measure plasma waves in space and of some of the unique problems associated with this type of research. Low-altitude electric and magnetic field data, primarily obtained with the OV3-3 (1966-70A) spacecraft experiment, are presented. Preliminary results obtained from Pioneer 3 and OGO 5 are very briefly discussed. M.M.

A70-18530*

A STUDY OF THE INFLUENCE OF MAGNETIC ACTIVITY ON THE LOCATION OF THE PLASMAPAUSE AS MEASURED BY OGO-5

C. R. Chappell, K. K. Harris, and G. W. Sharp (Lockheed Missiles and Space Co., Palo Alto, Calif.) 1 Jan. 1970 7 p refs Journal of Geophysical Research, vol. 75, p. 50-56. (Contract NAS5-9092)

The plasmopause position has been measured quite well by the light ion mass spectrometer aboard OGO 5, which measures the concentrations of H(+), He(+), and O(+) ions as a function of L and local time. The influence of magnetic activity on this plasmopause position has been studied for the local-time regions at 1000 plus or minus 2 hours and 0200 plus or minus 2 hours. The plasmopause location shows a general decrease in radius with increasing activity in both regions. The time lag between the onset of magnetic activity and the change in plasmopause radius is found to be about 2 to 6 hours for the 0200 local-time region. However, the time lag for the 1000 local-time region is not well defined, although the 6-hour lag time seemed to fit some of the cases better than 12- or 24-hour periods that were examined. By using the 2- to 6-hour response time, the plasmopause density profiles in the 0200 local-time region were grouped according to magnetic activity. This grouping displays the typical plasmopause reaction in this local-time region to increasing magnetic activity with the knee position moving to lower L values, the sharpness of the knee increasing, and

the total concentration levels inside and outside the knee remaining approximately the same at 1000 ions/cu cm and 1 ion/cu cm, respectively. (Author)

A70-18532*

SATELLITE OBSERVATIONS OF EQUATORIAL PHENOMENA AND DEFOCUSING OF VLF ELECTROMAGNETIC WAVES.

R. R. Scarabucci (Stanford U., Stanford, Calif.) 1 Jan. 1970 16 p refs Journal of Geophysical Research, vol. 75, p. 69-84.

(Contract NAS5-3093; Grants NGL-05-020-008; NSF GP-948)

Amplitude measurements of whistlers and signals from VLF transmitters have been made with the low altitude, polar-orbiting OGO 4 satellite. Two aspects of these measurements related to the behavior of the waves near the magnetic equator are described and interpreted: (1) Daytime spectrograms taken near the magnetic equator show a remarkable high frequency cutoff in the amplitude of the VLF whistler waves. The cutoff frequency decreases as the satellite approaches the magnetic equator, and sometimes all signals drop below the equipment threshold. This feature is also present when the signals from different VLF transmitters are simultaneously observed. It is shown that the above phenomenon is explained primarily by absorption in the D and E regions of the ionosphere and by the daytime ray trajectories near the equator. (2) During the night, absorption becomes relatively small, but nevertheless an abrupt amplitude cutoff of signals from VLF transmitters may still occur. This nighttime cutoff is explained primarily by defocusing near the equator, which is enhanced for nighttime ionization profiles. The defocusing of the VLF waves depends strongly upon the rapid change of ionization gradient occurring between 500 and 1000 km of height and also upon the curvature of the earth's magnetic field around the magnetic equator. (Author)

A70-18534*

COMPARISON OF CERTAIN VLF NOISE PHENOMENA WITH THE LOWER HYBRID RESONANCE FREQUENCY CALCULATED FROM SIMULTANEOUS ION COMPOSITION MEASUREMENTS.

T. Laaspere (Dartmouth Coll., Hanover, N.H.) and H. A. Taylor, Jr. (NASA, Goddard Space Flight Center, Lab. for Atmospheric and Biological Sciences, Greenbelt, Md.) 1 Jan. 1970 10 p refs Journal of Geophysical Research, vol. 75, p. 97-106.

(Contract NAS5-3092)

Certain vlf noise phenomena commonly observed with electric dipole antennas on the Alouette, OGO, and Injun 5 spacecraft have been associated with the lower hybrid resonance frequency of the ionospheric medium in the vicinity of the spacecraft. By using simultaneous vlf and ion mass spectrometer data from OGO 4, it has now become possible to compare the characteristic frequencies of these noise bands with the lower hybrid resonance frequency $f_{sub LH}$ calculated directly from ion composition measurements. The results of the study show a clear correspondence between the independent observations over a wide range of variation of $f_{sub LH}$. Some differences between the vlf and the spectrometer results are also evident and suggest that the characteristic frequencies of lower hybrid resonance noise phenomena observed by satellite-borne vlf receivers may not always be determined in the immediate vicinity of the spacecraft. (Author)

A70-18546*

OBSERVATIONS OF THE PLASMAPAUSE FROM OGO-5.

C. R. Chappell (Lockheed Missiles and Space Co., Palo Alto, Calif.), K. K. Harris, and G. W. Sharp 1 Jan. 1970 6 p refs Journal of Geophysical Research, vol. 75, p. 219-224.

(Contract NAS5-9092)

The data from the ion spectrometer aboard the OGO 5

vehicle have been analyzed for the early orbits. The profiles of O(+), He(+), and H(-) ion concentrations have been obtained as a function of the geomagnetic parameter L. The detailed character of the plasmapause has been observed. It is found that the concentration change at the plasmapause location is highly variable being at times gradual and at other times very abrupt. The diameter of the plasmasphere is found to depend upon the magnetic activity, showing a significant decrease when the magnetic activity is high. The plasmapause is found to occur independently in all ion species at precisely the same location. An interesting 'wavelike' structure in the ion concentration is observed in the vicinity of L = 6. (Author)

**A70-19630
HARMONIC ION CYCLOTRON RESONANCES
OBSERVED BY THE OGO-4 SATELLITE.**

H. Kikuchi (Max-Planck-Institut fuer Aeronomie, Lindau ueber Northeim, West Germany) 17 Jan. 1970 2 p Nature, vol. 225, p. 257, 258.

Discussion of a new phenomenon associated with proton whistlers which has been observed in the VLF recordings from the OGO 4 satellite. The new effect appears on a frequency-time spectrogram as several separated, narrow, steady bands of noise whose center lines are located at multiples of the ion cyclotron frequency. G.R.

**A70-21377*
INITIAL DECELERATION OF SOLAR WIND POSITIVE
IONS IN THE EARTH'S BOW SHOCK.**

M. Neugebauer (California Inst. of Tech., Jet Propulsion Lab., Pasadena, Calif.) 1 Feb. 1970 17 p refs Journal of Geophysical Research, vol. 75, p. 717-733.

Assessment of high-time-resolution plasma measurements made on the upstream edge of the earth's bow shock by the combination of a Faraday cup with modulation grid and a curved-plate analyzer on the satellite OGO 5. These observations show that the solar-wind positive ions often undergo a substantial deceleration just upstream of the shock's steep gradient of magnetic-field strength. This deceleration, which is not necessarily accompanied by a temperature increase, may be caused by a charge-separation electric field on the upstream side of the bow shock. (Author)

**A70-21380*
OGO 3 OBSERVATIONS OF ELF NOISE IN THE
MAGNETOSPHERE.**

R. E. Holzer (California, U., Los Angeles, Calif.), C. T. Russell, and E. J. Smith (California Inst. of Tech., Jet Propulsion Lab., Pasadena, Calif.) 1 Feb. 1970 14 p refs Journal of Geophysical Research, vol. 75, p. 755-768. (Contract JPL-950403; Grant NGR-05-007-235)

Examination of the noise present between 1 and 1000 Hz at the magnetic equator with the OGO 3 search coil magnetometer, revealing a previously unobserved class of signals existing only in the outer plasmasphere. These waves are propagating nearly perpendicular to the magnetic field, probably within less than 1 deg of perpendicular to it; they exist only between about twice the proton gyrofrequency and half the lower hybrid resonant frequency. The waves are confined to a region within about 2 deg of the equator and therefore have a large amplitude gradient along the magnetic field lines. They are resonant with harmonics of the electron bounce frequency and have sufficient amplitude (approximately 10 milligammas rms) to cause the observed pitch-angle diffusion of electrons mirroring near the equator. (Author)

**A70-23490*
DIRECT DETECTION OF ASYMMETRIC INCREASES
OF EXTRATERRESTRIAL 'RING CURRENT' PROTON
INTENSITIES IN THE OUTER RADIATION ZONE.**

L. A. Frank (Iowa, U., Iowa City, Iowa) 1 Mar. 1970 6 p refs Journal of Geophysical Research, vol. 75, p. 1263-1268.

(Contract NAS5-2054; Grants Nonr-1509(06);

NGL-16-001-002)

Measurements of the spatial distributions and temporal variations of the extraterrestrial ring current proton intensities near the magnetic equator during selected phases of two moderate magnetic storms on July 9 and September 8, 1966, provide direct evidence of asymmetric enhancement of these proton intensities deep in the outer radiation zone, during the early development of the latter magnetic storm. Increases of these low energy proton (from 5 to 50 keV) intensities in the evening-midnight quadrant of the outer radiation zone on L shells of about 3.5 to 5.0 were accompanied by a substantial polar magnetic substorm observed during similar local times. However, no increases of proton intensities at levels above those typical of the quiescent ring current centered at L of about 6.5, were yet observed near local noon, several hours later. Several implications that concern the origin and motions of this plasma during the early development phase of the magnetic storm are discussed. (Author)

**A70-23491*
OMNIDIRECTIONAL INTENSITY CONTOURS OF
LOW-ENERGY PROTONS /0.5 TO 50 keV/ IN THE
EARTH'S OUTER RADIATION ZONE AT THE
MAGNETIC EQUATOR.**

L. A. Frank and H. D. Owens (Iowa, U., Iowa City, Iowa) 1 Mar. 1970 10 p refs Journal of Geophysical Research, vol. 75, p. 1269-1278.

(Contracts NAS5-2054; Nonr-1509(06); Grants NGL-16-001-002; NSG-233-62)

Observations of low-energy proton intensities within seven selected energy bandpasses spanning the energy range from 0.5 to 50 keV are summarized in diagrams of L versus time for the period of June 10 through July 23, 1966. These contours of omnidirectional, differential proton intensities were calculated via measurements of the directional, differential spectrums of the proton intensities with a sensitive electrostatic analyzer array borne on the earth satellite OGO 3 at mid- and low latitudes in the outer radiation zone and are normalized to a geomagnetic latitude of 0 deg (magnetic equator). Diagrams of L versus time provide a compact, useful summary of these unique observations of proton intensities over L values ranging from 3.0 to 12 and promote further insight into the morphological features of one of the most dynamically important components of magnetospheric plasma. (Author)

**A70-23493*
OBSERVATIONS OF THE AURORA IN THE FAR
ULTRAVIOLET FROM OGO 4.**

T. A. Chubb and G. T. Hicks (U.S. Navy, E. O. Hulburt Center for Space Research, Washington, D. C.) 1 Mar. 1970 22 p refs Journal of Geophysical Research, vol. 75, p. 1290-1311. NASA supported research.

Observations of the aurora have been made from the OGO 4 spacecraft in the far ultraviolet. Auroral arcs were found to be easily detectable even in full sunlight, and the aurora was observed to be continuously present with little difference between Southern and Northern Hemispheres. The morphology of the far ultraviolet aurora is quite similar to that of the visible aurora. The middle day aurora was observed to be about 40% as bright as the middle night aurora and to occur at about 8 deg higher invariant latitude. Minimum relative brightness seems to occur in late morning. The center of the auroral oval was generally observed to be dark. Lyman alpha rich arcs were frequently observed on evening crossings of the oval and were observed equatorward of arcs of normal color; in three morning crossings of the oval, Lyman alpha rich arcs were observed poleward of arcs of more normal color. At high Kp the auroral display brightened and moved equatorward. Displays with considerable stability in arc structure for periods of up to 5 hours were observed, whereas other displays showed significant change from orbit to orbit. Arcs were observed with maximum contrast relative to the dayglow in the 1350- to 1550-A band. (Author)

A70-25746*

IDENTIFICATION OF THE HARD X-RAY PULSE IN THE FLARE OF SEPTEMBER 11-12, 1968.

J. Vorpahl (California, U., Berkeley, Calif.) and H. Zirin (Mount Wilson and Palomar Observatories, Pasadena, Calif.) Feb. 1970 6 p refs Solar Physics, vol. 11, p. 285-290. NSF supported research.

(Contract NASS-9094; Grant NGL-05-002-071)

Comparison of the optical and X-ray data on the flare development sequence of Sept. 11-12, 1968. The comparison leads to the identification of a hard X-ray pulse with the formation of a brilliant kernel. Each stage in the X-ray event is shown to correspond to a definite phase in the development of the flare.

M.V.E.

A70-26568*

VARIATION OF THE ION-TEMPERATURE GRADIENT ALONG FIELD LINES IN THE OUTER PLASMASPHERE.

J. M. Grebowsky and N. K. Rahman (NASA, Goddard Space Flight Center, Lab. for Atmospheric and Biological Sciences, Greenbelt, Md.) Mar. 1970 6 p refs Planetary and Space Science, vol. 18, p. 417-422.

The equations of thermal diffusion are used to explore the variation of the ion-temperature in the outer plasmasphere, where H(+) is the dominant positive ion. The ion-temperature gradient component in the direction of the magnetic field is a function of only the ratio of the H(+) scale height to the He(+) scale height along the field direction and the gravitational acceleration when the ion and electron temperatures are equal. However, if the scale heights are equal then the ion-temperature gradient is independent of the temperature and depends only on the gravitational acceleration. The ion-temperature gradients are determined throughout the plasmasphere where the H(+), He(+) concentration ratio is assumed to be spatially invariant. At an altitude of 1000 km in the protonosphere, the magnitude of the computed upward directed ion temperature gradient component along the field line increases from 0.9 deg K/km near L 1.3 to 1.5 deg K/km at L 5. The computed ion-temperature variations are in general agreement with electron-temperature observations in the topside ionosphere and the outer plasmasphere.

(Author)

A70-27181*

OGO 3 OBSERVATIONS OF THE LYMAN ALPHA INTENSITY AND THE HYDROGEN CONCENTRATION BEYOND 5 R SUB E

P. Mange and R. R. Meier (U.S. Navy, Naval Research Lab., Washington, D. C.) 1 Apr. 1970 11 p refs Journal of Geophysical Research, vol. 75, p. 1837-1847. NASA supported research.

The intensity of Lyman alpha was measured from the OGO 3 spacecraft at altitudes from 5 to 19 R sub E (Earth radii). The variation of intensity with distance reveals a mean hydrogen density at 50,000 km of about 20 atoms per cu cm for the summer 1966 epoch and negligible contribution to the signal from geocoronal hydrogen beyond 12 radii. An extraterrestrial background of some 750 rayleighs was observed at apogee. Asymmetry of intensity variations on either side of apogee suggest an enhancement of the background from regions near the galactic plane, and correlation of the background with solar activity over a 40-day period suggests that a portion of the background is solar-related.

(Author)

A70-27183*

LOW-FREQUENCY NOISE OBSERVED IN THE DISTANT MAGNETOSPHERE WITH OGO-1.

N. Duncel, B. Ficklin (Stanford U., Stanford, Stanford Research Inst., Menlo Park, Calif. Develco, Inc., Mountain View, Calif.), R. A. Helliwell (Stanford U., Stanford, Calif.), and L. Rorden 1 Apr. 1970 9 p refs Journal of Geophysical Research, vol. 75, p. 1854-1862.

(Contract NASS-2131; Grants NGR-05-020-288; NGL-05-020-008; NSG-174)

Discussion of two new types of low-frequency noise, designated broad-band and highpass, which have been detected in the distant magnetosphere by the VLF/LF experiment on the OGO 1 satellite. Broadband noise extends over the entire range of observations from 0.2 to 100 kHz and the intensity decreases with increasing frequency. It occurs in bursts having durations of a few minutes or less. It shows no connection with any of the expected plasma cutoff or resonance frequencies and is believed to be a nonpropagating disturbance generated in the vicinity of the satellite. Highpass noise extends from a characteristic low-frequency cutoff to above 100 kHz and occurs in bursts lasting tens of minutes.

G.R.

A70-27594#

LUNAR LIMB SHOCK WAVE.

J. V. Hollweg (Max-Planck-Institut fuer Physik und Astrophysik, Garching, West Germany) 1969 5 p refs Astronomische Gesellschaft, Mitteilungen, no. 27, p. 222-226. Astronomische Gesellschaft, Versammlung, 51st, Mannheim, West Germany, Sep. 15-19, 1969.

Investigation of a weak shock wave at the lunar limb as observed by the Lunar Explorer 35 measurements, defined with respect to the solar wind flow direction, and characterized by weak increases in the magnetic field strength and plasma density just outside of the lunar wake and by an outward deflection of the plasma flow of the order of 3 to 6 deg. A mechanism for the formation of this shock wave which is viable over the entire lunar limb and which accounts for the intermittency of the observations in a natural way, is presented.

O.H.

A70-29111*

FAST TIME-RESOLVED SPECTRA OF ELECTROSTATIC TURBULENCE IN THE EARTH'S BOW SHOCK.

F. V. Coroniti, R. W. Fredricks, C. F. Kennel (TRW Systems Group, Redondo Beach, California, U., Los Angeles, Calif.), and F. L. Scarf (TRW Systems Group, Redondo Beach, Calif.) 4 May 1970 5 p refs Physical Review Letters, vol. 24, p. 994-998.

(Contract NAS5-9278)

Examination of fine details of electrostatic turbulence in the earth's bow shock structure. Based on the broad band analog electric data from the OGO 5 experiment, a fast time resolution spectral analysis was performed which allows a complete turbulence spectrum over a selected passband to be formed each 12.5 msec. Spectral details on scales for a few Debye lengths indicate that single modes or their groups dominate the turbulence spectrum. The character of the modes is discussed.

O.H.

A70-29185*

OBSERVATIONS OF IRREGULAR STRUCTURE IN THERMAL ION DISTRIBUTIONS IN THE DUSK SIDE MAGNETOSPHERE.

H. C. Brinton (NASA, Goddard Space Flight Center, Greenbelt, Md.), A. R. Deshmukh (Aero Geo Astro Co., Beltsville, Md.), and H. A. Taylor 1 May 1970 9 p refs Journal of Geophysical Research, vol. 75, p. 2481-2489.

Discussion of the variability in the position and structure of the plasmopause revealed by the measured distribution of the thermal positive ions H(+) and He(+) in the magnetosphere. Such variability is found to be most pronounced in the afternoon-dusk local time sector and is indicative of magnetospheric irregularities in the same region. As the OGO 3 satellite made progressive duskside (1500-1900 LT) and nightside (2200-0100 LT) passes during June-July 1966, the duskside plasmasphere was observed to exhibit an outward expansion or bulge, accompanied in some cases by considerable fine structure. In particular, the plasmopause was observed at L positions as distant as L = 7.8 in the afternoon-dusk sector in contrast to positions near L = 5-6 observed near midnight on the same day and at comparable levels of moderate magnetic activity. This variability is superimposed on an average diurnal distribution

A70-29924

of the plasmopause that is similar in shape to that deduced from whistler data during 1963, although the 1966-1967 results place the plasmopause at a position generally more distant by about 152 L. M.V.E.

A70-29924*

OBSERVATIONS OF NATURALLY OCCURRING VLF AND MAN-MADE HF PLASMA WAVES IN AURORAL REGIONS OF THE IONOSPHERE.

F. T. Bell (Stanford U., Stanford, Calif.) and T. S. Jorgensen (Danske Meteorologiske Institut, Charlottenlund, Denmark) New York, American Elsevier Publishing Co., 1970 11 p refs In: Plasma Waves in Space and in the Lab., NATO, Advanced Study Inst., Roros, Norway, Apr. 17-26, 1968, Proceedings, Volume 2, p. 377-387. (Contract NAS5-3093; Grant NSG-174)

Discussion of two methods for detecting the position of the auroral oval in the polar ionosphere and for monitoring the auroral activity with high time and space resolution. Both methods involve satellite observations. The first method consists in satellite observation of naturally occurring VLF auroral noise. Satellite observation of man-made HF plasma waves in the auroral region makes up the second method. It is shown that a study of the day to day behavior of the auroral oval can be carried out by one or two satellites, but that five to six satellites are needed for studies of phenomena with time scales of about 2 hours. A good reason for carrying out observations of the auroral oval by means of various satellite methods is felt to be the circumstance that with the existing relatively thin network of all-sky cameras and because of poor meteorological conditions in the Arctic, it is seldom possible to select a grouping of stations from which the entire auroral oval can be observed. M.V.E.

A70-30045*

MAGNETOMETERS FOR SPACE MEASUREMENTS OVER A WIDE RANGE OF FIELD INTENSITIES.

B. G. Ledley (NASA, Goddard Space Flight Center, Greenbelt, Md.) Feb. 1970 5 p refs Revue de Physique Appliquee, vol. 5, p. 164-168. (Centre National d'Etudes Spatiales, Colloque International sur les Champs Magnetiques Faibles d'Interet Geophysique et Spatial, Paris, France, May 20-23, 1969.)

Discussion of some of the wide range magnetometers developed by the Goddard Space Flight Center taking into consideration a rubidium vapor magnetometer and a fluxgate magnetometer. Magnetometers of both types are flown on the fifth Orbiting Geophysical Observatory (OGO 5). For scalar measurements the rubidium vapor magnetometer, with a range of three gammas to fifty thousand gammas, has an error which reaches a maximum of 1.5 gamma at fifty thousand gammas. Present development is directed toward reducing the electronic phase shifts and the experiment weight. A fluxgate system is being developed to achieve an accuracy of 0.01% up to 60,000 gammas. G.R.

A70-30059

ENTRY OF SOLAR COSMIC RAYS INTO THE EARTH'S MAGNETOSPHERE

K. A. Anderson (California, U., Berkeley, Calif.) Dordrecht, D. Reidel Publishing Co. 1970 15 p refs In: Particles and Fields in the Magnetosphere, Summer Advanced Study Inst., Symposium, U. of California, Santa Barbara, Calif., Aug. 4-15, 1969, Proceedings, p. 3-17. Symposium Supported by the U.S. Army, the Defense Atomic Support Agency, the Lockheed Aircraft Corp., the U.S. Navy, and the U. of California. (Astrophysics and Space Science Library, Volume 17), 1970.

Examination of the origin and mechanism of entry of cosmic electrons and protons into the earth's magnetosphere. The models of closed and open magnetospheres are examined in detail, and several recent theories and observations concerning this problem are reviewed and analyzed. It is concluded that the source of these particles entering the magnetosphere is the sun, and that the sun is also the direct source feeding the magnetotail. The particles enter the

magnetosphere on smoothly connected field lines. No conclusive experimental demonstration exists that diffusion occurs in the tail which suggests the validity of the model of an open magnetosphere. O.H.

A70-30069*

AC ELECTRIC AND MAGNETIC FIELDS AND COLLISIONLESS SHOCK STRUCTURES.

R. W. Fredricks (TRW Systems Groups, Redondo Beach, Calif.), C. F. Kennel (TRW Systems Group, Redondo Beach, California, U., Los Angeles, Calif.), and F. L. Scarf Dordrecht, D. Reidel Publishing Co. 1970 7 p refs In: Particles and Fields in the Magnetosphere, Summer Advanced Study Inst., Symposium, U. of California, Santa Barbara, Calif., Aug. 4-15, 1969, Proceedings, p. 102-108. Symposium Supported by the U.S. Army, the Defense Atomic Support Agency, the Lockheed Aircraft Corp., the U.S. Navy, and the U. of California. (Astrophysics and Space Science Library, Volume 17), - 1970.

(Contracts NAS5-9278; NAS2-4673; Grant NASw-1598) Instruments on board Pioneer 8 and 9, and OGO 5 have provided high time resolution plasma diagnostics from which the gross and fine structure of collision-free shocks can be deduced. We have found several types of shock structures in the high-beta (about 1) high Mach number (about 10) flows of solar wind plasma impinging upon the magnetospheric obstacle and in the low Mach number interplanetary shocks. By far the most common structure is a large amplitude MHD pulse structure having a characteristic length of the initial gradient and trailing wavetrain corresponding to a few times the electron inertial length. The dissipation mechanism in such shock structures is provided by electrostatic wave turbulence arising apparently from current driven electron-proton or proton-proton two stream instabilities which saturate nonlinearly. Nonlinear whistler mode waves also occur in some shock structures, but provide much less efficient dissipation or proton thermalization compared with that due to the electrostatic turbulence. (Author)

A70-30074*

THE REACTION OF THE PLASMAPAUSE TO VARYING MAGNETIC ACTIVITY.

C. R. Chappell, K. K. Harris, and G. W. Sharp (Lockheed Research Labs., Palo Alto, Calif.) Dordrecht, D. Reidel Publishing Co. 1970 6 p refs In: Particles and Fields in the Magnetosphere, Summer Advanced Study Inst., Symposium, U. of California, Santa Barbara, Calif., Aug. 4-15, 1969, Proceedings, p. 148-153. Symposium Supported by the U.S. Army, the Defense Atomic Support Agency, the Lockheed Aircraft Corp., the U.S. Navy, and the U. of California. (Astrophysics and Space Science Library, Volume 17), 1970. (Contract NAS5-9092)

Analysis of ion concentration measurements conducted by the OGO 5 spacecraft in order to characterize the position and density profile of the plasmopause as a function of local time and the L parameter. The L parameter represents the equatorial crossing distance of the field line at which a particular plasmopause measurement was taken. It is shown that there exists a fair correlation between an increase in the magnetic activity and a decrease in the plasmopause position within plus or minus two hours of 1000 and 0200 LT. T.M.

A70-30076*

MAGNETIC FIELD OBSERVATIONS IN HIGH BETA REGIONS OF THE MAGNETOSPHERE

J. P. Heppner (NASA, Goddard Space Flight Center, Greenbelt, Md.), B. G. Ledley, T. L. Skillman, and M. Sugiura Dordrecht, D. Reidel Publishing Co. 1970 6 p refs In: Particles and Fields in the Magnetosphere, Summer Advanced Study Inst., Symposium, U. of California, Santa Barbara, Calif., Aug. 4-15, 1969, Proceedings, p. 165-170. Symposium Support by the U.S. Army, the Defense Atomic Support Agency, the Lockheed Aircraft Corp., the U.S. Navy, and the U. of California. (Astrophysics and Space Science Library,

Volume 17), 1970.

Description of the characteristics of geomagnetic field distortion in the magnetosphere on the basis of magnetic observations conducted by the OGO 1, 3, and 5 satellites. Approximate distributions of ΔB (the magnitude of the measured field minus the magnitude of the reference field) are given in the noon and midnight sectors of the magnetosphere for magnetically quiet and slightly disturbed conditions. A sudden decrease in the magnetic field, followed by irregular variations, was often observed near midnight on low-latitude inbound orbits of OGO 3. Additional data show that following the onset of a magnetic bay disturbance on the ground the magnetic field in the tail collapses near the meridional plane of the bay onset. T.M.

A70-30078*

AC MAGNETIC FIELDS.

R. E. Holzer (California, U., Los Angeles, Calif.) and C. T. Russell Dordrecht, D. Reidel Publishing Co. 1970 18 p refs In: Particles and Fields in the Magnetosphere, Summer Advanced Study Inst., Symposium, U. of California, Santa Barbara, Calif., Aug. 4-15, 1969, Proceedings, p. 195-212. Symposium supported by the U.S. Army, the Defense Atomic Support Agency, the Lockheed Aircraft Corp., the U.S. Navy, and the U. of California. (Astrophysics and Space Science Library, Volume 17), 1970. (Contract NAS5-9098; Grants NGR-05-007-235; NGR-05-007-004)

Magnetic fluctuations have been observed by ground observatories from the Pc5 band to the VLF band. Not all these fluctuations have been observed also in space however. The precision of satellite-borne instruments, data rates and orbital characteristics have restricted observations in the past, so that only the lowest and the highest frequencies have been examined extensively. Preliminary results from recent experiments are beginning to fill this gap. Some of these new results are presented together with a review of past work. These latest results suggest first that the large amplitude 100 to 300 sec period waves are field line resonances driven by waves generated by the motion of the magnetopause and second that ELF hiss and chorus are the result of a plasma instability in the equatorial region of the magnetosphere. (Author)

A70-30082*

VARIATIONS IN ELECTRIC FIELDS FROM POLAR ORBITING SATELLITES.

J. P. Heppner (NASA, Goddard Space Flight Center, Greenbelt, Md.) and N. C. Maynard Dordrecht, D. Reidel Publishing Co. 1970 7 p refs In: Particles and Fields in the Magnetosphere, Summer Advanced Study Inst., Symposium, U. of California, Santa Barbara, Calif., Aug. 4-15, 1969, Proceedings, p. 247-253. Symposium supported by the U.S. Army, the Defense Atomic Support Agency, the Lockheed Aircraft Corp., the U.S. Navy, and the U. of California. (Astrophysics and Space Science Library, Volume 17), 1970.

Further definition of the characteristics of the electric fields inferred from the measurements performed on the OVI 10 satellite. Preliminary data from the OGO 6 satellite, launched in June 1969, are used in this redefinition. The OGO 6 data substantiate the OVI 10 indications on spatial irregularities and waves in the ELF-VLF regime. M.V.E.

A70-30083*

HIGH FREQUENCY ELECTROSTATIC WAVES IN THE MAGNETOSPHERE.

R. W. Fredricks, C. F. Kennel (California, U., Los Angeles, Calif.), and F. L. Scarf (TRW Systems Group, Redondo Beach, Calif.) Dordrecht, D. Reidel Publishing Co. 1970 9 p refs In: Particles and Fields in the Magnetosphere, Summer Advanced Study Inst., Symposium, U. of California, Santa Barbara, Calif., Aug. 4-15, 1969, Proceedings, p. 257-265. Symposium supported by the U.S. Army, the Defense Atomic Support Agency, the Lockheed Aircraft Corp., the U.S. Navy, and the U. of California. (Astrophysics and Space Science Library, Volume 17), 1970.

(Grant NGR-05-007-190)

Brief review of several theories of instabilities in which high frequency electrostatic waves are generated by electrons. Examples of several magnetospheric electrostatic emissions observed on OGO 5 are discussed. The theoretical discussion indicates that several difficult experimental questions must be resolved before a definitive understanding of magnetospheric electrostatic emissions becomes possible. M.V.E.

A70-30085*

AC FIELDS AND WAVE PARTICLE INTERACTIONS.

G. M. Crook (TRW Systems Group, Redondo Beach, Calif.), R. W. Fredricks, I. M. Green, C. F. Kennel (TRW Systems Group, Redondo Beach, California, U., Los Angeles Calif.), and F. L. Scarf Dordrecht, D. Reidel Publishing Co., 1970 9 p refs In: Particles and Fields in the Magnetosphere, Summer Advanced Study Inst., Symposium, U. of California, Santa Barbara, Calif., Aug. 4-15, 1969, Proceedings, p. 275-283. Symposium supported by the U.S. Army, the Defense Atomic Support Agency, the Lockheed Aircraft Corp., the U.S. Navy, and the U. of California. (Astrophysics and Space Science Library, Volume 17), 1970. (Contracts NAS2-4673; NAS5-9278; Grant NASw-1589)

Survey of recent experiments which provided detailed information on electrostatic and electromagnetic plasma waves in the outer magnetosphere, magnetosheath, and solar wind. Nonwhistler-mode electrostatic noise is very frequently detected on the nightside auroral lines of force, and strong emissions that appear to be related to the Bernstein modes are found beyond the plasmopause very near the magnetic equator. On Pioneer 8 and 9 spacecraft, low-frequency electrostatic waves are found near the nightside magnetopause boundary. In the magnetosheath and the solar wind, other types of wave-particle interactions are observed. Magnetic null regions at filament boundaries generally involve excitation of intense high frequency electrostatic noise, and locally trapped electromagnetic waves are sometimes detected in density troughs. T.M.

A70-30089*

FURTHER COMMENTS CONCERNING LOW ENERGY CHARGED PARTICLE DISTRIBUTIONS WITHIN THE EARTH'S MAGNETOSPHERE AND ITS ENVIRONS.

L. A. Frank (Iowa, U., Iowa City, Iowa) Dordrecht, D. Reidel Publishing Co., 1970 13 p refs In: Particles and Fields in the Magnetosphere, Summer Advanced Study Inst., Symposium, U. of California, Santa Barbara, Calif., Aug. 4-15, 1969, Proceedings, p. 319-331. Symposium supported by the U.S. Army, the Defense Atomic Support Agency, the Lockheed Aircraft Corp., the U.S. Navy, and the U. of California. (Astrophysics and Space Science Library, Volume 17), 1970. (Contracts NAS5-2054; NAS5-9074; Nonr-1509(06); Grants NGL-16-001-002; NsG-233-62)

Several recent observations of the distributions of low-energy charged particles (100 eV to 50 keV) within the earth's magnetosphere and its environs are examined for evidences of source (acceleration) mechanisms. Proton (0.5 to 50 keV) intensities in the outer radiation zone and plasma sheet are concentrated upon since this population forms the largest charged particle energy reservoir in the magnetospheric system. To date no source mechanism for these proton intensities with broad differential energy spectrums (i.e., of the plasma sheet and the storm time and quiescent ring currents) has been delineated clearly. It is suggested herein that at least the storm time ring current protons are of solar origin and are convected into the magnetotail under the influence of magnetospheric electrostatic fields or via a diffusion process driven by fluctuating magnetic and/or electric fields. (Author)

A70-30090*

THE ORIGIN AND DISTRIBUTION OF ENERGETIC ELECTRONS IN THE VAN ALLEN RADIATION BELTS.

J. R. Winckler (Minnesota, U., Minneapolis, Minn.)

Dordrecht, D. Reidel Publishing Co. 1970 21 p refs In: Particles and Fields in the Magnetosphere, Summer Advanced Study Inst., Symposium, U. of California, Santa Barbara, Calif., Aug. 4-15, 1969, Proceedings, p. 332-352. Symposium supported by the U.S. Army, the Defense Atomic Support Agency, the Lockheed Aircraft Corp., the U.S. Navy, and the U. of California. (Astrophysics and Space Science Library, Volume 17) 1970.

(Grant NGL-24-005-008)

Discussion of some new results on the injection and distribution of the energetic electron component in the Van Allen radiation belts as a result of magnetic storms. The results described were obtained from magnetic storms. The results described were obtained from magnetic deflection electron spectrometers carried in the OGO 1 and OGO 3 satellites in elliptical orbits penetrating both the inner and outer zone regions and in the ATS 1 geostationary orbit satellite in the outer zone. Correlations with ground based magnetic and auroral measurements, as well as with observations from high altitude balloons have contributed to the interpretation of the results described. Special attention is given to long term variations of the inner zone and inner zone injection characteristics, as well as to substorm correlated electron increases in the outer radiation belt and acceleration of electrons near midnight. M.V.F.

A70-30358*

ON THE STRUCTURE OF THE INNER MAGNETOSPHERE.

R. M. Thorne (California, U., Los Angeles, Calif.) Apr. 1970 23 p refs Cosmic Electrodynamics, vol. 1, p. 67-89. Research supported by the U. of California. (Contract NAS5-9098)

Investigation of the morphology of the thermal and energetic particles in the inner magnetosphere. The motion and relative position of several well defined features of the particle distribution are followed during geomagnetic disturbances and over the solar cycle. It is found that ring current protons build up just outside the storm-time plasmopause and subsequently decay at a rate such that their flux maximum approximately coincides with the expanding plasmopause. Low energy electrons also appear just outside the plasmopause during the main phase of the storm. Their subsequent decay is much slower than that of the protons, and the net effect of the storm is an injection of these electrons well into the plasmopause. Even during periods of severe geomagnetic disturbances, the energetic electrons are distributed into two distinct zones. The pronounced and persistent slot between the inner and outer electron zones is better defined and occurs at lower L values for higher electron energies. The profile of the inner edge remains unchanged during geomagnetic storms, and it also appears to be unaffected over the solar cycle. The outer edge of the slot is probably controlled by a balance between inward diffusion and loss. M.V.E.

A70-31902*

THE ALTITUDE DEPENDENCE OF THE QUIETTIME COSMIC RAY IONIZATION OVER THE POLAR REGIONS AT SOLAR MINIMUM.

M. J. George (California Inst. of Tech., Pasadena, Calif.) 1 Jun. 1970 5 p refs Journal of Geophysical Research, vol. 75, p. 3154-3158.

(Contract NAS5-9317; NAS5-3095; Grant NGL-05-002-007)

The integrating ionization chamber on the OGO 2 satellite has measured the quiet time cosmic ray ionization from 430 to 1540 km over the polar regions. After correction for time variations and spacecraft radioactivity, ionization averages have been fitted to analytical functions, which describe the primary and splash-albedo components of the cosmic rays. Extrapolating to the top of the atmosphere and to infinity, the ionizations are 550 plus or minus 10 and 985 plus or minus 6 ion pairs/cu cm sec atm, respectively, and splash albedo contributes 10.4 plus or minus 2.3% of the total ionization at the top of the atmosphere. These results apply to early November 1965 and are compared with balloon

and interplanetary values obtained for similar intensity levels with similar instruments. An interesting side result is another estimate of the radial gradient of the ionization, 8.5 plus or minus 3.1%/AU. (Author)

A70-31903*

OBSERVATIONS OF THE COSMIC RAY KNEE WITH A POLAR ORBITING IONIZATION CHAMBER

M. J. George (California Inst. of Tech., Pasadena, Calif.) 1 Jun. 1970 8 p refs Journal of Geophysical Research, vol. 75, p. 3159-3166.

(Contracts NAS5-9317; NAS5-3095; Grant NGL-05-002-007)

The cosmic ray knee has been observed with the ion chambers on the OGO 2 (October 1965-February 1966) and OGO 4 (August 1967) polar orbiting satellites, using the same graphical definition that applies to balloon observations. The knee is interpreted as a position in the geomagnetic field, which depends on the cosmic ray rigidity spectrum at the time of observation, where the cosmic ray cutoff rigidity has a particular value and is about 1.2 bV for the OGO 2 measurements. The invariant latitude of the knee decreases with altitude of observations at the rate of .0025 (plus or minus .0005) degree/km and had the value 59.1 deg at the surface of the earth in 1965-1966. This invariant latitude should be independent of longitude; in fact, however, a slight longitude dependence of the order of plus or minus 1 deg is observed. Knee latitudes were 0.6 deg lower (toward the equator) in 1967, according to OGO 4, and 4 to 5 deg lower in 1961 as measured by other observers. We find a north-south latitude difference of 0.6 (plus or minus 0.4) deg, which suggests a seasonal variation with the knee slightly closer to the pole during winter. A small diurnal variation of the knee latitude with amplitude 0.5 (plus or minus 0.4) deg is indicated; this appears to be consistent with calculations and observations for higher latitudes. (Author)

A70-31905

DEFORMATION OF A MAGNETIC DIPOLE FIELD BY TRAPPED PARTICLES.

K. Lackner (ESRO, European Space Research Inst., Frascati, Italy) 1 Jun. 1970 13 p refs Journal of Geophysical Research, vol. 75, p. 3180-3192.

Description of a model for the stormtime ring current, based on a self-consistent steady state solution of Vlasov's and Maxwell's equations for a finite pressure plasma immersed in the earth's dipole field. The model is used to calculate a set of self-consistent equilibrium configurations that correspond to increasing dipole moments of the ring current. These calculations prove the existence of equilibrium solutions that contain a neutral point and regions in which the particle energy density exceeds the undisturbed magnetic field energy density for a factor up to 27. M.V.E.

A70-34835*

DYNAMIC SPECTRA OF TYPE III SOLAR BURSTS FROM 4 TO 2 MHZ OBSERVED BY OGO-3.

T. E. Graedel (Radio Astronomy Observatory, Ann Arbor, Mich.) and F. T. Haddock Apr. 1970 12 p refs Astrophysical Journal, vol. 160, Pt.-1, p. 293-300.

(Contract NAS5-2051; Grant NGL-23-005-017)

Summary of the characteristics of Type III solar bursts from 4 to 2 MHz, as determined from 218 bursts detected by an antenna/radiometer package aboard OGO-3. These data represent the first large sample of information on low frequency solar bursts and the first dynamic spectra with high time resolution obtained below ionospheric cutoff frequencies. Type V continuum followed the Type III bursts in 1.8 per cent of the cases studied. No Type II or Type IV events were observed at these frequencies, evidence for Type I radiation is inconclusive. M.V.E.

A70-35303*

EVOLUTION IN DESIGN OF THE ORBITING GEOPHYSICAL OBSERVATORIES.

W. E. Scull (NASA, Goddard Space Flight Center, Greenbelt,

Md.) Tokyo, Agne Publishing Inc. 1969 9 p In: International Symposium on Space Technology and Science, 8th Tokyo, Japan, Aug. 25-30, 1969 Proceedings p. 1053-1061.

Description of the design of OGOs and its evolution from OGO-I to OGO-VI with respect to missions for which they were designed. It is concluded that fulfillment of mission objectives of the sun- and earth-oriented OGOs was evolutionary, with each mission contributing to following missions. Starting with OGO-I, still operating after 5 years in orbit, orbital experience of each mission resulted in changes in design of the spacecraft or ground system. Although some factors had degrading effects on their particular missions, the OGOs were successfully modified to correct these problems. The spacecraft and ground system underwent continuous evolution from a design based on concepts of years from 1961 to 1964 to result in 5 of 6 missions currently operating which accumulated almost 1.4 million experiment hours of scientific data. Z.W.

A70-35764*

GECORONAL HYDROGEN: AN ANALYSIS OF THE LYMAN-ALPHA AIRGLOW OBSERVED FROM OGO-4. P. Mange (U.S. Navy, E. O. Hulbert Center for Space Research, Washington, D. C.) and R. R. Meier Jun. 1970 19 p refs Planetary and Space Science, vol. 18, p. 803-821.

(NASA Order S-32327-G; NASA Order S-43340-G; NASA Order S-20613-G; Grants NSF GP-7890; NSF GP-6354)

Results of observations of the hydrogen Lyman alpha glow surrounding the earth, carried out from the OGO 4 spacecraft. The dependence of this emission feature on solar zenith angle was measured in the altitude range of about 400 to 900 km. The Lyman-alpha is attributed to radiative transport of solar Lyman alpha photons through the hydrogen geocorona. The data are analyzed by solving the spherical radiative transport problem for selected hydrogen models. The principal features of the observations can be explained by a combination of the models of Kockarts and Nicolet, and Chamberlain, normalized to 3×10 to the 7th power hydrogen atoms per cu cm at 100 km for the fall 1967 epoch. This implies an optical depth of 1.33 above 650 km. Theory and observation establish an upper limit of a factor of four for the diurnal variation of the hydrogen concentration at high altitude. (Author)

A70-35771*

OGO SATELLITE WAKE STRUCTURE DEDUCED FROM ANTENNA IMPEDANCE MEASUREMENTS.

H. Well and R. G. Yorks (Radioastronomy Observatory, Ann Arbor, Mich.) Jun. 1970 17 p refs Planetary and Space Science, vol. 18, p. 901-916.

(Grants NGR-23-005-068; NGR-23-005-371)

Measurements of the complex impedance of an 18-m monopole antenna at 2.5 MHz are used to study the electron densities in and out of the wake of a large spinning satellite in the earth's upper ionosphere. Some spacecraft orientation information is also obtained from the impedance data. The ratios of the wake electron densities, averaged over the length of the antenna, to the unperturbed local densities are calculated for all angles of attack of the satellite. Electron density distributions along the antenna are derived. (Author)

A70-36005*

OGO-5 OBSERVATIONS OF QUASI-TRAPPED ELECTROMAGNETIC WAVES IN THE SOLAR WIND.

R. W. Fredricks, I. M. Green (TRW Systems Group, Redondo Beach Calif.), M. Neugebauer (California Inst. of Tech., Jet Propulsion Lab., Pasadena, Calif.), and F. L. Scarf 1 Jul. 1970 16 p refs Journal of Geophysical Research, vol. 75, p. 3735-3750.

(Contract NAS5-9278)

Discussion of the observations of quasi-trapped electromagnetic waves made by the OGO 5 on Apr. 5, 1968, in the solar wind at a frequency of 70 kHz. The existence of a

relation between these electromagnetic waves and the ones reported previously at 20 to 30 kHz by Zond 3, Venus 2, Pioneer 8 and 9, and Luna 11 and 12 is suggested. The problem of distinguishing electromagnetic waves of this type from electrostatic plasma oscillations is analyzed. V.Z.

A70-36006*

OGO-5 OBSERVATIONS OF ELECTROSTATIC TURBULENCE IN BOW SHOCK MAGNETIC STRUCTURES.

P. J. Coleman, G. M. Crook, R. W. Fredricks, I. M. Green, C. F. Kennel (TRW Systems Group, Redondo Beach, California, U., Los Angeles, Calif.), C. T. Russell (California, U., Los Angeles, Calif.), and F. L. Scarf (TRW Systems Group, Redondo Beach, Calif.) 1 Jul. 1970 18 p refs Journal of Geophysical Research, vol. 75, p. 3751-3768.

(Contracts NAS5-9278; NAS5-9098)

Measurement of magnetic field, vlf electric field, and directed positive flux made during passage of OGO 5 through many bow shock structures both inbound and outbound on Mar. 12, 1968. These shocks were chosen because the period Mar. 11 to 13, 1968, was one of a reasonably quiet solar wind. The data are correlated on time scales greater than or equal to 144 msec and show that electrostatic wave turbulence is generated in the shock front by diamagnetic currents flowing on scale lengths equal to about the electron inertial length. This electrostatic turbulence builds to high levels near or in the regions of large jumps in the absolute value of B and then decays rapidly downstream. A jump in the absolute value of B and the scattering or randomization of protons are observed to occur only after a strong level of electrostatic turbulence is achieved; this leads to the conclusion that the electrostatic turbulence is a major contributor to the shock dissipative process. This turbulence is best explained as the ion acoustic or Buneman mode due to two-stream instability. One very thick shock structure is displayed which contains many very large amplitude and nearly reversible magnetic field pulsations. (Author)

A70-36014*

THE MORPHOLOGY OF THE BULGE REGION OF THE PLASMASPHERE.

C. R. Chappell, K. K. Harris, and G. W. Sharp (Lockheed Research Labs., Palo Alto, Calif.) 1 Jul. 1970 14 p refs Journal of Geophysical Research, vol. 75, p. 3848-3861.

(Contract NAS5-9092)

Study of the morphology of the bulge region of the plasmasphere by measuring the concentration of H(\pm) ions by means of a mass spectrometer flown on OGO 5. Many representative profiles made in the bulge region are presented. The equatorial location of the plasmopause in the bulge region and its apparent movement with changing magnetic activity is examined. The shape of the typical bulge profile and its reaction both to magnetic storms and to periods of quieting are examined. Finally the observed profiles are compared with the profiles predicted by a magnetospheric convection model. Z.W.

A70-36016*

OGO-4 OBSERVATIONS OF ION COMPOSITION AND TEMPERATURES IN THE TOPSIDE IONOSPHERE.

R. E. Bourdeau (NASA, Goddard Space Flight Center, Lab. for Planetary Atmospheres, Greenbelt, Md.), S. Chandra, J. L. Donley, and B. E. Troy, Jr. 1 Jul. 1970 12 p refs Journal of Geophysical Research, vol. 75, p. 3867-3878.

Direct measurement of the densities of ionic constituents H(+), He(+), and O(-) and the temperatures of ions and electrons from the OGO 4 planar retarding potential analyzer in the altitude range from 400 to 900 km. Results are presented from day and night passes in the middle and low latitudes near the 1967 fall equinox. The passes are selected to emphasize the latitudinal rather than the height dependence of the measurements. The main results can be summarized as follows: (1) above 800 km at night, there is a deep equatorial trough in He(+) and a corresponding rise in O(-), suggesting a charge exchange between He(+) and O as an important loss mechanism for He(-), (2) the dominant ion in the night

at these altitudes between plus or minus 40 deg geomagnetic latitudes is H(+) followed generally by O(+) and He(+); outside this latitude region O(+) becomes the dominant constituent, increasing continuously toward the pole; (3) the major ionic constituent in the daytime is O(+) throughout the altitude and latitude range of observations; in the height range from 400 to 500 km, the latitudinal variation in O(+) shows the well-known feature of the geomagnetic anomaly; and (4) both electron and ion temperatures generally increase poleward from their low-latitude values, attaining maxima between 40 and 50 deg geomagnetic latitude. (Author)

A70-37483*

MAGNETIC AND ELECTRIC FIELD CHANGES ACROSS THE SHOCK AND IN THE MAGNETOSHEATH.

P. J. Coleman, R. W. Fredricks (TRW Systems Group, Redondo Beach, Calif), C. F. Kennel, C. T. Russell (California, U., Los Angeles, Calif.), and F. L. Scarf Dordrecht, D. Reidel Publishing Co. 1970 9 p refs In: Intercorrelated Satellite Observations Related to Solar Events, European Space Research Organization, Annual ESLAB/ESRIN, Symposium, 3rd, Noordwijk, Netherlands, Sep. 16-19, 1969, Proceedings. p. 181-189 Astrophysics and Space Science Library. Volume 19, 1970.

(Contracts NAS5-9278; NAS5-9098; NAS2-4673)

Discussion of observations regarding the structure of the earth's bow shock and of a number of closely related topics. Intercorrelated spacecraft observations of solar events are discussed using Pioneer 8 and OGO-5 data from March 14 and April 5, 1968. It is also shown that the two-stream current instability can be triggered by strong magnetic field compressions that are not directly associated with the bow shock. Field configurations that yield intense VLF electrostatic turbulence include those near null regions and those associated with large amplitude oblique magnetosonic waves. G.R.

A70-37487

TRAPPED PARTICLE POPULATION CHANGES ASSOCIATED WITH SOLAR EVENTS.

J. G. Roederer (Denver, U., Denver, Colo.) Dordrecht, D. Reidel Publishing Co. 1970 12 p refs In: Intercorrelated Satellite Observations Related to Solar Events, European Space Research Organization, Annual ESLAB/ESRIN, Symposium, 3rd, Noordwijk, Netherlands, Sep. 16-19, 1969, Proceedings. p. 239-250 Astrophysics and Space Science Library. Volume 19, 1970.

Discussion of trapped particle population changes associated with solar events and caused by the effects of solar wind discontinuities on the magnetosphere. It is pointed out that the most drastic sequence of such time variations occurs during a magnetospheric storm. The changes in the energetic particle population are discussed and the morphology of trapped particle variations during storms is considered. Prospects for future research are examined. G.R.

A70-37513

ELECTRON DENSITY MEASUREMENTS IN THE THERMAL PLASMA OF THE MAGNETOSPHERE USING A LANGMUIR PROBE.

R. Freeman, K. Norman, and A.P. Willmore (U. Coll., London, England) Dordrecht, D. Reidel Publishing Co. 1970 11 p refs In: Intercorrelated Satellite Observations Related to Solar Events, European Space Research Organization, Annual ESLAB/ESRIN, Symposium, 3rd, Noordwijk, Netherlands, Sep. 16-19, 1969, Proceedings. p. 524-534 Astrophysics and Space Science Library. Volume 19, 1970.

Discussion of the results obtained at the time of the solar flare of February 1969 in an experiment designed to measure the ambient electron density and temperature in the magnetosphere. The experiment is included in the payload of the NASA Orbiting Geophysical Observatory satellite, OGO-5. The results obtained are compared with earlier satellite passes during periods of different geomagnetic activity. The data consist of unrefined electron density

profiles plotted directly from the processed data tapes.

G.R.

A70-37522

OGO-5 MEASUREMENTS OF ELECTRONS ABOVE 500 MeV.

B. N. Swanenburg (Leiden, Rijksuniversiteit, Leiden, Netherlands) Dordrecht D. Reidel Publishing Co. 1970 4 p In: Intercorrelated Satellite Observations Related to Solar Events, European Space Research Organization, Annual ESLAB/ESRIN, Symposium, 3rd, Noordwijk, Netherlands, Sep. 16-19, 1969 Proceedings. p. 610-613 Astrophysics and Space Science Library. Volume 19, 1970.

Discussion of the data obtained with a cosmic ray electron detector which is flown on board the OGO-5 satellite. A chronological account of the observations during 1968 is given. A clearly positive correlation is seen between the neutron monitor, proton and alpha-rate and the integral electron rate. The data obtained support the diffusion-convection theory of the solar modulation mechanism.

G.R.

A70-38096**

COSMIC RAY ELECTRONS AND POSITRONS OF ENERGIES 2 TO 9.5 MeV OBSERVED IN INTERPLANETARY SPACE.

T. L. Cline and G. Porreca (NASA, Goddard Space Flight Center, Greenbelt, Md.) Budapest Akademiai Kiado, 1970 5 p refs In: International Conference on Cosmic Rays, 11th, Budapest, Hungary, Aug. 25-Sep. 4, 1969, Proceedings. Volume 1 - Origin and Galactic Phenomena. p. 145-149 Conference sponsored by the International Union of Pure and Applied Physics and the Hungarian Academy of Sciences.

Study of the differential energy spectra of electrons and positrons in the 2 to 9.5 MeV interval performed in interplanetary space during solar quiet times following March 1968 with the OGO 5 satellite. The observed quiet time electron spectrum roughly agrees with the expected unmodulated cosmic ray knock-on electron spectrum. The positron to electron ratio, totaled for the energy interval from 2 to 9.5 MeV, is only 1.8 per cent. There are indications of a moderate modulation of the positron intensity in the medium energy region, having a detailed energy dependence yet to be determined. M.V.E.

A70-38098**

INTERPLANETARY POSITRONS NEAR 1 MeV FROM OTHER THAN THE PION TO MUON TO ELECTRON PROCESS.

T. L. Cline and E. W. Hones, Jr. (NASA, Goddard Space Flight Center, Greenbelt, Md., California, U., Los Alamos, N. Mex.) Budapest Akademiai Kiado, 1970 6 p In: International Conference on Cosmic Rays, 11th, Budapest, Hungary, Aug. 25-Sep. 4, 1969, Proceedings, Volume 1 - Origin and Galactic Phenomena. p. 159-164 Conference sponsored by the International Union of Pure and Applied Physics and the Hungarian Academy of Sciences.

Evidence is presented for a spectral component of interplanetary positrons separate from that produced by the decay of interstellar mesons from cosmic-ray interactions. Results from observations made with the OGO 3 satellite indicate the detection of greater than 0.5 MeV positrons with a differential intensity near 100 per sq m per sec per ster per MeV, two decades higher than the maximum expected from cosmic-ray meson production. Data accumulated for nearly two years, have been examined for the existence of temporal or spatial variations; accelerator exposures of the detector are also being made in order to determine if the particles observed in space might be local secondaries. To date, there is no indication of any solar or geophysical production mechanism, or effect local to the detector, which would account for the observed positron rate. The observed cosmic-ray positron intensity taken, to be of cosmic-ray origin, is compared with the calculated values of interstellar beta emission by cosmic-ray excited nuclei; qualitative agreement

exists only if a high, possibly local, low-energy cosmic-ray intensity is used. A heliocentric acceleration or some quite different source may instead be required to provide the observed intensity. (Author)

A70-38105*#
TIME VARIATIONS IN THE COSMIC RAY ELECTRON SPECTRUM ABOVE 500 MeV.

J. A. M. Bleeker, J. J. Burger, A. J. M. Deerenberg, A. Scheepmaker, B. N. Swanenburg (Leiden, Rijksuniversiteit, Leiden, Netherlands), Y. Tanaka (Nagoya U., Nagoya, Japan), and H. C. VanDeHulst Budapest, Akademiai Kiado 1970 7 p refs In: International Conference on Cosmic Rays, 11th, Budapest, Hungary, Aug. 25-Sep. 4, 1969, Proceedings. Volume 1 - Origin and Galactic Phenomena. p. 209-215 Conference sponsored by the International Union of Pure and Applied Physics and the Hungarian Academy of Sciences.

Measurement of magnetic field, vlf electric field, and directed positive ion flux made during passage of OGO 5 through many bow shock structures both inbound and outbound on Mar. 12, 1968. These shocks were chosen because the period Mar. 11 to 13, 1968, was one of a reasonably quiet solar wind. The data are correlated on time scales greater than or equal to 144 msec and show that electrostatic wave turbulence is generated in the shock front by diamagnetic currents flowing on scale lengths equal to about the electron inertial length. This electrostatic turbulence builds to high levels near or in the regions of large jumps in the absolute value of B and then decays rapidly downstream. A jump in the absolute value of B and the scattering or randomization of protons are observed to occur only after a strong level of electrostatic turbulence is achieved; this leads to the conclusion that the electrostatic turbulence is a major contributor to the shock dissipative process. This turbulence is best explained as the ion acoustic or Buneman mode due to two-stream instability. One very thick shock structure is displayed which contains many very large amplitude and nearly reversible magnetic field pulsations. (Author)

A70-38106#
THE COSMIC RAY ELECTRON SPECTRUM BETWEEN 0.5 AND 10 GeV OBSERVED ON BOARD OGO-5.

J. A. M. Bleeker, J. J. Burger, A. J. M. Deerenberg, A. Scheepmaker, B. N. Swanenburg (Leiden, Rijksuniversiteit, Leiden, Netherlands), Y. Tanaka (Nagoya U., Nagoya, Japan), and H. C. VanDeHulst Budapest Akademiai Kiado 1970 5 p refs In: International Conference on Cosmic Rays, 11th, Budapest, Hungary, Aug. 25-Sep. 4, 1969, Proceedings. Volume 1 - Origin and Galactic Phenomena. p. 217-221 Conference sponsored by the International Union of Pure and Applied Physics and the Hungarian Academy of Sciences. Research supported by the Dutch Ministry of Education and Sciences.

A cosmic ray detector sensitive to electrons with energies between 0.5 and 10 GeV is flown on board the OGO-5 satellite. The instrument is operating at altitudes between 80,000 and 150,000 km. The cosmic ray electron presented over the period April 15 to May 5, 1968. A considerable flattening of the spectrum at energies below 3 GeV is observed. A substantial part of this flattening is considered to be a genuine property of the interstellar cosmic ray electron spectrum. (Author)

A70-38127*#
SPECTRA AND CHARGE COMPOSITION OF THE LOW ENERGY GALACTIC COSMIC RADIATION FROM Z EQUALS 2 TO 14.

V. K. Balasubrahmanyam (NASA, Goddard Space Flight Center, Greenbelt, Md.), F. J. McDonald, and B. J. Teegarden Budapest, Akademiai Kiado 1970 7 p refs In: International Conference on Cosmic Rays, 11th, Budapest, Hungary, Aug. 25-Sep. 4, 1969, Proceedings. Volume 1 - Origin and Galactic Phenomena. p. 345-351 Conference sponsored by the International Union of Pure and Applied Physics and

the Hungarian Academy of Sciences.

Results from the Goddard Cosmic Ray Experiment on OGO-5 for the study of charge and energy spectra. The detector system, designed to study the energy range from 5 to 800 MeV/nucleon and charge range from 1 to 14 consists of three different detectors for low, medium, and high energies. Some new features were seen in C/O, C/He, and O/He ratios which seem to favor the hypothesis of a two-component model for the origin of cosmic rays. F.R.L.

A70-38377*
COMPARISON OF COINCIDENT OGO-3 AND OGO-4 HYDROGEN ION COMPOSITION MEASUREMENTS.

J. M. Grebowsky, N. K. Rahman (NASA, Goddard Space Flight Center, Greenbelt, Md., Maryland, U., College Park, Md.), and H. A. Taylor, Jr. (NASA, Goddard Space Flight Center, Greenbelt, Md.) Jul. 1970 12 p refs Planetary and Space Science, vol. 18, p. 965-976.
 Comparison of ion composition measurements made on Aug. 8 and Aug. 28, 1967, by the topside ionospheric polar orbiting satellite OGO 4, and simultaneously by the eccentric orbiting magnetospheric satellite OGO 3 on nightside passes through the plasmasphere. Throughout most of the mid-latitude regions sampled, an isothermal diffusive equilibrium model at an ion temperature of 1000 K provides a good approximation for coupling these ionospheric regions. In agreement with previous studies of the average local time asymmetry of the plasmasphere boundary, the plasmopause L coordinates measured by OGO 3 near midnight were greater than the L coordinates associated with the light ion troughs observed near dawn on the coincident OGO 4 pass. F.R.L.

A70-39326*
LATITUDE AND ALTITUDE DEPENDENCE OF THE COSMIC RAY ALBEDO NEUTRON FLUX.

E. L. Chupp (New Hampshire, U., Durham, N. H.), S. O. Ifedili, R. W. Jenkins, and J. A. Lockwood 1 Aug. 1970 8 p refs Journal of Geophysical Research, vol. 75, p. 4197-4204.
 (Contract NAS5-9313)

Description of the preliminary measurements of the cosmic ray albedo neutron flux from a neutron detector on board the orbiting geophysical observatory OGO 6, a polar-orbiting satellite with altitudes between 400 and 1100 km. Following a description of the detector and its efficiency, the results of measurements performed for the period June 7 to 17, 1969 are reported. From these measurements, the latitude and altitude dependence of the neutron flux is determined. In particular, the neutron leakage flux at the top of the atmosphere is examined and analyzed. O.H.

A70-39338*
OGO-4 SPECTROMETER MEASUREMENTS OF THE TROPICAL ULTRAVIOLET AIRGLOW

C. A. Barth and S. Schaffner (Colorado, U., Boulder, Colo.) 1 Aug. 1970 8 p refs Journal of Geophysical Research, vol. 75, p. 4299-4306.
 (Contract NAS5-9315; Grant NGL-06-003-052)

The OGO 4 ultraviolet spectrometer measured the ultraviolet nightglow at tropical latitudes. The spectrum consists of the 1304 and 1356-A lines of atomic oxygen. The Lyman-Birge-Hopfield bands of molecular nitrogen and the ultraviolet lines of atomic nitrogen do not appear. The tropical ultraviolet airglow occurs in two bands north and south of the geomagnetic equator under satellite observation conditions that are best correlated with a local time of 2100 to 2130. When the intensity of this airglow is maximum, the ratio of the intensity of the 1304-A to the 1356-A line is 1.8. The most likely source of excitation of the tropical ultraviolet airglow appears to be an ionospheric recombination mechanism. (Author)

A70-39344*
A COMPARISON OF THE OXYGEN ION-ION NEUTRALIZATION AND RADIATIVE RECOMBINATION

MECHANISMS FOR PRODUCING THE ULTRAVIOLET NIGHTGLOW.

W. B. Hanson (Texas, U., Dallas, Tex.) 1 Aug. 1970 4 p refs Journal of Geophysical Research, vol. 75, p. 4343-4346.
(Grant NGL-44-004-001)

Recently, Knudsen suggested that oxygen ion-ion neutralization might provide an important contribution to the ultraviolet oxygen nightglow observed on OGO 4. The relative contribution of this process is compared with that provided by radiative recombination, and it is concluded that radiative recombination should always be dominant, unless presently accepted values of the pertinent rate coefficients are in error. When the F region electron concentrations are not abnormally large, the two mechanisms contribute comparable amounts of ultraviolet emission. It is also concluded that, unless certain of these coefficients are underestimated, the two mechanisms will not provide the observed intensity of the ultraviolet nightglow. (Author)

A70-39349*

MAGNETIC FIELD MAPPING OF THE INNER MAGNETOSPHERE.

J. C. Cain and R. E. Sweeney (NASA, Goddard Space Flight Center, Magnetic and Electric Fields Branch, Greenbelt, Md.) 1 Aug. 1970 3 p Journal of Geophysical Research, vol. 75, p. 4360-4362. Symposium on Quantitative Magnetospheric Models, Boulder, Colo., Mar. 18, 1970

Description of a model, labeled pogo (8/69), which was derived by fitting all the data of the total ambient magnetic field taken during quiet intervals from Oct. 1965 through May 1968 with a series of internal spherical harmonics and their first derivatives in time. It is worth while to use this model to determine the magnitude of errors in earlier models. M.M.

A70-40479

IONOSPHERIC STORMS AT MIDLATITUDES.

J. A. Klobuchar, M. Mendillo, and M. D. Papagiannis (Boston U., Boston, Mass.) 01(USAF, Cambridge Research Labs, Bedford, Mass.) Jun. 1970 4 p refs Radio Science, vol. 5, p. 895-898. U.S. Air Force, Symposium on the Application of Atmospheric Studies to Satellite Transmission, Boston, Mass., Sep. 35, 1969.

The total electron content of the ionosphere often responds in a dramatic way to increase in geomagnetic activity. By monitoring the VHF signets from the geostationary satellite ATS 3, it has been possible to study in detail the very pronounced increases in total content often found during the afternoon hours on the day of the commencement of a magnetic storm. Comparisons with magnetic field data show that the enhancements in electron content coincide with increases in the total magnetic field. This simultaneity suggests that, when the magnetosphere is compressed during the initial phase of a storm, the ionization stored in the magnetic tubes of force may be dumped into the topside of the F region. Such a depletion of the protonosphere is in agreement with whistler measurements, which indicate that a contraction of the plasmasphere occurs during periods of increased magnetic activity. (Author)

A70-40690

SEARCH FOR GALACTIC GAMMA-RAYS WITH ENERGIES GREATER THAN 500 MEV ON BOARD OGO-5.

J. A. M. Bleeker, J. J. Burger, A. J. M. Deerenberg, A. Scheepmaker, B. N. Swanenburg (Leiden, Rijksuniversiteit, Leiden, Netherlands), Y. Tanaka (Nagoya U., Nagoya, Japan), and H. C. VanDeHulst Dordrecht, D. Reidel Publishing Co. 1970 3 p In: Non-Solar X- and Gamma-Ray Astronomy, International Astronomical Union, Symposium, Rome Italy, May 8-10, 1969, Proceedings, p. 297-299. Symposium supported by the Consiglio Nazionale delle Ricerche. (IAU Symposium No. 37), 1970.

Description of a search for an increase in counting rate toward the galactic plane in gamma-rays on board OGO-5.

The observed counting rates of gamma-rays with energies greater than 900 MeV are tabulated, together with the observed rates of charged particles, which could contribute to the background and the guard counter rates. M.M.

A70-40691

SPARK-CHAMBER OBSERVATION OF GALACTIC GAMMA-RADIATION.

G. W. Hutchinson, A. J. Pearce, D. Ramsden, and R. D. Wills (Southampton, U., Southampton, England) Dordrecht, D. Reidel Publishing Co. 1970 6 p In: Non-Solar X- and Gamma-Ray Astronomy, International Astronomical Union, Symposium, Rome, Italy, May 8-10, 1969, Proceedings, p. 300-305. Symposium supported by the Consiglio Nazionale delle Ricerche. Research supported by the Science Research Council. (IAU Symposium no. 37), 1970.

A gamma-ray telescope incorporating an acoustic spark chamber is included in the payload of the OGO-5 spacecraft. The performance of the instrument, which is sensitive to photons of energy 25 to 100 MeV, is discussed. Observations are limited to a portion of the sky near Cygnus, but the first month's data indicate a variation of intensity showing a maximum in the direction of the galactic plane. If this plane contains a line source of radiation, its intensity is found to be 9 (plus or minus 5) times 10 to the minus 4th power photons per sq cm per sec per rad above an energy of 40 MeV. (Author)

A70-41057*

STUDY OF THE THERMAL PLASMA ON CLOSED FIELD LINES OUTSIDE THE PLASMASPHERE.

J. M. Grebowsky, H. G. Mayr, and H. A. Taylor, Jr. (NASA, Goddard Space Flight Center, Greenbelt, Md.) Aug. 1970 13 p refs Planetary and Space Science, vol. 18, p. 1123-1135.

Using OGO 4 ion composition measurements near the midlatitude light ion trough below 1000 km, a model for the plasma state along the magnetic field lines is developed which produces, in the equatorial plane, the sharp density gradient characteristic of the plasmapause. In this model the field aligned plasmasphere boundary is a boundary across which the characteristics of the proton flux along the field lines change. Within the plasmasphere the proton fluxes along the field lines are of small or vanishing magnitude and may be directed either away from or towards the earth. By contrast, the small equatorial ion densities (about 1 per cu cm) known to exist on closed field lines outside the plasmasphere are consistent with the measured low altitude densities only if large proton fluxes, of the order of the critical flux, are directed along the field lines. These latter fluxes are directed away from the earth and correspond to the attainment of supersonic proton flow velocities on closed field lines outside the plasmasphere. This is consistent with the model of a supersonic polar wind convecting onto closed field lines. (Author)

A70-41087

THEORY OF SPACECRAFT SHEATH STRUCTURE, POTENTIAL, AND VELOCITY EFFECTS ON ION MEASUREMENTS BY TRAPS AND MASS SPECTROMETERS.

L. W. Parker (Mt. Auburn Research Associates, Cambridge, Mass.) and E. C. Whipple, Jr. (Essa, Aeronomy Lab., Boulder, Colo.) 1 Sep. 1970 14 p refs Journal of Geophysical Research, vol. 75, p. 4720-4733.
(Contract E-22-8-70N)

Extension of a previously developed theory for the behavior of an electron trap with an attractive aperture grid on a charged spacecraft to include ion collection and to make the theory applicable to ion traps and mass spectrometers. The ion current for specific class of spacecraft experiments including mass spectrometer with attractive apertures and ion traps is computed. The investigation is based on the computation of trajectories in the electric fields due to the spacecraft potential, the drawing in potential of the experimental aperture and the space charge. Two values of

the Debye length namely an infinite length (Laplace field) and a length comparable to the experiment dimensions and H(+), He(+), and O(+) ion currents are considered. The current is shown to be enhanced by a large factor either by an attractive satellite potential or an attractive drawing in potential. Another effect of the satellite potential is to reduce the amplitude of the current modulation caused by the spacecraft spin. For large Debye lengths and no drawing in potential, the current is found to depend in a simple manner on a parameter that is the ratio of the work done on the ion by the electric field to the unperturbed ion kinetic energy in the spacecraft reference frame. The current voltage characteristic of an internal repelling collector in the case of an ion trap with no drawing in potential is also investigated. It is found that the temperature can be inferred from the shape of the retarded current voltage characteristic at sufficiently large retarding potential regardless of the Debye length. O.H.

A70-42468#

OBSERVATIONS OF THE COMET BENNETT (1969 i), OBSERVATIONS DE LA COMETE BENNETT (1969 I)
Ch. Bertaud (Meudon, Observatoire, Meudon, Hauts-de-Seine, France) Sep. 1970 14 p L'Astronomie, vol. 84, p. 361-374. In FRENCH

Observational results for the comet Bennett (1969 i) and discussion of the spectrograms obtained. The linear diameter of the comet was optically estimated to be about 50,000 km, eccentricity of the trajectory was equal to 0.996 and the period was estimated to be about 1600 years. The spectrograms obtained by means of the satellite OGO 5 made it possible to reveal Lyman-alpha emission of very high intensity. In the neighborhood of the comet head this intensity attained 24 kR. The hydrogen emission envelope was found to be about 13,000,000 km in diameter. The hydrogen mass was estimated in a first approximation to be about 2,000,000 tons. Z.W.

A70-43301*

THE SOLAR VARIATION OF SOFT X-RAY EMISSION.
R. W. Kreplin (U.S. Navy, E. O. Hulburt Center for Space Research, Washington, D.C.) Jun. 1970 8 p refs Annales de Geophysique, vol. 26, p 567-575. Navy-NASA supported research.

Review of the daily average solar X-ray emission levels in the bands 44 to 60 A, 8 to 20 A and 1 to 8 A obtained from the nearly continuous records provided by the NRI, Solrad satellites since January 1964. These records show increases of a factor of 20 in the 44 to 60 A band between the solar minimum in 1964 and the solar maximum in 1969. For the same period an increase of a factor of 200 has been observed in the 8 to 20 A band. Short term fluctuations are observed to correspond to the presence of active regions on the disk. The X-ray emission history of one such region, McMath 8207 is examined in detail and it is shown that the emission levels vary with the complexity of the magnetic fields of the spot group. Observation of X-ray emission 36 hours prior to the appearance of the active region on the limb indicates emission from altitudes as great as 50,000 km in the lower corona. M.V.E.

A70-43834*

ELECTRON OBSERVATIONS BETWEEN THE INNER EDGE OF THE PLASMA SHEET AND THE PLASMASPHERE.

L. A. Frank (Iowa, U., Iowa City, Iowa) and M. A. Schield 1 Oct. 1970 14 p refs Journal of Geophysical Research, vol. 75, p. 5401-5414.
(Contracts NAS5-2054; Nonr-1509(06); Grant NGL-16-001-002)

Review of the results of measurements of electron densities over the energy range of about 100 eV to 50 keV for magnetic-shell-parameter values between 3 and 10 earth radii near local midnight at low magnetic latitudes, obtained over the period June 11 through July 23, 1966, with an array of electrostatic analyzers borne on earth satellite OGO 3. It

has been found that the earthward edge of the plasma sheet is characterized by severe decreases in electron energy densities with decreasing geocentric radial distance. These decreases have a distinct structure with fluxes of higher energy electrons decreasing further from the earth for the electron energy range of about 700 eV to 20 keV. The plasmapause is usually observed to be located at the minimum of the energy density profile for electrons with energies above 700 eV. At electron energies of about 200 eV, a plasmapause structure comprising a sharp radially outward boundary and a broader inward boundary is observed. Kilovolt electron intensities between the plasmasphere and the earthward edge of the plasma sheet decreased more rapidly and fell to typically quiescent values within the satellite's orbital period of 48 hours. Simultaneous observations of the angular distributions of electron intensities at two pitch angles in the plasma sheet revealed that these angular distributions approached isotropy for the several plasma sheet crossings that were examined. M.V.E.

A70-43840*

PLASMA MEASUREMENTS WITH THE RETARDING POTENTIAL ANALYZER ON OGO-6.

T. W. Flowerday (Texas, U., Dallas, Tex.), W. B. Hanson, S. Sanatani, and D. Zuccaro 1 Oct. 1970 19 p refs Journal of Geophysical Research, vol. 75, p 5483-5501.
(Contract NAS5-9311)

Description of the nature of the results from the retarding potential analyzer on the OGO 6 satellite. The device appears capable of measuring ion temperature to an accuracy of better than 10% in a quiet ionosphere. In the dawn dusk plane, the ion temperature is observed to vary from 1000 to 4000 K. The higher temperatures are associated with higher altitudes in the winter hemisphere. Molecular ions are detected near the perigee (400 km), but their concentrations seldom exceed 1% of the atomic oxygen ion concentration. The device also operates in a mode that examines the horizontal changes in ion concentrations (fractional changes as small as 0.001 can be observed) with a spatial resolution from 350 to as small as 40 meters depending on the telemetry rate. M.V.E.

A70-43841*

METEORIC IONS ABOVE THE F2 PEAK.

W. B. Hanson and S. Sanatani (Texas, U., Dallas, Tex.) 1 Oct. 1970 7 p refs Journal of Geophysical Research, vol. 75, p. 5503-5509.
(Contract NAS5-9311)

Observation of heavy ions of about mass 56 amu (probably iron ions) at heights well above the F2 peak at concentrations of the order of 100 per cu cm. Another ion (or ions) of intermediate mass (about 30 amu) and comparable concentration is also observed, but its identification is now obscure. The heavy ions are a common feature of the nighttime ionosphere, and it is suggested that they arise from meter disintegration near 100 km and are then lifted by the dynamo electric field to greater heights. Readily resolvable structure in the variation of ion temperature with latitude is also observed, and it is postulated that these enhancements in ion temperature may be caused by the relative drift motions of ions with respect to the neutral atmosphere. (Author)

A70-43851*

THE ALFVEN VELOCITY IN THE MAGNETOSPHERE AND ITS RELATIONSHIP TO ELF EMISSIONS.

R. K. Burton, C. R. Chappell (Lockheed Research Labs., Palo Alto, Calif.), and C. T. Russell (California, U., Los Angeles, Calif.) 1 Oct. 1970 5 p refs Journal of Geophysical Research, vol. 75, p. 5582-5586.
(Contracts NAS5-9092; NAS5-9098; JPL-950403; Grant NGR-05-007-235)

OGO 5 measurements of the ion density and magnetic field strength near the equator in the dawn quadrant of the magnetosphere have been used to determine the Alfvén velocity. The Alfvén velocity in the outer magnetosphere ranges between 1000 and 2000 km/sec. At decreasing radial

distances the Alfvén velocity increases to a maximum (average, 4800 km/sec) and drops to a minimum (average, 490 km/sec) just inside the plasmasphere. ELF emissions are well ordered by the Alfvén velocity profiles. ELF chorus from 100 to 1000 Hz exists in the outer magnetosphere only for Alfvén velocities below about 3000 km/sec. ELF hiss is found immediately inside the plasmapause. This relationship between ELF emissions and the Alfvén velocity is further support for unstable wave generation by Doppler shifted cyclotron resonance. (Author)

A70-43852*

ON THE DIURNAL VARIATION OF THE EXOSPHERIC NEUTRAL HYDROGEN TEMPERATURE.

M. A. Clark (Aerospace Corp., Los Angeles, Calif.) and P. H. Metzger 1 Oct. 1970 5 p refs *Journal of Geophysical Research*, vol. 75, p. 5587-5591. (NASA Order S-99813-G)

Evaluation of resonance filter data obtained from OGO 6 implying a mean exospheric temperature of 900 K for June 8, 1969, with a 200 K variation dawn to dusk between 0600 and 1800 LT near the equator. Owing to the tilt of the orbit plane by approximately 1 hour toward the summer pole, a north-south asymmetry of about 75 K is also seen. These data strongly suggest that sources of Lyman alpha external to the geocorona are smaller than previously thought. (Author)

A70-45768

TEMPERATURE AND EMISSION-MEASURE PROFILES OF TWO SOLAR X-RAY FLARES.

C. S. Bowyer (California, U., Berkeley, Calif.), S. W. Kahler, R. W. Kreplin (U.S. Navy, E. O. Hulburt Center for Space Research, Washington, D.C.), and J. F. Meekins Oct. 1970 12 p refs *Astrophysical Journal*, vol. 162, Pt-1, p. 293-304.

(Grant NSF GP-11406)

Data from the NRL 2- to 20-keV X-ray detector on the OGO-5 satellite are discussed. A detailed study of two solar X-ray flares shows that the 3- to 12-keV flux is thermal in origin, with emission measures which vary by two orders of magnitude during the course of the flares analyzed. A physical interpretation of the energy dispersion of the times of peak X-ray fluxes is given. Heating of a flare region by nonthermal electrons is proposed for the flare of June 9, 1968. (Author)

A70-45769

IMPLICATIONS OF THE OBSERVED SOLAR MODULATION OF COSMIC-RAY ELECTRONS.

J. J. Burger (Leiden, Rijksuniversiteit, Leiden, Netherlands) and Y. Tanaka (Nagoya U., Nagoya, Japan) Oct. 1970 10 p refs *Astrophysical Journal*, vol. 162, Pt-1, p. 305-314.

The observed variation of the primary electron intensity above 500 MeV between 1966 and 1968 is compared with those of protons and alpha particles. The modulation feature of these three components is consistent with the simple diffusion convection theory. On the other hand, a generalized diffusion convection theory developed by Gleason and Axford which includes effective energy losses does not explain simultaneously the modulation of the three different species. The disagreement may imply that the effect of energy loss is insignificant in accounting for the solar modulation. The interstellar electron spectrum is derived by using the simple diffusion convection theory, under the assumption that the cosmic ray diffusion coefficient is a separable function of heliocentric radius and rigidity. Comparison of the result with the nonthermal galactic radio spectrum, and also the observed positron flux indicate a significant underestimate of the modulation below 1 GeV. This casts serious doubt on the separability of the diffusion coefficient. (Author)

A71-11491*

SPECTROMETER OBSERVATIONS IN THE REGION NEAR THE BOW SHOCK ON MARCH 12, 1968.

K. K. Harris (Lockheed Research Labs., Palo Alto, Calif.),

S. L. Ossakow, and G. W. Sharp 1 Nov. 1970 13 p refs *Journal of Geophysical Research*, vol. 75, p. 6024-6036. (Contract NAS5-9092)

Review of the measurements of directed proton fluxes in the 0-600 eV range performed by means of an ion spectrometer on the OGO 5 satellite in a cone angle of 10 deg with respect to the spectrometer normal and in a fixed direction with respect to the satellite-sun line in the bow shock and adjacent regions of the magnetosheath and solar wind. The data presented for the multiple shock crossings of Mar. 12, 1968, indicate that the fluxes measured by the spectrometer are some 3 orders of magnitude higher in the magnetosheath than in the solar wind. The abrupt increase in directed proton flux, in going from the solar wind into the magnetosheath, identifies the position of the bow shock in the satellite orbit. The higher proton fluxes, in passing through the bow shock to the magnetosheath, are accompanied by steep gradients in the magnetic field as measured by a magnetometer and saturation of electrostatic wave turbulence as measured by a plasma wave detector. For the most part, these measurements correlate very well with the bow shock crossings observed by means of the light-ion spectrometer. M.V.E.

A71-11494

DIFFUSIVE ENTRY OF SOLAR-FLARE PARTICLES INTO GEOMAGNETIC TAIL.

A. J. Dessler (Rice U., Houston, Tex.) and F. C. Michel 1 Nov. 1970 12 p refs *Journal of Geophysical Research*, vol. 75, p. 6061-6072.

(Contract AF 19(628)-70-C-0184)

Extension and modification of Michel and Dessler's (1965) diffusion model, accounting for certain findings about the access of electrons and protons to the polar caps. The diffusion model utilizes a magnetospheric structure in which the tail is described as being composed of filaments, each having slightly different plasma and field properties. It is shown that an energy-independent access of protons into such a tail model is possible over a broad range of proton energies. Diffusion results from the fluctuating fields about the protons in cyclotron motion. This diffusion mechanism is ineffective for the electrons. The electrons enter further down the tail where the tail becomes flattened and the filaments intermingle with the interplanetary field lines. Depending on the circumstances, the latter mechanism could be important for proton entry as well. Access to the distant tail regions should be sensitive to the direction of the interplanetary field relative to the tail field, which is believed to account for the observed north-south polar-cap asymmetry. M.V.E.

A71-11498*

OBSERVATIONS FROM OGO-5 OF THE THERMAL ION DENSITY AND TEMPERATURE WITHIN THE MAGNETOSPHERE.

E. J. R. Maier (NASA, Goddard Space Flight Center, Lab. for Planetary Atmospheres, Greenbelt, Md.) and G. P. Serbu 1 Nov. 1970 12 p refs *Journal of Geophysical Research*, vol. 75, p. 6102-6113.

Discussion of some recent simultaneous measurements of ion density and temperature performed in the dawn and morning quadrants of the magnetosphere by means of the OGO 5 satellite. Some preliminary results of ion temperature profiles, as measured for the first time in the outer protonosphere, are presented. The ion temperature observations show that within the plasmapause the day to night temperature ratio is about a factor of 2. The relatively high observed density of about 100 ions per cu cm at 4 earth radii and an apparent temperature of 30 to 50 thousand deg K are not consistent with a simple diffusive equilibrium distribution along a closed magnetic field line. The self-collision life time of 0.5-eV particles in a plasma of a 100-ions/cu cm density is 2400 sec, and the majority of such ionospheric particles with a Maxwellian velocity distribution would be lost rapidly. However, the self-collision time for 5-eV particles in a plasma of the same density is 80,000 sec. The computed bounce

periods for the 0.5- and 5-eV particles are 3000 and 1000 sec. Thus the 5-eV particles will survive 40 or more bounces, whereas the 0.5-eV particles will be Coulomb-scattered into the loss cone in one bounce period. The discrimination of this process against low-energy particles is suggested as an explanation for the apparent high temperature of the ions.

M.V.E.

A71-11499***WHISTLER DUCT PROPERTIES DEDUCED FROM VLF OBSERVATIONS MADE WITH THE OGO-3 SATELLITE NEAR THE MAGNETIC EQUATOR.**

J. J. Angerami (Stanford U., Stanford, Calif.) 1 Nov. 1970 21 p refs Journal of Geophysical Research, vol. 75, p. 6115-6135.

(Contract NAS5-2131; Grants NGR-05-020-288; NGL-05-020-008; NSF GP-948; NSF GA-1151)

Discussion of the first direct evidence on the nature of ducting, based on in situ whistler observations made by the OGO 3 satellite. The interpretation of the data strongly supports both the cutoff theoretically predicted by Smith (1961) at one half minimum gyrofrequency along the path and the Angerami (1966) hydrostatic model of magnetospheric ionization. For the cases studied, it is found that the overall thermal damping is not an important process near half the local gyrofrequency. The data lead to estimates of the L shell thicknesses of whistler ducts, their elongation or extent in longitude, and minimum enhancements needed for trapping. The data also confirm the validity of using the longitudinal approximation to calculate travel times and nose frequencies of ducted whistlers. The data give further evidence that whistler ducts are indeed enhancements, rather than depressions, of ionization.

M.V.E.

A71-11500***VLF ELECTRIC FIELD OBSERVATIONS IN THE MAGNETOSPHERE.**

F. V. Coroniti (TRW Systems Group, Redondo Beach, California, U., Los Angeles, Calif.), R. W. Fredricks, C. F. Kennel, J. H. McGehee (TRW Systems Group, Redondo Beach, Calif.), and F. L. Scarf 1 Nov. 1970 17 p refs Journal of Geophysical Research, vol. 75, p. 6136-6152 (Contract NAS5-9278; Grant NGR-05-007-190)

New types of magnetospheric electric field emissions have been detected by OGO 5 with wave frequencies (f) above the local electron cyclotron frequency (f_c). The most common emissions occur between the lowest electron cyclotron harmonics ($f = 3f_c/2$), followed by emissions at high frequencies (f much greater than f_c). A few signals have been observed slightly above the local f_c . The strong emissions with f about or more than $3f_c/2$ appear to be localized within a few degrees of the geomagnetic equator. More than 60% of the equator crossings between L values of 4 and 10 in the 0000-1200 LT sector have such activity. The waves have large electric field amplitudes (1-10 mv/m), which suggests they may be sources of pitch angle diffusion and turbulent energization of auroral zone electrons. (Author)

A71-11503***DEPRESSIONS IN THE FAR-ULTRAVIOLET AIRGLOW OVER THE POLES.**

R. R. Meier (U.S. Navy, E. O. Hulburt Center for Space Research, Washington, D.C.) 1 Nov. 1970 15 p refs Journal of Geophysical Research, vol. 75, p. 6218-6232 (NASA Order S-32327-G; NASA Order S-45340-G; NASA Order S-20613-G)

Observations of the ultraviolet emissions of atomic hydrogen (Lyman alpha) and atomic oxygen (1304 A) over the polar regions from the OGO 4 satellite show that the airglows are sometimes depressed relative to the nonpolar levels. The Lyman alpha decreases are a manifestation of a reduction in the polar hydrogen concentration, apparently associated with the region of open magnetic field lines. The polar hydrogen concentration is estimated to be approximately 37% below the nonpolar level for a Lyman alpha depression of 10%, and 27% below the nonpolar level for a

5% depression. The 1304-A decreases are apparently related to a change in the exciting photoelectron concentration, when either the field lines are open or the conjugate ionosphere is in shadow. (Author)

A71-11504***EQUATORIAL AURORA/AIRGLOW IN THE FAR ULTRAVIOLET.**

T. A. Chubb (U.S. Navy, E. O. Hulburt Center for Space Research, Washington, D.C.) and G. T. Hicks 1 Nov. 1970 16 p refs Journal of Geophysical Research, vol. 75, p. 6233-6248

(NASA Order S-32327-G)

Discussion of an experiment performed aboard the OGO 4 polar-orbiting satellite, during which far ultraviolet emissions in the equatorial zone were detected at altitudes of less than 500 km. The occurrence frequency reached a maximum in late October and early March during the period from August 1967 to May 1968. Both maxima occurred near 2130 local time. Low values during June 1968 indicate a strong seasonal dependence. The emissions were seen quite symmetrically in position at 12 to 15 deg on either side of the magnetic dip equator, completely encircling the earth. Frequently, the peak intensity of the emissions was the same north and south of the equator, but in some cases the intensity was three or four times greater on one side than on the other. In rare cases, emission was totally lacking on one side while clearly present on the other. Simultaneous comparisons of quick-look scanning spectrometer data of Barth from OGO 4 show that the emissions are oxygen lines at 1304 and 1356. Possible mechanism for production of the emissions are discussed.

V.P.

A71-13475***IDENTIFICATION AND RELATIVE ABUNDANCES OF C, N, AND O NUCLEI TRAPPED IN THE GEOMAGNETIC FIELD.**

A. Mogro-Campero and J. A. Simpson (Chicago, U., Chicago, Ill.) 7 Dec. 1970 5 p refs Physical Review Letters, vol. 25, p. 1631-1635

(Contract NAS5-9366; Grant NGL-14-001-006)

Determination of the relative abundances of C, N, and O nuclei, with energies ranging from 13 to 33 MeV/nucleon, trapped in the radiation belt near the geomagnetic equator. The data were obtained over a 10-month period in 1968 by means of the OGO 5 satellite. The measured abundance ratio O/C for these nuclei is equal to about 0.5; this ratio is consistent only with an extraterrestrial origin of these nuclei.

Z.W.

A71-14014***PICOGRAM DUST PARTICLE FLUX: 1967-1968 MEASUREMENTS IN SELENOCENTRIC, CISLUNAR AND INTERPLANETARY SPACE.**

W. M. Alexander, C. W. Arthur, J. L. Bohn (Temple U., Philadelphia, Pa.), and J. D. Corbin (Baylor U., Waco, Tex.) Amsterdam, North Holland Publishing Co. 1970 8 p refs In: Space Research X, COSPAR, Plenary Meeting, 12th, and Symposium on Thermospheric Properties Concerning Temperatures and Dynamics with Special Application to H and He, Prague, Czechoslovakia, May 11-24, 1969, Proceedings, p. 252-259 Symposium co-sponsored by the International Assn. of Geomagnetism and Aeronomy, the International Union of Geodesy and Geophysics, and the International Union of Radio Science.

(Contract NAS5-9352; NAS5-9128; Grant NsG-39-012-001)

Review and interpretation of data showing the mean cumulative flux of interplanetary dust particles from day 130 to 345, 1967, as measured by Mariner 4, with discussion of special events detected by Mariner 4 during this period. Data are also presented showing the mean cumulative flux of dust particles in cislunar space as measured by OGO 3, as well as data Lunar Explorer 35 showing the fluctuation of the mean cumulative dust particle flux in selenocentric space for day 201, 1967, to day 201, 1968. Selected data

obtained during the times of several meteor showers occurring both in 1967 and 1968 are given. F.R.L.

A71-14028*

OBSERVATIONS OF LYMAN-ALPHA AND THE ATOMIC HYDROGEN DISTRIBUTION IN THE THERMOSPHERE AND EXOSPHERE.

R. R. Meier (U.S. Navy, E. O. Hulburt Center for Space Research, Washington, D.C.) Amsterdam, North Holland Publishing Co. 1970 10 p refs In: Space Research X, COSPAR, Plenary Meeting, 12th, and Symposium on Thermospheric Properties Concerning Temperatures and Dynamics with Special Application to H and He, Prague, Czechoslovakia, May 11-24, 1969. Proceedings, p. 572-581 Symposium co-sponsored by the International Assn. of Geomagnetism and Aeronomy, the International Union of Geodesy and Geophysics, and the International Union of Radio Science.

(NASA Order S-32327-G; NASA Order S-45340-G; NASA Order S-20613-G; Grants NSF GP-6354; NSF GP-7890)

Analysis of observations of Lyman-alpha from the OGO 3, OGO 4, and OSO 4 satellites and Balmer-alpha measurements in the night sky by assuming that the radiation is principally due to resonance scattering of solar photons in the atomic hydrogen geocorona. After correction for the extraterrestrial background, the OGO 4 and OSO 4 observations yield typical nadir-zenith intensity ratios of 0.84 and 1.20 for night and day (solar zenith angles of 180 and 10 deg), respectively, in the autumn 1967 epoch. Nadir intensities of 1.1 and 24 kR for night and day were characteristic of that period. To interpret these data numerical solutions of radiative transfer equations have been obtained for various models of the geocorona. The results of this analysis indicate that if the solar Lyman-alpha flux is 4.0×10 to the 11th protons/sq cm-sec-A, then the mean optical depth above 650 km is about 1.3 (or 7.0×10 to the 12th atoms/sq cm) for an 100 K exospheric temperature. Radiative transfer methods were also applied to the Lyman-beta problem, and solutions were compared with experimental observations of Balmer-alpha. The conclusions of this analysis are in agreement with the Lyman-alpha results if a nonterrestrial Balmer-alpha background of some 3.0 to 4 R is present in addition to the airglow, and if the solar Lyman-beta flux is higher than previously reported.

A71-14046

FLARE X-RAY AND RADIO WAVE EMISSION.

J. P. Castelli (USAF Cambridge Research Labs., Bedford, Mass.), R. W. Kreplin, and P. J. Moser (U.S. Navy, E. O. Hulburt Center for Space Research, Washington, D. C.) Amsterdam, North Holland Publishing Co. 1970 8 p refs In: Space Research X, COSPAR, Plenary Meeting, 12th, and Symposium on Thermospheric Properties Concerning Temperatures and Dynamics with Special Application to H and He, Prague, Czechoslovakia, May 11-24, 1969. Proceedings, p. 920-927 Symposium co-sponsored by the International Assn. of Geomagnetism and Aeronomy, the International Union of Geodesy and Geophysics, and the International Union of Radio Science.

Measurement of solar X-ray emission since July 1967 with the aid of SOLRAD 9 (1968-17A) and OGO 5 (1967-73A). A number of X-ray flares, for which there are accompanying cm radio burst data from Sagamore Hill-Radio Observatory and from Manila, have been examined in an attempt to clarify the relationship between the emission processes for the two wavelength ranges. Whereas flare X rays of photon energy greater than 20 keV appear to match microwave outbursts closely in time and duration, a steep rise of X-ray intensities in the band from 0 to 3 A consistently leads the microwave flash by several minutes. For most flares classified 1B or greater, the 0.3 A X-ray flux has risen by an order of magnitude before the sharp rise in microwave emission. Generally, the microwave flash is short-lived, but followed by the postburst slow decay which matches the duration of soft X-ray emission. (Author)

A71-14068*

MICROSCOPIC STRUCTURE OF THE SOLAR WIND@

F. L. Scarf (TRW Systems Group, Redondo Beach, Calif.) Oct. 1970 37 p refs Space Science Reviews, vol. 11, p. 234-270

(Contracts NAS5-9278; NAS2-4673)

As the solar wind flows out from the coronal base the Coulomb collision frequencies rapidly become small and particle-particle collisions can no longer maintain local statistical equilibrium. At 1 AU the particle distribution functions have important non-Maxwellian characteristics and the firehose instability, a cyclotron resonance whistler-mode instability, and several heat flux current instabilities should be operative. Superthermal particle populations also provide large wave levels, and other forms of enhanced plasma turbulence develop at shock fronts and discontinuities. This report contains a review of the theoretical concepts and a progress report on the experimental study of interplanetary wave-particle interactions. (Author)

A71-14212

ELECTRON INTENSITY VARIATIONS IN THE INNER BELT FOLLOWING A GEOMAGNETIC STORM.

R. W. Kreplin (U.S. Navy, Naval Research Lab., Washington, D.C.) and F. F. Tomblin (Bellcomm, Inc., Washington, D.C.) 5 Dec. 1970 3 p refs Nature, vol. 228, p. 988-990.

Discussion of electron flux variations in the inner belt following geomagnetic storms taking into consideration data obtained with OGO 4 ionization chambers. OGO 4 ionization chamber characteristics are described. The study of electron flux levels following the May 1967 event for a three month period starting in August 1967 is reported. Electron flux levels above 120 keV were monitored by ionization chambers also used as solar X-ray monitors on OGO 4 in polar orbit. Supplementary electron data above 280 keV were obtained from the C1 detector on the 1963 38C satellite also in polar orbit. G.R.

A71-14515*

INWARD MOTION OF THE MAGNETOPAUSE BEFORE A SUBSTORM.

M. P. Aubry, M. G. Kivelson (California, U., Los Angeles, Calif.), and C. T. Russell 1 Dec. 1970 14 p refs Journal of Geophysical Research, vol. 75, p. 7018-7031. ESRO supported research.

(Contract NAS5-9098)

Study of an inward motion of the magnetopause by about 2 earth radii in two hours recorded on Mar. 27, 1968, by the UCLA magnetometer on board the inbound OGO 5 satellite. It is shown that this inward motion was associated with a reversal of the vertical component of the interplanetary field from northward to southward, the solar wind momentum flux remaining constant. The inward shift did not produce any compression of the magnetospheric cavity, which implies a transfer of magnetic flux from the dayside magnetosphere to the tail: the IMP 4 satellite saw the magnetic tail field increasing at the end of this interval and later the substorm-associated collapse of this field. The substorm was also recorded on the ground. It is emphasized that the position of the magnetopause after the inward shift cannot be explained in terms of the available numerical models. (Author)

A71-14538*

POLARIZATION OF PROTON WHISTLERS.

R. L. Smith (Stanford U., Stanford, Calif.) 1 Dec. 1970 6 p refs Journal of Geophysical Research, vol. 75, p. 7261-7266.

(Contract NAS5-9309)

An experiment that separates whistler-mode waves into characteristic right and left-hand circularly polarized components on a broad-band basis has shown that electron whistlers are nearly right-hand polarized and proton whistlers are nearly left-hand polarized, as is predicted by whistler theories. The method has application to the study of broad-band phenomena such as hiss and chorus, and should

allow improved accuracy of ion density as measured from proton whistlers. (Author)

A71-14550*
DIRECT CORRELATIONS OF LARGE-AMPLITUDE WAVES WITH SUPRATHERMAL PROTONS IN THE UPSTREAM SOLAR WIND.

P. J. Coleman, Jr. (California U., Los Angeles), L. A. Frank (Iowa, U., Iowa City, Iowa), R. W. Fredricks (TRW Systems Group, Redondo Beach, Calif.), M. Neugebauer (California Inst. of Tech., Jet Propulsion Lab., Pasadena, Calif.), C. T. Russell, and F. L. Scarf 1 Dec. 1970 7 p refs Journal of Geophysical Research, vol. 75, p. 7316-7322. (Contracts NAS5-9278; NAS5-9196; NAS5-9098)

Results of direct correlations of magnetometer, plasma probe, and Lepedea proton data taken simultaneously by experiments aboard OGO 5 during a large upstream wave event on March 10, 1968. Direct correlation of Lepedea fluxes with magnetometer fluctuations shows that the large upstream wave amplitudes occur when enhanced fluxes of protons with $E_{sub p}$ approximating 4 to 7 keV are present. This suggests that such suprathermal proton streams drive the hydromagnetic fluctuations. The presence or absence of electrostatic plasma wave turbulence in these regions has been correlated with the degree of anisotropy of the 4- to 7-keV protons, and also with density gradients detected by the solar wind plasma probe. F.R.L.

A71-15937*
SPECTRAL CHARACTERISTICS OF IMPULSIVE SOLAR-FLARE X-RAYS GREATER THAN OR APPROXIMATELY 10 keV.

K. A. Anderson (California, U., Berkeley, Calif.) and S. R. Kane Dec. 1970 16 p refs Astrophysical Journal, vol. 162, Pt. 1, p. 1003-1018. (Contract NAS5-9094)

Deduction of the characteristics of the impulsive solar-flare X-ray component from thirteen bursts of hard X-rays observed with the OGO-5 satellite during the period from Mar. 21 to June 30, 1968. Most of these impulsive X-ray bursts were associated with impulsive microwave bursts and optical flares of importance smaller than or approximately 1. For approximately 40 keV, X rays the e-folding rise and decay time are found to be 2 to 5 and 3 to 10 sec, respectively. The spectrum of the energetic electrons in the X-ray source region has been deduced under the assumption that electron-proton bremsstrahlung is the mechanism for X-ray production. The short rise time, the power-law energy spectrum, and the time of occurrence relative to the optical flare indicate that the impulse X rays greater than or approximately 10 keV are a nonthermal flash-phase phenomenon. There is evidence that the injection of energetic electrons into the X-ray source region occurs more or less continuously throughout the impulse X-ray burst. This injection, combined with the loss of energetic electrons through escape and collisions, probably determines the time-intensity profile of an impulsive X-ray burst. M.M.

A71-17258*
MAGNETOPAUSE CROSSING OF THE GEOSTATIONARY SATELLITE ATS 5 AT 6.6 RE.

T. L. Skillman and M. Sugiura (NASA, Goddard Space Flight Center, Lab. for Space Physics, Greenbelt, Md.) 1 Jan. 1971 7 p refs Journal of Geophysical Research, vol. 76, p. 44-50

Discussion of the unusually large magnetic field decrease preceded by an impulsive increase of about 100 gammas observed by the geostationary satellite ATS 5 during the moderate magnetic storm of September 29-30, 1969. The field remained low for about 1 min and returned to the preevent level as abruptly as it decreased. From the ATS 1 and ATS 5 observations and magnetograms from ground observatories, it has been inferred that the magnetosphere was greatly compressed before the event; the magnetopause distance was probably near 7 earth radii at the subsolar point. By comparing the changes observed by ATS 5 with

the field measured by ATS 1, which was 3 hours behind ATS 5 in local time, the event is interpreted as a magnetopause crossing of ATS 5 caused by a localized rapid inward motion of the magnetopause and its subsequent recession, temporarily creating an indentation on the magnetopause surface and briefly exposing ATS 5 to the magnetosheath field. M.V.E.

A71-17261*
ENERGY SPECTRUMS FOR PROTON (200 EV LESS THAN OR EQUAL TO E LESS THAN OR EQUAL TO 1 MEV) INTENSITIES IN THE OUTER RADIATION ZONE.

L. A. Frank (Iowa, U., Iowa City, Iowa) and G. Pizzella 1 Jan. 1971 4 p refs Journal of Geophysical Research, vol. 76, p. 88-91. (Contracts NAS5-2054; N00014-68-A-0196-0003; Grant NGL-16-001-002)

Derivation of the directional differential spectrums of proton intensities mirroring near the magnetic equator in the outer radiation zone for the energy range 200 eV less than or equal to E less than or equal to 1 MeV with measurements from the spacecrafts OGO 3, Explorer 12 and 14, and Mariner 4. The average proton spectrum is characterized by a single maximum of differential intensities at 5 to 10 keV and monotonically decreasing intensities with lower and higher proton energy. It is suggested that the appropriate boundary region for models of radial diffusion of protons into the outer radiation zone is located in the vicinity of the earthward edge of the quiet-time extraterrestrial ring current at L approximately equal to 6.5 earth radii. (Author)

A71-17263*
THE RELATION OF THE Pc 1 MICROPULSATION SOURCE REGION TO THE PLASMAPAUSE.

R. R. Heacock (Alaska, U., College, Alaska) 1 Jan. 1971 10 p refs Journal of Geophysical Research, vol. 76, p. 100-109. (Contracts NAS9-8945; AF 19(628)-68-C-0120; Grants NSF GA-1591; NSF GA-1514)

Amplitude and polarization measurements of structured Pc 1 micropulsations obtained in Alaska and in Finland imply that the Pc 1 source lines are near or inside the plasmopause. The measurements give the source lines significantly closer to the earth than are given by Pc 1 dispersion calculations. Specific Pc 1 events are compared with plasmopause positions determined by the OGO 3 and OGO 5 satellites. We present some evidence that implies that structured Pc 1 source lines corotate with the earth. (Author)

A71-17279*
OBSERVATIONS OF CONJUGATE EXCITATION OF THE O I 1304-A AIRGLOW.

R. R. Meier (U.S. Navy, E. E. Hulburt Center for Space Research, Washington, D.C.) 1 Jan. 1971 6 p refs Journal of Geophysical Research, vol. 76, p. 242-247. (NASA Order S-32327-G; NASA Order S-45340-G; NASA Order S-20613-G)

Discussion of the first observations of conjugate excitation of the O I 1304-A airglow made from the OGO 4 spacecraft in August 1967. The observational data are presented, discussed, and analyzed. It is shown that the emission was observed only when the conjugate ionosphere was still sunlit, thus suggesting excitation by photoelectrons traveling along magnetic field lines to the night hemisphere. O.H.

A71-17686#
MAGNETOSPHERIC SUDDEN IMPULSES.

T. Ondoh May 1970 15 p refs Radio Research Laboratories, Journal, vol. 17, p. 199-213

Discussion of magnetospheric distributions of amplitudes and rise times of sudden impulses observed by the satellites OGO 3 and OGO 5. Seventy-six sudden impulses are analyzed in order to determine the magnetospheric distribution for sudden impulse amplitudes and rise times as a function of

A71-17918

location. The observed amplitudes and rise times are compared with theoretical sudden impulse amplitude and rise time data which are derived from the magnetic field of the model magnetosphere proposed by Mead (1964). G.R.

A71-17918*

THE EMISSION AND PROPAGATION OF APPROXIMATELY 40 keV SOLAR FLARE ELECTRONS. 2: THE ELECTRON EMISSION STRUCTURE OF LARGE ACTIVE REGIONS.

R. P. Lin (California, U., Berkeley, Calif.) Dec. 1970 26 p refs Solar Physics, vol. 15, p. 453-478. (Contracts NAS5-9077; NAS5-9091)

Mapping of the emission structure of a large electron-active region, McMath plage 8905, which crossed the visible solar disk in July-Aug. 1967, using electrons of approximately 40 keV energy observed at 1 AU as tracers. The acceleration of 10 to 100 keV electrons is found to be a property of active regions with a certain stage of development, and is signaled by the emission of greater than or approximately 20 keV X rays. The emission of electrons into the interplanetary medium may be separate from the acceleration of the electrons. M.M.

A71-17975*

OBSERVATION OF EARLY-TYPE STARS FROM OGO-6.

M. A. Clark (Aerospace Corp., El Segundo, Calif.) and P. H. Metzger Jan. 1971 4 p refs Astronomy and Astrophysics, vol. 10, no. 1, p. 155-158. (NASA Order S-99813-G; Contracts AF 04(701)-69-C-0066; AF 04(701)-70-C-0059)

Observation of stellar fluxes of the order of 10 to the minus eighth power erg s cm to the minus second power A for 10 eV photons for several bright UV emitting stars. These observations were made from the OGO 6 scanning Ly-alpha experiment whose resonance absorption filter suppressed the strong H Ly-alpha airglow, making possible the observation of weak external enhancements. Five separate orbits of data revealed point-source enhancements. M.M.

A71-18127*#

THE 'QUIET TIME' FLUXES OF PROTONS AND ALPHA-PARTICLES IN THE ENERGY RANGE OF 2-20 MeV/NUCLEON IN 1967.

C. Y. Fan (Arizona, U., Tucson, Ariz.), G. Gloeckler, R. B. McKibben, and J. A. Simpson (Chicago, U., Chicago, Ill.) Budapest, Akademiai Kiado, 1970 7 p refs In: International Conference on Cosmic Rays, 11th, Budapest, Hungary, Aug. 25-Sep. 4, 1969, Proceedings. Volume 2 - Solar Cosmic Rays, Modulation of Galactic Radiation, Magnetospheric and Atmospheric Effects, p. 261-267 Conference Sponsored by the International Union of Pure and Applied Physics and the Hungarian Academy of Sciences. (Acta Physica, vol. 29, Supplement 2), 1970. (Grants NGL-14-001-006; NGR-03-002-107; Contract AF 49(638)-1642)

The quiet time fluxes and different spectra of protons and alpha particles in the energy range 2-20 MeV/nucleon were measured in 1967 with cosmic ray detectors on the OGO-3 satellite. These measurements are the continuation of similar studies, begun in 1964, of the temporal variation of the spectra of these particles. The results obtained from the period 1964 to 1966 indicated that these particles were a mixture of particles of galactic and solar origin. The 1967 measurements show that, despite an increase in solar activity and modulation of relativistic cosmic rays, the 2 to 20 MeV fluxes of protons and alpha particles remained relatively unchanged. The implications of this result are discussed. (Author)

A71-18128*#

MODULATION AND HELIOCENTRIC GRADIENT OF LOW ENERGY COSMIC RAYS NEAR SOLAR MINIMUM, 1965.

S. R. Kane and J. R. Winckler (Minnesota, U., Minneapolis,

Minn.) Budapest, Akademiai Kiado, 1970 6 p refs In: International Conference on Cosmic Rays, 11th, Budapest, Hungary, Aug. 25-Sep. 4, 1969, Proceedings. Volume 2 - Solar Cosmic Rays, Modulation of Galactic Radiation Magnetospheric and Atmospheric Effects, p. 269-274 Conference Sponsored by the International Union of Pure and Applied Physics and the Hungarian Academy of Sciences. (Acta Physica, vol. 29, Supplement 2), 1970. (Contract NAS5-2071)

Comparison of cosmic ray total ionization measurements made in space with the OGO-1 and OGO-2 ion chambers with other cosmic ray measurements in space and on the ground. The data were acquired at geocentric distances between 15 and 25 earth radii during the period September 1964 to May 1968. Long-term and short-term variations are examined, and attention is given to the hysteresis effect. F.R.L.

A71-18137#

SPECTRAL VARIATIONS IN SHORT TERM FORBUSH DECREASES AND IN LONG TERM CHANGES IN COSMIC RAY INTENSITY.

V. K. Balasubrahmanyam (NASA, Goddard Space Flight Center, Greenbelt, Md.) and D. Venkatesan (Calgary, U., Calgary, Alberta, Canada, NASA Goddard Space Flight Center, Greenbelt, Md.) Budapest, Akademiai Kiado, 1970 10 p refs In: International Conference on Cosmic Rays, 11th, Budapest, Hungary, Aug. 25-Sep. 4, 1969, Proceedings. Volume 2 - Solar Cosmic Rays, Modulation of Galactic Radiation, Magnetospheric and Atmospheric Effects, p. 327-336 Conference sponsored by the International Union of Pure and Applied Physics and the Hungarian Academy of Sciences. (Acta Physica, vol. 29, Supplement 2). (Grant NRC A-3685)

Summary of data from satellite IMP A, B, and C and OGO A on a continuous basis over the period from November 1963 to May 1967. The cosmic ray intensity registered by GM counters on these satellites, of energy greater than or equal to 50 MeV is compared with the intensities recorded by neutron monitors, at the equatorial station, Huancayo, at the high-altitude station, Deep River, and at the polar station, Alert. Spectral variations during the Forbush decreases and during long-term changes in cosmic ray intensity are investigated, and the results are discussed in terms of current ideas. (Author)

A71-18158*#

A DISCUSSION OF SOLAR COSMIC RAY ACTIVITY NEAR SUNSPOT MAXIMUM.

A. J. Masley and P. R. Satterblom (McDonnell Douglas Astronautics Co., Santa Monica, Calif.) Budapest, Akademiai Kiado, 1970 7 p In: International Conference on Cosmic Rays, 11th, Budapest, Hungary, Aug. 25-Sep. 4, 1969, Proceedings. Volume 2 - Solar Cosmic Rays, Modulation of Galactic Radiation, Magnetospheric and Atmospheric Effects, p. 513-519 Conference sponsored by the International Union of Pure and Applied Physics and the Hungarian Academy of Sciences. NSF-NASA sponsored research.

Discussion of 16 solar cosmic ray events observed during 1968 and 12 during the first seven months of 1969. This represents an increase in activity as the peak in the solar cosmic ray cycle is reached. The events ranged in maximum intensity from 0.5 to 12.5 dB absorption at 30 MHz for protons with energy greater than 10 MeV. The two largest events observed during the period were the event of Nov. 18, 1968, with 12.5 dB, and the event of April 11, 1969 with 12 dB. The latter event is particularly interesting because it was apparently due to solar activity behind the east limb. F.R.L.

A71-18170*#

ELECTRONS FROM SOLAR FLARES IN THE 10 TO 200 MeV REGION.

D. Datlowe, J. Lheureux, and P. Meyer (Chicago, U., Chicago, Ill.) Budapest, Akademiai Kiado, 1970 6 p refs In: International Conference on Cosmic Rays, 11th,

Nov. 10, 1975

Budapest, Hungary, Aug. 25-Sep. 4, 1969, Proceedings, Volume 2 - Solar Cosmic Rays, Modulation of Galactic Radiation, Magnetospheric and Atmospheric Effects, p. 643-648. Conference sponsored by the International Union of Pure and Applied Physics and the Hungarian Academy of Sciences. (Acta Physica, vol. 29, Supplement 2), 1970. (Contract NAS5-9096; Grant NGR-14-001-005)

The emission of electrons in association with solar flares has now frequently been observed at energies around 50 keV and occasionally between 5 and 10 MeV. With an instrument on board the satellite OGO-5 we have, during 1968, searched for solar electrons with energy in excess of 10 MeV. On several occasions we have measured an excess flux of high energy electrons associated with solar flare activity. We shall report on these observations and discuss the energy spectra and time history for some of the events. (Author)

A71-19656*

OGO 5 OBSERVATIONS OF UPSTREAM WAVES IN THE INTERPLANETARY MEDIUM: DISCRETE WAVE PACKETS.

D. D. Childers, P. J. Coleman, Jr. (California, U., Los Angeles, Calif.), and C. T. Russell 1 Feb. 1971 17 p refs Journal of Geophysical Research, vol. 76, p. 845-861. (Contract NAS5-9098)

Consideration of the waves observed in the interplanetary medium within several earth radii of the earth's bow shock, consisting of discrete wave packets with amplitudes that are a significant fraction of the background magnetic field. By using the measured solar wind density and cold plasma dispersion theory, it is shown that these wave packets must be right-handed in the plasma frame at frequencies from about 2 to 4 times the proton gyrofrequency. The propagation vector of these waves is found to point away from the earth's bow shock and to lie between the solar wind flow direction and the average spiral field. The waves are being carried away from the sun by the solar wind, since their velocity is less than the solar wind speed, but they appear to be associated with the intersection of the field line with the earth's bow shock. M.V.E.

A71-19663*

SUBAURORAL RED ARCS AND ASSOCIATED IONOSPHERIC PHENOMENA.

S. Chandra, E. J. R. Maier, B. C. Narasinga Rao (NASA, Goddard Space Flight Center, Lab. for Planetary Atmospheres, Greenbelt, Md.), and B. E. Troy, Jr. 1 Feb. 1971 6 p refs Journal of Geophysical Research, vol. 76, p. 920-925.

Review of the measurements performed of the properties of ionospheric plasma during the subauroral red arc of September 28-29, 1967, and discussion of the merits of some hypotheses about the red arc phenomenon. In the light of the observational data presented on the flux of suprathermal electrons and electron temperature, it is shown that the thermal conduction hypothesis, proposed by Cole (1965) as the mechanism for heating the ambient plasma during the subauroral red arc condition, has to be accepted. In the absence of any significant increase in the flux of suprathermal electrons, the soft electron hypothesis must be ruled out from consideration. It is concluded that the subauroral red arc is caused by a combination of thermal conduction of energy from the magnetosphere and changes in the neutral compositions in the lower atmosphere. M.V.E.

A71-19724*

THE ASSOCIATION OF SOLAR OPTICAL FLARES WITH TYPE 3 SOLAR BURSTS FROM 4 TO 2 MHz OBSERVED BY OGO-3.

T. E. Graedel (Radio Astronomy Observatory, Ann Arbor, Mich.) Apr. 1970 7 p refs Astrophysical Journal, vol. 160, Pt-1, p. 301-307. (Contract NAS5-2051; Grant NSG-572)

Study in which type 3 solar radio bursts from 4 to 2 MHz observed by OGO-3 were associated with optical flares, hence, with solar plage regions. A radio burst was

considered to be flare associated if it occurred within 10 min of the reported flare maximum. With this criterion, 70% of the radio bursts were found to be associated with flares or subflares. On the average, the burst preceded the reported flare maximum by 1.45 min. The plage regions associated with the greatest number of radio bursts were, in general, those which were largest, brightest, and of greatest sunspot area and field strength. Since radio bursts are thought to originate in coronal streamers, it is inferred that these plage regions are associated with coronal streamers with a radius of 5 solar radii or greater. The data suggest that a major change in filament or sunspot structure in a large plage region can temporarily create or enhance the conditions necessary for the propagation of electron streams to large radial distances and that well-established streamers maintain their integrity and magnetic-field structure for as long as two solar rotations. (Author)

A71-19825*

IMPULSIVE HARD X-RAY AND ULTRAVIOLET EMISSION DURING SOLAR FLARES.

R. F. Donnelly (ESSA, Space Disturbances Lab., Boulder, Colo.) and S. R. Kane (California, U., Berkeley, Calif.) 15 Feb. 1971 15 p refs Astrophysical Journal, vol. 164, Pt-1, p. 151-163. (Contract NAS5-9094)

Study of the relation between the impulsive hard X-rays, observed by the satellites OGO 1, 3, and 5, and the concurrent enhancement of the extreme-ultraviolet (10 to 1030 A) radiation, observed by means of sudden frequency deviations, and investigation of the physical restraints imposed by this relation on the characteristics of energetic electrons produced during the flash phase of solar flares. It is found that the impulsive components of hard X-rays, extreme ultraviolet emission, and microwave radio emission associated with solar flares are well correlated in time. There is an overall decrease in the ratio of extreme-ultraviolet flux to hard X-ray flux with increase in central meridian distance (CMD) of the associated H-alpha flare. This effect is believed to be due to the increase in extreme-ultraviolet absorption by the solar atmosphere with any increase in CMD of the flare. The total kinetic energy of the energetic electrons in the flare region as deduced from the observed X-ray spectrum is comparable to that which must be deposited in the denser chromospheric regions to explain the observed enhancement of the 10 to 1030 A flux. M.V.E.

A71-20318

THE TREND OF IONOSPHERIC ABSORPTION DURING SHORTWAVE FADE-OUTS RELATED TO THE TREND OF ENHANCEMENT OF SOLAR X-RAY FLUX

G. Hartmann (Max-Planck-Institut fuer Aeronomie, Lindau ueber Northeim, West Germany), R. W. Kreplin (U.S. Navy, Naval Research Lab., Washington, D.C.), and H. Schwentek Jan. 1971 6 p refs Radio Science, vol. 6, p. 35-40.

Observation of short-wave fadeouts during the period from July 1967 to July 1968 through simultaneous use of several short-wave paths particularly established for absorption measurements. The frequencies used were 2.50, 2.614, 2.775, and 6.09 MHz. The data were obtained from satellites OGO 4 and Solrad 9 in the wavelength ranges 0.5 to 3, 1 to 8, 8 to 20, and 44 to 60 A. A very good correlation is found between the enhancements of solar X-ray flux and the enhancements of ionospheric absorption. The beginning and maximum of the short-wave fadeouts are delayed by 0.5 to 4 minutes in relation to the beginning and maximum of the bursts, with the longer delay corresponding to the shorter wavelength. The end of the effects cannot be determined so definitely; the time differences between bursts and short-wave fadeouts vary between plus or minus 7 minutes. Usually, the trend and detail of the short-wave fadeouts very nearly follow the trend of the bursts; thus bursts may be considered equivalent to short-wave fadeouts. A.B.K.

A71-20945

A71-20945

A MODEL FOR THE SOURCE OF SOLAR-FLARE X-RAYS.

M. D. Papagiannis (Boston, U., Boston, Mass.) and F. M. Strauss 1 Mar. 1971 10 p refs *Astrophysical Journal*, vol. 164, Pt-1, p. 369-378.
(Contract AF 19(628)-68-C-0097)

A solar flare model by Sturrock is used to compute quantitatively the thermal X-ray emission during a small flare. The results are in good agreement with actual X-ray data obtained with the OGO-5 satellite. The microwave and optical emissions are also discussed. (Author)

A71-21037*

SIMULTANEOUS OBSERVATIONS OF SOLAR-FLARE ELECTRON SPECTRA IN INTERPLANETARY SPACE AND WITHIN EARTH'S MAGNETOSPHERE.

A. L. Vampola (Aerospace Corp., Los Angeles, Calif.) and H. I. West, Jr. (California, U., Livermore, Calif.) 22 Feb. 1971 6 p refs *Physical Review Letters*, vol. 26, p. 458-463. AEC-NASA sponsored research.
(Contract AF 04(701)-69-C-0066)

Magnetic electron spectrometers on satellites OGO 5 and OVI-19 were used to make simultaneous measurements in interplanetary space and over the polar caps during the intense solar particle event of April 1969. The absolute intensities and energy spectra measured on the two satellites tracked within experimental error for the entire history of the event. The results are examined in terms of the open and closed methods of earth's magnetosphere. (Author)

A71-21631*

MOTION AND STRUCTURE OF THE MAGNETOPAUSE.

M. P. Aubry, M. G. Kivelson, and C. T. Russell (California, U., Los Angeles, Calif.) 1 Mar. 1971 24 p refs *Journal of Geophysical Research*, vol. 76, p. 1673-1696. Research supported by the European Space Research Organization.
(Contract NAS5-9098)

Data obtained during a 2-hr sequence of multiple crossings of the magnetopause in the equatorial plane with the OGO 5 UCLA triaxial fluxgate magnetometer and electron spectrometer show that the magnetopause motion was composed to two different oscillation: large amplitude oscillations with periods from 3.5 to 6 min. and smaller amplitude oscillations with periods as short as 10 sec. The amplitude of the short-period oscillation increased abruptly when the magnetosheath field turned 90 deg southward, producing an extremely variable boundary. The particle boundary showed the same oscillations as the magnetic field boundary, but the two were not coincident and their relative position was quite variable. The direction of the normal to the magnetopause during successive crossings shows that these oscillations do not represent pulsation of the whole boundary but are ripples moving tailward with a velocity of the same order as the plasma flow velocity. M.M.

A71-21643*

MAGNETIC FIELD VARIATIONS IN THE NEAR GEOMAGNETIC TAIL ASSOCIATED WITH WEAK SUBSTORM ACTIVITY.

P. J. Coleman, Jr. (California, U., Los Angeles, Calif.), R. L. McPherron, and C. T. Russell 1 Mar. 1971 7 p refs *Journal of Geophysical Research*, vol. 76, p. 1823-1829.
(Contract NAS5-9098)

Use of magnetic field observations obtained with the UCLA OGO 5 fluxgate magnetometer on an inbound pass, during which the satellite remained close to the magnetic meridian and traveled almost parallel to and approximately two earth radii above the expected position of the neutral sheet, to illustrate the variations in the configuration of the tail field during weak substorm activity. Beyond ten earth radii from the earth, changes to dipolar fields are accompanied by a reduction in field strength presumably due to accompanied by a reduction in field strength presumably due to plasma sheet expansion. Within approximately ten earth

radii, changes to a more dipolar field are accompanied by no change by an increase in field strength. In both regions, these changes are accompanied by turbulence or noise. Occasional twisting of the field out of the usual magnetic meridian is also observed. (Author)

A71-21647*

HORIZONTAL DISTRIBUTION OF HELIUM IN THE EARTH'S UPPER ATMOSPHERE.

D. N. Harpold, A. E. Hedin (NASA, Goddard Space Flight Center, Greenbelt, Md.), R. Horowitz, and C. A. Reber 1 Mar. 1971 4 p refs *Journal of Geophysical Research*, vol. 76, p. 1845-1848.

Study of the helium distribution in June 1969 by using data from the mass spectrometer on OGO 6 (perigee, 400 km; apogee, 1100 km). After normalizing for altitude effects by use of the Jacchia model atmosphere, the densities show an order of magnitude difference between the Southern (winter) Hemisphere and the Northern (summer) Hemisphere, with the maximum density occurring near .55 deg latitude. The exact location of the maximum varies between .40 deg and .70 deg geographic latitude and is apparently correlated with the geomagnetic dipole latitude of .53 deg. This correlation is consistent with the idea that the helium distribution is quite sensitive to thermospheric winds. (Author)

A71-22801*

INTERPLANETARY DECELERATION OF SOLAR COSMIC RAYS.

S. S. Murray, E. C. Stone, and R. E. Vogt (California Inst. of Tech., Pasadena, Calif.) 15 Mar. 1971 4 p refs *Physical Review Letters*, vol. 26, p. 663-666.
(Contract NAS5-9312; Grants NGR-05-002-160; NGL-05-002-007)

Use of observations of solar-flare proton fluxes of low energies (1 to 10 MeV) during the June, 1969, event to study the effects of energy-change processes on particles propagating in interplanetary space. It is found that the proton energies are decreasing with time at a rate which is consistent with an exponential-decay time constant of 210 plus or minus 10 hr. Since adiabatic deceleration in a uniform solar wind would result in a faster decay (78 plus or minus 4 hr), additional processes such as Fermi acceleration or a more general deceleration process must be considered. (Author)

A71-23635*

A PRELIMINARY SURVEY OF THE DISTRIBUTION OF MICROPULSATIONS IN THE MAGNETOSPHERE FROM OGO'S 3 AND 5.

J. P. Heppner, B. G. Ledley, T. L. Skillman, and M. Sugiura Sep. 1970 9 p refs *Annales de Geophysique*, vol. 26, p. 709-717 International Assn. of Geomagnetism and Aeronomy, General Scientific Assembly, Madrid, Spain, Sep. 1-12, 1969.

Systematic analysis of magnetic field data received by the OGO 3 and 5 satellites in order to determine the magnetospheric distribution of micropulsations in 7 bands, and incoherent irregularities in two categories (time constants T less than 5 sec, and 5 sec less than T less than 45 sec). Although incomplete, the principal features of the distributions are sufficiently evident near the equatorial plane to make preliminary results significant. Waves and recurrent pulses with Pc-3 periodicities frequently constitute the dominant large amplitude fluctuations in the magnetosheath sunward from the dayside magnetopause. It is believed that these waves and recurrent pulses are closely related to the Pc-3 oscillations within the dayside magnetosphere. Support is given to the suggestion that a Pc-3 activity index based on surface observations should be derived and be made available as an international service. F.R.L.

A71-23711*

THE PIONEER 9 ELECTRIC FIELD EXPERIMENT.

G. M. Crook (TRW Systems Group, Redondo Beach, Calif.), I. M. Green, and F. L. Scarf Feb. 1971 17 p refs *Cosmic Electrodynamics*, vol. 1, p. 496-512.

(Contract NAS2-4673)

The Pioneer 9 electric field experiment is described and the near-earth observations (r less than or equal to 100 R sub e) are discussed. It is shown that in the region of the magnetopause the OGO-5 plasma wave experiment and the Pioneer 9 electric field experiment detected very similar changes in the noise spectrum and these variations may be related to the presence of a diffusive plasma layer. Large and intermittent signal enhancements were also found in the outer magnetosheath and these are shown to be associated with traversals of current sheets resembling X-type nulls.

(Author)

A71-24438

EVIDENCE FOR A SOURCE OF AN EXTRATERRESTRIAL HYDROGEN LYMAN-ALPHA EMISSION: THE INTERSTELLAR WIND.

J. L. Bertaux and J. E. Blamont (CNRS, Service d'Aeronomie, Verrieres-le-Busson, Essonne, France) Mar. 1971 18 p refs Astronomy and Astrophysics, vol. 11, no. 2, p. 200-217. (Contracts CNES-65-003; CNES-66-011; CNES-67-201; CNES-68-202; CNES-69-225; CNES-70-299)

A series of maneuvers commanded to the OGO satellite made it possible to map the intensity of the 1216 A Lyman-alpha emission coming from outside the geocorona, as measured by a photometer with a 80 A bandwidth and a 0.66 deg circular field of view. The spatial distribution of this emission, presented in celestial and galactic coordinates, has no small-scale features, but shows a maximum of 530 Rayleighs near the ecliptic plane and a minimum of 200 Rayleighs in the opposite direction. These results give support to the theory that in its motion toward the apex, the sun crosses neutral atomic hydrogen of interstellar origin, giving rise to an apparent interstellar wind.

Z.W.

A71-24439*

OGO-5 MEASUREMENTS OF THE LYMAN ALPHA SKY BACKGROUND.

R. F. Krassa (Colorado, U., Boulder, Colo.) and G. E. Thomas Mar. 1971 16 p refs Astronomy and Astrophysics, vol. 11, no. 2, p. 218-233. (Contract NAS5-9327; Grant NGR-06-003-052)

A two-channel UV photometer on OGO 5, responding to the spectral regions ranging from 1050 to 1800 A and from 1225 to 1800 A, measured the spatial variations of the 1216 A background during three spin-up maneuvers in September 1969, December 1969, and April 1970. It is shown that a weighted difference of the signals from the two channels represents the Lyman-alpha 1216 A background, free from the contribution of unresolved stars. A prominent maximum in intensity (570 Rayleighs) and a less pronounced minimum (240 Rayleighs) were discovered, both located near the ecliptic and separated by about 180 deg. The origin of the observed emission is suggested to be scattering of solar Lyman alpha from interstellar hydrogen that is swept into the vicinity of the earth from the direction of the apparent apex of motion of the solar system.

Z.W.

A71-24555*

EVIDENCE OF SOLAR GEOMAGNETIC SEASONAL CONTROL OF THE TOPSIDE IONOSPHERE.

H. A. Taylor, Jr. (NASA, Goddard Space Flight Center, Lab. for Planetary Atmospheres, Greenbelt, Md.) Jan. 1971 17 p refs Planetary and Space Science, vol. 19, p. 77-93.

Study of the pronounced longitudinal variation in the composition of the topside ionosphere as revealed by ion composition results obtained from the polar orbiting OGO-4 satellite. This variation is in the form of a large-scale wobble or shift in the latitudinal distributions of the major topside ions, observed as the earth rotates beneath the fixed satellite orbit. Both the location and prominence of distinct ionospheric features are found to change significantly between longitudes for which the angle between the earth-sun line and the dipole equator has its greatest variation. Similarly, it is found that the ambient ion concentrations at a given latitude may change by as much as an order of magnitude

between contrasting longitudes. The overall result is that seasonal variations, such as the decrease in production of ionization at winter latitudes, are minimized at the location of extreme solar-geomagnetic season. The persistence of the longitudinal asymmetry over a range of local times, seasons, and magnetic conditions reveals that the topside ionosphere is dependent upon a solar-geomagnetic rather than simply a solar seasonal control.

O.H.

A71-24781*

RELATIONSHIP OF THE PLASMA SHEET, RING CURRENT, TRAPPING BOUNDARY, AND PLASMA-PAUSE NEAR THE MAGNETIC EQUATOR AND LOCAL MIDNIGHT.

L. A. Frank (Iowa, U., Iowa City, Iowa) 1 Apr. 1971 11 p refs Journal of Geophysical Research, vol. 76, p. 2265-2275.

(Contracts NAS5-2054; N00014-68-A-0196-0003; Grant NGL-16-001-002)

Near-magnetic equator observations of the plasma-sheet structure in the pre- and postmidnight sectors of the magnetosphere on the sensitive electrostatic analyzer array of the OGO 3 satellite in June and July, 1966. The trapping boundary of energetic electrons with energies from 40 keV was located within the extraterrestrial proton ring current and near its outer edge. The earthward edge of the plasma sheet was located in the postmidnight sector, its inner boundary being coincident with the position of the plasma-pause. Measurements during a polar magnetic substorm and during a main-phase magnetic storm showed the absence in the premidnight sector of a frequently observed electron trough and the structural features similar to those observed in the postmidnight sector.

V.Z.

A71-24787*

OGO-5 MEASUREMENTS OF THE PLASMASPHERE DURING OBSERVATIONS OF STABLE AURORAL RED ARCS

C. R. Chappell, K. K. Harris, and G. W. Sharp (Lockheed Research Labs., Palo Alto, Calif.) 1 Apr. 1971 9 p refs Journal of Geophysical Research, vol. 76, p. 2357-2365. (Contract NAS5-9092)

Ambient H(+) ion concentration was measured in the plasmasphere during two intense magnetic storms that were accompanied by occurrences of stable auroral red (SAR) arcs. The H(+) ion density profiles were measured by the ion mass spectrometer on OGO 5 during the periods Oct. 29 to Nov. 7, and Oct. 10 to 17, 1968. Correlations of the H(+) ion densities in the plasmasphere were made with the D sub st and Kp magnetic indices and with ground observations of the 6300-A SAR arcs. This study shows that the SAR arcs are observed in the rapid recovery phase of the storm in the 10-20 hours following injection of ring current particles, and that the plasmasphere is drastically reduced in size during the storm, with the SAR arc located in L value near the position of the plasmapause. The arc is found to occur in the ionosphere at the base of flux tubes that have ambient H(+) ion densities of 100-1000 ions/cu cm near the magnetic equatorial plane.

(Author)

A71-24788*

FAST TIME RESOLVED SPECTRAL ANALYSIS OF VLF BANDED EMISSIONS.

F. V. Coroniti, R. W. Fredricks, C. F. Kennel (TRW Systems Group, Space Sciences Lab., Redondo Beach, California, U., Los Angeles, Calif.), and F. L. Scarf (TRW Systems Group, Space Sciences Lab., Redondo Beach, Calif.) 1 Apr. 1971 16 p refs Journal of Geophysical Research, vol. 76, p. 2366-2381.

(Contract NAS5-9278)

High time resolution spectral techniques are used for taking statistically independent spectra every 12.5 microsec in a study of the several classes of VLF banded emissions acquired by the short antenna OGO 5 electric field detector. Single and/or multiple FM bursts and discrete single modes with stable center frequencies are established in the VLF

banded rising chorus spectra. Such bursts and modes of higher structural complexity are also indicated in inverted or falling banded chorus spectra. The spectrum of a banded hisslike emission was found to be dominated by multiple single discrete modes having constant center frequencies. A narrow band emission with frequencies slightly above half the local electron cyclotron frequency consisted of single modes and groups of unresolved modes free of frequency modulation.

V.Z.

A71-26144*

INSTRUMENTATION FOR MEASUREMENT OF COSMIC NOISE AT 2.0 AND 2.5 MHz FROM A POLAR ORBITING GEOPHYSICAL OBSERVATORY.

R. G. Yorks (Radio Astronomy Observatory, Ann Arbor, Mich.) May 1971 9 p refs IEEE Transactions on Instrumentation and Measurement, vol. IM-20, p. 86-94. (Contract NAS5-3099)

This paper describes the radio astronomy instrument flown on both Polar Orbiting Geophysical Observatories 2 and 4 (OGO-2 and OGO-4). The instrument was designed to map the brightness distribution of cosmic noise over the sky at 2.0 and 2.5 MHz by using the theoretically predicted ionospheric focusing of an electrically short antenna. An antenna impedance bridge was included as a necessary part of the system. The system is unusual because the impedance bridge and the 2.5-MHz radiometer operate simultaneously at the same frequency. OGO-2 was launched on October 14, 1965, and the instrument operated normally until the spacecraft was turned off November 1, 1967. During this period the instrument was operated for 4495 hours with many on-off cycles. OGO-4 was launched July 28, 1967, and the instrument operated properly for 18,330 hours prior to termination of spacecraft operations on October 23, 1969. Results of these experiments are published separately.

(Author)

A71-27654*

CHARACTERISTICS OF SOFT SOLAR X-RAY BURSTS.

J. F. Drake (Iowa, U., Iowa City, Iowa) Jan. 1971 34 p refs Solar Physics, vol. 16, p. 152-185. (Contracts NAS5-9076; N00014-68-A-0196-0003; Grant NGL-16-001-002)

The burst component of the solar X-ray flux in the soft wavelength range 2-12 Å observed from Explorer 33 and Explorer 35 from July 1966 to September 1968 was analyzed. In this period 4028 burst peaks were identified. The differential distributions of the temporal and intensity parameters of the bursts revealed no separation into more than one class bursts. The most frequently observed value for rise time was 4 min and for decay time was 12 min. The distribution of the ratio of rise to decay time can be represented by an exponential with exponent -2.31 from a ratio of 0.3 to 2.7; the maximum in this distribution occurred at a ratio of 0.3. The values of the total observed flux, divided by the background flux at burst maximum, can be represented by a power law with exponent -2.62 for ratios between 1.5 and 32. The distribution of peak burst fluxes can be represented by a power law with exponent -1.75 over the range 1-100 milli-erg/sq cm sec. The flux time integral values are given by a power law with exponent -1.44 over the range 1-50 erg sq cm.

M.M.

A71-27911*

PRIMARY ELECTRON INFLUX TO DAYSIDE AURORAL OVAL.

F. W. Berko (NASA, Goddard Space Flight Center, Greenbelt, Md.) and R. A. Hoffman 1 May 1971 10 p refs Journal of Geophysical Research, vol. 76, p. 2967-2976.

Data from the OGO 4 auroral particles experiment were analyzed to determine properties of the higher latitude region of electron precipitation in the dayside hemisphere. From 7 months of data a probability map of occurrence of this structured low-energy precipitation was compiled. The highest

probabilities are concentrated predominantly between 0500 and 1400 hours magnetic local time, and from 75 to 82-1/2 deg invariant latitude. There is excellent congruity of these high probabilities of occurrence and the high probability of occurrence of discrete auroral optical emissions, which define the auroral oval in these hours. The soft energy spectrums measured and the estimated total energy influx during typical precipitation events are appropriate for producing the type of aurora observed in these hours. It is concluded that the structured low-energy electron precipitation is the primary energy source for the dayside auroral oval. (Author)

A71-27913*

SATELLITE OBSERVATIONS OF BAND-LIMITED MICROPULSATIONS DURING A MAGNETOSPHERIC SUBSTORM.

P. J. Coleman, Jr. (California, U., Los Angeles, Calif.) and R. L. McPherron 1 May 1971 12 p refs Journal of Geophysical Research, vol. 76, p. 3010-3021. (Contract NAS5-9098)

Band-limited micropulsations have been observed in space by the UCLA fluxgate magnetometer on OGO 5. Throughout the event the satellite was inbound on the dawn meridian between 7 and 5 earth radii just below the magnetic equatorial plane. These pulsations were quasi-sinusoidal, with a period of 20 sec and rms amplitude of 0.3 gamma. Their average polarization was transverse to the main magnetic field, with the major axis azimuthal in the equatorial plane. The average ellipticity was 0.3 and the predominant sense of rotation was right-handed with respect to the main magnetic field. Instantaneously these parameters were quite variable, with the pulsations occurring in bursts propagating at various angles to the field. During the pulsation event the main field was essentially dipolar; however, the waves were first observed just inside a sharp transition from a region in which the field magnitude had been constant for several earth radii.

M.M.

A71-28700

DETECTION OF MICROMETEOROID FLUX ON SATELLITES.

C. S. Nilsson and F. W. Wright (Smithsonian Astrophysical Observatory, Cambridge, Mass.) 10 May 1971 2 p Journal of Geophysical Research, vol. 76, p. 3424, 3425.

Analysis of data from the Orbiting Geophysical Observatory (OGO) emphasizing certain noise-control procedures as developed by Nilsson et al. (1969). In about 4300 hr of available data (including those previously obtained), with no obvious noise generally present, 282 events were observed. The importance of these data is in demonstrating the need for more than one noise control procedure.

F.R.L.

A71-29057*

RELATIVISTIC ELECTRONS ASSOCIATED WITH SOLAR PARTICLE EVENTS, MEASURING OCCURRENCE FREQUENCY, ELECTRON PROPAGATION AND DIFFUSION ANISOTROPY.

D. Dattlowe (California, U., San Diego, Calif.) Apr. 1971 23 p refs Solar Physics, vol. 17, p. 436-458. (Contract NAS5-9096; Grant NGL-14-001-005)

The results are presented of the first systematic study of electrons of energies greater than 10 MeV associated with solar flares. Direct measurements were made of the frequency of occurrence of these particles in solar flare related events. The spectra of the particles were made of the frequency of occurrence of these particles in solar flare related events. The spectra of the particles were studied, as well as the evolution of the spectra in the course of these events. In addition the propagation of the electrons is investigated, and the degree of anisotropy in their diffusion is measured for the first time. It is found that electrons in the energy range 12-45 MeV are normally present in major solar particle events. The time-intensity profiles of the fluxes indicate diffusive propagation; and the time-to-maximum intensity is found to vary with solar longitude in a way which can only

be the result of anisotropic propagation with the perpendicular diffusion coefficient comparable in magnitude to, but smaller than, the parallel diffusion coefficient. M.V.E.

A71-29903*
GEOMAGNETIC MODELS FROM SATELLITE SURVEYS.

J. C. Cain (NASA, Goddard Space Flight Center, Greenbelt, Md.) May 1971 15 p refs Reviews of Geophysics and Space Physics, vol. 9, p. 259-273.

The use of satellite scalar magnetic field data to produce geomagnetic field models is reviewed. There have been nine separate spacecraft that have acquired observations of the geomagnetic field from low (less than 1500 km) satellite altitudes since 1958. The magnetic field models produced from such data have not been sufficiently compared with surface vector data to firmly establish their validity. One comparison has indicated that satellite-derived models are as valid over-all as those produced from surface data. Variations in the field components are shown to be larger than those in scalar field by factors of 4-10. Recent satellite models indicate an increase in dipole decay to -27 gammas/year, a value that may be plausible, judging from extrapolation of earlier surface-derived models. Also noted is a recent slowing of eccentric dipole westward drift. (Author)

A71-30028*
THE MAGNETIC FIELD OF THE MAGNETOSPHERE AND TAIL.

D. H. Fairfield (NASA, Goddard Space Flight Center, Greenbelt, Md.) New York, Gordon and Breach, Science Publishers, Inc. 1970 24 p refs In: The Polar Ionosphere and Magnetospheric Processes, NATO, Advanced Study Inst., Kjeller, Norway, Apr. 9-18, 1969, Proceedings, p. 1-24.

Analysis of spacecraft measurements of the solar wind-compressed magnetic field in the sunward magnetosphere and the extended magnetic field of the geomagnetic tail indicates that, in an average magnetosphere, field lines crossing the earth above 78 plus or minus 3 deg and 69 plus or minus 2 deg geomagnetic latitude in the noon and midnight meridians, respectively, are extended into the geomagnetic tail. Field lines in the northern and southern hemispheres of the tail are generally oriented parallel or antiparallel to the earth-sun line with the two regions being separated by a neutral sheet or current sheet less than 1 earth radius thick. The observation of tail-like fields almost 1000 earth radii behind the earth by Pioneer 7 sets a lower limit on the radial extent of tail-associated effects. Departures from the average magnetosphere field configuration occur at the time of magnetic storms and bay events. Storms are associated with higher tail fields and the extension of additional field lines to the tail. M.M.

A71-30029*
LOW ENERGY PARTICLE FLUXES IN THE GEOMAGNETIC TAIL.

V. M. Vasyliunas (MIT, Cambridge, Mass.) New York, Gordon and Breach, Science Publishers, Inc. 1970 23 p refs In: The Polar Ionosphere and Magnetospheric Processes, NATO, Advanced Study Inst., Kjeller, Norway, Apr. 9-18, 1969, Proceedings, p. 25-47. (Grant NGL-22-009-015)

Intense fluxes of low energy particles exist within the geomagnetic tail. They are confined to the equatorial region of the tail and form a plasma sheet several earth radii thick and centered about the magnetic neutral sheet. The mean energy of electrons within the plasma sheet typically ranges from a few hundred eV to a few keV; the mean energy of protons is appreciably higher. The electron and proton number densities are equal. Low energy proton fluxes extend from the magnetotail earthward to well within the outer radiation belt, where during magnetic storms they become very intense and form the ring current responsible for the storm's main phase. The inner boundary of the plasma sheet has now been traced in latitude to -55 deg and shown

to coincide with magnetic field lines through the equatorward boundary of the aurora oval. M.M.

A71-30032*
OGO 4 SATELLITE MEASUREMENTS OF LOW ENERGY-HIGH LATITUDE ELECTRON PRECIPITATION.

R. A. Hoffman (NASA, Goddard Space Flight Center, Greenbelt, Md.) New York, Gordon and Breach, Science Publishers, Inc. 1970 13 p refs In: The Polar Ionosphere and Magnetospheric Processes, NATO, Advanced Study Inst., Kjeller, Norway, Apr. 9-18, 1969, Proceedings, p. 79-91.

Data from the Auroral Particles Experiment aboard OGO-4 have indicated four regions of low-energy electron precipitation at high latitudes. These have been designated by the terms band region, burst region, polar cavity, and premidnight region. The band region is characterized by a relatively structureless, moderately hard precipitation pattern which generally follows the auroral oval, except that it extends to lower latitudes at noon. It is especially prevalent in the dawn hemisphere. The burst region begins within the band region and extends polewards, reaching up to 85 deg at noon, and is usually characterized by a very soft spectrum and large structure in the precipitation pattern. The polar cavity is an area of no detectable fluxes, while the premidnight region displays structured electron fluxes with widely varying spectra. M.M.

A71-30037*
TEMPERATURE AND COMPOSITION STUDIES IN THE POLAR IONOSPHERE.

S. J. Bauer (NASA, Goddard Space Flight Center, Greenbelt, Md.) New York, Gordon and Breach, Science Publishers, Inc. 1970 13 p refs In: The Polar Ionosphere and Magnetospheric Processes, NATO, Advanced Study Inst., Kjeller, Norway, Apr. 9-18, 1969 Proceedings, p. 161-173.

A geomagnetic latitude of approximately 60 deg appears to represent the demarcation between the mid-latitude and polar ionosphere. At this latitude the abundance of light ions, H(+) and He(+), decrease abruptly, leading to a polar ionosphere consisting primarily of O(+). The light ions seem to be escaping via the tail of the magnetosphere; an outward bulk motion of H(+) over the polar cap has been observed by the ion-mass spectrometer on Explorer 31. The plasma density over the polar region decreases much faster with altitude than according to a diffusive equilibrium distribution. The charged particle temperatures, of which the electron temperature has been primarily measured, show a gradient with altitude and latitude. A maximum of electron temperature is often observed near 60 deg geomagnetic latitude, with lower temperature over the poles. At an altitude of a few thousand km, the electron temperature in the polar ionosphere is approximately 3000-4000 K, reaching values as high as 6000-8000 K at an altitude of 6000 km. M.M.

A71-30951*#
SATELLITE MEASUREMENTS OF THE COLD PLASMA IN THE MAGNETOSPHERE.

S. J. Bauer (NASA, Goddard Space Flight Center, Greenbelt, Md.) Brussels, International Union of Radio Science, 1970 7 p refs In: Progress in Radio Science 1966-1969, International Union of Radio Science, General Assembly, 16th, Ottawa, Canada, Aug. 18-29, 1969, Proceedings, Volume 1 - Ionosphere, Magnetosphere, Radio Noise, p. 159-165.

Satellite data for electron and ion distributions in the magnetosphere are reviewed, and the validity of different methods for direct measurement of plasma density is evaluated. Factors affecting the accuracy of Langmuir probe measurements are described to illustrate the precautions which must be taken when interpreting in situ measurements. Whistler data and in situ measurements are compared to demonstrate discrepancies concerning plasma density distributions and the existence of a plasmopause. T.M.

A71-30952#
VLF EMISSION AND ELECTRON INSTABILITIES

J. M. Cornwall (Los Angeles, U. Coll., Los Angeles, Aerospace Corp., El Segundo, Calif.) Brussels, International Union of Radio Science 1970 12 p refs In: Progress in Radio Science 1966-1969, International Union of Radio Science, General Assembly, 16th, Ottawa, Canada, Aug. 18-29, 1969, Proceedings, Volume 1 - Ionosphere, Magnetosphere, Radio Noise, p. 171-182.

Satellite data on VLF electromagnetic emissions delineate the location of their source regions as mostly equatorial above the plasmopause. OGO 5 measurements show that large-amplitude electrostatic waves are generated in the same source regions. Questions of wave-particle correlation and electron precipitation are discussed, and recent theoretical explanations for electrostatic instabilities, triggered emissions, and plasma echoes are reviewed. T.M.

A71-30956*#

INTERPLANETARY WAVES AND THEIR EFFECTS ON THE MAGNETOSPHERE.

F. L. Scarf (TRW Systems Group, Redondo Beach, Calif.) Brussels, International Union of Radio Science, 1970 13 p refs In: Progress in Radio Science 1966-1969, International Union of Radio Science, General Assembly, 16th, Ottawa, Canada, Aug. 18-29, 1969, Proceedings, Volume 1 - Ionosphere, Magnetosphere, Radio Noise, p. 233-245. (Contracts NAS2-4673; NAS5-9278; Grant NASw-1598)

Recent measurements show that all of the microscopic properties and many of the bulk or fluid characteristics of the collisionless solar wind near the earth are determined by wave-particle interactions. Pitch-angle anisotropies continuously develop as the plasma carries the extended solar magnetic field outward from the corona, and associated nonresonant instabilities produce growth of Alfvén and magnetosonic waves. It has been found that the dominant particle dissipation mechanisms for low Mach number interplanetary shocks, high Mach number bow shocks, and magnetic null regions at filament boundaries generally involve the excitation of intense high-frequency electrostatic noise. However, some shocks governed by electromagnetic whistler mode dissipation have also been detected. Strong local waves are less frequently excited in the solar wind, but weak electron plasma oscillations are found at shock boundaries and in other regions where the plasma distribution functions are perturbed. Very large amplitude electromagnetic waves have also been detected in interplanetary space. T.M.

A71-31754*

MAGNETIC FIELD AND ELECTRON OBSERVATIONS NEAR THE DAWN MAGNETOPAUSE.

K. W. Ogilvie, J. D. Scudder, and M. Sugiura (NASA, Goddard Space Flight Center, Lab. for Extraterrestrial Physics, Greenbelt, Md.) 1 Jun. 1971 13 p refs Journal of Geophysical Research, vol. 76, p. 3574-3586.

Observations of electron fluxes between 25 eV and several kiloelectronvolts by the triaxial electron spectrometer and of the magnetic field by the fluxgate magnetometer on the satellite OGO 5 are used to study the structure and movement of the magnetopause. The observations were made at both quiet and fairly disturbed times between 6.4 and 7.6 hr local time and at geomagnetic latitudes between 16 and 40 deg. The boundary layer electron fluxes for velocities smaller than 8000 km/sec are typical of the magnetosheath. The non-Maxwellian tails of the spectra for velocities greater than 8000 km/sec resemble those observed in the magnetosphere. The magnetic field in the boundary layer has either magnetospheric or transitional characteristics. These observations suggest the possibility of mixing of the magnetosheath plasma with the magnetospheric plasma, which would be important in determining the structure of the boundary layer. Z.W.

A71-31757*

OGO-2 AND 4 VLF OBSERVATIONS OF THE ASYMMETRIC PLASMAPAUSE NEAR THE TIME OF SAR ARC EVENTS.

J. L. Carpenter (Stanford U., Stanford, Calif.) 1 Jun. 1971 p refs Journal of Geophysical Research, vol. 76,

p. 3644-3650.

(Grants NGR-05-020-288; NSF GA-12317; NSF GA-1485; NSF GA-10719; NSF GA-18128;)

Comparison of OGO 2 and OGO 4 VLF data on plasmopause crossings with SAR arc observations reported on Sept. 29, 1967, and on Oct. 31 and Nov. 1, 1968. The positions of the plasmopause and SAR arcs were found to agree within plus or minus 1 deg in invariant latitude. OGO 4 evidence from the 0900 to 2100 magnetic local time plane showed that the known local-time asymmetry in plasmopause L value (evening maximum, dawn minimum) could explain some of the apparent motions of the arcs as viewed from ground stations. Some other details of the arc motions are apparently due to substorm-related convection events in the outer plasmasphere. (Author)

A71-31774*

ION THERMALIZATION IN THE EARTH'S BOW SHOCK.

K. Papadopoulos (Maryland, U., College Park, Md., U.S. Navy, Naval Research Lab., Washington, D.C.) 1 Jun. 1971 5 p refs Journal of Geophysical Research, vol. 76, p. 3806-3810. (Grant NGL-21-002-005)

The role of the counterstreaming ion instability in thermalizing the solar wind ions in the earth's bow shock is discussed. The interplanetary magnetic field plays an important role in the development of this instability. Comparison with recent experimental data shows that it can be the dominant mechanism of ion thermalization. (Author)

A71-33741*#

RESULTS OF A 1970 GEMINID DUST PARTICLE ROCKET EXPERIMENT AND ANALYSIS OF OGO III DUST PARTICLE VELOCITY MEASUREMENTS.

W. M. Alexander (Baylor U., Waco, Tex.), C. W. Arthur (California, U., Los Angeles), J. L. Bohn (Temple U., Philadelphia), B. J. Farmer (Advanced Technology Center, Inc., Grand Prairie, Tex.), and J. H. Johnson Jun. 1971 25 p refs COSPAR, Plenary Meeting, 14th, Seattle, Wash., Jun. 18-Jul. 2, 1971, Paper. (Grant NGR-39-012-001)

Results of a dust particle experiment carried on a Black Brant VB upper atmosphere research rocket launched from Churchill, Canada, Dec. 14, 1970. Hypervelocity calibrations showed that the experiment would detect particles with masses greater than 0.5 picogram and provide coincident detection of particles greater than 5 picograms. Control sensors for detection of electromagnetic and mechanical noise were included in the instrumentation. Three coincident events have been identified indicating an event rate during the 1970 occurrence of the Geminid shower that was greater than the normal sporadic flux. The velocity and orbital elements of four dust particles have been determined by measurements from the OGO 3 dust particle experiment. A study of the results from OGO 3 and OGO 1 indicates that the OGO 1 velocity measurements were the result of spacecraft noise. From OGO 3 flux measurements, an expectation of 5 plus or minus 2 velocity measurements are predicted. Four events were detected between July 1966 and December 1967. The mean flux from the OGO 3 measurement is in excellent agreement with that measured from the Radiation Satellite. (Author)

A71-33762*#

OBSERVED SOLAR GEOMAGNETIC CONTROL OF THE IONOSPHERE: IMPLICATIONS FOR REFERENCE IONOSPHERES.

H. A. Taylor (NASA, Goddard Space Flight Center, Greenbelt, Md.) Jun. 1971 42 p refs COSPAR, Plenary Meeting, 14th, Seattle, Wash., Jun. 18-Jul. 2, 1971, Paper.

Data sets from the OGO-6 spectrometer during the period 1969-1970 are used to study the previously observed dominant longitudinal variations superimposed upon the latitudinal distributions of each ion specie in the ionosphere. The results reveal that seasonal variations in the ion distributions are

generally repeatable, and that the annual variation in the topside O(+) and H(+) content and distribution during the period examined was minimal. The importance of magnetic field control in regulating the ion distributions is emphasized, and the need is suggested for the use of improved coordinate systems for the correlation of satellite observations and the development of atmospheric models. O.H.

A71-33802*#
SEASONAL VARIATIONS IN THE THERMOSPHERE AND EXOSPHERE, 1968-1970.

G. M. Keating, J. S. Levine, J. A. Mullins (NASA, Langley Research Center, Hampton, Va.), and E. J. Prior Jun. 1971 23 p refs COSPAR, Plenary Meeting, 14th, Seattle, Wash., Jun. 18-Jul. 2, 1971, Paper.

Recent simultaneous drag measurements of Explorers 19 and 39 near opposite poles are used to obtain an improved description of the seasonal density variations near and below 1000 km. The winter helium bulge is measured in both the Northern and Southern Hemispheres. An improved model of these density variations is compared with recently published OGO-6 mass spectrometer measurements of the winter helium bulge. To obtain consistency between these measurements and drag measurements, it is necessary to make major revisions in both the generally assumed global distribution of exospheric temperature and the global distribution of atomic oxygen. Two temperature maxima are required: the major one at latitudes higher than the subsolar point in the summer hemisphere, and a secondary one near the winter pole. This distribution is consistent with satellite drag measurements, if maximum oxygen concentrations near 120 km occur at low latitudes in the winter hemisphere rather than concentrations at these altitudes being invariant as is generally assumed. O.H.

A71-33834#
OGO-5 DETERMINATION OF THE LOCAL INTERSTELLAR WIND PARAMETERS.

A. Ammar, J. L. Bertaux, and J. E. Blamont (CNRS, Service d'Aeronomie, Verrieres-le-Buisson, Essonne, France) Jun. 1971 26 p refs COSPAR, Plenary Meeting, 14th, Seattle, Wash., Jun. 18-Jul. 2, 1971, Paper.

The Lyman-alpha sky background measured outside the geocorona by two independent photometers on OGO-5 suggested that an interstellar wind of neutral hydrogen penetrates into the heliosphere, where solar wind and solar ultraviolet create an ionization cavity. The shape of this cavity is a function of the interstellar density, the relative velocity, the temperature, and also the solar Lyman-alpha radiation pressure which may overcompensate the gravitation. For two different values of the solar Lyman-alpha flux, one which equilibrates the gravitation, and one which corresponds to recent measurements and overcompensates the gravitation, the interstellar wind parameters are adjusted to agree with the sky background measurements. Even if a uniform galactic component is present with its maximum allowable value, temperatures are found to be in the range from 1000 to 10,000 deg K, densities in the range from 0.2 to 0.5 atoms per cu cm, and the relative wind velocity between 3 and 9 km/s. O.H.

A71-33943*
CORRELATED OBSERVATIONS OF ELECTRONS AND MAGNETIC FIELDS AT THE EARTH'S BOW SHOCK.

M. Neugebauer (California Inst. of Tech., Jet Propulsion Lab., Pasadena, Calif.), J. V. Olson (California, U., Los Angeles, Calif.), and C. T. Russell 1 Jul. 1971 15 p refs Journal of Geophysical Research, vol. 76, p. 4366-4380. (Contracts NAS5-9098; JPL-950403)

The internal structure of the earth's bow shock has been studied by using simultaneous observations made on board the OGO 5 satellite of the magnetic field (0-3 Hz), the ELF magnetic fluctuations (10-1000 Hz), and the suprathermal electrons (100-800 eV). The results indicate an extreme complexity in the interactions occurring at the earth's bow shock. There is an interplay of many physical processes

involving charged particles, electric and magnetic field structures, and electromagnetic and electrostatic waves.

M.V.E.

A71-33944*
MAGNETOTAIL CHANGES IN RELATION TO THE SOLAR WIND MAGNETIC FIELD AND MAGNETOSPHERIC SUBSTORMS.

M. P. Aubry and R. L. McPherron (California, U., Los Angeles, Calif.) 1 Jul. 1971 21 p refs Journal of Geophysical Research, vol. 76, p. 4381-4401. Research supported by the European Space Research Organization. (Contracts NAS5-9098; N00014-69-A-0200-4016; Grant NGR-05-007-004)

Analysis of data from several satellites and ground magnetic observatories shows that the magnetotail responds to both magnetospheric substorm activity and to changes in the north-south orientation of the interplanetary field. A change from a northward to a southward interplanetary field causes a slow increase of the field within the lobe of the tail and a thinning of the plasma sheet. A change from a southward to a northward interplanetary field causes the plasma sheet to expand. In contrast, it seems that in the inner magnetosphere the distortion of the magnetic field due to a period of southward interplanetary field is not relieved by an interval of a northward field, but only through the occurrence of a substorm expansion. A substorm expansion causes a slow decrease of the field within the lobe of the tail and an expansion of the plasma sheet. T.M.

A71-33946*
ASYMMETRIC RING CURRENT AT TWILIGHT LOCAL TIME.

R. A. Langel and R. E. Sweeney (NASA, Goddard Space Flight Center, Greenbelt, Md.) 1 Jul. 1971 8 p refs Journal of Geophysical Research, vol. 76, p. 4420-4427.

OGO 2 rubidium vapor magnetometer measurements are compared with surface magnetic observatory data collected during three magnetic storms of March 13-15, 22-25, and 28-29, 1966. The analysis of these data demonstrates that the main sources of mid-latitude-field depressions are not in the ionosphere for dip latitudes less than 45 deg and twilight local times. M.V.E.

A71-33948*
RELATIVISTIC ELECTRON PRECIPITATION DURING MAGNETIC STORM MAIN PHASE.

C. F. Kennel and R. M. Thorne (California, U., Los Angeles, Calif.) 1 Jul. 1971 8 p refs Journal of Geophysical Research, vol. 76, p. 4446-4453. (Contract AF 19(628)-71-C-0075; Grants NGR-05-007-190; NSF GA-28045)

Demonstration that relativistic electrons can have cyclotron resonances with electromagnetic ion-cyclotron waves. The resonant energy is generally well above 1 Mev throughout the magnetosphere, but it can fall to near 1 Mev just within the plasmapause. This also corresponds to the region where ring current (10 to 50 keV) protons are expected to be strongly unstable. The resulting ion-cyclotron wave amplitude necessary to precipitate ring current protons leads to electron lifetimes near the strong diffusion limit. Thus, greater than 1 Mev electrons whose drift orbits intersect the stormtime plasmapause should rapidly be precipitated in the region 3 less than L less than 5 during the initial phase of a magnetic storm. (Author)

A71-33951*
OBSERVATIONS OF AURORAL HISS, LHR NOISE, AND OTHER PHENOMENA IN THE FREQUENCY RANGE 20 Hz-540 kHz ON OGO-6.

W. C. Johnson, T. Laaspere, and L. C. Semprebon (Dartmouth Coll., Hanover, N. H.) 1 Jul. 1971 17 p refs Journal of Geophysical Research, vol. 76, p. 4477-4493. (Contract NAS5-9305)

The characteristics of ionospheric electric and electromagnetic waves were studied over a broad frequency range by

the OGO 6 spacecraft launched on June 5, 1969 into a polar orbit with a perigee of 400 km and an apogee of 1100 km. Lower hybrid resonance (LHR) noise bands observed below auroral latitudes in the range from a few to about 20 kHz are among the most intense phenomena revealed by the experiment. The broadband intensities of the signals often exceed the full-scale reading of about 3 mV/m of the broadband detector. New information is obtained on the intensity of auroral hiss over a wide range of frequencies, and the results suggest that the power flux of auroral hiss may decrease more rapidly with frequency than predicted. The occurrence pattern of auroral hiss in space very definitely suggests a correlation with soft electron fluxes. The possible correlation of electric fields near zero frequency with the fine structure of LHR bands is a new result that will be pursued further. The observation of intense vlf hiss near the equator is another new result. T.M.

A71-33956*
EQUATORIAL ION TEMPERATURE: A COMPARISON OF CONFLICTING INCOHERENT SCATTER AND OGO-4 RETARDING POTENTIAL ANALYZER VALUES.

J. P. McClure (Texas, U., Dallas, Tex.) and B. E. Troy, Jr. (NASA, Goddard Space Flight Center, Lab. for Planetary Atmospheres, Greenbelt, Md.) 1 Jul. 1971 7 p refs Journal of Geophysical Research, vol. 76, p. 4534-4540. (NASA Order R-06-012-008; Grant NGL-44-004-001)

During October and November 1967, the satellite OGO 4 crossed the geomagnetic equator near the Jicamarca Radar Observatory between altitudes of 400 and 650 km at night. For this period, comparisons are made between the radar values of ion temperature and those obtained by the retarding potential analyzer (RPA) on OGO 4. There is general disagreement between the two sets of data, with the RPA values exceeding the radar values by as much as 40%. Although there is nothing obviously wrong with either set of data, this discrepancy cannot be accommodated within the error bars placed on each data set. Typical examples of the conflicting measurements are presented, and the conflicting geophysical implications of these data with regard to the heating of the equatorial ionosphere at night are discussed. T.M.

A71-34777#
HYDROMAGNETIC INTERPRETATION OF HIGH LATITUDE SUDDEN IMPULSE.

T. Ondoh Jan. 1971 15 p refs Radio Research Laboratories, Journal, vol. 18, p. 19-33.

The hydromagnetic behavioral characteristics of high-latitude sudden impulses (si) are studied by comparing observations with the theoretical si inferred from solar wind compression characteristics. The amplitude of transverse hydromagnetic waves propagating from the magnetosphere equatorial plane into high latitudes is calculated. The latitudinal variations of the theoretical wave amplitude agree well with the steep increase in the si amplitude observed at about 60 to 70 deg geomagnetic latitude when the effect of the ionosphere on the hydromagnetic waves is taken into account. V.Z.

A71-35409*
THE GUM NEBULA: FURTHER EVIDENCE FROM SPACECRAFT AND GROUND-BASED INSTRUMENTS.

J. K. Alexander, J. C. Brandt, S. P. Maran, and T. P. Stecher (NASA, Goddard Space Flight Center, Greenbelt, Md.) 1 Aug. 1971 4 p refs Astrophysical Journal, vol. 167, Pt-1 p. 487-490.

Measurements by the RAE-1 and OGO-5 satellites are combined with data from ground-based telescopes to yield more accurate parameters for the Gum Nebula, including a somewhat smaller size and an estimate of the electron temperature. The supernova that ionizes the nebula must have been observed at the earth, and it is possible that records exist that can be deciphered by archeologists. Archeological

records from the Southern Hemisphere would be of the greatest interest. M.V.E.

A71-37353*
NONTHERMAL ELECTRONS AND HIGH-FREQUENCY WAVES IN THE UPSTREAM SOLAR WIND

L. A. Frank (Iowa, U., Iowa City, Iowa), R. W. Fredricks (TRW Systems Group, Redondo Beach, Calif.), M. Neugebauer (California Inst. of Tech., Jet Propulsion Lab., Space Science Div., Pasadena, Calif.), and F. L. Scarf 1 Aug. 1971 10 p refs Journal of Geophysical Research, vol. 76, p. 5162-5171. (Contracts NAS5-9278; NAS5-9196)

Use of OGO 5 interplanetary particle and wave observations from Mar. 11 and 12, 1968, to demonstrate that oscillations near the characteristic upper hybrid and electron plasma frequencies are produced when nonthermal electrons (energies greater than or equal to 700 to 800 eV) flow upstream. The results are discussed in terms of resonant interactions, with the streaming particle speed set equal to the wave phase speed. The nonthermal electrons can interact with long-wavelength longitudinal electron plasma oscillations, or with relatively short-wavelength transverse waves. Other OGO 5 measurements favoring the electromagnetic wave-particle interaction are cited, and the relations between these observations and some theories of type II solar radio bursts are discussed briefly. (Author)

A71-37368*
PLASMA INSTABILITY AT $(n \text{ PLUS } 1/2)f \text{ SUB } c$ AND ITS RELATIONSHIP TO SOME SATELLITE OBSERVATIONS.

R. W. Fredricks (TRW Systems Group, Redondo Beach, Calif.) 1 Aug. 1971 5 p refs Journal of Geophysical Research, vol. 76, p. 5344-5348. Research supported by the TRW Systems Group Independent Research Program. (Contract NAS5-9278; Grant NASw-1598)

Attempt to develop a plausible plasma physical explanation for two separate experimental observations of electric field fluctuations in the magnetospheric plasma at multiples of the local electron gyrofrequency. Although these two observations appear quite different at first glance, it is considered that they are basically due to the same plasma instability. F.R.L.

A71-39711**
RESPONSE OF THE NEUTRAL ATMOSPHERE TO GEOMAGNETIC DISTURBANCES.

G. R. Carignan (Michigan, U., Ann Arbor, Mich.), C. A. Reber (NASA, Goddard Space Flight Center, Greenbelt, Md.), and D. R. Tausch Berlin, East Germany, Akademie-Verlag, 1971 8 p refs In: Space Research XI, COSPAR, Plenary Meeting, 13th, and Symposium on Remote Sounding of the Atmosphere, Leningrad, USSR, May 20-29, 1970, Proceedings, Volume 2, p. 995-1002 Meeting and Symposium co-sponsored by the International Union of Geodesy and Geophysics and the World Meteorological Organization.

Data obtained from a quadrupole mass analyzer launched on the OGO-6 satellite on June 5, 1969 have been used in a study of neutral atmospheric composition variations during geomagnetic disturbances. Specifically studied was the period between Sept. 27, 1969 and Oct. 1, 1969, during which time several magnetic storms occurred and a maximum Kp of 80 was recorded. The composition data obtained during this period indicate that the densities of O and N₂, and most likely the temperatures, are enhanced in the high-latitude regions of the earth and relatively unaffected in the equatorial regions. The time lag between a given magnetic disturbance and the atmospheric response at high latitudes is very short, apparently less than one hour. (Author)

A71-39746#
DRIFTING WHISTLER CUT-OFF PHENOMENA STRIATIONS - OBSERVED BY POGO SATELLITES.
 I. Kimura (Kyoto U., Kyoto, Japan) Berlin, East Germany, Akademie-Verlag, 1971 6 p refs In: Space Research XI,

COSPAR, Plenary Meeting, 13th, and Symposium on Remote Sounding of the Atmosphere, Leningrad, USSR, May 20-29, 1970, Proceedings, Volume 2, p. 1331-1336 Meeting and Symposium co-sponsored by the International Union of Geodesy and Geophysics and the World Meteorological Organization.

An interesting whistler phenomenon has been found in low latitudes by POGO satellites (OGO 2 and 4) which is similar to the equatorial erosion but is characterized by continuously increasing lower and upper cut-off frequencies as the satellite moves towards higher latitudes from the magnetic equator. This phenomenon was observed in a magnetic latitude range between 5 and 25 deg in the local evening and mostly in the fall season. This is now called rising striation. A similar phenomenon which may be identical with 'walking trace whistlers' has also been observed in the middle latitudes, around 30-40 deg geomagnetic, where falling striations were detected. In the present paper, characteristics of the rising striations are reported, and an interpretation of the phenomenon based on the propagation effect is given. According to ray tracing, a horizontal gradient in the ionospheric electron density distribution in low latitudes, as well as the effect of ions, shows a frequency dependence for the ray paths which are responsible for the occurrence of the rising striation. (Author)

A71-39833*

THE RELATIONSHIP OF THE PLASMASPHERE AND THE STABLE AURORAL RED ARCS IN THE MAGNETIC STORM OF OCTOBER 29 TO NOVEMBER 7, 1968. C. R. Chappell, K. K. Harris, and G. W. Sharp (Lockheed Research Labs., Palo Alto, Calif.) Dordrecht, D. Reidel Publishing Co., 1971 8 p refs In: The Radiating Atmosphere, Summer Advanced Study Inst., Symposium, Queen's U., Kingston, Ontario, Canada, Aug. 3-14, 1970, Proceedings, p. 73-89 Symposium supported by the Advanced Research Projects Agency, the Defense Atomic Support Agency, the Lockheed Aircraft Corp., and the U.S. Navy. (Astrophysics and Space Science Library, Volume 24), 1971. (Contract NAS5-9092)

The densities of ambient H⁺ and He⁺ ions in the plasmasphere were measured by the Lockheed light ion mass spectrometer on OGO 5 during the magnetic storm of Oct. 29 to Nov. 7, 1968. Three occurrences of red arcs were reported during this storm period. In one satellite pass during the storm, the ion densities were measured on an L shell at the base of which an intense red arc was being simultaneously observed by a ground station. The ion measurements are discussed in terms of a general change in the size of the plasmasphere associated with this period of stable auroral red (SAR) arc observation. The size changes are correlated with the ground-based measurements of 6300 A SAR arc emissions and with the magnetic activity over this period. The results indicate that there must be at least two ingredients necessary for the production of a SAR arc. First, there must be an injection of ring current particles which is probably the source of energy for the arcs. Second, the plasmasphere must be greatly reduced in size to the L values characteristic of the location of the SAR arcs. T.M.

A71-43158*

NONTHERMAL ELECTRONS AND HIGH-FREQUENCY WAVES IN THE UPSTREAM SOLAR WIND. 2: ANALYSIS AND INTERPRETATION.

L. A. Frank (Iowa, U., Iowa City, Iowa), R. W. Fredricks, and F. L. Scarf (TRW Systems Group, Redondo Beach, Calif.) 1 Oct. 1971 9 p refs Journal of Geophysical Research, vol. 76, p. 6691-6699. (Contracts NAS5-9278; NAS5-9196)

Investigation of a streaming instability caused by suprathermal electrons with a bulk energy of about 1 keV and random widths from about 60 eV to 4 keV as a model to explain to OGO 5 observations of electric-field fluctuations with frequencies at or near the local electron plasma frequency upstream from the earth's bow shock. In a previous paper, it was shown that the waves appeared in direct correlation

with enhanced anisotropic electron fluxes having electron numbers greater than or about equal to 700 eV. It is now shown that the streaming instability produced by this type of suprathermal electron beam leads to a wave frequency nearly equal to the local electron plasma frequency, whereas the growth rates are still significant even if the beam thermal speed becomes comparable to the bulk speed. (Author)

A71-43161*

MAGNETOPAUSE ATTITUDES DURING OGO-5 CROSSINGS.

B. G. Ledley (NASA, Goddard Space Flight Center, Greenbelt, Md.) 1 Oct. 1971 7 p refs Journal of Geophysical Research, vol. 76, p. 6736-6742.

Determination of the attitude of the magnetopause current layer for 31 OGO 5 crossings located at subsatellite local times between 0430 and 1020 and solar magnetospheric latitudes between -8.5 and +40 deg. A consistent difference in this attitude is observed between crossings in which the satellite leaves the magnetosphere and crossings in which it enters. The magnitude of this difference appears to be independent of the sun-earth-satellite angle. The ratio of the component of the magnetic field normal to the magnetopause to the total adjacent magnetospheric field is computed for each crossing. Ratios ranging from +0.1 to -0.2 are obtained, where a plus sign signifies an outward directed component. The average ratio for those crossings in which the magnetosheath and magnetospheric fields subtended angles greater than 90 deg is -0.3 plus or minus 0.09. (Author)

A71-43162*

OGO-5 OBSERVATIONS OF THE POLAR CUSP ON NOVEMBER 1, 1968.

C. R. Chappell (Lockheed Res. Labs., Palo Alto), M. D. Montgomery (California, U., Los Alamos), M. Neugebauer (California Inst. of Tech., Pasadena, Calif.), C. T. Russell (California, U., Los Angeles), and F. L. Scarf (TRW Systems Group, Redondo Beach, Calif.) 1 Oct. 1971 22 p refs Journal of Geophysical Research, vol. 76, p. 6743-6764. ARPA-AEC sponsored research. (Contracts NAS5-9098; NAS5-9092; NAS5-9278)

Discussion of an apparent direct penetration of magnetosheath plasma into the dayside magnetosphere at magnetic latitudes as low as 43 deg encountered by the OGO 5 spacecraft during the large magnetic storm of Nov. 1, 1968. Because this region of magnetosheath plasma occurred on magnetospheric field lines immediately adjacent to the zone of trapped energetic particles, it is interpreted to be the polar cusp. The temperature of the electrons in the polar cusp was four times greater than the electron temperature measured simultaneously by Vela 4B in the downstream magnetosheath at local dusk, and the electron energy distribution in the cusp was similar to the distribution observed later when OGO 5 entered the magnetosheath. During the encounters with the polar cusp the amount of depression of the magnetic field implies the presence of magnetosheath protons together with the directly measured electrons. During this period of time the polar cusp was very turbulent at both ULF (magnetic) and VLF (electric) frequencies. Energetic (greater than or equal to 50 keV) electrons were also observed in the cusp. The cusp moved equatorward and poleward in response to changes in the north-south components of the interplanetary magnetic field. (Author)

A71-43166*

STRUCTURED VARIATIONS OF THE PLASMAPAUSE: EVIDENCE OF A COROTATING PLASMA TAIL.

J. M. Grebowsky (NASA, Goddard Space Flight Center, Greenbelt, Md.), H. A. Taylor, Jr., and W. J. Walsh (Aero Geo Astro Co., Beltsville, Md.) 1 Oct. 1971 9 p refs Journal of Geophysical Research, vol. 76, p. 6806-6814.

Review of a nearly complete set of high-resolution proton distributions obtained from OGO 4 during September 1967. These results, obtained during the recovery phase of

a magnetic storm that occurred on September 20-21, indicate that under appropriate magnetic- and electric-field conditions the plasmasphere may exhibit a tail-like structure that appears to corotate with the earth and results in a singular pattern of depleted and nondepleted plasma regions, which complicates the description of the plasmopause. A time-dependent analysis of the plasmopause motion using a simple plasma convection model is expected to provide evidence that a plasma tail may be formed by the tendency of plasma associated with the storm-distorted duskside plasmasphere bulge to corotate with the earth during a period of quieting magnetic activity. M.V.E.

A71-43176

INTERPLANETARY-PARTICLE ASSOCIATIONS WITH TYPE 3 SOLAR BURSTS.

T. E. Graedel (Bell Telephone Labs., Inc., Whippany, N.J.) and L. J. Lanzerotti (Bell Telephone Labs., Inc., Murray Hill, N.J.) 1 Oct. 1971 7 p refs Journal of Geophysical Research, vol. 76, p. 6932-6938.

Use of interplanetary proton (E equal to approximately 0.6 and E equal to approximately 1.2 MeV) and electron (E greater than 40 keV; E greater than 3000 keV) data from May 28 to Nov. 30, 1967, to study the association of particle data with solar radio-burst data in the dekametric band from OGO 3 and with data reported in Solar Geophysical Data and the IAU Quarterly Bulletin. By using reasonable particle- and radio-burst association criteria, it is concluded that the observed associations during this time period do not support the common belief that interplanetary-particle observations confirm the association of electrons with type 3 radio bursts. (Author)

A72-10361

CONCENTRATION OF NEUTRAL HYDROGEN IN THE UPPER ATMOSPHERE ACCORDING TO DATA ON THE IONIC COMPOSITION OF THE MEDIUM.

M. N. Fatkullin Oct. 1971 12 p refs Kosmicheskije Issledovaniia, vol. 9, Mar.-Apr. 1971, p. 246-259 Cosmic Research, vol. 9, Oct. 1971, p. 228-239. Translation.

The vertical and diurnal variations of the hydrogen atom concentration in the upper atmosphere during periods of near minimum solar activity are calculated on the basis of measurements of the concentration of thermal-energy positive hydrogen and oxygen ions in the medium. The data employed are selected from rocket and satellite mass-spectrometric measurements, observations of noncoherent radiowave scattering, and satellite observations of proton whistlers. A comparison with model calculations shows that the latter tend to underestimate the neutral hydrogen concentration at heights between 300 and 500 km. V.P.

A72-10877*

THE ENERGY DEPENDENCE OF THE COSMIC-RAY NEUTRON LEAKAGE FLUX IN THE RANGE 0.01-10 MeV.

R. W. Jenkins, S. O. Ifedili, J. A. Lockwood (New Hampshire, University, Durham, N.H.), and H. Razdan 1 Nov. 1971 9 p refs Journal of Geophysical Research, vol. 76, Nov. 1, 1971, p. 7470-7478.

(Contract NAS5-9313)

Measurement of the cosmic-ray neutron leakage flux and energy spectrum in the range 1 to 10 MeV by a neutron detector on the OGO 6 satellite from June 7 to Sept. 30, 1969. The same detector simultaneously measured the total leakage flux, having 75% of its response to the leakage flux in the interval from 1 keV to 1 MeV. For a neutron energy spectrum of the form AE to the minus gamma in the range from 1 to 10 MeV, the upper limit to gamma for polar regions was found to be 1.0 and for the equatorial regions was 1.2. For the polar regions, the lower limit to gamma was found to be 0.8. This energy spectrum at 1 to 10 MeV is slightly flatter than Newkirk (1963) predicted. (Author)

A72-10886*

MAGNETOSPHERIC-FIELD DISTORTIONS OBSERVED

BY OGO 3 AND 5.

M. Sugiura, B. G. Ledley, T. L. Skillman, and J. P. Heppner (NASA, Goddard Space Flight Center, Laboratory for Space Physics, Greenbelt, Md.) 1 Nov. 1971 14 p refs Journal of Geophysical Research, vol. 76, Nov. 1, 1971, p. 7552-7565.

The rubidium vapor magnetometer data of the scalar magnetic-field intensity obtained by the OGO 3 and 5 satellites are analyzed to study the magnetospheric-field distortions in terms of the observed field magnitude under quiet and slightly disturbed conditions minus the magnitude of the reference geomagnetic field (ΔB). Average contours of equal ΔB s are shown in the geomagnetic noon-midnight and dawn-dusk meridian planes for magnetically quiet and slightly disturbed conditions. The equatorial distribution of observed ΔB s as a function of geocentric distance differs substantially from that expected from the well-known models of the quiet-time ring current. Other findings suggest that there must be a population of low-energy particles with substantial total energy near the equator at distances of 2 to 5 earth radii that has not been recognized as having sufficient energy to inflate the magnetic field. M.V.E.

A72-10892*

THE DAYSIDE OF THE PLASMASPHERE.

C. R. Chappell, K. K. Harris, and G. W. Sharp (Lockheed Research Laboratories, Palo Alto, Calif.) 1 Nov. 1971 16 p refs Journal of Geophysical Research, vol. 76, Nov. 1, 1971, p. 7632-7647.

(Contract NAS5-9092)

The concentrations of H(+) ions in the dayside region of the plasmasphere, measured from March 1968 through February 1969 by the Lockheed light-ion mass spectrometer aboard the OGO 5 satellite, are presented and analyzed. The position of the plasmopause on the dayside appears to be determined by the level of magnetic activity present during the previous corotation of the dayside sector through the formative nightside region. Observations of the buildup of H(+) density versus local time following magnetic storms indicate that H(+) ions flow from the dayside ionosphere into the plasmasphere and plasma trough. Plasmopause density profiles in the afternoon-dusk sector show the effects of the dayside filling from the ionosphere. In addition, several of the dayside profiles display a steep drop in the H(+) density of about a factor of 10 inside the plasmopause position. O.H.

A72-10902*

RELATIONSHIP BETWEEN Fe (+) IONS AND EQUATORIAL SPREAD F.

W. B. Hanson and S. Sanatani (Texas, University, Dallas, Tex.) 1 Nov. 1971 8 p refs Journal of Geophysical Research, vol. 76, Nov. 1, 1971, p. 7761-7768.

(Contract NAS5-9311)

Evaluation of observations from the retarding potential analyzer on OGO 6 near the magnetic equator, demonstrating an intimate relationship between the presence of Fe(+) ions and irregularities in the total ion concentration. The ionospheric irregularities (or structure) are probably another manifestation of equatorial spread F, although this has not yet been verified. Nearly half the nighttime equatorial crossings below 700 km exhibit both Fe(+) and structure, but only 10% of the passes without Fe(+) have structure. Approximately one-third of the passes with Fe(+) are not structured, which indicates that Fe(+) may be a necessary but not sufficient condition for structure formation. The Atlantic region shows an extremely high and detailed correlation between Fe(+) ions and the irregularities. (Author)

A72-12081#

GEOMAGNETIC SURVEY BY THE POLAR ORBITING GEOPHYSICAL OBSERVATORIES.

J. C. Cain and R. A. Langel (NASA, Goddard Space Flight Center, Greenbelt, Md.) 1971 11 p refs In: World magnetic survey 1957-1969, Paris, International Union of Geodesy and

Geophysics, 1971, p. 65-75.

Summary of reduced data from the polar Orbiting Geophysical Observatories OGO 2 and 4, spanning the time period from Oct. 14, 1965 to the end of 1967. A brief discussion of the accuracy of the observations is followed by a description of the data extent. It is shown that the quantity of data acquired by the OGO magnetometers far exceeds the total for all other magnetic survey sources. Data acquisition for only about a two-week interval gives virtually complete global coverage. Procedures and considerations underlying the data analysis performed are discussed. Suggestions for further work are presented. M.V.E.

A72-12084*#**RESULTS OF MAGNETIC SURVEYS OF THE MAGNETOSPHERE AND ADJACENT REGIONS.**

M. Sugiura (NASA, Goddard Space Flight Center, Laboratory for Space Sciences, Greenbelt, Md.) 1971 1 p refs In: World magnetic survey 1957-1969, Paris, International Union of Geodesy and Geophysics, 1971, p. 81-94.

Review of the gross features of the magnetic fields in the magnetosphere and its vicinity that have been explored in the past several years by extensive spacecraft observations. The magnetopause, the bow shock, the magnetosheath, and the geomagnetic tail are discussed. Results of a recent study of the OGO 1 and 3 satellite data taken in the near tail region, the magnetic field disturbances observed in the magnetosphere, and brief accounts of quantitative models of the magnetosphere are also reviewed. Special attention is given to the storm-time ring current and the to polar substorms or magnetic bays. M.V.E.

A72-13428*#**BIDIRECTIONAL REFLECTANCE OF THE MOONLIT EARTH.**

W. B. Fowler, E. I. Reed (NASA, Goddard Space Flight Center, Laboratory for Planetary Atmospheres, Greenbelt, Md.), and J. E. Blamont (CNRS, Paris, France) Dec. 1971 4 p refs Applied Optics, vol. 10, Dec. 1971, p. 2657-2660.

Use of OGO-4 airglow photometer data and computed lunar spectral irradiances at the subsatellite point to examine the highest radiance over clouds and lowest radiance over open ocean near 3914, 5577, 5893, 6225, and 6300 Å in terms of bidirectional reflectance. The results are compared to and are consistent with mathematical models of the atmosphere developed by Plass and Kattawar (1968, 1970) and with daytime measurements from OSO-3 by Neel et al. (1969). (Author)

A72-13507***ELECTRON ENERGY FLUX IN THE SOLAR WIND.**

K. W. Ogilvie, J. D. Scudder, and M. Sugiura (NASA, Goddard Space Flight Center, Greenbelt, Md.) 1 Dec. 1971 9 p refs Journal of Geophysical Research, vol. 76, Dec. 1, 1971, p. 8165-8173.

Description of studies of electrons between 10 eV and 9.9 keV in the solar wind. The transport of energy in the rest frame of the plasma is evaluated and shown to be parallel to the interplanetary magnetic field. The presence of electrons from solar events causes this energy-flux density to exceed the heat flow due to thermal electrons. In one such event, the observations are shown to be consistent with the solar-electron observations made at higher energies. When observations are made at a point connected to the earth's bow shock by an interplanetary-field line, a comparatively large energy flux along the field toward the sun is observed, but the heat flow remains outwardly directed during this time interval. In either situation the heat flow is found to be consistent with measurements made on Velsa satellites by a different method. These values, less than .01 ergs/sq cm/sec, are sufficiently low to require modifications to the Spitzer-Harm conductivity formula for use in solar-wind theories. (Author)

A72-13518***NEUTRAL COMPOSITION VARIATION ABOVE 400****KILOMETERS DURING A MAGNETIC STORM.**

D. R. Taesch, G. R. Carignan (Michigan, University, Ann Arbor, Mich.), and C. A. Reber (NASA, Goddard Space Flight Center, Laboratory for Planetary Atmospheres, Greenbelt, Md.) 1 Dec. 1971 8 p refs Journal of Geophysical Research, vol. 76, Dec. 1, 1971, p. 8318-8325. (Contract NAS5-9328)

Examination of data from the neutral atmospheric composition experiment launched aboard OGO 6, June 5, 1969, for the period from Sept. 27 through Oct. 3, 1969. Several magnetic storms occurred during this time, and the response of the neutral atmosphere to the energy deposition causing these storms was studied. The data indicate that the major portion of the energy is deposited at high latitudes, causing enhancements in N₂ densities corresponding to Jacchia (1970) temperature increases on the order of 400 to 500 K. The time difference between atmospheric response and magnetic activity appears to be very short at high latitudes. The O/N₂ ratio variations suggest dynamic processes that cause a circulation in the atmosphere that is upward at the pole with subsidence at the equator. (Author)

A72-14561***AN UPPER LIMIT ON THE HARDNESS OF THE NONTHERMAL ELECTRON SPECTRA PRODUCED DURING THE FLASH PHASE OF SOLAR FLARES.**

S. R. Kane (California, University, Berkeley, Calif.) 15 Dec. 1971 5 p refs Astrophysical Journal, vol. 170, Dec. 15, 1971, pt. 1, p. 587-591. (Contract NAS5-9094)

The observations of impulsive solar-flare X-rays above 10 keV made with OGO 5 satellite have been analyzed in order to study the variation of the nonthermal electron spectrum from one flare to another. The X-ray spectrum at the maxima of 129 impulsive X-ray bursts is represented by KE to the minus-gamma power photons per sq cm per sec per keV, and the frequency of occurrence of bursts with different values of gamma is studied. It is found that for gamma less than 4.0 the frequency of bursts rapidly decreases with the decrease in the value of gamma. The probability of occurrence of a burst with gamma less than 2.3 is extremely small. (Author)

A72-15366***ENRICHMENT OF VERY HEAVY NUCLEI IN THE COMPOSITION OF SOLAR ACCELERATED PARTICLES.**

A. Mogro-Campero and J. A. Simpson (Chicago, University, Chicago, Ill.) 1 Jan. 1972 5 p refs Astrophysical Journal, vol. 171, Jan. 1, 1972, pt. 2, p. L5-L9. (Contract NAS5-9366; Grants NGL-14-001-006; NSF GA-18368X)

Measurement of the abundances of the nuclei, C, N, O, Ne, Mg, Si, Ar, and Ca and the group Cr-Co relative to oxygen from seven solar energetic-particle events in the energy range from about 14 to 61 MeV per nucleon with a solid-state detector telescope on the OGO-5 satellite, 1968-1971. The differential energy spectra of O (14 to 29 MeV per nucleon) and Cr-Co (3 to 61 MeV per nucleon) have a spectral index of about (-3) for a power law in kinetic energy. The relative abundances of C, N, O, and Ne are in excellent agreement with emulsion studies. However, when compared with the solar photospheric and coronal abundances, the OGO-5 measurements show a large enhancement of relative abundances beginning with Si, and extending to the Cr-Co group. The enhancement over the solar and universal abundances is in rough agreement with the composition of the galactic cosmic radiation. (Author)

A72-16719***THE QUIET-TIME SPECTRA OF COSMIC-RAY ELECTRONS OF ENERGIES BETWEEN 10 AND 200 MeV OBSERVED ON OGO-5.**

J. L'Heureux, C. Y. Fan (Arizona, University, Tucson, Ariz.), and P. Meyer (Chicago, University, Chicago, Ill.) 15 Jan.

1972 14 p refs *Astrophysical Journal*, vol. 171, Jan. 15, 1972, pt. 1, p. 363-376.
(Contracts : NASS-9096; NASS-11444; Grants
NGL-14-001-005; NGR-03-002-107)

Measurement of spectra of cosmic-ray electrons of energies between 10 and 100 MeV over a one-year period starting 1968 March. The measurement was made with a detector system on board the OGO-5 satellite. The instrument consists of a solid-state dE/dx detector, a total-energy CsI detector, a gas Cerenkov threshold detector, and two-scintillation guard counters. Time periods during which no solar-flare events were recorded were selected for the study. It was found that during these quiet periods there were numerous intensity variations of the electron flux. These variations, which are seen only below 25 MeV do not show marked correlation with any solar or interplanetary-medium parameters. The flux of the electrons of energies above 25 MeV on the other hand, showed a gradual decrease over the one-year period, paralleling the neutron monitor intensity. The parameter describing this long-term modulation is almost independent of the rigidity of the electrons in the reported energy range. The physical implication of the finding is discussed. (Author)

A72-17453*
IRREGULAR STRUCTURE OF THERMAL ION PLASMA NEAR THE PLASMAPAUSE OBSERVED FROM OGO-3 AND Pc 1 MEASUREMENTS.

H. Kikuchi and H. A. Taylor, Jr. (NASA, Goddard Space Flight Center, Greenbelt, Md.) 1 Jan. 1972 12 p refs *Journal of Geophysical Research*, vol. 77, Jan. 1, 1972, p. 131-142.

Independent measurements of the plasmopause and associated thermal plasma structure from OGO 3 are compared with ground-based Pc 1 observations from the period 1966-67. Substantial agreement between the plasmopause crossing identified on the satellite and the Pc 1 occurrence positions observed on the ground at midlatitudes during the nighttime (including dawn and dusk) indicates that these nighttime Pc 1 events are closely associated with the plasmopause. A correlation of selected closely spaced events obtained in the nighttime under quiet to moderate activity provides good agreement in the proton concentrations near the plasmopause boundary. Preliminary results indicate Pc 1 excitation is associated with plasma irregularities near the plasmopause and is particularly favorable in the region of post-storm recovery and in the region of diurnal 'plasma bulge' in the afternoon-dusk sector. (Author)

A72-19145*
OGO-5 MAGNETIC-FIELD DATA NEAR THE EARTH'S BOW SHOCK: A CORRELATION WITH THEORY.

J. K. Guha, D. L. Judge, and J. H. Marburger (Southern California, University, Los Angeles, Calif.) 1 Feb. 1972 7 p refs *Journal of Geophysical Research*, vol. 77, Feb. 1, 1972, p. 604-610.
(Contract NASS-9098)

Magnetic-field data obtained in the earth's bow-shock region with a high-resolution triaxial fluxgate magnetometer aboard the OGO 5 satellite have been correlated with a theory of Tidman and Northrop (1968). These authors have shown that either of two hypotheses about the nature of low-frequency magnetic waves could be invoked to explain previous observations. We have observed exponentially decaying upstream waves that are consistent with only one of these hypotheses. This observation allows use of the theory to infer the local shock velocity and frequency of driving currents within the shock. This method of finding the shock velocity is less sensitive to errors in the plasma parameters than is the method based on the Rankine-Hugoniot relations. (Author)

A72-19148*
MEASUREMENT OF THE WAVE-NORMAL VECTOR OF PROTON WHISTLERS ON OGO-6.

K. W. Chan, R. K. Burton, R. E. Holzer (California,

University, Los Angeles, Calif.), and E. J. Smith (California Institute of Technology, Jet Propulsion Laboratory, Pasadena, Calif.) 1 Feb. 1972 5 p refs *Journal of Geophysical Research*, vol. 77, Feb. 1, 1972, p. 635-639.
(Contract JPL-950403; Grant NGR-05-007-276)

Description of the first experimental determination of the wave-normal vector of proton whistlers in the ionosphere. Between the crossover frequency and the proton gyrofrequency, both right-hand and left-hand modes of propagation can occur for upgoing waves. Theoretically, the amount of energy in the respective modes depends on theta, the angle between the wave normal and the magnetic field. For proton whistlers with only left-hand mode energy between the crossover and proton gyrofrequency, theta ranged from 36 to 51 deg. For proton whistlers with strong right-hand and left-hand mode signals, theta ranged from 24 to 29 deg. The result is in good agreement with Wang's (1971) collisionless mode-coupling model. The angle between the wave normal and the vertical is found to increase with increasing altitude. (Author)

A72-19149*
COMPARISON OF VERY-LOW-FREQUENCY AURORAL HISS WITH PRECIPITATING LOW-ENERGY ELECTRONS BY THE USE OF SIMULTANEOUS DATA FROM TWO OGO-4 EXPERIMENTS.

R. A. Hoffman (NASA, Goddard Space Flight Center, Greenbelt, Md.) and T. Laaspere (Dartmouth College, Hanover, N.H.) 1 Feb. 1972 11 p refs *Journal of Geophysical Research*, vol. 77, Feb. 1, 1972, p. 640-650.
(Grant NGR-30-001-030)

Determination of the origin of auroral hiss by comparing the records of a VLF experiment (0.3 to 18 kHz) with simultaneous data obtained by an auroral-particle experiment having detectors for precipitating electrons at 0.7, 2.3 and 7.3 keV. It is found that, on the dayside of the earth, the occurrence of VLF hiss correlates well with precipitation events at 0.7 keV, but in general very poorly with activity in the higher-energy channels. Exact correlation between variations in VLF hiss intensity and in electron fluxes is rare even at 0.7 keV. In addition, VLF hiss tends to be observed over a somewhat larger spatial region than precipitating 0.7-keV electrons. It is concluded that, on the dayside, auroral hiss is generated by soft (E less than 1 keV) cusp region electrons and that the lack of detailed correlation between the two phenomena is caused by propagation effects as the hiss travels downward and spreads from the generation region. (Author)

A72-21189
FLUCTUATING MAGNETIC FIELDS IN THE MAGNETOSPHERE.

C. T. Russell, R. L. McPherron, and P. J. Coleman, Jr. (California, University, Los Angeles, Calif.) Jan. 1972 47 p refs *Space Science Reviews*, vol. 12, Jan. 1972, p. 810-856.

Magnetic fluctuations in the extremely low frequency (ELF) and very low frequency (VLF) waves in space are studied. The experiments and instrumentation designed to measure natural ELF and VLF are described. Two observed classes of wave phenomena are considered: whistlers and emissions. The various whistler phenomena, their characteristics, their formation, and their uses in probing the magnetosphere are discussed in detail. Emissions are studied principally in two separate altitude ranges: near the ionosphere from about 200 to 2000 km altitude, and at high altitudes in the magnetosphere near the magnetic equator. The individual emission phenomena are characterized. O.H.

A72-21223*
CORRELATIONS OF OGO-5 PLASMAPAUSE CROSSING WITH OBSERVATIONS OF TYPE Pi MICROPULSATIONS ON THE GROUND.

R. R. Heacock, A. J. Mullen, V. P. Hessler (Alaska, University, College, Alaska), C. Sucksdorff, M. Kivinen (Finnish Meteorological Institute, Helsinki, Finland), and E. Kataja (Sodankyla Geophysical Observatory, Sodankyla,

Finland) Dec. 1971 6 p refs *Annales de Geophysique*, vol. 27, Oct.-Dec. 1971, p. 477-482. NSF supported research.

(Contract NAS5-9092)

Comparison of plasmopause positions with Pi micropulsation events observed at College (L = 5.4) or at Sodankyla (L = 5.1), showing that in almost all cases the plasmopause was inside the field line of the observing site when the Pi event was recorded. Strong Pi events were seen at Nurmijaarvi (L = 3.4) only when Kp was very high, when the plasmopause would be expected to be inside L = 3.4. When Pi events and structure Pc 1 events were observed nearly simultaneously, the Pi activity was always more prominent at the poleward site. A demarcation line seems to exist, separating the Pi and structured Pc 1 source regions. This line may be the plasmopause, with structure Pc 1 inside and Pi outside.

F.R.L.

A72-21510*
ELECTRON SCATTERING EFFECTS IN TYPICAL COSMIC RAY TELESCOPES.

J. E. Lupton (California Institute of Technology, Pasadena, Calif.) and E. C. Stone Feb. 1972 7 p refs *IEEE Transactions on Nuclear Science*, vol. NS-19, Feb. 1972, p. 562-568. Institute of Electrical and Electronics Engineers, Nuclear Science Symposium, 18th, San Francisco, Calif., Nov. 3-5, 1971

(Contracts NAS5-3095; NAS5-9312; Grants NGR-05-002-160; NGL-05-002-007)

Laboratory measurements have been made of the response of two typical cosmic ray detector systems to electrons between 0.2 and 2.0 MeV. Working Laboratory versions of each of these particle telescopes were exposed to the monoenergetic electron beam from a magnetic spectrometer. The results of pulse height and counting rate measurements indicate that electrons scattered from the anti-coincidence cup comprise about 25% of the total number arriving at the top of the detector stack. In certain cases, the contribution of these scattered particles to the total number of electrons detected can reach 65%.

(Author)

A72-23004*
LARGE-SCALE COHERENCE AND HIGH VELOCITIES OF THE EARTH'S BOW SHOCK ON FEBRUARY 12, 1969.

E. W. Greenstadt (TRW Systems Group, Redondo Beach, Calif.), P. C. Hedgecock (Imperial College of Science and Technology, London, England), and C. T. Russell (California University, Los Angeles, Calif.) 1 Mar. 1972 7 p refs *Journal of Geophysical Research*, vol. 77, Mar. 1, 1972, p. 1116-1122.

(Contract NAS5-9098; Grant NASw-2186)

The earth's bow shock exhibited a clean laminar profile at low Mach number as it crossed and recrossed OGO 5, HEOS 1, and Explorer 33 on February 12, 1969. The approximate 120 earth radii distance between HEOS and Explorer during one set of crossings indicated the abrupt character of the laminar shock front and the absence of magnetosheath turbulence both in the dayside hemisphere above the ecliptic and in the flank of the shock 75 earth radii behind the earth and below the ecliptic. The abruptness of the shock and coplanarity of the loci of OGO and HEOS with the local shock normal permit the most reliable estimates yet obtained of shock velocities along the normal. These mean velocities ranged from 11 to at least 100 km/sec over distances of 2-7 earth radii.

(Author)

A72-23008*
OGO-4 OBSERVATIONS OF EXTREMELY LOW FREQUENCY HISS.

J. L. R. Muzzio and J. J. Angerami (Stanford University, Stanford, Calif.) 1 Mar. 1972 17 p refs *Journal of Geophysical Research*, vol. 77, Mar. 1, 1972, p. 1157-1173.

(Contract NAS5-3093; Grants NGR-05-020-288; NGL-05-020-008; NSF GP-948)

Analysis of ELF and VLF data from the Stanford

University experiment on OGO 4 revealed an ELF hiss band with characteristics not previously identified. The band, referred to as band-limited ELF hiss, is seen from low to medium latitudes. On the basis of wave-propagation properties, it is proposed that the BLH is generated at large wave normal angles in the equatorial region near L = 4. This model can be used to explain the characteristics of the BLH. Two mechanisms for the generation of BLH based on radiation from energetic electrons are considered.

M.V.E.

A72-23011*
THERMAL POSITIVE IONS IN THE OUTER IONOSPHERE AND MAGNETOSPHERE FROM OGO 1.

M. Ahmed (Regis College, Weston, Mass.) and R. C. Sagalyn (USAF, Cambridge Research Laboratories, Bedford, Mass.) 1 Mar. 1972 16 p refs *Journal of Geophysical Research*, vol. 77, Mar. 1, 1972, p. 1205-1220.

(NASA Order DPR-S-70015-G)
(AD-742186; AFCRL-72-0244)

Study of the positive thermal ion densities measured with a spherical electrostatic analyzer aboard OGO 1 between September and October, 1964. A high variability of charged-particle distributions is established within and beyond the plasmopause boundary. The density gradient was in an inverse relation to the plasmopause L position and was consistently about one order of magnitude higher for the afternoon sector orbits than for the nightside orbits. Irregularities of different types were observed in the positive thermal ion densities within the plasmasphere and outside it, showing no correlation with the magnetic activity level. A delay of 3 to 9 hr was observed in the movement of the plasmopause following an increase in the magnetic activity level on the nightside.

V.Z.

A72-23019*
DISTRIBUTIONS OF ELECTRON PLASMA OSCILLATIONS UPSTREAM FROM THE EARTH'S BOW SHOCK.

R. W. Fredricks, F. L. Scarf, and I. M. Green (TRW Systems Group, Redondo Beach, Calif.) 1 Mar. 1972 6 p refs *Journal of Geophysical Research*, vol. 77, Mar. 1, 1972, p. 1300-1305.

(Contract NAS5-9278)

Evaluation of data from the 14.5- and 30-kHz plasma-wave detector channels aboard OGO 5 for the period Dec. 2, 1968, to Apr. 8, 1969, demonstrating the relatively isotropic occurrence of electron plasma oscillations upstream from the bow shock. These plasma oscillations were shown previously to correlate with streams of electrons having energy greater than 700 eV. The present study implies the presence of such streams, most probably electrons reflected by the bow shock, irrespective of spacecraft longitude in the upstream solar wind.

(Author)

A72-23520*
RF SHEATH AND ADMITTANCE CHARACTERISTICS OF A SPHERICAL PLASMA PROBE.

J. R. Kan (Dartmouth College, Hanover, N.H.) Feb. 1972 8 p refs *Radio Science*, vol. 7, Feb. 1972, p. 301-308.

(Contract NAS5-9305)

Development of a radio-frequency sheath model for a spherical probe in a collisionless plasma. The method of solution is based on the quasi-static approximation and the electrostatic probe theory of Bernstein and Rabinowitz (1959). The resistive part of the admittance is ascribed to the sheath transit-time collisionless dissipation mechanism suggested by Mayer (1963) and developed by Gould (1964). Expressions are obtained for the effective sheath thickness and the equivalent resistance of the transit-time dissipation. The sheath model and, hence, the admittance are completely determined in terms of the bias potential, the probe radius, the plasma frequency, and the Debye length - i.e., there are no adjustable parameters in the proposed theory which are to be determined by experiment. The results obtained agree favorably with Cohen and Bekefi's (1971) experimental data

A72-24957

on the conductance resonant frequency and the width of the conductance peak. (Author)

A72-24957*

MAGNETIC STORM EFFECTS IN THE NEUTRAL COMPOSITION.

H. G. Mayr (NASA, Goddard Space Flight Center, Thermosphere and Exosphere Branch, Greenbelt, Md.) and H. Volland (NASA, Goddard Space Flight Center, Thermosphere and Exosphere Branch, Greenbelt, Md.; Bonn, Universitaet, Bonn, West Germany) Mar. 1972 15 p refs Planetary and Space Science, vol. 20, Mar. 1972, p. 379-393.

Demonstration that the thermospheric wind circulation excited during magnetic storms, presumably by Joule heating within the auroral zone, is an effective mechanism for removing atomic oxygen at high latitudes. Wind-induced variations in O exceed the temperature effects up to 250 km. The calculated depletion is most pronounced at around 180 km, where the density can decrease by as much as a factor of two, consistent with the observed storm time variations in the ionosphere. At higher altitudes, this effect is canceled by the thermal expansion in atomic oxygen, thus explaining the negligible response in the concentration of this atmospheric constituent under disturbed conditions, when N₂ increased by as much as a factor of ten. (Author)

A72-26399*

OGO-5 OBSERVATIONS OF LHR NOISE, EMISSIONS, AND WHISTLERS NEAR THE PLASMAPAUSE AT SEVERAL EARTH RADII DURING A LARGE MAGNETIC STORM.

F. L. Scarf, R. W. Fredricks (TRW Systems Group, Redondo Beach, Calif.), E. J. Smith, A. M. A. Frandsen (California Institute of Technology, Jet Propulsion Laboratory, Pasadena, Calif.), and G. P. Serbu (NASA, Goddard Space Flight Center, Greenbelt, Md.) 1 Apr. 1972 18 p refs Journal of Geophysical Research, vol. 77, Apr. 1, 1972, p. 1776-1793.

(Contract NAS5-9278; Project OGO)

On May 15, 1969, OGO 5 crossed the plasmopause during a major storm that produced severe geomagnetic disturbances (K_p up to 8-), large and rapid variations in ring-current intensity (as measured by Dst), intense low-latitude aurora, and persistent SAR arcs. Near the highly structured plasmasphere boundary, the electric- and magnetic-field sensors on OGO 5 detected lower-hybrid-resonance noise bursts, whistlers, ELF hiss, and other discrete signals or emissions. Some LHR noise bursts were associated with whistlers, and these high-altitude phenomena resembled the corresponding ionospheric ones. This report contains a description of the VLF observations. We also show that intense ULF magnetic signals were present near the plasmopause, and we attempt to relate these observations to the predictions of various theories of proton ring-current decay and SAR-arc formation. (Author)

A72-26402*

AURORAL SPECTRUM BETWEEN 1200 AND 4000 ANGSTROMS.

W. E. Sharp (Michigan, University, Ann Arbor, Mich.) and M. H. Rees (Colorado, University, Boulder, Colo.) 1 Apr. 1972 10 p refs Journal of Geophysical Research, vol. 77, Apr. 1, 1972, p. 1810-1819.

(Grant NGR-06-003-110)

Results of spectroscopic observations of an auroral event made simultaneously by airborne and satellite-borne scanning spectrometers in the wavelength region between 1200 and 4000 Å. Photon emission rates of several vibrational bands of the N₂ 2nd positive, Vegard-Kaplan, and Lyman-Birge-Hopfield systems, the N I lines at 1200 and 3466 Å, and O I lines at 1304, 1356, and 2972 Å were recorded. Model calculations of the emission rates of the observed features are found to be in reasonable agreement with the measurements. Electron impact excites the nitrogen band systems, as well as the O I 1356-Å line. A spectral

feature at 2150 Å is tentatively identified as the (1,0) gamma band of N O. Author

A72-26407*

NEUTRAL DENSITY MEASUREMENTS NEAR 400 KILOMETERS BY A MICROPHONE DENSITY GAGE ON OGO-6 DURING JULY 12-15, 1969.

A. D. Anderson and G. W. Sharp (Lockheed Research Laboratories, Palo Alto, Calif.) 1 Apr. 1972 7 p refs Journal of Geophysical Research, vol. 77, Apr. 1, 1972, p. 1878-1884.

(Contract NAS5-9334)

Analysis of persistent density peaks (maxima) measured near 400 km during daytime (1425 LT) by a microphone density gauge on OGO 6 during July 12 to 15, 1969. Most of the density peaks occurred between geomagnetic latitudes 50 and 61 N and L values 2.3 and 4.7. The average density change in the peaks was 27%. Most of the peaks appeared in the longitude sector from 150 to 350 E. No density peaks were measured in the 50 to 130 E sector during the 3-1/2 day observation period. A persistent pair of density peaks was present on seven successive orbits during July 13 and July 14 (both geomagnetically disturbed days) near geomagnetic latitudes 53 and 61 N respectively. (Author)

A72-26411*

ERRORS IN RETARDING POTENTIAL ANALYZERS CAUSED BY NONUNIFORMITY OF THE GRID-PLANE POTENTIAL.

W. B. Hanson, D. R. Frame, and J. E. Midgley (Texas, University, Dallas, Tex.) 1 Apr. 1972 9 p refs Journal of Geophysical Research, vol. 77, Apr. 1, 1972, p. 1914-1922.

(Contracts NAS5-9311; NSR-44-004-029)

One aspect of the degradation in performance of retarding potential analyzers caused by potential depressions in the retarding grid is quantitatively estimated from laboratory measurements and theoretical calculations. A simple expression is obtained that permits the use of laboratory measurements of grid properties to make first-order corrections to flight data. Systematic positive errors in ion temperature of approximately 16% for the OGO 4 instrument and 3% for the OGO 6 instrument are deduced. The effects of the transverse electric fields arising from the grid potential depressions are not treated. (Author)

A72-29378*

DISSIPATION MECHANISMS IN A PAIR OF SOLAR-WIND DISCONTINUITIES.

T. W. J. Unti, M. Neugebauer (California Institute of Technology, Jet Propulsion Laboratory, Pasadena, Calif.), G. Atkinson (Department of Communications, Communications Research Centre, Ottawa, Canada), and C.-S. Wu (Maryland, University, College Park, Md.) 1 May 1972 14 p refs Journal of Geophysical Research, vol. 77, May 1, 1972, p. 2250-2263.

(Grant NGL-21-002-005)

A pair of sharp closely spaced discontinuities in the solar wind was recorded by the high time resolution instruments aboard OGO 5 on Mar. 14, 1968. There is plasma turbulence within the double structure, and there appear to be small-amplitude hydromagnetic waves radiating from the discontinuities. The generation of the plasma turbulence is discussed in terms of magnetic drift waves. Although it seems probable that the surfaces are tangential discontinuities, arguments are also advanced that the double structure may represent the Petschek mechanism in which rapid field-line merging occurs between standing waves. (Author)

A72-29379*

STUDY OF WAVES IN THE EARTH'S BOW SHOCK.

R. E. Holzer, J. V. Olson, C. T. Russell (California, University, Los Angeles, Calif.), and T. G. Northrop 1 May 1972 10 p refs Journal of Geophysical Research, vol. 77, May 1, 1972, p. 2264-2273.

(Contract JPL-950403; Grant NGR-05-007-276)

NOV. 10, 1975

Results of an examination of the perturbation vectors of waves upstream and downstream from the region of maximum compression in the bow shock on OGO 5 under particularly steady solar-wind conditions. The polarization of the upstream waves was right-hand circular, and that of the downstream waves left-hand elliptical in the spacecraft frame. By observing that the polarization of the waves remained unchanged as the shock motion swept the wave structure back and forth across the satellite three times in eight minutes, it was found that the waves were not stationary in the shock frame. A study of the methods of determining the shock normal indicates that the normal estimated from a shock model should be superior to the normal based on magnetic coplanarity. The propagation vectors of the waves examined did not coincide with the shock-model normal, the average magnetic field, or the plasma-flow velocity. However, the major axis of the polarization ellipse of the downstream wave was nearly parallel to the upstream propagation vector. (Author)

A72-29380*

PLASMA WAVES IN THE DAYSIDE POLAR CUSP. I: MAGNETOSPHERIC OBSERVATIONS.

F. L. Scarf, R. W. Fredricks, I. M. Green (TRW Systems Group, Redondo Beach, Calif.), and C. T. Russell (California, University, Los Angeles, Calif.) 1 May 1972 20 p refs Journal of Geophysical Research, vol. 77, May 1, 1972, p. 2274-2293.

(Contracts NAS5-9278; NAS5-9098)

General survey of the OGO 5 plasma-wave measurements for the dayside polar-cusp encounters of Nov. 1, 1968, and detailed analysis of the observations at the low-altitude (r approximately 3 to 5 earth radii) cusp boundaries. The survey section contains an overall discussion of the ULF magnetic-field wave levels and the VLF electric-field amplitude ranges measured from perigee out to 9 earth radii on Nov. 1, 1968. These cusp-associated observations are compared with those made on Oct. 27 and Nov. 6, 1968, when OGO 5 traversed the dayside magnetosphere without encountering the cusp. It is shown that at the November 1 low-altitude cusp boundaries intense wave levels were detected over a broad spectral region at the steep gradients in cusp plasma density and thermal energy. The results are interpreted in terms of drift instabilities for low-beta plasmas with hot ions, and associated wave-particle and wave-wave interactions are briefly discussed. (Author)

A72-29384*

SATELLITE OBSERVATIONS OF WHISTLER-MODE SIGNALS IN THE CONJUGATE REGION OF A 200-KILOHERTZ STATION.

T. Laaspere and S. C. Orphanoudakis (Dartmouth College, Hanover, N.H.) 1 May 1972 9 p refs Journal of Geophysical Research, vol. 77, May 1, 1972, p. 2319-2327. (Contract NAS5-9305)

Study of the signals recorded by a narrow-band (about 200 Hz) receiver at a broadcast station operating at 200 kHz and in the conjugate region of Ashkhabad. The latitude of the station is nearly low enough for propagation of a 200-kHz signal in the ducted whistler mode to the conjugate hemisphere along field lines terminating at the station. In the dawn-dusk orbital plane signals are indeed relatively often observed in the conjugate region, but the source of the signals and their path of propagation is not completely clear. The pattern of observations is consistent with propagation over the long magnetospheric path in field-aligned ducts spread in longitude near 22 deg invariant latitude, but an interpretation involving nonducted propagation is preferred, in which the occasionally high electric-field intensities encountered (greater than 10 microvolts/m) result from focusing effects or from propagation near the resonance angle. (Author)

A72-31965**

SIMULTANEOUS SATELLITE AND RIOMETER MEASUREMENTS OF PARTICLES DURING SOLAR COSMIC RAY EVENTS.

M. B. Baker, P. R. Satterblom, A. J. Masley, and A. D. Goedeke (McDonnell Douglas Astronautics Co., Huntington Beach, Calif.) May 1972 13 p refs COSPAR, Plenary Meeting, 15th, Madrid, Spain, May 10-24, 1972, Paper 13 p Research supported by the McDonnell Douglas Independent Research and Development Program.

(Contract NAS5-9324; Grant NSF C-393)

The expected 30 and 50 MHz riometer absorptions have been calculated for three events in 1969 using data from the MDAC-W charged particle experiment on OGO 6. Several times during each event, the satellite passed over the MDAC-W Arctic and Antarctic Geophysical Observatories. The calculated total absorption (using 2 minute averages of the data) agrees well with the measured absorption for the overpasses. The alpha particle and electron contributions usually amount to less than a few percent of the proton absorption. During the large November 2, 1969 event, however, the electrons produced the major part of the absorption up to the peak and a significant contribution during virtually its entire duration. With the two frequencies for which simultaneous riometer data were taken, it is possible to detect the softening of the particle spectra during the events, and the relative hardness differences between events. (Author)

A72-32955*

LYMAN-ALPHA MEASUREMENTS OF NEUTRAL HYDROGEN IN THE OUTER GEOCORONA AND IN INTERPLANETARY SPACE.

G. E. Thomas and R. C. Bohlin (Colorado, University, Boulder, Colo.) 1 Jun. 1972 10 p refs Journal of Geophysical Research, vol. 77, June 1, 1972, p. 2752-2761. (Contract NAS5-9327; Grant NGR-06-003-052)

Results of hydrogen Lyman-alpha (1216 A) measurements made on a continuous basis by a two-channel photometer on OGO 5 from March 1968 to June 1971. The highly elliptical orbit provided measurements of both the outer geocorona and of the 1216-A sky background emission, since geocoronal scattering is minimal at the apogee distance of 150,000 km. Selected data (through 1970) are presented, as well as an interpretation of the three principal discoveries to date - namely, (1) a pronounced antisolar enhancement of the geocoronal scattering beyond 70,000 km which is regarded as evidence for a hydrogen geotail produced by solar Lyman-alpha radiation pressure; (2) a clear correlation of periodic variations in the sky background emission with solar activity associated with solar rotation; and (3) an annual variation of the 1216-A sky background emission, caused by the earth's orbital motion within the cavity created by the solar wind in the nearby interstellar hydrogen. (Author)

A72-32959*

GEOMAGNETICALLY TRAPPED CARBON, NITROGEN, AND OXYGEN NUCLEI.

A. Mogro-Campero (Chicago, University, Chicago, Ill.) 1 Jun. 1972 20 p refs Journal of Geophysical Research, vol. 77, June 1, 1972, p. 2799-2818.

(Contract NAS5-9366; Grants NSF GA-28368X; NGL-14-001-006)

Results of measurements carried out with the University of Chicago nuclear composition telescope on the OGO 5 satellite, establishing the presence of 13- to 33-MeV/nucleon geomagnetically trapped C and O nuclei, with some evidence for N nuclei. These trapped nuclei were found at L less than or equal to 5 and near the geomagnetic equator. The data cover the period from Mar. 3, 1968, to Dec. 31, 1969. The distribution of CNO flux as a function of L is given. No change in the intensity of the average trapped CNO flux was detected by comparing data for 1968 and 1969. The results reported set a new value for the observed high energy limit of trapping as described by the critical adiabaticity parameter. The penetration of solar flare CNO up to L = 4 was observed twice in 1968, in disagreement with Stormer theory predictions. The effects of these results on some models for the origin of the trapped radiation are discussed. (Author)

A72-32964*
LONGITUDINAL VARIATIONS OF THERMOSPHERIC COMPOSITION INDICATING MAGNETIC CONTROL OF POLAR HEAT INPUT.

A. E. Hedin and C. A. Reber (NASA, Goddard Space Flight Center, Greenbelt, Md.) 1 Jun. 1972 9 p refs *Journal of Geophysical Research*, vol. 77, June 1, 1972, p. 2871-2879.

Measurement of neutral N₂, O, and He densities from OGO 6 over the south polar region during magnetically quiet periods in late August and early September 1969. It is found that N₂ densities, when they are extrapolated to a common altitude, maximize at about 0800 UT near 70 deg invariant latitude. The density of He has a minimum at this time, and the density of O has a slight maximum. It is proposed that these phenomena are the result of cyclic variations in soft electron precipitation, which heats the thermosphere either directly or through enhanced Joule heating. This heat energy would increase the gas temperature, the increase in the gas temperature leading to the N₂ increase, and would vary the composition by generation of a wind system.

(Author)

A72-33869#
COSMIC-RAY ELECTRONS.

H. C. VanDeHulst Mar. 1972 15 p refs *Royal Astronomical Society, Quarterly Journal*, vol. 13, Mar. 1972, p. 10-24.

Some aspects of the search and study of cosmic ray electrons are discussed. The near-earth spectrum of cosmic-ray electrons in 1968 is compared with the interstellar spectrum derived from radio astronomy in 1971. The restriction of measurements to one year, or to a set of years, is shown to be judicious because of solar minimum. Methods of electron detection are described, including that of observing and isolating X-rays that arise from inverse Compton scattering of a photon off a cosmic ray electron. D.F.L.

A72-35089
SOFT X-RAY AND MICROWAVE OBSERVATIONS OF HOT REGIONS IN SOLAR FLARES.

H. S. Hudson (Tokyo Astronomical Observatory, Tokyo, Japan; California, University, La Jolla, Calif.) and K. Ohki (Tokyo Astronomical Observatory, Tokyo, Japan) Mar. 1972 14 p refs *Solar Physics*, vol. 23, Mar. 1972, p. 155-168. NSF supported research.

A72-35591*
HIGH-ENERGY ELECTRON SPIKES AT HIGH LATITUDES.

J. W. Brown (California Institute of Technology, Pasadena, Calif.) and E. C. Stone 1 Jul. 1972 13 p refs *Journal of Geophysical Research*, vol. 77, July 1, 1972, p. 3384-3396. NSF supported research. (Contract NAS5-3095; Grants NGL-05-002-007; NGR-05-002-160)

Observation of over 750 spikes of precipitating electrons with E greater than or equal to 425 keV aboard the low-altitude polar orbiter OGO 4 between July 30 and Dec. 31, 1967. The spikes may be divided into three distinct populations, depending on whether they occur at latitudes below, at, or above the local limit of trapping. These spikes are designated type 1, 2, and 3, respectively. Type 3 spikes occur in a narrow latitude band about 3 deg wide, centered at invariant latitude Lambda approximately equal to 78 deg at 1000 MLT (magnetic local time) and 68 deg at 2000 MLT. Type 3 spikes appear to be associated with spikes observed near the magnetopause and the neutral sheet. Type 2 spikes also occur in a latitude band about 3 deg wide, centered at about 71 deg at 1000 MLT and 67 deg at 2200 MLG. Type 2 spikes appear to be related to island fluxes in the neutral sheet, although they occur on closed field lines and may persist for many hours. Type 1 spikes occur in a wider band of latitudes, from about 62 deg to 68 deg near midnight and 66 deg to 68 deg near noon. Although they are observed on closed field lines, type 1 spikes do not persist for periods longer than about 1 hour, and it is concluded that they are

produced by strong pitch-angle scattering from the stably trapped population. (Author)

A72-35597*
PITCH-ANGLE DIFFUSION OF RADIATION BELT ELECTRONS WITHIN THE PLASMASPHERE.

L. R. Lyons, R. M. Thorne, and C. F. Kennel (California, University, Los Angeles, Calif.) 1 Jul. 1972 20 p refs *Journal of Geophysical Research*, vol. 77, July 1, 1972, p. 3455-3474.

(Contract F19628-71-C-0075; Grants NGR-05-007-190; NSF GA-28045)

Study of the formation of the quiet-time electron slot, which divides the radiation belt electrons into an inner and an outer zone. The pitch-angle diffusion of radiation belt electrons resulting from resonant interactions with the observed plasmaspheric whistler-mode wave band is quantitatively investigated. The effects of wave propagation obliquely to the geomagnetic field direction with the resulting diffusion at all cyclotron-harmonic resonances and the Landau resonance are evaluated along with the effects of interactions occurring at all geomagnetic latitudes. The results obtained account for the long-term stability of the inner radiation zone, the location of its outer edge as a function of electron energy, and the removal of electrons to levels near zero throughout the slot. Computed pitch-angle distributions and precipitation decay rates are in good agreement with slot-region observations. (Author)

A72-35599*
TURBULENCE OF ELECTROSTATIC ELECTRON CYCLOTRON HARMONIC WAVES OBSERVED BY OGO-5.

H. Oya (NASA, Goddard Space Flight Center, Greenbelt, Md.) 1 Jul. 1972 12 p refs *Journal of Geophysical Research*, vol. 77, July 1, 1972, p. 3483-3494.

Analysis of VLF emissions that have been observed near 3/2, 5/2, and 7/2 f sub H by OGO 5 in the magnetosphere (f sub H is the electron cyclotron frequency) in the light of the mechanism used for the diffuse plasma resonance f sub Dn observed by Alouette 2 and Isis 1. The VLF emission is considered to be generated by nonlinear coupling mechanisms in certain portions of the observation as the f sub Dn is enhanced by its association with nonlinear wave-particle interaction of the electrostatic electron cyclotron harmonic wave, including the instability due to the nonlinear inverse Landau damping mechanism in the turbulence. The difference between the two observations is in the excitation mechanism of the turbulence; the turbulence in the plasma trough detected by OGO 5 is due to natural origins, whereas the ionospheric topside sounder makes the plasma wave turbulence artificially by submitting strong stimulation pulses. Electron density values in the plasma trough are deduced by applying the f sub Dn-f sub N/f sub H relationship obtained from the Alouette 2 experiment as well as by applying the condition for the wave-particle nonlinear interactions. The electron density values reveal good agreement with the ion density values observed simultaneously by the highly sensitive ion mass spectrometer. (Author)

A72-35603
GEOMAGNETIC EFFECT ON THE NEUTRAL TEMPERATURE OF THE F REGION DURING THE MAGNETIC STORM OF SEPTEMBER 1969.

J. E. Blamont and J. M. Luton (CNRS, Service d'Aeronomie, Verrieres-le-Buisson, Essonne, France) 1 Jul. 1972 23 p refs *Journal of Geophysical Research*, vol. 77, July 1, 1972, p. 3534-3556.

(Contracts CNES-65-008; CNES-66-011; CNES-67-201; CNES-68-202; CNES-69-225; CNES-70-299; CNES-71-201)

A72-35604*
ANALYSIS OF OGO-6 OBSERVATIONS OF THE O I

A577-A TROPICAL NIGHTGLOW.

R. J. Thomas and T. M. Donahue (Pittsburgh, University, Pittsburgh, Pa.) 1 Jul. 1972 9 p refs Journal of Geophysical Research, vol. 77, July 1, 1972, p. 3557-3565. (Contract NAS5-11077)

Atomic oxygen green line data from the horizon scanning photometer on OGO 6 have been examined. Unfolding the satellite data from the tropical F region yields altitude and latitude variations of the O(1S) emissions. The spatial variations of the tropical F-region electron density are then calculated by assuming dissociative recombination and using a model atmosphere. Where comparisons to ground based data are possible the results are good. Thus, the satellite observations constitute a form of topside sounding of the ionosphere below the F peak and provide synoptic data about this portion of the ionosphere that are otherwise impractical to obtain. (Author)

A72-35619***DETECTION OF SOLAR-WIND ELECTRON PLASMA FREQUENCY FLUCTUATIONS IN AN OBLIQUE NONLINEAR MAGNETOHYDRODYNAMIC WAVE.**

R. W. Fredricks, F. L. Scarf (TRW Systems Group, Redondo Beach, Calif.), C. T. Russell (California, University, Los Angeles, Calif.), and M. Neugebauer (California Institute of Technology, Jet Propulsion Laboratory, Pasadena, Calif.) 1 Jul. 1972 4 p refs Journal of Geophysical Research, vol. 77, July 1, 1972, p. 3598-3601. (Contracts NAS5-9278; NAS5-9098)

Millimeter-wavelength signals are being investigated to determine their possible use in a near earth environment for remote detection purposes. Both radiometric and radar systems concepts are being considered. A typical radiometric application is discussed. Severe attenuation of the signal occurs in the atmospheric propagation path at certain wavelengths as a result of resonance absorption by water vapor and oxygen molecules. Undesirable radar reflections from the terrain occur when operating at low grazing angles. The magnitude of the interference is a function of antenna beamwidth and reflectivity of the intervening terrain. The effect of these multipath signals on the 70 GHz antenna pointing error is treated. The objects to be detected are often partially obscured by foliage and trees. Radar and radiometric measurements of this effect at 35, 70, and 140 GHz are discussed. M.M.

A72-35989***SATELLITE AND GROUND-BASED OBSERVATIONS OF A RED ARC.**

A. F. Nagy (Michigan, University, Ann Arbor, Mich.), W. B. Hanson (Texas, University, Dallas, Tex.), R. J. Hoch (Battelle Pacific Northwest Laboratories, Richland, Wash.), and T. L. Aggson (NASA, Goddard Space Flight Center, Greenbelt, Md.) 1 Jul. 1972 5 p refs Journal of Geophysical Research, vol. 77, July 1, 1972, p. 3613-3617. (Contracts NAS5-9306; NAS5-9311; AT(45-1)-1830; Grant NSF GA-31464)

The results of simultaneous satellite and ground-based observations carried out during the red-arc period of August 8-9, 1970, are discussed in the light of present day theory. The formation of the arc at the electron temperature peak and density trough seems to support the thermal-conduction theory of red-arc formation. M.V.E.

A72-38728***GEOMAGNETIC CUTOFFS FOR COSMIC-RAY PROTONS FOR SEVEN ENERGY INTERVALS BETWEEN 1.2 AND 39 Mev**

J. L. Faselow (California Institute of Technology, Jet Propulsion Laboratory, Pasadena, Calif.) and E. C. Stone (California Institute of Technology, Pasadena, Calif.) 1 Aug. 1972 11 p refs Journal of Geophysical Research, vol. 77, Aug. 1, 1972, p. 3999-4009. (Contract NAS5-3095; Grants NGL-05-002-007; NGR-05-002-160)

A72-39401***MEASUREMENTS OF ELECTRON DETECTION EFFICIENCIES IN SOLID STATE DETECTORS.**

J. E. Lupton and E. C. Stone (California Institute of Technology, Pasadena, Calif.) Jan. 1972 3 p refs Nuclear Instruments and Methods, vol. 98, Jan. 1972, p. 189-191. (Contracts NAS5-3095; NAS5-9315; Grants NGR-05-002-160; NGL-05-002-007)

Detailed laboratory measurement of the electron response of solid state detectors as a function of incident electron energy, detector depletion depth, and energy-loss discriminator threshold. These response functions were determined by exposing totally depleted silicon surface barrier detectors with depletion depths between 50 and 1000 microns to the beam from a magnetic beta-ray spectrometer. The data were extended to 5000 microns depletion depth using the results of previously published Monte Carlo electron calculations. When the electron counting efficiency of a given detector is plotted as a function of energy-loss threshold for various incident energies, the efficiency curves are bounded by a smooth envelope which represents the upper limit to the detection efficiency. These upper limit curves, which scale in a simple way, make it possible to easily estimate the electron sensitivity of solid-state detector systems. (Author)

A72-39541***PROPERTIES OF LOW ENERGY PARTICLE IMPACTS IN THE POLAR DOMAIN IN THE DAWN AND DAYSIDE HOURS.**

R. A. Hoffman (NASA, Goddard Space Flight Center, Greenbelt, Md.) 1972 22 p refs In: Magnetosphere-ionosphere interactions; Proceedings of the Advanced Study Institute, Dalseter, Norway, April 14-23, 1971, Oslo, Universitetsforlaget, 1972, p. 117-138.

A72-39544***THE PLASMAPAUSE AS MEASURED IN POSITIVE IONS.**

G. W. Sharp, C. R. Chappell, and K. K. Harris (Lockheed Research Laboratories, Palo Alto, Calif.) 1972 15 p refs In: Magnetosphere-ionosphere interactions; Proceedings of the Advanced Study Institute, Dalseter, Norway, April 14-23, 1971 Oslo, Universitetsforlaget, 1972, p. 169-183. (Contract NAS5-9092)

Use of extensions of the existing theory of magnetospheric convection to describe the dynamics of the plasmasphere and the variation in the plasmapause location. The equatorial local time plane is divided into three separate and physically distinct regions, the bulge region, the nightside region, and the dayside region, corresponding to local times of 1500 to 2200 hrs, 2200 to 0600 hrs, and 0600 to 1500 hrs, respectively. The characteristics predicted by the model in the bulge region are: presence of the bulge at dust, 1/R to the 4th power radial dependence of plasma concentration, and large fluctuations in plasma density at the plasmapause and plasma detachment. In the nightside region the predicted characteristics are: rapid response to magnetic activity changes, formative region for plasmasphere ripples, and the formative region for the dayside plasmapause location. The model also predicts the dayside plasmasphere characteristics, such as the slow response to magnetic activity changes, and filling of the plasmasphere from the ionosphere, including the formation of a double plasmapause. (Author)

A72-39980***THE HARANG DISCONTINUITY IN AURORAL BELT IONOSPHERIC CURRENTS.**

J. P. Heppner (NASA, Goddard Space Flight Center, Greenbelt, Md.) Jun. 1972 16 p refs Geofysiske Publikasjoner (Geophysica Norvegica), vol. 22, June 1972, p. 105-120.

Discussion of the nature of a discontinuity in the ionospheric current of the auroral belt whose existence was suggested by Harang in 1946. Convection characteristics, time variability, and current continuity in the auroral belt are

considered in a context of observations and arguments supporting the reality of Harang's discontinuity. V.Z.

A72-42016*

MOLECULAR IONS IN THE F2 LAYER.

H. Rishbeth (Science Research Council, Radio and Space Research Station, Slough, Bucks., England), P. Bauer (CNET, Issy-les-Moulineaux, Hauts-de-Seine, France), and W. B. Hanson (Texas, University, Dallas, Tex.) Aug. 1972 11 p refs Planetary and Space Science, vol. 20, Aug. 1972, p. 1287-1297.

(Contract NASS-9311; Grant NGL-44-004-001)

Data on ion concentrations at heights of 400-500 km, obtained by the OGO 6 satellite, suggest that the $O(+)$ and molecular ion concentrations are sometimes anticorrelated. To assist in explaining this phenomenon, a table of the chemical reactions most likely to control the molecular ion concentrations is drawn up, and its validity tested with the aid of data from rocket-borne mass spectrometers at heights of 220-400 km. The anticorrelation of $O(+)$ and $NO(+)$ ions by day is thought to be due to the importance of a reaction between $N_2(+)$ ions and O atoms; the main source of $N_2(+)$ above 300 km is probably charge-exchange between N_2 and $O(+)$, the latter being produced by photoionization. However, at night another source of $NO(+)$ ions is required, which may be $N(+)$ ions that are either stored in the magnetosphere or are produced from $He(+)$ and N_2 .

(Author)

A72-42043*

TYPE 3 SOLAR NOISE OBSERVED BELOW 100 kHz ON OGO-3.

N. Dunckel, R. A. Helliwell (Stanford University, Stanford, Calif.), and J. Vesecky (Stanford University, Stanford; Stanford Research Institute, Menlo Park, Calif.) Jul. 1972 13 p refs Solar Physics, vol. 25, July 1972, p. 197-209.

(Contract NASS-11387; Grants NGR-05-020-288; NGL-05-020-014)

Type III solar noise bursts have been observed in the frequency range 25-100 kHz with VLF detector on OGO 3. The bursts decrease in frequency from 100 kHz (the highest frequency of observation) to as low as 25 kHz in approximately 45 min. The intensity at 100 kHz increases for about 20 min, then decays over a period of approximately 1 hr. The variation of the intensity with time becomes less regular at lower frequencies. Bursts are predominantly associated with west-limb flares. Their commencement 100 kHz tends to follow type III bursts observed at 2-4 MHz by about 10 min. Observed drift rates and decay times correspond roughly to those extrapolated from higher frequency measurements.

(Author)

A72-42406*

SPATIAL DISTRIBUTION OF ENERGETIC PLASMA SHEET ELECTRONS.

R. J. Walker and T. A. Farley (California, University, Los Angeles, Calif.) 1 Sep. 1972 11 p refs Journal of Geophysical Research, vol. 77, Sept. 1, 1972, p. 4650-4660. (Contract NASS-9097)

The spatial distribution of energetic plasma sheet electrons (E greater than 50 keV) out to a radial distance of 24 earth radii using data from electron spectrometer and fluxgate magnetometer experiments on OGO 5 is presented. A comparison of distributions in geocentric solar magnetospheric coordinates (GSM) prepared with and without the use of a neutral sheet model indicates that the use of such a model facilitates organization of plasma sheet data. The percentage of flux occurrence above a given flux threshold falls off rapidly with distance from the neutral sheet. Contours of constant percentage of occurrence diverge slightly from the neutral sheet at local times away from midnight. This effect decreases with increasing flux threshold. (Author)

A72-42416

POWER-LAW WAVENUMBER SPECTRUM DEDUCED FROM IONOSPHERIC SCINTILLATION OBSERVA-

TIONS.

C. L. Rufenach (NOAA, Space Environment Laboratory, Boulder, Colo.) 1 Sep. 1972 12 p refs Journal of Geophysical Research, vol. 77, Sept. 1, 1972, p. 4761-4772. ARPA supported research. (ARPA Order 1361)

Ionospheric scintillation observations near Boulder, Colorado, from the radio source Cygnus A were spectral analyzed at 26 MHz. The scintillation spectral features are used to calculate the diffraction effects and hence deduce the F-region irregularity wavenumber spectrum for sizes from about 4 to 0.6 km. An example based on the Gaussian spectrum shows that the extrapolation to radio frequencies much higher than 26 MHz will not explain the observed equatorial and auroral scintillations. Abrupt changes in electron density are required to support the higher-wavenumber spectral densities that cause these higher-frequency scintillations. These abrupt density changes can be represented by a power-law wavenumber spectrum.

(Author)

A72-42418

THEORETICAL CALCULATIONS OF THE F-REGION TROPICAL ULTRAVIOLET AIRGLOW INTENSITY.

D. N. Anderson (Cooperative Institute for Research in Environmental Sciences, Boulder, Colo.) 1 Sep. 1972 8 p refs Journal of Geophysical Research, vol. 77, Sept. 1, 1972, p. 4782-4789.

Far ultraviolet airglow emissions at 1304 and 1356 Å from atomic oxygen have been observed to exist in two bands or arcs 12 to 15 deg north and south of the magnetic equator, the height-integrated intensity of the emissions maximizing between 2100 and 2200 LT during equinox. Two of the mechanisms thought to be responsible for producing the excited states of atomic oxygen are neutralization and radiative recombination. To investigate the contribution made by each process, the daily variation of the column emission rate from 20 deg N to 20 deg S dip latitude in the ionospheric F region is theoretically calculated by numerically solving the time-dependent electron continuity equation, taking into account the effects of production, loss, ambipolar diffusion, and neutral winds. Of the two mechanisms, radiative recombination produces results that are in better agreement with the observations, although the calculated emission rates are still lower than the observed values. (Author)

A72-42431*

NEUTRAL COMPOSITION IN THE THERMOSPHERE.

D. R. Tausch and G. R. Carignan (Michigan, University, Ann Arbor, Mich.) 1 Sep. 1972 7 p refs Journal of Geophysical Research, vol. 77, Sept. 1, 1972, p. 4870-4876. (Contract NASS-9328)

Data obtained from the OGO 6 neutral atmospheric composition (NAC) experiment for a period of more than 1 year are used to compare the average constituent composition at an altitude of 400 km with that predicted by the Jacchia 1971 and 1965 models. The comparison shows that the Jacchia 1971 model underestimates the molecular nitrogen densities at 400 km by a factor of 2. An atmosphere is constructed down to 120 km by means of the Stein and Walker technique. A fit is made with (1) the 400-km total densities from drag measurements and the composition from OGO 6 NAC, (2) the 250-km measured molecular nitrogen densities, and (3) the 150-km total densities from drag. This fit shows that the Jacchia 1971 model overestimates the atomic oxygen content at 150 km. (Author)

A72-42432*

POLAR-CAP ELECTRIC FIELD DISTRIBUTIONS RELATED TO THE INTERPLANETARY MAGNETIC FIELD DIRECTION.

J. P. Heppner (NASA, Goddard Space Flight Center, Greenbelt, Md.) 1 Sep. 1972 11 p refs Journal of Geophysical Research, vol. 77, Sept. 1, 1972, p. 4877-4887.

Data from successive OGO-6 passes over southern and northern high latitudes are presented to illustrate how grossly

asymmetric the distribution of electric field magnitudes can sometimes be. They are also shown to provide an example of the anticorrelation between southern and northern polar-cap magnitude distributions. Signature classification, correlations, and possible relations with interplanetary magnetic fields are discussed. M.V.E.

A72-42901*
SATELLITE MEASUREMENTS OF HIGH LATITUDE CONVECTION ELECTRIC FIELDS.

D. P. Cauffman and D. A. Gurnett (Iowa, University, Iowa City, Iowa) Jul. 1972 42 p refs Space Science Reviews, vol. 13, July 1972, p. 369-410.
 (Contracts NASS-10625; NAS1-8141; NAS1-8144; NAS1-8150; N00014-68-A-0196-0003; Grant NGL-16-001-043)
 (AD-750221)

This paper reviews the first results of satellite experiments to measure magnetospheric convection electric fields using the double-probe technique. The earliest successful measurements were made with the low-altitude (680-2530 km) polar orbiting Injun-5 spacecraft. The Injun-5 results are compared with the initial findings of the electric field experiment on the polar orbiting OGO-6 satellite. Electric field measurements from the OGO-6 satellite have substantiated many of the initial Injun-5 observations with improved accuracy and sensitivity. The OGO-6 detector revealed the persistent occurrence of anti-sunward convection across the polar cap region at velocities not generally detectable with the Injun-5 experiment. The OGO-6 observations also provided information indicating that the location of the electric field reversal shifts equatorward during periods of increased magnetic activity. The implications of the electric field measurements of magnetospheric and auroral structure are summarized, and a list of specific recommendations for improving future experiments is presented. (Author)

A72-42902*
FLUCTUATING MAGNETIC FIELDS IN THE MAGNETOSPHERE. 2: ULF WAVES.

R. L. McPherron, C. T. Russell, and P. J. Coleman, Jr. (California, University, Los Angeles, Calif.) Jul. 1972 44 p refs Space Science Reviews, vol. 13, July 1972, p. 411-454.
 (Contract NASS-9098; Grants NSF GA-28907; NGL-05-007-004)

At the present time the existing satellite observations of ULF waves suggest that the level of geomagnetic activity controls the types of waves which occur within the magnetosphere. Consequently, we consider separately quiet times, times of magnetospheric substorms, and times of magnetic storms. Within each of these categories, there are distinctly different wave modes distinguished by their polarization: either transverse or parallel to the ambient field. In addition, these wave phenomena occur in distinct frequency bands. In terms of the standard nomenclature of ground micropulsation studies ULF wave types observed in the magnetosphere include quiet time transverse Pc 1, Pc 3, Pc 4, Pc 5; quiet time compressional - Pc 1 and Pi 1 sub storm compressional Pi 1 and Pi 2; storm transverse - Pc 1; storm compressional Pc 4, 5. (Author)

A72-44513*
OUTER MAGNETOSPHERE NEAR MIDNIGHT AT QUIET AND DISTURBED TIMES.

M. P. Aubry, M. G. Kivelson, R. L. McPherron, and C. T. Russell (California, University, Los Angeles, Calif.) 1 Oct. 1972 16 p refs Journal of Geophysical Research, vol. 77, Oct. 1, 1972, p. 5487-5502. Research supported by the European Space Research Organization.
 (Contracts NASS-9097; NASS-9098; Grant NGR-05-007-305)

OGO 5 magnetic-field and energetic-electron (E greater than 50 keV) data are used to study both the quiet-time, steady-state configuration of the outer magnetosphere or near tail region near midnight and the disturbed time changes of

this configuration. The nighttime cusp is found to be a distinct feature within the plasma sheet at quiet times but indistinguishable from the plasma sheet at disturbed times. The sequence of thinning and expansion of the plasma sheet in this region in association with the substorms is studied. The response of the plasma sheet in the near tail at about 10 earth radii is found to be similar to that in the more distant tail at more than 20 earth radii. Finally, the nature of field-aligned currents flowing on the plasma-sheet boundary is investigated. Assuming infinite current sheets, the sheet current density at OGO 5 is found to be approximately .01 A/m. (Author)

A72-44516*
SOURCE AND IDENTIFICATION OF HEAVY IONS IN THE EQUATORIAL F LAYER.

W. B. Hanson, D. L. Sterling (Texas, University, Dallas, Tex.), and R. F. Woodman (Jicamarca Radio Observatory, Lima, Peru) 1 Oct. 1972 12 p refs Journal of Geophysical Research, vol. 77, Oct. 1, 1972, p. 5530-5541.
 (Contract NASS-9311; Grant NGL-44-004-001)

Further evidence is presented to show that the interpretation of some OGO 6 retarding potential analyzer (RPA) results in terms of ambient Fe⁺ ions is correct. The Fe⁺ ions are observed only within dip latitudes of plus or minus 30 deg, and the reason for this latitudinal specificity is discussed in terms of a low-altitude source region and F region diffusion and electrodynamic drift. It is shown that the polarization field associated with the equatorial electrojet will raise ions to 160 km out of a chemical source region below 100 km but it will do so only in a narrow region centered on the dip equator. Subsequent vertical ExB drift, coupled with motions along the magnetic fields, can move the ions to greater heights and greater latitudes. There should be a resultant fountain of metallic ions rising near the equator that subsequently descends back to the E and D layers at tropical latitudes. (Author)

A72-44522*
ELECTRON POLAR CAP AND THE BOUNDARY OF OPEN GEOMAGNETIC FIELD LINES.

L. C. Evans (California Institute of Technology, Pasadena; NASA, Ames Research Center, Moffett Field, Calif.) and E. C. Stone 1 Oct. 1972 5 p refs Journal of Geophysical Research, vol. 77, Oct. 1, 1972, p. 5580-5584.
 (Contract NASS-3095; Grant NGR-05-002-160)

A total of 333 observations of the boundary of the polar access region for electrons (energies greater than 530 keV) provides a comprehensive map of the electron polar cap. The boundary of the electron polar cap, which should occur at the latitude separating open and closed field lines, is consistent with previously reported closed field line limits determined from trapped-particle data. The boundary, which is sharply defined, seems to occur at one of three discrete latitudes. Although the electron flux is generally uniform across the polar cap, a limited region of reduced access is observed about 10% of the time. (Author)

A72-44523*
CYCLOTRON DRIFT INSTABILITY IN THE BOW SHOCK.

C. S. Wu (Maryland, University, College Park, Md.) and R. W. Fredricks (TRW Systems Group, Redondo Beach, Calif.) 1 Oct. 1972 5 p refs Journal of Geophysical Research, vol. 77, Oct. 1, 1972, p. 5585-5589.
 (Contract NASS-9278; Grant NGL-21-002-005)

It is argued that the cyclotron drift instability (coupled ion waves and electron Bernstein modes) can explain many structural features of the weak electrostatic turbulence observed in bow shock magnetic-field gradients and thus that it provides a more attractive speculation than the ion acoustic or Buneman instabilities previously suggested as weak turbulence sources. (Author)

A72-44850*
BEHAVIOR OF OUTER RADIATION ZONE AND A NEW

MODEL OF MAGNETOSPHERIC SUBSTORM.

G. K. Parks (Washington, University, Seattle, Wash.), G. Laval, and R. Pellat (Commissariat a l'Energie Atomique, Centre d'Etudes Nucleaires de Fontenay-aux-Roses, Fontenay-aux-Roses, Hauts-de-Seine, France) Sep. 1972 18 p refs Planetary and Space Science, vol. 20, Sept. 1972, p. 1391-1408. International Union of Geodesy and Geophysics, Symposium on the Morphology and Physics of Magnetospheric Substorms, Moscow, USSR, Aug. 3, 1971, (Contract NAS5-9542; Grant NSF GU-2655)

This paper presents particle data obtained from synchronous altitudes and attempts to evaluate the origin and nature of particle flux variations observed during substorms. The correlated particle intensities, time variations, and energy spectrums are compared between the equatorial and auroral zones. The correlated particle and field observations during substorms are tied together and a model of magnetospheric substorms is derived. Among the features predicted by the model is the poleward expansion of visual auroras observed at the onset of magnetospheric substorms. The model also explains how substorms are triggered in a few minutes time scale during sudden commencements.

(Author)

A72-44854*

ELECTRIC FIELD VARIATIONS DURING SUBSTORMS: OGO-6 MEASUREMENTS.

J. P. Heppner (NASA, Goddard Space Flight Center, Greenbelt, Md.) Sep. 1972 24 p refs Planetary and Space Science, vol. 20, Sept. 1972, p. 1475-1498. International Union of Geodesy and Geophysics, Symposium on the Morphology and Physics of Magnetospheric Substorms, Moscow, USSR, Aug. 3, 1971

The general pattern of high electric fields in magnetic-time invariant latitude coordinates is reviewed in the light of OGO-6 electric field measurements. This pattern is found to show little variability and, when unusual variations or field distributions occur, they are relatively isolated in time and space. Significant indications of direct correlation between electric field behavior and stages of magnetic bay development have not been found.

M.V.E.

A72-44856*

SUBSTORM RELATED CHANGES IN THE GEOMAGNETIC TAIL: THE GROWTH PHASE.

R. L. McPherron (California, University, Los Angeles, Calif.) Sep. 1972 19 p refs Planetary and Space Science, vol. 20, Sept. 1972, p. 1521-1539. International Union of Geodesy and Geophysics, Symposium on the Morphology and Physics of Magnetospheric Substorms, Moscow, USSR, Aug. 3, 1971

(Grant NGR-05-007-305)

The details of two substorms of August 15, 1968, are discussed, and the sequence of events occurring during a magnetospheric substorm is established. Special attention is given to the substorm effects on the geometry of the near tail region and, particularly, to the growth and expansion phases.

M.V.E.

A72-44857*

NOISE IN THE GEOMAGNETIC TAIL.

C. T. Russell (California, University, Los Angeles, Calif.) Sep. 1972 13 p refs Planetary and Space Science, vol. 20, Sept. 1972, p. 1541-1553. International Union of Geodesy and Geophysics, Symposium on the Morphology and Physics of Magnetospheric Substorms, Moscow, USSR, Aug. 3, 1971.

(Contract NAS5-9098)

Present observations have revealed a variety of magnetic wave phenomena in the tail, from ULF to ELF frequencies. However, only VLF measurements of electric fields have been made. These measurements reveal that the tail is electrically quiet at VLF frequencies, except in the near-earth plasma sheet during substorm expansion phases. The magnetic waves observed include: waves with periods of about 2 min which cause the plasma sheet boundary position and the

neutral sheet location to oscillate; waves from .1 to 1 Hz which occur throughout the plasma sheet during plasma sheet expansions; and ELF waves which occur sporadically in the plasma sheet.

(Author)

A72-45593

DISTRIBUTION OF HYDROGEN AND HELIUM IN THE UPPER ATMOSPHERE.

G. Kockarts (Institut d'Aeronomie Spatiale de Belgique, Brussels, Belgium) Oct. 1972 15 p refs Journal of Atmospheric and Terrestrial Physics, vol. 34, Oct. 1972, p. 1729-1743. Conference on Theoretical Ionospheric Models, University Park, Pa., June 14-16, 1971

A73-10878

GLOBAL SATELLITE MEASUREMENTS OF NITRIC OXIDE.

D. W. Rusch and C. A. Barty (Colorado, University, Boulder, Colo.) 1972 3 p In: Symposium on D- and E-Region Ion Chemistry, Urbana, Ill., July 6-8, 1971, Informal Record Urbana, University of Illinois, 1972, p. 32-34.

An Ebert-Fastie scanning spectrometer mounted on board the polar orbiting satellite OGO 4 was used to measure nitric oxide (1.0) gamma emission at 2150 A in twilight orbits. Local phenomena in the polar regions are judged to be responsible for high variations in the emission rate with respect to time and latitude in these regions. A regular nitric-oxide emission increase is seen during the summer and winter months as a function of latitude.

T.M.

A73-11389*

THE IMPULSIVE X-RAY BURST OF OCTOBER 10, 1970.

S. R. Kane (California, University, Berkeley, Calif.), S. W. Kahler, and J. D. Kurfess (U.S. Navy, E. O. Hulburt Center for Space Research, Washington, D.C.) Aug. 1972 7 p refs Solar Physics, vol. 25, Aug. 1972, p. 418-424. (Contract NAS5-9094; Grants NSF GP-29794; NSF GP-27215)

An impulsive burst of 100-400 keV solar X-rays associated with a small solar flare was observed on October 10, 1970 with a large area scintillator aboard a balloon. The X-ray burst was also observed simultaneously in 10-80 keV range by the OGO 5 satellite and in 8-20 A range by the SOLRAD 9 satellite. The event is attributed to an H-alpha subflare located approximately at S13, E88 on the solar disk. The spectral characteristics of this event are examined in the light of the earlier X-ray observations of small solar flares.

(Author)

A73-11391

THE ROLE OF ENERGETIC ELECTRONS IN THE CORRELATION OF METER AND DECIMETER TYPE III BURSTS WITH 4 KEV X-RAY EMISSION.

S. W. Kahler (U.S. Navy, E. O. Hulburt Center for Space Research, Washington, D.C.) Aug. 1972 17 p refs Solar Physics, vol. 25, Aug. 1972, p. 435-451. (Grant NSF GP-29794)

A73-11732*

EQUATORIAL CURRENT SHEET IN THE MAGNETOSPHERE.

M. Sugiura (NASA, Goddard Space Flight Center, Laboratory for Space Physics, Greenbelt, Md.) 1 Nov. 1972 11 p refs Journal of Geophysical Research, vol. 77, Nov. 1, 1972, p. 6093-6103.

The delta B distribution deduced from the OGO 3 and 5 satellites shows large field depressions in the equatorial region inside the plasmasphere. On the basis of the delta B distribution, it is shown that what is usually considered the quiet-time ring current is an equatorial sheet current that is an extension of the neutral sheet current in the magnetospheric tail. The primary source of the large field reductions inside the plasmasphere is a population of protons with energies

of 0.1-1 Mev initially detected by Davis and Williamson (1963) and Davis (1965) on Explorer 12, 14, and 15. Low-energy protons extensively measured on OGO 3 by Frank (1967, 1971) are primarily responsible for the current near and outside the plasmopause. (Author)

A73-11904*

THE LIGHT ION TROUGH.

H. A. Taylor, Jr. (NASA, Goddard Space Flight Center, Laboratory for Planetary Atmospheres, Greenbelt, Md.) Oct. 1972 14 p refs Planetary and Space Science, vol. 20, Oct. 1972, p. 1593-1605.

A distinct feature of the ion composition results from the OGO 2, 4 and 6 satellites is the light ion trough, wherein the mid-latitude concentrations of H(+) and He(+) decrease sharply with latitude. In contrast to the 'main trough' in electron density observed primarily as a nightside phenomenon, the light ion trough persists during both day and night. For daytime winter hemisphere conditions and for all seasons during night, the mid-latitude light ion concentration decrease is a pronounced feature. In the dayside summer and equinox hemispheres, the rate of light ion decrease with latitude is comparatively gradual, and the trough boundary is less well defined, particularly for quiet magnetic conditions. In response to magnetic storms, the light ion trough minimum moves equatorward, and deepens, consistent with earlier evidence of the contraction of the plasmasphere in response to storm time enhancements in magnetospheric plasma convection. (Author)

A73-12320#

PLASMASPHERE DYNAMICS INFERRED FROM OGO-5 OBSERVATIONS.

C. R. Chappell, K. K. Harris, and G. W. Sharp (Lockheed Research Laboratories, Palo Alto, Calif.) 1972 9 p refs In: Space research XII; Proceedings of the Fourteenth Plenary Meeting, Seattle, Wash., June 18-July 2, 1971. Volume 2, Berlin, East Germany, Akademie-Verlag GmbH, 1972, p. 1513-1521.

Data from the light ion mass spectrometer aboard OGO 5 during the period from March 1968 through February 1969 has given a complete local time coverage of the plasmasphere. Inbound and outbound profiles of H(+) He(+) and $O(+)+N(+)$ ions have been measured once every 2-1/2 days from an initial perigee height of 300 km to an apogee of about 23 earth radii during this year period. Although the ion motion cannot be directly measured by the instrument, the plasmasphere dynamics can be inferred through an examination of the changes in plasmasphere profile between consecutive orbits. These dynamics are discussed, and a model of the plasmasphere is developed. Examples of these dynamic processes include dayside filling of the plasmasphere, peeling away of the outer portions of the plasmasphere in the afternoon-dusk sector, and inward convective motions of the plasmasphere on the nightside. (Author)

A73-12323*#

NEW INTERPRETATIONS OF EXTRATERRESTRIAL LYMAN-ALPHA OBSERVATIONS.

P. W. Blum (NASA, Goddard Space Flight Center, Greenbelt, Md.) and H. J. Fahr (Bonn, Universitaet, Bonn, West Germany) 1972 9 p refs In: Space research XII; Proceedings of the Fourteenth Plenary Meeting, Seattle, Wash., June 18-July 2, 1971. Volume 2, Berlin, East Germany, Akademie-Verlag GmbH, 1972, p. 1569-1577.

The solar Lyman-alpha radiation pressure affects the orbits and the velocities of the interstellar particles entering the solar system. This leads to enhanced particle losses in the heliosphere, since particles spend a longer time crossing it. This causes a stronger decrease of the density with decreasing distances from the sun than had been calculated without accounting for the radiation pressure. Furthermore, the emission pattern of the solar Lyman-alpha radiation is anisotropic and rotates with the sun in a 27-day period. This causes a temporal change in the location of the intensity

extrema. At the same time it produces hydrogen density anisotropies with extreme deviating in their directions from those which had been calculated without consideration of the radiation pressure. (Author)

A73-12442

SHADOWING OF ELECTRON AZIMUTHAL-DRIFT MOTIONS NEAR THE NOON MAGNETOPOUSE.

H. I. West, Jr., R. M. Buck, and J. R. Walton (California, University, Livermore, Calif.) 6 Nov. 1972 2 p Nature Physical Science, vol. 240, Nov. 6, 1972, p. 6, 7.

A73-13719*

THE ABUNDANCES OF SOLAR ACCELERATED NUCLEI FROM CARBON TO IRON.

A. Mogro-Campero (Chicago, University, Chicago, Ill.) and J. A. Simpson 1 Oct. 1972 5 p refs Astrophysical Journal, vol. 177, Oct. 1, 1972, pt. 2, p. L37-L41. (Contract NAS5-9366; Grants NSF GA-28368XA; NGL-14-001-006)

Revised observation periods and new data are found to confirm previous evidence that the overabundance of solar-flare nuclei with respect to solar photospheric and coronal abundances increases with increasing atomic number. It is also verified that enhancements can vary from flare to flare and that this variability is large enough to explain the differences observed by various investigators regarding the magnitude of solar-flare high-Z particle enhancements. Additional evidence for a two-stage solar acceleration mechanism is obtained. It is shown that the galactic cosmic-ray source composition displays a similar overabundance as a function of atomic number. V.P.

A73-13855*

MAGNETIC AND ELECTRIC WAVES IN SPACE.

C. T. Russell (California, University, Los Angeles, Calif.) Dordrecht, D. Reidel Publishing Co., 1972, p. 39-50 1972 12 p refs In: Earth's magnetospheric processes; Proceedings of the Symposium, Cortina, Italy, August 30-September 10, 1971.

(Contract NAS5-9098)

Waves play a fundamental role in many processes occurring in the solar wind and in the magnetosphere. These waves have been observed by a variety of experiments on many different spacecraft and analyzed with an increasing number of different techniques. In this review, we examine a number of the recent observations of waves in space, discussing the role of waves in the various regions and their characteristics, and illustrating some of their techniques used in their analysis. (Author)

A73-13871*

REVIEW OF MAGNETIC FIELD OBSERVATIONS.

N. F. Ness (NASA, Goddard Space Flight Center, Laboratory for Extraterrestrial Physics, Greenbelt, Md.) Dordrecht D. Reidel Publishing Co., 1972, p. 189-199. 1972 11 p refs In: Earth's magnetospheric processes; Proceedings of the Symposium, Cortina, Italy, August 30-September 10, 1971.

Recent observations in previously unexplored regions of the magnetosphere, particularly in the polar-cusp region, compliment and reinforce emphasis on particle access to the plasma sheet via the polar neutral points. Significant distortions of the geomagnetic field in the polar-cusp region suggest field-aligned currents at large geocentric distances which can be related to low-altitude polar-cap phenomena. Studies of the microstructure of the field reversal region of the plasma sheet embedded in the geomagnetic tail suggest a periodic structure of more complexity than earlier assumed simplified single neutral-line models. (Author)

A73-13883*

ELECTROSTATIC WAVES IN THE MAGNETOSPHERE

F. L. Scarf and R. W. Fredricks (TRW Systems Group, Redondo Beach, Calif.) Dordrecht D. Reidel Publishing

Co., 1972, p. 329-339. 1972 11 p refs In: Earth's magnetospheric processes; Proceedings of the Symposium, Cortina, Italy, August 30-September 10, 1971. (Contract NAS5-9278; Project OGO)

Electric dipole antennas on magnetospheric spacecraft measure E field components of many kinds of electromagnetic waves. In addition, lower hybrid resonance emissions are frequently observed well above the ionosphere. The OGO 5 plasma wave experiment has also detected new forms of electrostatic emissions that appear to interact very strongly with the local plasma particles. Greatly enhanced wave amplitudes have been found during the expansion phases of substorms, and analysis indicates that these emissions produce strong pitch angle diffusion. Intense broadband electrostatic turbulence is also detected at current layers containing steep magnetic field gradients. This current-driven instability is operative at the bow shock and also at field null regions just within the magnetosheath, and at the magnetopause near the dayside polar cusp. The plasma turbulence appears to involve ion acoustic waves, and the wave particle scattering provides an important collisionless dissipation mechanism for field merging. (Author)

A73-14962

SOLAR PROTON INTENSITY STRUCTURES IN THE MAGNETOSPHERE DURING INTERPLANETARY ANISOTROPIES.

G. Morfill and M. Scholer (Max-Planck-Institut fuer Physik und Astrophysik, Garching, West Germany) Dec. 1972 11 p refs Planetary and Space Science, vol. 20, Dec. 1972, p. 2113-2123.

A73-15526*

COSMIC-RAY SCINTILLATIONS. I: INSIDE THE MAGNETOSPHERE.

A. J. Owens and J. R. Jokipii (California Institute of Technology, Pasadena, Calif.) 1 Dec. 1972 17 p refs Journal of Geophysical Research, vol. 77, Dec. 1, 1972, p. 6639-6655. Research supported by the Alfred P. Sloan Foundation and NSF (Grant NGR-05-002-160)

A73-15531*

PRECIPITATION OF LOW-ENERGY ELECTRONS AT HIGH LATITUDES: EFFECTS OF INTERPLANETARY MAGNETIC FIELD AND DIPOLE TILT ANGLE.

J. L. Burch (NASA, Goddard Space Flight Center, Greenbelt, Md.) 1 Dec. 1972 12 p refs Journal of Geophysical Research, vol. 77, Dec. 1, 1972, p. 6696-6707.

A73-15533*

THE LIGHT-ION TROUGH, THE MAIN TROUGH, AND THE PLASMAPAUSE.

H. A. Taylor, Jr. (NASA, Goddard Space Flight Center, Laboratory for Planetary Atmospheres, Greenbelt, Md.) and W. J. Walsh (Aero Geo Astro Corp., Beltsville, Md.) 1 Dec. 1972 8 p refs

Although the plasmopause has been detected as a global phenomenon by both VLF and ion composition measurements, the electron and ion density troughs have been identified primarily as nightside features. This problem, as well as the difficulty in explaining various inconsistencies in relating the position of the plasmopause and the ionization trough, is explained by a close examination of the ion composition, generally unavailable in previous trough studies. In particular, ion composition results from the polar-orbiting OGO satellites identify the persistence of a pronounced light-ion trough (LIT) in H(+) and He(-), often identified by order-of-magnitude decreases in the light-ion concentrations, that occurs within a few degrees of latitude and reaches residual concentration levels of 100 to 1000 ions/cm³ near 60 deg dipole latitude. The LIT, observed both within the thermosphere and at high latitudes in the magnetosphere,

has been correlated directly with the VLF whistler identification of the plasmopause. (Author)

A73-15538*

THEORETICAL MODEL FOR THE LATITUDE DEPENDENCE OF THE THERMOSPHERIC ANNUAL AND SEMIANNUAL VARIATIONS.

H. G. Mayr (NASA, Goddard Space Flight Center, Thermosphere and Exosphere Branch, Greenbelt, Md.) and H. Volland (Bonn, Universitaet, Bonn, West Germany) 1 Dec. 1972 17 p refs Journal of Geophysical Research, vol. 77, Dec. 1, 1972, p. 6774-6790.

A73-17041*

X-RADIATION (E GREATER THAN 10 keV), H-ALPHA AND MICROWAVE EMISSION DURING THE IMPULSIVE PHASE OF SOLAR FLARES.

J. A. Vorpahl (California, University, Berkeley, Calif.) Oct. 1972 17 p refs Solar Physics, vol. 26, Oct. 1972, p. 397-413.

(Contract NAS5-9094; Grants NSF GA-31587; NGL-05-003-017)

A study has been made of the variation in hard (E greater than 10 keV) X-radiation, H-alpha and microwave emission during the impulsive phase of solar flares. Analysis shows that the rise-time in the 20-30-keV X-ray spike depends on the electron hardness. The impulsive phase is also marked by an abrupt, very intense increase in H-alpha emission in one or more knots of the flare. Properties of these H-alpha kernels include: (1) a luminosity several times greater than the surrounding flare, (2) an intensity rise starting about 20-30 sec before, peaking about 20-25 sec after, and lasting about twice as long as the hard spike, (3) a location lower in the chromosphere than the remaining flare, (4) essentially no expansion prior to the hard spike, and (5) a position within 6000 km of the boundary separating polarities, usually forming on both sides of the neutral line near both feet of the same tube of force. Correspondingly, impulsive microwave events are characterized by: (1) great similarity in burst structure with 20-32 keV X-rays but only above 5000 MHz, (2) typical low frequency burst cutoff between 1400-3800 MHz, and (3) maximum emission above 7500 MHz. (Author)

A73-17047*

EVIDENCE FOR ELECTRON EXCITATION OF TYPE 3 RADIO BURST EMISSION.

H. Alvarez, F. Haddock (Radio Astronomy Observatory, Ann Arbor, Mich.), and R. P. Lin (California, University, Berkeley, Calif.) Oct. 1972 6 p refs Solar Physics, vol. 26, Oct. 1972, p. 468-473.

(Contracts NAS5-9099; NAS5-9091; Grant NGL-05-003-017)

Type 3 radio bursts observed at kilometric wavelengths (less than or about equal to 0.35 MHz) by the OGO 5 spacecraft are compared with greater than 45 keV solar electron events observed near 1 AU by the IMP 5 and Explorer 35 spacecraft for the period from March 1968 to November 1969. Fifty-six distinct type 3 bursts extending to less than or about equal to 0.35 MHz were observed above the threshold of the OGO 5 detector; all but two were associated with solar flares. Twenty-six of the bursts were followed less than or about equal to 40 min later by greater than 45 keV solar electron events observed at 1 AU. All of these 26 bursts were identified with flares located west of W09 longitude. Of the bursts not associated with electron events only three were identified with flares west of W09, 18 were located east of W09, and seven occurred during times when electron events would be obscured by high background particle fluxes. (Author)

A73-19233

INTERPRETATION OF OGO-5 LYMAN ALPHA MEASUREMENTS IN THE UPPER GEOCORONA.

J. L. Bertaux and J. E. Blamont (CNRS, Service d'Aeronomie,

Verrieres-le-Buisson, Essonne, France) 1 Jan. 1973 12 p refs Journal of Geophysical Research, vol. 78, Jan. 1, 1973, p. 80-91.

(Contracts CNES-69-225; CNES-70-299)

Lyman alpha intensity measurements (1216 A) were obtained by a photometer on board the OGO 5 spacecraft outside the geocorona. The Lyman alpha emission originating from hydrogen atoms in the upper part of the geocorona was derived from the total measured intensity after subtraction of the extraterrestrial emission. The hydrogen density distribution between 5 and 16 earth radii was deduced. This distribution is consistent with the evaporative atmospheric model of Chamberlain (1963) on the night side. A depletion of atoms found above a distance of 6 earth radii on the day side could be accounted for by the action on satellite particles of charge exchange with solar wind protons and by the solar Lyman alpha radiation pressure, according to numerical computations of both effects. It was also calculated that orbits with a perigee of 2 earth radii are rapidly distorted by radiation pressure. The mean time spent in the exosphere by satellite particles on such orbits is only 500,000 sec, one-half the ionization lifetime. (Author)

A73-19241*
COMPARISON OF TE AND TI FROM OGO-6 AND FROM VARIOUS INCOHERENT SCATTER RADARS.

J. P. McClure, W. B. Hanson (Texas, University, Dallas, Tex.), A. F. Nagy, R. J. Cicerone (Michigan, University, Ann Arbor, Mich.), L. H. Brace (NASA, Goddard Space Flight Center, Aeronomy Branch, Greenbelt, Md.), M. Baron (Stanford Research Institute, Menlo Park, Calif.), P. Bauer (CNET, Departement Recherches Spatiales Radioelectriques, Issy-les-Moulineaux, Hauts-de-Seine, France), H. C. Carlson (Arecibo Observatory, Arecibo, P.R.), J. V. Evans (MIT, Lexington, Mass.); G. N. Taylor (Royal Radar Establishment, Malvern, Worcs., England) et al 1 Jan. 1973 9 p refs Journal of Geophysical Research, vol. 78, Jan. 1, 1973, p. 197-205.

(Contract NAS5-9311; Grants NGR-52-158-001; NGL-44-004-001)

Langmuir probe and retarding potential analyzer (RPA) data on the electron and ion temperatures Te and Ti obtained from OGO 6 are compared with Te and Ti values obtained from the incoherent scatter network. The satellite to radar temperature ratio TeS/TeR is 1.15 on the average for these comparisons. This discrepancy is larger than the uncertainties usually placed on the probe and radar Te values. The ion temperature ratio TiS/TiR approximately 1.0, independent of the particular radar examined. This comparison serves as an intercalibration of the incoherent scatter network.

(Author)

A73-19252
ENERGY DEPENDENT TIME LAG IN THE LONG-TERM MODULATION OF COSMIC RAYS.

J. J. Burger and B. N. Swanenburg (Leiden, Rijksuniversiteit, Leiden, Netherlands) 1 Jan. 1973 14 p refs Journal of Geophysical Research, vol. 78, Jan. 1, 1973, p. 292-305.

The intensity variations in the cosmic ray electron spectrum above 500 Mev observed outside the radiation belts from March 1968 to August 1971 are reported. The data show the existence of a large energy dependent hysteresis in the long-term modulation and two different types of steplike changes in the modulation parameter at rigidities below those observed with neutron monitors. The data indicate further that changes in the rigidity dependence of the modulation parameter occur mainly at rigidities above roughly 2 GV. The assumption that time lag phenomena in the solar modulation reflect the effective size of the solar cavity is questioned, and alternative explanations of the energy dependent time lags are qualitatively investigated. (Author)

A73-19254*
RECENT STUDIES OF MAGNETOSPHERIC ELECTRIC FIELD EMISSIONS ABOVE THE ELECTRON GYROFREQUENCY.

R. W. Fredricks and F. L. Scarf (TRW Systems Group, Space Sciences Dept., Redondo Beach, Calif.) 1 Jan. 1973 5 p refs Journal of Geophysical Research, vol. 78, Jan. 1, 1973, p. 310-314.

(Contract NAS5-9278; Project OGO)

A73-19255*
PARAMETRIC DESCRIPTION OF THERMOSPHERIC ION COMPOSITION RESULTS

H. A. Taylor, Jr. (NASA, Goddard Space Flight Center, Laboratory for Planetary Atmospheres, Greenbelt, Md.) 1 Jan. 1973 5 p refs Journal of Geophysical Research, vol. 78, Jan. 1, 1973, p. 315-319.

Results of an attempt to accumulate an ion composition data base for an international reference ionosphere (IRI) with the aid of polar-orbiting satellites. A progress report is presented on the preparation of the results from the Bennett RF ion spectrometer experiment on OGO 4 and 6 using the most extensive set of thermospheric ion composition data yet available. An example of the pole-to-pole distributions of all ions detected by the spectrometer on OGO 6 is given which shows considerable structure resulting from both altitude and latitude variations. Also, an example is given of the type of analysis made possible by the combined scope of the OGO ion composition data base and the IRI statistical sorting routine. A.B.K.

A73-20652*
CORRELATION OF GROUND-BASED MEASUREMENTS OF STRUCTURED PC 1 MICROPULSATIONS WITH OGO-V PLASMAPAUSE OBSERVATIONS.

A. J. Mullen and R. R. Heacock (Alaska, University, College, Alaska) Sep. 1972 7 p refs Annales de Geophysique, vol. 28, July-Sept. 1972, p. 519-525.

(Contract NAS5-9092; NSF Grants GA-27664; NSF GA-16496)

A73-20766*
EVIDENCE FOR A COMMON ORIGIN OF THE ELECTRONS RESPONSIBLE FOR THE IMPULSIVE X-RAY AND TYPE 3 RADIO BURSTS.

S. R. Kane (California, University, Berkeley, Calif.) Nov. 1972 8 p refs Solar Physics, vol. 27, Nov. 1972, p. 174-181. 23 refs

(Contract NAS5-9094; Grant NGL-05-003-017)

Observations of impulsive solar flare X-rays greater than or about equal to 10 keV made with the OGO 5 satellite are compared with ground-based measurements of type 3 solar radio bursts in 10 to 580-MHz range. It is shown that the times of maxima of these two emissions, when detectable, agree within about 18 sec. This maximum time difference is comparable to that between the maxima of the impulsive X-ray and impulsive microwave bursts. In view of the various observational uncertainties, it is argued that the observations are consistent with the impulsive X-ray, impulsive microwave, and type 3 radio bursts being essentially simultaneous. The observations are also consistent with 10- to 100-keV electron streams being responsible for the type 3 emission. The observations indicate that the nonthermal electron groups responsible for the impulsive X-ray, impulsive microwave, and type 3 radio bursts are accelerated simultaneously in essentially the same region of the solar atmosphere. (Author)

A73-22054*
PROTON SCATTERING IN THE REGION NEAR THE EARTH'S BOW SHOCK.

S. L. Ossakow (U.S. Navy, Naval Research Laboratory, Washington, D.C.) and G. W. Sharp (Lockheed Research Laboratories, Palo Alto, Calif.) 1 Feb. 1973 10 p refs Journal of Geophysical Research, vol. 78, Feb. 1, 1973, p. 607-616.

(Contract NAS5-9092)

Lockheed spectrometer data from orbits 1 through 20

of OGO 5 are used to study proton scattering near the bow shock. Correlative UCLA fluxgate magnetometer data from the satellite are used to complete motion studies of the bow shock when spectrometer data are missing. Thirty-eight analyzable sets of multiple shock crossings show 358 shock encounters ranging from 10 to 22 earth radii and spanning sun-earth-satellite angles from 30 to 90 deg. Gross features of the study show that the location and shape of the bow shock are in good agreement with the hydrodynamic model of the bow shock. (Author)

A73-22066*

OGO-6 MEASUREMENTS OF SUPERCOOLED PLASMA IN THE EQUATORIAL EXOSPHERE.

W. B. Hanson (Texas, University, Dallas, Tex.), A. F. Nagy (Michigan, University, Ann Arbor, Mich.), and R. J. Moffett (Sheffield, University, Sheffield, England) 1 Feb. 1973 6 p ref. Journal of Geophysical Research, vol. 78, Feb. 1, 1973, p. 751-756.

(Contracts NAS5-9311; NAS5-9306; Grant NGL-44-004-001)

Plasma measurements performed on OGO 6 reveal electron and ion temperature values that on occasion appear to be well below the expected neutral gas temperature. The phenomenon is observed only at night above 500 km near the magnetic equator. It is suggested that the expansion cooling of the plasma is accomplished by downward motions of the F region plasma induced by winds or diffusion, by outward $E \times B$ drift, or more probably by the upward flow of plasma during interhemisphere transport along magnetic field lines. It is also suggested that preferential cooling of electrons because of their greater thermal conductivity should tend to give ion temperatures greater than electron temperatures during the postsunset cooling of the plasmasphere when photoelectrons are absent. (Author)

A73-22069

NONLINEAR THEORY OF PLASMA INSTABILITY AT HALF-HARMONICS OF THE ELECTRON GYROFREQUENCY.

M. Nambu (Kyorin University, Tokyo, Japan) 1 Feb. 1973 3 p refs. Journal of Geophysical Research, vol. 78, Feb. 1, 1973, p. 769-771.

Study of some naturally occurring emissions observed by OGO 5 near the geomagnetic equator outside the plasmapause. The investigation is performed within the framework of nonlinear plasma theory, and the nonlinear frequency correction to a previous Fredricks (1971) linear instability analysis is obtained. Splitting of frequency spectra is not found to occur for high-frequency cyclotron waves, in contrast to low-frequency drift waves. M.V.E.

A73-23538*

MEASUREMENTS OF THE IRON-GROUP ABUNDANCE IN ENERGETIC SOLAR PARTICLES.

D. L. Bertsch, C. E. Fichtel, C. J. Pellerin, and D. V. Reames (NASA, Goddard Space Flight Center, Greenbelt, Md.) 1 Mar. 1973 7 p refs. Astrophysical Journal, vol. 180, Mar. 1, 1973, pt. 1, p. 583-589.

A73-23539*

DIRECT MEASUREMENTS OF SOLAR-WIND FLUCTUATIONS BETWEEN 0.0048 AND 13.3 Hz.

T. W. J. Unti, M. Neugebauer, and B. E. Goldstein (California Institute of Technology, Jet Propulsion Laboratory, Pasadena, Calif.) 1 Mar. 1973 8 p refs. Astrophysical Journal, vol. 180, Mar. 1, 1973, pt. 1, p. 591-598.

A73-24727*

SOLAR FLARE PARTICLE PROPAGATION: COMPARISON OF A NEW ANALYTIC SOLUTION WITH SPACECRAFT MEASUREMENTS.

J. E. Lupton and E. C. Stone (California Institute of Technology, Pasadena, Calif.) 1 Mar. 1973 12 p refs.

Journal of Geophysical Research, vol. 78, Mar. 1, 1973, p. 1007-1018.

(Contract NAS5-9312; Grants NGR-05-002-160; NGL-05-002-007)

A73-24732*

ELECTRON PITCH ANGLE DISTRIBUTIONS THROUGHOUT THE MAGNETOSPHERE AS OBSERVED ON OGO-5.

H. I. West, Jr., R. M. Buck, and J. R. Walton (California, University, Livermore, Calif.) 1 Mar. 1973 18 p refs. Journal of Geophysical Research, vol. 78, Mar. 1, 1973, p. 1064-1081. AEC-NASA supported research (NASA Order S-70014-G)

A survey of the equatorial pitch angle distributions of energetic electrons is provided for all local times out to radial distances of 20 earth radii on the night side of the earth and to the magnetopause on the day side of the earth. In much of the inner magnetosphere and in the outer magnetosphere on the day side of the earth, the normal loss cone distribution prevails. The effects of drift shell splitting - i.e., the appearance of pitch angle distributions with minimums at 90 deg, called butterfly distributions - become apparent in the early afternoon magnetosphere at extended distances, and the distribution is observed in to 5.5 earth radii in the nighttime magnetosphere. Inside about 9 earth radii the pitch angle effects are quite energy-dependent. Beyond about 9 earth radii in the premidnight magnetosphere during quiet times the butterfly distribution is often observed. It is shown that these electrons cannot survive a drift to dawn without being considerably modified. The role of substorm activity in modifying these distributions is identified. (Author)

A73-24738*

LARGE ION CONCENTRATION GRADIENTS BELOW THE EQUATORIAL F PEAK.

W. B. Hanson and S. Sanatani (Texas, University, Dallas, Tex.) 1 Mar. 1973 7 p refs. Journal of Geophysical Research, vol. 78, Mar. 1, 1973, p. 1167-1173. (Contract NAS5-9311; Grants NSF GA-31318; NGL-44-004-001)

Very large vertical and longitudinal gradients in the ion concentrations are observed below the F peak near the magnetic equator with the retarding potential analyzer on OGO 6. Ion concentration bite outs of up to a factor of 1000 are observed above 400 km. They appear to be associated with the bottom side of the nighttime F layer. The ion composition in the minima may contain large fractions of ions heavier than O^{+} (e.g., NO^{+} and Fe^{+}). It is suggested that convective electric fields associated with spread F steepen the bottomside of the F layer and also introduce longitudinal irregularities in the vertical ion concentration profiles. (Author)

A73-24744

ULTRALOW FREQUENCY FLUCTUATIONS AT THE POLAR CUSP BOUNDARIES.

N. D'Angelo (Danish Space Research Institute, Lyngby, Denmark) 1 Mar. 1973 4 p refs. Journal of Geophysical Research, vol. 78, Mar. 1, 1973, p. 1206-1209.

Analysis of OGO 5 observations of ULF magnetic fluctuations at the polar cusp boundaries in terms of a drift wave instability and a Kelvin-Helmholtz instability. In the light of the analysis results obtained, it appears plausible that the latitudinal extent of the plasma cusp at low altitudes is affected by the presence of large-amplitude fluctuations at the cusp boundaries. Analogy with laboratory observations on the effect of the Kelvin-Helmholtz instability on diffusion suggests that this instability may be of great importance in determining the structure of the polar cusp. M.V.E.

A73-25753

ISIS-1 SATELLITE OBSERVATIONS OF THE IONOSPHERE AT HIGH SOUTHERN LATITUDES.

D. Eccles, J. W. King, and A. J. Slater (Science Research

Council, Radio and Space Research Station, Slough, Bucks., England) Apr. 1973 8 p refs Journal of Atmospheric and Terrestrial Physics, vol. 35, Apr. 1973, p. 625-632.

Topside sounder data from consecutive passes of ISIS-1 over the south polar region during November 1969 have been used to produce contour maps of the F2 critical frequency and these are compared with observations of the neutral N2 and electron concentrations reported by other workers. It is shown that at night at longitudes near 90 deg W large values of the F2 critical frequency occur at latitudes lower than 70 deg S, but that at higher latitudes the critical frequency decreases rapidly, forming an ionization cliff at approximately 60 deg invariant latitude. Evidence is presented which indicates that on the poleward side of the cliff appreciable heating of the atmosphere occurs and that the low values of the F2 critical frequency are caused by an increase in the electron loss rate associated with an enhancement of the N2 concentration in the polar region.

(Author)

A73-26985*

AN ASSOCIATION OF MAGNETOSPHERIC WHISTLER DISPERSION CHARACTERISTICS WITH CHANGES IN LOCAL PLASMA DENSITY.

F. L. Scarf (TRW Systems Group, Redondo Beach, Calif.) and C. R. Chappell (Lockheed Research Laboratories, Palo Alto, Calif.) 1 Apr. 1973 6 p refs Journal of Geophysical Research, vol. 78, Apr. 1, 1973, p. 1597-1602.

(Contracts NAS5-9278; NAS5-23106)

We use OGO 5 measurements made within the plasmopause on May 15, 1969, to investigate the possible association between changes in lightning whistler dispersion characteristics and local density fluctuations. It is shown that groups of whistlers with relatively constant dispersions tended to be detected in regions where the local ion concentration was significantly enhanced. It is assumed that these local density fluctuations represent characteristics of large-scale field-aligned variations. The results are then compared with ray refraction estimates appropriate for low-frequency whistler mode propagation (wave components with frequencies comparable to the local lower hybrid frequency) in a nonuniform medium.

(Author)

A73-26988*

DISTRIBUTIONS AND CHARACTERISTICS OF HIGH-LATITUDE FIELD-ALIGNED ELECTRON PRECIPITATION.

F. W. Berko (NASA, Goddard Space Flight Center, Laboratory for Space Physics, Greenbelt, Md.) 1 Apr. 1973 12 p refs Journal of Geophysical Research, vol. 78, Apr. 1, 1973, p. 1615-1626.

Satellite measurements of field-aligned auroral electron precipitation have been analyzed using 16 months of data from the OGO 4 auroral particles experiment. As can be seen from the moving satellite, the anisotropies are of short duration and are most likely to occur when particle fluxes are high. Field-aligned 2.3-keV electron precipitation is found in an oval-shaped region primarily in the nighttime hours; maximum probability is at about 70 deg invariant latitude near midnight, congruent to and poleward of the auroral optical emissions in these hours. This precipitation is found to be associated with the high-latitude boundary of auroral electron precipitation during substorm expansion and is characterized by a slightly harder and considerably more intense energy spectrum than typical isotropic precipitation.

(Author)

A73-26997*

MAGNETIC CONTROL OF THE NEAR EQUATORIAL NEUTRAL THERMOSPHERE.

A. E. Hedin and H. G. Mayr (NASA, Goddard Space Flight Center, Greenbelt, Md.) 1 Apr. 1973 4 p refs Journal of Geophysical Research, vol. 78, Apr. 1, 1973, p. 1688-1691.

Neutral density data between 400 and 500 km obtained with the OGO 6 neutral mass spectrometer indicate that at

all longitudes the daytime N2 and O densities have latitudinal minimums at the magnetic equator that are about 20 and 10%, respectively, below maximums observed between plus and minus 20 deg magnetic latitude. Our calculations suggest that this anomaly could result from latitudinal variations in ion drag associated with the 'equatorial anomaly' in F region ionization. At latitudes of enhanced electron density the energy flow from the dayside to the nightside of the earth is damped, and thus the amplitude of the temperature and density variations is enhanced, and the time of maximum is shifted to later local times.

(Author)

A73-27602*

AURORAL HEATING AND THE COMPOSITION OF THE NEUTRAL ATMOSPHERE.

P. B. Hays, R. A. Jones, and M. H. Rees (Colorado, University, Boulder, Colo.) Apr. 1973 15 p refs Planetary and Space Science, vol. 21, Apr. 1973, p. 559-573.

(Grants NSF GA-16290A1; NGR-23-005-360)

Heating of the neutral atmosphere by auroral particle fluxes and by orthogonal electric fields is responsible for large changes in the thermospheric composition that have been observed by satellite mass spectrometers. Vertical winds of a few meters per second are produced in the region subject to auroral heating; this vertical upwelling drives circulation cells that extend the effects of heating in the auroral region on a global scale. Our analysis focuses on the initial phase of a magnetic storm within the auroral region.

(Author)

A73-29964*

FIELD-ALIGNED CURRENTS, PLASMA WAVES, AND ANOMALOUS RESISTIVITY IN THE DISTURBED POLAR CUSP.

R. W. Fredricks, F. L. Scarf (TRW Systems Group, Redondo Beach, Calif.), and C. T. Russell (California, University, Los Angeles, Calif.) 1 May 1973 9 p refs Journal of Geophysical Research, vol. 78, May 1, 1973, p. 2133-2141.

(Contracts NAS5-9278; NAS5-9098)

During the magnetic storm of November 1, 1968, the OGO 5 spacecraft encountered the polar cusp region at low magnetic latitudes. We show that the region just outside the last closed field lines contained a warm magnetosheath plasma, magnetic field perturbations interpretable as field-aligned current layers, and electrostatic waves possibly due to plasma instabilities driven by these currents. Estimates of anomalous resistivity extrapolated along the field lines due to these electrostatic waves lead to estimates of field-aligned potential drops between OGO 5 and ionosphere on the order of 2 kV.

(Author)

A73-29966*

OBSERVATION OF A CURRENT-DRIVEN PLASMA INSTABILITY AT THE OUTER ZONE-PLASMA SHEET BOUNDARY.

F. L. Scarf, R. W. Fredricks (TRW Systems Group, Redondo Beach, Calif.), C. T. Russell, M. Kivelson (California, University, Los Angeles, Calif.), M. Neugebauer (California Institute of Technology, Jet Propulsion Laboratory, Pasadena, Calif.), and C. R. Chappell (Lockheed Research Laboratories, Palo Alto, Calif.) 1 May 1973 16 p refs Journal of Geophysical Research, vol. 78, May 1, 1973, p. 2150-2165.

(Contracts NAS5-9278; NAS5-9098; NAS5-9092; NAS7-100; NASw-2357)

Several spacecraft experimenters have reported on the detection of large temporal variations in trapped electron fluxes near L = 5 to 6 at midlatitudes in the night hemisphere. In this report we describe in detail the particle, wave, and field changes measured when OGO 5 traversed an outer-zone trapping boundary of this type on September 7, 1968. It is shown that thermal proton concentrations and E greater than 50-keV electron fluxes abruptly decreased when electrons with (1-4) keV mean energy were detected. It is also shown that currents flowed along the average geomagnetic field direction near the plasma boundaries and that these were accompanied by intense VLF electrostatic waves. It is proposed that turbulent resistivity produced by current-driven plasma

instabilities allows parallel dc electric fields to develop along this boundary. (Author)

A73-29975*

MAGNETIC STORM CHARACTERISTICS OF THE THERMOSPHERE.

H. G. Mayr (NASA, Goddard Space Flight Center, Greenbelt, Md.) and H. Volland (Bonn, Universitaet, Bonn, West Germany) 1 May 1973 14 p refs Journal of Geophysical Research, vol. 78, May 1, 1973, p. 2251-2264.

Energy and diffusive mass transport associated with the thermospheric circulation are considered in a self-consistent, though mathematically relatively simple, form to describe in a three-dimensional two-constituent model magnetic storm characteristics in composition (N₂, O, and He), temperature, and mass-density. It is shown that during disturbed conditions the latitudinal variations of composition and gas temperature reflect the local nature of the magnetic storm heat input assumed to be primarily confined to the auroral zones. Thereby gas temperature and N₂ increase, He decreases, and O remains constant through the auroral zones at exospheric heights (due to the superposition of temperature and diffusion effects) in agreement with OGO 6 mass spectrometer measurements. In contrast, the magnetic storm response in the total mass density is characterized by a strong world-wide component and a relatively insignificant increase toward the poles. (Author)

A73-29988*

ON THE CAUSE OF EQUATORIAL SPREAD F.

W. B. Hanson, J. P. McClure, and D. L. Sterling (Texas, University, Dallas, Tex.) 1 May 1973 4 p refs Journal of Geophysical Research, vol. 78, May 1, 1973, p. 2353-2356.

(Contract NAS5-9311; Grants NSF GA-31318; NGL-44-004-001)

It is suggested that convective electric fields in the equatorial ionosphere are generated by neutral winds (zonal or meridional) which act on regions having structure in their field aligned Pedersen conductivity integrals. The conductivity structure is presumably caused by long-lived metallic ions concentrated irregularly below the F layer at altitudes where their collision and gyrofrequencies are comparable. The resulting plasma convection leads to large-scale irregularities and sets up gradients in the electric field that drive other instability mechanisms to produce small-scale irregularities. The mechanism proposed requires a different velocity above and below 200 km for winds in the magnetic east-west direction, but for winds in the magnetic meridian direction, an altitude gradient is not required. V.P.

A73-31767*

EQUATORIAL PHENOMENA IN NEUTRAL THERMOSPHERIC COMPOSITION

C. A. Reber, A. E. Hedin, and S. Chandra (NASA, Goddard Space Flight Center, Laboratory for Planetary Atmospheres, Greenbelt, Md.) Jun. 1973 6 p refs (International Symposium on Equatorial Aeronomy, 4th, Ibadan, Nigeria, Sept. 4-9, 1972.) Journal of Atmospheric and Terrestrial Physics, vol. 35, June 1973, p. 1223-1228

Several interesting phenomena relating to the equatorial ionosphere have been observed in the data from the OGO-6 mass spectrometer. The diurnal variations during equinox at an altitude of 450 km show the N₂ and O densities peaking near 1500 hr while He peaks near 1000 hr. The latitudinal variation in N₂ during the day is very similar to the F-region electron density exhibiting the well known features of the ionospheric anomaly. During periods of intense geomagnetic disturbance (e.g. the large storm of 8 March 1970), the low latitude thermospheric temperature increases on the order of 50-150 K, while at mid latitudes, increases of more than 1000 K are observed. (Author)

A73-31768*

THE POGO DATA.

J. C. Cain and R. E. Sweeney (NASA, Goddard Space Flight

Center, Laboratory for Space Physics, Greenbelt, Md.) Jun. 1973 17 p (International Symposium on Equatorial Aeronomy, 4th, Ibadan, Nigeria, Sept. 4-9, 1972.) Journal of Atmospheric and Terrestrial Physics, vol. 35, June 1973, p. 1231-1247.

During intervals in 1967-1970, the OGO-4 and 6 spacecraft made over 2000 traversals over the equatorial electrojet in the altitude range 400-800 km when local times were between 9 and 15 hr. These spacecraft carried total field magnetometers making measurements to an accuracy of 2 gammas with a sample rate greater than once a second. Delta-F values, the deviations of these observations from an internal reference model, were plotted for a 30 deg band about the Equator, and the characteristics of the electrojet effect in the data investigated. This effect was characterized by a sharp negative V-signature of some 16-19 deg in width and a variable amplitude. (Author)

A73-31769

COMPARISON OF GEOMAGNETIC CHANGES IN INDIA AND THE POGO DATA.

R. P. Kane (Physical Research Laboratory, Ahmedabad, India) Jun. 1973 4 p Journal of Atmospheric and Terrestrial Physics, vol. 35, June 1973, p. 1249-1252. (International Symposium on Equatorial Aeronomy, 4th, Ibadan, Nigeria, Sept. 4-9, 1972.) Research supported by the Department of Space of India.

The best estimate of the amplitude of the electrojet signature at any particular local time when the POGO satellite traversed the electrojet region as given by Cain and Sweeney (1972) should be directly comparable to the ground-observed electrojet strength at the same local time. For ground observations the equatorial station Trivandrum and the low latitude station Alibag were used. The results of the comparison are presented in a graph, taking also into account the subjective estimates of the amplitude uncertainty. G.R.

A73-31772

ON THE CORRELATION OF THE GROUND DATA AT IBADAN WITH POGO SATELLITE RESULTS.

E. Oni (Ibadan, University, Ibadan, Nigeria) Jun. 1973 5 p Journal of Atmospheric and Terrestrial Physics, vol. 35, June 1973, p. 1267-1271. (International Symposium on Equatorial Aeronomy, 4th, Ibadan, Nigeria, Sept. 4-9, 1972.)

POGO satellite data are compared with the ground data at Ibadan. Results show poor correlation. The ratio ground/POGO obtained from the scatter diagrams and extrapolated to the value of the jet axis is compared with other ratios from India, Addis Ababa and Huancayo. The variation in the ratios from different zones is discussed in the light of the results of the preliminary work on the upper mantle conductivity structure in Nigeria. It is concluded that the conventional model of image plane approximation used by Chapman and others in deducing the induction part of the electrojet is unrealistic in the face of recent results of solid earth physics study. (Author)

A73-31773

ELECTROJET MEASUREMENTS FROM SATELLITE AND GROUND.

D. G. Osborne (University, College, London, England) Jun. 1973 7 p Journal of Atmospheric and Terrestrial Physics, vol. 35, June 1973, p. 1273-1279. (International Symposium on Equatorial Aeronomy, 4th, Ibadan, Nigeria, Sept. 4-9, 1972.) Research supported by the University of Dar es Salaam.

Of the 2000 OGO-4 and OGO-6 equatorial passes, 112 were within 10 deg either side of Addis Ababa. Twenty-five passes happened during magnetically quiet periods when the index Ap was less than 4. Correlations were sought between the effect of the equatorial electrojet at satellite altitude and ground measurements. When the ground values Delta-H (AA) were read at the LT corresponding to the local time at the longitude of the satellite, the correlation is very good for 80 per cent of the observations. The inverse slope of the ground effect versus satellite effect is about 3.8 for Addis

Ababa. A Delta-H (AA) threshold of about 40 gammas was found below which the satellite did not register any electrojet effect. (Author)

A73-32964*

THE PREVALENCE OF SECOND HARMONIC RADIATION IN TYPE 3 BURSTS OBSERVED AT KILOMETRIC WAVELENGTHS.

F. T. Haddock and H. Alvarez (Radio Astronomy Observatory, Ann Arbor, Mich.) Mar. 1973 14 p refs Solar Physics, vol. 29, Mar. 1973, p. 183-196. (Contract NAS5-9099)

We present the analysis of 64 type 3 solar bursts that drifted from 3.5 MHz down to the range 350-50 kHz between March 1968 and February 1970. Bursts arrival times were predicted by a simple model and then compared with observations. The results show that, as the bursts drift, the fundamental often disappears below a certain frequency range while the second harmonic remains. Below about 1 MHz, the second harmonic occurrence predominates. Recognizing this fact we deduce a mean velocity of $0.32c$ plus or minus $0.02c$ for the exciter particles, where the uncertainty is the standard error and c the velocity of light in vacuum; the electron density model used is comparable to a solar wind model. (Author)

A73-32965*

SOLAR WIND DENSITY MODEL FROM KM-WAVE TYPE 3 BURSTS.

H. Alvarez and F. T. Haddock (Radio Astronomy Observatory, Ann Arbor, Mich.) Mar. 1973 13 p refs Solar Physics, vol. 29, Mar. 1973, p. 197-209. (Contract NAS5-9099)

The analysis of type 3 bursts observed from the OGO 5 satellite between 3.5 MHz and 50 kHz gives an empirical expression for the frequency drift rate as a function of frequency that is valid from 75 kHz to 550 MHz. Using this expression and some simplifying assumptions we obtain indirectly an empirical formula for the electron density distribution of the solar wind to 1 AU which is consistent with published values of electron density and with observed type 3 burst drift rates. (Author)

A73-33293#

PRIMARY COSMIC RAY ELECTRONS

P. Meyer (Chicago, University, Chicago, Ill.) 1972 19 p refs In: International Conference on Cosmic Rays, 12th, Hobart, Tasmania, Australia, August 16-25, 1971. Invited and Rapporteur Papers, Hobart, Australia, University of Tasmania, 1972, p. 235-251; Discussion, p. 252, 253.

Solar electrons with energies from a few keV to about 100 MeV are frequently observed. Questions of the modulation of galactic electrons are discussed, giving attention to an application of the transport equation, the 11 year solar cycle modulation, quiet time intensity changes of low energy electrons, and Forbush decreases. It is pointed out that any measurement of the spectrum of high energy cosmic ray electrons is an exceedingly difficult experimental task. The specific manner in which high-energy cosmic ray electrons lose energy during their life in the galaxy is investigated. G.R.

A73-33436

ERRORS IN ION AND ELECTRON TEMPERATURE MEASUREMENTS DUE TO GRID PLANE POTENTIAL NONUNIFORMITIES IN RETARDING POTENTIAL ANALYZERS

P. D. Goldan, E. J. Yadlowsky, and E. C. Whipple, Jr. (NOAA, Aeronomy Laboratory, Boulder, Colo.) 1 Jun. 1973 10 p refs Journal of Geophysical Research, vol. 78, June 1, 1973, p. 2907-2916.

A73-33437*

ION CYCLOTRON WAVES OBSERVED IN THE POLAR SP.

R. W. Fredricks (TRW Systems Group, Redondo Beach, Calif.) and C. T. Russell (California, University, Los Angeles, Calif.) 1 Jun. 1973 9 p refs Journal of Geophysical Research, vol. 78, June 1, 1973, p. 2917-2925. (Contracts NAS5-9278 NAS5-9098)

During the penetration by OGO 5 of the low-latitude disturbed polar cusp region on Nov. 1, 1968, while a major magnetic storm was in progress, a variety of plasma wave activity was observed. Observations of waves with amplitudes less than 2% of the background magnetic field intensity and having frequencies between approximately 0.67 and 0.87 times the local proton gyrofrequency are described. The polarization of these waves indicates that they are propagating at an appreciable angle to the local geomagnetic field line direction. The source of these waves has not been determined, but currents and gradient drifts are suggested as possible agents. (Author)

A73-33438*

ADDITIONAL RESULTS FROM AN OGO-6 EXPERIMENT CONCERNING IONOSPHERIC ELECTRIC AND ELECTROMAGNETIC FIELDS IN THE RANGE 20 Hz TO 540 kHz.

T. Laaspere and W. C. Johnson (Dartmouth College, Hanover, N.H.) 1 Jun. 1973 19 p refs Journal of Geophysical Research, vol. 78, June 1, 1973, p. 2926-2944. (Contract NAS5-9305; Grant NGR-30-001-041)

A73-33441*

THERMOSPHERIC WIND EFFECTS ON THE DISTRIBUTION OF HELIUM AND ARGON IN THE EARTH'S UPPER ATMOSPHERE.

C. A. Reber (NASA, Goddard Space Flight Center, Greenbelt, Md.) and P. B. Hays (Michigan, University, Ann Arbor, Mich.) 1 Jun. 1973 15 p refs Journal of Geophysical Research, vol. 78, June 1, 1973, p. 2977-2991.

A73-33449*

SATELLITE STUDIES OF MAGNETOSPHERIC SUBSTORMS ON AUGUST 15, 1968. 1: STATE OF THE MAGNETOSPHERE.

R. L. McPherron (California, University, Los Angeles, Calif.) 1 Jun. 1973 10 p refs Journal of Geophysical Research, vol. 78, June 1, 1973, p. 3044-3053. (Grant NGL-05-007-004)

The state of the magnetosphere on August 15, 1968, as defined by magnetic indices and ground magnetograms, is described. Onset times of various phases of two magnetospheric substorms are determined. These substorms occurred while the OGO 5 satellite was inbound on the midnight meridian through the cusp region of the geomagnetic tail. It is concluded that at least two worldwide substorm expansions were preceded by growth phases. M.V.E.

A73-33450*

SATELLITE STUDIES OF MAGNETOSPHERIC SUBSTORMS ON AUGUST 15, 1968. 2: SOLAR WIND AND OUTER MAGNETOSPHERE.

R. L. McPherron (California, University, Los Angeles, Calif.), G. K. Parks (Washington, University, Seattle, Wash.), D. S. Colburn (NASA, Ames Research Center, Moffett Field, Calif.), and M. D. Montgomery (California, University, Los Alamos, N. Mex.) 1 Jun. 1973 8 p refs Journal of Geophysical Research, vol. 78, June 1, 1973, p. 3054-3061. AEC-ARPA supported research. (Contract N00014-69-A-0200-4016; Grants NSF GA-487; NGL-05-007-004; NGR-05-007-305)

Investigation of the changes in the solar wind and the outer magnetosphere associated with two substorms that occurred on August 15, 1968. The results of the study suggest that trapped particles in the magnetosphere may be redistributed by perturbations well before an auroral expansion. This gives support to the assumed existence of a magnetospheric substorm growth phase. M.V.E.

A73-33451*

SATELLITE STUDIES OF MAGNETOSPHERIC SUBSTORMS ON AUGUST 15, 1968. 3: SOME FEATURES OF MAGNETOSPHERIC CONVECTION.

D. L. Carpenter (Stanford University, Stanford, Calif.) and C. R. Chappell (Lockheed Research Laboratories, Palo Alto, Calif.) 1 Jun. 1973 6 p refs Journal of Geophysical Research, vol. 78, June 1, 1973, p. 3062-3067.

(Contract NAS5-9092; Grants NSF GA-12317; NSF GA-19608; NSF GA-18128; NGR-05-020-288; NGL-05-020-008)

New details of unsteady magnetospheric convection and gradual erosion of the plasmasphere during a weak magnetic storm are revealed in the light of presented ground data and OGO 4 and OGO 5 data for August 13-15, 1968. These new findings suggest that westward electric fields of the order of 0.5 mv/m were present in the midnight sector during the substorms studied. M.V.E.

A73-33452*

SATELLITE STUDIES OF MAGNETOSPHERIC SUBSTORMS ON AUGUST 15, 1968. 4: OGO-5 MAGNETIC FIELD OBSERVATIONS.

R. L. McPherron, C. T. Russell, P. J. Coleman, Jr. (California University, Los Angeles, Calif.), and M. P. Aubry 1 Jun. 1973 11 p refs Journal of Geophysical Research, vol. 78, June 1, 1973, p. 3068-3078. Research supported by the European Space Research Organization.

(Contract NAS5-9098)

A73-33453*

SATELLITE STUDIES OF MAGNETOSPHERIC SUBSTORMS ON AUGUST 15, 1968. 5: ENERGETIC ELECTRONS, SPATIAL BOUNDARIES, AND WAVE-PARTICLE INTERACTIONS AT OGO-5.

M. G. Kivelson, T. A. Farley, and M. P. Aubry (California University, Los Angeles, Calif.) 1 Jun. 1973 14 p refs Journal of Geophysical Research, vol. 78, June 1, 1973, p. 3097-3092.

(Contract NAS5-9097)

A73-33454*

SATELLITE STUDIES OF MAGNETOSPHERIC SUBSTORMS ON AUGUST 15, 1968. 6: OGO 5 ENERGETIC ELECTRON OBSERVATIONS. PITCH ANGLE DISTRIBUTIONS IN THE NIGHTTIME MAGNETOSPHERE

H. I. West, Jr., R. M. Buck, and J. R. Walton (California University, Livermore, Calif.) 1 Jun. 1973 10 p refs Journal of Geophysical Research, vol. 78, June 1, 1973, p. 3093-3102. AEC-NASA supported research.

(NASA Order S-70014-G)

A73-33455*

SATELLITE STUDIES OF MAGNETOSPHERIC SUBSTORMS ON AUGUST 15, 1968. 7: OGO-5 ENERGETIC PROTON OBSERVATIONS. SPATIAL BOUNDARIES

R. M. Buck, H. I. West, Jr. (California University, Livermore, Calif.), and R. G. D'Arcy, Jr. (Bartol Research Foundation, Swarthmore, Pa.) 1 Jun. 1973 16 p refs Journal of Geophysical Research, vol. 78, June 1, 1973, p. 3103-3118. AEC-NASA supported research.

(NASA Order S-70014-G)

A73-33456*

SATELLITE STUDIES OF MAGNETOSPHERIC SUBSTORMS ON AUGUST 15, 1968. 8: OGO-5 PLASMA WAVE OBSERVATIONS.

F. L. Scarf, R. W. Fredricks (TRW Systems Group, Redondo Beach, Calif.), C. F. Kennel, and F. V. Coroniti (California University, Los Angeles, Calif.) 1 Jun. 1973 12 p refs Journal of Geophysical Research, vol. 78, June 1, 1973, p. 3119-3130.

(Contract NAS5-9278)

A73-33457*

SATELLITE STUDIES OF MAGNETOSPHERIC SUBSTORMS ON AUGUST 15, 1968. 9: PHENOMENOLOGICAL MODEL FOR SUBSTORMS.

R. L. McPherron, C. T. Russell (California University, Los Angeles, Calif.), and M. P. Aubry (CNET, Issy-les-Moulineaux, Hauts-de-Seine, France) 1 Jun. 1973 19 p refs Journal of Geophysical Research, vol. 78, June 1, 1973, p. 3131-3149.

(Grant NGR-05-007-004)

Observations made during three substorms on August 15, 1968, are shown to be consistent with current theoretical ideas about the cause of substorms. The phenomenological model described in several preceding papers is further expanded. This model follows closely the theoretical ideas presented more quantitatively in recent papers by Coronti and Kennel (1972 and 1973). M.V.E.

A73-33464*

QUIET TIME MAGNETOSPHERIC FIELD DEPRESSION AT 2.3-3.6 EARTH RADII.

M. Sugiura (NASA, Goddard Space Flight Center, Laboratory for Space Physics, Greenbelt, Md.) 1 Jun. 1973 4 p refs Journal of Geophysical Research, vol. 78, June 1, 1973, p. 3182-3185.

Flux gate magnetometer data from OGO 5 are presented that establish the existence of large field depressions under conditions of varying degree of disturbance at distances ranging from 2.3 to 3.6 earth radii at all local times. For this study, flux gate data obtained near perigee during the period of approximately one year from Jan. 21, 1969, to Feb. 23, 1970, were used. M.V.E.

A73-33876*

THE PLASMASPHERE DURING A MAGNETIC RECOVERY PERIOD: A COMBINED STUDY OF THE OGO-4 AND OGO-5 SATELLITE DATA AND OF WHISTLERS RECEIVED AT THE GROUND. [LA PLASMASPHERE EN PERIODE DE RECOUVREMENT MAGNETIQUE: ETUDE COMBINEE DES DONNEES DES SATELLITES OGO-4, OGO-5 ET DES SIFFLEMENTS RECUS AU SOL]

P. Corcuff, Y. Corcuff (Poitiers, Universite, Poitiers, France), D. L. Cappentier (Stanford University, Stanford, Calif.), C. R. Chappell (Lockheed Research Laboratories, Palo Alto, Calif.), J. Vigneron (Groupe de Recherches Ionospheriques, Saint-Maur-des-Fosses, Val-de-Marne, France), and N. Kleimenova (Akademiia Nauk SSSR, Institut Fiziki Zemli, Moscow, USSR) Dec. 1972 17 p refs Annales de Geophysique, vol. 28, Oct.-Dec. 1972, p. 679-695. In FRENCH; In French Research supported by the Centre National de la Recherche Scientifique et Administration des Terres Australes et Antarctiques Francaises.

(Contract NAS5-9092; Grants NSF GV-28840X; NSF GA-18128; NSF GA-32590X; NGL-05-020-008; NGR-05-020-288)

A73-34783*

ELECTRON DEPLETION IN THE WAKE OF IONOSPHERIC SPACECRAFT: A COMPARISON BETWEEN RESULTS FROM LANGMUIR PROBES AND ANTENNAS.

U. Samir (Michigan University, Ann Arbor, Mich.; Tel Aviv University, Tel Aviv, Israel) and H. Weil (Michigan University, Ann Arbor, Mich.) Jun. 1973 8 p refs Planetary and Space Science, vol. 21, June 1973, p. 993-1000. (Grant NGR-23-005-320)

A73-36273*

DEPENDENCE OF THE POLAR CUSP ON THE NORTH-SOUTH COMPONENT OF THE INTERPLANETARY MAGNETIC FIELD.

M. G. Kivelson, C. T. Russell (California, University, Los Angeles, Calif.), M. Neugebauer (California Institute of Technology, Jet Propulsion Laboratory, Pasadena, Calif.), F. L. Scarf, and R. W. Fredricks (TRW Systems Group, Redondo Beach, Calif.) 1 Jul. 1973 12 p refs Journal of Geophysical Research, vol. 78, July 1, 1973, p. 3761-3772. (Contracts NAS5-9097; NAS5-9278; NAS7-100; Grant NGR-05-007-305)

A73-36275

SYNOPTIC SURVEY FOR THE NEUTRAL LINE IN THE MAGNETOTAIL DURING THE SUBSTORM EXPANSION PHASE.

A. Nishida and N. Nagayama (Tokyo, University, Tokyo, Japan) 1 Jul. 1973 17 p refs Journal of Geophysical Research, vol. 78, July 1, 1973, p. 3782-3798.

A self-consistent tail current sheet model described by an exact analytic solution of the time-independent Vlasov-Maxwell equations is presented. The model has a slingshot field configuration with field lines outside the plasma sheet slightly flared in the antisolar direction. It is pointed out that when the model parameters are adjusted to agree with the spatial variation along the tail the required thickness of the neutral sheet must be about 2.5 earth radii, instead of less than or equal to 1 earth radius, as indicated by observations. Furthermore, it is shown qualitatively that a considerable velocity shear must be present in the tail current sheet if the plasma sheet is indeed much thicker than the neutral sheet. (Author)

A73-36645*

NEUTRON MEASUREMENTS IN SPACE.

J. A. Lockwood (New Hampshire, University, Durham, N.H.) Jun. 1973 57 p refs Space Science Reviews, vol. 14, June 1973, p. 663-719.

(Contract NAS5-9313; Grants NSF GA-33858; NGR-30-002-074)

The experimental measurements of the neutron flux and energy spectrum in space since 1964 are reviewed and related to the theoretical predictions. A discussion of the neutron sources is presented. The difficulties associated with neutron measurements of both the atmospheric neutron leakage flux and solar neutrons are included. Particular emphasis is placed upon the neutron leakage flux and energy measurements at energies greater than about 1 MeV. The possibilities of CRAND as a source for the energetic trapped protons are discussed in light of recent measurements of the 10- to 100-MeV neutron flux. The current status of the solar neutron flux observations is also presented. An attempt is made to interpret and discuss recent neutron measurements. In order to understand these results, the theoretical predictions of the neutron fluxes and energy spectra from possible neutron sources are briefly presented. (Author)

A73-38939*

EQUATORIAL AIRGLOW AND THE IONOSPHERIC GEOMAGNETIC ANOMALY.

S. Chandra, E. I. Reed, B. E. Troy, Jr. (NASA, Goddard Space Flight Center, Laboratory for Planetary Atmospheres, Greenbelt, Md.), and J. E. Blamont (CNRS, Service d'Aeronomie, Verrieres-le-Buisson, Essonne, France) 1 Aug. 1973 11 p refs Journal of Geophysical Research, vol. 78, Aug. 1, 1973, p. 4630-4640.

OGO 4 observations of the O I (6300-A) emissions have revealed a global pattern hitherto undetected from the ground-based observations. It is seen that the postsunset emission of O I (6300 A) in October 1967 is very asymmetrical with respect to the geomagnetic equator in certain longitude regions and shows poor correlation with the electron density measured simultaneously from the same spacecraft. This asymmetry is less marked in the UV airglow. O I (1356 A), which appears to vary as the square of the maximum electron density in the F region. The horizon scan data of the 6300-A airglow reveal that the latitudinal asymmetry is associated with asymmetry in the height of

the O I (6300-A) emission and hence with the altitude of the F2 peak. From the correlative studies of the airglow and the ionospheric measurements the mechanisms of the UV and the 6300 A emissions are discussed in terms of the processes involving radiative and dissociative recombination. Theoretical expressions are developed which relate the airglow data to the ionospheric parameters. (Author)

A73-38941*

ROLE OF GAS-SURFACE INTERACTIONS IN THE REDUCTION OF OGO-6 NEUTRAL PARTICLE MASS SPECTROMETER DATA.

A. E. Hedin (NASA, Goddard Space Flight Center, Greenbelt, Md.), B. B. Hinton, and G. A. Schmitt (Michigan, University, Ann Arbor, Mich.) 1 Aug. 1973 18 p Journal of Geophysical Research, vol. 78, Aug. 1, 1973, p. 4651-4668.

(Contract NAS5-9328; Grant NGR-23-005-651)

Data obtained with the quadrupole mass spectrometer aboard the OGO 6 satellite show the effects of significant surface interaction processes, including nearly complete recombination of incoming atomic oxygen on the walls of the instrument antechamber plus adsorption and desorption of oxygen and carbon monoxide. The observed data are fit by solving the time-dependent continuity equations accounting for production and loss of atomic oxygen, molecular oxygen, and (in the case of mass 28) carbon monoxide. The surface parameters that best fit the data are selected and applied to the determination of ambient densities and their estimated errors. (Author)

A73-39074#

EXTRATERRESTRIAL ULTRAVIOLET RADIATION AND THE PARAMETER OF THE HI MEDIUM NEAR THE SUN. [EXTRATERRESTRICHE ULTRAVIOLETT-STRAHLUNG UND DIE PARAMETER DES SONNENNAHEN HI-MEDIUMS]

H. J. Fahr and G. Lay (Bonn, Universitaet, Bonn, West Germany) 1973 5 p refs Astronomische Gesellschaft, Wissenschaftliche Tagung, Vienna, Austria, Sept. 18-23, 1972 In GERMAN; In German. Astronomische Gesellschaft, Mitteilungen, no. 32, 1973, p. 198-202.

It is indicated that extraterrestrial UV radiation at 1216 A can be interpreted as a result of solar radiation scattering at the same wavelength on interstellar neutral hydrogen in interplanetary space. It is theorized that the interstellar HI medium penetrates into the solar system from a certain direction and that its density becomes there anisotropic, the anisotropy level being dependent on the parameters of the HI medium at the time of penetration. This direction and the HI medium velocity can be determined from the structure of Lyman-alpha isophots as measured by the OGO-5 satellite. V.Z.

A73-41374#

THE DETECTION OF 'INTERMEDIATE' SIZE MAGNETIC ANOMALIES IN COSMOS 49 AND OGO-2, 4, 6 DATA.

R. D. Regan, W. M. Davis (U.S. Geological Survey, Silver Spring, Md.), and J. C. Cain (NASA, Goddard Space Flight Center, Greenbelt, Md.) 1973 5 p refs In: Space research 13: Proceedings of the Fifteenth Plenary Meeting, Madrid, Spain, May 10-24, 1972. Volume 2, Berlin, East Germany, Akademie-Verlag GmbH, 1973, p. 619-623.

Benkova, Dolginov and Simonenko have recently reported the presence of intermediate size magnetic anomalies from Cosmos 49 data and hypothesized a crustal and/or upper mantle origin for these. We have examined the spherical harmonic models of the internal potential function, based on the OGO 2, 4 and 6 data and verified the locations and amplitudes of those anomalies with wavelengths of approximately 4000 km. The patterns of delta-F so computed were then compared with the IZMIRAN maps and also were analyzed statistically, in both the spatial and frequency domains, using residuals computed from the raw Cosmos 49 data. The two sets of data were thus derived from

A73-41497

completely independent sets of observations and field references. The two patterns are shown to agree very well over the whole earth surface up to the 50 deg latitude limit of Cosmos 49. (Author)

A73-41497*
DECAY TIME OF TYPE 3 SOLAR BURSTS OBSERVED AT KILOMETRIC WAVELENGTHS

H. Alvarez and F. T. Haddock (Michigan, University, Ann Arbor, Mich.) May 1973 8 p refs Solar Physics, vol. 30, May 1973, p. 175-182. (Contract NAS5-9099)

Type 3 bursts were observed between 3.5 MHz and 50 kHz by the University of Michigan radio astronomy experiment aboard the OGO 5 satellite. Decay times were measured and then combined with published data ranging up to about 200 MHz. The observed decay times increase with decreasing frequency, but at a rate considerably slower than that expected from electron-proton Coulomb collisions. At 50 kHz, values differ by about a factor of 100. Using Hartle and Sturrock's solar wind model, Coulomb collisional frequencies were computed and compared with the apparent collisional frequencies deduced from the observations. It was found that the ratio of observed to computed values varies with heliocentric distance according to an inverse 0.71 power. (Author)

A73-41498*
UPPER LIMIT TO THE 1-20 MEV SOLAR NEUTRON FLUX.

J. A. Lockwood, S. O. Ifedili, and R. W. Jenkins (New Hampshire, University, Durham, N.H.) May 1973 9 p refs Solar Physics, vol. 30, May 1973, p. 183-191. (Contract NAS5-9313; Grant NGR-30-003-008)

The upper limit on the quiet time solar neutron flux from 1 to 20 MeV has been measured to be less than .002 neutrons at the 95% confidence level. This result is deduced from the OGO 6 neutron detector measurements of the day-night effect near the equator at low altitudes for the period from June 7 to Dec. 23, 1969. The OGO 6 detector had very low (less than 4%) counting rate contributions from locally produced neutrons in the detecting system and the spacecraft and from charged-particle interactions in the neutron sensor. (Author)

A73-41912*
ELECTRON CONCENTRATIONS CALCULATED FROM TYE LOWER HYBRID RESONANCE NOISE BAND OBSERVED BY OGO-3

W. J. Burtis (Stanford University, Stanford, Calif.) 1 Sep. 1973 9 p refs Journal of Geophysical Research, vol. 78, Sept. 1, 1973, p. 5515-5523. (Grants NGL-05-020-008; NGR-05-020-288)

A noise band at the lower hybrid resonance (LHR) is often detected by the VLF and ELF receivers on OGO 3, using the electric antenna. In some cases the noise band is at the geometric mean gyrofrequency as measured by the Goddard Space Flight Center (GSFC) magnetometer, and local LHR in a dense H(+) plasma is indicated. In such cases, electron concentration can be calculated, if it is assumed that heavy ions are negligible. Observations at midlatitudes and altitudes of a few earth radii show local concentrations as low as 1.4 electrons/cu cm. In one case the concentrations obtained from the LHR noise band agree with those measured simultaneously by the GSFC ion mass spectrometer within a factor of 2. In another case the concentration is observed to fall by a factor of 2 in 150 km and then to decrease roughly as R to the minus fourth power, in agreement with whistler measurements outside the plasmopause. (Author)

A73-41914
LATITUDE AND LOCAL TIME DEPENDENCE OF PRECIPITATED LOW-ENERGY ELECTRONS AT HIGH LATITUDES.

G. Gustafsson 1 Sep. 1973 16 p refs Journal of Geophysical Research, vol. 78, Sept. 1, 1973, p. 5537-5552.

Data from particle detectors on board the satellite OGO 4 were used to study the precipitation of electrons in the energy range from 0.7 to 24 keV. The latitude dependence of these particles in the local time region from midnight to dawn has been investigated in detail. The analysis shows that the precipitation of particles with energies from 2.3 to 24 keV is centered at an invariant latitude of about 68 deg at midnight with a clear shift in latitude with increasing local time, and that this shift is more pronounced for lower energies. The highest fluxes of particles in this energy interval are measured at midnight, and they decrease rapidly with local time. In the dawn region, the location of the maximum precipitation for different energies varies about 1 deg of latitude for each unit of Kp, but the relative distribution remains almost unchanged. The fact that different energies have their maximums at different latitudes implies that the flux spectrum of precipitated particles, when measured at a certain latitude, has a peak at an energy corresponding to the energy of maximum precipitation at the latitude. (Author)

A73-41919*
EFFECTS OF INTERHEMISPHERE TRANSPORT ON PLASMA TEMPERATURES AT LOW LATITUDES.

G. J. Bailey, R. J. Moffett (Sheffield, University, Sheffield, England), W. B. Hanson, and S. Sanatani (Texas, University, Dallas, Tex.) 1 Sep. 1973 14 p refs Journal of Geophysical Research, vol. 78, Sept. 1, 1973, p. 5597-5610. (Contract NAS5-9311; Grant NSR-44-004-029)

The thermal balance of the equatorial plasma between 300 and 800 km is examined. Steady state nighttime calculations are made for O+, H+, and electrons. The following features are included: collisional heat transfer between ions, electrons, and neutrals; ion and electron thermal conduction along the field lines; curvature of the field lines; nonlinear advection due to field-aligned ion and electron motions; and convective compression or expansion due to field-aligned and E x B motions. The ion velocities necessary to calculate the effects of convection are obtained from the work of Moffett and Hanson, who include a meridional wind across the magnetic equator in their calculations. It is shown that field-aligned interhemisphere plasma flows appreciably affect the plasma temperatures. (Author)

A73-41925*
SATELLITE ULTRAVIOLET MEASUREMENTS OF NITRIC OXIDE FLUORESCENCE WITH A DIFFUSIVE TRANSPORT MODEL.

D. W. Rusch (Colorado, University, Boulder, Colo.) 1 Sep. 1973 11 p refs Journal of Geophysical Research, vol. 78, Sept. 1, 1973, p. 5676-5686. (Contract NAS5-9315)

Twilight measurements of fluorescence in the (1, 0) gamma band of nitric oxide were made from June 1967 to January 1969 by an ultraviolet scanning spectrometer on board the polar orbiting satellite Ogo 4. Nitric oxide vertical column emission rates were measured between solar zenith angles of 93 and 98 deg. Seasonal and latitudinal variations were found to be less than a factor of 1.3, the scatter and uncertainty in the data prohibiting more precise determinations from being made. Time independent chemical diffusion models for the vertical distribution of nitric oxide agree well with profiles measured from sounding rockets. The column emission rates calculated from the theoretical models are larger than the satellite measurements by a factor of 3. (Author)

A73-43693*
A MAGNETOSPHERIC FIELD MODEL INCORPORATING THE OGO-3 AND 5 MAGNETIC FIELD OBSERVATIONS.

M. Sugiura (NASA, Goddard Space Flight Center, Laboratory for Space Physics, Greenbelt, Md.) and D. J. Poros (Computer Sciences Corp., Silver Spring, Md.) Oct. 1973 11 p refs Planetary and Space Science, vol. 21, Oct. 1973, p. 1763-1773.

A magnetospheric field model is presented in which the usually assumed toroidal ring current is replaced by a circular disk current of finite thickness that extends from the tail to geocentric distances less than 3 earth radii. The drastic departure of this model from the concept of the conventional ring current lies in that the current is continuous from the tail to the inner magnetosphere. This conceptual change was required to account for the recent results of analysis of the OGO 3 and 5 magnetic field observations. In the present model the cross-tail current flows along circular arcs concentric with the earth and completes circuit via surface currents on the magnetopause. Apart from these return currents in the tail magnetopause, Mead's (1964) model is used for the field from the magnetopause current. The difference scalar field, Delta B, defined as the difference between the scalar field calculated from the present model and the magnitude of the dipole field, is found to be in gross agreement with the observed Delta B. (Author)

A73-45112*

ELECTRON OBSERVATIONS IN THE SOLAR WIND AND MAGNETOSHEATH.

J. D. Scudder, K. W. Ogilvie (NASA, Goddard Space Flight Center, Laboratory for Extraterrestrial Physics, Greenbelt, Md.), and D. L. Lind (NASA, Johnson Space Center, Astronaut Office, Houston, Tex.) 1 Oct. 1973 14 p refs Journal of Geophysical Research, vol. 78, Oct. 1, 1973, p. 6535-6548

Electron temperature measurements taken by a triaxial electron analyzer on OGO 5 in the solar wind and in the magnetosheath are interpreted. In the interplanetary medium, observations made on the bow shock connected lines of magnetic force have been separated from those made on non-bow-shock connected lines. The dependence of electron thermal properties on the local field geometry is discussed together with features of electron temperature and density discontinuities across the bow shock. The velocity distribution function is characterized together with temperature and density variations in a part of the dawn magnetosheath.

T.M.

A73-45121*

DISTRIBUTION OF ATOMIC OXYGEN IN THE UPPER ATMOSPHERE DEDUCED FROM OGO-6 AIRGLOW OBSERVATIONS.

T. M. Donahue, B. Guenther, and R. J. Thomas (Pittsburgh, University, Pittsburgh, Pa.) 1 Oct. 1973 28 p ref Journal of Geophysical Research, vol. 78, Oct. 1, 1973, p. 6662-6689.

(Contract NAS5-11077; Grant NSF GA-27638)

The atomic oxygen distribution as a function of altitude between 80 and 120 km and as a function of latitude has been deduced from OGO 6 557.7-nm airglow photometer data obtained between August 1969 and April 1970. The results indicate that the density ranges from 15 to 50 billion per cu cm at 120 km; that there is a semiannual variation by a factor of 3 in the global average density near 100 km in phase with the satellite drag semiannual effect; and that large latitudinal variations occur with maximums between 40 and 60 deg in the winter hemisphere and sometimes deep minimums in the tropics. The implication of these results for meridional and vertical transport patterns is discussed.

(Author)

A74-12627*

SHOCK SYSTEM OF FEBRUARY 2, 1969

T. Unti, M. Neugebauer (California Institute of Technology, Jet Propulsion Laboratory, Pasadena, Calif.), and C.-S. Wu (Maryland, University, College Park, Md.) 1 Nov. 1973 20 p refs Journal of Geophysical Research, vol. 78, Nov. 1, 1973, p. 7237-7256.

(Contract NAS7-100)

The shock system observed in the solar wind by Pioneer 9 and Ogo 5 on Feb. 2, 1969, consisted of the following major discontinuities: a forward slow shock; a forward fast shock; a tangential discontinuity at which the density dropped

sharply and the flow direction changed; a tangential discontinuity at which the magnetic field strength jumped to an unusually high value; two closely spaced tangential discontinuities that bracketed a region of even greater field strength and that fronted a region of very cool, very dense, helium-enriched plasma; a reverse fast shock of low Mach number; and a second reverse fast shock of very low Mach number. The event had aspects of both corotating and flare-induced shock systems; it is suggested that the source of the disturbances was a flare occurring at or near an M region. (Author)

A74-12640*

A CATALOG OF IONOSPHERIC F REGION IRREGULARITY BEHAVIOR BASED ON OGO-6 RETARDING POTENTIAL ANALYZER DATA

J. P. McClure and W. B. Hanson (Texas, University, Dallas, Tex.) 1 Nov. 1973 10 p refs Journal of Geophysical Research, vol. 78, Nov. 1, 1973, p. 7431-7440. Research supported by the University of Texas (Contract NAS5-9311; NAS5-23184; Grants NSF GA-31318; NGL-44-004-001)

Review of in situ data obtained with the aid of the retarding potential analyzer on board OGO 6 which reveal the nature of ionospheric irregularities in the total ion concentration above 400 km. Except for the high-latitude regions, the ionosphere is usually observed to be very smooth in the daytime, but considerable structure is observed at night, particularly near the equator and at Atlantic longitudes. Although most of the irregularities observed appear to be stochastic in nature, many nearly monochromatic waveforms are observed near the equator. The topics discussed include the midlatitude scintillation boundary, large-amplitude equatorial irregularities, the fluctuation spectrum of typical F region irregularities, the lower edge of the equatorial F region, sinusoidal waveforms, ground glass irregularities, breaking wave irregularities, and regions of smooth and irregular ionization inside the polar cap. A.B.K.

A74-14219*

THE RELATION BETWEEN LOW-LATITUDE NEUTRAL DENSITY VARIATIONS NEAR 400 km AND MAGNETIC ACTIVITY INDICES.

A. D. Anderson (Lockheed Research Laboratories, Palo Alto, Calif.) Dec. 1973 12 p refs Planetary and Space Science, vol. 21, Dec. 1973, p. 2049-2060. (Contract NAS5-9334)

A74-14274*

RATE OF EROSION OF DAYSIDE MAGNETIC FLUX BASED ON A QUANTITATIVE STUDY OF THE DEPENDENCE OF POLAR CUSP LATITUDE ON THE INTERPLANETARY MAGNETIC FIELD.

J. L. Burch (NASA, Goddard Space Flight Center, Laboratory for Space Physics, Greenbelt, Md.) Nov. 1973 7 p refs Radio Science, vol. 8, Nov. 1973, p. 955-961. (AGU, NCAR, and NOAA, Chapman Memorial Symposium on Magnetospheric Motions, Boulder, Colo., June 18-22, 1973.)

A74-14283*

ACTIVE EXPERIMENTS, MAGNETOSPHERIC MODIFICATION, AND A NATURALLY OCCURRING ANALOGUE.

M. G. Kivelson and C. T. Russell (California, University, Los Angeles, Calif.) Nov. 1973 14 p ref Radio Science, vol. 8, Nov. 1973, p. 1035-1048. (AGU, NCAR, and NOAA, Chapman Memorial Symposium on Magnetospheric Motions, Boulder, Colo., June 18-22, 1973.) (Contracts NAS5-9097; NAS5-9098; N00014-73-C-0130; Grant NGR-05-007-305)

Recently, a scheme has been proposed which would modify the magnetosphere by injecting plasma near the equator beyond the plasmapause and initiating wave-particle instabilities. The expected effects have been examined

theoretically. Injection of plasma into this region is also a naturally occurring phenomenon produced by the cross-tail electric fields which are associated with geomagnetic activity. For further investigation of magnetospheric instabilities the advantages of examining artificially injected plasma (control of time and location of injection and of the volume of plasma injected) contrast with the advantages of studying natural enhancements (no extra payload, frequent occurrence). Thus, the two types of experiments are complementary. In preliminary studies of natural plasma enhancements both ULF and ELF emissions have been observed. The ELF noise is consistent with generation by the electron cyclotron instability. (Author)

A74-14811*

HELIOGRAPHIC LONGITUDE DISTRIBUTION OF THE FLARES ASSOCIATED WITH TYPE 3 BURSTS OBSERVED AT KILOMETRIC WAVELENGTHS

H. Alvarez, F. T. Haddock, and W. H. Potter (Michigan, University, Ann Arbor, Mich.) Aug. 1973 8 p refs Solar Physics, vol. 31, Aug. 1973, p. 493-500. (Contract NAS5-11174)

A74-15356*

MEASUREMENTS OF THE ATMOSPHERIC NEUTRON LEAKAGE RATE

J. A. Lockwood, S. O. Ifedili, and R. W. Jenkins (New Hampshire, University, Durham, N.H.) 1 Dec. 1973 8 p refs Journal of Geophysical Research, vol. 78, Dec. 1, 1973, p. 7978-7985.

(Contract NAS5-9313; Grant NGR-30-002-088)

The atmospheric neutron leakage rate in the energy range from 0.01 to 10,000,000 eV has been measured as a function of latitude, altitude, and time with a neutron detector on board the OGO 6 satellite. The latitude dependence of the neutron leakage is in reasonable agreement with that predicted by Lingenfelter (1963) and Light et al. (1973) if the neutron energy spectrum has the shape calculated by Newkirk (1963). The change in the neutron latitude dependence with the cosmic ray modulation agrees with the predictions of Lingenfelter and Light et al. For several solar proton events enhancements were observed in the neutron counting rates at lambda greater than or equal to 70 deg. Such events, however, provide an insignificant injection of protons at E less than or equal to 20 MeV into the radiation belts. An isotropic angular distribution of the neutron leakage in the energy range from 0.1 keV to 10 MeV best fits the observed altitude dependence of the neutron leakage flux. (Author)

A74-15496*

DETERMINATION OF THE SOLAR LYMAN-ALPHA FLUX INDEPENDENT OF CALIBRATION BY ULTRAVIOLET OBSERVATIONS OF COMET BENNETT

H. U. Keller and G. E. Thomas (Colorado, University, Boulder, Colo.) 1 Dec. 1973 4 p Astrophysical Journal, vol. 186, Dec. 1, 1973, pt. 2, p. L87-L90.

(Contract NAS5-9327; Grants NGR-06-003-201 NGL-06-003-052)

A74-17648

ENERGY DISTRIBUTION OF PHOTOELECTRONS EMITTED FROM A SURFACE ON THE OGO-5 SATELLITE AND MEASUREMENTS OF SATELLITE POTENTIAL

K. Norman and R. M. Freeman (London, University College, Holmbury St. Mary, Surrey, England) Dordrecht, D. Reidel Publishing Co., 1973, p. 231-243; Discussion, p. 243, 244, 1973 14 p In: Photon and particle interactions with surfaces in space; Proceedings of the Sixth ESLAB Symposium, Noordwijk, Netherlands, September 26-29, 1972.

A74-17742*

THE MAGNETOTAIL AND SUBSTORMS.

C. T. Russell and R. L. McPherron (California, University, Los Angeles, Calif.) Dec. 1973 62 p refs Space Science Reviews, vol. 15, Nov.-Dec. 1973, p. 205-266.

(Contracts NAS5-9097; NAS5-9098; Grants NSF GA-34148X; NGR-05-007-004; NGR-05-007-305)

The tail plays a very active and important role in substorms. Magnetic flux eroded from the dayside magnetosphere is stored here. As more and more flux is transported to the magnetotail and stored, the boundary flares more, the field strength in the tail increases, and the currents strengthen and move closer to the earth. Further, the plasma sheet thins and the magnetic flux crossing the neutral sheet lessens. The experimental evidence for these processes is discussed and a phenomenological or qualitative model of the substorm sequence is presented. In this model, the flux transport is driven by the merging of the magnetospheric and interplanetary magnetic fields. During the growth phase of substorms the merging rate on the dayside magnetosphere exceeds the reconnection rate in the neutral sheet. F.R.L.

A74-18364*

POSTMIDNIGHT CHORUS: A SUBSTORM PHENOMENON.

B. T. Tsurutani and E. J. Smith (California Institute of Technology, Jet Propulsion Laboratory, Pasadena, Calif.) 1 Jan. 1974 10 p refs Journal of Geophysical Research, vol. 79, Jan. 1, 1974, p. 118-127.

(Contract NAS7-100)

The ELF emissions were detected in the midnight sector of the magnetosphere in conjunction with magnetospheric substorms. The emissions were observed at local midnight and early morning hours and are accordingly called post-midnight chorus. The characteristics of these emissions such as their frequency time structure, emission frequency with respect to the local equatorial electron gyro-frequency, intensity-time variation, and the average intensity were investigated. The occurrence of the chorus in the nightside magnetosphere was investigated as a function of local time, L shell, magnetic latitude, and substorm activity, and the results of this analysis are presented. Specific features of postmidnight chorus are discussed in the context of possible wave-particle interactions occurring during magnetospheric substorms. F.R.L.

A74-18372*

EFFECT OF SATELLITE POTENTIAL ON DIRECT ION DENSITY MEASUREMENTS THROUGH THE PLASMA-PAUSE.

E. C. Whipple, J. M. Warnock, and R. H. Winkler (NOAA, Aeronomy Laboratory, Boulder, Colo.) 1 Jan. 1974 8 p refs Journal of Geophysical Research, vol. 79, Jan. 1, 1974, p. 179-186. NASA supported research

(Contract NOAA-E-22-1-72(G))

A simplified theory has been developed for calculating the effect of satellite potential on the ion current measured by an experiment such as an ion mass spectrometer or an ion trap. The theory is based on the use of a spherically symmetric Debye potential distribution in the sheath around the satellite and is particularly appropriate for use in regions where the Debye length is large, such as in the plasmasphere and magnetosphere. Ion data obtained from the ion trap on the OGO 3 satellite during a pass through the plasmasphere show excellent agreement with the theory. The inferred ion densities from this analysis are as much as 1 order of magnitude different from what would be inferred from previous analyses. (Author)

A74-18376*

EMPIRICAL MODEL OF GLOBAL THERMOSPHERIC TEMPERATURE AND COMPOSITION BASED ON DATA FROM THE OGO-6 QUADRUPOLE MASS SPECTROMETER.

A. E. Hedin, H. G. Mayr, C. A. Reber, N. W. Spencer (NASA, Goddard Space Flight Center, Greenbelt, Md.), and G. R. Carignan (Michigan, University, Ann Arbor, Mich.) 1 Jan. 1974 11 p refs Journal of Geophysical Research,

vol. 79, Jan. 1, 1974, p. 215-225.

A74-18754*#

GEOPHYSICAL PROPERTIES OF THE IONOSPHERIC IRREGULARITIES RESPONSIBLE FOR RADIO SCINTILLATION.

J. P. McClure (Texas, University, Dallas, Tex.) Jan. 1974 9 p refs American Institute of Aeronautics and Astronautics, Aerospace Sciences Meeting, 12th, Washington, D.C., Jan. 30-Feb. 1, 1974, 9 p.
(Contracts NAS5-9311; NAS5-23184; Grants NSF GA-31318; NGL-44-004-026)
(AIAA Paper 74-53)

The properties of F-region ionospheric irregularities are described based on in-situ measurements of the actual waveforms of ion concentration. The spectral properties of the irregularities are discussed. In high, middle and low latitudes most of the irregularities observed fall into a single noise-like category having power spectra which can be approximated by f to the negative n -th power and S to the n -th power, where S is the irregularity scale size and n is approximately 2. Thus the spectral components have a maximum gradient which is almost independent of their size. Other categories of irregularities are also observed occasionally. (Author)

A74-21679*

OBSERVATIONS OF THE INTERNAL STRUCTURE OF THE MAGNETOPAUSE.

M. Neugebauer, E. J. Smith (California Institute of Technology, Jet Propulsion Laboratory, Pasadena, Calif.), and C. T. Russell (California, University, Los Angeles, Calif.) 1 Feb. 1974 12 p Journal of Geophysical Research, vol. 79, Feb. 1, 1974, p. 499-510.
(Contracts NAS7-100; NAS5-9098)

Magnetic field, plasma flux, and ELF wave data have been studied for several encounters of OGO 5 with the earth's magnetopause. In one case of a crossing in the near-earth region of the geomagnetic tail, the structure agreed closely with a simple Chapman-Ferraro type of model with nearly complete neutralization of the charge separation electric field. Departures from the simple structure were observed at other magnetopause crossings. One crossing revealed a well-defined double structure with a large change in field direction closer to the earth than the ion flux and field strength gradients. The thickness of the magnetopause often depended on whether the change in field strength, the change in field direction, or the change in ion flux was being considered. Bursts of ELF waves were occasionally observed at the magnetopause. T.M.

A74-21680*

PLASMA WAVES IN THE DAYSIDE POLAR CUSP. 2: MAGNETOPAUSE AND POLAR MAGNETOSHEATH.

F. L. Scarf, R. W. Fredricks (TRW Systems Group, Redondo Beach, Calif.), M. Neugebauer (California Institute of Technology, Jet Propulsion Laboratory, Pasadena, Calif.), and C. T. Russell (California, University, Los Angeles, Calif.) 1 Feb. 1974 10 p refs Journal of Geophysical Research, vol. 79, Feb. 1, 1974, p. 511-520.
(Contracts NAS5-9278; NAS5-9098; NAS7-100; Grant NASw-2357)

During the outbound pass of Nov. 1, 1968, OGO 5 sporadically encountered the low-altitude polar cusp at low magnetic latitudes. The spacecraft remained in the cusp beyond six earth radii, and it then traversed the interface region between the magnetospheric cusp and the magnetosheath. Two large scale discontinuities were detected in this sheath-cusp transition region, and several possible interpretations are evaluated here. At 1427 UT, local changes in magnetic field orientation and the variation in ULF magnetic power spectral density were typical of shifts detected at the magnetopause, although the spacecraft did not traverse a true boundary of warm plasma at this point. The second discontinuity, detected at 1456 UT, resembled a collisionless shock, and it was characterized by observations

of intense, impulsive VLF electric field bursts and rapid local variations in both total ion flux and differential electron flux. The simplest interpretation is that OGO 5 had traversed a standing shock within the sheath. T.M.

A74-21693*

GLOBAL CHARACTERISTICS IN THE DIURNAL VARIATIONS OF THE THERMOSPHERIC TEMPERATURE AND COMPOSITION.

H. G. Mayr, A. E. Hedin, C. A. Reber, and G. R. Carignan (NASA, Goddard Space Flight Center, Greenbelt, Md.) 1 Feb. 1974 10 p refs Journal of Geophysical Research, vol. 79, Feb. 1, 1974, p. 619-628.

A74-22345*

OGO-5 MEASUREMENTS OF THE LYMAN-ALPHA SKY BACKGROUND IN 1970 AND 1971.

G. E. Thomas and R. F. Krassa (Colorado, University, Boulder, Colo.) Jan. 1974 10 p refs Astronomy and Astrophysics, vol. 30, no. 2, Jan. 1974, p. 223-232.
(Contract NAS5-9327; Grants NGR-06-003-201; NGL-06-003-052)

The results of measurements of the Lyman-alpha sky background emission at 1216 A, made by two different UV photometers during the last three 'spin-up' maneuvers (enabling more than 50% of the sky to be observed) are examined. The processed data revealed a smooth variation of Lyman-alpha brightness from a broad maximum near RA = 269 deg, declination = -20 deg to a broader minimum near RA = 50 deg, declination = +20 deg. The maximum/minimum intensity ratio is found to be on the order of 4. V.P.

A74-23679*

GLOBAL TEMPERATURE DISTRIBUTIONS FROM OGO-6 6300 A AIRGLOW MEASUREMENTS.

J. E. Blamont, J. M. Luton (CNRS, Service d'Aeronomie, Verrieres-le-Buisson, Essonne, France), and J. S. Nisbet (Pennsylvania State University, University Park, Pa.) Feb. 1974 5 p refs Radio Science, vol. 9, Feb. 1974, p. 247-251. Union Radio Scientifique Internationale, Symposium on Incoherent Scatter, Tromso, Norway, June 12-16, 1973.
(Grant NGL-39-009-003)

The OGO-6 6300 A airglow temperature measurements have been used to develop models of the global temperature distributions under solstice and equinox conditions for the altitude region from 240 to 300 km and for times ranging from dawn in this altitude region to shortly after sunset. The distributions are compared with models derived from satellite orbital decay and incoherent scatter sounding. The seasonal variation of the temperature as a function of latitude is shown to be very different from that derived from static diffusion models with constant boundary conditions. (Author)

A74-24766*

A CORRELATED STUDY OF ELF WAVES AND ELECTRON PRECIPITATION ON OGO-6.

R. E. Holzer, T. A. Farley, R. K. Burton (California, University, Los Angeles, Calif.), and M. C. Chapman (TRW Systems Group, Redondo Beach, Calif.) 1 Mar. 1974 7 p refs Journal of Geophysical Research, vol. 79, Mar. 1, 1974, p. 1007-1013.
(Contracts NAS7-100; NAS5-9308; JPL-950403; Grant NGR-05-007-276)

The OGO 6 ELF chorus records from the search coil magnetometer have been compared with simultaneous electron precipitation records. The chorus signals observed in the vicinity of field lines passing through the outer magnetosphere were characteristically accompanied by electron precipitation in the same region. Both the chorus and the precipitation records consisted of a series of sharp peaks. Although in some cases chorus and precipitation peaks appeared to be associated, the observed peaks did not in general coincide. Comparison of the chorus

A74-24767

measurements on OGO 6 and OGO 5 suggests a model in which the chorus is ducted along field lines to within less than 1 earth radius above the OGO 6 orbit after which it diverges from the field lines and is deflected toward the local vertical. The result is equatorward skewing of the average wave pattern with respect to the precipitation pattern.

(Author)

A74-24767*

TYE ORIGIN AND PROPAGATION OF CHORUS IN THE OUTER MAGNETOSPHERE.

R. K. Burton and R. E. Holzer (California, University, Los Angeles, Calif.) 1 Mar. 1974 10 p refs Journal of Geophysical Research, vol. 79, Mar. 1, 1974, p. 1014-1023. (Contracts NAS7-100; JPL-950403; Grant NGR-05-007-276)

Wave normals of chorus in the outer magnetosphere have been determined for the first time from data obtained with OGO 5 search coil magnetometer. These measurements combined with simultaneous information concerning geomagnetic field, plasma density, and the electron energy and pitch angle distributions provide a consistent picture of the generation, propagation, and subsequent damping of chorus in agreement with theory. Specifically, the data are consistent with chorus generation within 25 deg of the equatorial plane on the dayside and within 2 deg on the nightside. Chorus is generated by a Doppler-shifted cyclotron resonance with electrons between 5 and 150 keV but only when the pitch angle distribution is peaked at 90 deg to the local magnetic field and the anisotropy exceeds a critical value.

(Author)

A74-27695*

IN SITU MEASUREMENTS OF THE SPECTRAL CHARACTERISTICS OF F REGION IONOSPHERIC IRREGULARITIES.

P. L. Dyson (Texas, University, Dallas, Tex.; La Trobe University, Bundoora, Victoria, Australia), J. P. McClure, and W. B. Hanson (Texas, University, Dallas, Tex.) 1 Apr. 1974 6 p refs Journal of Geophysical Research, vol. 79, Apr. 1, 1974, p. 1497-1502. (Contracts NAS5-9311; NAS5-23184; Grants NSF GA-31318; NGL-44-004-001)

The retarding potential analyzer aboard OGO 6 has provided high-resolution observations of the ion concentration along the satellite path. Changes in ion concentration as small as 0.03% and at times as small as 0.01% could be measured. Spatial resolution varied from 35 to 380 m. Samples of data have been analyzed to determine the spectral properties of the F region irregularities observed. The most common frequency spectrum observed suggests that the responsible irregularities result from the turbulent dissipation of larger irregularities. At the equator, the larger irregularities are probably produced by convective electric fields. At high latitudes, electric fields may also be involved, but other factors such as precipitating particles may contribute to, or be primarily responsible for, the production of large irregularities. Examples of other types of spectra associated with wavelike irregularities and with ground glass (high-frequency noise) irregularities are also shown.

(Author)

A74-27700

THE 1972 COSMIC RAY ELECTRON SPECTRUM ABOVE 0.5 GeV.

J. J. Burger and B. N. Swarnburg (Kamerlingh Onnes Laboratorium, Leiden, Netherlands) 1 Apr. 1974 2 p refs Journal of Geophysical Research, vol. 79, Apr. 1, 1974, p. 1533, 1534.

The cosmic ray electron spectrum above 0.5 GeV measured outside the radiation belts during a special operation of the OGO 5 satellite from June 30 to July 13, 1972, is presented in a table. This table shows for comparison the intensities measured with the same instrument over the period from March 1968 to August 1971. The implications of the presented data for gaining some understanding of the solar modulation process are discussed.

M.V.E.

A74-27713*

COMPARISON OF ATOMIC OXYGEN MEASUREMENTS BY INCOHERENT SCATTER AND SATELLITE-BORNE MASS SPECTROMETER TECHNIQUES.

A. E. Hedin (NASA, Goddard Space Flight Center, Greenbelt, Md.) and D. Alcayde (Toulouse, Universite, Toulouse, France) 1 Apr. 1974 3 p refs Journal of Geophysical Research, vol. 79, Apr. 1, 1974, p. 1579-1581.

Atomic oxygen densities determined by the incoherent scatter technique are compared to densities deduced from satellite-borne mass spectrometer measurements and are found to agree within experimental error. The diurnal variations inferred from the incoherent scatter measurements do show, however, some departure from diurnal variations found by modeling the mass spectrometer results. Some implications of these departures are briefly discussed.

(Author)

A74-29960#

THE AIR COMPOSITION IN THE THERMOSPHERE. [DIE LUFTZUSAMMENSETZUNG IN DER THERMOSPHAERE]

U. Von Zahn (Bonn, Universitaet, Bonn, West Germany) 1974 14 p refs Kleinheubacher Berichte, vol. 17, 1974, p. 113-126. In GERMAN: In German Arbeitsgemeinschaft Ionosphaere, URSI, and Nachrichtentechnische Gesellschaft, Gemeinsame Tagung, Kleinheubach, West Germany, Oct. 8-13, 1973.

Review of the processes affecting the air composition in the region from 80 to 500 km, and evaluation of recent aircraft and satellite measurements of the air composition in this region. A number of heat-generating processes occurring in the thermosphere are discussed, including elementary dynamic processes, absorption of solar wave radiation, dissipation of solar wind energy, meteorological dynamic processes, interactions between lower and upper atmosphere, escape processes involving H and He, and interactions between neutral and ionized components of the upper atmosphere. Aircraft measurements of the oxygen density in the lower thermosphere are described, as well as mass-spectrometric measurements of the air composition in the thermosphere performed on board the OGO 6 and ESRO 4 satellites.

A.B.K.

A74-30149*#

SEARCH FOR BRIEF CELESTIAL X-RAY BURSTS.

T. L. Cline and U. D. Desai (NASA, Goddard Space Flight Center, Greenbelt, Md.) Denver University of Denver, 1974, p. 80-85. 1974 6 p refs In: International Cosmic Ray Conference, 13th, Denver, Colo., August 17-30, 1973, Proceedings, Volume 1.

The occurrence of intense bursts of 0.1- to 1.5-MeV photons from space has been confirmed with observations from IMP-6. This is the first positive result of an extensive data comparison, in which a search was made of OGO and IMP records for time coincidences between brief X- or gamma-ray increases and a variety of other transient phenomena. The IMP-6 measurements provided the first differential energy spectra of these events, the shapes of which indicate that photons predominantly in the gamma-ray domain are released into space. Whether these bursts originate in distant supernovae or in some new class of relatively nearby gamma-ray flare stars, they reveal a process which is new to high-energy astrophysics, not only because of the unusual spectrum, but also because of the brief time scales involved and because of the intense fluxes observed.

(Author)

A74-30156*#

ON THE ORIGIN OF LOW ENERGY HEAVY NUCLEI BELOW APPROXIMATELY 30 MEV PER NUCLEON OBSERVED IN INTERPLANETARY SPACE DURING QUIET TIMES, 1968-72.

A. Mogro-Campero, N. Schofield, and J. A. Simpson (Chicago, University, Chicago, Ill.) Denver University of Denver, 1974, p. 140-145. 1974 6 p refs In: International

Cosmic Ray Conference, 13th, Denver, Colo., August 17-30, 1973, Proceedings, Volume 1.
(Contract NAS5-9366; Grants NSF GA-28368X; NGL-14-001-006)

A74-30190**

THE ELEMENTAL ABUNDANCE RATIOS OF INTERSTELLAR SECONDARY AND PRIMARY COSMIC RAYS.

J. W. Brown, E. C. Stone, and R. E. Vogt (California Institute of Technology, Pasadena, Calif.) Denver University of Denver, 1974, p. 556-561. 1974 6 p refs In: International Cosmic Ray Conference, 13th, Denver, Colo., August 17-30, 1973, Proceedings, Volume 1.
(Contract NAS5-9312; Grant NGR-05-002-160)

We report new observations of abundances in the charge range (Z) between 2 and 10, which were obtained with a dE/dx-Cerenkov detector launched into a polar orbit on OGO 6 as part of the Caltech Solar and Galactic Cosmic Ray Experiment. Integral rigidity spectra of all the elements observed have shapes similar to that of the helium spectrum in the rigidity range of 2 to 14 GV, approaching a power law with exponent -1.6 above 8 GV. Calculations of interstellar propagation assuming a steady-state model and including the presence of interstellar helium and the effects of solar modulation predict a variation with rigidity of ratios such as Be/O and B/O, which is not observed. The data can be explained by assuming a rigidity-dependent confinement of cosmic rays within the galaxy. (Author)

A74-30204**

THE COSMIC RAY ELECTRON SPECTRUM AND ITS MODULATION FROM 1968 THROUGH 1972.

G. Fulks, P. Meyer (Chicago, University, Chicago, Ill.), and J. Lheureux (Arizona, University, Tucson, Ariz.) Denver University of Denver, 1974, p. 753-758. 1974 6 p refs In: International Cosmic Ray Conference, 13th, Denver, Colo., August 17-30, 1973, Proceedings, Volume 2.
(Contracts NAS5-9096; NAS5-11444; Grant NSF GA-31767X1)

Over the past five years we have measured the energy spectrum of primary cosmic ray electrons with both a balloon-borne and a satellite absorption spectrometer. All of the balloon flights used identical equipment that was launched each summer from Fort Churchill, Manitoba, Canada. The satellite, OGO 5, has been in an eccentric orbit since March 1968. Together these instruments provide the electron spectrum over a range of energy from 20 MeV to 20 GeV. This wide range and the substantial span of time covered by the measurements permit a detailed study of the solar modulation of electrons. These results are compared with the modulation of the nuclear components as observed by a neutron monitor and interpreted using the cosmic ray transport equation. (Author)

A74-30263**

SIMULTANEOUS SATELLITE AND RIOMETER STUDIES.

M. B. Baker, A. J. Masley, and P. R. Satterblom (McDonnell Douglas Astronautics Co., Huntington Beach, Calif.) Denver University of Denver, 1974, p. 1440-1445. 1974 6 p refs In: International Cosmic Ray Conference, 13th, Denver, Colo., August 17-30, 1973, Proceedings, Volume 2. Research supported by the McDonnell Douglas Independent Research and Development Program.
(Contract NAS5-9324; Grant NSF C-393)

The expected 30 and 50 MHz riometer absorption was calculated for the 7 June, 25 September and 2 November 1969 solar events using data from the McDonnell Douglas charged particle experiment on the polar orbiting OGO 6 satellite. Excellent agreement was found between measured polar cap riometer absorption during the events and absorption calculated from detailed particle data obtained on the satellite passing over the riometer. Electrons are found to contribute the greater part of the 30 MHz absorption

before the peak of the 2 November 1969 event; at all other times protons produce most of the absorption. The alpha-particle contribution is negligible in all cases. (Author)

A74-30287**

ACCELERATION OF ELECTRONS DURING THE FLASH PHASE OF SOLAR FLARES.

S. R. Kane (California, University, Berkeley, Calif.) Denver University of Denver, 1974, p. 1607-1612. 1974 6 p refs In: International Cosmic Ray Conference, 13th, Denver, Colo., August 17-30, 1973, Proceedings, Volume 2.
(Contract NAS5-9094; Grant NGL-05-003-017)

The characteristics of the electron acceleration process operating during the flash phase of solar flares are deduced from the high time resolution observations of impulsive solar X-rays greater than or equal to 10 keV and other flash phase emissions from small solar flares. The implications of these findings are discussed. (Author)

A74-30670*

SPATIAL AND TEMPORAL BEHAVIOR OF ATOMIC OXYGEN DETERMINED BY OGO 6 AIRGLOW OBSERVATIONS.

T. M. Donahue, B. Guenther, and R. J. Thomas (Pittsburgh, University, Pittsburgh, Pa.) 1 May 1974 6 p refs Journal of Geophysical Research, vol. 79, May 1, 1974, p. 1959-1964.
(Grants NSF GA-37744; NGR-39-001-155)

Maps are produced of the atomic oxygen density near 97 km showing a strong variation in latitude, longitude, universal time, and time of year. These densities are deduced from atomic oxygen green nightglow observations carried out from OGO 6. Meridional wind patterns needed to support the asymmetries observed in local oxygen production and loss rates are deduced. (Author)

A74-30908**

ACCELERATION OF ELECTRONS IN SOLAR FLARES.

R. P. Lin (California, University, Berkeley, Calif.) 1973 34 p refs In: Solar terrestrial relations; Proceedings of the International Conference, Calgary, Alberta, Canada, August 28-September 1, 1972, Calgary, Alberta, Canada, University of Calgary, 1973, p. 307-340.
(Contracts NAS5-2989; NAS5-9077; NAS5-9091; NAS5-9094; NAS5-3177; Grant NGL-05-003-017)

Observations pertaining to the acceleration and emission of 10 to 100 keV electrons in small solar flares are reviewed. The energy spectrum of the accelerated electrons is obtained from observations of X-rays and escaping electrons. The loss of the electrons through various processes, such as collisions with the ambient medium, escape to the interplanetary medium, and emission of X-rays and radio waves, is considered, and quantitative energy loss estimates obtained for each process. The role of the accelerated electrons in the overall flare mechanism is examined and an attempt is made to develop a consistent picture of a small electron flare. (Author)

A74-31903**

SHORT-TERM INTENSITY FLUCTUATION OF COSMIC-RAY ELECTRONS BETWEEN 0.5 AND 10 GeV.

J. J. Burger and B. N. Swanenburg (Leiden, Rijksuniversiteit, Leiden, Netherlands) Denver University of Denver, 1974, p. 3117-3122. 1974 6 p refs In: International Cosmic Ray Conference, 13th, Denver, Colo., August 17-30, 1973, Proceedings, Volume 5.

The cosmic-ray electron spectrum between 0.5 and 10 GeV has been monitored continuously from March 1968 until August 1971 aboard the OGO 5 satellite. These observations permit a detailed assessment of the long-term intensity variations (11-year cycle) as well as the short-term fluctuations (e.g. Forbush decreases). The results show a distinct difference in the rigidity dependence between these two effects. The implications for the description of the

transport of cosmic rays in the solar cavity are discussed. (Author)

A74-31942*
COSMIC GAMMA-RAY BURST DETECTED WITH AN INSTRUMENT ON BOARD THE OGO-5 SATELLITE.
 J. L'Heureux (Arizona, University, Tucson, Ariz.) 15 Jan. 1974 4 p refs Astrophysical Journal, vol. 187, Jan. 15, 1974, pt. 2, p. L53-L56.
 (Contracts NASS-9096; NASS-11444)

Gamma-ray bursts of cosmic origin have recently been detected by instruments on the Vela satellites. We now confirm the detection of the June 20, 1971 event with an instrument on board the OGO 5 satellite. The intensity of this burst is calculated to be approximately 100-200 photons per sq cm/sec for photons of energy greater than 150 keV with an upper limit of 50 photons per sq cm/sec for the intensity above 5 MeV. An upper limit of one-third of the intensity of the June 30, 1971 event is set for 10 other events studied. (Author)

A74-34019*
NEAR-EARTH MAGNETIC DISTURBANCE IN TOTAL FIELD AT HIGH LATITUDES. 1: SUMMARY OF DATA FROM OGO-2, 4, AND 6. 2: INTERPRETATION OF DATA FROM OGO-2, 4, AND 6.
 R. A. Langel (NASA, Goddard Space Flight Center, Geophysics Branch, Greenbelt, Md.) 1 Jun. 1974 29 p refs Journal of Geophysical Research, vol. 79, June 1, 1974, p. 2363-2371; 2373-2392.

A complete survey of the near-earth magnetic field magnitude was carried out by the Polar Orbiting Geophysical Observatories (OGO 2, 4, and 6). The average properties of variations in total magnetic field strength at invariant latitudes greater than 55 deg are given. Data from all degrees of magnetic disturbance are included, the emphasis being on periods when $K_p = 2-$ to $3+$. Although individual satellite passes at low altitudes confirm the existence of electrojet currents, neither individual satellite passes nor contours of average delta B are consistent with latitudinally narrow electrojet currents as the principal source of delta B at the satellite. The total field variations at the satellite form a region of positive delta B between about 2200 and 1000 MLT and a region of negative delta B between about 1000 and 2200 MLT. The ratio of delta B magnitudes in these positive and negative regions is variable. F.R.L.

A74-34020*
THE GLOBAL DISTRIBUTION OF NATURAL AND MAN-MADE IONOSPHERIC ELECTRIC FIELDS AT 200 KHZ AND 540 KHZ AS OBSERVED BY OGO-6.
 T. Laaspere and L. C. Sempere (Dartmouth College, Hanover, N.H.) 1 Jun. 1974 9 p refs Journal of Geophysical Research, vol. 79, June 1, 1974, p. 2393-2401.
 (Contract NASS-9305; Grant NGR-30-001-041)

An experiment on the polar-orbiting OGO 6 spacecraft yielded real-time analog data in several broadband channels and essentially continuous tape-recorded data from two narrow-band (200-Hz) receivers operating at 200 and 540 kHz. The results show that the worldwide distributions of signals at 200 and 540 kHz falls into a number of different categories: (1) naturally generated broadband (auroral) hiss at polar latitudes with typical 200-kHz intensities of around 0.1 microvolt per meter per Hz to the 1/2 power, maximum intensities of up to several microvolt per meter per Hz to the 1/2 power, and generally lower intensities at 540 kHz; (2) nighttime midlatitude enhancements of a few microvolts per meter, which probably result either from a superposition of signals from a number of 200- and 540-kHz stations or from interference from intense signals of much higher frequencies; (3) well-defined signal peaks associated with individual ground stations operating at 200 kHz; (4) striking signal enhancements in the conjugate region of a low-latitude 200-kHz station (Ashkhabad), suggesting propagation in the whistler mode to the opposite hemisphere; and (5) occasional signal enhancements at the magnetic equator. (Author)

A74-34027*
HEATING OF THE HIGH-LATITUDE THERMOSPHERE DURING MAGNETICALLY QUIET PERIODS.

C. A. Reber and A. E. Hedin (NASA, Goddard Space Flight Center, Greenbelt, Md.) 1 Jun. 1974 5 p refs Journal of Geophysical Research, vol. 79, June 1, 1974, p. 2457-2461.

A persistent mid- to high-latitude heating phenomenon is observed in both hemispheres in data from the OGO 6 quadrupole mass spectrometer. The phenomenon is evidenced by an increase in N_2 density (indicative of a thermospheric temperature rise) and a depletion in helium (indicating an upwelling of air). The composition changes maximize near 0900 and 2100 UT, appear to corotate with the local magnetic pole, and are larger near equinox than near the summer solstice. The variation in latitude of the peak in the winter helium density (as a function of UT) is a specific manifestation of this general heating phenomenon. (Author)

A74-34038*
PLASMASPHERIC HISS INTENSITY VARIATIONS DURING MAGNETIC STORMS.

E. J. Smith, A. M. A. Frandsen, B. T. Tsurutani (California Institute of Technology, Jet Propulsion Laboratory, Pasadena, Calif.), R. M. Thorne, and K. W. Chan (California, University, Los Angeles, Calif.) 1 Jun. 1974 4 p refs Journal of Geophysical Research, vol. 79, June 1, 1974, p. 2507-2510.

(Contract NAS7-100; Grant NSF GA-34148)

The storm time intensity variations of ELF electromagnetic emissions have been studied by using the OGO 6 search coil magnetometer. Low-latitude signals exhibit a sharp low-frequency cutoff and are identified as plasmaspheric hiss. Such waves show pronounced intensification during the recovery phase of magnetic storms but remain close to background levels during the storm main phase. This behavior is consistent with cyclotron resonant generation within the plasmasphere as the latter expands into the intensified belt of outer zone electrons during the storm recovery. (Author)

A74-34042*
OBSERVATIONS OF THE CONJUGATE SAR ARCS OF SEPTEMBER 28-30, 1967

E. I. Reed (NASA, Goddard Space Flight Center, Laboratory for Planetary Atmospheres, Greenbelt, Md.) and J. E. Blamont (CNRS, Service d'Aeronomie, Verrieres-le-Buisson, Essonne, France) 1 Jun. 1974 2 p refs Journal of Geophysical Research, vol. 79, June 1, 1974, p. 2524, 2525/.

Stable subauroral red arcs (SAR arcs) were observed in both the northern and southern hemispheres on Sept. 28 to 30, 1967. For each pass the universal time and the longitude of the spacecraft as it crossed the magnetic equator are given. The SAR arc was noted to be worldwide in its extent and located on the same L shell in the northern and southern hemispheres. It appeared near L equals 3, moved equatorward to L equals 2.4, and later moved to, or reformed, near L equals 2.9. Its intensities were variable over the nearly two days of observations and, apparently influenced by the composition of the lower thermosphere, averaged 60 per cent greater in the northern hemisphere. F.R.L.

A74-38468*
RISE TIME IN 20-32 KEV IMPULSIVE X-RADIATION.

J. A. Vorpahl (California, University, San Diego; Sacramento City College, Sacramento, Calif.) and T. Takakura (Tokyo, University, Tokyo, Japan) 15 Jul. 1974 3 p refs Astrophysical Journal, vol. 191, July 15, 1974, pt. 1, p. 563-565.
 (Contracts NASS-9094; NASS-11080; Grants NGL-05-003-017 NSF GA-31587; NGL-05-003-017)

A new property of the X-ray impulsive component observed in solar flares is discussed, giving attention to the relation between the slope of the electron power spectrum and the rise time in the 20-32 keV X-ray spike. This particular energy range was chosen because it offered the greatest number of impulsive events while being sufficiently high to

avoid contamination by soft X radiation. It is found for the thin-target model that the electron spectrum tends to be softer when the acceleration rate is smaller. G.R.

A74-43688*

A NEW MODEL FOR THE HIGH-FREQUENCY DECA-METRIC RADIATION FROM JUPITER

F. L. Scarf (TRW Systems Group, Redondo Beach, Calif.)
1 Sep. 1974 5 p refs Journal of Geophysical Research, vol. 79, Sept. 1, 1974, p. 3835-3839. Research supported by the TRW Systems Group Independent Research and Development Program
(Contract NAS5-9278)

It is generally accepted that the Jupiter decametric noise bursts occur at frequencies directly related to the electron gyrofrequencies in the Jupiter ionosphere, and it is frequently suggested that the radiation occurs at the gyrofrequency. The recent Pioneer 10 measurement of a $4-G-(R \text{ sub } 5)$ cubed dipole moment provides some basis for a more detailed analysis of the local wave mode involved in the radiation. The direct measurement of a relatively small planetary dipole moment suggests that phenomena associated with local ionospheric wave modes having frequencies higher than lokal gyrofrequencies should be considered for at least some of the emissions. A possible explanation for certain intense high-frequency Jupiter noise bursts is discussed which is based on a wave-wave coupling mechanism that involves the radiation field and the $(n + 1/2)$ gyrofrequency electrostatic modes. (Author)

B. Literature Cited in STAR

The "N" at the beginning of these accession numbers which end with a five digit number less than 70001 represents a series announced in *Scientific and Technical Aerospace Reports (STAR)*. This series contains scientific and technical reports issued by NASA and its contractors, other Government agencies, corporations, universities, and research organizations throughout the world.

N62-15053*# National Aeronautics and Space Administration. Goddard Space Flight Center, Greenbelt, Md.
THE ORBITING GEOPHYSICAL OBSERVATORY: A NEW TOOL FOR SPACE RESEARCH.
George H. Ludwig and E. Scull. Wilfred Washington NASA. Aug. 1962 18 p
(NASA-TN-D-1450) Avail: NTIS

In early spacecraft, the systems and experiments were highly integrated assemblies designed to fully utilize the limited weight capabilities of the launching vehicles. This high degree of mechanical and electrical integration required that each satellite or probe be completely redesigned for each new mission. Now that larger launching vehicles are available, observatory-type spacecraft are being developed which make the integration of large numbers of complex experiments more practical. These spacecraft consist of basic structures, electrical power, thermal control, attitude control, and data handling systems. Typical of these is the Orbiting Geophysical Observatory (OGO) which will carry 150 pounds of experiments to conduct investigations within and immediately outside the earth's magnetosphere and exosphere. It is being developed with well defined, simple interfaces between the experiments and spacecraft systems so that experiments developed at different laboratories may be integrated into the spacecraft with a minimum of effort. The capabilities of OGO are discussed and the experiments which are being developed for the first OGO launching are listed. Author

N64-13388# Iowa State Univ. of Science and Technology, Ames. Ames Lab.
POGO REFERENCE MANUAL
D. R. Fitzwater, E. H. Hietbrink, M. M. Ledet, D. E. McFarland, and C. E. Runge Nov. 1963 54 p
(Contract W-7405-eng-82)
(IS-769) Avail: NTIS

This programmers manual for POGO supplies the necessary background information for the use of the various system functions, as well as program descriptions for each system function, and examples of their use. Author

N64-23517*# National Aeronautics and Space Administration. Goddard Space Flight Center, Greenbelt, Md.
OGO EARTH ACQUISITION
R. A. Devaney, H. E. Montgomery, and S. J. Paddack May 1964 164 p refs
(NASA-TM-X-55002; X-643-64-101) Avail: NTIS

To acquire the earth means that the earth will be visible to the satellite in a certain fashion. The technique for predicting earth acquisition is a mathematical method that is developed into a computer program. Through the use of the program it is possible to predict when, after a reference time, the earth can be acquired by a particular satellite in a

given orbit. The technique is a function of the kind of earth-search and acquisition device, the orbit, the launch date and the time of day. The technique is applied and results are shown for two satellites in the OGO family-namely, for the Eccentric Orbiting Geophysical Observatory, EGO S-49 and for the Polar Orbiting Geophysical Observatory, POGO S-50. Author

N64-27251*# National Aeronautics and Space Administration. Goddard Space Flight Center, Greenbelt, Md.
SHADES OF EGO, S-49
H. E. Montgomery, S. J. Paddack, and F. B. Shaffer Jan. 1964 103 p refs
(Contract NAS5-2535)
(NASA-TM-X-55014; X-640-19) Avail: NTIS

This report presents shadow data and heat input data for the S-49 EGO. It gives times for which each experiment is in the shadow of either the earth, the satellite's main box, or the solar array. It also gives the heat inputs to the experiments as a function of time from launch for one complete orbit. The heat inputs include direct solar radiation, reflected solar radiation, and earth-emitted radiation. Author

N64-27355* National Aeronautics and Space Administration. Goddard Space Flight Center, Greenbelt, Md.
THE WORLD MAGNETIC SURVEY
J. P. Heppner and D. Reidel 20 May 1963 42 p refs
Repr. from Space Sci. Rev. (Dordrecht), v. 2, 1963 p 315-354
(NASA-RP-277)

The mathematical and graphical description of the earth's main field has been, and is, a data-limited problem. The World Magnetic Survey (WMS) is an endeavor to minimize this limitation by rapidly and comprehensively blanketing the earth with magnetic field measurements. Satellite surveys, which will play a key role in the WMS, are the principal topic of this paper. Existing magnetic field descriptions, the expected results from new surveys, and the methods of obtaining these results with the POGO satellite are emphasized. Author

N64-27813*# National Aeronautics and Space Administration. Goddard Space Flight Center, Greenbelt, Md.
GEGENSCHN ORBITAL PARAMETERS AND OPERATIONAL SCHEDULE
S. J. Paddack Jun. 1964 67 p refs
(NASA-TM-X-55032; X-643-133) Avail: NTIS

A technique for defining the location of the Eccentric Orbiting Geophysical Observatory (EGO), S-49, in the gegenschnein reference frame is presented. The gegenschnein reference frame is an orthogonal coordinate system with its origin at the center of the earth and its fundamental plane lying in the ecliptic plane with one of the axes in this plane pointing directly away from the sun. An operational schedule

for the gegenschein experiment is predicted. Since the experiment device cannot tolerate direct or reflected sunlight, the gegenschein experiment package is placed on the dark side of the solar array. The position of the satellite in the gegenschein coordinate system is a function of the orbit and position of the sun. The field of view problem is a function of the location of the satellite, earth and moon, and solar array position, the latter because the gegenschein experiment package rotates with the solar array. As a result of the application of these techniques in computer programs, the position in the gegenschein coordinate system versus time of the EGO is derived, and an operational schedule as a function of solar array angle is presented. Author

N65-14504# Comstock and Wescott, Inc., Cambridge, Mass. INVESTIGATION OF ULTRAVIOLET SOLAR RADIATION AND ITS INFLUENCE ON THE AEROSPACE ENVIRONMENT Final Report

J. F. McGrath, J. D. Sullivan, and W. J. Thorburn 31 Aug. 1964 262 p refs
(Contract AF 19(604)-7496)
(AFCRL-64-773; AD-608680)

CONTENTS:

1. RETARDING POTENTIAL ANALYZER 55p ref
2. EUV TELEMETERING ROCKET MONOCHROMATOR 80 p
3. EXTREME ULTRAVIOLET SATELLITE TELEMETERING MONOCHROMATORS 39 p
4. XUV SPECTROPHOTOMETER FOR POGO SATELLITES 40 p refs
5. PROPORTIONAL COUNTER SPECTROMETER 33 p

N65-18269*# National Aeronautics and Space Administration. Goddard Space Flight Center, Greenbelt, Md.

SHADES OF POGO

C. Herron and H. E. Montgomery Nov. 1964 22 p refs
(NASA-TM-X-55153; X-640-64-349) Avail: NTIS

Shadow data are presented for the S-50 (POGO) for a launch date of March 14, 1965 at 14.5 hours U. T. They show the amount of time per orbit that experiments spend in the shadow of the earth, the shadow of the main satellite structure, or the shadow of the solar array. Solar, solar reflected and earth emitted heat input data are given for an epoch time of September 12, 1965 at 1.5 U.T. R.L.K.

N65-21656*# National Aeronautics and Space Administration. Goddard Space Flight Center, Greenbelt, Md.

POWER STUDY OF SPIN STABILIZED EGO /S-49/

H. Montgomery and F. B. Shaffer Mar. 1965 13 p refs
(NASA-TM-X-55186; X-643-65-14) Avail: NTIS

An analysis is performed to determine the solar array angle which will provide maximum power output for the Orbiting Geophysical Observatory satellite. Considered are the effects of shadowing by the box and deviation of solar cell short circuit current from a cosine curve. It is assumed: (1) The geometry of the satellite is given. (2) The satellite is spinning about the k(-) sub B axis. (3) The solar cells have uniform input-output behavior, and (4) The deviation of the output from a cosine curve as the angle of incidence of sunlight is varied. Equations for the ratio of average to maximum current generated by the solar array are given. The possible ranges for the angle between the satellite's k(-) sub B axis and the vector which points from the satellite to the sun, and for the solar array angle are 0 to 180 deg and 90 to 270 deg, respectively. G.G.

N65-29296*# National Aeronautics and Space Administration. Goddard Space Flight Center, Greenbelt, Md. VISUAL PRESENTATION OF THE MOTION AND ORIENTATION OF AN ORBITING SPACECRAFT /OGO/

M. Mahoney and J. Quann Jul. 1965 17 p
(NASA-TN-D-2918) Avail: NTIS

The motion and orientation of an orbiting spacecraft are normally represented by vectors and angles in the various coordinate systems (celestial inertial coordinates, spacecraft coordinates, geodetic coordinates, etc) and it is difficult to interpret spacecraft behavior in terms of actual orbital position and attitude. Motion and orientation information for a particular satellite (OGO) have been analyzed by the 1107 computer (Univac) and the 4020 microfilm plotter (Stromberg-Carlson) and numerical data on satellite behavior were made available. The data were then used to create a motion picture film illustrating satellite attitude in orbit. Author

N65-29678*# ADCOLE Corp., Waltham, Mass. ELECTRONIC INSTRUMENTATION FOR IONOSPHERIC AND EXTREME ULTRAVIOLET RADIATION MEASUREMENTS Final Report

R. S. Hills 1 Mar. 1965 162 p refs Sponsored in parts by NASA

(Contract AF 19/628/-2464)

(NASA-CR-64074; AFCRL-65-417) CSCL 09C

This report describes the design, construction test and flight use of the electronic portions of research instruments used on rockets and satellites for the investigation of ultraviolet solar radiation. These instruments include grating monochromators for measurements in the 55-1300 Angstrom range and proportional counter spectrometers in the 1-10 Angstrom range. Also described is work done on retarding potential analyzers used for analysis of environmental charged particles, including measurement of electron temperature. All the instruments are of a telemetering type. Associated equipment used for calibration and testing of the instruments in both the laboratory and the launch phases is described. Automatic data reduction equipment was developed and used successfully. Experiments involved OSO, OGO and Air Force satellites and Aerobee-150 and Black Brant rockets. Author

N65-29783*# National Aeronautics and Space Administration. Goddard Space Flight Center, Greenbelt, Md.

RELATIVE ADVANTAGES OF SMALL AND OBSERVATORY TYPE SATELLITES

G. H. Ludwig May 1965 26 p Presented at the COSPAR Symp., Buenos Aires, 13-19 May 1965

(NASA-TM-X-55261; X-611-65-189) Avail: NTIS CSCL 22B

Both the relatively small explorer and the large Orbiting Observatory classes of scientific satellite have advantages which need to be considered carefully when a new space experiment is to be performed. The small satellite offers greater choice in tailoring the orbit to the experiments. The smaller size simplifies the electrical, magnetic, and radiated interference problem, since fewer operating components are involved. It provides greater ease in testing and scheduling and permits a shorter pre-launch lead time. The larger observatory permits the conduct of more complex or larger numbers of related experiments for the more detailed study of the co-relationships between the numerous space phenomena. Since it is less highly integrated, standard experiment/spacecraft interfaces can be defined to simplify the experiment design and integration problems. The larger size permits the use of higher capacity and more flexible data systems and more precise active orientation systems. Operational efficiency is higher, since the data from a large number of experiments can be recorded and processed simultaneously. It is concluded that both types should continue to be used to meet the varied requirements of the space sciences program. Author

N65-30651*# National Aeronautics and Space Administration. Goddard Space Flight Center, Greenbelt, Md.

ORBITAL PARAMETERS FOR THE OGO-E GEOCORONAL HYDROGEN EXPERIMENT

S. J. Paddack Jul. 1965 34 p refs

(NASA-TM-X-55276; X-643-65-294) Avail: NTIS CSCL 22C

This document presents and applies methods for obtaining certain necessary orbital and spacecraft parameters for meaningful data analysis of the geo-coronal hydrogen

measurement experiment (Experiment No. 22) on the fifth in Orbiting Geophysical Observatory Series, namely the OGO-E. Techniques are presented for determining as a function of time: (1) orbit inclination with respect to the ecliptic plane; (2) the angle between the orbit's angular momentum vector and the sun's position vector; (3) the half angular dimension of the earth viewed from the satellite; (4) the solar array angle; and (5) the angle between the projection of the sun on the x-y plane of the experiment's coordinate system and the x-axis of that system. The calculations were made using a numerical integration general purpose interplanetary trajectory program (ITEM). Consequently, the changes in the orbit due to perturbations are reflected in the calculations of the quantities mentioned above. The results of computer runs are presented in this document.

Author

N66-12993* Stanford Univ., Calif. Radioscience Lab. **ECCENTRIC GEOPHYSICAL-OBSERVATORY SATELLITE S-49 WITH INTERPRETATION OF THE RADIO-BEACON EXPERIMENT TECHNICAL REPORT NO. 1** A. V. DaRosa Jun. 1965 63 p refs (Contract NASr-136)

(NASA-CR-68307; SEL-65-063) Avail: NTIS CSCL 04A
The S-49 satellite, launched on 5 September 1964 carried a pair of radio beacons operating at harmonically related frequencies modulated by 20 and 200-kc signals. The radio-beacon experiment was designed to investigate the exosphere by studying the behavior of the columnar electron content between ground and satellite as the latter moves from perigee to apogee in its highly eccentric orbit. To avoid errors arising from over-simplified assumptions about the dense ionosphere which would mask the effects in the exosphere simultaneous measurements were made of the differential-Doppler frequency and the Faraday rotation angle. The former provides columnar-content information from ground to transmitter while the latter yields columnar content information determined mainly by the ionization in the lower ionosphere. The difference between the contents thus obtained can be attributed to the columnar content of the exosphere up to satellite height and should be essentially independent of variations in the lower ionosphere. The objective of the present report is to describe the underlying principles and the techniques for translating the rad data received from the EGO beacon experiment into curves of slant columnar content in the exosphere vs time. These curves are the starting point for an analysis of the exospheric behavior. Such an analysis, however, is not a part of the present report. The usual first order analysis of the differential Doppler frequency and the Faraday rotation angle data is complicated in the present case by the rotation of the satellite antenna. The effect of this rotation is investigated and methods for taking into account are developed. The effects of various approximations usually made in the first order analysis are investigated and, when necessary, proper corrections are introduced. In brief, the use of this report will permit the specification of scaling techniques for the records bearing the raw data from the satellite and the writing of computer programs that will yield exospheric columnar contents.

Author

N66-13640* State Univ. of Iowa, Iowa City. Dept. of Physics and Astronomy. **LOW-ENERGY PROTON AND ELECTRON EXPERIMENTS FOR THE ORBITING GEOPHYSICAL OBSERVATORIES B AND E** L. A. Frank Jul. 1965 35 p (Grant NSG-233-62; Contract NONR-1509/06/) (NASA-CR-68558; Rept-65-22) Avail: NTIS CSCL 20H

The instrumentation and calibrations of the University of Iowa low-energy proton and electron experiment for the Orbiting Geophysical Laboratories (OGO) B and E are described. The experiment utilizes cylindrical curved-plate electrostatic analyzers to provide measurements of the differential energy spectrums of protons and electrons within and in the vicinity of the earth's magnetosphere. Continuous

channel multipliers (Bendix Channeltrons) are used to count individual charged particles accepted by the analyzers and provide the instrument with a dynamic range in proton and electron intensities extending from 10,000 to 10 to the 10th power/ (sq cm-sec-sr) in a given energy bandpass of the electrostatic analyzer. The widths of the energy bandpasses of the electrostatic analyzers are sufficiently wide to cover the entire energy range extending from 90 eV to 70,000 eV (protons and electrons separately) in 14 voltage steps on the curved plates. The four electrostatic analyzers (two analyzers each for protons and electrons covering the above energy range) complete with signal conditioner, high-voltage power supplies, and thermal shield require an average power of 2 watts and an instrumentation weight of 6.3 pounds.

Author

N66-21006* National Aeronautics and Space Administration. Goddard Space Flight Center, Greenbelt, Md. **EGO ORBITAL PARAMETERS AND HEAT INPUTS** H. E. Montgomery and S. J. Paddock 1 Apr. 1963 79 p refs (NASA-TM-X-55428; X-643-63-61) Avail: NTIS CSCL 22A

Methods of analysis for computing orbital, spacecraft angle, and spacecraft heat input data for OGO (Orbiting Geophysical Observatory) are presented. Specific results are given for the S-49, Eccentric Orbiting Geophysical Observatory (EGO). The orbital data include the transient behavior of true anomaly, the flight path angle, the distance from the center of the earth to the satellite, the angle between the line of apsides and the ecliptic plane, and the angle between the projection of the line of apsides on the ecliptic plane and the earth-sun line. The spacecraft angle data include the transient behavior of solar array angle, the orbital plane experiment package (OPEP) angle, and the OPEP velocity vector angle. The transient heat input data include earth emitted heat, direct solar heat, and earth reflected solar heat inputs to all the faces of the main OGO box, the solar array, and the OPEP. The calculated results are consistent with the previously conducted EGO Launch Window Study insofar as the perigee restraint is concerned. The present data are for launch times for which the perigee will not go below its initial value for a whole year. L.S.

N66-35685* Aerospace Corp., El Segundo, Calif. **MODELS OF THE TRAPPED RADIATION ENVIRONMENT. VOLUME 2: INNER AND OUTER ZONE ELECTRONS** A. B. Lucero, J. I. Vette, and J. A. Wright Washington NASA 1966 100 p refs Supported in part by NASA (Contract AF 04(695)-469) (NASA-SP-3024-Vol-2) Avail: NTIS

Graphs and tables of data for the electron environment AE2, which cover both inner and outer zone out to L=60 for the time period around August 1964 are presented. Data for electron energy spectra, distribution and orbital integrations are included. N.E.N.

N67-13710* Minnesota Univ., Minneapolis. Cosmic Ray Group. **THE CONSTRUCTION, CALIBRATION AND OPERATION OF THE UNIVERSITY OF MINNESOTA EXPERIMENTS FOR OGO-1 AND OGO-3** S. R. Kane, K. A. Pfitzer, and J. R. Winckler Sep. 1966 48 p refs (CR-87)

Response characteristics of the ionization chamber and electron spectrometer experiments flown on the OGO-1 and OGO-3 satellites are considered in the outer radiation belt. The ion chamber response is attributed entirely to energetic electrons that penetrate the chamber wall. Here, the ion chamber constitutes a stable, sensitive counter with a dynamic range for electrons above 600 kV energy. Calculation of absolute fluxes of particles from the counting rates of the OGO instruments is described, and instrumental constants for these flux determinations are summarized.

Cross-calibration between the ion chamber and spectrometer and sampled data in the outer radiation belts is included. Responses to electrons, X-rays, protons, and heavier nuclei, and cosmic rays in free space are detailed for the OGO-1 ion chamber experiment, and attention is given to the normalization and calibration of the ion chamber correction for dead-time of the reset switch and the dynamic range and linearity of response. M.W.R.

N67-18763*# National Aeronautics and Space Administration, Goddard Space Flight Center, Greenbelt, Md.

A REPRESENTATION OF THE PERIGEE MOTION OF A SATELLITE AS A FUNCTION OF LOCAL TIME

R. A. Langel Feb. 1967 12 p
(NASA-TM-X-55703; X-612-67-34) Avail: NTIS CSCL 22C

A procedure was developed for a graphic display of one specialized feature of a satellite orbit—the relationship of the perigee of the orbit to latitude and to local time. From this plot it is a very simple matter to see exactly when in a satellite lifetime it will encounter a particular sunlight configuration. At what latitude the satellite approaches closest to the earth can also be readily seen. Obvious applications are predictions of eclipse times and periods of maximum drag. From a geophysical viewpoint, one may predict when satellite data should be examined for effects which are local time and/or latitude dependent. Author

N67-19899* Aerospace Corp., El Segundo, Calif.
MODELS OF THE TRAPPED RADIATION ENVIRONMENT, VOLUME 3: ELECTRONS AT SYNCHRONOUS ALTITUDES

A. B. Lucero, J. I. Vette, and J. A. Wright Washington
NASA 1967 111 p refs
(Contracts NASA Order W-11683; AF 04(695)-469)
(NASA-SP-3024-Vol-3) Avail: NTIS

In order to produce the trapped electron environment in sufficient detail, data was examined from particle detectors flown on IMP A, OGO A, FRS-17, and Explorers 6, 12, and 14. The model environment is confined to L=6.6; B/B sub o and local time variations as well as the energy spectrum are presented. Time variations are discussed in terms of a solar cycle variation, occasional 27-day variations, and in a completely statistical way. Since the elliptical satellites sample the L=6.6 shell twice each orbit, the time between samples varies from three hours up to four days. It is shown that if a large number of these samples are treated as independent events, the logarithm of the flux displays a Gaussian distribution in which the standard deviation increases with energy. The construction of the model is discussed and graphical and analytical representations are given. R.N.A.

N67-22257*# Advanced Technology Labs., Mountain View, Calif.

HIGH ALTITUDE LIMITATION STUDY ADVANCED HORIZON SENSOR FOR OGO Final Report, 4 Apr. - 15 Jul. 1966

R. K. Ronald 30 Aug. 1966 100 p refs
(Contract NASS-9109)
(NASA-CR-83567; ATD-R-1405) Avail: NTIS CSCL 17H

High altitude or small earth limitations are investigated for the advanced horizon sensor of the Orbiting Geophysical Observatory OGO-A. Small earth limitation is considered as the extreme nonlinearity in the three-tracker mode of attitude angle calculation when the earth disk subtends a small angle and it is shown that at a satellite altitude of more than 80,000 nautical miles a reliable maximum pitch attitude angle of only one degree results and the tracking check logic breaks track when the horizon temperature is less than 214 K. Effects of finite field of view of the infrared beam, de offset, and horizon temperature on the tracking point are considered, while small earth climatic variations are excluded. Horizon convolution and horizon-gradient tracking computer programs are discussed, and summing amplifier output accuracy as well as space bias

and square earth effect are considered. Optical characteristics of the OGO-A telescope transfer functions numerical values for circuit constant and a space bias study are treated. M.W.R.

N67-27576*# National Aeronautics and Space Administration, Goddard Space Flight Center, Greenbelt, Md.
METHODS OF DATA REDUCTION FOR THE OPEP AIRGLOW PHOTOMETER ON OGO-2

J. Pacquet (Centre Natl. de la Rech. Sci., Verrieres-le-Buisson) May 1967 59 p
(NASA-TM-X-55794; X-613-67-218) CSCL 20B

A brief description is given of the methods used in the reduction of the data from the OPEP airglow photometer on OGO-II. For selected portions of the data, computers have been used to apply instrumental corrections, to reduce an oscillatory component dependent on the position of the OPEP container, and to solve a system of linear equations to compute a vertical emission profile from the observed horizon profiles. Author

N67-27578*# National Aeronautics and Space Administration, Goddard Space Flight Center, Greenbelt, Md.
SOME EFFECTS OF MEV ELECTRONS ON THE OGO 2 (POGO) AIRGLOW PHOTOMETERS

C. W. Aitken (Vitro Corp. of Am.), J. F. Brun (Centre Natl. de la Rech. Sci., Paris), W. B. Fowler, and E. I. Reed Mar. 1967 58 p refs
(NASA-TM-X-55791; X-613-67-132) CSCL 20B

After noting the high levels of background current in the Main Body Airglow Photometer on OGO-II, a Polar Orbiting Geophysical Observatory, a series of laboratory tests were made to indicate the sources of interference and methods of prevention. Tests with 2.6 MeV electrons confirmed that such electrons in space could account for the observed signals. Other tests were made which (1) showed that the most sensitive portion of the photometer was the cathode-window combination in the photomultiplier, (2) indicated the effectiveness of various methods of shielding, and (3) studied the presence and decay time of radiation-induced phosphorescence. Further laboratory tests confirmed that a similar OPEP photometer on the same satellite, with a different photomultiplier, a more limited spectral range, and greater shielding, was relatively insensitive to the same environment. Author

N67-30147*# National Aeronautics and Space Administration, Goddard Space Flight Center, Greenbelt, Md.
PROCESSING OF THE TOTAL FIELD MAGNETOMETER DATA FROM THE OGO-2 SATELLITE

R. A. Langel Jun. 1967 82 p refs
(NASA-TM-X-55822; X-612-67-272) Avail: NTIS

The process of reducing the OGO-2 magnetic field data from the original data acquisition and recording (pulse code modulation data only) to the preparation of the final data set used for analysis is described in detail. The OGO-2 telemetry system, magnetometer, and associated instrumentation are also described. An effort is made to point out both the unsuccessful and successful data reduction techniques used as well as what procedures would be used now if the processing were to begin afresh and how to best utilize the new generation of computer hardware which is becoming available. R.N.A.

N67-30831*# Stanford Univ., Calif. Radioscience Lab.
OBSERVATIONS OF WHISTLER-MODE SIGNALS IN THE OGO SATELLITES FROM VLF GROUND STATION TRANSMITTERS

R. L. Heyborne Nov. 1966 113 p refs
(Contract NASS-2131; NASS-3093; Grant NSF GP-2247)
(NASA-CR-84869; TR-3415/3418-1; SEL-66-094) CSCL 04A

Amplitude calibrated receivers aboard two satellites (OGO-1 and OGO-2) are used to receive signals propagating in the whistler mode from vlf ground stations. Existing theory is utilized to calculate the expected intensities of these signals. Measured and calculated intensities are then compared. The

two satellites effectively sub-divide the whistler mode path into two main parts: (1) the earth-ionosphere waveguide loss, the boundary and excitation loss, and the absorption loss through the ionosphere to the altitudes of OGO-2, and (2) losses due to divergence of the signal between OGO-2 and the higher altitudes of OGO-1 plus any additional absorption above OGO-2. These data are utilized to determine more precisely the major features and loss characteristics of whistler-mode paths inferred from previous experiments, and to determine the accuracy of attenuation rates predicted earlier by theoretical means. It is concluded that the average intensity of VLF whistler-mode signals in the magnetosphere may usually be predicted to an accuracy of + or - 10 db by the use of available models and existing theory. Author

N67-30930# California Univ., Livermore. Lawrence Radiation Lab.

A LOW-POWERED MAGNETIC HALL PROBE FOR SPACE APPLICATIONS

J. H. McQuaid 10 Jan. 1966 20 p refs
(Contract W-7405-eng-48)

(UCRL-14650-T) Avail: NTIS

A magnetic Hall probe was developed for use in a spectrometer system aboard NASA's OGO-E Satellite. The probe is to monitor the flux in each of the two spectrometer magnets. This flux is in the order of 800-900 gauss for the small magnet and 2500-2700 gauss for the large magnet. When measuring long term variations in the magnetic field it is not necessary to continuously monitor the flux; therefore the Hall generator in this system operates on current pulses of short duration. The pulsed current mode of operation affords high efficiency and low power consumption. In the system described, the Hall generator is placed in the magnetic field and driven by a pulse generator. The resulting Hall voltage (which is proportional to the magnetic flux) is amplified and fed to a pulse stretcher. The stretcher circuit preserves the pulse amplitude for a time which is suitable for accurate readout. Author (NSA)

N67-31362*# State Univ. of Iowa, Iowa City. Dept. of Physics and Astronomy.

STUDY OF THE TEMPORAL VARIATIONS OF 40 keV ELECTRONS IN THE MAGNETOSPHERE DURING AND AFTER THE MAGNETIC STORM ON APRIL 18, 1965 Progress Report, May 1967

C. S. R. Rao May 1967 60 p

(Grant NsG-233-62; Contract NONR-1509/06/)

(NASA-CR-85905; Rept-67-16) Avail: NTIS CSCL 20A

Temporal variations of the intensities of electrons $E > 40$ keV during the main phase and post-storm period of a large magnetic storm which occurred on April 18, 1965 are studied using data obtained at high latitudes by the University of Iowa Satellite Injun IV and at low latitudes by the NASA satellite OGO 1. The high latitude observations show a large inward movement of the cutoff boundary for trapped electrons to lower latitudes by as much as 8 deg. On the storm day and during the post-storm period, the cutoff latitude shows a close and direct correlation with D_{st} and inverse correlation with 3 hour index. The slot which is present at an invariant latitude of 61 before the storm disappears on the storm day and is replaced by a peak. The post-storm variations of these storm induced electrons at higher latitudes are uncorrected with the $K_{sub} \rho$ index. The intensities decay according to an exponential law. There appears to be an injection and inward diffusion of fresh electrons during the post storm period leading to the formation of the normal quiet day profile. Variations for precipitated electrons are generally similar. Author

N67-32070*# Smithsonian Astrophysical Observatory, Cambridge, Mass.

MEASUREMENTS OF RED VELOCITIES OF INTERPLANETARY DUST PARTICLES FROM OGO-1

W. M. Alexander (Temple Univ.) and C. S. Nilsson 1967 5 p In NASA, Washington Meteor Orbits and Dust p 301-305 refs Sponsored by NASA and NAS

Details are given on the instrumentation, the impact parameter data, and the probable orbits of three particles. The method of calculating the orbital elements is discussed, and probability distributions are shown for orbital inclinations and eccentricities. It is suggested that the particles were in heliocentric orbits. N.E.N.

N67-35595*# National Aeronautics and Space Administration, Goddard Space Flight Center, Greenbelt, Md.

PROCESSING THE DATA FROM THE OGO-III GEGENSCHHEIM PHOTOMETRY EXPERIMENT

J. H. Quann Aug. 1967 159 p

(NASA-TM-X-55907; X-565-67-403) CSCL 20B

The objectives, apparatus, data generation and display, and data analysis system of the Geggenschheim Photometry Experiment performed aboard the OGO-B spacecraft, are discussed. The experiment is intended to provide information for gaining a better understanding of the earth and earth-sun relationships. The procedure for using the system is described. Program control user options, run execution, control card formats, subroutines, and computation procedures are discussed. Output examples are given. L.S.

N67-37021*# Stanford Research Inst., Menlo Park, Calif. OGO-1 VLF EXPERIMENT A-17 DIGITAL DATA PROCESSING SYSTEM Final Report

W. E. Blair, B. P. Ficklin, M. E. Mills, N. D. Schlosser, J. H. Wensley, W. H. Zwisler et al Apr. 1967 112 p

(Contract NAS5-2131)

(NASA-CR-88618) CSCL 20F

The digital data processing technique of the VLF radio noise and propagation experiment (A-17) aboard the OGO-1 satellite is examined. Descriptions, operational procedures, and details of the instrument and satellite are given as required for understanding of the data processing system. Data acquisition, decommutation, and processing systems are briefly described. The input, output, and operation of the four-phase data-processing system are presented in detail. The computer display system and 16-mm cine film presentation are also described, and examples are shown. On more than 200,000 frames of film 2x10 to the 8th power experimental digital data bits of information covering 99 satellite revolutions have been plotted and stored. This accumulation of data represents more than 100,000 bits of information per frame and was computer processed at approximately three frames per second. This cine film technique provides capability for significant data compacting, quick data scanning, discrimination between signals and interference, recognition of unique data characteristics, and simultaneous data comparison. Author

N67-37398* National Aeronautics and Space Administration, Goddard Space Flight Center, Greenbelt, Md.

THE GEOMAGNETIC SECULAR VARIATION, 1900 - 1965

J. C. Cain and S. J. Hendricks Sep. 1967 231 p refs

(NASA-TM-X-55944; X-612-67-479) CSCL 08N

The main geomagnetic field model uses linear and parabolic terms in time to represent secular change over the interval 1900-1965. The predicted field is compared with observatory annual means to investigate systematic residuals. Deviations of the order of 100 gamma are noted for short spans of years and are observed to occur only in limited regions. Otherwise, the trends of the computed field parallel the observations. Comparisons of secular change charts with those drawn by earlier analyses show good agreement. The westward drift is generally noted in the vector representation of the harmonic coefficients except that a few terms are seen to undergo predominantly an amplitude change. The components below $(g(6), h(6))$ that show a recognizable eastward drift are the (3,2) and (5,2) terms. Both dip poles are noted to move smoothly northward over the interval whereas the dipole position initially drifts eastward, reverses direction near 1920, and then moves westward at a rate up to about 0.7 deg/year. Its 1965 position is found to be 78.8 deg N and 70.0 deg W. Author

N67-40126* State Univ. of Iowa, Iowa City. Dept. of Physics and Astronomy.

INVESTIGATION OF ENERGETIC ELECTRON INTENSITIES IN THE EARTH'S OUTER RADIATION ZONE WITH OGO 1 M.S. Thesis

H. K. Hills Aug. 1967 117 p refs

(Contract NAS5-2054)

(NASA-CR-89652) Avail: NTIS CSCL 04A

Observations of intensities of outer zone electrons obtained with instrumentation borne on the earth-satellite OGO-1 during the period September through December, 1964 are presented. Omnidirectional intensities near the magnetic equatorial plane are given for electrons of energy $E > 40$ keV, $E > 130$ keV, and $E > 2$ MeV, and are characterized by short term variations superimposed upon an over-all long term decrease. The pitch angle distributions of electrons ($E > 40$ keV and $E > 130$ keV) may be approximated by the function $\sin(n)\alpha$ with n generally found to be less than or about unity throughout the outer zone ($3 < \text{or} = L < \text{or} = 7$). Computations of the effects of geomagnetic storms upon the distribution of intensities of these electrons with energies above the detector thresholds are summarized. Adiabatic motions are shown to be capable of causing large temporal variations in electron intensities during a magnetic storm. Author

N68-10422* Minnesota Univ., Minneapolis. Cosmic Ray Group.

APPLICATION OF AN INTEGRATING TYPE IONIZATION CHAMBER TO MEASUREMENTS OF RADIATION IN SPACE Ph.D. Thesis

S. R. Kane Sep. 1967 221 p refs

(Contract NAS5-2071)

(NASA-CR-90060; CR-106) Avail: NTIS CSCL 22B

An integrating type ion chamber experiment, using a resetting drift-type electrometer and designed to fly on the OGO-1 and 111 satellites is described. The chamber is demonstrated to have an accuracy and stability of approximately 1% during its operation in space over a period of nearly three years. The minimum energy for penetration by protons and electrons is 12 and 0.6 MeV respectively. The response to 40 keV electrons (through bremsstrahlung) is about 10 to the minus 7th power x (response at energies > 600 keV). The response to X-rays in 10-150 keV range is peaked at approximately 20 keV; below 10 keV the response is approximately 0.01 x (response at 20 keV). For 1 particle on $\text{cm}^2 \text{ sec}^{-1}$ of 20 keV photons, electrons with energy $>$ or $=$ to 1 MeV and minimum ionizing nuclei with charge Z_e the pulsing rate of the chamber is respectively 0.2, 7.0, and 5.5 $z(2)$ NPPS (Normalized Pulses Per Second) x 1,000. Author

N68-14025* Stanford Research Inst., Menlo Park, Calif. **RESONANCES IN THE DRIVING-POINT IMPEDANCE OF AN ELECTRIC DIPOLE IN THE IONOSPHERE**

W. E. Blair Mar. 1967 33 p refs Prepared for Stanford Univ., Calif.

(Contract NAS5-9309)

(NASA-CR-91620; TR-1) Avail: NTIS CSCL 20N

The resonances in the driving-point impedance of a center-fed cylindrical electric dipole imbedded in the ionosphere are analyzed. The ionospheric model is a lossy, anisotropic, homogeneous neutral plasma containing various ionic constituents. It is found that there are zeros in the reactance at the upper and lower hybrid frequencies and poles at the electron and ion gyrofrequencies. These critical frequencies are independent of antenna length and orientation (parallel or perpendicular to the earth's magnetic field) to the first-order approximation. It is shown that pole-zero frequencies could be used to determine the earth's magnetic field strength, electron density, and ion masses and densities at any point in the ionosphere at which the impedance was measured. Author

N68-15232* State Univ. of Iowa, Iowa City. Dept. of Physics and Astronomy.

A CINEMATOGRAPHIC DISPLAY OF OBSERVATIONS OF LOW-ENERGY PROTON AND ELECTRON SPECTRA IN THE TERRESTRIAL MAGNETOSPHERE Progress Report, Nov. 1967

L. A. Frank and W. L. Shope Nov. 1967 27 p refs

(Contract NAS5-2054; Grant NSG-233-62; Contract

Nonr-1509/06)

(NASA-CR-91871; Rept-67-67; AD-662228) Avail: NTIS

A massive series of observations of the differential energy spectra of proton and electron intensities over the energy range of approximately 300 eV to 50 keV within the earth's magnetosphere and its environs has been obtained with an array of electrostatic analyzers borne on the earth-satellite OGO 3. In order to supplement the presently existing publications derived from these observations and to provide further insight into the distributions of low-energy charged particles within the earth's radiation zones over geocentric radial distances of approximately 2 to 20 RE (RE, earth radii) we have utilized a SC 4020 microfilm plotter to construct a cinematographic display of the differential energy spectra of proton and electron intensities which spans a complete circuit of the spacecraft around the earth, or about 50 hours of substantially continuous observations beginning at 1330 U.T. on July 14, 1966. This cinematographic display comprises approximately 18,000 individual frames and summarizes some 550,000 intensity measurements. A description of the methods and graphic results is furnished as an aid in interpretation of this visual presentation of the observations. Author (TAB)

N68-17981* Stanford Univ., Calif. Radioscience Lab. **WHISTLER PROPAGATION IN MAGNETOSPHERIC DUCTS**

J. J. Angerami and R. L. Smith Jul. 1967 9 p. In ESSA Conjugate Point Symp., vol. 2, Session 3 Jul. 1967

(Contract NAS5-2131; Grants NSG-174; NSF GP-948)

CSCL 04A

Reviewed are some of the theories of propagation of whistlers in field-aligned ducts and their relation to recent observations. Features of propagation are discussed which were deduced from the ray theory approach and then verified by recent ground and satellite observations. These observations have led to further ray tracing studies which explain some high frequency leakage effects and suggest an indirect experimental determination of duct dimensions and enhancement factors. In addition to ray tracing techniques, the review covers the mode theory of propagation as developed for tropospheric ducting, and the full wave treatment using Maxwell's equations directly. K.W.

N68-23026* Minnesota Univ., Minneapolis. School of Physics and Astronomy.

AN ATLAS OF 10-50 keV SOLAR FLARE X-RAYS OBSERVED BY THE OGO SATELLITES, 5 SEPTEMBER 1964 TO 31 DECEMBER 1966

R. L. Arnoldy, S. R. Kane, and J. R. Winckler Jan. 1968 82 p refs

(Contract NAS5-2071)

(NASA-CR-94429; ; CR-108) Avail: NTIS CSCL 03B

Ionization rate profiles are presented for about 70 solar events that represent almost all of the cases detected by the ion chambers during the observing times of OGO-1 and OGO-3 through the end of 1966. Some data on the instrumentation are included for these preliminary studies relating to X-ray phenomena in radio emission. Besides listing of frequency and the observing station, the presence of the radio emission is indicated on the plots by a horizontal line with a vertical arrow marking the reported time of maximum. Although radio information is quite complete, the absence of an indicated radio burst in some cases is due to the unavailability of information and does not necessarily mean a radio burst did not occur. M.W.R.

N68-35999* National Aeronautics and Space Administration. Goddard Space Flight Center, Greenbelt, Md. **PHOTOELECTRON FLUX IN THE TOPSIDE IONO-**

N69-12899

SPHERE MEASURED BY RETARDING POTENTIAL ANALYZERS

J. L. Donley and B. C. N. Rao Sep. 1968 15 p refs
(NASA-TM-X-63358; X-615-68-381) Avail: NTIS CSCL 04A

Reported are results of measurements of photoelectron flux in the topside ionosphere which were made using retarding potential analyzers aboard the Explorer 31 and OGO-4 satellites. S.C.W.

N69-12899 Iowa Univ., Iowa City.
INVESTIGATION OF ENERGETIC ELECTRON INTENSITIES IN THE EARTH'S OUTER RADIATION ZONE WITH OGO 1 Ph.D. Thesis

H. K. Hills 1967 117 p
Avail: Univ. Microfilms Order No. 68-941

Intensities of outer zone electrons obtained with instrumentation borne on the earth-satellite OGO 1 are presented. Omnidirectional intensities near the magnetic equatorial plane are given for electrons of energy $E > 40$ keV, $E > 130$ keV, and $E > 2$ MeV, and are characterized by short-term variations superimposed upon an over-all long-term decrease. The pitch angle distributions of electrons ($E > 40$ keV and $E > 130$ keV) are approximated, and effects of geomagnetic storms upon the distribution of intensities of these electrons with energies above the detector thresholds are summarized. These results are compared with observations in order to distinguish between adiabatic and non-adiabatic particle behavior. Adiabatic motions are shown to be capable of causing large temporal variations in electron intensities during a magnetic storm. Dissert. Abstr.

N69-14392*# Michigan Univ., Ann Arbor. Radio Astronomy Observatory.
INSTRUMENTATION FOR RADIO ASTRONOMY MEASUREMENTS ABOARD THE OGO-5 SPACECRAFT

B. D. MacRae 20 Sep. 1968 142 p refs
(Contract NAS5-9099)
(NASA-CR-98670) Avail: NTIS CSCL 22A

This report describes the design considerations and performance characteristics of a satellite-borne instrumentation system designed and constructed at the University of Michigan Radio Astronomy Observatory. The system is designed to make radio astronomy measurements at eight discrete frequencies from 50 kHz to 3.5 MHz. These measurements are to detect solar and Jovian radio frequency bursts and to determine the relative average level of cosmic background radiation down to 50 kHz. Procedures used for preflight and in-flight noise calibrations are discussed. A description of the ground support equipment used for preflight testing is given. The instrument was successfully launched aboard the OGO-5(E) spacecraft on 4 March 1968 into an elliptical orbit having the following approximate parameters: perigee, 292 kilometers; apogee, 147,000 kilometers; inclination to the equator, 31 deg; period, 63 hours, 25 minutes. The initial data from the instrument look excellent and the instrument should successfully fulfill its missions. The scientific aspects and results of this program will be published separately. Author

N69-14393*# Michigan Univ., Ann Arbor. Radio Astronomy Observatory.
DATA REDUCTION AND ANALYSIS REPORT FOR THE RADIO ASTRONOMY EXPERIMENT ABOARD THE OGO-2 SPACECRAFT

Aug. 1968 24 p refs
(Contract NAS5-3099)
(NASA-CR-98669; Rept-68-12) Avail: NTIS CSCL 22A

The Radio Astronomy Observatory of the University of Michigan has identical experiments on the OGO-2 and OGO-4 spacecraft, whose primary objective is to generate a map of the cosmic noise background at a frequency of 2.5 MHz, using ionospheric focussing to provide resolution. Because of various spacecraft problems, it does not appear that the OGO-2 experiment will achieve this objective. Therefore, the

data from this experiment has not been fully processed. It is possible, however, that OGO-2 data may be of some value to supplement that obtained from OGO-4, or may yield valuable information on the earth's ionosphere. Author

N69-17412*# Iowa Univ., Iowa City. Dept. of Physics and Astronomy.
SOLAR X-RAY CONTROL OF THE E LAYER OF THE IONOSPHERE

P. R. Sengupta Jan. 1969 46 p refs
(NGL-16-001-002)
(NASA-CR-73884; Rept-69-3) Avail: NTIS CSCL 04A

Solar X-ray control of the E layer of the ionosphere is investigated. Electron production rates between 100 and 140 km above the earth due to 31-100 A solar X-ray flux extrapolated from X-ray data recorded by Explorer 30, OGO-4, and OSO-4, and due to reported Lyman alpha flux from rocket and satellite experiments are calculated to show that about 70% of the E-layer ionization is contributed by the X-rays. Calculated E-layer electron densities due to solar X-ray flux on two typical days are compared with the E-layer electron density profile. It is concluded that 31-100 A solar X-rays which contribute about 70% of the E-layer ionization on a day of moderate solar activity are responsible for day-to-day variations in the E-layer index. Contribution of 10-30 A solar flux to the E-layer ionization is small except on a day of high solar activity. Author

N69-17928*# Dartmouth Coll., Hanover, N.H. Radiophysics Lab.

AN EXPERIMENT TO STUDY WHISTLERS AND AUDIO-FREQUENCY EMISSIONS WITH A RECEIVING SYSTEM ON BOARD THE POGO S-50 SATELLITE (OGO-C/2) IN CONJUNCTION WITH AN EXISTING NETWORK OF GROUND-BASED OBSERVING STATIONS Final Report, 30 May 1963 - 29 Feb. 1968

T. Laaspere and M. G. Morgan 29 Feb. 1968 60 p refs
(Contract NAS5-3092)
(NASA-CR-97605) Avail: NTIS CSCL 04A

Technical specifications developed by the contractor for the experiment are cited and a chronological account is given of the production of the experiment by a subcontractor and its acceptance by Goddard Space Flight Center. The launch and the results obtained with the experiment are described, and a paper discussing observations of lower-hybrid-resonance phenomena by Dartmouth's OGO-2 experiment is included. Consideration given to means of acquiring data from the spacecraft over Labrador is also described. Author

N69-18074*# National Aeronautics and Space Administration. Goddard Space Flight Center, Greenbelt, Md.
EFFECTS OF ENERGETIC PARTICLES ON PHOTOMULTIPLIERS IN EARTH ORBITS UP TO 1500 km

J. E. Blamont (CNRS, Paris), W. B. Fowler, and E. I. Reed Dec. 1968 19 p refs
(NASA-TM-X-63419; X-613-68-486) Avail: NTIS CSCL 09A

The response of several types of photomultipliers to energetic particles is discussed in terms of observed background current. Examples are drawn primarily from photometers for observation of the earth's airglow on two Polar Orbiting Geophysical Observatories, OGO-2 and OGO-4; brief reference is made to other OGO photometers. The largest background current was observed on OGO-2 from an EMR541E, a sapphire end-window tube with S-20 photocathode. At a maximum of the inner electron belt, cathode current exceeded 10 to the minus 9th power amperes at about 1500 km. Several components were noted in the background current, with the most prominent due to the inner radiation belt and a component with the latitude distribution characteristic of cosmic rays. Estimated instantaneous proton and electron fluxes are compared with background current in order to obtain an approximate responsivity to energetic particles. Author

N69-19899* Minnesota Univ., Minneapolis. School of Physics and Astronomy.
AN EXPERIMENTAL STUDY OF ELECTRON FLUXES FROM 50 KEV TO 4 MEV IN THE INNER RADIATION BELT Ph.D. Thesis

K. A. Pfizter Aug. 1968 166 p refs Submitted for publication
 (Contract NAS5-2071)
 (NASA-CR-100648) Avail: NTIS CSCL 04A

A five channel magnetic electron spectrometer which is capable of accurately measuring the electron spectrum from 40 keV to 4 MeV is described. The spectrometer consists of two separate detectors operating together to provide double energy selection. The first of these is an electromagnet with a collimating slit having a geometry factor of 8.64×0.001 sterad-sq cm. The second detector consists of a heavily shielded scintillation crystal and photomultiplier tube. The electron spectrometers were flown on the Orbiting Geophysical Observatories (OGO) 1 and 3. The two spectrometers, which have been cross calibrated in space and shown to agree to within 10% observe the continuing decay of the electrons injected into the inner zone by the nuclear explosion, Starfish, on July 9, 1962. The spectrometers observe a factor of ten decrease in the electron flux over a period of two years from September 1964 to August 1966 in the inner zone below $L = 1.8$ for electrons of $E > 290$ keV.

Author

N69-20849* Iowa Univ., Iowa City. Dept. of Physics and Astronomy.

LOCAL TIME ASYMMETRIES IN THE INCREASE OF ELECTRON FLUXES IN THE OUTER VAN ALLEN ZONE DURING SUBSTORMS

C. S. R. Rao Feb. 1969 35 p refs
 (Contract NAS5-3097; Grant NGL-16-001-002)
 (NASA-CR-100419; Rept-69-8) Avail: NTIS CSCL 04A

The increase was studied in the fluxes of electrons $E_{sub e} >$ or approximately 40 keV and $E_{sub e} >$ or approximately 120 keV in the outer Van Allen zone at different local times during night-time magnetic bay activity. Electrons $E_{sub e} >$ or approximately 40 keV show increases in the midnight to afternoon sectors but not in the evening sector during bay activity. Electrons $E_{sub e} >$ or approximately 120 keV do not, however, show significant increases at these times. Also, whereas the increase in the midnight sector occurs immediately after the onset of a bay, a significant increase in the morning sector occurs only later, i.e., during peak or recovery phase of the bay. This time delay is attributed to the time taken by the electrons that are freshly energized in the midnight sector to drift in longitude so as to appear in the morning sector. The absence of increase in the evening sector is believed due to the fact that the freshly energized electrons disappear by the time they drift to that sector.

Author

N69-23367* Smithsonian Astrophysical Observatory, Cambridge, Mass.

THE MICROMETEOROID EXPERIMENT ON THE OGO 2 SATELLITE

C. S. Nilsson and D. Wilson Feb. 1969 38 p refs
 (Contract NAS5-11007)
 (NASA-CR-100683; Rept-902-41) Avail: NTIS CSCL 03C

The aim of this experiment was to measure the velocities, masses, and orbits of dust particles in the earth's dust cloud. The negative results obtained were instrumental in bringing about a reappraisal of the magnitude of this dust concentration. No orbits were determined, and it is questionable whether any micrometeoroids of mass > 10 to the minus 12th power g impacted on the sensors during the 1300 hr in which good data were obtained. Two possible impacts were recorded, but these were more likely due to experiment noise. These two events give an upper limit to the flux of particles of mass > 10 to the minus 12th power g of 3×10 to the minus 10th power particles/sq m sec 2π ster. This figure is compared with data from other experiments.

Author

N69-23730 California Univ., Berkeley.
THE PROPAGATION OF SOLAR PROTONS Ph.D. Thesis

S. W. Kahler 1968 141 p
 Avail: Univ. Microfilms Order No. 68-13919

Data from a scintillation counter experiment on the OGO-C spacecraft were used to analyze twelve energetic ($3 < E < 32$ MeV) solar proton events. The spacecraft, the performance of the experiment and methods of data analysis are discussed. The proton events presented were divided into four groups, each with well defined properties. The diffusive event follows an impulsive injection of particles at the sun and decays exponentially in time. The onset phase may be smooth or irregular, but the spectrum grows progressively softer during the decay phase. The storm particle event is a low energy event associated with a geomagnetic storm. During this event the spectrum first grows softer, then becomes harder. The halo structure is a stream of particles confined to the interplanetary lines of force which connect to the flare region at the sun. Recurrent proton events are due to the gradual release of particles from an active region in which a flare has occurred during a previous solar rotation. The two examples reported here showed narrow ($<$ or $=$ to 10 hours) interplanetary spatial confinement. Representative fluxes and modified spectral behavior are presented for these events as a basis for describing a model of a typical solar proton event.

Dissert. Abstr.

N69-24521* Stanford Univ., Calif. Electronics Labs.
PROTONOSPHERIC ELECTRON CONCENTRATION PROFILES Final Report

A. V. DaRosa and O. K. Garriott Mar. 1969 51 p refs
 (Contract NASr-136)
 (NASA-CR-100778; SU-SEL-68-044) Avail: NTIS CSCL 04B

The local electron concentration was calculated along portions of the orbit of OGO-1, based on differential Doppler frequency and Faraday polarization rotation measurements of harmonic radio beacon transmissions. Since it is not possible to make these calculations with sufficient accuracy for most satellite orbits, an extensive error analysis is included, to establish the sources and magnitudes of the uncertainties in the computations. Values of protonospheric electron concentration were obtained between altitudes of about 6,000 and 15,000 km on a number of orbits. The uncertainties in the computed values result principally from scaling errors in the Faraday polarization rotation angle and from horizontal gradients in the ionosphere; they typically total less than \pm or $-$ 600 electrons/cu cm. A number of concentration profiles are shown and are compared with direct probe measurements, with whistler results and with extrapolated values of electron concentration obtained from Alouette I near 1000 km.

Author

N69-25437* Michigan Univ., Ann Arbor.
OGO SPACECRAFT ELECTROMAGNETIC INTERFERENCE IN THE 50-KHz TO 4-MHz FREQUENCY RANGE

R. G. Peltzer 15 Dec. 1968 10 p refs In JPL Proc. of the Spacecraft Electromagnetic Interference Workshop P 139-148 Supported by NASA

Avail: NTIS Copyright. Avail: NTIS CSCL 09C
 The interference generating capability of the OGO spacecraft is reviewed. The most obvious potential sources of interference generated in the spacecraft were the transmitters, data handling systems, and power converters. After briefly describing the signals generated in the craft, the distribution of the signals through the spacecraft wiring was examined. The skin and overall structural material was then considered as a potentially inherent EMI container. The radio probing objectives of the OGOS are briefly discussed. Procedures for ground testing for EMI and for spacecraft generated interference testing are briefly enumerated; recommendations are made for future design considerations and for more effective testing.

B.P.

N69-26549# Colorado Univ., Boulder. Dept. of Astro-Geophysics.

THE VERTICAL DISTRIBUTION OF OZONE BETWEEN 35 AND 55 KM AS DETERMINED FROM SATELLITE ULTRAVIOLET MEASUREMENTS M.S. Thesis

G. P. Anderson 1969 66 p refs

Avail: Issuing Activity

An Ebert-Fastie ultraviolet spectrometer mounted on a polar-orbiting satellite was used to observe back-scattered radiation in the spectral region 2550 to 3100Å. The data were calibrated using a coordinated rocket sounding to determine the effective solar flux. A modified Phillip-Twomey inversion technique was then applied, yielding a reasonable vertical ozone distribution between 35 and 55 km. Author

N69-29659# National Aeronautics and Space Administration. Goddard Space Flight Center, Greenbelt, Md. **PROPAGATION OF SOLAR COSMIC RAYS IN THE INTERPLANETARY MAGNETIC FIELD**

E. C. Roelof 1969 25 p refs In Its Lectures in High Energy Astrophys. p 111-135

Avail: NTIS CSCL 04A

A diffusion-convection theory is developed to explain solar cosmic ray propagation in the interplanetary plasma and the distorted production spectrum by the time the particles arrive at earth. It is shown that irregularities of the interplanetary magnetic field carried out into space by the expanding corona cause this distortion and randomize the trajectories of the particles. G.G.

N69-31345# Michigan Univ., Ann Arbor. Dept. of Astronomy.

RESULTS FROM ORBITING GEOPHYSICAL OBSERVATORY I Final Scientific Report

F. T. Haddock 1969 6 p

(Contract NAS5-2051)

(NASA-CR-103321) Avail: NTIS CSCL 03A

The OGO-1 spacecraft encountered difficulties shortly after launch and the antenna erection command for this instrument was delayed for some time. When the erection attempt was made the antenna only erected an estimated four to six feet instead of the intended 30 feet. The complete shutdown of the experiment was not requested since there existed a chance that a very large solar flare event would be observed with the greatly reduced antenna sensitivity. However, reduction of the data tapes for 1/1/66, 3/19/66, and 3/25/66 have yielded nothing. Data tape reduction was delayed by computer costs. This experiment was finally judged a scientific failure. The OGO-3 (OGO-B) experiment performed satisfactorily and provided good scientific results. Author

N69-32730# Naval Research Lab., Washington, D.C. **USING SOLAR X-RAYS AS INDICATORS OF SOLAR-FLARE ACTIVITY Interim Report**

D. M. Horan, R. W. Kreplin, A. T. McClinton, Jr., and L. C. Schneider Mar. 1969 24 p refs

(AD-686662; NRL-6884) Avail: NTIS CSCL 14B

X-ray and particle emission during solar flares can sufficiently increase the electron density in the lower regions of the ionosphere to cause disruption of high-frequency radio communications. Criteria have been established to predict periods of high solar activity during which solar flares capable of disrupting communications might occur. A study of solar-flare occurrence and solar X-ray flux levels over 14 months has shown that solar flares are three times more likely to occur when the criteria are met than when they are not met. Author (TAB)

N69-33963# California Univ., Los Angeles. **DIGITAL OFFSET FIELD GENERATOR FOR SPACECRAFT MAGNETOMETERS**

R. C. Snare and G. N. Spellman (Marshall Labs.) 1967 12 p refs In Nev. Univ. Space Magnetic Exploration and Technol. p 155-166

(Contracts NAS5-9570; NAS5-9098)

Avail: NTIS CSCL 03B

A digital offset field generator has been developed which accurately extends the dynamic range of a sensitive magnetometer. This system enables the use of a sensitive magnetometer to resolve small magnetic field fluctuations in the presence of fields of large value. The circuitry is described in some detail and its application in instruments for the first Applications Technology Satellite and the fifth Orbiting Geophysical Observatory is discussed. Author

N69-33977# TRW Systems, Redondo Beach, Calif. Space Sciences Lab.

MAGNETIC TESTS OF THE OGO AND ERS SATELLITES

G. T. Inouye 1967 14 p In Nev. Univ. Space Magnetic Exploration and Technol. p 363-378

(Contract NAS5-3900)

Avail: NTIS CSCL 22B

This paper presents the results and methods used to test for the magnetic properties of the OGO and ERS satellites. The magnetic property of the spacecraft of paramount interest is the spacecraft magnetic field at the position of the on-board magnetic sensor, both permanent and induced. Also of interest is the proportion of this field which is hard or permanent, and the proportion which is soft which may be changed by normal magnetizing environments to which the spacecraft may be subjected before being launched into orbit. Another magnetic property of interest is an overall map of the spacecraft field, and its characterization in terms of dipole and higher order multipoles, both permanent and induced, located at the center of the spacecraft. The testing techniques used in both the coil and coil-less methods involve the rotation of the spacecraft about two axes relative to fixed tri-axial fluxgate sensors. The fluxgate sensor outputs are recorded on both a multichannel Sanborn chart recorder and an X-Y plotter. The X-Y plot permits an immediate scaling of the magnitude of the magnetic moment in the plane of rotation, as well as giving its orientation in spacecraft coordinates. Rotation of the spacecraft about another orthogonal axis provides data for obtaining the total moment vector. Author

N69-34536# California Inst. of Tech., Pasadena. **NEW MEASUREMENTS OF THE ABSOLUTE COSMIC RAY IONIZATION FROM SEA LEVEL TO 1540 KILOMETERS ALTITUDE** Ph.D. Thesis

M. J. George 25 Apr. 1969 174 p refs

(Contracts NAS5-3095; NAS5-9317; NAS7-100; Grant Nonr-220(53); Contract NGL-05-002-007)

(NASA-CR-104068) Avail: NTIS CSCL 03B

The construction of an air filled ionization chamber is described. This chamber was flown along with an older, argon filled, balloon type chamber in a C-135 aircraft from 1,000 to 40,000 feet altitude, and other measurements of sea level cosmic ray ionization were made. The calibrations of the two instruments were found to agree within 1 percent, and the airplane data were consistent with previous balloon measurements in the upper atmosphere. Ionization due to radon gas in the atmosphere was investigated. Absolute ionization data in the lower atmosphere have been compared with results of other observers, and discrepancies have been discussed. Also, data from a polar orbiting ion chamber on the OGO-2, 4 spacecraft have been analyzed. The problem of radioactivity produced on the spacecraft during passes through high fluxes of trapped protons has been investigated, and some corrections determined. Author

N69-38983# National Aeronautics and Space Administration. Goddard Space Flight Center, Greenbelt, Md. **COSMIC RAY AND SOLAR FLARE ELECTRONS**

T. L. Cline 1969 5 p In Its Significant Accomplishments in Sci., 1968 p 131-135

Avail: NTIS CSCL 04A

Comparisons between observed and calculated interplanetary electrons of energies above 1 MeV are made

and related to the identification and source of solar electrons. Observations from IMP 3, and more recently supported by IMP 4 and OGO 5, have yielded the first directly detected interplanetary solar flare electrons of relativistic energies. From these data, several implications regarding the solar electron population also responsible for microwave and X-ray bursts at dawn. Charts of original data from the satellites showing cosmic ray electron distributions and solar flare particle distributions are included. M.H.E.

N69-38984*# National Aeronautics and Space Administration, Goddard Space Flight Center, Greenbelt, Md.
GALACTIC AND SOLAR COSMIC RAYS
F. B. McDonald 1969 6 p In Its Significant Accomplishments in Sci., 1968 p 136-141
Avail: NTIS CSCL 04A

The detection system of OGO 5 consisting of a Cerenkov counter and a mass spectrometer is explained in terms of the multiple parameter analysis used to compute the precise chemical composition of galactic and solar cosmic radiation traveling at relativistic velocities. An analysis of a representative sample for charge distribution is provided and the analytical steps with underlying mathematical assumptions are demonstrated. M.H.E.

N70-11147*# Michigan Univ., Ann Arbor. Radio Astronomy Observatory.
DYNAMIC SPECTRA OF 4-2 MHz SOLAR BURSTS: RESULTS FROM ORBITING GEOPHYSICAL OBSERVATORY 3 Final Report, part 1: Scientific; Ph.D. Thesis
T. E. Graedel 1968 213 p refs
(Contract NAS5-2051)
(NASA-CR-106640) Avail: NTIS CSCL 04A

The data collected by OGO-3 in detecting solar bursts are analyzed quantitatively at selected frequencies. The burst data are plotted as graphs of output voltage against time. The OGO-3 spacecraft, the radio astronomy experiment, and observed properties of the solar radio bursts are described. The physical conditions of the corona, and the evidence for a plasma frequency burst hypothesis are reviewed. Conclusions which were drawn are summarized as follows: (1) Solar fast drift radio bursts with peak flux densities in the 4 to 2 MHz band were observed at the rate of one burst for 50 hours of observation, (2) Type V continuum was observed in 2% of all cases following fast drift bursts at low frequencies, and (3) The detection of a reverse drift burst at low frequencies may indicate the presence of significant magnetic fields transverse to the radial direction at distances of approximately 5 solar R. F.O.S.

N70-11727*# Stanford Research Inst., Menlo Park, Calif.
RESEARCH RELATED TO MEASUREMENTS OF ATOMIC SPECIES IN THE EARTH'S UPPER ATMOSPHERE
B. R. Baker and B. J. Wood 1 Sep. 1969 11 p refs
(Contract NASr-49/30/)
(NASA-CR-106805; QSR-9) Avail: NTIS CSCL 04A

Oxygen atom reactions with solid surfaces were investigated to improve data interpretation of atomic oxygen composition reported by mass spectrometers in upper atmospheric flight. Interaction rates were observed with metal surfaces in a reaction vessel. Atom removal by recombination as indicated by the steady, high ratio of mass 32/mass 16 measured by the OGO-F mass spectrometer at perigee was confirmed by the experimentally determined behavior of gold. A precise correction for the atom removal term is suggested based on recombination coefficients derived from rate data to provide an absolute evaluation of the oxygen atom particle density being sampled. Similar corrections are recommended for the oxygen data from the Explorer 32 satellite. M.H.E.

N70-12221*# Michigan Univ., Ann Arbor. Dept. of Astronomy.
OGO 3 DATA ANALYSIS - DYNAMIC SPECTRA OF SOLAR BURSTS Final Scientific Report
T. E. Graedel 1968 74 p refs

(Grant NGR-23-005-312)
(NASA-CR-107031) Avail: NTIS CSCL 04A

The computation of solar burst time profiles and dynamic spectra, utilizing a model of the form described can produce theoretical values for Type 3 burst characteristics which agree quite well with observational values. The parameters which have been used in the model can then be regarded as indicative of coronal physical conditions and of Type 3 solar burst radiation mechanisms. A high level of accuracy was obtained in matching observations, even though the model which was used did not treat the difficult plasma physics problems in a realistic way. The results presented refer to average Type 3 bursts. Any individual event, likely to result from an electron velocity spectrum which differs from the average may occur with a density enhancement differing from the model described. Author

N70-14425*# Michigan Univ., Ann Arbor. High Altitude Engineering Lab.
THE OGO-2 NEUTRAL AND ION MASS SPECTROMETER EXPERIMENT
B. B. Hinton, R. J. Leite, and C. J. Mason Oct. 1969 15 p refs
(Contract NAS5-3098)
(NASA-CR-107408; Rept-05465-1-F) Avail: NTIS CSCL 14B

The experiment is described from the data processing point of view. A brief description of the quadrupole spectrometer is given. The approach to data processing is reviewed and related to the OGO-2 data. A brief review of the spacecraft malfunctions and their influence upon the experiment is included. The only significant data obtained indicated that large spacecraft probably expell large amounts of water vapor over extended periods of time and precautions should be taken to prevent damage to instruments and degradation of their data. Author

N70-15525*# Stanford Univ., Calif. Radioscience Lab.
NONDUCTED VLF PROPAGATION IN THE MAGNETOSPHERE
F. Walter Oct. 1969 155 p refs
(Contract NAS5-3093; Grant NSG-020-008; Contract N00014-67-A-0112-0012; Grants NSF GA-1151; NSF GA-1485)
(NASA-CR-107614; SU-SEL-69-061; TR-3418-1) Avail: NTIS CSCL 17B

Evidence for nonducted VLF propagation between conjugate hemispheres has been found in records from the broadband VLF receivers aboard the polar satellites OGO 2 and OGO 4. The nonducted signals are received in the ionosphere between 47 deg and 56 deg invariant latitude. They have never been observed on the ground and include natural whistlers and fixed-frequency signals from Omega transmitters. In a frequency-time spectrogram, these nonducted whistlers appear as rising tones with a lower cutoff frequency in the approximate range of 5 to 8 kHz. A train of WT whistlers exhibits a nearly constant lower cutoff frequency which is equal to the maximum value of the lower hybrid resonance (LHR) frequency above the satellite, and an upper cutoff frequency that decreases with increasing satellite latitude. Fixed frequency Omega signals exhibit two features that are not apparent in the natural whistlers: an enhancement of signal strength and a Doppler shift that increases with latitude and may reach hundreds of Hertz. Author

N70-15678*# Stanford Univ., Calif. Radioscience Lab.
MAGNETIC RADIATION OBSERVED BY OGO-1 AND OGO-3 BROADBAND VLF RECEIVERS
W. J. Burtis Aug. 1969 63 p refs
(Contract NAS5-2131; Grant NGR-05-020-288)
(NASA-CR-107653; SU-SEL-69-019; TR-3438-1) Avail: NTIS CSCL 04A

A continuing study of the properties of VLF emissions, using observations from the OGO satellites as well as from ground stations, is presented. It is concerned specifically with

radiation observed by the broadband VLF receivers onboard OGO 1 and OGO 3 primarily during 1966. Three distinct classes of emissions are defined and illustrated: banded chorus, banded hiss, and low-frequency noise. The occurrence of radiation in each class is investigated as a function of magnetic shell, dipole latitude, local time, and magnetic activity. The relation of this radiation to VLF emissions observed on the ground and in the topside ionosphere is discussed. Energies are calculated for gyroresonant electrons which may generate banded chorus. The amplitude of banded chorus radiation is estimated and rise and fall times of discrete emissions are illustrated. Author

N70-15768*# Stanford Univ., Calif. Radioscience Lab. INTERPRETATION OF VLF SIGNALS OBSERVED ON THE OGO-4 SATELLITE

R. R. Scarabucci Oct. 1969 169 p refs
(Contract NASS-3093; Grant NGR-020-008)
(NASA-CR-107654; SU-SEL-69-065; TR-3418-2) Avail: NTIS CSCL 17B

The main purpose is to present and interpret measurements of very low frequency signals observed with the low altitude, polar orbiting, OGO-4 satellite. The interpretations of the measurements are based on amplitude and spectrum analysis of the received signals as well as on the related position of the satellite. The phenomena to be discussed are observed on nearly all revolutions of OGO-4. The present study is mainly concerned with signals generated on the ground by lightning strokes and by VLF transmitters. This research may also be classified as a global study of very low frequency propagation in the ionosphere and in the magnetosphere of the earth. It includes the general problem of excitation of waves through the lower ionosphere under different conditions and the characteristics of propagation inside the anisotropic plasma above the earth. The study covers a variety of situations, including signals received when OGO-4 is relatively close to the ground sources and signals received at low, middle, and high latitudes. The differences between daytime and nighttime propagation are also included. Author

N70-17448*# Minnesota Univ., Minneapolis. School of Physics and Astronomy.

A SURVEY OF THE TOTAL RADIATION IN SPACE OBSERVED BY THE OGO SATELLITES, 5 SEPTEMBER 1964 - 27 MAY 1968

S. R. Kane and J. R. Winckler Sep. 1969 210 p refs
(Contract NASS-2071; Grant NGL-24-005-008)
(NASA-CR-107886; CR-135) Avail: NTIS CSCL 04A

Graphical and tabular summaries of the ionization rates in space recorded by the large spherical ion chambers on the OGO-1 and OGO-3 spacecraft are presented. The survey begins with the launch of OGO-1 in September, 1964 and ends with the last reduced data furnished on a regular basis by the Data Reduction Facility at Goddard Space Flight Center in May 1968, although some samples of data are given in July and August, 1968 from special runs. The ionization chambers are sensitive to all types of particle and photon radiation which can penetrate the aluminum shell. The hourly average rates of the ion chambers have been computed without regard to the location of the satellite and as a function of universal time for the entire period. Background radiation is measured outside the magnetosphere during periods of solar quiet. On each pass of the satellite the radiation belts are shown as large spikes with the radiation zones in general unresolved with the one hour averages and with the peak rates consistent with an average over this time period. Author

N70-17624*# Minnesota Univ., Minneapolis. Cosmic Ray Group.

DESCRIPTION OF DATA PLOTS FROM THE UNIVERSITY OF MINNESOTA ION CHAMBER AND ELECTRON SPECTROMETER ON OGO-1 AND OGO-3

S. R. Kane, K. A. Pfitzer, and J. R. Winckler Oct. 1969 40 p

(Contract NASS-2071; Grant NGR-24-005-008)

(NASA-CR-107885; CR-147) Avail: NTIS CSCL 04A

Samples of computer plots and their explanations are presented for electron spectrometer and ionization chamber data on radiation belts, solar radiation, and galactic cosmic rays. The electron spectrometer data are plotted against such factors as time, range, and L-values. All of the spectrometer data are plotted in the same arbitrary scale which must be multiplied by the conversion factor to obtain the electron fluxes or the differential energy spectra. The data for the five energy channels are background corrected and plotted against a normalized scale. A list of completed data plots is presented. J.M.

N70-19313*# National Aeronautics and Space Administration. Goddard Space Flight Center, Greenbelt, Md. COORDINATE TRANSFORMATIONS USED IN OGO SATELLITE DATA ANALYSIS

Jan. 1970 15 p
(NASA-TM-X-63826; X-645-70-29) Avail: NTIS CSCL 08E

Graphical presentations are shown for: (1) geocentric celestial inertial coordinates; (2) geographic distance coordinates; (3) topographic coordinates; (4) geomagnetic coordinates; (5) solar geomagnetic coordinates; (6) solar magnetospheric coordinates; and (7) solar ecliptic coordinates. Matrices for coordinate transformations from the geocentric celestial inertial coordinate system to other coordinates are developed and a vector expression by magnitude and two angles with respect to the solar ecliptic coordinate system is formed.

N70-23999*# Michigan Univ., Ann Arbor. Radio Astronomy Observatory.

OGO-2 DATA ANALYSIS SATELLITE PLASMA WAKE STUDY. Final Report

H. Weil and R. G. Yorks Feb. 1970 76 p ref
(Contract NGR-23-005-314)

(NASA-CR-109457; Rept-70-1) Avail: NTIS CSCL 20I

The plasma wake of the spinning OGO-2 satellite is studied using the 2.5 MHz antenna impedance data. The method for measuring antenna impedance is described. The very strong wake modulation recorded in the inductive region up to the time the reactance goes capacitive is considered as significant wake feature, and is believed to be an impedance effect caused by the continually varying angle between the antenna and the magnetic field lines as the spacecraft spins. The paper OGO satellite wake structure deduced from antenna impedance measurement, and the outlines of computer programs written for this study are included. F.O.S.

N70-27302*# National Aeronautics and Space Administration. Goddard Space Flight Center, Greenbelt, Md. DISCREPANCIES IN THE OBSERVED PLASMA-TROUGH DENSITY

E. J. R. Maier and G. P. Serbu Mar. 1970 14 p refs
(NASA-TM-X-63905; X-621-70-71) Avail: NTIS CSCL 20I

Observations of the plasmapause have now been achieved by a variety of techniques: ground based reception of whistlers, in-situ observations by mass spectrometers retarding analyzers and VLF receivers. Comparisons of some of these observations are made and it is concluded that the details of the plasmasphere boundary and the thermal plasma density beyond the plasmasphere are more variable than the idealized plasmasphere model would suggest. Author

N70-28003# Applied Systems Corp., Freeport, N.Y. INVESTIGATION OF ELECTRICAL STRUCTURE IN THE NEAR EARTH REGION AS MEASURED BY ORBITING SPHERICAL ELECTROSTATIC ANALYZERS, OR PLASMA PROBES Final Report, 1 Jul. 1968 - 31 Oct. 1969

B. R. Greene, A. Lieberman, and W. J. Snapp 28 Nov. 1969 86 p refs

(Contract F19628-68-C-0382)

(AD-700804; AFCRL-70-0017) Avail: NTIS CSCL 04/1

The report contains a study and analysis of several scientific experiments for the study of the distribution of charged particles in the near earth regions. The experiments under study consist of spherical electrostatic analyzers or probes, flown on OGO satellites. Scientific and numerical techniques for the study and analysis of the data produced by these experiments and a system of computer programs for converting the recorded raw data into the desired physical results are given. Author (TAB)

N70-28103*# California Univ., Livermore. Lawrence Radiation Lab.

THE LRL ELECTRON AND PROTON SPECTROMETER ON NASA'S ORBITING GEOPHYSICAL OBSERVATORY 5(E): INSTRUMENTATION AND CALIBRATION

R. M. Bogdanowicz, R. G. Darcy, Jr., R. W. Hill, N. C. Jensen, J. H. McQuaid, H. I. West, Jr., and J. H. Wujec 2 Jun. 1969 110 p

(NASA Order S-70014-G)

(NASA-CR-109962; UCRL-50572) Avail: NTIS CSCL 20F

The design construction and calibration of the electron and proton experiment on the OGO-V satellite are described. A brief account of post-launch results is included. The electron spectrometer consists of two small permanent magnets used for energy analysis with electron detection provided by solid-state detectors. Background detectors are also provided. The energy range covered is approximately 60 to 2950 keV in 7 differential energy channels. The proton spectrometer consists of a single solid-state detector and a range-energy telescope of four solid-state detectors situated in line with the entrance aperture of the larger of the electron spectrometer magnets. The energy range is 0.1 to 94 MeV in 7 differential energy channels. Data handling in the experiment is primarily digital using a binary floating point compressional scheme. The experiment apertures are scanned relative to the stabilized spacecraft for obtaining pitch-angle distributions. Author

N70-29987*# National Aeronautics and Space Administration. Goddard Space Flight Center, Greenbelt, Md.

AURORAL ELECTRON DRIFT AND PRECIPITATION: CAUSE OF THE MANTLE AURORA

R. A. Hoffman Jun. 1970 42 p refs Submitted for Publication

(NASA-TM-X-63941; X-646-70-205) Avail: NTIS CSCL 04A

Data from the Auroral Particles Experiment on OGO-D were analyzed to determine the properties of the band region of low energy electron precipitation in the late morning hours. The existence of this precipitation is consistent with a scheme involving a release of a body of electrons on closed magnetic field lines in the vicinity of midnight at the time of a magnetospheric substorm with a subsequent drift in local time through the morning hours at least as far as noon. While drifting the electrons encounter a strong pitch angle diffusion mechanism which precipitates them into the atmosphere to produce the mantle aurora. This mechanism seems to exist independent of substorm magnetic activity. The diffusion coefficient must be larger than 0.001/second and the resulting lifetime of the electrons is about 6.000 seconds. The energy density of the source electrons in the midnight region would not be unreasonably large if the source is in the cusp. Author

N70-32928*# Stanford Univ., Calif. Radioscience Lab. **EXPERIMENTS C02 (OGO 2) AND D02 (OGO 4) Final Report, 2 Nov. 1962 - 31 Jul. 1969**

J. J. Angerami and R. A. Helliwell 31 Jul. 1969 109 p refs

(Contract NAS5-3093)

(NASA-CR-110658) Avail: NTIS CSCL 20N

The main results are summarized of the research data from the experiments flown on OGO 2 and OGO 4 to make

VLF measurements on propagation and wave-particle interactions in the magnetosphere and ionosphere and to survey the ionospheric noise in a range of frequencies from 200 Hz to 100 kHz. The orbits and attitudes of both satellites, and the main features of the experiments are briefly described, and the calibration curves of the corresponding receivers are given. A concise account of the results obtained to date on each of several topics is given, and illustrated abstracts of work in progress are included. Author

N70-33156*# Stanford Univ., Calif. Radioscience Lab. **EXPERIMENTS A17 (OGO 1) AND B17 (OGO 3) Final Report, 16 Feb. 1962 - 30 Jun. 1968**

R. A. Helliwell 30 Jun. 1968 81 p refs

(Contract NAS5-2131)

(NASA-CR-110716) Avail: NTIS CSCL 12B

The main results of the research data form the VLF experiments flown on OGO 1 (A 17) and OGO 3 (B 17) are summarized. The orbits and attitudes of both satellites are briefly described and the main features of the VLF experiments A 17 and B 17 are presented. The calibration curves of the corresponding receivers are given along with a concise account of the results obtained to date in each of several topics. Author

N70-33175*# National Aeronautics and Space Administration. Goddard Space Flight Center, Greenbelt, Md.

NEW RESULTS AND TECHNIQUES IN SPACE RADIO ASTRONOMY

J. K. Alexander Jul. 1970 51 p refs Presented at the IAU Symp. no. 41, Munich, 10-14 Aug. 1970

(NASA-TM-X-63976; X-693-70-267) Avail: NTIS CSCL 03A

A summary of all space radio astronomy experiments is presented. Major advances in space radio astronomy have come mainly from experiments conducted on the satellites Alouette-2, Luna-11 and 12, OGO-3 and 5, ATS-2, and RAE-1. Among the most significant technological developments has been the continuing refinement in the accuracy of absolute intensity measurements from approximately + or - 50 percent in the early experiments to + or - 15 to 25 percent in more recent ones. Another important new technique has been the successful use of 229 meter long traveling wave V antennas on the RAE-1 to obtain directive observations of a large portion of the sky at low frequencies. The planned launching of a second RAE spacecraft into a lunar orbit will permit radio astronomical measurements at frequencies down to 30 kHz, facilitate use of the moon as an occulting disk for source position measurements, and provide new information on the cislunar noise environment required to assess the feasibility of future lunar radio observatories. Author

N70-42352*# Michigan Univ., Ann Arbor. Radio Astronomy Observatory.

THE REDUCTION AND ANALYSIS OF DATA FROM THE LOW-FREQUENCY RADIO ASTRONOMY EXPERIMENT ABOARD THE OGO-4 SPACECRAFT Final Report

W. H. Potter Jul. 1970 89 p refs

(Contract NAS5-3099; NGR-23-005-371)

(NASA-CR-110796; UM/RAO-70-5) Avail: NTIS CSCL 22A

The purpose of the OGO-D radio astronomy experiment was to map the brightness temperature of the sky at a frequency of 2.5 MHz, using a short monopole antenna on the spacecraft, and depending upon the ionospheric focusing effect to achieve angular resolution. The experiment operated for the life of the spacecraft returning data from radiometers operating at 2.0 and 2.5 MHz and measurements of the complex impedance of the antenna at 2.5 MHz as the spacecraft passed up and down through the ionosphere. Radio frequency interference generated within the spacecraft makes the interpretation of the radiometer data difficult, and it appears to be impractical to extract mapping information. The antenna impedance measurements are not

affected by the interference and represent a useful body of data for the study of the properties of the ionosphere and the behavior of antennas in plasma. Theoretical investigations were carried out in such fields as the behavior of antennas in plasma and the propagation of electromagnetic waves in plasma. Author

N71-10358*# ADCOLE Corp., Waltham, Mass.
ELECTRONIC INSTRUMENTATION FOR SOLAR RADIATION MEASUREMENTS Final Report, 1 Feb. 1965 - 31 Jul. 1969
R. S. Hills 1 Oct. 1969 189 p refs
(NASA Order S-35349-G; NASA Order S-99821-G; Contract AF 19(628)-5042)
(NASA-CR-110906; AD-700780; AFCRL-69-0450) Avail: NTIS CSCL 03B

The report describes the design, construction, test and flight use of the electronic portions of research instruments used on rockets and satellites for the investigation of extreme solar ultraviolet radiation. These instruments include grating monochromators for measurements in the 30-1300 Angstrom range and proportional counter spectrometers in the 1-10 Angstrom range. Also described is work done on retarding potential analyzers used for analysis of environmental charged particles. All the instruments are of a telemetering type. Associated equipment used for calibration and testing of the instruments in both the laboratory and the launch phases is described. Automatic data reduction equipment was developed and used successfully. Experiments were flown on OSO and OGO satellites, and Aerobee-150 rockets.

Author (TAB)

N71-10588*# Texas Univ., Dallas.
OGO-F-06 ION MASS SPECTROMETER Final Report, Mar. 1966 - Jun. 1970
W. B. Hanson and J. F. Metrailler Aug. 1970 109 p
(Contract NASS-9310)
(NASA-CR-111146) Avail: NTIS CSCL 20F

Covered is the theory of operation, design history, test history, and post launch results of the OGO-F-06 ion mass spectrometer which was mounted in OPEP I (Orbital Plane Experiment Package) of OGO-VI (Orbiting Geophysical Observatory) and launched on June 5, 1969. This experiment incurred a catastrophic failure early in the flight as a result of high voltage arcing. With this failure there were no scientific results obtained from the instrument. Author

N71-20207*# Faraday Labs., Inc., La Jolla, Calif.
SPACE MEASUREMENTS OF THE CONTAMINATION OF SURFACES BY OGO-6 OUTGASSING AND THEIR CLEANING BY SPUTTERING AND DESORPTION
W. E. Corbin, Jr. and D. McKeown Oct. 1970 15 p refs
In NBS Space Simulation Oct. 1970 p 113-127
(Contracts NAS5-11163; N00014-68-C-0373)
(NASA-CR-117138) Avail: NTIS CSCL 11F

Results of the contamination of surfaces by outgassing of the OGO-6 satellite and the rates at which these surfaces are now being cleaned by sputtering and desorption after being in space for five months are given. It was found that the primary source of outgassing on the satellite was its two solar panels baking out in the sun. The time constant for the exponential decay of the outgassing is 1.000 hours. The maximum amount of contamination adsorbed by the surfaces exposed to the outgassing was reached after five months in orbit and is 96 mg/sq cm for the Al surface and 52 mg/sq m for the Au surface. The contamination has a desorption activation energy of 26 kcal/g mol which falls into the energy range of materials, such as epoxies and vacuum oils. The surfaces are undergoing cleaning by desorption and sputtering by upper atmospheric neutral impacts.

Author (TAB)

N71-20638*# Michigan Univ., Ann Arbor. Dept. of Electrical Engineering.
EMPIRICAL MODEL OF POLAR THERMOSPHERE STORM Final Technical Report

D. R. Tausch Jan. 1971 31 p refs
(Contract NAS8-26243)
(NASA-CR-103080; Rept-03756-1-F) Avail: NTIS CSCL 04A

Satellite neutral atmospheric composition measurement data are studied for: (1) the latitudinal extent of the neutral response to the storm; (2) the magnitude of the response versus quiet conditions; (3) the longitudinal variations in the auroral oval, and (4) the time responses of the atmospheric parameters to the solar activity as indicated by the solar-geomagnetic indices. Author

N71-21544*# Michigan Univ., Ann Arbor. High Altitude Engineering Lab.
REDUCTION AND ANALYSIS OF DATA FROM OGO-4 EXPERIMENT 15 Final Report, 1 Nov. 1969 - 30 Nov. 1970

R. J. Leite, C. J. Mason, and J. Spencer Jan. 1971 19 p refs
(Grant NGR-23-005-383)
(NASA-CR-117525; Rept-033460-1-F) Avail: NTIS CSCL 09B

The procedures used to process the atmospheric composition data obtained through the use of a sweeping quadrupole mass spectrometer on OGO-4 satellite are described. These data were stored in digital form on magnetic tape. Attitude-orbital data were provided in digital form on magnetic tape also. These two sets of data are correlated in time through date-time comparison. A discussion of conclusions concerning reduction of commutated spectral data and the difficulties associated with interpretation of these data are included. It is shown that use of an electronic computer of appropriate capacity provides the only realistic approach to the processing of commutated spectral data. Author

N71-23238*# Michigan Univ., Ann Arbor. High Altitude Engineering Lab.
PERTURBATIONS TO OBSERVED AMBIENT NEUTRAL DENSITIES DUE TO PRESENCE OF AN ORBITING GEOPHYSICAL OBSERVATORY

B. B. Hinton and R. J. Leite Jan. 1971 22 p refs
(Grant NGR-23-005-383)
(NASA-CR-117897; Rept-03346-2-T) Avail: NTIS CSCL 03B

The perturbation by a spacecraft in the density of ions and neutral particles as it moves through the upper atmosphere was studied. Estimates are given for the resultant perturbations on measured values of ambient neutral particle densities for mass spectrometer experiments mounted in an Orbital Plane Experiment Package of an Orbiting Geophysical Observatory (OGO). Author

N71-25265*# National Aeronautics and Space Administration. Goddard Space Flight Center, Greenbelt, Md.
DIURNAL PHASE ANOMALY IN THE EARTH'S UPPER ATMOSPHERE

S. Chandra 1970 4 p In Its Significant Accomplishments in Sci. and Technol. at Goddard Space Flight Center 1970 p 41-44
Avail: NTIS CSCL 04B

Discrepancies between the phase and the diurnal amplitude of the thermospheric temperatures inferred from satellite drag and Thompson backscatter results are discussed. It is shown that the introduction of a dynamic diffusion concept for computing the temperature from density leads to a reasonable agreement between both sets of observational data and that the assumption of an invariant boundary is not valid. G.G.

N71-25267*# National Aeronautics and Space Administration. Goddard Space Flight Center, Greenbelt, Md.
LATITUDINAL DISPERSION OF GASES IN THE UPPER ATMOSPHERE

C. A. Reber 1970 4 p In Its Significant Accomplishments in Sci. and Technol. at Goddard Space Flight Center 1970 p 49-52

Avail: NTIS CSCL 04A

Mass spectrometer data from OGO-F satellite trajectory through the symmetrical atmosphere establish a separation of the densities of the major gases from the He density, with the He peak occurring later in the orbit. The perigee was between the N₂ and the O peaks, and the difference in latitude between the peaks of the major gases and the He was about 50 degrees. G.G.

N71-25268*# National Aeronautics and Space Administration, Goddard Space Flight Center, Greenbelt, Md.

AIRGLOW OBSERVATIONS FROM OGO 4

E. I. Reed 1970 5 p In Its Significant Accomplishments in Sci. and Technol. at Goddard Space Flight Center 1970 p 53-57

Avail: NTIS CSCL 04A

OGO 4 photometric airglow measurements on the 6300 Å red line of atomic oxygen below 40 degrees of latitude are related to neutral and charged components in the atmosphere. This arc of the red airglow with intensities of up to more than 1,000 rayleighs is closely related to the ionospheric equatorial anomaly of the daytime F-region. Absence of the southern arc over much of the Pacific is attributed to energy loss through molecular collisions or insufficient charge exchange reactions. G.G.

N71-25270*# National Aeronautics and Space Administration, Goddard Space Flight Center, Greenbelt, Md.

THERMAL PLASMA NEAR THE PLASMAPAUSE

J. M. GREBOWSKY 1970 3 p In Its Significant Accomplishments In Sci. and Technol. at Goddard Space Flight Center 1970 p 63-65

Avail: NTIS CSCL 04A

A schematic model of the mechanism responsible for the formation of the plasmopause near the equatorial plane is formulated. The rapid drop of electron density with increasing altitude is associated with troughs in the latitudinal distribution of light ions and electrons as well as with a change in the plasma's state of motion along the magnetic field lines. Also incorporated into this model are plasma fluxes which continually move upward as an ionospherically produced plasma replenishes the plasma loss. Comparison of model computations with OGO-D measurements on a H⁺ ion trough at 900 km showed good agreement. G.G.

N71-25271*# National Aeronautics and Space Administration, Goddard Space Flight Center, Greenbelt, Md.

THE INFLATION OF THE INNER MAGNETOSPHERE

M. Sugiura 1970 3 p In Its Significant Accomplishments in Sci. and Technol. at Goddard Space Flight Center 1970 p 66-68

Avail: NTIS CSCL 04A

OGO-B and OGO-E magnetic field measurements are used to map magnetospheric field magnitudes and disturbances in the geomagnetic noon-to-midnight meridian plane for a slightly disturbed condition. Established is the existence of a large positive field region at middle to high latitudes and the large decrease of the field in the inner magnetosphere. These phenomena are attributed to an inflation of the inner magnetosphere by a ring of particles; intensities of the quiet time ring currents are greater by a factor of 2 or 3 than generally supposed and vary considerably, even during slight disturbances. G.G.

N71-25272*# National Aeronautics and Space Administration, Goddard Space Flight Center, Greenbelt, Md.

AURORAL PARTICLE INJECTION AND DRIFT

R. A. Hoffman 1970 4 p In Its Significant Accomplishments in Sci. and Technol. at Goddard Space Flight Center 1970 p 69-72

Avail: NTIS CSCL 04A

The source location of electrons that cause the aurora in the auroral oval is attributed to bombardment of the upper atmosphere by electrons with energies from about 1 to 10 kV. Measurements by satellite borne detectors in low altitude polar orbits show that electrons precipitate not only

at midnight but in a region extending from a few hours before midnight through the morning hours to local noon. These electrons are injected onto magnetic field lines emanating from the earth during substorms and subsequently drift on closed field lines through the morning hours to local noon where they are measured later precipitating into the atmosphere. G.G.

N71-25273*# National Aeronautics and Space Administration, Goddard Space Flight Center, Greenbelt, Md.

OGO 5 MEASUREMENTS OF ELECTRONS NEAR THE MAGNETOPAUSE.

K. W. Oglivie 1970 3 p In Its Significant Accomplishments in Sci. and Technol. at Goddard Space Flight Center 1970 p 73-75

Avail: NTIS CSCL 04A

Observations of low energy electrons by OGO-E differential electrostatic spectrometer show a sharp increase in 45 eV flux time coincident with the magnetopause crossing. Flux curve evaluations indicate that the magnetopause does not always move and that if it is stationary, a thickness at the unstable region of about 100 km is the correct order of magnitude. G.G.

N71-32190*# National Aeronautics and Space Administration, Goddard Space Flight Center, Greenbelt, Md.

DERIVATION OF THE INTERNATIONAL GEOMAGNETIC REFERENCE FIELD, IGRF(10/68)

J. C. Cain and S. J. Cain Washington Aug. 1971 38 p refs

(NASA-TN-D-6237; G-1023) Avail: NTIS CSCL 20C

The results are summarized of the testing of the various magnetic field models against the available World Magnetic Survey data and details are given on the method by which the first International Geomagnetic Reference Field /IGRF(10/68)/ was derived. The IGRF(10/68) was composed of contributions from the field models derived by Goddard Space Flight Center, Air Force Cambridge Research Laboratories, Royal Greenwich Observatory, Institute of Terrestrial Magnetism and Radiowave Propagation (IZMIRAN), and the U.S. Coast and Geodetic Survey. IGRF(10/68) is a set of 80 internal, spherical harmonic coefficients and their first time derivatives, epoch 1965.0, referenced to a sphere of radius 6371.2 km. The rms residuals to surface and airborne magnetic-survey data taken between 1961 and 1965 average approximately 200 gamma. The rms deviations from selected Cosmos 49 (1964.7) and POGO (1965.8-1967.9) satellite observations of total field range from 30 gamma to 60 gamma. Author

N71-32436*# National Aeronautics and Space Administration, Goddard Space Flight Center, Greenbelt, Md.

PLASMA PARAMETER BETA IN THE MIDNIGHT MAGNETOSPHERE: FROM THE NEAR-EARTH PLASMA SHEET TO THE PLASMAPAUSE

M. Sugiura Jul. 1971 20 p refs

(NASA-TM-X-65640; X-645-71-280) Avail: NTIS CSCL 04A

Rb magnetometer observations on OGO-B and estimates of plasma energy density based on proton and electron flux measurements on the same satellite, were used to evaluate plasma parameter beta (the ratio of plasma energy density to the magnetic field energy density), in the magnetosphere near midnight. The observations were made near the dipole equator. It was shown that near midnight, beta normally exceeded unity just outside the plasmopause even during magnetically quiet periods. Existence of a peak in beta near the inner edge of the high beta region appeared to be a part of the structure of this plasma region. The proton belt was not the main cause of the equatorial depression of the magnetic field in the inner magnetosphere, because the distribution of Delta B, defined as the deviation of the scalar B from the magnitude of a reference field, was entirely different from that expected from the proton belt. Both the radial distribution and the magnitude of beta were highly

variable from one pass to the next over a time span of approximately two days. Author

N71-32519* National Aeronautics and Space Administration, Goddard Space Flight Center, Greenbelt, Md. Lab. for Space Physics.

ANALOGY BETWEEN MAGNETOSPHERIC RESONANCE AND THE VIBRATION OF A STRINGED MUSICAL INSTRUMENT

M. Sugiura Jul. 1971 15 p refs
(NASA-TM-X-65644; X-645-71-279) Avail: NTIS CSCL 03B

The production of resonant oscillations of the earth's magnetic field is discussed using as an analogy a violin playing. The magnetosphere resonates as the body of the violin and the solar wind acts as the bow. The frictional force assumed to produce a drag that drives the convection in the magnetosphere is considered to be created by the solar wind. The magnetosphere resonates differently depending on the solar wind pressure, speed, and other factors creating the frictional force on the magnetopause. Satellite data in agreement with the theory are discussed. N.E.N.

N71-33768* Temple Univ., Philadelphia, Pa.
OGO-3 DUST PARTICLE EXPERIMENT: DATA REDUCTION AND ANALYSIS Final Report

J. L. Bohn 1971 82 p refs
(Contract NAS5-9352)
(NASA-CR-121477) Avail: NTIS CSCL 14B

The OGO 3 spacecraft contained an experiment to measure various physical parameters of picogram size dust particles in cis-lunar and near earth space. Information concerning the scientific objectives of the experiment, the basic sensors and detector array, the sensor calibration, electronic instrumentation, and experiment data are presented. Author

N71-34333* Lockheed Missiles and Space Co., Palo Alto, Calif.

NIGHT GLOW OF THE ATMOSPHERE IN THE WAVELENGTH 1304 Å OXYGEN LINE AT LOW GEOMAGNETIC LATITUDES

E. K. Sheffer 1971 8 p refs Transl. into ENGLISH from Kosmich. Issled. Akad. Nauk SSSR (Moscow), v. 9, no. 1, 1971 p 74-80

Avail: NTIS National Translations Center, John Crerar Library, Chicago, Ill. 60616

An analysis of nightglow in the 1225 to 1350 Å range, belonging to the triplet atomic oxygen lines, recorded in equatorial domains during the flight of Cosmos-215 is presented. A description is given of the orbital elements and experimental equipment onboard the satellite. Peak values of the glow intensity as a function of local observation time are shown. The results from Cosmos-215 are compared with those obtained on the OGO-4 satellite. J.M.

N71-35437* Instituto Geofisico del Peru, Lima. Radio Observatorio de Jicamarca.

COORDINATED SATELLITE AND INCOHERENT SCATTER OBSERVATIONS Progress Report

R. F. Woodman and C. P. Lagos Aug. 1971 74 p refs
(Grant NGR-52-158-001)

(NASA-CR-121984) Avail: NTIS CSCL 03B

Four types of information are presented: (1) electron density and temperature profiles collected at the Jicamarca Radar Observatory, Lima, Peru, located near the magnetic equator coincident with twenty near-overhead passes of OGO-6; (2) films of Spread-F structure coincident with seven near-overhead passes of OGO-6; (3) electron density contours and vertical plasma drifts coincident with five 6300 Å nightglow emission intensities measured at the Huancayo Observatory; and (4) references to papers completed and prepared for publication which are connected with nightglow studies and special events such as a magnetic storm and a solar eclipse. Author

N71-36131* National Physical Lab., New Delhi (India). Radio Science Div.

IONOSPHERIC EFFECTS OF SOLAR FLARES. 5: THE FLARE EVENT OF JANUARY 30, 1968 AND ITS IMPLICATIONS

S. D. Deshpande, S. Ganguly, V. C. Jain, and A. P. Mitra
Apr. 1971 33 p refs

(RSD-63; PL-480-11) Avail: NTIS

From riometer and pulse absorption measurements on three frequencies for the large X-ray flare event that occurred on 30 January 1968, electron density profiles were derived for the entire course of the flare. The time variation of the electron production rate was obtained for the event from satellite measurements of X-rays in the bands 0-3 Å, 0-8 Å and 8-20 Å. A comparison of the profiles with the electron production rates deduced from the X-rays revealed a decrease in the effective recombination coefficient or of the negative ion to electron ratio which is in agreement with other results. Author

N71-36136* Aerospace Corp., El Segundo, Calif. Lab. Operations.

A FLIGHT CALIBRATION DEVICE FOR ABSOLUTE MEASUREMENTS AT THE LYMAN-ALPHA WAVELENGTH

P. H. Metzger and M. A. Clark 12 Jun. 1971 18 p refs
(Contract FO471-70-C-0059)

(AD-726567; TR-0059(6260-10)-9; SAMSO-TR-71-36) Avail: NTIS CSCL 20/6

A small device consisting of a lamp, filter, and external photodiode has been used successfully to monitor the sensitivity of a Lyman-alpha photometer on OGO-6 as well as a number of Air Force satellites. The operation of this calibration device is independent of lamp filter or window decay. Author (GRA)

N72-11325* National Aeronautics and Space Administration, Goddard Space Flight Center, Greenbelt, Md.
MAGNETIC FIELD FLUCTUATIONS DURING SUBSTORMS

D. H. Fairfield Sep. 1971 45 p refs Presented at the Moscow Symp. on Magnetospheric Substorms, Aug. 1971
Submitted for publication

(NASA-TM-X-65748; X-692-71-453) Avail: NTIS CSCL 03B

Before a magnetospheric substorm and during its early phases the magnetic field magnitude in the geomagnetic tail increases and field lines in the nighttime hemisphere assume a more tail-like configuration. Before the substorm onset a minimum amount of magnetic flux is observed to cross the neutral sheet which means that the neutral sheet currents attain their most earthward locations and their greatest current densities. This configuration apparently results from an increased transport of magnetic flux to the tail caused by a southward interplanetary magnetic field. The field begins relaxing toward a more dipolar configuration at the time of a substorm onset with the recovery probably occurring first between 6 and 10 R sub E. This recovery must be associated with magnetospheric convection which restores magnetic flux to the dayside hemisphere. Field aligned currents appear to be required to connect magnetospheric currents to the auroral electrojets, implying that a net current flows in a limited range of longitudes. Space measurements supporting current systems are limited. More evidence exists for the occurrence of double current sheets which do not involve net current at a given longitude. Author

N72-14808* Jet Propulsion Lab., Calif. Inst. of Tech., Pasadena.

COMPUTATION OF SOLAR WIND PARAMETERS FROM THE OGO-5 PLASMA SPECTROMETER DATA USING HERMITE POLYNOMIALS

M. Neugebauer 15 Dec. 1971 59 p refs

(Contract NAS7-100)

(NASA-CR-125063; JPL-TM-33-519) Avail: NTIS CSCL 03B

The method used to calculate the velocity, temperature, and density of the solar wind plasma is presented from spectra obtained by attitude-stabilized plasma detectors on the earth satellite OGO 5. The method, which used expansions in terms of Hermite polynomials, is very inexpensive to implement on an electronic computer compared to the least-squares and other iterative methods often used for similar problems. Author

N72-18715*# Massachusetts Inst. of Tech., Cambridge. Center for Space Research.
OGO-1 AND OGO-3 MIT PLASMA EXPERIMENTS S4903 Final Project Report

30 Jun. 1968 208 p refs

(Contract NAS5-2053)

(NASA-CR-122351) Avail: NTIS CSCL 20I

Plasma proton and plasma electron prototype and flight models were designed, fabricated, and tested. Ground support equipment for the models was also prepared. The flight models were launched aboard the first and third Orbiting Geophysical Observatories on 4 Sept. 1964 and 6 June 1966. These experiments have generally functioned in accordance with the design specifications and useful data are still being received. K.P.D.

N72-22383*# TRW Systems Group, Redondo Beach, Calif. Space Sciences Lab.

COMPLEX ELECTRIC FIELD EMISSIONS OBSERVED BY OGO-5 ON 15 AUGUST 1968

C. F. Kennel, F. L. Scarf, F. V. Coroniti, R. W. Fredricks, and J. H. McGhee, Jr. Mar. 1971 10 p refs In ESRO The ESRO Geostationary Magnetospheric Satellite p 91-100

(Contract NAS5-9278; Grant NGR-05-007-190)

(NASA-CR-126238) Avail: NTIS CSCL 03B

OGO-5 results from the first broad-band electric field experiment to operate successfully beyond the plasmopause are presented, indicating that processes similar to those encountered in the laboratory may also operate in the magnetosphere. The wave electric and magnetic field data are discussed from a complex event observed on 15 August 1968, in which various types of electric field emissions above the electron cyclotron frequency, as well as electromagnetic chorus activity, occurred near the geomagnetic equator on auroral lines of force near local midnight. Details of the plasma wave detector and the dc and wave magnetic field diagnostics are also given. Author (ESRO)

N72-23118*# Michigan Univ., Ann Arbor. Radio Astronomy Observatory.

ANALYSIS OF TYPE 3 SOLAR RADIO BURSTS OBSERVED AT KILOMETRIC WAVELENGTHS FROM THE OGO-5 SATELLITE Final Scientific Report

H. Alvarez Dec. 1971 301 p refs

(Contract NAS5-9099)

(NASA-CR-122393; UM/RAO-71-9) Avail: NTIS CSCL 20N

Research was conducted to analyze the data on solar radio bursts obtained by the OGO-5 satellite. Since the wavelengths corresponding to the three lowest frequencies of observations exceeded one kilometer, the bursts detected in those channels were designated as kilometer-waves. The data search covered approximately 9200 hours between March 1968 and February 1970, and included the maximum of solar cycle No. 20. The study concentrated on 64 Type 3 solar radio events reaching frequencies equal or lower than 0.35 MHz. This selection criteria led to the choice of the most intense radio events. Measurements included: times of start, times of decay, and amplitudes of the 64 events. The consistency of the results, within the accuracy of the measurements, lends support to some of the assumptions made for the analysis, notably, the validity of the local plasma hypothesis, the constancy of the exciter particles velocity, and spiral shape of their trajectory. Author

N72-23334*# National Aeronautics and Space Administration. Goddard Space Flight Center, Greenbelt, Md.

THE IONOSPHERE DURING A SUBAURORAL RED ARC

E. J. R. Maier 1972 6 p In its Significant Accomplishments in Sci., 1970 p 46-51

Avail: NTIS CSCL 04A

The enhancements of the red 6300 A line in the mid-latitudes during maximum solar activity are discussed. From Explorer 31 and OGO-4 satellite data, electron and ion temperatures were obtained at altitudes of 880 km and 2500 km. It was found that there is an increased plasma temperature in the region of the optical emissions, a difference of 1000 K between the plasma temperature at 880 km and that at 2100 km, and the ion temperatures are less than the electron temperatures. It is concluded that red arcs are observed only when there is heat flow from above, combined with decreased density caused by composition changes at the lower boundary. F.O.S.

N72-23341*# National Aeronautics and Space Administration. Goddard Space Flight Center, Greenbelt, Md.

CRUSTAL ANOMALIES

J. Cain 1972 6 p ref In its Significant Accomplishments in Sci., 1970 p 86-91 Original contains color illustrations

Avail: NTIS CSCL 08G

Crustal or magnetic anomaly component effects on Cosmos-49 and POGO measurements of the ambient geomagnetic field for North America are presented graphically. A.L.

N72-23429*# Aerospace Corp., El Segundo, Calif.

SPECTRAL VARIATIONS OF THE L ALPHA SKY: A FINAL REPORT OF OBSERVATIONS FROM OGO-6 Research Report, Jun. 1969 - Sep. 1970

P. H. Metzger and M. A. Clark 1 Mar. 1972 73 p refs (Contract F04701-71-C-0172)

(AD-736816; TR-0172(2260-10)-4; SAMSO-TR-72-4) Avail: NTIS CSCL 04/1

Data obtained in June 1969 from OGO-6 (400 x 1100 km, inclination 82 deg) reveal a consistent pattern in the observed variations of the spectral width of Lyman alpha radiation as seen by a sky-scanning photometer equipped with a resonance filter. These data have been interpreted in terms of the diurnal variation of the exospheric hydrogen temperature showing a temperature maximum near 1800 hours local time and a dawn-to-dusk difference of 200K. Evidence is presented that indicates the major source of the observed variation is local hydrogen. An analysis based on this assumption is given. Sky maps are presented that show the apparent temperature distribution across the sky, and, from these, a region is identified that appears to be aligned with the earth's magnetotail and consistently appears as a hot region. The contribution of the external UV sources is discussed. Author (GRA)

N72-25727*# California Inst. of Tech., Pasadena.

MAGNETOSPHERIC ACCESS OF SOLAR PARTICLES AND THE CONFIGURATION OF THE DISTANT GEOMAGNETIC FIELD, VOLUME 2 Ph.D. Thesis

L. C. Evans 1972 120 p refs

(Contract NAS5-3095)

(NASA-CR-122360) Avail: NTIS CSCL 03B

A summary is provided of all proton events observed with OGO-4 and observed flux profiles for several events. Pertinent data are indicated relating to the orientation of the interplanetary magnetic field. The events whose profiles are presented are divided into three classes: EDP events (normally associated with co-rotating features), solar flare events, and events having characteristics of both EDP events and flare events (class C events). A description of these classes of events and the criteria used to distinguish between EDP events and flare events are discussed. In addition, the 1 December 1967 EDP event and the 2 November 1967 solar flare event are discussed in some detail. Accompanying the profiles of each event is a brief list of notable observational

features of the event. Events are presented chronologically.

Author

N72-26309*# National Aeronautics and Space Administration, Goddard Space Flight Center, Greenbelt, Md.
AN ATLAS OF LOW LATITUDE 6300A (01) NIGHT AIRGLOW FROM OGO-4 OBSERVATIONS
E. I. Reed, W. B. Fowler (Centre Natl. de Rech. Sci., Verrieres-le-Buisson, France), and J. E. Blamont May 1972 52 p refs Submitted for publication
(NASA-TM-X-65913; X-625-72-171) Avail: NTIS CSCL 04A

The atomic oxygen emission line at 6300 A, measured in the nadir direction by a photometer on the polar orbiting satellite OGO-4, was plotted between 40 deg N and 40 deg S latitude on a series of maps for the moon-free periods between 30 August 1967 and 10 January 1968. The longitudinal and local time variations which occur during the northern fall-winter season are indicated. The northern tropical arc is more widespread while the southern arc is not present at all longitudes. The conditions under which the observations were made are described, and four airglow maps were selected to show the local time variations.

Author

N72-27423*# National Aeronautics and Space Administration, Goddard Space Flight Center, Greenbelt, Md.
FUNCTIONAL CHARACTERISTICS OF THE OGO MAIN BODY AIRGLOW PHOTOMETER
E. I. Reed, W. B. Fowler, and J. E. Blamont (Centre Natl. de la Rech. Sci., Verrieres-le-Buisson, France) May 1972 24 p refs
(NASA-TM-X-65926; X-625-72-174) Avail: NTIS CSCL 14B

The OGO-4 main body airglow photometer used a trialkali cathode photomultiplier to sense light at selected wavelengths between 2500 and 6300A corresponding to important emissions in the aurora and night airglow at emission rates ranging from a few rayleighs to about 200 kilorayleighs. The optical, electronic, and mechanical systems are described in terms of their functional characteristics.

Author

N72-27829 California Inst. of Tech., Pasadena.
PROPAGATION OF 1-10 MEV SOLAR FLARE PROTONS IN INTERPLANETARY SPACE Ph.D. Thesis
S. S. Murray 1971 227 p
Avail: Univ. Microfilms Order No. 72-479

Observations of 1 to 10 MeV solar flare protons associated with the 7 June 1969 solar event were used in an investigation of the physical processes affecting particle propagation in interplanetary space. The observations were made with the solar and galactic cosmic ray experiment on board the OGO-F, a low altitude polar-orbiting satellite. It was found during the decay of the event that the processes of diffusion, convection, and energy change must be considered to obtain satisfactory agreement between the observations and theoretical predictions. For this event, there is clear evidence for energy change processes occurring in interplanetary space. The observed energy change is not simply due to adiabatic deceleration in a uniformly expanding solar wind. During the decay the effects of diffusion are consistent with an energy-independent diffusion coefficient from 1 to 10 MeV.

Dissert. Abstr.

N72-28353*# National Aeronautics and Space Administration, Goddard Space Flight Center, Greenbelt, Md.
OGO-4 OBSERVATIONS OF THE 6300 A NIGHT AIRGLOW FROM 40 DEG N TO 40 DEG S: A SET OF 19 COLOR MAPS
E. I. Reed and J. E. Blamont (CNRS, Verrieres-le-Buisson, France) May 1972 27 p Original contains color illustrations
(NASA-TM-X-65954; X-625-72-173) Avail: NTIS CSCL 04A

Data for the 6300 A line of atomic oxygen from the

main body airglow photometer on the OGO-D satellite are summarized in a set of 19 maps for various local times at night between 30 August 1967 and 10 January 1968.

Author

N72-28467*# Lockheed Missiles and Space Co., Palo Alto, Calif. Research Labs.
MICROPHONE DENSITY GAGE EXPERIMENT FOR OGO-F Final Report
Jul. 1972 87 p refs
(Contract NAS5-9334)
(NASA-CR-130082; LMSC/L-73-72-1) Avail: NTIS CSCL 14B

A description is given of the fabrication, installation, and operation of the microphone density gage instrument. An analysis of the resulting problems and minor failures is also given. The approach to the data analysis is discussed and the significant results obtained are presented. Author

N72-28802*# McDonnell-Douglas Astronautics Co., Huntington Beach, Calif. Space Sciences Dept.
ANALYSIS OF INNER AND OUTER ZONE: OGO-1 AND OGO-2 ELECTRON SPECTROMETER AND ION CHAMBER DATA Final Report
K. A. Pfitzer 12 May 1972 46 p refs
(Contract NASw-2203)
(NASA-CR-127455; MDC-G2960) Avail: NTIS CSCL 03B

The dynamic processes governing the acceleration and loss of electrons in the radiation zones are investigated. The radial diffusion coefficient was determined for a McIlwain parameter between 1.6 and 2.2 for electrons having a first adiabatic invariant of 12 MeV/gauss. The coefficient is larger than earlier values and suggests that there exists a lower limit to the fluxes in the inner zone. The agreement between observed and calculated magnetic fields and particle fluxes is improved by using solar wind pressure as input to the magnetic field models. Changes in the plasma pressure can cause apparent local time asymmetries in particle flux. A comparison of the magnetic field models with observed location of the trapping boundary also indicates the need for including distributed currents within the magnetosphere. The high latitude trapping boundary is only weakly dependent on A sub p, and the trapping boundary data are improved by including in the models a stand-off distance which varies with the plasma pressure. N.E.N.

N72-28812*# California Univ., Berkeley.
ENERGETIC RADIATIONS FROM SOLAR FLARES Final Report, Mar. 1968 - Aug. 1971
K. A. Anderson Aug. 1971 42 p refs
(Contract NAS5-9094)
(NASA-CR-122509; SSL-Ser-13-Issue 50) Avail: NTIS CSCL 03B

An experiment designed to measure energetic X-rays, electrons, protons and alpha particles from solar flares aboard OGO 5 is reported. A brief statement of the objectives of the experiment is followed by a description of the instrumentation including detector characteristics and associated electronics. The data handling system is then described and the operational history of the experiment is discussed. This is followed by a description of the format of the magnetic data tapes and a summary of the major computer processing programs. The measurements made with this experiment within the first year of its operation have led to several basic results regarding the role of non-thermal electrons in the physics of solar flares. These results are described in the papers listed in the bibliography given at the end of this report. Author

N72-29818*# California Inst. of Tech., Pasadena.
SOLAR FLARE PARTICLE PROPAGATION: COMPARISON OF A NEW ANALYTIC SOLUTION WITH SPACECRAFT MEASUREMENTS Ph.D. Thesis
J. E. Lupton 1972 188 p refs
(Contract NAS5-9312; Grants NGR-05-002-160;

NGL-05-002-007)

(NASA-CR-122406) Avail: NTIS CSCL 03B

A new analytic solution has been obtained to the complete Fokker-Planck equation for solar flare particle propagation including the effects of convection, energy-change, corotation, and diffusion. It is assumed that the particles are injected impulsively at a single point in space, and that a boundary exists beyond which the particles are free to escape. Several solar flare particle events have been observed with the Caltech Solar and Galactic Cosmic Ray Experiment aboard OGO-6. Detailed comparisons of the predictions of the new solution with these observations of 1-70 MeV protons show that the model adequately describes both the rise and decay times. The model gives reasonable fits to the time-profile of 1-10 MeV protons from classical flare-associated events. It is not necessary to invoke a scatter-free region near the sun in order to reproduce the fast rise times observed for directly-connected events. The new solution also yields a time-evolution for the vector anisotropy which agrees well with previously reported observations. Author

N72-30823* National Aeronautics and Space Administration. Goddard Space Flight Center, Greenbelt, Md.
POGO OBSERVATIONS OF THE EQUATORIAL ELECTROJET

J. C. Cain and R. E. Sweeney Aug. 1972 146 p refs
(NASA-TM-X-65995; X-645-72-299) Avail: NTIS CSCL 22C

During intervals in 1967 to 1970, the OGO-4 and 6 spacecraft made over 2000 traversals over the equatorial electrojet in the altitude range 400-800 km when local times were between 9 and 15 hours. These spacecraft carried total field magnetometers making measurements to an accuracy of 2 gamma with a sample rate greater than once a second. Delta F values, the deviations from these observations, were formed from an internal reference model. The results were plotted for a 30 deg band about the equator, and the characteristics of the electrojet effect in the data were investigated. This effect was characterized by a sharp negative V-signature of some 16-19 deg in width and a variable amplitude. The position of this minimum was found to lie within 0.5 deg of the dip equator. A slight northward shift was noted at the longitude of Huancayo. The jet amplitudes were normalized to 400 km amplitudes and observed to be highly variable in time. Amplitudes over the longitude range 50 to 90 deg W averaged 60% higher than elsewhere, as expected, due to the weaker main field. However, though the scatter of amplitudes is high, the expected minima in east Asia were not evident. It was speculated that this could be due to a less conducting upper mantle in this area. Author

N72-32390* Lockheed Missiles and Space Co., Palo Alto, Calif. Research Lab.

VARIATIONS OF ATMOSPHERIC DENSITY NEAR 400 KM WITH MAGNETIC ACTIVITY DURING THE STORM PERIOD OF 28 SEPTEMBER TO 2 OCTOBER 1969

A. D. Anderson Apr. 1972 38 p refs
(Contract NAS5-9334)

(NASA-CR-122479; LMSC/D266900) Avail: NTIS CSCL 04A

Neutral density data were obtained near 400 km (1600 Lt) from a microphone density gage on OGO-6 from 0 to 40 deg N geomagnetic latitude for 25 September through 3 October 1969. Several geomagnetic storms occurred during this period. Least squares fits were made to data points on density scatter diagrams. An equation representing the least squares fit was computed for each delay time. The equation of best fit (and the corresponding time delay between the density and the magnetic index which resulted in this best fit) was found by choosing the equation that gave the minimum standard error. The implications of the time differences associated with the best fits at various latitudes and longitudes are discussed with regard to the time delays

involved in geomagnetic heating of the neutral upper atmosphere. Author

N73-10392* National Aeronautics and Space Administration. Goddard Space Flight Center, Greenbelt, Md.

A SYNOPTIC STUDY OF THE NATURE AND EFFECTS OF FIELD ALIGNED LOW ENERGY ELECTRON PRECIPITATION IN THE AURORAL REGIONS Ph.D. Thesis - Catholic Univ. of America

F. W. Berko Oct. 1972 108 p refs

(NASA-TM-X-66065; X-646-72-384) Avail: NTIS CSCL 04A

A synoptic study is presented of field-aligned precipitation events observed during a 16-month period, representing a full 4 pi precession of the satellite orbital plane in magnetic local time. The morphology of this type of precipitation, its nature, and relationships between this phenomenon and other geophysical events are discussed in the context of the 16-month data base. Author

N73-10789* TRW Systems Group, Redondo Beach, Calif. Space Sciences Lab.

ELECTRON PLASMA OSCILLATIONS IN THE NEAR-EARTH SOLAR WIND: PRELIMINARY OBSERVATIONS AND INTERPRETATIONS

R. W. Fredricks, F. L. Scarf, and I. M. Green 1972 7 p refs In NASA. Ames Res. Center Solar Wind p 353-359
(Contract NAS5-9278)

CSCL 03B

Preliminary results and conclusions of a study of electric field oscillations in the upstream solar wind are reported. The OGO-5 orbits are on the dusk (three) and on the dawn (one) sides of the earth-sun line. It is concluded that there are electron streams produced at or near the bow shock. These streams penetrate the incoming solar wind plasma, and generate quasi-electromagnetic waves. The streams (as inferred from the wave levels) occur without regard to dawn-dusk location, as opposed to the low-frequency MHD upstream disturbances driven by backstreaming protons, which show a definitely strong preference for the dawn-noon sector. The presence of the suprathermal electron streams and associated wave turbulence indicates that some near-earth electron distributions are probably not representative of true solar wind distributions far away from the earth. Author

N73-10791* California Univ., Los Angeles. Inst. of Geophysics and Planetary Physics.

COMMENTS ON THE MEASUREMENT OF POWER SPECTRA OF THE INTERPLANETARY MAGNETIC FIELD

C. T. Russell 1972 10 p refs In NASA. Ames Res. Center Solar Wind p 365-374

(Contract NAS5-9098)

CSCL 03B

Examination of possible noise sources in the measurement of the power spectrum of fluctuations in the interplanetary magnetic field shows that most measurements by fluxgate magnetometers are limited by digitization noise whereas the search coil magnetometers is limited by instrument noise. The folding of power about the Nyquist frequency or aliasing can be a serious problem at times for many magnetometers, but it is not serious during typical solar wind conditions except near the Nyquist frequency. Waves in the solar wind associated with the presence of the earth's bow shock can contaminate the interplanetary spectrum in the vicinity of the earth. However, at times the spectrum in this region is the same as far from the earth. Doppler shifting caused by the convection of waves by the solar wind makes the interpretation of interplanetary spectra difficult. Author

N73-10792* California Univ., Los Angeles. Dept. of Planetary and Space Science.

POWER SPECTRA OF THE INTERPLANETARY MAGNETIC FIELD NEAR THE EARTH

D. D. Childers and C. T. Russell 1972 7 p refs In

N73-10795

NASA. Ames Res. Center Solar Wind p 375-381
CSCL 03B

Power spectra of the interplanetary magnetic field measured by near-earth satellites upstream from the earth's bow shock are free from terrestrial contamination provided the field at the satellite does not intersect the bow shock. Considerable spectral enhancement for the range of frequencies 0.01 to 1.00 Hz, due to turbulence caused by the shock, may occur if the field observed at the satellite intersects the shock. This turbulence occurs frequently in both the morning and afternoon quadrants. In the frequency band from 0.07 to 1 Hz, this noise decreases in amplitude with radial distance from the shock with an attenuation length of 4 R sub E.

Author

N73-10795* TRW Systems Group, Redondo Beach, Calif. Space Sciences Lab.
COMPARISON OF DEEP SPACE AND NEAR-EARTH OBSERVATIONS OF PLASMA TURBULENCE AT SOLAR WIND DISCONTINUITIES

F. L. Scarf, R. W. Fredricks, and I. M. Green 1972 9 p refs *In* NASA. Ames Res. Center Solar Wind p 421-429

(Contracts NASw-2113; NAS5-9278; NAS2-4573)
CSCL 03B

Simultaneous observations of plasma waves from the electric field instruments on Pioneer 9 and OGO 5 are used to illustrate the difference between near-earth and deep space conditions. It is shown that the experimental study of true interplanetary wave-particle interactions is difficult to carry out from an earth orbiter because the earth provides significant fluxes of nonthermal particles that generate intense plasma turbulence in the upstream region.

Author

N73-10812* Centre National de la Recherche Scientifique, Verrieres-le-Buisson (France). Service d'Aeronomie.
OBSERVATION OF LYMAN-ALPHA EMISSION IN INTERPLANETARY SPACE

J. L. Bertaux and J. E. Blamont 1972 7 p refs *In* NASA. Ames Res. Center Solar Wind p 661-667

CSCL 03B

The extraterrestrial Lyman-alpha emission was mapped by the OGO 5 satellite, when it was outside the geocorona. Three maps, obtained at different periods of the year, are presented and analyzed. The results suggest that at least half of the emission takes place in the solar system, and give strong support to the theory that in its motion toward the apex, the sun crosses neutral atomic hydrogen of interstellar origin, giving rise to an apparent interstellar wind.

Author

N73-10813* Colorado Univ., Boulder. Dept. of Astro-Geophysics.
PROPERTIES OF NEARBY INTERSTELLAR HYDROGEN DEDUCED FROM LYMAN-ALPHA SKY BACKGROUND MEASUREMENTS

G. E. Thomas 1972 16 p refs *In* NASA. Ames Res. Center Solar Wind p 668-683

(Contract NAS5-9327; Grant NGR-06-003-052)
CSCL 03B

For a sufficiently rapid relative motion of the solar system and the nearby interstellar gas, neutral atoms may be expected to penetrate the heliosphere before becoming ionized. Recent satellite measurements of the Lyman alpha emission above the geocorona indicate such an interstellar wind of neutral hydrogen emerging from the direction of Sagittarius and reaching to within a few astronomical units of the sun. A detailed model of the scattering of solar Lyman alpha from the spatial distribution of neutral hydrogen in interplanetary space is presented. This asymmetric distribution is established by solar wind and solar ultraviolet ionization processes along the trajectories of the incoming hydrogen atoms. The values of the interstellar density, the relative velocity, and the gas temperature are adjusted to agree with the Lyman alpha measurements. The results may be interpreted in terms of two models, the cold model and the

hot model of the interstellar gas, depending on whether galactic Lyman alpha emission is present at its maximum allowable value or negligibly small.

Author

N73-11345*# National Aeronautics and Space Administration. Goddard Space Flight Center, Greenbelt, Md.

SEASONAL AND ALTITUDE VARIATIONS IN FIELD-ALIGNED PRECIPITATION OCCURRENCE

F. W. Berko Oct. 1972 24 p refs

(NASA-TM-X-66099; X-646-72-405) Avail: NTIS CSCL 04A

Data from more than 7500 orbits of the polar-orbiting satellite OGO-4 have been analyzed to determine the existence of seasonal, altitude, or universal time differences in the occurrence of field-aligned electrons. Unexpected variations in frequency of occurrence have been found at different altitudes and in different seasons. In particular, the probability of observing this phenomenon at high latitudes was found to be greatest in the winter months at the highest altitudes attained by OGO-4. A localized parallel electric field acceleration mechanism is presented which could account for the particle observations.

Author

N73-13376*# Michigan Univ., Ann Arbor. Space Physics Research Lab.

OGO-F-02 DATA ANALYSIS Final Report

A. F. Nagy, W. M. Silvis, and E. C. Foust Nov. 1972 37 p refs

(Contract NAS5-9306; ORA Proj. 078900)

(NASA-CR-130128) Avail: NTIS CSCL 04A

The OGO-6 satellite, which was launched on June 5, 1969 carried a complement of twenty-six experiments. One of those instruments, the F-02 package, was a cylindrical Langmuir probe experiment whose primary purpose was to measure ionospheric electron temperatures and densities. This report briefly describes the F-02 experiment itself, outlines the computer programs developed to analyze the raw data, and gives a summary of the scientific information obtained, with the aid of this experiment.

Author

N73-15837*# California Inst. of Tech., Pasadena.

A QUANTITATIVE INVESTIGATION OF THE SOLAR MODULATION OF COSMIC-RAY PROTONS AND HELIUM NUCLEI Ph.D. Thesis

F. L. Garrard 19 Jun. 1972 233 p refs

(Contract NAS5-9312; Grant NGR-05-002-160)

(NASA-CR-130298) Avail: NTIS CSCL 03B

The differential energy spectra of cosmic ray protons and He nuclei were measured at energies up to 315 MeV/nucleon using balloon-borne and satellite-borne instruments. These spectra are presented for solar quiet times for the years 1966 through 1970. The data analysis is verified by extensive accelerator calibrations of the detector systems and by calculations and measurements of the production of secondary protons in the atmosphere. The spectra of protons and He nuclei in this energy range are dominated by the solar modulation of the local interstellar spectra. Numerical solutions to the transport equation are presented for a wide range of parameters.

Author

N73-15863*# California Univ., Los Angeles. Space Science Center.

TRAPPED AND PRECIPITATING ELECTRONS EXPERIMENT (F-16) ON THE ORBITING GEOPHYSICAL OBSERVATORIES PROGRAM OGO-6 MISSION Final Report, Mar. 1966 - Jun. 1972

T. A. Farley 27 Nov. 1972 14 p

(Contract NAS5-9308)

(NASA-CR-130137) Avail: NTIS CSCL 03B

An electron spectrometer instrument for the Orbiting Geophysical Observatories program (OGO 6) was built. The data reduction and analysis of the experiment data are discussed.

Author

N73-16126*# Stanford Univ., Calif. Radioscience Lab.
ELF PROPAGATION IN THE PLASMASPHERE BASED

ON SATELLITE OBSERVATIONS OF DISCRETE AND CONTINUOUS FORMS

J. L. R. Muzzio Dec. 1971 124 p refs
(Contract NAS5-3093; Grants NGR-05-020-288;
NGL-05-020-008)

(NASA-CR-130351; TR-3439-2; SU-SEL-71-055) Avail:
NTIS CSCL 20N

The propagation of electromagnetic waves in a nonhomogeneous anisotropic medium is examined from the point of view of geometrical optics. In particular, the propagation of ELF waves in the magnetosphere is described in terms of the electron and ion densities and the intensity and inclination of the earth's magnetic field. The analysis of the variations of wave normal angle along the ray path is extended to include the effects of ions. A comparison of the relative importance of each of the above parameters in controlling the orientation of the wave normals is made in the region of the magnetosphere where most of the ion whistlers have been detected. Author

N73-16344*# Stanford Univ., Calif. Radioscience Lab. THE STRUCTURE OF THE MAGNETOSPHERE AS DEDUCED FROM MAGNETOSPHERICALLY REFLECTED WHISTLERS

B. C. Edgar Mar. 1972 195 p refs
(Contract NAS5-2131; Grants NGR-05-020-288;
NGL-05-020-008)

(NASA-CR-130352; SU-TR-3438-2; SU-SEL-71-070) Avail:
NTIS CSCL 04A

Very low frequency (VLF) electromagnetic wave phenomenon called the magnetospherically reflected (MR) whistler was investigated. VLF (0.3 to 12.5 kHz) data obtained from the Orbiting Geophysical Observatories 1 and 3 from October 1964 to December 1966 were used. MR whistlers are produced by the dispersive propagation of energy from atmospheric lightning through the magnetosphere to the satellite along ray paths which undergo one or more reflections due to the presence of ions. The gross features of MR whistler frequency-time spectrograms are explained in terms of propagation through a magnetosphere composed of thermal ions and electrons and having small density gradients across L-shells. Irregularities observed in MR spectra were interpreted in terms of propagation through field-aligned density structures. Trough and enhancement density structures were found to produce unique and easily recognizable signatures in MR spectra. Sharp cross-field density dropoff produces extra traces in MR spectrograms. Author

N73-16432*# Lockheed Missiles and Space Co., Palo Alto, Calif. Research Lab. CONTINUED DATA ANALYSIS FOR EXPERIMENT E-18 ON OGO-5 Final Report

K. K. Harris Nov. 1972 36 p refs
(Contract NAS5-23106)

(NASA-CR-130156) Avail: NTIS CSCL 04A

The processing of all useful data acquired from the light ion mass spectrometer experiment on OGO-E is reported and results obtained from specific interpretations of the data are discussed. The work was confined primarily to processing the raw data to a form in which the specific light ion densities were obtained as a function of universal time. The data were then reproduced on magnetic tape as a function of both universal time and the important geomagnetic parameters, such as, L, B, magnetic latitude, magnetic longitude, geodetic latitude, geodetic longitude, altitude, etc. Author

N73-16436*# Pittsburgh Univ., Pa. THE ALTITUDE OF THE SCATTERING LAYER NEAR THE MESOPAUSE OVER THE SUMMER POLES

T. M. Donahue and B. Guenther Dec. 1972 11 p ref
(Contract NAS5-11077; Grant NSF GA-27638)

(NASA-CR-130271; SRCC-182) Avail: NTIS CSCL 04A

The variation in radiance and altitude with time and latitude is reported for the dense scattering layers observed over the summer poles by the OGO 6 airglow photometer. The average altitude was 84.3 km with a tendency for higher

values on the night side than on the day side of the polar cap. The average radiance increased by a factor of 5 between day 163 and day 180, 1969, but decreased thereafter.

Author

N73-16795*# McDonnell-Douglas Astronautics Co., Huntington Beach, Calif. Space Sciences Dept. MDAC SOLAR COSMIC RAY EXPERIMENT ON OGO-6 Final Report, Mar. 1966 - Jan. 1973

A. J. Masley Jan. 1973 47 p refs
(Contract NAS5-9324)

(NASA-CR-130155; MDC-G4351) Avail: NTIS CSCL 03B

The instrumentation of the OGO-F solar cosmic ray experiment is described and results of data obtained during the satellite lifetime from launch on June 5, 1969, through September, 1970, are discussed. Author

N73-17946* National Aeronautics and Space Administration. Goddard Space Flight Center, Greenbelt, Md. MAGNETIC CONTROL OF THE HIGH LATITUDE THERMOSPHERE

A. E. Hedin 1972 4 p In its Significant Accomplishments in Sci., 1971 p 58-61
CSCL 04A

The thermospheric composition and density were measured by a neutral mass spectrometer onboard OGO 6 satellite. The observations were made during a quiet magnetic period in late August and early September 1969 when the satellite perigee was near the South Pole. Gas densities at 430 km altitude and contours of constant N₂ and He densities were plotted. J.A.M.

N73-17948* National Aeronautics and Space Administration. Goddard Space Flight Center, Greenbelt, Md. THE MAGNETOSPHERIC PLASMA TAIL

J. M. Grebowsky 1972 4 p In its Significant Accomplishments in Sci., 1971 p 67-70

Thermal proton density measurements by the RF ion mass spectrometer on the low altitude, polar orbiting, satellite OGO 4 were compared on five consecutive nightside passes during the early recovery stage of an intense storm occurring in September 1967. The observations showed the existence of an elongated plasma tail during the recovery phase of the storm. J.A.M.

N73-19841*# New Hampshire Univ., Durham. Space Science Center. NEUTRON MEASUREMENTS OF THE OGO-VI SPACECRAFT Final Scientific Report

J. A. Lockwood Jan. 1973 60 p refs
(Contract NAS5-9313; Grant NGR-30-002-008)
(NASA-CR-130181) Avail: NTIS CSCL 03B

The neutron measurements with the OGO-6 spacecraft are reported. Topics discussed include: the design and calibration of a neutron monitor for measuring the cosmic ray neutron leakages from the earth's atmosphere, determination of latitude dependence of cosmic ray leakage flux, determination of the angular distribution of neutron leakage flux as deduced by measurements of the altitude dependence, and verification of the solar modulation of the cosmic ray source for the neutron leakage. F.O.S.

N73-20498*# California Univ., Los Angeles. A SUMMARY OF THE RESULTS FROM THE UCLA OGO-5 FLUXGATE MAGNETOMETER Final Report, Feb. 1965 - Dec. 1972

P. J. Coleman, Jr. and C. T. Russell Feb. 1973 42 p refs
(Contract NAS5-9098)
(NASA-CR-130205; IGPP-Publ-1173-18) Avail: NTIS CSCL 14B

The OGO-5 fluxgate magnetometer experiment (E-14) was designed to measure the vector magnetic field over the full range of the OGO-5 orbit. Thus, it has a dynamic range of + or - 64,000 gamma yet it maintained a precision of + or - 1/16 gamma at all times. This enabled a broad spectrum

of problems to be attached. Studies of the magnetospheric waves, currents, waves-particle interactions, pitch angle distributions and wave normal directions were made. The structure of the magnetopause, the magnetotail, and bow shock were probed, waves and discontinuities in the solar wind were examined and the various phases of substorms were examined in depth. Author

N73-20842* National Aeronautics and Space Administration. Goddard Space Flight Center, Greenbelt, Md. **A MODEL OF THE STARFISH FLUX IN THE INNER RADIATION ZONE**
M. J. Teague (KMS Technol. Center) and E. G. Stasinopoulos Dec. 1972 66 p refs
(NASA-TM-X-66211; X-601-72-487) Avail: NTIS CSCL 03B

A model of the Starfish electrons injected into the radiation belt in July 1962 was determined for epoch September 1964. This model distinguishes between artificial and natural electrons and provides the artificial unidirectional electron flux as a function of equatorial pitch angle, energy, and L value. The model is based primarily upon data from the OGO-1, OGO-3, OGO-5, 1963-38C, and the OV3-3 satellites. Decay times for the Starfish electrons are given as a function of energy and L value. These decay times represent the best compromise between a number of independently determined values. The times at which the artificial Starfish flux component had become insignificant in comparison to the natural flux component are determined as functions of energy and L value. These times are determined by two separate methods, and averaged values are presented. It is shown that Starfish electrons, by the present time have become insignificant for all energies and L values. Author

N73-20866* National Aeronautics and Space Administration. Goddard Space Flight Center, Greenbelt, Md. **THE EQUATORIAL ELECTROJET SATELLITE AND SURFACE COMPARISON**
J. C. Cain, ed. and R. E. Sweeney, ed. Dec. 1972 87 p refs A collection of Papers presented to the 4th Intern. Symp. on Equatorial Aeronomy Submitted for publication (NASA-TM-X-66218; X-645-73-5) Avail: NTIS CSCL 03B

The OGO 4 and 6 (POGO) magnetic field results for the equatorial electrojet indicate that while the present models are approximately correct, the possibility of a westward component must be incorporated. The scatter diagrams of POGO amplitudes and surface data show a correlation. The ratios between the amplitudes estimated from surface data and those at 400 km altitude are as follows: India 5 to 8, East Africa (Addis Ababa) 4, Central Africa 3, West Africa (Nigeria) 3, South America (Huancaayo) 5, and Philippines 5. The variation in the ratio is due to the conductivity structure of the earth in various zones. Author

N73-21367* National Aeronautics and Space Administration. Goddard Space Flight Center, Greenbelt, Md. **SIMULTANEOUS PARTICLE AND FIELD OBSERVATIONS OF FIELD-ALIGNED CURRENTS**
F. W. Berko, R. A. Hoffman, R. K. Burton (Calif. Univ., Los Angeles), and R. E. Holzer (Calif. Univ., Los Angeles) Apr. 1973 34 p refs Submitted for publication (NASA-TM-X-66224; X-646-73-45) Avail: NTIS CSCL 08N

Simultaneous measurements of low energy precipitating electrons and magnetic fluctuations from the low altitude polar orbiting satellite OGO-4 have been compared. Analysis of the two sets of experimental data for isolated events led to the classification of high latitude field-aligned currents as purely temporal or purely spatial variations. Magnetic field disturbances calculated using these simple current models and the measured particle fluxes were in good agreement with measured field values. While fluxes of greater than 1 keV electrons are detected primarily on the nightside, magnetometer disturbances indicative of field-aligned currents were seen at all local times, both in the visual auroral regions and dayside polar cusp. Thus electrons with energies less than

approximately 1 keV are the prime charge carriers in high latitude dayside field-aligned currents. The satellite measurements are in good agreement with previously measured field-aligned current values and with values predicted from several models involving magnetospheric field-aligned currents. Author

N73-22079* Stanford Univ., Calif. Radioscience Lab. **BANDED WHISTLERS OBSERVED ON OGO-4**
E. M. Paymar Jan. 1972 53 p refs
(Grant NGR-05-020-288)
(NASA-CR-131495; SU-SEL-71-054; SU-TR-3439-1) Avail: NTIS CSCL 03B

Inspection of broadband VLF records from OGO-4 shows that some whistlers exhibit a banded structure in which one or more bands of frequencies are missing from the whistler's spectrum. The phenomenon is commonly observed by satellites on midlatitude field lines at all local times and at various longitudes around the world. The dispersion of banded whistlers (BW) is of several tens of sec to the 1/2 power, indicating that they originated in the opposite hemisphere and are propagating downward at the satellite. BW are generally spread in time (tenths of seconds) rather than sharply defined and tend to occur at random. The frequency spacing of the bands may be either uniform or irregular, and may vary radically between successive events. Several possible explanations for BW are considered. In particular, an analysis of the interaction of plane electromagnetic waves traveling in an anisotropic plasma with a field aligned slab of enhanced ionization is presented with promising results. Author

N73-25868* National Aeronautics and Space Administration. Goddard Space Flight Center, Greenbelt, Md. **DEPENDENCE OF FIELD-ALIGNED ELECTRON PRECIPITATION ON SEASON, ALTITUDE AND PITCH ANGLE**
F. W. Berko and R. A. Hoffman May 1973 30 p refs Submitted for publication
(NASA-TM-X-66260; X-646-73-153) Avail: NTIS CSCL 03B

The occurrence of field-aligned 2.3 keV electron precipitation was examined by using data from more than 7500 orbits of the polar-orbiting satellite, OGO-4. The frequency of occurrence of field aligned precipitation was highest at actual pitch angles between 7 and 10 deg, being highest in the winter months, at highest satellite altitudes. Acceleration by a localized parallel electric field established by electrostatic charge layers is proposed to explain particle observations. Author

N73-25870* Chicago Univ., Ill. Lab. for Astrophysics and Space Research. **DATA PROCESSING AND ANALYSIS FROM THE UNIVERSITY OF CHICAGO CHARGED PARTICLE EXPERIMENT ON THE OGO-5 SPACECRAFT Final Report**
J. A. Simpson 25 May 1973 5 p refs
(Contract NAS5-9366)
(NASA-CR-132761) Avail: NTIS CSCL 03B

The data processing and analysis performed for the charged particle experiment are summarized, and the principal scientific results obtained from the analysis are reported. A bibliography is included of conference reports, and publications based on these results. Author

N73-31150* California Univ., Livermore. Lawrence Livermore Lab. **LLL ELECTRON AND PROTON SPECTROMETER ON NASA'S ORBITING GEOPHYSICAL OBSERVATORY 5, THE DATA USER'S GUIDE TO THE MICROFILM RECORDS**
H. I. West, Jr. 20 Dec. 1972 60 p refs
(Contract W-7405-eng-48)
(UCRL-51307) Avail: NTIS

Background is provided for using data from the energetic-

particle experiment conducted on OGO-5. These data were plotted on both 20-minute and 2-hour scales. Data from the UCLA magnetometer experiment were plotted to the 20-minute scale for correlative purposes. In addition, tables of pertinent attitude orbit data were plotted. Many of these data are available on microfilm from the National Space Science Data Center. Author (NSA)

N73-32286* Texas Univ., Dallas.
OGO 6 ION CONCENTRATION IRREGULARITY STUDIES Final Report

J. P. McClure Sep. 1973 91 p refs
(Contract NAS5-23184)

(NASA-CR-132814) Avail: NTIS CSCL 04A

Research is reported concerning the ionospheric F-region irregularities. The results are based on in-situ OGO-6 measurements of the total ion concentration $N_{\text{sub } i}$. A proposed mechanism for the generation of equatorial F-region irregularities and the morphological results, and the occurrence of Fe(+) ions in the equatorial F-region are discussed. Related research papers are included. F.O.S.

N73-32639 New Hampshire Univ., Durham.
NEUTRON MEASUREMENTS IN SPACE WITH OGO-6 Ph.D. Thesis

S. O. Ifedili 1973 261 p

Avail: Univ. Microfilms Order No. 73-16742

An experiment has been performed with a neutron detector on the OGO-6 satellite to search for solar neutrons, to measure the solar proton albedo neutron flux, and to determine the flux, latitude dependence, angular distribution, energy spectrum and the solar modulation of the cosmic ray albedo neutrons. Solar proton albedo neutron fluxes, both at high and low latitudes and for several solar proton events, were measured. The total cosmic ray leakage flux has been measured to be about 0.7 times the Lingenfelter (1963) flux while the latitude dependence is in good agreement with that calculated by Lingenfelter (1963). The form of the angular distribution of the cosmic ray albedo neutrons at the top of the atmosphere was deduced from the comparison of the measured and calculated altitude dependence of the cosmic ray albedo neutron flux. Finally, the solar modulation of the cosmic ray albedo neutrons has been observed.

Dissert. Abstr.

N73-33320* Michigan Univ., Ann Arbor. Space Physics Research Lab.

OGO-6 NEUTRAL ATMOSPHERIC COMPOSITION EXPERIMENT Final Report

D. R. Tausch Sep. 1973 7 p refs

(Grant NGR-23-005-561)

(NASA-CR-135798) Avail: NTIS CSCL 04A

The continued analysis of data obtained from the neutral atmospheric composition experiment flown on OGO-V6 is discussed. The effort was directed toward the study of five specific areas of interest for which the OGO-V6 data were especially useful. Author

N73-33321* Texas Univ., Dallas.
INVESTIGATION INTO THE MECHANISM AND RATES OF ATMOSPHERIC MIXING IN THE LOWER THERMOSPHERE Semiannual Status Report, period ending 15 Mar. 1973

F. S. Johnson et al 5 Oct. 1973 25 p refs

(Grant NGL-44-004-026)

(NASA-CR-135789) Avail: NTIS CSCL 04A

Three separate studies are reported which include: (1) an analysis of energy input to the lower thermosphere, (2) data analyses of OGO-6 onboard retarding potential analyzer measurements, and (3) an investigation of the sharp cutoff in plasma density of the Venus ionosphere as observed by Mariner 5. D.L.G.

N73-33777* California Inst. of Tech., Pasadena.
A SATELLITE MEASUREMENT OF COSMIC-RAY ABUNDANCES AND SPECTRA IN THE CHARGE

RANGE 2 LESS THAN OR EQUAL TO 7 LESS THAN OR EQUAL TO 10 Ph.D. Thesis

J. W. Brown Jun. 1973 118 p refs

(Contract NAS5-9312; Grant NGR-05-002-160)

(NASA-CR-135786; SRL-73-2) Avail: NTIS CSCL 03B

The composition of the nuclear component of the cosmic radiation was studied to yield information concerning the source, propagation, and confinement of cosmic rays within the galaxy. The first comprehensive satellite measurement is presented of cosmic-ray composition and spectra in the charge range 2 equal to or less than Z equal to or less than 10 using the geomagnetic field as a rigidity analyzer through the entire range of vertical cutoffs. The results indicate that the spectra of all the elements in the observed range are similar, and thus that various ratios of elemental abundances are nearly independent of rigidity over the range 2 equal to or less than P equal to or less than 15 GV. Calculations of the propagation of cosmic rays through the interstellar and interplanetary media predict that there should be a variation with rigidity of ratios of various elements, because of the charge-dependent effects of ionization of the interstellar gas by the cosmic rays. The absence of this variation can be explained by assuming a rigidity-dependent confinement of the cosmic rays in the galaxy.

Author

N74-10255* National Aeronautics and Space Administration. Marshall Space Flight Center, Huntsville, Ala.

THERMOELECTRICALLY-COOLED QUARTZ CRYSTAL MICROBALANCE

D. McKeown (Faraday, Labs., Inc.), W. E. Corbin, Jr. (Faraday, Labs., Inc.), and R. J. Naumann 1973 12 p refs In its Space Simulation, 7th p 345-356

(Contracts NAS8-27879; NAS5-11163)

CSCL 14B

A quartz crystal microbalance is of limited value in monitoring surface contamination on satellites or in space simulation chambers because it operates several degrees above ambient temperatures. The amount of contamination adsorbed on a surface is highly temperature dependent and the higher temperature of the microbalance will significantly reduce the amount of contamination it absorbs. To overcome this problem a thermoelectrically cooled quartz crystal microbalance has been developed to monitor surface contamination as a function of temperature. Author

N74-10366* National Aeronautics and Space Administration. Goddard Space Flight Center, Greenbelt, Md.

DYNAMICS OF MIDLATITUDE LIGHT ION TROUGH AND PLASMATAILS

A. J. Chen, J. M. Grebowsky, and H. A. Taylor, Jr. Aug. 1973 31 p refs Submitted for publication

(NASA-TM-X-70494; X-621-73-275) Avail: NTIS CSCL 03B

Light ion trough measurements near midnight made by the RF ion mass spectrometer on OGO-4 operating in the high resolution mode in Feb. 1968 reveal the existence of irregular structure on the low latitude side of the midlatitude trough. Using two different relations between the equatorial convection electric field, assumed spatially invariant and directed from dawn to dusk, and K_p (one based on plasmopause measurements, the other on polar cap E field measurements) a model development was made of the outer plasmasphere. The model calculations produced multiple plasmatail extensions of the plasmasphere which compare favorably with the observed irregularities. Due to magnetic local time differences between the Northern and Southern Hemisphere along OGO's orbit, the time dependent irregularity structure observed is not symmetrical about the equator. The model development produces an outer plasmasphere boundary location which varies similarly to the observed minimum density point of the light ion trough. However, the measurements are not extensive enough to yield conclusive proof that one of the electric field models is better than the other. Author

N74-12109 Stanford Univ., Calif.
OGO-4 SATELLITE OBSERVATIONS OF WHISTLER-MODE PROPAGATION EFFECTS ASSOCIATED WITH CAUSTICS IN THE MAGNETOSPHERE Ph.D. Thesis
 N. H. Dantas 1973 158 p
 Avail: Univ. Microfilms Order No. 73-14886

Whistler striations, a phenomenon observed aboard the polar orbiting OGO-4 satellite, are described and interpreted. The phenomenon is characterized either by amplitude enhancements in bands of frequencies or by a high-frequency cutoff of whistler signals received at low latitudes. The center frequency of the bands or the cutoff frequency increases or decreases as the satellite approaches the magnetic equator, giving rise to a striated visual effect on frequency-vs-time displays. The explanation for the occurrence of the striations is based on the behavior of VLF ray paths in the region of the ionosphere characterized by the so-called equatorial anomaly of electron distribution. Ray tracing studies in this case predict the presence of caustic surfaces whose properties, combined with absorption results, account for the several details associated with the striations such as: local time of occurrence, rate of change of the cutoff frequency with latitude, minimum in cutoff frequency and its day-night variation, etc. Dissert. Abstr.

N74-12459* Smithsonian Astrophysical Observatory, Cambridge, Mass.
VARIATIONS IN THERMOSPHERIC COMPOSITION: A MODEL BASED ON MASS-SPECTROMETER AND SATELLITE-DRAG DATA
 L. G. Jacchia 30 Nov. 1973 28 p refs
 (Grant NGR-09-015-002)
 (NASA-CR-136192; SAO-Special-Rept-354) Avail: NTIS CSCL 03B

The seasonal-latitudinal and the diurnal variations of composition observed by mass spectrometers on the OGO 6 satellite are represented by two simple empirical formulae, each of which uses only one numerical parameter. The formulae are of a very general nature and predict the behavior of these variations at all heights and for all levels of solar activity; they yield a satisfactory representation of the corresponding variations in total density as derived from satellite drag. It is suggested that a seasonal variation of hydrogen might explain the abnormally low hydrogen densities at high northern latitudes in July 1964. Author

N74-12842* Stanford Univ., Calif. Radioscience Lab.
MEASUREMENTS OF VLF POLARIZATION AND WAVE NORMAL DIRECTION ON OGO-F Final Report
 R. A. Helliwell 1973 40 p refs
 (Contract NAS5-9309)
 (NASA-CR-132882) Avail: NTIS CSCL 20N

A major achievement of the F-24 experiment on OGO 6 was a verification of the polarization of proton whistlers. As predicted, the electron whistler was found to be right-hand polarized and the proton whistler left hand polarized. The transition from right- to left-hand polarization was found to occur very rapidly. Thus it appears that the experimental technique may allow great accuracy in the measurement of the cross-over frequency, a frequency that provides information on the ionic composition of the ionosphere. Author

N74-13165* California Univ., Livermore. Lawrence Livermore Lab.
LLL ELECTRON AND PROTON SPECTROMETER ON NASA'S ORBITING GEOPHYSICAL OBSERVATORY 5 Final Report for Experiment 6
 H. I. West, Jr., R. M. Buck, and J. R. Walton 29 May 1973 66 p refs
 (NASA Order S-70014-G; Contract W-7405-eng-48)
 (NASA-CR-136218; UCRL-51385) Avail: NTIS CSCL 14B

The LLL energetic electron and proton spectrometer on NASA's Orbiting Geophysical Observatory 5 (OGO-5) operated successfully from launch - March 4, 1968 - until retirement in August 1971. Data recovery during this time

was about 95% of the orbit except for the last few months. The electron spectrometer used a magnetic field for electron momentum selection which served also as an electron broom for a proton range-energy telescope. The energy range was approximately 60 to 2950 keV for electrons (seven channels) and 0.10 to approximately 94 MeV for protons (seven channels). The experiment was scanned relative to the stabilized OGO-5 for obtaining directional information. Excellent data were taken throughout the magnetosphere and in the interplanetary region. Studies were carried out in the areas of equatorial pitch-angle distributions, substorm dynamics and field topology, particle spectra (time history), particle spatial distributions, and solar particle events. Author

N74-13566* National Aeronautics and Space Administration, Goddard Space Flight Center, Greenbelt, Md.
VARIATION WITH INTERPLANETARY SECTOR OF THE TOTAL MAGNETIC FIELD MEASURED AT THE OGO 2, 4, AND 6 SATELLITES
 R. A. Langel Nov. 1973 32 p refs
 (NASA-TM-X-70531; X-645-73-356) Avail: NTIS CSCL 03B

Variations in the scalar magnetic field (δB) from the polar orbiting OGO 2, 4, and 6 spacecraft are examined as a function of altitude for times when the interplanetary magnetic field is toward the sun and for times when the interplanetary magnetic field is away from the sun. This morphology is basically the same as that found when all data, irrespective of interplanetary magnetic sector, are averaged together. Differences in δB occur, both between sectors and between seasons, which are similar in nature to variations in the surface δZ found by Langel (1973c). The altitude variation of δB at sunlit local times together with δZ at the earth's surface, demonstrates that the δZ and δB which varies with sector has an ionospheric source. Langel (1973b) showed that the positive δB region in the dark portion of the hemisphere is due to at least two sources, the westward electrojet and an unidentified non-ionospheric source(s). Comparison of magnetic variations between season/sector at the surface and at the satellite, in the dark portion of the hemisphere, indicates that these variations are caused by variations in the latitudinally narrow electrojet currents and not by variations in the non-ionospheric source of δB . Author

N74-15857* Develco, Inc., Mountain View, Calif.
THE FEASIBILITY OF A SUB-LF SATELLITE-TO-SUBMARINE COMMUNICATION DOWNLINK VLF NOISE LEVELS IN THE IONOSPHERE Technical Report, 13 Dec. 1971 - 27 Nov. 1972
 N. Dunkel 27 Nov. 1972 15 p refs
 (Contract N00014-72-C-0113)
 (AD-769139; Rept-532-721127; TR-2) Avail: NTIS CSCL 17/2

The electromagnetic noise environment of satellite-borne ELF, VLF and LF receivers was investigated. Noise data obtained from a number of satellite and rocket experiments (maximum altitude 3000 km) have been reviewed and summarized. The intensity of whistlers equatorial hiss, and man-made signals as a function of latitude, time of day and state of the ionosphere were examined and typical noise environment curves were presented. These data suggest that areas near the magnetic equator and over the polar cap provide the lowest ionospheric noise environment. Author (GRA)

N74-16064* National Aeronautics and Space Administration, Goddard Space Flight Center, Greenbelt, Md.
HIGH LATITUDE MINOR ION ENHANCEMENTS: A CLUE FOR STUDIES OF MAGNETOSPHERE-ATMOSPHERE COUPLING
 H. A. Taylor, Jr. Dec. 1973 25 p refs Submitted for publication
 (NASA-TM-X-70582; X-621-74-28) Avail: NTIS CSCL 04A

Unexpectedly abrupt and pronounced distributions of the thermal molecular ions $\text{NO}(+)$, $\text{O}_2(+)$ and $\text{N}_2(+)$ were observed at mid and high latitudes by the OGO-6 ion mass spectrometer. These minor ions may reach concentration levels exceeding 1000 ions/cu cm at altitudes as great as 1000 km, suggestive of scale heights well in excess of those inferred from low and mid-latitude measurements, under relatively undisturbed conditions. The high latitude ion enhancements were observed to be narrowly defined in time and space, with molecular ion concentrations changing by as much as an order of magnitude between successive orbits. Author

N74-16072# Max-Planck-Institut fuer Aeronomie, Lindau Uber Northeim (West Germany). Inst. fuer Stratosphaer-physik.

A MULTISATELLITE STUDY OF AURORAL-ZONE PHENOMENA.

L. Possberg, E. Lammers (Brunswick Univ.), W. Riedler (Tech. Hochschule, Graz), G. Skovli (Norweg. Defence Res. Estab., Kjeller), F. Soeraas (Bergen Univ.), P. Stauning (Tech. Univ., Lyngby, Den.), B. Theile (Brunswick Univ.), and G. R. Thomas (Radio and Space Res. Sta., Slough, Engl.) Paris ESRO May 1973 56 p refs Sponsored in part by Bundesmin. fuer Forsch. und Technol., Danish Space Res. Inst., Roy. Norweg. Council for Sci. and Technol., Sci. Res. Council, Engl., Space Res. Inst. of the Austrian Acad. of Sci., Swed. Nat. Sci. Res. Council and ESRO (ESRO-SR-23-Pt-1) Avail: NTIS

Multisatellite observations of particles and transverse magnetic field variations in and near the auroral zone were studied for moderately disturbed magnetic conditions during 11 November 1969. Particle and field data in the outer magnetosphere and in interplanetary space were also included in the study. The results show that, whereas most but not all of the nightside auroral zone disturbances can be related to changes in the distant magnetosphere, the dayside disturbances are not easily interpreted in terms of such changes. Author (ESRO)

N74-16940*# Analysis and Computer Systems, Inc., Burlington, Mass.

DATA PROCESSING SYSTEM FOR THE INTENSITY MONITORING SPECTROMETER FLOWN ON THE ORBITING GEOPHYSICAL OBSERVATORY-F (OGO-F) SATELLITE Final Report, 1 Jul. 1970 - 30 Jun. 1973

A. G. Cronin and J. R. Delaney Jul. 1973 87 p refs (NASA Order S-99821; Contract F19628-70-C-0298; AF Proj. 6688) (NASA-CR-136827; AFCRL-TR-73-0655) Avail: NTIS CSCL 09B

The system is discussed which was developed to process digitized telemetry data from the intensity monitoring spectrometer flown on the Orbiting Geophysical Observatory (OGO-F) satellite. Functional descriptions and operating instructions are included for each program in the system. Author

N74-17058 Maryland Univ., College Park.
A STUDY OF HIGH LATITUDE MAGNETIC DISTURBANCE Ph.D. Thesis

R. A. Langel 1973 218 p
Avail: Univ. Microfilms Order No. 73-28879

Variations in the total (i.e., scalar) magnetic field data from the polar orbiting OGO 2, 4, and 6 spacecraft (altitudes 400-1510km.), with supporting vector magnetic field data from observatories at the earth's surface, are analyzed for dipole latitudes above 55 deg. Data from all degrees of magnetic disturbance are included, but emphasis is placed on periods when K sub $p = 2(-)$ to $3(+)$. The principal total field variations are: (1) a positive Delta B (Delta B = measured field magnitude minus the field magnitude from a mathematical model of the quiet field) region between about 22(h) and 10(h) magnetic local time (MLT) with its maximum near 3(h) and 72 deg, and (2) a negative Delta B region between about 10(h) and 22(h) MLT with its maximum near 15(h) and 75 deg. Individual satellite passes, at low altitudes,

indicate the presence of a westward electrojet at about 23-6(h) MLT and eastward electrojet at about 19-2323(h) MLT. Neither average Delta B patterns nor individual satellite passes are consistent with electrojet currents as the primary source. Dissert. Abstr.

N74-17126# Lockheed Missiles and Space Co., Palo Alto, Calif. Research Lab.

MAGNETOSPHERIC CHEMICAL RELEASE STUDY

Final Technical Report
B. M. McCormac, J. E. Evans, S. B. Mende, and G. T. Davidson 1. Nov. 1973 107 p refs
(Contract N00014-73-C-0130; ARPA Order 2260) (AD-769979) Avail: NTIS CSCL 04/1

Wave particle interactions in the magnetosphere can produce ULF and VLF amplification, affect the diffusion of energy from the magnetosphere to the ionosphere, and may affect the trapping of energetic electrons and protons. Chemical releases of barium or lithium may modify the wave particle interactions in the magnetosphere such that the phenomena can be better investigated and may lead to techniques for producing desired wave particle interactions. Under this study results of a barium release in the outer magnetosphere and OGO-5 satellite results have been reviewed to obtain guidance in planning future satellite experiments. The possibility of using cold plasma chemical releases to reduce trapped betas from nuclear detonations has been studied. Data on previous observations of electrons and protons in the magnetosphere have been collected. General requirements for satellite experiments are given. Author (GRA)

N74-18420*# Wyoming Univ., Laramie. Dept. of Physics and Astronomy.

MAGNETOSPHERIC MODULATION EFFECTS ON SOLAR COSMIC RAYS FROM SIMULTANEOUS OGO 1 AND 3 ION CHAMBER DATA IN 1968 AND 1969

D. J. Hofmann Oct. 1973 158 p refs
(Grant NGR-51-001-033) (NASA-CR-137075) Avail: NTIS CSCL 03B

Simultaneous observations by identical ionization chambers aboard the satellites OGO-1 and OGO-3 are utilized to investigate spatial variations in particle intensity near and inside the magnetosphere during the solar cosmic ray events of September 1966. Cross-correlation of the absolute proton flux computed from the chamber rate during three solar particle events shows good agreement with the measurements by the IMP-F Solar Proton Monitor during the same events. The chamber has a dynamic range of over six orders of magnitude. Before launch it was calibrated in the laboratory with radiation dosages in the range 1 R/hr-6000 R/hr. The OGO-1 and OGO-3 chambers, which were normalized in the laboratory prior to the launch, are found to maintain their normalization within approximately equal to 1 per cent during their flight. The high sensitivity and absolute inter-comparability of the instruments allow small intensity differences to be detected and it is established that the observed differences can be explained by a magnetospheric screening effect when an anisotropic beam of particles is present in space. Evidence is presented to show that the screening is at times complete for a duration of as much as 110 min in the tail of the magnetosphere so that during this period the solar cosmic rays (E approximately equal to 15 MeV) have virtually no access to that region of the magnetosphere. Small intensity fluctuations of temporal nature observed are found to be subjected to a damping effect inside the magnetosphere. Author

N74-19023*# National Aeronautics and Space Administration, Goddard Space Flight Center, Greenbelt, Md.

ELECTRIC FIELD MEASUREMENTS ACROSS THE HARANG DISCONTINUITY

N. C. Maynard Feb. 1974 41 p refs
(NASA-TM-X-70613; X-625-74-67) Avail: NTIS CSCL 04A

The Harang discontinuity, the area separating the

N74-19088

positive and negative bay regions in the midnight sector of the auroral zone, is a focal point for changes in behavior of many phenomena. Through this region the electric field rotates through the west from a basically northward field in the positive bay region to a basically southward field in the negative bay region appearing as a reversal in a single axis measurement. 32 of these reversals have been identified in the OGO-6 data from November and December, 1969. The discontinuity is dynamic in nature, moving southward and steepening its latitudinal profile as magnetic activity is increased. As activity decreases it relaxes poleward and spreads out in latitudinal width. It occurs over several hours of magnetic local time. The boundary in the electric field data is consistent with the reversal of ground magnetic disturbances from a positive to negative bay condition. The discontinuity is present in the electric field data both during substorms and during quiet times and appears to define a pattern on which other effects can occur. (AUTHOR)

N74-19088*# Minnesota Univ., Minneapolis. Dept. of Physics.

COSMIC RAY TELESCOPE FOR OGO 2 AND 4 SPACECRAFT Final Report, 1 Jul. 1962 - Jul. 1969

W. R. Webber 26 Mar. 1974 4 p

(Contract NAS5-3096)

(NASA-CR-137238) Avail: NTIS CSCL 20F

The construction and subsequent flight are described of a cosmic ray telescope aboard the OGO-2 and 4 spacecraft. This instrument was a combination Cerenkov-scintillation counter telescope designed to measure the cosmic ray energy spectrum from 1-15 GV and charge composition from $Z = 1-8$. OGO-2 was launched in October 1965; however, attitude control problems caused a rapid loss control gas, so that after approximately 2 weeks it was no longer possible to point the spacecraft. This mission was officially declared a failure. The cosmic ray instrument appeared to work well during this time. OGO-4 was launched in July 1967, with a similar telescope aboard. It operated successfully approximately one year. The details of the experiment, its operation, and the results are given. Author

N74-20502*# National Aeronautics and Space Administration, Goddard Space Flight Center, Greenbelt, Md.

THE INNER ZONE ELECTRON MODEL AE-5

M. J. Teague and J. I. Vette Nov. 1972 200 p refs

(NASA-TM-X-69987; NSSDC-72-10) Avail: NTIS CSCL 03B

A description is given of the work performed in the development of the inner radiation zone electron model, AE-5. A complete description of the omnidirectional flux model is given for energy thresholds $E_{sub T}$ in the range $4.0 > E_{sub T} / (MeV) > 0.04$ and for L values in the range $2.8 > L > 1.2$ for an epoch of October 1967. Confidence codes for certain regions of B-L space and certain energies are given based on data coverage and the assumptions made in the analysis. The electron model programs that can be supplied to a user are referred to. One of these, a program for accessing the model flux at arbitrary points in B-L space and arbitrary energies, includes the latest outer zone electron model and proton model. The model AE-5, is based on data from five satellites, OGO-1, OGO-3 1963-38C, OV3-3, and Explorer 26, spanning the period December 1964 to December 1967. Author

N74-20503*# National Aeronautics and Space Administration, Goddard Space Flight Center, Greenbelt, Md.

A MODEL ENVIRONMENT FOR OUTER ZONE ELECTRONS

G. W. Singley and J. I. Vette Dec. 1972 127 p refs

(NASA-TM-X-69989; NSSDC-72-13) Avail: NTIS CSCL 03B

A brief morphology of outer zone electrons is given to illustrate the nature of the phenomena that we are attempting to model. This is followed by a discussion of the data processing that was done with the various data received from the experimenters before incorporating it into the data base

from which this model was ultimately derived. The details of the derivation are given, and several comparisons of the final model with the various experimental measurements are presented. Author

N74-20542*# Texas Univ., Dallas.

OGO-6 EXPERIMENT F-03 Final Report

W. B. Hanson and S. Sanatani 15 Jul. 1973 11 p refs

(Contract NAS5-9311)

(NASA-CR-132943) Avail: NTIS CSCL 22C

The results obtained with the retarding potential analyzer on the OGO-6 satellite are discussed. The information obtained during the OGO-6 flight concerned the following subjects: (1) measurement of electron flux density in the plasmaphere, (2) latitudinal variations of ion temperature, (3) heating in the nighttime ionosphere by conjugate photoelectrons, (4) longitudinal variation in equatorial ion temperature at low altitude, and (5) identification of heavy ions in the upper F region. Author

N74-20982*# National Aeronautics and Space Administration, Goddard Space Flight Center, Greenbelt, Md.

A GLOBAL MAGNETIC ANOMALY MAP

R. D. Regan (USGS, Silver Spring, Md.), W. M. Davis (USGS, Silver Spring, Md.), and J. C. Cain Apr. 1974

24 p refs Submitted for publication Original contains color illustrations

(NASA-TM-X-70628; X-922-74-98) Avail: NTIS CSCL 08E

A subset of POGO satellite magnetometer data has been formed that is suitable for analysis of crustal magnetic anomalies. Using a thirteenth order field model, fit to these data, magnetic residuals have been calculated over the world to latitude limits of plus 50 deg. These residuals averaged over one degree latitude-longitude blocks represent a detailed global magnetic anomaly map derived solely from satellite data. Preliminary analysis of the map indicates that the anomalies are real and of geological origin. Author

N74-21445* California Univ., Berkeley. Space Sciences Lab.

CHARACTERISTICS OF NONTHERMAL ELECTRONS ACCELERATED DURING THE FLASH PHASE OF SMALL SOLAR FLARES

S. R. Kane 1973 23 p refs In NASA, Washington High Energy Phenomena on the Sun p 55-77

(Contract NAS5-9094; Grant NGL-05-003-017)

CSCL 03B

Observations of impulsive hard X-rays and other flash phase emissions from small solar flares are analyzed in order to determine the characteristics of energetic electrons accelerated during the flash phase. The electron spectrum and its time variation are deduced from a model of the X-ray source in which the electron injection is continuous, and the electron energy loss is primarily due to collisions with the ambient plasma and escape into the corona. The instantaneous electron spectrum in the X-ray source, as well as the acceleration spectrum, are found to be nonthermal. The observations are consistent with a flare model having the following properties: (1) the acceleration region is located in the lower corona where the ion density is less than 10^{10} to the 9th power per cubic centimeter, (2) the total kinetic energy of the nonthermal electron is approximately 10 percent of the total flare energy, so that the efficiency of the acceleration process is very high, (3) the nonthermal electrons (and protons) provide energy for all flash phase emissions, (4) the acceleration is a continuous process with a time constant less than 1 second, or a continuous series of impulses each lasting less than 1 second and a total duration of approximately 100 seconds, (5) the electron spectrum continuously hardens during the increasing phase of the X-ray burst and softens during the decreasing phase and, (6) the more energetic flares do not necessarily produce a harder electron spectrum. Author

Nov. 10, 1975

N74-21450* American Science and Engineering, Inc.,
Cambridge, Mass.

**POSSIBLE LOW ENERGY (E LESS THAN KEV)
NONTHERMAL X-RAY EVENTS**

S. W. Kahler 1973 8 p refs In NASA, Washington
High Energy Phenomena on the Sun p 124-131
CSCL 03B

A search of the 3-to 30-keV data from the NRL proportional counter detector on the Orbiting Geophysical Observatory-5 (OGO-5) satellite has yielded several events which may be nearly completely nonthermal in the E greater than 3 and less than 10 keV range. In each case an impulsive hard X-ray burst accompanied by an impulsive microwave burst was associated with a low energy X-ray burst whose profile was a simple rise and fall. The lack of a two component nature in the low energy range argues that the low energy X-ray flux is due to a single physical mechanism, in this case nonthermal bremsstrahlung from accelerated electrons. However, the spectra and time profiles are quite consistent with a thermal interpretation. Polarization measurements are probably necessary to resolve the physical origin of such bursts.
Author

N74-21458* Hale Observatories, Pasadena, Calif.

**OPTICAL, HARD X-RAY, AND MICROWAVE EMIS-
SION DURING THE IMPULSIVE PHASE OF FLARES**

J. A. Vorpahl 1973 7 p refs In NASA, Washington
High Energy Phenomena on the Sun p 221-227
(Contract NAS5-9094a Grants NGL-05-003-017;
NGL-05-002-034; NSF GA-31587)
CSCL 03B

A study was made of the variation in hard (E greater than or equal to 10 keV) X-radiation, H-alpha, and microwave emission during the impulsive phase of solar flares. Most important, the observations showed that there is an optical impulsive component in addition to the well-known hard X-ray and microwave spikes. Properties of these H-alpha kernels are given. Further analysis shows that the rise time in the 20- to 32-keV X-ray spike depends on the slope in the electron spectrum. A picture of the impulsive phase is given that is consistent with observations of the three above emissions.
Author

N74-21466* California Inst. of Tech., Pasadena.

**THE ISOTOPES OF H AND HE IN SOLAR COSMIC
RAYS**

T. L. Garrard, E. C. Stone, and R. E. Vogt 1973 14 p
refs In NASA, Washington High Energy Phenomena on
the Sun p 341-354
(NAS5-9312; NGR-05-002-160)
CSCL 03B

The isotopic composition of H and He in solar cosmic rays was studied with the solar galactic cosmic ray experiment on the Orbiting Geophysical Observatory, OGO-6. Averaging over 20 days of data seven flare events during 1969, the ratios He-3/He-4 = 0.10 + or - 0.02, D/H (76) .0003 and T/H (76) .0001 in the 4 to 5 MeV/nucleon energy range were obtained. In addition, large variations were found in the relative abundance of He-3 from event, with a maximum ratio of He-3/He-4 = 0.26 + or - 0.08 observed on October 14 and 15, 1969. The relative abundance of He-3 and D during this event does not seem to be consistent with existing calculations of the nuclear interaction origin of these isotopes.
Author

C. Literature Cited in Other Series

The following "N" series citations identified by accession numbers N...-70001 through N...-89999 for the years 1967 through the present year represent technical reports that were relatively old at the time of processing or those that contained preliminary or fragmentary information.

N69-72494* Jet Propulsion Lab., Calif. Inst. of Tech., Pasadena.
EOGO TRIAXIAL SEARCH COIL MAGNETOMETER FINAL ENGINEERING REPORT
N. Katz, G. Mohler, R. Reynolds, D. Sassa, and G. Takahashi
Pasadena, Calif. JPL 1 Jun. 1964 82 p Prepared by JPL
(Contracts NAS7-100; JPL-950257)
(NASA-CR-100619; ML/TN-2000.341)

N74-74623* TRW Systems Group, Redondo Beach, Calif.
ORBITING GEOPHYSICAL OBSERVATORIES, 1, 2, AND 3 Final Report
19 Dec. 1966 474 p
(Contract NAS5-899 NASA-CR-139254;
TRW-00063-6009-R0-00)
Avail: NTIS

N74-74624* Rice Univ., Houston, Tex.
RESPONSE TO ENVIRONMENT AND RADIATION OF AN IONIZATION CHAMBER AND MATCHED GEIGER TUBE USED ON SPACECRAFT
H. R. Anderson, L. G. Despain, and H. V. Neher 2 Jul. 1966 9 p refs Repr. from Nucl. Instrum. Methods (Netherlands), v. 47, 1967 p 1-9 Sponsored by NASA
(NASA-CR-139255) Avail: NTIS

N74-74625+ Aerospace Corp., El Segundo, Calif. Space Physics Lab.
INSTRUMENT REPORT FOR LYMAN-ALPHA EXPERIMENT (OGO-F-12)
M. A. Clark 31 Mar. 1969 23 p
Avail: NTIS

N74-74626* TRW Systems Group, Redondo Beach, Calif. Space Sciences Dept.
DISTRIBUTIONS OF HIGH FREQUENCY WAVES UPSTREAM FROM EARTH'S BOW SHOCK
R. W. Fredricks, F. L. Scarf, and I. M. Green 1 Jul. 1971 21 p refs
(NAS5-9278)
(NASA-CR-139256; TRW-05402-6029-R0-00) Avail: NTIS

N74-74627* National Aeronautics and Space Administration, Goddard Space Flight Center, Greenbelt, Md.
REPLY
J. P. Heppner 21 Feb. 1973 2 p refs Repr. from J. Geophys. Res., v. 78, no. 19, 1 Jul. 1973 p 4003-4004
(NASA-TM-X-70215) Avail: NTIS

N74-74628* National Aeronautics and Space Administration, Goddard Space Flight Center, Greenbelt, Md.
OGO-4 AURORAL PARTICLES EXPERIMENT AND CALIBRATION
R. A. Hoffman and D. S. Evans Dec. 1967 59 p refs
(NASA-TM-X-70216; X-611-67-632) Avail: NTIS

N74-74629 Catholic Univ. of America, Washington, D.C. Graduate School of Arts and Sciences.
CORONAL ELECTRON TEMPERATURE ASSOCIATED WITH SOLAR FLARES Ph.D. Thesis
D. M. HORAN 1970 133 p refs
(OGO-4-67-100A-06; OGO-4-67-73A-21) Avail: NTIS

N74-74630* National Aeronautics and Space Administration, Goddard Space Flight Center, Greenbelt, Md.
SHADES OF OGO-B (S-49A)
H. E. Montgomery and C. Herron Apr. 1965 18 p refs
(NASA-TM-X-70214; X-640-65-150) Avail: NTIS

N74-74631* Michigan Univ., Ann Arbor. Dept. of Astronomy.
INSTRUMENTATION FOR RADIO ASTRONOMY MEASUREMENTS ABOARD THE OGO-1 AND OGO-3 SPACECRAFT. PART 2: TECHNICAL Final Report
F. T. Haddock and R. G. Peltzer 31 Dec. 1969 186 p refs
(Contract NAS5-2051)
(NASA-CR-139257) Avail: NTIS

N74-74632* California Univ., Los Angeles.
COMMENTS ON A PAPER BY J. P. HEPPNER, POLAR CAP ELECTRIC FIELD DISTRIBUTIONS RELATED TO INTERPLANETARY MAGNETIC FIELD DIRECTION
C. T. Russell and G. Atkinson 21 Feb. 1973 2 p refs
Repr. from J. Geophys. Res., v. 78, no. 19, 1 Jul. 1973 p 4001-4002
(Grant NGR-05-007-004)
(NASA-CR-139259)

N74-74633* California Univ., Los Angeles. Inst. of Geophysics and Planetary Physics.
OGO-5 ORBITAL PLOTS GENERATED BY THE UCLA FLUXGATE MAGNETOMETER GROUP
C. T. Russell Sep. 1969 24 p refs
(Contract NAS5-9098)
(NASA-CR-139260; Publ-792) Avail: NTIS

N74-74634* National Aeronautics and Space Administration. Goddard Space Flight Center, Greenbelt, Md.
OGO-5 OBSERVATIONS OF DISCRETE WHISTLERS AND EMISSIONS DURING A LARGE MAGNETIC STORM
 F. L. Scarf, R. W. Fredricks, E. J. Smith, A. M. A. Frandsen, and G. P. Serbu Aug. 1971 48 p refs Prepared jointly with TRW Systems Group, Redondo Beach, Calif. and JPL.
 (Contract NAS5-9278)
 (NASA-TM-X-70213; TRW-05402-6031-RO-00) Avail: NTIS

N74-74635 Pittsburgh Univ., Pa. Space Magnetism.
A MODEL IONOSPHERE FOR MID-DAY AND MID-LATITUDE DURING SUNSPOT MINIMUM
 D. L. Shaeffer and Y. Inoue Jul. 1968 43 p refs (SMUP-4) Avail: NTIS

N74-74636* National Aeronautics and Space Administration. Goddard Space Flight Center, Greenbelt, Md.
THE REDUCTION AND ANALYSIS OF ELECTRON DATA FOR OUTER ZONE ELECTRON MODEL AE-4. VOLUME 3: OGO-1 AND 3 UNIVERSITY OF MINNESOTA EXPERIMENT DATA
 G. W. Singley Mar. 1971 52 p refs
 (NASA-TM-X-70212; NSSDC-71-08) Avail: NTIS

N74-74637* Battelle Memorial Inst., Richland, Wash.
OGO-4 STUDY Final Report, Jun. 1968 - Jul. 1970
 Jul. 1970 31 p refs
 (NASA Order Y-40670)
 (NASA-CR-139261) Avail: NTIS

N74-74638* Institute for Telecommunication Sciences and Aeronomy, Boulder, Colo.
A SATELLITE ION-ELECTRON COLLECTOR: EXPERIMENTAL EFFECTS OF GRID TRANSPARENCY, PHOTOEMISSION, AND SECONDARY EMISSION
 E. C. Whipple, Jr., J. W. Hirman, and R. ROSS 1970 40 p refs
 (NASA Order S-9919-G)
 (NASA-CR-139262) Avail: NTIS

N74-74639* Minnesota Univ., Minneapolis. School of Physics and Astronomy.
ELECTRON SPECTROMETER AND INTEGRATING ION CHAMBER FOR THE OGO-1 AND OGO-3 MISSIONS Final Report, 6 Feb. 1962 - 30 Jun. 1968
 J. R. Winckler Dec. 1969 23 p refs
 (Contract NAS5-2071)
 (NASA-CR-139263; CR-148) Avail: NTIS

N74-74659* Faraday Labs., Inc., La Jolla, Calif.
REMOVAL OF SURFACE CONTAMINATION BY PLASMA SPUTTERING
 D. McKeown and W. E. Corbin, Jr. 1971 18 p Presented at AIAA 6th Thermophys. Conf., Tullahoma, Tenn., 26-28 Apr. 1971
 (Contract NAS5-11163)
 (NASA-CR-139264) Avail: NTIS

N74-74660 Michigan Univ., Ann Arbor. Radio Astronomy Observatory.
INITIAL RESULTS FROM RADIO ASTRONOMY-EXPERIMENT NO. 18, OGO-3
 T. E. Graedel 1967 24 p
 (UM/RAO-67-9) Avail: NTIS

N74-74661 California Inst. of Tech., Pasadena. Space Radiation Lab.
OGO-C ORIENTATION STUDY
 P. E. Dimotakis 1972 61 p
 (Rept-9; OGO-2) Avail: NTIS

N74-74662* California Univ., Livermore. Lawrence Radiation Lab.
ENERGETIC ELECTRONS AND PROTONS OBSERVED ON OGO-5, MARCH 6-10, 1970
 H. I. West, Jr., J. R. Walton, R. M. Buck, and R. G. Darcy, Jr. 1970 6 p
 (NASA Order S-70014-G)
 (NASA-CR-139265) Avail: NTIS

N74-74663* California Univ., Livermore. Lawrence Livermore Lab.
ENERGETIC ELECTRON AND PROTON SOLAR PARTICLE OBSERVATIONS ON OGO-5, JANUARY 24-30, 1971
 H. I. West, Jr., R. M. Buck, J. R. Walton, and R. G. Darcy, Jr. 1971 7 p
 (NASA Order S-70014-G)
 (NASA-CR-139266) Avail: NTIS

N74-74765* Stanford Research Inst., Menlo Park, Calif.
INSTRUMENTS FOR THE STANFORD UNIVERSITY/STANFORD RESEARCH INSTITUTE VLF EXPERIMENT (4917) ON THE EOGO SATELLITE
 L. H. Rorden, L. E. Orsak, B. P. Ficklin, and R. H. Stehle May 1966 112 p
 (Contract NAS5-2131; S-142)
 (NASA-CR-139258) Avail: NTIS

N74-76907* Michigan Univ., Ann Arbor. Dept. of Astronomy.
DATA USER'S NOTES: OGO-3 EXPERIMENT NO. 18 LOW FREQUENCY RADIO ASTRONOMY, APPENDICES A AND B
 T. E. Graedel 1969 73 p Sponsored by NASA
 (NASA-CR-140526; UM/RAO-69-8-APP-A; UM/RAO-69-8; APP B) Avail: NTIS

N74-76909* Iowa Univ., Iowa City. Dept. of Physics and Astronomy.
OGO-2 EXPERIMENT 5010 AND OGO-4 EXPERIMENT 5010A Final Report
 R. H. Gabel, ed. and J. A. VanAllen Aug. 1972 67 p refs
 (Contract NAS5-3097)
 (NASA-CR-140527) Avail: NTIS

N74-76910* Bendix Field Engineering Corp., Columbia, Md.
PROGRAM DESCRIPTION OF THE DATA REDUCTION PROGRAM FOR EXPERIMENT 19 OF OGO-D
 W. K. Michael 1 Apr. 1970 60 p
 (Contract NAS5-11720)
 (NASA-TM-X-70372) Avail: NTIS

N74-76911* State Univ. of Iowa, Iowa City. Dept. of Physics and Astronomy.
INSTRUMENT REPORT FOR A TRAPPED RADIATION EXPERIMENT FOR EGO (S-49) (OGO-1)
 J. A. VanAllen and G. Crossett, Jr., ed. 29 Jan. 1963 36 p
 (Contract NAS5-2054)
 (NASA-CR-140528) Avail: NTIS

N74-76912

N74-76912* National Aeronautics and Space Administration. Goddard Space Flight Center, Greenbelt, Md.
OGO ATTITUDE COMPUTATIONS
W. D. Wiard Mar. 1966 80 p
(NASA-TM-X-63373; X-564-66-90) Avail: NTIS

N74-76913* National Aeronautics and Space Administration, Washington, D.C.
ORBITING GEOPHYSICAL OBSERVATORIES S-49, S-50
1 May 1962 54 p
(NASA-TM-X-50488) Avail: NTIS

N74-76914* Lockheed Missiles and Space Co., Palo Alto, Calif. Research Labs.
A LIGHT ION MASS SPECTROMETER EXPERIMENT FOR OGO-E Final Report
1971 242 p refs
(NAS5-9092)
(NASA-CR-122291; LMSC/D243393) Avail: NTIS

N74-76923* Rice Univ., Houston, Tex.
REDUCTION AND ANALYSIS OF DATA FROM OGO-C,D ION CHAMBER EXPERIMENT Final Report
H. R. Anderson Nov. 1969 30 p refs
(Contract NAS5-9317)
(NASA-CR-107184) Avail: NTIS

N74-76932* TRW Systems Group, Redondo Beach, Calif.
ORBITING GEOPHYSICAL OBSERVATORIES Final Report
1 Sep. 1969 415 p refs
(NAS5-3900; NAS5-899)
(NASA-CR-140524; TRW-02648-6088-RO-00) Avail: NTIS

N74-77109* TRW Systems Group, Redondo Beach, Calif.
DATA ANALYSIS PROGRAM FOR THE OGO E-24 PLASMA WAVE DETECTOR Progress Report
G. M. Crook, F. L. Scari, R. W. Fredricks, and I. M. Green 25 Mar. 1970 20 p refs
(Contract NAS5-9278)
(NASA-CR-140523; TRW-05402-6020-RO-00) Avail: NTIS

N74-77446* National Aeronautics and Space Administration. Goddard Space Flight Center, Greenbelt, Md.
A DOUBLE GAMMA-RAY SPECTROMETER TO SEARCH FOR POSITRONS IN SPACE
T. L. Cline, P. Serlemitsos, and E. W. Hones, Jr. Jun. 1962 6 p In Inst. of Radio Engr. IRE Trans. on Nucl. Sci., Vol. NS-9, No. 3 p 370-375

N74-77515 Tokyo Univ. (Japan).
MAGNETOSPHERIC SUBSTORM, 1972
1972 113 p Partly in JAPANESE and partly in ENGLISH
Avail: NTIS

N74-77537* Michigan Univ., Ann Arbor. Dept. of Aeronautical and Astronautical Engineering.
NEUTRAL AND ION MASS SPECTROMETER EXPERIMENT S5015
R. J. Leite, C. J. Mason, and R. D. Kistler 15 May 1964 78 p
(Contract NAS5-3098)
(NASA-CR-96663) Avail: NTIS

VI-110

NOV. 10, 1975

D. Literature Not Cited in the NASA System

There were a number of articles deemed suitable for the OGO Bibliography which were not in the NASA system. The "B" series citations presented here were provided by the NSSDC TRF. As opposed to the "A" and "N" numbers, the "B" number serves merely as an accession number for the TRF. In the interest of having the bibliography as up-to-date as possible, the major journals were searched up through the February 1, 1975 issues. Since a number of weeks are required to process documents into the NASA system, many of the journal articles listed here will have "A" numbers in the near future. However, there are certain documents which will never get a NASA number. These documents will be pointed out by the use of the word "No" at the end of the citation. The two main reasons for this are that NSSDC did not have a suitable copy or microfiche to provide to the NASA Facility for processing or that the Facility did not break down a document into its component parts written by separate authors and assign individual numbers to each part. In this latter case, the citation will always indicate the "A" or "N" numbered document in which the article can be found.

There are four articles listed in VI.B which have recently appeared as journal articles. The citations for these should now read:

- N73-21367: J. Geophys. Res. 80, 37-46, Jan. 1975
N74-16064: J. Atmos. Terr. Phys. 36, 1815-1823, Nov. 1974
N74-19023: J. Geophys. Res. 79, 4620-4631, Nov. 1974
N74-13566: Planet. Space Sci. 22, 1413-1425, Oct. 1974

B00570-000 Martin Co., Denver, Colo.
DYNAMIC ANALYSIS OF LONGITUDINAL OSCILLATIONS OF SM-68B STAGE 1 (POGO)
F. E. Bikle and J. B. Rohrs Mar. 1964 NO.

B00969-000 Iowa Univ., Iowa City.
REDUCING RADIO-FREQUENCY-INTERFERENCE FROM SPACECRAFTS IN THE FREQUENCY RANGE FROM 20Hz TO 200 KHz
D. A. Gurnett Jun. 1967 NO.

B01263-000 Stanford Univ., Calif.
SUMMARY OF DIGITAL DATA-PROCESSING SYSTEMS FOR THE OGO SU/SRI VERY-LOW-FREQUENCY EXPERIMENTS Summary Report
W. E. Blair and B. P. Eicklin Jul. 1967 NO.

B01265-000 Stanford Research Inst., Calif.
INSTRUMENTATION FOR THE STANFORD UNIVERSITY/STANFORD RESEARCH INSTITUTE VLF EXPERIMENT (B-17) ON THE OGO-3 SATELLITE Supplemental Report
B. P. Ficklin, R. H. Stehle, C. Barnes, and M. E. Mills May 1967 NO.

B01634-000 National Aeronautics and Space Administration, Goddard Space Flight Center, Greenbelt, Md.
EARTH SATELLITE EXPERIMENT FOR MEASURING THE CHARGE AND ENERGY SPECTRA OF THE PRIMARY COSMIC RAYS
G. H. Ludwig Nov. 1963 NO.
(Bf-611-63-253)

B03716-000 Chicago Univ., Ill.
DESCRIPTION OF OGO-1 AND OGO-3 COUNTING RATE PROCESSING AND RESULTING DATA. COSMIC RAY SPECTRA AND FLUXES EXPERIMENT ON OGO-1 AND OGO-3
W. Mixon and B. McKibben Feb. 1969 NO.

B03937-000 California Univ., Berkeley. Space Science Lab.
SOLAR COSMIC RAY EXPERIMENT FOR THE FIRST ORBITING GEOPHYSICAL OBSERVATORIES Consolidated Progress Report, Ser. 9, Issue 50, p 134-135
K. A. Anderson Oct. 1968 NO.

B03940-000 California Univ., Berkeley. Space Science Lab.
ENERGETIC RADIATION FROM SOLAR FLARES Consolidated Progress Report, Ser. 9, Issue 50, p 142
K. A. Anderson Oct. 1968 NO.

B03943-000 California Univ., Berkeley. Space Science Lab.
EXPERIMENT DATA ANALYSIS REPORT OGO-3: EXPERIMENT NO. 1
K. A. Anderson Dec. 1968 NO. Ser. 9, Issue 55

B03944-000 California Univ., Berkeley. Space Science Lab.
EXPERIMENT DATA ANALYSIS REPORT OGO-A: EXPERIMENT NO. 1
K. A. Anderson Jun. 1968 NO. Ser. 9, Issue 30

B04201-000
MICROMETEOROID EXPERIMENT ON THE OGO 4 SATELLITE
C. S. Nilsson, F. W. Wright, and D. Wilson Jul. 1969
Presented in SAO, p 907-132, Jul. 1969 NO.

B05000-000 Michigan Univ., Ann Arbor. High Altitude Engineering Lab.
EXPERIMENT DATA ANALYSIS REPORT FOR THE OGO-4 NEUTRAL AND ION MASS SPECTROMETER EXPERIMENT
R. J. Leite, B. B. Hinton, and C. J. Mason Oct. 1969 NO.
(Rept-05465-2-F)

B07587-000 National Oceanic and Atmospheric Administration, Boulder, Colo. World Data Center A.
ENERGETIC ELECTRONS AND PROTONS OBSERVED ON OGO-5, MARCH 6-10, 1970 Data on Solar-Geophysics Activity Association with the Major Geomagnetic Storm of

B08373-000

Mar. 8, 1970, UAG-12, Pt-1, p 124-129
H. I. West, Jr., J. R. Walton, R. M. Buck, and R. G. D'Arcy, Jr. Apr. 1971 (Preprint is N74-74662).
(UAG-12-Pt-1)

B08373-000 Tasmania Univ., Hobart (Australia).
MEASUREMENTS OF THE PRIMARY COSMIC RAY ELECTRON SPECTRUM BETWEEN 20 MeV AND 20 GeV AND ITS CHANGES WITH TIME
P. Meyer, P. J. Schmidt, and J. L'Heureux Aug. 1971
Presented in the Proceedings of the 12th Intern. Conf. on Cosmic Rays, v. 2, p 548-553 1971 Conf. held at Hobart Australia, Aug. 1971 (In A73-11375). NO.

B10763-000 Tasmania Univ., Hobart (Australia).
TRANSPORT OF SOLAR FLARE PROTONS: COMPARISON OF A NEW ANALYTIC MODEL WITH SPACECRAFT MEASUREMENTS
J. E. Lupton and E. C. Stone 1971 Presented in Cosmic Ray Conf. Papers, 2, p 492-497, Jul. 1971 Proceedings of the 12th Intern. Conf. on Cosmic Rays, Hobart Australia, 16-25 Aug. 1971 (In A73-11375). NO.

B11181-000
SOLAR COSMIC RAY OBSERVATIONS
A. J. Masley, J. W. McDonough, and P. R. Satterbloom
Oct. 1972 Presented in the Antarctic Journal of the U.S., 5, no. 5, Sep.- Oct. 1970 p 172 NO.

B12880-000 California Univ., Berkeley. Inst. of Geophysics and Planetary Physics.
PRODUCTION PROCESSING OF THE DATA OBTAINED BY THE UCLA OGO-5 FLUXGATE MAGNETOMETER
C. T. Russell Mar. 1971 NO.
(Rept-95)

B13262-000
RELATIVISTIC ELECTRONS IN SPACE
G. M. Simnett 1973 Presented in Space Research, 13, v. 2, 1973 p 745-762 Proceedings of the 15th COSPAR Plenary Meeting, Madrid, 10-24 May 1972

B14580-000
DYNAMICAL CHARACTERISTICS OF PULSATING SUBSTORM, PS6
T. Saito 1972 Presented in Magnetospheric Substorms, 4, no. 20-21, 1972, p 34-39 NO.

B14583-000
PLASMA WAVE-PARTICLE INTERACTION INSIDE THE NEUTRAL SHEET (IN JAPANESE)
T. Oya 1972 Presented in Magnetospheric Substorm, 4, no. 20-21, 1972, p 87-91 NO.

B14718-000 Michigan Univ., Ann Arbor. Radio Astronomy Obs.
UNIVERSITY OF MICHIGAN RADIO ASTRONOMY EXPERIMENT ABOARD THE OGO-5 SPACECRAFT
F. I. Haddock Apr. 1970 NO.
(UM/RAO-70-3)

B14744-000 Tasmania Univ., Hobart (Australia).
ENERGY SPECTRUM OF COSMIC-RAY ELECTRONS FROM 0.5 TO 10 GeV
B. N. Swanenburg, J. J. Burger, and P. A. J. DeKorte Aug. 1971 Presented at the 12th Intern. Conf. on Cosmic Rays, Hobart Australia, 16-25 Aug. 1971 (In A73-11375). NO.
Presented in Conf. Papers, 5, of the 12th Intern. Conf. on Cosmic Rays, 1971, p 1714-1719
(A73-11375)

B14745-000 Cosmic Ray Working Group.
OBSERVATION OF COSMIC-RAY ELECTRONS WITH THE OGO-5 SATELLITE
B. N. Swanburgh 1971 NO.

B15152-000
ENERGETIC ELECTRON AND PROTON SOLAR PARTICLE OBSERVATIONS ON OGO-5, 24-34 JANUARY 1971
H. I. West, Jr., R. M. Buck, J. R. Walton, and R. G. Darcy, Jr. Dec. 1972 Phys., UAG-24, Pt. 1, 113-119, Boulder, Colo., Dec. 1972 In World Data Center A for Solar-Terrest. Preprint N74-74663
(B15152-000)

B15846-000
CORRELATION OF SATELLITE ESTIMATES OF THE EQUATORIAL ELECTROJET INTENSITY WITH GROUND OBSERVATIONS AT ADDIS ABABA
P. Guoin Jun. 1973 J. Atmos. and Terr. Phys., 35, p 1257-1264

B15849-000
SUMMARY AND FUTURE WORK (OGO-4 AND OGO-6)
J. C. Cain, I. A. Onwumechilli, P. N. Mayaud, and E. Oni 1973 Presented in Journal of Atmospheric and Terrestrial Physics, 35, Jun. 1973, p 1231-1247

B15918-000
FOUR YEARS OF DUST PARTICLE MEASUREMENTS IN CISLUNAR AND SELENOCENTRIC SPACE FROM LUNAR EXPLORER 35 AND OGO 3
W. M. Alexander, J. C. Smith, C. W. Arthur, and J. L. Bohn 1973 Proceedings of the 15th COSPAR Plenary Meeting, Madrid, 10-24 May 1972 Presented in Space Res., 13, v. 2, 1973, p 1037-1046

B16248-000
GLOBAL EMPIRICAL MODEL OF THERMOSPHERIC COMPOSITION BASED ON OGO-6 MASS SPECTROMETER MEASUREMENTS
A. E. Hedin, H. G. Mayr, C. A. Reber, N. W. Spencer, and G. R. Carignan 1973 Proceedings of the 15th COSPAR Plenary Meeting, Madrid, 10-24 May 1972 Presented in Space Res., 13, v. 1, 1973, p 315-320

B16756-000
ELECTRON PRECIPITATION PATTERNS AND SUBSTORM MORPHOLOGY
R. A. Hoffman Jun. 1973 J. Geophys. Res. 78, 2867-2884, June 1973 In A73-33434

VI-112

NOV. 10, 1975

B17665-000
RELATIVISTIC ELECTRON EVENTS IN INTERPLANETARY SPACE

G. M. Simnett Jul. 1974 Space Sci. Rev. 16, 257-323, July 1974 In A74-37632

B17973-000 Dartmouth Coll., Hanover, N.H. Radiophysics Lab.
RESULTS FROM AN EXPERIMENT ON OGO-6 TO STUDY ELECTRIC AND ELECTROMAGNETIC FIELDS IN THE RANGE 20 Hz - 540 KHz

I. Laaspere Sep. 1972 NO.

B18269-000
OGO-5 OBSERVATIONS OF THE PHYSICAL PROCESSES OCCURRING IN THE DISTURBED POLAR CUSP AND THE CUSP-MAGNETOSHEATH INTERFACE

C. T. Russell, M. G. Kivelson, R. W. Fredricks, F. L. Scarf, M. Neugebauer, M. J. Rycroft, ed., and R. D. Reasenber, ed. 1974 Proceedings of the 16th COSPAR Plenary Meeting, Konstanz, West Germany, 23 May - 5 Jun. 1973 Presented in Space Res., 14, 1974, p 335-342

B18277-000
OGO-5 SPARK-CHAMBER TELESCOPE FOR GAMMA-RAY ASTRONOMY

A. J. Dean, G. W. Hutchinson, D. Ramsden, B. G. Taylor, and R. D. Wills 1968 NO. Presented in Nuclear Instr. and Methods, 65, 1968 p 293-300

B18378-000
ASYMMETRY OF THE RING CURRENT

O. A. Troshichev and Ya. I. Feldshtein Jun. 1971 NO. Presented in Kosmich. Issled., 9, no. 3, May-Jun. 1971 p 408-412

B18548-000 Stanford Univ., Calif. Radio Science Lab.
MEASUREMENT OF IONOSPHERIC AND EXOSPHERIC ELECTRON CONTENT USING RADIO BEACONS ON ORBITING GEOPHYSICAL OBSERVATORIES: COMPILATION OF DATA AND FINAL REPORT

R. B. Fritz and J. K. Hargreaves Dec. 1973 NO. Prepared in part by NOAA, Boulder, Colo.

B19906-000 National Aeronautics and Space Administration. Goddard Space Flight Center, Greenbelt, Md.
NEAR VIEW OF THE RING CURRENT

M. Sugiura 1972 Presented at Symp. held at NASA, Goddard Space Flight Center, Greenbelt, Md., 10 Nov. 1971 Presented in Significant Accomplishments in Sci., 1971, NASA-SP-312, 1972 p 62-66 (NASA-SP-312)

B19920-000
NEUTRAL WIND VELOCITIES CALCULATED FROM TEMPERATURE MEASUREMENTS DURING A MAGNETIC STORM AND THE OBSERVED IONOSPHERIC EFFECTS

O. P. Saxena, K. K. Mahajan, M. J. Rycroft, ed., and R. D. Reasenber, ed. 1974 Proceedings of the 16th COSPAR Plenary Meeting, Konstanz, West Germany, 23 May - 5 Jun.

1973 Presented in Space Res., 14, 1974 p 241-246

B20296-000 Faraday Labs., Inc., La Jolla, Calif.
GAS-SURFACE INTERACTION STUDIES Final Report for OGO-6 Gas-Surface Energy Transfer Experiment, 1-25 Dec. 1973

D. McKeown, J. M. Bowyer, Jr., and R. S. Dummer Dec. 1973 (In N74-25869). NO.

B20297-000 Faraday Labs., Inc., La Jolla, Calif.
BOMBARDMENT OF OGO-6 SURFACES BY HIGH-ENERGY PARTICLES Final Report for OGO-6 Gas-Surface Energy Transfer Experiment, 26-31 Dec. 1973

J. M. Bowyer, Jr. and D. McKeown Dec. 1973 (In N74-25869). NO.

B20340-000 Texas Univ., Dallas.
IN SITU MEASUREMENTS OF AMPLITUDE AND SCALE SIZE CHARACTERISTICS OF IONOSPHERIC IRREGULARITIES: OGO-6 ION CONCENTRATION IRREGULARITY STUDIES Final Report

P. L. Dyson, J. P. McClure, and W. B. Hanson Sep. 1973 (In N73-32286). NO. (Contract NAS5-23184) (NASA-CR-132814)

B20951-000
PLASMA TAIL INTERPRETATIONS OF PRONOUNCED DETACHED PLASMA REGIONS MEASURED WITH OGO-5

A. J. Chen and J. M. Grebowsky Sep. 1974 Presented in Journal of Geophysical Res., 79, Sep. 1974 p 3851-3856

B20953-000 General Dynamics Corp., San Diego, Calif.
INSTRUMENT REPORT FOR DESIGN OF THE GAS-SURFACE ENERGY TRANSFER EXPERIMENTS FOR OGO-F

D. McKeown, J. N. Miller, Jr., and M. G. Fox Aug. 1969 NO. (GDC-DBE-69-005)

B20954-000 Faraday Labs., Inc., La Jolla, Calif.
INITIAL RESULTS FROM OGO-6 GAS-SURFACE EXPERIMENT

D. McKeown and W. E. Corbin, Jr. Oct. 1969 (FAR-15-69)

B21207-000 Marshall Labs., Torrance, Calif.
POGO TRIAXIAL SEARCH COIL MAGNETOMETER Final Engineering Report

N. Katz, G. Mohler, R. Reynolds, D. Sassa, and G. Takshashi Sep. 1964 NO. (ML/TN-2000.372)

B22062-000
NON-RELATIVISTIC SOLAR ELECTRONS

R. P. Lin Jul. 1974 Space Sci. Rev. 16, 189-256, July 1974 (In A74-37631).

B22333-000
HIGH LATITUDE PROTON PRECIPITATION AND LIGHT ION DENSITY PROFILES DURING THE

B22334-000

MAGNETIC STORM INITIAL PHASE

J. L. Burch Oct. 1973 J. Geophys. Res. 78, 6569-6578, Oct. 1973 In A73-45114

B22334-000

THE EQUATORIAL HELIUM ION TROUGH AND THE GEOMAGNETIC ANOMALY

S. Chandra Feb. 1975 J. Atmospheric and Terrest. Phys., 359-367, Feb. 1975

B22600-000 Lockheed Missiles and Space Co., Palo Alto, Calif. Research Lab.

A MULTI-SATELLITE STUDY OF THE NATURE OF WAVELIKE STRUCTURES IN THE MAGNETOSPHERE PLASMA Final Report

E. G. Shelley Aug. 1974
(Contract NASw-2551)

B22601-000

DIURNAL VARIATION OF THE NEUTRAL THERMOSPHERIC WINDS DETERMINED FROM INCOHERENT SCATTER RADAR DATA

R. G. Roble, B. A. Emery, J. E. Salah, and P. B. Hays Jul. 1974 J. Geophys. Res. 79, 2868-2876, July 1974 (In A74-36375).

B22603-000

INTENSITY VARIATION OF ELF HISS AND CHORUS DURING ISOLATED SUBSTORMS

R. M. Thorne, E. J. Smith, K. J. Fiske, and S. R. Church Sep. 1974 Geophys. Res. Letters 1, 193-196, Sep. 1974 (In A74-44202).

B22604-000

MAGNETOPOUSE ROTATIONAL FORMS

B. U. O. Sonnerup and B. G. Ledley Oct. 1974 J. Geophys. Res. 79, 4309-4314, Oct. 1974 (In A75-11221).

B22605-000

IS THE RED ARC A GOOD INDICATOR OF IONOSPHERE-MAGNETOSPHERE CONDITIONS

A. F. Nagy, L. H. Brace, N. C. Maynard, and W. B. Hanson Oct. 1974 J. Geophys. Res. 79, 4331-4333, Oct. 1974 (In A75-11226).

B22606-000

AN UPPER LIMIT TO THE PRODUCT OF NO AND O DENSITIES FROM 105 TO 120 Km

T. M. Donahue Oct. 1974 J. Geophys. Res. 79, 4337-4339, Oct. 1974 (In A75-11227).

B22607-000

ACCELERATION OF ELECTRONS IN THE ABSENCE OF DETECTABLE OPTICAL FLARES DEDUCED FROM TYPE 3 RADIO BURSTS, H-ALPHA ACTIVITY AND SOFT X-RAY EMISSION

S. R. Kane, R. W. Kreplin, M. J. Martres, M. Pick, and I. Soru-Escout Oct. 1974 Solar Phys. 38, 483-497, Oct. 1974 (In A75-16217).

B22608-000

A SEARCH FOR SOLAR NEUTRONS DURING SOLAR FLARES

S. O. Ifedili Nov. 1974 Solar Phys. 39, 233-241, Nov. 1974

B22609-000

THE SOLAR CYCLE VARIATION OF THE SOLAR WIND HELIUM ABUNDANCE

K. W. Ogilvie and J. Hirshberg Nov. 1974 J. Geophys. Res. 79, 4595-4602, Nov. 1974 (In A75-16631).

B22610-000

THE MEASUREMENT OF COLD ION DENSITIES IN THE PLASMA TROUGH

K. K. Harris Nov. 1974 J. Geophys. Res. 79, 4654-4660, Nov. 1974 (In A75-16637).

B22611-000

SUBSTORM AND INTERPLANETARY MAGNETIC FIELD EFFECTS ON THE GEOMAGNETIC TAIL LOBES

M. V. Caan, R. L. McPherron, and C. T. Russell Jan. 1975 J. Geophys. Res. 80, 191-194, Jan. 1975

B22612-000

STRUCTURE OF THE QUASI-PERPENDICULAR LAMINAR BOW SHOCK

E. W. Greenstadt, C. T. Russell, F. T. Scarf, V. Formisano, and M. Neugebauer Feb. 1975 J. Geophys. Res. 80, 502-514, Feb. 1975

B22613-000

ELECTROMAGNETIC HISS AND RELATIVISTIC ELECTRON LOSSES IN THE INNER ZONE

B. T. Tsurutani, E. J. Smith, and R. M. Thorne Feb. 1975 J. Geophys. Res. 80, 600-607, Feb. 1975

B22614-000

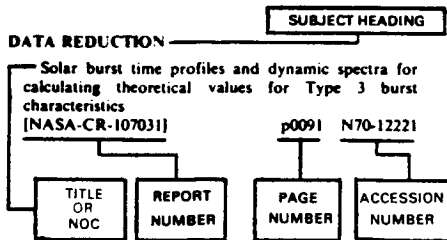
OBSERVED VARIATIONS OF THE EXOSPHERIC HYDROGEN DENSITY WITH EXOSPHERIC TEMPERATURE

J. L. Bertaux Feb. 1975 J. Geophys. Res. 80, 639-642, Feb. 1975

VII. INDEXES TO LITERATURE CITATIONS AND ABSTRACTS

A. SUBJECT INDEX

Typical Subject Index Listing



This index is arranged alphabetically by subject term. A brief description of the document, e.g., title plus title extension, or Notation of Content, (NOC) is included in each subject entry to indicate the type of document cited. The page number identifies the page in the abstract section (VI) on which the citation appears.

A

ABUNDANCE

Cosmic ray nuclei energy spectra and abundances above 20 Mev/nucleon determined by OGO-1 satellite experiment, considering He, B, C, N, O, Ne, Mg, Si, Mn, Fe, Co and Ni

p0019 A69-20067

The abundances of solar accelerated nuclei from carbon to iron.

p0065 A73-13719

The elemental abundance ratios of interstellar secondary and primary cosmic rays.

p0079 A74-30190

The solar cycle variation of the solar wind helium abundance [B22609-000]

p0114

ACOUSTIC SIMULATION

Orbiting Geophysical Observatory vibration magnitude and spectra due to launch acoustic environment determined from simulation tests

p0002 A65-19503

AERONOMY

Description of satellite instrumentation for atmospheric composition measurements

p0001 A63-12209

AEROSPACE SYSTEMS

Discussion of a management program for evaluation of aerospace systems design - Orbiting Geophysical Observatory (OGO) is used as an example

p0001⁷ A63-13537

AIRGLOW

Airglow lines measured through photometers on OGO-2 satellite, noting nadir and zenith airglow

p0007 A67-23278

UV OGO observations of atomic hydrogen and oxygen in airglow, comparing results to exospheric models of hydrogen geocorona

p0022 A69-31400

OGO 4 UV airglow spectrometer consisting of Ebert-Fastie monochromator and photomultipliers with cesium telluride and cesium iodide channels

p0025 A69-36682

Satellite multispectral photometry data in airglow bands correlated with cloud characteristics and surface albedo variations

p0028 A70-15522

In-flight radiometric calibration of low brightness OGO 4 airglow photometer

p0029 A70-15645

OGO-4 observations of hydrogen Lyman-alpha airglow surrounding earth, measuring dependence on solar zenith angle

p0035 A70-35764

Lyman alpha and atomic oxygen 1304 A airglow depressions over poles from OGO 4 satellite observations

p0041 A71-11503

Far UV equatorial airglow and aurora intensities and occurrence frequencies from satellite observation

p0041 A71-11504

O I 1304-A airglow, observing conjugate excitation with OGO 4 spacecraft

p0043 A71-17279

Bidirectional reflectance at several wavelengths from moonlit earth observations by airglow photometer on OGO-4 satellite

p0055 A72-13428

Theoretical calculations of the F-region tropical ultraviolet airglow intensity.

p0062 A72-42418

Asymmetrical global O I airglow emission pattern with respect to magnetic equator from OGO 4 observations, noting poor correlation with ionospheric electron density

p0073 A73-38939

Distribution of atomic oxygen in the upper atmosphere deduced from OGO-6 airglow observations.

p0075 A73-45121

Global temperature distributions from OGO-6 6300 A airglow measurements.

p0077 A74-23679

Data reduction methods for OGO airglow photometer measurements [NASA-TM-X-55794]

p0085 N67-27576

Laboratory tests on interference sensitivity of polar OGO airglow photometer

p0085 N67-27578

OGO-D photometric airglow measurements

p0095 N71-25268

Functional characteristics of OGO-4 main body airglow photometer utilizing cathode photomultiplier to sense light at selected wavelengths

p0098 N72-27423

Airglow maps for atomic oxygen 6300 A line from OGO-D satellite

p0098 N72-28353

ALPHA PARTICLES

Alpha particle proton ratio of geomagnetic field from data from charged-particle telescope on OGO 1 satellite

p0009 A67-37412

Proton and He nuclei differential energy spectra and intensity variations in interplanetary space in 1-20 MeV per nucleon energy range

p0015 A68-41420

Geomagnetically trapped protons and alpha particles, analyzing OGO 4 data

p0027 A69-43184

Quiet time fluxes and differential energy spectra of protons and alpha particles at 2-20 MeV measured by cosmic ray detectors on OGO-3

p0044 A71-18127

Simultaneous satellite and riometer studies. -- for solar cosmic ray events

p0079 A74-30263

AMPLITUDES

In situ measurements of amplitude and scale size characteristics of ionospheric irregularities: OGO-6 ion concentration irregularity studies [B20340-000]

p0113

ANGULAR DISTRIBUTION

Electron pitch angle distributions throughout the magnetosphere as observed on OGO-5.

p0068 A73-24732

ANNUAL VARIATIONS

Hydrogen and He ion distribution measurements, noting seasonal and local magnetic time variability

p0022 A69-31326

Solar geomagnetic seasonal ionization control of upper ionosphere longitudinal composition variations from polar satellite observations

p0047 A71-24555

Seasonal and annual longitudinal variations in ionospheric ion distribution, stressing solar geomagnetic control importance

p0050 A71-33762

Seasonal density variations in thermosphere and exosphere, obtaining model from Explorers 19 and 39 drag measurements for comparison with OGO-6 mass spectroscopy

p0051 A71-33802

Theoretical model for the latitude dependence of the thermospheric annual and semiannual variations.

p0066 A73-15538

Seasonal, altitude, and universal time differences in field-aligned electrons [NASA-TM-X-66099]

p0100 N73-11345

Variations in thermospheric composition: A model based on mass-spectrometer and satellite-drag data [NASA-CR-136192]

p0104 N74-12459

ANTARCTIC REGIONS

Thermospheric composition variations in south polar regions during magnetically quiet periods from OGO-6 observations, considering atmospheric heating by electron precipitation cyclic variations

p0060 A72-32964

ISIS-1 satellite observations of the ionosphere at high southern latitudes.

p0068 A73-25753

ANTENNA COUPLERS

OGO 5 spacecraft detector instrumentation for measuring electrostatic and electromagnetic waves electric fields with coupled antennas, describing in-flight operation

p0025 A69-36683

APPLICATIONS OF MATHEMATICS

World magnetic survey (WMS) method for minimizing limitations of mathematical and graphical descriptions of earth's magnetic field

p0082 N64-27355

ARGON

Thermospheric wind effects on the distribution of helium and argon in the earth's upper atmosphere.

p0071 A73-33441

ARTIFICIAL CLOUDS

Active experiments, magnetospheric modification, and a naturally occurring analogue.

p0075 A74-14283

ASTRONOMICAL MAPS

OGO radio astronomy instrument for cosmic noise sky brightness distribution mapping by electrically short antenna ionospheric focusing

p0048 A71-26144

ASTRONOMICAL MODELS

Solar flare model, computing thermal X ray emission

p0046 A71-20945

The prevalence of second harmonic radiation in type 3 bursts observed at kilometric wavelengths.

p0071 A73-32964

Solar wind density model from km-wave type 3 bursts.

p0071 A73-32965

Observations of the internal structure of the magnetopause.

p0077 A74-21679

A new model for the high-frequency decametric radiation from Jupiter

p0081 A74-43688

ASTRONOMICAL OBSERVATORIES

Data user's notes: OGO-3 experiment no. 18 low frequency radio astronomy, appendices A and B [NASA-CR-140526]

p0109 N74-76907

ASTRONOMICAL PHOTOMETRY

ASTRONOMICAL PHOTOMETRY

Neutral hydrogen interstellar wind parameters from Lyman alpha sky background measurements outside geocorona by photometers on OGO 5

p0051 A71-33834

OGO-D photometric airglow measurements

p0095 N71-25268

ASTRONOMICAL TELESCOPES

OGO-5 spark-chamber telescope for gamma-ray astronomy [B18277-000]

p0113

ASYMMETRY

Solar protons delayed access into polar regions during 2 November 1967 solar particle event, discussing north-south asymmetry

p0027 A69-43183

Asymmetry of the ring current [B18378-000]

p0113

ATMOSPHERIC ATTENUATION

Latitudinal cut-off of manmade VLF signals in short path through ionosphere to OGO 2 satellite, noting strong noise following signal cut-off

p0021 A69-28958

ATMOSPHERIC CIRCULATION

Theoretical model for the latitude dependence of the thermospheric annual and semiannual variations.

p0066 A73-15538

Energy and diffusive mass transport relation to thermospheric circulation, composition, temperature and mass density from three dimensional two constituent magnetic storm model

p0070 A73-29975

Mechanism and rates of atmospheric mixing in lower thermosphere including heat input [NASA-CR-135789]

p0103 N73-33321

ATMOSPHERIC COMPOSITION

Description of satellite instrumentation for atmospheric composition measurements

p0001 A63-12209

Earth satellite sweeping mass spectrometer for measuring atmospheric neutral particle and positive ion concentration

p0025 A69-36681

Horizontal He distribution in upper atmosphere from OGO 6 mass spectrometric data normalization for altitude by Jacchia model atmosphere

p0046 A71-21647

Solar geomagnetic seasonal ionization control of upper ionosphere longitudinal composition variations from polar satellite observations

p0047 A71-24555

Neutral atmospheric composition and density variations during geomagnetic disturbances from OGO-6 satellite quadrupole mass analyzer measurements

p0052 A71-39711

Neutral H concentration in upper atmosphere during solar minimum, using ion thermal energies from rocket and satellite mass spectrometric, radio and proton whistler measurements

p0054 A72-10361

Magnetic storm effects on neutral atmospheric composition above 400 km, discussing energy deposition

p0055 A72-13518

Magnetic storm effects in atmospheric neutral composition, noting thermospheric wind circulation role due to Joule heating within auroral zone

p0058 A72-24957

Thermospheric composition variations in south polar regions during magnetically quiet periods from OGO-6 observations, considering atmospheric heating by electron precipitation cyclic variations

p0060 A72-32964

Distribution of hydrogen and helium in the upper atmosphere.

p0064 A72-45593

Equatorial ionospheric anomaly related neutral thermospheric composition variation observation from OGO-6 mass spectroscopic data, noting static diffusion model limitations

p0070 A73-31767

Global characteristics in the diurnal variations of the thermospheric temperature and composition.

p0077 A74-21693

Comparison of atomic oxygen measurements by incoherent scatter and satellite-borne mass spectrometer techniques.

p0078 A74-27713

The air composition in the thermosphere.

p0078 A74-29960

Spatial and temporal behavior of atomic oxygen determined by OGO 6 airglow observations.

p0079 A74-30670

Heating of the high-latitude thermosphere during magnetically quiet periods.

p0080 A74-34027

Procedures for processing atmospheric composition data obtained through use of sweeping quadrupole mass spectrometer on OGO-4 satellite [NASA-CR-117525]

p0094 N71-21544

OGO-6 neutral atmospheric composition experiment [NASA-CR-135798]

p0103 N73-33320

Neutral and ion mass spectrometer experiment S5015 [NASA-CR-96663]

p0110 N74-77537

ATMOSPHERIC DENSITY

Probe for measuring energy transfer between satellite and upper atmosphere

p0004 A66-15922

Seasonal density variations in thermosphere and exosphere, obtaining model from Explorers 19 and 39 drag measurements for comparison with OGO-6 mass spectroscopy

p0051 A71-33802

Neutral atmospheric composition and density variations during geomagnetic disturbances from OGO-6 satellite quadrupole mass analyzer measurements

p0052 A71-39711

Atmospheric neutral density measurement near 400 km during daytime by microphone density gage on OGO 6

p0058 A72-26407

Magnetic control of near equatorial neutral thermosphere, calculating F region ionization anomaly and molecular nitrogen and atomic oxygen density latitudinal variations

p0069 A73-26997

The relation between low-latitude neutral density variations near 400 km and magnetic activity indices.

p0075 A74-14219

Observed variations of the exospheric hydrogen density with exospheric temperature [B22614-000]

p0114

Fabrication, installation, and operation of microphone density gage experiment onboard OGO-F [NASA-CR-130082]

p0088 N72-28467

Neutral density data from OGO-F and geomagnetic storms [NASA-CR-122479]

p0099 N72-32390

ATMOSPHERIC DIFFUSION

Energy and diffusive mass transport relation to thermospheric circulation, composition, temperature and mass density from three dimensional two constituent magnetic storm model

p0070 A73-29975

ATMOSPHERIC ELECTRICITY

Ionospheric electric fields variations in ELF-VLF, confirming OV-1 satellite measurements with OGO 6 data

p0033 A70-30082

Magnetospheric VLF electric field emissions above electron cyclotron frequency from OGO 5 observation at magnetic equator

p0041 A71-11500

Ionospheric electric and electromagnetic waves broadband characteristics, investigating auroral hiss and LHR noise

p0051 A71-33951

The global distribution of natural and man-made ionospheric electric fields at 200 kHz and 540 kHz as observed by OGO-6.

p0080 A74-34020

Thermospheric composition variations in south polar regions during magnetically quiet periods from OGO-6 observations, considering atmospheric heating by electron precipitation cyclic variations

p0060 A72-32964

Auroral heating and the composition of the neutral atmosphere.

p0069 A73-27602

Heating of the high-latitude thermosphere during magnetically quiet periods.

p0080 A74-34027

Mechanism and rates of atmospheric mixing in lower thermosphere including heat input [NASA-CR-135789]

p0103 N73-33321

SUBJECT INDEX

ATMOSPHERIC IONIZATION

Magnetospheric ionization distribution determined by ducted and nonducted whistler propagation modes and reflection as observed by OGO 1

p0010 A68-17728

High latitude ionization spikes observed by POGO spacecraft, noting frequency correlation with magnetic disturbances and development by high energy electron injections

p0021 A69-28950

Hysteresis effect on cosmic ray modulation and gradient ionization near solar minimum from measurements made near earth with OGO 1 and 3 ion chambers

p0028 A70-15106

Quiet time cosmic ray ionization altitude dependence over polar regions from measurements by integrating ionization chamber on OGO-2

p0034 A70-31902

Magnetic control of near equatorial neutral thermosphere, calculating F region ionization anomaly and molecular nitrogen and atomic oxygen density latitudinal variations

p0069 A73-26997

Absolute cosmic ray ionization measurements in upper and lower atmosphere [NASA-CR-104068]

p0090 N69-34536

Aurora formation by electron injection and drift in upper atmosphere

p0095 N71-25272

Magnetosphere temperature distribution model noting heat fluxes due to low electron density, large mean free path, turbulent heat transfer, etc.

p0015 A68 38423

Hydrogen Lyman alpha nightglow models, discussing solar photon scattering in geocorona and hydrogen vertical distribution

p0022 A69-30191

Solar cosmic rays entry into magnetosphere, showing entrance on smoothway connected field lines

p0032 A70-30059

Inner magnetosphere magnetic field mapping, deriving pogo model

p0038 A70-39349

Thermal plasma model along magnetic field lines outside plasmasphere with sharp density gradient in equatorial plane, using OGO-4 ion composition measurements

p0038 A70-41057

Solar flare particles entrance into geomagnetic tail, modifying diffusion model

p0040 A71-11494

Horizontal He distribution in upper atmosphere from OGO 6 mass spectrometric data normalization for altitude by Jacchia model atmosphere

p0046 A71-21647

Geomagnetic field models validity from satellite data

p0049 A71-29903

Seasonal density variations in thermosphere and exosphere, obtaining model from Explorers 19 and 39 drag measurements for comparison with OGO-6 mass spectroscopy

p0051 A71-33802

OGO 4 satellite observed band limited ELF hiss characteristics explanation by model based on generation at large wave normal angle in equatorial region

p0057 A72-23008

Plasmapause nightside, dayside and bulge positive ion concentration measurements with OGO 5 mass spectrometer compared with magnetospheric convection model

p0061 A72-39544

Thermospheric atomic oxygen and molecular nitrogen densities from OGO 6 neutral atmospheric composition experiment, comparing with prediction by Jacchia models

p0062 A72-42431

Solar wind interaction with geomagnetic field, discussing magnetosphere polar cusp region and geomagnetic tail neutral sheet structure

p0065 A73-13871

Solar proton intensity structures in the magnetosphere during interplanetary anisotropies.

p0066 A73-14962

Theoretical model for the latitude dependence of the thermospheric annual and semiannual variations.

p0066 A73-15538

SUBJECT INDEX

Equatorial ionospheric anomaly related neutral thermospheric composition variation observation from OGO-6 mass spectroscopic data, noting static diffusion model limitations

p0070 A73-31767

POGO satellite observation of electrojet profiles compared with H variation around measurements, interpreting data by classical band current model

p0070 A73-31773

Satellite studies of magnetospheric substorms on August 15, 1968. 9: Phenomenological model for substorms.

p0072 A73-33457

A magnetospheric field model incorporating the OGO-3 and 5 magnetic field observations.

p0074 A73-43693

The magnetotail and substorms. --- magnetic flux transport model

p0076 A74-17742

Empirical model of global thermospheric temperature and composition based on data from the OGO-6 quadrupole mass spectrometer.

p0076 A74-18376

Global temperature distributions from OGO-6 6300 A airglow measurements.

p0077 A74-23679

OGO-D atmospheric composition data for polar thermospheric storm model [NASA-CR-103080]

p0094 N71-20638

Atmospheric model for thermal plasma near equatorial plasmopause

p0095 N71-25270

A model ionosphere for mid-day and mid-latitude during sunspot minimum [SMUP-4]

p0109 N74-74635

ATMOSPHERIC PHYSICS
Measurements of the atmospheric neutron leakage rate

p0076 A74-15356

The air composition in the thermosphere.

p0078 A74-29960

ATMOSPHERIC RADIATION
Atmospheric VLF electromagnetic emissions and electron instabilities data from satellite observation, detailing source regions, large amplitude electrostatic waves and wave-particle correlation.

p0049 A71-30952

Asymmetrical global O I airglow emission pattern with respect to magnetic equator from OGO 4 observations, noting poor correlation with ionospheric electron density

p0073 A73-38939

Satellite ultraviolet measurements of nitric oxide fluorescence with a diffusive transport model.

p0074 A73-41925

Plasmaspheric hiss intensity variations during magnetic storms.

p0080 A74-34038

ATMOSPHERIC SCATTERING
Disposition of scattering layers over polar-regions as observed by OGO-6 airglow photometer [NASA-CR-130271]

p0101 N73-16436

ATMOSPHERIC TEMPERATURE
Magnetosphere temperature distribution model noting heat fluxes due to low electron density, large mean free path, turbulent heat transfer, etc.

p0015 A68-38423

Exospheric neutral hydrogen temperature diurnal variation from satellite resonance filter data, suggesting Lyman alpha source external to geocorona

p0040 A70-43852

Empirical model of global thermospheric temperature and composition based on data from the OGO-6 quadrupole mass spectrometer.

p0076 A74-18376

Global characteristics in the diurnal variations of the thermospheric temperature and composition.

p0077 A74-21693

Observed variations of the exospheric hydrogen density with exospheric temperature [B22614-000]

p0114

ATMOSPHERICS
Magnetospheric ELF noise, discussing OGO 3 spectrum analysis

p0019 A69-18834

Magnetic equator ELF noise examined with OGO 3 magnetometer, indicating unique signals in plasmasphere

p0030 A70-21380

Broadband and highpass LF noise in distant magnetosphere detected by VLF/LF experiment on OGO 1 satellite

p0031 A70-27183

Magnetosphere Alfvén velocity profile relation to ELF chorus and hiss, indicating unstable wave generation by cyclotron resonance

p0039 A70-43851

Postmidnight chorus: A substorm phenomenon. --- outer magnetosphere

p0076 A74-18364

The feasibility of a sub-LF satellite-to-submarine communication downlink VLF noise levels in the ionosphere [AD-769139]

p0104 N74-15857

ATOM CONCENTRATION
Comparison of atomic oxygen measurements by incoherent scatter and satellite-borne mass spectrometer techniques.

p0078 A74-27713

ATOMIC EXCITATIONS
O I 1304-A airglow, observing conjugate excitation with OGO 4 spacecraft

p0043 A71-17279

ATOMIC RECOMBINATION
Radiative recombination of atomic oxygen ions in nighttime F region UV radiation detected by polar-orbiting OGO 4 satellite

p0023 A69-34957

Oxygen atom recombination reactions with solid surfaces for mass spectrometer atomic oxygen composition correction in upper atmosphere [NASA-CR-106805]

p0091 N70-11727

ATS
OGO 3 search coil magnetometer data correlated with magnetopause crossing by ATS 1 satellite, discussing OGO 3 crossing of outer magnetosphere into interplanetary medium

p0017 A68-41693

ATS 5
Magnetopause crossing observation of ATS 5 satellite during magnetic storm

p0043 A71-17258

AUDIO FREQUENCIES
Continuous and triggered audio frequency noise bands associated with ionospheric lower hybrid resonance frequency observed on OGO 2

p0018 A69-16257

Studying whistlers and audio frequency emissions with receiving system on POGO satellite in conjunction with ground based observing stations [NASA-CR-97605]

p0088 N69-17928

AURORAL ARCS
Auroral arcs far UV observations by OGO 4, discussing luminosity, morphology, position, etc.

p0030 A70-23493

The Harang discontinuity in auroral belt ionospheric currents.

p0061 A72-39980

AURORAL SPECTROSCOPY
Auroral electron energy spectra measured from 180 to 250 km using electrostatic analyzer and channeltron detector, discussing electron flux

p0012 A68-25969

Auroral spectrum analysis in 1200-4000 A band, obtaining photon emission rates

p0058 A72-26402

Observations of the conjugate SAR arcs of September 28-30, 1967. --- subauroral red arcs

p0080 A74-34042

AURORAL TEMPERATURE
Auroral heating and the composition of the neutral atmosphere.

p0069 A73-27602

AURORAL ZONES
VLF and LF emission characteristic features and origin mechanism in auroral regions of ionosphere, discussing satellite observation of noise spectrum in space

p0025 A69-38495

High latitude regions of low energy electron precipitation from OGO 4 satellite auroral particle experiment

p0049 A71-30032

Magnetic storm effects in atmospheric neutral composition, noting thermospheric wind circulation role due to Joule heating within auroral zone

p0058 A72-24957

The Harang discontinuity in auroral belt ionospheric currents.

p0061 A72-39980

Distributions and characteristics of high-latitude field-aligned electron precipitation.

p0069 A73-26988

A multisatellite study of auroral-zone phenomena. [ESRO-SR-23-PT-1]

p0105 N74-16072

BOLTZMANN TRANSPORT EQUATION

AURORAS

Electron measurements near weak aurora during rocket flight

p0008 A67-33595

LF and VLF wideband noise called auroral hiss observed by Byrd ground station and OGO 2, proposing incoherent Cerenkov radiation from 1 kev electrons

p0011 A68-19752

Polar ionosphere auroral oval position detection by satellite observations of naturally occurring VLF and man-made HF plasma waves

p0032 A70-29924

Far UV equatorial airglow and aurora intensities and occurrence frequencies from satellite observation

p0041 A71-11504

Properties of higher latitude region of structured low energy electron precipitation in noon hemisphere, relating radiation with optical emissions in dayside auroral oval

p0048 A71-27911

Low energy electron and proton fluxes in geomagnetic tail of equatorial magnetosphere forming plasma sheet related to auroral oval

p0049 A71-30029

VLF auroral hiss comparison with low energy electron precipitation, using OGO 4 data

p0056 A72-19149

Type 3 solar burst distinction from auroral type high pass noise via spectrum analysis

p0062 A72-42043

Mantle aurora caused by auroral electron drift and precipitation [NASA-TM-X-63941]

p0093 N70-29987

Aurora formation by electron injection and drift in upper atmosphere

p0095 N71-25272

Synoptic study of field-aligned electron precipitation in auroral regions [NASA-TM-X-66065]

p0099 N73-10392

Electric field measurements across the Harang discontinuity --- of the auroral zone [NASA-TM-X-70613]

p0105 N74-19023

OGO-4 auroral particles experiment and calibration [NASA-TM-X-70216]

p0108 N74-74628

AZIMUTH

Shadowing of electron azimuthal-drift motions near the noon magnetopause.

p0065 A73-12442

B

BACKGROUND RADIATION

Lyman alpha sky background measurements by OGO 5 satellite, discussing absolute emission rate, spatial variations and origin

p0047 A71-24439

Neutral hydrogen interstellar wind parameters from Lyman alpha sky background measurements outside geocorona by photometers on OGO 5

p0051 A71-33834

OGO-5 measurements of the Lyman-alpha sky background in 1970 and 1971.

p0077 A74-22345

BALLOON SOUNDING

Skyhook balloon flight Geiger counter cosmic ray monitor measurements of energy and charge spectra of galactic rays at solar minimum

p0006 A66-34847

BATTERY CHARGERS

Orbiting Geophysical Observatory electric power subsystem design innovations including power supply, solar array output and battery charge control

p0003 A65-19528

BETA PARTICLES

Beta particle observations between inner edge of plasma sheet to plasmapause in midnight earth magnetosphere [NASA-TM-X-65640]

p0095 N71-32436

BIBLIOGRAPHIES

Experiment data analysis report OGO-A: Experiment no. 1 [B03944-000]

p0111

BOLTZMANN TRANSPORT EQUATION

Differential energy spectra of cosmic ray protons and helium nuclei dominated by solar modulation of local interstellar spectra, and numerical solutions to transport equation [NASA-CR-130298]

p0100 N73-15837

BOUNDARY LAYERS

BOUNDARY LAYERS

Magnetic field measurements in outer magnetosphere, emphasizing boundary regions and shock front characteristics

p0010 A68-12172

Plasmapause position measurements by ion mass spectrometers and broadband VLF receivers on OGO 1 and OGO 3 and by broadband recordings at Antarctica

p0021 A69-25153

BOW WAVES

Magnetic field observations by OGO-1, with profiles of bow shock and magnetopause encounters

p0010 A68-11011

IMP-2 and OGO-1 investigations of bow shock large scale motions during magnetic storms result from magnetosphere-magnetosheath compression by solar wind dynamic pressure

p0011 A68-17768

Detection of electric field turbulence in earth bow shock, noting wave amplitude correlation with magnetic field structure

p0018 A69-14681

Magnetic fluctuations in various frequency ranges, associated with earth bow shock, detected with search coil magnetometer on OGO 3

p0026 A69-40501

Fluctuating electric fields relations to MHD bow shock structure, using LF fluxgate magnetometer aboard OGO 5

p0026 A69-42693

Initial deceleration of solar wind positive ions upstream of earth bow shock determined from OGO 5 high time resolution plasma measurements

p0030 A70-21377

Fast time-resolved spectra of earth bow shock electrostatic turbulence based on broadband analog electric data from OGO-5

p0031 A70-29111

Electrostatic turbulence in bow shock magnetic structures observed by OGO 5, explaining turbulence as ion acoustic or Buneman mode due to two stream instability

p0035 A70-36006

Magnetic and electric field changes across earth bow shock and magnetosheath, discussing Pioneer 8 and OGO-5 data

p0036 A70-37483

Directed proton fluxes measurements in bow shock, magnetosheath and solar wind by OGO 5 satellite ion spectrometer

p0040 A71-11491

Solar wind ion thermalization in earth bow shock by counterstreaming instability related to interplanetary magnetic field

p0050 A71-31774

Earth bow shock internal structure based on correlated observations of magnetic field, ELF magnetic fluctuations and suprathermal electrons by OGO 5 satellite

p0051 A71-33943

Suprathermal electron beam induced HF wave instability in solar wind upstream from earth bow shock, interpreting OGO 5 observations

p0053 A71-43158

Earth bow shock magnetic field data correlation with OGO 5 flux gate magnetometer, using Tidman-Northrop theory

p0056 A72-19145

Earth bow shock laminar profile at low Mach number by crossing satellites on 12 February 1969, determining mean velocity along normal

p0057 A72-23004

Electron plasma oscillations distribution upstream from earth bow shock, evaluating OGO-5 plasma wave detector data

p0057 A72-23019

Earth-solar wind bow shock structure from OGO-5 observations during passage from interplanetary medium into magnetosheath

p0058 A72-29379

Weak electrostatic turbulence observation in earth bow shock magnetic field gradient, suggesting cyclotron drift instability role

p0063 A72-44523

Proton scattering in the region near the earth's bow shock

p0067 A73-22054

Solar wind and magnetosheath electron temperature measurements by triaxial electron analyzer onboard OGO-5, presenting data for bow shock

p0075 A73-45112

Structure of the quasi-perpendicular laminar bow shock

[B22612-000] p0114

Distributions of high frequency waves upstream from earth's bow shock

[NASA-CR-139256] p0108 N74-74626

BREMSSTRAHLUNG

Highest differential energy range of X rays during July 1966 solar flare suggests nonthermal bremsstrahlung origin of hard flare X rays

p0011 A68-17769

Center to limb variation of solar hard X ray bursts, suggesting inverse Compton effect and bremsstrahlung from anisotropic electrons

p0023 A69-33055

Impulsive solar flare X rays spectral characteristics, examining electron energy, bremsstrahlung, microwave bursts and particle escape, collisions and injection

p0043 A71-15937

BRIGHTNESS TEMPERATURE

Reduction and analysis of data on low frequency brightness temperature of sky from OGO-4 radio astronomy experiment

[NASA-CR-110796] p0093 N70-42352

BROADBAND AMPLIFIERS

Nonducted very low frequency propagation in magnetosphere from broadband VLF receivers on OGO 2 and OGO 4 polar satellites

[NASA-CR-107614] p0091 N70-15525

C

CALIBRATING

In-flight radiometric calibration of low brightness OGO 4 airglow photometer

p0029 A70-15645

Flight calibration device for absolute measurements of photometer at Lyman alpha wavelength on OGO-6 and other satellites

[AD-726567] p0096 N71-36136

CATIONS

Earth satellite sweeping mass spectrometer for measuring atmospheric neutral particle and positive ion concentration

p0025 A69-36681

Initial deceleration of solar wind positive ions upstream of earth bow shock determined from OGO 5 high time resolution plasma measurements

p0030 A70-21377

Plasmapause irregular structure and position indicated by measured distributions of hydrogen and helium thermal positive ions in duskside magnetosphere

p0031 A70-29185

CERENKOV RADIATION

LF and VLF wideband noise called auroral hiss observed by Byrd ground station and OGO 2, proposing incoherent Cerenkov radiation from 1 keV electrons

p0011 A68-19752

CHARGE DISTRIBUTION

Earth satellite experiment for measuring the charge and energy spectra of the primary cosmic rays

[B01634-000] p0111

Multiple parameter analysis of galactic and solar cosmic rays for chemical composition and charge distribution

p0091 N69-38984

CHARGED PARTICLES

Measurement of differential energy spectra of protons, helium nuclei and heavy nuclei by cosmic radiation telescopes mounted on POGO and Pioneer satellites

p0004 A66-23684

Skyhook balloon flight Geiger counter cosmic ray monitor measurements of energy and charge spectra of galactic rays at solar minimum

p0006 A66-34847

Solar and galactic particle spectra and composition measured with cosmic ray telescope mounted on satellite

p0008 A67-27249

Charged particles of extraterrestrial ring current during geomagnetic storms, with OGO 3 measurements of proton and electron differential energy spectra

p0009 A67-37401

Primary cosmic ray energy spectra and charge composition during 1965 solar modulation minimum, using scintillator photomultiplier detector on OGO 1

p0016 A68-41431

Low energy charged particles in earth magnetosphere observed by OGO satellite

p0019 A69-19358

Charged particles injection into captured radiation zone of Van Allen belts during main phase of magnetic storm indicated by proton data analysis

p0025 A69-37967

Low energy charged particle distribution within earth magnetosphere and environs, suggesting solar origin for storm time ring current protons

p0033 A70-30089

Low energy galactic cosmic radiation energy spectra and charge composition in 2-14 Z range by OGO-5, suggesting two component model for origin

p0037 A70-38127

Proton energy change effects on charged particles propagating in interplanetary space, using low energy solar flare proton fluxes observations

p0046 A71-22801

Satellite charged particle observations and polar cap riometer absorption measurements during solar cosmic ray events, noting electron and proton contributions

p0059 A72-31965

Charged particle distribution study in near earth region using orbiting spherical electrostatic analyzers or plasma probes

[AD-700804] p0092 N70-28003

Design of OGO-E experiment to measure energetic X-rays, electrons, protons, and alphaparticle emissions from solar flares

[NASA-CR-122509] p0098 N72-28812

Data processing and analysis of charged particle experiment on OGO-5 spacecraft

[NASA-CR-132761] p0102 N73-25870

CHEMICAL COMPOSITION

Low energy galactic cosmic radiation energy spectra and charge composition in 2-14 Z range by OGO-5, suggesting two component model for origin

p0037 A70-38127

C, N and O nuclei abundances in radiation belt near geomagnetic equator, using data obtained by OGO-5 satellite in 1968

p0041 A71-13475

Multiple parameter analysis of galactic and solar cosmic rays for chemical composition and charge distribution

p0091 N69-38984

CHEMICAL ELEMENTS

Chemical abundances and energy spectra of nuclei in galactic radiation measured in interplanetary space by OGO-1 satellite

p0006 A66-34833

Energy spectra and abundances of elements He through Si of galactic cosmic ray above 20 Mev per nucleon in nuclear charge range between 2 and 26

p0006 A67-11687

CHEMICAL ENERGY

Magnetospheric chemical release study --- modifications of wave particle interactions in magnetosphere

[AD-769979] p0105 N74-17126

CHIRP SIGNALS

A correlated study of ELF waves and electron precipitation on OGO-6.

p0077 A74-24766

CHROMOSPHERE

Soft X-ray and microwave observations of hot regions in solar flares.

p0060 A72-35089

CINEMATOGRAPHY

Cinematographic display of observations of low energy proton and electron spectra in terrestrial magnetosphere

[NASA-CR-91871] p0087 N68-15232

CIRCULAR POLARIZATION

Whistler-mode waves circular polarization measurement by OGO 6 satellite, noting application to hiss, chorus and ion density studies

p0042 A71-14538

CISLUNAR SPACE

Earth-sun relationship data obtained by Orbiting Geophysical Observatory experiments concerning the atmosphere of the earth, the magnetosphere, and cislunar space

p0001 A63-21527

Velocities of dust particles in cislunar space

p0004 A66-15266

Zodiacal dust particle flux measurements from OGO 3 and Mariner 4 spacecraft in cislunar and interplanetary space

p0013 A68-29457

Picogram dust particle flux measurements in selenocentric, cislunar and interplanetary space by Mariner 4, OGO 3 and Explorer 35

p0041 A71-14014

Four years of dust particle measurements in cislunar and selenocentric space from Lunar Explorer 35 and OGO 3
[B15918-000] p0112
 OGO 3 experiment to measure physical parameters of picogram size dust particles in cislunar and near earth space
[NASA-CR-121477] p0096 N71-33768

CLOUDS (METEOROLOGY)
 Satellite multispectral photometry data in airglow bands correlated with cloud characteristics and surface albedo variations
 p0028 A70-15522

COILS
 POGO triaxial search coil magnetometer
[B21207-000] p0113 B75-21207

COLD PLASMAS
 Satellite measurements of cold plasma density and plasmopause in magnetosphere, comparing whistler, Langmuir probe and ion trap data
 p0049 A71-30951

COLLISIONLESS PLASMAS
 Collision free earth shock wave gross and fine structure deduced from OGO 5 plasma diagnostics
[AIAA PAPER 69-676] p0023 A69-33452
 Collisionless plasma spherical probe RF sheath model based on quasi-static approximation and electrostatic theory
 p0057 A72-23520

COMET TAILS
 Determination of the solar Lyman-alpha flux independent of calibration by ultraviolet observations of Comet Bennett)
 p0076 A74-15496

COMETS
 Comet Bennett /1969 i/ spectrograms, discussing linear diameter, trajectory, Lyman alpha emission and hydrogen mass
 p0039 A70-42468

COMPRESSION WAVES
 IMP-2 and OGO-1 investigations of bow shock large scale motions during magnetic storms result from magnetosphere-magnetosheath compression by solar wind dynamic pressure
 p0011 A68-17768
 Resonant compression waves in geomagnetic tail estimated for frequency and spatial distribution by single layered two dimensional model
 p0028 A70-15127

COMPTON EFFECT
 Center to limb variation of solar hard X ray bursts, suggesting inverse Compton effect and bremsstrahlung from anisotropic electrons
 p0023 A69-33055

COMPUTER PROGRAMMING
 Orbiting Geophysical Observatory programming system consisting of real time quick-look monitor and data processors
[AIAA PAPER 64-218] p0002 A64-24447
 Programmer manual for Polar Orbiting Geophysical Observatory
[IS-769] p0082 N64-13388

COMPUTER PROGRAMS
 Analytical determination of earth visibility from orbiting satellite - OGO and POGO
[NASA-TM-X-55002] p0082 N64-23517
 F-02 experiment onboard OGO-6, and computer program for analysis of raw data
[NASA-CR-130128] p0100 N73-13376
 The inner zone electron model AE-5
[NASA-TM-X-69987] p0106 N74-20502
 Program description of the data reduction program for experiment 19 of OGO-D
[NASA-TM-X-70372] p0109 N74-76910

CONJUGATE POINTS
 O 1 1304-A airglow, observing conjugate excitation with OGO 4 spacecraft
 p0043 A71-17279
 Whistler mode signals observation in conjugate region of 200 kHz broadcast station by satellite-borne narrow band receiver, considering field-aligned ducted and nonducted propagation
 p0059 A72-29384

CONJUGATES
 Observations of the conjugate SAR arcs of September 28-30, 1967, --- subauroral red arcs
 p0080 A74-34042

CONTAMINATION
 Thermoelectrically-cooled quartz crystal microbalance --- monitor of surface contamination as function of temperature
 p0103 N74-10255

CONTROL SIMULATION
 Single axis test program and simulator for vehicle dynamics in free space to test attitude control system of Orbiting Geophysical Observatory (OGO)
 p0002 A64-27303

CONVECTION
 Cosmic ray electrons solar modulation, considering diffusion-convection theory
 p0040 A70-45769

CONVECTION CURRENTS
 Injun 5 satellite measurements of magnetospheric convection electric fields via double probe technique, discussing substantiation with OGO 6 results
[AD-750221] p0063 A72-42901

CONVECTIVE FLOW
 Satellite studies of magnetospheric substorms on August 15, 1968. 3: Some features of magnetospheric convection.
 p0072 A73-33451
 Diffusion-convection theory for solar cosmic ray propagation in interplanetary magnetic field
 p0090 N69-29659

COORDINATE TRANSFORMATIONS
 Coordinate transformations for OGO satellite data reduction
[NASA-TM-X-63826] p0092 N70-19313

CORPUSCULAR RADIATION
 Hysteresis effect on cosmic ray modulation and gradient ionization near solar minimum from measurements made near earth with OGO 1 and 3 ion chambers
 p0028 A70-15106
 Initial deceleration of solar wind positive ions upstream of earth bow shock determined from OGO 5 high time resolution plasma measurements
 p0030 A70-21377

CORRELATION
 Oxygen ion anticorrelation to molecular ion concentrations from OGO 6 observations in F 2 region
 p0062 A72-42016

COSMIC DUST
 Temperature gradient and thermal effects on ceramic transducer sensors used on spacecraft for cosmic dust experiments
 p0013 A68-29467
 Sensors used in cosmic dust experiments studied for response to microparticle hypervelocity impacts, noting relationship to velocity
 p0013 A68-29468
 OGO 3 experiment to measure physical parameters of picogram size dust particles in cislunar and near earth space
[NASA-CR-121477] p0096 N71-33768

COSMIC NOISE
 OGO radio astronomy instrument for cosmic noise sky brightness distribution mapping by electrically short antenna ionospheric focusing
 p0048 A71-26144
 Design considerations and performance characteristics for radio astronomy instrumentation system aboard OGO-5 spacecraft
[NASA-CR-98670] p0088 N69-14392
 Data reduction and analysis report for radio astronomy experiment aboard OGO-2 spacecraft
[NASA-CR-98669] p0088 N69-14393

COSMIC PLASMA
 Low altitude electric and magnetic measurements of plasma waves in space from OV3-3, Pioneer 8 and OGO 5 satellite observations
 p0029 A70-17376
 Neutral hydrogen interstellar wind parameters from Lyman alpha sky background measurements outside geocorona by photometers on OGO 5
 p0051 A71-33834

COSMIC RAY ALBEDO
 Cosmic ray albedo neutron flux latitude and altitude dependence, using OGO-6 polar orbiting satellite
 p0037 A70-39326

COSMIC RAYS
 Cosmic ray experiments for Explorer 12 and the Orbiting Geophysical Observatory using GeigerMuller counters, and scintillation counter telescopes
 p0001 A63-20022
 Orbiting Geophysical Observatory (OGO) for cosmic ray, radio astronomy and Gegenschein experiments including satellite description and orbit data
 p0003 A65-22431
 Differential response curves and mean rigidity of response of ion chambers aboard balloons and satellites in free space during long-term cosmicray variation from 1960 to 1965
 p0003 A65-33664

Measurement of differential energy spectra of protons, helium nuclei and heavy nuclei by cosmic radiation telescopes mounted on POGO and Pioneer satellites
 p0004 A66-23684

Explorer 18 satellite measurements of proton energy spectra in region corotating with sun, noting modulation of galactic cosmic radiation and source of continuous particle accelerations
 p0005 A66-34754

Energy spectra and abundances of elements He through Si of galactic cosmic ray above 20 Mev per nucleon in nuclear charge range between 2 and 26
 p0006 A67-11687

Solar modulation of galactic protons and He nuclei during last solar cycle analyzed according to Parker theory
 p0007 A67-19913

Solar and galactic particle spectra and composition measured with cosmic ray telescope mounted on satellite
 p0008 A67-27249

Hydrogen and helium cosmic ray nuclei isotopic composition measured to clarify abundance ratios energy dependence below 75 MeV/nucleon
 p0015 A68-41421

Low energy interplanetary positrons detection by OGO satellites, discussing possible existence of equilibrium charge ratio
 p0015 A68-41427

Low energy cosmic ray nuclei propagating in interstellar space analyzed by telescope onboard OGO 1
 p0016 A68-41434

Balloon and satellite measurement of quiet time cut-off rigidities for cosmic ray particles
 p0016 A68-41562

OGO-6 neutron monitor for measuring cosmic ray neutron flux near earth, locating sensor on boom to minimize spacecraft produced neutrons
 p0024 A69-36678

Hysteresis effect on cosmic ray modulation and gradient ionization near solar minimum from measurements made near earth with OGO 1 and 3 ion chambers
 p0028 A70-15106

Quiet time cosmic ray ionization altitude dependence over polar regions from measurements by integrating ionization chamber on OGO-2
 p0034 A70-31902

Cosmic ray knee interpretation using polar orbiting ionization chambers data from OGO-2/4
 p0034 A70-31903

Cosmic ray electron and positron differential energy spectra during solar quiet times from OGO5 satellite observations in interplanetary space
 p0036 A70-38096

Interplanetary cosmic ray positrons energy spectral component with origin different from interstellar mesons decay
 p0036 A70-38098

Long term variations of cosmic ray electron spectrum above 500 MeV from balloon and satellite observations, noting reduction during Forbush decreases
 p0037 A70-38105

Interstellar cosmic ray electron spectrum flattening below 3 GeV from OGO-5 observations
 p0037 A70-38106

Low energy galactic cosmic radiation energy spectra and charge composition in 2-14 Z range by OGO-5, suggesting two component model for origin
 p0037 A70-38127

Cosmic ray electrons solar modulation, considering diffusion-convection theory
 p0040 A70-45769

Quiet time fluxes and differential energy spectra of protons and alpha particles at 2-20 MeV measured by cosmic ray detectors on OGO-3
 p0044 A71-18127

Low energy cosmic rays modulation and heliocentric gradient during solar minimum, comparing OGO 1 and 2 ion chamber measurements with other space and ground observations
 p0044 A71-18128

Forbush decreases and long term cosmic ray particle intensity changes, investigating spectral variations
 p0044 A71-18137

Cosmic ray neutron leakage flux and energy spectrum measurements in 0.01-10 MeV range by OGO 6 satellite-borne neutron detector
 p0054 A72-10877

Nov. 10, 1975

Heavy nuclei enrichment in solar accelerated particles, discussing differential energy spectra, photospheric and coronal abundances, satellite observation and agreement with galactic cosmic rays
p0055 A72-15366

OGO-5 measurement of 10-200 MeV cosmic ray electron energy spectra, discussing quiet time flux intensity
p0055 A72-16719

Electron scattering effects on response of cosmic ray particle telescopes from pulse height and counting rate measurements
p0057 A72-21510

Cosmic ray electron search and study, comparing near earth to interstellar spectrum
p0060 A72-33869

Geomagnetic cutoffs for cosmic-ray protons for seven energy intervals between 1.2 and 39 Mev
p0061 A72-38728

Cosmic-ray scintillations. I. Inside the magnetosphere.
p0066 A73-15526

Energy dependent time lag in the long-term modulation of cosmic rays.
p0067 A73-19252

The 1972 cosmic ray electron spectrum above 0.5 GeV. -- mechanism for distortion by solar modulation
p0078 A74-27700

Short-term intensity fluctuation of cosmic-ray electrons between 0.5 and 10 GeV.
p0079 A74-31903

Cosmic gamma-ray burst detected with an instrument on board the OGO-5 satellite.
p0080 A74-31942

Description of OGO-1 and OGO-3 counting rate processing and resulting data. Cosmic ray spectra and fluxes experiment on OGO-1 and OGO-3
[B03716-000] p0111

Energy spectrum of cosmic-ray electrons from 0.5 to 10 GeV
[B14744-000] p0112

Observation of cosmic-ray electrons with the OGO-5 satellite
[B14745-000] p0112

Absolute cosmic ray ionization measurements in upper and lower atmosphere
[NASA-CR-104068] p0090 N69-34536

Cosmic ray electrons and solar flare particles from OGO-E and Explorer 33 data for identifying solar flare electrons
p0090 N69-38983

Differential energy spectra of cosmic ray protons and helium nuclei dominated by solar modulation of local interstellar spectra, and numerical solutions to transport equation
[NASA-CR-130298] p0100 N73-15837

Satellite measurement of cosmic ray abundances and spectra in charge range 2 equal to or less than 7 equal to or less than 10
[NASA-CR-135786] p0103 N73-33777

Cosmic ray telescope for OGO 2 and 4 spacecraft -- construction and flight of cosmic ray telescope on OGO-2 and 4 spacecraft
[NASA-CR-137238] p0106 N74-19088

Response to environment and radiation of an ionization chamber and matched geiger tube used on spacecraft
[NASA-CR-139255] p0108 N74-74624

COSMOS SATELLITES
Comparison of Cosmos-215 and OGO-D observations of nightglow in 1225 to 1350 A range at low geomagnetic latitudes
p0096 N71-34333

COUNTING RATE COMPUTERS
Description of OGO-1 and OGO-3 counting rate processing and resulting data. Cosmic ray spectra and fluxes experiment on OGO-1 and OGO-3
[B03716-000] p0111

CRITICAL FREQUENCIES
ISIS-1 satellite observations of the ionosphere at high southern latitudes.
p0068 A73-25753

CURRENT SHEETS
Magnetopause current layer deflection during OGO 5 crossings, noting independence on sun-earth-satellite angle
p0053 A71-43161

Magnetic field strength change in equatorial plasmasphere, considering quiet ring current as equatorial sheet current extension of neutral sheet current in magnetospheric tail
p0064 A73-11732

Field-aligned currents, plasma waves, and anomalous resistivity in the disturbed polar cusp.
p0069 A73-29964

A magnetospheric field model incorporating the OGO-3 and 5 magnetic field observations.
p0074 A73-43693

CU SPS
OGO 5 polar cusp observations showing dayside magnetosheath plasma penetration during magnetic storm
p0053 A71-43162

Dependence of the polar cusp on the north-south component of the interplanetary magnetic field.
p0072 A73-36273

OGO-5 observations of the physical processes occurring in the disturbed polar cusp and the cusp-magnetosheath interface
[B18269-000] p0113

CU T-OFF
Balloon and satellite measurement of quiet time cut-off rigidities for cosmic ray particles
p0016 A68-41562

CYCLOTRON FREQUENCY
Magnetospheric VLF electric field emissions above electron cyclotron frequency from OGO 5 observation at magnetic equator
p0041 A71-11500

Weak electrostatic turbulence observation in earth bow shock magnetic field gradient, suggesting cyclotron drift instability role
p0063 A72-44523

CYCLOTRON RADIATION
Turbulence of electrostatic electron cyclotron harmonic waves observed by OGO-5.
p0060 A72-35599

CYCLOTRON RESONANCE
Harmonic ion cyclotron resonances associated with proton whistlers observed from OGO-4 satellite VLF recordings
p0030 A70-19630

Relativistic electron precipitation during magnetic storms, showing cyclotron resonances with electromagnetic ion cyclotron waves
p0051 A71-33948

The origin and propagation of chorus in the outer magnetosphere.
p0078 A74-24767

D

DATA ACQUISITION
Geomagnetic survey by polar-orbiting OGO 2 and 4, discussing data acquisition and reduction results and accuracy
p0054 A72-12081

Equatorial electrojet characteristics observation during 1967-1970 with POGO satellite-borne magnetometers, noting anomaly characterized by sharp negative V-signature in width and variable amplitude
p0070 A73-31768

DATA CORRELATION
OGO-5 plasmopause crossing correlation with ground observations of Pi geomagnetic micropulsations
p0056 A72-21223

The relation between low-latitude neutral density variations near 400 km and magnetic activity indices.
p0075 A74-14219

Correlation of satellite estimates of the equatorial electrojet intensity with ground observations at Addis Ababa
[B15846-000] p0112

DATA PROCESSING
Main geomagnetic field data, discussing data conversion to computer-readable form
p0009 A67-36901

Summary of digital data-processing systems for the OGO SU/SRI very-low-frequency experiments
[B01263-000] p0111

Experiment data analysis report OGO-3: Experiment no. 1
[B03943-000] p0111

Experiment data analysis report OGO-A: Experiment no. 1
[B03944-000] p0111

Experiment data analysis report for the OGO-4 neutral and ion mass spectrometer experiment
[B05000-000] p0111

Production processing of the data obtained by the UCLA OGO-5 fluxgate magnetometer
[B12880-000] p0112

Geocoronal hydrogen measurement experiment on OGO-E - methods of obtaining orbital and spacecraft parameters for data analysis
[NASA-TM-X-55276] p0083 N65-30651

Processing of total field magnetometer data from OGO-2 satellite
[NASA-TM-X-55822] p0085 N67-30147

Display and processing program for data from gegenschein photometry experiment from OGO-B
[NASA-TM-X-55907] p0086 N67-35595

Digital data processing system for very low frequency radio noise and propagation experiment aboard OGO-1
[NASA-CR-88618] p0086 N67-37021

Solar burst time profiles and dynamic spectra for calculating theoretical values for Type 3 burst characteristics
[NASA-CR-107031] p0091 N70-12221

Reduction and analysis of data on low frequency brightness temperature of sky from OGO-4 radio astronomy experiment
[NASA-CR-110796] p0093 N70-42352

Procedures for processing atmospheric composition data obtained through use of sweeping quadrupole mass spectrometer on OGO-4 satellite
[NASA-CR-117525] p0094 N71-21544

Reduction and analysis of trapped and precipitating electron data from OGO 6 spectrometer experiment F-16
[NASA-CR-130137] p0100 N73-15863

Analysis of light ion mass spectrometer data from OGO-E experiment
[NASA-CR-130156] p0101 N73-16432

Data processing and analysis of charged particle experiment on OGO-5 spacecraft
[NASA-CR-132761] p0102 N73-25870

Data processing system for the intensity monitoring spectrometer flown on the Orbiting Geophysical Observatory-F (OGO-F) satellite
[NASA-CR-136827] p0105 N74-16940

Data analysis program for the OGO E-24 plasma wave detector
[NASA-CR-140523] p0110 N74-77109

DATA PROCESSING EQUIPMENT
Orbiting Geophysical Observatory programming system consisting of real time quick-look monitor and data processors
[AIAA PAPER 64-218] p0002 A64-24447

DATA RECORDING
Harmonic ion cyclotron resonances associated with proton whistlers observed from OGO-4 satellite VLF recordings
p0030 A70-19630

DATA REDUCTION
Main geomagnetic field data, discussing data conversion to computer-readable form
p0009 A67-36901

OGO 4 satellite micrometeoroid flux detection, emphasizing noise control procedures for data correlation
p0048 A71-28700

Geomagnetic survey by polar-orbiting OGO 2 and 4, discussing data acquisition and reduction results and accuracy
p0054 A72-12081

Role of gas-surface interactions in the reduction of OGO-6 neutral particle mass spectrometer data.
p0073 A73-38941

Geocoronal hydrogen measurement experiment on OGO-E - methods of obtaining orbital and spacecraft parameters for data analysis
[NASA-TM-X-55276] p0083 N65-30651

Data reduction methods for OGO airglow photometer measurements
[NASA-TM-X-55794] p0085 N67-27576

Processing of total field magnetometer data from OGO-2 satellite
[NASA-TM-X-55822] p0085 N67-30147

Design considerations and performance characteristics for radio astronomy instrumentation system aboard OGO-5 spacecraft
[NASA-CR-98670] p0088 N69-14392

Data reduction and analysis report for radio astronomy experiment aboard OGO-2 spacecraft
[NASA-CR-98669] p0088 N69-14393

Solar burst time profiles and dynamic spectra for calculating theoretical values for Type 3 burst characteristics
[NASA-CR-107031] p0091 N70-12221

Samples of electron spectroscopy and ionization chamber data plots from OGO-1 and OGO-3
[NASA-CR-107885] p0092 N70-17624

SUBJECT INDEX

Coordinate transformations for OGO satellite data reduction
 [NASA-TM-X-63826] p0092 N70-19313
 Reduction and analysis of trapped and precipitating electron data from OGO 6 spectrometer experiment F-16
 [NASA-CR-130137] p0100 N73-15863
 The reduction and analysis of electron data for outer zone electron model AE-4. Volume 3: OGO-1 and 3 University of Minnesota experiment data
 [NASA-TM-X-70212] p0109 N74-74636
 Program description of the data reduction program for experiment 19 of OGO-D
 [NASA-TM-X-70372] p0109 N74-76910
 Reduction and analysis of data from OGO-C,D ion chamber experiment
 [NASA-CR-107184] p0110 N74-76923

DATA SYSTEMS
 OGO structure and systems covering thermal and attitude controls, power plant, communications, tracking and data handling
 p0002 A65-14349

DAWN CHORUS
 Banded chorus, VLF discrete emissions in magnetosphere in single variable frequency band with frequency depending on equatorial electron gyrofrequency
 p0023 A69-31981
 The origin and propagation of chorus in the outer magnetosphere.
 p0078 A74-24767
 Intensity variation of elf hiss and chorus during isolated substorms
 [B22603-000] p0114

DAYTIME
 Plasma waves in the dayside polar cusp. 2: Magnetopause and polar magnetosheath.
 p0077 A74-21680

DECAMETRIC WAVES
 A new model for the high-frequency decametric radiation from Jupiter
 p0081 A74-43688

DECAY RATES
 Soft solar X-ray bursts characteristics, discussing temporal and intensity differential distributions, flux measurements and decay time
 p0048 A71-27654
 Decay time of type 3 solar bursts observed at kilometeric wavelengths
 p0074 A73-41497

DECELERATION
 Initial deceleration of solar wind positive ions upstream of earth bow shock determined from OGO 5 high time resolution plasma measurements
 p0030 A70-21377

DECIMETER WAVES
 The role of energetic electrons in the correlation of meter and decimeter type III bursts with 4 keV X-ray emission.
 p0064 A73-11391

DECONTAMINATION
 OGO-6 surface contamination by outgassing in space environment and decontamination by sputtering and desorption
 [NASA-CR-117138] p0094 N71-20207

DEGRADATION
 Continuous-channel electron multipliers degradation in spacecraft environment simulation laboratory equipment
 p0021 A69-29565

DEMAGNETIZATION
 Digital offset field generator for dynamic range extension of magnetometers
 p0090 N69-33963

DENSE PLASMAS
 Electron concentrations calculated from the lower hybrid resonance noise band observed by OGO-3
 p0074 A73-41912

DENSITY (MASS/VOLUME)
 An upper limit to the product of NO and O densities from 105 to 120 Km
 [B22606-000] p0114

DENSITY DISTRIBUTION
 Interpretation of OGO-5 Lyman alpha measurements in the upper geocorona.
 p0066 A73-19233
 An association of magnetospheric whistler dispersion characteristics with changes in local plasma density.
 p0069 A73-26985
 The relation between low-latitude neutral density variations near 400 km and magnetic activity indices.
 p0075 A74-14219

Spatial and temporal behavior of atomic oxygen determined by OGO 6 airglow observations.
 p0079 A74-30670

Latitudinal density distribution of gases in upper atmosphere
 p0094 N71-25267

DENSITY MEASUREMENT
 Satellite measurements of cold plasma density and plasmopause in magnetosphere, comparing whistler, Langmuir probe and ion trap data
 p0049 A71-30951
 Gum Nebula size, density and electron temperature data from RAE-1 and OGO-5 satellites and ground based telescopes observations, correlating with Vela X supernova outburst
 p0052 A71-35409
 Atmospheric neutral density measurement near 400 km during daytime by microphone density gage on OGO 6
 p0058 A72-26407
 Electron concentrations calculated from the lower hybrid resonance noise band observed by OGO-3
 p0074 A73-41912
 Effect of satellite potential on direct ion density measurements through the plasmopause.
 p0076 A74-18372
 The measurement of cold ion densities in the plasma trough
 [B22610-000] p0114
 Fabrication, installation, and operation of microphone density gage experiment onboard OGO-F
 [NASA-CR-130082] p0098 N72-28467

DETECTORS
 Data analysis program for the OGO E-24 plasma wave detector
 [NASA-CR-140523] p0110 N74-77109

DIGITAL DATA
 Summary of digital data-processing systems for the OGO SU/SRI very-low-frequency experiments
 [B01263-000] p0111 B75-01263
 Digital data processing system for very low frequency radio noise and propagation experiment aboard OGO-I
 [NASA-CR-88618] p0086 N67-37021

DIODES
 Low energy solar cosmic ray experiment for OGO-6 using double diffused depleted silicon diodes
 p0012 A68-27616

DIPOLE ANTENNAS
 Resonances in driving point impedance of electric dipole antenna in ionosphere
 [NASA-CR-91620] p0087 N68-14025

DIPOLE MOMENTS
 Geomagnetic dipole field disturbances by trapped particles, calculating self consistent equilibrium configuration for ring current dipole moments
 p0034 A70-31905

DIRECTIVITY
 Center to limb variation of solar hard X ray bursts, suggesting inverse Compton effect and bremsstrahlung from anisotropic electrons
 p0023 A69-33055

DISPLAY DEVICES
 Visual presentation of motion and orientation of Orbiting Geophysical Observatory
 [NASA-TN-D-2918] p0083 N65-29296
 Display and processing program for data from gegenschein photometry experiment from OGO-B
 [NASA-TM-X-55907] p0086 N67-35595

DIURNAL VARIATIONS
 Ionospheric electron density response to geomagnetic storms at midlatitudes, noting diurnal variations detected by ATS 3 VHF signals
 p0038 A70-40479
 Exospheric neutral hydrogen temperature diurnal variation from satellite resonance filter data, suggesting Lyman alpha source external to geocorona
 p0040 A70-43852
 Properties of low energy particle impacts in the polar domain in the dawn and dayside hours.
 p0061 A72-39541
 Plasmopause nighttime, dayside and bulge positive ion concentration measurements with OGO 5 mass spectrometer compared with magnetospheric convection model
 p0061 A72-39544
 Diurnal latitudinal composition variations in light ion trough from OGO mass spectrometric observations, noting magnetic storm effects
 p0065 A73-11904

EARTH ALBEDO

POGO satellite observed electrojet signature data comparison with daily geomagnetic variation amplitude measurement at equatorial ground station in India
 p0070 A73-31769

Global characteristics in the diurnal variations of the thermospheric temperature and composition.
 p0077 A74-21693
 Diurnal variation of the neutral thermospheric winds determined from incoherent scatter radar data
 [B22601-000] p0114
 Dynamic diffusion concept for calculating diurnal thermospheric temperature characteristics
 p0094 N71-25265
 Beta particle observations between inner edge of plasma sheet to plasmopause in midnight earth magnetosphere
 [NASA-TM-X-65640] p0095 N71-32436
 Diurnal variation of Lyman alpha spectral width as measured by OGO-6 sky-scanning photometer
 [AD-736816] p0097 N72-23429
 Variations in thermospheric composition: A model based on mass-spectrometer and satellite-drag data
 [NASA-CR-136192] p0104 N74-12459

DOPPLER EFFECT
 Nonducted VLF walking trace whistlers and Doppler shifts in fixed frequency transmissions identified on OGO midlatitude spectrographic records
 p0028 A70-15116
 Protonospheric electron concentration profiles based on Doppler and Faraday effects
 [NASA-CR-100778] p0089 N69-24521

DRIFT RATE
 Electron intensities and substorm drift effects in outer radiation belt using two satellite technique
 p0026 A69-43172
 Solar wind density model from km-wave type 3 bursts.
 p0071 A73-32965
 Mantle aurora caused by auroral electron drift and precipitation
 [NASA-TM-X-63941] p0093 N70-29987

DUCTS
 Whistler ducts as enhanced ionization from OGO 3 satellite observations near magnetic equator, noting magnetospheric ionization hydrostatic model and predicted cut-off
 p0041 A71-11499

DYNAMIC CHARACTERISTICS
 Dynamic analysis of longitudinal oscillations of SM-68B stage 1 (POGO)
 [B00570-000] p0111
 Dynamical characteristics of pulsating substorm, PS6
 [B14580-000] p0112

DYNAMIC MODELS
 Plasma proton and plasma electron prototype and flight models
 [NASA-CR-122351] p0097 N72-18715

E

E REGION
 Magnetic dip equator position at E layer and gradient with time and altitude, using geomagnetic field models
 p0026 A69-42428
 Solar X ray contribution to E layer ionization
 [NASA-CR-73884] p0088 N69-17412

EARLY STARS
 Early type stars radiant flux observation from OGO 6 satellite
 p0044 A71-17975

EARTH (PLANET)
 Analytical determination of earth visibility from orbiting satellite - OGO and POGO
 [NASA-TM-X-55002] p0082 N64-23517
 Micrometeoroids in earth dust cloud obtained from OGO-B satellite
 [NASA-CR-100683] p0089 N69-23367
 Power spectra of interplanetary magnetic field near earth bow shock
 p0099 N73-10792

EARTH ALBEDO
 Satellite multispectral photometry data in airglow bands correlated with cloud characteristics and surface albedo variations
 p0028 A70-15522
 Bidirectional reflectance at several wavelengths from moonlit earth observations by airglow photometer on OGO-4 satellite
 p0055 A72-13428

NOV. 10, 1975

EARTH ATMOSPHERE

EARTH ATMOSPHERE

Earth-sun relationship data obtained by Orbiting Geophysical Observatory experiments concerning the atmosphere of the earth, the magnetosphere, and cislunar space

Thermospheric wind effects on the distribution of helium and argon in the earth's upper atmosphere. p0001 A63-21527

Beta particle observations between inner edge of plasma sheet to plasmopause in midnight earth magnetosphere. p0071 A73-33441

A double gamma-ray spectrometer to search for positrons in space. [NASA-TM-X-65640] p0095 N71-32436

p0110 N74-77446

EARTH CRUST

Effects of crustal anomalies on satellite measurements of ambient geomagnetic field. p0097 N72-23341

EARTH MANTLE

POGO satellite observed electrojet current data comparison with ground measurement at Ibadan, discussing data ratios variation by upper earth mantle conductivity structure. p0070 A73-31772

The detection of 'intermediate' size magnetic anomalies in Cosmos 49 and OGO-2, 4, 6 data. p0073 A73-41374

EARTH MOTION

Magnetic fluctuations in various frequency ranges, associated with earth bow shock, detected with search coil magnetometer on OGO 3. p0026 A69-40501

EARTH ORBITS

Instrumentation and calibrations of low energy proton and electron experiment for Orbiting Geophysical Observatories. [NASA-CR-68558] p0084 N66-13640

Effects of energetic particles on photomultipliers in earth orbits up to 1500 km. [NASA-TM-X-63419] p0088 N69-18074

EARTH SATELLITES

Rubidium vapor magnetometer used for near earth orbiting spacecraft, instrumentation and in-flight performance. p0008 A67-36513

Earth satellite sweeping mass spectrometer for measuring atmospheric neutral particle and positive ion concentration. p0025 A69-36681

ELECTRIC EQUIPMENT

Orbiting geophysical observatory spacecraft and its qualification and acceptance testing. p0002 A63-23249

ELECTRIC FIELD STRENGTH

Fluctuating electric fields relations to MHD bow shock structure, using LF fluxgate magnetometer aboard OGO 5. p0026 A69-42693

Geomagnetic tail magnetic and electric fields ULF, VLF and ELF fluctuations, considering relationship to substorm processes. p0064 A72-44857

Recent studies of magnetospheric electric field emissions above the electron gyrofrequency. p0067 A73-19254

Electric field measurements across the Harang discontinuity -- of the auroral zone. [NASA-TM-X-70613] p0105 N74-19023

ELECTRIC FIELDS

High latitude electron bursts observed by OGO 4, postulating electric field acceleration mechanism beyond 3 earth radii for ambient thermal plasma electrons. p0017 A68-43443

Detection of electric field turbulence in earth bow shock, noting wave amplitude correlation with magnetic field structure. p0018 A69-14681

OGO 5 spacecraft detector instrumentation for measuring electrostatic and electromagnetic waves electric fields with coupled antennas, describing in-flight operation. p0025 A69-36683

Satellite plasma diagnostics for electric and magnetic fields and fine structure of collisionless shocks in solar wind plasma flows and interplanetary shocks. p0032 A70-30069

Ionospheric electric fields variations in ELF-VLF, confirming OV-1 satellite measurements with OGO 6 data. p0033 A70-30082

Plasma wave particle interactions in outer magnetosphere, magnetosheath and solar wind, noting role of AC electric fields. p0033 A70-30085

Magnetospheric VLF electric field emissions above electron cyclotron frequency from OGO 5 observation at magnetic equator. p0041 A71-11500

Pioneer 9 space probe electric field experiment and near earth observations of noise spectra variations related to diffusive plasma layer. p0046 A71-23711

Electric field fluctuations in magnetospheric plasma at multiples of local electron gyrofrequency due to plasma instability. p0052 A71-37368

Plasma wave measurements during OGO-5 dayside magnetosphere polar cusp encounters, discussing ULF magnetic field wave levels and VLF electric field amplitude ranges. p0059 A72-29380

Polar-cap electric field distributions related to the interplanetary magnetic field direction. p0062 A72-42432

Injun 5 satellite measurements of magnetospheric convection electric fields via double probe technique, discussing substantiation with OGO 6 results. [AD-750221] p0063 A72-42901

Electric field variations during substorms: OGO-6 measurements. p0064 A72-44854

Electromagnetic wave observation in interplanetary medium and in magnetosphere, emphasizing magnetic and electric field measurements. p0065 A73-13855

Equatorial spread F formation convective electric fields generation by neutral winds and conductivity caused by metallic ion concentrations. p0070 A73-29988

Additional results from an OGO-6 experiment concerning ionospheric electric and electromagnetic fields in the range 20 Hz to 540 kHz. p0071 A73-33438

Results from an experiment on OGO-6 to study electric and electromagnetic fields in the range 20 Hz - 540 KHz. [B17973-000] p0113

OGO-E study of electric field emissions at geomagnetic equator. [NASA-CR-126238] p0097 N72-22383

Electric field oscillations in upstream solar wind, using OGO-5 observations. p0099 N73-10789

Simultaneous observations of plasma waves from electric field instruments on Pioneer 9 and OGO 5 to illustrate difference between near-earth and deep space conditions. p0100 N73-10795

Seasonal, altitude, and universal time differences in field-aligned electrons. [NASA-TM-X-66099] p0100 N73-11345

Comments on a paper by J. P. Heppner. Polar cap electric field distributions related to interplanetary magnetic field direction. [NASA-CR-139259] p0108 N74-74632

ELECTRIC POTENTIAL
Electron trap behavior on charged spacecraft, obtaining expressions for current to aperture and internal retarding electrodes for all apertures and spacecraft potentials. p0022 A69-31976

Retarding potential analyzer errors and performance degradation due to grid plane potential depressions. p0058 A72-26411

Energy distribution of photoelectrons emitted from a surface on the OGO-5 satellite and measurements of satellite potential. p0076 A74-17648

ELECTRICAL IMPEDANCE
Resonances in driving point impedance of electric dipole antenna in ionosphere. p0087 N68-14025

Applying impedance data to plasma wake of spinning OGO-C satellite. [NASA-CR-109457] p0092 N70-23999

ELECTRICAL MEASUREMENT
Injun 5 satellite measurements of magnetospheric convection electric fields via double probe technique, discussing substantiation with OGO 6 results. [AD-750221] p0063 A72-42901

SUBJECT INDEX

ELECTRICAL RESISTIVITY

Field-aligned currents, plasma waves, and anomalous resistivity in the disturbed polar cusp. p0069 A73-29964

ELECTROMAGNETIC ABSORPTION

Ionospheric absorption relation to solar X-ray flux enhancement during short wave fade-outs from OGO-4 and Solrad 9 satellites. p0045 A71-20318

ELECTROMAGNETIC FIELDS

Additional results from an OGO-6 experiment concerning ionospheric electric and electromagnetic fields in the range 20 Hz to 540 kHz. p0071 A73-33438

Results from an experiment on OGO-6 to study electric and electromagnetic fields in the range 20 Hz - 540 KHz. [B17973-000] p0113

ELECTROMAGNETIC INTERFERENCE

OGO spacecraft EMI in 50 kHz to 4 MHz range. p0089 N69-25437

ELECTROMAGNETIC MEASUREMENT

OGO-6 electric and electromagnetic fields measurement for ionosphere using dipole antenna, emphasizing broadband observation covering whistler mode waves. p0024 A69-36677

Low altitude electric and magnetic measurements of plasma waves in space from OV3-3, Pioneer 8 and OGO 5 satellite observations. p0029 A70-17376

ELECTROMAGNETIC NOISE

Satellite observation of natural VLF phenomena in ionosphere and magnetosphere stressing radio noise frequency-time characteristics. p0010 A68-14098

VLF noise phenomena observed with satellite electric dipole antennas compared with lower hybrid resonance frequency of ionospheric medium in vicinity. p0029 A70-18534

OGO-5 observation of lower hybrid resonance noise, bursts, VLF hiss and whistlers near plasmopause during large magnetic storm. p0058 A72-26399

Type 3 solar burst distinction from auroral type high pass noise via spectrum analysis. p0062 A72-42043

Geomagnetic tail magnetic and electric fields ULF, VLF and ELF fluctuations, considering relationship to substorm processes. p0064 A72-44857

OGO-1 and OGO-3 VLF emission records of magnetospheric electromagnetic noise. [NASA-CR-107653] p0091 N70-15678

ELECTROMAGNETIC RADIATION

Electromagnetic emissions in vicinity of proton gyrofrequency from OGO 2 satellite measurements, noting sweep frequency receiver PCM and Rayspan special purpose data. p0013 A68-31481

OGO 5 observations of quasi-trapped electromagnetic waves in solar wind at 70 kHz. p0035 A70-36005

Atmospheric VLF electromagnetic emissions and electron instabilities data from satellite observation, detailing source regions, large amplitude electrostatic waves and wave-particle correlation. p0049 A71-30952

Electromagnetic waves in interplanetary space and effects on magnetosphere, considering solar wind characteristics due to wave interactions. p0050 A71-30956

Ionospheric electric and electromagnetic waves broadband characteristics, investigating auroral hiss and LHR noise. p0051 A71-33951

Electromagnetic wave observation in interplanetary medium and in magnetosphere, emphasizing magnetic and electric field measurements. p0065 A73-13855

Whistler propagation in magnetospheric ducts studies based on ray tracings verified by ground and satellite observations. p0087 N68-17981

OGO-1 and OGO-3 VLF emission records of magnetospheric electromagnetic noise. [NASA-CR-107653] p0091 N70-15678

ELECTROMAGNETIC SCATTERING

OGO 5 satellite measurements of intensity and width of Lyman alpha line scattered by hydrogen geocorona. p0022 A69-31412

SUBJECT INDEX

ELECTROMAGNETIC WAVE TRANSMISSION

Satellite observations of equatorial erosion and defocusing of VLF waves propagating at low magnetic latitudes

p0029 A70-18532

OGO-D electromagnetic wave propagation measurements with whistler and hiss formations in plasmasphere

[NASA-CR-130351] p0100 N73-16126

ELECTRON ACCELERATORS

Rise time in 20-32 keV impulsive X-radiation.

p0080 A74-38468

ELECTRON BEAMS

Suprathermal electron beam induced HF wave instability in solar wind upstream from earth bow shock, interpreting OGO 5 observations

p0053 A71-43158

ELECTRON BOMBARDMENT

Aurora formation by electron injection and drift in upper atmosphere

p0095 N71-25272

ELECTRON COUNTERS

Low energy electrons on day side of magnetosphere observed with MIT electron detector on OGO 3 satellite

p0018 A69-14027

Electron detector for OGO-E to measure flux and energy spectrum of electrons in primary cosmic rays [IEEE PAPER 3C-4]

p0019 A69-19198

Solid state detector for electron spatial distribution measurements on OGO-6 satellite, discussing design emphasizing reliability

p0024 A69-36676

Electron intensity long term variations above 500 MeV by OGO-5 satellite-borne cosmic ray electron detector, supporting diffusion-convection theory of solar modulation

p0036 A70-37522

ELECTRON DECAY RATE

Model of electrons artificially injected into inner radiation belt by Starfish nuclear explosion [NASA-TM-X-66211]

p0102 N73-20842

ELECTRON DENSITY (CONCENTRATION)

Low energy electron spatial distribution in magnetosphere obtained with OGO 1 and 3 indicate lower energies and higher densities occur during geomagnetic disturbances

p0012 A68-28348

Low energy electrons on day side of magnetosphere observed with MIT electron detector on OGO 3 satellite

p0018 A69-14027

Electron densities between inner edge plasma sheet and plasmasphere as function of geocentric radial distance from OGO-3 electrostatic measurements

p0039 A70-43834

The prevalence of second harmonic radiation in type 3 bursts observed at kilometric wavelengths.

p0071 A73-32964

Solar wind density model from km-wave type 3 bursts.

p0071 A73-32965

Electron concentrations calculated from the lower hybrid resonance noise band observed by OGO-3

p0074 A73-41912

Measurement of ionospheric and exospheric electron content using radio beacons on orbiting geophysical observatories: Compilation of data and final report [B18548-000]

p0113

A model environment for outer zone electrons [NASA-TM-X-69989]

p0106 N74-20503

OGO-6 experiment F-03 --- analysis of data obtained with retarding potential analyzer [NASA-CR-132943]

p0106 N74-20542

ELECTRON DENSITY PROFILES

Flux, energy distribution and density of ions and electrons in magnetosphere plasma during solar activity period determined by OGO-3 electrostatic probes

p0012 A68-29421

Magnetosphere low energy proton and electron density spatial distributions and temporal variations from OGO 3 satellite observations

p0013 A68-34245

Magnetospheric plasmopause shape, changes of electron density and wave phenomena

p0014 A68-37940

Solid state detector for electron spatial distribution measurements on OGO-6 satellite, discussing design emphasizing reliability

p0024 A69-36676

Solar X ray contribution to E layer ionization [NASA-CR-73884]

p0088 N69-17412

Protonospheric electron concentration profiles based on Doppler and Faraday effects

[NASA-CR-100778] p0089 N69-24521

Jicamarca radio observations of temperature and electron density profiles, films of Spread F structure, and nightglow emission intensities

[NASA-CR-121984] p0096 N71-35437

ELECTRON DIFFUSION

Electron injection and diffusion into electron inner radiation belt after solar flare, measuring electron fluxes by OGO 3 spectrometer

p0017 A68-41697

Cosmic ray electrons solar modulation, considering diffusion-convection theory

p0040 A78-45769

Pitch-angle diffusion of radiation belt electrons within the plasmasphere.

p0060 A72-35597

ELECTRON DISTRIBUTION

Drift shell splitting in nondipolar distorted magnetosphere tested with data from electron spectrometer on ATS 1 and OGO 3 satellites

p0026 A69-40508

Van Allen radiation belts energetic electrons injection and distribution due to magnetic storms, using satellite-borne spectrometers

p0033 A70-30090

High latitude observation of precipitating electron spikes by polar orbiter OGO 4 satellite, noting population dependence on local trapping limit

p0060 A72-35591

Satellite studies of magnetospheric substorms on August 15, 1968. 6: OGO 5 energetic electron observations. Pitch angle distributions in the nighttime magnetosphere

p0072 A73-33454

Temporal variations of 40 keV electrons in magnetosphere during and after magnetic storm on April 18, 1965

[NASA-CR-85905] p0086 N67-31362

ELECTRON EMISSION

Emission structure of large electron active region McMath plage 8905 mapped by 40 keV solar flare electrons

p0044 A71-17918

Type 3 radio bursts correlation with solar flares and electron events from OGO 5, IMP 5 and Explorer 35 observations

p0066 A73-17047

ELECTRON ENERGY

Electron energy spectra analyzed in earth magnetosphere using OGO 3, noting relation to radial distance

p0007 A67-19926

Auroral electron energy spectra measured from 180 to 250 km using electrostatic analyzer and channeltron detector, discussing electron flux

p0012 A68-25969

Low energy electron spatial distribution in magnetosphere obtained with OGO 1 and 3 indicate lower energies and higher densities occur during geomagnetic disturbances

p0012 A68-28348

Solid state detector system for electron measurements on OGO-6

p0014 A68-34540

Ambient electron energy spectrum secondary peak determined from unducted magnetospherically reflected whistler mode radiation measurements

p0015 A68-38428

Low energy interplanetary positrons detection by OGO satellites, discussing possible existence of equilibrium charge ratio

p0015 A68-41427

Low energy electrons in magnetosphere from OGO-1 and OGO-3 observations, discussing plasma sheet, magnetic bay activity, electron pressure, temperature and density gradient

p0019 A69-19373

Low energy electron precipitation data at northern high latitudes obtained from satellite low altitude polar orbit

p0021 A69-28964

Quiet time primary cosmic ray electron flux and energy spectrum from 10 to 200 Mev in interplanetary space observed by OGO 5 satellite

p0027 A70-12902

Hydrogen, He and oxygen ion density, and ion and electron temperatures in upper ionosphere from OGO 4 observations

p0035 A70-36016

ELECTRON FLUX DENSITY

Electron intensity long term variations above 500 MeV by OGO-5 satellite-borne cosmic ray electron detector, supporting diffusion-convection theory of solar modulation

p0036 A70-37522

Impulsive solar flare X rays spectral characteristics, examining electron energy, bremsstrahlung, microwave bursts and particle escape, collisions and injection

p0043 A71-15937

Suprathermal electron temperature and ion composition as function of geomagnetic latitude in polar ionosphere, using Explorer 31 mass spectrometer measurements

p0049 A71-30037

Gum Nebula size, density and electron temperature data from RAE-1 and OGO-5 satellites and ground based telescopes observations, correlating with Vela X supernova outburst

p0052 A71-35409

OGO-5 measurement of 10-200 MeV cosmic ray electron energy spectra, discussing quiet time flux intensity

p0055 A72-16719

Measurements of electron detection efficiencies in solid state detectors.

p0061 A72-39401

The role of energetic electrons in the correlation of meter and decimeter type III bursts with 4 keV X-ray emission.

p0064 A73-11391

Comparison of Te and Ti from OGO-6 and from various incoherent scatter radars.

p0067 A73-19241

OGO-6 measurements of supercooled plasma in the equatorial exosphere.

p0068 A73-22066

Errors in ion and electron temperature measurements due to grid plane potential, nonuniformities in retarding potential analyzers

p0071 A73-33436

Effects of interhemisphere transport on plasma temperatures at low latitudes.

p0074 A73-41919

Solar wind and magnetosheath electron temperature measurements by triaxial electron analyzer onboard OGO-5, presenting data for bow shock

p0075 A73-45112

Energy distribution of photoelectrons emitted from a surface on the OGO-5 satellite and measurements of satellite potential.

p0076 A74-17648

The 1972 cosmic ray electron spectrum above 0.5 GeV. --- mechanism for distortion by solar modulation

p0078 A74-27700

The cosmic ray electron spectrum and its modulation from 1968 through 1972.

p0079 A74-30908

Acceleration of electrons in solar flares.

p0079 A74-30908

Rise time in 20-32 keV impulsive X-radiation.

p0080 A74-38468

Energetic electrons and protons observed on OGO-5, March 6-10, 1970 [B07587-000]

p0111

Instrumentation and calibrations of low energy proton and electron experiment for Orbiting Geophysical Observatories

p0084 N66-13640

Trapped electron environment in inner and outer radiation belts - tables and graphs

p0084 N66-35685

Cinematographic display of observations of low energy proton and electron spectra in terrestrial magnetosphere

p0087 N68-15232

Energetic electron intensities in outer radiation zone of earth measured by OGO-1 satellite

p0088 N69-12899

F-02 experiment onboard OGO-6, and computer program for analysis of raw data [NASA-CR-130128]

p0100 N73-13376

Coronal electron temperature associated with solar flares

p0108 N74-74629

ELECTRON FLUX DENSITY

Electron injection and diffusion into electron inner radiation belt after solar flare, measuring electron fluxes by OGO 3 spectrometer

p0017 A68-41697

Low energy electron precipitation data at northern high latitudes obtained from satellite low altitude polar orbit

p0021 A69-28964

ELECTRON PLASMA

Quiet time primary cosmic ray electron flux and energy spectrum from 10 to 200 MeV in interplanetary space observed by OGO 5 satellite

p0027 A70-12902

Electron intensity long term variations above 500 MeV by OGO-5 satellite-borne cosmic ray electron detector, supporting diffusion-convection theory of solar modulation

p0036 A70-37522

Inner belt electron flux variations following geomagnetic storms from satellite instrument data

p0042 A71-14212

Low energy electron and proton fluxes in geomagnetic tail of equatorial magnetosphere forming plasma sheet related to auroral oval

p0049 A71-30029

Solar wind 10-9900 eV electron flux, evaluating energy transport in plasma rest frame

p0055 A72-13507

OGO-5 measurement of 10-200 MeV cosmic ray electron energy spectra, discussing quiet time flux intensity

p0055 A72-16719

Electron polar cap and the boundary of open geomagnetic field lines.

p0063 A72-44522

Evidence for a common origin of the electrons responsible for the impulsive X-ray and type 3 radio bursts.

p0067 A73-20766

Short-term intensity fluctuation of cosmic-ray electrons between 0.5 and 10 GeV.

p0079 A74-31903

Temporal variations of 40 keV electrons in magnetosphere during and after magnetic storm on April 18, 1965

[NASA-CR-85905] p0086 N67-31362

OGO outer zone observational data on electron intensities of earth geomagnetic field

[NASA-CR-89652] p0087 N67-40126

Photoelectron flux measurements in topside ionosphere using retarding potential analyzers

[NASA-TM-X-63358] p0087 N68-35999

Energetic electron intensities in outer radiation zone of earth measured by OGO-1 satellite

p0088 N69-12899

Cosmic ray electrons and solar flare particles from OGO-E and Explorer 33 data for identifying solar flare electrons

p0090 N69-38983

OGO-E electrostatic spectrometer measurements on electron flux near magnetopause

p0095 N71-25273

ELECTRON PLASMA

Low energy electrons in magnetosphere from OGO-1 and OGO-3 observations, discussing plasma sheet, magnetic bay activity, electron pressure, temperature and density gradient

p0019 A69-19373

Magnetic field and electron plasma observations near dawn magnetopause by triaxial spectrometer and fluxgate magnetometer on satellite OGO 5

p0050 A71-31754

Nonthermal electrons interaction with electron plasma oscillations and HF transverse waves in upstream solar wind.

p0052 A71-37353

Electron plasma oscillations distribution upstream from earth bow shock, evaluating OGO-5 plasma wave detector data

p0057 A72-23019

Detection of solar-wind electron plasma frequency fluctuations in an oblique nonlinear magnetohydrodynamic wave.

p0061 A72-35610

Nonlinear frequency correction to plasma instability at half harmonics of electron gyrofrequency as observed by OGO 5 near geomagnetic equator outside plasmopause

p0068 A73-22069

ELECTRON PRECIPITATION

Low energy electron precipitation data at northern high latitudes obtained from satellite low altitude polar orbit

p0021 A69-28964

Properties of higher latitude region of structured low energy electron precipitation in noon hemisphere, relating radiation with optical emissions in dayside auroral oval

p0048 A71-27911

High latitude regions of low energy electron precipitation from OGO 4 satellite auroral particle experiment

p0049 A71-30032

Atmospheric VLF electromagnetic emissions and electron instabilities data from satellite observation, detailing source regions, large amplitude electrostatic waves and wave-particle correlation.

p0049 A71-30952

Relativistic electron precipitation during magnetic storms, showing cyclotron resonances with electromagnetic ion cyclotron waves

p0051 A71-33948

VLF auroral hiss comparison with low energy electron precipitation, using OGO 4 data

p0056 A72-19149

Thermospheric composition variations in south polar regions during magnetically quiet periods from OGO-6 observations, considering atmospheric heating by electron precipitation cyclic variations

p0060 A72-32964

High latitude observation of precipitating electron spikes by polar orbiter OGO 4 satellite, noting population dependence on local trapping limit

p0060 A72-35591

Pitch-angle diffusion of radiation belt electrons within the plasmasphere.

p0060 A72-35597

Properties of low energy particle impacts in the polar domain in the dawn and dayside hours.

p0061 A72-39541

Precipitation of low-energy electrons at high latitudes: Effects of interplanetary magnetic field and dipole tilt angle.

p0066 A73-15531

Distributions and characteristics of high-latitude field-aligned electron precipitation.

p0069 A73-26988

Latitude and local time dependence of precipitated low-energy electrons at high latitudes.

p0074 A73-41914

A correlated study of ELF waves and electron precipitation on OGO-6.

p0077 A74-24766

Electron precipitation patterns and substorm morphology [B16756-000]

p0112

Synoptic study of field-aligned electron precipitation in auroral regions [NASA-TM-X-66065]

p0099 N73-10392

Reduction and analysis of trapped and precipitating electron data from OGO 6 spectrometer experiment F-16

p0100 N73-15863

Effects of season altitude and pitch angle on electron precipitation from OGO-D data [NASA-TM-X-66260]

p0102 N73-25868

ELECTRON PROBES

Triaxial electron spectrometer, mounted on OGO-5 spacecraft, measures flux and energy distributions of electrons, noting electron multiplier

p0005 A66-23689

ELECTRON RADIATION

LF and VLF wideband noise called auroral hiss observed by Byrd ground station and OGO 2, proposing incoherent Cerenkov radiation from 1 keV electrons

p0011 A68-19752

High latitude electron bursts observed by OGO 4, postulating electric field acceleration mechanism beyond 3 earth radii for ambient thermal plasma electrons

p0017 A68-43443

Cosmic ray electron search and study, comparing near earth to interstellar spectrum

p0060 A72-33869

Electron pitch angle distributions throughout the magnetosphere as observed on OGO-5.

p0068 A73-24732

Solar electrons, galactic electron radiation modulation and spectrum of high energy cosmic ray electrons.

p0071 A73-33293

Samples of electron spectroscopy and ionization chamber data plots from OGO-1 and OGO-3 [NASA-CR-107885]

p0092 N70-17624

ELECTRON SCATTERING

Interplanetary electron associations with type 3 solar bursts, using decametric OGO 3 and solar geophysical observations

p0054 A71-43176

Electron scattering effects on response of cosmic ray particle telescopes from pulse height and counting rate measurements

p0057 A72-21510

Electromagnetic hiss and relativistic electron losses in the inner zone [B22613-000]

p0114

ELECTRON SOURCES

High latitude electron bursts observed by OGO 4, postulating electric field acceleration mechanism beyond 3 earth radii for ambient thermal plasma electrons

p0017 A68-43443

ELECTRON TRAJECTORIES

Shadowing of electron azimuthal-drift motions near the noon magnetopause.

p0065 A73-12442

The reduction and analysis of electron data for outer zone electron model AE-4. Volume 3: OGO-1 and 3 University of Minnesota experiment data [NASA-TM-X-70212]

p0109 N74-74636

ELECTRONIC EQUIPMENT TESTS

OGO triaxial search coil magnetometer Final Engineering Report [NASA-CR-100619]

p0108 N69-72494

ELECTRONIC SPECTRA

Long term variations of cosmic ray electron spectrum above 500 MeV from balloon and satellite observations, noting reduction during Forbush decreases

p0037 A70-38105

Interstellar cosmic ray electron spectrum flattening below 3 GeV from OGO-5 observations

p0037 A70-38106

Solar flare electron spectra in interplanetary space and within earth magnetosphere, investigating simultaneous observations by satellite-borne magnetic electron spectrometers

p0046 A71-21037

Nonthermal electron spectra hardness limit during flash phase of solar flares from OGO-5 observation

p0055 A72-14561

ELECTRONS

Electron and proton spectrometer detector mounted on OGO-5, measurements cover seven differential energy channels

p0005 A66-23690

Electron spectra, pitch angle distributions and total ionization measured throughout radiation belts by satellite magnetic spectrometer and integrating ionization chamber

p0008 A67-25807

OGO 3 observation of low energy protons and electrons in earth magnetosphere, noting narrow peak of relatively high low-energy particle intensities

p0008 A67-26312

Electron measurements near weak aurora during rocket flight

p0008 A67-33595

Auroral electron energy spectra measured from 180 to 250 km using electrostatic analyzer and channeltron detector, discussing electron flux

p0012 A68-25969

Electron detector for OGO-E to measure flux and energy spectrum of electrons in primary cosmic rays [IEEE PAPER 3C-4]

p0019 A69-19198

HF electrostatic waves generation by electrons in magnetosphere

p0033 A70-30083

Cosmic ray electron and positron differential energy spectra during solar quiet times from OGO5 satellite observations in interplanetary space

p0036 A70-38096

Earth bow shock internal structure based on correlated observations of magnetic field, ELF magnetic fluctuations and suprathermal electrons by OGO 5 satellite

p0051 A71-33943

Measurements of the primary cosmic ray electron spectrum between 20 MeV and 20 GeV and its changes with time [B08373-000]

p0112

Relativistic electrons in space [B13262-000]

p0112

Energy spectrum of cosmic-ray electrons from 0.5 to 10 GeV [B14744-000]

p0112

Observation of cosmic-ray electrons with the OGO-5 satellite [B14745-000]

p0112

Relativistic electron events in interplanetary space [B17665-000]

p0113

SUBJECT INDEX

Acceleration of electrons in the absence of detectable optical flares deduced from type 3 radio bursts, H-alpha activity and soft X-ray emission [B22607-000] p0114

Models of trapped electron environment of inner radiation belt at synchronous orbit altitudes [NASA-SP-3024-VOL-3] p0085 N67-19899

Laboratory tests on interference sensitivity of polar OGO airglow photometer [NASA-TM-X-55791] p0085 N67-27578

Effects of energetic particles on photomultipliers in earth orbits up to 1500 km [NASA-TM-X-63419] p0089 N69-18074

Electron fluxes from 50 keV to 4 MeV in inner radiation belt by spectrometer on OGO 1 and 3 [NASA-CR-100648] p0089 N69-19899

Local time asymmetries in increase of electron fluxes in outer Van Allen zone during substorms [NASA-CR-100419] p0089 N69-20849

Plasma proton and plasma electron prototype and flight models [NASA-CR-122351] p0097 N72-18715

OGO 1 and 3 spectrometer and ion chamber data on dynamic processes governing electrons in radiation belts, and applicability of diffusion theories and magnetic field models [NASA-CR-127455] p0098 N72-28802

Comparison of simultaneous particle detector and search coil magnetometer measurements of precipitating particles and field aligned currents from OGO-D [NASA-TM-X-66224] p0102 N73-21367

User guide to microfilm records of data obtained in energetic particle experiment with OGO-5 [UCRL-51307] p0102 N73-31150

The inner zone electron model AE-5 [NASA-TM-X-69987] p0106 N74-20502

Energetic electrons and protons observed on OGO-5, March 6-10, 1970 [NASA-CR-139265] p0109 N74-74662

Energetic electron and proton solar particle observations on OGO-5, January 24-30, 1971 [NASA-CR-139266] p0109 N74-74663

ELECTROSTATIC GENERATORS

HF electrostatic waves generation by electrons in magnetosphere p0033 A70-30083

ELECTROSTATIC PROBES

Electron depletion in the wake of ionospheric spacecraft: A comparison between results from Langmuir probes and antennas. p0072 A73-34783

Energy distribution of photoelectrons emitted from a surface on the OGO-5 satellite and measurements of satellite potential. p0076 A74-17648

Instrumentation and calibrations of low energy proton and electron experiment for Orbiting Geophysical Observatories [NASA-CR-68558] p0084 N66-13640

OGO-E electrostatic spectrometer measurements on electron flux near magnetopause p0095 N71-25273

A satellite ion-electron collector: Experimental effects of grid transparency, photoemission, and secondary emission [NASA-CR-139262] p0109 N74-74638

ELECTROSTATIC WAVES

Fast time-resolved spectra of earth bow shock electrostatic turbulence based on broadband analog electric data from OGO-5 p0031 A70-29111

HF electrostatic waves generation by electrons in magnetosphere p0033 A70-30083

Electrostatic turbulence in bow shock magnetic structures observed by OGO 5, explaining turbulence as ion acoustic or Buneman mode due to two stream instability p0035 A70-36006

Atmospheric VLF electromagnetic emissions and electron instabilities data from satellite observation, detailing source regions, large amplitude electrostatic waves and wave-particle correlation p0049 A71-30952

Turbulence of electrostatic electron cyclotron harmonic waves observed by OGO-5. p0060 A72-35599

Magnetospheric observations in OGO 5 plasma wave experiment, emphasizing electrostatic wave particles interaction with plasma p0065 A73-13883

Field-aligned currents, plasma waves, and anomalous resistivity in the disturbed polar cusp. p0069 A73-29964

ELECTROSTATICS

Weak electrostatic turbulence observation in earth bow shock magnetic field gradient, suggesting cyclotron drift instability role p0063 A72-44523

Charged particle distribution study in near earth region using orbiting spherical electrostatic analyzers or plasma probes [AD-700804] p0092 N70-28003

EMISSION SPECTRA

Electromagnetic emissions in vicinity of proton gyrofrequency from OGO 2 satellite measurements, noting sweep frequency receiver PCM and Rayspan special purpose data p0013 A68-31481

Magnetospheric VLF banded emissions spectral analysis, investigating OGO-5 data by high time resolution spectral techniques p0047 A71-24788

Global nitric oxide and gamma emission measurements with Ebert-Fastie scanning spectrometer onboard polar orbiting OGO 4 satellite p0064 A73-10878

Atomic oxygen emission line at 6300 A for low latitudes observed by OGO-D satellite [NASA-TM-X-65913] p0098 N72-26309

Possible low energy (E less than keV) nonthermal X-ray events --- analysis of proportional counter detector data from OGO-5 p0107 N74-21450

Optical, hard X-ray, and microwave emission during the impulsive phase of flares --- analysis of optical impulsive component in solar flares p0107 N74-21458

ENERGY ABSORPTION

Quiet-time solar neutron flux upper limit from OGO-6 neutron detector, evaluating solar cosmic ray acceleration, nuclear reaction and energy region p0074 A73-41498

ENERGY DISSIPATION

Measurements of electron detection efficiencies in solid state detectors. p0061 A72-39401

ENERGY DISTRIBUTION

Triaxial electron spectrometer, mounted on OGO-5 spacecraft, measures flux and energy distributions of electrons, noting electron multiplier p0005 A66-23689

OGO 3 observation of low energy protons and electrons in earth magnetosphere, noting narrow peak of relatively high low-energy particle intensities p0008 A67-26312

Flux, energy distribution and density of ions and electrons in magnetosphere plasma during solar activity period determined by OGO-3 electrostatic probes p0012 A68-29421

Energetic radiation from solar flares [B03940-000] p0111

ENERGY LEVELS

Low energy cosmic rays modulation and heliocentric gradient during solar minimum, comparing OGO 1 and 2 ion chamber measurements with other space and ground observations p0044 A71-18128

ENERGY SPECTRA

Measurement of differential energy spectra of protons, helium nuclei and heavy nuclei by cosmic radiation telescopes mounted on POGO and Pioneer satellites p0004 A66-23684

Primary cosmic ray charge and energy spectra for helium through oxygen during 1965 minimum solar modulation effect p0005 A66-26348

Explorer 18 satellite measurements of proton energy spectra in region corotating with sun, noting modulation of galactic cosmic radiation and source of continuous particle accelerations p0005 A66-34754

Chemical abundances and energy spectra of nuclei in galactic radiation measured in interplanetary space by OGO-1 satellite p0006 A66-34833

Skyhook balloon flight Geiger counter cosmic ray monitor measurements of energy and charge spectra of galactic rays at solar minimum p0006 A66-34847

Energy spectra and abundances of elements He through Si of galactic cosmic ray above 20 Mev per nucleon in nuclear charge range between 2 and 26 p0006 A67-11687

Electron energy spectra analyzed in earth magnetosphere using OGO 3, noting relation to radial distance p0007 A67-19926

Nuclear abundances of galactic and solar cosmic rays, discussing detector electronics system for measurement of particle energy spectrum p0008 A67-25852

OGO 3 observation of low energy protons and electrons in earth magnetosphere, noting narrow peak of relatively high low-energy particle intensities p0008 A67-26312

Solar and galactic particle spectra and composition measured with cosmic ray telescope mounted on satellite p0008 A67-27249

Electron measurements near weak aurora during rocket flight p0008 A67-33595

Charged particles of extraterrestrial ring current during geomagnetic storms, with OGO 3 measurements of proton and electron differential energy spectra p0009 A67-37401

Highest differential energy range of X rays during July 1966 solar flare suggests nonthermal bremsstrahlung origin of hard flare X rays p0011 A68-17769

Differential energy spectra of low energy protons and positive ions in earth inner radiation zone, using electrostatic analyzers aboard OGO-3 satellite p0011 A68-17771

Auroral electron energy spectra measured from 180 to 250 km using electrostatic analyzer and channeltron detector, discussing electron flux p0012 A68-25969

Low energy solar cosmic ray experiment for OGO-6 using double diffused depleted silicon diodes p0012 A68-27616

Ambient electron energy spectrum secondary peak determined from unducted magnetospherically reflected whistler mode radiation measurements p0015 A68-38428

Proton and He nuclei differential energy spectra and intensity variations in interplanetary space in 1-20 MeV per nucleon energy range p0015 A68-41420

Primary cosmic ray energy spectra and charge composition during 1965 solar modulation minimum, using scintillator photomultiplier detector on OGO 1 p0016 A68-41431

Low energy cosmic ray nuclei propagating in interstellar space analyzed by telescope onboard OGO 1 p0016 A68-41434

Electron detector for OGO-E to measure flux and energy spectrum of electrons in primary cosmic rays [IEEE PAPER 3C-4] p0019 A69-19198

Cosmic ray nuclei energy spectra and abundances above 20 Mev/nucleon determined by OGO-1 satellite experiment, considering He, B, C, N, O, Ne, Mg, Si, Mn, Fe, Co and Ni p0019 A69-20067

Solar protons in magnetospheric tail after flare of July 7, 1966 with isotropic pitch angle distribution, expressing energy spectrum as exponential in rigidity p0020 A69-21699

Quiet time primary cosmic ray electron flux and energy spectrum from 10 to 200 Mev in interplanetary space observed by OGO 5 satellite p0027 A70-12902

Cosmic ray electron and positron differential energy spectra during solar quiet times from OGO5 satellite observations in interplanetary space p0036 A70-38096

Interplanetary cosmic ray positrons energy spectral component with origin different from interstellar mesons decay p0036 A70-38098

Long term variations of cosmic ray electron spectrum above 500 MeV from balloon and satellite observations, noting decrease during Forbush decreases p0037 A70-38105

Low energy galactic cosmic radiation energy spectra and charge composition in 2-14 Z range by OGO-5, suggesting two component model for origin p0037 A70-38127

Directional differential energy spectra for proton intensities in outer radiation zone near magnetic equator from satellite observations p0043 A71-17261

Quiet time fluxes and differential energy spectra of protons and alpha particles at 2-20 MeV measured by cosmic ray detectors on OGO-3

p0044 A71-18127

Solar flare electrons at 10-200 MeV region, discussing energy spectra and time history

p0044 A71-18170

Cosmic ray neutron leakage flux and energy spectrum measurements in 0.01-10 MeV range by OGO 6 satellite-borne neutron detector

p0054 A72-10877

Nonthermal electron spectra hardness limit during flash phase of solar flares from OGO-5 observation

p0055 A72-14561

Heavy nuclei enrichment in solar accelerated particles, discussing differential energy spectra, photospheric and coronal abundances, satellite observation and agreement with galactic cosmic rays

p0055 A72-15366

OGO-5 measurement of 10-200 MeV cosmic ray electron energy spectra, discussing quiet time flux intensity

p0055 A72-16719

Behavior of outer radiation zone and a new model of magnetospheric substorm.

p0063 A72-44850

The 1972 cosmic ray electron spectrum above 0.5 GeV. --- mechanism for distortion by solar modulation

p0078 A74-27700

On the origin of low energy heavy nuclei below approximately 30 MeV per nucleon observed in interplanetary space during quiet times, 1968-72.

p0078 A74-30156

The cosmic ray electron spectrum and its modulation from 1968 through 1972.

p0079 A74-30204

Earth satellite experiment for measuring the charge and energy spectra of the primary cosmic rays

[B01634-000] p0111

Energy spectrum of cosmic-ray electrons from 0.5 to 10 GeV

[B14744-000] p0112

Trapped electron environment in inner and outer radiation belts - tables and graphs

[NASA-SP-3024-VOL-2] p0084 N66-35685

Propagation of high energy solar protons as observed by OGO C spacecraft

p0089 N69-23730

Differential energy spectra of cosmic ray protons and helium nuclei dominated by solar modulation of local interstellar spectra, and numerical solutions to transport equation

[NASA-CR-130298] p0100 N73-15837

Satellite measurement of cosmic ray abundances and spectra in charge range 2 equal to or less than 7 equal to or less than 10

[NASA-CR-135786] p0103 N73-33777

ENERGY STORAGE

Magnetic storm effects on neutral atmospheric composition above 400 km, discussing energy deposition

p0055 A72-13518

ENERGY TRANSFER

Probe for measuring energy transfer between satellite and upper atmosphere

p0004 A66-15922

Gas-surface energy transfer experiment on OGO-6 satellite, measuring upper atmosphere kinetic energy flux to determine accommodation and drag coefficients, density, etc.

p0024 A69-36680

Solar wind 10-9900 eV electron flux, evaluating energy transport in plasma rest frame

p0055 A72-13507

Energy and diffusive mass transport relation to thermospheric circulation, composition, temperature and mass density from three dimensional two constituent magnetic storm model

p0070 A73-29975

Gas-surface interaction studies

[B20296-000] p0113

Bombardment of OGO-6 surfaces by high-energy particles

[B20297-000] p0113

Instrument report for design of the gas-surface energy transfer experiments for OGO-F

[B20953-000] p0113

ENVIRONMENT MODELS

Models of trapped electron environment of inner radiation belt at synchronous orbit altitudes

[NASA-SP-3024-VOL-3] p0085 N67-19899

ENVIRONMENTAL RESEARCH SATELLITES

Magnetic property tests on OGO and environmental research satellites

p0090 N69-33977

ENVIRONMENTAL TESTS

Continuous-channel electron multipliers degradation in spacecraft environment simulation laboratory equipment

p0021 A69-29565

EQUATORIAL ELECTROJET

Equatorial electrojet characteristics observation during 1967-1970 with POGO satellite-borne magnetometers, noting anomaly characterized by sharp negative V-signature in width and variable amplitude

p0070 A73-31768

POGO satellite observed electrojet signature data comparison with daily geomagnetic variation amplitude measurement at equatorial ground station in India

p0070 A73-31769

POGO satellite observed electrojet current data comparison with ground measurement at Ibadan, discussing data ratios variation by upper earth mantle conductivity structure

p0070 A73-31772

POGO satellite observation of electrojet profiles compared with H variation around measurements, interpreting data by classical band current model

p0070 A73-31773

Correlation of satellite estimates of the equatorial electrojet intensity with ground observations at Addis Ababa

[B15846-000] p0112

Results of OGO 4 and 6 spacecraft observations of equatorial electrojet

[NASA-TM-X-65995] p0099 N72-30823

EQUATORIAL ORBITS

C, N and O nuclei abundances in radiation belt near geometric equator, using data obtained by OGO-5 satellite in 1968

p0041 A71-13475

EQUATORS

Far UV equatorial airglow and aurora intensities and occurrence frequencies from satellite observation

p0041 A71-11504

ESCAPE VELOCITY

Measurements of the atmospheric neutron leakage rate

p0076 A74-15356

EXOSPHERE

Response of ionospheric and exospheric electron contents to partial solar eclipse, using OGO 1 satellite

p0015 A68-38439

Latitudinal variations in exosphere thermal ion composition, examining evidence of solar and geomagnetic control of ion distribution

p0016 A68-41673

Ion depletion in high latitude exosphere, considering OGO 2 simultaneous observations of positive ion concentration, VLF signal propagation and whistlers

p0023 A69-34939

Exospheric neutral hydrogen temperature diurnal variation from satellite resonance filter data, suggesting Lyman alpha source external to geocorona

p0040 A70-43852

Lyman alpha radiation scattering observation by satellites, obtaining geocoronal atomic hydrogen distribution in thermosphere and exosphere

p0042 A71-14028

Seasonal density variations in thermosphere and exosphere, obtaining model from Explorers 19 and 39 drag measurements for comparison with OGO-6 mass spectroscopy

p0051 A71-33802

OGO-6 measurements of supercooled plasma in the equatorial exosphere.

p0068 A73-22066

Measurement of ionospheric and exospheric electron content using radio beacons on orbiting geophysical observatories: Compilation of data and final report

[B18548-000] p0113

Observed variations of the exospheric hydrogen density with exospheric temperature

[B22614-000] p0114

Evaluation of radio beacon data from satellite observation of earth exosphere - data scaling techniques

[NASA-CR-68307] p0084 N66-12993

EXPERIMENTAL DESIGN

OGO triaxial search coil magnetometer for measuring earth magnetic fluctuations, discussing design rationale and observation results

p0024 A69-36675

Solar cosmic ray experiment for the first Orbiting Geophysical Observatories

[B03937-000] p0111

Experiment data analysis report OGO-3: Experiment no. 1

[B03943-000] p0111

Experiment data analysis report OGO-A: Experiment no. 1

[B03944-000] p0111

Micrometeoroid experiment on the OGO 4 satellite

[B04201-000] p0111

University of Michigan radio astronomy experiment aboard the OGO-5 spacecraft

[B14718-000] p0112

Summary and future work (OGO-4 and OGO-6)

[B15849-000] p0112

The Orbiting Geophysical Observatory - tool for space research

[NASA-TN-D-1450] p0082 N62-15053

Small Explorer and large orbiting observatory classes of scientific satellites

[NASA-TM-X-55261] p0083 N65-29783

Response characteristics of ionization chamber and spectrometer experiments aboard Orbiting Geophysical Observatory (OGO)

[CR-87] p0084 N67-13710

Design of OGO-E experiment to measure energetic X-rays, electrons, protons, and alphas particle emissions from solar flares

[NASA-CR-122509] p0098 N72-28812

EXPLORER SATELLITES

Small Explorer and large orbiting observatory classes of scientific satellites

[NASA-TM-X-55261] p0083 N65-29783

EXPLORER 12 SATELLITE

Cosmic ray experiments for Explorer 12 and the Orbiting Geophysical Observatory using GeigerMuller counters, and scintillation counter telescopes

p0001 A63-20022

EXPLORER 18 SATELLITE

Explorer 18 satellite measurements of proton energy spectra in region corotating with sun, noting modulation of galactic cosmic radiation and source of continuous particle accelerations

p0005 A66-34754

EXPLORER 31 SATELLITE

Enhancements of red arc during maximum solar activity

p0097 N72-23334

EXPLORER 33 SATELLITE

Cosmic ray electrons and solar flare particles from OGO-E and Explorer 33 data for identifying solar flare electrons

p0090 N69-38983

Reply

[NASA-TM-X-70215] p0108 N74-74627

EXPLORER 35 SATELLITE

Four years of dust particle measurements in cislunar and selenocentric space from Lunar Explorer 35 and OGO 3

[B15918-000] p0112

EXTRATERRESTRIAL RADIATION

Fluxgate magnetometer for OGO-E spacecraft in observing MHD waves and magnetic field structures in space

p0007 A67-15724

Extraterrestrial hydrogen Lyman alpha emission source, investigating interstellar wind with OGO 5 satellite

p0047 A71-24438

New interpretations of extraterrestrial Lyman-alpha observations.

p0065 A73-12323

Extraterrestrial ultraviolet radiation and the parameter of the HI medium near the sun.

p0073 A73-39074

Integrating type ionization chamber applied to measurements of radiation in space

[NASA-CR-90060] p0087 N68-10422

Measurement of extraterrestrial Lyman alpha emission by OGO 5 satellite while outside geocorona

p0100 N73-10812

Development of model of scattering of solar Lyman alpha from spatial distribution of neutral hydrogen in interplanetary space

p0100 N73-10813

A model environment for outer zone electrons

[NASA-TM-X-69989] p0106 N74-20503

EXTRATERRESTRIAL RADIO WAVES

Magnetic fluctuations in ELF and VLF waves in space, discussing whistler phenomena and applications to magnetospheric probes

p0056 A72-21189

EXTREMELY LOW FREQUENCIES

OGO 5 observation of ULF geomagnetic fluctuation at polar cusp boundaries in terms of ionospheric drift wave and Kelvin-Helmholtz instabilities
p0068 A73-24744
Postmidnight chorus: A substorm phenomenon. --- outer magnetosphere
p0076 A74-18364
Intensity variation of elf hiss and chorus during isolated substorms
[B22603-000] p0114
OGO-D electromagnetic wave propagation measurements with whistler and hiss formations in plasmasphere
[NASA-CR-130351] p0100 N73-16126

EXTREMELY LOW RADIO FREQUENCIES

Magnetospheric ELF noise, discussing OGO 3 spectrum analysis
p0019 A69-18834
OGO 4 satellite observed band limited ELF hiss characteristics explanation by model based on generation at large wave normal angle in equatorial region
p0057 A72-23008
A correlated study of ELF waves and electron precipitation on OGO-6.
p0077 A74-24766

F

F REGION

Radiative recombination of atomic oxygen ions in nighttime F region UV radiation detected by polar-orbiting OGO 4 satellite
p0023 A69-34957
Geomagnetic effect on the neutral temperature of the F region during the magnetic storm of September 1969.
p0060 A72-35603
Atomic oxygen green line emission in nightglow from OGO-F photometer observations, calculating tropical F region electron density spatial distribution
p0060 A72-35604
Theoretical calculations of the F-region tropical ultraviolet airglow intensity.
p0062 A72-42418
Source and identification of heavy ions in the equatorial F layer.
p0063 A72-44516
OGO-6 measurements of supercooled plasma in the equatorial exosphere.
p0068 A73-22066
OGO 6 retarding potential analyzer observation of vertical and longitudinal gradients in ion concentrations below F region peak near magnetic equator
p0068 A73-24738
Magnetic control of near equatorial neutral thermosphere, calculating F region ionization anomaly and molecular nitrogen and atomic oxygen density latitudinal variations
p0069 A73-26997
A catalog of ionospheric F region irregularity behavior based on OGO-6 retarding potential analyzer data
p0075 A74-12640
Geophysical properties of the ionospheric irregularities responsible for radio scintillation.
[AIAA PAPER 74-53] p0077 A74-18754
In situ measurements of the spectral characteristics of F region ionospheric irregularities.
p0078 A74-27695
OGO-6 ion concentration irregularity studies
[NASA-CR-132814] p0103 N73-32286
OGO-6 experiment F-03 --- analysis of data obtained with retarding potential analyzer
[NASA-CR-132943] p0106 N74-20542

F 2 REGION

Meteoritic metallic ions above F 2 peak, discussing current density and transport mechanisms
p0039 A70-43841
Oxygen ion anticorrelation to molecular ion concentrations from OGO 6 observations in F 2 region
p0062 A72-42016
ISIS-1 satellite observations of the ionosphere at high southern latitudes.
p0068 A73-25753

FACT LAE

Emission structure of large electron active region McMath plage 8905 mapped by 40 keV solar flare electrons
p0044 A71-17918

FAILURE ANALYSIS

Design, test evaluation, and performance failure analysis of ion mass spectrometer for OGO-F
[NASA-CR-111146] p0094 N71-10588

FAR ULTRAVIOLET RADIATION

Auroral arcs far UV observations by OGO 4, discussing luminosity, morphology, position, etc.
p0030 A70-23493
Far UV equatorial airglow and aurora intensities and occurrence frequencies from satellite observation
p0041 A71-11504
Impulsive hard X ray and far UV emission during solar flares
p0045 A71-19825
Auroral spectrum analysis in 1200-4000 Å band, obtaining photon emission rates
p0058 A72-26402
Theoretical calculations of the F-region tropical ultraviolet airglow intensity.
p0062 A72-42418

FARADAY EFFECT

Protonospheric electron concentration profiles based on Doppler and Faraday effects
[NASA-CR-100778] p0089 N69-24521

FIELD EMISSION

OGO-E study of electric field emissions at geomagnetic equator
[NASA-CR-126238] p0097 N72-22383

FIELD STRENGTH

Fluxgate and Ru vapor magnetometers for space measurements over wide field intensities, reducing electronic phase shift and experiment weight
p0032 A70-30045

FIELD THEORY (PHYSICS)

Solar cosmic rays entry into magnetosphere, showing entrance on smoothly connected field lines
p0032 A70-30059
Effects of season altitude and pitch angle on electron precipitation from OGO-D data
[NASA-TM-X-66260] p0102 N73-25868

FINE STRUCTURE

Collision free earth shock wave gross and fine structure deduced from OGO 5 plasma diagnostics [AIAA PAPER 69-676] p0023 A69-33452
Satellite plasma diagnostics for electric and magnetic fields and fine structure of collisionless shocks in solar wind plasma flows and interplanetary shocks
p0032 A70-30069

FLUORESCENCE

Satellite ultraviolet measurements of nitric oxide fluorescence with a diffusive transport model.
p0074 A73-41925

FLUX (RATE)

Explorer 18 satellite measurements of proton energy spectra in region corotating with sun, noting modulation of galactic cosmic radiation and source of continuous particle accelerations
p0005 A66-34754
Electron spectra, pitch angle distributions and total ionization measured throughout radiation belts by satellite magnetic spectrometer and integrating ionization chamber
p0008 A67-25807
Electron measurements near weak aurora during rocket flight
p0008 A67-33595
Auroral electron energy spectra measured from 180 to 250 km using electrostatic analyzer and channeltron detector, discussing electron flux
p0012 A68-25969
Solid state detector system for electron measurements on OGO-6
p0014 A68-34540
Electron detector for OGO-E to measure flux and energy spectrum of electrons in primary cosmic rays [IEEE PAPER 3C-4] p0019 A69-19198
Description of OGO-1 and OGO-3 counting rate processing and resulting data. Cosmic ray spectra and fluxes experiment on OGO-1 and OGO-3
[B03716-000] p0111
Models of trapped electron environment of inner radiation belt at synchronous orbit altitudes
[NASA-SP-3024-VOL 3] p0085 N67-19899
Electron fluxes from 50 keV to 4 MeV in inner radiation belt by spectrometer on OGO 1 and 3
[NASA-CR-100648] p0089 N69-19899
Local time asymmetries in increase of electron fluxes in outer Van Allen zone during substorms
[NASA-CR-100419] p0089 N69-20849
Electron density profiles and production rates associated with 30 Jan. 1968 large X ray flare event [RSD-63] p0096 N71-36131
The inner zone electron model AE-5
[NASA-TM-X-69987] p0106 N74-20502

FLUX DENSITY

Meteors and micrometeoroids influx near earth (1965-1967)
p0014 A68-35397
Production processing of the data obtained by the UCLA OGO-5 fluxgate magnetometer
[B12880-000] p0112
Digital offset field generator for dynamic range extension of magnetometers
p0090 N69-33963

FOKKER-PLANCK EQUATION

Solar flare particle propagation: Comparison of a new analytic solution with spacecraft measurements.
p0068 A73-24727
Analytic solution to complete Fokker-Planck equation for solar flare particle propagation
[NASA-CR-122406] p0098 N72-29818

FORBUSH DECREASES

Long term variations of cosmic ray electron spectrum above 500 MeV from balloon and satellite observations, noting reduction during Forbush decreases
p0037 A70-38105
Forbush decreases and long term cosmic ray particle intensity changes, investigating spectral variations
p0044 A71-18137
Short-term intensity fluctuation of cosmic-ray electrons between 0.5 and 10 GeV.
p0079 A74-31903

FREE ELECTRONS

Solar flare injection and propagation of low energy protons and electrons in 7-9 July 1966 solar particle event
p0014 A68-37148

FREQUENCY DISTRIBUTION

Magnetic fluctuations in various frequency ranges, associated with earth bow shock, detected with search coil magnetometer on OGO 3
p0026 A69-40501

FREQUENCY RANGES

OGO-6 electric and electromagnetic fields measurement for ionosphere using dipole antenna, emphasizing broadband observation covering whistler mode waves
p0024 A69-36677

FREQUENCY RESPONSE

Drifting whistler frequency cutoff phenomena (striations) observation in low latitude by POGO satellites, discussing interpretation based on propagation effect
p0052 A71-39746

FREQUENCY SHIFT

Nonducted VLF walking trace whistlers and Doppler shifts in fixed frequency transmissions identified on OGO midlatitude spectrographic records
p0028 A70-15116

G

GALACTIC RADIATION

Differential response curves and mean rigidity of response of ion chambers aboard balloons and satellites in free space during long-term cosmicray variation from 1960 to 1965
p0003 A65-33664
Chemical abundances and energy spectra of nuclei in galactic radiation measured in interplanetary space by OGO-1 satellite
p0006 A66-34833
Skyhook balloon flight Geiger counter cosmic ray monitor measurements of energy and charge spectra of galactic rays at solar minimum
p0006 A66-34847
Energy spectra and abundances of elements He through Si of galactic cosmic ray above 20 Mev per nucleon in nuclear charge range between 2 and 26
p0006 A67-11687
Solar modulation of galactic protons and He nuclei during last solar cycle analyzed according to Parker theory
p0007 A67-19913
Nuclear abundances of galactic and solar cosmic rays, discussing detector electronics system for measurement of particle energy spectrum
p0008 A67-25852
Solar and galactic particle spectra and composition measured with cosmic ray telescope mounted on satellite
p0008 A67-27249
OGO cosmic ray measuring device involving charged particle detectors to measure spectra and chemical composition over selected energy intervals
p0012 A68-27615

GAMMA RAYS

Low energy galactic cosmic radiation energy spectra and charge composition in 2-14 Z range by OGO-5, suggesting two component model for origin

p0037 A70-38127

High energy galactic gamma rays search onboard OGO-5, tabulating results

p0038 A70-40690

Galactic gamma ray intensity near Cygnus by OGO-5 spacecraft-borne telescope with acoustic spark chamber, discussing source intensity

p0038 A70-40691

Heavy nuclei enrichment in solar accelerated particles, discussing differential energy spectra, photospheric and coronal abundances, satellite observation and agreement with galactic cosmic rays

p0055 A72-15366

Solar electrons, galactic electron radiation modulation and spectrum of high energy cosmic ray electrons.

p0071 A73-33293

Multiple parameter analysis of galactic and solar cosmic rays for chemical composition and charge distribution

p0091 N69-38984

GAMMA RAYS

High energy galactic gamma rays search onboard OGO-5, tabulating results

p0038 A70-40690

Galactic gamma ray intensity near Cygnus by OGO-5 spacecraft-borne telescope with acoustic spark chamber, discussing source intensity

p0038 A70-40691

Global nitric oxide and gamma emission measurements with Ebert-Fastie scanning spectrometer onboard polar orbiting OGO 4 satellite

p0064 A73-10878

Search for brief celestial X-ray bursts. --- supernovae or gamma ray flare stars origins

p0078 A74-30149

Cosmic gamma-ray burst detected with an instrument on board the OGO-5 satellite.

p0080 A74-31942

OGO-5 spark-chamber telescope for gamma-ray astronomy [B18277-000]

p0113

A double gamma-ray spectrometer to search for positrons in space

p0110 N74-77446

GAS DENSITY

Thermospheric atomic oxygen and molecular nitrogen densities from OGO 6 neutral atmospheric composition experiment, comparing with prediction by Jacchia models

p0062 A72-42431

Spatial and temporal behavior of atomic oxygen determined by OGO 6 airglow observations.

p0079 A74-30670

Latitudinal density distribution of gases in upper atmosphere

p0094 N71-25267

GAS-METAL INTERACTIONS

Gas-surface energy transfer experiment on OGO-6 satellite, measuring upper atmosphere kinetic energy flux to determine accommodation and drag coefficients, density, etc.

p0024 A69-36680

GAS-SOLID INTERFACES

Role of gas-surface interactions in the reduction of OGO-6 neutral particle mass spectrometer data.

p0073 A73-38941

GASES

Gas-surface interaction studies [B20296-000]

p0113

Instrument report for design of the gas-surface energy transfer experiments for OGO-F

[B20953-000]

p0113

Initial results from OGO-6 gas-surface experiment [B20954-000]

p0113

GEGENSCHNEIN

Orbiting Geophysical Observatory (OGO) for cosmic ray, radio astronomy and Gegenschein experiments including satellite description and orbit data

p0003 A65-22431

Display and processing program for data from gegenschein photometry experiment from OGO-B [NASA-TM-X-55907]

p0086 N67-35595

GEIGER COUNTERS

Cosmic ray experiments for Explorer 12 and the Orbiting Geophysical Observatory using GeigerMuller counters, and scintillation counter telescopes

p0001 A63-20022

Skyhook balloon flight Geiger counter cosmic ray monitor measurements of energy and charge spectra of galactic rays at solar minimum

p0006 A66-34847

Response to environment and radiation of an ionization chamber and matched geiger tube used on spacecraft

[NASA-CR-139255] p0108 N74-74624

GEMINID METEORIODS

Geminid meteoroid dust particles detection, determining velocity and orbital elements from OGO 3 flux measurements

p0050 A71-33741

GEOCENTRIC COORDINATES

Position and shape of neutral sheet in geocentric solar magnetospheric coordinate system from geomagnetic tail measurements

p0010 A68-13469

Electron densities between inner edge plasma sheet and plasmasphere as function of geocentric radial distance from OGO-3 electrostatic measurements

p0039 A70-43834

GEOCORONAL EMISSIONS

Solar Lyman-alpha radiation observed by OGO 4 spacecraft showing short term fluctuations superimposed with monthly variation

p0028 A70-15128

Exospheric neutral hydrogen temperature diurnal variation from satellite resonance filter data, suggesting Lyman alpha source external to geocorona

p0040 A70-43852

Lyman alpha radiation scattering observation by satellites, obtaining geocoronal atomic hydrogen distribution in thermosphere and exosphere

p0042 A71-14028

Neutral hydrogen Lyman-alpha measurements in outer geocorona and in interplanetary space by two channel photometer on OGO 5

p0059 A72-32955

Interpretation of OGO-5 Lyman alpha measurements in the upper geocorona.

p0066 A73-19233

Geocoronal hydrogen measurement experiment on OGO-E - methods of obtaining orbital and spacecraft parameters for data analysis

[NASA-TM-X-55276] p0083 N65-30651

Development of model of scattering of solar Lyman alpha from spatial distribution of neutral hydrogen in interplanetary space

p0100 N73-10813

GEOELECTRICITY

High latitude electron bursts observed by OGO 4, postulating electric field acceleration mechanism beyond 3 earth radii for ambient thermal plasma electrons

p0017 A68-43443

Magnetic and electric field changes across earth bow shock and magnetosheath, discussing Pioneer 8 and OGO-5 data

p0036 A70-37483

GEOMAGNETIC HOLLOW

OGO-B and OGO-E measurements on magnetospheric field magnitudes and disturbances caused by ring currents

p0095 N71-25271

GEOMAGNETIC LATITUDE

Suprathermal electron temperature and ion composition as function of geomagnetic latitude in polar ionosphere, using Explorer 31 mass spectrometer measurements

p0049 A71-30037

Rate of erosion of dayside magnetic flux based on a quantitative study of the dependence of polar cusp latitude on the interplanetary magnetic field.

p0075 A74-14274

Latitudinal density distribution of gases in upper atmosphere

p0094 N71-25267

GEOMAGNETIC MICROPULSATIONS

Pc i micropulsation source region relation to plasmopause, using amplitude and polarization measurements

p0043 A71-17263

Geomagnetic micropulsations distribution in magnetosphere, using OGO 3 and 5 data

p0046 A71-23635

Band limited micropulsations observed in space during magnetospheric substorm by fluxgate magnetometer on OGO 5

p0048 A71-27913

SUBJECT INDEX

Nighttime plasmopause and thermal ion plasma structures relationship to micropulsations, considering excitation in post storm recovery and diurnal plasma bulge regions

p0056 A72-17453

OGO-5 plasmopause crossing correlation with ground observations of Pi geomagnetic micropulsations

p0056 A72-21223

Correlation of ground-based measurements of structured Pc I micropulsations with OGO-V plasmopause observations.

p0067 A73-20652

GEOMAGNETIC PULSATIONS

Magnetic fluctuations in various frequency ranges, associated with earth bow shock, detected with search coil magnetometer on OGO 3

p0026 A69-40501

OGO 5 observation of ULF geomagnetic fluctuation at polar cusp boundaries in terms of ionospheric drift wave and Kelvin-Helmholtz instabilities

p0068 A73-24744

Postmidnight chorus: A substorm phenomenon. --- outer magnetosphere

p0076 A74-18364

GEOMAGNETIC TAIL

Resonant compression waves in geomagnetic tail estimated for frequency and spatial distribution by single layered two dimensional model

p0028 A70-15127

Solar flare particles entrance into geomagnetic tail, modifying diffusion model

p0040 A71-11494

Substorm related magnetic field variations in near geomagnetic tail from OGO 5 inbound pass

p0046 A71-21643

Solar wind compressed magnetic field in sunward magnetosphere and extended geomagnetic tail observation by Pioneer 7 spacecraft

p0049 A71-30028

Low energy electron and proton fluxes in geomagnetic tail of equatorial magnetosphere forming plasma sheet related to auroral oval

p0049 A71-30029

Magnetotail changes relationship to solar wind magnetic field and magnetospheric substorms from ground and satellite data

p0051 A71-33944

Earth corotating plasma tail evidence in plasmopause variations from high resolution proton distribution data obtained by OGO 4 satellite during magnetic storm

p0053 A71-43166

Magnetosphere and adjacent regions magnetic surveys by OGO 1 and 3 satellites, discussing magnetopause, bow shock, magnetosheath, geomagnetic tail, ring current and polar substorms

p0055 A72-12084

Outer magnetosphere near midnight at quiet and disturbed times.

p0063 A72-44513

Substorm related changes in the geomagnetic tail: The growth phase.

p0064 A72-44856

Geomagnetic tail magnetic and electric fields ULF, VLF and ELF fluctuations, considering relationship to substorm processes

p0064 A72-44857

Magnetic field strength change in equatorial plasmasphere, considering quiet ring current as equatorial sheet current extension of neutral sheet current in magnetospheric tail

p0064 A73-11732

Solar wind interaction with geomagnetic field, discussing magnetosphere polar cusp region and geomagnetic tail neutral sheet structure

p0065 A73-13871

Satellite studies of magnetospheric substorms on August 15, 1968. I: State of the magnetosphere.

p0071 A73-33449

Synoptic survey for the neutral life in the magnetotail during the substorm expansion phase.

p0073 A73-36275

The magnetotail and substorms. --- magnetic flux transport model

p0076 A74-17742

Observations of the internal structure of the magnetopause.

p0077 A74-21679

Plasma tail interpretations of pronounced detached plasma regions measured with OGO-5 [B20951-000]

p0113

SUBJECT INDEX

Substorm and interplanetary magnetic field effects on the geomagnetic tail lobes [B22611-000] p0114

Magnetospheric plasma tail study, using thermal proton density measurements from OGO 4 p0101 N73-17948

GEOMAGNETISM

IMP-2 and OGO-1 measurements on plasma characteristics in transition region between solar wind and geomagnetic field p0003 A65-25921

Geomagnetic field values obtained from OGO-2 satellite-mounted rubidium vapor magnetometer p0007 A67-23244

Main geomagnetic field data, discussing data conversion to computer-readable form p0009 A67-36901

Alpha particle proton ratio of geomagnetic field from data from charged-particle telescope on OGO 1 satellite p0009 A67-37412

Magnetic field observations by OGO-1, with profiles of bow shock and magnetopause encounters p0010 A68-11011

Magnetic field measurements in outer magnetosphere, emphasizing boundary regions and shock front characteristics p0010 A68-12172

International geomagnetic reference field model described by spherical harmonic coefficients with first and second time derivatives p0012 A68-26625

Plasmasphere thermal positive ion structure, determining distribution of hydrogen and helium positive ions in magnetosphere from OGO p0014 A68-37114

Latitudinal variations in exosphere thermal ion composition, examining evidence of solar and geomagnetic control of ion distribution p0016 A68-41673

Geomagnetic field minimum in southern Brazil, comparing satellites data maps p0017 A68-42083

Sudden magnetic field increase associated with July 8, 1966 sudden commencement observed by OGO 3 satellite in magnetotail p0018 A69-11226

OGO triaxial search coil magnetometer for measuring earth magnetic fluctuations, discussing design rationale and observation results p0024 A69-36675

Geomagnetic field model (POGO) to confirm eccentric dipole westward velocity secular decrease predicted by day length changes p0025 A69-37490

Magnetic dip equator position at E layer and gradient with time and altitude, using geomagnetic field models p0026 A69-42428

Ion temperature gradient along magnetic field lines in outer plasmasphere by thermal diffusion equations compared with electron temperature observations p0031 A70-26568

Geomagnetic field distortion in high beta magnetospheric regions from OGO observations for quiet and slightly disturbed conditions p0032 A70-30076

Geomagnetic dipole field disturbances by trapped particles, calculating self consistent equilibrium configuration for ring current dipole moments p0034 A70-31905

Magnetic and electric field changes across earth bow shock and magnetosheath, discussing Pioneer 8 and OGO-5 data p0036 A70-37483

Inner magnetosphere magnetic field mapping, deriving pogo model p0038 A70-39349

Solar geomagnetic seasonal ionization control of upper ionosphere longitudinal composition variations from polar satellite observations p0047 A71-24555

Geomagnetic field models validity from satellite data p0049 A71-29903

Earth bow shock internal structure based on correlated observations of magnetic field, ELF magnetic fluctuations and suprathermal electrons by OGO 5 satellite p0051 A71-33943

Magnetospheric magnetic field distortions under quiet and slightly disturbed conditions, obtaining scalar intensity with OGO 3 and 5 rubidium vapor magnetometer p0054 A72-10886

Earth bow shock magnetic field data correlation with OGO 5 flux gate magnetometer, using Tidman-Northrop theory p0056 A72-19145

Geomagnetic cutoffs for cosmic-ray protons for seven energy intervals between 1.2 and 39 Mev p0061 A72-38728

ULF wave observation by satellite, considering geomagnetic activity control of magnetospheric wave occurrence p0063 A72-42902

Electron polar cap and the boundary of open geomagnetic field lines. p0063 A72-44522

Weak electrostatic turbulence observation in earth bow shock magnetic field gradient, suggesting cyclotron drift instability role p0063 A72-44523

Satellite studies of magnetospheric substorms on August 15, 1968. 2: Solar wind and outer magnetosphere. p0071 A73-33450

Quiet time magnetospheric field depression at 2.3-3.6 earth radii. p0072 A73-33464

A magnetospheric field model incorporating the OGO-3 and 5 magnetic field observations. p0074 A73-43693

Near-earth magnetic disturbance in total field at high latitudes. 1: Summary of data from OGO-2, 4, and 6. 2: Interpretation of data from OGO-2, 4, and 6. p0080 A74-34019

World magnetic survey (WMS)- method for minimizing limitations of mathematical and graphical descriptions of earths magnetic field [NASA-RP-277] p0082 N64-27355

Geomagnetic secular variations, 1900-1965 [NASA-TM-X-55944] p0086 N67-37398

OGO outer zone observational data on electron intensities of earth geomagnetic field [NASA-CR-89652] p0087 N67-40126

Cinematographic display of observations of low energy proton and electron spectra in terrestrial magnetosphere p0087 N68-15232

Derivation of International Geomagnetic Reference Field with tables of spherical harmonic coefficients and test results of various magnetic field models [NASA-TN-D-6237] p0095 N71-32190

Resonant oscillations of geomagnetic field in magnetosphere caused by solar wind [NASA-TM-X-65644] p0096 N71-32519

Effects of crustal anomalies on satellite measurements of ambient geomagnetic field p0097 N72-23341

GEOMORPHOLOGY

Morphology of thermal and energetic particles in inner magnetosphere during geomagnetic disturbances and solar cycles p0034 A70-30358

GEOPHYSICAL SATELLITES

OGO-2 experiment 5010 and OGO-4 experiment 5010A [NASA-CR-140527] p0109 N74-76909

Orbiting Geophysical Observatories S-49, S-50 [NASA-TM-X-50488] p0110 N74-76913

Orbiting Geophysical Observatories [NASA-CR-140524] p0110 N74-76932

GEOPHYSICS

Detection of electric field turbulence in earth bow shock, noting wave amplitude correlation with magnetic field structure p0018 A69-14681

GRAPHS (CHARTS)

World magnetic survey (WMS)- method for minimizing limitations of mathematical and graphical descriptions of earths magnetic field [NASA-RP-277] p0082 N64-27355

Trapped electron environment in inner and outer radiation belts - tables and graphs [NASA-SP-3024-VOL-2] p0084 N66-35685

Graphical and tabular summaries of ionization rates in space recorded by OGO spacecraft ion chambers [NASA-CR-107886] p0092 N70-17448

GRATINGS (SPECTRA)

Nonfocusing grazing incidence monochromator which utilizes planar gratings and collimating slit systems p0005 A66-27326

HEAVY NUCLEI

GROUND STATIONS

Magnetic field data from OGO-2 spacecraft and surface magnetic observatories, noting magnetic storm occurrence and magnetosphere inflation and detection of polar ionospheric currents p0018 A69-11125

Correlation of satellite estimates of the equatorial electrojet intensity with ground observations at Addis Ababa [B15846-000] p0112

Observations of whistler mode signal propagation by OGO satellites from very low frequency ground station transmitters [NASA-CR-84869] p0085 N67-30831

A study of high latitude magnetic disturbance --- from magnetic field data obtained with OGO spacecraft and ground observatories p0105 N74-17058

GYROFREQUENCY

Electromagnetic emissions in vicinity of proton gyrofrequency from OGO 2 satellite measurements, noting sweep frequency receiver PCM and Rayspan special purpose data p0013 A68-31481

Banded chorus, VLF discrete emissions in magnetosphere in single variable frequency band with frequency depending on equatorial electron gyrofrequency p0023 A69-31981

Electric field fluctuations in magnetospheric plasma at multiples of local electron gyrofrequency due to plasma instability p0052 A71-37368

Nonlinear frequency correction to plasma instability at half harmonics of electron gyrofrequency as observed by OGO 5 near geomagnetic equator outside plasmopause p0068 A73-22069

H

H ALPHA LINE

Extraterrestrial hydrogen Lyman alpha emission source, investigating interstellar wind with OGO 5 satellite p0047 A71-24438

H alpha subflare associated X-ray burst of 10 October 1970 observed by balloon-borne scintillator and OGO 5 and SOLRAD 9 satellites p0064 A73-11389

X-radiation (E greater than 10 keV), H-alpha and microwave emission during the impulsive phase of solar flares p0066 A73-17041

Acceleration of electrons in the absence of detectable optical flares deduced from type 3 radio bursts, H-alpha activity and soft X-ray emission [B22607-000] p0114

HALL GENERATORS

Magnetic Hall probe developed for use in spectrometer system aboard OGO-E satellite [UCRL-14650-T] p0086 N67-30930

HARMONIC RADIATION

Turbulence of electrostatic electron cyclotron harmonic waves observed by OGO-5. p0060 A72-35599

Nonlinear frequency correction to plasma instability at half harmonics of electron gyrofrequency as observed by OGO 5 near geomagnetic equator outside plasmopause p0068 A73-22069

The prevalence of second harmonic radiation in type 3 bursts observed at kilometeric wavelengths. p0071 A73-32964

HAWAII

OGO-4 study [NASA-CR-139261] p0109 N74-74637

HEAT FLUX

Computation methods and results for orbital data, spacecraft angle, and heat input for OGO and specifically for EGO [NASA-TM-X-55428] p0084 N66-21006

HEAVY IONS

Source and identification of heavy ions in the equatorial F layer. p0063 A72-44516

HEAVY NUCLEI

Chemical abundances and energy spectra of nuclei in galactic radiation measured in interplanetary space by OGO-1 satellite p0006 A66-34833

NOV. 10, 1975

HELIUM

C, N and O nuclei abundances in radiation belt near geomagnetic equator, using data obtained by OGO-5 satellite in 1968

p0041 A71-13475

Heavy nuclei enrichment in solar accelerated particles, discussing differential energy spectra, photospheric and coronal abundances, satellite observation and agreement with galactic cosmic rays

p0055 A72-15366

Measurements of the iron-group abundance in energetic solar particles.

p0068 A73-23538

On the origin of low energy heavy nuclei below approximately 30 MeV per nucleon observed in interplanetary space during quiet times, 1968-72.

p0078 A74-30156

HELIUM

Explorer 18 satellite measurements of proton energy spectra in region corotating with sun, noting modulation of galactic cosmic radiation and source of continuous particle accelerations

p0005 A66-34754

Horizontal He distribution in upper atmosphere from OGO 6 mass spectrometric data normalization for altitude by Jacchia model atmosphere

p0046 A71-21647

Distribution of hydrogen and helium in the upper atmosphere.

p0064 A72-45593

Thermospheric wind effects on the distribution of helium and argon in the earth's upper atmosphere.

p0071 A73-33441

The solar cycle variation of the solar wind helium abundance

[B22609-000] p0114

HELIUM IONS

Light ion abundance measurements of OGO satellites and field aligned diffusive equilibrium theory with temperature and concentration latitudinal variations

p0021 A69-25157

Hydrogen and He ion distribution measurements, noting seasonal and local magnetic time variability

p0022 A69-31326

OGO 5 ion spectrometer for measuring oxygen, He and hydrogen ion concentration, noting functions as energetic particle analyzer and proton energy distribution measurement capability

p0024 A69-36679

Plasmaspheric ambient hydrogen and helium atomic cations density measurement by OGO 5 ion mass spectrometer during magnetic storm, noting relationship to auroral red arcs

p0053 A71-39833

The equatorial helium ion trough and the geomagnetic anomaly

[B22334-000] p0114

HELIUM ISOTOPES

Hydrogen and helium cosmic ray nuclei isotopic composition measured to clarify abundance ratios energy dependence below 75 MeV/nucleon

p0015 A68-41421

The isotopes of H and He in solar cosmic rays --- as observed by OGO-6

p0107 N74-21466

HIGH ENERGY ELECTRONS

Energetic solar proton and electron event observed in July 1966 by Explorer 33 and OGO-3, noting association with invisible solar hemisphere flare

p0020 A69-22181

Van Allen radiation belts energetic electrons injection and distribution due to magnetic storms, using satellite-borne spectrometers

p0033 A70-30090

Solar flare electrons at 10-200 MeV region, discussing energy spectra and time history

p0044 A71-18170

Relativistic electrons associated with solar particle events, measuring occurrence frequency, electron propagation and diffusion anisotropy.

p0048 A71-29057

Relativistic electron precipitation during magnetic storms, showing cyclotron resonances with electromagnetic ion cyclotron waves

p0051 A71-33948

Nonthermal electron spectra hardness limit during flash phase of solar flares from OGO-5 observation

p0055 A72-14561

High latitude observation of precipitating electron spikes by polar orbiter OGO 4 satellite, noting population dependence on local trapping limit

p0060 A72-35591

High energy electron spatial distribution in plasma sheet from OGO 5 magnetometer experiments

p0062 A72-42406

Satellite studies of magnetospheric substorms on August 15, 1968. 5: Energetic electrons, spatial boundaries, and wave-particle interactions at OGO-5.

p0072 A73-33453

Satellite studies of magnetospheric substorms on August 15, 1968. 6: OGO 5 energetic electron observations. Pitch angle distributions in the nighttime magnetosphere

p0072 A73-33454

Acceleration of electrons during the flash phase of solar flares.

p0079 A74-30287

HIGH ENERGY INTERACTIONS

Bombardment of OGO-6 surfaces by high-energy particles

[B20297-000] p0113

Characteristics of nonthermal electrons accelerated during the flash phase of small solar flares

p0106 N74-21445

Optical, hard X-ray, and microwave emission during the impulsive phase of flares --- analysis of optical impulsive component in solar flares

p0107 N74-21458

HIGH FREQUENCIES

HF electrostatic waves generation by electrons in magnetosphere

p0033 A70-30083

Distributions of high frequency waves upstream from earth's bow shock

[NASA-CR-139256] p0108 N74-74626

HISS

LF and VLF wideband noise called auroral hiss observed by Byrd ground station and OGO 2, proposing incoherent Cerenkov radiation from 1 kev electrons

p0011 A68-19752

VLF auroral hiss comparison with low energy electron precipitation, using OGO 4 data

p0056 A72-19149

OGO 4 satellite observed band limited ELF hiss characteristics explanation by model based on generation at large wave normal angle in equatorial region

p0057 A72-23008

OGO-5 observation of lower hybrid resonance noise, bursts, VLF hiss and whistlers near plasmapause during large magnetic storm

p0058 A72-26399

Plasmaspheric hiss intensity variations during magnetic storms.

p0080 A74-34038

Intensity variation of eif hiss and chorus during isolated substorms

[B22603-000] p0114

Electromagnetic hiss and relativistic electron losses in the inner zone

[B22613-000] p0114

OGO-D electromagnetic wave propagation measurements with whistler and hiss formations in plasmasphere

[NASA-CR-130351] p0100 N73-16126

HORIZON SCANNERS

High-altitude or small-earth limitations for advanced horizon sensor of Orbiting Geophysical Observatory /OGO-A/

[NASA-CR-83567] p0085 N67-22257

HYDROGEN

Hydrogen Lyman alpha nightglow models, discussing solar photon scattering in geocorona and hydrogen vertical distribution

p0022 A69-30191

Solar Lyman-alpha radiation observed by OGO 4 spacecraft showing short term fluctuations superimposed with monthly variation

p0028 A70-15128

Lyman alpha intensity and hydrogen concentration at 5 to 19 earth radii determined from OGO 3 spacecraft measurements

p0031 A70-27181

OGO 4 observations of hydrogen Lyman-alpha airglow surrounding earth, measuring dependence on solar zenith angle

p0035 A70-35764

Exospheric neutral hydrogen temperature diurnal variation from satellite resonance filter data, suggesting Lyman alpha source external to geocorona

p0040 A70-43852

Neutral hydrogen interstellar wind parameters from Lyman alpha sky background measurements outside geocorona by photometers on OGO 5

p0051 A71-33834

Neutral hydrogen Lyman-alpha measurements in outer geocorona and in interplanetary space by two channel photometer on OGO 5

p0059 A72-32955

Distribution of hydrogen and helium in the upper atmosphere.

p0064 A72-45593

Observed variations of the exospheric hydrogen density with exospheric temperature

[B22614-000] p0114

Geocoronal hydrogen measurement experiment on OGO-E - methods of obtaining orbital and spacecraft parameters for data analysis

[NASA-TM-X-55276] p0083 N65-30651

HYDROGEN ATOMS

UV OGO observations of atomic hydrogen and oxygen in airglow, comparing results to exospheric models of hydrogen geocorona

p0022 A69-31400

Lyman alpha radiation scattering observation by satellites, obtaining geocoronal atomic hydrogen distribution in thermosphere and exosphere

p0042 A71-14028

Neutral H concentration in upper atmosphere during solar minimum, using ion thermal energies from rocket and satellite mass spectrometric, radio and proton whistler measurements

p0054 A72-10361

Interpretation of OGO-5 Lyman alpha measurements in the upper geocorona.

p0066 A73-19233

Extraterrestrial ultraviolet radiation and the parameter of the HI medium near the sun.

p0073 A73-39074

HYDROGEN IONS

Light ion abundance measurements of OGO satellites and field aligned diffusive equilibrium theory with temperature and concentration latitudinal variations

p0021 A69-25157

Hydrogen and He ion distribution measurements, noting seasonal and local magnetic time variability

p0022 A69-31326

OGO 5 ion spectrometer for measuring oxygen, He and hydrogen ion concentration, noting functions as energetic particle analyzer and proton energy distribution measurement capability

p0024 A69-36679

Plasmasphere bulge region morphology from hydrogen ion concentration measurement by mass spectrometer on OGO 5 satellite

p0035 A70-36014

Simultaneous hydrogen ion composition measurements by upper ionospheric polar orbiting OGO 4 and eccentric orbiting magnetospheric OGO 3 at midlatitude

p0037 A70-38377

Hydrogen ion concentration measurements by OGO 5 in plasmasphere during intense magnetic storms accompanied by stable auroral red arcs

p0047 A71-24787

Plasmaspheric ambient hydrogen and helium atomic cations density measurement by OGO 5 ion mass spectrometer during magnetic storm, noting relationship to auroral red arcs

p0053 A71-39833

Hydrogen ions concentration in dayside region of plasmasphere from OGO 5 satellite mass spectrometry, noting plasmapause position as function of magnetic activity

p0054 A72-10892

HYDROGEN ISOTOPES

Hydrogen and helium cosmic ray nuclei isotopic composition measured to clarify abundance ratios energy dependence below 75 MeV/nucleon

p0015 A68-41421

The isotopes of H and He in solar cosmic rays --- as observed by OGO-6

p0107 N74-21466

HYDROGEN PLASMA

Electron concentrations calculated from the lower hybrid resonance noise band observed by OGO-3

p0074 A73-41912

HYPERSONIC WAKES

Complex impedance measurements for monopole antenna for electron densities in/out of OGO satellite wake in upper ionosphere

p0035 A70-35771

HYPERVELOCITY IMPACT

Sensors used in cosmic dust experiments studied for response to microparticle hypervelocity impacts, noting relationship to velocity

p0013 A68-29468

SUBJECT INDEX

NOV. 10, 1975

SUBJECT INDEX

HYSTERESIS

Hysteresis effect on cosmic ray modulation and gradient ionization near solar minimum from measurements made near earth with OGO 1 and 3 ion chambers

p0028 A70-15106

I

IMP

IMP-2 and OGO-1 measurements on plasma characteristics in transition region between solar wind and geomagnetic field

p0003 A65-25921

IMPEDANCE MEASUREMENTS

Complex impedance measurements for monopole antenna for electron densities in/out of OGO satellite wake in upper ionosphere

p0035 A70-35771

Electron depletion in the wake of ionospheric spacecraft: A comparison between results from Langmuir probes and antennas.

p0072 A73-34783

IN-FLIGHT MONITORING

In-flight radiometric calibration of low brightness OGO 4 airglow photometer

p0029 A70-15645

INCOHERENT SCATTERING

Geomagnetic equatorial ionospheric temperature, comparing incoherent scatter radar and OGO-D retarding potential analyzer values

p0052 A71-33956

Comparison of Te and Ti from OGO-6 and from various incoherent scatter radars.

p0067 A73-19241

Comparison of atomic oxygen measurements by incoherent scatter and satellite-borne mass spectrometer techniques.

p0078 A74-27713

Diurnal variation of the neutral thermospheric winds determined from incoherent scatter radar data [B22601-000]

p0114

INNER RADIATION BELT

Differential energy spectra of low energy protons and positive ions in earth inner radiation zone, using electrostatic analyzers aboard OGO-3 satellite

p0011 A68-17771

Electron injection and diffusion into electron inner radiation belt after solar flare, measuring electron fluxes by OGO 3 spectrometer

p0017 A68-41697

Inner belt electron flux variations following geomagnetic storms from satellite instrument data

p0042 A71-14212

Models of trapped electron environment of inner radiation belt at synchronous orbit altitudes [NASA-SP-3024-VOL-3]

p0085 N67-19899

Electron fluxes from 50 keV to 4 MeV in inner radiation belt by spectrometer on OGO 1 and 3 [NASA-CR-100648]

p0089 N69-19899

The inner zone electron model AE-5 [NASA-TM-X-69987]

p0106 N74-20502

INSTRUMENT ERRORS

Retarding potential analyzer errors and performance degradation due to grid plane potential depressions

p0058 A72-26411

Errors in ion and electron temperature measurements due to grid plane potential, nonuniformities in retarding potential analyzers

p0071 A73-33436

INTERACTIONS

Gas-surface interaction studies [B20296-000]

p0113

INTERFACES

OGO-5 observations of the physical processes occurring in the disturbed polar cusp and the cusp-magnetosheath interface [B18269-000]

p0113

INTERNATIONAL QUIET SUN YEAR

Orbiting Geophysical Observatory (OGO) for cosmic ray, radio astronomy and Gegenschein experiments including satellite description and orbit data

p0003 A65-22431

INTERPLANETARY DUST

Velocities of dust particles in cislunar space [B2004 A66-15266]

p0041 A71-14014

Picogram dust particle flux measurements in selenocentric, cislunar and interplanetary space by Mariner 4, OGO 3 and Explorer 35

p0041 A71-14014

Four years of dust particle measurements in cislunar and selenocentric space from Lunar Explorer 35 and OGO 3 [B15918-000]

p0112

Speeds, directions of arrival, and mass of dust particles measured from OGO-1 satellite to determine orbits of dust particles

p0086 N67-32070

INTERPLANETARY GAS

Extraterrestrial ultraviolet radiation and the parameter of the H I medium near the sun.

p0073 A73-39074

INTERPLANETARY MAGNETIC FIELDS

Explorer 18 satellite measurements of proton energy spectra in region corotating with sun, noting modulation of galactic cosmic radiation and source of continuous particle accelerations

p0005 A66-34754

Interplanetary magnetic field measurements from Mariner and OGO satellites at various paths, regions and intervals, finding dominant polarity effect dependent on sun latitude

p0027 A70-13980

Magnetopause inward motion before substorm, showing association with interplanetary field vertical component reversal

p0042 A71-14515

Solar wind compressed magnetic field in sunward magnetosphere and extended geomagnetic tail observation by Pioneer 7 spacecraft

p0049 A71-30028

Solar wind ion thermalization in earth bow shock by counterstreaming instability related to interplanetary magnetic field

p0050 A71-31774

Magnetotail changes relationship to solar wind magnetic field and magnetospheric substorms from ground and satellite data

p0051 A71-33944

Large amplitude interplanetary solar wind discontinuities observed by OGO-5 plasma spectrometer and magnetometers, considering magnetic drift waves mechanism for plasma turbulence generation

p0058 A72-29378

Polar-cap electric field distributions related to the interplanetary magnetic field direction.

p0062 A72-42432

Precipitation of low-energy electrons at high latitudes: Effects of interplanetary magnetic field and dipole tilt angle.

p0066 A73-15531

Dependence of the polar cusp on the north-south component of the interplanetary magnetic field.

p0072 A73-36273

Rate of erosion of dayside magnetic flux based on a quantitative study of the dependence of polar cusp latitude on the interplanetary magnetic field.

p0075 A74-14274

Substorm and interplanetary magnetic field effects on the geomagnetic tail lobes [B22611-000]

p0114

Diffusion-convection theory for solar cosmic ray propagation in interplanetary magnetic field

p0090 N69-29659

Possible noise sources in power spectra measurement of interplanetary magnetic field

p0099 N73-10791

Power spectra of interplanetary magnetic field near earth bow shock

p0099 N73-10792

Variation with interplanetary sector of the total magnetic field measured at the OGO 2, 4, and 6 satellites [NASA-TM-X-70531]

p0104 N74-13566

Reply [NASA-TM-X-70215]

p0108 N74-74627

Comments on a paper by J. P. Heppner. Polar cap electric field distributions related to interplanetary magnetic field direction [NASA-CR-139259]

p0108 N74-74632

INTERPLANETARY MEDIUM

Interplanetary cosmic ray positrons energy spectral component with origin different from interstellar mesons decay

p0036 A70-38098

Solar wind microscopic structure, examining interplanetary wave-particle interactions

p0042 A71-14068

Upstream discrete wave packets propagation interplanetary medium from OGO 5 observation

p0045 A71-19656

INTERSTELLAR RADIATION

Interplanetary electron associations with type 3 solar bursts, using decametric OGO 3 and solar geophysical observations

p0054 A71-43176

Large amplitude interplanetary solar wind discontinuities observed by OGO-5 plasma spectrometer and magnetometers, considering magnetic drift waves mechanism for plasma turbulence generation

p0058 A72-29378

Earth-solar wind bow shock structure from OGO-5 observations during passage from interplanetary medium into magnetosheath

p0058 A72-29379

Electromagnetic wave observation in interplanetary medium and in magnetosphere, emphasizing magnetic and electric field measurements

p0065 A73-13855

Direct measurements of solar-wind fluctuations between 0.0048 and 13.3 Hz.

p0068 A73-23539

Differential energy spectra of cosmic ray protons and helium nuclei dominated by solar modulation of local interstellar spectra, and numerical solutions to transport equation [NASA-CR-130298]

p0100 N73-15837

INTERPLANETARY SPACE

Zodiacal dust particle flux measurements from OGO 3 and Mariner 4 spacecraft in cislunar and interplanetary space

p0013 A68-29457

Proton and He nuclei differential energy spectra and intensity variations in interplanetary space in 1-20 MeV per nucleon energy range

p0015 A68-41420

Low energy interplanetary positrons detection by OGO satellites, discussing possible existence of equilibrium charge ratio

p0015 A68-41427

Quiet time primary cosmic ray electron flux and energy spectrum from 10 to 200 Mev in interplanetary space observed by OGO 5 satellite

p0027 A70-12902

Solar flare electron spectra in interplanetary space and within earth magnetosphere, investigating simultaneous observations by satellite-borne magnetic electron spectrometers

p0046 A71-21037

Proton energy change effects on charged particles propagating in interplanetary space, using low energy solar flare proton fluxes observations

p0046 A71-22801

Electromagnetic waves in interplanetary space and effects on magnetosphere, considering solar wind characteristics due to wave interactions

p0050 A71-30956

Neutral hydrogen Lyman-alpha measurements in outer geocorona and in interplanetary space by two channel photometer on OGO 5

p0059 A72-32955

On the origin of low energy heavy nuclei below approximately 30 MeV per nucleon observed in interplanetary space during quiet times, 1968-72.

p0078 A74-30156

Relativistic electron events in interplanetary space [B17665-000]

p0113

Multiple parameter analysis of galactic and solar cosmic rays for chemical composition and charge distribution

p0091 N69-38984

Solar flare protons and physical processes affecting particle propagation in interplanetary space

p0098 N72-27829

INTERSTELLAR GAS

Development of model of scattering of solar Lyman alpha from spatial distribution of neutral hydrogen in interplanetary space

p0100 N73-10813

INTERSTELLAR MATTER

Neutral hydrogen interstellar wind parameters from Lyman alpha sky background measurements outside geocorona by photometers on OGO 5

p0051 A71-33834

New interpretations of extraterrestrial Lyman-alpha observations.

p0065 A73-12323

INTERSTELLAR RADIATION

Extraterrestrial hydrogen Lyman alpha emission source, investigating interstellar wind with OGO 5 satellite

p0047 A71-24438

NOV. 10, 1975

INTERSTELLAR SPACE

The elemental abundance ratios of interstellar secondary and primary cosmic rays.
p0079 A74-30190

INTERSTELLAR SPACE

Interstellar cosmic ray electron spectrum flattening below 3 GeV from OGO-5 observations
p0037 A70-38106

Low frequency space radio astronomy
[NASA-TM-X-63976] p0093 N70-33175

ION CONCENTRATION

Latitudinal variations in exosphere thermal ion composition, examining evidence of solar and geomagnetic control of ion distribution
p0016 A68-41673

OGO 5 ion spectrometer for measuring oxygen, He and hydrogen ion concentration, noting functions as energetic particle analyzer and proton energy distribution measurement capability
p0024 A69-36679

Plasmapause observations by ion spectrometer aboard OGO-5 vehicle for early orbits, obtaining O, He and H ion concentration profiles for geomagnetic parameter
p0029 A70-18546

Hydrogen ion concentration measurements by OGO 5 in plasmasphere during intense magnetic storms accompanied by stable auroral red arcs
p0047 A71-24787

Hydrogen ions concentration in dayside region of plasmasphere from OGO 5 satellite mass spectrometry, noting plasmapause position as function of magnetic activity
p0054 A72-10892

Oxygen ion anticorrelation to molecular ion concentrations from OGO 6 observations in F 2 region
p0062 A72-42016

OGO-6 ion concentration irregularity studies
[NASA-CR-132814] p0103 N73-32286

ION CURRENTS

Spacecraft sheath structure, potential and velocity effects on ion current measurements by traps and mass spectrometers
p0038 A70-41087

ION CYCLOTRON RADIATION

Relativistic electron precipitation during magnetic storms, showing cyclotron resonances with electromagnetic ion cyclotron waves
p0051 A71-33948

Ion cyclotron waves observed in the polar cusp.
p0071 A73-33437

ION DENSITY (CONCENTRATION)

Light ion abundance measurements of OGO satellites and field aligned diffusive equilibrium theory with temperature and concentration latitudinal variations
p0021 A69-25157

Plasmapause position and density profile from ion concentration measurements by OGO-5, determining reaction to magnetic variations
p0032 A70-30074

Magnetosphere thermal ion density and temperature in dawn and morning quadrants from OGO 5 satellite measurements
p0040 A71-11498

Thermal positive ion densities measurement in outer ionosphere and magnetosphere by OGO 1 satellite, relating plasmapause distribution and magnetic activity level
p0057 A72-23011

Effect of satellite potential on direct ion density measurements through the plasmapause.
p0076 A74-18372

In situ measurements of amplitude and scale size characteristics of ionospheric irregularities: OGO-6 ion concentration irregularity studies
[B20340-000] p0113

High latitude proton precipitation and light ion density profiles during the magnetic storm initial phase
[B22333-000] p0113

The measurement of cold ion densities in the plasma trough
[B22610-000] p0114

Perturbations in density of ions and neutral particles in upper atmosphere due to OGO
[NASA-CR-117897] p0094 N71-23238

Analysis of light ion mass spectrometer data from OGO-E experiment
[NASA-CR-130156] p0101 N73-16432

High latitude minor ion enhancements: A clue for studies of magnetosphere-atmosphere coupling --- using OGO 6 ion mass spectrometer
[NASA-TM-X-70582] p0104 N74-16064

ION DISTRIBUTION

OGO-1 first results on mass spectrometry measurements of thermal positive ion composition at high altitudes
p0004 A66-14781

Differential energy spectra of low energy protons and positive ions in earth inner radiation zone, using electrostatic analyzers aboard OGO-3 satellite
p0011 A68-17771

Response of ionospheric and exospheric electron contents to partial solar eclipse, using OGO 1 satellite
p0015 A68-38439

Latitudinal variations in exosphere thermal ion composition, examining evidence of solar and geomagnetic control of ion distribution
p0016 A68-41673

Earth thermal plasmasphere contraction subsequent to solar flare obtained from ion mass spectrometers on OGO satellites
p0020 A69-23777

Hydrogen and He ion distribution measurements, noting seasonal and local magnetic time variability
p0022 A69-31326

Plasmapause irregular structure and position indicated by measured distributions of hydrogen and helium thermal positive ions in duskside magnetosphere
p0031 A70-29185

Seasonal and annual longitudinal variations in ionospheric ion distribution, stressing solar geomagnetic control importance
p0050 A71-33762

Plasmasphere hydrogen, helium, oxygen and nitrogen ions inbound and outbound profiles from OGO 5 mass spectrometric measurements
p0065 A73-12320

ION INJECTION

Solar flare injection and propagation of low energy protons and electrons in 7-9 July 1966 solar particle event
p0014 A68-37148

Active experiments, magnetospheric modification, and a naturally occurring analogue.
p0075 A74-14283

ION PRODUCTION RATES

OGO ion chamber measurement of ionization by penetrating radiation, discussing spike intensity
p0017 A68-43450

Graphical and tabular summaries of ionization rates in space recorded by OGO spacecraft ion chambers
[NASA-CR-107886] p0092 N70-17448

ION RECOMBINATION

Radiative recombination of atomic oxygen ions in nighttime F region UV radiation detected by polar-orbiting OGO 4 satellite
p0023 A69-34957

UV oxygen nightglow observation by OGO-4, examining ion-ion neutralization and radiative recombination production mechanisms
p0037 A70-39344

ION SOURCES

Source and identification of heavy ions in the equatorial F layer.
p0063 A72-44516

ION TEMPERATURE

Ion temperature gradient along magnetic field lines in outer plasmasphere by thermal diffusion equations compared with electron temperature observations
p0031 A70-26568

Hydrogen, He and oxygen ion density, and ion and electron temperatures in upper ionosphere from OGO 4 observations
p0035 A70-36016

Ionospheric ion temperature measurements by retarding potential analyzer on OGO-6 satellite
p0039 A70-43840

Magnetosphere thermal ion density and temperature in dawn and morning quadrants from OGO 5 satellite measurements
p0040 A71-11498

Solar wind ion thermalization in earth bow shock by counterstreaming instability related to interplanetary magnetic field
p0050 A71-31774

Geomagnetic equatorial ionospheric ion temperature, comparing incoherent scatter radar and OGO-D retarding potential analyzer values
p0052 A71-33956

Nighttime plasmapause and thermal ion plasma structures relationship to micropulsations, considering excitation in post storm recovery and diurnal plasma bulge regions
p0056 A72-17453

SUBJECT INDEX

Comparison of Te and Ti from OGO-6 and from various incoherent scatter radars.
p0067 A73-19241

OGO-6 measurements of supercooled plasma in the equatorial exosphere.
p0068 A73-22066

Errors in ion and electron temperature measurements due to grid plane potential, nonuniformities in retarding potential analyzers
p0071 A73-33436

ION TRAPS (INSTRUMENTATION)

Electron trap behavior on charged spacecraft, obtaining expressions for current to aperture and internal retarding electrodes for all apertures and spacecraft potentials
p0022 A69-31976

Spacecraft sheath structure, potential and velocity effects on ion current measurements by traps and mass spectrometers
p0038 A70-41087

Effect of satellite potential on direct ion density measurements through the plasmapause.
p0076 A74-18372

A satellite ion-electron collector: Experimental effects of grid transparency, photoemission, and secondary emission
[NASA-CR-139262] p0109 N74-74638

IONIC DIFFUSION

Light ion abundance measurements of OGO satellites and field aligned diffusive equilibrium theory with temperature and concentration latitudinal variations
p0021 A69-25157

IONIC MOBILITY

Plasmasphere hydrogen, helium, oxygen and nitrogen ions inbound and outbound profiles from OGO 5 mass spectrometric measurements
p0065 A73-12320

IONIZATION CHAMBERS

Differential response curves and mean rigidity of response of ion chambers aboard balloons and satellites in free space during long-term cosmic ray variation from 1960 to 1965
p0003 A65-33664

Studies of primary cosmic rays with ionization chambers. --- rigidity response of ionization chambers in high atmosphere and deep space for study of rigidity dependence of solar cycle modulation of primary cosmic ray
p0006 A66-34768

Electron spectra, pitch angle distributions and total ionization measured throughout radiation belts by satellite magnetic spectrometer and integrating ionization chamber
p0008 A67-25807

Solar flare energetic X-ray events detected by onboard satellite ionization chambers, studying relationship to radio burst and space particle emission
p0009 A67-41232

Cosmic ray knee interpretation using polar orbiting ionization chambers data from OGO-2/4
p0034 A70-31903

Response characteristics of ionization chamber and spectrometer experiments aboard Orbiting Geophysical Observatory (OGO)
[CR-87] p0084 N67-13710

Integrating type ionization chamber applied to measurements of radiation in space
[NASA-CR-90060] p0087 N68-10422

Absolute cosmic ray ionization measurements in upper and lower atmosphere
[NASA-CR-104068] p0090 N69-34536

Graphical and tabular summaries of ionization rates in space recorded by OGO spacecraft ion chambers
[NASA-CR-107886] p0092 N70-17448

Samples of electron spectroscopy and ionization chamber data plots from OGO-1 and OGO-3
[NASA-CR-107885] p0092 N70-17624

OGO 1 and 3 spectrometer and ion chamber data on dynamic processes governing electrons in radiation belts, and applicability of diffusion theories and magnetic field models
[NASA-CR-127455] p0098 N72-28802

Magnetospheric modulation effects on solar cosmic rays from simultaneous OGO 1 and 3 ion chamber data in 1968 and 1969
[NASA-CR-137075] p0105 N74-18420

Response to environment and radiation of an ionization chamber and matched geiger tube used on spacecraft
[NASA-CR-139255] p0108 N74-74624

Electron spectrometer and integrating ion chamber for the OGO-1 and OGO-3 missions
[NASA-CR-139263] p0109 N74-74639

SUBJECT INDEX

Reduction and analysis of data from OGO-C,D ion chamber experiment [NASA-CR-107184] p0110 N74-76923

IONIZATION CROSS SECTIONS

Quiet time cosmic ray ionization altitude dependence over polar regions from measurements by integrating ionization chamber on OGO-2 p0034 A70-31902

IONIZATION FREQUENCIES

High latitude ionization spikes observed by POGO spacecraft, noting frequency correlation with magnetic disturbances and development by high energy electron injections p0021 A69-28950

Ionization rate profiles from solar flare X rays observed by ion chambers aboard OGO 1 and OGO 3 [NASA-CR-94429] p0087 N68-23026

IONIZED GASES

Plasmapause irregular structure and position indicated by measured distributions of hydrogen and helium thermal positive ions in duskside magnetosphere p0031 A70-29185

IONOSPHERE

OGO-1 first results on mass spectrometry measurements of thermal positive ion composition at high altitudes p0004 A66-14781

Thermal positive ion densities measurement in outer ionosphere and magnetosphere by OGO 1 satellite, relating plasmapause distribution and magnetic activity level [AD-742186] p0057 A72-23011

Additional results from an OGO-6 experiment concerning ionospheric electric and electromagnetic fields in the range 20 Hz to 540 kHz. p0071 A73-33438

Measurement of ionospheric and exospheric electron content using radio beacons on orbiting geophysical observatories: Compilation of data and final report [B18548-000] p0113

Is the red arc a good indicator of ionosphere-magnetosphere conditions [B22605-000] p0114

An upper limit to the product of NO and O densities from 105 to 120 Km [B22606-000] p0114

Electromagnetic hiss and relativistic electron losses in the inner zone [B22613-000] p0114

A model ionosphere for mid-day and mid-latitude during sunspot minimum [SMUP-4] p0109 N74-74635

A light ion mass spectrometer experiment for OGO-E [NASA-CR-122291] p0110 N74-76914

IONOSPHERIC COMPOSITION

Ion cut-off whistlers observed during VLF experiment aboard OGO 2 and OGO 4, noting possible application to relative ionospheric proton concentration determination p0018 A69-14029

Hydrogen, He and oxygen ion density, and ion and electron temperatures in upper ionosphere from OGO 4 observations p0035 A70-36016

Suprathermal electron temperature and ion composition as function of geomagnetic latitude in polar ionosphere, using Explorer 31 mass spectrometer measurements p0049 A71-30037

Seasonal and annual longitudinal variations in ionospheric composition distribution, stressing solar geomagnetic control importance p0050 A71-33762

Thermospheric atomic oxygen and molecular nitrogen densities from OGO 6 neutral atmospheric composition experiment, comparing with prediction by Jacchia models p0062 A72-42431

Diurnal latitudinal composition variations in light ion trough from OGO mass spectrometric observations, noting magnetic storm effects p0065 A73-11904

The light-ion trough, the main trough, and the plasmapause. p0066 A73-15533

Parametric description of thermospheric ion composition results p0067 A73-19255

Auroral heating and the composition of the neutral atmosphere. p0069 A73-27602

Solar X ray contribution to E layer ionization [NASA-CR-73884] p0088 N69-17412

OGO-6 experiment F-03 --- analysis of data obtained with retarding potential analyzer [NASA-CR-132943] p0106 N74-20542

A model ionosphere for mid-day and mid-latitude during sunspot minimum [SMUP-4] p0109 N74-74635

IONOSPHERIC CURRENTS

Magnetic field data from OGO-2 spacecraft and surface magnetic observatories, noting magnetic storm occurrence and magnetosphere inflation and detection of polar ionospheric currents p0018 A69-11125

Ionospheric electric and electromagnentic waves broadband characteristics, investigating auroral hiss and LHR noise p0051 A71-33951

The Harang discontinuity in auroral belt ionospheric currents. p0061 A72-39980

POGO satellite observed electrojet current data comparison with ground measurement at Ibadan, discussing data ratios variation by upper earth mantle conductivity structure p0070 A73-31772

IONOSPHERIC DISTURBANCES

Power-law wavenumber spectrum deduced from ionospheric scintillation observations. p0062 A72-42416

In situ measurements of the spectral characteristics of F region ionospheric irregularities. p0078 A74-27695

Neutral wind velocities calculated from temperature measurements during a magnetic storm and the observed ionospheric effects [B19920-000] p0113

In situ measurements of amplitude and scale size characteristics of ionospheric irregularities: OGO-6 ion concentration irregularity studies [B20340-000] p0113

IONOSPHERIC DRIFT

OGO 5 observation of ULF geomagnetic fluctuation at polar cusp boundaries in terms of ionospheric drift wave and Kelvin-Helmholtz instabilities p0068 A73-24744

IONOSPHERIC ELECTRON DENSITY

Radio propagation experiment using transmitted VHF waves from OGO-1 to deduce electron density in ionosphere and magnetosphere p0004 A66-10892

Response of ionospheric and exospheric electron contents to partial solar eclipse, using OGO 1 satellite p0015 A68-38439

Complex impedance measurements for monopole antenna for electron densities in/out of OGO satellite wake in upper ionosphere p0035 A70-35771

Ionospheric electron density response to geomagnetic storms at midlatitudes, noting diurnal variations detected by ATS 3 VHF signals p0038 A70-40479

Atomic oxygen green line emission in nightglow from OGO-F photometer observations, calculating tropical F region electron density spatial distribution p0060 A72-35604

The light-ion trough, the main trough, and the plasmapause. p0066 A73-15533

Electron depletion in the wake of ionospheric spacecraft: A comparison between results from Langmuir probes and antennas. p0072 A73-34783

Asymmetrical global O 1 airglow emission pattern with respect to magnetic equator from OGO 4 observations, noting poor correlation with ionospheric electron density p0073 A73-38939

Geophysical properties of the ionospheric irregularities responsible for radio scintillation. [AIAA PAPER 74-53] p0077 A74-18754

Photoelectron flux measurements in topside ionosphere using retarding potential analyzers [NASA-TM-X-63358] p0087 N68-35999

Protonospheric electron concentration profiles based on Doppler and Faraday effects [NASA-CR-100778] p0089 N69-24521

Atmospheric model for thermal plasma near equatorial plasmapause p0095 N71-25270

IONOSPHERIC PROPAGATION

Electron density profiles and production rates associated with 30 Jan. 1968 large X ray flare event [RSD-63] p0096 N71-36131

IONOSPHERIC ION DENSITY

Ion depletion in high latitude exosphere, considering OGO 2 simultaneous observations of positive ion concentration, VLF signal propagation and whistlers p0023 A69-34939

Hydrogen, He and oxygen ion density, and ion and electron temperatures in upper ionosphere from OGO 4 observations p0035 A70-36016

Simultaneous hydrogen ion composition measurements by upper ionospheric polar orbiting OGO 4 and eccentric orbiting magnetospheric OGO 3 at midlatitude p0037 A70-38377

Positive Fe ion concentration relationship to equatorial spread F from OGO 6 satellite observation near magnetic equator p0054 A72-10902

Source and identification of heavy ions in the equatorial F layer. p0063 A72-44516

Diurnal latitudinal composition variations in light ion trough from OGO mass spectrometric observations, noting magnetic storm effects p0065 A73-11904

OGO 6 retarding potential analyzer observation of vertical and longitudinal gradients in ion concentrations below F region peak near magnetic equator p0068 A73-24738

Equatorial spread F formation convective electric fields generation by neutral winds and conductivity caused by metallic ion concentrations p0070 A73-29988

Effects of interhemisphere transport on plasma temperatures at low latitudes. p0074 A73-41919

A catalog of ionospheric F region irregularity behavior based on OGO-6 retarding potential analyzer data p0075 A74-12640

In situ measurements of the spectral characteristics of F region ionospheric irregularities. p0078 A74-27695

IONOSPHERIC NOISE

Continuous and triggered audio frequency noise bands associated with ionospheric lower hybrid resonance frequency observed on OGO 2 p0018 A69-16257

VLF and LF emission characteristic features and origin mechanism in auroral regions of ionosphere, discussing satellite observation of noise spectrum in space p0025 A69-38495

VLF data from OGO 2 and OGO 4 on propagation, wave-particle interactions, and noise in ionosphere and magnetosphere [NASA-CR-110658] p0093 N70-32928

IONOSPHERIC PROPAGATION

Satellite observation of natural VLF phenomena in ionosphere and magnetosphere stressing radio noise frequency-time characteristics p0010 A68-14098

Sudden magnetic field increase associated with July 8, 1966 sudden commencement observed by OGO 3 satellite in magnetotail p0018 A69-11226

Latitudinal cut-off of manmade VLF signals in short path through ionosphere to OGO 2 satellite, noting strong noise following signal cut-off p0021 A69-28958

Nonducted VLF walking trace whistlers and Doppler shifts in fixed frequency transmissions identified on OGO midlatitude spectrographic records p0028 A70-15116

VLF noise phenomena observed with satellite electric dipole antennas compared with lower hybrid resonance frequency of ionospheric medium in vicinity p0029 A70-18534

Magnetospheric sudden impulses amplitude and rise time distributions observation by OGO 3 and 5 satellites p0043 A71-17686

Ionospheric absorption relation to solar X-ray flux enhancement during short wave fade-outs from OGO-4 and Solrad 9 satellites p0045 A71-20318

Nov. 10, 1975

Drifting whistler frequency cutoff phenomena (striations) observation in low latitude by POGO satellites, discussing interpretation based on propagation effect

OGO 6 ionospheric measurement of proton whistlers wave-normal vector, investigating propagation modes

Geophysical properties of the ionospheric irregularities responsible for radio scintillation.

[AIAA PAPER 74-53] Resonances in driving point impedance of electric dipole antenna in ionosphere

[NASA-CR-91620] Very low frequency signals observed by OGO-4 measured and interpreted, and global ionospheric propagation study

[NASA-CR-107654] VLF data from OGO 2 and OGO 4 on propagation, wave-particle interactions, and noise in ionosphere and magnetosphere

[NASA-CR-110658] IONOSPHERIC SOUNDING

OGO-6 electric and electromagnetic fields measurement for ionosphere using dipole antenna, emphasizing broadband observation covering whistler mode waves

Polar ionosphere auroral oval position detection by satellite observations of naturally occurring VLF and man-made HF plasma waves

Ionospheric electric fields variations in ELF-VLF, confirming OV-1 satellite measurements with OGO 6 data

Magnetospheric thermal plasma electron density measurement during solar flare by OGO-5 satellite

Ionospheric ion temperature measurements by retarding potential analyzer on OGO-6 satellite

Subauroral red arcs phenomenon hypotheses based on associated ionospheric plasma properties measurements

Geomagnetic effect on the neutral temperature of the F region during the magnetic storm of September 1969.

Midlatitude red arc observations by satellite and ground station, suggesting thermal conduction theory of formation from ionospheric electron and ion temperatures and densities

ISIS-1 satellite observations of the ionosphere at high southern latitudes.

IONOSPHERIC TEMPERATURE
Suprathermal electron temperature and ion composition as function of geomagnetic latitude in polar ionosphere, using Explorer 31 mass spectrometer measurements

Geomagnetic equatorial ionospheric temperature, comparing incoherent scatter radar and OGO-D retarding potential analyzer values

Geomagnetic effect on the neutral temperature of the F region during the magnetic storm of September 1969.

Global temperature distributions from OGO-6 6300 A airglow measurements.

IONOSPHERICS
The global distribution of natural and man-made ionospheric electric fields at 200 kHz and 540 kHz as observed by OGO-6.

IONS
Experiment data analysis report for the OGO-4 neutral and ion mass spectrometer experiment

IRON
Positive Fe ion concentration relationship to equatorial spread F from OGO 6 satellite observation near magnetic equator

Measurements of the iron-group abundance in energetic solar particles.

J

JUPITER (PLANET)

A new model for the high-frequency decametric radiation from Jupiter

K

KINETIC ENERGY

Gas-surface energy transfer experiment on OGO-6 satellite, measuring upper atmosphere kinetic energy flux to determine accommodation and drag coefficients, density, etc.

L

LAMINAR FLOW

Structure of the quasi-perpendicular laminar bow shock

LATITUDE

Properties of higher latitude region of structured low energy electron precipitation in noon hemisphere, relating radiation with optical emissions in dayside auroral oval

Theoretical model for the latitude dependence of the thermospheric annual and semiannual variations.

Latitude and local time dependence of precipitated low-energy electrons at high latitudes.

LATITUDE MEASUREMENT

Relationship of perigee motion of satellite orbit to latitude and local time

LEAKAGE

Measurements of the atmospheric neutron leakage rate

LIGHT EMISSION

LF and VLF wideband noise called auroral hiss observed by Byrd ground station and OGO 2, proposing incoherent Cerenkov radiation from 1 keV electrons

Properties of higher latitude region of structured low energy electron precipitation in noon hemisphere, relating radiation with optical emissions in dayside auroral oval

Auroral spectrum analysis in 1200-4000 A band, obtaining photon emission rates

Distributions and characteristics of high-latitude field-aligned electron precipitation.

LIGHT SCATTERING

Extraterrestrial ultraviolet radiation and the parameter of the HI medium near the sun.

LINES OF FORCE

Ion temperature gradient along magnetic field lines in outer plasmasphere by thermal diffusion equations compared with electron temperature observations

Thermal plasma model along magnetic field lines outside plasmasphere with sharp density gradient in equatorial plane, using OGO-4 ion composition measurements

Electron polar cap and the boundary of open geomagnetic field lines.

LONG TERM EFFECTS

Forbush decreases and long term cosmic ray particle intensity changes, investigating spectral variations

LONGITUDINAL STABILITY

Seasonal and annual longitudinal variations in ionospheric ion distribution, stressing solar geomagnetic control importance

Dynamic analysis of longitudinal oscillations of SM-68B stage 1 (POGO)

LOW FREQUENCIES

Broadband and highpass LF noise in distant magnetosphere detected by VLF/LF experiment on OGO 1 satellite

The prevalence of second harmonic radiation in type 3 bursts observed at kilometric wavelengths.

Low frequency space radio astronomy

LOW FREQUENCY BANDS

Decay time of type 3 solar bursts observed at kilometric wavelengths

LOWER ATMOSPHERE

Absolute cosmic ray ionization measurements in upper and lower atmosphere

LUMINOUS INTENSITY

Electron measurements near weak aurora during rocket flight

Far UV equatorial airglow and aurora intensities and occurrence frequencies from satellite observation

LUNAR DUST

Four years of dust particle measurements in cislunar and selenocentric space from Lunar Explorer 35 and OGO 3

LUNAR LIMB

Lunar limb shock wave observed by Explorer 35 satellite defined with respect to solar wind flow direction, discussing formation mechanism

LYMAN ALPHA RADIATION

Hydrogen Lyman alpha nightglow models, discussing solar photon scattering in geocorona and hydrogen vertical distribution

OGO 5 satellite measurements of intensity and width of Lyman alpha line scattered by hydrogen geocorona

Solar Lyman-alpha radiation observed by OGO 4 spacecraft showing short term fluctuations superimposed with monthly variation

Lyman alpha intensity and hydrogen concentration at 5 to 19 earth radii determined from OGO 3 spacecraft measurements

OGO-4 observations of hydrogen Lyman-alpha airglow surrounding earth, measuring dependence on solar zenith angle

Comet Bennett /1969 i/ spectrograms, discussing linear diameter, trajectory, Lyman alpha emission and hydrogen mass

Exospheric neutral hydrogen temperature diurnal variation from satellite resonance filter data, suggesting Lyman alpha source external to geocorona

Lyman alpha and atomic oxygen 1304 A airglow depressions over poles from OGO 4 satellite observations

Lyman alpha radiation scattering observation by satellites, obtaining geocoronal atomic hydrogen distribution in thermosphere and exosphere

Extraterrestrial hydrogen Lyman alpha emission source, investigating interstellar wind with OGO 5 satellite

Lyman alpha sky background measurements by OGO 5 satellite, discussing absolute emission rate, spatial variations and origin

Neutral hydrogen interstellar wind parameters from Lyman alpha sky background measurements outside geocorona by photometers on OGO 5

Neutral hydrogen Lyman-alpha measurements in outer geocorona and in interplanetary space by two channel photometer on OGO 5

New interpretations of extraterrestrial Lyman-alpha observations.

Interpretation of OGO-5 Lyman alpha measurements in the upper geocorona.

SUBJECT INDEX

Determination of the solar Lyman-alpha flux independent of calibration by ultraviolet observations of Comet Bennett) p0076 A74-15496

OGO-5 measurements of the Lyman-alpha sky background in 1970 and 1971. p0077 A74-22345

Flight calibration device for absolute measurements of photometer at Lyman alpha wavelength on OGO-6 and other satellites [AD-726567] p0096 N71-36136

Diurnal variation of Lyman alpha spectral width as measured by OGO-6 sky-scanning photometer [AD-736816] p0097 N72-23429

Measurement of extraterrestrial Lyman alpha emission by OGO 5 satellite while outside geocorona p0100 N73-10812

Development of model of scattering of solar Lyman alpha from spatial distribution of neutral hydrogen in interplanetary space p0100 N73-10813

Instrument report for Lyman-alpha experiment (OGO-F-12) p0108 N74-74625

LYMAN SPECTRA

Diurnal variation of Lyman alpha spectral width as measured by OGO-6 sky-scanning photometer [AD-736816] p0097 N72-23429

M

MAGNETIC ANOMALIES

Geomagnetic field minimum in southern Brazil, comparing satellites data maps p0017 A68-42083

Equatorial electrojet characteristics observation during 1967-1970 with POGO satellite-borne magnetometers, noting anomaly characterized by sharp negative V-signature in width and variable amplitude p0070 A73-31768

The detection of 'intermediate' size magnetic anomalies in Cosmos 49 and OGO-2, 4, 6 data. p0073 A73-41374

The equatorial helium ion trough and the geomagnetic anomaly [B22334-000] p0114

Effects of crustal anomalies on satellite measurements of ambient geomagnetic field p0097 N72-23341

A global magnetic anomaly map --- obtained from POGO satellite data [NASA-TM-X-70628] p0106 N74-20982

MAGNETIC CONTROL

Seasonal and annual longitudinal variations in ionospheric distribution, stressing solar geomagnetic control importance p0050 A71-33762

Magnetic control of near equatorial neutral thermosphere, calculating F region ionization anomaly and molecular nitrogen and atomic oxygen density latitudinal variations p0069 A73-26997

Digital offset field generator for dynamic range extension of magnetometers p0090 N69-33963

MAGNETIC DIPOLES

Geomagnetic field model (POGO) to confirm eccentric dipole westward velocity secular decrease predicted by day length changes p0025 A69-37490

MAGNETIC DISTURBANCES

Sudden magnetic field increase associated with July 8, 1966 sudden commencement observed by OGO 3 satellite in magnetotail p0018 A69-11226

High latitude ionization spikes observed by POGO spacecraft, noting frequency correlation with magnetic disturbances and development by high energy electron injections p0021 A69-28950

Morphology of thermal and energetic particles in inner magnetosphere during geomagnetic disturbances and solar cycles p0034 A70-30358

Geomagnetic dipole field disturbances by trapped particles, calculating self consistent equilibrium configuration for ring current dipole moments p0034 A70-31905

Electrostatic turbulence in bow shock magnetic structures observed by OGO 5, explaining turbulence as ion acoustic or Buneman mode due to two stream instability p0035 A70-36006

Earth bow shock internal structure based on correlated observations of magnetic field, ELF magnetic fluctuations and suprathermal electrons by OGO 5 satellite p0051 A71-33943

High latitude sudden impulses, calculating transverse hydromagnetic waves propagation from magnetosphere equatorial plane p0052 A71-34777

Neutral atmospheric composition and density variations during geomagnetic disturbances from OGO-6 satellite quadrupole mass analyzer measurements p0052 A71-39711

The Harang discontinuity in auroral belt ionospheric currents. p0061 A72-39980

Outer magnetosphere near midnight at quiet and disturbed times. p0063 A72-44513

Geomagnetic tail magnetic and electric fields ULF, VLF and ELF fluctuations, considering relationship to substorm processes p0064 A72-44857

Near-earth magnetic disturbance in total field at high latitudes. 1: Summary of data from OGO-2, 4, and 6. 2: Interpretation of data from OGO-2, 4, and 6. p0080 A74-34019

A multisatellite study of auroral-zone phenomena. [ESRO-SR-23-PT-1] p0105 N74-16072

A study of high latitude magnetic disturbance --- from magnetic field data obtained with OGO spacecraft and ground observatories p0105 N74-17058

Electric field measurements across the Harang discontinuity --- of the auroral zone [NASA-TM-X-70613] p0105 N74-19023

MAGNETIC EFFECTS

Magnetic activity effect on magnetospheric plasmopause position, measuring ion concentrations as function of local time from OGO 5 observations p0029 A70-18530

Soft solar X rays cyclic variation from satellite observation, noting relation to sunspot group magnetic field complexity p0039 A70-43301

Geomagnetic effect on the neutral temperature of the F region during the magnetic storm of September 1969. p0060 A72-35603

Geomagnetic cutoffs for cosmic-ray protons for seven energy intervals between 1.2 and 39 Mev p0061 A72-38728

Polar-cap electric field distributions related to the interplanetary magnetic field direction. p0062 A72-42432

ULF wave observation by satellite, considering geomagnetic activity control of magnetospheric wave occurrence p0063 A72-42902

Satellite studies of magnetospheric substorms on August 15, 1968. I: State of the magnetosphere. p0071 A73-33449

Dependence of the polar cusp on the north-south component of the interplanetary magnetic field. p0072 A73-36273

Heating of the high-latitude thermosphere during magnetically quiet periods. p0080 A74-34027

MAGNETIC EQUATOR

Geomagnetic field minimum in southern Brazil, comparing satellites data maps p0017 A68-42083

Magnetic dip equator position at E layer and gradient with time and altitude, using geomagnetic field models p0026 A69-42428

Satellite observations of equatorial erosion and defocusing of VLF waves propagating at low magnetic latitudes p0029 A70-18532

Magnetic equator ELF noise examined with OGO 3 magnetometer, indicating unique signals in plasmasphere p0030 A70-21380

Low energy protons omnidirectional intensity contours in outer radiation zone at magnetic equator p0030 A70-23491

MAGNETIC FIELDS

Whistler ducts as enhanced ionization from OGO 3 satellite observations near magnetic equator, noting magnetospheric ionization hydrostatic model and predicted cut-off p0041 A71-11499

Magnetospheric VLF electric field emissions above electron cyclotron frequency from OGO 5 observation at magnetic equator p0041 A71-11500

Directional differential energy spectra for proton intensities in outer radiation zone near magnetic equator from satellite observations p0043 A71-17261

Plasma sheet proton ring current, trapping boundary and plasmopause interrelations near magnetic equator and local midnight by satelliteborne analyzer array p0047 A71-24781

Geomagnetic equatorial ionospheric ion temperature, comparing incoherent scatter radar and OGO-D retarding potential analyzer values p0052 A71-33956

Positive Fe ion concentration relationship to equatorial spread F from OGO 6 satellite observation near magnetic equator p0054 A72-10902

OGO-6 measurements of supercooled plasma in the equatorial exosphere. p0068 A73-22066

OGO 6 retarding potential analyzer observation of vertical and longitudinal gradients in ion concentrations below F region peak near magnetic equator p0068 A73-24738

Magnetic control of near equatorial neutral thermosphere, calculating F region ionization anomaly and molecular nitrogen and atomic oxygen density latitudinal variations p0069 A73-26997

Equatorial ionospheric anomaly related neutral thermospheric composition variation observation from OGO-6 mass spectroscopic data, noting static diffusion model limitations p0070 A73-31767

Asymmetrical global O I airglow emission pattern with respect to magnetic equator from OGO 4 observations, noting poor correlation with ionospheric electron density p0073 A73-38939

The equatorial helium ion trough and the geomagnetic anomaly [B22334-000] p0114

OGO-E study of electric field emissions at geomagnetic equator [NASA-CR-126238] p0097 N72-22383

MAGNETIC FIELDS

Magnetic design of OGO and Pioneer solar probe including data on instrumentation, mechanical equipment, permanent magnets, test methods, etc p0004 A66-15919

Fluxgate magnetometer for OGO-E spacecraft in observing MHD waves and magnetic field structures in space p0007 A67-15724

Rapid magnetic field variations observed in magnetosheath evaluated in terms of transverse modes of plasma wave propagation [JPL-TR-32-1199] p0009 A67-40804

Magnetic field data from OGO-2 spacecraft and surface magnetic observatories, noting magnetic storm occurrence and magnetosphere inflation and detection of polar ionospheric currents p0018 A69-11125

Satellite plasma diagnostics for electric and magnetic fields and fine structure of collisionless shocks in solar wind plasma flows and interplanetary shocks p0032 A70-30069

Thermal plasma model along magnetic field lines outside plasmasphere with sharp density gradient in equatorial plane, using OGO-4 ion composition measurements p0038 A70-41057

Magnetic field and electron plasma observations near dawn magnetopause by triaxial spectrometer and fluxgate magnetometer on satellite OGO 5 p0050 A71-31754

Plasma wave measurements during OGO-5 dayside magnetosphere polar cusp encounters, discussing ULF magnetic field wave levels and VLF electric field amplitude ranges p0059 A72-29380

Solar wind interaction with geomagnetic field, discussing magnetosphere polar cusp region and geomagnetic tail neutral sheet structure p0065 A73-13871

NOV. 10, 1975

MAGNETIC FLUX

Processing of total field magnetometer data from OGO-2 satellite
 [NASA-TM-X-55822] p0085 N67-30147
 OGO-B and OGO-E measurements on magnetospheric field magnitudes and disturbances caused by ring currents p0095 N71-25271
 Seasonal, altitude, and universal time differences in field-aligned electrons
 [NASA-TM-X-66099] p0100 N73-11345
 OGO-5 fluxgate magnetometer for measuring magnetic field over range of OGO-5 orbit
 [NASA-CR-130205] p0101 N73-20498
 OGO D and F magnetic field results and surface data comparison p0102 N73-20866
MAGNETIC FLUX

Magnetospheric magnetic field distortions under quiet and slightly disturbed conditions, obtaining scalar intensity with OGO 3 and 5 rubidium vapor magnetometer p0054 A72-10886
 Magnetic field strength change in equatorial plasmasphere, considering quiet ring current as equatorial sheet current extension of neutral sheet current in magnetospheric tail p0064 A73-11732
 Quiet time magnetospheric field depression at 2.3-3.6 earth radii. p0072 A73-33464
 Rate of erosion of dayside magnetic flux based on a quantitative study of the dependence of polar cusp latitude on the interplanetary magnetic field. p0075 A74-14274
 The magnetotail and substorms. --- magnetic flux transport model p0076 A74-17742
 Comparison of simultaneous particle detector and search coil magnetometer measurements of precipitating particles and field aligned currents from OGO-D [NASA-TM-X-66224] p0102 N73-21367

MAGNETIC MEASUREMENT

OGO 3 search coil magnetometer data correlated with magnetopause crossing by ATS 1 satellite, discussing OGO 3 crossing of outer magnetosphere into interplanetary medium p0017 A68-41693
 Interplanetary magnetic field measurements from Mariner and OGO satellites at various paths, regions and intervals, finding dominant polarity effect dependent on sun latitude p0027 A70-13980
 Geomagnetic field distortion in high beta magnetospheric regions from OGO observations for quiet and slightly disturbed conditions p0032 A70-30076
 Electromagnetic wave observation in interplanetary medium and in magnetosphere, emphasizing magnetic and electric field measurements p0065 A73-13855
 Satellite studies of magnetospheric substorms on August 15, 1968. 4: OGO-5 magnetic field observations. p0072 A73-33452

Near-earth magnetic disturbance in total field at high latitudes. 1: Summary of data from OGO-2, 4, and 6. 2: Interpretation of data from OGO-2, 4, and 6. p0080 A74-34019
 World magnetic survey (WMS)- method for minimizing limitations of mathematical and graphical descriptions of earth's magnetic field [NASA-RP-277] p0082 N64-27355
 Magnetic property tests on OGO and environmental research satellites p0090 N69-33977

MAGNETIC PROBES

Magnetic Hall probe developed for use in spectrometer system aboard OGO-E satellite [UCRL-14650-T] p0086 N67-30930

MAGNETIC PROPERTIES

Magnetic property tests on OGO and environmental research satellites p0090 N69-33977

MAGNETIC RIGIDITY

Differential response curves and mean rigidity of response of ion chambers aboard balloons and satellites in free space during long-term cosmic ray variation from 1960 to 1965 p0003 A65-33664
 Balloon and satellite measurement of quiet time cut-off rigidities for cosmic ray particles p0016 A68-41562

MAGNETIC STORMS

Charged particles of extraterrestrial ring current during geomagnetic storms, with OGO 3 measurements of proton and electron differential energy spectra p0009 A67-37401
 IMP-2 and OGO-1 investigations of bow shock large scale motions during magnetic storms result from magnetosphere-magnetosheath compression by solar wind dynamic pressure p0011 A68-17768
 Plasmasphere behavior during solar flare events compared with satellite data from storm-time and plasmopause p0011 A68-19744

Directional differential intensities of protons injected into outer radiation zone coincident with initial phase of geomagnetic storm and monitored by OGO 3 p0016 A68-41684
 Magnetic field data from OGO-2 spacecraft and surface magnetic observatories, noting magnetic storm occurrence and magnetosphere inflation and detection of polar ionospheric currents p0018 A69-11125

Charged particles injection into captured radiation zone of Van Allen belts during main phase of magnetic storm indicated by proton data analysis p0025 A69-37967
 Electron intensities and substorm drift effects in outer radiation belt using two satellite technique p0026 A69-43172
 Extraterrestrial ring current proton intensities asymmetric increases in outer radiation belt during magnetic storms p0030 A70-23490

Van Allen radiation belts energetic electrons injection and distribution due to magnetic storms, using satellite-borne spectrometers p0033 A70-30090
 Ionospheric electron density response to geomagnetic storms at midlatitudes, noting diurnal variations detected by ATS 3 VHF signals p0038 A70-40479

Inner belt electron flux variations following geomagnetic storms from satellite instrument data p0042 A71-14212
 Magnetopause inward motion before substorm, showing association with interplanetary field vertical component reversal p0042 A71-14515
 Magnetopause crossing observation of ATSS satellite during magnetic storm p0043 A71-17258

Substorm related magnetic field variations in near geomagnetic tail from OGO 5 inbound pass p0046 A71-21643
 Hydrogen ion concentration measurements by OGO 5 in plasmasphere during intense magnetic storms accompanied by stable auroral red arcs p0047 A71-24787
 Band limited micropulsations observed in space during magnetospheric substorm by fluxgate magnetometer on OGO 5 p0048 A71-27913

Magnetotail changes relationship to solar wind magnetic field and magnetospheric substorms from ground and satellite data p0051 A71-33944
 OGO-2 rubidium vapor magnetometer measurements comparison with surface magnetic observatory data during geomagnetic storms, considering asymmetric ring current p0051 A71-33946

Relativistic electron precipitation during magnetic storms, showing cyclotron resonances with electromagnetic ion cyclotron waves p0051 A71-33948
 Plasmaspheric ambient hydrogen and helium atomic cations density measurement by OGO 5 ion mass spectrometer during magnetic storm, noting relationship to auroral red arcs p0053 A71-39833

OGO 5 polar cusp observations showing dayside magnetosheath plasma penetration during magnetic storm p0053 A71-43162
 Earth corotating plasma tail evidence in plasmopause variations from high resolution proton distribution data obtained by OGO 4 satellite during magnetic storm p0053 A71-43166
 Magnetic storm effects on neutral atmospheric composition above 400 km, discussing energy deposition p0055 A72-13518

SUBJECT INDEX

Magnetic storm effects in atmospheric neutral composition, noting thermospheric wind circulation role due to Joule heating within auroral zone p0058 A72-24957
 OGO-5 observation of lower hybrid resonance noise, bursts, VLF hiss and whistlers near plasmopause during large magnetic storm p0058 A72-26399
 Geomagnetic effect on the neutral temperature of the F region during the magnetic storm of September 1969. p0060 A72-35603
 Behavior of outer radiation zone and a new model of magnetospheric substorm. p0063 A72-44850
 Electric field variations during substorms: OGO-6 measurements. p0064 A72-44854
 Diurnal latitudinal composition variations in light ion trough from OGO mass spectrometric observations, noting magnetic storm effects p0065 A73-11904
 Field-aligned currents, plasma waves, and anomalous resistivity in the disturbed polar cusp. p0069 A73-29964
 Energy and diffusive mass transport relation to thermospheric circulation, composition, temperature and mass density from three dimensional two constituent magnetic storm model p0070 A73-29975
 Ion cyclotron waves observed in the polar cusp. p0071 A73-33437
 Satellite studies of magnetospheric substorms on August 15, 1968. 1: State of the magnetosphere. p0071 A73-33449
 Satellite studies of magnetospheric substorms on August 15, 1968. 2: Solar wind and outer magnetosphere. p0071 A73-33450
 Satellite studies of magnetospheric substorms on August 15, 1968. 3: Some features of magnetospheric convection. p0072 A73-33451
 Satellite studies of magnetospheric substorms on August 15, 1968. 4: OGO-5 magnetic field observations. p0072 A73-33452
 Satellite studies of magnetospheric substorms on August 15, 1968. 5: Energetic electrons, spatial boundaries, and wave-particle interactions at OGO-5. p0072 A73-33453
 Satellite studies of magnetospheric substorms on August 15, 1968. 6: OGO 5 energetic electron observations. Pitch angle distributions in the nighttime magnetosphere p0072 A73-33454
 Satellite studies of magnetospheric substorms on August 15, 1968. 7: OGO-5 energetic proton observations. Spatial boundaries p0072 A73-33455
 Satellite studies of magnetospheric substorms on August 15, 1968. 8: OGO-5 plasma wave observations. p0072 A73-33456
 Satellite studies of magnetospheric substorms on August 15, 1968. 9: Phenomenological model for substorms. p0072 A73-33457
 Synoptic survey for the neutral line in the magnetotail during the substorm expansion phase. p0073 A73-36275
 The relation between low-latitude neutral density variations near 400 km and magnetic activity indices. p0075 A74-14219
 The magnetotail and substorms. --- magnetic flux transport model p0076 A74-17742
 Postmidnight chorus: A substorm phenomenon. --- outer magnetosphere p0076 A74-18364
 Plasmaspheric hiss intensity variations during magnetic storms. p0080 A74-34038
 Energetic electrons and protons observed on OGO-5, March 6-10, 1970 [B07587-000] p0111
 Dynamical characteristics of pulsating substorm, PS6 [B14580-000] p0112
 Plasma wave-particle interaction inside the neutral sheet (in Japanese) [B14583-000] p0112

NOV. 10, 1975

Neutral wind velocities calculated from temperature measurements during a magnetic storm and the observed ionospheric effects
[B19920-000] p0113

High latitude proton precipitation and light ion density profiles during the magnetic storm initial phase
[B22333-000] p0113

Intensity variation of elf hiss and chorus during isolated substorms
[B22603-000] p0114

Substorm and interplanetary magnetic field effects on the geomagnetic tail lobes
[B22611-000] p0114

Temporal variations of 40 keV electrons in magnetosphere during and after magnetic storm on April 18, 1965
[NASA-CR-85905] p0086 N67-31362

OGO outer zone observational data on electron intensities of earth geomagnetic field
[NASA-CR-89652] p0087 N67-40126

Local time asymmetries in increase of electron fluxes in outer Van Allen zone during substorms
[NASA-CR-100419] p0089 N69-20849

Propagation of high energy solar protons as observed by OGO C spacecraft
p0089 N69-23730

OGO-D atmospheric composition data for polar thermospheric storm model
[NASA-CR-103080] p0094 N71-20638

Magnetic field fluctuations during magnetospheric substorms and field aligned currents in magnetosphere, based on satellite observations
[NASA-TM-X-65748] p0096 N72-11325

Enhancements of red arc during maximum solar activity
p0097 N72-23334

Neutral density data from OGO-F and geomagnetic storms
[NASA-CR-122479] p0099 N72-32390

OGO-5 observations of discrete whistlers and emissions during a large magnetic storm
[NASA-TM-X-70213] p0109 N74-74634

Magnetospheric substorm, 1972
p0110 N74-77515

MAGNETIC SURVEYS

Geomagnetic survey by polar-orbiting OGO 2 and 4, discussing data acquisition and reduction results and accuracy
p0054 A72-12081

Magnetosphere and adjacent regions magnetic surveys by OGO 1 and 3 satellites, discussing magnetopause, bow shock, magnetosheath, geomagnetic tail, ring current and polar substorms
p0055 A72-12084

World magnetic survey (WMS)- method for minimizing limitations of mathematical and graphical descriptions of earths magnetic field
[NASA-RP-277] p0082 N64-27355

Derivation of International Geomagnetic Reference Field with tables of spherical harmonic coefficients and test results of various magnetic field models
[NASA-TN-D-6237] p0095 N71-32190

MAGNETIC VARIATIONS

Rapid magnetic field variations observed in magnetosheath evaluated in terms of transverse modes of plasma wave propagation
[JPL-TR-32-1199] p0009 A67-40804

OGO triaxial search coil magnetometer for measuring earth magnetic fluctuations, discussing design rationale and observation results
p0024 A69-36675

Geomagnetic field model (POGO) to confirm eccentric dipole westward velocity secular decrease predicted by day length changes
p0025 A69-37490

Plasmapause position and density profile from ion concentration measurements by OGO-5, determining reaction to magnetic variations
p0032 A70-30074

Geomagnetic field distortion in high beta magnetospheric regions from OGO observations for quiet and slightly disturbed conditions
p0032 A70-30076

Magnetic fluctuations observed by ground observatories, suggesting large amplitude waves as field line resonances driven by magnetopause motion
p0033 A70-30078

Magnetic and electric field changes across earth bow shock and magnetosheath, discussing Pioneer 8 and OGO-5 data
p0036 A70-37483

Substorm related magnetic field variations in near geomagnetic tail from OGO 5 inbound pass
p0046 A71-21643

Magnetic fluctuations in ELF and VLF waves in space, discussing whistler phenomena and applications to magnetospheric probes
p0056 A72-21189

POGO satellite observed electrojet signature data comparison with daily geomagnetic variation amplitude measurement at equatorial ground station in India
p0070 A73-31769

POGO satellite observation of electrojet profiles compared with H variation around measurements, interpreting data by classical band current model
p0070 A73-31773

Near-earth magnetic disturbance in total field at high latitudes. 1: Summary of data from OGO-2, 4, and 6. 2: Interpretation of data from OGO-2, 4, and 6.
p0080 A74-34019

Geomagnetic secular variations, 1900-1965
[NASA-TM-X-55944] p0086 N67-37398

MAGNETICALLY TRAPPED PARTICLES

Beta particle observations between inner edge of plasma sheet to plasmapause in midnight earth magnetosphere
[NASA-TM-X-65640] p0095 N71-32436

MAGNETOHYDRODYNAMIC FLOW

Lunar limb shock wave observed by Explorer 35 satellite defined with respect to solar wind flow direction, discussing formation mechanism
p0031 A70-27594

MAGNETOHYDRODYNAMIC STABILITY

HF electrostatic waves generation by electrons in magnetosphere
p0033 A70-30083

Electric field fluctuations in magnetospheric plasma at multiples of local electron gyrofrequency due to plasma instability
p0052 A71-37368

Suprathermal electron beam induced HF wave instability in solar wind upstream from earth bow shock, interpreting OGO 5 observations
p0053 A71-43158

Nonlinear frequency correction to plasma instability at half harmonics of electron gyrofrequency as observed by OGO 5 near geomagnetic equator outside plasmapause
p0068 A73-22069

OGO 5 observation of ULF geomagnetic fluctuation at polar cusp boundaries in terms of ionospheric drift wave and Kelvin-Helmholtz instabilities
p0068 A73-24744

Observation of a current-driven plasma instability at the outer zone-plasma sheet boundary.
p0069 A73-29966

MAGNETOHYDRODYNAMIC WAVES

Fluxgate magnetometer for OGO-E spacecraft in observing MHD waves and magnetic field structures in space
p0007 A67-15724

Fluctuating electric fields relations to MHD bow shock structure, using LF fluxgate magnetometer aboard OGO 5
p0026 A69-42693

Magnetosphere Alfvén velocity profile relation to ELF chorus and hiss, indicating unstable wave generation by cyclotron resonance
p0039 A70-43851

High latitude sudden impulses, calculating transverse hydromagnetic waves propagation from magnetosphere equatorial plane
p0052 A71-34777

Detection of solar-wind electron plasma frequency fluctuations in an oblique nonlinear magnetohydrodynamic wave.
p0061 A72-35610

ULF wave observation by satellite, considering geomagnetic activity control of magnetospheric wave occurrence
p0063 A72-42902

MAGNETOMETERS

Magnetopause location, boundary positions and magnetic noise spectral data obtained with triaxial search coil magnetometer aboard OGO 1 satellite
p0004 A66-23148

Fluxgate magnetometer for OGO-E spacecraft in observing MHD waves and magnetic field structures in space
p0007 A67-15724

Geomagnetic field values obtained from OGO-2 satellite-mounted rubidium vapor magnetometer
p0007 A67-23244

Electron spectra, pitch angle distributions and total ionization measured throughout radiation belts by satellite magnetic spectrometer and integrating ionization chamber
p0008 A67-25807

Rubidium vapor magnetometer used for near earth orbiting spacecraft, instrumentation and in-flight performance
p0008 A67-36513

Rapid magnetic field variations observed in magnetosheath evaluated in terms of transverse modes of plasma wave propagation
[JPL-TR-32-1199] p0009 A67-40804

OGO triaxial search coil magnetometer for measuring earth magnetic fluctuations, discussing design rationale and observation results
p0024 A69-36675

Fluxgate and Ru vapor magnetometers for space measurements over wide field intensities, reducing electronic phase shift and experiment weight
p0032 A70-30045

OGO-2 rubidium vapor magnetometer measurements comparison with surface magnetic observatory data during geomagnetic storms, considering asymmetric ring current
p0051 A71-33946

Earth bow shock magnetic field data correlation with OGO 5 flux gate magnetometer, using Tidman-Northrop theory
p0056 A72-19145

Quiet time magnetospheric field depression at 2.3-3.6 earth radii.
p0072 A73-33464

Production processing of the data obtained by the UCLA OGO-5 fluxgate magnetometer
[B1280-000] p0112

POGO triaxial search coil magnetometer
[B21207-000] p0113

Processing of total field magnetometer data from OGO-2 satellite
[NASA-TM-X-55822] p0085 N67-30147

Digital offset field generator for dynamic range extension of magnetometers
p0090 N69-33963

OGO-5 fluxgate magnetometer for measuring magnetic field over range of OGO-5 orbit
[NASA-CR-130205] p0101 N73-20498

Comparison of simultaneous particle detector and search coil magnetometer measurements of precipitating particles and field aligned currents from OGO-D
[NASA-TM-X-66224] p0102 N73-21367

OGO triaxial search coil magnetometer Final Engineering Report
[NASA-CR-100619] p0108 N69-72494

MAGNETOPAUSE

Magnetopause location, boundary positions and magnetic noise spectral data obtained with triaxial search coil magnetometer aboard OGO 1 satellite
p0004 A66-23148

Magnetospheric plasmapause shape, changes of electron density and wave phenomena
p0014 A68-37940

OGO 3 search coil magnetometer data correlated with magnetopause crossing by ATS 1 satellite, discussing OGO 3 crossing of outer magnetosphere into interplanetary medium
p0017 A68-41693

Magnetic fluctuations observed by ground observatories, suggesting large amplitude waves as field line resonances driven by magnetopause motion
p0033 A70-30078

Magnetopause inward motion before substorm, showing association with interplanetary field vertical component reversal
p0042 A71-14515

Magnetopause crossing observation of ATS 5 satellite during magnetic storm
p0043 A71-17258

Multiple magnetopause crossings in equatorial plane by OGO 5, showing magnetopause motion composed of two oscillations
p0046 A71-21631

Magnetic field and electron plasma observations near dawn magnetopause by triaxial spectrometer and fluxgate magnetometer on satellite OGO 5
p0050 A71-31754

Magnetopause current layer deflection during OGO 5 crossings, noting independence on sun-earth-satellite angle
p0053 A71-43161

Shadowing of electron azimuthal-drift motions near the noon magnetopause.
p0065 A73-12442

MAGNETOSPHERE

Correlation of ground-based measurements of structured Pc 1 micropulsations with OGO-V plasmapause observations. p0067 A73-20652

Observations of the internal structure of the magnetopause. p0077 A74-21679

Plasma waves in the dayside polar cusp. 2: Magnetopause and polar magnetosheath. p0077 A74-21680

Magnetopause rotational forms (B22604-000) p0114

OGO-E electrostatic spectrometer measurements on electron flux near magnetopause p0095 N71-25273

MAGNETOSPHERE

Radio propagation experiment using transmitted VHF waves from OGO-1 to deduce electron density in ionosphere and magnetosphere p0004 A66-10892

OGO-1 first results on mass spectrometry measurements of thermal positive ion composition at high altitudes p0004 A66-14781

Fluxgate magnetometer for OGO-E spacecraft in observing MHD waves and magnetic field structures in space p0007 A67-15724

Electron energy spectra analyzed in earth magnetosphere using OGO 3, noting relation to radial distance p0007 A67-19926

OGO 3 observation of low energy protons and electrons in earth magnetosphere, noting narrow peak of relatively high low-energy particle intensities p0008 A67-26312

Magnetic field measurements in outer magnetosphere, emphasizing boundary regions and shock front characteristics p0010 A68-12172

Position and shape of neutral sheet in geocentric solar magnetospheric coordinate system from geomagnetic tail measurements p0010 A68-13469

Satellite observation of natural VLF phenomena in ionosphere and magnetosphere stressing radio noise frequency-time characteristics p0010 A68-14098

Magnetospheric ionization distribution determined by ducted and nonducted whistler propagation modes and reflection as observed by OGO 1 p0010 A68-17728

Plasmasphere behavior during solar flare events compared with satellite data from storm-time and plasmapause p0011 A68-19744

Low energy electron spatial distribution in magnetosphere obtained with OGO 1 and 3 indicate lower energies and higher densities occur during geomagnetic disturbances p0012 A68-28348

Flux, energy distribution and density of ions and electrons in magnetosphere plasma during solar activity period determined by OGO-3 electrostatic probes p0012 A68-29421

Magnetosphere low energy proton and electron density spatial distributions and temporal variations from OGO 3 satellite observations p0013 A68-34245

Magnetosphere temperature distribution model noting heat fluxes due to low electron density, large mean free path, turbulent heat transfer, etc. p0015 A68-38423

Ambient electron energy spectrum secondary peak determined from unducted magnetospherically reflected whistler mode radiation measurements p0015 A68-38428

Spatial variations in particle intensity near and inside magnetosphere during September 1966 solar cosmic ray events, noting magnetosphere screening effectiveness p0018 A69-12740

Low energy electrons on day side of magnetosphere observed with MIT electron detector on OGO 3 satellite p0018 A69-14027

Magnetospheric ELF noise, discussing OGO 3 spectrum analysis p0019 A69-18834

Low energy charged particles in earth magnetosphere observed by OGO satellite p0019 A69-19358

Low energy electrons in magnetosphere from OGO-1 and OGO-3 observations, discussing plasma sheet, magnetic bay activity, electron pressure, temperature and density gradient p0019 A69-19373

Solar protons in magnetospheric tail after flare of July 7, 1966 with isotropic pitch angle distribution, expressing energy spectrum as exponential in rigidity p0020 A69-21699

Earth thermal plasmasphere contraction subsequent to solar flare obtained from ion mass spectrometers on OGO satellites p0020 A69-23777

Plasmapause position measurements by ion mass spectrometers and broadband VLF receivers on OGO 1 and OGO 3 and by broadband recordings at Antarctica p0021 A69-25153

Light ion abundance measurements of OGO satellites and field aligned diffusive equilibrium theory with temperature and concentration latitudinal variations p0021 A69-25157

Banded chorus, VLF discrete emissions in magnetosphere in single variable frequency band with frequency depending on equatorial electron gyrofrequency p0023 A69-31981

Drift shell splitting in nondipolar distorted magnetosphere tested with data from electron spectrometer on ATS 1 and OGO 3 satellites p0026 A69-40508

Magnetospheric observations of whistler mode emissions by OGO 1 satellite over VLF and LF ranges p0028 A70-15117

Plasmapause observations by ion spectrometer aboard OGO-5 vehicle for early orbits, obtaining O, He and H ion concentration profiles for geomagnetic parameter p0029 A70-18546

Magnetic equator ELF noise examined with OGO 3 magnetometer, indicating unique signals in plasmasphere p0030 A70-21380

Plasmapause irregular structure and position indicated by measured distributions of hydrogen and helium thermal positive ions in duskside magnetosphere p0031 A70-29185

Solar cosmic rays entry into magnetosphere, showing entrance on smoothly connected field lines p0032 A70-30059

Plasmapause position and density profile from ion concentration measurements by OGO-5, determining reaction to magnetic variations p0032 A70-30074

Geomagnetic field distortion in high beta magnetospheric regions from OGO observations for quiet and slightly disturbed conditions p0032 A70-30076

HF electrostatic waves generation by electrons in magnetosphere p0033 A70-30083

Plasma wave particle interactions in outer magnetosphere, magnetosheath and solar wind, noting role of AC electric fields p0033 A70-30085

Low energy charged particle distribution within earth magnetosphere and environs, suggesting solar origin for storm time ring current protons p0033 A70-30089

Morphology of thermal and energetic particles in inner magnetosphere during geomagnetic disturbances and solar cycles p0034 A70-30358

Trapped particle population changes associated with solar events, discussing solar wind discontinuity effects on magnetosphere p0036 A70-37487

Inner magnetosphere magnetic field mapping, deriving pogo model p0038 A70-39349

Electron densities between inner edge plasma sheet and plasmasphere as function of geocentric radial distance from OGO-3 electrostatic measurements p0039 A70-43834

Magnetosphere Alfvén velocity profile relation to ELF chorus and hiss, indicating unstable wave generation by cyclotron resonance p0039 A70-43851

SUBJECT INDEX

Directed proton fluxes measurements in bow shock, magnetosheath and solar wind by OGO 5 satellite ion spectrometer p0040 A71-11491

Magnetosphere thermal ion density and temperature in dawn and morning quadrants from OGO 5 satellite measurements p0040 A71-11498

Magnetospheric VLF electric field emissions above electron cyclotron frequency from OGO 5 observation at magnetic equator p0041 A71-11500

Magnetospheric sudden impulses amplitude and rise time distributions observation by OGO 3 and 5 satellites p0043 A71-17686

Solar flare electron spectra in interplanetary space and within earth magnetosphere, investigating simultaneous observations by satellite-borne magnetic electron spectrometers p0046 A71-21037

Geomagnetic micropulsations distribution in magnetosphere, using OGO 3 and 5 data p0046 A71-23635

Magnetospheric VLF banded emissions spectral analysis, investigating OGO-5 data by high time resolution spectral techniques p0047 A71-24788

Solar wind compressed magnetic field in sunward magnetosphere and extended geomagnetic tail observation by Pioneer 7 spacecraft p0049 A71-30028

Low energy electron and proton fluxes in geomagnetic tail of equatorial magnetosphere forming plasma sheet related to auroral oval p0049 A71-30029

Satellite measurements of cold plasma density and plasmapause in magnetosphere, comparing whistler, Langmuir probe and ion trap data p0049 A71-30951

Electromagnetic waves in interplanetary space and effects on magnetosphere, considering solar wind characteristics due to wave interactions p0050 A71-30956

Magnetotail changes relationship to solar wind magnetic field and magnetospheric substorms from ground and satellite data p0051 A71-33944

High latitude sudden impulses, calculating transverse hydromagnetic waves propagation from magnetosphere equatorial plane p0052 A71-34777

Electric field fluctuations in magnetospheric plasma at multiples of local electron gyrofrequency due to plasma instability p0052 A71-37368

OGO 5 polar cusp observations showing dayside magnetosheath plasma penetration during magnetic storm p0053 A71-43162

Magnetospheric magnetic field distortions under quiet and slightly disturbed conditions, obtaining scalar intensity with OGO 3 and 5 rubidium vapor magnetometer p0054 A72-10886

Magnetosphere and adjacent regions magnetic surveys by OGO 1 and 3 satellites, discussing magnetopause, bow shock, magnetosheath, geomagnetic tail, ring current and polar substorms p0055 A72-12084

Magnetic fluctuations in ELF and VLF waves in space, discussing whistler phenomena and applications to magnetospheric probes p0056 A72-21189

Thermal positive ion densities measurement in outer ionosphere and magnetosphere by OGO 1 satellite, relating plasmapause distribution and magnetic activity level [AD-742186] p0057 A72-23011

Earth-solar wind bow shock structure from OGO-5 observations during passage from interplanetary medium into magnetosheath p0058 A72-29379

Plasma wave measurements during OGO-5 dayside magnetosphere polar cusp encounters, discussing ULF magnetic field wave levels and VLF electric field amplitude ranges p0059 A72-29380

Pitch-angle diffusion of radiation belt electrons within the plasmasphere. p0060 A72-35597

NOV. 10, 1975

SUBJECT INDEX

Turbulence of electrostatic electron cyclotron harmonic waves observed by OGO-5.

p0060 A72-35599
Injun 5 satellite measurements of magnetospheric convection electric fields via double probe technique, discussing substantiation with OGO 6 results [AD-750221] p0063 A72-42901

ULF wave observation by satellite, considering geomagnetic activity control of magnetospheric wave occurrence p0063 A72-42902

Outer magnetosphere near midnight at quiet and disturbed times. p0063 A72-44513

Behavior of outer radiation zone and a new model of magnetospheric substorm. p0063 A72-44850

Electromagnetic wave observation in interplanetary medium and in magnetosphere, emphasizing magnetic and electric field measurements p0065 A73-13855

Solar wind interaction with geomagnetic field, discussing magnetosphere polar cusp region and geomagnetic tail neutral sheet structure p0065 A73-13871

Magnetospheric observations in OGO 5 plasma wave experiment, emphasizing electrostatic wave particles interaction with plasma p0065 A73-13883

Solar proton intensity structures in the magnetosphere during interplanetary anisotropies. p0066 A73-14962

Cosmic-ray scintillations. I: Inside the magnetosphere. p0066 A73-15526

Recent studies of magnetospheric electric field emissions above the electron gyrofrequency. p0067 A73-19254

Electron pitch angle distributions throughout the magnetosphere as observed on OGO-5. p0068 A73-24732

An association of magnetospheric whistler dispersion characteristics with changes in local plasma density. p0069 A73-26985

Satellite studies of magnetospheric substorms on August 15, 1968. 2: Solar wind and outer magnetosphere. p0071 A73-33450

Satellite studies of magnetospheric substorms on August 15, 1968. 4: OGO-5 magnetic field observations p0072 A73-33452

Satellite studies of magnetospheric substorms on August 15, 1968. 5: Energetic electrons, spatial boundaries, and wave-particle interactions at OGO-5. p0072 A73-33453

Satellite studies of magnetospheric substorms on August 15, 1968. 6: OGO 5 energetic electron observations. Pitch angle distributions in the nighttime magnetosphere p0072 A73-33454

Satellite studies of magnetospheric substorms on August 15, 1968. 9: Phenomenological model for substorms. p0072 A73-33457

Quiet time magnetospheric field depression at 2.3-3.6 earth radii. p0072 A73-33464

Dependence of the polar cusp on the north-south component of the interplanetary magnetic field. p0072 A73-36273

A magnetospheric field model incorporating the OGO-3 and 5 magnetic field observations. p0074 A73-43693

Solar wind and magnetosheath electron temperature measurements by triaxial electron analyzer onboard OGO-5, presenting data for bow shock p0075 A73-45112

Rate of erosion of dayside magnetic flux based on a quantitative study of the dependence of polar cusp latitude on the interplanetary magnetic field. p0075 A74-14274

The magnetotail and substorms. --- magnetic flux transport model p0076 A74-17742

A correlated study of ELF waves and electron precipitation on OGO-6. p0077 A74-24766

The origin and propagation of chorus in the outer magnetosphere. p0078 A74-24767

Plasmaspheric hiss intensity variations during magnetic storms. p0080 A74-34038

Dynamical characteristics of pulsating substorm. p0112

[B14580-000] OGO-5 observations of the physical processes occurring in the disturbed polar cusp and the cusp-magnetosheath interface p0113

[B18269-000] A multi-satellite study of the nature of wavelike structures in the magnetosphere plasma p0114

[B22600-000] Is the red arc a good indicator of ionosphere-magnetosphere conditions p0114

[B22605-000] Cinematographic display of observations of low energy proton and electron spectra in terrestrial magnetosphere p0087 N68-15232

[NASA-CR-91871] Whistler propagation in magnetospheric ducts studies based on ray tracings verified by ground and satellite observations p0087 N68-17981

OGO-1 and OGO-3 VLF emission records of magnetospheric electromagnetic noise p0091 N70-15678

[NASA-CR-107653] Comparison of observation data by whistlers and mass spectrometers of plasmopause p0092 N70-27302

[NASA-TM-X-63905] VLF data from OGO 2 and OGO 4 on propagation, wave-particle interactions, and noise in ionosphere and magnetosphere p0093 N70-32928

[NASA-CR-110658] Resonant oscillations of geomagnetic field in magnetosphere caused by solar wind p0096 N71-32519

[NASA-TM-X-65644] Magnetic field fluctuations during magnetospheric substorms and field aligned currents in magnetosphere, based on satellite observations p0096 N72-11325

[NASA-TM-X-65748] Observation of magnetospherically reflected whistlers made by OGO-A and OGO-C p0101 N73-16344

[NASA-CR-130352] OGO-4 satellite observations of whistler-mode propagation effects associated with caustics in the magnetosphere p0104 N74-12109

Variation with interplanetary sector of the total magnetic field measured at the OGO 2, 4, and 6 satellites p0104 N74-13566

[NASA-TM-X-70531] Magnetospheric chemical release study --- modifications of wave particle interactions in magnetosphere p0105 N74-17126

[AD-769979] Magnetospheric modulation effects on solar cosmic rays from simultaneous OGO 1 and 3 ion chamber data in 1968 and 1969 p0105 N74-18420

[NASA-CR-137075] Instruments for the Stanford University/Stanford Research Institute VLF experiment(4917) on the EOGO satellite p0109 N74-74765

[NASA-CR-139258] Magnetospheric substorm, 1972 p0110 N74-77515

MAGNETOSPHERIC ELECTRON DENSITY

Electron intensities and substorm drift effects in outer radiation belt using two satellite technique p0026 A69-43172

Spacecraft surface secondary electron emission effects on electron trap measurements in magnetosphere and solar wind, noting agreement with positive ion densities p0027 A70-13994

Magnetospheric thermal plasma electron density measurement during solar flare by OGO-5 satellite p0036 A70-37513

Magnetic field and electron plasma observations near dawn magnetopause by triaxial spectrometer and fluxgate magnetometer on satellite OGO 5 p0050 A71-31754

Properties of low energy particle impacts in the polar domain in the dawn and dayside hours. p0061 A72-39541

Precipitation of low-energy electrons at high latitudes: Effects of interplanetary magnetic field and dipole tilt angle. p0066 A73-15531

The plasmasphere during a magnetic recovery period: A combined study of the OGO-4 and OGO-5 satellite data and of whistlers received at the ground. p0072 A73-33876

Temporal variations of 40 keV electrons in magnetosphere during and after magnetic storm on April 18, 1965 [NASA-CR-85905] p0086 N67-31362

MAGNETOSPHERIC ION DENSITY

Mantle aurora caused by auroral electron drift and precipitation [NASA-TM-X-63941] p0093 N70-29987

MAGNETOSPHERIC INSTABILITY

Magnetospheric plasmopause shape, changes of electron density and wave phenomena p0014 A68-37940

Broadband and highpass LF noise in distant magnetosphere detected by VLF/LF experiment on OGO 1 satellite p0031 A70-27183

Observation of a current-driven plasma instability at the outer zone-plasma sheet boundary. p0069 A73-29966

Satellite studies of magnetospheric substorms on August 15, 1968. 1: State of the magnetosphere. p0071 A73-33449

Satellite studies of magnetospheric substorms on August 15, 1968. 3: Some features of magnetospheric convection. p0072 A73-33451

Satellite studies of magnetospheric substorms on August 15, 1968. 7: OGO-5 energetic proton observations. Spatial boundaries p0072 A73-33455

Satellite studies of magnetospheric substorms on August 15, 1968. 8: OGO-5 plasma wave observations. p0072 A73-33456

Active experiments, magnetospheric modification, and a naturally occurring analogue. p0075 A74-14283

Postmidnight chorus: A substorm phenomenon. --- outer magnetosphere p0076 A74-18364

OGO-B and OGO-E measurements on magnetospheric field magnitudes and disturbances caused by ring currents p0095 N71-25271

Beta particle observations between inner edge of plasma sheet to plasmopause in midnight earth magnetosphere [NASA-TM-X-65640] p0095 N71-32436

MAGNETOSPHERIC ION DENSITY

Plasmasphere thermal positive ion structure, determining distribution of hydrogen and helium positive ions in magnetosphere from OGO p0014 A68-37114

Magnetic activity effect on magnetospheric plasmopause position, measuring ion concentrations as function of local time from OGO 5 observations p0029 A70-18530

Plasmasphere bulge region morphology from hydrogen ion concentration measurement by mass spectrometer on OGO 5 satellite p0035 A70-36014

Simultaneous hydrogen ion composition measurements by upper ionospheric polar orbiting OGO 4 and eccentric orbiting magnetospheric OGO 3 at midlatitude p0037 A70-38377

Whistler ducts as enhanced ionization from OGO 3 satellite observations near magnetic equator, noting magnetospheric ionization hydrostatic model and predicted cut-off p0041 A71-11499

Hydrogen ion concentration measurements by OGO 5 in plasmasphere during intense magnetic storms accompanied by stable auroral red arcs p0047 A71-24787

Plasmaspheric ambient hydrogen and helium atomic cations density measurement by OGO 5 ion mass spectrometer during magnetic storm, noting relationship to auroral red arcs p0053 A71-39833

Hydrogen ions concentration in dayside region of plasmasphere from OGO 5 satellite mass spectrometry, noting plasmopause position as function of magnetic activity p0054 A72-10892

Plasmopause nightside, dayside and bulge positive ion concentration measurements with OGO 5 mass spectrometer compared with magnetospheric convection model p0061 A72-39544

Plasmasphere hydrogen, helium, oxygen and nitrogen ions inbound and outbound profiles from OGO 5 mass spectrometric measurements p0065 A73-12320

The light-ion trough, the main trough, and the plasmopause. p0066 A73-15533

MAGNETOSPHERIC PROTON DENSITY

The plasmasphere during a magnetic recovery period: A combined study of the OGO-4 and OGO-5 satellite data and of whistlers received at the ground.

p0072 A73-33876

Dynamics of midlatitude light ion trough and plasmatails --- from data obtained on OGO-4 [NASA-TM-X-70494]

p0103 N74-10366

MAGNETOSPHERIC PROTON DENSITY

Solar protons in magnetospheric tail after flare of July 7, 1966 with isotropic pitch angle distribution, expressing energy spectrum as exponential in rigidity

p0020 A69-21699

MANAGEMENT PLANNING

Discussion of a management program for evaluation of aerospace systems design - Orbiting Geophysical Observatory (OGO) is used as an example

p0001 A63-13537

MAPPING

Inner magnetosphere magnetic field mapping, deriving pogo model

p0038 A70-39349

A global magnetic anomaly map --- obtained from POGO satellite data [NASA-TM-X-70628]

p0106 N74-20982

MAPS

Geomagnetic field minimum in southern Brazil, comparing satellites data maps

p0017 A68-42083

MASS SPECTRA

Analysis of light ion mass spectrometer data from OGO-E experiment [NASA-CR-130156]

p0101 N73-16432

MASS SPECTROMETERS

OGO-1 first results on mass spectrometry measurements of thermal positive ion composition at high altitudes

p0004 A66-14781

Earth satellite sweeping mass spectrometer for measuring atmospheric neutral particle and positive ion concentration

p0025 A69-36681

Spacecraft sheath structure, potential and velocity effects on ion current measurements by traps and mass spectrometers

p0038 A70-41087

Role of gas-surface interactions in the reduction of OGO-6 neutral particle mass spectrometer data.

p0073 A73-38941

Experiment data analysis report for the OGO-4 neutral and ion mass spectrometer experiment [B05000-000]

p0111

Global empirical model of thermospheric composition based on OGO-6 mass spectrometer measurements

[B16248-000] p0112

Comparison of observation data by whistlers and mass spectrometers of plasmopause

[NASA-TM-X-63905] p0092 N70-27302

Design, test evaluation, and performance failure analysis of ion mass spectrometer for OGO-F [NASA-CR-111146]

p0094 N71-10588

Thermospheric composition and density, measured by neutral mass spectrometer onboard OGO-6 satellite

p0101 N73-17946

High latitude minor ion enhancements: A clue for studies of magnetosphere-atmosphere coupling --- using OGO 6 ion mass spectrometer [NASA-TM-X-70582]

p0104 N74-16064

A light ion mass spectrometer experiment for OGO-E

[NASA-CR-122291] p0110 N74-76914

Neutral and ion mass spectrometer experiment S5015

[NASA-CR-96663] p0110 N74-77537

MASS SPECTROSCOPY

Empirical model of global thermospheric temperature and composition based on data from the OGO-6 quadrupole mass spectrometer.

p0076 A74-18376

Comparison of atomic oxygen measurements by incoherent scatter and satellite-borne mass spectrometer techniques.

p0078 A74-27713

Oxygen atom recombination reactions with solid surfaces for mass spectrometer atomic oxygen composition correction in upper atmosphere

[NASA-CR-106805] p0091 N70-11727

Statistical analysis of neutral and ion mass spectroscopy data for OGO-2

[NASA-CR-107408] p0091 N70-14425

MASS TRANSFER

Energy and diffusive mass transport relation to thermospheric circulation, composition, temperature and mass density from three dimensional two constituent magnetic storm model

p0070 A73-29975

MATHEMATICAL MODELS

International geomagnetic reference field model described by spherical harmonic coefficients with first and second time derivatives

p0012 A68-26625

Resonant compression waves in geomagnetic tail estimated for frequency and spatial distribution by single layered two dimensional model

p0028 A70-15127

Collisionless plasma spherical probe RF sheath model based on quasi-static approximation and electrostatic theory

p0057 A72-23520

Global empirical model of thermospheric composition based on OGO-6 mass spectrometer measurements [B16248-000]

p0112

Resonances in driving point impedance of electric dipole antenna in ionosphere [NASA-CR-91620]

p0087 N68-14025

The inner zone electron model AE-5 [NASA-TM-X-69987]

p0106 N74-20502

The reduction and analysis of electron data for outer zone electron model AE-4. Volume 3: OGO-1 and 3 University of Minnesota experiment data [NASA-TM-X-70212]

p0109 N74-74636

MATRIX METHODS

Coordinate transformations for OGO satellite data reduction

[NASA-TM-X-63826] p0092 N70-19313

MEASURING INSTRUMENTS

Retarding potential analyzer errors and performance degradation due to grid plane potential depressions

p0058 A72-26411

MESONS

Interplanetary cosmic ray positrons energy spectral component with origin different from interstellar mesons decay

p0036 A70-38098

MESOPAUSE

Disposition of scattering layers over polar-regions as observed by OGO-6 airglow photometer [NASA-CR-130271]

p0101 N73-16436

METAL IONS

Meteoric metallic ions above F 2 peak, discussing current density and transport mechanisms

p0039 A70-43841

Positive Fe ion concentration relationship to equatorial spread F from OGO 6 satellite observation near magnetic equator

p0054 A72-10902

Equatorial spread F formation convective electric fields generation by neutral winds and conductivity caused by metallic ion concentrations

p0070 A73-29988

METAL SURFACES

Oxygen atom recombination reactions with solid surfaces for mass spectrometer atomic oxygen composition correction in upper atmosphere

[NASA-CR-106805] p0091 N70-11727

METEOR TRAILS

Meteors and micrometeoroids influx near earth (1965-1967)

p0014 A68-35397

METEOROID CONCENTRATION

Meteors and micrometeoroids influx near earth (1965-1967)

p0014 A68-35397

METEOROID DUST CLOUDS

Micrometeoroid experiments on OGO 2 and OGO 4 satellites, measuring velocity, masses and particle orbits in earth dust cloud

p0027 A70-10444

Geminid meteoroid dust particles detection, determining velocity and orbital elements from OGO 3 flux measurements

p0050 A71-33741

Micrometeoroids in earth dust cloud obtained from OGO-B satellite

[NASA-CR-100683] p0089 N69-23367

METEOROLOGY

Is the red arc a good indicator of ionosphere-magnetosphere conditions

[B22605-000] p0114

SUBJECT INDEX

MICROBALANCES

Thermoelectrically-cooled quartz crystal microbalance --- monitor of surface contamination as function of temperature

p0103 N74-10255

MICROFILMS

User guide to microfilm records of data obtained in energetic particle experiment with OGO-5 [UCRL-51307]

p0102 N73-31150

MICROMETEORIODS

Inconclusiveness of satellite measurements of micrometeoroid fluxes using piezoelectric microphone detectors in supporting hypothesis of cloud of dust surrounding earth

p0006 A66-41213

Meteors and micrometeoroids influx near earth (1965-1967)

p0014 A68-35397

Micrometeoroid experiments on OGO 2 and OGO 4 satellites, measuring velocity, masses and particle orbits in earth dust cloud

p0027 A70-10444

Meteoric metallic ions above F 2 peak, discussing current density and transport mechanisms

p0039 A70-43841

OGO 4 satellite micrometeoroid flux detection, emphasizing noise control procedures for data correlation

p0048 A71-28700

Micrometeoroid experiment on the OGO 4 satellite [B04201-000]

p0111

Micrometeoroids in earth dust cloud obtained from OGO-B satellite [NASA-CR-100683]

p0089 N69-23367

MICROPHONES

Fabrication, installation, and operation of microphone density gage experiment onboard OGO-F [NASA-CR-130082]

p0098 N72-28467

MICROSTRUCTURE

Solar wind microscopic structure, examining interplanetary wave-particle interactions

p0042 A71-14068

MICROWAVE EMISSION

X-radiation (E greater than 10 keV), H-alpha and microwave emission during the impulsive phase of solar flares.

p0066 A73-17041

Possible low energy (E less than keV) nonthermal X ray events --- analysis of proportional counter detector data from OGO-5

p0107 N74-21450

MICROWAVE SPECTRA

Soft X-ray and microwave observations of hot regions in solar flares.

p0060 A72-35089

Evidence for a common origin of the electrons responsible for the impulsive X-ray and type 3 radio bursts.

p0067 A73-20766

MIDLATITUDE ATMOSPHERE

Simultaneous hydrogen ion composition measurements by upper ionospheric polar orbiting OGO 4 and eccentric orbiting magnetospheric OGO 3 at midlatitude

p0037 A70-38377

Midlatitude red arc observations by satellite and ground station, suggesting thermal conduction theory of formation from ionospheric electron and ion temperatures and densities

p0061 A72-35989

Dynamics of midlatitude light ion trough and plasmatails --- from data obtained on OGO-4 [NASA-TM-X-70494]

p0103 N74-10366

A model ionosphere for mid-day and mid-latitude during sunspot minimum [SMUP-3]

p0109 N74-74635

MISSION PLANNING

OGOs design evolution with respect to scientific mission requirements

p0034 A70-35303

Orbiting Geophysical Observatories S-49, S-50 [NASA-TM-X-50488]

p0110 N74-76913

MODELS

Transport of solar flare protons: Comparison of a new analytic model with spacecraft measurements [B10763-000]

p0112

MOLECULAR IONS

Oxygen ion anticorrelation to molecular ion concentrations from OGO 6 observations in F 2 region

p0062 A72-42016

MONITORS

Orbiting Geophysical Observatory programming system consisting of real time quick-look monitor and data processors

[AIAA PAPER 64-218] p0002 A64-24447

MONOCHROMATORS

Nonfocusing grazing incidence monochromator which utilizes planar gratings and collimating slit systems

p0005 A66-27326

Ultraviolet solar radiation research instruments for space vehicles

[AFRL-64-773] p0083 N65-14504

Telemetry instruments aboard space vehicles for study of solar ultraviolet radiation monochromator, spectrometer, and radiation counter

[NASA-CR-64074] p0083 N65-29678

MONOPOLE ANTENNAS

Complex impedance measurements for monopole antenna for electron densities in/out of OGO satellite wake in upper ionosphere

p0035 A70-35771

MORPHOLOGY

Electron precipitation patterns and substorm morphology

[B16756-000] p0112

A model environment for outer zone electrons

[NASA-TM-X-69989] p0106 N74-20503

N

NASA PROGRAMS

NASA electrostatic solar plasma instruments for Orbiting Geophysical Observatory and Interplanetary Monitoring Platform measuring flux, energy spectrum, etc.

p0003 A65-29239

NEAR WAKES

Electron depletion in the wake of ionospheric spacecraft: A comparison between results from Langmuir probes and antennas.

p0072 A73-34783

NEBULAE

Gum Nebula size, density and electron temperature data from RAE-1 and OGO-5 satellites and ground based telescopes observations, correlating with Vela X supernova outburst

p0052 A71-35409

NEUTRAL PARTICLES

Earth satellite sweeping mass spectrometer for measuring atmospheric neutral particle and positive ion concentration

p0025 A69-36681

Neutral atmospheric composition and density variations during geomagnetic disturbances from OGO-6 satellite quadrupole mass analyzer measurements

p0052 A71-39711

Atmospheric neutral density measurement near 400 km during daytime by microphone density gage on OGO 6

p0058 A72-26407

Auroral heating and the composition of the neutral atmosphere.

p0069 A73-27602

Experiment data analysis report for the OGO-4 neutral and ion mass spectrometer experiment

[B05000-000] p0111

NEUTRAL SHEETS

A magnetospheric field model incorporating the OGO-3 and 5 magnetic field observations.

p0074 A73-43693

NEUTRON COUNTERS

OGO-6 neutron monitor for measuring cosmic ray neutron flux near earth, locating sensor on boom to minimize spacecraft produced neutrons

p0024 A69-36678

Neutron measurements on OGO-6 spacecraft

[NASA-CR-130181] p0101 N73-19841

NEUTRON FLUX DENSITY

OGO-6 neutron monitor for measuring cosmic ray neutron flux near earth, locating sensor on boom to minimize spacecraft produced neutrons

p0024 A69-36678

Cosmic ray albedo neutron flux latitude and altitude dependence, using OGO-6 polar orbiting satellite

p0037 A70-39326

Cosmic ray neutron leakage flux and energy spectrum measurements in 0.01-10 MeV range by OGO 6 satellite-borne neutron detector

p0054 A72-10877

Neutron flux and energy spectra measurements in space related to theoretical predictions, discussing neutron leakage flux, solar neutron observations and radiation detector configurations

p0073 A73-36645

Quiet-time solar neutron flux upper limit from OGO-6 neutron detector, evaluating solar cosmic ray acceleration, nuclear reaction and energy region

p0074 A73-41498

NEUTRON SPECTRA

Neutron flux and energy spectra measurements in space related to theoretical predictions, discussing neutron leakage flux, solar neutron observations and radiation detector configurations

p0073 A73-36645

NEUTRONS

Measurements of the atmospheric neutron leakage rate

p0076 A74-15356

A search for solar neutrons during solar flares

[B22608-000] p0114

OGO-6 measurements of solar neutrons

p0103 N73-32639

NIGHT SKY

Radiative recombination of atomic oxygen ions in nighttime F region UV radiation detected by polar-orbiting OGO 4 satellite

p0023 A69-34957

Nighttime plasmopause and thermal ion plasma structures relationship to micropulsations, considering excitation in post storm recovery and diurnal plasma bulge regions

p0056 A72-17453

Outer magnetosphere near midnight at quiet and disturbed times.

p0063 A72-44513

Satellite studies of magnetospheric substorms on August 15, 1968. 6: OGO 5 energetic electron observations. Pitch angle distributions in the nighttime magnetosphere

p0072 A73-33454

Effects of interhemisphere transport on plasma temperatures at low latitudes.

p0074 A73-41919

Local time asymmetries in increase of electron fluxes in outer Van Allen zone during substorms

[NASA-CR-100419] p0089 N69-20849

NIGHTGLOW

Hydrogen Lyman alpha nightglow models, discussing solar photon scattering in geocorona and hydrogen vertical distribution

p0022 A69-30191

Tropical UV nightglow measurement by Ogo-4 spectrometer, considering ionospheric recombination excitation mechanism

p0037 A70-39338

UV oxygen nightglow observation by OGO-4, examining ion-ion neutralization and radiative recombination production mechanisms

p0037 A70-39344

Atomic oxygen green line emission in nightglow from OGO-F photometer observations, calculating tropical F region electron density spatial distribution

p0060 A72-35604

Spatial and temporal behavior of atomic oxygen determined by OGO 6 airglow observations.

p0079 A74-30670

Comparison of Cosmos-215 and OGO-D observations of nightglow in 1225 to 1350 A range at low geomagnetic latitudes

p0096 N71-34333

Jicamarca radio observations of temperature and electron density profiles, films of Spread F structure, and nightglow emission intensities

[NASA-CR-121984] p0096 N71-35437

NITRIC OXIDE

Global nitric oxide and gamma emission measurements with Ebert-Fastie scanning spectrometer onboard polar orbiting OGO 4 satellite

p0064 A73-10878

Satellite ultraviolet measurements of nitric oxide fluorescence with a diffusive transport model.

p0074 A73-41925

NITROGEN

Thermospheric atomic oxygen and molecular nitrogen densities from OGO 6 neutral atmospheric composition experiment, comparing with prediction by Jacchia models

p0062 A72-42431

NITROGEN OXIDES

An upper limit to the product of NO and O densities from 105 to 120 Km

[B22606-000] p0114

NOISE (SOUND)

Digital data processing system for very low frequency radio noise and propagation experiment aboard OGO-1

[NASA-CR-88618] p0086 N67-37021

NOISE INTENSITY

Intensity variation of elf hiss and chorus during isolated substorms

[B22603-000] p0114

NOISE SPECTRA

Magnetopause location, boundary positions and magnetic noise spectral data obtained with triaxial search coil magnetometer aboard OGO 1 satellite

p0004 A66-23148

Continuous and triggered audio frequency noise bands associated with ionospheric lower hybrid resonance frequency observed on OGO 2

p0018 A69-16257

Magnetospheric ELF noise, discussing OGO 3 spectrum analysis

p0019 A69-18834

VLF and LF emission characteristic features and origin mechanism in auroral regions of ionosphere, discussing satellite observation of noise spectrum in space

p0025 A69-38495

Broadband and highpass LF noise in distant magnetosphere detected by VLF/LF experiment on OGO 1 satellite

p0031 A70-27183

Pioneer 9 space probe electric field experiment and near earth observations of noise spectra variations related to diffusive plasma layer

p0046 A71-23711

NONUNIFORM MAGNETIC FIELDS

Magnetospheric magnetic field distortions under quiet and slightly disturbed conditions, obtaining scalar intensity with OGO 3 and 5 rubidium vapor magnetometer

p0054 A72-10886

NORTHERN HEMISPHERE

Low energy electron precipitation data at northern high latitudes obtained from satellite low altitude polar orbit

p0021 A69-28964

NUCLEAR EXPLOSIONS

Model of electrons artificially injected into inner radiation belt by Starfish nuclear explosion

[NASA-TM-X-66211] p0102 N73-20842

NUCLEI (NUCLEAR PHYSICS)

Energy spectra and abundances of elements He through Si of galactic cosmic ray above 20 Mev per nucleon in nuclear charge range between 2 and 26

p0006 A67-11687

Cosmic ray nuclei energy spectra and abundances above 20 Mev/nucleon determined by OGO-1 satellite experiment, considering He, B, C, N, O, Ne, Mg, Si, Mn, Fe, Co and Ni

p0020 A69-20067

Low energy multiply charged cosmic ray nuclei propagation and source characteristics, considering two component model based on OGO satellite measurements

p0020 A69-20068

The abundances of solar accelerated nuclei from carbon to iron.

p0065 A73-13719

OBSERVATORIES

The Orbiting Geophysical Observatory - tool for space research

[NASA-TN-D-1450] p0082 N62-15053

OPERATIONAL PROBLEMS

Operational performance of radiometer antenna on OGO-A

[NASA-CR-103321] p0090 N69-31345

OPTICAL EQUIPMENT

Photoelectric optical imaging system survival in earth radiation belt, noting noise level and total energy absorption

p0007 A67-12055

OPTICAL RESONANCE

Solar flare model, computing thermal X ray emission

p0046 A71-20945

ORBIT CALCULATION

Computation methods and results for orbital data, spacecraft angle, and heat input for OGO and specifically for EGO

[NASA-TM-X-55428] p0084 N66-21006

ORBITAL ELEMENTS

- OGO-5 orbital plots generated by the UCLA fluxgate magnetometer group
[NASA-CR-139260] p0108 N74-74633
- ORBITAL ELEMENTS**
Geminid meteoroid dust particles detection, determining velocity and orbital elements from OGO 3 flux measurements p0050 A71-33741
- ORBITAL MECHANICS**
OGO attitude computations [NASA-TM-X-63373] p0110 N74-76912
- OSCILLATIONS**
Multiple magnetopause crossings in equatorial plane by OGO 5, showing magnetopause motion composed of two oscillations p0046 A71-21631
- OUTER RADIATION BELT**
Directional differential intensities of protons injected into outer radiation zone coincident with initial phase of geomagnetic storm and monitored by OGO 3 p0016 A68-41684
POGO ion chamber measurement of ionization by penetrating radiation, discussing spike intensity p0017 A68-43450
Electron intensities and substorm drift effects in outer radiation belt using two satellite technique p0026 A69-43172
Extraterrestrial ring current proton intensities asymmetric increases in outer radiation belt during magnetic storms p0030 A70-23490
Low energy protons omnidirectional intensity contours in outer radiation zone at magnetic equator p0030 A70-2349i
Directional differential energy spectra for proton intensities in outer radiation zone near magnetic equator from satellite observations p0043 A71-17261
Plasmaspheric hiss intensity variations during magnetic storms. p0080 A74-34038
Trapped electron environment in inner and outer radiation belts - tables and graphs [NASA-SP-3024-VOL-2] p0084 N66-35685
OGO outer zone observational data on electron intensities of earth geomagnetic field [NASA-CR-89652] p0087 N67-40126
Energetic electron intensities in outer radiation zone of earth measured by OGO-1 satellite p0088 N69-12899
Local time asymmetries in increase of electron fluxes in outer Van Allen zone during substorms [NASA-CR-100419] p0089 N69-20849
- OUTGASSING**
OGO-6 surface contamination by outgassing in space environment and decontamination by sputtering and desorption [NASA-CR-117138] p0094 N71-20207
- OV-1 SATELLITES**
Ionospheric electric fields variations in ELF-VLF, confirming OV-1 satellite measurements with OGO 6 data p0033 A70-30082
- OXYGEN**
OGO 5 ion spectrometer for measuring oxygen, He and hydrogen ion concentration, noting functions as energetic particle analyzer and proton energy distribution measurement capability p0024 A69-36679
An upper limit to the product of NO and O densities from 105 to 120 Km [B22606-000] p0114
Atomic oxygen emission line at 6300 A for low latitudes observed by OGO-D satellite [NASA-TM-X-65913] p0098 N72-26309
Airglow maps for atomic oxygen 6300 A line from OGO-D satellite [NASA-TM-X-65954] p0098 N72-28353
- OXYGEN ATOMS**
UV OGO observations of atomic hydrogen and oxygen in airglow, comparing results to exospheric models of hydrogen geocorona p0022 A69-31400
Radiative recombination of atomic oxygen ions in nighttime F region UV radiation detected by polar-orbiting OGO 4 satellite p0023 A69-34957
Thermospheric atomic oxygen and molecular nitrogen densities from OGO 6 neutral atmospheric composition experiment, comparing with prediction by Jacchia models p0062 A72-42431

- Distribution of atomic oxygen in the upper atmosphere deduced from OGO-6 airglow observations. p0075 A73-45121
Comparison of atomic oxygen measurements by incoherent scatter and satellite-borne mass spectrometer techniques. p0078 A74-27713
Spatial and temporal behavior of atomic oxygen determined by OGO 6 airglow observations. p0079 A74-30670
Oxygen atom recombination reactions with solid surfaces for mass spectrometer atomic oxygen composition correction in upper atmosphere [NASA-CR-106805] p0091 N70-11727
- OXYGEN SPECTRA**
UV oxygen nightglow observation by OGO-4, examining ion-ion neutralization and radiative recombination production mechanisms p0037 A70-39344
Lyman alpha and atomic oxygen 1304 A airglow depressions over poles from OGO 4 satellite observations p0041 A71-11503
O I 1304-A airglow, observing conjugate excitation with OGO 4 spacecraft p0043 A71-17279
Atomic oxygen green line emission in nightglow from OGO-F photometer observations, calculating tropical F region electron density spatial distribution p0060 A72-35604
Theoretical calculations of the F-region tropical ultraviolet airglow intensity. p0062 A72-42418
Asymmetrical global O I airglow emission pattern with respect to magnetic equator from OGO 4 observations, noting poor correlation with ionospheric electron density p0073 A73-38939

OZONE

- Ozone vertical distribution in upper stratosphere determined from OGO 4 observations, describing calibration of satellite data and onboard instrumentation p0023 A69-32645
Stratospheric ozone vertical distribution as determined by ultraviolet spectrometer on polar orbiting OGO-4 satellite p0090 N69-26549

P

PARTICLE ACCELERATION

- Heavy nuclei enrichment in solar accelerated particles, discussing differential energy spectra, photospheric and coronal abundances, satellite observation and agreement with galactic cosmic rays p0055 A72-15366
The abundances of solar accelerated nuclei from carbon to iron. p0065 A73-13719
Quiet-time solar neutron flux upper limit from OGO-6 neutron detector, evaluating solar cosmic ray acceleration, nuclear reaction and energy region p0074 A73-41498
Acceleration of electrons during the flash phase of solar flares. p0079 A74-30287
Acceleration of electrons in solar flares. p0079 A74-30908
Acceleration of electrons in the absence of detectable optical flares deduced from type 3 radio bursts, H-alpha activity and soft X-ray emission [B22607-000] p0114
- PARTICLE DENSITY (CONCENTRATION)**
Low energy charged particle distribution within earth magnetosphere and environs, suggesting solar origin for storm time ring current protons p0033 A70-30089
- PARTICLE DIFFUSION**
Diffusion-convection theory for solar cosmic ray propagation in interplanetary magnetic field p0090 N69-29659
- PARTICLE EMISSION**
Solar flare energetic X-ray events detected by onboard satellite ionization chambers, studying relationship to radio burst and space particle emission p0009 A67-41232

PARTICLE ENERGY

- OGO 3 observation of low energy protons and electrons in earth magnetosphere, noting narrow peak of relatively high low-energy particle intensities p0008 A67-26312
Magnetosphere low energy proton and electron density spatial distributions and temporal variations from OGO 3 satellite observations p0013 A68-34245
Low energy charged particles in earth magnetosphere observed by OGO satellite p0019 A69-19358
Cosmic ray nuclei energy spectra and abundances above 20 Mev/nucleon determined by OGO-1 satellite experiment, considering He, B, C, N, O, Ne, Mg, Si, Mn, Fe, Co and Ni p0019 A69-20067
Low energy charged particle distribution within earth magnetosphere and environs, suggesting solar origin for storm time ring current protons p0033 A70-30089
Properties of low energy particle impacts in the polar domain in the dawn and dayside hours. p0061 A72-39541
On the origin of low energy heavy nuclei below approximately 30 MeV per nucleon observed in interplanetary space during quiet times, 1968-72. p0078 A74-30156

PARTICLE FLUX DENSITY

- Spatial variations in particle intensity near and inside magnetosphere during September 1966 solar cosmic ray events, noting magnetosphere screening effectiveness p0018 A69-12740
Trapped particle population changes associated with solar events, discussing solar wind discontinuity effects on magnetosphere p0036 A70-37487
Picogram dust particle flux measurements in selenocentric, ecliptic and interplanetary space by Mariner 4, OGO 3 and Explorer 35 p0041 A71-14014
Quiet time fluxes and differential energy spectra of protons and alpha particles at 2-20 MeV measured by cosmic ray detectors on OGO-3 p0044 A71-18127
OGO 4 satellite micrometeoroid flux detection, emphasizing noise control procedures for data correlation p0048 A71-28700
High latitude regions of low energy electron precipitation from OGO 4 satellite auroral particle experiment p0049 A71-30032
Geminid meteoroid dust particles detection, determining velocity and orbital elements from OGO 3 flux measurements p0050 A71-33741
Behavior of outer radiation zone and a new model of magnetospheric substorm. p0063 A72-44850
Direct measurements of solar-wind fluctuations between 0.0048 and 13.3 Hz. p0068 A73-23539
Distributions and characteristics of high-latitude field-aligned electron precipitation. p0069 A73-26988
Measurements of the atmospheric neutron leakage rate p0076 A74-15356
- PARTICLE INTENSITY**
Forbush decreases and long term cosmic ray particle intensity changes, investigating spectral variations p0044 A71-18137
- PARTICLE INTERACTIONS**
Solar wind microscopic structure, examining interplanetary wave-particle interactions p0042 A71-14068
Nonthermal electrons interaction with electron plasma oscillations and HF transverse waves in upstream solar wind. p0052 A71-37353
Plasma wave-particle interaction inside the neutral sheet (in Japanese) [B14583-000] p0112
Bombardment of OGO-6 surfaces by high-energy particles [B20297-000] p0113
Magnetospheric chemical release study -- modifications of wave particle interactions in magnetosphere [AD-769979] p0105 N74-17126

Characteristics of nonthermal electrons accelerated during the flash phase of small solar flares p0106 N74-21445

PARTICLE MOTION

Sensors used in cosmic dust experiments studied for response to microparticle hypervelocity impacts, noting relationship to velocity p0013 A68-29468

Drift shell splitting in nondipolar distorted magnetosphere tested with data from electron spectrometer on ATS 1 and OGO 3 satellites p0026 A69-40508

Geminid meteoroid dust particles detection, determining velocity and orbital elements from OGO 3 flux measurements p0050 A71-33741

PARTICLE TELESCOPES

Electron and proton spectrometer detector mounted on OGO-5, measurements cover seven differential energy channels p0005 A66-23690

Low energy cosmic ray nuclei propagating in interstellar space analyzed by telescope onboard OGO 1 p0016 A68-41434

Electron scattering effects on response of cosmic ray particle telescopes from pulse height and counting rate measurements p0057 A72-21510

Nuclear composition telescope measurements onboard OGO 5 satellite, observing presence of geomagnetically trapped carbon, nitrogen and oxygen nuclei p0059 A72-32959

PARTICLE TRAJECTORIES

Speeds, directions of arrival, and mass of dust particles measured from OGO-1 satellite to determine orbits of dust particles p0086 N67-32070

PARTICLES

Energetic electron and proton solar particle observations on OGO-5, 24-34 January 1971 [B15152-000] p0112

PAYLOADS

Orbiting geophysical observatories p0001 A63-10333

PERIGEE

Relationship of perigee motion of satellite orbit to latitude and local time [NASA-TM-X-55703] p0085 N67-18763

PERIODIC VARIATIONS

Solar Lyman-alpha radiation observed by OGO 4 spacecraft showing short term fluctuations superimposed with monthly variation p0028 A70-15128

PERTURBATION THEORY

Perturbations in density of ions and neutral particles in upper atmosphere due to OGO [NASA-CR-117897] p0094 N71-23238

PHOTOELECTRIC EMISSION

Energy distribution of photoelectrons emitted from a surface on the OGO-5 satellite and measurements of satellite potential. p0076 A74-17648

A satellite ion-electron collector: Experimental effects of grid transparency, photoemission, and secondary emission [NASA-CR-139262] p0109 N74-74638

PHOTOELECTRICITY

Photoelectric optical imaging system survival in earth radiation belt, noting noise level and total energy absorption p0007 A67-12055

PHOTOELECTRONS

Photoelectron flux measurements in topside ionosphere using retarding potential analyzers [NASA-TM-X-63358] p0087 N68-35999

PHOTOMETERS

Airglow lines measured through photometers on OGO-2 satellite, noting nadir and zenith airglow p0007 A67-23278

In-flight radiometric calibration of low brightness OGO 4 airglow photometer p0029 A70-15645

Global temperature distributions from OGO-6 6300 A airglow measurements. p0077 A74-23679

Data reduction methods for OGO airglow photometer measurements [NASA-TM-X-55794] p0085 N67-27576

Laboratory tests on interference sensitivity of polar OGO airglow photometer [NASA-TM-X-55791] p0085 N67-27578

Flight calibration device for absolute measurements of photometer at Lyman alpha wavelength on OGO-6 and other satellites [AD-726567] p0096 N71-36136

Diurnal variation of Lyman alpha spectral width as measured by OGO-6 sky-scanning photometer [AD-736816] p0097 N72-23429

Functional characteristics of OGO-4 main body airglow photometer utilizing cathode photomultiplier to sense light at selected wavelengths [NASA-TM-X-65926] p0098 N72-27423

PHOTOMETRY

Orbiting Geophysical Observatory satellite /OGO 3/ photometric measurements, establishing daytime sky brightness upper limit p0010 A68-12548

Display and processing program for data from gegenschein photometry experiment from OGO-B [NASA-TM-X-55907] p0086 N67-35595

PHOTOMULTIPLIER TUBES

Triaxial electron spectrometer, mounted on OGO-5 spacecraft, measures flux and energy distributions of electrons, noting electron multiplier p0005 A66-23689

Continuous-channel electron multipliers degradation in spacecraft environment simulation laboratory equipment p0021 A69-29565

Effects of energetic particles on photomultipliers in earth orbits up to 1500 km [NASA-TM-X-63419] p0088 N69-18074

PIEZOELECTRIC CRYSTALS

Inconclusiveness of satellite measurements of micrometeoroid fluxes using piezoelectric microphone detectors in supporting hypothesis of cloud of dust surrounding earth p0006 A66-41213

PIONEER SPACE PROBES

Magnetic design of OGO and Pioneer solar probe including data on instrumentation, mechanical equipment, permanent magnets, test methods, etc p0004 A66-15919

Measurement of differential energy spectra of protons, helium nuclei and heavy nuclei by cosmic radiation telescopes mounted on POGO and Pioneer satellites p0004 A66-23684

PIONEER 7 SPACE PROBE

Solar wind compressed magnetic field in sunward magnetosphere and extended geomagnetic tail observation by Pioneer 7 spacecraft p0049 A71-30028

PIONEER 9 SPACE PROBE

Pioneer 9 space probe electric field experiment and near earth observations of noise spectra variations related to diffusive plasma layer p0046 A71-23711

Simultaneous observations of plasma waves from electric field instruments on Pioneer 9 and OGO 5 to illustrate difference between near-earth and deep space conditions p0100 N73-10795

PITCH (INCLINATION)

Drift shell splitting in nondipolar distorted magnetosphere tested with data from electron spectrometer on ATS 1 and OGO 3 satellites p0026 A69-40508

Pitch-angle diffusion of radiation belt electrons within the plasmasphere. p0060 A72-35597

Shadowing of electron azimuthal-drift motions near the noon magnetopause. p0065 A73-12442

Electron pitch angle distributions throughout the magnetosphere as observed on OGO-5. p0068 A73-24732

Effects of season altitude and pitch angle on electron precipitation from OGO-D data [NASA-TM-X-66260] p0102 N73-25868

PLANETARY RADIATION

A new model for the high-frequency decametric radiation from Jupiter p0081 A74-43688

PLASMA CONDUCTIVITY

Equatorial spread F formation convective electric fields generation by neutral winds and conductivity caused by metallic ion concentrations p0070 A73-29988

PLASMA CONTROL

Nuclear composition telescope measurements onboard OGO 5 satellite, observing presence of geomagnetically trapped carbon, nitrogen and oxygen nuclei p0059 A72-32959

Shadowing of electron azimuthal-drift motions near the noon magnetopause. p0065 A73-12442

PLASMA DENSITY

Satellite measurements of cold plasma density and plasmopause in magnetosphere, comparing whistler, Langmuir probe and ion trap data p0049 A71-30951

PLASMA DIAGNOSTICS

OGO-5 plasma spectrometers for measuring total flux below 12 keV and energy (spectral density) of plasma p0017 A68-42739

Collision free earth shock wave gross and fine structure deduced from OGO 5 plasma diagnostics [AIAA PAPER 69-676] p0023 A69-33452

Satellite plasma diagnostics for electric and magnetic fields and fine structure of collisionless shocks in solar wind plasma flows and interplanetary shocks p0032 A70-30069

Ionospheric ion temperature measurements by retarding potential analyzer on OGO-6 satellite p0039 A70-43840

Pioneer 9 space probe electric field experiment and near earth observations of noise spectra variations related to diffusive plasma layer p0046 A71-23711

High energy electron spatial distribution in plasma sheet from OGO 5 magnetometer experiments p0062 A72-42406

Correlation of ground-based measurements of structured Pc 1 micropulsations with OGO-V plasmopause observations. p0067 A73-20652

Active experiments, magnetospheric modification, and a naturally occurring analogue. p0075 A74-14283

PLASMA DIFFUSION

Pioneer 9 space probe electric field experiment and near earth observations of noise spectra variations related to diffusive plasma layer p0046 A71-23711

PLASMA FLUX MEASUREMENTS

Plasmasphere thermal positive ion structure, determining distribution of hydrogen and helium positive ions in magnetosphere from OGO p0014 A68-37114

OGO-5 plasma spectrometers for measuring total flux below 12 keV and energy (spectral density) of plasma p0017 A68-42739

Observations of the internal structure of the magnetopause. p0077 A74-21679

PLASMA FREQUENCIES

Detection of solar-wind electron plasma frequency fluctuations in an oblique nonlinear magnetohydrodynamic wave. p0061 A72-35610

Nonlinear frequency correction to plasma instability at half harmonics of electron gyrofrequency as observed by OGO 5 near geomagnetic equator outside plasmopause p0068 A73-22069

PLASMA INTERACTIONS

Detection of solar-wind electron plasma frequency fluctuations in an oblique nonlinear magnetohydrodynamic wave. p0061 A72-35610

Solar wind interaction with geomagnetic field, discussing magnetosphere polar cusp region and geomagnetic tail neutral sheet structure p0065 A73-13871

PLASMA LAYERS

Pioneer 9 space probe electric field experiment and near earth observations of noise spectra variations related to diffusive plasma layer p0046 A71-23711

Plasma sheet proton ring current, trapping boundary and plasmopause interrelations near magnetic equator and local midnight by satelliteborne analyzer array p0047 A71-24781

High energy electron spatial distribution in plasma sheet from OGO 5 magnetometer experiments p0062 A72-42406

PLASMA OSCILLATIONS

PLASMA OSCILLATIONS

Nonthermal electrons interaction with electron plasma oscillations and HF transverse waves in upstream solar wind.

p0052 A71-37353

Electron plasma oscillations distribution upstream from earth bow shock, evaluating OGO-5 plasma wave detector data

p0057 A72-23019

PLASMA PHYSICS

Electric field fluctuations in magnetospheric plasma at multiples of local electron gyrofrequency due to plasma instability

p0052 A71-37368

Solar wind 10-9900 eV electron flux, evaluating energy transport in plasma rest frame

p0055 A72-13507

Plasma proton and plasma electron prototype and flight models [NASA-CR-122351]

p0097 N72-18715

PLASMA POTENTIALS

Energy distribution of photoelectrons emitted from a surface on the OGO-5 satellite and measurements of satellite potential.

p0076 A74-17648

Effect of satellite potential on direct ion density measurements through the plasmopause.

p0076 A74-18372

PLASMA PROBES

IMP-2 and OGO-1 measurements on plasma characteristics in transition region between solar wind and geomagnetic field

p0003 A65-25921

Flux, energy distribution and density of ions and electrons in magnetosphere plasma during solar activity period determined by OGO-3 electrostatic probes

p0012 A68-29421

Electron trap behavior on charged spacecraft, obtaining expressions for current to aperture and internal retarding electrodes for all apertures and spacecraft potentials

p0022 A69-31976

Collisionless plasma spherical probe RF sheath model based on quasi-static approximation and electrostatic theory

p0057 A72-23520

Charged particle distribution study in near earth region using orbiting spherical electrostatic analyzers or plasma probes

[AD-700804] p0092 N70-28003

PLASMA RESONANCE

Resonances in driving point impedance of electric dipole antenna in ionosphere [NASA-CR-91620]

p0087 N68-14025

PLASMA SHEATHS

Magnetospheric plasmopause shape, changes of electron density and wave phenomena

p0014 A68-37940

Spacecraft sheath structure, potential and velocity effects on ion current measurements by traps and mass spectrometers

p0038 A70-41087

Electron densities between inner edge plasma sheet and plasmasphere as function of geocentric radial distance from OGO-3 electrostatic measurements

p0039 A70-43834

OGO 5 polar cusp observations showing dayside magnetosheath plasma penetration during magnetic storm

p0053 A71-43162

Collisionless plasma spherical probe RF sheath model based on quasi-static approximation and electrostatic theory

p0057 A72-23520

Plasma waves in the dayside polar cusp. 2: Magnetopause and polar magnetosheath.

p0077 A74-21680

PLASMA SPECTRA

OGO-5 plasma spectrometers for measuring total flux below 12 keV and energy (spectral density) of plasma

p0017 A68-42739

PLASMA SPRAYING

Removal of surface contamination by plasma sputtering [NASA-CR-139264]

p0109 N74-74659

PLASMA TEMPERATURE

OGO-6 measurements of supercooled plasma in the equatorial exosphere.

p0068 A73-22066

Effects of interhemisphere transport on plasma temperatures at low latitudes.

p0074 A73-41919

PLASMA TURBULENCE

Large amplitude interplanetary solar wind discontinuities observed by OGO-5 plasma spectrometer and magnetometers, considering magnetic drift waves mechanism for plasma turbulence generation

p0058 A72-29378

Turbulence of electrostatic electron cyclotron harmonic waves observed by OGO-5.

p0060 A72-35599

Weak electrostatic turbulence observation in earth bow shock magnetic field gradient, suggesting cyclotron drift instability role

p0063 A72-44523

Observation of a current-driven plasma instability at the outer zone-plasma sheet boundary.

p0069 A73-29966

PLASMA WAVES

Rapid magnetic field variations observed in magnetosheath evaluated in terms of transverse modes of plasma wave propagation [JPL-TR-32-1199]

p0009 A67-40804

OGO 5 spacecraft detector instrumentation for measuring electrostatic and electromagnetic waves electric fields with coupled antennas, describing in-flight operation

p0025 A69-36683

Low altitude electric and magnetic measurements of plasma waves in space from OV3-3, Pioneer 8 and OGO 5 satellite observations

p0029 A70-17376

Polar ionosphere auroral oval position detection by satellite observations of naturally occurring VLF and man-made HF plasma waves

p0032 A70-29924

Plasma wave particle interactions in outer magnetosphere, magnetosheath and solar wind, noting role of AC electric fields

p0033 A70-30085

OGO 5 observations of quasi-trapped electromagnetic waves in solar wind at 70 kHz

p0035 A70-36005

Large amplitude upstream wave solar wind event of 10 March 1968 with suprathermal protons, correlating magnetometer plasma probe and Lepede proton data

p0043 A71-14550

Electron plasma oscillations distribution upstream from earth bow shock, evaluating OGO-5 plasma wave detector data

p0057 A72-23019

Plasma wave measurements during OGO-5 dayside magnetosphere polar cusp encounters, discussing ULF magnetic field wave levels and VLF electric field amplitude ranges

p0059 A72-29380

Magnetospheric observations in OGO 5 plasma wave experiment, emphasizing electrostatic wave particles interaction with plasma

p0065 A73-13883

Ion cyclotron waves observed in the polar cusp.

p0071 A73-33437

Satellite studies of magnetospheric substorms on August 15, 1968. 8: OGO-5 plasma wave observations.

p0072 A73-33456

Plasma waves in the dayside polar cusp. 2: Magnetopause and polar magnetosheath.

p0077 A74-21680

Plasma wave-particle interaction inside the neutral sheet (in Japanese) [B14583-000]

p0112

A multi-satellite study of the nature of wavelike structures in the magnetosphere plasma [B22600-000]

p0114

Data analysis program for the OGO E-24 plasma wave detector [NASA-CR-140523]

p0110 N74-77109

PLASMA-ELECTROMAGNETIC INTERACTION

Magnetospheric sudden impulses amplitude and rise time distributions observation by OGO 3 and 5 satellites

p0043 A71-17686

Observation of a current-driven plasma instability at the outer zone-plasma sheet boundary.

p0069 A73-29966

PLASMA-PARTICLE INTERACTIONS

Plasma wave particle interactions in outer magnetosphere, magnetosheath and solar wind, noting role of AC electric fields

p0033 A70-30085

SUBJECT INDEX

Morphology of thermal and energetic particles in inner magnetosphere during geomagnetic disturbances and solar cycles

p0034 A70-30358

Pitch-angle diffusion of radiation belt electrons within the plasmasphere.

p0060 A72-35597

Magnetospheric observations in OGO 5 plasma wave experiment, emphasizing electrostatic wave particles interaction with plasma

p0065 A73-13883

Observation of a current-driven plasma instability at the outer zone-plasma sheet boundary.

p0069 A73-29966

PLASMAPAUSE

Pc 1 micropulsation source region relation to plasmopause, using amplitude and polarization measurements

p0043 A71-17263

Plasma sheet proton ring current, trapping boundary and plasmopause interrelations near magnetic equator and local midnight by satelliteborne analyzer array

p0047 A71-24781

Satellite measurements of cowl plasma density and plasmopause in magnetosphere, comparing whistler, Langmuir probe and ion trap data

p0049 A71-30951

Stable auroral red arcs on 29 September 1967, 31 October and 1 November 1968, comparing OGO 2 and OGO 4 VLF data on plasmopause crossings

p0050 A71-31757

Earth corotating plasma tail evidence in plasmopause variations from high resolution proton distribution data obtained by OGO 4 satellite during magnetic storm

p0053 A71-43166

Hydrogen ions concentration in dayside region of plasmasphere from OGO 5 satellite mass spectrometry, noting plasmopause position as function of magnetic activity

p0054 A72-10892

Nighttime plasmopause and thermal ion plasma structures relationship to micropulsations, considering excitation in post storm recovery and diurnal plasma bulge regions

p0056 A72-17453

OGO-5 plasmopause crossing correlation with ground observations of Pi geomagnetic micropulsations

p0056 A72-21223

Thermal positive ion densities measurement in outer ionosphere and magnetosphere by OGO 1 satellite, relating plasmopause distribution and magnetic activity level [AD 742186]

p0057 A72-23011

OGO-5 observation of lower hybrid resonance noise, bursts, VLF hiss and whistlers near plasmopause during large magnetic storm

p0058 A72-26399

Plasmopause nightside, dayside and bulge positive ion concentration measurements with OGO 5 mass spectrometer compared with magnetospheric convection model

p0061 A72-39544

The light-ion trough, the main trough, and the plasmopause.

p0066 A73-15533

An association of magnetospheric whistler dispersion characteristics with changes in local plasma density.

p0069 A73-26985

Satellite studies of magnetospheric substorms on August 15, 1968. 3: Some features of magnetospheric convection.

p0072 A73-33451

The plasmasphere during a magnetic recovery period: A combined study of the OGO-4 and OGO-5 satellite data and of whistlers received at the ground.

p0072 A73-33876

Active experiments, magnetospheric modification, and a naturally occurring analogue.

p0075 A74-14283

Effect of satellite potential on direct ion density measurements through the plasmopause.

p0076 A74-18372

Atmospheric model for thermal plasma near equatorial plasmopause

p0095 N71-25270

Dynamics of midlatitude light ion trough and plasmatails --- from data obtained on OGO-4 [NASA-TM-X-70494]

p0103 N74-10366

A light ion mass spectrometer experiment for OGO-E [NASA-CR-122291]

p0110 N74-76914

SUBJECT INDEX

PLASMAS (PHYSICS)

Plasmapause observations by ion spectrometer aboard OGO-5 vehicle for early orbits, obtaining O, He and H ion concentration profiles for geomagnetic parameter p0029 A70-18546

Plasma tail interpretations of pronounced detached plasma regions measured with OGO-5 [B20951-000] p0113

A multi-satellite study of the nature of wavelike structures in the magnetosphere plasma [B22600-000] p0114

The measurement of cold ion densities in the plasma trough [B22610-000] p0114

Applying impedance data to plasma wake of spinning OGO-C satellite [NASA-CR-109457] p0092 N70-23999

Comparison of observation data by whistlers and mass spectrometers of plasmapause [NASA-TM-X-63905] p0092 N70-27302

POLAR CAP ABSORPTION

Satellite charged particle observations and polar cap riometer absorption measurements during solar cosmic ray events, noting electron and proton contributions p0059 A72-31965

POLAR CAPS

Polar-cap electric field distributions related to the interplanetary magnetic field direction. p0062 A72-42432

Electron polar cap and the boundary of open geomagnetic field lines. p0063 A72-44522

POLAR ORBITS

Cosmic ray knee interpretation using polar orbiting ionization chambers data from OGO-2/4 p0034 A70-31903

Geomagnetic survey by polar-orbiting OGO 2 and 4, discussing data acquisition and reduction results and accuracy p0054 A72-12081

Global nitric oxide and gamma emission measurements with Ebert-Fastie scanning spectrometer onboard polar orbiting OGO 4 satellite p0064 A73-10878

POLAR REGIONS

High latitude electron bursts observed by OGO 4, postulating electric field acceleration mechanism beyond 3 earth radii for ambient thermal plasma electrons p0017 A68-43443

Solar protons nonuniformity over polar caps observed by OGO 2 ionization chamber during 24 March 1966 solar proton events p0022 A69-31967

Ion depletion in high latitude exosphere, considering OGO 2 simultaneous observations of positive ion concentration, VLF signal propagation and whistlers p0023 A69-34939

Solar protons delayed access into polar regions during 2 November 1967 solar particle event, discussing north-south asymmetry p0027 A69-43183

Polar ionosphere auroral oval position detection by satellite observations of naturally occurring VLF and man-made HF plasma waves p0032 A70-29924

Quiet time cosmic ray ionization altitude dependence over polar regions from measurements by integrating ionization chamber on OGO-2 p0034 A70-31902

Lyman alpha and atomic oxygen 1304 A airglow depressions over poles from OGO 4 satellite observations p0041 A71-11503

High latitude regions of low energy electron precipitation from OGO 4 satellite auroral particle experiment p0049 A71-30032

Suprathermal electron temperature and ion composition as function of geomagnetic latitude in polar ionosphere, using Explorer 31 mass spectrometer measurements p0049 A71-30037

High latitude sudden impulses, calculating transverse hydromagnetic waves propagation from magnetosphere equatorial plane p0052 A71-34777

OGO 5 polar cusp observations showing dayside magnetosheath plasma penetration during magnetic storm p0053 A71-43162

Plasma wave measurements during OGO-5 dayside magnetosphere polar cusp encounters, discussing ULF magnetic field wave levels and VLF electric field amplitude ranges p0059 A72-29380

High latitude observation of precipitating electron spikes by polar orbiter OGO 4 satellite, noting population dependence on local trapping limit p0060 A72-35591

Properties of low energy particle impacts in the polar domain in the dawn and dayside hours. p0061 A72-39541

Precipitation of low-energy electrons at high latitudes: Effects of interplanetary magnetic field and dipole tilt angle. p0066 A73-15531

OGO 5 observation of ULF geomagnetic fluctuation at polar cusp boundaries in terms of ionospheric drift wave and Kelvin-Helmholtz instabilities p0068 A73-24744

Distributions and characteristics of high-latitude field-aligned electron precipitation. p0069 A73-26988

Field-aligned currents, plasma waves, and anomalous resistivity in the disturbed polar cusp. p0069 A73-29964

Ion cyclotron waves observed in the polar cusp. p0071 A73-33437

Dependence of the polar cusp on the north-south component of the interplanetary magnetic field. p0072 A73-36273

Latitude and local time dependence of precipitated low-energy electrons at high latitudes. p0074 A73-41914

Rate of erosion of dayside magnetic flux based on a quantitative study of the dependence of polar cusp latitude on the interplanetary magnetic field. p0075 A74-14274

Plasma waves in the dayside polar cusp. 2: Magnetopause and polar magnetosheath. p0077 A74-21680

Near-earth magnetic disturbance in total field at high latitudes. 1: Summary of data from OGO-2, 4, and 6. 2: Interpretation of data from OGO-2, 4, and 6. p0080 A74-34019

Heating of the high-latitude thermosphere during magnetically quiet periods. p0080 A74-34027

OGO-5 observations of the physical processes occurring in the disturbed polar cusp and the cusp-magnetosheath interface [B18269-000] p0113

High latitude proton precipitation and light ion density profiles during the magnetic storm initial phase [B22333-000] p0113

OGO-D atmospheric composition data for polar thermospheric storm model [NASA-CR-103080] p0094 N71-20638

Disposition of scattering layers over polar-regions as observed by OGO-6 airglow photometer [NASA-CR-130271] p0101 N73-16436

POLAR SUBSTORMS
Magnetosphere and adjacent regions magnetic surveys by OGO 1 and 3 satellites, discussing magnetopause, bow shock, magnetosheath, geomagnetic tail, ring current and polar substorms p0055 A72-12084

Behavior of outer radiation zone and a new model of magnetospheric substorm. p0063 A72-44850

Substorm related changes in the geomagnetic tail: The growth phase. p0064 A72-44856

Precipitation of low-energy electrons at high latitudes: Effects of interplanetary magnetic field and dipole tilt angle. p0066 A73-15531

Synoptic survey for the neutral line in the magnetotail during the substorm expansion phase. p0073 A73-36275

POLARIZATION (WAVES)
Measurements of VLF polarization and wave normal direction on OGO-F [NASA-CR-132882] p0104 N74-12842

POLARIZATION CHARACTERISTICS
Pe 1 micropulsation source region relation to plasmapause, using amplitude and polarization measurements p0043 A71-17263

PRIMARY COSMIC RAYS

POLES

Geomagnetic dipole field disturbances by trapped particles, calculating self consistent equilibrium configuration for ring current dipole moments p0034 A70-31905

POSITION (LOCATION)

Plasmapause position measurements by ion mass spectrometers and broadband VLF receivers on OGO 1 and OGO 3 and by broadband recordings at Antarctica p0021 A69-25153

Magnetic dipole position at E layer and gradient with time and altitude, using geomagnetic field models p0026 A69-42428

Location and scheduling of operation of Eccentric Geophysical Observatory /EGO/ in gegenschein reference system [NASA-TM-X-55032] p0082 N64-27813

POSITRONS

Low energy interplanetary positrons detection by OGO satellites, discussing possible existence of equilibrium charge ratio p0015 A68-41427

Cosmic ray electron and positron differential energy spectra during solar quiet times from OGO5 satellite observations in interplanetary space p0036 A70-38096

Interplanetary cosmic ray positrons energy spectral component with origin different from interstellar mesons decay p0036 A70-38098

A double gamma-ray spectrometer to search for positrons in space p0110 N74-77446

POSTFLIGHT ANALYSIS

Data reduction and analysis report for radio astronomy experiment aboard OGO-2 spacecraft [NASA-CR-98669] p0088 N69-14393

POTENTIAL FIELDS

Retarding potential analyzer errors and performance degradation due to grid plane potential depressions p0058 A72-26411

Photoelectron flux measurements in topside ionosphere using retarding potential analyzers [NASA-TM-X-63358] p0087 N68-35999

POWER EFFICIENCY

Orbiting Geophysical Observatory electric power subsystem design innovations including power supply, solar array output and battery charge control p0003 A65-19528

POWER SPECTRA

Rapid magnetic field variations observed in magnetosheath evaluated in terms of transverse modes of plasma wave propagation [JPL-TR-32-1199] p0009 A67-40804

Hydrogen and helium cosmic ray nuclei isotopic composition measured to clarify abundance ratios energy dependence below 75 MeV/nucleon p0015 A68-41421

Cosmic-ray scintillations. I: Inside the magnetosphere. p0066 A73-15526

Direct measurements of solar-wind fluctuations between 0.0048 and 13.3 Hz. p0068 A73-23539

Rise time in 20-32 keV impulsive X-radiation. p0080 A74-38468

Possible noise sources in power spectra measurement of interplanetary magnetic field p0099 N73-10791

Power spectra of interplanetary magnetic field near earth bow shock p0099 N73-10792

POWER SUPPLIES

OGO structure and systems covering thermal and attitude controls, power plant, communications, tracking and data handling p0002 A65-14349

PRIMARY COSMIC RAYS

Primary cosmic ray charge and energy spectra for helium through oxygen during 1965 minimum solar modulation effect p0005 A66-26348

Studies of primary cosmic rays with ionization chambers, --- rigidity response of ionization chambers in high atmosphere and deep space for study of rigidity dependence of solar cycle modulation of primary cosmic ray p0006 A66-34768

NOV. 10, 1975

PROGRAMMERS

Chemical abundances and energy spectra of nuclei in galactic radiation measured in interplanetary space by OGO-1 satellite

p0006 A66-34833

Primary cosmic ray energy spectra and charge composition during 1965 solar modulation minimum, using scintillator photomultiplier detector on OGO 1

p0016 A68-41431

Electron detector for OGO-E to measure flux and energy spectrum of electrons in primary cosmic rays [IEEE PAPER 3C-4]

p0020 A69-19198

Cosmic ray nuclei energy spectra and abundances above 20 Mev/nucleon determined by OGO-1 satellite experiment, considering He, B, C, N, O, Ne, Mg, Si, Mn, Fe, Co and Ni

p0020 A69-20067

Low energy multiply charged cosmic ray nuclei propagation and source characteristics, considering two component model based on OGO satellite measurements

p0020 A69-20068

Quiet time primary cosmic ray electron flux and energy spectrum from 10 to 200 Mev in interplanetary space observed by OGO 5 satellite

p0027 A70-12902

Solar electrons, galactic electron radiation modulation and spectrum of high energy cosmic ray electrons.

p0071 A73-33293

The elemental abundance ratios of interstellar secondary and primary cosmic rays.

p0079 A74-30190

The cosmic ray electron spectrum and its modulation from 1968 through 1972.

p0079 A74-30204

Earth satellite experiment for measuring the charge and energy spectra of the primary cosmic rays [B01634-000]

p0111

Measurements of the primary cosmic ray electron spectrum between 20 MeV and 20 GeV and its changes with time [B08373-000]

p0112

PROGRAMMERS

Programmer manual for Polar Orbiting Geophysical Observatory [IS-769]

p0082 N64-13388

PROJECT MANAGEMENT

Discussion of a management program for evaluation of aerospace systems design - Orbiting Geophysical Observatory (OGO) is used as an example

p0001 A63-13537

PROPAGATION

Solar flare protons and physical processes affecting particle propagation in interplanetary space

p0098 N72-27829

PROPAGATION MODES

Magnetospheric ionization distribution determined by ducted and nonducted whistler propagation modes and reflection as observed by OGO 1

p0010 A68-17728

Low energy multiply charged cosmic ray nuclei propagation and source characteristics, considering two component model based on OGO satellite measurements

p0020 A69-20068

Nonducted VLF walking trace whistlers and Doppler shifts in fixed frequency transmissions identified on OGO midlatitude spectrographic records

p0028 A70-15116

OGO 6 ionospheric measurement of proton whistlers wave-normal vector, investigating propagation modes

p0056 A72-19148

Whistler mode signals observation in conjugate region of 200 kHz broadcast station by satellite-borne narrow band receiver, considering field-aligned ducted and nonducted propagation

p0059 A72-29384

PROPAGATION VELOCITY

Magnetosphere Alfvén velocity profile relation to ELF chorus and hiss, indicating unstable wave generation by cyclotron resonance

p0039 A70-43851

PROTON BEAMS

Electromagnetic emissions in vicinity of proton gyrofrequency from OGO 2 satellite measurements, noting sweep frequency receiver PCM and Rayspan special purpose data

p0013 A68-31481

PROTON DENSITY (CONCENTRATION)

Directional differential intensities of protons injected into outer radiation zone coincident with initial phase of geomagnetic storm and monitored by OGO 3

p0016 A68-41684

Ion cut-off whistlers observed during VLF experiment aboard OGO 2 and OGO 4, noting possible application to relative ionospheric proton concentration determination

p0018 A69-14029

Directional differential energy spectra for proton intensities in outer radiation zone near magnetic equator from satellite observations

p0043 A71-17261

Earth corotating plasma tail evidence in plasmopause variations from high resolution proton distribution data obtained by OGO 4 satellite during magnetic storm

p0053 A71-43166

Magnetospheric plasma tail study, using thermal proton density measurements from OGO 4

p0101 N73-17948

PROTON ENERGY

Proton and He nuclei differential energy spectra and intensity variations in interplanetary space in 1-20 MeV per nucleon energy range

p0015 A68-41420

Charged particles injection into captured radiation zone of Van Allen belts during main phase of magnetic storm indicated by proton data analysis

p0025 A69-37967

Low energy protons omnidirectional intensity contours in outer radiation zone at magnetic equator

p0030 A70-23491

Directional differential energy spectra for proton intensities in outer radiation zone near magnetic equator from satellite observations

p0043 A71-17261

Proton energy change effects on charged particles propagating in interplanetary space, using low energy solar flare proton fluxes observations

p0046 A71-22801

Geomagnetic cutoffs for cosmic-ray protons for seven energy intervals between 1.2 and 39 Mev

p0061 A72-38728

Energetic electrons and protons observed on OGO-5, March 6-10, 1970

p0111

Instrumentation and calibrations of low energy proton and electron experiment for Orbiting Geophysical Observatories

p0084 N66-13640

Cinematographic display of observations of low energy proton and electron spectra in terrestrial magnetosphere

p0087 N68-15232

PROTON FLUX DENSITY

Differential energy spectra of low energy protons and positive ions in earth inner radiation zone, using electrostatic analyzers aboard OGO-3 satellite

p0011 A68-17771

Magnetosphere low energy proton and electron density spatial distributions and temporal variations from OGO 3 satellite observations

p0013 A68-34245

Proton and He nuclei differential energy spectra and intensity variations in interplanetary space in 1-20 MeV per nucleon energy range

p0015 A68-41420

Extraterrestrial ring current proton intensities asymmetric increases in outer radiation belt during magnetic storms

p0030 A70-23490

Low energy protons omnidirectional intensity contours in outer radiation zone at magnetic equator

p0030 A70-23491

Directed proton fluxes measurements in bow shock, magnetosheath and solar wind by OGO 5 satellite ion spectrometer

p0040 A71-11491

Quiet time fluxes and differential energy spectra of protons and alpha particles at 2-20 MeV measured by cosmic ray detectors on OGO-3

p0044 A71-18127

Proton energy change effects on charged particles propagating in interplanetary space, using low energy solar flare proton fluxes observations

p0046 A71-22801

Low energy electron and proton fluxes in geomagnetic tail of equatorial magnetosphere forming plasma sheet related to auroral oval

p0049 A71-30029

Solar proton intensity structures in the magnetosphere during interplanetary anisotropies.

p0066 A73-14962

Proton scattering in the region near the earth's bow shock.

p0067 A73-22054

SUBJECT INDEX

Satellite studies of magnetospheric substorms on August 15, 1968. 7: OGO-5 energetic proton observations. Spatial boundaries

p0072 A73-33455

Proton events observed with OGO-D and some observed flux profiles [NASA-CR-122360]

p0097 N72-25727

PROTON IRRADIATION

Explorer 18 satellite measurements of proton energy spectra in region corotating with sun, noting modulation of galactic cosmic radiation and source of continuous particle accelerations

p0005 A66-34754

PROTON PRECIPITATION

High latitude proton precipitation and light ion density profiles during the magnetic storm initial phase [B22333-000]

p0113

Measurements of VLF polarization and wave normal direction on OGO-F [NASA-CR-132882]

p0104 N74-12842

PROTON SCATTERING

Proton scattering in the region near the earth's bow shock.

p0067 A73-22054

PROTON-PROTON REACTIONS

Hydrogen and helium cosmic ray nuclei isotopic composition measured to clarify abundance ratios energy dependence below 75 MeV/nucleon

p0015 A68-41421

PROTONS

Electron and proton spectrometer detector mounted on OGO-5, measurements cover seven differential energy channels

p0005 A66-23690

OGO 3 observation of low energy protons and electrons in earth magnetosphere, noting narrow peak of relatively high low-energy particle intensities

p0008 A67-26312

Alpha particle proton ratio of geomagnetic field from data from charged-particle telescope on OGO 1 satellite

p0009 A67-37412

Energetic protons from March 24, 1966 solar flare observed with OGO 1 satellite scintillation counter

p0010 A67-41233

Geomagnetically trapped protons and alpha particles, analyzing OGO 4 data

p0027 A69-43184

OGO 6 ionospheric measurement of proton whistlers wave-normal vector, investigating propagation modes

p0056 A72-19148

Transport of solar flare protons: Comparison of a new analytic model with spacecraft measurements [B10763-000]

p0112

Effects of energetic particles on photomultipliers in earth orbits up to 1500 km [NASA-TM-X-63419]

p0088 N69-18074

Plasma proton and plasma electron prototype and flight models

p0097 N72-18715

Proton events observed with OGO-D and some observed flux profiles

p0097 N72-25727

User guide to microfilm records of data obtained in energetic particle experiment with OGO-5 [UCRL-51307]

p0102 N73-31150

PULSE AMPLITUDE

High latitude ionization spikes observed by POGO spacecraft, noting frequency correlation with magnetic disturbances and development by high energy electron injections

p0021 A69-28950

PULSED RADIATION

Hard X-ray pulse identification with formation of brilliant kernel (11-12 September 1968) flare by comparison with optical data

p0030 A70-25746

Q

QUADRUPOLES

Empirical model of global thermospheric temperature and composition based on data from the OGO-6 quadrupole mass spectrometer.

p0076 A74-18376

QUARTZ CRYSTALS

Thermoelectrically-cooled quartz crystal microbalance -- monitor of surface contamination as function of temperature

p0103 N74-10255

RADAR DATA

Diurnal variation of the neutral thermospheric winds determined from incoherent scatter radar data [B22601-000] p0114

RADAR MEASUREMENT

Geomagnetic equatorial ionospheric ion temperature, comparing incoherent scatter radar and OGO-D retarding potential analyzer values p0052 A/1-33956

RADAR SCATTERING

Comparison of Te and Ti from OGO-6 and from various incoherent scatter radars. p0067 A73-19241

Diurnal variation of the neutral thermospheric winds determined from incoherent scatter radar data [B22601-000] p0114

RADIANT FLUX DENSITY

Lyman alpha intensity and hydrogen concentration at 5 to 19 earth radii determined from OGO 3 spacecraft measurements p0031 A70-27181

Galactic gamma ray intensity near Cygnus by OGO-5 spacecraft-borne telescope with acoustic spark chamber, discussing source intensity p0038 A70-40691

Soft solar X-ray bursts characteristics, discussing temporal and intensity differential distributions, flux measurements and decay time p0048 A71-27654

Plasmaspheric hiss intensity variations during magnetic storms. p0080 A74-34038

RADIATION BELTS

Photoelectric optical imaging system survival in earth radiation belt, noting noise level and total energy absorption p0007 A67-12055

Electron spectra, pitch angle distributions and total ionization measured throughout radiation belts by satellite magnetic spectrometer and integrating ionization chamber p0008 A67-25807

Alpha particle proton ratio of geomagnetic field from data from charged-particle telescope on OGO 1 satellite p0009 A67-37412

Magnetosphere low energy proton and electron density spatial distributions and temporal variations from OGO 3 satellite observations p0013 A68-34245

Charged particles injection into captured radiation zone of Van Allen belts during main phase of magnetic storm indicated by proton data analysis p0025 A69-37967

Geomagnetically trapped protons and alpha particles, analyzing OGO 4 data p0027 A69-43184

Van Allen radiation belts energetic electrons injection and distribution due to magnetic storms, using satellite-borne spectrometers p0033 A70-30090

C, N and O nuclei abundances in radiation belt near geomagnetic equator, using data obtained by OGO-5 satellite in 1968 p0041 A71-13475

Pitch-angle diffusion of radiation belt electrons within the plasmasphere. p0060 A72-35597

Energy dependent time lag in the long-term modulation of cosmic rays. p0067 A73-19252

Cinematographic display of observations of low energy proton and electron spectra in terrestrial magnetosphere [NASA-CR-91871] p0087 N68-15232

OGO 1 and 3 spectrometer and ion chamber data on dynamic processes governing electrons in radiation belts, and applicability of diffusion theories and magnetic field models [NASA-CR-127455] p0098 N72-28802

Model of electrons artificially injected into inner radiation belt by Starfish nuclear explosion [NASA-TM-X-66211] p0102 N73-20842

RADIATION COUNTERS

Triaxial electron spectrometer, mounted on OGO-5 spacecraft, measures flux and energy distributions of electrons, noting electron multiplier p0005 A66-23689

Inconclusiveness of satellite measurements of micrometeoroid fluxes using piezoelectric microphone detectors in supporting hypothesis of cloud of dust surrounding earth p0006 A66-41213

Ground based riometer and satellite-borne particle detector data on May 23 and 28, 1967 solar cosmic ray events p0013 A68-31924

Low energy interplanetary positrons detection by OGO satellites, discussing possible existence of equilibrium charge ratio p0015 A68-41427

Latitude and local time dependence of precipitated low-energy electrons at high latitudes. p0074 A73-41914

Cosmic gamma-ray burst detected with an instrument on board the OGO-5 satellite. p0080 A74-31942

Telemetry instruments aboard space vehicles for study of solar ultraviolet radiation monochromator, spectrometer, and radiation counter [NASA-CR-64074] p0083 N65-29678

Comparison of simultaneous particle detector and search coil magnetometer measurements of precipitating particles and field aligned currents from OGO-D [NASA-TM-X-66224] p0102 N73-21367

RADIATION DAMAGE

Photoelectric optical imaging system survival in earth radiation belt, noting noise level and total energy absorption p0007 A67-12055

RADIATION DETECTORS

Measurement of differential energy spectra of protons, helium nuclei and heavy nuclei by cosmic radiation telescopes mounted on POGO and Pioneer satellites p0004 A66-23684

OGO cosmic ray measuring device involving charged particle detectors to measure spectra and chemical composition over selected energy intervals p0012 A68-27615

Low energy electrons on day side of magnetosphere observed with MIT electron detector on OGO 3 satellite p0018 A69-14027

Solar X-ray flare temperature and emission measure profiles using OGO 5 satellite detector, interpreting energy dispersion of peak times p0040 A70-45768

Measurements of electron detection efficiencies in solid state detectors. p0061 A72-39401

Recent studies of magnetospheric electric field emissions above the electron gyrofrequency p0067 A73-19254

RADIATION DISTRIBUTION

Center to limb variation of solar hard X ray bursts, suggesting inverse Compton effect and bremsstrahlung from anisotropic electrons p0023 A69-33055

Electron pitch angle distributions throughout the magnetosphere as observed on OGO-5. p0068 A73-24732

A model environment for outer zone electrons [NASA-TM-X-69989] p0106 N74-20503

RADIATION MEASUREMENT

OGO-6 neutron monitor for measuring cosmic ray neutron flux near earth, locating sensor on boom to minimize spacecraft produced neutrons p0024 A69-36678

Hysteresis effect on cosmic ray modulation and gradient ionization near solar minimum from measurements made near earth with OGO 1 and 3 ion chambers p0028 A70-15106

Cosmic ray knee interpretation using polar orbiting ionization chambers data from OGO-2/4 p0034 A70-31903

High energy galactic gamma rays search onboard OGO-5, tabulating results p0038 A70-40690

Cosmic ray neutron leakage flux and energy spectrum measurements in 0.01-10 MeV range by OGO 6 satellite-borne neutron detector p0054 A72-10877

Absolute cosmic ray ionization measurements in upper and lower atmosphere [NASA-CR-104068] p0090 N69-34536

Design of OGO-E experiment to measure energetic X-rays, electrons, protons, and alpha particle emissions from solar flares [NASA-CR-122509] p0098 N72-28812

Instrumentation and measurement data of OGO-F solar cosmic ray experiment [NASA-CR-130155] p0101 N73-16795

RADIATION MEASURING INSTRUMENTS

Integrating type ionization chamber applied to measurements of radiation in space [NASA-CR-90060] p0087 N68-10422

Instrumentation and measurement data of OGO-F solar cosmic ray experiment [NASA-CR-130155] p0101 N73-16795

RADIATION PRESSURE

New interpretations of extraterrestrial Lyman-alpha observations. p0065 A73-12323

RADIATION SOURCES

Low energy multiply charged cosmic ray nuclei propagation and source characteristics, considering two component model based on OGO satellite measurements p0020 A69-20068

Galactic gamma ray intensity near Cygnus by OGO-5 spacecraft-borne telescope with acoustic spark chamber, discussing source intensity p0038 A70-40691

Extraterrestrial hydrogen Lyman alpha emission source, investigating interstellar wind with OGO 5 satellite p0047 A71-24438

Lyman alpha sky background measurements by OGO 5 satellite, discussing absolute emission rate, spatial variations and origin p0047 A71-24439

RADIATION SPECTRA

Dynamic spectra of type 3 solar bursts from OGO-3 antenna/radiometer observations p0034 A70-34835

Long term variations of cosmic ray electron spectrum above 500 MeV from balloon and satellite observations, noting reduction during Forbush decreases p0037 A70-38105

Cosmic ray electron search and study, comparing near earth to interstellar spectrum p0060 A72-33869

RADIATIVE RECOMBINATION

Radiative recombination of atomic oxygen ions in nighttime F region UV radiation detected by polar-orbiting OGO 4 satellite p0023 A69-34957

UV oxygen nightglow observation by OGO-4, examining ion-ion neutralization and radiative recombination production mechanisms p0037 A70-39344

RADIO ASTRONOMY

Orbiting Geophysical Observatory (OGO) for cosmic ray, radio astronomy and Gegenschein experiments including satellite description and orbit data p0003 A65-22431

OGO radio astronomy instrument for cosmic noise sky brightness distribution mapping by electrically short antenna ionospheric focusing p0048 A71-26144

Heliographic longitude distribution of the flares associated with type 3 bursts observed at kilometeric wavelengths p0076 A74-14811

University of Michigan radio astronomy experiment aboard the OGO-5 spacecraft [B14718-000] p0112

Design considerations and performance characteristics for radio astronomy instrumentation system aboard OGO-5 spacecraft [NASA-CR-98670] p0088 N69-14392

Data reduction and analysis report for radio astronomy experiment aboard OGO-2 spacecraft [NASA-CR-98669] p0088 N69-14393

Low frequency space radio astronomy [NASA-TM-X-63976] p0093 N70-33175

Instrumentation for radio astronomy measurements aboard the OGO-1 and OGO-3 spacecraft. Part 2: Technical [NASA-CR-139257] p0108 N74-74631

Initial results from radio astronomy-experiment no. 18, OGO-3 [UM-RAO-67-9] p0109 N74-74660

Data user's notes: OGO-3 experiment no. 18 low frequency radio astronomy, appendices A and B [NASA-CR-140526] p0109 N74-76907

RADIO AURORAS

The global distribution of natural and man-made ionospheric electric fields at 200 kHz and 540 kHz as observed by OGO-6. p0080 A74-34020

RADIO BEACONS

RADIO BEACONS

Evaluation of radio beacon data from satellite observation of earth exosphere - data scaling techniques

[NASA-CR-68307] p0084 N66-12993

RADIO BURSTS

Solar flare X ray bursts detected by OGO spacecraft correlated with radio emission and solar flare electron and proton events

p0011 A68-22450

RADIO COMMUNICATION

The feasibility of a sub-LF satellite-to-submarine communication downlink VLF noise levels in the ionosphere

[AD-769139] p0104 N74-15857

RADIO ECHOES

Ambient electron energy spectrum secondary peak determined from unducted magnetospherically reflected whistler mode radiation measurements

p0015 A68-38428

RADIO EMISSION

Solar flare X ray and radio wave emission measurement by OGO-4 and Solrad-9 satellites

p0042 A71-14046

Solar flare model, computing thermal X ray emission

p0046 A71-20945

Studying whistlers and audio frequency emissions with receiving system on POGO satellite in conjunction with ground based observing stations

[NASA-CR-97605] p0088 N69-17928

RADIO FREQUENCIES

Nonducted very low frequency propagation in magnetosphere from broadband VLF receivers on OGO 2 and OGO 4 polar satellites

[NASA-CR-107614] p0091 N70-15525

Analysis of data on Type 3 bursts measured by OGO-5 satellite

[NASA-CR-122393] p0097 N72-23118

Neutral and ion mass spectrometer experiment S5015

[NASA-CR-96663] p0110 N74-77537

RADIO FREQUENCY INTERFERENCE

Reducing radio-frequency-interference from spacecrafts in the frequency range from 20Hz to 200 KHz

[B00969-000] p0111

RADIO OBSERVATION

Jicamarca radio observations of temperature and electron density profiles, films of Spread F structure, and nightglow emission intensities

[NASA-CR-121984] p0096 N71-35437

RADIO SIGNALS

The global distribution of natural and man-made ionospheric electric fields at 200 kHz and 540 kHz as observed by OGO-6.

p0080 A74-34020

Observations of whistler mode signal propagation by OGO satellites from very low frequency ground station transmitters

[NASA-CR-84869] p0085 N67-30831

RADIO SPECTRA

Power-law wavenumber spectrum deduced from ionospheric scintillation observations.

p0062 A72-42416

RADIO TRANSMISSION

Whistler mode signals observation in conjugate region of 200 kHz broadcast station by satellite-borne narrow band receiver, considering field-aligned ducted and nonducted propagation

p0059 A72-29384

A correlated study of ELF waves and electron precipitation on OGO-6.

p0077 A74-24766

The origin and propagation of chorus in the outer magnetosphere.

p0078 A74-24767

Observations of whistler mode signal propagation by OGO satellites from very low frequency ground station transmitters

[NASA-CR-84869] p0085 N67-30831

Digital data processing system for very low frequency radio noise and propagation experiment aboard OGO-1

[NASA-CR-88618] p0086 N67-37021

RADIO TRANSMITTERS

Observations of whistler mode signal propagation by OGO satellites from very low frequency ground station transmitters

[NASA-CR-84869] p0085 N67-30831

RADIO WAVES

Radio propagation experiment using transmitted VHF waves from OGO-1 to deduce electron density in ionosphere and magnetosphere

p0004 A66-10892

Solar flare X ray and radio wave emission measurement by OGO-4 and Solrad-9 satellites

p0042 A71-14046

RADIOMETERS

Operational performance of radiometer antenna on OGO-A

[NASA-CR-103321] p0090 N69-31345

RANGE (EXTREMES)

Nonthermal electron spectra hardness limit during flash phase of solar flares from OGO-5 observation

p0055 A72-14561

Quiet-time solar neutron flux upper limit from OGO-6 neutron detector, evaluating solar cosmic ray acceleration, nuclear reaction and energy region

p0074 A73-41498

RAY TRACING

Whistler propagation in magnetospheric ducts studies based on ray tracings verified by ground and satellite observations

p0087 N68-17981

REACTION KINETICS

Oxygen atom recombination reactions with solid surfaces for mass spectrometer atomic oxygen composition correction in upper atmosphere

[NASA-CR-106805] p0091 N70-11727

REAL TIME OPERATION

Orbiting Geophysical Observatory programming system consisting of real time quick-look monitor and data processors

[AIAA PAPER 64-218] p0002 A64-24447

RECEIVERS

Nonducted very low frequency propagation in magnetosphere from broadband VLF receivers on OGO 2 and OGO 4 polar satellites

[NASA-CR-107614] p0091 N70-15525

RECOMBINATION REACTIONS

Tropical UV nightglow measurement by Ogo-4 spectrometer, considering ionospheric recombination excitation mechanism

p0037 A70-39338

RED ARCS

Subauroral red arcs phenomenon hypotheses based on associated ionospheric plasma properties measurements

p0045 A71-19663

Hydrogen ion concentration measurements by OGO 5 in plasmasphere during intense magnetic storms accompanied by stable auroral red arcs

p0047 A71-24787

Stable auroral red arcs on 29 September 1967, 31 October and 1 November 1968, comparing OGO 2 and OGO 4 VLF data on plasmopause crossings

p0050 A71-31757

Plasmaspheric ambient hydrogen and helium atomic cations density measurement by OGO 5 ion mass spectrometer during magnetic storm, noting relationship to auroral red arcs

p0053 A71-39833

Midlatitude red arc observations by satellite and ground station, suggesting thermal conduction theory of formation from ionospheric electron and ion temperatures and densities

p0061 A72-35989

Observations of the conjugate SAR arcs of September 28-30, 1967. --- subauroral red arcs

p0080 A74-34042

Is the red arc a good indicator of ionosphere-magnetosphere conditions

[B22605-000] p0114

Enhancements of red arc during maximum solar activity

p0097 N72-23334

REFERENCE ATMOSPHERES

Parametric description of thermospheric ion composition results

p0067 A73-19255

REFERENCE SYSTEMS

Location and scheduling of operation of Eccentric Geophysical Observatory (EGO) in eegenschein reference system

[NASA-TM-X-55032] p0082 N64-27813

RELATIVISTIC PARTICLES

Relativistic electrons associated with solar particle events, measuring occurrence frequency, electron propagation and diffusion anisotropy.

p0048 A71-29057

Relativistic electron precipitation during magnetic storms, showing cyclotron resonances with electromagnetic ion cyclotron waves

p0051 A71-33948

Relativistic electrons in space

[B13262-000] p0112

Relativistic electron events in interplanetary space and other satellites

[B17665-000] p0113

Electromagnetic hiss and relativistic electron losses in the inner zone

[B22613-000] p0114

REMOTE SENSORS

Flight calibration device for absolute measurements of photometer at Lyman alpha wavelength on OGO-6 and other satellites

[AD-726567] p0096 N71-36136

RESONANT FREQUENCIES

Continuous and triggered audio frequency noise bands associated with ionospheric lower hybrid resonance frequency observed on OGO 2

p0018 A69-16257

Resonant compression waves in geomagnetic tail estimated for frequency and spatial distribution by single layered two dimensional model

p0028 A70-15127

VLF noise phenomena observed with satellite electric dipole antennas compared with lower hybrid resonance frequency of ionospheric medium in vicinity

p0029 A70-18534

RESONANT VIBRATION

Resonant oscillations of geomagnetic field in magnetosphere caused by solar wind

[NASA-TM-X-65644] p0096 N71-32519

RING CURRENTS

Charged particles of extraterrestrial ring current during geomagnetic storms, with OGO 3 measurements of proton and electron differential energy spectra

p0009 A67-37401

Extraterrestrial ring current proton intensities asymmetric increases in outer radiation belt during magnetic storms

p0030 A70-23490

Geomagnetic dipole field disturbances by trapped particles, calculating self consistent equilibrium configuration for ring current dipole moments

p0034 A70-31905

Plasma sheet proton ring current, trapping boundary and plasmopause interrelations near magnetic equator and local midnight by satelliteborne analyzer array

p0047 A71-24781

OGO-2 rubidium vapor magnetometer measurements comparison with surface magnetic observatory data during geomagnetic storms, considering asymmetric ring current

p0051 A71-33946

Magnetosphere and adjacent regions magnetic surveys by OGO 1 and 3 satellites, discussing magnetopause, bow shock, magnetosheath, geomagnetic tail, ring current and polar substorms

p0055 A72-12084

Magnetic field strength change in equatorial plasmasphere, considering quiet ring current as equatorial sheet current extension of neutral sheet current in magnetospheric tail

p0064 A73-11732

Asymmetry of the ring current

[B18378-000] p0113

Near view of the ring current

[B19906-000] p0113

OGO-B and OGO-E measurements on magnetospheric field magnitudes and disturbances caused by ring currents

p0095 N71-25271

RADIOMETERS

Ground based riometer and satellite-borne particle detector data on May 23 and 28, 1967 solar cosmic ray events

p0013 A68-31924

Satellite charged particle observations and polar cap riometer absorption measurements during solar cosmic ray events, noting electron and proton contributions

p0059 A72-31965

ROCKET SOUNDING

Electron measurements near weak aurora during rocket flight

p0008 A67-33595

ROCKET-BORNE INSTRUMENTS

Ultraviolet solar radiation research instruments for space vehicles

[AFCR1-64-773] p0083 N65-14504

SUBJECT INDEX

ROTATING PLASMAS

Earth corotating plasma tail evidence in plasmopause variations from high resolution proton distribution data obtained by OGO 4 satellite during magnetic storm p0053 A71-43166

ROTATION

Magnetopause rotational forms [B22604-000] p0114

RUBIDIUM

Rubidium vapor magnetometer used for near earth orbiting spacecraft, instrumentation and in-flight performance p0008 A67-36513
OGO-2 rubidium vapor magnetometer measurements comparison with surface magnetic observatory data during geomagnetic storms, considering asymmetric ring current p0051 A71-33946

S

SATELLITE ANTENNAS

OGO-6 electric and electromagnetic fields measurement for ionosphere using dipole antenna, emphasizing broadband observation covering whistler mode waves p0024 A69-36677

Complex impedance measurements for monopole antenna for electron densities in/out of OGO satellite wake in upper ionosphere p0035 A70-35771

Electron depletion in the wake of ionospheric spacecraft: A comparison between results from Langmuir probes and antennas. p0072 A73-34783

Evaluation of radio beacon data from satellite observation of earth exosphere - data scaling techniques [NASA-CR-68307] p0084 N66-12993

Operational performance of radiometer antenna on OGO-A [NASA-CR-103321] p0090 N69-31345

SATELLITE ATTITUDE CONTROL

Design of a simple attitude positioning control system for an orbiting geophysical observatory p0002 A64-10864

Single axis test program and simulator for vehicle dynamics in free space to test attitude control system of Orbiting Geophysical Observatory (OGO) p0002 A64-27303

OGO structure and systems covering thermal and attitude controls, power plant, communications, tracking and data handling p0002 A65-14349

High-altitude or small-earth limitations for advanced horizon sensor of Orbiting Geophysical Observatory /OGO-A/ [NASA-CR-83567] p0085 N67-22257

VLF experiments flown on OGO 1 (A17) and OGO 3 (B17) including orbits and attitudes of both satellites [NASA-CR-110716] p0093 N70-33156

OGO-C orientation study [REPT-9] p0109 N74-74661

SATELLITE DESIGN

Orbiting geophysical observatories p0001 A63-10333

Earth-sun relationship data obtained by Orbiting Geophysical Observatory experiments concerning the atmosphere of the earth, the magnetosphere, and cislunar space p0001 A63-21527

Magnetic design of OGO and Pioneer solar probe including data on instrumentation, mechanical equipment, permanent magnets, test methods, etc. p0004 A66-15919

OGO for conducting diversified measurements to study earth atmosphere, earth-sun relationship, etc. p0024 A69-36674

OGO-6 design, research program, orbits and instrumentation, emphasizing relationship between particle activity, aurora and airglow, geomagnetic field, atmospheric and solar energy interrelations p0026 A69-43132

SATELLITE DRAG

Seasonal density variations in thermosphere and exosphere, obtaining model from Explorers 19 and 39 drag measurements for comparison with OGO-6 mass spectroscopy p0051 A71-33802

SATELLITE INSTRUMENTS

Description of instrumentation on the Orbiting Geophysical Observatory (OGO) p0001 A63-13629

Cosmic ray experiments for Explorer 12 and the Orbiting Geophysical Observatory using GeigerMuller counters, and scintillation counter telescopes p0001 A63-20022

Power requirements for satellites or spacecraft carrying communications or data-processing equipment p0002 A64-11240

Orbiting Geophysical Observatory (OGO) for cosmic ray, radio astronomy and Gegenschein experiments including satellite description and orbit data p0003 A65-22431

NASA electrostatic solar plasma instruments for Orbiting Geophysical Observatory and Interplanetary Monitoring Platform measuring flux, energy spectrum, etc. p0003 A65-29239

Differential response curves and mean rigidity of response of ion chambers aboard balloons and satellites in free space during long-term cosmicray variation from 1960 to 1965 p0003 A65-33664

Velocities of dust particles in cislunar space p0004 A66-15266

Magnetic design of OGO and Pioneer solar probe including data on instrumentation, mechanical equipment, permanent magnets, test methods, etc. p0004 A66-15919

Magnetopause location, boundary positions and magnetic noise spectral data obtained with triaxial search coil magnetometer aboard OGO 1 satellite p0004 A66-23148

Airglow lines measured through photometers on OGO-2 satellite, noting nadir and zenith airglow p0007 A67-23278

Nuclear abundances of galactic and solar cosmic rays, discussing detector electronics system for measurement of particle energy spectrum p0008 A67-25852

Alpha particle proton ratio of geomagnetic field from data from charged-particle telescope on OGO 1 satellite p0009 A67-37412

Solar flare energetic X-ray events detected by onboard satellite ionization chambers, studying relationship to radio burst and space particle emission p0009 A67-41232

OGO-6 design, research program, orbits and instrumentation, emphasizing relationship between particle activity, aurora and airglow, geomagnetic field, atmospheric and solar energy interrelations p0026 A69-43132

In-flight radiometric calibration of low brightness OGO 4 airglow photometer p0029 A70-15645

Instrumentation for the Stanford University/Stanford Research Institute VLF experiment (B-17) on the OGO-3 satellite [B01265-000] p0111

Instrument report for design of the gas-surface energy transfer experiments for OGO-F [B20953-000] p0113

High-altitude or small-earth limitations for advanced horizon sensor of Orbiting Geophysical Observatory /OGO-A/ [NASA-CR-83567] p0085 N67-22257

Data reduction methods for OGO airglow photometer measurements [NASA-TM-X-55794] p0085 N67-27576

Laboratory tests on interference sensitivity of polar OGO airglow photometer [NASA-TM-X-55791] p0085 N67-27578

Magnetic Hall probe developed for use in spectrometer system aboard OGO-E satellite [UCRL-14650-T] p0086 N67-30930

Instrument report for Lyman-alpha experiment (OGO-F-12) p0108 N74-74625

A light ion mass spectrometer experiment for OGO-E [NASA-CR-122291] p0110 N74-76914

SATELLITE OBSERVATION

Orbiting geophysical observatories p0001 A63-10333

Earth-sun relationship data obtained by Orbiting Geophysical Observatory experiments concerning the atmosphere of the earth, the magnetosphere, and cislunar space p0001 A63-21527

SATELLITE OBSERVATION

NASA electrostatic solar plasma instruments for Orbiting Geophysical Observatory and Interplanetary Monitoring Platform measuring flux, energy spectrum, etc. p0003 A65-29239

OGO-1 first results on mass spectrometry measurements of thermal positive ion composition at high altitudes p0004 A66-14781

Magnetopause location, boundary positions and magnetic noise spectral data obtained with triaxial search coil magnetometer aboard OGO 1 satellite p0004 A66-23148

Electron energy spectra analyzed in earth magnetosphere using OGO 3, noting relation to radial distance p0007 A67-19926

Geomagnetic field values obtained from OGO-2 satellite-mounted rubidium vapor magnetometer p0007 A67-23244

Airglow lines measured through photometers on OGO-2 satellite, noting nadir and zenith airglow p0007 A67-23278

Orbiting Geophysical Observatory satellite /OGO 3/ photometric measurements, establishing daytime sky brightness upper limit p0010 A68-12548

Satellite observation of natural VLF phenomena in ionosphere and magnetosphere stressing radio noise frequency-time characteristics p0010 A68-14098

Magnetospheric ionization distribution determined by ducted and nonducted whistler propagation modes and reflection as observed by OGO 1 p0010 A68-17728

IMP-2 and OGO-1 investigations of bow shock large scale motions during magnetic storms result from magnetosphere-magnetosheath compression by solar wind dynamic pressure p0011 A68-17768

Plasmasphere behavior during solar flare events compared with satellite data from storm-time and plasmopause p0011 A68-19744

Solar flare X ray bursts detected by OGO spacecraft correlated with radio emission and solar flare electron and proton events p0011 A68-22450

Low energy electron spatial distribution in magnetosphere obtained with OGO 1 and 3 indicate lower energies and higher densities occur during geomagnetic disturbances p0012 A68-28348

Zodiacal dust particle flux measurements from OGO 3 and Mariner 4 spacecraft in cislunar and interplanetary space p0013 A68-29457

Electromagnetic emissions in vicinity of proton gyrofrequency from OGO 2 satellite measurements, noting sweep frequency receiver PCM and Rayspan special purpose data p0013 A68-31481

Ground based riometer and satellite-borne particle detector data on May 23 and 28, 1967 solar cosmic ray events p0013 A68-31924

Magnetosphere low energy proton and electron density spatial distributions and temporal variations from OGO 3 satellite observations p0013 A68-34245

Response of ionospheric and exospheric electron contents to partial solar eclipse, using OGO 1 satellite p0015 A68-38439

Low energy cosmic ray nuclei propagating in interstellar space analyzed by telescope onboard OGO 1 p0016 A68-41434

Directional differential intensities of protons injected into outer radiation zone coincident with initial phase of geomagnetic storm and monitored by OGO 3 p0016 A68-41684

Electron injection and diffusion into electron inner radiation belt after solar flare, measuring electron fluxes by OGO 3 spectrometer p0017 A68-41697

Geomagnetic field minimum in southern Brazil, comparing satellites data maps p0017 A68-42083

Magnetic field data from OGO-2 spacecraft and surface magnetic observations, noting magnetic storm occurrence and magnetosphere inflation and detection of polar ionospheric currents p0018 A69-11125

Sudden magnetic field increase associated with July 8, 1966 sudden commencement observed by OGO 3 satellite in magnetotail

p0018 A69-11226

Low energy electrons on day side of magnetosphere observed with MIT electron detector on OGO 3 satellite

p0018 A69-14027

Continuous and triggered audio frequency noise bands associated with ionospheric lower hybrid resonance frequency observed on OGO 2

p0018 A69-16257

Low energy electrons in magnetosphere from OGO-1 and OGO-3 observations, discussing plasma sheet, magnetic bay activity, electron pressure, temperature and density gradient

p0019 A69-19373

Spectral intensity of high energy solar X rays observed during July 7, 1966 polar event with satellite OGO 3, suggesting nonthermal bremsstrahlung origin

p0020 A69-23753

High latitude ionization spikes observed by POGO spacecraft, noting frequency correlation with magnetic disturbances and development by high energy electron injections

p0021 A69-28950

UV OGO observations of atomic hydrogen and oxygen in airglow, comparing results to exospheric models of hydrogen geocorona

p0023 A69-31400

OGO 5 satellite measurements of intensity and width of Lyman alpha line scattered by hydrogen geocorona

p0023 A69-31412

Solar protons nonuniformity over polar caps observed by OGO 2 ionization chamber during 24 March 1966 solar proton events

p0023 A69-31967

Banded chorus, VLF discrete emissions in magnetosphere in single variable frequency band with frequency depending on equatorial electron gyrofrequency

p0023 A69-31981

Ozone vertical distribution in upper stratosphere determined from OGO 4 observations, describing calibration of satellite data and onboard instrumentation

p0023 A69-32645

Collision free earth shock wave gross and fine structure deduced from OGO 5 plasma diagnostics [AIAA PAPER 69-676]

p0023 A69-33452

Ion depletion in high latitude exosphere, considering OGO 2 simultaneous observations of positive ion concentration, VLF signal propagation and whistlers

p0023 A69-34939

OGO for conducting diversified measurements to study earth atmosphere, earth-sun relationship, etc.

p0024 A69-36674

OGO triaxial search coil magnetometer for measuring earth magnetic fluctuations, discussing design rationale and observation results

p0024 A69-36675

Solid state detector for electron spatial distribution measurements on OGO-6 satellite, discussing design emphasizing reliability

p0024 A69-36676

OGO 5 ion spectrometer for measuring oxygen, He and hydrogen ion concentration, noting functions as energetic particle analyzer and proton energy distribution measurement capability

p0024 A69-36679

Satellite observations of solar proton events with halo structure or energetic storm proton event and SSC, noting similarity in origin

p0025 A69-37555

VLF and LF emission characteristic features and origin mechanism in auroral regions of ionosphere, discussing satellite observation of noise spectrum in space

p0025 A69-38495

Drift shell splitting in nondipolar distorted magnetosphere tested with data from electron spectrometer on ATS 1 and OGO 3 satellites

p0026 A69-40508

Solar X ray detector aboard OGO 5 satellite observing two components in energetic solar X ray bursts, attributing impulsive component to bremsstrahlung

p0026 A69-40775

Fluctuating electric fields relations to MHD bow shock structure, using LF fluxgate magnetometer aboard OGO 5

p0026 A69-42693

OGO-6 design, research program, orbits and instrumentation, emphasizing relationship between particle activity, aurora and airglow, geomagnetic field, atmospherics and solar energy interrelations

p0026 A69-43132

Electron intensities and substorm drift effects in outer radiation belt using two satellite technique

p0026 A69-43172

Geomagnetically trapped protons and alpha particles, analyzing OGO 4 data

p0027 A69-43184

Solar X ray flux measurements from OGO 4, comparing peak fluxes before, during and after flares with IQSY data

p0027 A69-43611

Micrometeoroid experiments on OGO 2 and OGO 4 satellites, measuring velocity, masses and particle orbits in earth dust cloud

p0027 A70-10444

Quiet time primary cosmic ray electron flux and energy spectrum from 10 to 200 Mev in interplanetary space observed by OGO 5 satellite

p0027 A70-12902

Interplanetary magnetic field measurements from Mariner and OGO satellites at various paths, regions and intervals, finding dominant polarity effect dependent on sun latitude

p0027 A70-13980

Magnetospheric observations of whistler mode emissions by OGO 1 satellite over VLF and LF ranges

p0028 A70-15117

Solar Lyman-alpha radiation observed by OGO 4 spacecraft showing short term fluctuations superimposed with monthly variation

p0028 A70-15128

Satellite multispectral photometry data in airglow bands correlated with cloud characteristics and surface albedo variations

p0028 A70-15522

Low altitude electric and magnetic measurements of plasma waves in space from OV3-3, Pioneer 8 and OGO 5 satellite observations

p0029 A70-17376

Magnetic activity effect on magnetospheric plasmapause position, measuring ion concentrations as function of local time from OGO 5 observations

p0029 A70-18530

Satellite observations of equatorial erosion and defocusing of VLF waves propagating at low magnetic latitudes

p0029 A70-18532

VLF noise phenomena observed with satellite electric dipole antennas compared with lower hybrid resonance frequency of ionospheric medium in vicinity

p0029 A70-18534

Plasmapause observations by ion spectrometer aboard OGO-5 vehicle for early orbits, obtaining O, He and H ion concentration profiles for geomagnetic parameter

p0029 A70-18546

Harmonic ion cyclotron resonances associated with proton whistlers observed from OGO-4 satellite VLF recordings

p0030 A70-19630

Magnetic equator ELF noise examined with OGO 3 magnetometer, indicating unique signals in plasmasphere

p0030 A70-21380

Auroral arcs far UV observations by OGO 4, discussing luminosity, morphology, position, etc.

p0030 A70-23493

Lyman alpha intensity and hydrogen concentration at 5 to 19 earth radii determined from OGO 3 spacecraft measurements

p0031 A70-27181

Broadband and highpass VLF noise in distant magnetosphere detected by VLF/LF experiment on OGO 1 satellite

p0031 A70-27183

Lunar limb shock wave observed by Explorer 35 satellite defined with respect to solar wind flow direction, discussing formation mechanism

p0031 A70-27594

Polar ionosphere auroral oval position detection by satellite observations of naturally occurring VLF and man-made HF plasma waves

p0032 A70-29924

Plasmapause position and density profile from ion concentration measurements by OGO-5, determining reaction to magnetic variations

p0032 A70-30074

Geomagnetic field distortion in high beta magnetospheric regions from OGO observations for quiet and slightly disturbed conditions

p0032 A70-30076

Van Allen radiation belts energetic electrons injection and distribution due to magnetic storms, using satellite-borne spectrometers

p0033 A70-30090

Quiet time cosmic ray ionization altitude dependence over polar regions from measurements by integrating ionization chamber on OGO-2

p0034 A70-31902

Cosmic ray knee interpretation using polar orbiting ionization chambers data from OGO-2/4

p0034 A70-31903

Dynamic spectra of type 3 solar bursts from OGO-3 antenna radiometer observations

p0034 A70-34835

OGO-4 observations of hydrogen Lyman-alpha airglow surrounding earth, measuring dependence on solar zenith angle

p0035 A70-35764

OGO 5 observations of quasi-trapped electromagnetic waves in solar wind at 70 kHz

p0035 A70-36005

Plasmasphere bulge region morphology from hydrogen ion concentration measurement by mass spectrometer on OGO 5 satellite

p0035 A70-36014

Magnetospheric thermal plasma electron density measurement during solar flare by OGO-5 satellite

p0036 A70-37513

Electron intensity long term variations above 500 MeV by OGO-5 satellite-borne cosmic ray electron detector, supporting diffusion-convection theory of solar modulation

p0036 A70-37522

Simultaneous hydrogen ion composition measurements by upper ionospheric polar orbiting OGO 4 and eccentric orbiting magnetospheric OGO 3 at midlatitude

p0037 A70-38377

Cosmic ray albedo neutron flux latitude and altitude dependence, using OGO-6 polar orbiting satellite

p0037 A70-39326

Tropical UV nightglow measurement by Ogo-4 spectrometer, considering ionospheric recombination excitation mechanism

p0037 A70-39338

High energy galactic gamma rays search onboard OGO-5, tabulating results

p0038 A70-40690

Galactic gamma ray intensity near Cygnus by OGO-5 spacecraft-borne telescope with acoustic spark chamber, discussing source intensity

p0038 A70-40691

Ionospheric ion temperature measurements by retarding potential analyzer on OGO-6 satellite

p0039 A70-43840

Directed proton fluxes measurements in bow shock, magnetosheath and solar wind by OGO 5 satellite ion spectrometer

p0040 A71-11491

Whistler ducts as enhanced ionization from OGO 3 satellite observations near magnetic equator, noting magnetospheric ionization hydrostatic model and predicted cut-off

p0041 A71-11499

Magnetospheric VLF electric field emissions above electron cyclotron frequency from OGO 5 observation at magnetic equator

p0041 A71-11500

Lyman alpha and atomic oxygen 1304 A airglow depressions over poles from OGO 4 satellite observations

p0041 A71-11503

C, N and O nuclei abundances in radiation belt near geomagnetic equator, using data obtained by OGO-5 satellite in 1968

p0041 A71-13475

Picogram dust particle flux measurements in seleno-centric, cislunar and interplanetary space by Mariner 4, OGO 3 and Explorer 35

p0041 A71-14014

Lyman alpha radiation scattering observation by satellites, obtaining geocoronal atomic hydrogen distribution in thermosphere and exosphere

p0042 A71-14028

Whistler-mode waves circular polarization measurement by OGO 6 satellite, noting application to hiss, chorus and ion density studies

p0042 A71-14538

SUBJECT INDEX

Magnetopause crossing observation of ATS 5 satellite during magnetic storm
 p0043 A71-17258

Magnetospheric sudden impulses amplitude and rise time distributions observation by OGO 3 and 5 satellites
 p0043 A71-17686

Early type stars radiant flux observation from OGO 6 satellite
 p0044 A71-17975

Quiet time fluxes and differential energy spectra of protons and alpha particles at 2-20 MeV measured by cosmic ray detectors on OGO-3
 p0044 A71-18127

Upstream discrete wave packets propagation interplanetary medium from OGO 5 observation
 p0045 A71-19656

Solar optical flares association with type 3 bursts from OGO-3 observations, suggesting temporary creation or enhancement of electron stream propagation by filament or sunspot structure change
 p0045 A71-19724

Solar geomagnetic seasonal ionization control of upper ionosphere longitudinal composition variations from polar satellite observations
 p0047 A71-24555

Plasma sheet proton ring current, trapping boundary and plasmopause interrelations near magnetic equator and local midnight by satelliteborne analyzer array
 p0047 A71-24781

Band limited micropulsations observed in space during magnetospheric substorm by fluxgate magnetometer on OGO 5
 p0048 A71-27913

OGO 4 satellite micrometeoroid flux detection, emphasizing noise control procedures for data correlation
 p0048 A71-28700

Geomagnetic field models validity from satellite data
 p0049 A71-29903

Satellite measurements of cold plasma density and plasmopause in magnetosphere, comparing whistler, Langmuir probe and ion trap data
 p0049 A71-30951

Atmospheric VLF electromagnetic emissions and electron instabilities data from satellite observation, detailing source regions, large amplitude electrostatic waves and wave-particle correlation.
 p0049 A71-30952

Earth bow shock internal structure based on correlated observations of magnetic field, ELF magnetic fluctuations and suprathermal electrons by OGO 5 satellite
 p0051 A71-33943

Geomagnetic equatorial ionospheric temperature, comparing incoherent scatter radar and OGO-D retarding potential analyzer values
 p0052 A71-33956

Drifting whistler frequency cutoff phenomena (striations) observation in low latitude by POGO satellites, discussing interpretation based on propagation effect
 p0052 A71-39746

Plasmaspheric ambient hydrogen and helium atomic cations density measurement by OGO 5 ion mass spectrometer during magnetic storm, noting relationship to auroral red arcs
 p0053 A71-39833

Earth corotating plasma tail evidence in plasmopause variations from high resolution proton distribution data obtained by OGO 4 satellite during magnetic storm
 p0053 A71-43166

Cosmic ray neutron leakage flux and energy spectrum measurements in 0.01-10 MeV range by OGO 6 satellite-borne neutron detector
 p0054 A72-10877

Positive Fe ion concentration relationship to equatorial spread F from OGO 6 satellite observation near magnetic equator
 p0054 A72-10902

Magnetosphere and adjacent regions magnetic surveys by OGO 1 and 3 satellites, discussing magnetopause, bow shock, magnetosheath, geomagnetic tail, ring current and polar substorms
 p0055 A72-12084

Bidirectional reflectance at several wavelengths from moonlit earth observations by arglow photometer on OGO-4 satellite
 p0055 A72-13428

OGO 6 ionospheric measurement of proton whistlers wave-normal vector, investigating propagation modes
 p0056 A72-19148

Earth bow shock laminar profile at low Mach number by crossing satellites on 12 February 1969, determining mean velocity along normal
 p0057 A72-23004

OGO 4 satellite observed band limited ELF hiss characteristics explanation by model based on generation at large wave normal angle in equatorial region
 p0057 A72-23008

Atmospheric neutral density measurement near 400 km during daytime by microphone density gage on OGO 6
 p0058 A72-26407

Whistler mode signals observation in conjugate region of 200 kHz broadcast station by satellite-borne narrow band receiver, considering field-aligned ducted and nonducted propagation
 p0059 A72-29384

Satellite charged particle observations and polar cap riometer absorption measurements during solar cosmic ray events, noting electron and proton contributions
 p0059 A72-31965

High latitude observation of precipitating electron spikes by polar orbiter OGO 4 satellite, noting population dependence on local trapping limit
 p0060 A72-35591

Turbulence of electrostatic electron cyclotron harmonic waves observed by OGO-5.
 p0060 A72-35599

Atomic oxygen green line emission in nightglow from OGO-F photometer observations, calculating tropical F region electron density spatial distribution
 p0060 A72-35604

Midlatitude red arc observations by satellite and ground station, suggesting thermal conduction theory of formation from ionospheric electron and ion temperatures and densities
 p0061 A72-35989

Geomagnetic cutoffs for cosmic-ray protons for seven energy intervals between 1.2 and 39 Mev
 p0061 A72-38728

High energy electron spatial distribution in plasma sheet from OGO 5 magnetometer experiments
 p0062 A72-42406

Thermospheric atomic oxygen and molecular nitrogen densities from OGO 6 neutral atmospheric composition experiment, comparing with prediction by Jacchia models
 p0062 A72-42431

Injun 5 satellite measurements of magnetospheric convection electric fields via double probe technique, discussing substantiation with OGO 6 results [AD-750221]
 p0063 A72 42901

ULF wave observation by satellite, considering geomagnetic activity control of magnetospheric wave occurrence
 p0063 A72-42902

Outer magnetosphere near midnight at quiet and disturbed times.
 p0063 A72-44513

Source and identification of heavy ions in the equatorial F layer.
 p0063 A72-44516

Electron polar cap and the boundary of open geomagnetic field lines.
 p0063 A72-44522

Electric field variations during substorms: OGO-6 measurements.
 p0064 A72-44854

Plasmasphere hydrogen, helium, oxygen and nitrogen ions inbound and outbound profiles from OGO 5 mass spectrometric measurements
 p0065 A73-12320

New interpretations of extraterrestrial Lyman-alpha observations.
 p0065 A73-12323

Magnetospheric observations in OGO 5 plasma wave experiment, emphasizing electrostatic wave particles interaction with plasma
 p0065 A73-13883

Type 3 radio bursts correlation with solar flares and electron events from OGO 5, IMP 5 and Explorer 35 observations
 p0066 A73-17047

Interpretation of OGO-5 Lyman alpha measurements in the upper geocorona.
 p0066 A73-19233

Recent studies of magnetospheric electric field emissions above the electron gyrofrequency.
 p0067 A73-19254

SATELLITE OBSERVATION

Correlation of ground-based measurements of structured Pc 1 micropulsations with OGO-V plasmopause observations.
 p0067 A73-20652

Evidence for a common origin of the electrons responsible for the impulsive X-ray and type 3 radio bursts.
 p0067 A73-20766

Proton scattering in the region near the earth's bow shock.
 p0067 A73-22054

Nonlinear frequency correction to plasma instability at half harmonics of electron gyrofrequency as observed by OGO 5 near geomagnetic equator outside plasmopause
 p0068 A73-22069

Direct measurements of solar-wind fluctuations between 0.0048 and 13.3 Hz.
 p0068 A73-23539

Solar flare particle propagation: Comparison of a new analytic solution with spacecraft measurements.
 p0068 A73-24727

OGO 6 retarding potential analyzer observation of vertical and longitudinal gradients in ion concentrations below F region peak near magnetic equator
 p0068 A73-24738

OGO 5 observation of ULF geomagnetic fluctuation at polar cusp boundaries in terms of ionospheric drift wave and Kelvin-Helmholtz instabilities
 p0068 A73-24744

ISIS-1 satellite observations of the ionosphere at high southern latitudes.
 p0068 A73-25753

Distributions and characteristics of high-latitude field-aligned electron precipitation.
 p0069 A73-26988

Auroral heating and the composition of the neutral atmosphere.
 p0069 A73-27602

Observation of a current-driven plasma instability at the outer zone-plasma sheet boundary.
 p0069 A73-29966

Equatorial ionospheric anomaly related neutral thermospheric composition variation observation from OGO-6 mass spectroscopic data, noting static diffusion model limitations
 p0070 A73-31767

Equatorial electrojet characteristics observation during 1967-1970 with POGO satellite-borne magnetometers, noting anomaly characterized by sharp negative V-signature in width and variable amplitude
 p0070 A73-31768

POGO satellite observed electrojet signature data comparison with daily geomagnetic variation amplitude measurement at equatorial ground station in India
 p0070 A73-31769

POGO satellite observed electrojet current data comparison with ground measurement at Ibadan, discussing data ratios variation by upper earth mantle conductivity structure
 p0070 A73-31772

POGO satellite observation of electrojet profiles compared with H variation around measurements, interpreting data by classical band current model
 p0070 A73-31773

Ion cyclotron waves observed in the polar cusp.
 p0071 A73-33437

Additional results from an OGO-6 experiment concerning ionospheric electric and electromagnetic fields in the range 20 Hz to 540 kHz.
 p0071 A73-33438

Satellite studies of magnetospheric substorms on August 15, 1968. 2: Solar wind and outer magnetosphere.
 p0071 A73-33450

Satellite studies of magnetospheric substorms on August 15, 1968. 4: OGO-5 magnetic field observations.
 p0072 A73-33452

Satellite studies of magnetospheric substorms on August 15, 1968. 5: Energetic electrons, spatial boundaries, and wave-particle interactions at OGO-5.
 p0072 A73-33453

Satellite studies of magnetospheric substorms on August 15, 1968. 6: OGO 5 energetic electron observations. Pitch angle distributions in the nighttime magnetosphere
 p0072 A73-33454

Satellite studies of magnetospheric substorms on August 15, 1968. 7: OGO-5 energetic proton observations. Spatial boundaries
 p0072 A73-33455

Nov. 10, 1975

Satellite studies of magnetospheric substorms on August 15, 1968. 8: OGO-5 plasma wave observations.

p0072 A73-33456

Satellite studies of magnetospheric substorms on August 15, 1968. 9: Phenomenological model for substorms.

p0072 A73-33457

Quiet time magnetospheric field depression at 2.3-3.6 earth radii.

p0072 A73-33464

The plasmasphere during a magnetic recovery period: A combined study of the OGO-4 and OGO-5 satellite data and of whistlers received at the ground.

p0072 A73-33876

The detection of 'intermediate' size magnetic anomalies in Cosmos 49 and OGO-2, 4, 6 data.

p0073 A73-41374

Electron concentrations calculated from the lower hybrid resonance noise band observed by OGO-3

p0074 A73-41912

Latitude and local time dependence of precipitated low-energy electrons at high latitudes.

p0074 A73-41914

A magnetospheric field model incorporating the OGO-3 and 5 magnetic field observations.

p0074 A73-43693

Distribution of atomic oxygen in the upper atmosphere deduced from OGO-6 airglow observations.

p0075 A73-45121

Shock system of February 2, 1969 --- solar wind observations

p0075 A74-12627

A catalog of ionospheric F region irregularity behavior based on OGO-6 retarding potential analyzer data

p0075 A74-12640

The relation between low-latitude neutral density variations near 400 km and magnetic activity indices.

p0075 A74-14219

Heliographic longitude distribution of the flares associated with type 3 bursts observed at kilometric wavelengths

p0076 A74-14811

Determination of the solar Lyman-alpha flux independent of calibration by ultraviolet observations of Comet Bennett)

p0076 A74-15496

Observations of the internal structure of the magnetopause.

p0077 A74-21679

Plasma waves in the dayside polar cusp. 2: Magnetopause and polar magnetosheath.

p0077 A74-21680

Global characteristics in the diurnal variations of the thermospheric temperature and composition.

p0077 A74-21693

OGO-5 measurements of the Lyman-alpha sky background in 1970 and 1971.

p0077 A74-22345

A correlated study of ELF waves and electron precipitation on OGO-6.

p0077 A74-24766

The origin and propagation of chorus in the outer magnetosphere.

p0078 A74-24767

In situ measurements of the spectral characteristics of F region ionospheric irregularities.

p0078 A74-27695

The air composition in the thermosphere.

p0078 A74-29960

Search for brief celestial X-ray bursts. --- supernovae or gamma ray flare stars origins

p0078 A74-30149

On the origin of low energy heavy nuclei below approximately 30 MeV per nucleon observed in interplanetary space during quiet times, 1968-72.

p0078 A74-30156

The elemental abundance ratios of interstellar secondary and primary cosmic rays.

p0079 A74-30190

Simultaneous satellite and riometer studies. --- for solar cosmic ray events

p0079 A74-30263

Spatial and temporal behavior of atomic oxygen determined by OGO 6 airglow observations.

p0079 A74-30670

Acceleration of electrons in solar flares.

p0079 A74-30908

Short-term intensity fluctuation of cosmic-ray electrons between 0.5 and 10 GeV.

p0079 A74-31903

Near-earth magnetic disturbance in total field at high latitudes. 1: Summary of data from OGO-2, 4, and 6. 2: Interpretation of data from OGO-2, 4, and 6.

p0080 A74-34019

The global distribution of natural and man-made ionospheric electric fields at 200 kHz and 540 kHz as observed by OGO-6.

p0080 A74-34020

Heating of the high-latitude thermosphere during magnetically quiet periods.

p0080 A74-34027

Transport of solar flare protons: Comparison of a new analytic model with spacecraft measurements [B10763-000]

p0112

Solar cosmic ray observations [B11181-000]

p0112

Observation of cosmic-ray electrons with the OGO-5 satellite [B14745-000]

p0112

Correlation of satellite estimates of the equatorial electrojet intensity with ground observations at Addis Ababa [B15846-000]

p0112

Summary and future work (OGO-4 and OGO-6) [B15849-000]

p0112

Observations of whistler mode signal propagation by OGO satellites from very low frequency ground station transmitters [NASA-CR-84869]

p0085 N67-30831

Photoelectron flux measurements in topside ionosphere using retarding potential analyzers [NASA-TM-X-63358]

p0087 N68-35999

Magnetic field fluctuations during magnetospheric substorms and field aligned currents in magnetosphere, based on satellite observations [NASA-TM-X-65748]

p0096 N72-11325

Satellite measurement of cosmic ray abundances and spectra in charge range 2 equal to or less than 7 equal to or less than 10 [NASA-CR-135786]

p0103 N73-33777

A multisatellite study of auroral-zone phenomena. [ESRO-SR-23-PT-1]

p0105 N74-16072

OGO-5 observations of discrete whistlers and emissions during a large magnetic storm [NASA-TM-X-70213]

p0109 N74-74634

OGO-4 study [NASA-CR-139261]

p0109 N74-74637

SATELLITE ORBITS

OGO-6 design, research program, orbits and instrumentation, emphasizing relationship between particle activity, aurora and airglow, geomagnetic field, atmospherics and solar energy interrelations

p0026 A69-43132

Electron depletion in the wake of ionospheric spacecraft: A comparison between results from Langmuir probes and antennas.

p0072 A73-34783

Analytical determination of earth visibility from orbiting satellite - OGO and POGO [NASA-TM-X-55002]

p0082 N64-23517

Shadow and heat input data for S-50 (POGO) [NASA-TM-X-55153]

p0083 N65-18269

Geocoronal hydrogen measurement experiment on OGO-E - methods of obtaining orbital and spacecraft parameters for data analysis [NASA-TM-X-55276]

p0083 N65-30651

Computation methods and results for orbital data, spacecraft angle, and heat input for OGO and specifically for EGO [NASA-TM-X-55428]

p0084 N66-21006

Relationship of perigee motion of satellite orbit to latitude and local time [NASA-TM-X-55703]

p0085 N67-18763

VLF experiments flown on OGO 1 (A17) and OGO 3 (B17) including orbits and attitudes of both satellites [NASA-CR-110716]

p0093 N70-33156

OGO-5 fluxgate magnetometer for measuring magnetic field over range of OGO-5 orbit [NASA-CR-130205]

p0101 N73-20498

OGO-5 orbital plots generated by the UCLA fluxgate magnetometer group [NASA-CR-139260]

p0108 N74-74633

SATELLITE ORIENTATION

Design of a simple attitude positioning control system for an orbiting geophysical observatory

p0002 A64-10864

Visual presentation of motion and orientation of Orbiting Geophysical Observatory [NASA-TN-D-2918]

p0083 N65-29296

OGO-C orientation study [REPT-9]

p0109 N74-74661

SATELLITE ROTATION

Evaluation of radio beacon data from satellite observation of earth exosphere - data scaling techniques [NASA-CR-68307]

p0084 N66-12993

SATELLITE-BORNE INSTRUMENTS

Measurement of differential energy spectra of protons, helium nuclei and heavy nuclei by cosmic radiation telescopes mounted on POGO and Pioneer satellites

p0004 A66-23684

Triaxial electron spectrometer, mounted on OGO-5 spacecraft, measures flux and energy distributions of electrons, noting electron multiplier

p0005 A66-23689

Electron and proton spectrometer detector mounted on OGO-5, measurements cover seven differential energy channels

p0005 A66-23690

Inconclusiveness of satellite measurements of micrometeoroid fluxes using piezoelectric microphone detectors in supporting hypothesis of cloud of dust surrounding earth

p0006 A66-41213

Geomagnetic field values obtained from OGO-2 satellite-mounted rubidium vapor magnetometer

p0007 A67-23244

Electron spectra, pitch angle distributions and total ionization measured throughout radiation belts by satellite magnetic spectrometer and integrating ionization chamber

p0008 A67-25807

Solar and galactic particle spectra and composition measured with cosmic ray telescope mounted on satellite

p0008 A67-27249

Rubidium vapor magnetometer used for near earth orbiting spacecraft, instrumentation and in-flight performance

p0008 A67-36513

Cosmic ray neutron leakage flux and energy spectrum measurements in 0.01-10 MeV range by OGO 6 satellite-borne neutron detector

p0054 A72-10877

Global nitric oxide and gamma emission measurements with Ebert-Fastie scanning spectrometer onboard polar orbiting OGO 4 satellite

p0064 A73-10878

Role of gas-surface interactions in the reduction of OGO 6 neutral particle mass spectrometer data.

p0073 A73-38941

Satellite ultraviolet measurements of nitric oxide fluorescence with a diffusive transport model.

p0074 A73-41925

Global temperature distributions from OGO-6 6300 A airglow measurements.

p0077 A74-23679

Comparison of atomic oxygen measurements by incoherent scatter and satellite-borne mass spectrometer techniques.

p0078 A74-27713

Cosmic gamma-ray burst detected with an instrument on board the OGO-5 satellite.

p0080 A74-31942

The Orbiting Geophysical Observatory - tool for space research [NASA-TN-D-1450]

p0082 N62-15053

World magnetic survey (WMS) - method for minimizing limitations of mathematical and graphical descriptions of earths magnetic field [NASA-RP-277]

p0082 N64-27355

Location and scheduling of operation of Eccentric Geophysical Observatory / EGO/ in gegenschein reference system [NASA-TM-X-55032]

p0082 N64-27813

Ultraviolet solar radiation research instruments for space vehicles [AFCRE-64-773]

p0083 N65-14504

Telemetry instruments aboard space vehicles for study of solar ultraviolet radiation monochromator, spectrometer, and radiation counter [NASA-CR-64074]

p0083 N65-29678

Instrumentation and calibrations of low energy proton and electron experiment for Orbiting Geophysical Observatories [NASA-CR-68558]

p0084 N66-13640

Response characteristics of ionization chamber and spectrometer experiments aboard Orbiting Geophysical Observatory (OGO) [CR-87]

p0084 N67-13710

SUBJECT INDEX

Speeds, directions of arrival, and mass of dust particles measured from OGO-1 satellite to determine orbits of dust particles p0086 N67-32070

OGO outer zone observational data on electron intensities of earth geomagnetic field [NASA-CR-89652] p0087 N67-40126

OGO-6 measurements of solar neutrons p0103 N73-32639

SCHEDULING
Location and scheduling of operation of Eccentric Geophysical Observatory /EGO/ in gegenschein reference system [NASA-TM-X-55032] p0082 N64-27813

SCIENTIFIC SATELLITES
OGO for conducting diversified measurements to study earth atmosphere, earth-sun relationship, etc. p0024 A69-36674

Small Explorer and large orbiting observatory classes of scientific satellites [NASA-TM-X-55261] p0083 N65-29783

Design, construction, test and flight use of electronic portions of research instruments on rockets and satellites for solar ultraviolet radiation [NASA-CR-110906] p0094 N71-10358

SCINTILLATION
Power-law wavenumber spectrum deduced from ionospheric scintillation observations. p0062 A72-42416

Cosmic-ray scintillations. I: Inside the magnetosphere. p0066 A73-15526

Geophysical properties of the ionospheric irregularities responsible for radio scintillation. [AIAA PAPER 74-53] p0077 A74-18754

SCINTILLATION COUNTERS
Cosmic ray experiments for Explorer 12 and the Orbiting Geophysical Observatory using GeigerMuller counters, and scintillation counter telescopes p0001 A63-20022

Energetic protons from March 24, 1966 solar flare observed with OGO 1 satellite scintillation counter p0010 A67-41233

SECONDARY COSMIC RAYS
The elemental abundance ratios of interstellar secondary and primary cosmic rays. p0079 A74-30190

SECONDARY EMISSION
Spacecraft surface secondary electron emission effects on electron trap measurements in magnetosphere and solar wind, noting agreement with positive ion densities p0027 A70-13994

A satellite ion-electron collector: Experimental effects of grid transparency, photoemission, and secondary emission [NASA-CR-139262] p0109 N74-74638

SECULAR VARIATIONS
Geomagnetic secular variations, 1900-1965 [NASA-TM-X-55944] p0086 N67-37398

SELENOLOGY
Four years of dust particle measurements in cislunar and selenocentric space from Lunar Explorer 35 and OGO 3 [B15918-000] p0112

SENSORS
Sensors used in cosmic dust experiments studied for response to microparticle hypervelocity impacts, noting relationship to velocity p0013 A68-29468

SHADOWS
Shadow time and heat input of EGO satellite [NASA-TM-X-55014] p0082 N64-27251

Shadow and heat input data for S-50 (POGO) [NASA-TM-X-55153] p0083 N65-18269

Solar cell array angle to provide maximum power for spin stabilized Orbiting Geophysical Observatory [NASA-TM-X-55186] p0083 N65-21656

Shades of OGO-B (S-49A) [NASA-TM-X-70214] p0108 N74-74630

SHEATHS
OGO-5 observations of the physical processes occurring in the disturbed polar cusp and the cusp-magnetosheath interface [B18269-000] p0113

SHOCK FRONTS
Magnetic field measurements in outer magnetosphere, emphasizing boundary regions and shock front characteristics p0010 A68-12172

SHOCK SPECTRA
Collision free earth shock wave gross and fine structure deduced from OGO 5 plasma diagnostics [AIAA PAPER 69-676] p0023 A69-33452

SHOCK WAVE INTERACTION
Proton scattering in the region near the earth's bow shock. p0067 A73-22054

SHOCK WAVE PROFILES
Magnetic field observations by OGO-1, with profiles of bow shock and magnetopause encounters p0010 A68-11011

Electrostatic turbulence in bow shock magnetic structures observed by OGO 5, explaining turbulence as ion acoustic or Buneman mode due to two stream instability p0035 A70-36006

Earth bow shock laminar profile at low Mach number by crossing satellites on 12 February 1969, determining mean velocity along normal p0057 A72-23004

SHOCK WAVES
IMP-2 and OGO-1 investigations of bow shock large scale motions during magnetic storms result from magnetosphere-magnetosheath compression by solar wind dynamic pressure p0011 A68-17768

Detection of electric field turbulence in earth bow shock, noting wave amplitude correlation with magnetic field structure p0018 A69-14681

Magnetic fluctuations in various frequency ranges, associated with earth bow shock, detected with search coil magnetometer on OGO 3 p0026 A69-40501

Fluctuating electric fields relations to MHD bow shock structure, using LF fluxgate magnetometer aboard OGO 5 p0026 A69-42693

Initial deceleration of solar wind positive ions upstream of earth bow shock determined from OGO 5 high time resolution plasma measurements p0030 A70-21377

Lunar limb shock wave observed by Explorer 35 satellite defined with respect to solar wind flow direction, discussing formation mechanism p0031 A70-27594

Fast time-resolved spectra of earth bow shock electrostatic turbulence based on broadband analog electric data from OGO-5 p0031 A70-29111

Electrostatic turbulence in bow shock magnetic structures observed by OGO 5, explaining turbulence as ion acoustic or Buneman mode due to two stream instability p0035 A70-36006

Magnetic and electric field changes across earth bow shock and magnetosheath, discussing Pioneer 8 and OGO-5 data p0036 A70-37483

Directed proton fluxes measurements in bow shock, magnetosheath and solar wind by OGO 5 satellite ion spectrometer p0040 A71-11491

Solar wind ion thermalization in earth bow shock by counterstreaming instability related to interplanetary magnetic field p0050 A71-31774

Earth bow shock internal structure based on correlated observations of magnetic field, ELF magnetic fluctuations and suprathermal electrons by OGO 5 satellite p0051 A71-33943

Earth bow shock magnetic field data correlation with OGO 5 flux gate magnetometer, using Tidman-Northrop theory p0056 A72-19145

Electron plasma oscillations distribution upstream from earth bow shock, evaluating OGO-5 plasma wave detector data p0057 A72-23019

Earth-solar wind bow shock structure from OGO-5 observations during passage from interplanetary medium into magnetosheath p0058 A72-29379

Weak electrostatic turbulence observation in earth bow shock magnetic field gradient, suggesting cyclotron drift instability role p0063 A72-44523

Shock system of February 2, 1969 --- solar wind observations p0075 A74-12627

SOLAR ACTIVITY EFFECTS
Structure of the quasi-perpendicular laminar bow shock [B22612-000] p0114

Distributions of high frequency waves upstream from earth's bow shock [NASA-CR-139256] p0108 N74-74626

SHORT WAVE RADIO TRANSMISSION
Ionospheric absorption relation to solar X-ray flux enhancement during short wave fade-outs from OGO-4 and Sofrad 9 satellites p0045 A71-20318

SIGNAL FADING
Latitudinal cut-off of manmade VLF signals in short path through ionosphere to OGO 2 satellite, noting strong noise following signal cut-off p0021 A69-28958

SIGNAL PROCESSING
Very low frequency signals observed by OGO-4 measured and interpreted, and global ionospheric propagation study [NASA-CR-107654] p0092 N70-15768

SIZE DETERMINATION
Gum Nebula size, density and electron temperature data from RAE-1 and OGO-5 satellites and ground based telescopes observations, correlating with Vela X supernova outburst p0052 A71-35409

SKY BRIGHTNESS
Orbiting Geophysical Observatory satellite /OGO 3/ photometric measurements, establishing daytime sky brightness upper limit p0010 A68-12548

OGO radio astronomy instrument for cosmic noise sky brightness distribution mapping by electrically short antenna ionospheric focusing p0048 A71-26144

OGO-5 measurements of the Lyman-alpha sky background in 1970 and 1971. p0077 A74-22345

Reduction and analysis of data on low frequency brightness temperature of sky from OGO-4 radio astronomy experiment [NASA-CR-110796] p0093 N70-42352

SKY RADIATION
Lyman alpha sky background measurements by OGO 5 satellite, discussing absolute emission rate, spatial variations and origin p0047 A71-24439

SOLAR ACTIVITY
Flux energy distribution and density of ions and electrons in magnetosphere plasma during solar activity period determined by OGO-3 electrostatic probes p0012 A68-29421

Primary cosmic ray energy spectra and charge composition during 1965 solar modulation minimum, using scintillator photomultiplier detector on OGO 1 p0016 A68-41431

Latitudinal variations in exosphere thermal ion composition, examining evidence of solar and geomagnetic control of ion distribution p0016 A68-41673

Neutral H concentration in upper atmosphere during solar minimum, using ion thermal energies from rocket and satellite mass spectrometric, radio and proton whistler measurements p0054 A72-10361

Simultaneous satellite and riometer studies. --- for solar cosmic ray events p0079 A74-30263

Enhancements of red arc during maximum solar activity p0097 N72-23334

SOLAR ACTIVITY EFFECTS
Primary cosmic ray charge and energy spectra for helium through oxygen during 1965 minimum solar modulation effect p0005 A66-26348

Solar modulation of galactic protons and He nuclei during last solar cycle analyzed according to Parker theory p0007 A67-19913

Hysteresis effect on cosmic ray modulation and gradient ionization near solar minimum from measurements made near earth with OGO 1 and 3 ion chambers p0028 A70-15106

Trapped particle population changes associated with solar events, discussing solar wind discontinuity effects on magnetosphere p0036 A70-37487

SOLAR ARRAYS

Cosmic ray electron and positron differential energy spectra during solar quiet times from OGO5 satellite observations in interplanetary space

p0036 A70-38096

Cosmic ray electrons solar modulation, considering diffusion-convection theory

p0040 A70-45769

Quiet time fluxes and differential energy spectra of protons and alpha particles at 2-20 MeV measured by cosmic ray detectors on OGO-3

p0044 A71-18127

Low energy cosmic rays modulation and heliocentric gradient during solar minimum, comparing OGO 1 and 2 ion chamber measurements with other space and ground observations

p0044 A71-18128

Solar geomagnetic seasonal ionization control of upper ionosphere longitudinal composition variations from polar satellite observations

p0047 A71-24555

Energy dependent time lag in the long-term modulation of cosmic rays.

p0067 A73-19252

The 1972 cosmic ray electron spectrum above 0.5 GeV. -- mechanism for distortion by solar modulation

p0078 A74-27700

The cosmic ray electron spectrum and its modulation from 1968 through 1972.

p0079 A74-30204

Short-term intensity fluctuation of cosmic-ray electrons between 0.5 and 10 GeV.

p0079 A74-31903

Solar X ray indication of flare activity [AD-686662]

p0090 N69-32730

SOLAR ARRAYS

Orbiting Geophysical Observatory electric power subsystem design innovations including power supply, solar array output and battery charge control

p0003 A65-19528

Location and scheduling of operation of Eccentric Geophysical Observatory /EGO/ in gegenschein reference system

p0082 N64-27813

Solar cell array angle to provide maximum power for spin stabilized Orbiting Geophysical Observatory [NASA-TM-X-55186]

p0083 N65-21656

Shades of OGO-B (S-49A)

p0108 N74-74630

SOLAR CELLS

Solar cell array angle to provide maximum power for spin stabilized Orbiting Geophysical Observatory [NASA-TM-X-55186]

p0083 N65-21656

SOLAR CORONA

Solar burst time profiles and dynamic spectra for calculating theoretical values for Type 3 burst characteristics

p0091 N70-12221

Coronal electron temperature associated with solar flares

p0108 N74-74629

SOLAR CORPUSCULAR RADIATION

Relativistic electrons associated with solar particle events, measuring occurrence frequency, electron propagation and diffusion anisotropy.

p0048 A71-29057

Heavy nuclei enrichment in solar accelerated particles, discussing differential energy spectra, photospheric and coronal abundances, satellite observation and agreement with galactic cosmic rays

p0055 A72-15366

The abundances of solar accelerated nuclei from carbon to iron.

p0065 A73-13719

Measurements of the iron-group abundance in energetic solar particles.

p0068 A73-23538

Solar flare particle propagation. Comparison of a new analytic solution with spacecraft measurements.

p0068 A73-24727

Acceleration of electrons during the flash phase of solar flares.

p0079 A74-30287

SOLAR COSMIC RAYS

Skyhook balloon flight Geiger counter cosmic ray monitor measurements of energy and charge spectra of galactic rays at solar minimum

p0006 A66-34847

Nuclear abundances of galactic and solar cosmic rays, discussing detector electronics system for measurement of particle energy spectrum

p0008 A67-25852

OGO cosmic ray measuring device involving charged particle detectors to measure spectra and chemical composition over selected energy intervals

p0012 A68-27615

Low energy solar cosmic ray experiment for OGO-6 using double diffused depleted silicon diodes

p0012 A68-27616

Ground based riometer and satellite-borne particle detector data on May 23 and 28, 1967 solar cosmic ray events

p0013 A68-31924

Spatial variations in particle intensity near and inside magnetosphere during September 1966 solar cosmic ray events, noting magnetosphere screening effectiveness

p0018 A69-12740

Peaks and time intensity profile of energetic X rays and cosmic rays observed by OGO-3 ion chamber on May 23, 1967 flare event

p0020 A69-22182

Solar cosmic rays entry into magnetosphere, showing entrance on smoothly connected field lines

p0032 A70-30059

Solar cosmic ray activity near sunspot maximum, discussing events of 18 November 1968 and 11 April 1969

p0044 A71-18158

Proton energy change effects on charged particles propagating in interplanetary space, using low energy solar flare proton fluxes observations

p0046 A71-22801

Satellite charged particle observations and polar cap riometer absorption measurements during solar cosmic ray events, noting electron and proton contributions

p0059 A72-31965

Measurements of the iron-group abundance in energetic solar particles.

p0068 A73-23538

Solar electrons, galactic electron radiation modulation and spectrum of high energy cosmic ray electrons.

p0071 A73-33293

Quiet-time solar neutron flux upper limit from OGO-6 neutron detector, evaluating solar cosmic ray acceleration, nuclear reaction and energy region

p0074 A73-41498

Simultaneous satellite and riometer studies. -- for solar cosmic ray events

p0079 A74-30263

Solar cosmic ray experiment for the first Orbiting Geophysical Observatories

[B03937-000] p0111

Solar cosmic ray observations

[B11181-000] p0112

Diffusion-convection theory for solar cosmic ray propagation in interplanetary magnetic field

p0090 N69-29659

Multiple parameter analysis of galactic and solar cosmic rays for chemical composition and charge distribution

p0091 N69-38984

Instrumentation and measurement data of OGO-F solar cosmic ray experiment

[NASA-CR-130155] p0101 N73-16795

The isotopes of H and He in solar cosmic rays -- as observed by OGO-6

p0107 N74-21466

SOLAR CYCLES

Morphology of thermal and energetic particles in inner magnetosphere during geomagnetic disturbances and solar cycles

p0034 A70-30358

Soft solar X rays cyclic variation from satellite observation, noting relation to sunspot group magnetic field complexity

p0039 A70-43301

Solar cosmic ray activity near sunspot maximum, discussing events of 18 November 1968 and 11 April 1969

p0044 A71-18158

The solar cycle variation of the solar wind helium abundance

[B22609-000] p0114

SOLAR ECLIPSES

Response of ionospheric and exospheric electron contents to partial solar eclipse, using OGO 1 satellite

p0015 A68-38439

SOLAR ELECTRONS

Solar electrons, galactic electron radiation modulation and spectrum of high energy cosmic ray electrons.

p0071 A73-33293

Acceleration of electrons in solar flares.

p0079 A74-30908

Energetic electron and proton solar particle observations on OGO-5, 24-34 January 1971

[B15152-000] p0112

Non-relativistic solar electrons

[B22602-000] p0113

SOLAR FLARES

Solar flare energetic X-ray events detected by onboard satellite ionization chambers, studying relationship to radio burst and space particle emission

p0009 A67-41232

Energetic protons from March 24, 1966 solar flare observed with OGO 1 satellite scintillation counter

p0010 A67-41233

Highest differential energy range of X rays during July 1966 solar flare suggests nonthermal bremsstrahlung origin of hard flare X rays

p0011 A68-17769

Solar flare X ray bursts detected by OGO spacecraft correlated with radio emission and solar flare electron and proton events

p0011 A68-22450

10-50 keV solar flare X ray bursts observed by OGO satellites and correlated with radio bursts and energetic particle emission

p0014 A68-35480

Solar flare injection and propagation of low energy protons and electrons in 7-9 July 1966 solar particle event

p0014 A68-37148

Electron injection and diffusion into electron inner radiation belt after solar flare, measuring electron fluxes by OGO 3 spectrometer

p0017 A68-41697

Solar protons in magnetospheric tail after flare of July 7, 1966 with isotropic pitch angle distribution, expressing energy spectrum as exponential in rigidity

p0020 A69-21699

Energetic solar proton and electron event observed in July 1966 by Explorer 33 and OGO-3, noting association with invisible solar hemisphere flare

p0020 A69-22181

Peaks and time intensity profile of energetic X rays and cosmic rays observed by OGO-3 ion chamber on May 23, 1967 flare event

p0020 A69-22182

Spectral intensity of high energy solar X rays observed during July 7, 1966 polar event with satellite OGO 3, suggesting nonthermal bremsstrahlung origin

p0020 A69-23753

Earth thermal plasmasphere contraction subsequent to solar flare obtained from ion mass spectrometers on OGO satellites

p0020 A69-23777

Geomagnetic crochets time relations to solar X rays, radio bursts and flares

p0023 A69-34227

Solar X ray flux measurements from OGO 4, comparing peak fluxes before, during and after flares with IQSY data

p0027 A69-43611

Hard X-ray pulse identification with formation of brilliant kernel (11-12 September 1968) flare by comparison with optical data

p0030 A70-25746

Magnetospheric thermal plasma electron density measurement during solar flare by OGO-5 satellite

p0036 A70-37513

Solar X-ray flare temperature and emission measure profiles using OGO 5 satellite detector, interpreting energy dispersion of peak times

p0040 A70-45768

Solar flare particles entrance into geomagnetic tail, modifying diffusion model

p0040 A71-11494

Solar flare X ray and radio wave emission measurement by OGO-4 and Solrad-9 satellites

p0042 A71-14046

Impulsive solar flare X rays spectral characteristics, examining electron energy, bremsstrahlung, microwave bursts and particle escape, collisions and injection

p0043 A71-15937

Emission structure of large electron active region McMath plage 8905 mapped by 40 keV solar flare electrons

p0044 A71-17918

Solar flare electrons at 10-200 MeV region, discussing energy spectra and time history

p0044 A71-18170

Solar optical flares association with type 3 bursts from OGO-3 observations, suggesting temporary creation or enhancement of electron stream propagation by filament or sunspot structure change

p0045 A71-19724

SUBJECT INDEX

SUBJECT INDEX

Impulsive hard X ray and far UV emission during solar flares p0046 A71-19825

Solar flare model, computing thermal X ray emission p0046 A71-20945

Solar flare electron spectra in interplanetary space and within earth magnetosphere, investigating simultaneous observations by satellite-borne magnetic electron spectrometers p0046 A71-21037

Proton energy change effects on charged particles propagating in interplanetary space, using low energy solar flare proton fluxes observations p0046 A71-22801

Relativistic electrons associated with solar particle events, measuring occurrence frequency, electron propagation and diffusion anisotropy. p0048 A71-29057

Nonthermal electron spectra hardness limit during flash phase of solar flares from OGO-5 observation p0055 A72-14561

Soft X-ray and microwave observations of hot regions in solar flares. p0060 A72-35089

H alpha subflare associated X-ray burst of 10 October 1970 observed by balloon-borne scintillator and OGO 5 and SOLRAD 9 satellites p0064 A73-11389

The abundances of solar accelerated nuclei from carbon to iron. p0065 A73-13719

X-radiation (E greater than 10 keV), H-alpha and microwave emission during the impulsive phase of solar flares. p0066 A73-17041

Type 3 radio bursts correlation with solar flares and electron events from OGO 5, IMP 5 and Explorer 35 observations p0066 A73-17047

Solar flare particle propagation: Comparison of a new analytic solution with spacecraft measurements. p0068 A73-24727

Heliographic longitude distribution of the flares associated with type 3 bursts observed at kilometric wavelengths p0076 A74-14811

Acceleration of electrons during the flash phase of solar flares. p0079 A74-30287

Acceleration of electrons in solar flares. p0079 A74-30908

Rise time in 20-32 keV impulsive X-radiation. p0080 A74-38468

Energetic radiation from solar flares [B03940-000] p0111

Transport of solar flare protons: Comparison of a new analytic model with spacecraft measurements [B10763-000] p0112

Acceleration of electrons in the absence of detectable optical flares deduced from type 3 radio bursts, H-alpha activity and soft X-ray emission [B22607-000] p0114

A search for solar neutrons during solar flares [B22608-000] p0114

Propagation of high energy solar protons as observed by OGO C spacecraft p0089 N69-23730

Solar X ray indication of flare activity [AD-686662] p0090 N69-32730

Cosmic ray electrons and solar flare particles from OGO-E and Explorer 33 data for identifying solar flare electrons p0090 N69-38983

Electron density profiles and production rates associated with 30 Jan. 1968 large X ray flare event [RSD-63] p0096 N71-36131

Solar flare protons and physical processes affecting particle propagation in interplanetary space p0098 N72-27829

Design of OGO-E experiment to measure energetic X-rays, electrons, protons, and alphaparticle emissions from solar flares [NASA-CR-122509] p0098 N72-28812

Analytic solution to complete Fokker-Planck equation for solar flare particle propagation [NASA-CR-122406] p0098 N72-29818

Characteristics of nonthermal electrons accelerated during the flash phase of small solar flares p0106 N74-21445

Optical, hard X-ray, and microwave emission during the impulsive phase of flares --- analysis of optical impulsive component in solar flares p0107 N74-21458

Coronal electron temperature associated with solar flares [OGO-4-67-100A-06] p0108 N74-74629

SOLAR HEATING

Shadow time and heat input of EGO satellite [NASA-TM-X-55014] p0082 N64-27251

Shadow and heat input data for S-50 (POGO) [NASA-TM-X-55153] p0083 N65-18269

SOLAR MAGNETIC FIELD

Soft solar X rays cyclic variation from satellite observation, noting relation to sunspot group magnetic field complexity p0039 A70-43301

Seasonal and annual longitudinal variations in ionospheric distribution, stressing solar geomagnetic control importance p0050 A71-33762

Substorm related changes in the geomagnetic tail: The growth phase. p0064 A72-44856

Reply [NASA-TM-X-70215] p0108 N74-74627

SOLAR PHYSICS

Characteristics of nonthermal electrons accelerated during the flash phase of small solar flares p0106 N74-21445

SOLAR PROMINENCES

Characteristics of nonthermal electrons accelerated during the flash phase of small solar flares p0106 N74-21445

SOLAR PROTONS

10-50 kev solar flare X ray bursts observed by OGO satellites and correlated with radio bursts and energetic particle emission p0014 A68-35480

Solar flare injection and propagation of low energy protons and electrons in 7-9 July 1966 solar particle event p0014 A68-37148

Solar protons in magnetospheric tail after flare of July 7, 1966 with isotropic pitch angle distribution, expressing energy spectrum as exponential in rigidity p0020 A69-21699

Energetic solar proton and electron event observed in July 1966 by Explorer 33 and OGO-3, noting association with invisible solar hemisphere flare p0020 A69-22181

Spectral intensity of high energy solar X rays observed during July 7, 1966 polar event with satellite OGO 3, suggesting nonthermal bremsstrahlung origin p0020 A69-23753

Solar protons nonuniformity over polar caps observed by OGO 2 ionization chamber during 24 March 1966 solar proton events p0022 A69-31967

Satellite observations of solar proton events with halo structure or energetic storm proton event and SSC, noting similarity in origin p0025 A69-37555

Solar protons delayed access into polar regions during 2 November 1967 solar particle event, discussing north-south asymmetry p0027 A69-43183

Low energy charged particle distribution within earth magnetosphere and environs, suggesting solar origin for storm time ring current protons p0033 A70-30089

Large amplitude upstream wave solar wind event of 10 March 1968 with suprathermal protons, correlating magnetometer plasma probe and Lepedea proton data p0043 A71-14550

Solar proton intensity structures in the magnetosphere during interplanetary anisotropies. p0066 A73-14962

Simultaneous satellite and riometer studies. --- for solar cosmic ray events p0079 A74-30263

Energetic electron and proton solar particle observations on OGO-5, 24-34 January 1971 [B15152-000] p0112 B75-15152

Propagation of high energy solar protons as observed by OGO C spacecraft p0089 N69-23730

Solar flare protons and physical processes affecting particle propagation in interplanetary space p0098 N72-27829

Analytic solution to complete Fokker-Planck equation for solar flare particle propagation [NASA-CR-122406] p0098 N72-29818

Energetic electrons and protons observed on OGO-5, March 6-10, 1970 [NASA-CR-139265] p0109 N74-74662

Energetic electron and proton solar particle observations on OGO-5, January 24-30, 1971 [NASA-CR-139266] p0109 N74-74663

SOLAR RADIATION

Solar Lyman-alpha radiation observed by OGO 4 spacecraft showing short term fluctuations superimposed with monthly variation p0028 A70-15128

Neutron flux and energy spectra measurements in space related to theoretical predictions, discussing neutron leakage flux, solar neutron observations and radiation detector configurations p0073 A73-36645

Extraterrestrial ultraviolet radiation and the parameter of the HI medium near the sun. p0073 A73-39074

Determination of the solar Lyman-alpha flux independent of calibration by ultraviolet observations of Comet Bennett) p0076 A74-15496

Energetic radiation from solar flares [B03940-000] p0111

Energetic electron and proton solar particle observations on OGO-5, 24-34 January 1971 [B15152-000] p0112

Non-relativistic solar electrons [B22602-000] p0113

Acceleration of electrons in the absence of detectable optical flares deduced from type 3 radio bursts, H-alpha activity and soft X-ray emission [B22607-000] p0114

A search for solar neutrons during solar flares [B22608-000] p0114

Shadow time and heat input of EGO satellite [NASA-TM-X-55014] p0082 N64-27251

Ultraviolet solar radiation research instruments for space vehicles [AFCRL-64-773] p0083 N65-14504

Shadow and heat input data for S-50 (POGO) [NASA-TM-X-55153] p0083 N65-18269

Telemetry instruments aboard space vehicles for study of solar ultraviolet radiation monochromator, spectrometer, and radiation counter [NASA-CR-64074] p0083 N65-29678

Computation methods and results for orbital data, spacecraft angle, and heat input for OGO and specifically for EGO [NASA-TM-X-55428] p0084 N66-21006

Design, construction, test and flight use of electronic portions of research instruments on rockets and satellites for solar ultraviolet radiation [NASA-CR-110906] p0094 N71-10358

Magnetospheric modulation effects on solar cosmic rays from simultaneous OGO 1 and 3 ion chamber data in 1968 and 1969 [NASA-CR-137075] p0105 N74-18420

Possible low energy (E less than keV) nonthermal X-ray events --- analysis of proportional counter detector data from OGO-5 p0107 N74-21450

Optical, hard X-ray, and microwave emission during the impulsive phase of flares --- analysis of optical impulsive component in solar flares p0107 N74-21458

SOLAR RADIO BURSTS

Solar flare energetic X-ray events detected by onboard satellite ionization chambers, studying relationship to radio burst and space particle emission p0009 A67-41232

10-50 kev solar flare X ray bursts observed by OGO satellites and correlated with radio bursts and energetic particle emission p0014 A68-35480

Geomagnetic crochets time relations to solar X rays, radio bursts and flares p0023 A69-34227

Ionization rate profiles from solar flare X rays observed by ion chambers aboard OGO 1 and OGO 3 [NASA-CR-94429] p0087 N68-23026

Design considerations and performance characteristics for radio astronomy instrumentation system aboard OGO-5 spacecraft [NASA-CR-98670] p0088 N69-14392

Data collected by OGO-3 in detecting solar bursts [NASA-CR-106640] p0091 N70-11147

SOLAR RADIO EMISSION

Peaks and time intensity profile of energetic X rays and cosmic rays observed by OGO-3 ion chamber on May 23, 1967 flare event p0020 A69-22182

Soft X-ray and microwave observations of hot regions in solar flares. p0060 A72-35089

SOLAR SPECTRA

SOLAR SPECTRA

Solar and galactic particle spectra and composition measured with cosmic ray telescope mounted on satellite

p0008 A67-27249

Impulsive solar flare X rays spectral characteristics, examining electron energy, bremsstrahlung, microwave bursts and particle escape, collisions and injection

p0043 A71-15937

Solar flare electron spectra in interplanetary space and within earth magnetosphere, investigating simultaneous observations by satellite-borne magnetic electron spectrometers

p0046 A71-21037

Determination of the solar Lyman-alpha flux independent of calibration by ultraviolet observations of Comet Bennett)

p0076 A74-15496

Possible low energy (E less than keV) nonthermal X-ray events --- analysis of proportional counter detector data from OGO-5

p0107 N74-21450

SOLAR STORMS

Satellite observations of solar proton events with halo structure or energetic storm proton event and SSC, noting similarity in origin

p0025 A69-37555

SOLAR TEMPERATURE

Solar X-ray flare temperature and emission measure profiles using OGO 5 satellite detector, interpreting energy dispersion of peak times

p0040 A70-45768

Solar flare model, computing thermal X ray emission

p0046 A71-20945

SOLAR WIND

Orbiting Geophysical Observatory (OGO) for cosmic ray, radio astronomy and Gegenschein experiments including satellite description and orbit data

p0003 A65-22431

IMP-2 and OGO-1 measurements on plasma characteristics in transition region between solar wind and geomagnetic field

p0003 A65-25921

NASA electrostatic solar plasma instruments for Orbiting Geophysical Observatory and Interplanetary Monitoring Platform measuring flux, energy spectrum, etc.

p0003 A65-29239

Solar modulation of galactic protons and He nuclei during last solar cycle analyzed according to Parker theory

p0007 A67-19913

Position and shape of neutral sheet in geocentric solar magnetospheric coordinate system from geomagnetic tail measurements

p0010 A68-13469

IMP-2 and OGO-1 investigations of bow shock large scale motions during magnetic storms result from magnetosphere-magnetosheath compression by solar wind dynamic pressure

p0011 A68-17768

Spacecraft surface secondary electron emission effects on electron trap measurements in magnetosphere and solar wind, noting agreement with positive ion densities

p0027 A70-13994

Magnetic activity effect on magnetospheric plasmopause position, measuring ion concentrations as function of local time from OGO 5 observations

p0029 A70-18530

Initial deceleration of solar wind positive ions upstream of earth bow shock determined from OGO 5 high time resolution plasma measurements

p0030 A70-21377

Lunar limb shock wave observed by Explorer 35 satellite defined with respect to solar wind flow direction, discussing formation mechanism

p0031 A70-27594

Satellite plasma diagnostics for electric and magnetic fields and fine structure of collisionless shocks in solar wind plasma flows and interplanetary shocks

p0032 A70-30069

Plasma wave particle interactions in outer magnetosphere, magnetosheath and solar wind, noting role of AC electric fields

p0033 A70-30085

OGO 5 observations of quasi-trapped electromagnetic waves in solar wind at 70 kHz

p0035 A70-36005

Trapped particle population changes associated with solar events, discussing solar wind discontinuity effects on magnetosphere

p0036 A70-37487

Directed proton fluxes measurements in bow shock, magnetosheath and solar wind by OGO 5 satellite ion spectrometer

p0040 A71-11491

Solar wind microscopic structure, examining interplanetary wave-particle interactions

p0042 A71-14068

Large amplitude upstream wave solar wind event of 10 March 1968 with suprathermal protons, correlating magnetometer plasma probe and Lepedea proton data

p0043 A71-14550

Solar wind compressed magnetic field in sunward magnetosphere and extended geomagnetic tail observation by Pioneer 7 spacecraft

p0049 A71-30028

Solar wind ion thermalization in earth bow shock by counterstreaming instability related to interplanetary magnetic field

p0050 A71-31774

Magnetotail changes relationship to solar wind magnetic field and magnetospheric substorms from ground and satellite data

p0051 A71-33944

Nonthermal electrons interaction with electron plasma oscillations and HF transverse waves in upstream solar wind.

p0052 A71-37353

Suprathermal electron beam induced HF wave instability in solar wind upstream from earth bow shock, interpreting OGO 5 observations

p0053 A71-43158

Solar wind 10-9900 eV electron flux, evaluating energy transport in plasma rest frame

p0055 A72-13507

Large amplitude interplanetary solar wind discontinuities observed by OGO-5 plasma spectrometer and magnetometers, considering magnetic drift waves mechanism for plasma turbulence generation

p0058 A72-29378

Earth-solar wind bow shock structure from OGO-5 observations during passage from interplanetary medium into magnetosheath

p0058 A72-29379

Detection of solar-wind electron plasma frequency fluctuations in an oblique nonlinear magnetohydrodynamic wave.

p0061 A72-35610

Substorm related changes in the geomagnetic tail: The growth phase.

p0064 A72-44856

Solar wind interaction with geomagnetic field, discussing magnetosphere polar cusp region and geomagnetic tail neutral sheet structure

p0065 A73-13871

Direct measurements of solar-wind fluctuations between 0.0048 and 13.3 Hz.

p0068 A73-23539

The prevalence of second harmonic radiation in type 3 bursts observed at kilometric wavelengths.

p0071 A73-32964

Solar wind density model from km-wave type 3 bursts.

p0071 A73-32965

Satellite studies of magnetospheric substorms on August 15, 1968. 2: Solar wind and outer magnetosphere.

p0071 A73-33450

Solar wind and magnetosheath electron temperature measurements by triaxial electron analyzer onboard OGO-5, presenting data for bow shock

p0075 A73-45112

Shock system of February 2, 1969 --- solar wind observations

p0075 A74-12627

The solar cycle variation of the solar wind helium abundance [B22609-000]

p0114

Computation of velocity, temperature, and density of solar wind plasma, using attitude-stabilized plasma detectors on OGO-5 [NASA-CR-125063]

p0096 N72-14808

Electric field oscillations in upstream solar wind, using OGO-5 observations

p0099 N73-10789

Development of model of scattering of solar Lyman alpha from spatial distribution of neutral hydrogen in interplanetary space

p0100 N73-10813

Differential energy spectra of cosmic ray protons and helium nuclei dominated by solar modulation of local interstellar spectra, and numerical solutions to transport equation

[NASA-CR-130298] p0100 N73-15837

Reply [NASA-TM-X-70215]

p0108 N74-74627

SOLAR X-RAYS

Solar flare energetic X-ray events detected by onboard satellite ionization chambers, studying relationship to radio burst and space particle emission

p0009 A67-41232

Highest differential energy range of X rays during July 1966 solar flare suggests nonthermal bremsstrahlung origin of hard flare X rays

p0011 A68-17769

Solar flare X ray bursts detected by OGO spacecraft correlated with radio emission and solar flare electron and proton events

p0011 A68-22450

10-50 keV solar flare X ray bursts observed by OGO satellites and correlated with radio bursts and energetic particle emission

p0014 A68-35480

Peaks and time intensity profile of energetic X rays and cosmic rays observed by OGO-3 ion chamber on May 23, 1967 flare event

p0020 A69-22182

Spectral intensity of high energy solar X rays observed during July 7, 1966 polar event with satellite OGO 3, suggesting nonthermal bremsstrahlung origin

p0020 A69-23753

Center to limb variation of solar hard X ray bursts, suggesting inverse Compton effect and bremsstrahlung from anisotropic electrons

p0023 A69-33055

Geomagnetic crochets time relations to solar X rays, radio bursts and flares

p0023 A69-34227

Solar X ray detector aboard OGO 5 satellite observing two components in energetic solar X ray bursts, attributing impulsive component to bremsstrahlung

p0026 A69-40775

Solar X ray flux measurements from OGO 4, comparing peak fluxes before, during and after flares with IQSY data

p0027 A69-43611

Hard X-ray pulse identification with formation of brilliant kernel (11-12 September 1968) flare by comparison with optical data

p0030 A70-25746

Soft solar X rays cyclic variation from satellite observation, noting relation to sunspot group magnetic field complexity

p0039 A70-43301

Solar X-ray flare temperature and emission measure profiles using OGO 5 satellite detector, interpreting energy dispersion of peak times

p0040 A70-45768

Solar flare X ray and radio wave emission measurement by OGO-4 and Solrad-9 satellites

p0042 A71-14046

Impulsive solar flare X rays spectral characteristics, examining electron energy, bremsstrahlung, microwave bursts and particle escape, collisions and injection

p0043 A71-15937

Impulsive hard X ray and far UV emission during solar flares

p0046 A71-19825

Ionospheric absorption relation to solar X-ray flux enhancement during short wave fade-outs from OGO-4 and Solrad 9 satellites

p0046 A71-20318

Solar flare model, computing thermal X ray emission

p0046 A71-20945

Soft solar X-ray bursts characteristics, discussing temporal and intensity differential distributions, flux measurements and decay time

p0048 A71-27654

Soft X-ray and microwave observations of hot regions in solar flares.

p0060 A72-35089

H alpha subflare associated X-ray burst of 10 October 1970 observed by balloon-borne scintillator and OGO 5 and SOLRAD 9 satellites

p0064 A73-11389

The role of energetic electrons in the correlation of meter and decimeter type III bursts with 4 keV X-ray emission. p0064 A73-11391

X-radiation (E greater than 10 keV), H-alpha and microwave emission during the impulsive phase of solar flares. p0066 A73-17041

Evidence for a common origin of the electrons responsible for the impulsive X-ray and type 3 radio bursts. p0067 A73-20766

Acceleration of electrons during the flash phase of solar flares. p0079 A74-30287

Rise time in 20-32 keV impulsive X-radiation. p0080 A74-38468

Solar X ray contribution to E layer ionization [NASA-CR-73884] p0088 N69-17412

Solar X ray indication of flare activity [AD-686662] p0090 N69-32730

Electron density profiles and production rates associated with 30 Jan. 1968 large X ray flare event [RSD-63] p0096 N71-36131

SOLID STATE DEVICES

Energy spectra and abundances of elements He through Si of galactic cosmic ray above 20 Mev per nucleon in nuclear charge range between 2 and 26 p0006 A67-11687

Solid state detector for electron spatial distribution measurements on OGO-6 satellite, discussing design emphasizing reliability p0024 A69-36676

Measurements of electron detection efficiencies in solid state detectors. p0061 A72-39401

SOUNDING ROCKETS

Design, construction, test and flight use of electronic portions of research instruments on rockets and satellites for solar ultraviolet radiation [NASA-CR-110906] p0094 N71-10358

Neutral and ion mass spectrometer experiment SS015 [NASA-CR-96663] p0110 N74-77537

SPACE ENVIRONMENT SIMULATION

Continuous-channel electron multipliers degradation in spacecraft environment simulation laboratory equipment p0021 A69-29565

SPACE EXPLORATION

The Orbiting Geophysical Observatory - tool for space research [NASA-TN-D-1450] p0082 N62-15053

Small Explorer and large orbiting observatory classes of scientific satellites [NASA-TM-X-55261] p0083 N65-29783

SPACE VEHICLE CHECKOUT PROGRAM

Orbiting geophysical observatory spacecraft and its qualification and acceptance testing p0002 A63-23249

SPACECRAFT COMMUNICATION

Description of instrumentation on the Orbiting Geophysical Observatory (OGO) p0001 A63-13629

OGO structure and systems covering thermal and attitude controls, power plant, communications, tracking and data handling p0002 A65-14349

Latitudinal cut-off of manmade VLF signals in short path through ionosphere to OGO 2 satellite, noting strong noise following signal cut-off p0021 A69-28958

Reducing radio-frequency-interference from spacecrafts in the frequency range from 20Hz to 200 KHz [B00969-000] p0111

The feasibility of a sub-LF satellite-to-submarine communication downlink VLF noise levels in the ionosphere [AD-769139] p0104 N74-15857

SPACECRAFT CONTAMINATION

OGO-6 surface contamination by outgassing in space environment and decontamination by sputtering and desorption [NASA-CR-117138] p0094 N71-20207

Removal of surface contamination by plasma sputtering [NASA-CR-139264] p0109 N74-74659

SPACECRAFT DESIGN

Orbiting Geophysical Observatories, 1, 2, and 3 p0108 N74-74623

SPACECRAFT ELECTRONIC EQUIPMENT

OGO spacecraft EMI in 50 kHz to 4 MHz range p0089 N69-25437

OGO 3 experiment to measure physical parameters of picogram size dust particles in cislunar and near earth space [NASA-CR-121477] p0096 N71-33768

SPACECRAFT ENVIRONMENTS

Continuous-channel electron multipliers degradation in spacecraft environment simulation laboratory equipment p0021 A69-29565

Energy distribution of photoelectrons emitted from a surface on the OGO-5 satellite and measurements of satellite potential. p0076 A74-17648

SPACECRAFT INSTRUMENTS

Description of satellite instrumentation for atmospheric composition measurements p0001 A63-12209

OGO cosmic ray measuring device involving charged particle detectors to measure spectra and chemical composition over selected energy intervals p0012 A68-27615

Temperature gradient and thermal effects on ceramic transducer sensors used on spacecraft for cosmic dust experiments p0013 A68-29467

Electron trap behavior on charged spacecraft, obtaining expressions for current to aperture and internal retarding electrodes for all apertures and spacecraft potentials p0022 A69-31976

OGO 4 UV airglow spectrometer consisting of Ebert-Fastie monochromator and photomultipliers with cesium telluride and cesium iodide channels p0025 A69-36682

OGO 5 spacecraft detector instrumentation for measuring electrostatic and electromagnetic waves electric fields with coupled antennas, describing in-flight operation p0025 A69-36683

Spacecraft surface secondary electron emission effects on electron trap measurements in magnetosphere and solar wind, noting agreement with positive ion densities p0027 A70-13994

Fluxgate and Ru vapor magnetometers for space measurements over wide field intensities, reducing electronic phase shift and experiment weight p0032 A70-30045

Spacecraft sheath structure, potential and velocity effects on ion current measurements by traps and mass spectrometers p0038 A70-41087

EOGO triaxial search coil magnetometer Final Engineering Report [NASA-CR-100619] p0108 N69-72494

Instrumentation for radio astronomy measurements aboard the OGO-1 and OGO-3 spacecraft. Part 2: Technical [NASA-CR-139257] p0108 N74-74631

SPACECRAFT LAUNCHING

Orbiting Geophysical Observatory vibration magnitude and spectra due to launch acoustic environment determined from simulation tests p0002 A65-19503

Shadow and heat input data for S-50 (POGO) [NASA-TM-X-55153] p0083 N65-18269

SPACECRAFT MOTION

Spacecraft sheath structure, potential and velocity effects on ion current measurements by traps and mass spectrometers p0038 A70-41087

Visual presentation of motion and orientation of Orbiting Geophysical Observatory [NASA-TN-D-2918] p0083 N65-29296

Relationship of perigee motion of satellite orbit to latitude and local time [NASA-TM-X-55703] p0085 N67-18763

SPACECRAFT POWER SUPPLIES

Power requirements for satellites or spacecraft carrying communications or data-processing equipment p0002 A64-11240

Orbiting Geophysical Observatory electric power subsystem design innovations including power supply, solar array output and battery charge control p0003 A65-19528

Orbiting Geophysical Observatory (OGO) for cosmic ray, radio astronomy and Gegendheim experiments including satellite description and orbit data p0003 A65-22431

Solar cell array angle to provide maximum power for spin stabilized Orbiting Geophysical Observatory [NASA-TM-X-55186] p0083 N65-21656

SPARK CHAMBERS

OGO-5 spark-chamber telescope for gamma-ray astronomy [B18277-000] p0113

SPATIAL DISTRIBUTION

Low energy electron spatial distribution in magnetosphere obtained with OGO 1 and 3 indicate lower energies and higher densities occur during geomagnetic disturbances p0012 A68-28348

Spatial variations in particle intensity near and inside magnetosphere during September 1966 solar cosmic ray events, noting magnetosphere screening effectiveness p0018 A69-12740

Resonant compression waves in geomagnetic tail estimated for frequency and spatial distribution by single layered two dimensional model p0028 A70-15127

Low energy protons omnidirectional intensity contours in outer radiation zone at magnetic equator p0030 A70-23491

Magnetospheric sudden impulses amplitude and rise time distributions observation by OGO 3 and 5 satellites p0043 A71-17686

Horizontal He distribution in upper atmosphere from OGO 6 mass spectrometric data normalization for altitude by Jacchia model atmosphere p0046 A71-21647

Lyman alpha sky background measurements by OGO 5 satellite, discussing absolute emission rate, spatial variations and origin p0047 A71-24439

High energy electron spatial distribution in plasma sheet from OGO 5 magnetometer experiments p0062 A72-42406

Diurnal latitudinal composition variations in light ion trough from OGO mass spectrometric observations, noting magnetic storm effects p0065 A73-11904

Thermospheric wind effects on the distribution of helium and argon in the earth's upper atmosphere. p0071 A73-33441

SPECTRA

Description of OGO-1 and OGO-3 counting rate processing and resulting data. Cosmic ray spectra and fluxes experiment on OGO-1 and OGO-3 [B03716-000] p0111

Measurements of the primary cosmic ray electron spectrum between 20 MeV and 20 GeV and its changes with time [B06373-000] p0112

SPECTRAL BANDS

Banded chorus, VLF discrete emissions in magnetosphere in single variable frequency band with frequency depending on equatorial electron gyrofrequency p0023 A69-31981

SPECTRAL LINE WIDTH

OGO 5 satellite measurements of intensity and width of Lyman alpha line scattered by hydrogen geocorona p0022 A69-31412

SPECTRAL REFLECTANCE

Bidirectional reflectance at several wavelengths from moonlit earth observations by airglow photometer on OGO-4 satellite p0055 A72-13428

SPECTRAL RESOLUTION

Dynamic spectra of type 3 solar bursts from OGO-3 antenna/radiometer observations p0034 A70-34835

SPECTROHELIOGRAPHS

Heliographic longitude distribution of the flares associated with type 3 bursts observed at kilometric wavelengths p0076 A74-14811

SPECTROMETERS

Triaxial electron spectrometer, mounted on OGO-5 spacecraft, measures flux and energy distributions of electrons, noting electron multiplier p0005 A66-23689

Electron and proton spectrometer detector mounted on OGO-5, measurements cover seven differential energy channels p0005 A66-23690

Nonfocusing grazing incidence monochromator which utilizes planar gratings and collimating slit systems p0005 A66-27326

OGO-5 plasma spectrometers for measuring total flux below 12 keV and energy (spectral density) of plasma p0017 A68-42739

SPECTROPHOTOMETERS

OGO 5 ion spectrometer for measuring oxygen, He and hydrogen ion concentration, noting functions as energetic particle analyzer and proton energy distribution measurement capability

p0024 A69-36679

Ultraviolet solar radiation research instruments for space vehicles

p0083 N65-14504

Response characteristics of ionization chamber and spectrometer experiments aboard Orbiting Geophysical Observatory (OGO)

[CR-87] p0084 N67-13710

Magnetic Hall probe developed for use in spectrometer system aboard OGO-E satellite

[UCRL-14650-T] p0086 N67-30930

Electron fluxes from 50 keV to 4 MeV in inner radiation belt by spectrometer on OGO 1 and 3

[NASA-CR-100648] p0089 N69-19899

Systems analysis of electron and proton spectrometer on OGO-E

[NASA-CR-109962] p0093 N70-28103

Computation of velocity, temperature, and density of solar wind plasma, using attitude-stabilized plasma detectors on OGO-5

[NASA-CR-125063] p0096 N72-14808

OGO 1 and 3 spectrometer and ion chamber data on dynamic processes governing electrons in radiation belts, and applicability of diffusion theories and magnetic field models

[NASA-CR-127455] p0098 N72-28802

LLL electron and proton spectrometer on NASA's Orbiting Geophysical Observatory 5

[NASA-CR-136218] p0104 N74-13165

Data processing system for the intensity monitoring spectrometer flown on the Orbiting Geophysical Observatory-F (OGO-F) satellite

[NASA-CR-136827] p0105 N74-16940

Electron spectrometer and integrating ion chamber for the OGO-1 and OGO-3 missions

[NASA-CR-139263] p0109 N74-74639

A double gamma-ray spectrometer to search for positrons in space

p0110 N74-77446

SPECTROPHOTOMETERS

Ultraviolet solar radiation research instruments for space vehicles

[AFCLR-64-773] p0083 N65-14504

SPECTROPHOTOMETRY

Satellite multispectral photometry data in airglow bands correlated with cloud characteristics and surface albedo variations

p0028 A70-15522

SPECTRUM ANALYSIS

Fast time-resolved spectra of earth bow shock electrostatic turbulence based on broadband analog electric data from OGO-5

p0031 A70-29111

Forbush decreases and long term cosmic ray particle intensity changes, investigating spectral variations

p0044 A71-18137

Magnetospheric VLF banded emissions spectral analysis, investigating OGO-5 data by high time resolution spectral techniques

p0047 A71-24788

Auroral spectrum analysis in 1200-4000 A band, obtaining photon emission rates

p0058 A72-26402

Type 3 solar burst distinction from auroral type high pass noise via spectrum analysis

p0062 A72-42043

Solar electrons, galactic electron radiation modulation and spectrum of high energy cosmic ray electrons.

p0071 A73-33293

Geophysical properties of the ionospheric irregularities responsible for radio scintillation.

[AIAA PAPER 74-53] p0077 A74-18754

In situ measurements of the spectral characteristics of F region ionospheric irregularities.

p0078 A74-27695

Comparison of Cosmos-215 and OGO-D observations of nightglow in 1225 to 1350 A range at low geomagnetic latitudes

p0096 N71-34333

SPHERICAL HARMONICS

Geomagnetic field values obtained from OGO-2 satellite-mounted rubidium vapor magnetometer

p0007 A67-23244

International geomagnetic reference field model described by spherical harmonic coefficients with first and second time derivatives

p0012 A68-26625

Derivation of International Geomagnetic Reference Field with tables of spherical harmonic coefficients and test results of various magnetic field models

[NASA-TN-D-6237] p0095 N71-32190

SPIKE POTENTIALS

POGO ion chamber measurement of ionization by penetrating radiation, discussing spike intensity

p0017 A68-43450

SPIKES

High latitude ionization spikes observed by POGO spacecraft, noting frequency correlation with magnetic disturbances and development by high energy electron injections

p0021 A69-28950

SPIN STABILIZATION

Solar cell array angle to provide maximum power for spin stabilized Orbiting Geophysical Observatory

[NASA-TM-X-55186] p0083 N68-21656

SPREAD F

Positive Fe ion concentration relationship to equatorial spread F from OGO 6 satellite observation near magnetic equator

p0054 A72-10902

Equatorial spread F formation convective electric fields generation by neutral winds and conductivity caused by metallic ion concentrations

p0070 A73-29988

Jicamarca radio observations of temperature and electron density profiles, films of Spread F structure, and nightglow emission intensities

[NASA-CR-121984] p0096 N71-35437

SPUTTERING

Removal of surface contamination by plasma sputtering

[NASA-CR-139264] p0109 N74-74659

STATISTICAL ANALYSIS

Data collected by OGO-3 in detecting solar bursts

[NASA-CR-106640] p0091 N70-11147

Statistical analysis of neutral and ion mass spectroscopy data for OGO-2

[NASA-CR-107408] p0091 N70-14425

Cosmic ray telescope for OGO 2 and 4 spacecraft --- construction and flight of cosmic ray telescope on OGO-2 and 4 spacecraft

[NASA-CR-137238] p0106 N74-19088

Reduction and analysis of data from OGO-C.D ion chamber experiment

[NASA-CR-107184] p0110 N74-76923

STATISTICAL CORRELATION

Correlation of ground-based measurements of structured Pc 1 micropulsations with OGO-V plasmopause observations

p0067 A73-20652

STELLAR LUMINOSITY

Early type stars radiant flux observation from OGO 6 satellite

p0044 A71-17975

STELLAR RADIATION

Early type stars radiant flux observation from OGO 6 satellite

p0044 A71-17975

STORMS

Electron precipitation patterns and substorm morphology

[B16756-000] p0112

STRATOSPHERE

Ozone vertical distribution in upper stratosphere determined from OGO 4 observations, describing calibration of satellite data and onboard instrumentation

p0023 A69-32645

STRIATION

Drifting whistler frequency cutoff phenomena (striations) observation in low latitude by POGO satellites, discussing interpretation based on propagation effect

p0052 A71-39746

STRUCTURAL DESIGN

Design, test evaluation, and performance failure analysis of ion mass spectrometer for OGO-F

[NASA-CR-111146] p0094 N71-10588

SUDDEN IONOSPHERIC DISTURBANCES

Sudden magnetic field increase associated with July 8, 1966 sudden commencement observed by OGO 3 satellite in magnetotail

p0018 A69-11226

Geomagnetic crochets time relations to solar X rays, radio bursts and flares

p0023 A69-34227

Magnetospheric substorm, 1972

p0110 N74-77515

SUBJECT INDEX

SUNSPOT CYCLE

Studies of primary cosmic rays with ionization chambers. --- rigidity response of ionization chambers in high atmosphere and deep space for study of rigidity dependence of solar cycle modulation of primary cosmic ray

p0006 A66-34768

A model ionosphere for mid-day and mid-latitude during sunspot minimum

p0109 N74-74635

SUNSPOTS

Soft solar X rays cyclic variation from satellite observation, noting relation to sunspot group magnetic field complexity

p0039 A70-43301

Solar cosmic ray activity near sunspot maximum, discussing events of 18 November 1968 and 11 April 1969

p0044 A71-18158

Solar optical flares association with type 3 bursts from OGO-3 observations, suggesting temporary creation or enhancement of electron stream propagation by filament or sunspot structure change

p0045 A71-19724

A model ionosphere for mid-day and mid-latitude during sunspot minimum

p0109 N74-74635

SUPERCOOLING

OGO-6 measurements of supercooled plasma in the equatorial exosphere.

p0068 A73-22066

SUPERNOVAE

Gum Nebula size, density and electron temperature data from RAE-1 and OGO-5 satellites and ground based telescopes observations, correlating with Vela X supernova outburst

p0052 A71-35409

Search for brief celestial X-ray bursts. --- supernovae or gamma ray flare stars origins

p0078 A74-30149

SURFACE REACTIONS

Probe for measuring energy transfer between satellite and upper atmosphere

p0004 A66-15922

Gas-surface energy transfer experiment on OGO-6 satellite, measuring upper atmosphere kinetic energy flux to determine accommodation and drag coefficients, density, etc.

p0024 A69-36680

Role of gas-surface interactions in the reduction of OGO-6 neutral particle mass spectrometer data.

p0073 A73-38941

Gas-surface interaction studies

p0113

Instrument report for design of the gas-surface energy transfer experiments for OGO-F

p0113

Initial results from OGO-6 gas-surface experiment

p0113

Oxygen atom recombination reactions with solid surfaces for mass spectrometer atomic oxygen composition correction in upper atmosphere

p0091 N70-11727

SYNOPTIC MEASUREMENT

Synoptic survey for the neutral line in the magnetotail during the substorm expansion phase.

p0073 A73-36275

SYNOPTIC METEOROLOGY

Global characteristics in the diurnal variations of the thermospheric temperature and composition.

p0077 A74-21693

SYSTEMS ANALYSIS

Systems analysis of electron and proton spectrometer on OGO-E

p0093 N70-28103

Discussion of a management program for evaluation of aerospace systems design - Orbiting Geophysical Observatory (OGO) is used as an example

p0001 A63-13537

Design of a simple attitude positioning control system for an orbiting geophysical observatory

p0002 A64-10864

Orbiting Geophysical Observatories, 1, 2, and 3

p0108 N74-74623

T

TABLES (DATA)

Trapped electron environment in inner and outer radiation belts - tables and graphs

p0084 N66-35685

SUBJECT INDEX

Graphical and tabular summaries of ionization rates in space recorded by OGO spacecraft ion chambers [NASA-CR-107886] p0092 N70-17448

Derivation of International Geomagnetic Reference
Field with tables of spherical harmonic coefficients and test results of various magnetic field models. [NASA-TN-D-6237] p0095 N71-32190

TELEMETRY
Description of instrumentation on the Orbiting Geophysical Observatory (OGO) p0001 A63-13629

Recent studies of magnetospheric electric field emissions above the electron gyrofrequency. p0067 A73-19254

Ultraviolet solar radiation research instruments for space vehicles [AFRL-64-773] p0083 N65-14504

Processing of total field magnetometer data from OGO-2 satellite [NASA-TM-X-55822] p0085 N67-30147

TEMPERATE REGIONS
Ionospheric electron density response to geomagnetic storms at midlatitudes, noting diurnal variations detected by ATS 3 VHF signals p0038 A70-40479

TEMPERATURE CONTROL
OGO structure and systems covering thermal and attitude controls, power plant, communications, tracking and data handling p0002 A65-14349

TEMPERATURE DISTRIBUTION
Magnetosphere temperature distribution model noting heat fluxes due to low electron density, large mean free path, turbulent heat transfer, etc. p0015 A68-38423

Global temperature distributions from OGO-6 6300 A airglow measurements. p0077 A74-23679

Dynamic diffusion concept for calculating diurnal thermospheric temperature characteristics p0094 N71-25265

TEMPERATURE EFFECTS
Temperature gradient and thermal effects on ceramic transducer sensors used on spacecraft for cosmic dust experiments p0013 A68-29467

Soft X-ray and microwave observations of hot regions in solar flares. p0060 A72-35089

TEMPERATURE GRADIENTS
Temperature gradient and thermal effects on ceramic transducer sensors used on spacecraft for cosmic dust experiments p0013 A68-29467

TEMPERATURE MEASUREMENT
Ionospheric ion temperature measurements by retarding potential analyzer on OGO-6 satellite p0039 A70-43840

Solar X-ray flare temperature and emission measure profiles using OGO 5 satellite detector, interpreting energy dispersion of peak times p0040 A70-45768

Errors in ion and electron temperature measurements due to grid plane potential, nonuniformities in retarding potential analyzers p0071 A73-33436

Solar wind and magnetosheath electron temperature measurements by triaxial electron analyzer onboard OGO-5, presenting data for bow shock p0075 A73-45112

Neutral wind velocities calculated from temperature measurements during a magnetic storm and the observed ionospheric effects [B19920-000] p0113

TEMPERATURE PROFILES
Jicamarca radio observations of temperature and electron density profiles, films of Spread F structure, and nightglow emission intensities [NASA-CR-121984] p0096 N71-35437

TERRESTRIAL DUST BELT
Inconclusiveness of satellite measurements of micrometeoroid fluxes using piezoelectric microphone detectors in supporting hypothesis of cloud of dust surrounding earth p0006 A66-41213

Micrometeoroid experiments on OGO 2 and OGO 4 satellites, measuring velocity, masses and particle orbits in earth dust cloud p0027 A70-10444

TEST EQUIPMENT
Orbiting geophysical observatory spacecraft and its qualification and acceptance testing p0002 A63-23249

Single axis test program and simulator for vehicle dynamics in free space to test attitude control system of Orbiting Geophysical Observatory (OGO) p0002 A64-27303

TEST FACILITIES
Orbiting Geophysical Observatory vibration magnitude and spectra due to launch acoustic environment determined from simulation tests p0002 A65-19503

THERMAL CONDUCTIVITY
Midlatitude red arc observations by satellite and ground station, suggesting thermal conduction theory of formation from ionospheric electron and ion temperatures and densities p0061 A72-35989

THERMAL DIFFUSION
Ion temperature gradient along magnetic field lines in outer plasmasphere by thermal diffusion equations compared with electron temperature observations p0031 A70-26568

THERMAL EMISSION
Solar flare model, computing thermal X ray emission p0046 A71-20945

THERMAL PLASMAS
Earth thermal plasmasphere contraction subsequent to solar flare obtained from ion mass spectrometers on OGO satellites p0020 A69-23777

Plasmapause irregular structure and position indicated by measured distributions of hydrogen and helium thermal positive ions in duskside magnetosphere p0031 A70-29185

Magnetospheric thermal plasma electron density measurement during solar flare by OGO-5 satellite p0036 A70-37513

Thermal plasma model along magnetic field lines outside plasmasphere with sharp density gradient in equatorial plane, using OGO-4 ion composition measurements p0038 A70-41057

Nighttime plasmapause and thermal ion plasma structures relationship to micropulsations, considering excitation in post storm recovery and diurnal plasma bulge regions p0056 A72-17453

Atmospheric model for thermal plasma near equatorial plasmapause p0095 N71-25270

THERMAL RADIATION
Shadow time and heat input of EGO satellite [NASA-TM-X-55014] p0082 N64-27251

THERMALIZATION (ENERGY ABSORPTION)
Solar wind ion thermalization in earth bow shock by counterstreaming instability related to interplanetary magnetic field p0050 A71-31774

THERMODYNAMIC EQUILIBRIUM
Light ion abundance measurements of OGO satellites and field aligned diffusive equilibrium theory with temperature and concentration latitudinal variations p0021 A69-25157

THERMOELECTRIC COOLING
Thermoelectrically-cooled quartz crystal microbalance --- monitor of surface contamination as function of temperature p0103 N74-10255

THERMOSPHERE
Lyman alpha radiation scattering observation by satellites, obtaining geocoronal atomic hydrogen distribution in thermosphere and exosphere p0042 A71-14028

Seasonal density variations in thermosphere and exosphere, obtaining model from Explorers 19 and 39 drag measurements for comparison with OGO-6 mass spectroscopy p0051 A71-33802

Magnetic storm effects in atmospheric neutral composition, noting thermospheric wind circulation role due to Joule heating within auroral zone p0058 A72-24957

Thermospheric composition variations in south polar regions during magnetically quiet periods from OGO-6 observations, considering atmospheric heating by electron precipitation cyclic variations p0060 A72-32964

Theoretical model for the latitude dependence of the thermospheric annual and semiannual variations. p0066 A73-15538

Parametric description of thermospheric ion composition results p0067 A73-19255

TRANSDUCERS

Magnetic control of near equatorial neutral thermosphere, calculating F region ionization anomaly and molecular nitrogen and atomic oxygen density latitudinal variations p0069 A73-26997

Auroral heating and the composition of the neutral atmosphere. p0069 A73-27602

Energy and diffusive mass transport relation to thermospheric circulation, composition, temperature and mass density from three dimensional two constituent magnetic storm model p0070 A73-29975

Equatorial ionospheric anomaly related neutral thermospheric composition variation observation from OGO-6 mass spectroscopic data, noting static diffusion model limitations p0070 A73-31767

Empirical model of global thermospheric temperature and composition based on data from the OGO-6 quadrupole mass spectrometer. p0076 A74-18376

Global characteristics in the diurnal variations of the thermospheric temperature and composition. p0077 A74-21693

The air composition in the thermosphere. p0078 A74-29960

Heating of the high-latitude thermosphere during magnetically quiet periods. p0080 A74-34027

Global empirical model of thermospheric composition based on OGO-6 mass spectrometer measurements [B16248-000] p0112

Diurnal variation of the neutral thermospheric winds determined from incoherent scatter radar data [B22601-000] p0114

An upper limit to the product of NO and O densities from 105 to 120 Km [B22606-000] p0114

Dynamic diffusion concept for calculating diurnal thermospheric temperature characteristics p0094 N71-25265

Thermospheric composition and density, measured by neutral mass spectrometer onboard OGO-6 satellite p0101 N73-17946

Mechanism and rates of atmospheric mixing in lower thermosphere including heat input [NASA-CR-135789] p0103 N73-33321

Variations in thermospheric composition: A model based on mass-spectrometer and satellite-drag data [NASA-CR-136192] p0104 N74-12459

TIME DEPENDENCE
Geomagnetic crochets time relations to solar X rays, radio bursts and flares p0023 A69-34227

Magnetic activity effect on magnetospheric plasmapause position, measuring ion concentrations as function of local time from OGO 5 observations p0029 A70-18530

Latitude and local time dependence of precipitated low-energy electrons at high latitudes. p0074 A73-41914

TIME FUNCTIONS
Relationship of perigee motion of satellite orbit to latitude and local time [NASA-TM-X-55703] p0085 N67-18763

TIME LAG
Solar protons delayed access into polar regions during 2 November 1967 solar particle event, discussing north-south asymmetry p0027 A69-43183

Energy dependent time lag in the long-term modulation of cosmic rays. p0067 A73-19252

TIME RESPONSE
Solar flare electrons at 10-200 MeV region, discussing energy spectra and time history p0044 A71-18170

TRAJECTORY ANALYSIS
Comet Bennett /1969 i/ spectrograms, discussing linear diameter, trajectory, Lyman alpha emission and hydrogen mass p0039 A70-42468

Shadowing of electron azimuthal-drift motions near the noon magnetopause. p0065 A73-12442

TRANSDUCERS
Temperature gradient and thermal effects on ceramic transducer sensors used on spacecraft for cosmic dust experiments p0013 A68-29467

Nov. 10, 1975

TRANSPORT PROPERTIES

TRANSPORT PROPERTIES

Transport of solar flare protons: Comparison of a new analytic model with spacecraft measurements [B10763-000] p0112

TRANSVERSE WAVES

Nonthermal electrons interaction with electron plasma oscillations and HF transverse waves in upstream solar wind. p0052 A71-37353

TRAPPED PARTICLES

Alpha particle proton ratio of geomagnetic field from data from charged-particle telescope on OGO 1 satellite p0009 A67-37412

Geomagnetically trapped protons and alpha particles, analyzing OGO 4 data p0027 A69-43184

Spacecraft surface secondary electron emission effects on electron trap measurements in magnetosphere and solar wind, noting agreement with positive ion densities p0027 A70-13994

Geomagnetic dipole field disturbances by trapped particles, calculating self consistent equilibrium configuration for ring current dipole moments p0034 A70-31905

Trapped particle population changes associated with solar events, discussing solar wind discontinuity effects on magnetosphere p0036 A70-37487

High latitude observation of precipitating electron spikes by polar orbiter OGO 4 satellite, noting population dependence on local trapping limit p0060 A72-35591

Electron polar cap and the boundary of open geomagnetic field lines. p0063 A72-44522

Trapped electron environment in inner and outer radiation belts - tables and graphs [NASA-SP-3024-VOL-2] p0084 N66-35685

Models of trapped electron environment of inner radiation belt at synchronous orbit altitudes [NASA-SP-3024-VOL-3] p0085 N67-19899

Temporal variations of 40 keV electrons in magnetosphere during and after magnetic storm on April 18, 1965 p0086 N67-31362

Reduction and analysis of trapped and precipitating electron data from OGO 6 spectrometer experiment F-16 [NASA-CR-130137] p0100 N73-15863

Instrument report for a trapped radiation experiment for EGO (S-49) (OGO-1) [NASA-SP-3024-VOL-2] p0109 N74-76911

TRIAxIAL STRESSES

POGO triaxial search coil magnetometer [B21207-000] p0113

TROPICAL METEOROLOGY

Effects of interhemispheric transport on plasma temperatures at low latitudes. p0074 A73-41919

TROPICAL REGIONS

Tropical UV nightglow measurement by Ogo-4 spectrometer, considering ionospheric recombination excitation mechanism p0037 A70-39338

C, N and O nuclei abundances in radiation belt near geometric equator, using data obtained by OGO-5 satellite in 1965 p0041 A71-13475

Multiple magnetopause crossings in equatorial plane by OGO 5, showing magnetopause motion composed of two oscillations p0046 A71-21631

Atomic oxygen green line emission in nightglow from OGO-F photometer observations, calculating tropical F region electron density spatial distribution p0060 A72-35604

Theoretical calculations of the F-region tropical ultraviolet airglow intensity. p0062 A72-42418

Magnetic field strength change in equatorial plasmasphere, considering quiet ring current as equatorial sheet current extension of neutral sheet current in magnetospheric tail p0064 A73-11732

TROUGHS

The equatorial helium ion trough and the geomagnetic anomaly [B22334-000] p0114

The measurement of cold ion densities in the plasma trough [B22610-000] p0114

TURBULENCE

TURBULENCE

Fast time-resolved spectra of earth bow shock electrostatic turbulence based on broadband analog electric data from OGO-5 p0031 A70-29111

TWILIGHT GLOW

Satellite ultraviolet measurements of nitric oxide fluorescence with a diffusive transport model. p0074 A73-41925

TYPE 3 BURSTS

Dynamic spectra of type 3 solar bursts from OGO-3 antenna/radiometer observations p0034 A70-34835

Solar optical flares association with type 3 bursts from OGO-3 observations, suggesting temporary creation or enhancement of electron stream propagation by filament or sunspot structure change p0045 A71-19724

Interplanetary electron associations with type 3 solar bursts, using decametric OGO 3 and solar geophysical observations p0054 A71-43176

Type 3 solar burst distinction from auroral type high pass noise via spectrum analysis p0062 A72-42043

The role of energetic electrons in the correlation of meter and decimeter type III bursts with 4 keV X-ray emission. p0064 A73-11391

Type 3 radio bursts correlation with solar flares and electron events from OGO 5, IMP 5 and Explorer 35 observations p0066 A73-17047

Evidence for a common origin of the electrons responsible for the impulsive X-ray and type 3 radio bursts. p0067 A73-20766

The prevalence of second harmonic radiation in type 3 bursts observed at kilometric wavelengths. p0071 A73-32964

Solar wind density model from km-wave type 3 bursts. p0071 A73-32965

Decay time of type 3 solar bursts observed at kilometric wavelengths p0074 A73-41497

Heliographic longitude distribution of the flares associated with type 3 bursts observed at kilometric wavelengths p0076 A74-14811

Acceleration of electrons in the absence of detectable optical flares deduced from type 3 radio bursts, H-alpha activity and soft X-ray emission [B22607-000] p0114

Solar burst time profiles and dynamic spectra for calculating theoretical values for Type 3 burst characteristics [NASA-CR-107031] p0091 N70-12221

Analysis of data on Type 3 bursts measured by OGO-5 satellite [NASA-CR-122393] p0097 N72-23118

U

ULTRAVIOLET PHOTOMETRY

Determination of the solar Lyman-alpha flux independent of calibration by ultraviolet observations of Comet Bennett) p0076 A74-15496

ULTRAVIOLET RADIATION

Nonfocusing grazing incidence monochromator which utilizes planar gratings and collimating slit systems p0005 A66-27326

UV oxygen nightglow observation by OGO-4, examining ion-ion neutralization and radiative recombination production mechanisms p0037 A70-39344

Extraterrrestrial ultraviolet radiation and the parameter of the HI medium near the sun. p0073 A73-39074

Ultraviolet solar radiation research instruments for space vehicles [AFCL-64-773] p0083 N65-14594

Design, construction, test and flight use of electronic portions of research instruments on rockets and satellites for solar ultraviolet radiation [NASA-CR-110906] p0094 N71-10358

SUBJECT INDEX

ULTRAVIOLET SPECTRA

UV OGO observations of atomic hydrogen and oxygen in airglow, comparing results to exospheric models of hydrogen geocorona p0022 A69-31400

ULTRAVIOLET SPECTROMETERS

OGO 4 UV airglow spectrometer consisting of Ebert-Fastie monochromator and photomultipliers with cesium telluride and cesium iodide channels p0025 A69-36682

Satellite ultraviolet measurements of nitric oxide fluorescence with a diffusive transport model. p0074 A73-41925

Telemetry instruments aboard space vehicles for study of solar ultraviolet radiation monochromator, spectrometer, and radiation counter [NASA-CR-64074] p0083 N65-29678

Stratospheric ozone vertical distribution as determined by ultraviolet spectrometer on polar orbiting OGO-4 satellite p0090 N69-26549

ULTRAVIOLET SPECTROSCOPY

Tropical UV nightglow measurement by Ogo-4 spectrometer, considering ionospheric recombination excitation mechanism p0037 A70-39338

UPPER ATMOSPHERE

Probe for measuring energy transfer between satellite and upper atmosphere p0004 A66-15922

Hydrogen and He ion distribution measurements, noting seasonal and local magnetic time variability p0022 A69-31326

Gas-surface energy transfer experiment on OGO-6 satellite, measuring upper atmosphere kinetic energy flux to determine accommodation and drag coefficients, density, etc. p0024 A69-36680

Horizontal He distribution in upper atmosphere from OGO 6 mass spectrometric data normalization for altitude by Jacchia model atmosphere p0046 A71-21647

Neutral H concentration in upper atmosphere during solar minimum, using ion thermal energies from rocket and satellite mass spectrometric, radio and proton whistler measurements p0054 A72-10361

Distribution of hydrogen and helium in the upper atmosphere. p0064 A72-45593

Thermospheric wind effects on the distribution of helium and argon in the earth's upper atmosphere. p0071 A73-33441

Distribution of atomic oxygen in the upper atmosphere deduced from OGO-6 airglow observations. p0075 A73-45121

The relation between low-latitude neutral density variations near 400 km and magnetic activity indices. p0075 A74-14219

Absolute cosmic ray ionization measurements in upper and lower atmosphere [NASA-CR-104068] p0090 N69-34536

Charged particle distribution study in near earth region using orbiting spherical electrostatic analyzers or plasma probes [AD-700804] p0092 N70-28003

Perturbations in density of ions and neutral particles in upper atmosphere due to OGO [NASA-CR-117897] p0094 N71-23238

Latitudinal density distribution of gases in upper atmosphere p0094 N71-25267

Aurora formation by electron injection and drift in upper atmosphere p0095 N71-25272

Neutral density data from OGO-F and geomagnetic storms [NASA-CR-122479] p0099 N72-32390

UPPER IONOSPHERE

Ion temperature gradient along magnetic field lines in outer plasmasphere by thermal diffusion equations compared with electron temperature observations p0031 A70-26568

Hydrogen, He and oxygen ion density, and ion and electron temperatures in upper ionosphere from OGO 4 observations p0035 A70-36016

Solar geomagnetic seasonal ionization control of upper ionosphere longitudinal composition variations from polar satellite observations p0047 A71-24555

SUBJECT INDEX

WHISTLERS

Atmospheric neutral density measurement near 400 km during daytime by microphone density gage on OGO 6 p0058 A72-26407

USER MANUALS (COMPUTER PROGRAMS)
 Programmer manual for Polar Orbiting Geophysical Observatory [IS-769] p0082 N64-13388

V

VARIABLE STARS
 Search for brief celestial X-ray bursts, --- supernovae or gamma ray flare stars origins p0078 A74-30149

VELOCITY DISTRIBUTION
 Earth bow shock laminar profile at low Mach number by crossing satellites on 12 February 1969, determining mean velocity along normal p0057 A72-23004

VELOCITY MEASUREMENT
 Velocities of dust particles in cislunar space p0004 A66-15266
 Geminid meteoroid dust particles detection, determining velocity and orbital elements from OGO 3 flux measurements p0050 A71-33741
 Speeds, directions of arrival, and mass of dust particles measured from OGO-1 satellite to determine orbits of dust particles p0086 N67-32070

VERTICAL DISTRIBUTION
 Hydrogen Lyman alpha nightglow models, discussing solar photon scattering in geocorona and hydrogen vertical distribution p0022 A69-30191
 Ozone vertical distribution in upper stratosphere determined from OGO 4 observations, describing calibration of satellite data and onboard instrumentation p0023 A69-32645
 Cosmic ray knee interpretation using polar orbiting ionization chambers data from OGO-2/4 p0034 A70-31903
 Distribution of hydrogen and helium in the upper atmosphere p0064 A72-45593
 Stratospheric ozone vertical distribution as determined by ultraviolet spectrometer on polar orbiting OGO-4 satellite p0090 N69-26549

VERY LOW FREQUENCIES
 Satellite observation of natural VLF phenomena in ionosphere and magnetosphere stressing radio noise frequency-time characteristics p0010 A68-14098
 Latitudinal cut-off of manmade VLF signals in short path through ionosphere to OGO 2 satellite, noting strong noise following signal cut-off p0021 A69-28958
 Nonducted VLF walking trace whistlers and Doppler shifts in fixed frequency transmissions identified on OGO midlatitude spectrographic records p0028 A70-15116
 Magnetospheric observations of whistler mode emissions by OGO 1 satellite over VLF and LF ranges p0028 A70-15117
 Satellite observations of equatorial erosion and defocusing of VLF waves propagating at low magnetic latitudes p0029 A70-18532
 VLF noise phenomena observed with satellite electric dipole antennas compared with lower hybrid resonance frequency of ionospheric medium in vicinity p0029 A70-18534
 Magnetic fluctuations observed by ground observatories, suggesting large amplitude waves as field line resonances driven by magnetopause motion p0033 A70-30078
 Magnetospheric VLF banded emissions spectral analysis, investigating OGO-5 data by high time resolution spectral techniques p0047 A71-24788
 Atmospheric VLF electromagnetic emissions and electron instabilities data from satellite observation, detailing source regions, large amplitude electrostatic waves and wave-particle correlation p0049 A71-30952

Stable auroral red arcs on 29 September 1967, 31 October and 1 November 1968, comparing OGO 2 and OGO 4 VLF data on plasmopause crossings p0050 A71-31757
 Geomagnetic tail magnetic and electric fields ULF, VLF and ELF fluctuations, considering relationship to substorm processes p0064 A72-44857
 Summary of digital data-processing systems for the OGO SU/SRI very-low-frequency experiments [B01263-000] p0111
 Instrumentation for the Stanford University/Stanford Research Institute VLF experiment (B-17) on the OGO-3 satellite [B01265-000] p0111
 Digital data processing system for very low frequency radio noise and propagation experiment aboard OGO-1 [NASA-CR-88618] p0086 N67-37021
 Nonducted very low frequency propagation in magnetosphere from broadband VLF receivers on OGO 2 and OGO 4 polar satellites [NASA-CR-107614] p0091 N70-15525
 Very low frequency signals observed by OGO-4 measured and interpreted, and global ionospheric propagation study [NASA-CR-107654] p0092 N70-15768
 VLF experiments flown on OGO 1 (A17) and OGO 3 (B17) including orbits and attitudes of both satellites [NASA-CR-110716] p0093 N70-33156
 OGO-4 observation of banded whistlers using broadband VLF instrumentation p0102 N73-22079
 Measurements of VLF polarization and wave normal direction on OGO-F [NASA-CR-132882] p0104 N74-12842
 The feasibility of a sub-LF satellite-to-submarine communication downlink VLF noise levels in the ionosphere [AD-769139] p0104 N74-15857
 Instruments for the Stanford University/Stanford Research Institute VLF experiment (4917) on the OGO satellite [NASA-CR-139258] p0109 N74-74765

VIBRATION MODE
 Rapid magnetic field variations observed in magnetosheath evaluated in terms of transverse modes of plasma wave propagation [JPL-TR-32-1199] p0009 A67-40804

VIBRATION TESTS
 Orbiting Geophysical Observatory vibration magnitude and spectra due to launch acoustic environment determined from simulation tests p0002 A65-19503

VISIBILITY
 Analytical determination of earth visibility from orbiting satellite - OGO and POGO [NASA-TM-X-55002] p0082 N64-23517

VISUAL PHOTOMETRY
 Observations of the conjugate SAR arcs of September 28-30, 1967, --- subauroral red arcs p0080 A74-34042

VLF EMISSION RECORDERS
 OGO-1 and OGO-3 VLF emission records of magnetospheric electromagnetic noise [NASA-CR-107653] p0091 N70-15678

VOLT-AMPERE CHARACTERISTICS
 Electron trap behavior on charged spacecraft, obtaining expressions for current to aperture and internal retarding electrodes for all apertures and spacecraft potentials p0022 A69-31976

W

WAKES
 Applying impedance data to plasma wake of spinning OGO-C satellite [NASA-CR-109457] p0092 N70-23999

WAVE DIFFRACTION
 Power-law wavenumber spectrum deduced from ionospheric scintillation observations p0062 A72-42416

WAVE DISPERSION
 An association of magnetospheric whistler dispersion characteristics with changes in local plasma density p0069 A73-26985

WAVE GENERATION
 Magnetosphere Alfvén velocity profile relation to ELF chorus and hiss, indicating unstable wave generation by cyclotron resonance p0039 A70-43851
 The origin and propagation of chorus in the outer magnetosphere p0078 A74-24767

WAVE INTERACTION
 Solar wind microscopic structure, examining interplanetary wave-particle interactions p0042 A71-14068
 Electromagnetic waves in interplanetary space and effects on magnetosphere, considering solar wind characteristics due to wave interactions p0050 A71-30956
 Magnetospheric observations in OGO 5 plasma wave experiment, emphasizing electrostatic wave particles interaction with plasma p0065 A73-13883
 Magnetospheric chemical release study --- modifications of wave particle interactions in magnetosphere [AD-769979] p0105 N74-17126

WAVE PROPAGATION
 Radio propagation experiment using transmitted VHF waves from OGO-1 to deduce electron density in ionosphere and magnetosphere p0004 A66-10892
 Rapid magnetic field variations observed in magnetosheath evaluated in terms of transverse modes of plasma wave propagation [JPL-TR-32-1199] p0009 A67-40804
 Magnetic equator ELF noise examined with OGO 3 magnetometer, indicating unique signals in plasmasphere p0030 A70-21380
 Upstream discrete wave packets propagation interplanetary medium from OGO 5 observation p0045 A71-19656
 High latitude sudden impulses, calculating transverse hydromagnetic waves propagation from magnetosphere equatorial plane p0052 A71-34777
 Whistler propagation in magnetospheric ducts studies based on ray tracings verified by ground and satellite observations p0087 N68-17981
 Very low frequency signals observed by OGO-4 measured and interpreted, and global ionospheric propagation study [NASA-CR-107654] p0092 N70-15768
 OGO-4 satellite observations of whistler-mode propagation effects associated with caustics in the magnetosphere p0104 N74-12109

WAVEGUIDES
 Whistler ducts as enhanced ionization from OGO 3 satellite observations near magnetic equator, noting magnetospheric ionization hydrostatic model and predicted cut-off p0041 A71-11499

WHISTLERS
 Magnetospheric ionization distribution determined by ducted and nonducted whistler propagation modes and reflection as observed by OGO 1 p0010 A68-17728
 Ambient electron energy spectrum secondary peak determined from unducted magnetospherically reflected whistler mode radiation measurements p0015 A68-38428
 Ion cut-off whistlers observed during VLF experiment aboard OGO 2 and OGO 4, noting possible application to relative ionospheric proton concentration determination p0018 A69-14029
 OGO-6 electric and electromagnetic fields measurement for ionosphere using dipole antenna, emphasizing broadband observation covering whistler mode waves p0024 A69-36677
 Nonducted VLF walking trace whistlers and Doppler shifts in fixed frequency transmissions identified on OGO midlatitude spectrographic records p0028 A70-15116
 Magnetospheric observations of whistler mode emissions by OGO 1 satellite over VLF and LF ranges p0028 A70-15117
 Harmonic ion cyclotron resonances associated with proton whistlers observed from OGO-4 satellite VLF recordings p0030 A70-19630

NOV. 10, 1975

WIND (METEOROLOGY)

Whistler ducts as enhanced ionization from OGO 3 satellite observations near magnetic equator, noting magnetospheric ionization hydrostatic model and predicted cut-off

p0041 A71-11499

Whistler-mode waves circular polarization measurement by OGO 6 satellite, noting application to hiss, chorus and ion density studies

p0042 A71-14538

Drifting whistler frequency cutoff phenomena (striations) observation in low latitude by POGO satellites, discussing interpretation based on propagation effect

p0052 A71-39746

OGO 6 ionospheric measurement of proton whistlers wave-normal vector, investigating propagation modes

p0056 A72-19148

Magnetic fluctuations in ELF and VLF waves in space, discussing whistler phenomena and applications to magnetospheric probes

p0056 A72-21189

OGO-5 observation of lower hybrid resonance noise, bursts, VLF hiss and whistlers near plasmopause during large magnetic storm

p0058 A72-26399

Whistler mode signals observation in conjugate region of 200 kHz broadcast station by satellite-borne narrow band receiver, considering field-aligned ducted and nonducted propagation

p0059 A72-29384

An association of magnetospheric whistler dispersion characteristics with changes in local plasma density.

p0069 A73-26985

The plasmasphere during a magnetic recovery period: A combined study of the OGO-4 and OGO-5 satellite data and of whistlers received at the ground.

p0072 A73-33876

The global distribution of natural and man-made ionospheric electric fields at 200 kHz and 540 kHz as observed by OGO-6.

p0080 A74-34020

Observations of whistler mode signal propagation by OGO satellites from very low frequency ground station transmitters

[NASA-CR-84869] p0085 N67-30831

Whistler propagation in magnetospheric ducts studies based on ray tracings verified by ground and satellite observations

p0087 N68-17981

Studying whistlers and audio frequency emissions with receiving system on POGO satellite in conjunction with ground based observing stations

[NASA-CR-97605] p0088 N69-17928

Comparison of observation data by whistlers and mass spectrometers of plasmopause

[NASA-TM-X-63905] p0092 N70-27302

OGO-D electromagnetic wave propagation measurements with whistler and hiss formations in plasmasphere

[NASA-CR-130351] p0100 N73-16126

Observation of magnetospherically reflected whistlers made by OGO-A and OGO-C

[NASA-CR-130352] p0101 N73-16344

OGO-4 observation of banded whistlers using broadband VLF instrumentation

[NASA-CR-131495] p0102 N73-22079

OGO-4 satellite observations of whistler-mode propagation effects associated with caustics in the magnetosphere

p0104 N74-12109

Measurements of VLF polarization and wave normal direction on OGO-F

[NASA-CR-132882] p0104 N74-12842

OGO-5 observations of discrete whistlers and emissions during a large magnetic storm

[NASA-TM-X-70213] p0109 N74-74634

WIND (METEOROLOGY)

Equatorial spread F formation convective electric fields generation by neutral winds and conductivity caused by metallic ion concentrations

p0070 A73-29988

Diurnal variation of the neutral thermospheric winds determined from incoherent scatter radar data

[B22601-000] p0114

WIND EFFECTS

Magnetic storm effects in atmospheric neutral composition, noting thermospheric wind circulation role due to Joule heating within auroral zone

p0058 A72-24957

Thermospheric wind effects on the distribution of helium and argon in the earth's upper atmosphere.

p0071 A73-33441

WIND VELOCITY MEASUREMENT

Neutral wind velocities calculated from temperature measurements during a magnetic storm and the observed ionospheric effects

[B19920-000] p0113

X

X RAY ASTRONOMY

Solar flare X ray bursts detected by OGO spacecraft correlated with radio emission and solar flare electron and proton events

p0011 A68-22450

X RAY DENSITY MEASUREMENT

Solar X ray flux measurements from OGO 4, comparing peak fluxes before, during and after flares with IQSY data

p0027 A69-43611

X RAY SOURCES

Search for brief celestial X-ray bursts. --- supernovae or gamma ray flare stars origins

p0078 A74-30149

X RAY SPECTROSCOPY

Spectral intensity of high energy solar X rays observed during July 7, 1966 polar event with satellite OGO 3, suggesting nonthermal bremsstrahlung origin

p0020 A69-23753

X RAYS

Acceleration of electrons in the absence of detectable optical flares deduced from type 3 radio bursts, H-alpha activity and soft X-ray emission

[B22607-000] p0114

Ionization rate profiles from solar flare X rays observed by ion chambers aboard OGO 1 and OGO 3

[NASA-CR-94429] p0087 N68-23026

Possible low energy (E less than keV) nonthermal X-ray events --- analysis of proportional counter detector data from OGO-5

p0107 N74-21450

Optical, hard X-ray, and microwave emission during the impulsive phase of flares --- analysis of optical impulsive component in solar flares

p0107 N74-21458

Z

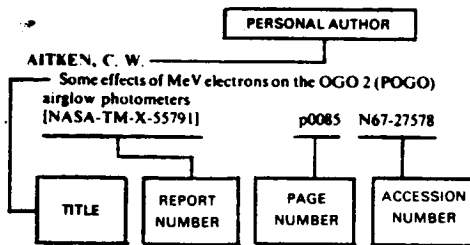
ZODIACAL DUST

Zodiacal dust particle flux measurements from OGO 3 and Mariner 4 spacecraft in cislunar and interplanetary space

p0013 A68-29457

B. PERSONAL AUTHOR INDEX

Typical Personal Author Index Listing



Listings in this index are arranged alphabetically by personal author. The title of the document provides a brief description of the subject matter. The report number helps to indicate the type of document cited. The page number identifies the page in the abstract section (VI) on which the citation appears while the accession number denotes the number by which the citation is identified on that page. Under each author's name the accession numbers are arranged in ascending alphanumeric order.

A

- AGGSON, T. L.**
Satellite and ground-based observations of a red arc.
p0061 A72-35989
- AHMED, M.**
Thermal positive ions in the outer ionosphere and magnetosphere from OGO I.
[AD-742186] p0057 A72-23011
- AITKEN, C. W.**
Some effects of MeV electrons on the OGO 2 (POGO) airglow photometers
[NASA-TM-X-55791] p0085 N67-27578
- ALCAYDE, D.**
Comparison of atomic oxygen measurements by incoherent scatter and satellite-borne mass spectrometer techniques.
p0078 A74-27713
- ALEXANDER, J. K.**
• The Gum Nebula: Further evidence from spacecraft and ground-based instruments.
p0052 A71-35409
New results and techniques in space radio astronomy
[NASA-TM-X-63976] p0093 N70-33175
- ALEXANDER, W. M.**
Measured velocities of interplanetary dust particles.
p0004 A66-15266
Zodiacal dust measurements in cis-lunar and interplanetary space from OGO-3 and Mariner 4 experiments between June and December 1966.
p0013 A68-29457
Results of studies of thermal gradient effects on ceramic transducer sensors used in cosmic dust experiments.
p0013 A68-29467
Results of recent microparticle hypervelocity impact studies related to sensors of cosmic dust experiments.
p0013 A68-29468
Picogram dust particle flux: 1967-1968 measurements in selenocentric, cislunar and interplanetary space.
p0041 A71-14014
Results of a 1970 Geminid dust particle rocket experiment and analysis of OGO III dust particle velocity measurements.
p0050 A71-33741

- Four years of dust particle measurements in cislunar and selenocentric space from Lunar Explorer 35 and OGO 3
[B15918-000] p0112
Measured velocities of interplanetary dust particles from OGO-1 p0086 N67-32070
- ALFONSI, P. J.**
A simulation of the response of the OGO spacecraft structure to the launch acoustic environment.
p0002 A65-19503
- ALLISON, L. J.**
Meteorological results from multi-spectral photometry in airglow bands by the OGO-4 satellite.
p0028 A70-15522
- ALTHOUSE, W. E.**
A solar and galactic cosmic ray satellite experiment.
p0012 A68-27615
- ALVAREZ, H.**
Evidence for electron excitation of type 3 radio burst emission.
p0066 A73-17047
The prevalence of second harmonic radiation in type 3 bursts observed at kilometric wavelengths.
p0071 A73-32964
Solar wind density model from km-wave type 3 bursts.
p0071 A73-32965
Decay time of type 3 solar bursts observed at kilometric wavelengths
p0074 A73-41497
Heliographic longitude distribution of the flares associated with type 3 bursts observed at kilometric wavelengths
p0076 A74-14811
Analysis of type 3 solar radio bursts observed at kilometric wavelengths from the OGO-5 satellite
[NASA-CR-122393] p0097 N72-23118
- AMMAR, A.**
OGO-5 determination of the local interstellar wind parameters.
p0051 A71-33834
- ANDERSON, A. D.**
Neutral density measurements near 400 kilometers by a microphone density gage on OGO-6 during July 12-15, 1969.
p0058 A72-26407
The relation between low-latitude neutral density variations near 400 km and magnetic activity indices.
p0075 A74-14219
Variations of atmospheric density near 400 km with magnetic activity during the storm period of 28 September to 2 October 1969
[NASA-CR-122479] p0099 N72-32390
- ANDERSON, D. N.**
Theoretical calculations of the F-region tropical ultraviolet airglow intensity.
p0062 A72-42418
- ANDERSON, G. P.**
Satellite observations of the vertical ozone distribution in the upper stratosphere.
p0023 A69-32645
The vertical distribution of ozone between 35 and 55 km as determined from satellite ultraviolet measurements
p0090 N69-26549
- ANDERSON, H. R.**
Observations of POGO ion chamber experiment in the outer radiation zone.
p0017 A68-43450
Nonuniformity of solar protons over the polar caps on March 24, 1966.
p0022 A69-31967
Response to environment and radiation of an ionization chamber and matched geiger tube used on spacecraft
[NASA-CR-139255] p0108 N74-74624
Reduction and analysis of data from OGO-C,D ion chamber experiment
[NASA-CR-107184] p0110 N74-76923

- ANDERSON, K. A.**
Energetic protons from the solar flare of March 24, 1966.
p0010 A67-41233
Entry of solar cosmic rays into the earth's magnetosphere
p0032 A70-30059
Spectral characteristics of impulsive solar-flare X-rays greater than or approximately 10 keV.
p0043 A71-15937
Solar cosmic ray experiment for the first Orbiting Geophysical Observatories
[B03937-000] p0111
Energetic radiation from solar flares
[B03940-000] p0111
Experiment data analysis report OGO-3: Experiment no. 1
[B03943-000] p0111
Experiment data analysis report OGO-A: Experiment no. 1
[B03944-000] p0111
Energetic radiations from solar flares
[NASA-CR-122509] p0098 N72-28812
- ANGERAMI, J. J.**
Magnetospheric properties deduced from OGO-1 observations of ducted and nonducted whistlers.
p0010 A68-17728
Nonducted mode of VLF propagation between conjugate hemispheres: Observations on OGO's 2 and 4 of the "walking-trace" whistler and of Doppler shifts in fixed frequency transmissions.
p0028 A70-15116
Whistler duct properties deduced from VLF observations made with the OGO-3 satellite near the magnetic equator.
p0041 A71-11499
OGO-4 observations of extremely low frequency hiss.
p0057 A72-23008
Whistler propagation in magnetospheric ducts
p0087 N68-17981
Experiments C02 (OGO 2) and D02 (OGO 4)
[NASA-CR-110658] p0093 N70-32928
- ARNOLDY, R. L.**
Response of ion chambers in free space to the long-term cosmic-ray variation from 1960 to 1965.
p0003 A65-33664
Studies of primary cosmic rays with ionization chambers.
p0006 A66-34768
A study of energetic solar flare X-rays.
p0009 A67-41232
Energetic solar flare X-rays observed by satellite and their correlation with solar radio and energetic particle emission.
p0011 A68-22450
The observation of 10-50 keV solar flare X-rays by the OGO satellites and their correlation with solar radio and energetic particle emission.
p0014 A68-35480
An atlas of 10-50 keV solar flare X-rays observed by the OGO satellites, 5 September 1964 to 31 December 1966
[NASA-CR-94429] p0087 N68-23026
- ARTHUR, C. W.**
Picogram dust particle flux: 1967-1968 measurements in selenocentric, cislunar and interplanetary space.
p0041 A71-14014
Results of a 1970 Geminid dust particle rocket experiment and analysis of OGO III dust particle velocity measurements.
p0050 A71-33741
Four years of dust particle measurements in cislunar and selenocentric space from Lunar Explorer 35 and OGO 3
[B15918-000] p0112
- ATRINSON, G.**
Dissipation mechanisms in a pair of solar-wind discontinuities.
p0058 A72-29378

NOV. 10, 1975

Comments on a paper by J. P. Heppner. Polar cap electric field distributions related to interplanetary magnetic field direction
[NASA-CR-139259] p0108 N74-74632

AUBRY, M. P.
Inward motion of the magnetopause before a substorm. p0042 A71-14515
Motion and structure of the magnetopause. p0046 A71-21631
Magnetotail changes in relation to the solar wind magnetic field and magnetospheric substorms. p0051 A71-33944
Outer magnetosphere near midnight at quiet and disturbed times. p0063 A72-44513
Satellite studies of magnetospheric substorms on August 15, 1968. 4: OGO-5 magnetic field observations. p0072 A73-33452
Satellite studies of magnetospheric substorms on August 15, 1968. 5: Energetic electrons, spatial boundaries, and wave-particle interactions at OGO-5. p0072 A73-33453
Satellite studies of magnetospheric substorms on August 15, 1968. 9: Phenomenological model for substorms. p0072 A73-33457

B

BAILEY, G. J.
Effects of interhemisphere transport on plasma temperatures at low latitudes. p0074 A73-41919

BAKER, B. R.
Research related to measurements of atomic species in the earth's upper atmosphere [NASA-CR-106305] p0091 N70-11727

BAKER, M. B.
Simultaneous satellite and riometer measurements of particles during solar cosmic ray events. p0059 A72-31965
Simultaneous satellite and riometer studies. p0079 A74-30263

BALASUBRAHMANYAN, V. K.
The multiply charged primary cosmic radiation at solar minimum, 1965. p0005 A66-26348
Galactic cosmic rays at solar minimum, 1965. p0006 A66-34847
Solar modulation of galactic cosmic rays. p0007 A67-19913
The composition of low-energy cosmic rays in 1965. p0016 A68-41431
Spectra and charge composition of the low energy galactic cosmic radiation from Z equals 2 to 14. p0037 A70-38127
Spectral variations in short term Forbush decreases and in long term changes in cosmic ray intensity. p0044 A71-18137

BALL, R. H.
Prediction of geomagnetic secular change, confirmed. p0025 A69-37490

BARNES, C.
Instrumentation for the Stanford University/Stanford Research Institute VLF experiment (B-17) on the OGO-3 satellite [B01265-000] p0111

BARON, M.
Comparison of Te and Ti from OGO-6 and from arious incoherent scatter radars. p0067 A73-19241

BARTH, C. A.
Satellite observations of the vertical ozone distribution in the upper stratosphere. p0023 A69-32645
OGO-4 ultraviolet airglow spectrometer. p0025 A69-36682
OGO-4 spectrometer measurements of the tropical ultraviolet airglow p0037 A70-39338

BARTJ, C. A.
Global satellite measurements of nitric oxide. p0064 A73-10878

BAUER, P.
Molecular ions in the F2 layer. p0062 A72-42016
Comparison of Te and Ti from OGO-6 and from various incoherent scatter radars. p0067 A73-19241

BAUER, S. J.
Temperature and composition studies in the polar ionosphere. p0049 A71-30037

Satellite measurements of the cold plasma in the magnetosphere. p0049 A71-30951

BEACHLEY, N. H.
Testing OGO's attitude controls. p0002 A64-27303

BECK, C. W., II
Solar wind measurement techniques. 2: Solar plasma energy spectrometers. p0003 A65-29239

BEDO, D. E.
Collimating grating monochromators for the vacuum ultraviolet. p0005 A66-27326

BELL, F. T.
Observations of naturally occurring VLF and man-made hf plasma waves in auroral regions of the ionosphere. p0032 A70-29924

BENJAMIN, C. R.
A magnetic field instrument for the OGO-E spacecraft. p0007 A67-15724

BERG, O. E.
Measured velocities of interplanetary dust particles. p0004 A66-15266

BERKO, F. W.
Primary electron influx to dayside auroral oval. p0048 A71-27911
Distributions and characteristics of high-latitude field-aligned electron precipitation. p0069 A73-26988
A synoptic study of the nature and effects of field aligned low energy electron precipitation in the auroral regions [NASA-TM-X-66065] p0099 N73-10392
Seasonal and altitude variations in field-aligned precipitation occurrence [NASA-TM-X-66099] p0100 N73-11345
Simultaneous particle and field observations of field-aligned currents [NASA-TM-X-66224] p0102 N73-21367
Dependence of field-aligned electron precipitation on season, altitude and pitch angle [NASA-TM-X-66260] p0102 N73-25868

BERTAUD, CH.
Observations of the comet Bennett (1969i). p0039 A70-42468

BERTAUX, J. L.
OGO-5 measurements of Lyman-alpha intensity distribution and linewidth up to 6 earth radii. p0022 A69-31412
Evidence for a source of an extraterrestrial hydrogen Lyman-alpha emission: The interstellar wind. p0047 A71-24438
OGO-5 determination of the local interstellar wind parameters. p0051 A71-33834
Interpretation of OGO-5 Lyman alpha measurements in the upper geocorona. p0066 A73-19233
Observed variations of the exospheric hydrogen density with exospheric temperature [B22614-000] p0114
Observation of Lyman-alpha emission in interplanetary space p0100 N73-10812

BERTSCH, D. L.
Measurements of the iron-group abundance in energetic solar particles. p0068 A73-23538

BIKLE, F. E.
Dynamic analysis of longitudinal oscillations of SM-68B stage 1 (POGO) [B00570-000] p0111

BINGHAM, R. G.
Two satellite-borne cosmic radiation detectors. p0004 A66-23684
Direct measurements of geomagnetic cutoffs for cosmic-ray particles in the latitude range 45 deg to 70 deg using balloons and satellites. p0016 A68-41562

BINSACK, J. H.
Simultaneous IMP 2 and OGO 1 observations of bow shock compression. p0011 A68-17768

BLAIR, W. F.
Proton gyrofrequency band emissions observed aboard OGO 2. p0013 A68-31481

Summary of digital data-processing systems for the OGO SU/SRI very-low-frequency experiments [B01263-000] p0111
OGO-1 VLF experiment A-17 digital data processing system [NASA-CR-88618] p0086 N67-37021
Resonances in the driving-point impedance of an electric dipole in the ionosphere [NASA-CR-91620] p0087 N68-14025

BLAMONT, J. E.
Some results concerning the principal airglow lines as measured from the OGO-2 satellite. p0007 A67-23278
OGO-5 measurements of Lyman-alpha intensity distribution and linewidth up to 6 earth radii. p0022 A69-31412
Meteorological results from multi-spectral photometry in airglow bands by the OGO-4 satellite. p0028 A70-15522
Inflight radiometric calibration of OGO-IV airglow photometer. p0029 A70-15645
Evidence for a source of an extraterrestrial hydrogen Lyman-alpha emission: The interstellar wind. p0047 A71-24438
OGO-5 determination of the local interstellar wind parameters. p0051 A71-33834
Bidirectional reflectance of the moonlit earth. p0055 A72-13428
Geomagnetic effect on the neutral temperature of the F region during the magnetic storm of September 1969. p0060 A72-35603
Interpretation of OGO-5 Lyman alpha measurements in the upper geocorona. p0066 A73-19233
Equatorial airglow and the ionospheric geomagnetic anomaly. p0073 A73-38939
Global temperature distributions from OGO-6 6300 A airglow measurements. p0077 A74-23679
Observations of the conjugate SAR arcs of September 28-30, 1967. p0080 A74-34042
Effects of energetic particles on photomultipliers in earth orbits up to 1500 km [NASA-TM-X-63419] p0088 N69-18074
An atlas of low latitude 6300A (01) night airglow from OGO-4 observations [NASA-TM-X-65913] p0098 N72-26309
Functional characteristics of the OGO main body airglow photometer [NASA-TM-X-65926] p0098 N72-27423
OGO-4 observations of the 6300A night airglow from 40 deg N to 40 deg S: A set of 19 color maps [NASA-TM-X-65954] p0098 N72-28353
Observation of Lyman-alpha emission in interplanetary space p0100 N73-10812

BLEEKER, J. A. M.
Time variations in the cosmic ray electron spectrum above 500 MeV. p0037 A70-38105
The cosmic ray electron spectrum between 0.5 and 10 GeV observed on board OGO-5. p0037 A70-38106
Search for galactic gamma-rays with energies greater than 500 MeV on board OGO-5. p0038 A70-40690

BLUM, P. W.
New interpretations of extraterrestrial Lyman-alpha observations. p0065 A73-12323

BOGDANOWICZ, R. M.
The LRL electron and proton spectrometer on NASA's Orbiting Geophysical Observatory 5 (E): Instrumentation and calibration [NASA-CR-109962] p0093 N70-28103

BOHLIN, R. C.
Lyman-alpha measurements of neutral hydrogen in the outer geocorona and in interplanetary space. p0059 A72-32955

BOHN, J. L.
Zodiacal dust measurements in cis-lunar and interplanetary space from OGO-3 and Mariner 4 experiments between June and December 1966. p0013 A68-29457
Results of studies of thermal gradient effects on ceramic transducer sensors used in cosmic dust experiments. p0013 A68-29467

- Results of recent microparticle hypervelocity impact studies related to sensors of cosmic dust experiments. p0013 A68-29468
- Picogram dust particle flux: 1967-1968 measurements** in selenocentric, cislunar and interplanetary space. p0041 A71-14014
- Results of a 1970 Geminid dust particle rocket experiment and analysis of OGO III dust particle velocity measurements. p0050 A71-33741
- Four years of dust particle measurements in cislunar and selenocentric space from Lunar Explorer 35 and OGO 3 [B15918-000] p0112
- OGO-3 dust particle experiment: Data reduction and analysis [NASA-CR-121477] p0096 N71-33768
- BOLDT, E.**
Solar modulation of galactic cosmic rays. p0007 A67-19913
- BONNER, F. M.**
Ion depletion in the high-latitude exosphere: Simultaneous OGO-2 observations of the light ion trough and the VLF cutoff. p0023 A69-34939
- BOURDEAU, R. E.**
OGO-4 observations of ion composition and temperatures in the topside ionosphere. p0035 A70-36016
- BOWYER, C. S.**
Temperature and emission-measure profiles of two solar X-ray flares. p0040 A70-45768
- BOWYER, J. M., JR.**
Gas-surface interaction studies [B20296-000] p0113
- Bombardment of OGO-6 surfaces by high-energy particles [B20297-000] p0113
- BRACE, L. H.**
Comparison of Te and Ti from OGO-6 and from various incoherent scatter radars. p0067 A73-19241
- Is the red arc a good indicator of ionosphere-magnetosphere conditions [B22605-000] p0114
- BRANDT, J. C.**
The Gum Nebula: Further evidence from spacecraft and ground-based instruments. p0052 A71-35409
- BRINTON, H. C.**
Instrumentation for atmospheric composition measurements. p0001 A63-12209
- Positive ion composition in the magnetosheath obtained from the OGO-A satellite. p0004 A66-14781
- Contraction of the plasmasphere during geomagnetically disturbed periods. p0011 A68-19744
- Thermal ion structure of the plasmasphere. p0014 A68-37114
- Thermal ions in the exosphere: Evidence of solar and geomagnetic control. p0016 A68-41673
- Evidence of contraction of the earth's thermal plasmasphere subsequent to the solar flare events of 7 and 9 July 1966. p0020 A69-23777
- Multi-experiment detection of the plasmopause from EOGO satellites and antarctic ground stations. p0021 A69-25153
- Observations of hydrogen and helium ions during a period of rising solar activity. p0022 A69-31326
- Ion depletion in the high-latitude exosphere: Simultaneous OGO-2 observations of the light ion trough and the VLF cutoff. p0023 A69-34939
- Observations of irregular structure in thermal ion distributions in the duskside magnetosphere. p0031 A70-29185
- BRODY, K. I.**
Some remarks on the position and shape of the neutral sheet. p0010 A68-13469
- BROWN, J. W.**
High-energy electron spikes at high latitudes. p0060 A72-35591
- The elemental abundance ratios of interstellar secondary and primary cosmic rays. p0079 A74-30190
- A satellite measurement of cosmic-ray abundances and spectra in the charge range 2 less than or equal to 7 less than or equal to 10 [NASA-CR-135786] p0103 N73-33777
- BRUN, J. F.**
Some effects of MeV electrons on the OGO 2 (POGO) airglow photometers [NASA-TM-X-55791] p0085 N67-27578
- BUCK, R. M.**
Shadowing of electron azimuthal-drift motions near the noon magnetopause. p0065 A73-12442
- Electron pitch angle distributions throughout the magnetosphere as observed on OGO-5. p0068 A73-24732
- Satellite studies of magnetospheric substorms on August 15, 1968. 6: OGO 5 energetic electron observations. Pitch angle distributions in the nighttime magnetosphere p0072 A73-33454
- Satellite studies of magnetospheric substorms on August 15, 1968. 7: OGO-5 energetic proton observations. Spatial boundaries p0072 A73-33455
- Energetic electrons and protons observed on OGO-5, March 6-10, 1970 [B07587-000] p0111
- Energetic electron and proton solar particle observations on OGO-5, 24-34 January 1971 [B15152-000] p0112
- LLL electron and proton spectrometer on NASA's Orbiting Geophysical Observatory 5 [NASA-CR-136218] p0104 N74-13165
- Energetic electrons and protons observed on OGO-5, March 6-10, 1970 [NASA-CR-139265] p0109 N74-74662
- Energetic electron and proton solar particle observations on OGO-5, January 24-30, 1971 [NASA-CR-139266] p0109 N74-74663
- BURCH, J. L.**
Precipitation of low-energy electrons at high latitudes: Effects of interplanetary magnetic field and dipole tilt angle. p0066 A73-15531
- Rate of erosion of dayside magnetic flux based on a quantitative study of the dependence of polar cusp latitude on the interplanetary magnetic field. p0075 A74-14274
- High latitude proton precipitation and light ion density profiles during the magnetic storm initial phase [B22333-000] p0113
- BURGER, J. J.**
Time variations in the cosmic ray electron spectrum above 500 MeV. p0037 A70-38105
- The cosmic ray electron spectrum between 0.5 and 10 GeV observed on board OGO-5. p0037 A70-38106
- Search for galactic gamma-rays with energies greater than 500 MeV on board OGO-5. p0038 A70-40690
- Implications of the observed solar modulation of cosmic-ray electrons. p0040 A70-45769
- Energy dependent time lag in the long-term modulation of cosmic rays. p0067 A73-19252
- The 1972 cosmic ray electron spectrum above 0.5 GeV. p0078 A74-27700
- Short-term intensity fluctuation of cosmic-ray electrons between 0.5 and 10 GeV. p0079 A74-31903
- Energy spectrum of cosmic-ray electrons from 0.5 to 10 GeV [B14744-000] p0112
- BURROU, S. C. N.**
Solar wind measurement techniques. 2. Solar plasma energy spectrometers. p0003 A65-29239
- BURTIS, D. W.**
A low energy solar cosmic ray experiment for OGO-F. p0012 A68-27616
- BURTIS, W. J.**
Banded chorus: A new type of VLF radiation observed in the magnetosphere by OGO-1 and OGO-3. p0023 A69-31981
- Electron concentrations calculated from the lower hybrid resonance noise band observed by OGO-3 p0074 A73-41912
- Magnetic radiation observed by OGO-1 and OGO-3 broadband VLF receivers [NASA-CR-107653] p0091 N70-15678
- BURTON, R. K.**
The Alfvén velocity in the magnetosphere and its relationship to ELF emissions. p0039 A70-43851
- Measurement of the wave-normal vector of proton whistlers on OGO-6. p0056 A72-19148
- A correlated study of ELF waves and electron precipitation on OGO-6. p0077 A74-24766
- The origin and propagation of chorus in the outer magnetosphere. p0078 A74-24767
- Simultaneous particle and field observations of field-aligned currents [NASA-TM-X-66224] p0102 N73-21367
- CAAN, M. V.**
Substorm and interplanetary magnetic field effects on the geomagnetic tail lobes [B22611-000] p0114
- CAIN, J.**
Crustal anomalies p0097 N72-23341
- CAIN, J. C.**
First magnetic field results from the OGO-2 satellite. p0007 A67-23244
- The main geomagnetic field. p0009 A67-36901
- A proposed model for the international geomagnetic reference field, 1965. p0012 A68-26625
- Magnetic chart of the Brazilian anomaly: A verification. p0017 A68-42083
- OGO-2 magnetic field observations during the magnetic storm of March 13-15, 1966. p0018 A69-11125
- Prediction of geomagnetic secular change confirmed. p0025 A69-37490
- The location of the dip equator at E-layer altitude. p0026 A69-42428
- Magnetic field mapping of the inner magnetosphere. p0038 A70-39349
- Geomagnetic models from satellite surveys. p0049 A71-29903
- Geomagnetic survey by the polar Orbiting Geophysical Observatories. p0054 A72-12081
- The POGO data. p0070 A73-31768
- The detection of 'intermediate' size magnetic anomalies in Cosmos 49 and OGO-2, 4, 6 data. p0073 A73-41374
- Summary and future work (OGO-4 and OGO-6) [B15849-000] p0112
- The geomagnetic secular variation, 1900 - 1965 [NASA-TM-X-55944] p0086 N67-37398
- Derivation of the International Geomagnetic Reference Field, IGRF(10/68) [NASA-TN-D-6237] p0095 N71-32190
- POGO observations of the equatorial electrojet [NASA-TM-X-65995] p0099 N72-30823
- The equatorial electrojet satellite and surface comparison [NASA-TM-X-66218] p0102 N73-20866
- A global magnetic anomaly map [NASA-TM-X-70628] p0106 N74-20982
- CAIN, S. J.**
Derivation of the International Geomagnetic Reference Field, IGRF(10/68) [NASA-TN-D-6237] p0095 N71-32190
- CAMPBELL, M.**
OGO-A magnetic field observations. p0010 A68-11011
- CAPPENTIER, D. L.**
The plasmasphere during a magnetic recovery period: A combined study of the OGO-4 and OGO-5 satellite data and of whistlers received at the ground. p0072 A73-33876
- CARDEN, R. C.**
An experiment to study electric and electromagnetic fields in the frequency range 10 Hz to 540 kHz on OGO-F. p0024 A69-36677

C

CARIGNAN, G. R.

Response of the neutral atmosphere to geomagnetic disturbances.

p0052 A71-39711

Neutral composition variation above 400 kilometers during a magnetic storm.

p0055 A72-13518

Neutral composition in the thermosphere.

p0062 A72-42431

Empirical model of global thermospheric temperature and composition based on data from the OGO-6 quadrupole mass spectrometer.

p0076 A74-18376

Global characteristics in the diurnal variations of the thermospheric temperature and composition.

p0077 A74-21693

Global empirical model of thermospheric composition based on OGO-6 mass spectrometer measurements

[B16248-000] p0112

CARLSON, H. C.

Comparison of Te and Ti from OGO-6 and from various incoherent scatter radars.

p0067 A73-19241

CARPENTER, D. L.

Recent research on the magnetospheric plasmopause.

p0014 A68-37940

Multi-experiment detection of the plasmopause from EOGO satellites and antarctic ground stations.

p0021 A69-25153

Ion depletion in the high-latitude exosphere: Simultaneous OGO-2 observations of the light ion trough and the VLF cutoff.

p0023 A69-34939

OGO-2 and 4 vlf observations of the asymmetric plasmopause near the time of SAR arc events.

p0050 A71-31757

Satellite studies of magnetospheric substorms on August 15, 1968. 3: Some features of magnetospheric convection.

p0072 A73-33451

CASTELLI, J. P.

Flare X-ray and radio wave emission.

p0042 A71-14046

CAUFFMAN, D. P.

Satellite measurements of high latitude convection electric fields.

[AD-750221] p0063 A72-42901

CAYLA, F.

Satellite observations of the vertical ozone distribution in the upper stratosphere.

p0023 A69-32645

CHAN, K. W.

Measurement of the wave-normal vector of proton whistlers on OGO-6.

p0056 A72-19148

Plasmaspheric hiss intensity variations during magnetic storms.

p0080 A74-34038

CHANDRA, S.

OGO-4 observations of ion composition and temperatures in the topside ionosphere.

p0035 A70-36016

Subauroral red arcs and associated ionospheric phenomena.

p0045 A71-19663

Equatorial phenomena in neutral thermospheric composition

p0070 A73-31767

Equatorial airglow and the ionospheric geomagnetic anomaly.

p0073 A73-38939

The equatorial helium ion trough and the geomagnetic anomaly

[B22334-000] p0114

Diurnal phase anomaly in the earth's upper atmosphere

p0094 N71-25265

CHAPMAN, M. C.

A correlated study of ELF waves and electron precipitation on OGO-6.

p0077 A74-24766

CHAPPELL, C. R.

A study of the influence of magnetic activity on the location of the plasmopause as measured by OGO-5

p0029 A70-18530

Observations of the plasmopause from OGO-5.

p0029 A70-18546

The reaction of the plasmopause to varying magnetic activity.

p0032 A70-30074

The morphology of the bulge region of the plasmasphere.

p0035 A70-36014

The Alfvén velocity in the magnetosphere and its relationship to ELF emissions.

p0039 A70-43851

OGO-5 measurements of the plasmasphere during observations of stable auroral red arcs

p0047 A71-24787

The relationship of the plasmasphere and the stable auroral red arcs in the magnetic storm of October 29 to November 7, 1968.

p0053 A71-39833

OGO-5 observations of the polar cusp on November 1, 1968.

p0053 A71-43162

The dayside of the plasmasphere.

p0054 A72-10892

The plasmopause as measured in positive ions.

p0061 A72-39544

Plasmasphere dynamics inferred from OGO-5 observations.

p0065 A73-12320

An association of magnetospheric whistler dispersion characteristics with changes in local plasma density.

p0069 A73-26985

Observation of a current-driven plasma instability at the outer zone-plasma sheet boundary.

p0069 A73-29966

Satellite studies of magnetospheric substorms on August 15, 1968. 3: Some features of magnetospheric convection.

p0072 A73-33451

The plasmasphere during a magnetic recovery period: A combined study of the OGO-4 and OGO-5 satellite data and of whistlers received at the ground.

p0072 A73-33876

CHEN, A. J.

Plasma tail interpretations of pronounced detached plasma regions measured with OGO-5

[B20951-000] p0113

Dynamics of midlatitude light ion trough and plasmatails

[NASA-TM-X-70494] p0103 N74-10366

CHILDERS, D. D.

OGO 5 observations of upstream waves in the interplanetary medium: Discrete wave packets.

p0045 A71-19656

Power spectra of the interplanetary magnetic field near the earth

p0099 N73-10792

CHIBB, T. A.

Measurements of solar X-ray emission from the OGO-4 spacecraft.

p0027 A69-43611

Observations of the aurora in the far ultraviolet from OGO 4.

p0030 A70-23493

Equatorial aurora/airglow in the far ultraviolet.

p0041 A71-11504

CHUPP, E. L.

Cosmic ray neutron monitor for OGO-F.

p0024 A69-36678

Latitude and altitude dependence of the cosmic ray albedo neutron flux.

p0037 A70-39326

CHURCH, S. R.

Intensity variation of elf hiss and chorus during isolated substorms

[B22603-000] p0114

CICERONE, R. J.

Comparison of Te and Ti from OGO-6 and from various incoherent scatter radars.

p0067 A73-19241

CLARK, M. A.

On the diurnal variation of the exospheric neutral hydrogen temperature.

p0040 A70-43852

Observation of early-type stars from OGO-6.

p0044 A71-17975

A flight calibration device for absolute measurements at the Lyman-alpha wavelength

[AD-726567] p0096 N71-36136

Spectral variations of the L alpha sky: A final report of observations from OGO-6

[AD-736816] p0097 N72-23429

Instrument report for Lyman-alpha experiment (OGO-F-12)

p0108 N74-74625

CLINE, T. L.

High-energy X-rays from the solar flare of July 7, 1966.

p0011 A68-17769

Search for low-energy interplanetary positrons.

p0015 A68-41427 Very high energy solar X-rays observed during the proton event of 7 July 1966.

p0020 A69-23753 Cosmic ray electrons and positrons of energies 2 to 9.5 MeV observed in interplanetary space.

p0036 A70-38096 Interplanetary positrons near 1 MeV from other than the pion to muon to electron process.

p0036 A70-38098 Search for brief celestial X-ray bursts.

p0078 A74-30149 Cosmic ray and solar flare electrons

p0090 N69-38983 A double gamma-ray spectrometer to search for positrons in space

p0110 N74-77446

COLBURN, D. S.

Satellite studies of magnetospheric substorms on August 15, 1968. 2: Solar wind and outer magnetosphere.

p0071 A73-33450

COLEMAN, P. J.

OGO-5 observations of electrostatic turbulence in bow shock magnetic structures.

p0035 A70-36006 Magnetic and electric field changes across the shock and in the magnetosheath.

p0036 A70-37483

COLEMAN, P. J., JR.

Observations of the microstructure of the earth's bow shock.

p0026 A69-42693 Heliographic latitude dependence of the dominant polarity of the interplanetary magnetic field.

p0027 A70-13980 Direct correlations of large-amplitude waves with suprathermal protons in the upstream solar wind.

p0043 A71-14550 OGO 5 observations of upstream waves in the interplanetary medium: Discrete wave packets.

p0045 A71-19656 Magnetic field variations in the near geomagnetic tail associated with weak substorm activity.

p0046 A71-21643 Satellite observations of band-limited micropulsations during a magnetospheric substorm.

p0048 A71-27913 Fluctuating magnetic fields in the magnetosphere.

p0056 A72-21189 Fluctuating magnetic fields in the magnetosphere. 2: ULF waves.

p0063 A72-42902 Satellite studies of magnetospheric substorms on August 15, 1968. 4: OGO-5 magnetic field observations.

p0072 A73-33452 A summary of the results from the UCLA OGO-5 fluxgate magnetometer

[NASA-CR-130205] p0101 N73-20498

COLIN, I.

An interpretation of OGO light ion abundance measurements.

p0021 A69-25157

COMSTOCK, G.

Composition and spectra of charged particles of solar and cosmic origin measured on satellites.

p0008 A67-27249

COMSTOCK, G. M.

Abundances and energy spectra for nuclei of galactic origin above 20 MeV per nucleon.

p0006 A66-34833 Abundances and energy spectra of galactic cosmic-ray nuclei above 20 MeV per nucleon in the nuclear charge range 2 less than or equal to Z less than or equal to 26.

p0006 A67-11687 The low-energy cosmic-ray nuclei and their propagation in interstellar space.

p0016 A68-41434 Energy spectra and abundances of the cosmic-ray nuclei helium to iron from the OGO-1 satellite experiment.

p0020 A69-20067 Propagation and source characteristics derived from the low-energy, multiply charged, cosmic-ray nuclei.

p0020 A69-20068

CORBIN, J. D.

Picogram dust particle flux: 1967-1968 measurements in selenocentric, cislunar and interplanetary space.

p0041 A71-14014

- CORBIN, W. E., JR.**
Initial results from OGO-6 gas-surface experiment [B20954-000] p0113 B75-20954
Space measurements of the contamination of surfaces by OGO-6 outgassing and their cleaning by sputtering and desorption [NASA-CR-117138] p0094 N71-20207
Thermoelectrically-cooled quartz crystal microbalance p0103 N74-10255
Removal of surface contamination by plasma sputtering [NASA-CR-139264] p0109 N74-74659
- CORCUFF, P.**
The plasmasphere during a magnetic recovery period: A combined study of the OGO-4 and OGO-5 satellite data and of whistlers received at the ground. p0072 A73-33876
- CORCUFF, Y.**
The plasmasphere during a magnetic recovery period: A combined study of the OGO-4 and OGO-5 satellite data and of whistlers received at the ground. p0072 A73-33876
- CORNWALL, J. M.**
VLF emission and electron instabilities p0049 A71-30952
- CORONITI, F. V.**
Fast time-resolved spectra of electrostatic turbulence in the earth's bow shock. p0031 A70-29111
VLF electric field observations in the magnetosphere. p0041 A71-11500
Fast time resolved spectral analysis of VLF banded emissions. p0047 A71-24788
Satellite studies of magnetospheric substorms on August 15, 1968. 8: OGO-5 plasma wave observations. p0072 A73-33456
Complex electric field emissions observed by OGO-5 on 15 August 1968 [NASA-CR-126238] p0097 N72-22383
- COYLE, R. J.**
Real time quick-look analysis for the OGO satellites. [AIAA PAPER 64-218] p0002 A64-24447
- CRONIN, A. G.**
Data processing system for the intensity monitoring spectrometer flown on the Orbiting Geophysical Observatory-F (OGO-F) satellite [NASA-CR-136827] p0105 N74-16940
- CROOK, G. M.**
Detection of electric-field turbulence in the earth's bow shock. p0018 A69-14681
The OGO-5 plasma wave detector-instrumentation and in-flight operation. p0025 A69-36683
Observations of plasma waves in space. p0029 A70-17376
Ac fields and wave particle interactions. p0033 A70-30085
OGO-5 observations of electrostatic turbulence in bow shock magnetic structures. p0035 A70-36006
The Pioneer 9 electric field experiment. p0046 A71-23711
Data analysis program for the OGO E-24 plasma wave detector [NASA-CR-140523] p0110 N74-77109
- CROSSETT, G., JR.**
Instrument report for a trapped radiation experiment for EGO (S-49) (OGO-1) [NASA-CR-140528] p0109 N74-76911
- CRYSTAL, T. L.**
Proton gyrofrequency band emissions observed aboard OGO 2. p0013 A68-31481
- D**
- DANGELO, N.**
Ultralow frequency fluctuations at the polar cusp boundaries. p0068 A73-24744
- DANTAS, N. H.**
OGO-4 satellite observations of whistler-mode propagation effects associated with caustics in the magnetosphere p0104 N74-12109
- DARCY, R. G., JR.**
Satellite studies of magnetospheric substorms on August 15, 1968. 7: OGO-5 energetic proton observations. Spatial boundaries p0072 A73-33455
Energetic electrons and protons observed on OGO-5, March 6-10, 1970 [B07587-000] p0111
Energetic electron and proton solar particle observations on OGO-5, 24-34 January 1971 [B15152-000] p0112
The LRL electron and proton spectrometer on NASA's Orbiting Geophysical Observatory 5(E): Instrumentation and calibration [NASA-CR-109962] p0093 N70-28103
Energetic electrons and protons observed on OGO-5, March 6-10, 1970 [NASA-CR-139265] p0109 N74-74662
Energetic electron and proton solar particle observations on OGO-5, January 24-30, 1971 [NASA-CR-139266] p0109 N74-74663
- DAROSA, A. V.**
Eccentric Geophysical-Observatory Satellite S-49 with interpretation of the radiobeacon experiment Technical Report No. 1 [NASA-CR-68307] p0084 N66-12993
Protonospheric electron concentration profiles [NASA-CR-100778] p0089 N69-24521
- DATLOWE, D.**
Electrons from solar flares in the 10 to 200 MeV region. p0044 A71-18170
Relativistic electrons associated with solar particle events, measuring occurrence frequency, electron propagation and diffusion anisotropy. p0048 A71-29057
- DAVIDSON, G. T.**
Magnetospheric chemical release study [AD-769979] p0105 N74-17126
- DAVIS, W. M.**
The detection of 'intermediate' size magnetic anomalies in Cosmos 49 and OGO-2, 4, 6 data. p0073 A73-41374
A global magnetic anomaly map [NASA-TM-X-70628] p0106 N74-20982
- DEAN, A. J.**
OGO-5 spark-chamber telescope for gamma-ray astronomy [B18277-000] p0113
- DEERENBERG, A. J. M.**
Time variations in the cosmic ray electron spectrum above 500 MeV. p0037 A70-38105
The cosmic ray electron spectrum between 0.5 and 10 GeV observed on board OGO-5. p0037 A70-38106
Search for galactic gamma-rays with energies greater than 500 MeV on board OGO-5. p0038 A70-40690
- DEKORTE, P. A. J.**
Energy spectrum of cosmic-ray electrons from 0.5 to 10 GeV [B14744-000] p0112
- DELANEY, J. R.**
Data processing system for the intensity monitoring spectrometer flown on the Orbiting Geophysical Observatory-F (OGO-F) satellite [NASA-CR-136827] p0105 N74-16940
- DESAL, U. D.**
Search for brief celestial X-ray bursts. p0078 A74-30149
- DESHMUKH, A. R.**
Observations of irregular structure in thermal ion distributions in the duskside magnetosphere. p0031 A70-29185
- DESHPANDE, S. D.**
Ionospheric effects of solar flares. 5: The flare event of January 30, 1968 and its implications [RSD-63] p0096 N71-36131
- DESPAIN, L. G.**
Response to environment and radiation of an ionization chamber and matched geiger tube used on spacecraft [NASA-CR-139255] p0108 N74-74624
- DESSLER, A. J.**
Diffusive entry of solar-flare particles into geomagnetic tail. p0040 A71-11494
- DEVANEY, R. A.**
OGO earth acquisition [NASA-TM-X-55002] p0082 N64-23517
- DIMOFAKIS, P. F.**
OGO-C orientation study [REPT-9] p0109 N74-74661
- DODSON, H. W.**
The solar particle event of July 16-19, 1966 and its possible association with a flare on the invisible solar hemisphere. p0020 A69-22181
- DONAHUE, T. M.**
Analysis of OGO-6 observations of the O 1557-A tropical nightglow. p0060 A72-35604
Distribution of atomic oxygen in the upper atmosphere deduced from OGO-6 airglow observations. p0075 A73-45121
Spatial and temporal behavior of atomic oxygen determined by OGO 6 airglow observations. p0079 A74-30670
An upper limit to the product of NO and O densities from 105 to 120 Km [B22606-000] p0114
The altitude of the scattering layer near the mesopause over the summer poles [NASA-CR-130271] p0101 N73-16436
- DONLEY, J. L.**
OGO-4 observations of ion composition and temperatures in the topside ionosphere. p0035 A70-36016
Photoelectron flux in the topside ionosphere measured by retarding potential analyzers [NASA-TM-X-63358] p0087 N68-35999
- DONNELLY, R. F.**
Impulsive hard X-ray and ultraviolet emission during solar flares. p0045 A71-19825
- DRAKE, J. F.**
Characteristics of soft solar X-ray bursts. p0048 A71-27654
- DUFUR, S. W.**
An interpretation of OGO light ion abundance measurements. p0021 A69-25157
- DUMMER, R. S.**
Gas-surface energy transfer experiment for OGO-F. p0024 A69-36680
Gas-surface interaction studies [B226296-000] p0113
- DUNCKEL, N.**
Whistler-mode emissions on the OGO-1 satellite. p0028 A70-15117
Low-frequency noise observed in the distant magnetosphere with OGO-1. p0031 A70-27183
Type 3 solar noise observed below 100 kHz on OGO-1. p0062 A72-42043
The feasibility of a sub-LF satellite-to-submarine communication downlink VLF noise levels in the ionosphere [AD-769139] p0104 N74-15857
- DYSON, P. L.**
In situ measurements of the spectral characteristics of E region ionospheric irregularities. p0078 A74-27695
In situ measurements of amplitude and scale size characteristics of ionospheric irregularities: OGO-6 ion concentration irregularity studies [B20340-000] p0113
- E**
- ECCLES, D.**
ISIS-1 satellite observations of the ionosphere at high southern latitudes. p0068 A73-25753
- EDGAR, B. C.**
The structure of the magnetosphere as deduced from magnetospherically reflected whistlers [NASA-CR-130352] p0101 N73-16344
- EICKEN, B. P.**
Summary of digital data-processing systems for the OGO 5U/SRI very-low-frequency experiments [B01263-000] p0111
- EMERY, B. A.**
Diurnal variation of the neutral thermospheric winds determined from incoherent scatter radar data [B27601-000] p0114
- ERICKSON, W. C.**
Two satellite-borne cosmic radiation detectors. p0004 A66-23684
- EVANS, D. S.**
Field-aligned electron bursts at high latitudes observed by OGO-4. p0017 A68-43443

EVANS, J. E.

- OGO-4 auroral particles experiment and calibration [NASA-TM-X-70216] p0108 N74-74628
- EVANS, J. E.
Magnetospheric chemical release study [AD-769979] p0105 N74-17126
- EVANS, J. V.
Comparison of Te and Ti from OGO-6 and from various incoherent scatter radars. p0067 A73-19241
- EVANS, L. C.
Access of solar protons into the polar cap: A persistent north-south asymmetry. p0027 A69-43183
- Electron polar cap and the boundary of open geomagnetic field lines. p0063 A72-44522
- Magnetospheric access of solar particles and the configuration of the distant geomagnetic field, volume 2 [NASA-CR-122360] p0097 N72-25727

F

- FAHR, H. J.
New interpretations of extraterrestrial Lyman-alpha observations. p0065 A73-12323
- Extraterrestrial ultraviolet radiation and the parameter of the H I medium near the sun. p0073 A73-39074
- FAIRFIELD, D. H.
The magnetic field of the magnetosphere and tail. p0049 A71-30028
- Magnetic field fluctuations during substorms [NASA-TM-X-65748] p0096 N72-11325
- FAN, C. Y.
Protons and helium nuclei within interplanetary magnetic regions which co-rotate with the sun. p0005 A66-34754
- Abundances and energy spectra for nuclei of galactic origin above 20 MeV per nucleon. p0006 A66-34833
- Abundances and energy spectra of galactic cosmic-ray nuclei above 20 MeV per nucleon in the nuclear charge range 2 less than or equal to Z less than or equal to 26. p0006 A67-11687
- Composition and spectra of charged particles of solar and cosmic origin measured on satellites. p0008 A67-27249
- Differential energy spectra and intensity variation of 1-20 MeV/nucleon protons and helium nuclei in interplanetary space (1964-66). p0015 A68-41420
- Energy spectra and abundances of the cosmic-ray nuclei helium to iron from the OGO-1 satellite experiment. p0019 A69-20067
- Primary cosmic-ray electron energy spectrum from 10 to 200 Mev observed in interplanetary space. p0027 A70-12902
- The 'quiet time' fluxes of protons and alpha-particles in the energy range of 2-20 MeV/nucleon in 1967. p0044 A71-18127
- The quiet-time spectra of cosmic-ray electrons of energies between 10 and 200 Mev observed on OGO-5. p0055 A72-16719
- FANSELOW, J. L.
Geomagnetic cutoffs for cosmic-ray protons for seven energy intervals between 1.2 and 39 Mev p0061 A72-38728
- FARLEY, T. A.
Spatial distribution of energetic plasma sheet electrons. p0062 A72-42406
- Satellite studies of magnetospheric substorms on August 15, 1968. 5: Energetic electrons, spatial boundaries, and wave-particle interactions at OGO-5. p0072 A73-33453
- A correlated study of ELF waves and electron precipitation on OGO-6. p0077 A74-24766
- Trapped and precipitating electrons experiment (F-16) on the Orbiting Geophysical Observatories program OGO-6 mission [NASA-CR-130137] p0100 N73-15863
- FARMER, B. J.
Results of a 1970 Geminid dust particle rocket experiment and analysis of OGO III dust particle velocity measurements. p0050 A71-33741

- FARTHING, W. H.
Rubidium vapor magnetometer for near earth orbiting spacecraft. p0008 A67-36513
- FATKULLIN, M. N.
Concentration of neutral hydrogen in the upper atmosphere according to data on the ionic composition of the medium. p0054 A72-10361
- FELDSHTEIN, Y. I.
Asymmetry of the ring current [B18378-000] p0113
- FENTON, K. B.
A search for alpha particles trapped in the geomagnetic field. p0009 A67-37412
- FICHTEL, C. E.
Measurements of the iron-group abundance in energetic solar particles. p0068 A73-23538
- FICKLIN, B.
Low-frequency noise observed in the distant magnetosphere with OGO-1. p0031 A70-27183
- FICKLIN, B. P.
Proton gyrofrequency band emissions observed aboard OGO 2. p0013 A68-31481
- Instrumentation for the Stanford University/Stanford Research Institute VLF experiment (B-17) on the OGO-3 satellite [B01265-000] p0111
- OGO-1 VLF experiment A-17 digital data processing system [NASA-CR-88618] p0086 N67-37021
- Instruments for the Stanford University/Stanford Research Institute VLF experiment (4917) on the EOGO satellite [NASA-CR-139258] p0109 N74-74765
- FISKE, K. J.
Intensity variation of elf hiss and chorus during isolated substorms [B22603-000] p0114
- FITZWATER, D. R.
POGO reference manual [IS-769] p0082 N64-13388
- FLOWERDAY, T. W.
Plasma measurements with the retarding potential analyzer on OGO-6. p0039 A70-43840
- FOLZ, W. C.
Rubidium vapor magnetometer for near earth orbiting spacecraft. p0008 A67-36513
- FORMISANO, V.
Structure of the quasi-perpendicular laminar bow shock [B22612-000] p0114
- FOUST, E. C.
OGO-F-02 data analysis [NASA-CR-130128] p0100 N73-13376
- FOWLER, W. B.
Meteorological results from multi-spectral photometry in airglow bands by the OGO-4 satellite. p0028 A70-15522
- Inflight radiometric calibration of OGO-IV airglow photometer. p0029 A70-15645
- Bidirectional reflectance of the moonlit earth. p0055 A72-13428
- Some effects of M eV electrons on the OGO 2 (POGO) airglow photometer: [NASA-TM-X-55791] p0085 N67-27578
- Effects of energetic particles on photomultipliers in earth orbits up to 1500 km [NASA-TM-X-63419] p0088 N69-18074
- An atlas of low latitude 6300A (01) night airglow from OGO-4 observations [NASA-TM-X-65913] p0098 N72-26309
- Functional characteristics of the OGO main body airglow photometer [NASA-TM-X-65926] p0098 N72-27423
- FOX, M. G.
Probe for measuring energy transfer between a satellite and the upper atmosphere. p0004 A66-15922
- Instrument report for design of the gas-surface energy transfer experiments for OGO-F [B20953-000] p0113
- FRAME, D. R.
Errors in retarding potential analyzers caused by nonuniformity of the grid-plane potential. p0058 A72-26411

PERSONAL AUTHOR INDEX

- FRANSEN, A. M. A.
OGO search coil magnetometer experiments. p0024 A69-36675
- OGO-5 observations of LHR noise, emissions, and whistlers near the plasmopause at several earth radii during a large magnetic storm. p0058 A72-26399
- Plasmaspheric hiss intensity variations during magnetic storms. p0080 A74-34038
- OGO-5 observations of discrete whistlers and emissions during a large magnetic storm [NASA-TM-X-70213] p0109 N74-74634
- FRANK, L. A.
Initial observations of low-energy electrons in the earth's magnetosphere with OGO-3. p0007 A67-19926
- Several observations of low-energy protons and electrons in the earth's magnetosphere with OGO-3. p0008 A67-26312
- On the extraterrestrial ring current during geomagnetic storms. p0009 A67-37401
- Energy fluxes of low-energy protons and positive ions in the earth's inner radiation zone. p0011 A68-17771
- On the distributions of low-energy protons and electrons in the earth's magnetosphere. p0013 A68-34245
- Lifetimes for low-energy protons in the outer radiation zone. p0016 A68-41684
- Recent observations of low-energy charged particles in the earth's magnetosphere. p0019 A69-19358
- Degradation of continuous-channel electron multipliers in a laboratory operating environment. p0021 A69-29565
- Direct detection of asymmetric increases of extraterrestrial 'ring current' proton intensities in the outer radiation zone. p0030 A70-23490
- Omnidirectional intensity contours of lowenergy protons /0.5 to 50 keV/ in the earth's outer radiation zone at the magnetic equator. p0030 A70-23491
- Further comments concerning low energy charged particle distributions within the earth's magnetosphere and its environs. p0033 A70-30089
- Electron observations between the inner edge of the plasma sheet and the plasmasphere. p0039 A70-43834
- Direct correlations of large-amplitude waves with suprathermal protons in the upstream solar wind. p0043 A71-14550
- Energy spectrums for proton (200 eV less than or equal to E less than or equal to 1 MeV) intensities in the outer radiation zone. p0043 A71-17261
- Relationship of the plasma sheet, ring current, trapping boundary, and plasmopause near the magnetic equator and local midnight. p0047 A71-24781
- Nonthermal electrons and high-frequency waves in the upstream solar wind p0052 A71-37353
- Nonthermal electrons and high-frequency waves in the upstream solar wind. 2: Analysis and interpretation. p0053 A71-43158
- Low-energy proton and electron experiment for the Orbiting Geophysical Observatories B and E [NASA-CR-68558] p0084 N66-13640
- A cinematographic display of observations of low-energy proton and electron spectra in the terrestrial magnetosphere [NASA-CR-91871] p0087 N68-15232
- FREDRICKS, R. W.
Detection of electric-field turbulence in the earth's bow shock. p0018 A69-14681
- The fine structure of the earth's collisionless shock wave. [AIAA PAPER 69-676] p0023 A69-33452
- The OGO-5 plasma wave detector-instrumentation and in-flight operation. p0025 A69-36683
- Observations of the microstructure of the earth's bow shock. p0026 A69-42693
- Observations of plasma waves in space. p0029 A70-17376

- Fast time-resolved spectra of electrostatic turbulence in the earth's bow shock. p0031 A70-29111
- Ac electric and magnetic fields and collisionless shock structures.** p0032 A70-30069
- High frequency electrostatic waves in the magnetosphere. p0033 A70-30083
- Ac fields and wave particle interactions.** p0033 A70-30085
- OGO-5 observations of quasi-trapped electromagnetic waves in the solar wind. p0035 A70-36005
- OGO-5 observations of electrostatic turbulence in bow shock magnetic structures. p0035 A70-36006
- Magnetic and electric field changes across the shock and in the magnetosheath. p0036 A70-37483
- VII electric field observations in the magnetosphere.** p0041 A71-11500
- Direct correlations of large-amplitude waves with suprathermal protons in the upstream solar wind. p0043 A71-14550
- Fast time resolved spectral analysis of VLF banded emissions. p0047 A71-24788
- Nonthermal electrons and high-frequency waves in the upstream solar wind p0052 A71-37353
- Plasma instability at $(n \pm 1/2)f$ sub c and its relationship to some satellite observations. p0052 A71-37368
- Nonthermal electrons and high-frequency waves in the upstream solar wind. 2: Analysis and interpretation. p0053 A71-43158
- Distributions of electron plasma oscillations upstream from the earth's bow shock. p0057 A72-23019
- OGO-5 observations of LHR noise, emissions, and whistlers near the plasmopause at several earth radii during a large magnetic storm. p0058 A72-26399
- Plasma waves in the dayside polar cusp. I: Magnetospheric observations. p0059 A72-29380
- Detection of solar-wind electron plasma frequency fluctuations in an oblique nonlinear magnetohydrodynamic wave. p0061 A72-35610
- Cyclotron drift instability in the bow shock. p0063 A72-44523
- Electrostatic waves in the magnetosphere p0065 A73-13883
- Recent studies of magnetospheric electric field emissions above the electron gyrofrequency. p0067 A73-19254
- Field-aligned currents, plasma waves, and anomalous resistivity in the disturbed polar cusp. p0069 A73-29964
- Observation of a current-driven plasma instability at the outer zone-plasma sheet boundary. p0069 A73-29966
- Ion cyclotron waves observed in the polar cusp. p0071 A73-33437
- Satellite studies of magnetospheric substorms on August 15, 1968. 8: OGO-5 plasma wave observations. p0072 A73-33456
- Dependence of the polar cusp on the north-south component of the interplanetary magnetic field. p0072 A73-36273
- Plasma waves in the dayside polar cusp. 2: Magnetopause and polar magnetosheath. p0077 A74-21680
- OGO-5 observations of the physical processes occurring in the disturbed polar cusp and the cusp-magnetosheath interface p0113
- [B18269-000] p0097 N72-22383
- Complex electric field emissions observed by OGO-5 on 15 August 1968 [NASA-CR-126238] p0099 N73-10789
- Electron plasma oscillations in the near-earth solar wind: Preliminary observations and interpretations p0099 N73-10789
- Comparison of deep space and near-earth observations of plasma turbulence at solar wind discontinuities p0100 N73-10795
- Distributions of high frequency waves upstream from earth's bow shock [NASA-CR-139256] p0109 N74-74626
- OGO-5 observations of discrete whistlers and emissions during a large magnetic storm [NASA-TM-X-70213] p0109 N74-74634
- Data analysis program for the OGO E-24 plasma wave detector [NASA-CR-140523] p0110 N74-77109
- FREEMAN, R. M. Energy distribution of photoelectrons emitted from a surface on the OGO-5 satellite and measurements of satellite potential. p0076 A74-17648
- FREEMAN, R. M. OZNORMAN, K. Electron density measurements in the thermal plasma of the magnetosphere using a Langmuir probe. p0036 A70-37513
- FRIEDMAN, H. Measurements of solar X-ray emission from the OGO-4 spacecraft. p0027 A69-43611
- FRTZ, R. B. Response of ionospheric and exospheric electron contents to a partial solar eclipse. p0015 A68-38439
- Measurement of ionospheric and exospheric electron content using radio beacons on orbiting geophysical observatories: Compilation of data and final report [B18548-000] p0113
- FRTZ, T. A. Initial observations of geomagnetically trapped protons and alpha particles with OGO 4. p0027 A69-43184
- FRYER, T. B. Solar wind measurement techniques. 2: Solar plasma energy spectrometers. p0003 A65-29239
- FULKS, G. The cosmic ray electron spectrum and its modulation from 1968 through 1972. p0079 A74-30204
- G**
- GABEL, R. H. OGO-2 experiment 5010 and OGO-4 experiment 5010A [NASA-CR-140527] p0109 N74-76909
- GANGULY, S. Ionospheric effects of solar flares. 5: The flare event of January 30, 1968 and its implications [RSD-63] p0096 N71-36131
- GARRARD, T. L. A quantitative investigation of the solar modulation of cosmic-ray protons and helium nuclei [NASA-CR-130298] p0100 N73-13837
- The isotopes of H and He in solar cosmic rays p0107 N74-21466
- GARRIOTT, O. K. Protonospheric electron concentration profiles [NASA-CR-100778] p0089 N69-24521
- GEORGE, M. J. The altitude dependence of the quiettime cosmic ray ionization over the polar regions at solar minimum. p0034 A70-31902
- Observations of the cosmic ray knee with a polar orbiting ionization chamber p0034 A70-31903
- New measurements of the absolute cosmic ray ionization from sea level to 1540 kilometers altitude [NASA-CR-104068] p0090 N69-34536
- GILLAND, J. R. Primary electron detector experiment for OGO-E. [IEEE PAPER 3C-4] p0019 A69-19198
- GLASER, P. F. Inside the Orbiting Geophysical Observatory. p0001 A63-13629
- GLEGHORN, G. J. Magnetic considerations in the design and testing of the OGO and Pioneer spacecraft. p0004 A66-15919
- GLOECKLER, G. Protons and helium nuclei within interplanetary magnetic regions which co-rotate with the sun. p0005 A66-34754
- Composition and spectra of charged particles of solar and cosmic origin measured on satellites. p0008 A67-27249
- Differential energy spectra and intensity variation of 1-20 MeV/nucleon protons and helium nuclei in interplanetary space (1964-66). p0015 A68-41420
- The 'quiet time' fluxes of protons and alpha-particles in the energy range of 2-20 MeV/nucleon in 1967. p0044 A71-18127
- GOEDEKE, A. D. The 23 and 28 May 1967 solar cosmic ray events. p0013 A68-31924
- Simultaneous satellite and riometer measurements of particles during solar cosmic ray events. p0059 A72-31965
- GOLDAN, P. D. Errors in ion and electron temperature measurements due to grid plane potential. nonuniformities in retarding potential analyzers p0071 A73-33436
- GOLDSTEIN, B. E. Direct measurements of solar-wind fluctuations between 0.0048 and 13.3 Hz. p0068 A73-23539
- GOUIN, P. Correlation of satellite estimates of the equatorial electrojet intensity with ground observations at Addis Ababa [B15846-000] p0112
- GRAEDEL, T. E. Dynamic spectra of type III solar bursts from 4 to 2 MHz observed by OGO-3. p0034 A70-34835
- The association of solar optical flares with type 3 solar bursts from 4 to 2 MHz observed by OGO-3. p0045 A71-19724
- Interplanetary-particle associations with type 3 solar bursts. p0054 A71-43176
- Dynamic spectra of 4-2 MHz solar bursts: Results from Orbiting Geophysical Observatory 3 [NASA-CR-106640] p0091 N70-11147
- Initial results from radio astronomy-experiment no. 18. OGO-3 [UM/RAO-67-9] p0109 N74-74660
- Data user's notes: OGO-3 experiment no. 18 low frequency radio astronomy, appendices A and B [NASA-CR-140526] p0109 N74-76907
- GRAEDEL, T. F. OGO 3 data analysis - Dynamic spectra of solar bursts [NASA-CR-107031] p0091 N70-12221
- GRAHAM, R. A. OGO-E plasma spectrometer. p0017 A68-42739
- GREBOWSKY, J. M. Variation of the ion-temperature gradient along field lines in the outer plasmasphere. p0031 A70-26568
- Comparison of coincident OGO-3 and OGO-4 hydrogen ion composition measurements. p0037 A70-38377
- Study of the thermal plasma on closed field lines outside the plasmasphere. p0038 A70-41057
- Structured variations of the plasmopause: Evidence of a corotating plasma tail. p0053 A71-43166
- Plasma tail interpretations of pronounced detached plasma regions measured with OGO-5 [B20951-000] p0113
- Thermal plasma near the plasmopause p0095 N71-25270
- The magnetospheric plasma tail p0101 N73-17948
- Dynamics of midlatitude light ion trough and plasmatails [NASA-TM-X-70494] p0103 N74-10366
- GREEN, I. M. Detection of electric-field turbulence in the earth's bow shock. p0018 A69-14681
- The OGO-5 plasma wave detector-instrumentation and in-flight operation. p0025 A69-36683
- Observations of plasma waves in space. p0029 A70-17376
- Ac fields and wave particle interactions. p0033 A70-30085
- OGO-5 observations of quasi-trapped electromagnetic waves in the solar wind. p0035 A70-36005
- OGO-5 observations of electrostatic turbulence in bow shock magnetic structures. p0035 A70-36006
- The Pioneer 9 electric field experiment. p0046 A71-23711
- Distributions of electron plasma oscillations upstream from the earth's bow shock. p0057 A72-23019
- Plasma waves in the dayside polar cusp. I: Magnetospheric observations. p0059 A72-29380

GREENE, B. R.

Electron plasma oscillations in the near-earth solar wind: Preliminary observations and interpretations p0099 N73-10789
 Comparison of deep space and near-earth observations of plasma turbulence at solar wind discontinuities p0100 N73-10795
 Distributions of high frequency waves upstream from earth's bow shock [NASA-CR-139256] p0108 N74-74626
 Data analysis program for the OGO E-24 plasma wave detector [NASA-CR-140523] p0110 N74-77109

GREENE, B. R.

Investigation of electrical structure in the near earth region as measured by orbiting spherical electrostatic analyzers, or plasma probes [AD-700804] p0092 N70-28003

GREENSTADT, E. W.

Large-scale coherence and high velocities of the earth's bow shock on February 12, 1969. p0057 A72-23004
 Structure of the quasi-perpendicular laminar bow shock [B22612-000] p0114

GUENTHER, B.

Distribution of atomic oxygen in the upper atmosphere deduced from OGO-6 airglow observations. p0075 A73-45121
 Spatial and temporal behavior of atomic oxygen determined by OGO 6 airglow observations. p0079 A74-30670
 The altitude of the scattering layer near the mesopause over the summer poles [NASA-CR-130271] p0101 N73-16436

GUHA, J. K.

OGO-5 magnetic-field data near the earth's bow shock: A correlation with theory. p0056 A72-19145

GURNETT, D. A.

Satellite measurements of high latitude convection electric fields. [AD-750221] p0063 A72-42901
 Reducing radio-frequency-interference from spacecrafts in the frequency range from 20Hz to 200 KHz [B00969-000] p0111

GUSTAFSSON, G.

Latitude and local time dependence of precipitated low-energy electrons at high latitudes. p0074 A73-41914

GUTHART, H.

Proton gyrofrequency band emissions observed aboard OGO 2. p0013 A68-31481

H

HADDOCK, F.

Evidence for electron excitation of type 3 radio burst emission. p0066 A73-17047

HADDOCK, F. I.

University of Michigan radio astronomy experiment aboard the OGO-5 spacecraft [B14718-000] p0112

HADDOCK, F. T.

Dynamic spectra of type III solar bursts from 4 to 2 MHz observed by OGO-3. p0034 A70-34835
 The prevalence of second harmonic radiation in type 3 bursts observed at kilometric wavelengths. p0071 A73-32964
 Solar wind density model from km-wave type 3 bursts. p0071 A73-32965
 Decay time of type 3 solar bursts observed at kilometric wavelengths p0074 A73-41497

Heliographic longitude distribution of the flares associated with type 3 bursts observed at kilometric wavelengths p0076 A74-14811

Results from Orbiting Geophysical Observatory 1 [NASA-CR-103321] p0090 N69-31345

Instrumentation for radio astronomy measurements aboard the OGO-1 and OGO-3 spacecraft. Part 2: Technical [NASA-CR-139257] p0108 N74-74631

HAGGE, D. E.

The multiply charged primary cosmic radiation at solar minimum, 1965. p0005 A66-26348
 Galactic cosmic rays at solar minimum, 1965. p0006 A66-34847
 Measurement and interpretation of the isotopic composition of hydrogen and helium cosmic-ray nuclei below 75 MeV/nucleon. p0015 A68-41421
 The composition of low-energy cosmic rays in 1965. p0016 A68-41431

HANSON, W. B.

Radiative recombination of atomic oxygen ions in the nighttime F region. p0023 A69-34957
 A comparison of the oxygen ion-ion neutralization and radiative recombination mechanisms for producing the ultraviolet nightglow. p0037 A70-39344
 Plasma measurements with the retarding potential analyzer on OGO-6. p0039 A70-43840

Meteoric ions above the F2 peak. p0039 A70-43841
 Relationship between Fe (+) ions and equatorial spread F. p0054 A72-10902

Errors in retarding potential analyzers caused by nonuniformity of the grid-plane potential. p0058 A72-26411
 Satellite and ground-based observations of a red arc. p0061 A72-35989

Molecular ions in the F2 layer. p0062 A72-42016
 Source and identification of heavy ions in the equatorial F layer. p0063 A72-44516
 Comparison of Te and Ti from OGO-6 and from various incoherent scatter radars. p0067 A73-19241

OGO-6 measurements of supercooled plasma in the equatorial exosphere. p0068 A73-22066
 Large ion concentration gradients below the equatorial F peak. p0068 A73-24738

On the cause of equatorial spread F p0070 A73-29988
 Effects of interhemisphere transport on plasma temperatures at low latitudes. p0074 A73-41919

A catalog of ionospheric F region irregularity behavior based on OGO-6 retarding potential analyzer data p0075 A74-12640
 In situ measurements of the spectral characteristics of F region ionospheric irregularities. p0078 A74-27695

In situ measurements of amplitude and scale size characteristics of ionospheric irregularities: OGO-6 ion concentration irregularity studies [B20340-000] p0113

Is the red arc a good indicator of ionosphere-magnetosphere conditions [B22605-000] p0114
 OGO-F-06 ion mass spectrometer [NASA-CR-111146] p0094 N71-10588
 OGO-6 experiment F-03 [NASA-CR-132943] p0106 N74-20542

HARGREAVES, J. K.

Response of ionospheric and exospheric electron contents to a partial solar eclipse. p0015 A68-38439
 Measurement of ionospheric and exospheric electron content using radio beacons on orbiting geophysical observatories: Compilation of data and final report [B18548-000] p0113

HARPOLD, D. N.

Horizontal distribution of helium in the earth's upper atmosphere. p0046 A71-21647

HARRINGTON, T. H.

A solar and galactic cosmic ray satellite experiment. p0012 A68-27615

HARRIS, K. K.

OGO-5 ion spectrometer. p0024 A69-36679
 A study of the influence of magnetic activity on the location of the plasmopause as measured by OGO-5 p0029 A70-18530

PERSONAL AUTHOR INDEX

Observations of the plasmopause from OGO-5. p0029 A70-18546
 The reaction of the plasmopause to varying magnetic activity. p0032 A70-30074

The morphology of the bulge region of the plasmasphere. p0035 A70-36014
 Spectrometer observations in the region near the bow shock on March 12, 1968. p0040 A71-11491

OGO-5 measurements of the plasmasphere during observations of stable auroral red arcs p0047 A71-24787
 The relationship of the plasmasphere and the stable auroral red arcs in the magnetic storm of October 29 to November 7, 1968. p0053 A71-39833

The dayside of the plasmasphere. p0054 A72-10892
 The plasmopause as measured in positive ions. p0061 A72-39544
 Plasmasphere dynamics inferred from OGO-5 observations. p0065 A73-12320

The measurement of cold ion densities in the plasma trough [B22610-000] p0114
 Continued data analysis for Experiment E-18 on OGO-5 [NASA-CR-130156] p0101 N73-16432

HARTMANN, G.

The trend of ionospheric absorption during shortwave fade-outs related to the trend of enhancement of solar X-ray flux p0045 A71-20318

HAYS, P. B.

Auroral heating and the composition of the neutral atmosphere. p0069 A73-27602

Thermospheric wind effects on the distribution of helium and argon in the earth's upper atmosphere. p0071 A73-33441
 Diurnal variation of the neutral thermospheric winds determined from incoherent scatter radar data [B22601-000] p0114

HEACOCK, R. R.

The relation of the Pc 1 micropulsation source region to the plasmasphere. p0043 A71-17263

Correlations of OGO-5 plasmopause crossing with observations of type Pi micropulsations on the ground. p0056 A72-21223
 Correlation of ground-based measurements of structured Pc 1 micropulsations with OGO-V plasmopause observations. p0067 A73-20652

HEDEMAN, E. R.

The solar particle event of July 16-19, 1966 and its possible association with a flare on the invisible solar hemisphere. p0020 A69-22181

HEDGECOCK, P. C.

Large-scale coherence and high velocities of the earth's bow shock on February 12, 1969. p0057 A72-23004

HEDIN, A. E.

Horizontal distribution of helium in the earth's upper atmosphere. p0046 A71-21647

Longitudinal variations of thermospheric composition indicating magnetic control of polar heat input. p0060 A72-32964

Magnetic control of the near equatorial neutral thermosphere. p0069 A73-26997

Equatorial phenomena in neutral thermospheric composition p0070 A73-31767

Role of gas-surface interactions in the reduction of OGO-6 neutral particle mass spectrometer data. p0073 A73-38941

Empirical model of global thermospheric temperature and composition based on data from the OGO-6 quadrupole mass spectrometer. p0076 A74-18376

Global characteristics in the diurnal variations of the thermospheric temperature and composition. p0077 A74-21693

- Comparison of atomic oxygen measurements by incoherent scatter and satellite-borne mass spectrometer techniques. p0078 A74-27713
- Heating of the high-latitude thermosphere during magnetically quiet periods. p0080 A74-34027
- Global empirical model of thermospheric composition based on OGO-6 mass spectrometer measurements [B16248-000] p0112
- Magnetic control of the high latitude thermosphere p0101 N73-17946
- HEDLUND, R. C.**
Solar wind measurement techniques. 2: Solar plasma energy spectrometers. p0003 A65-29239
- HELLIWELL, R. A.**
Latitudinal cutoff of VLF signals in the ionosphere. p0021 A69-28958
- Banded chorus: A new type of VLF radiation observed in the magnetosphere by OGO-1 and OGO-3. p0023 A69-31981
- Whistler-mode emissions on the OGO-1 satellite. p0028 A70-15117
- Low-frequency noise observed in the distant magnetosphere with OGO-1. p0031 A70-27183
- Type 3 solar noise observed below 100 kHz on OGO-3. p0062 A72-42043
- Experiments C02 (OGO 2) and D02 (OGO 4) [NASA-CR-110658] p0093 N70-32928
- Experiments A17 (OGO 1) and B17 (OGO 3) [NASA-CR-110716] p0093 N70-33156
- Measurements of VLF polarization and wave normal direction on OGO-F [NASA-CR-132882] p0104 N74-12842
- HENNERSON, N. K.**
Radiation of continuous-channel electron multipliers in a laboratory operating environment. p0021 A69-29565
- HENDRICKS, S. J.**
First magnetic field results from the OGO-2 satellite. p0007 A67-23244
- A proposed model for the international geomagnetic reference field, 1965. p0012 A68-26625
- Magnetic chart of the Brazilian anomaly: A verification. p0017 A68-42083
- The geomagnetic secular variation, 1900 - 1965 [NASA-TM-X-55944] p0086 N67-37398
- HEPPNER, J. P.**
OGO-A magnetic field observations. p0010 A68-11011
- Recent measurements of the magnetic field in the outer magnetosphere and boundary regions. p0010 A68-12172
- Propagation of the sudden commencement of July 8, 1966, to the magnetotail. p0018 A69-11226
- Magnetic field observations in high beta regions of the magnetosphere p0032 A70-30076
- Variations in electric fields from polar orbiting satellites. p0033 A70-30082
- A preliminary survey of the distribution of micropulsations in the magnetosphere from OGO's-3 and 5. p0046 A71-23635
- Magnetospheric-field distortions observed by OGO 3 and 5. p0054 A72-10886
- The Harang discontinuity in auroral belt ionospheric currents. p0061 A72-39980
- Polar-cap electric field distributions related to the interplanetary magnetic field direction. p0062 A72-42432
- Electric field variations during substorms: OGO-6 measurements. p0064 A72-44854
- The world magnetic survey [NASA-RP-277] Repl. p0082 N64-27355
- [NASA-TM-X-70215] p0108 N74-74627
- HERRON, C.**
Shades of POGO [NASA-TM-X-55153] p0083 N65-18269
- Shades of OGO-B (S-49A) [NASA-TM-X-70214] p0108 N74-74630
- HESSLER, V. P.**
Correlations of OGO-5 plasmopause crossing with observations of type Pi micropulsations on the ground. p0056 A72-21223
- HEYBORNE, R. L.**
Latitudinal cutoff of VLF signals in the ionosphere. p0021 A69-28958
- Ion depletion in the high-latitude exosphere: Simultaneous OGO-2 observations of the light ion trough and the VLF cutoff. p0023 A69-34939
- Observations of whistler-mode signals in the OGO satellites from VLF ground station transmitters [NASA-CR-84869] p0085 N67-30831
- HICKS, D. B.**
Primary electron detector experiment for OGO-E. [IEEE PAPER 3C-4] p0019 A69-19198
- HICKS, G. T.**
Observations of the aurora in the far ultraviolet from OGO 4. p0030 A70-23493
- Equatorial aurora/airglow in the far ultraviolet. p0041 A71-11504
- HIETBRINK, E. H.**
POGO reference manual [IS-769] p0082 N64-13388
- HILL, R. W.**
The LRL electron and proton spectrometer on NASA's Orbiting Geophysical Observatory 5(E): Instrumentation and calibration [NASA-CR-109962] p0093 N70-28103
- HILLS, H. K.**
Investigation of energetic electron intensities in the earth's outer radiation zone with OGO 1 [NASA-CR-89652] p0087 N67-40126
- Investigation of energetic electron intensities in the earth's outer radiation zone with OGO 1 p0088 N69-12899
- HILLS, R. S.**
Electronic instrumentation for ionospheric and extreme ultraviolet radiation measurements [NASA-CR-64074] p0083 N65-29678
- Electronic instrumentation for solar radiation measurements [NASA-CR-110906] p0094 N71-10358
- HINTEREGGER, H. E.**
Collimating grating monochromators for the vacuum ultraviolet. p0005 A66-27326
- HINTON, B. B.**
A sweeping neutral and positive ion mass spectrometer for atmospheric composition at satellite altitudes. p0025 A69-36681
- Role of gas-surface interactions in the reduction of OGO-6 neutral particle mass spectrometer data. p0073 A73-38941
- Experiment data analysis report for the OGO-4 neutral and ion mass spectrometer experiment [B05000-000] p0111
- The OGO-2 neutral and ion mass spectrometer experiment [NASA-CR-107408] p0091 N70-14425
- Perturbations to observed ambient neutral densities due to presence of an Orbiting Geophysical Observatory [NASA-CR-117897] p0094 N71-23238
- HIRMAN, J. W.**
A satellite ion-electron collector: Experimental effects of grid transparency, photoemission, and secondary emission [NASA-CR-139262] p0109 N74-74638
- HIRSHBERG, J.**
The solar cycle variation of the solar wind helium abundance [B22609-000] p0114
- HOCH, R. J.**
Satellite and ground-based observations of a red arc. p0061 A72-35989
- HOFFMAN, R. A.**
Field-aligned electron bursts at high latitudes observed by OGO-4. p0017 A68-43443
- Low-energy electron precipitation at high latitudes. p0021 A69-28964
- Primary electron influx to dayside auroral oval. p0048 A71-27911
- OGO 4 satellite measurements of low energy-high latitude electron precipitation. p0049 A71-30032
- Comparison of very-low-frequency auroral hiss with precipitating low-energy electrons by the use of simultaneous data from two OGO-4 experiments. p0056 A72-19149
- Properties of low energy particle impacts in the polar domain in the dawn and dayside hours. p0061 A72-39541
- Electron precipitation patterns and substorm morphology [B16756-000] p0112
- Auroral electron drift and precipitation: Cause of the mantle aurora [NASA-TM-X-63941] p0093 N70-29987
- Auroral particle injection and drift p0095 N71-25272
- Simultaneous particle and field observations of field-aligned currents [NASA-TM-X-66224] p0102 N73-21367
- Dependence of field-aligned electron precipitation on season, altitude and pitch angle [NASA-TM-X-66260] p0102 N73-25868
- OGO-4 auroral particles experiment and calibration [NASA-TM-X-70216] p0108 N74-74628
- HOFMANN, D. J.**
Observations of the screening of solar cosmic rays by the outer magnetosphere. p0018 A69-12740
- Magnetospheric modulation effects on solar cosmic rays from simultaneous OGO 1 and 3 ion chamber data in 1968 and 1969 [NASA-CR-137075] p0105 N74-18420
- HOLLWEG, J. V.**
Lunar limb shock wave. p0031 A70-27594
- HOLT, S. S.**
High-energy X-rays from the solar flare of July 7, 1966. p0011 A68-17769
- Very high energy solar X-rays observed during the proton event of 7 July 1966. p0020 A69-23753
- HOLZER, R. E.**
Preliminary results from the OGO-1 search coil magnetometer: Boundary positions and magnetic noise spectra. p0004 A66-23148
- Magnetic noise in the magnetosheath in the frequency range 3-300 Hz. [JPL-TR-32-1199] p0009 A67-40804
- OGO-3 search coil magnetometer data correlated with the reported crossing of the magnetopause at 6.6 R_{sub E} by ATS 1. p0017 A68-41693
- OGO 3 observations of ELF noise in the magnetosphere, I. p0019 A69-18834
- OGO search coil magnetometer experiments. p0024 A69-36675
- High-frequency magnetic fluctuations associated with the earth's bow shock. p0026 A69-40501
- OGO 3 observations of ELF noise in the magnetosphere. p0030 A70-21380
- Ac magnetic fields. p0033 A70-30078
- Measurement of the wave-normal vector of proton whistlers on OGO-6. p0056 A72-19148
- Study of waves in the earth's bow shock. p0058 A72-29379
- A correlated study of ELF waves and electron precipitation on OGO-6. p0077 A74-24766
- The origin and propagation of chorus in the outer magnetosphere. p0078 A74-24767
- Simultaneous particle and field observations of field-aligned currents [NASA-TM-X-66224] p0102 N73-21367
- HONES, E. W., JR.**
High-energy X-rays from the solar flare of July 7, 1966. p0011 A68-17769
- Search for low-energy interplanetary positrons. p0015 A68-41427
- Very high energy solar X-rays observed during the proton event of 7 July 1966. p0020 A69-23753
- Interplanetary positrons near 1 MeV from other than the pion to muon to electron process. p0036 A70-38098

HORAN, D. M.

A double gamma-ray spectrometer to search for positrons in space

p0110 N74-77446

HORAN, D. M.

Measurements of solar X-ray emission from the OGO-4 spacecraft.

p0027 A69-43611

Using solar X-rays as indicators of solar-flare activity

[AD-686662] p0090 N69-32730

Coronal electron temperature associated with solar flares

[OGO-4-67-100A-06] p0108 N74-74629

Horizontal distribution of helium in the earth's upper atmosphere.

p0046 A71-21647

Two satellite-borne cosmic radiation detectors.

p0004 A66-23684

Soft X-ray and microwave observations of hot regions in solar flares.

p0060 A72-35089

Observations of POGO ion chamber experiment in the outer radiation zone.

p0017 A68-43450

Nonuniformity of solar protons over the polar caps on March 24, 1966.

p0022 A69-31967

A proposed model for the international geomagnetic reference field, 1965.

p0012 A68-26625

Spark-chamber observation of galactic gamma-radiation.

p0038 A70-40691

OGO-5 spark-chamber telescope for gamma-ray astronomy

[B18277-000] p0113

I

IFEDILI, S. O.

Latitude and altitude dependence of the cosmic ray albedo neutron flux.

p0037 A70-39326

The energy dependence of the cosmic-ray neutron leakage flux in the range 0.01-10 MeV.

p0054 A72-10877

Upper limit to the 1-20 MeV solar neutron flux.

p0074 A73-41498

Measurements of the atmospheric neutron leakage rate

p0076 A74-15356

A search for solar neutrons during solar flares

[B22608-000] p0114

Neutron measurements in space with OGO-6

p0103 N73-32639

A model ionosphere for mid-day and mid-latitude during sunspot minimum

[SMUP-4] p0109 N74-74635

Magnetic tests of the OGO and ERS satellites

p0090 N69-33977

J

JACCHIA, L. G.

Variations in thermospheric composition: A model based on mass-spectrometer and satellite-drag data

[NASA-CR-136192] p0104 N74-12459

Ionospheric effects of solar flares. 5: The flare event of January 30, 1968 and its implications

[RSD-63] p0096 N71-36131

Cosmic ray neutron monitor for OGO-F.

p0024 A69-36678

Latitude and altitude dependence of the cosmic ray albedo neutron flux.

p0037 A70-39326

The energy dependence of the cosmic-ray neutron leakage flux in the range 0.01-10 MeV.

p0054 A72-10877

Upper limit to the 1-20 MeV solar neutron flux.

p0074 A73-41498

Measurements of the atmospheric neutron leakage rate

p0076 A74-15356

JENSEN, N. C.

The LRL electron and proton spectrometer on NASA's Orbiting Geophysical Observatory 5(E): Instrumentation and calibration

[NASA-CR-109962] p0093 N70-28103

Investigation into the mechanism and rates of atmospheric mixing in the lower atmosphere

[NASA-CR-135789] p0103 N73-33321

Results of a 1970 Geminid dust particle rocket experiment and analysis of OGO III dust particle velocity measurements.

p0050 A71-33741

JOHNSON, W. C.

Observations of lower hybrid resonance phenomena on the OGO 2 spacecraft.

p0018 A69-16257

Observations of auroral hiss, LHR noise, and other phenomena in the frequency range 20 Hz-540 kHz on OGO-6.

p0051 A71-33951

Additional results from an OGO-6 experiment concerning ionospheric electric and electromagnetic fields in the range 20 Hz to 540 kHz.

p0071 A73-33438

Cosmic-ray scintillations. I: Inside the magnetosphere.

p0066 A73-15526

Auroral heating and the composition of the neutral atmosphere.

p0069 A73-27602

OGO-E cosmic radiation: Nuclear abundance experiment.

p0008 A67-25852

Interpretation of auroral hiss measured on OGO 2 and at Byrd station in terms of incoherent Cerenkov radiation.

p0011 A68-19752

VLF and LF emissions in auroral regions of the ionosphere.

p0025 A69-38495

Observations of naturally occurring VLF and man-made hf plasma waves in auroral regions of the ionosphere.

p0032 A70-29924

OGO-5 magnetic-field data near the earth's bow shock: A correlation with theory.

p0056 A72-19145

K

KAHLE, A. B.

Prediction of geomagnetic secular change confirmed.

p0107 A69-37490

Energetic protons from the solar flare of March 24, 1966.

p0010 A67-41233

Solar flare injection and propagation of lowenergy protons and electrons in the event of 7-9 July, 1966.

p0014 A68-37148

The solar particle event of July 16-19, 1966 and its possible association with a flare on the invisible solar hemisphere.

p0020 A69-22181

A comparison of energetic storm protons to halo protons.

p0025 A69-37555

Temperature and emission-measure profiles of two solar X-ray flares.

p0040 A70-45768

The impulsive X-ray burst of October 10, 1970.

p0064 A73-11389

The role of energetic electrons in the correlation of meter and decimeter type III bursts with 4 keV X-ray emission.

p0064 A73-11391

The propagation of solar protons

p0089 N69-23730

Possible low energy (E less than keV) nonthermal X-ray events

p0106 N74-21450

KAN, J. R.

RF sheath and admittance characteristics of a spherical plasma probe.

p0057 A72-23520

KANE, R. F.

Comparison of geomagnetic changes in India and the POGO data.

p0070 A73-31769

KANE, S. R.

Response of ion chambers in free space to the long-term cosmic-ray variation from 1960 to 1965.

p0003 A65-33664

Studies of primary cosmic rays with ionization chambers.

p0006 A66-34768

The spectra and intensity of electrons in the radiation belts.

p0008 A67-25807

A study of energetic solar flare X-rays.

p0009 A67-41232

Energetic solar flare X-rays observed by satellite and their correlation with solar radio and energetic particle emissions.

p0011 A68-22450

The observation of 10-50 kev solar flare X-rays by the OGO satellites and their correlation with solar radio and energetic particle emission.

p0014 A68-35480

Observations of the screening of solar cosmic rays by the outer magnetosphere.

p0018 A69-12740

Observations of energetic X-rays and solar cosmic rays associated with the 23 May 1967 solar flare event.

p0020 A69-22182

Observations of two components in energetic solar X-ray bursts.

p0026 A69-40775

"Hysteresis" effects in cosmic ray modulation and the cosmic ray gradient near solar minimum.

p0028 A70-15106

Spectral characteristics of impulsive solar-flare X-rays greater than or approximately 10 keV.

p0043 A71-15937

Modulation and heliocentric gradient of low energy cosmic rays near solar minimum, 1965.

p0044 A71-18128

Impulsive hard X-ray and ultraviolet emission during solar flares.

p0045 A71-19825

An upper limit on the hardness of the nonthermal electron spectra produced during the flash phase of solar flares.

p0055 A72-14561

The impulsive X-ray burst of October 10, 1970.

p0064 A73-11389

Evidence for a common origin of the electrons responsible for the impulsive X-ray and type 3 radio bursts.

p0067 A73-20766

Acceleration of electrons during the flash phase of solar flares.

p0079 A74-30287

Acceleration of electrons in the absence of detectable optical flares deduced from type 3 radio bursts, H-alpha activity and soft X-ray emission

[B22607-000] p0114

The construction, calibration and operation of the University of Minnesota experiments for OGO-1 and OGO-3

[CR-87] p0084 N67-13710

Application of an integrating type ionization chamber to measurements of radiation in space

[NASA-CR-90060] p0087 N68-10422

An atlas of 10-50 keV solar flare X-rays observed by the OGO satellites, 5 September 1964 to 31 December 1966

[NASA-CR-94429] p0087 N68-23026

A survey of the total radiation in space observed by the OGO satellites, 5 September 1964 - 27 May 1968

[NASA-CR-107886] p0092 N70-17448

Description of data plots from the University of Minnesota ion chamber and electron spectrometer on OGO-1 and OGO-3

[NASA-CR-107885] p0092 N70-17624

Characteristics of nonthermal electrons accelerated during the flash phase of small solar flares

p0106 N74-21445

KATAJA, E.

Correlations of OGO-5 plasmopause crossing with observations of type Pi micropulsations on the ground.

p0056 A72-21223

PERSONAL AUTHOR INDEX

LAY, G.

- AVZ, N.**
POGO triaxial search coil magnetometer [B21207-000] p0113
EOGO triaxial search coil magnetometer Final Engineering Report [NASA-CR-100619] p0108 N69-72494
- BEATING, G. M.**
Seasonal variations in the thermosphere and exosphere, 1968-1970. p0051 A71-33802
- BELLER, H. U.**
Determination of the solar Lyman-alpha flux independent of calibration by ultraviolet observations of Comet Bennett) p0076 A74-15496
- BENNETT, C. F.**
Detection of electric-field turbulence in the earth's bow shock. p0018 A69-14681
Observations of plasma waves in space. p0029 A70-17376
Fast time-resolved spectra of electrostatic turbulence in the earth's bow shock. p0031 A70-29111
Ac electric and magnetic fields and collisionless shock structures. p0032 A70-30069
High frequency electrostatic waves in the magnetosphere. p0033 A70-30083
Ac fields and wave particle interactions. p0033 A70-30085
OGO-5 observations of electrostatic turbulence in bow shock magnetic structures. p0035 A70-36006
Magnetic and electric field changes across the shock and in the magnetosheath. p0036 A70-37483
Vlf electric field observations in the magnetosphere. p0041 A71-11500
Fast time resolved spectral analysis of VLF banded emissions. p0047 A71-24788
Relativistic electron precipitation during magnetic storm main phase. p0051 A71-33948
Pitch-angle diffusion of radiation belt electrons within the plasmasphere. p0060 A72-35597
Satellite studies of magnetospheric substorms on August 15, 1968. 8: OGO-5 plasma wave observations. p0072 A73-33456
Complex electric field emissions observed by OGO-5 on 15 August 1968 [NASA-CR-126238] p0097 N72-22383
- KIKUCHI, H.**
Harmonic ion cyclotron resonances observed by the OGO-4 satellite. p0030 A70-19630
Irregular structure of thermal ion plasma near the plasmapause observed from OGO-3 and Pc 1 measurements. p0056 A72-17453
- KIMURA, I.**
Drifting whistler cut-off phenomena striations - observed by POGO satellites. p0052 A71-39746
- KING, J. W.**
ISIS-1 satellite observations of the ionosphere at high southern latitudes. p0068 A73-25753
- KISTLER, R. D.**
A sweeping neutral and positive ion mass spectrometer for atmospheric composition at satellite altitudes. p0025 A69-36681
Neutral and ion mass spectrometer experiment S5015 [NASA-CR-96663] p0110 N74-77537
- KIVELSON, M.**
Observation of a current-driven plasma instability at the outer zone-plasma sheet boundary. p0069 A73-29966
- KIVELSON, M. G.**
Inward motion of the magnetopause before a substorm. p0042 A71-14515
Motion and structure of the magnetopause. p0046 A71-21631
Outer magnetosphere near midnight at quiet and disturbed times. p0063 A72-44513
- Satellite studies of magnetospheric substorms on August 15, 1968. 5: Energetic electrons, spatial boundaries, and wave-particle interactions at OGO-5. p0072 A73-33453
Dependence of the polar cusp on the north-south component of the interplanetary magnetic field. p0072 A73-36273
Active experiments, magnetospheric modification, and a naturally occurring analogue. p0075 A74-14283
OGO-5 observations of the physical processes occurring in the disturbed polar cusp and the cusp-magnetosheath interface [B18269-000] p0113
- KIVINEN, M.**
Correlations of OGO-5 plasmapause crossing with observations of type Pi micropulsations on the ground. p0056 A72-21223
- KLEIMENOVA, N.**
The plasmasphere during a magnetic recovery period: A combined study of the OGO-4 and OGO-5 satellite data and of whistlers received at the ground. p0072 A73-33876
- KLOBUCHAR, J. A.**
Ionospheric storms at midlatitudes. p0038 A70-40479
- KOCKARTS, G.**
Distribution of hydrogen and helium in the upper atmosphere. p0064 A72-45593
- KONRADI, A.**
The 135-1650 kev solar protons after the flare of July 7, 1966, observed in the magnetotail and magnetosheath. p0020 A69-21699
- KRASSA, R. F.**
OGO-5 measurements of the Lyman alpha sky background. p0047 A71-24439
OGO-5 measurements of the Lyman-alpha sky background in 1970 and 1971. p0077 A74-22345
- KRAUSZ, A.**
Power sources. p0002 A64-11240
The electric power supply of the Orbiting Geophysical Observatory. p0003 A65-19528
- KREINS, E. R.**
Meteorological results from multi-spectral photometry in airglow bands by the OGO-4 satellite. p0028 A70-15522
- KREPLIN, R. W.**
Measurements of solar X-ray emission from the OGO-4 spacecraft. p0027 A69-43611
The solar variation of soft X-ray emission. p0039 A70-43301
Temperature and emission-measure profiles of two solar X-ray flares. p0040 A70-45768
Flare X-ray and radio wave emission. p0042 A71-14046
Electron intensity variations in the inner belt following a geomagnetic storm. p0042 A71-14212
The trend of ionospheric absorption during shortwave fade-outs related to the trend of enhancement of solar X-ray flux p0045 A71-20318
Acceleration of electrons in the absence of detectable optical flares deduced from type 3 radio bursts, H-alpha activity and soft X-ray emission [B22607-000] p0114
Using solar X-rays as indicators of solar-flare activity [AD-686662] p0090 N69-32730
- KRIMIGIS, S. M.**
Initial observations of geomagnetically trapped protons and alpha particles with OGO 4. p0027 A69-43184
- KURFESS, J. D.**
The impulsive X-ray burst of October 10, 1970. p0064 A73-11389
- LAASPERE, I.**
Results from an experiment on OGO-6 to study electric and electromagnetic fields in the range 20 Hz - 540 KHz [B17973-000] p0113
- LAASPERE, I.**
Observations of lower hybrid resonance phenomena on the OGO 2 spacecraft. p0018 A69-16257
An experiment to study electric and electromagnetic fields in the frequency range 10 Hz to 540 kHz on OGO-6. p0024 A69-36677
Comparison of certain VLF noise phenomena with the lower hybrid resonance frequency calculated from simultaneous ion composition measurements. p0029 A70-18534
Observations of auroral hiss, LHR noise, and other phenomena in the frequency range 20 Hz-540 kHz on OGO-6. p0051 A71-33951
Comparison of very-low-frequency auroral hiss with precipitating low-energy electrons by the use of simultaneous data from two OGO-4 experiments. p0056 A72-19149
Satellite observations of whistler-mode signals in the conjugate region of a 200-kilohertz station. p0059 A72-29384
Additional results from an OGO-6 experiment concerning ionospheric electric and electromagnetic fields in the range 20 Hz to 540 kHz. p0071 A73-33438
The global distribution of natural and man-made ionospheric electric fields at 200 kHz and 540 kHz as observed by OGO-6. p0080 A74-34020
An experiment to study whistlers and audio-frequency emissions with a receiving system on board the POGO S-50 satellite (OGO-C/2) in conjunction with an existing network of ground-based observing stations [NASA-CR-97605] p0088 N69-17928
- LACKNER, K.**
Deformation of a magnetic dipole field by trapped particles. p0034 A70-31905
- LAGOS, C. P.**
Coordinated satellite and incoherent scatter observations [NASA-CR-121984] p0096 N71-35437
- LAMMERS, E.**
A multisatellite study of auroral-zone phenomena. [ESRO-SR-23-PT-1] p0105 N74-16072
- LANGFEL, R. A.**
First magnetic field results from the OGO-2 satellite. p0007 A67-23244
A proposed model for the international geomagnetic reference field, 1965. p0012 A68-26625
Magnetic chart of the Brazilian anomaly: A verification. p0017 A68-42083
OGO-2 magnetic field observations during the magnetic storm of March 13-15, 1966. p0018 A69-11125
Asymmetric ring current at twilight local time. p0051 A71-33946
Geomagnetic survey by the polar Orbiting Geophysical Observatories. p0054 A72-12081
Near-earth magnetic disturbance in total field at high latitudes. 1: Summary of data from OGO-2, 4, and 6. 2: Interpretation of data from OGO-2, 4, and 6. p0080 A74-34019
A representation of the perigee motion of a satellite as a function of local time [NASA-TM-X-55703] p0085 N67-18763
Processing of the total field magnetometer data from the OGO-2 satellite [NASA-TM-X-55822] p0085 N67-30147
Variation with interplanetary sector of the total magnetic field measured at the OGO 2, 4, and 6 satellites [NASA-TM-X-70531] p0104 N74-13566
A study of high latitude magnetic disturbance p0105 N74-17058
- LANZEROTTI, L. J.**
Interplanetary-particle associations with type 3 solar bursts. p0054 A71-43176
- LAVAL, G.**
Behavior of outer radiation zone and a new model of magnetospheric substorm. p0063 A72-44850
- LAY, G.**
Extraterrestrial ultraviolet radiation and the parameter of the H1 medium near the sun. p0073 A73-39074

NOV. 10, 1975

LEDET, M. M.

- LEDET, M. M.
POGO reference manual
[IS-769] p0082 N64-13388
- LEDLAY, B. G.
Magnetic field observations in high beta regions of the magnetosphere p0032 A70-30076
- LEDLEY, B. G.
OGO-A magnetic field observations. p0010 A68-11011
Propagation of the sudden commencement of July 8, 1966, to the magnetotail. p0018 A69-11226
Magnetometers for space measurements over a wide range of field intensities. p0032 A70-30045
A preliminary survey of the distribution of micropulsations in the magnetosphere from OGO's-3 and 5. p0046 A71-23635
Magnetopause attitudes during OGO-5 crossings. p0053 A71-43161
Magnetospheric-field distortions observed by OGO 3 and 5. p0054 A72-10886
Magnetopause rotational forms [B22604-000] p0114
- LEITE, R. J.
A sweeping neutral and positive ion mass spectrometer for atmospheric composition at satellite altitudes. p0025 A69-36681
Experiment data analysis report for the OGO-4 neutral and ion mass spectrometer experiment [B05000-000] p0111
The OGO-2 neutral and ion mass spectrometer experiment [NASA-CR-107408] p0091 N70-14425
Reduction and analysis of data from OGO-4 experiment 15 [NASA-CR-117525] p0094 N71-21544
Perturbations to observed ambient neutral densities due to presence of an Orbiting Geophysical Observatory [NASA-CR-117897] p0094 N71-23238
Neutral and ion mass spectrometer experiment S5015 [NASA-CR-96663] p0110 N74-77537
- LEVINE, J. S.
Seasonal variations in the thermosphere and exosphere, 1968-1970. p0051 A71-33802
- LEZNIAK, J.
Two satellite-borne cosmic radiation detectors. p0004 A66-23684
- LEZNIAK, T. W.
Experimental verification of drift-shell splitting in the distorted magnetosphere. p0026 A69-40508
- LHEUREUX, J.
Primary cosmic-ray electron energy spectrum from 10 to 200 Mev observed in interplanetary space. p0027 A70-12902
Electrons from solar flares in the 10 to 200 MeV region. p0044 A71-18170
The quiet-time spectra of cosmic-ray electrons of energies between 10 and 200 MeV observed on OGO-5. p0055 A72-16719
The cosmic ray electron spectrum and its modulation from 1968 through 1972. p0079 A74-30204
Cosmic gamma-ray burst detected with an instrument on board the OGO-5 satellite. p0080 A74-31942
Measurements of the primary cosmic ray electron spectrum between 20 MeV and 20 GeV and its changes with time [B08373-000] p0112
- LIEBERMAN, A.
Investigation of electrical structure in the near earth region as measured by orbiting spherical electrostatic analyzers, or plasma probes [AD-700804] p0092 N70-28003
- LIN, R. P.
Solar flare injection and propagation of lowenergy protons and electrons in the event of 7-9 July, 1966. p0014 A68-37148
The solar particle event of July 16-19, 1966 and its possible association with a flare on the invisible solar hemisphere. p0020 A69-22181

- The emission and propagation of approximately 40 keV solar flare electrons. 2: The electron emission structure of large active regions. p0044 A71-17918
- Evidence for magnet excitation of type 3 radio burst emission. p0066 A73-17047
Acceleration of electrons in solar flares. p0079 A74-30908
Non-relativistic solar electrons [B22602-000] p0113
- LIND, D. L.
Plasma electron detector using an open electron multiplier. p0005 A66-23689
Electron measurements near a weak aurora. p0008 A67-33595
Electron observations in the solar wind and magnetosheath. p0075 A73-45112
- LINDNER, J. W.
Magnetic considerations in the design and testing of the OGO and Pioneer spacecraft. p0004 A66-15919
- LOCKWOOD, J. A.
Cosmic ray neutron monitor for OGO-F. p0024 A69-36678
Latitude and altitude dependence of the cosmic ray albedo neutron flux. p0037 A70-39326
The energy dependence of the cosmic-ray neutron leakage flux in the range 0.01-10 MeV. p0054 A72-10877
Neutron measurements in space. p0073 A73-36645
Upper limit to the 1-20 MeV solar neutron flux. p0074 A73-41498
Measurements of the atmospheric neutron leakage rate p0076 A74-15356
Neutron measurements of the OGO-VI Spacecraft [NASA-CR-130181] p0101 N73-19841
- LONDON, J.
Satellite observations of the vertical ozone distribution in the upper stratosphere. p0023 A69-32645
- LUCERO, A. B.
Models of the trapped radiation environment. Volume 2: Inner and outer zone electrons [NASA-SP-3024-VOL-2] p0084 N66-35685
Models of the trapped radiation environment. Volume 3: Electrons at synchronous altitudes [NASA-SP-3024-VOL-3] p0085 N67-19899
- LUDWIG, G. H.
The orbiting geophysical observations. p0001 A63-10333
Cosmic ray experiments for Explorer 12 and the Orbiting Geophysical Observatory. p0001 A63-20022
The multiply charged primary cosmic radiation at solar minimum, 1965. p0005 A66-26348
Galactic cosmic rays at solar minimum, 1965. p0006 A66-34847
OGO-E cosmic radiation: Nuclear abundance experiment. p0008 A67-25852
Earth satellite experiment for measuring the charge and energy spectra of the primary cosmic rays [B01634-000] p0111
The Orbiting Geophysical Observatory: A new tool for space research. p0082 N62-15053
Relative advantages of small and observatory type satellites [NASA-TM-X-55261] p0083 N65-29783
- LUKAS, P.
The OGO-5 plasma wave detector-instrumentation and in-flight operation. p0025 A69-36683
- LUPTON, J. E.
Electron scattering effects in typical cosmic ray telescopes. p0057 A72-21510
Measurements of electron detection efficiencies in solid state detectors. p0061 A72-39401
Solar flare particle propagation: Comparison of a new analytic solution with spacecraft measurements. p0068 A73-24727
Transport of solar flare protons: Comparison of a new analytic model with spacecraft measurements [B10763-000] p0112

PERSONAL AUTHOR INDEX

- Solar flare particle propagation: Comparison of a new analytic solution with spacecraft measurements [NASA-CR-122406] p0098 N72-29818
- LUPTON, J. M.
Geomagnetic effect on the neutral temperature of the F region during the magnetic storm of September 1969. p0060 A72-35603
Global temperature distributions from OGO-6 6300 A airglow measurements. p0077 A74-23679
- LYONS, I. R.
Pitch-angle diffusion of radiation belt electrons within the plasmasphere. p0060 A72-35597
- M**
- MACKEY, E. F.
OGO-4 ultraviolet airglow spectrometer. p0025 A69-36682
- MACRAE, B. D.
Instrumentation for radio astronomy measurements aboard the OGO-5 spacecraft [NASA-CR-98670] p0088 N69-14392
- MAHAJAN, K. K.
Neutral wind velocities calculated from temperature measurements during a magnetic storm and the observed ionospheric effects [B19920-000] p0113
- MAHONEY, M.
Visual presentation of the motion and orientation of an orbiting spacecraft /OGO/ [NASA-TN-D-2918] p0083 N65-29296
- MAIER, E. J. R.
Observations from OGO-5 of the thermal ion density and temperature within the magnetosphere. p0040 A71-11498
Subauroral red arcs and associated ionospheric phenomena. p0045 A71-19663
Discrepancies in the observed plasma-trough density [NASA-TM-X-63905] p0092 N70-27302
The ionosphere during a subauroral red arc p0097 N72-23334
- MANGE, P.
OGO-3 observations of the Lyman alpha intensity and the hydrogen concentration beyond 5 R sub E p0031 A70-27181
Geocoronal hydrogen: An analysis of the Lyman-alpha airglow observed from OGO-4. p0035 A70-35764
- MARAN, S. P.
The Gum Nebula. Further evidence from spacecraft and ground-based instruments. p0052 A71-35409
- MARBURGER, J. H.
OGO-5 magnetic-field data near the earth's bow shock: A correlation with theory. p0056 A72-19145
- MARTIN, L. B.
Testing OGO's attitude controls. p0002 A64-27303
- MARTRES, M. J.
Acceleration of electrons in the absence of detectable optical flares deduced from type 3 radio bursts, H-alpha activity and soft X-ray emission [B22607-000] p0114
- MASLEY, A. J.
A low energy solar cosmic ray experiment for OGO-F. p0012 A68-27616
The 23 and 28 May 1967 solar cosmic ray events. p0013 A68-31924
A discussion of solar cosmic ray activity near sunspot maximum. p0044 A71-18158
Simultaneous satellite and riometer measurements of particles during solar cosmic ray events. p0059 A72-31965
Simultaneous satellite and riometer studies. p0079 A74-30263
Solar cosmic ray observations [B11181-000] p0112
MDAC solar cosmic ray experiment on OGO-6 [NASA-CR-130155] p0101 N73-16795
- MASON, C. J.
A sweeping neutral and positive ion mass spectrometer for atmospheric composition at satellite altitudes. p0025 A69-36681

- Experiment data analysis report for the OGO-4 neutral and ion mass spectrometer experiment [B05000-000] p0111
- The OGO-2 neutral and ion mass spectrometer experiment [NASA-CR-107408] p0091 N70-14425
- Reduction and analysis of data from OGO-4 experiment 15 [NASA-CR-117525] p0094 N71-21544
- Neutral and ion mass spectrometer experiment S5015 [NASA-CR-96663] p0110 N74-77537
- MAYAUD, P. N.
Summary and future work (OGO-4 and OGO-6) [B15849-000] p0112
- MAYNARD, N. C.
Variations in electric fields from polar orbiting satellites. p0033 A70-30082
- Is the red arc a good indicator of ionosphere-magnetosphere conditions [B22605-000] p0114
- Electric field measurements across the Harang discontinuity [NASA-TM-X-70613] p0105 N74-19023
- MAYR, H. G.
Model of magnetospheric temperature distribution. p0015 A68-38423
- Observations of hydrogen and helium ions during a period of rising solar activity. p0022 A69-31326
- Study of the thermal plasma on closed field lines outside the plasmasphere. p0038 A70-41057
- Magnetic storm effects in the neutral composition. p0058 A72-24957
- Theoretical model for the latitude dependence of the thermospheric annual and semiannual variations. p0066 A73-15538
- Magnetic control of the near equatorial neutral thermosphere. p0069 A73-26997
- Magnetic storm characteristics of the thermosphere. p0070 A73-29975
- Empirical model of global thermospheric temperature and composition based on data from the OGO-6 quadrupole mass spectrometer. p0076 A74-18376
- Global characteristics in the diurnal variations of the thermospheric temperature and composition. p0077 A74-21693
- Global empirical model of thermospheric composition based on OGO-6 mass spectrometer measurements [B16248-000] p0112
- MCCLINTON, A. T., JR.
Using solar X-rays as indicators of solar-flare activity [AD-686662] p0090 N69-32730
- MCCLURE, J. P.
Equatorial ion temperature: A comparison of conflicting incoherent scatter and OGO-4 retarding potential analyzer values. p0052 A71-33956
- Comparison of Te and Ti from OGO-6 and from various incoherent scatter radars. p0067 A73-19241
- On the cause of equatorial spread F. p0070 A73-29988
- A catalog of ionospheric F region irregularity behavior based on OGO-6 retarding potential analyzer data p0075 A74-12640
- Geophysical properties of the ionospheric irregularities responsible for radio scintillation. [AIAA PAPER 74-53] p0077 A74-18754
- In situ measurements of the spectral characteristics of F region ionospheric irregularities. p0078 A74-27695
- In situ measurements of amplitude and scale size characteristics of ionospheric irregularities: OGO-6 ion concentration irregularity studies [B20340-000] p0113
- OGO 6 ion concentration irregularity studies [NASA-CR-132814] p0103 N73-32286
- MCCORMAC, B. M.
Magnetospheric chemical release study [AD-769979] p0105 N74-17126
- MCCOY, J. E.
Observations of POGO ion chamber experiment in the outer radiation zone. p0017 A68-43450
- High-latitude ionization spikes observed by the POGO ion chamber experiment. p0021 A69-28950
- MCCRACKEN, C. W.
Measured velocities of interplanetary dust particles. p0004 A66-15266
- MCDONALD, F. B.
Cosmic ray experiments for Explorer 12 and the Orbiting Geophysical Observatory. p0001 A63-20022
- The multiply charged primary cosmic radiation at solar minimum, 1965. p0005 A66-26348
- Galactic cosmic rays at solar minimum, 1965. p0006 A66-34847
- Measurement and interpretation of the isotopic composition of hydrogen and helium cosmic-ray nuclei below 75 MeV/nucleon. p0015 A68-41421
- The composition of low-energy cosmic rays in 1965. p0016 A68-41431
- Galactic and solar cosmic rays p0091 N69-38984
- MCDONALD, F. J.
Spectra and charge composition of the low energy galactic cosmic radiation from Z equals 2 to 14. p0037 A70-38127
- MCDONOUGH, J. W.
Solar cosmic ray observations [B11181-000] p0112
- MCFARLAND, D. E.
POGO reference manual [IS-769] p0082 N64-13388
- MCGEHEE, J. H.
Vii electric field observations in the magnetosphere. p0041 A71-11500
- MCGEHEE, J. H., JR.
Complex electric field emissions observed by OGO-5 on 15 August 1968 [NASA-CR-126238] p0097 N72-22383
- MCGRATH, J. F.
Investigation of ultraviolet solar radiation and its influence on the aerospace environment [AFCR-64-773] p0083 N65-14504
- MCILWRAITH, N.
Plasma electron detector using an open electron multiplier. p0005 A66-23689
- Electron measurements near a weak aurora. p0008 A67-33595
- MCKEOWN, D.
Probe for measuring energy transfer between a satellite and the upper atmosphere p0004 A66-15922
- Gas-surface energy transfer experiment for OGO-F. p0024 A69-36680
- Gas-surface interaction studies [B20296-000] p0113
- Bombardment of OGO-6 surfaces by high-energy particles [B20297-000] p0113
- Instrument report for design of the gas-surface energy transfer experiments for OGO-F [B20953-000] p0113
- Initial results from OGO-6 gas-surface experiment [B20954-000] p0113
- Space measurements of the contamination of surfaces by OGO-6 outgassing and their cleaning by sputtering and desorption [NASA-CR-117138] p0094 N71-20207
- Thermoelectrically-cooled quartz crystal microbalance p0103 N74-10255
- Removal of surface contamination by plasma sputtering [NASA-CR-139264] p0109 N74-74659
- MCKIBBEN, B.
Differential energy spectra and intensity variation of 1-20 MeV/nucleon protons and helium nuclei in interplanetary space (1964-66). p0015 A68-41420
- Description of OGO-1 and OGO-3 counting rate processing and resulting data. Cosmic ray spectra and fluxes experiment on OGO-1 and OGO-3 [B03716-000] p0111
- MCKIBBEN, R. B.
The 'quiet time' fluxes of protons and alpha-particles in the energy range of 2-20 MeV/nucleon in 1967. p0044 A71-18127
- MCLEOD, M. G.
Preliminary results from the OGO-1 search coil magnetometer. Boundary positions and magnetic noise spectra. p0004 A66-23148
- Magnetic noise in the magnetosheath in the frequency range 3-300 Hz. [JPL-TR-32-1199] p0009 A67-40804
- MCPHERRON, R. L.
Magnetic field variations in the near geomagnetic tail associated with weak substorm activity. p0046 A71-21643
- Satellite observations of band-limited micropulsations during a magnetospheric substorm. p0048 A71-27913
- Magnetotail changes in relation to the solar wind magnetic field and magnetospheric substorms. p0051 A71-33944
- Fluctuating magnetic fields in the magnetosphere. p0056 A72-21189
- Fluctuating magnetic fields in the magnetosphere. 2: ULF waves. p0063 A72-42902
- Outer magnetosphere near midnight at quiet and disturbed times. p0063 A72-44513
- Substorm related changes in the geomagnetic tail: The growth phase. p0064 A72-44856
- Satellite studies of magnetospheric substorms on August 15, 1968. 1: State of the magnetosphere. p0071 A73-33449
- Satellite studies of magnetospheric substorms on August 15, 1968. 2: Solar wind and outer magnetosphere. p0071 A73-33450
- Satellite studies of magnetospheric substorms on August 15, 1968. 4: OGO-5 magnetic field observations. p0072 A73-33452
- Satellite studies of magnetospheric substorms on August 15, 1968. 9: Phenomenological model for substorms. p0072 A73-33457
- The magnetotail and substorms. p0076 A74-17742
- Substorm and interplanetary magnetic field effects on the geomagnetic tail lobes [B27641-000] p0114
- MICQUARD, J. H.
An electron and proton spectrometer detector system for an OGO-F satellite experiment. p0005 A66-23690
- A low powered magnetic Hall probe for space applications [UCRL-14650-11] p0086 N67-30930
- The LRI electron and proton spectrometer on NASA's Orbiting Geophysical Observatory 5(E): Instrumentation and calibration [NASA-CR-109962] p0093 N70-28103
- MEEKINS, J. F.
Temperature and emission-measure profiles of two solar X-ray flares. p0040 A70-45768
- MEIER, R. R.
The hydrogen Lyman-alpha airglow. p0022 A69-30191
- Temporal variations of solar Lyman alpha p0028 A70-15128
- OGO-3 observations of the Lyman alpha intensity and the hydrogen concentration beyond 5 R sub E p0031 A70-27181
- Geocoronal hydrogen: An analysis of the Lyman-alpha airglow observed from OGO-4. p0035 A70-35764
- Depressions in the far-ultraviolet airglow over the poles p0041 A71-11503
- Observations of Lyman-alpha and the atomic hydrogen distribution in the thermosphere and exosphere. p0042 A71-14028
- Observations of conjugate excitation of the O I 1304-A airglow. p0043 A71-17279
- MENDE, S. B.
Magnetospheric chemical release study [AD-769979] p0105 N74-17126
- MENDELIC, M.
Ionospheric storms at midlatitudes. p0038 A70-40479
- METRAILER, J. F.
OGO-F-06 ion mass spectrometer [NASA-CR-111146] p0094 N71-10588

METZGER, P. H.

On the diurnal variation of the exospheric neutral hydrogen temperature.

p0040 A70-43852

Observation of early-type stars from OGO-6.

p0044 A71-17975

A flight calibration device for absolute measurements at the Lyman-alpha wavelength

[AD-726567] p0096 N71-36136

Spectral variations of the L alpha sky: A final report of observations from OGO-6

[AD-736816] p0097 N72-23429

MEYER, J. P.

Measurement and interpretation of the isotopic composition of hydrogen and helium cosmic-ray nuclei below 75 MeV/nucleon.

p0015 A68-41421

MEYER, P.

Primary cosmic-ray electron energy spectrum from 10 to 200 Mev observed in interplanetary space.

p0027 A70-12902

Electrons from solar flares in the 10 to 200 MeV region.

p0044 A71-18170

The quiet-time spectra of cosmic-ray electrons of energies between 10 and 200 MeV observed on OGO-5.

p0055 A72-16719

Primary cosmic ray electrons

p0071 A73-33293

The cosmic ray electron spectrum and its modulation from 1968 through 1972.

p0079 A74-30204

Measurements of the primary cosmic ray electron spectrum between 20 MeV and 20 GeV and its changes with time

[B08373-000] p0112

MICHAEL, W. K.

Program description of the data reduction program for experiment 19 of OGO-D

[NASA-TM-X-70372] p0109 N74-76910

MICHEL, F. C.

Diffusive entry of solar-flare particles into geomagnetic tail.

p0040 A71-11494

MIDGLEY, J. E.

Errors in retarding potential analyzers caused by nonuniformity of the grid-plane potential.

p0058 A72-26411

MILLER, J. N., JR.

Instrument report for design of the gas-surface energy transfer experiments for OGO-F

[B20953-000] p0113

MILLS, M. E.

Instrumentation for the Stanford University/Stanford Research Institute VLF experiment (B-17) on the OGO-3 satellite

[B01265-000] p0111

OGO-1 VLF experiment A-17 digital data processing system

[NASA-CR-88618] p0086 N67-37021

MITRA, A. P.

Ionospheric effects of solar flares. 5: The flare event of January 30, 1968 and its implications

[RSD-63] p0096 N71-36131

MIXON, W.

Description of OGO-1 and OGO-3 counting rate processing and resulting data. Cosmic ray spectra and fluxes experiment on OGO-1 and OGO-3

[B03716-000] p0111

MOFFETT, R. J.

OGO-6 measurements of supercooled plasma in the equatorial exosphere.

p0068 A73-22066

Effects of interhemisphere transport on plasma temperatures at low latitudes.

p0074 A73-41919

MOGRO-CAMPERO, A.

Identification and relative abundances of C, N, and O nuclei trapped in the geomagnetic field.

p0041 A71-13475

Enrichment of very heavy nuclei in the composition of solar accelerated particles.

p0055 A72-15366

Geomagnetically trapped carbon, nitrogen, and oxygen nuclei.

p0059 A72-32959

The abundances of solar accelerated nuclei from carbon to iron.

p0065 A73-13719

On the origin of low energy heavy nuclei below approximately 30 MeV per nucleon observed in interplanetary space during quiet times, 1968-72.

p0078 A74-30156

MOHLER, G.

POGO triaxial search coil magnetometer

[B21207-000] p0113

OGO triaxial search coil magnetometer Final Engineering Report

[NASA-CR-100619] p0108 N69-72494

MONTGOMERY, H.

Power study of spin stabilized EGO /S-49/

[NASA-TM-X-55186] p0083 N65-21656

MONTGOMERY, H. E.

OGO earth acquisition

[NASA-TM-X-55002] p0082 N64-23517

Shades of EGO, S-49

[NASA-TM-X-55014] p0082 N64-27251

Shades of POGO

[NASA-TM-X-55153] p0083 N65-18269

OGO orbital parameters and heat inputs

[NASA-TM-X-55428] p0084 N66-21006

Shades of OGO-B (S-49A)

[NASA-TM-X-70214] p0108 N74-74630

MONTGOMERY, M. D.

OGO-5 observations of the polar cusp on November 1, 1968.

p0053 A71-43162

Satellite studies of magnetospheric substorms on August 15, 1968. 2: Solar wind and outer magnetosphere.

p0071 A73-33450

MORFILL, G.

Solar proton intensity structures in the magnetosphere during interplanetary anisotropies.

p0066 A73-14962

MORGAN, M. G.

Observations of lower hybrid resonance phenomena on the OGO 2 spacecraft.

p0018 A69-16257

An experiment to study whistlers and audio-frequency emissions with a receiving system on board the POGO S-50 satellite (OGO-C/2) in conjunction with an existing network of ground-based observing stations

[NASA-CR-97605] p0088 N69-17928

MOSER, P. J.

Flare X-ray and radio wave emission.

p0042 A71-14046

MULLEN, A. J.

Correlations of OGO-5 plasmopause crossing with observations of type Pi micropulsations on the ground.

p0056 A72-21223

Correlation of ground-based measurements of structured Pc 1 micropulsations with OGO-V plasmopause observations.

p0067 A73-20652

MULLINS, J. A.

Seasonal variations in the thermosphere and exosphere, 1968-1970.

p0051 A71-33802

MURRAY, S. S.

Interplanetary deceleration of solar cosmic rays.

p0046 A71-22801

Propagation of 1-10 MeV solar flare protons in interplanetary space

p0098 N72-27829

MUZZIO, J. L. R.

Ion cutoff whistlers.

p0018 A69-14029

OGO-4 observations of extremely low frequency hiss.

p0057 A72-23008

ELF propagation in the plasmasphere based on satellite observations of discrete and continuous forms

[NASA-CR-130351] p0100 N73-16126

MYERS, M. A.

Preliminary results from the Ames Research Center plasma probe observations of the solar-wind-geomagnetic field interaction region on IMP-2 and OGO-1.

p0003 A65-25921

NAGAYAMA, N.

Synoptic survey for the neutral line in the magnetotail during the substorm expansion phase.

p0073 A73-36275

NAGY, A. F.

Satellite and ground-based observations of a red arc.

p0061 A72-35989

Comparison of Te and Ti from OGO-6 and from various incoherent scatter radars.

p0067 A73-19241

OGO-6 measurements of supercooled plasma in the equatorial exosphere.

p0068 A73-22066

Is the red arc a good indicator of ionosphere-magnetosphere conditions

[B22605-000] p0114

OGO-F-02 data analysis

[NASA-CR-130128] p0100 N73-13376

NAMBA, M.

Nonlinear theory of plasma instability at half-harmonics of the electron gyrofrequency.

p0068 A73-22069

NARASINGA RAO, B. C.

Subauroral red arcs and associated ionospheric phenomena.

p0045 A71-19663

NAUMANN, R. J.

Thermoelectrically-cooled quartz crystal microbalance

p0103 N74-10255

NEHER, H. V.

Response to environment and radiation of an ionization chamber and matched geiger tube used on spacecraft

[NASA-CR-139255] p0108 N74-74624

NESS, N. F.

Review of magnetic field observations.

p0065 A73-13871

NEUGEBAUER, M.

Initial deceleration of solar wind positive ions in the earth's bow shock.

p0030 A70-21377

OGO-5 observations of quasi-trapped electromagnetic waves in the solar wind.

p0035 A70-36005

Direct correlations of large-amplitude waves with suprathermal protons in the upstream solar wind.

p0043 A71-14550

Correlated observations of electrons and magnetic fields at the earth's bow shock.

p0051 A71-33943

Nonthermal electrons and high-frequency waves in the upstream solar wind

p0052 A71-37353

OGO-5 observations of the polar cusp on November 1, 1968

p0053 A71-43162

Dissipation mechanisms in a pair of solar-wind discontinuities.

p0058 A72-29378

Detection of solar-wind electron plasma frequency fluctuations in an oblique nonlinear magnetohydrodynamic wave.

p0061 A72-35610

Direct measurements of solar-wind fluctuations between 0.0048 and 13.3 Hz.

p0068 A73-23539

Observation of a current-driven plasma instability at the outer zone-plasma sheet boundary.

p0069 A73-29966

Dependence of the polar cusp on the north-south component of the interplanetary magnetic field.

p0072 A73-36273

Shock system of February 2, 1969

p0075 A74-12627

Observations of the internal structure of the magnetopause.

p0077 A74-21679

Plasma waves in the dayside polar cusp. 2: Magnetopause and polar magnetosheath.

p0077 A74-21680

OGO-5 observations of the physical processes occurring in the disturbed polar cusp and the cusp-magnetosheath interface

[B18269-000] p0113

Structure of the quasi-perpendicular laminar bow shock

[B22612-000] p0114

Computation of solar wind parameters from the OGO-5 plasma spectrometer data using Hermite polynomials

[NASA-CR-125063] p0096 N72-14808

NILSSON, C.

Some doubts about the earth's dust cloud.

p0006 A66-41213

NILSSON, C. S.

Measured velocities of interplanetary dust particles.

p0004 A66-15266

The flux of meteors and micrometeoroids in the neighborhood of the earth.

p0014 A68-35397

Attempts to measure micrometeoroid flux on the OGO 2 and OGO 4 satellites.

p0027 A70-10444

N

PERSONAL AUTHOR INDEX

PINTER, S.

Detection of micrometeoroid flux on satellites.
p0048 A71-28700
Micrometeoroid experiment on the OGO 4 satellite
[B04201-000] p0111
Measured velocities of interplanetary dust particles
from OGO-1 p0086 N67-32070
The micrometeoroid experiment on the OGO 2
satellite
[NASA-CR-100683] p0089 N69-23367
NISBET, J. S.
Global temperature distributions from OGO-6 6300
A airglow measurements. p0077 A74-23679
NISHIDA, A.
Synoptic survey for the neutral line in the magnetotail
during the substorm expansion phase. p0073 A73-36275
NORMAN, K.
Energy distribution of photoelectrons emitted from
a surface on the OGO-5 satellite and measurements
of satellite potential. p0076 A74-17648
NORTHROP, T. G.
Study of waves in the earth's bow shock.
p0058 A72-29379

O

OBAYASHI, T.
Ionospheric experiment using the orbiting
geophysical observatory (OGO-A) at the Ionosphere
Research Laboratory, Kyoto University. p0004 A66-10892
OGILVIE, K. W.
Electron measurements near a weak aurora.
p0008 A67-33595
Auroral electron energy spectra. p0012 A68-25969
Magnetic field and electron observations near the
dawn magnetopause. p0050 A71-31754
Electron energy flux in the solar wind. p0055 A72-13507
Electron observations in the solar wind and
magnetosheath. p0075 A73-45112
The solar cycle variation of the solar wind helium
abundance [B22609-000] p0114
OGLIVIE, K. W.
OGO 5 measurements of electrons near the
magnetopause. p0095 N71-25273
OHKI, K.
Soft X-ray and microwave observations of hot regions
in solar flares. p0060 A72-35089
OHKI, K.-I.
Directivity of solar hard X-ray bursts. p0023 A69-33055
OLSON, J. V.
OGO-3 search coil magnetometer data correlated
with the reported crossing of the magnetopause at 6.6
R sub E by ATS 1. p0017 A68-41693
High-frequency magnetic fluctuations associated with
the earth's bow shock. p0026 A69-40501
Correlated observations of electrons and magnetic
fields at the earth's bow shock. p0051 A71-33943
Study of waves in the earth's bow shock. p0058 A72-29379
ONDOH, T.
Magnetospheric sudden impulses. p0043 A71-17686
Hydromagnetic interpretation of high latitude sudden
impulse. p0052 A71-34777
ONI, E.
On the correlation of the ground data at Ibadan with
POGO satellite results. p0070 A73-31772
Summary and future work (OGO-4 and OGO-6)
[B15849-000] p0112
ONWU MECHILL, I. A.
Summary and future work (OGO-4 and OGO-6)
[B15849-000] p0112

ORMES, J. F.
Direct measurements of geomagnetic cutoffs for
cosmic-ray particles in the latitude range 45 deg to 70
deg using balloons and satellites. p0016 A68-41562
ORPHANOU DAKIS, S. C.
Satellite observations of whistler-mode signals in the
conjugate region of a 200-kilohertz station. p0059 A72-29384
ORSAK, L. E.
Instruments for the Stanford University/Stanford
Research Institute VLF Experiment (4917) on the EOGO
satellite [NASA-CR-139258] p0109 N74-74765
OSBORNE, D. G.
Electrojet measurements from satellite and ground. p0070 A73-31773
OSSAKOW, S. L.
Spectrometer observations in the region near the bow
shock on March 12, 1968. p0040 A71-11491
Proton scattering in the region near the earth's bow
shock. p0067 A73-22054
OTTEN, D. D.
Attitude control for an orbiting observatory:
OGO. p0002 A64-10864
Testing OGO's attitude controls. p0002 A64-27303
OWENS, A. J.
Cosmic-ray scintillations. I: Inside the
magnetosphere. p0066 A73-15526
OWENS, H. D.
Omnidirectional intensity contours of lowenergy
protons /0.5 to 50 keV/ in the earth's outer radiation
zone at the magnetic equator. p0030 A70-23491
OYA, H.
Turbulence of electrostatic electron cyclotron
harmonic waves observed by OGO-5. p0060 A72-35599
OYA, T.
Plasma wave-particle interaction inside the neutral
sheet (in Japanese) [B14583-000] p0112
PACQUET, J.
Methods of data reduction for the OPEP Airglow
photometer on OGO-2 [NASA-TM-X-55794] p0085 N67-27576
PADDACK, S. J.
OGO earth acquisition [NASA-TM-X-55002] p0052 N64-23517
Shades of EGO. S-49 [NASA-TM-X-55014] p0082 N64-27251
Gegenschein orbital parameters and operational
schedule [NASA-TM-X-55032] p0082 N64-27813
Orbital parameters for the OGO-E geocoronal
hydrogen experiment [NASA-TM-X-55276] p0083 N65-30651
EGO orbital parameters and heat inputs [NASA-TM-X-55428] p0084 N66-21006
PALMEIRA, R. A. R.
Solar modulation of galactic cosmic rays. p0007 A67-19913
PAPADOPOULOS, K.
Ion thermalization in the earth's bow shock. p0050 A71-31774
PAPAGIANNIS, M. D.
Ionospheric storms at midlatitudes. p0046 A70-40479
A model for the source of solar-flare X-rays. p0045 A71-20945
PARK, C. G.
Multi-experiment detection of the plasmapause from
EOGO satellites and antarctic ground stations. p0021 A69-25153
PARKER, L. W.
Theory of an electron trap on a charged spacecraft. p0022 A69-31976
Effects of secondary electron emission on electron
trap measurements in the magnetosphere and solar
wind. p0027 A70-13994
Theory of spacecraft sheath structure, potential, and
velocity effects on ion measurements by traps and mass
spectrometers. p0038 A70-41087

P

PARKER, P. J.
Last of the OGO's. p0026 A69-43132
PARKS, G. K.
Behavior of outer radiation zone and a new model
of magnetospheric substorm. p0063 A72-44850
Satellite studies of magnetospheric substorms on
August 15, 1968. 2: Solar wind and outer
magnetosphere. p0071 A73-33450
PAYMAR, E. M.
Banded whistlers observed on OGO-4
[NASA-CR-131495] p0102 N73-22079
PEARCE, A. J.
Spark-chamber observation of galactic
gamma-radiation. p0038 A70-40691
PELLAT, R.
Behavior of outer radiation zone and a new model
of magnetospheric substorm. p0063 A72-44850
PELLERIN, C. J.
Measurements of the iron-group abundance in
energetic solar particles. p0068 A73-23538
PELTZER, R. G.
OGO spacecraft electromagnetic interference in the
50-kHz to 4-MHz frequency range p0089 N69-25437
Instrumentation for radio astronomy measurements
aboard the OGO-1 and OGO-3 spacecraft. Part 2:
Technical [NASA-CR-139257] p0108 N74-74631
PETERSON, M. C.
The Orbiting Geophysical Observatory Test
Program. p0002 A63-23249
PFITZER, K.
The spectra and intensity of electrons in the radiation
belts. p0008 A67-25807
PFITZER, K. A.
Experimental observation of a large addition to the
electron inner radiation belt after a solar flare event.
p0017 A68-41697
Experimental verification of drift-shell splitting in the
distorted magnetosphere. p0026 A69-40508
Intensity correlations and substorm electron drift
effects in the outer radiation belt measured with the
OGO 3 and ATS 1 satellites. p0026 A69-43172
The construction, calibration and operation of the
University of Minnesota experiments for OGO-1 and
OGO-3 [CR-87] p0084 N67-13710
An experimental study of electron fluxes from 50 keV
to 4 MeV in the inner radiation belt [NASA-CR-100648] p0089 N69-19899
Description of data plots from the University of
Minnesota ion chamber and electron spectrometer on
OGO-1 and OGO-3 [NASA-CR-107885] p0092 N70-17624
Analysis of inner and outer zone: OGO-1 and OGO-2
electron spectrometer and ion chamber data [NASA-CR-127455] p0098 N72-28802
PHARO, M. W., III
Contraction of the plasmasphere during
geomagnetically disturbed periods. p0011 A68-19744
Thermal ions in the exosphere: Evidence of solar
and geomagnetic control. p0016 A68-41673
Evidence of contraction of the earth's thermal
plasmasphere subsequent to the solar flare events of 7
and 9 July 1966. p0020 A69-23777
PICK, M.
Acceleration of electrons in the absence of detectable
optical flares deduced from type 3 radio bursts, H-alpha
activity and soft X-ray emission [B22607-000] p0114
PICKETT, R. A.
Thermal ion structure of the plasmasphere. p0014 A68-37114
PINTER, S.
Some relations between 3 cm solar radio bursts, flares,
X-rays and geomagnetic crochets. p0023 A69-34227

PIZZELLA, G.

PIZZELLA, G.

Energy spectrums for proton (200 eV less than or equal to E less than or equal to 1 MeV) intensities in the outer radiation zone.

p0043 A71-17261

POROS, D. J.

A magnetospheric field model incorporating the OGO-3 and 5 magnetic field observations.

p0074 A73-43693

PORRECA, G.

Cosmic ray electrons and positrons of energies 2 to 9.5 MeV observed in interplanetary space.

p0036 A70-38096

POSSBERG, L.

A multisatellite study of auroral-zone phenomena. [ESRO-SR-23-PT-1]

p0105 N74-16072

POTTER, W. H.

Heliographic longitude distribution of the flares associated with type 3 bursts observed at kilometric wavelengths

p0076 A74-14811

The reduction and analysis of data from the low-frequency radio astronomy experiment aboard the OGO-4 spacecraft

[NASA-CR-110796] p0093 N70-42352

PRATT, B.

An experiment to study electric and electromagnetic fields in the frequency range 10 Hz to 540 kHz on OGO-F.

p0024 A69-36677

PRIMBSCH, J. H.

Energetic protons from the solar flare of March 24, 1966.

p0010 A67-41233

PRIOR, E. J.

Seasonal variations in the thermosphere and exosphere, 1968-1970.

p0051 A71-33802

PYLE, K. R.

Differential energy spectra and intensity variation of 1-20 MeV/nucleon protons and helium nuclei in interplanetary space (1964-66)

p0015 A68-41420

Q

QUANN, J.

Visual presentation of the motion and orientation of an orbiting spacecraft /OGO/

[NASA-TN-D-2918] p0083 N65 29296

QUANN, J. H.

Processing the data from the OGO-III GEGENSCHHEIM photometry experiment

[NASA-TM-X-55907] p0086 N67-35595

R

RAHMAN, N. K.

Thermal ions in the exosphere: Evidence of solar and geomagnetic control.

p0016 A68-41673

Variation of the ion-temperature gradient along field lines in the outer plasmasphere.

p0031 A70-26568

Comparison of coincident OGO-3 and OGO-4 hydrogen ion composition measurements.

p0037 A70-38377

RAMSDEN, D.

Spark-chamber observation of galactic gamma-radiation.

p0038 A70-40691

OGO-5 spark-chamber telescope for gamma-ray astronomy

[B18277-000] p0113

RAO, B. C. N.

Photoelectron flux in the topside ionosphere measured by retarding potential analyzers

[NASA-TM-X-61358] p0087 N68-35999

RAO, C. S. R.

Study of the temporal variations of 40 keV electrons in the magnetosphere during and after the magnetic storm on April 18, 1965

[NASA-CR-85905] p0086 N67-31362

Local time asymmetries in the increase of electron fluxes in the outer Van Allen zone during substorms

[NASA-CR-100419] p0089 N69-20849

RAZDAN, H.

The energy dependence of the cosmic-ray neutron leakage flux in the range 0.01-10 MeV.

p0054 A72-10877

RFAMES, D. V.

Measurements of the iron-group abundance in energetic solar particles.

p0068 A73-23538

REASENBERG, R. D.

OGO-5 observations of the physical processes occurring in the disturbed polar cusp and the cusp-magnetosheath interface

[B18269-000] p0113

Neutral wind velocities calculated from temperature measurements during a magnetic storm and the observed ionospheric effects

[B19920-000] p0113

REBER, C. A.

Horizontal distribution of helium in the earth's upper atmosphere.

p0046 A71-21647

Response of the neutral atmosphere to geomagnetic disturbances.

p0052 A71-39711

Neutral composition variation above 400 kilometers during a magnetic storm.

p0055 A72-13518

Longitudinal variations of thermospheric composition indicating magnetic control of polar heat input.

p0060 A72-32964

Equatorial phenomena in neutral thermospheric composition

p0070 A73-31767

Thermospheric wind effects on the distribution of helium and argon in the earth's upper atmosphere.

p0071 A73-33441

Empirical model of global thermospheric temperature and composition based on data from the OGO-6 quadrupole mass spectrometer.

p0076 A74-18376

Global characteristics in the diurnal variations of the thermospheric temperature and composition.

p0077 A74-21693

Heating of the high-latitude thermosphere during magnetically quiet periods.

p0080 A74-34027

Global empirical model of thermospheric composition based on OGO-6 mass spectrometer measurements

[B16248-000] p0112

Latitudinal dispersion of gases in the upper atmosphere

p0094 N71-25267

REED, E. I.

Meteorological results from multi-spectral photometry in airglow bands by the OGO-4 satellite.

p0028 A70-15522

Inflight radiometric calibration of OGO-IV airglow photometer.

p0029 A70-15645

Bidirectional reflectance of the moonlit earth.

p0055 A72-13428

Equatorial airglow and the ionospheric geomagnetic anomaly.

p0073 A73-38939

Observations of the conjugate SAR arcs of September 28-30, 1967.

p0080 A74-34042

Some effects of MeV electrons on the OGO 2 (POGO) airglow photometers

[NASA-TM-X-55791] p0085 N67-27578

Effects of energetic particles on photomultipliers in earth orbits up to 1500 km

[NASA-TM-X-63419] p0088 N69-18074

Airglow observations from OGO 4

p0095 N71-25268

An atlas of low latitude 6300A (01) night airglow from OGO-4 observations

[NASA-TM-X-65913] p0098 N72-26309

Functional characteristics of the OGO main body airglow photometer

[NASA-TM-X-65926] p0098 N72-27423

OGO-4 observations of the 6300 A night airglow from 40 deg N to 40 deg S: A set of 19 color maps

[NASA-TM-X-65954] p0098 N72-28353

REED, E. I.

Some results concerning the principal airglow lines as measured from the OGO-2 satellite.

p0007 A67-23278

REES, M. H.

Auroral spectrum between 1200 and 4000 angstroms.

p0058 A72-26402

Auroral heating and the composition of the neutral atmosphere.

p0069 A73-27602

PERSONAL AUTHOR INDEX

REGAN, R. D.

The detection of 'intermediate' size magnetic anomalies in Cosmos 49 and OGO-2, 4, 6 data.

p0073 A73-41374

A global magnetic anomaly map

[NASA-TM-X-70628] p0106 N74-20982

REIDEL, D.

The world magnetic survey

[NASA-RP-277] p0082 N64-27355

REYNOLDS, R.

POGO triaxial search coil magnetometer

[B21207-000] p0113

EOGO triaxial search coil magnetometer Final Engineering Report

[NASA-CR-100619] p0108 N69-72494

RIEDLER, W.

A multisatellite study of auroral-zone phenomena. [ESRO-SR-23-PT-1]

p0105 N74-16072

Molecular ions in the F2 layer.

p0062 A72-42016

ROBINSON, R. L.

The electric power supply of the Orbiting Geophysical Observatory.

p0003 A65-19528

ROBLE, R. G.

Diurnal variation of the neutral thermospheric winds determined from incoherent scatter radar data

[B22601-000] p0114

ROEDERER, J. G.

Trapped particle population changes associated with solar events.

p0036 A70-37487

ROELOF, E. C.

Solar flare injection and propagation of lowenergy protons and electrons in the event of 7-9 July, 1966.

p0014 A68-37148

Propagation of solar cosmic rays in the interplanetary magnetic field

p0090 N69-29659

ROGOWSKI, L. K.

Primary electron detector experiment for OGO-E.

[IEEE PAPER 3C-4] p0019 A69-19198

ROHRS, J. B.

Dynamic analysis of longitudinal oscillations of SM-68B stage 1 (POGO)

[B00570-000] p0111

RONALD, R. K.

High altitude limitation study advanced horizon sensor for OGO

[NASA-CR-83567] p0085 N67-22257

RORDEN, L.

Low-frequency noise observed in the distant magnetosphere with OGO-1.

p0031 A70-27183

RORDEN, I. H.

Instruments for the Stanford University/Stanford Research Institute VLF experiment (4917) on the EOGO satellite

[NASA-CR-139258] p0109 N74-74765

ROSENBERG, R. L.

Heliographic latitude dependence of the dominant polarity of the interplanetary magnetic field.

p0027 A70-13980

ROSS, R.

A satellite ion-electron collector: Experimental effects of grid transparency, photoemission, and secondary emission

[NASA-CR-139262] p0109 N74-74638

RUFINACH, C. L.

Power-law wavenumber spectrum deduced from ionospheric scintillation observations.

p0062 A72-42416

RUNGE, C. E.

POGO reference manual

[IS-768] p0082 N64-13388

RUSCH, D. W.

Global satellite measurements of nitric oxide.

p0064 A73-10878

Satellite ultraviolet measurements of nitric oxide fluorescence with a diffusive transport model.

p0074 A73-41925

RUSSSEL, C. T.

Active experiments, magnetospheric modification, and a naturally occurring analogue.

p0075 A74-14283

RUSSSEL, C. T.

Magnetic noise in the magnetosheath in the frequency range 300 Hz.

[JPL-TR-32-1199] p0009 A67-40804

Some remarks on the position and shape of the neutral sheet.

p0010 A68-13469

PERSONAL AUTHOR INDEX

SCARF, F. L.

OGO-3 search coil magnetometer data correlated with the reported crossing of the magnetopause at 6.6 R sub E by ATS 1.

p0017 A68-41693

OGO 3 observations of ELF noise in the magnetosphere. 1.

p0019 A69-18834

OGO 3 observations of ELF noise in the magnetosphere.

p0030 A70-21380

Ac magnetic fields.

p0033 A70-30078

OGO-5 observations of electrostatic turbulence in bow shock magnetic structures.

p0035 A70-36006

Magnetic and electric field changes across the shock and in the magnetosheath.

p0036 A70-37483

The Alfvén velocity in the magnetosphere and its relationship to ELF emissions.

p0039 A70-43851

Inward motion of the magnetopause before a substorm.

p0042 A71-14515

Direct correlations of large-amplitude waves with suprathermal protons in the upstream solar wind.

p0043 A71-14550

OGO 5 observations of upstream waves in the interplanetary medium: Discrete wave packets.

p0045 A71-19656

Motion and structure of the magnetopause.

p0046 A71-21631

Magnetic field variations in the near geomagnetic tail associated with weak substorm activity.

p0046 A71-21643

Correlated observations of electrons and magnetic fields at the earth's bow shock.

p0051 A71-33943

OGO-5 observations of the polar cusp on November 1, 1968.

p0053 A71-43162

Fluctuating magnetic fields in the magnetosphere.

p0056 A72-21189

Large-scale coherence and high velocities of the earth's bow shock on February 12, 1969.

p0057 A72-23004

Study of waves in the earth's bow shock.

p0058 A72-29379

Plasma waves in the dayside polar cusp. 1: Magnetospheric observations.

p0059 A72-29380

Detection of solar wind electron plasma frequency fluctuations in an oblique nonlinear magneto-hydrodynamic wave.

p0061 A72-35610

Fluctuating magnetic fields in the magnetosphere. 2: ULF waves.

p0063 A72-42902

Outer magnetosphere near midnight at quiet and disturbed times.

p0063 A72-44513

Noise in the geomagnetic tail.

p0064 A72-44857

Magnetic and electric waves in space.

p0065 A73-13855

Field-aligned currents, plasma waves, and anomalous resistivity in the polar cusp.

p0069 A73-29964

Observation of a current-driven plasma instability at the outer zone-plasma sheet boundary.

p0069 A73-29966

Ion cyclotron waves observed in the polar cusp.

p0071 A73-33437

Satellite studies of magnetospheric substorms on August 15, 1968. 4: OGO-5 magnetic field observations.

p0072 A73-33452

Satellite studies of magnetospheric substorms on August 15, 1968. 9: Phenomenological model for substorms.

p0072 A73-33457

Dependence of the polar cusp on the north-south component of the interplanetary magnetic field.

p0072 A73-36273

The magnetotail and substorms.

p0076 A74-17742

Observations of the internal structure of the magnetopause.

p0077 A74-21679

Plasma waves in the dayside polar cusp. 2: Magnetopause and polar magnetosheath.

p0077 A74-21680

Production processing of the data obtained by the UCLA OGO-5 fluxgate magnetometer [B12880-000]

p0112

OGO-5 observations of the physical processes occurring in the disturbed polar cusp and the cusp-magnetosheath interface

[B18269-000] p0113

Substorm and interplanetary magnetic field effects on the geomagnetic tail lobes

[B22611-000] p0114

Structure of the quasi-perpendicular laminar bow shock

[B22612-000] p0114

Comments on the measurement of power spectra of the interplanetary magnetic field

Power spectra of the interplanetary magnetic field near the earth

[NASA-CR-139260] p0099 N73-10791

A summary of the results from the UCLA OGO-5 fluxgate magnetometer

[NASA-CR-130205] p0101 N73-20498

Comments on a paper by J. P. Heppner, Polar cap electric field distributions related to interplanetary magnetic field direction

[NASA-CR-139259] p0108 N74-74632

OGO-5 orbital plots generated by the UCLA fluxgate magnetometer group

[NASA-CR-139260] p0108 N74-74633

A review of satellite observations of V.L.F. phenomena in the magnetosphere.

[NASA-CR-107654] p0010 A68-14098

OGO-5 observations of the physical processes occurring in the disturbed polar cusp and the cusp-magnetosheath interface

[B18269-000] p0113

Neutral wind velocities calculated from temperature measurements during a magnetic storm and the observed ionospheric effects

[B19920-000] p0113

S

SAGALYN, R. C.

Magnetosphere plasma properties during a period of rising solar activity, OGO-3.

p0012 A68-29421

Thermal positive ions in the outer ionosphere and magnetosphere from OGO 1.

[AD-742186] p0057 A72-23011

SAITO, T.

Dynamical characteristics of pulsating substorm, PS6

[B14580-000] p0112

SALAH, J. E.

Diurnal variation of the neutral thermospheric winds determined from incoherent scatter radar data

[B22601-000] p0114

SAMIR, U.

Electron depletion in the wake of ionospheric spacecraft: A comparison between results from Langmuir probes and antennas.

p0072 A73-34783

SANATANI, S.

Plasma measurements with the retarding potential analyzer on OGO-6.

p0039 A70-43840

Meteoric ions above the F2 peak.

p0039 A70-43841

Relationship between Fe (+) ions and equatorial spread F.

p0054 A72-10902

Large ion concentration gradients below the equatorial F peak.

p0068 A73-24738

Effects of interhemisphere transport on plasma temperatures at low latitudes.

p0074 A73-41919

OGO-6 experiment F-03

[NASA-CR-132943] p0106 N74-20542

SASSA, D.

POGO triaxial search coil magnetometer

[B21207-000] p0113

OGO triaxial search coil magnetometer Final Engineering Report

[NASA-CR-100619] p0108 N69-72494

SATTERBLOM, P. R.

A low energy solar cosmic ray experiment for OGO-F.

p0012 A68-27616

A discussion of solar cosmic ray activity near sunspot maximum.

p0044 A71-18158

Simultaneous satellite and riometer measurements of particles during solar cosmic ray events.

p0059 A72-31965

Simultaneous satellite and riometer studies.

p0079 A74-30263

SATTERBLOM, P. R.

Solar cosmic ray observations

[B11181-000] p0112

SAWYER, D.

Two satellite-borne cosmic radiation detectors.

p0004 A66-23684

SAWYER, D. M.

Direct measurements of geomagnetic cutoffs for cosmic-ray particles in the latitude range 45 deg to 70 deg using balloons and satellites.

p0016 A68-41562

SAXENA, O. P.

Neutral wind velocities calculated from temperature measurements during a magnetic storm and the observed ionospheric effects

[B19920-000] p0113

SCARABUCCI, R. R.

Satellite observations of equatorial phenomena and defocusing of VLF electromagnetic waves.

p0029 A70-18532

Interpretation of VLF signals observed on the OGO-4 satellite

[NASA-CR-107654] p0092 N70-15768

SCARD, F. L.

Detection of electric-field turbulence in the earth's bow shock.

p0018 A69-14681

SCARF, F. L.

The fine structure of the earth's collisionless shock wave.

[AIAA PAPER 69-676] p0023 A69-33452

The OGO-5 plasma wave detector-instrumentation and in-flight operation.

p0025 A69-36683

Observations of plasma waves in space.

p0029 A70-17376

Fast time-resolved spectra of electrostatic turbulence in the earth's bow shock.

p0031 A70-29111

Ac electric and magnetic fields and collisionless shock structures.

p0032 A70-30069

High frequency electrostatic waves in the magnetosphere.

p0033 A70-30083

Ac fields and wave particle interactions.

p0033 A70-30085

OGO-5 observations of quasi-trapped electromagnetic waves in the solar wind.

p0035 A70-36005

OGO-5 observations of electrostatic turbulence in bow shock magnetic structures.

p0035 A70-36006

Magnetic and electric field changes across the shock and in the magnetosheath.

p0036 A70-37483

Vlf electric field observations in the magnetosphere.

p0041 A71-11500

Microscopic structure of the solar wind

p0042 A71-14068

Direct correlations of large-amplitude waves with suprathermal protons in the upstream solar wind.

p0043 A71-14550

The Pioneer 9 electric field experiment.

p0046 A71-23711

Fast time resolved spectral analysis of VLF banded emissions.

p0047 A71-24788

Interplanetary waves and their effects on the magnetosphere.

p0050 A71-30956

Nonthermal electrons and high-frequency waves in the upstream solar wind. 2: Analysis and interpretation.

p0052 A71-37353

Nonthermal electrons and high-frequency waves in the upstream solar wind. 2: Analysis and interpretation.

p0053 A71-43158

OGO-5 observations of the polar cusp on November 1, 1968.

p0053 A71-43162

Distributions of electron plasma oscillations upstream from the earth's bow shock.

p0057 A72-23019

OGO-5 observations of LHR noise, emissions, and whistlers near the plasmapause at several earth radii during a large magnetic storm.

p0058 A72-26399

NOV. 10, 1975

- Plasma waves in the dayside polar cusp. I: Magnetospheric observations. p0059 A72-29380
 Detection of solar-wind electron plasma frequency fluctuations in an oblique nonlinear magnetohydrodynamic wave. p0061 A72-35610
 Electrostatic waves in the magnetosphere p0065 A73-13883
 Recent studies of magnetospheric electric field emissions above the electron gyrofrequency. p0067 A73-19254
 An association of magnetospheric whistler dispersion characteristics with changes in local plasma density. p0069 A73-26985
 Field-aligned currents, plasma waves, and anomalous resistivity in the disturbed polar cusp. p0069 A73-29964
 Observation of a current-driven plasma instability at the outer zone-plasma sheet boundary. p0069 A73-29966
 Satellite studies of magnetospheric substorms on August 15, 1968. 8: OGO-5 plasma wave observations. p0072 A73-33456
 Dependence of the polar cusp on the north-south component of the interplanetary magnetic field. p0072 A73-36273
 Plasma waves in the dayside polar cusp. 2: Magnetopause and polar magnetosheath. p0077 A74-21680
 A new model for the high-frequency decametric radiation from Jupiter p0081 A74-43688
 OGO-5 observations of the physical processes occurring in the disturbed polar cusp and the cusp-magnetosheath interface [B18269-000] p0113
 Complex electric field emissions observed by OGO-5 on 15 August 1968 [NASA-CR-126239] p0097 N72-22383
 Electron plasma oscillations in the near-earth solar wind: Preliminary observations and interpretations p0099 N73-10789
 Comparison of deep space and near-earth observations of plasma turbulence at solar wind discontinuities p0100 N73-10795
 Distributions of high frequency waves upstream from earth's bow shock [NASA-CR-139256] p0109 N74-74626
 OGO-5 observations of discrete whistlers and emissions during a large magnetic storm [NASA-TM-X-70213] p0109 N74-74634
 Data analysis program for the OGO E-24 plasma wave detector [NASA-CR-140523] p0110 N74-77109
- SCARF, F. T.
 Structure of the quasi-perpendicular laminar bow shock [B22612-000] p0114
- SCHAFFNER, S.
 OGO-4 spectrometer measurements of the tropical ultraviolet airglow p0037 A70-39338
- SCHEEPMACKER, A.
 Time variations in the cosmic ray electron spectrum above 500 MeV. p0037 A70-38105
 The cosmic ray electron spectrum between 0.5 and 10 GeV observed on board OGO-5. p0037 A70-38106
 Search for galactic gamma-rays with energies greater than 500 MeV on board OGO-5. p0038 A70-40690
- SCHILD, M. A.
 Electron observations between the inner edge of the plasma sheet and the plasmasphere. p0039 A70-43834
- SCHIFFMACHER, E. R.
 Response of ionospheric and exospheric electron contents to a partial solar eclipse. p0015 A68-38439
- SCHLOSSER, N. D.
 OGO-1 VLF experiment A-17 digital data processing system [NASA-CR-88618] p0086 N67-37021
- SCHMIDT, P. J.
 Measurements of the primary cosmic ray electron spectrum between 20 MeV and 20 GeV and its changes with time [B08373-000] p0112
- SCHMITT, G. A.
 Role of gas-surface interactions in the reduction of OGO-6 neutral particle mass spectrometer data. p0073 A73-38941
- SCHNEIDER, L. C.
 Using solar X-rays as indicators of solar-flare activity [AD-686662] p0090 N69-32730
- SCHOFIELD, N.
 On the origin of low energy heavy nuclei below approximately 30 MeV per nucleon observed in interplanetary space during quiet times, 1968-72. p0078 A74-30156
- SCHOLER, M.
 Solar proton intensity structures in the magnetosphere during interplanetary anisotropies. p0066 A73-14962
- SCHWENK, H.
 The trend of ionospheric absorption during shortwave fade-outs related to the trend of enhancement of solar X-ray flux p0045 A71-20318
- SCUDDER, J. D.
 Magnetic field and electron observations near the dawn magnetopause. p0050 A71-31754
 Electron energy flux in the solar wind. p0055 A72-13507
 Electron observations in the solar wind and magnetosheath. p0075 A73-45112
- SCULL, W. E.
 The orbiting geophysical observatories. p0001 A63-10333
 The mission of the Orbiting Geophysical Observatories. p0001 A63-21527
 The Orbiting Geophysical Observatories. p0002 A65-14349
 The Orbiting Geophysical Observatories. p0024 A69-36674
 Evolution in design of the orbiting geophysical observatories. p0034 A70-35303
- SECRETAN, L.
 Measured velocities of interplanetary dust particles. p0004 A66-15266
- SEMPREBON, L. C.
 Observations of auroral hiss, LHR noise, and other phenomena in the frequency range 20 Hz-540 kHz on OGO-6. p0051 A71-34951
 The global distribution of natural and man-made ionospheric electric fields at 200 kHz and 540 kHz as observed by OGO-6. p0080 A74-34020
- SENGUPTA, P. R.
 Solar X-ray control of the E layer of the ionosphere [NASA-CR-73884] p0088 N69-17412
- SERBU, G. P.
 Observations from OGO-5 of the thermal ion density and temperature within the magnetosphere. p0040 A71-11498
 OGO-5 observations of LHR noise, emissions, and whistlers near the plasmopause at several earth radii during a large magnetic storm. p0058 A72-26399
 Discrepancies in the observed plasma-trough density [NASA-TM-X-63905] p0092 N70-27302
 OGO-5 observations of discrete whistlers and emissions during a large magnetic storm [NASA-TM-X-70213] p0109 N74-74634
- SERLEMITSOS, P.
 A double gamma-ray spectrometer to search for positrons in space p0110 N74-77446
- SHAEFFER, D. I.
 A model ionosphere for mid-day and mid-latitude during sunspot minimum [SMUP-4] p0109 N74-74635
- SHAEFFER, F. B.
 Shades of EGO. S-49 [NASA-TM-X-55014] p0082 N64-27251
 Power study of spin stabilized EGO /S-49/ [NASA-TM-X-55186] p0083 N65-21656
- SHALIMOV, V. P.
 Possible injection of charged particles into a radiation zone during the main phase of a magnetic storm. p0025 A69-37967
- SHARP, G. W.
 OGO-5 ion spectrometer. p0024 A69-36679
- A study of the influence of magnetic activity on the location of the plasmopause as measured by OGO-5 p0029 A70-18530
 Observations of the plasmopause from OGO-5. p0029 A70-18546
 The reaction of the plasmopause to varying magnetic activity. p0032 A70-30074
 The morphology of the bulge region of the plasmasphere. p0035 A70-36014
 Spectrometer observations in the region near the bow shock on March 12, 1968. p0040 A71-11491
 OGO-5 measurements of the plasmasphere during observations of stable auroral red arcs p0047 A71-24787
 The relationship of the plasmasphere and the stable auroral red arcs in the magnetic storm of October 29 to November 7, 1968. p0053 A71-39833
 The dayside of the plasmasphere. p0054 A72-10892
 Neutral density measurements near 400 kilometers by a microphone density gage on OGO-6 during July 12-15, 1969. p0058 A72-26407
 The plasmopause as measured in positive ions. p0061 A72-39544
 Plasmasphere dynamics inferred from OGO-5 observations. p0065 A73-12320
 Proton scattering in the region near the earth's bow shock. p0067 A73-22054
- SHARP, W. E.
 Auroral spectrum between 1200 and 4000 angstroms. p0058 A72-26402
- SHEFFER, E. K.
 Night glow of the atmosphere in the wavelength 1304 A oxygen line at low geomagnetic latitudes p0096 N71-34333
- SHELLEY, E. G.
 A multi-satellite study of the nature of wavelike structures in the magnetosphere plasma [B22600-000] p0114
- SHOPE, W. L.
 A cinematographic display of observations of low energy proton and electron spectra in the terrestrial magnetosphere [NASA-CR-91871] p0087 N68-15232
- SILVA, R. W.
 Preliminary results from the Ames Research Center plasma probe observations of the solar-wind-geomagnetic field interaction region on IMP-2 and OGO-1. p0003 A65-25921
- SILVIS, W. M.
 OGO-F-02 data analysis [NASA-CR-130128] p0100 N73-13376
- SIMMONS, W. F.
 Results of studies of thermal gradient effects on ceramic transducer sensors used in cosmic dust experiments. p0013 A68-29467
- SIMNETT, G. M.
 Relativistic electrons in space [B13262-000] p0112
 Relativistic electron events in interplanetary space [B17665-000] p0113
- SIMPSON, J. A.
 Protons and helium nuclei within interplanetary magnetic regions which co-rotate with the sun. p0005 A66-34754
 Abundances and energy spectra for nuclei of galactic origin above 20 MeV per nucleon. p0006 A66-34833
 Abundances and energy spectra of galactic cosmic-ray nuclei above 20 MeV per nucleon in the nuclear charge range 2 less than or equal to Z less than or equal to 26. p0006 A67-11687
 Composition and spectra of charged particles of solar and cosmic origin measured on satellites. p0008 A67-27249
 Differential energy spectra and intensity variation of 1-20 MeV/nucleon protons and helium nuclei in interplanetary space (1964-66). p0015 A68-41420
 Energy spectra and abundances of the cosmic-ray nuclei helium to iron from the OGO-1 satellite experiment. p0019 A69-20067

- Identification and relative abundances of C, N, and O nuclei trapped in the geomagnetic field.
p0041 A71-13475
- The 'quiet time' fluxes of protons and alpha-particles in the energy range of 2-20 MeV/nucleon in 1967.
p0044 A71-18127
- Enrichment of very heavy nuclei in the composition of solar accelerated particles.
p0055 A72-15366
- The abundances of solar accelerated nuclei from carbon to iron.
p0065 A73-13719
- On the origin of low energy heavy nuclei below approximately 30 MeV per nucleon observed in interplanetary space during quiet times, 1968-72.
p0078 A74-30156
- Data processing and analysis from the University of Chicago charged particle experiment on the OGO-5 spacecraft
[NASA-CR-132761] p0102 N73-25870
- SINGLEY, G. W.
A model environment for outer zone electrons
[NASA-TM-X-69989] p0106 N74-20503
The reduction and analysis of electron data for outer zone electron model AE-4. Volume 3: OGO-1 and 3 University of Minnesota experiment data
[NASA-TM-X-70212] p0109 N74-74636
- SISCOE, G. L.
Resonant compressional waves in the geomagnetic tail.
p0028 A70-15127
- SKILLMAN, T. L.
OGO-A magnetic field observations.
p0010 A68-11011
Propagation of the sudden commencement of July 8, 1966, to the magnetotail.
p0018 A69-11226
Magnetic field observations in high beta regions of the magnetosphere
p0032 A70-30076
Magnetopause crossing of the geostationary satellite ATS 5 at 6.6 RE.
p0043 A71-17258
A preliminary survey of the distribution of micropulsations in the magnetosphere from OGO's-3 and 5.
p0046 A71-23635
Magnetospheric-field distortions observed by OGO 3 and 5.
p0054 A72-10886
- SKOVLI, G.
A multisatellite study of auroral zone phenomena
[ESRO-SR-23-PT-1] p0105 N74-16072
- SLATER, A. J.
ISIS-1 satellite observations of the ionosphere at high southern latitudes.
p0068 A73-25753
- SMIDDY, M.
Magnetosphere plasma properties during a period of rising solar activity, OGO-3.
p0012 A68-29421
- SMITH, C. R.
Instrumentation for atmospheric composition measurements.
p0001 A63-12209
Positive ion composition in the magnetosphere obtained from the OGO-A satellite.
p0004 A66-14781
- SMITH, E. J.
Preliminary results from the OGO-1 search coil magnetometer: Boundary positions and magnetic noise spectra.
p0004 A66-23148
Magnetic noise in the magnetosheath in the frequency range 3-300 Hz.
[JPL-TR-32-1199] p0009 A67-40804
OGO-3 search coil magnetometer data correlated with the reported crossing of the magnetopause at 6.6 R sub E by ATS 1.
p0017 A68-41693
OGO 3 observations of ELF noise in the magnetosphere. I.
p0019 A69-18834
OGO search coil magnetometer experiments.
p0024 A69-36675
High-frequency magnetic fluctuations associated with the earth's bow shock.
p0026 A69-40501
OGO 3 observations of ELF noise in the magnetosphere.
p0030 A70-21380
Measurement of the wave-normal vector of proton whistlers on OGO-6.
p0056 A72-19148
- OGO-5 observations of LHR noise, emissions, and whistlers near the plasmapause at several earth radii during a large magnetic storm.
p0058 A72-26399
Postmidnight chorus: A substorm phenomenon.
p0076 A74-18364
Observations of the internal structure of the magnetopause.
p0077 A74-21679
Plasmaspheric hiss intensity variations during magnetic storms.
p0080 A74-34038
Intensity variation of elf hiss and chorus during isolated substorms
[B22603-000] p0114
Electromagnetic hiss and relativistic electrop losses in the inner zone
[B22613-000] p0114
OGO-5 observations of discrete whistlers and emissions during a large magnetic storm
[NASA-TM-X-70213] p0109 N74-74634
- SMITH, J. C.
Four years of dust particle measurements in cislunar and selenocentric space from Lunar Explorer 35 and OGO 3
[B15918-000] p0112
- SMITH, R. L.
Magnetospheric properties deduced from OGO-1 observations of ducted and nonducted whistlers.
p0010 A68-17728
Latitudinal cutoff of VLF signals in the ionosphere.
p0021 A69-28958
Polarization of proton whistlers.
p0042 A71-14538
Whistler propagation in magnetospheric ducts
p0087 N68-17981
- SNAPP, W. J.
Investigation of electrical structure in the near earth region as measured by orbiting spherical electrostatic analyzers, or plasma probes
[AD-700804] p0092 N70-28003
- SNARE, R. C.
A magnetic field instrument for the OGO-E spacecraft.
p0007 A67-15724
Digital offset field generator for spacecraft magnetometers
p0090 N69-33963
- SOERAAS, F.
A multisatellite study of auroral-zone phenomena.
[ESRO-SR-23-PT-1] p0105 N74-16072
- SÖNNERUP, B. U. Ö.
Magnetopause rotational forms
[B22604-000] p0114
- SORU-ESCAUT, I.
Acceleration of electrons in the absence of detectable optical flares deduced from type 3 radio bursts, H-alpha activity and soft X-ray emission
[B22607-000] p0114
- SOUTHWORTH, R. B.
The flux of meteors and micrometeoroids in the neighborhood of the earth.
p0014 A68-35397
- SPANGLER, E. R.
Inside the Orbiting Geophysical Observatory.
p0001 A63-13629
- SPELLMAN, G. N.
Digital offset field generator for spacecraft magnetometers
p0090 N69-33963
- SPENCER, J.
Reduction and analysis of data from OGO-4 experiment 15
[NASA-CR-117525] p0094 N71-21544
- SPENCER, N. W.
Empirical model of global thermospheric temperature and composition based on data from the OGO-6 quadrupole mass spectrometer.
p0076 A74-18376
Global empirical model of thermospheric composition based on OGO-6 mass spectrometer measurements
[B16248-000] p0112
- STASSINPOULOS, E. G.
A model of the Starfish flux in the inner radiation zone
[NASA-TM-X-66211] p0102 N73-20842
- STAUNING, P.
A multisatellite study of auroral-zone phenomena.
[ESRO-SR-23-PT-1] p0105 N74-16072
- STECHE, T. P.
The Gum Nebula: Further evidence from spacecraft and ground-based instruments.
p0052 A71-35409
- STEHLE, R. H.
Instrumentation for the Stanford University/Stanford Research Institute VLF experiment (B-17) on the OGO-3 satellite
[B01265-000] p0111
Instruments for the Stanford University/Stanford Research Institute VLF experiment (4917) on the EOGO satellite
[NASA-CR-139258] p0109 N74-74765
- STERLING, D. L.
Source and identification of heavy ions in the equatorial F layer.
p0063 A72-44516
On the cause of equatorial spread F.
p0070 A73-29988
- STEWART, J. K.
Real time quick-look analysis for the OGO satellites.
[ATAA PAPER 64-218] p0002 A64-24447
- STILWELL, D. E.
OGO-E cosmic radiation: Nuclear abundance experiment.
p0008 A67-25852
- STONE, E. C.
A solar and galactic cosmic ray satellite experiment.
p0012 A68-27615
Access of solar protons into the polar cap: A persistent north-south asymmetry.
p0027 A69-43183
Interplanetary deceleration of solar cosmic rays.
p0046 A71-22801
Electron scattering effects in typical cosmic ray telescopes.
p0057 A72-21510
High-energy electron spikes at high latitudes.
p0060 A72-35591
Geomagnetic cutoffs for cosmic-ray protons for seven energy intervals between 1.2 and 39 MeV
p0061 A72-38728
Measurements of electron detection efficiencies in solid state detectors.
p0061 A72-39401
Electron polar cap and the boundary of open geomagnetic field lines.
p0063 A72-44522
Solar flare particle propagation: Comparison of a new analytic solution with spacecraft measurements.
p0068 A73-24727
The elemental abundance ratios of interstellar secondary and primary cosmic rays.
p0079 A74-30190
Transport of solar flare protons: Comparison of a new analytic model with spacecraft measurements
[B10763-000] p0112
The isotopes of H and He in solar cosmic rays
p0107 N74-21466
- STRAUSS, F. M.
A model for the source of solar-flare X-rays.
p0046 A71-20945
- SUCKSDORFF, C.
Correlations of OGO-5 plasmapause crossing with observations of type Pi micropulsations on the ground.
p0056 A72-21223
- SUGIURA, M.
OGO-A magnetic field observations.
p0010 A68-11011
Propagation of the sudden commencement of July 8, 1966, to the magnetotail.
p0018 A69-11226
Magnetic field observations in high beta regions of the magnetosphere
p0032 A70-30076
Magnetopause crossing of the geostationary satellite ATS 5 at 6.6 RE.
p0043 A71-17258
A preliminary survey of the distribution of micropulsations in the magnetosphere from OGO's-3 and 5.
p0046 A71-23635
Magnetic field and electron observations near the dawn magnetopause.
p0050 A71-31754
Magnetospheric-field distortions observed by OGO 3 and 5.
p0054 A72-10886
Results of magnetic surveys of the magnetosphere and adjacent regions.
p0055 A72-12084
Electron energy flux in the solar wind.
p0055 A72-13507
Equatorial current sheet in the magnetosphere.
p0064 A73-11732

- Quiet time magnetospheric field depression at 2.3-3.6 earth radii. p0072 A73-33464
- A magnetospheric field model incorporating the OGO-3 and 5 magnetic field observations. p0074 A73-43693
- Near view of the ring current [B19906-000] p0113
- The inflation of the inner magnetosphere p0095 N71-25271
- Plasma parameter beta in the midnight magnetosphere: From the near-earth plasma sheet to the plasmapause [NASA-TM-X-65640] p0095 N71-32436
- Analogy between magnetospheric resonance and the vibration of a stringed musical instrument [NASA-TM-X-65644] p0096 N71-32519
- SULLIVAN, J. D.**
- Investigation of ultraviolet solar radiation and its influence on the aerospace environment [AFCRL-64-773] p0083 N65-14504
- SWANENBURGH, B. N.**
- Primary electron detector experiment for OGO-E. [IEEE PAPER 3C-4] p0019 A69-19198
- OGO-5 measurements of electrons above 500 MeV. p0036 A70-37522
- Time variations in the cosmic ray electron spectrum above 500 MeV. p0037 A70-38105
- The cosmic ray electron spectrum between 0.5 and 10 GeV observed on board OGO-5. p0037 A70-38106
- Search for galactic gamma-rays with energies greater than 500 MeV on board OGO-5. p0038 A70-40690
- Energy dependent time lag in the long-term modulation of cosmic rays. p0067 A73-19252
- The 1972 cosmic ray electron spectrum above 0.5 GeV. p0078 A74-27700
- Short-term intensity fluctuation of cosmic-ray electrons between 0.5 and 10 GeV. p0079 A74-31903
- Energy spectrum of cosmic-ray electrons from 0.5 to 10 GeV [B14744-000] p0112
- SWANENBURGH, B. N.**
- Observation of cosmic-ray electrons with the OGO-5 satellite [B14745-000] p0112
- SWEENEY, R. E.**
- Magnetic field mapping of the inner magnetosphere. p0038 A70-39349
- Asymmetric ring current at twilight local time. p0051 A71-33946
- The POGO data. p0070 A73-31768
- POGO observations of the equatorial electrojet [NASA-TM-X-65995] p0099 N72-30823
- The equatorial electrojet satellite and surface comparison [NASA-TM-X-66218] p0102 N73-20866
- SWISHER, R. L.**
- Energy fluxes of low-energy protons and positive ions in the earth's inner radiation zone. p0011 A68-17771
- Lifetimes for low-energy protons in the outer radiation zone. p0016 A68-41684
- Degradation of continuous-channel electron multipliers in a laboratory operating environment. p0021 A69-29565

T

- TAEUSCH, D. R.**
- Response of the neutral atmosphere to geomagnetic disturbances. p0052 A71-39711
- Neutral composition variation above 400 kilometers during a magnetic storm. p0055 A72-13518
- Neutral composition in the thermosphere. p0062 A72-42431
- Empirical model of polar thermosphere storm [NASA-CR-103080] p0094 N71-20638
- OGO-6 neutral atmospheric composition experiment [NASA-CR-135798] p0103 N73-33320

- TAKAHASHI, G.**
- OGO triaxial search coil magnetometer Final Engineering Report [NASA-CR-100619] p0108 N69-72494
- TAKAKI RA, T.**
- Rise time in 20-32 keV impulsive X-radiation. p0080 A74-38468
- TAKHASHI, G.**
- OGO triaxial search coil magnetometer [B21207-000] p0113
- TANAKA, Y.**
- Time variations in the cosmic ray electron spectrum above 500 MeV. p0037 A70-38105
- The cosmic ray electron spectrum between 0.5 and 10 GeV observed on board OGO-5. p0037 A70-38106
- Search for galactic gamma-rays with energies greater than 500 MeV on board OGO-5. p0038 A70-40690
- Implications of the observed solar modulation of cosmic-ray electrons. p0040 A70-45769
- TAYLOR, B. G.**
- OGO-5 spark-chamber telescope for gamma-ray astronomy [B18277-000] p0113
- TAYLOR, G. N.**
- Comparison of Te and Ti from OGO-6 and from various incoherent scatter radars. p0067 A73-19241
- TAYLOR, H. A.**
- Thermal ions in the exosphere: Evidence of solar and geomagnetic control. p0016 A68-41673
- Observations of irregular structure in thermal ion distributions in the duskside magnetosphere. p0031 A70-29185
- Observed solar geomagnetic control of the ionosphere: Implications for reference ionospheres. p0050 A71-33762
- TAYLOR, H. A., JR.**
- Instrumentation for atmospheric composition measurements. p0001 A63-12209
- Positive ion composition in the magnetosphere obtained from the OGO-A satellite. p0004 A66-14781
- Contraction of the plasmasphere during geomagnetically disturbed periods. p0011 A68-19744
- Thermal ion structure of the plasmasphere p0014 A68-37114
- Evidence of contraction of the earth's thermal plasmasphere subsequent to the solar flare events of 7 and 9 July 1966. p0020 A69-23777
- Multi-experiment detection of the plasmapause from OGO satellites and antarctic ground stations. p0021 A69-25153
- Observations of hydrogen and helium ions during a period of rising solar activity. p0022 A69-31326
- Ion depletion in the high-latitude exosphere: Simultaneous OGO-2 observations of the light ion trough and the VLF cutoff. p0023 A69-34939
- Comparison of certain VLF noise phenomena with the lower hybrid resonance frequency calculated from simultaneous ion composition measurements. p0029 A70-18534
- Comparison of coincident OGO-3 and OGO-4 hydrogen ion composition measurements. p0037 A70-38377
- Study of the thermal plasma on closed field lines outside the plasmasphere. p0038 A70-41057
- Evidence of solar geomagnetic seasonal control of the topside ionosphere. p0047 A71-24555
- Structured variations of the plasmapause: Evidence of a corotating plasma tail. p0053 A71-43166
- Irregular structure of thermal ion plasma near the plasmapause observed from OGO-3 and Pc 1 measurements. p0056 A72-17453
- The light ion trough. p0065 A73-11904
- The light-ion trough, the main trough, and the plasmapause. p0066 A73-15533

- Parametric description of thermospheric ion composition results p0067 A73-19255
- Dynamics of midlatitude light ion trough and plasmatails [NASA-TM-X-70494] p0103 N74-10366
- High latitude minor ion enhancements: A clue for studies of magnetosphere-atmosphere coupling [NASA-TM-X-70582] p0104 N74-16064
- TEAGUE, M. J.**
- A model of the Starfish flux in the inner radiation zone [NASA-TM-X-66211] p0102 N73-20842
- The inner zone electron model AE-5 [NASA-TM-X-69987] p0106 N74-20502
- TEEGARDEN, B. J.**
- Spectra and charge composition of the low energy galactic cosmic radiation from Z equals 2 to 14. p0037 A70-38127
- THEILE, B.**
- A multisatellite study of auroral-zone phenomena. [ESRO-SR-23-PT-1] p0105 N74-16072
- THOMAS, G. F.**
- Ultraviolet observations of atomic hydrogen and oxygen from the OGO satellites. p0022 A69-31400
- OGO-5 measurements of the Lyman alpha sky background. p0047 A71-24439
- Lyman-alpha measurements of neutral hydrogen in the outer geocorona and in interplanetary space. p0059 A72-32955
- Determination of the solar Lyman-alpha flux independent of calibration by ultraviolet observations of Comet Bennett) p0076 A74-15496
- OGO-5 measurements of the Lyman-alpha sky background in 1970 and 1971. p0077 A74-22345
- Properties of nearby interstellar hydrogen deduced from Lyman-alpha sky background measurements p0100 N73-10813
- THOMAS, G. R.**
- A multisatellite study of auroral-zone phenomena. [ESRO-SR-23-PT-1] p0105 N74-16072
- THOMAS, R. J.**
- Analysis of OGO-6 observations of the O 1 5577-A tropical nightglow. p0060 A72-35604
- Distribution of atomic oxygen in the upper atmosphere deduced from OGO-6 airglow observations p0075 A73-45121
- Spatial and temporal behavior of atomic oxygen determined by OGO 6 airglow observations p0079 A74-30670
- THORBURN, W. J.**
- Investigation of ultraviolet solar radiation and its influence on the aerospace environment [AFCRL-64-773] p0083 N65-14504
- THORNE, R. M.**
- Unducted whistler evidence for a secondary peak in the electron energy spectrum near 10 kev. p0015 A68-38428
- On the structure of the inner magnetosphere. p0034 A70-30358
- Relativistic electron precipitation during magnetic storm main phase. p0051 A71-33948
- Pitch-angle diffusion of radiation belt electrons within the plasmasphere. p0060 A72-35597
- Plasmaspheric hiss intensity variations during magnetic storms. p0080 A74-34038
- Intensity variation of elf hiss and chorus during isolated substorms [B22603-000] p0114
- Electromagnetic hiss and relativistic electron losses in the inner zone [B22613-000] p0114
- TOMBLIN, F. F.**
- Electron intensity variations in the inner belt following a geomagnetic storm. p0042 A71-14212
- TRAINOR, J. H.**
- OGO-E cosmic radiation: Nuclear abundance experiment p0008 A67-25852
- A solid state detector experiment for electron measurements on OGO-F. p0014 A68-34540

- Design of a long-life reliable nuclear experiment for space flight. p0024 A69-36676
- TROSHICHEV, O. A.**
Asymmetry of the ring current [B18378-000] p0113
- TROY, B. E., JR.**
OGO-4 observations of ion composition and temperatures in the topside ionosphere. p0035 A70-36016
Subauroral red arcs and associated ionospheric phenomena. p0045 A71-19663
Equatorial ion temperature: A comparison of conflicting incoherent scatter and OGO-4 retarding potential analyzer values. p0052 A71-33956
Equatorial airglow and the ionospheric geomagnetic anomaly. p0073 A73-38939
- TSURUTANI, B. T.**
Postmidnight chorus: A substorm phenomenon. p0076 A74-18364
Plasmaspheric hiss intensity variations during magnetic storms. p0080 A74-34038
Electromagnetic hiss and relativistic electron losses in the inner zone [B22613-000] p0114
- U**
- UNTI, T.**
Shock system of February 2, 1969 p0075 A74-12627
- UNTI, T. W. J.**
Dissipation mechanisms in a pair of solar-wind discontinuities. p0058 A72-29378
Direct measurements of solar-wind fluctuations between 0.0048 and 13.3 Hz. p0068 A73-23539
- V**
- VAMPOLA, A. L.**
Simultaneous observations of solar-flare electron spectra in interplanetary space and within earth's magnetosphere. p0046 A71-21037
- VAN ALLEN, J. A.**
OGO-2 experiment 5010 and OGO-4 experiment 5010A [NASA-CR-140527] p0109 N74-76909
Instrument report for a trapped radiation experiment for EGO (S-49) (OGO-1) [NASA-CR-140528] p0109 N74-76911
- VANDEHULST, H. C.**
Time variations in the cosmic ray electron spectrum above 500 MeV. p0037 A70-38105
The cosmic ray electron spectrum between 0.5 and 10 GeV observed on board OGO-5. p0037 A70-38106
Search for galactic gamma-rays with energies greater than 500 MeV on board OGO-5. p0038 A70-40690
Cosmic-ray electrons. p0060 A72-33869
- VASYLIUNAS, V. M.**
Simultaneous IMP 2 and OGO 1 observations of bow shock compression. p0011 A68-17768
A survey of low-energy electrons in the evening sector of the magnetosphere with OGO-1 and OGO-3. p0012 A68-28348
Low-energy electrons on the day side of the magnetosphere. p0018 A69-14027
Low energy electrons in the magnetosphere as observed by OGO-1 and OGO-3. p0019 A69-19373
Low energy particle fluxes in the geomagnetic tail. p0049 A71-30029
- VENKATESAN, D.**
Spectral variations in short term Forbush decreases and in long term changes in cosmic ray intensity. p0044 A71-18137
- VESCELIUS, F. E.**
OGO-E plasma spectrometer. p0017 A68-42739
- VESECKY, J.**
Type 3 solar noise observed below 100 kHz on OGO-3. p0062 A72-42043
- VETTE, J. I.**
Models of the trapped radiation environment. Volume 2: Inner and outer zone electrons [NASA-SP-3024-VOL-2] p0084 N66-35685
Models of the trapped radiation environment. Volume 3: Electrons at synchronous altitudes [NASA-SP-3024-VOL-3] p0085 N67-19899
The inner zone electron model AE-5 [NASA-TM-X-69987] p0106 N74-20502
A model environment for outer zone electrons [NASA-TM-X-69989] p0106 N74-20503
- VIGNERON, J.**
The plasmasphere during a magnetic recovery period: A combined study of the OGO-4 and OGO-5 satellite data and of whistlers received at the ground. p0072 A73-33876
- VOGT, R. E.**
A solar and galactic cosmic ray satellite experiment. p0012 A68-27615
Interplanetary deceleration of solar cosmic rays. p0046 A71-22801
The elemental abundance ratios of interstellar secondary and primary cosmic rays. p0079 A74-30190
The isotopes of H and He in solar cosmic rays p0107 N74-21466
- VOLLAND, H.**
Model of magnetospheric temperature distribution. p0015 A68-38423
Magnetic storm effects in the neutral composition. p0058 A72-24957
Theoretical model for the latitude dependence of the thermospheric annual and semiannual variations. p0066 A73-15538
Magnetic storm characteristics of the thermosphere. p0070 A73-29975
- VON ZAHN, U.**
The air composition in the thermosphere. p0078 A74-29960
- VORPAHL, J.**
Identification of the hard X-ray pulse in the flare of September 11-12, 1968. p0030 A70-25746
- VORPAHL, J. A.**
X-radiation (E greater than 10 keV), H-alpha and microwave emission during the impulsive phase of solar flares. p0066 A71-17041
Rise time in 20-32 keV impulsive X-radiation. p0080 A74-38468
Optical, hard X-ray, and microwave emission during the impulsive phase of flares. p0107 N74-21458
- W**
- WALKER, R. J.**
Spatial distribution of energetic plasma sheet electrons. p0062 A72-42406
- WALSH, W. J.**
Structured variations of the plasmopause: Evidence of a corotating plasma tail. p0053 A71-43166
The light-ion trough, the main trough, and the plasmopause. p0066 A73-15533
- WALTER, F.**
Nonducted mode of VLF propagation between conjugate hemispheres: Observations on OGO's 2 and 4 of the "walking-trace" whistler and of Doppler shifts in fixed frequency transmissions. p0028 A70-15116
Nonducted VLF propagation in the magnetosphere [NASA-CR-107614] p0091 N70-15525
- WALTON, J. R.**
Shadowing of electron azimuthal-drift motions near the noon magnetopause. p0065 A73-12442
Electron pitch angle distributions throughout the magnetosphere as observed on OGO-5. p0068 A73-24732
Satellite studies of magnetospheric substorms on August 15, 1968. 6: OGO 5 energetic electron observations. Pitch angle distributions in the nighttime magnetosphere p0072 A73-33454
- Energetic electrons and protons observed on OGO-5, March 6-10, 1970 [B07587-000] p0111
Energetic electron and proton solar particle observations on OGO-5, 24-34 January 1971 [B15152-000] p0112
LLL electron and proton spectrometer on NASA's Orbiting Geophysical Observatory 5 [NASA-CR-136218] p0104 N74-13165
Energetic electrons and protons observed on OGO-5, March 6-10, 1970 [NASA-CR-139265] p0109 N74-74662
Energetic electron and proton solar particle observations on OGO-5, January 24-30, 1971 [NASA-CR-139266] p0109 N74-74663
- WARNECKE, G.**
Meteorological results from multi-spectral photometry in airglow bands by the OGO-4 satellite. p0028 A70-15522
- WARNOCK, J. M.**
Effect of satellite potential on direct ion density measurements through the plasmopause. p0076 A74-18372
- WAY, S. H.**
OGO-E cosmic radiation: Nuclear abundance experiment. p0008 A67-25852
- WEBBER, W. R.**
Two satellite-borne cosmic radiation detectors. p0004 A66-23684
Direct measurements of geomagnetic cutoffs for cosmic-ray particles in the latitude range 45 deg to 70 deg using balloons and satellites. p0016 A68-41562
Cosmic ray telescope for OGO 2 and 4 spacecraft [NASA-CR-137238] p0106 N74-19088
- WEIL, H.**
Electron depletion in the wake of ionospheric spacecraft: A comparison between results from Langmuir probes and antennas. p0072 A73-34783
OGO-2 data analysis satellite plasma wake study. [NASA-CR-109457] p0092 N70-23999
- WELL, H.**
OGO satellite wake structure deduced from antenna impedance measurements. p0035 A70-35771
- WENSLEY, J. H.**
OGO-1 VLF experiment A-17 digital data processing system [NASA-CR-88618] p0086 N67-37021
- WEST, H. I., JR.**
Simultaneous observations of solar-flare electron spectra in interplanetary space and within earth's magnetosphere. p0046 A71-21037
Shadowing of electron azimuthal-drift motions near the noon magnetopause. p0065 A73-12442
Electron pitch angle distributions throughout the magnetosphere as observed on OGO-5. p0068 A73-24732
Satellite studies of magnetospheric substorms on August 15, 1968. 6: OGO 5 energetic electron observations. Pitch angle distributions in the nighttime magnetosphere p0072 A73-33454
Satellite studies of magnetospheric substorms on August 15, 1968. 7: OGO-5 energetic proton observations. Spatial boundaries p0072 A73-33455
Energetic electrons and protons observed on OGO-5, March 6-10, 1970 [B07587-000] p0111
Energetic electron and proton solar particle observations on OGO-5, 24-34 January 1971 [B15152-000] p0112
The LRL electron and proton spectrometer on NASA's Orbiting Geophysical Observatory 5 (E): Instrumentation and calibration [NASA-CR-109962] p0093 N70-28103
LLL electron and proton spectrometer on NASA's Orbiting Geophysical Observatory 5, the data user's guide to the microfilm records [UCRL-51307] p0102 N73-31150
LLL electron and proton spectrometer on NASA's Orbiting Geophysical Observatory 5 [NASA-CR-136218] p0104 N74-13165
Energetic electrons and protons observed on OGO-5, March 6-10, 1970 [NASA-CR-139265] p0109 N74-74662
Energetic electron and proton solar particle observations on OGO-5, January 24-30, 1971 [NASA-CR-139266] p0109 N74-74663

WEVER, A.

WEVER, A.

Results of recent microparticle hypervelocity impact studies related to sensors of cosmic dust experiments. p0013 A68-29468

WHIPPLE, E. C.

Effect of satellite potential on direct ion density measurements through the plasmopause. p0076 A74-18372

WHIPPLE, E. C., JR.

Theory of an electron trap on a charged spacecraft. p0022 A69-31976
Effects of secondary electron emission on electron trap measurements in the magnetosphere and solar wind. p0027 A70-13994

Theory of spacecraft sheath structure, potential, and velocity effects on ion measurements by traps and mass spectrometers. p0038 A70-41087

Errors in ion and electron temperature measurements due to grid plane potential. nonuniformities in retarding potential analyzers p0071 A73-33436

A satellite ion-electron collector: Experimental effects of grid transparency, photoemission, and secondary emission [NASA-CR-139262] p0109 N74-74638

WARD, W. D.

OGO attitude computations [NASA-TM-X-63373] p0110 N74-76912

WILFRED, E. S.

The Orbiting Geophysical Observatory: A new tool for space research. [NASA-TN-D-1450] p0082 N62-15053

WILLIAMS, D. J.

A solid state detector experiment for electron measurements on OGO-F. p0014 A68-34540

Design of a long-life reliable nuclear experiment for space flight. p0024 A69-36676

WILLMORE, A. P.

Electron density measurements in the thermal plasma of the magnetosphere using a Langmuir probe. p0036 A70-37513

WILLOUGHBY, D. S.

An interpretation of OGO light ion abundance measurements. p0021 A69-25157

WILLS, R. D.

Spark-chamber observation of galactic gamma-radiation. p0038 A70-40691

OGO-5 spark-chamber telescope for gamma-ray astronomy [B18277-000] p0113

WILSON, D.

Attempts to measure micrometeoroid flux on the OGO 2 and OGO 4 satellites. p0027 A70-10444

Micrometeoroid experiment on the OGO 4 satellite [B04201-000] p0111

The micrometeoroid experiment on the OGO 2 satellite [NASA-CR-100683] p0089 N69-23367

WINCKLER, J. R.

Response of ion chambers in free space to the long-term cosmic-ray variation from 1960 to 1965. p0003 A65-33664

Studies of primary cosmic rays with ionization chambers. p0006 A66-34768

The spectra and intensity of electrons in the radiation belts. p0008 A67-25807

A study of energetic solar flare X-rays. p0009 A67-41232

Energetic solar flare X-rays observed by satellite and their correlation with solar radio and energetic particle emission. p0011 A68-22450

The observation of 10-50 keV solar flare X-rays by the OGO satellites and their correlation with solar radio and energetic particle emission. p0014 A68-35480

Experimental observation of a large addition to the electron inner radiation belt after a solar flare event. p0017 A68-41697

Observations of the screening of solar cosmic rays by the outer magnetosphere. p0018 A69-12740

Observations of energetic X-rays and solar cosmic rays associated with the 23 May 1967 solar flare event. p0020 A69-22182

Experimental verification of drift-shell splitting in the distorted magnetosphere. p0026 A69-40508

Intensity correlations and substorm electron drift effects in the outer radiation belt measured with the OGO 3 and ATS 1 satellites. p0026 A69-43172

"Hysteresis" effects in cosmic ray modulation and the cosmic ray gradient near solar minimum. p0028 A70-15106

The origin and distribution of energetic electrons in the Van Allen radiation belts. p0033 A70-30090

Modulation and heliocentric gradient of low energy cosmic rays near solar minimum, 1965. p0044 A71-18128

The construction, calibration and operation of the University of Minnesota experiments for OGO-1 and OGO-3 p0084 N67-13710

An atlas of 10-50 keV solar flare X-rays observed by the OGO satellites, 5 September 1964 to 31 December 1966 [NASA-CR-94429] p0087 N68-23026

A survey of the total radiation in space observed by the OGO satellites, 5 September 1964 - 27 May 1968 [NASA-CR-107886] p0092 N70-17448

Description of data plots from the University of Minnesota ion chamber and electron spectrometer on OGO-1 and OGO-3 [NASA-CR-107885] p0092 N70-17624

Electron spectrometer and integrating ion chamber for the OGO-1 and OGO-3 missions [NASA-CR-139263] p0109 N74-74639

Effect of satellite potential on direct ion density measurements through the plasmopause. p0076 A74-18372

Implementation of a design review. p0001 A63-13537

Preliminary results from the Ames Research Center plasma probe observations of the solar-wind-geomagnetic field interaction region on IMP-2 and OGO-1. p0003 A69-25921

The effect of the earth's radiation belts on an optical system. p0007 A67-12055

Optical environment about the OGO-3 satellite. p0010 A68-12548

A low energy solar cosmic ray experiment for OGO-F. p0012 A68-27616

Research related to measurements of atomic species in the earth's upper atmosphere [NASA-CR-106805] p0091 N70-11727

Source and identification of heavy ions in the equatorial F layer. p0063 A72-44516

Coordinated satellite and incoherent scatter observations [NASA-CR-121984] p0096 N71-35437

Attempts to measure micrometeoroid flux on the OGO 2 and OGO 4 satellites. p0027 A70-10444

Detection of micrometeoroid flux on satellites. p0048 A71-28700

Micrometeoroid experiment on the OGO 4 satellite [B04201-000] p0111

Models of the trapped radiation environment. Volume 2: Inner and outer zone electrons [NASA-SP-3024-VOL-2] p0084 N66-35685

Models of the trapped radiation environment. Volume 3: Electrons at synchronous altitudes [NASA-SP-3024-VOL-3] p0085 N67-19899

Cyclotron drift instability in the bow shock. p0063 A72-44523

WU, C.-S.

Dissipation mechanisms in a pair of solar-wind discontinuities. p0058 A72-29378

Shock system of February 2, 1969 p0075 A74-12627

WUJECK, J. H.

The LRL electron and proton spectrometer on NASA's Orbiting Geophysical Observatory 5(E): Instrumentation and calibration [NASA-CR-109962] p0093 N70-28103

Y

YADLOWSKY, E. J.

Errors in ion and electron temperature measurements due to grid plane potential. nonuniformities in retarding potential analyzers p0071 A73-33436

YORKS, R. G.

OGO satellite wake structure deduced from antenna impedance measurements. p0035 A70-35771

Instrumentation for measurement of cosmic noise at 2.0 and 2.5 MHz from a Polar Orbiting Geophysical Observatory. p0048 A71-26144

OGO-2 data analysis satellite plasma wake study. [NASA-CR-109457] p0092 N70-23999

YUNG, T. J.

Proton gyrofrequency band emissions observed aboard OGO 2. p0013 A68-31481

Z

ZIRIN, H.

Identification of the hard X-ray pulse in the flare of September 11-12, 1968. p0030 A70-25746

ZUCCARO, D.

Plasma measurements with the retarding potential analyzer on OGO-6. p0039 A70-43840

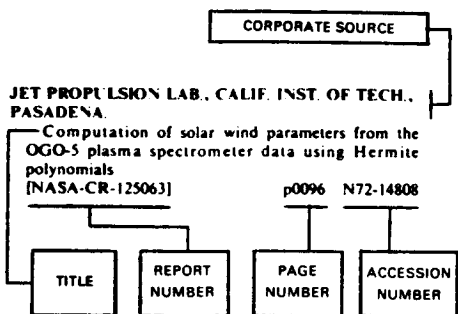
ZWISLER, W. H.

OGO-1 VLF experiment A-17 digital data processing system [NASA-CR-88618] p0086 N67-37021

PERSONAL AUTHOR INDEX

C. CORPORATE SOURCE INDEX

Typical Corporate Source Index Listing



Listings in this index are arranged alphabetically by corporate source. The title of the document provides the user with a brief description of the subject matter. The report number helps to indicate the type of document cited. The page number identifies the page in the abstract section (VI) on which the citation appears while the accession number denotes the number by which the citation is identified on that page. The titles are arranged under each corporate source in ascending accession number order.

A

ADCOLE CORP., WALTHAM, MASS.
Electronic instrumentation for ionospheric and extreme ultraviolet radiation measurements [NASA-CR-64074] p0083 N65-29678

Electronic instrumentation for solar radiation measurements
[NASA-CR-110906] p0094 N71-10358

ADVANCED TECHNOLOGY LABS., MOUNTAIN VIEW, CALIF.
High altitude limitation study advanced horizon sensor for OGO [NASA-CR-83567] p0085 N67-22257

AEROSPACE CORP., EL SEGUNDO, CALIF.
Models of the trapped radiation environment. Volume 2: Inner and outer zone electrons [NASA-SP-3024-VOL-2] p0084 N66-35685

Models of the trapped radiation environment. Volume 3: Electrons at synchronous altitudes [NASA-SP-3024-VOL-3] p0085 N67-19899

A flight calibration device for absolute measurements at the Lyman-alpha wavelength [AD-726567] p0096 N71-36136

Spectral variations of the L alpha sky: A final report of observations from OGO-6 [AD-736816] p0097 N72-23429

Instrument report for Lyman-alpha experiment (OGO-F-12) p0108 N74-74625

AMERICAN SCIENCE AND ENGINEERING, INC., CAMBRIDGE, MASS.
Possible low energy (E less than keV) nonthermal X-ray events p0107 N74-21450

ANALYSIS AND COMPUTER SYSTEMS, INC., BURLINGTON, MASS.
Data processing system for the intensity monitoring spectrometer flown on the Orbiting Geophysical Observatory-F (OGO-F) satellite [NASA-CR-136827] p0105 N74-16940

APPLIED SYSTEMS CORP., FREEPORT, N.Y.
Investigation of electrical structure in the near earth region as measured by orbiting spherical electrostatic analyzers, or plasma probes [AD-700804] p0092 N70-28003

B

BATTELLE MEMORIAL INST., RICHLAND, WASH.
OGO-4 study [NASA-CR-139261] p0109 N74-74637

BENDIX FIELD ENGINEERING CORP., COLUMBIA, MD.
Program description of the data reduction program for experiment 19 of OGO-D [NASA-TM-X-70372] p0109 N74-76910

C

CALIFORNIA INST. OF TECH., PASADENA.
New measurements of the absolute cosmic ray ionization from sea level to 1540 kilometers altitude [NASA-CR-104068] p0090 N69-34536

Magnetospheric access of solar particles and the configuration of the distant geomagnetic field, volume 2 [NASA-CR-122360] p0097 N72-25727

Propagation of 1-10 MeV solar flare protons in interplanetary space p0098 N72-27829

Solar flare particle propagation: Comparison of a new analytic solution with spacecraft measurements [NASA-CR-122406] p0098 N72-29818

A quantitative investigation of the solar modulation of cosmic-ray protons and helium nuclei [NASA-CR-130298] p0100 N73-15837

A satellite measurement of cosmic-ray abundances and spectra in the charge range 2 less than or equal to 7 less than or equal to 10 [NASA-CR-135786] p0103 N73-33777

The isotopes of H and He in solar cosmic rays p0107 N74-21466

OGO-C orientation study
[REF-91] p0109 N74-74661

CALIFORNIA UNIV., BERKELEY.
Solar cosmic ray experiment for the first Orbiting Geophysical Observatories [B03937-000] p0111

Energetic radiation from solar flares [B03940-000] p0111

Experiment data analysis report OGO-3: Experiment no. 1 [B03943-000] p0111

Experiment data analysis report OGO-A: Experiment no. 1 [B03944-000] p0111

Production processing of the data obtained by the UCLA OGO-5 fluxgate magnetometer [B12880-000] p0112

The propagation of solar protons p0089 N69-23730

Energetic radiations from solar flares [NASA-CR-122509] p0098 N72-28812

Characteristics of nonthermal electrons accelerated during the flash phase of small solar flares p0106 N74-21445

CALIFORNIA UNIV., LIVERMORE, LAWRENCE LIVERMORE LAB.
LLL electron and proton spectrometer on NASA's Orbiting Geophysical Observatory 5, the data user's guide to the microfilm records [UCRL-51307] p0102 N73-31150

LLL electron and proton spectrometer on NASA's Orbiting Geophysical Observatory 5 [NASA-CR-136218] p0104 N74-13165

Energetic electron and proton solar particle observations on OGO-5, January 24-30, 1971 [NASA-CR-139266] p0109 N74-74663

CALIFORNIA UNIV., LIVERMORE, LAWRENCE RADIATION LAB.
A low-powered magnetic Hall probe for space applications [UCRL-14650-T] p0086 N67-30930

The LRL electron and proton spectrometer on NASA's Orbiting Geophysical Observatory 5(E): Instrumentation and calibration [NASA-CR-109962] p0093 N70-28103

Energetic electrons and protons observed on OGO-5, March 6-10, 1970 [NASA-CR-139265] p0109 N74-74662

CALIFORNIA UNIV., LOS ANGELES.
Digital offset field generator for spacecraft magnetometers p0090 N69-33963

Comments on the measurement of power spectra of the interplanetary magnetic field p0099 N73-10791

Power spectra of the interplanetary magnetic field near the earth p0099 N73-10792

Trapped and precipitating electrons experiment (F-16) on the Orbiting Geophysical Observatories program OGO-6 mission [NASA-CR-130137] p0100 N73-15863

A summary of the results from the UCLA OGO-5 fluxgate magnetometer [NASA-CR-130205] p0101 N73-20498

Comments on a paper by J. P. Heppner, Polar cap electric field distributions related to interplanetary magnetic field direction p0108 N74-74632

OGO-5 orbital plots generated by the UCLA fluxgate magnetometer group [NASA-CR-139260] p0108 N74-74633

CATHOLIC UNIV. OF AMERICA, WASHINGTON, D.C.
Coronal electron temperature associated with solar flares [OGO-4-67-100A-06] p0108 N74-74629

CENTRE NATIONAL DE LA RECHERCHE SCIENTIFIQUE, VERRIFRES-LE-BUISSON (FRANCE).
Observation of Lyman-alpha emission in interplanetary space p0100 N73-10812

CHICAGO UNIV., ILL.
Description of OGO 1 and OGO-3 counting rate processing and resulting data. Cosmic ray spectra and fluxes experiment on OGO-1 and OGO-3 [B03716-000] p0111

Data processing and analysis from the University of Chicago charged particle experiment on the OGO-5 spacecraft [NASA-CR-132761] p0102 N73-25870

COLORADO UNIV., BOULDER.
The vertical distribution of ozone between 35 and 55 km as determined from satellite ultraviolet measurements p0090 N69-26549

Properties of nearby interstellar hydrogen deduced from Lyman-alpha sky background measurements p0100 N73-10813

COMSTOCK AND WESCOTT, INC., CAMBRIDGE, MASS.
Investigation of ultraviolet solar radiation and its influence on the aerospace environment [AFCLR-64-773] p0083 N65-14504

D

DARTMOUTH COLL., HANOVER, N.H.
Results from an experiment on OGO-6 to study electric and electromagnetic fields in the range 20 Hz - 540 KHz [B17973-000] p0113

An experiment to study whistlers and audio-frequency emissions with a receiving system on board the POGO S-50 satellite (OGO-C/2) in conjunction with an existing network of ground-based observing stations [NASA-CR-97605] p0088 N69-17928

DEVELCO, INC., MOUNTAIN VIEW, CALIF.

DEVELCO, INC., MOUNTAIN VIEW, CALIF.
The feasibility of a sub-LF satellite-to-submarine communication downlink VLF noise levels in the ionosphere
[AD-769139] p0104 N74-15857

F

FARADAY LABS., INC., LA JOLLA, CALIF.
Gas-surface interaction studies
[B20296-000] p0113
Bombardment of OGO-6 surfaces by high-energy particles
[B20297-000] p0113
Initial results from OGO-6 gas-surface experiment
[B20954-000] p0113
Space measurements of the contamination of surfaces by OGO-6 outgassing and their cleaning by sputtering and desorption
[NASA-CR-117138] p0094 N71-20207
Removal of surface contamination by plasma sputtering
[NASA-CR-139264] p0109 N74-74659

G

GENERAL DYNAMICS CORP., SAN DIEGO, CALIF.
Instrument report for design of the gas-surface energy transfer experiments for OGO-F
[B20953-000] p0113

H

HALE OBSERVATORIES, PASADENA, CALIF.
Optical, hard X-ray, and microwave emission during the impulsive phase of flares
p0107 N74-21458

I

INSTITUTE FOR TELECOMMUNICATION SCIENCES AND AERONOMY, BOULDER, COLO.
A satellite ion-electron collector: Experimental effects of grid transparency, photoemission, and secondary emission
[NASA-CR-139262] p0109 N74-74636
INSTITUTO GEOFISICO DEL PERU, LIMA
Coordinated satellite and incoherent scatter observations
[NASA-CR-121984] p0096 N71-35437
IOWA STATE UNIV. OF SCIENCE AND TECHNOLOGY, AMES
POGO reference manual
[IS-769] p0082 N64-13388
IOWA UNIV., IOWA CITY
Reducing radio-frequency-interference from spacecrafts in the frequency range from 20Hz to 200 KHz
[B00969-000] p0111
Investigation of energetic electron intensities in the earth's outer radiation zone with OGO 1
p0088 N69-12899
Solar X-ray control of the E layer of the ionosphere
[NASA-CR-73884] p0088 N69-17412
Local time asymmetries in the increase of electron fluxes in the outer Van Allen zone during substorms
[NASA-CR-100419] p0089 N69-20849
OGO-2 experiment 5010 and OGO-4 experiment 5010A
[NASA-CR-140527] p0109 N74-76909

J

JET PROPULSION LAB., CALIF. INST. OF TECH., PASADENA
Computation of solar wind parameters from the OGO-5 plasma spectrometer data using Hermite polynomials
[NASA-CR-125063] p0096 N72-14808
EOGO triaxial search coil magnetometer Final Engineering Report
[NASA-CR-100619] p0108 N69-72494

L

LOCKHEED MISSILES AND SPACE CO., PALO ALTO, CALIF.
A multi-satellite study of the nature of wavelike structures in the magnetosphere plasma
[B22600-000] p0114
Night glow of the atmosphere in the wavelength 1304 A oxygen line at low geomagnetic latitudes
p0096 N71-34333
Microphone density gage experiment for OGO-F
[NASA-CR-130082] p0098 N72-28467
Variations of atmospheric density near 400 km with magnetic activity during the storm period of 28 September to 2 October 1969
[NASA-CR-122479] p0099 N72-32390
Continued data analysis for Experiment E-18 on OGO-5
[NASA-CR-130156] p0101 N73-16432
Magnetospheric chemical release study
[AD-769979] p0105 N74-17126
A light ion mass spectrometer experiment for OGO-E
[NASA-CR-122291] p0110 N74-76914

M

MARSHALL LABS., TORRANCE, CALIF.
POGO triaxial search coil magnetometer
[B21207-000] p0113
EOGO triaxial search coil magnetometer Final Engineering Report
[NASA-CR-100619] p0108 N69-72494
MARTIN CO., DENVER, COLO.
Dynamic analysis of longitudinal oscillations of SM-68B stage 1 (POGO)
[B00570-000] p0111
MARYLAND UNIV., COLLEGE PARK
A study of high latitude magnetic disturbance
p0105 N74-17058
MASSACHUSETTS INST. OF TECH., CAMBRIDGE
OGO-1 and OGO-3 MIT plasma experiments S4903
[NASA-CR-122351] p0097 N72-18715
MAX-PLANCK-INSTITUT FUER AERONOMIE, LINDAU UBER NORTHEIM (WEST GERMANY)
A multisatellite study of auroral-zone phenomena.
[MSRO-SR-23-PT-1] p0105 N74-16072
MCDONNELL-DOUGLAS AERONAUTICS CO., HUNTINGTON BEACH, CALIF.
Analysis of inner and outer zone: OGO-1 and OGO-2 electron spectrometer and ion chamber data
[NASA-CR-127455] p0098 N72-28802
MDAC solar cosmic ray experiment on OGO-6
[NASA-CR-130155] p0101 N73-16795
MICHIGAN UNIV., ANN ARBOR
Experiment data analysis report for the OGO-4 neutral and ion mass spectrometer experiment
[B05000-000] p0111
University of Michigan radio astronomy experiment aboard the OGO-5 spacecraft
[B14718-000] p0112
Instrumentation for radio astronomy measurements aboard the OGO-5 spacecraft
[NASA-CR-98670] p0088 N69-14392
Data reduction and analysis report for the radio astronomy experiment aboard the OGO-2 spacecraft
[NASA-CR-98669] p0088 N69-14393
OGO spacecraft electromagnetic interference in the 50-kHz to 4-MHz frequency range
p0089 N69-25437
Results from Orbiting Geophysical Observatory 1
[NASA-CR-103321] p0090 N69-31345
Dynamic spectra of 4-2 MHz solar bursts: Results from Orbiting Geophysical Observatory 3
[NASA-CR-106640] p0091 N70-11147
OGO 3 data analysis - Dynamic spectra of solar bursts
[NASA-CR-107031] p0091 N70-12221
The OGO-2 neutral and ion mass spectrometer experiment
[NASA-CR-107408] p0091 N70-14425
OGO-2 data analysis satellite plasma wake study.
[NASA-CR-109457] p0092 N70-23999
The reduction and analysis of data from the low-frequency radio astronomy experiment aboard the OGO-4 spacecraft
[NASA-CR-110796] p0093 N70-42352
Empirical model of polar thermosphere storm
[NASA-CR-103080] p0094 N71-20638

CORPORATE SOURCE INDEX

Reduction and analysis of data from OGO-4 experiment 15
[NASA-CR-117525] p0094 N71-21544
Perturbations to observed ambient neutral densities due to presence of an Orbiting Geophysical Observatory
[NASA-CR-117897] p0094 N71-23238
A analysis of type 3 solar radio bursts observed at kilometeric wavelengths from the OGO-5 satellite
[NASA-CR-122393] p0097 N72-23118
OGO-F-02 data analysis
[NASA-CR-130128] p0100 N73-13376
OGO-6 neutral atmospheric composition experiment
[NASA-CR-135798] p0103 N73-33320
Instrumentation for radio astronomy measurements aboard the OGO-1 and OGO-3 spacecraft. Part 2: Technical
[NASA-CR-139257] p0108 N74-74631
Initial results from radio astronomy-experiment no. 18, OGO-3
[UM/RAO-67-9] p0109 N74-74660
Data user's notes: OGO-3 experiment no. 18 low frequency radio astronomy, appendices A and B
[NASA-CR-140526] p0109 N74-76907
Neutral and ion mass spectrometer experiment S5015
[NASA-CR-96663] p0110 N74-77537
MINNESOTA UNIV., MINNEAPOLIS
The construction, calibration and operation of the University of Minnesota experiments for OGO-1 and OGO-3
[CR-87] p0084 N67-13710
Application of an integrating type ionization chamber to measurements of radiation in space
[NASA-CR-90060] p0087 N68-10422
An atlas of 10-50 keV solar flare X-rays observed by the OGO satellites, 5 September 1964 to 31 December 1966
[NASA-CR-94429] p0087 N68-23026
An experimental study of electron fluxes from 50 keV to 4 MeV in the inner radiation belt
[NASA-CR-100648] p0089 N69-19899
A survey of the total radiation in space observed by the OGO satellites, 5 September 1964 - 27 May 1968
[NASA-CR-107886] p0092 N70-17448
Description of data plots from the University of Minnesota ion chamber and electron spectrometer on OGO 1 and OGO-3
[NASA-CR-107885] p0092 N70-17624
Cosmic ray telescope for OGO 2 and 4 spacecraft
[NASA-CR-137248] p0106 N74-19088
Electron spectrometer and integrating ion chamber for the OGO-1 and OGO-3 missions
[NASA-CR-139263] p0109 N74-74639

N

NATIONAL AERONAUTICS AND SPACE ADMINISTRATION, GODDARD SPACE FLIGHT CENTER, GREENBELT, MD.
Earth satellite experiment for measuring the charge and energy spectra of the primary cosmic rays
[B01634-000] p0111
Near view of the ring current
[B19906-000] p0113
The Orbiting Geophysical Observatory: A new tool for space research.
[NASA-TN-D-1450] p0082 N62-15053
OGO earth acquisition
[NASA-TM-X-55002] p0082 N64-23517
Shades of EGO, S-49
[NASA-TM-X-55014] p0082 N64-27251
The world magnetic survey
[NASA-RP-277] p0082 N64-27355
Gegenschein orbital parameters and operational schedule
[NASA-TM-X-55032] p0082 N64-27813
Shades of POGO
[NASA-TM-X-55153] p0083 N65-18269
Power study of spin stabilized EGO /S-49/
[NASA-TM-X-55186] p0083 N65-21656
Visual presentation of the motion and orientation of an orbiting spacecraft /OGO/
[NASA-TN-D-2918] p0083 N65-29296
Relative advantages of small and observatory type satellites.
[NASA-TM-X-55261] p0083 N65-29783
Orbital parameters for the OGO-E geocoronal hydrogen experiment
[NASA-TM-X-55276] p0083 N65-30651

NOV. 10, 1975

EGO orbital parameters and heat inputs
[NASA-TM-X-55428] p0084 N66-21006
A representation of the perigee motion of a satellite
as a function of local time
[NASA-TM-X-55703] p0085 N67-18763
Methods of data reduction for the OPEP Airglow
photometer on OGO-2
[NASA-TM-X-55794] p0085 N67-27576
Some effects of MeV electrons on the OGO 2 (POGO)
airglow photometers
[NASA-TM-X-55791] p0085 N67-27578
Processing of the total field magnetometer data from
the OGO-2 satellite
[NASA-TM-X-55822] p0085 N67-30147
Processing the data from the OGO-III
GEGENSCHHEIM photometry experiment
[NASA-TM-X-55907] p0086 N67-35595
The geomagnetic secular variation, 1900 - 1965
[NASA-TM-X-55944] p0086 N67-37398
Photoelectron flux in the topside ionosphere
measured by retarding potential analyzers
[NASA-TM-X-63358] p0087 N68-35999
Effects of energetic particles on photomultipliers in
earth orbits up to 1500 km
[NASA-TM-X-63419] p0088 N69-18074
Propagation of solar cosmic rays in the interplanetary
magnetic field
p0090 N69-29659
Cosmic ray and solar flare electrons
p0090 N69-38983
Galactic and solar cosmic rays
p0091 N69-38984
Coordinate transformations used in OGO satellite
data analysis
[NASA-TM-X-63826] p0092 N70-19313
Discrepancies in the observed plasma-trough
density
[NASA-TM-X-63702] p0092 N70-27302
Auroral electron drift and precipitation: Cause of
the mantle aurora
[NASA-TM-X-63941] p0093 N70-29987
New results and techniques in space radio
astronomy
[NASA-TM-X-63976] p0093 N70-33175
Diurnal phase anomaly in the earth's upper
atmosphere
p0094 N71-25265
Latitudinal dispersion of gases in the upper
atmosphere
p0094 N71-25267
Airglow observations from OGO-4
p0095 N71-25268
Thermal plasma near the plasmapause
p0095 N71-25270
The inflation of the inner magnetosphere
p0095 N71-25271
Auroral particle injection and drift
p0095 N71-25272
OGO 5 measurements of electrons near the
magnetopause.
p0095 N71-25273
Derivation of the International Geomagnetic
Reference Field, IGRF(10/68)
[NASA-TM-X-62377] p0095 N71-32190
Plasma parameter beta in the midnight
magnetosphere: From the near-earth plasma sheet to
the plasmapause
[NASA-TM-X-65640] p0095 N71-32436
Analogy between magnetospheric resonance and the
vibration of a stringed musical instrument
[NASA-TM-X-65644] p0096 N71-32519
Magnetic field fluctuations during substorms
[NASA-TM-X-65748] p0096 N72-11325
The ionosphere during a subauroral red arc
p0097 N72-23334
Crustal anomalies
p0097 N72-23341
An atlas of low latitude 6300A (01) night airglow
from OGO-4 observations
[NASA-TM-X-65913] p0098 N72-26309
Functional characteristics of the OGO main body
airglow photometer
[NASA-TM-X-65926] p0098 N72-27423
OGO-4 observations of the 6300A night airglow from
40 deg N to 40 deg S. A set of 19 color maps
[NASA-TM-X-65954] p0098 N72-28353
POGO observations of the equatorial electrojet
[NASA-TM-X-65995] p0099 N72-30823
A synoptic study of the nature and effects of field
aligned low energy electron precipitation in the auroral
regions
[NASA-TM-X-66065] p0099 N73-10392
Seasonal and altitude variations in field-aligned
precipitation occurrence
[NASA-TM-X-66099] p0100 N73-11345

Magnetic control of the high latitude thermosphere
p0101 N73-17946
The magnetospheric plasma tail
p0101 N73-17948
A model of the Starfish flux in the inner radiation
zone
[NASA-TM-X-66211] p0102 N73-20842
The equatorial electrojet satellite and surface
comparison
[NASA-TM-X-66218] p0102 N73-20866
Simultaneous particle and field observations of
field-aligned currents
[NASA-TM-X-66224] p0102 N73-21367
Dependence of field-aligned electron precipitation on
season, altitude and pitch angle
[NASA-TM-X-66260] p0102 N73-25868
Dynamics of midlatitude light ion trough and
plasmatails
[NASA-TM-X-70494] p0103 N74-10366
Variation with interplanetary sector of the total
magnetic field measured at the OGO 2, 4, and 6
satellites
[NASA-TM-X-70531] p0104 N74-13566
High latitude minor ion enhancements: A clue for
studies of magnetosphere-atmosphere coupling
[NASA-TM-X-70582] p0104 N74-16064
Electric field measurements across the Harang
discontinuity
[NASA-TM-X-70613] p0105 N74-19023
The inner zone electron model AE-5
[NASA-TM-X-69987] p0106 N74-20502
A model environment for outer zone electrons
[NASA-TM-X-69989] p0106 N74-20503
A global magnetic anomaly map
[NASA-TM-X-70628] p0106 N74-20982
Reply
[NASA-TM-X-70215] p0109 N74-74627
OGO-4 auroral particles experiment and calibration
[NASA-TM-X-70216] p0109 N74-74628
Shades of OGO-4 (S-49A)
[NASA-TM-X-70214] p0109 N74-74630
OGO-5 observations of discrete whistlers and
emissions during a large magnetic storm
[NASA-TM-X-70213] p0109 N74-74634
The reduction and analysis of electron data for outer
zone electron model AE-4. Volume 3: OGO-1 and 3
University of Minnesota experiment data
[NASA-TM-X-70212] p0109 N74-74636
OGO attitude computations
[NASA-TM-X-63373] p0110 N74-76912
A double gamma-ray spectrometer to search for
positrons in space
p0110 N74-77446
**NATIONAL AERONAUTICS AND SPACE
ADMINISTRATION, MARSHALL SPACE FLIGHT
CENTER, HUNTSVILLE, ALA.**
Thermoelectrically-cooled quartz crystal
microbalance
p0103 N74-10255
**NATIONAL AERONAUTICS AND SPACE
ADMINISTRATION, WASHINGTON, D.C.**
Orbiting Geophysical Observatories S-49, S-50
[NASA-TM-X-50488] p0110 N74-76913
**NATIONAL OCEANIC AND ATMOSPHERIC
ADMINISTRATION, BOULDER, COLO.**
Energetic electrons and protons observed on OGO-5,
March 6-10, 1970
[B07587-000] p0111
Measurement of ionospheric and exospheric electron
content using radio beacons on orbiting geophysical
observatories: Compilation of data and final report
[B18548-000] p0113
**NATIONAL PHYSICAL LAB., NEW DELHI
(INDIA).**
Ionospheric effects of solar flares. 5: The flare event
of January 30, 1968 and its implications
[RSD-63] p0096 N71-36131
NAVAL RESEARCH LAB., WASHINGTON, D.C.
Using solar X-rays as indicators of solar-flare
activity
[AD-686662] p0090 N69-32730
NEW HAMPSHIRE UNIV., DURHAM.
Neutron measurements of the OGO-VI Spacecraft
[NASA-CR-130181] p0101 N73-19841
Neutron measurements in space with OGO-6
p0103 N73-32639

P

PITTSBURGH UNIV., PA.
The altitude of the scattering layer near the mesopause
over the summer poles
[NASA-CR-130271] p0101 N73-16436

A model ionosphere for mid-day and mid-latitude
during sunspot minimum
[SMU P-4] p0109 N74-74635

R

RICE UNIV., HOUSTON, TEX.

Response to environment and radiation of an
ionization chamber and matched geiger tube used on
spacecraft
[NASA-CR-139255] p0108 N74-74624
Reduction and analysis of data from OGO-C,D ion
chamber experiment
[NASA-CR-107184] p0110 N74-76923

S

**SMITHSONIAN ASTROPHYSICAL
OBSERVATORY, CAMBRIDGE, MASS.**

Measured velocities of interplanetary dust particles
from OGO-1
p0086 N67-32070
The micrometeoroid experiment on the OGO 2
satellite
[NASA-CR-100683] p0089 N69-23367
Variations in thermospheric composition: A model
based on mass-spectrometer and satellite-drag data
[NASA-CR-136192] p0104 N74-12459
STANFORD RESEARCH INST., CALIF.
Instrumentation for the Stanford
University/Stanford Research Institute VLF
experiment (B-17) on the OGO-3 satellite
[B01265-000] p0111
**STANFORD RESEARCH INST., MENLO PARK,
CALIF.**
OGO-1 VLF experiment A-17 digital data processing
system
[NASA-CR-88618] p0086 N67-37021
Resonances in the driving-point impedance of an
electric dipole in the ionosphere
[NASA-CR-91620] p0087 N68-14025
Research related to measurements of atomic species
in the earth's upper atmosphere
[NASA-CR-106805] p0091 N70-11727
Instruments for the Stanford University/Stanford
Research Institute VLF experiment (4917) on the FOGO
satellite
[NASA-CR-139258] p0109 N74-74765
STANFORD UNIV., CALIF.
Summary of digital data-processing systems for the
OGO-SU/SRI very-low-frequency experiments
[B01263-000] p0111
Measurement of ionospheric and exospheric electron
content using radio beacons on orbiting geophysical
observatories: Compilation of data and final report
[B18548-000] p0113
Eccentric Geophysical-Observatory Satellite S-49
with interpretation of the radiobeacon experiment
Technical Report No. 1
[NASA-CR-68307] p0084 N66-12993
Observations of whistler-mode signals in the OGO
satellites from VLF ground station transmitters
[NASA-CR-84869] p0085 N67-30831
Whistler propagation in magnetospheric ducts
p0087 N68-17981
Protonospheric electron concentration profiles
[NASA-CR-100778] p0089 N69-24521
Noninduced VLF propagation in the magnetosphere
[NASA-CR-107614] p0091 N70-15525
Magnetic radiation observed by OGO-1 and OGO-3
broadband VLF receivers
[NASA-CR-107653] p0091 N70-15678
Interpretation of VLF signals observed on the OGO-4
satellite
[NASA-CR-107654] p0092 N70-15768
Experiments C02 (OGO 2) and D02 (OGO 4)
[NASA-CR-110658] p0093 N70-32928
Experiments A17 (OGO 1) and B17 (OGO 3)
[NASA-CR-110716] p0093 N70-33156
ELF propagation in the plasmasphere based on
satellite observations of discrete and continuous
forms
[NASA-CR-130351] p0100 N73-16126
The structure of the magnetosphere as deduced from
magnetospherically reflected whistlers
[NASA-CR-130352] p0101 N73-16344
Banded whistlers observed on OGO-4
[NASA-CR-131495] p0102 N73-22079
OGO-4 satellite observations of whistler-mode
propagation effects associated with caustics in the
magnetosphere
p0104 N74-12109

STATE UNIV. OF IOWA, IOWA CITY.

- Measurements of VLF polarization and wave normal direction on OGO-F
 [NASA-CR-132882] p0104 N74-12842
- STATE UNIV. OF IOWA, IOWA CITY.
 Low-energy proton and electron experiment for the Orbiting Geophysical Observatories B and E
 [NASA-CR-68558] p0084 N66-13640
- Study of the temporal variations of 40 keV electrons in the magnetosphere during and after the magnetic storm on April 18, 1965
 [NASA-CR-85905] p0086 N67-31362
- Investigation of energetic electron intensities in the earth's outer radiation zone with OGO 1
 [NASA-CR-89652] p0087 N67-40126
- A cinematographic display of observations of low-energy proton and electron spectra in the terrestrial magnetosphere
 [NASA-CR-91871] p0087 N68-15232
- Instrument report for a trapped radiation experiment for EGO (S-49) (OGO-1)
 [NASA-CR-140528] p0109 N74-76911

T

TASMANIA UNIV., HOBART (AUSTRALIA).

- Measurements of the primary cosmic ray electron spectrum between 20 MeV and 20 GeV and its changes with time
 [B08373-000] p0112
- Transport of solar flare protons: Comparison of a new analytic model with spacecraft measurements
 [B10763-000] p0112
- Energy spectrum of cosmic-ray electrons from 0.5 to 10 GeV
 [B14744-000] p0112

TEMPLE UNIV., PHILADELPHIA, PA.

- OGO-3 dust particle experiment: Data reduction and analysis
 [NASA-CR-121477] p0096 N71-33768
- TEXAS UNIV., DALLAS.

- In situ measurements of amplitude and scale size characteristics of ionospheric irregularities: OGO-6 ion concentration irregularity studies
 [B20340-000] p0113
- OGO-F-06 ion mass spectrometer
 [NASA-CR-111146] p0094 N71-10588
- OGO 6 ion concentration irregularity studies
 [NASA-CR-132814] p0103 N73-32286
- Investigation into the mechanism and rates of atmospheric mixing in the lower thermosphere
 [NASA-CR-135789] p0103 N73-33321
- OGO-6 experiment F-03
 [NASA-CR-132943] p0106 N74-20542

TOKYO UNIV. (JAPAN).

- Magnetospheric substorm, 1972
 p0110 N74-77515

TRW SYSTEMS GROUP, REDONDO BEACH, CALIF.

- Complex electric field emissions observed by OGO-5 on 15 August 1968
 [NASA-CR-126238] p0097 N72-22383
- Electron plasma oscillations in the near-earth solar wind: Preliminary observations and interpretations
 p0099 N73-10789
- Comparison of deep space and near-earth observations of plasma turbulence at solar wind discontinuities
 p0100 N73-10795
- Orbiting Geophysical Observatories, 1, 2, and 3
 p0108 N74-74623
- Distributions of high frequency waves upstream from earth's bow shock
 [NASA-CR-139256] p0108 N74-74626
- OGO-5 observations of discrete whistlers and emissions during a large magnetic storm
 [NASA-TM-X-70213] p0108 N74-74634
- Orbiting Geophysical Observatories
 [NASA-CR-140524] p0110 N74-76932
- Data analysis program for the OGO E-24 plasma wave detector
 [NASA-CR-140523] p0110 N74-77109
- TRW SYSTEMS, REDONDO BEACH, CALIF.
 Magnetic tests of the OGO and ERS satellites
 p0090 N69-33977

W

WYOMING UNIV., LARAMIE.

- Magnetospheric modulation effects on solar cosmic rays from simultaneous OGO 1 and 3 ion chamber data in 1968 and 1969
 [NASA-CR-137075] p0105 N74-18429

CORPORATE SOURCE INDEX

- Micrometeoroid experiment on the OGO 4 satellite
 [B04201-000] p0111
- Solar cosmic ray observations
 [B11181-000] p0112
- Relativistic electrons in space
 [B13262-000] p0112
- Dynamical characteristics of pulsating substorm, PS6
 [B14580-000] p0112
- Plasma wave-particle interaction inside the neutral sheet (in Japanese)
 [B14583-000] p0112
- Observation of cosmic-ray electrons with the OGO-5 satellite
 [B14745-000] p0112
- Energetic electron and proton solar particle observations on OGO-5, 24-34 January 1971
 [B15152-000] p0112
- Correlation of satellite estimates of the equatorial electrojet intensity with ground observations at Addis Ababa
 [B15846-000] p0112
- Summary and future work (OGO-4 and OGO-6)
 [B15849-000] p0112
- Four years of dust particle measurements in cislunar and selenocentric space from Lunar Explorer 35 and OGO 3
 [B15918-000] p0112
- Global empirical model of thermospheric composition based on OGO-6 mass spectrometer measurements
 [B16248-000] p0112
- Electron precipitation patterns and substorm morphology
 [B16756-000] p0112
- Relativistic electron events in interplanetary space
 [B17665-000] p0113
- OGO-5 observations of the physical processes occurring in the disturbed polar cusp and the cusp-magnetosheath interface
 [B18269-000] p0113
- OGO-5 spark-chamber telescope for gamma-ray astronomy
 [B18277-000] p0113
- Asymmetry of the ring current
 [B18378-000] p0113
- Neutral wind velocities calculated from temperature measurements during a magnetic storm and the observed ionospheric effects
 [B19920-000] p0113
- Plasma tail interpretations of pronounced detached plasma regions measured with OGO-5
 [B20951-000] p0113
- Non-relativistic solar electrons
 [B22602-000] p0113
- High latitude proton precipitation and light ion density profiles during the magnetic storm initial phase
 [B22333-000] p0113
- The equatorial helium ion trough and the geomagnetic anomaly
 [B22334-000] p0114
- Diurnal variation of the neutral thermospheric winds determined from incoherent scatter radar data
 [B22601-000] p0114
- Intensity variation of elf hiss and chorus during isolated substorms
 [B22603-000] p0114
- Magnetopause rotational forms
 [B22604-000] p0114
- Is the red arc a good indicator of ionosphere-magnetosphere conditions
 [B22605-000] p0114
- An upper limit to the product of NO and O densities from 105 to 120 Km
 [B22606-000] p0114
- Acceleration of electrons in the absence of detectable optical flares deduced from type 3 radio bursts, H-alpha activity and soft X-ray emission
 [B22607-000] p0114
- A search for solar neutrons during solar flares
 [B22608-000] p0114
- The solar cycle variation of the solar wind helium abundance
 [B22609-000] p0114
- The measurement of cold ion densities in the plasma trough
 [B22610-000] p0114
- Substorm and interplanetary magnetic field effects on the geomagnetic tail lobes
 [B22611-000] p0114

- Structure of the quasi-perpendicular laminar bow shock
 [B22612-000] p0114
- Electromagnetic hiss and relativistic electron losses in the inner zone
 [B22613-000] p0114
- Observed variations of the exospheric hydrogen density with exospheric temperature
 [B22614-000] p0114

VIII. GLOSSARY OF ACRONYMS AND ABBREVIATIONS

ABBREVIATIONS AND ACRONYMS

The abbreviations and acronyms listed in this section are some of the more common ones used in the context of space science and spacecraft experiments and include those used in all sections of this *Summary* except in Section VI. The list includes spacecraft name acronyms, experiment affiliation acronyms and abbreviations, agency acronyms and abbreviations, etc., which may be useful in reading this *Summary*. Note that the same abbreviation or acronym may indicate two different definitions, these are separated by a semicolon.

A

A	angstrom; atomic weight
ABMA	Army Ballistic Missile Agency
ACAD	Academy
ACIC	Aeronautical Chart and Information Center
ACS	attitude control system
a/d	analog to digital
AE	Atmosphere Explorer (satellite, NASA-GSFC)
AEC	Atomic Energy Commission
AEROPROPUL	aeropropulsion
AEROSAT	Aeronautical Satellite (NASA-ESRO)
AEROSP	aerospace
AFB	Air Force Base
AFCRL	Air Force Cambridge Research Laboratories
AFO	Announcements of Flight Opportunities
AFSC	Air Force Systems Command
AGC	automatic gain control
AGCY	agency
AIM	Automated Internal Management (File)
AIMP	Anchored Interplanetary Monitoring Platform (satellite, NASA-GSFC)
ALOSYN	Alouette topside sounder synoptic (data)
ALPO	Apollo Lunar Polar Orbiter (satellite, NASA); Association of Lunar and Planetary Observers
ALSEP	Apollo Lunar Surface Experiments Package (NASA)
alt	altitude
am	amplitude modulation
amp	ampere
AMPS	Atmosphere, Magnetosphere, and Plasmas in Space (satellite, NASA)
AMS	Army Map Service (now Defense Mapping Agency Topographic Center)
AMSAT	Radio Amateur Satellite Corporation

amu	atomic mass unit; astronaut maneuvering
ANIK	Canadian Telecommunications Satellite; also referred to as TELESAT
ANNA	Army, Navy, NASA, Air Force Geodetic Satellite
ANS	Astronomical Netherlands Satellite (Netherlands - NASA joint project)
AOSO	Advanced Orbiting Solar Observatory
Ap	magnetic activity index Ap
APL	Applied Physics Laboratory of Johns Hopkins University
APPL	application
apt	automatic picture transmission
a/r	acquisition/reference
ARC	Ames Research Center (NASA)
arc-min	arc-minute
arc-sec	arc-second
ARDC	Air Research and Development Command (now AFSC)
ARPA	Advanced Research Projects Agency
ARSP	Aerospace Research Support Program (USAF)
AS&E	American Science & Engineering, Inc.
ASOS	antimony-sulfide oxy-sulfide
ASTP	Apollo-Soyuz Test Project (USSR-NASA, joint project)
ASTROPHYS	astrophysics
AT	atomic
ATCOS	Atmospheric Composition Satellite (NASA); also referred to as OV3-5, OV3.6
AT&T	American Telephone & Telegraph
ATDA	Alternate Target Docking Adapter
ATM	Apollo Telescope Mount
atmos	atmosphere
ATS	Applications Technology Satellite (NASA)
au	astronomical unit
AVCS	advanced vidicon camera system
avg	average
AVHRR	advanced very high resolution radiometer
AWRE	Atomic Weapons Research Establishment

B

bcd	binary coded decimal
BE	Beacon Explorer (satellite, NASA)
BERK	Berkeley
BeV	billion electron volts
BIC	barium iodide cloud
BIOS	Biological Satellite (NASA)
BLH	band-limited (ELF) hiss
bpi	bits per inch
bps	bits per second
BTL	Bell Telephone Laboratories
BUV	backscatter ultraviolet
bv	billion volts
b/w	black and white

Abbreviations and Acronyms

BWF	Bundesminister für Wissenschaftliche Forschung (Fed Rep of Germany)	DANISH INST SPACE RSCH	Danish Institute for Space Research
	C	DAPP	Defense Acquisition and Processing Program (DOD)
c	centigrade	DASA	Defense Atomic Support Agency
cal	calorie	DATS	Despun Antenna Test Satellite (DOD)
calsphere	calibration sphere	db	decibel
Cal Tech	California Institute of Technology	dc	direct current
CAS	Cooperative Applications Satellite (France-NASA); also referred to as EOLE	DCP	data collection platform
		DCS	direct couple system; data collection system
CAV	composite analog video	DEF	defense
cc	cubic centimeter	deg	degree
CDA	command and data acquisition (station)	DENPA	Density Phenomena (satellite, Japan)
CDC	Control Data Corporation	DEV	development
CDS	cadmium sulfide	DFVLR	Deutsche Forschung und Versuchsanstalt für Luft-und Raumfahrt; English translation, Research Laboratory for Aeronautics and Astronautics, Germany
CENS	Centre d'Etudes Nucleaires de Saclay	DIAL/MIKA	Diamant Allemand/Mini Kapsel (satellite, Germany-France, joint project)
CHEM	chemical	DIAL/WIKA	Diamant Allemand/Wissenschaftliche Kapsel (satellite, Germany-France, joint project)
cm	centimeter	diam	diameter
CM	command module	DIAPO	Diapason (satellite, France)
CMD	command	DIT	Drexel Institute of Technology
CNES	Centre National d'Etudes Spatiales	DMAAC	Defense Mapping Agency Aerospace Center
CNET	Centre National d'Etudes des Telecommunications	DMATC	Defense Mapping Agency Topographic Center
CNRS	Centre National de la Recherche Scientifique	DME	Direct Measurements Explorer (satellite, NASA)
COMM	commission	DME-A	Direct Measurements Explorer A (satellite, NASA)
COMS	see COMSAT	DMSP	Defense Military Satellite Program (DOD)
COMSAT	Communications Satellite Corporation	DOD	Department of Defense
CONIE	Comision Nacional de Investigacion del Espacio (Spain)	DODGE	Department of Defense Gravity Experiment (satellite, DOD)
CORSA	Cosmic-Ray Satellite (Japan)	DRID	direct readout image dissector (camera system)
COS	Cosmic-Ray Satellite (ESRO); cosmic	DRIR	direct readout infrared radiometer
COSPAR	Committee on Space Research	DRTE	Defense Research Telecommunications Establishment (now CRC)
COUNC	council	DSAP	Defense System Applications Program (DOD)
CPKF	Cape Kennedy, Florida (also referred to as the Eastern Test Range)	DSCS	Defense Satellite Communications System (DOD)
cps	cycles per second	DSIR	Department of Science and Industrial Research
cpu	central processing unit	DSN	Deep Space Network
CRC	Communications Research Centre	DV	digital video
CRPL	Central Radio Propagation Laboratories (later ITSA; formerly part of ESSA; now a subdivision of NOAA)	DYN	dynamic
CRREL	Cold Region Research & Engineering Laboratories		E
CRS	Commission for Space Research (Italy)	E	energy
crt	cathode ray tube	EASEP	Early Apollo Scientific Experiment Package
CsI	cesium iodide	ECS	Experimental Communications Satellite (NASA)
CSM	command service module	EDS	Environmental Data Service (NOAA)
CTS	Canadian Telecommunications Satellite	EGO	Eccentric (Orbiting) Geophysical Observatory (satellite, NASA)
CTR	center		
CZCS	coastal zone ocean color scanner		
	D		
DAC	data acquisition camera		
DADE	Dual Air Density Explorer (satellite, NASA)		

Abbreviations and Acronyms

EGRS Engineers Satellite (DOD)
el electric
ELDO European Launch Development Organization
ELEC electric
ELECTR electronics
ELECTRO-OPT SYS Electro-Optikal Systems, Inc.
ELF extremely low frequency
EME environmental measurement experiment
ELMS Earth Limb Measurement Satellite (NASA-USAF)
EMR Electromechanical Research (Company, England)
ENVIRON environment; environmental
ENV RSCH & TECH INC Environmental Research & Technology, Inc.
EOF end-of-file
EOGO Eccentric Orbiting Geophysical Observatory
EOS Earth Observation Satellite (NASA)
EP Experiment Package
EPE Energetic Particle Explorer (satellite, NASA)
E/Q energy per unit charge
ERB earth radiation budget (experiment)
ERDC Earth Resources Data Center
ERGS Earth Geodetic Satellite (USAF)
ERL Environmental Research Laboratory (NOAA)
EROS Earth Resources Observation System
ERS Environmental Research Satellite (USAF)
ERT extended range telescope
ERTS Earth Resources Technology Satellite (NASA)
ESGEO see GEOS
ESMR electrically scanning microwave radiometer
ESOC European Space Operations Centre
ESRO European Space Research Organization
ESSA Environmental Science Services Administration (now NOAA)
ESTABL establishment
ESTEC European Space Technology Center
ETR Eastern Test Range (also referred to as Cape Kennedy)
ETS Engineering Test Satellite
euv extreme ultraviolet
eV electron volts
EVA extravehicular activity
EVM Earth viewing (equipment)module
EXOS Exospheric Satellite (Japan)
EXOSAT European X-ray Observation Satellite (ESRO)
EXTRATERR extraterrestrial

F

FARO Flare-Activated Radiobiological Observatory
FED Federal

FLT-SAT Fleet Satellite (USN)
FM frequency modulation
FMRT final meteorological radiation tape(s)
FOUND foundation
FOV field of view
FPR flat plate radiometer
FR French Research (satellite, France)
FRC Flight Research Center (NASA)
FSC FLEETSATCOM (satellite, USN-USAF)
FSK frequency shift key
FWHM full width at half maximum
FWS filter wedge spectrometer

G

gamma 10⁵ gauss
GARP Global Atmospheric Research Program
GCA Geophysics Corporation of America
GD General Dynamics Corp.
GE General Electric (Company)
.ge. greater than or equal to
GEMS Geostationary European Meteorological Satellite (ESRO)
GEOPHYS geophysical
GEOPHYSICS CORP Geophysics Corporation of America
GEOS Geodetic Earth-Orbiting Satellite (NASA); Geostationary Earth-orbiting Satellite (ESRO)
GES FUR WELTRAUMFO RSCH Gesellschaft fur Weltraumforschung (Center for Space Research, Fed Rep of Germany)
G.E.T. ground elapsed time
GeV gigaelectron volts
GGSE gravity gradient stabilization experiment
GGTS Gravity Gradient Test Satellite (NASA)
gHz gigahertz
GISS Goddard Institute for Space Studies (NASA)
gm gram
GM Geiger-Mueller (tube)
GMS Geostationary Meteorological Satellite (Japan)
GMT Greenwich Mean Time
GOES Geosynchronous Operational Environmental Satellite (NASA) (also called SMS)
GP Gravitational Redshift Space Probe (NASA)
GRAVR Gravitational Redshift Space Probe (NASA)
GRE ground reconstruction equipment
GREB Galactic Radiation Experiment Background (Navy transit satellite)
GRI Groupe de Recherche Ionospherique
GROC Netherlands Committee for Geophysics and Space Research
GRS German Research Satellite (NASA-Germany)

Abbreviations and Acronyms

JSC	Johnson Space Center (NASA)	MAPS	measurement of air pollution from satellite
		MARENTS	Modified Advanced Research Environmental Test Satellite (USAF)
	K	MAS	Ministry of Aviation Supply, UK
K	Kelvin	MASC	magnetic attitude spin coil
kb	kilobit	MATER	material
kbs	kilobits per second	MB	millibar
keV	kiloelectron volt	mc	megacycle
kg	kilogram	MD	McDonnell-Douglas (Corporation)
kHz	kilohertz	m/e	mass/energy
km	kilometer	MED	medicine; medical
Kp	magnetic activity index	METEC	Meteoroid Technology (satellite, NASA)
KPNO	Kit Peak National Observatory	METEOSAT	Meteorological Satellite (ESRO)
KSC	John F. Kennedy Space Center (NASA)	MeV	million electron volts
	L	mg	milligram
LA	Los Angeles	MHz	megahertz
LAB	laboratory	MIDAS	Missile Defense Alarm System (USAF)
LACATE	lower atmosphere composition and temperature	min	minute
LAGEOS	Laser Geodetic Earth-Orbiting Satellite (NASA-MSFC)	MIT	Massachusetts Institute of Technology
LAS	Large Astronomical Satellite (ESRO)	MJS	Mariner Jupiter/Saturn (spacecraft, NASA)
LASL	Los Alamos Scientific Laboratory (ESRO)	mm	millimeter
LCS	Lincoln Calibration Sphere	MOL	Manned Orbiting Laboratory (satellite, DOD)
.le.	less than or equal to	M-P	minus to plus
LED	low-energy detector	MPI, GARCHING	Max Planck Institute for Extraterrestrial Physics
LEM	lunar excursion module	MPI, HEIDELBG	Max Planck Institute for Nuclear Physics
LEPEDEA	low-energy proton and electron differential energy analyzer	MPI, LINDAU	Max Planck Institute for Aeronomy---Max Planck Institute for Stratospheric Physics
LeRC	Lewis Research Center (NASA)	MR	magnetospherically reflected; medium resolution
LES	Lincoln Experimental Satellite (DOD)	MRIR	medium-resolution infrared radiometer
LETS	low-energy telescope system	ms	microsecond
LHIR	lower hybrid resonance	MSC	Manned Spacecraft Center (now Johnson Space Center)
LL	Lincoln Laboratory (MIT)	msec	millisecond
LM	lunar module	MSFC	Marshall Space Flight Center (NASA)
LMD	Laboratory of Meteorological Dynamics	MSN	mission
LOCKHEED	Lockheed Palo Alto Research Laboratory	MSS	Magnetic Storm Satellite (AFCL-NASA); multispectral scanner
LOFTI	Low-Frequency Trans-Ionospheric Satellite (USN-NRL)	MSSCC	multicolor spin-scan cloudcover camera
LOGACS	Low-G Accelerometer Calibration System (USAF)	MTS	Meteoroid Technology Satellite (NASA)
LPSP	Laboratoire de Physique Stellaire et Planetaire (CNRS)	MULLARD SS	Mullard Space Science Laboratory, Dorking, Surrey, UK
LRC	Langley Research Center (NASA)	MUSE	monitor of ultraviolet solar energy
LRIR	limb radiance inversion radiometer; low-resolution infrared radiometer	mw	milliwatt
LRL	Lunar Receiving Laboratory (JSC)		N
LRV	lunar roving vehicle	NA	not applicable; Nora Alice (satellite, DOD)
LST	Large Space Telescope (satellite, NASA)	NACE	neutral atmosphere composition experiment
.lt.	less than	NADUC	Nimbus/ATS Data Utilization Center (now NESS)
LTV	Ling-Temco-Vought (company)	NaI	sodium iodide
	M	NASA	National Aeronautics and Space Administration
m	meter, milli- (prefix)		
MA	Mercury Atlas		
MAD	Madrid, Spain		

Abbreviations and Acronyms

NASA OFFICES:

NASA-OA	NASA Office of Applications
NASA-OART	NASA Office of Advanced Research and Technology
NASA-OAST	NASA Office of Aeronautics and Space Technology
NASA-OMSF	NASA Office of Manned Space Flight
NASA-OSS	NASA Office of Space Science
NASA-OSSA	NASA Office of Space Science and Applications (now two separate offices)
NASA-OTDA	NASA Office of Tracking and Data Acquisition

NASA Research Centers:

NASA-ARC	NASA-Ames Research Center
NASA-FRC	NASA-Flight Research Center
NASA-GISS	NASA-Goddard Institute for Space Studies
NASA-GSFC	NASA-Goddard Space Flight Center
NASA-JPL	NASA-Jet Propulsion Laboratory
NASA-JSC	NASA-Johnson Space Center
NASA-KSC	NASA-John F. Kennedy Space Center
NASA-LeRC	NASA-Lewis Research Center
NASA-LRC	NASA-Langley Research Center
NASA-MSFC	NASA-Marshall Space Flight Center
NASA-WS	NASA-Wallops Station
NASC	National Aeronautics and Space Council
NASDA	National Space Development Agency
NATL	national
NATL RSCY CNCL, ITALY	National Research Council, Italy
NATO	North Atlantic Treaty Organization
NBS	National Bureau of Standards
NCAR	National Center for Atmospheric Research
NCC	National Climatic Center
NDRE	Norwegian Defense Research Establishment
NEMS	Nimbus-E Microwave Spectrometer; Near-Earth Magnetospheric Satellite (ESRO)
NESC	National Environmental Satellite Center (now NESS)
NESS	National Environmental Satellite Service (NOAA)
NGSP	National Geodetic Satellite Program
NETHERLANDS INST	Netherlands Institute of Nuclear Physics Research
NHC	National Hurricane Center
NIH	National Institutes of Health
NMC	National Meteorological Center
NMRT	Nimbus meteorological radiation tape
NNN	no national name
NNSS	Navy Navigational Satellite System
NOAA	National Oceanographic and Atmospheric Administration (formerly ESSA)
NOMSS	National Operational Meteorological Satellite System
NORAD	North American Air Defense Command
NORWEGIAN INST	Norwegian Institute of Cosmic Physics
NOS	National Ocean Survey (NOAA)

NOTS CHLAKE

NRC	Naval Ordnance Test Station, China Lake
NRL	National Research Council
NRL	Naval Research Laboratory
NSA	National Security Agency
nsec	nanosecond
NSF	National Science Foundation
NSSDC	National Space Science Data Center
NUCL	nuclear
NWL	Naval Weapons Laboratory
NWRC	National Weather Records Center (presently NCC)

O

OA	Office of Applications (NASA)
OA0	Orbiting Astronomical Observatory (satellite, NASA-GSFC)
OAR	Office of Aerospace Research (USAF)
OART	Office of Aerospace Research and Technology
OAST	Office of Aeronautics and Space Technology (NASA)
OBS	observatory
OCC	OPWE Command Center
OFO	Orbiting Frog Otolith (NASA experimental spacecraft)
OGO	Orbiting Geophysical Observatory (satellite, NASA)
OI	other investigator
OMNI	low-resolution omnidirectional radiometer (on Explorer 7)
OMSF	Office of Manned Space Flight (NASA)
ONR	Office of Naval Research
OPFP	orbital-plane experiment package
OPLE	Omega position and location experiment
OP OFF	operational off
ORBIS	Orbiting Radio Beacon Ionospheric Satellite (NASA)
ORS	Octahedral Research Satellite (NASA); Orbiting Research Satellite
OSCAR	Orbiting Satellite Carrying Amateur Radio
OSO	Orbiting Solar Observatory (satellite, NASA-GSFC)
OSS	Office of Space Science (NASA)
OSSA	Office of Space Science and Applications (NASA; now two separate offices)
OSTARE	Old Scientific Technical Aerospace Reports Extended
OT	Operational Tiros (satellite, NASA-GSFC)
OTDA	Office of Tracking and Data Acquisition (NASA)
OV	Orbiting Vehicle (satellite, USAF)

P

PAC	Package Attitude Control (satellite, NASA-GSFC)
PAET	Planetary Atmosphere Experiment Test

Abbreviations and Acronyms

PAGEOS	Passive Geodetic Earth-Orbiting Satellite (NASA)	RSRS	Radio and Space Research Station (now Appleton Laboratory)
PAM	pulse amplitude modulation	RTD	Research Technology Division (USAF)
PCM	pulse coded modulation	RTG	radioisotope thermoelectric generator
PE	Planetary Explorer	RTTS	real-time transmission system
PEP	platform electronic packages		
PFM	pulse frequency modulation		
PHASR	Personnel Hazards Associated with Space Radiation (satellite, USAF)		
PHYS	physics		
PI	principal investigator		
PIXEL	picture element		
PL	prelaunch; pro-longitudinal (whistler mode)		
PM	pulse modulation; photomultiplier (tube)		
PMR	pressure modulation radiometer; Pacific Missile Range		
PMT	photomultiplier tube		
p-n	positive-negative (junction)		
POGO	Polar Orbiting Geophysical Observatory (satellite, NASA)		
pps	pulse per second		
PROT	protection		
PS	pressure sensor		
PSE	passive seismograph experiment		
PTL	Photographic Technology Laboratory		
	Q		
QOMAC	quarter-orbit magnetic attitude control (system)		
QUI	Quito, Ecuador		
	R		
R&D	research and development		
RA	Ranger		
rad	radian, radiation		
RADCAT	Radar Calibration Target (satellite, ARPA)		
RADOSE	Radiation Dosimeter (satellite, DOD)		
RAE	Radio Astronomy Explorer (NASA-GSFC)		
RAM	random access measurement (system)		
RBV	return beam vidicom (camera)		
RC	resistance capacitor		
RCA	Radio Corporation of America		
R _E	Earth radius		
REP	republic		
RES	research		
REXS	Radio Exploration Satellite (Japan)		
rf	radio frequency		
RM	Radiation Meteoroid (satellite, NASA-OART)		
rms	root mean square		
ROS	Rosman, North Carolina		
RPA	retarding potential analyzer		
rpm	revolutions per minute		
rps	revolutions per second		
RRL	Radio Research Laboratories		
RSCH	research		
			S
		SAR	Subauroral red (arcs)
		SAM	stratospheric aerosol measurement
		SAMOS	Satellite Mission Observation System
		SAMS	stratospheric and mesospheric sounder
		SAMSO	Space and Missile Systems Organization (USAF)
		SAO	Smithsonian Astrophysical Observatory
		SAS	Small Aeronomy Satellite (NASA); Soviet Academy of Sciences
		SATAR	Satellite for Aerospace Research (NASA); OVI-2
		SATELL	satellite
		SATS	Satellite Antenna Test System (NASA)
		SBRC	Santa Barbara Research Center
		SCAMS	scanning microwave spectrometer
		SCEL	Signal Corps Engineering Laboratories
		SCH	School
		SCI	science
		SCMR	surface composition mapping radiometer
		SCORE	Signal Communication by Orbiting Relay Equipment (satellite, DOD)
		SCR	selective chopper radiometer
		SE	Solar Explorer (satellite, NASA)
		SEA	spherical electrostatic analyzer
		SEASAT	Ocean Dynamic Satellite (NASA)
		sec	second
		SEC	secondary electron conduction (vidicon tube)
		SECOR	Sequential Collation of Range (satellite, USAF-USA)
		SEM	space environment monitor
		SERT	Spinning Satellite for Electric Rocket Test (NASA-LERC)
		SESP	Space Experiment Support Program
		SESPO	Space Environmental Support Project Office
		SHS	Soviet Hydrometeorological Service
		SIBS	Salk Institute for Biological Studies
		SIDS	Space Investigations Documentation System (NASA)
		SIM	scientific instrument module
		SIRS	satellite infrared spectrometer
		SKA	Fairbanks, Alaska
		SM	San Marco (satellite, NASA-Italy)
		SMMR	scanning multispectral microwave radiometer
		SMS	Synchronous Meteorological Satellite (NASA)
		SNAP	systems for nuclear auxiliary power

Abbreviations and Acronyms

PAGEOS Passive Geodetic Earth-Orbiting Satellite (NASA)
 PAM pulse amplitude modulation
 PCM pulse coded modulation
 PE Planetary Explorer
 PEP platform electronic packages
 PFM pulse frequency modulation
 PHASR Personnel Hazards Associated with Space Radiation (satellite, USAF)
 PHYS physics
 PI principal investigator
 PIXEL picture element
 PL prelaunch; pro-longitudinal (whistler mode)
 PM pulse modulation; photomultiplier (tube)
 PMR pressure modulation radiometer; Pacific Missile Range
 PMT photomultiplier tube
 p-n positive-negative (junction)
 POGO Polar Orbiting Geophysical Observatory (satellite, NASA)
 pps pulse per second
 PROT protection
 PS pressure sensor
 PSE passive seismograph experiment
 PTL Photographic Technology Laboratory

Q

QOMAC quarter-orbit magnetic attitude control (system)
 QUI Quito, Ecuador

R

R&D research and development
 RA Ranger
 rad radian, radiation
 RADCAT Radar Calibration Target (satellite, ARPA)
 RADOSE Radiation Dosimeter (satellite, DOD)
 RAE Radio Astronomy Explorer (NASA-GSFC)
 RAM random access measurement (system)
 RBV return beam vidicom (camera)
 RC resistance capacitor
 RCA Radio Corporation of America
 R_E Earth radius
 REP republic
 RES research
 REXS Radio Exploration Satellite (Japan)
 rf radio frequency
 RM Radiation Meteoroid (satellite, NASA-OART)
 rms root mean square
 ROS Rosman, North Carolina
 RPA retarding potential analyzer
 rpm revolutions per minute
 rps revolutions per second
 RRL Radio Research Laboratories
 RSCH research

RSRS Radio and Space Research Station (now Appleton Laboratory)
 RTD Research Technology Division (USAF)
 RTG radioisotope thermoelectric generator
 RTTS real-time transmission system

S

SAR Subauroral red (arcs)
 SAM' stratospheric aerosol measurement
 SAMOS Satellite Mission Observation System
 SAMS stratospheric and mesospheric sounder
 SAMSO Space and Missile Systems Organization (USAF)
 SAO Smithsonian Astrophysical Observatory
 SAS Small Aeronomy Satellite (NASA); Soviet Academy of Sciences
 SATAR Satellite for Aerospace Research (NASA); OVI-2
 SATELL satellite
 SATS Satellite Antenna Test System (NASA)
 SBRC Santa Barbara Research Center
 SCAMS scanning microwave spectrometer
 SCEL Signal Corps Engineering Laboratories
 SCH School
 SCI science
 SCMR surface composition mapping radiometer
 SCORE Signal Communication by Orbiting Relay Equipment (satellite, DOD)
 SCR selective chopper radiometer
 SE Solar Explorer (satellite, NASA)
 SEA spherical electrostatic analyzer
 SEASAT Ocean Dynamic Satellite (NASA)
 sec second
 SEC secondary electron conduction (vidicon tube)
 SFCOR Sequential Collation of Range (satellite, USAF-USA)
 SEM Sequential Collation of Range (satellite, USAF-USA)
 SEM space environment monitor
 SERT Spinning Satellite for Electric Rocket Test (NASA-LERC)
 SESP Space Experiment Support Program
 SESPO Space Environmental Support Project Office
 SHS Soviet Hydrometeorological Service
 SIBS Salk Institute for Biological Studies
 SIDS Space Investigations Documentation System (NASA)
 SIM scientific instrument module
 SIRS satellite infrared spectrometer
 SKA Fairbanks, Alaska
 SM San Marco (satellite, NASA-Italy)
 SMMR scanning multispectral microwave radiometer
 SMS Synchronous Meteorological Satellite (NASA)
 SNAP systems for nuclear auxiliary power

Nov. 10, 1975

Abbreviations and Acronyms

SNT	Santiago, Chile	TDRSS	tracking and data relay satellite system
SOEP	solar-oriented experiment package	tec	total electron content
SOLRAD	Solar Radiation (satellite, NASA)	TEC	telemetry and command; transearth coast (Apollo program)
SPHINX	Space Plasma High Voltage Interactive Experimenter (satellite, NASA)	TECH	technical
SPM	solar proton monitor	TEI	transearth injection
SR	Solar Radiation (satellite, NASA); scanning radiometer	TELESAT	Canadian Telecommunications Satellite; also referred to as ANIK
SRATS	Solar Radiation and Thermospheric Structure (satellite, Japan)	temp	temporal; temperature
SRC	Space Research Council, UK	TET	telescope and electron telescope
SRI	Stanford Research Institute	TETR	Test and Training (satellite, NASA)
SRT	supporting research and technology	THIR	temperature-humidity infrared radiometer
SSCC	spin-scan cloudcover camera	THORAD-AGE	Thor Augmented Delta Agena (launch vehicle)
SSD	Space Sciences Division (Jet Propulsion Laboratory)	TIMATION	Time Location System (USN)
SSS	Small Scientific Satellite (NASA)	TIP	Tracking Impact Prediction (satellite, DOD)
SST	satellite-to-satellite tracking	TIROS	Television and Infrared Observation Satellite (NASA)
STADAN	Space Tracking and Data Acquisition Network	TL	team leader
STAR	Scientific and Technical Aerospace Reports	TLI	translunar injection
STARAD	Starfish Radiation (satellite, NASA)	TM	team member
STD	standard	TOMS	total ozone mapping system
STDN	Spaceflight Tracking and Data Network (NASA)	TOPO	topographic
ster	steradian	TOPS	Thermal Noise Optical Optimization Communication System (NASA)
STL	Space Technology Laboratories (now TRW Systems Group)	TOPSI	topside (sounder) (satellite, NASA)
STN	station	TOS	Tiros Operational Satellite (or System) (NASA)
STP	Solar Terrestrial Probe (also known as HELIOCENTRIC or IME-4, satellite, NASA-GSFC)	TOVS	Tiros operational vertical sounder
STRATOS	stratosphere	TRAAC	Transit Research and Attitude Control (satellite, USN)
STUD	studies	TRANET	Doppler Tracking Network (USN)
SUI	State University of Iowa (now University of Iowa)	TRANSP	transportation
SURCAL	Surveillance Calibration (satellite, DOD-NRL)	TRF	Technical Reference File
SVC	service	TRS	Tetrahedral Research Satellite (USAF)
SW/CTR ADV STUDIES	Southwest Center for Advanced Studies	TRW	TRW Systems Group
SW	southwest	ITS	Test and Training Satellite (NASA); also called TATS, TETR
SWRF	Sine Wave Response Filter (program)	TWERLE	tropical wind energy conversion and reference level experiment
SYNCOM	Synchronous Communication Satellite (NASA-GSFC)		
SYST	system		
	T		U
T&DR	tracking & data relay	U	university
TAC	Technology Application Center	U OF CALIF, BERK	University of California at Berkeley
TACOMSAT	Tactical Communications Satellite (DOD)	U OF CALIF, LA	University of California at Los Angeles
TACSAT	Tactical Communications Satellite (DOD)	U OF CALIF, RIVER	University of California at Riverside
TAT	Thrust-augmented Thor	U OF CALIF, SD	University of California at San Diego
TATS	Test and Training Satellite (NASA)	UCLA	University of California at Los Angeles
TATSACOM	Tactical Satellite Communications (program, DOD)	UHF	ultra-high frequency
TD	Thor-Delta (satellite, ESRO); launch vehicle (NASA-USAF)	UK	United Kingdom
TDP	Tracking Data Processor (program)	ULF	ultra-low frequency
		US	United States
		USA	United States Army
		USA TOPO COM	United States Army Topographic Command

Abbreviations and Acronyms

SNT	Santiago, Chile
SOEP	solar-oriented experiment package
SOLRAD	Solar Radiation (satellite, NASA)
SPHINX	Space Plasma High Voltage Interactive Experimenter (satellite, NASA)
SPM	solar proton monitor
SR	Solar Radiation (satellite, NASA); scanning radiometer
SRATS	Solar Radiation and Thermospheric Structure (satellite, Japan)
SRC	Space Research Council, UK
SRI	Stanford Research Institute
SRT	supporting research and technology
SSCC	spin-scan cloudcover camera
SSD	Space Sciences Division (Jet Propulsion Laboratory)
SSS	Small Scientific Satellite (NASA)
SST	satellite-to-satellite tracking
STADAN	Space Tracking and Data Acquisition Network
STAR	Scientific and Technical Aerospace Reports
STARAD	Starfish Radiation (satellite, NASA)
STD	standard
STDN	Spaceflight Tracking and Data Network (NASA)
ster	steradian
STL	Space Technology Laboratories (now TRW Systems Group)
STN	station
STP	Solar Terrestrial Probe (also known as HELIOCENTRIC or IME-4, satellite, NASA-GSFC)
STRATOS	stratosphere
STUD	studies
SUI	State University of Iowa (now University of Iowa)
SURCAL	Surveillance Calibration (satellite, DOD-NRL)
SE CTR ADV STUDIES	Southwest Center for Advanced Studies
SVC	service
SW	southwest
SWRF	Sine Wave Response Filter (program)
SYNCOM	Synchronous Communication Satellite (NASA-GSFC)
SYST	system

T

T&DR	tracking & data relay
TAC	Technology Application Center
TACOMSAT	Tactical Communications Satellite (DOD)
TACSAT	Tactical Communications Satellite (DOD)
TAT	Thrust-augmented Thor
TATS	Test and Training Satellite (NASA)
TATSACOM	Tactical Satellite Communications (program, DOD)
TD	Thor-Delta (satellite, ESRO); launch vehicle (NASA-USAF)
TDP	Tracking Data Processor (program)

TDRSS	tracking and data relay satellite system
tec	total electron content
TEC	telemetry and command; transearth coast (Apollo program)
TECH	technical
TEI	transearth injection
TELESAT	Canadian Telecommunications Satellite; also referred to as ANIK
temp	temporal; temperature
TET	telescope and electron telescope
TETR	Test and Training (satellite, NASA)
THIR	temperature-humidity infrared radiometer
THORAD-AGE	Thor Augmented Delta Agena (launch vehicle)
TIMATION	Time Location System (USN)
TIP	Tracking Impact Prediction (satellite, DOD)
TIROS	Television and Infrared Observation Satellite (NASA)
TL	team leader
TLI	translunar injection
TM	team member
TOMS	total ozone mapping system
TOPO	topographic
TOPS	Thermal Noise Optical Optimization Communication System (NASA)
TOPSI	topside (sounder) (satellite, NASA)
TOS	Tiros Operational Satellite (or System) (NASA)
TOVS	Tiros operational vertical sounder
TRAAC	Transit Research and Attitude Control (satellite, USN)
TRANET	Doppler Tracking Network (USN)
TRANSP	transportation
TRF	Technical Reference File
TRS	Tetrahedral Research Satellite (USAF)
TRW	TRW Systems Group
TTS	Test and Training Satellite (NASA); also called TATS, TETR
TWERLE	tropical wind energy conversion and reference level experiment

U

U	university
U OF CALIF, BERK	University of California at Berkeley
U OF CALIF, LA	University of California at Los Angeles
U OF CALIF, RIVER	University of California at Riverside
U OF CALIF, SD	University of California at San Diego
UCLA	University of California at Los Angeles
UHF	ultra-high frequency
UK	United Kingdom
ULF	ultra-low frequency
US	United States
USA	United States Army
USA TOPO COM	United States Army Topographic Command

Abbreviations and Acronyms

USAFECOM	United States Army Electronics Command	WWW	World Weather Watch
USAF	United States Air Force		
USAF AEROPROPUL	United States Air Force Aeropropulsion Laboratory		Z
USAF MAT LAB	United States Air Force Materials Laboratory	Z	atomic number
USAF MDE	United States Air Force Medicine, Wright Patterson AFB		
USAF SAMSO	United States Air Force Space and Missile Systems Organization		
USAF SCH OF AEROS MED	United States Air Force School of Aerospace Medicine, Brooks AFB		
USN	United States Navy		
USN AEROS MED RSCH LAB	United States Navy Aerospace Medicine Research Laboratory		
USSR	Union of Soviet Socialist Republics		
US TOPO CMD	United States Army Topographic Command		
UT	universal time		
UTD	University of Texas at Dallas		
UV	ultraviolet		
UVNO	ultraviolet nitric-oxide experiment		
UVS	ultraviolet spectrometer		

V

v	volt
var	variation
VHF	very high frequency
VHRR	very high resolution radiometer
VISSR	visible infrared spin-scan radiometer
VLf	very low frequency
VNBC	Vandenberg AFB, California (also referred to as WTR, Western Test Range)
VTPR	vertical temperature profile radiometer

W

w	watt
WALI	Wallops Island
WBVTR	wideband video tape recorder
WDC	World Data Center
WDC-A-R&S	World Data Center A for Rockets and Satellites
WEFAX	weather facsimile
WFC	Wallops Flight Center (NASA)
WGSPR	Working Group for Space Physics Research
WKG GRP SPC PHYS RSCH	Working Group for Space Physics Research
WMO	World Meteorological Organization
WNK	Winkfield, England
wpm	words per minute
WRESAT	Weapons Research Establishment Satellite (Australia)
WS	Wallops Station (NASA)
WSMR	White Sands Missile Range
WT	walking-trace
WTR	Western Test Range (also referred to as Vandenberg AFB)

Nov. 10, 1975

1. Report No. NASA SP-7601		2. Government Accession No.		3. Recipient's Catalog No.	
4. Title and Subtitle OGO Program Summary				5. Report Date December 1975	
				6. Performing Organization Code	
7. Author(s) John E. Jackson and James I. Vette				8. Performing Organization Report No.	
9. Performing Organization Name and Address National Space Science Data Center Goddard Space Flight Center Greenbelt, MD 20771				10. Work Unit No.	
				11. Contract or Grant No.	
12. Sponsoring Agency Name and Address National Aeronautics and Space Administration Goddard Space Flight Center Greenbelt, MD 20771				13. Type of Report and Period Covered	
				14. Sponsoring Agency Code	
15. Supplementary Notes					
16. Abstract Six Orbiting Geophysical Observatories (OGO's) were launched, one per year, over the period 1964 to 1969. OGO's 1, 3, and 5 were placed in highly elliptical, low-inclination orbits to retrieve and transmit data on the interplanetary region, shock and transition zones, the magnetosphere, the radiation belts, the ionosphere, cosmic rays, micrometeorites and the geocorona. OGO's 2, 4, and 6 were placed in low-altitude, nearly polar orbits to study the neutral atmosphere, particle influence at poles, airglow and auroral emissions, solar flares, etc. A comprehensive overview of the OGO program with special emphasis on scientific and technological accomplishments, descriptions of spacecraft and experiment characteristics with specialized indexes and an acronym/abbreviation glossary are given. Also included is an experiment-related bibliography consisting mainly of accessions (citation and abstracts, when available) from the NASA data base, with customized subject, personal author, and corporate source indexes.					
17. Key Words (Suggested by Author(s)) Artificial Satellites NASA Programs Bibliographies OGO Earth Satellites Summaries Geophysical Observations			18. Distribution Statement Unclassified - Unlimited		
19. Security Classif. (of this report) Unclassified		20. Security Classif. (of this page) Unclassified		21. No. of Pages 318	22. Price* \$6.00 HC